Martin Bertau · Heribert Offermanns
Ludolf Plass · Friedrich Schmidt
Hans-Jürgen Wernicke *Editors*

Methanol: The Basic Chemical and Energy Feedstock of the Future

Asinger's Vision Today

Springer

Methanol: The Basic Chemical and Energy Feedstock of the Future

Martin Bertau · Heribert Offermanns
Ludolf Plass · Friedrich Schmidt
Hans-Jürgen Wernicke
Editors

Methanol: The Basic Chemical and Energy Feedstock of the Future

Asinger's Vision Today

Based on "Methanol - Chemie- und Energierohstoff: Die Mobilisation der Kohle" by Friedrich Asinger published in 1986. Includes contributions by more than 40 experts from Industry and Academia.

Springer

Editors
Martin Bertau
Institut für Technische Chemie
TU Bergakademie Freiberg
Freiberg
Germany

Heribert Offermanns
Hanau
Germany

Ludolf Plass
Kronberg
Germany

Friedrich Schmidt
Rosenheim
Germany

Hans-Jürgen Wernicke
Wolfratshausen
Germany

ISBN 978-3-642-39708-0 ISBN 978-3-642-39709-7 (eBook)
DOI 10.1007/978-3-642-39709-7
Springer Heidelberg New York Dordrecht London

Library of Congress Control Number: 2013945151

Preface

The world population is increasing dramatically; fossil fuels are finite, and farmland as well as pastureland is limited or even declining. Therefore, the question of how to supply mankind not just with raw materials, fuels and energy, but also with food has been a topic of importance to the scientific community for a long time. The discussion has even intensified since "The Limits to Growth" was published by the Club of Rome, since climate conferences (Montreal 2005 etc.) have taken place, and especially since Germany's nuclear power phase-out.

The pioneer of petrochemistry in research and teaching, Friedrich Asinger from RWTH in Aachen, Germany, very early drew attention on to the waste of fossil fuels and proposed alternative concepts to secure raw material supply for the chemical and energy industry. In his book, published in 1986, he recommended methanol as a suitable basic chemical that can be easily stored and used as fuel or a fuel additive, as well as a chemical or energy raw material. He worked on this book without any help. He searched for, found and selected (and commented on) every citation completely on his own. With his book's subtitle "The Mobilisation of Coal" he indicated a medium-term solution—doing without oil and gas as fuels in the shortest possible timeframe. He also developed visions for a time after coal, oil and gas.

When all fossil fuel sources are exhausted, only CO_2 will be left (in the atmosphere and in the oceans) and—up to a point—Biomass.

Because Asinger's book is out of print and has never been translated into English, and because the issue of methanol as a chemical and energy feedstock is—now more than ever—a "hot topic", the time for a new book (in memory of Asinger, in a broad sense) has come.

Heribert Offermanns, a former student and assistant to Friedrich Asinger, took the initiative to gather a team of five editors—four of them with industrial experience and one who is professor at Freiberg University of Mining and Technology—with the aim of publishing a second revised edition that comprehensively documents the latest state of development in the field of methanol generation and usage. Also playing an active part in authoring this book, the editors succeeded in finding 46 well known experts from industry, academia and governmental research facilities as authors for the new edition.

The book is divided into a general and a more specific part. The general part begins with Asinger's vita, a short history of methanol and its present importance, as well as visions for the future beyond oil and gas: "Fossil Raw Materials—What Comes Next?" by Willi Keim, Aachen and "Technical Photosynthesis" by Franz X. Effenberger, Stuttgart. The extensive specific part, with contributions from the respective experts, provides information on the raw materials and their conditioning for methanol synthesis, as well as methanol synthesis itself. New topics include the physical and toxicological properties and issues of transport and storage. Methanol use as fuel and energy feedstock is addressed, as is its potential as an oil and gas substitute and as chemical feedstock. The book comprises eight chapters, and the number of literature citations exceeds 3,000. In particular, Chap. 4 (dealing with methanol feedstock and its conditioning) and Chap. 6 (methanol use) were substantially extended in comparison to the "old" Asinger. Of special value is access to the 1,400 references of the "Asinger" of 1986.

Martin Bertau
Heribert Offermanns
Ludolf Plass
Friedrich Schmidt
Hans-Jürgen Wernicke

Acknowledgments

A book like this would not have been realised without the committed support of many colleagues, among whom we first and foremost wish to express our dedicated thanks to the authors. Their competence and experience in their fields made it possible for us to prepare and publish this book. Further thanks is owed to Elizabeth Hawkins and Birgit Münch, Springer-Verlag, who always had an open ear for yet another wish to be realised and for countless reasons why this book deserved countless issues to be included deadline after deadline. Thanks are expressed also to Marion Hertel, Springer-Verlag, with whom everything began and who from the very beginning shared and supported our passion for this methanol compendium.

From the Institute of Chemical Technology, Freiberg University of Mining and Technology, we wish to thank Valentin G. Greb and Ringo Heyde for skilled and sophisticated graphical illustrations. Particular thanks are also owed to Ramona Handrek, Sebastian Hippmann, Michael Kraft, Tom Lorenz, Gunter Martin, Carsten Pätzold, Lydia Reichelt, Martin Seifert and Eric Weingart for proofreading the manuscript and helpful discussions. Steffen Braun, Freiberg University of Mining and Technology, is thanked for installing and patiently maintaining electronic data exchange. Sincere thanks are due to Norbert Ringer, Clariant Produkte Deutschland GmbH, for reviewing the chapters related to methanol synthesis and synthesis gas generation. Wolfgang Hilsebein, a former Lurgi colleague, gave very helpful advice regarding syngas and methanol processes, and Sandra Schröder of Air Liquide Global E&C Solutions prepared many figures and schemes.

Last but not least, we wish to express our utmost thanks to our families for showing never-ending patience and understanding. Finishing this book took much more effort and time than originally scheduled, so thank you all very much!

Freiberg, Hanau, Kronberg, Rosenheim, Wolfratshausen in February 2014.

Martin Bertau
Heribert Offermanns
Ludolf Plass
Friedrich Schmidt
Hans-Jürgen Wernicke

Contents

About the Editors

Martin Bertau Chair of Chemical Technology at Freiberg University of Mining and Technology, received his Ph.D. in 1997 at the University of Freiburg. He then headed the biotechnology division of Rohner Ltd. (Dynamit-Nobel group) in Basel, Switzerland. In the year 2000, he moved to Dresden University of Technology, where he received his *venia legendi* as well as *facultas docendi* both for biochemistry and organic chemistry in 2005. Since 2006, he has been heading the Institute of Chemical Technology at Freiberg University of Mining and Technology. His key areas of activity comprise resource chemistry and white biotechnology with the aim of developing integrated processes (zero-waste concept) for producing and recycling of chemistry raw materials such as strategic metals (rare earth metals, lithium, indium and others) and phosphorous, but also utilising CO_2 as well as lignocellulose for the production of base chemicals. For his work on the first industrial process for phosphate recycling, in 2012 he was awarded the resource efficiency prize of the German Federal Ministry of Economics and Technology.

Heribert Offermanns studied Chemistry at the RWTH Aachen, where he received his diploma in 1963. His doctoral degree was earned at the Institute of Technical Chemistry and Petrochemistry of the RWTH Aachen (under Prof. Dr. Friedrich Asinger) in 1966. He joined Degussa AG, Frankfurt in 1968 and served in various positions (R&D of organic chemistry, drug research, production of fumed silica and corporate technology in Germany, Belgium and the United States). From 1976 until retirement in 1999, he was for nearly 25 years a member of the Executive Board, where he was responsible for Central Functions (R&D, Chemical Engineering),

operational activities (Industrial Chemicals) and regions (United States, South America). Under his leadership, Degussa entered very successfully the field of biotechnology (mainly amino acids). He was a member of the council of the Johann-Wolfgang-Goethe-University, Frankfurt, a board member of the "Freunde und Förderer" of the university, and honorary professor. He served as a senator of the German Science Foundation (DFG). He also was member and later on president of the Chemical Industry Fund (*Fonds der Chemischen Industrie*) and for 13 years was a member of the board of the German Chemical Society. He was awarded Dr.-Ing. E.h. of RWTH Aachen, honorary member of the *Physikalischer Vereins* (Frankfurt) and of the *Wilhelm-Ostwald-Gesellschaft* (Großbothen), the *Carl-Duisberg-Plakette der GDCh*, the *Karl-Winnacker-Preis* of the *Marburger Universitätsbund*, and the *Bundesverdienstkreuz First Class*.

Ludolf Plass studied Mechanical Engineering at the Technical University in Darmstadt and graduated with a Ph.D. in chemical engineering from the University of Erlangen-Nuremberg. He has been employed with Lurgi GmbH for 40 years, among others in charge of the Lurgi Division for Coal and Power Technologies and the Company Lurgi Energy and Environmental Technologies GmbH. For several years, he has taken the function of chief technology officer of the Lurgi Group as executive vice president, responsible for Lurgi's technological processes including R&D. In 2006, he took the responsibility for product management and in 2008 for special projects. He served as chairman and board member of several Lurgi Affiliates and Joint Ventures in Germany, France, Italy, the United Kingdom, Spain, China, Australia and South Africa. He retired from Lurgi in 2009. He continued to work as senior advisor to the management board of Air Liquide E&C Solutions until the end of 2013. Aside from his work with Lurgi, he was a member of the Board of Directors of DECHEMA, and worked in several VDMA organisations/functions.

His present assignments include chairman of the advisory board of Schaefer Kalk, Diez, Lahn; chairman of the advisory board of Techno-Physik GmbH, Essen; member of the industry council Finatem Beteiligungs Gesellschaft Frankfurt, Main; Chairman of the advisory board of Ecoloop GmbH, Duisburg/Elbingerode/Harz; and chairman of the supervisory board of Christopherus Heim, Welzheim. In addition he is member of the advisory board of FMW Industrieanlagen GmbH, Kirchstetten (Austria).

Friedrich Schmidt was born in Beuthen, Germany (today Bytom, Poland), in 1943. He studied chemistry at the University of Hamburg, where he received his Ph.D. in 1973. Thereafter, he was an academic assistant at the University of Hamburg. In 1982, he was awarded the *venia legendi* on completion of his habilitation in physical chemistry at the University of Hamburg. From 1983 to 1986, he was Professor of Physical Chemistry at the University of Hamburg, Germany. From 1986 to 1992, he held various positions at the Munich-based Süd-Chemie, Germany; in 1993, he was appointed Director of Süd-Chemie Catalyst Development. He retired in 2002. He was a founding member and (from 2002 to 2006) chairman of the board of CONNECAT, the German Network of Catalysis.

Hans-Jürgen Wernicke studied Chemistry at the University of Kiel and received his Ph.D. in 1976 (supported by a grant from the German Chemical Industry Association). From 1976 to 1984, he was employed with Linde AG, Munich, where he was involved in engineering and construction of petrochemical plants, and assisted with the startup of a coal-to-liquids complex in South Africa. In 1985, he changed to Süd-Chemie AG, München, where he held various positions in the catalyst division, was active as project manager of zeolite catalysts, and assisted with the startup of a gas-to-liquids complex in South Africa. He was business unit manager of petrochemical catalysts and vice president of sales at Süd-Chemie Inc., USA. From 1996 to 2011, he was member of the Süd-Chemie executive board, and from 2007 to 2011 he was vice chairman of the executive board. Since 2007, he has been a member of the board of DECHEMA, which he headed from 2010 to 2012 as chairman. From 2008 to 2010, he was founding board member of the German Catalysis Society; from 1997 to 2011, he was a member of the board of trustees of the Chemical Industry Fund. He is a member of the board of curators of the Leibniz Institute for Catalysis, Rostock and of the Council of the University of Bayreuth.

Contributors

Nicola Ballarini Clariant Catalysis Italia, Via G. Fauser, 36/B, 28100 Novara, Italy
e-mail: nicola.ballarini@clariant.com

Martin Bertau Institute of Chemical Technology, Freiberg University of Mining and Technology, Leipziger Straße 29, 09599 Freiberg, Germany
e-mail: martin.bertau@chemie.tu-freiberg.de

Matthias Blug Evonik Industries AG, Rodenbacher Chaussee 4, 63457 Hanau-Wolfgang, Germany
e-mail: matthias.blug@evonikindustries.com

Elisabeth Brandes Physikalisch-Technische Bundesanstalt, AG 3.41, Bundesallee 100, 38116 Braunschweig, Germany
e-mail: elisabeth.brandes@ptb.de

Stefan Buchholz Creavis Technologies & Innovation, Paul-Baumann-Straße 1, 45772 Marl, Germany
e-mail: stefan.buchholz@evonik.com

Gereon Busch Evonik Industries AG, Feldmühlestraße 3, 53859 Niederkassel-Luelsdorf, Germany
e-mail: gereon.busch@evonik.com

Franz Xaver Effenberger Institute of Organic Chemistry, University of Stuttgart, Pfaffenwaldring 55, 70569 Stuttgart, Germany
e-mail: franz.effenberger@oc.uni-stuttgart.de

Veronika Gronemann Air Liquide Global E&C Solutions c/o Lurgi GmbH, Lurgiallee 5, 60439 Frankfurt/M., Germany
e-mail: veronika.gronemann@lurgi.com

Armin Günther Air Liquide Global E&C Solutions c/o Lurgi GmbH, Lurgiallee 5, 60439 Frankfurt/M., Germany
e-mail: dr.armin.guenther@lurgi.com

Angelika Heinzel Institute of Energy and Environmental Process Engineering, University of Duisburg-Essen, Lotharstraße 1, 47048 Duisburg, Germany
e-mail: angelika.heinzel@uni-duisburg-essen.de

Ringo Heyde Institute of Chemical Technology, Freiberg University of Mining and Technology, Leipziger Straße 29, 09599 Freiberg, Germany
e-mail: ringo.heyde@chemie.tu-freiberg.de

Sebastian Hippmann Institute of Chemical Technology, Freiberg University of Mining and Technology, Leipziger Straße 29, 09599 Freiberg, Germany
e-mail: sebastian.hippmann@chemie.tu-freiberg.de

Dirk Holtmann DECHEMA Research Institute, Theodor-Heuss-Allee 25, 60468 Frankfurt/M., Germany
e-mail: holtmann@dechema.de

Willi Keim Institute of Chemical Technology and Macromolecular Chemistry, RWTH Aachen, Worringerweg 1, 52056 Aachen, Germany
e-mail: Keim@itmc.rwth-aachen.de

Christoph Kiener Untergasse 2, 09599 Freiberg, Germany
e-mail: christoph.kiener@gmx.de

Jens Leker Institute of Business Administration at the Department of Chemistry and Pharmacy, University of Münster, Leonardo-Campus 1, 48149 Münster, Germany
e-mail: leker@uni-muenster.de

Matthias Linicus Air Liquide Global E&C Solutions c/o Lurgi GmbH, Lurgiallee 5, 60439 Frankfurt/M., Germany
e-mail: matthias.linicus@lurgi.com

Tom Lorenz Institute of Chemical Technology, Freiberg University of Mining and Technology, Leipziger Straße 29, 09599 Freiberg, Germany
e-mail: tom.lorenz@chemie.tu-freiberg.de

Heribert Offermanns Grünaustraße 2, 63457 Hanau, Germany
e-mail: heppoff@gmx.de

Robert Pardemann Institute of Energy Process Engineering and Chemical Engineering, Freiberg University of Mining and Technology, Fuchsmühlenweg 9, 09599 Freiberg, Germany
e-mail: robert.pardemann@iec.tu-freiberg.de

Carsten Pätzold Institute of Chemical Technology, Freiberg University of Mining and Technology, Leipziger Straße 29, 09599 Freiberg, Germany
e-mail: carsten.paetzold@chemie.tu-freiberg.de

Ludolf Plass Parkstraße 11, 61476 Kronberg, Germany
e-mail: dr.ludolf.plass@t-online.de

Sven Pohl Air Liquide Global E&C Solutions c/o Lurgi GmbH, Lurgiallee 5, 60439 Frankfurt/M., Germany
e-mail: sven.pohl@lurgi.com

Konstantin Räuchle Institute of Chemical Technology, Freiberg University of Mining and Technology, Leipziger Straße 29, 09599 Freiberg, Germany
e-mail: konstantin.raeuchle@chemie.tu-freiberg.de

Lydia Reichelt Institute of Chemical Technology, Freiberg University of Mining and Technology, Leipziger Straße 29, 09599 Freiberg, Germany
e-mail: lydia.reichelt@chemie.tu-freiberg.de

Wladimir Reschetilowski Institute of Chemical Technology, Dresden University of Technology, 01062 Dresden, Germany
e-mail: wladimir.reschetilowski@chemie.tu-dresden.de

Norbert Ringer Clariant Products Germany GmbH, Ottostraße 3, 80333 Munich, Germany
e-mail: norbert.ringer@clariant.com

Jürgen Roes Institute of Energy and Environmental Process Engineering, University of Duisburg-Essen, Lotharstraße 1, 47048 Duisburg, Germany
e-mail: juergen.roes@uni-duisburg-essen.de

Jörn Rolker Evonik Industries AG, Rodenbacher Chaussee 4, 63457 Hanau-Wolfgang, Germany
e-mail: joern.rolker@evonik.com

Gerd Sandstede Esperantostraße 5, 50598 Frankfurt/M., Germany
e-mail: sandstede-consulting@arcor.de

Thomas Schendler Chemical Safety Engineering, Federal Institute for Materials Research and Testing, Unter den Eichen 87, 12205 Berlin, Germany
e-mail: thomas.schendler@bam.de

Friedrich Schmidt Angerbachstrasse 28, 83024 Rosenheim, Germany
e-mail: fs-ro@gmx.de

Jens Schrader DECHEMA Research Institute, Theodor-Heuss-Allee 25, 60468 Frankfurt/M., Germany
e-mail: schrader@dechema.de

Katja Schulz Medical Faculty Carl Gustav Carus, Institute of Legal Medicine, Dresden University of Technology, Fetscherstraße 74, 01307 Dresden, Germany
e-mail: katja.schulz@tu-dresden.de

Matthias Seiler Evonik Industries AG, Rodenbacher Chaussee 4, 63457 Hanau-Wolfgang, Germany
e-mail: matthias.seiler@evonik.com

Frank Seyfried Volkswagen Group Research, Volkswagen AG, Berliner Ring 2, 38436 Wolfsburg, Germany
e-mail: frank.seyfried@volkswagen.de

Frank Sonntag DECHEMA Research Institute, Theodor-Heuss-Allee 25, 60468 Frankfurt/M., Germany
e-mail: sonntag@dechema.de

Ulrich-Dieter Standt Volkswagen Group Research, Volkswagen AG, Berliner Ring 2, 38436 Wolfsburg, Germany
e-mail: ulrich-dieter.standt@volkswagen.de

Michael Steffen The fuel cell research centre ZBT GmbH, Carl-Benz Straße 201, 47057 Duisburg, Germany
e-mail: m.steffen@zbt-duisburg.de

Osman Turna Air Liquide Global E&C Solutions c/o Lurgi GmbH, Lurgiallee 5, 60439 Frankfurt/M., Germany
e-mail: osman.turna@lurgi.com

Thomas Veith DECHEMA Research Institute, Theodor-Heuss-Allee 25, 60468 Frankfurt/M., Germany
e-mail: veith@dechema.de

Eric Weingart Institute of Chemical Technology, Freiberg University of Mining and Technology, Leipziger Straße 29, 09599 Freiberg, Germany
e-mail: eric.weingart@chemie.tu-freiberg.de

Hans-Jürgen Wernicke Kardinal-Wendel-Straße 75 a, 82515 Wolfratshausen, Germany
e-mail: h.j.wernicke@t-online.de

Matthias S. Wiehn Evonik Industries AG, Feldmühlestraße 3, 53859 Niederkassel-Luelsdorf, Germany
e-mail: matthias.wiehn@evonik.com

Markus Winterberg Evonik Industries AG, Feldmühlestraße 3, 53859 Niederkassel-Luelsdorf, Germany
e-mail: markus.winterberg@evonik.com

Thomas Wurzel Air Liquide Global E&C Solutions c/o Lurgi GmbH, Lurgiallee 5, 60439 Frankfurt/M., Germany
e-mail: thomas.wurzel@lurgi.com

Abbreviations

AAGR	Average annual growth rate
ABB	Asea Brown Boveri, Zürich/CH
ACHEMA	Ausstellungstagung für chemisches Apparatewesen (Exhibition Congress on Chemical Engineering, Environmental Protection and Biotechnology)
ADH	Alcohol dehydrogenase
ADR	(European) Agreement concerning the International Carriage of Dangerous Goods by Road
ADN	(European) Agreement concerning the International Carriage of Dangerous Goods by Inland Waterways
AEE	Aminoethoxyethanol
AEL	Alkaline electrolysis
AFC	Alkaline fuel cell
AFI	Aluminophosphate-five (zeolite structure)
AGHR	Advanced gas heated reformer
AIDH	Aldehyde dehydrogenase
AIT	Automobile ignition temperature
ALPO	Aluminophosphate (zeolite)
ANG (plant)	American Natural Gas, now Dakota Gasification Comp. (plant)
AOX	Alcohole oxidase
ARC	Axial-radial converter
ASTM	American Society for Testing and Materials
ASU	Air separation unit
ATE	1. Approach to equilibrium 2. Acute toxicity equivalence
atm	pressure (1 atm = 1.01325 bar)
ATR	Autothermal reformer
B7	Diesel fuel containing 7 % Biodiesel
bar g	gauge pressure (absolute pressure minus atmospheric pressure)
BASF	Badische Anilin- & Soda-Fabrik SE, Ludwigshafen/D
bbl	barrel (used in petrochemical industry), equals approx. 0.159 m^3

BCG	Boston Consulting Group, Boston
BEL	Biological exposure limit
BET	Brunauer-Emmett-Teller (method to determine specific surfaces)
BEWAG	Berliner Städtische Elektrizitätswerke AG, (now part of Vattenfall Europe)
BFW	Boiler feed water
BGL	British Gas /Lurgi (gasifier)
bioliq®	Biomass-to-Liquids process of KTI, Karlsruhe
BMA	Blausäure aus Methan und Ammoniak (Hydrogen cyanide from methane and ammonia) process by DEGUSSA AG/D (now Evonik Industries AG/D)
BMFT	renamed to BMBF, Bundesministerium für Bildung und Forschung (German Federal Ministry of Education and Research)
b.p.	Boiling point
BP	British Petroleum p.l.c/UK (today also referred to as "beyond petroleum")
BPD	Barrels per day (1 barrel = 0.159 m^3)
BTL	Biomass-to-Liquids
BtM	Biomass-to-Methanol
BTU	British thermal unit (BTU or Btu), equal to about 1055 joules
BWR	Boiler water reactor
CAES	Compressed air energy storage
CAPEX	Capital expenditure
CC	Combined cycle
CCP	Clean coal power
CCS	Carbon capture and storage
CCU	Carbon capture and utilisation
CD	Catalytic Distillation
cf or ft^3	cubic feet (1 cf = 0.0283 m^3)
CFB	Circulating fluid bed (gasifier)
CFD	Computational Fluid Dynamics
CHA	Chabasite
CHG	Compressed hydrogen gas
CHP	Combined heat and power
CI	Compression ignition (engine)
CLP (regulation)	Classification, Labelling and Packaging regulation in the European Union
CMD	Collext-mix-distribute (concept)
CMG	Conversion of methanol to gasoline (catalyst)
COD	Conversion of olefins to diesel
CPA	Conversion of paraffins to aromatics
CPO	Catalytic partial oxidation

CRG	Catalytic rich gas (process)
CRI	Carbon Recycling International Inc., La Jolla CA, USA
CTF	Covalent triazine framework
CTP	Coal-to-Propylene
CW	Cooling water
DEA	Diethanolamine
DGA	Diglycolamine
DHA	Dihydroxyacetone
DHAP	Dihydroxyacetone phosphate
DI	Direct injection (engine)
DICP	Dalian Institue of Chemical Physics, Dalian/China
DIPA	Diisopropyl amine
DLR	Deutsches Zentrum für Luft- und Raumfahrt (German Aerospace Centre)
dm^3	cubic decimeter
DMC	Dimethyl carbonate
DME	Dimethyl ether
DMF	Dimethyl formamide
DMFC	Direct methanol fuel cell
DMM	Dimethoxy methane
DMS	Dimethyl sulphide
DMSO	Dimethyl sulphoxide
DMT	Dimethyl terephthalic acid
DMTO	(DICP technology for) Methanol-to-Olefins
DPT	Davy Process Technology, now Johnson Matthey Davy Technologies Ltd, London/UK
DRI	Direct Reduced Iron (process)
DVGW	Deutscher Verein des Gas- und Wasserfaches e.V. (German Technical and Scientific Association for Gas and Water)
ECU	Engine control unit
EEC	European Economic Community
EEG	Erneuerbare Energien Gesetz (German Renewable Energy Sources Act)
EDLC	Electrochemical double-layer capacitor
EF	Entrained flow (gasifier)
EFAL	Extra-framework aluminium (in zeolites)
EFOY	Fuel cell system of SFC Energy GmbH, Brunnthal, Germany
EG	Ethylene glycol
EJ	ExaJoule (about 278 TWh)
EPC	Engineering, procurement and construction
FaldDH	Formalehyde dehydrogenase
FAMe	Fatty acid methyl ester
FAO	United Nations Food and Agricultural Organization

FB	Fluidised bed (gasifier)
FBP	1. Final boiling point 2. Fructose-1,6-bisphosphate
FCC	Fluid catalytic cracking
FCCT	Freudenberg FCCT SE & Co. KG, Weinheim/D (fuel cells)
FCV	Fuel cell vehicle
FDBD	Fixed bed dry bottom (gasifier)
FDH	Formate dehydrogenase
FICFB	Fast internal circulating fluid bed (gasifier)
FZJ	Forschungszentrum Jülich GmbH, Jülich/D
F6P	Fructose-6-phosphate
GAP	Glyceraldehyde-3-phosphate
GCR	Gas cooled reactor
GDL	Gas diffusion layer
GHR	Gas heated reformer
GHSV	Gas hourly space velocity (Vol/Vol × h)
GIAP	Joint Stock Company, Scientific Research Institute of Nitrogen Industry, Moscow
GJ	GigaJoule (= 277.8 kWh)
GSH	Glutathione
GSP	1. "Gaskombinat Schwarze Pumpe" (now VSG Industriepark Schwarze Pumpe GmbH, Spreetal, D 2. Siemens gasifier
Gt	Gigatonne
GTI	Gas Technology Institute, Des Plaines, Il, USA
Gtoe	Gigatonnes of oil equivalent
GTL	Gas-to-Liquids
GTP	Gas-to-Propylene
GTR	Gas-to-Chemical resources (technology)
$\Delta_R G^\circ$	Standard free energy of reaction
H4MPT	Tetrahydromethanopterine
HER	Heat exchange reformer
HGT	Heavy gasoline treatment
HHV	Higher heating value
HM	Hydrogen from Methanol (process of Caloric GmbH)
HIAT	Hydrogen and Informatics Institue of Applied Techologies GmbH, Schwerin/D
HP Steam	High pressure steam
HTAS	Haldor Topsoe A/S, Lyngby/DK
HTEL	High temperature electrolysis
HTER	see HER
HTS	High temperature shift
HTW	High temperature Winkler (gasifier)

HYSOLAR	Hydrogen from Solar Energy (project led by Deutsches Zentrum für Luft- & Raumfahrt e.V.)
ΔH, ΔH_R	Enthalpy of reaction
$\Delta H°$, $\Delta_R H°$, $\Delta H°_R$	Standard enthalpy of reaction
$\Delta_v H$	Heat of evaporation
ICIS	Independent Chemical Information Service (a business unit of Reed Business Information)
ICT	Fraunhofer Institue for Chemical Technologies, Pfinztal/D
ICVT	Institute of Chemical Process Engineering, Stuttgart/D
IDGCC	Integrated drying gasification combined cycle
IEA	International Energy Agency, Paris/F
IGCC	Integrated gasification combined cycle
ILPM	Improved low pressure methanol (technology)
IMDG (code)	International Maritime Code for Dangerous Goods (issued by International Marine Organisation)
IMFC	Indirect methanol fuel cell
IRR	Internal rate of return
ISE	Fraunhofer Institute for Solar Energy Systems, Freiburg/D
JAMG	Jincheng Anthracite Mining Group
JFE	JFE (Japan Fe Engng.) Group, Tokyo/J (formerly NKK)
JM	Johnson Matthey PLC, London/UK
KBR	Kellogg Brown & Root Inc., Houston, Tx
KRW	Kellog-Rust-Westinghouse (gasifier)
L, l	Litre
LC_{50}	Median lethal concentration
LD_{50}	Median lethal dose
LDP	Low presssure difference (shape)
LEL	Lower explosion limit
LEP	Lower explosion point
LHSV	Liquid hourly space velocity (volume/volume × hour)
LPDME	Liquid phase dimethyl ether synthesis (process)
LPG	Liquid petroleum gas, also: liquefied petroleum gas
LPM	Low pressure methanol (synthesis)
LPMEOH	Liquid phase methanol synthesis (process)
LPSteam	Low pressure steam
LTEL	Low temperature electrolysis
LTS	Low temperature shift
M15	Gasoline based blended fuel containing 15 % of methanol plus solubility enhancers
M85	Gasoline based blended fuel containing 85 % of methanol plus solubility enhancers
M100	Blended fuel consisting of ~90 % methanol and ~10 % hydrocarbons plus solubility enhancers
m^3 (STP)	cubic metre at standard temperature and pressure (273.15 K, 100 kPa)

MA	Methyl acetate
MAC	Maximum allowable concentration
MAN	Maschinenfabrik Augsburg Nürnberg
MARS	Metal ash recovery system
MCFC	Molten carbonate fuel cell
MDEA	Methyldiethanolamine
MDI	Methylene diphenyl diisocyanate
MEA	Monoethanolamine
MEK	Methylethylketone
MeOH	Methanol
MESG	Maximum experimental safe gap
METHAPU	Methanol Auxiliary Power Unit (project consortium, on-board fuel cells for cargo vessels)
MGC	Mitsubishi Gas Chemical Co., Tokyo/J
MHI	Mitsubishi Heavy Industries Ltd
MIE	Minimum ignition energy
MMA	Methylmethacrylate
MMBTU, MmBTU, mmBTU	Million British thermal units (BTU or Btu)
MMO	Methane monooxygenase
MOGD	Mobil-Olefin-to Gasoline/Diesel (process)
MOI	Mobil olefins interconversion (process)
MON	Motor octane number
MP Steam	Medium pressure steam
MPG	Multi Purpose Gasification or Gasifier
MPa	Megapascal (= 10 bar)
MRDC	Mobil Research & Development Corp., Paulsboro/US
MRF	Multistage radial flow (reactor)
Mt	Megatonne (1 million tonnes)
Mt/a	Million tonnes per year
mt	metric tonne
mtpd	metric tonnes per day
MTA	Methanol-to-Aromatics (process)
MTBE	Methyl tert-butyl ether
mt/d	metric tonnes per day
MTG	Methanol-to-Gasoline
MTHC	Methanol-to-Hydrocarbon (process)
MTI (fuel cells)	MTI Micro Inc., Albany, NY
MTO	Methanol-to-Olefins
MTP	Methanol-to-Propylene
MTS, MTSynfuel	Methanol-to-Synfuel
MTU	MTU Engines, Munich/D (Motoren- und Turbinen-Union)
MUG	Make up gas (methanol process)
MW_{th}	Megawatt (thermal)
MW_e	Megawatt (electrical)

MWM (test engine)	Motorenwerke Mannheim/D (now Caterpillar Energy Solutions GmbH)
NADP	Nicotinamide adenine dinucleotide phosphate
NBP	Net biomass production
NET	Net ecosystem production
NG	Natural gas
NKK	Nippon Kokan K.K. (now part of JFE Group)
Nm^3	standard cubic metre: m^3 at standard temperature and pressure (273.15 K, 100 kPa)
NMP	N-methyl pyrrolidone
NMR	Nuclear magnetic resonance
NPP	Net primary production
OBATE	On-board alcohole-to-ether (process)
OCP	Olefin cracking process
OCV	Open circuit cell voltage
OMB	Opposed multiple burner (technology)
OPEX	Operating expense
PAFC	Phosphoric acid fuel cell
PCC^{sm}	(Exxon) Propylene catalytic cracking (technology)
PDH	Propane dehydrogenation
PDU	Process demonstration unit
PEMEL	Proton exchange membrane electrolysis
PEMFC	Polymer electrolyte membrane fuel cell
PERP (report)	Process evaluation/Research planning (reports by ChemSystems/Nexant Inc., White Plains/US
PET	Polyethylene terephthalate
PF	Pulverised fuel
PG	Propylene glycol
PGM	Platinum group metal
PHA	Polyhydroxyalkanoate
PHES	Pumped hydro energy system
PISI	Port-injection spark ignition (engine)
PMMA	Polymethylmethacrylate
POM	Polyoxymethylene
POMDME	Polyoxymethylene-dimethyl ether
POX	Partial oxidation
PP	Polypropylene
ppm_v or ppmv	Volume parts per million
ppm_w or ppmw	Weight parts per million
ppb_v or ppbv	Volume parts per billion
ppb_w or ppbw	Weight parts per billion
PSA	Pressure swing adsorption
psi	pound per square inch (1 psi = 0.06895 bar)
psia	pound per square inch (absolute)
PV	Photovoltaic

PVA	Polyvinyl alcohol
RDF	Refuse-derived fuel
RE	Renewable energy
RID	Regulations for international carriage of dangerous goods by rail (issued by the International Rail Transport Committee (CIT), Bern/CH)
RITE	Research Institute of Innovative Technology for the Earth, Kyoto/J
RM	Regenerative (renewable) methanol
RMFC	Reformed methanol fuel cell
RON	Research octane numer
R/P	(static) Reserves-to-Production ratio (of fossil sources)
RuMP	Ribulose monophosphate
RWGS	Reverse water gas shift
RWTH	Rheinisch-Westfälische Technische Hochschule, Aachen
SAPO	Silico-alumino phosphate (zeolithe)
SBU	Secondary building unit (in zeolites)
S/C	Steam to carbon ratio
SCF, scf	Standard cubic foot (at 60 degrees Fahrenheit (15.6 degrees Celsius) and 1 atm or 101.325 kPa)
SCOT	Shell Claus Off-Gas Treatment (process)
SCP	Single cell protein
SCR	Steam raising converter
SECA	Special environmental control area
SFC	SFC Energy AG, Brunnthal/D (fuel cells)
SGS	Sour gas shift
SMR	Steam methane reformer/reforming
SN	Stoichiometric number
SNG	Synthetic natural gas
SOEC	Solid oxide electrolysis cell
SOFC	Solid oxide fuel cell
SRK	Soave–Redlich–Kwong (equation)
SSZ	zeolite with chabazite structure
STD	Syngas-to-Dimethyl ether
STP	Standard temperature (273.15 K) and pressure (100 kPa or 1 bar)
STS	Syngas-to-Fuel
STY	Space-time-yield
SVZ	(former) Sekundärrohstoff-Verwertungszentrum Schwarze Pumpe, Spremberg/D
SWS	Sour water stripper
t, tonne	metric tonne
TAME	tert-Amyl methylether
TBA	tert-Butyl alcohol
TEA	Triethanolamine

TCC	Tube cooled converter (Davy Process Technology)
TCE	Total capital employed
tcf	Trillion cubic feet
tcm	Trillion cubic metre
TDG	Transport of dangerous goods (regulations by UNECE)
TGT	Tail gas treatment
THF	Tetrahydrofurane
TIC	Total installed costs
TIGAS	Topsoe's integrated gasoline synthesis (Haldor Topsoe A/S, Lyngby/DK)
TON	turn-over-number (moles of substrate per mole of catalyst before being deactivated)
TOS	Time-on-stream
tpd	(metric) tonnes per day
TRBS	"Technische Regeln für Betriebssicherheit" (Bundesanstalt für Arbeitsschutz und Arbeitsmedizin Federal Institute for Occupational Safety and Health, Dortmund/D)
TRGS	"Technische Regeln für Gefahrstoffe" (Bundesanstalt für Arbeitsschutz und Arbeitsmedizin/Federal Institute for Occupational Safety and Health, Dortmund/D)
UCC	Union Carbide Corp., Danbury/US (affiliate of Dow Chemical)
UEL	Upper explosion limit
VAM	Vinyl acetate monomer
WCR	Water cooled reactor
WGS	Water gas shift
WHB	Waste heat boiler
WHSV	Weight hourly space velocity (weight/weight × hour)
W/m^2	Heat flux (Watt per m^2)
WTY	Weight-time-yield
XTL	x -to -liquids (x = fossil or biomass feeds)
Xu5P	Xylulose-5-phosphate
ZBT	Zentrum für BrennstoffzellenTechnik GmbH, Duisburg/D (fuel cells)
ZnTPPS	Zinc tetraphenylporphyrin tetrasulphonate
ZSM	Zeolite Socony Mobil (class of zeolites)
ZSW	Zentrum für Sonnenenergie- und Wasserstoff-Forschung (ZSW) Baden-Württemberg, Stuttgart/D

Chapter 1
Introduction

1.1 From Raw Materials to Methanol, Chemicals and Fuels

Heribert Offermanns, Ludolf Plass and Martin Bertau

The planet Earth is a sphere with a limited surface of 5×10^{13} m^2, of which 71 % is water and only 29 % is land. A total of 27.5 % of the landmass (i.e. 11 % of earth's surface) is used as arable acreage, 20.8 % as pasture and 9.4 % is used to grow timber. The remaining surface, which mainly is made up of deserts and mountains, is unused: 10.1 % is a frozen surface and 2.0 % is inland water. Meanwhile, the human population requires not less than 7 % of the land—a number that is constantly growing at the expense of the arable landmass. In fact, the usable area has been diminishing for years.

Carbon is the 13th most common element. It is found in nature in the form of diamonds and graphite and it is chemically bound as CO_2, carbonate, natural gas, crude oil, coal, or biomass. However, carbon is highly unequally distributed in the earth's upper crust. Approximately 50,000,000 Gt (99.92 %) of carbon is fixed in the earth's crust, chiefly as carbonate rock. Only approximately 40,000 Gt

H. Offermanns (✉)
Grünaustraße 2, 63457 Hanau, Germany
e-mail: heppoff@gmx.de

L. Plass
Parkstraße 11, 61476 Kronberg, Germany
e-mail: dr.ludolf.plass@t-online.de

M. Bertau
Institute of Chemical Technology, Freiberg University of Mining and Technology, Leipziger Straße 29, 09599 Freiberg, Germany
e-mail: martin.bertau@chemie.tu-freiberg.de

M. Bertau et al. (eds.), *Methanol: The Basic Chemical and Energy Feedstock of the Future*,
DOI: 10.1007/978-3-642-39709-7_1,

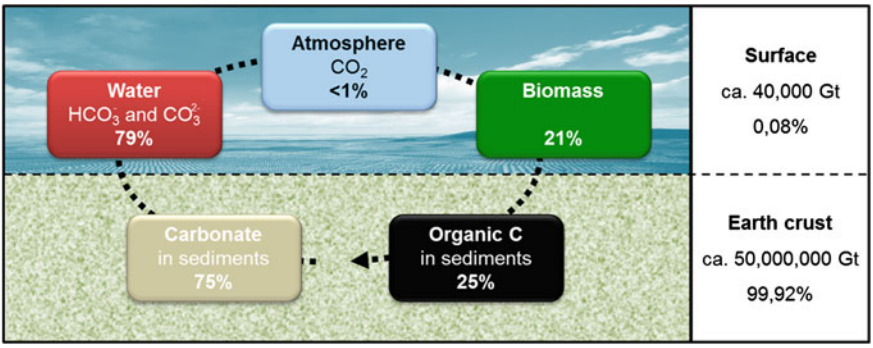

Fig. 1.1 Carbon distribution in the earth's crust. (Adapted from [3])

—a meager 0.08 %—is near the surface. The fact that 79 % of this latter amount is abundant as hydrogen carbonate and carbonate in water underscores the scarcity of economically exploitable carbon [1, 2]. Taking all this into account, one will inevitably come to the conclusion that the fraction of technically recoverable carbon is exceedingly rare but enriched in large-scale deposits (Fig. 1.1).

All natural carbon sources are exhaustible, but nature produces gargantuan amounts of renewable primary recourses. By means of photosynthesis, plants produce carbohydrates from atmospheric CO_2, sunlight and water. To a smaller extent, proteins and vegetable oils are also produced. The yearly production of biomass is estimated according to the U.S. Department of Energy (2005) to be approximately 150 Mt. Humans stand admiring this incredible performance while trying to understand how nature works. According to Primo Levi (see Fig. 1.2), the chemical leaf—technical photosynthesis—is the goal.

We use only small quantities of the long-existing and continuously accrued biomass ($\sim$4 %) for the production of food/fuel or as chemical or energy raw material. This usage (only 4 % human consumption) is not expected to substantially increase in the future.

Unlike the global population (currently 7 billion, estimated to be 9 billion in 2050), there will be no increase in the size of the earth. Therefore, every available acre of farmland should be prioritised for the production of food. However, there is a concerning downward trend in arable acreage because the growing population is consuming land for settling and concomitantly inappropriately using agricultural land. It should be common practice to use only the biomass that cannot serve as human nutrition as feedstock for energy and fuel, be it directly or indirectly.

Since the invention of fire, man has used biomass (wood) for heating. Wood used to play a considerable role in methanol production (wood alcohol), acetic acid (wood vinegar) and acetone. Also, hard coal and lignite have been (and are still) in use as feedstock for chemicals and energy. For instance, aromatics from tar distillation—a byproduct of coke production—served as raw materials for the production of dyes (I.G. Farben).

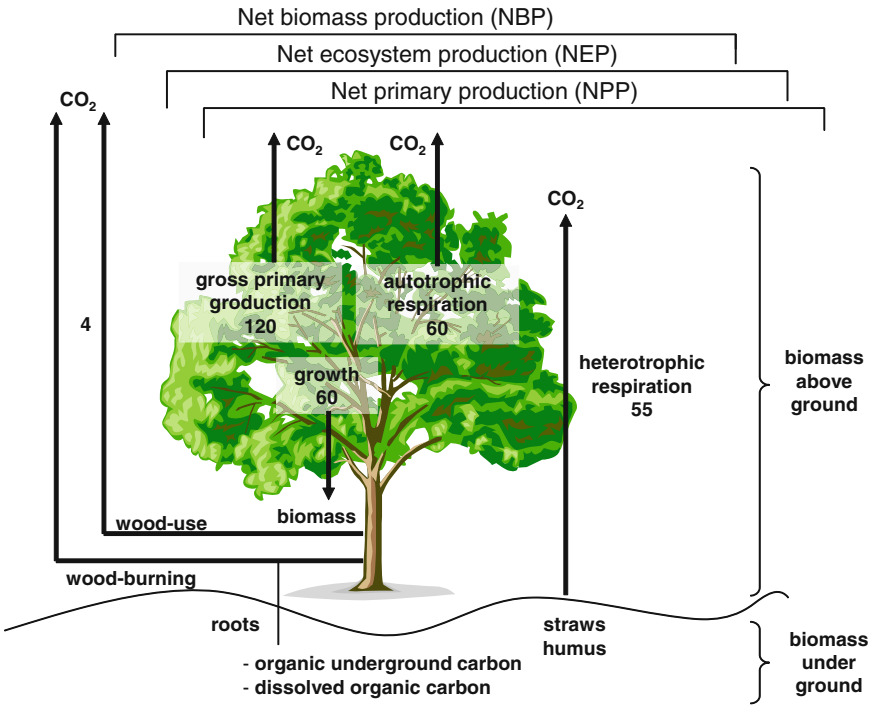

Fig. 1.2 Carbon loop in biomass production (numbers are in Gt). (Adapted from [4])

Crude oil (bitumen), which in some regions comes up to the surface, has been used for ages as cart grease and as an ingredient for ointment, among others. Until the middle of the 19th century, however, both natural gas and (especially) crude oil did not play any role as feedstock for chemicals or energy.

In 1853, the sleeping giant crude oil was woken up by the Galician pharmacist and chemist Ignazy Lukasiewicz (together with his associate Jan Zeh), as well as the physician, physicist and geologist Abraham P. Gessner, independently from each another. They tried to clean and distill crude oil to use it for oil lamps. The visions of the naturalist Benjamin Silliman of Yale University about the possible uses of the distillate were even surpassed. However, it still took decades until the era of crude oil began in the wake of inventions by Carl Benz and Rudolf Diesel, as well as Henry Ford's pioneering work.

The share of crude oil distillates for lamps decreased from 75 % in 1880 to 13 % in 1920, and the first refineries were built in Cleveland, Ohio in 1898. The driving force of crude oil processing was the production of gasoline and diesel fuel. Petrochemistry developed slowly, while natural gas and oil to a high degree began to replace hard coal and lignite as feedstock for power generation. The selection of carbon sources is broad, but the exhaustible fossil raw materials oil and gas—the consumption of which is an irreversible process—carry the greatest

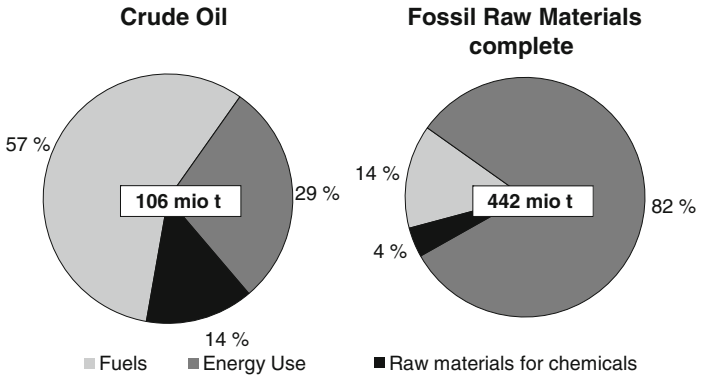

Fig. 1.3 Distribution of consumption of fossil raw materials and crude oil in Germany [6]

share of fulfilling the demand for energy, fuel and chemicals. For example in Germany, 80 % of all fossil raw materials (gas, oil and coal) are used for energy, 14 % for fuel, and only 4 % for chemicals (Fig. 1.3) [5].

The remaining static lifetimes of fossil raw materials are estimated as follows [6, 7]:

- Natural gas (reserves): 63 years
- Natural gas (resources): 74 years
- Crude oil (conventional reserves): 42 years
- Heavy oil, shale oil (nonconventional): 17 years
- Crude oil (conventional resources): 21 years
- Heavy oil, shale oil (nonconventional): 66 years

Brown coal (lignite) reserves are estimated to last for 227 years and hard coal reserves for 169 years, whereas the resources may last up to 1028 and 874 years, respectively. Reserves are proven deposits that can be economically exploited with known technology. Resources are deposits that cannot be exploited yet economically or are not proven for sure. The technical feasibility of their extraction requires improved technology; frequently, it is increasing world market prices that render resources into reserves [7].

Approximately 10 % of the world population consumes 90 % of the energy. With increasing qualities of life, the demands for showers/baths, heating and air conditioning will increase. There are many options to use carbon sources as feedstock for energy, fuel and basic chemicals, but carbon-rich fossil raw materials such as gas and oil have been preferred because their production is easier, logistics are simpler, and therefore the economics are better. It looks like predatory exploitation.

In the 1970s, critical voices were heard. In 1972, the Club of Rome published the book *The Limits to Growth* [8]. The Italian organic chemist, author and survivor of the Auschwitz concentration camp, Primo Levi, wrote the following in his book *Il Sistemo Periodico*:

> The human being has not yet tried consciously or unconsciously to compete with nature on this subject. That means, he has not yet taken the effort to withdraw the carbon from the air, that carbon which he needs badly for food, clothing, heating and to satisfy the hundreds of other requirements of modern life. He has not done anything, because there was no need to do so. He has found gigantic reserves of carbon easy to be used. But there is a vital question: for how many decades further? [9]

In the late 1950s, Friedrich Asinger—professor of Technical Chemistry and Petrochemistry at the Aachen RWTH, a pioneer in petrochemistry in research and teaching, and a commendable advisor of big chemical companies—called for a responsible handling of fossil raw materials. Although sometimes smiled at by students and colleagues, he taught that the crude oil—with its carbon chains formed over millions of years—should predominantly be used for the synthesis of chemicals, because the building of carbon chains is complicated and expensive.

After his retirement, Asinger dedicated special attention to the question of what comes after fossil raw materials, and methanol became the focus of his interest. He also expressed visions: "Once the fossil raw materials will become scarcer and more expensive or will dry out completely, there will remain as raw material, except for biomass, carbon dioxide only" [10]. However, Asinger ascribed special importance to coal for the time after the fossil raw materials with the shortest range (oil and gas) were exhausted, as indicated in the subtitle of his book "The Mobilisation of Coal".

Asinger and his Aachen colleague Rudolf Schulten developed a concept for the use of nuclear power that used coal as the carbon source. The nuclear heat of the pebble-bed reactor (developed by Schulten) served to split water, while the oxygen was used to combust coal in order to supply energy and pure carbon dioxide. The hydrogen obtained from nuclear thermal water splitting was envisaged to reduce the carbon dioxide to methanol. Although the fate of the pebble reactor is sealed, these early "Aachen visions" have lost none of their topicality and importance. Asinger and Schulten could not foresee that power generation by means of wind and solar energy would one day become of the great importance we witness today. The technical progress of wind mills and solar power, based on exceptionally high governmental subsidies, rendered this development possible—in particular in Germany, where in 2012, a total of 8.2 % of power was generated from renewables [11].

Instead of nuclear energy, wind and solar energy can be used to produce hydrogen via electrolysis, which is then either used for repowering or further converted to methanol or methane ("power to gas")—a topic that is dealt with in detail in Chap. 8. In fact, there are many options to reasonably combine water electrolysis, power generation and production of CO_2, as well as using the latter as a raw material. When Asinger published his book "Methanol - Chemie- und Energierohstoff" [10], the time for his visions had not come yet, and decision makers were not prepared to recognise the significance and consequences of what he proposed. The book was not translated into English and has been out of print for a long time. Meanwhile, the situation worsened, and now there is great public awareness for power generation based on fossil raw materials, as well as a

continued vigilance for the CO_2 issue. Thus, the time may have come to publish a second, revised edition of Asinger's book in English.

Methanol is the focal point of this book, in an attempt to address the question, "What comes next?".

The intensity of the discussion about the future supply of raw materials for the requirements of power generation, fuel and chemical industry, as well as the discussions about the greenhouse effect, have increased.

Many scientific and technical organisations, science academies, industry organisations and government commissions have demonstrated their point of view. For example, the nuclear power phaseout by the German government gave rise to further questions such as energy storage, for which methanol can play an important role (see Chaps. 7, 8) [12].

Around the world, South Africa is pursuing the further development of the Fischer–Tropsch process. China has established huge plants for the production of methanol on the basis of hard coal, with the aim of producing consecutive products. The Chinese production capacity for propylene on the basis of methanol (MTP), for instance, totaled up to 1 million tonnes in 2013 and will further increase substantially. One can see from this single example that Asinger's vision—the mobilisation of coal via methanol—has become reality indeed.

With the world's population approaching 9 billion people, the demand for energy, fuel and raw materials for chemistry and food production will increase rapidly. The same holds true for CO_2 emissions, which will also increase. Hence, the development of alternative technologies for producing energy is mandatory. In light of this strong increase in energy demand, special attention must be paid to reasonably utilising fossil carbon feedstock. Fossil raw materials with short "static ranges"—that is, the quotient of current reserves to annual output, such as with oil and gas—make easily convertible feedstock for chemical industry. Fossil raw materials with long ranges, such as hard coal, lignite and shale oil, will require additional efforts prior to use as chemical feedstock. In fact, methanol production from both CO_2 and long-range fossil raw materials may offer a solution to this dilemma. This approach may also provide new perspectives on biomass utilisation, which for the reasons outlined previously has to be prioritised for food production.

This book will not discuss all the advantages and disadvantages of future energy supplies. However, it goes without saying that methanol clearly has the potential to play a key role in the time beyond oil, gas and nuclear power. This book will therefore thoroughly discuss the following subjects:

- Raw materials for the synthesis of methanol and their conditioning
- Methods to produce methanol and their economics
- Properties of methanol (physical data, toxicology)
- Use of methanol as fuel, for the energy sector, and as chemical feedstock

Because methanol is a liquid with a boiling point of 65 °C, it can be distributed through pipeline grids and transported with big tankers. It is miscible with water so it is not as dangerous as crude oil. Likewise, storage in fuel depots does not cause any problems. With an energy density of 22.7 MJ/kg, methanol is well suited as

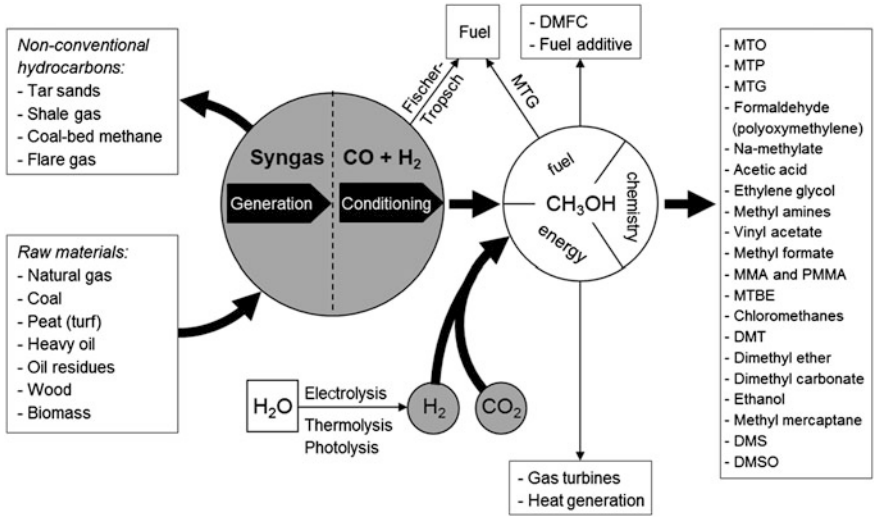

Fig. 1.4 From raw materials to synthesis gas (*syngas*), methanol, chemicals and fuels. Abbreviations: *DMFC* direct methanol fuel cell, *MTO* methanol-to-olefins, *MTP* methanol-to-propylene; *MTG* methanol-to-gasoline. (Adapted from [12])

energy storage compound. Chapter 8 provides a comparison of methanol versus methane in chemical storage for excess power from renewable resources, using Germany as an example.

It has been widely accepted that no energy store is superior to methanol's chemical bond. For comparison, the lead accumulator is 0.11 MJ/kg; in Li-ion batteries, it is 0.5–3.6 MJ/kg. Methanol has been recognised as a basis chemical for a long time. The first large scale plant for methanol production starting from synthesis gas (according to Pier and Mittasch) was put into operation in 1923 in Leuna, Germany. Not later than 1930, methanol production reached 100,000 tonnes/year. By means of zeolite catalysis, the whole range of second-generation petrochemicals is accessible starting from methanol. The compound is also a useful feedstock for specialty chemicals. For wood gasification, it is well known that methanol can be used as fuel, either in pure form or as an additive to gasoline. In direct methanol fuel cells, methanol is used to transform chemical energy directly into electrical energy (without the detour via reforming). Therefore, there are a number of reasons why Asinger should once again be given the opportunity to be heard when stating: "Should hydrogen be economically available, pure sulphur free carbon dioxide could serve as feedstock for the methanol synthesis." Chapters 7 and 8 provide analyses and data to enable the reader to develop a fact-based opinion on the possibilities of a methanol-driven economy.

The essential elements of methanol utilisation in chemistry and energy feedstock are summarised in Fig. 1.4.

Fig. 1.5 Friedrich Asinger, a pioneer in petrochemistry and mediator between basic and applied research

1.2 Friedrich Asinger

Heribert Offermanns

Grünaustraße 2, 63457 Hanau, Germany

Friedrich Asinger was an internationally respected researcher in the chemical and petrochemical industries. The name of Friedrich Asinger [13, 14] is not only linked to the Asinger reaction [15–18], which is a reaction of carbonyl compounds with elementary sulphur and ammonia to form nitrogen- and sulphur–containing heterocycles. He was also well known for teaching and research in petrochemistry at the Universities of Halle-Wittenberg, Dresden and Aachen, mainly thanks to his many textbooks [19–25]. It is no exaggeration to say that Asinger greatly influenced petrochemistry. Indeed, he considerably helped to shape the transition from the chemical raw material of coal to natural gas and oil (Fig. 1.5).

Asinger also was concerned about the overexploitation of the valuable raw materials gas and oil for energy production, and he became an advocate of nuclear energy and C_1-chemistry [12, 26]. As early as the 1960s, he advocated for the future use of methanol as an energy and chemical feedstock. His book *Methanol - Chemie- und Energierohstoff*, which he wrote after his retirement, has unfortunately not been translated into the English language. Twenty years before the currently much-debated book, *Beyond Oil and Gas: The Methanol Economy*, by Olah et al. [27] was published, in 1986. Asinger pointed out the usefulness of pure, sulphur-free

carbonic acid; together with cheaply available hydrogen, it could serve as a starting material for methanol synthesis. Furthermore, he said: "When raw material sources one day will become increasingly short in supply and more expensive or are even totally exhausted … there remains, apart from biomass, only carbonic acid as the source of raw materials for the organic chemical industry."

Born in Freiland, Austria, Friedrich ("Fritz") Asinger studied chemistry at Wien University of Technology and was granted his doctorate in 1932. For financial reasons, he had to turn down offers for a habilitation and for postdoctoral work at Columbia University in New York. He started his industrial career as chemist in a medium-sized chemical company in Vienna. In 1937, he took a position as research chemist at Leuna-Werke, founded in 1916 as Ammonia Works Merseburg by BASF; there, Asinger was promoted to group leader and later to head of research. Asinger was a successful inventor and innovator in the fields of sulphochlorination and sulphoxidation of paraffin, coal chemistry and new detergents.

Concurrent with his industrial activities, he received his habilitation from Graz University of Technology (Austria) and became an honorary lecturer at the Institute of Organic Chemistry at the University of Halle-Wittenberg under the directorship of the later Nobel Prize winner Karl Ziegler. In 1946, as part of the Operation Ossawakim—the forced deportation of skilled scientists from the Soviet-occupied eastern part of Germany—Asinger was displaced to the territory of the Soviet Union. Apart from his experimental work, which consisted of an order to develop rocket fuel, he wrote the manuscripts for the books *Chemie und Technologie der Paraffinkohlenwasserstoffe*, *Chemie und Technologie der Monoolefine and Einführung in die Petrolchemie*. In 1954, after 7 years in the Soviet Union, Asinger was released and allowed to return to the German Democratic Republic, where he resumed work at the Leuna company.

The Asinger books were published by the Akademie–Verlag Berlin in the years 1956–1959. English translations were published in 1967 for *Paraffins* and 1968 for *Monoolefins* by Pergamon Press Oxford, UK. In 1958, Asinger was appointed Professor of Organic Chemistry at the University of Halle–Wittenberg; also in 1958, he moved to Dresden University of Technology, where he became Professor and Director of the Institute of Organic Chemistry. In 1959, Asinger was appointed to a professorship at the Aachen RWTH and directorship at the Institute of Technical Chemistry and Petrochemistry.

As a citizen of Austria, Asinger had the chance to leave the German Democratic Republic, which was at that time separated by the "iron curtain" from the Federal Republic of Germany. It was for this reason why none of his coworkers could follow him. Therefore, Asinger had to establish a completely new research team. More than 150 students finished their studies with a doctoral degree under *Doktorvater* (Doctoral thesis supervisor) Friedrich Asinger. Students from 12 nations were members of the Institute, and more than 10 of the Asinger students took up an academic career. At Aachen, he wrote the books *Die Petrolchemische Industrie I + II* (Akademie–Verlag, Berlin, 1971) and *Methanol - Chemie- und Energierohstoff* (Springer-Verlag, Heidelberg, 1986). These books have never been

translated into the English language and therefore received no international recognition, particularly in the United States. Highlights of the Asinger books were the citations; for instance, there were more than 1,400 in his *Methanol* book, with most of them annotated with a commentary from the author.

1.3 The History of Methanol in the Chemical Industry

Heribert Offermanns

Grünaustraße 2, 63457 Hanau, Germany

For many decades, inorganic chemistry (e.g. Haber–Bosch process) and the chemistry of aromatics on the basis of coal tar dominated the chemical industry. F. F. Runge (1795–1867) isolated phenol and aniline from tar, which were cornerstones in the development of artificial dyestuffs. Fundamental research work by A. W. von Hofmann and A. Kekulé von Stradonitz and applied research of J. P. Gries, C. A. Martius, A. von Baeyer, H. Caro, C. Graebe, V. von Weinberg, C. Hagemann and others built the foundation of the most important dyestuff companies, which were joined stepwise to eventually form the IG Farbenindustrie AG, Frankfurt, in 1925–26. Similar developments occurred in Great Britain (W. A. Perkin) and in the United States [28–33].

The chemistry of aliphatic compounds lived in the shadows, with methanol (wood alcohol) and, less importantly, ethanol as raw materials. Today's most important polymers, such as polyolefins (more than 50 %) and polyamides with an overall yearly production of approximately 240 million t (according to Plastic Europe 2011) were not available because of the lack of basic petrochemical feedstock.

The growing importance of gold production (especially in South Africa) by means of the cyanide lixiviation process, which was developed by MacArthur and the Forrest brothers (1887), increased the demand for sodium cyanide so rapidly that the old production process (vinasse) could no longer cover the demand. Around the turn of the 20th century, H. Y. Castner and C. Kellner invented a process that was improved and finally was lead to technical maturity by chemists of the Deutsche Gold und Silberscheideanstalt (Degussa, later Degussa AG), and this new process replaced the old one.

In the Castner-Kellner process, charcoal reacts with ammonia and sodium metal. In order to secure the supply of the raw material charcoal, Degussa took part in the creation of the Holzverkohlungs-Industrie Konstanz (Hiag AG) in 1902. Hiag merged with its most important competitor, the Verein für Chemische Industrie AG (Frankfurt), in 1930. The companies were combined under the name HiagVerein GmbH and were absorbed 100 % by the Deutsche Gold und Silberscheideanstalt to become the department Hiag.

For logistical reasons and because of the forestry structure, many small manufactories for carbonising wood were established all over the beech woods in Germany. After the shutdown of smaller production facilities, 11 plants were still in operation in 1931. The carbonisation in retorts replaced the outdated technology of carbonising in heaps and made possible the production of organic chemicals in addition to the main product of charcoal. The first retorts had a capacity of 2.5 solid measures of timber, later ones had capacities of 10.0 solid measures of timber, and eventually the modern Reichert retorts reached a capacity of 40.0 solid measures of timber.

The byproducts of wood carbonisation in the bigger plants lead to the start of the organic chemistry business for Deutsche Gold und Silberscheideanstalt [34–36].

The carbonisation of natural seasoned beech wood yields the following:

- 26.7 % charcoal
- 4.4 % wood vinegar, mainly acetic acid
- 1.8 % wood alcohol, mainly methanol
- 7.1 % wood tar
- 16.2 % wood gas
- Residual water

At the beginning of the 20th century, the wood carbonisation industry in Germany was a monopoly [33]. The situation in Great Britain and the United States was similar. Wood gas and wood vinegar were important raw materials for major organic chemicals. There was no other access to formaldehyde (Paraform, Ultraform, Bakelit, urotropine, hexamethylenetetramine, pentaerythritol, etc.). Also, acrolein can be synthesised by condensation of acetaldehyde (from ethyl alcohol) and formaldehyde; it is one of the raw materials for the production of D,L-methionine, an amino acid important for animal feed.

A secondary product of wood vinegar was acetone, a raw material for methyl methacrylate and therefore for Plexiglas.

From wood tar, guaiacol and creosote were extracted.

Wood chemistry lost its importance after the introduction of coke-based C_1-chemistry with the development of the first technical synthesis of methanol in 1923 (Ammoniakwerk Merseburg of BASF; M. Pier, A. Mittasch) and with the advent of the chemistry of acetylene in the 1930s (W. Reppe); it was eventually supplanted by petrochemistry. During the first half of the 20th century, the chemistry of the aliphatics experienced an enormous boom (Fig. 1.6) (Table 1.1).

The first rail tank car of methanol left the Ammoniakwerk on September 26, 1923. It was at this plant where methanol production reached 100,000 tonnes per year in 1936 and 200,000 tonnes per year during World War II (Fig. 1.7) [37].

The Deutsche Gold und Silberscheideanstalt built a new chemistry complex in Fürstenberg/Oder and switched to a new route for methanol, acetylene and ethylene. However, this venture was abruptly stopped by the war. The plant was dismantled in 1945 and the apparatus were transported to the Soviet Union [34].

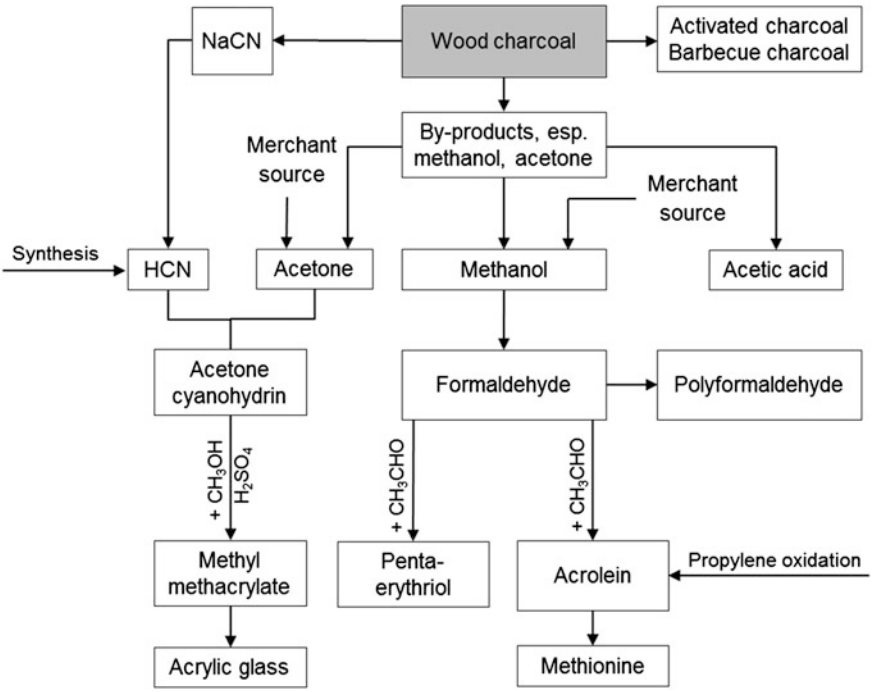

Fig. 1.6 Degussa's wood charcoal chemistry [36]

Table 1.1 Development of wood/charcoal based chemistry in Germany, 1933–1943 [36]

Wood-based products in metric tonnes (Hiag plants in post-war West Germany)[a]	1933	1938	1943
Charcoal	32,120	72,980	72,510
Activated charcoal	80	250	610
Wood tar	7,630	19,600	19,960
Tar oils	640	1,370	9,120
Guaiacol	0	20	60
Creosote	280	60	20
Flotation oils	0	50	810
Denatured wood alcohol	740	790	560
Solvent	600	890	600
Methanol	1,370	2,190	1,770
Formaldehyde	1,620	3,180	7,120
Paraformaldehyde	0	0	10
Acetates	3,100	6,940	9,770
Acetone	1,120	1,510	1,400
Acetone cyanohydrin	0	430	1,600

[a] Bodenfelde, Brilon-Wald, Bruchhausen, Brücken, Konstanz, Kredenbach, Lorch, Mombach, Oeventrop, Schleiden and Züschen. The figures include the totals for both charcoal and wood tar and the end products derived from them, but only the end products of wood vinegar and wood alcohol, which were entirely distilled into these by the plants

Fig. 1.7 The first tankwagon with methanol leaves Leuna on 26th September 1923 [38]

After the end of the war, petrochemicals became the dominating feedstock for organic chemicals and consequently also for typical Degussa products such as formaldehyde, pentaerythritol, acrolein, acetone, acetoncyanhydrin, methyl methacrylates (MMA) and polymethylmethacrylates (PMMA).

1.4 Methanol in Industrial Chemistry (General)

Heribert Offermanns[1], Ludolf Plass[2] and Ringo Heyde[3]

[1]*Grünaustraße 2, 63457 Hanau, Germany*

[2]*Parkstraße 11, 61476 Kronberg, Germany*

[3]*Institute of Chemical Technology, Freiberg University of Mining and Technology, Leipziger Straße 29, 09599 Freiberg, Germany*

Methanol (CH_3OH)—also named methyl alcohol, carbinol, or wood alcohol—is the first representative of the homologous series of alcohols that are correctly named by adding the syllable *-ol* to the corresponding paraffin. Methanol (molar mass 32.0429 g mol^{-1}) is a colourless, neutral, but polar liquid. It boils at 64.6 °C and freezes at −97.6 °C. For physical properties, see Sect. 5.1 for toxicology, see Sect. 5.2.

With a global annual consumption of 53 million tonnes in 2011 [39], methanol is one of the most important commodities of the chemical industry.

Figure 1.8 gives an overview of the value chain from methanol via its derivates to a large variety of products or end uses in many sectors [41]. The three major products produced from methanol are formaldehyde (36 %), methyl tertiary-butyl ether/ tertiary-amylmethylether (MTBE/TAME; 13 %) and acetic acid (9 %; Fig. 1.9). Formaldehyde production remains the largest single consumer of methanol.

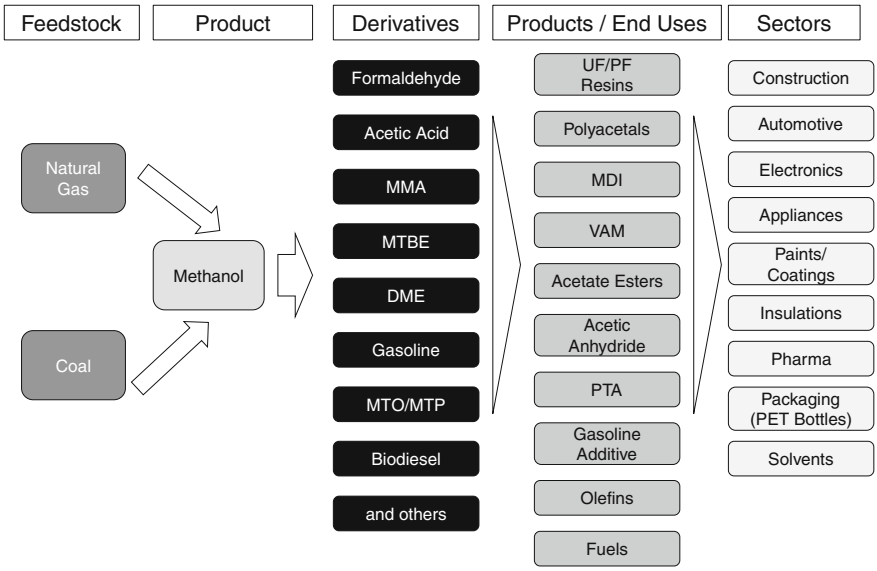

Fig. 1.8 Value chain of methanol [40]. A detailed description of methanol chemistry is given in chapter Chap. 6. Abbreviations: *MTO* methanol-to-olefins; *MTP* methanol-to-propylene

It is, among others, used for the production of plastics and resins, pharmaceuticals, chemical fibres, paint and pesticides. The production of MTBE/TAME is mainly used as an octane booster in gasoline, accounting for 16 % of the global annual consumption. However, the share of MTBE has decreased since 2003, when MTBE was replaced by ethanol as an antiknocking agent for fuels in California and 15 other U.S. states due to the contamination of water resources by MTBE from spilled fuels [41]. A large part of the acetic acid, which consumes approximately 9 % of global methanol production, is converted into vinyl acetate monomer (VAM).

The remaining 48 % of global methanol consumption is divided into the production of a large variety of chemical intermediates such as chloromethane, methylamine, methylmethacrylate and methylmercaptane, as well as the use of methanol or methanol derivatives such as dimethyl ether (DME) as a fuel or fuel blend (see Sects. 6.2 and 6.3). Overall, approximately one third of global methanol production is consumed in the fuel sector [42]. The chemicals produced from methanol stayed at approximately the same or slightly decreased levels on a percentage basis between 2009 and 2013 (Fig. 1.9). However, the fuel sector (MTBE/TAME/gasoline/DME) was estimated to increase from 30 % in 2009 to 40 % in 2013.

The so-called methanol-to-olefins (MTO) process, which allows for the production of feedstock for consumer plastics such as polyethylene and polypropylene, is starting to be a large-scale methanol consumer, increasing its share from 0 % in 2009 to 11 % in 2013. Ethylene and propylene are by far the two largest volume chemicals produced by the chemical industry. Approximately 120 Mio tonnes of

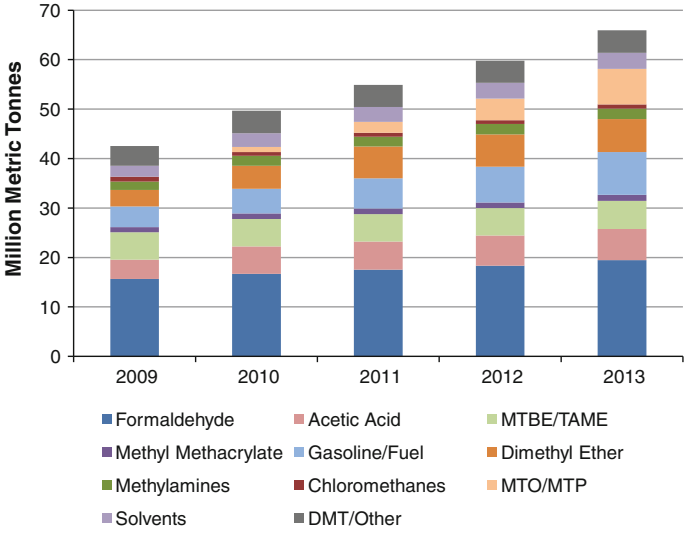

Fig. 1.9 Development of global methanol demand by sector (2013 forecast) [40]. Abbreviations: *MTBE/TAME* methyl tertiary-butyl ether/tertiary-amylmethylether; *MTO* methanol-to-olefins, *MTP* methanol-to-propylene

ethylene and 80 Mio tonnes of propylene were consumed worldwide in 2011. The demand for propylene is growing at a faster rate (approximately 4.5–5 % per annum; in China, approximately 6 % per annum) compared with that of ethylene (approximately 3–4 % per annum). Because the majority of both chemicals are still produced by steam cracking and fluid catalytic cracking, resulting in a given ratio of both chemicals, the increasing imbalance will need to be compensated for by the intentional production of propylene. Technologies used for intentional production are mainly propane dehydrogenation, metathesis, olefin cracking and to a growing extent methanol-to-propylene (MTP) technology, as further described in Sect. 6.4.3. The market price at which methanol is available for these processes is a decisive factor for the technology diffusion of these emerging applications [43]. Therefore, cost-efficient methanol production is a key objective for methanol producers and technology providers to maintain or improve profit margins in an increasingly competitive market (see chapter Chap. 7) (Fig. 1.10).

A study by Masih and coworkers conducted from 1998 to 2007 suggests that increasing natural gas prices are the driving force for methanol prices in Europe and the United States. In contrast, in the Asia–Pacific region, the surging demand for chemicals from growing consumer industries such as electronics, textiles, construction, leather and plastics processing was identified as the key driver for methanol prices [45]. Since 2006, the price of methanol has been extremely volatile. The steep increases in methanol prices in the second half of 2006 and in the last quarter of 2007 were caused by the shutdown of significant production

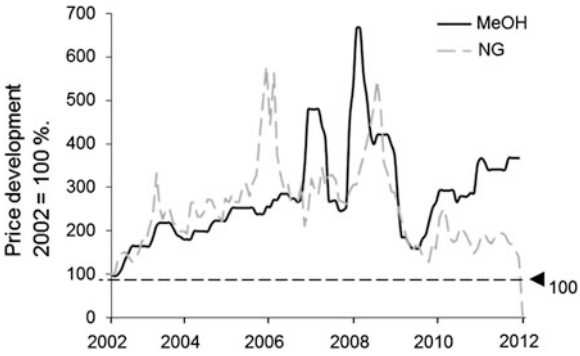

Fig. 1.10 Development of methanol *MeOH* [44] and natural gas *NG* prices [45] in the United States as a percentage of the reference price in January 2002

capacity due to technical problems and maintenance. High prices of natural gas have supported the high pricing level of methanol through 2008. In 2009, the methanol price dropped dramatically due to decreased demand because of the global economic crisis that followed the financial crisis. The methanol price increased to more than 350–400 € per tonnes in 2011, despite a relatively low natural gas cost in the United States, which is owed to the increasing availability of unconventional resources (shale gas).

Additionally, a regional shift has occurred in the production of methanol. Countries with large reserves of low-cost natural gas have invested into large-scale production facilities in order to monetise their "stranded gas" reserves, a byproduct from oil production. For example, because of the cost competition for products downstream of the methanol value chain, disfavoured plants in the United States were shut down. The Middle East and Asia, which have large reserves of natural gas and hard coal, have become the major methanol-producing regions [46]. With the increasing availability of shale gas in the United States, the price of natural gas has significantly dropped, leading to a higher profitability for the domestic production of base chemicals such as methanol. In recent years, China has become the world's largest consumer of methanol, with approximately 30 % of the global annual consumption (Fig. 1.11).

The expected annual growth rates in the range of 10–20 % are resulting from the plans of the Chinese government to reduce the dependency of China from costly crude oil, such as by blending gasoline with coal-based methanol [47]. The percentage of methanol used as gasoline/fuel is supposed to grow from 11 % in 2011 to 16 % 2016 (Figs. 1.12 and 1.13). As already indicated in Fig. 1.9, the MTO/MTP technology sector continues to show the strongest increase (from 6 % in 2011, to 11 % in 2013, and to 22 % in 2016). Such developments are even further enhanced by the low natural/shale gas prices in North America (Fig. 1.10), where a substantial number of projects, including MTO/MTP processes, are in the planning phase. In addition, methanol plants that had been shut down for raw material cost reasons may be put back into operation.

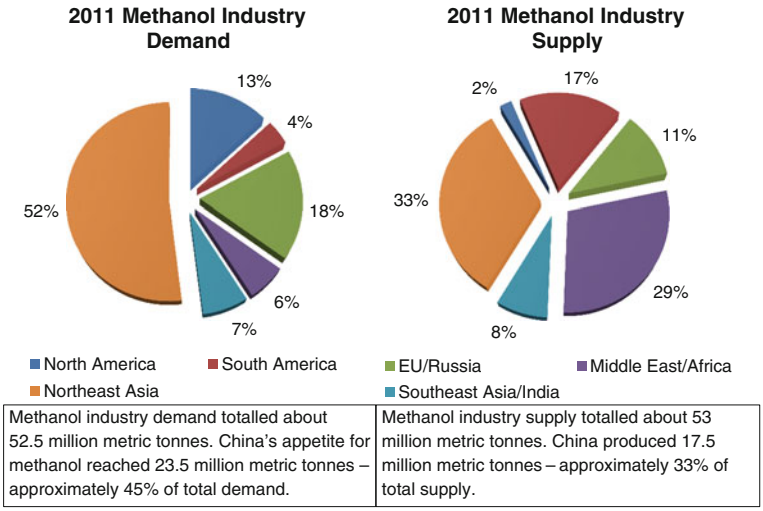

Fig. 1.11 Worldwide methanol supply and demand in 2011 [39]

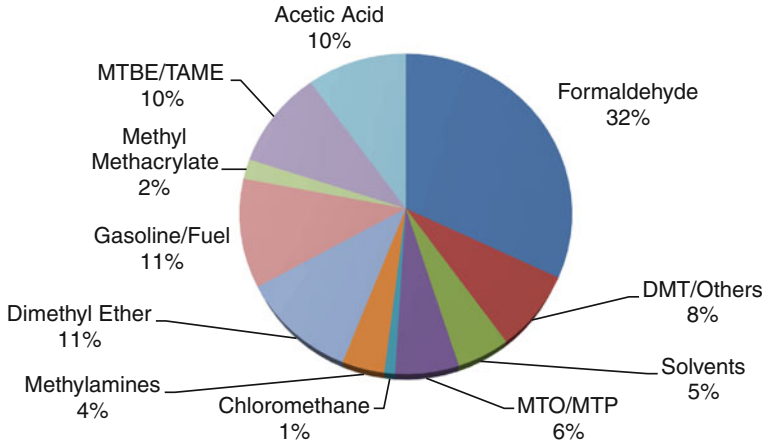

Fig. 1.12 Methanol demand by end use for 2011 [40]. Abbreviations: *MTBE/TAME* methyl tertiary-butyl ether/tertiary-amylmethylether; *MTO* methanol-to-olefins, *MTP* methanol-to-propylene

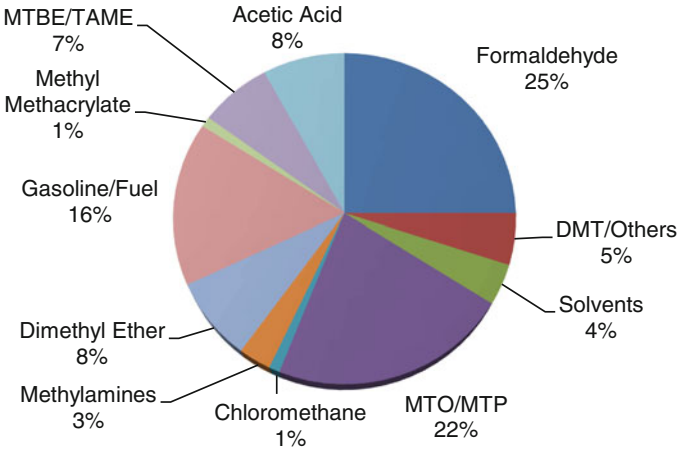

Fig. 1.13 Methanol demand and end use in 2016 [40]. Abbreviations: *MTBE/TAME* methyl tertiary-butyl ether/tertiary-amyl methylether, *MTO* methanol-to-olefins, *MTP* methanol-to-propylene

1.5 Methanol in Energy Storage and Carbon Recycling

Ludolf Plass[1] and Martin Bertau[2]

[1]*Parkstraße 11, 61476 Kronberg, Germany*
[2]*Institute of Chemical Technology, Freiberg University of Mining and Technology, Leipziger Straße 29, 09599 Freiberg, Germany*

Changing from a fossil/nuclear-based energy supply system to a renewable-based energy supply system poses substantial challenges regarding the necessary technological, economic and also social transformation processes. They all have to be synchronised within the limited timescale from today to the year 2050. As a forerunner in this process, Germany has to describe and compare the energy storage and carbon recycling processes, which are an essential element of this transformation process.

Some key parameters of the energy transformation are:

- Reduction of CO_2 emissions by >80 % in 2050
- Production of >90 % of electrical power via renewable resources by 2050
- Meeting stringent economic parameters
  - Securing a safe power supply at all times
  - Securing an affordable energy supply

For an increasingly renewable and strongly fluctuating power supply, the existing power storage capacities in Germany, as in most other countries, are far

underdeveloped. The only storage system for longer seasonal periods (4 weeks–3 months) is a chemical storage system. This means that electric power has to be converted via electrolysis to hydrogen as a first step.

Thereafter, essentially three chemical storage options are available, as discussed further in Chap. 8:

- Hydrogen storage:
  Results in the least conversion loss, but poses difficulties for longer-term storage and has high costs associated with a completely new infrastructure.
- Conversion from hydrogen to methane (SNG):
  Results in additional conversion losses, including in transport and storage. However, the existing infrastructure via the natural gas pipeline and power production system are attractive.
- Conversion from hydrogen to methanol:
  Again results in higher conversion losses. However, its lower storage and transport losses, higher repowering efficiency and most importantly, the potential to use "green" methanol in the chemical and fuel markets are attractive.

Important issues for chemical storage include the necessary capacity for grid stability and the necessary capacity to store "surplus power." Analysis has shown that the amount of surplus power far exceeds the amount of storage power for grid support from 2040 on. To avoid the shutdown of the power supply at certain times (and thus paying EEG compensation to the suppliers) or to export substantial power to other countries at marginal—sometimes even negative—prices (while again paying EEG compensation—a German scheme according to the Renewables Energy Sources Act—to the suppliers), a chemical storage system has to be designed for a foreseeable amount of surplus power.

The important question for the choice of the storage chemical is the question of what to do with the difference between surplus power and grid support power. In fact, there are two options:

Variant 1: Methane
Feeding the difference in energy as methane into the natural gas pipeline system.
Variant 2: Methanol
Feeding the difference in energy as methanol into the chemical/fuel market.

The "green methane" option implies that methane feed-in remuneration will be in accordance with the natural gas price, thus rendering this approach uneconomical for the foreseeable future until 2050. One has to bear in mind that natural gas prices have experienced a considerable drop due to the availability of shale gas. Because this amount will further increase, "green methane" will hardly have the potential to compete with shale gas prices.

The use of "green methanol," which has been produced from surplus power charged at 1 ct/kWh, as a chemical or in the fuel market provides the potential for an economical solution for the longer-term chemical storage of energy because the price levels for fossil resources will foreseeably further increase. In addition,

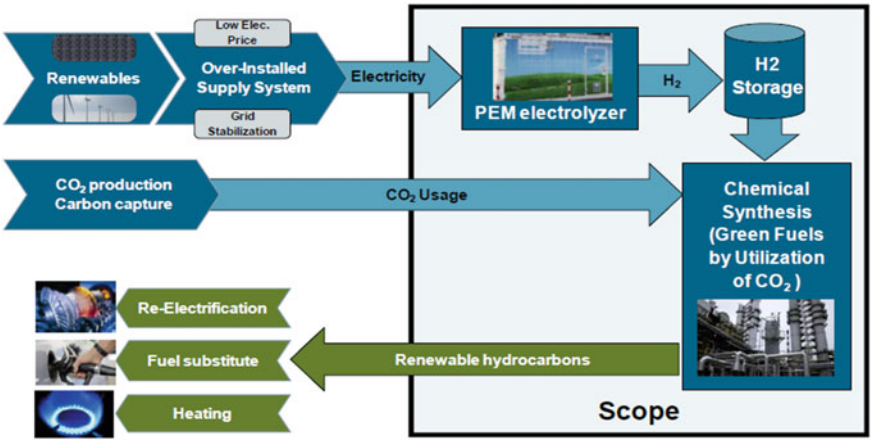

Fig. 1.14 Production of renewable hydrocarbons from surplus energy. (Courtesy of the authors) [48]

methanol has greater potential to recycle CO_2 obtained from combusting fossil or renewable resources than methane.

The "dualism" of methanol—that is, its property to be utilisable in both the chemistry and energy sectors—implies that chemical feedstock as well as combustibles for power generation and transportation/mobility purposes can be produced economically on a large scale from one source. Clearly, SNG can be used for mobility purposes, too; the same applies even for chemical feedstock. However, the overall efficiencies of (1) methane generation from renewables and (2) methane conversion to chemicals via synthesis gas or methanol are by far lower. For that reason, it is economically not competitive with methanol generation and utilisation.

The availability of "green methanol," a chemical entity that has been produced from CO_2, sunlight and water, will be an important contribution to the decarbonisation discussion. In addition to living things, the majority of consumer goods and combustibles are based on carbon. However, the decarbonisation discussion has been held in only in a few countries. For the benefit of their respective national economies, a switch to a methanol-based (i.e., "carbonised" economy) offers many more opportunities for more sustainable chemical production and power generation. The combustion of end-of-life products to CO_2 allows for the closing of the carbon loop for both green chemicals and biomass. This approach can be applied anywhere for the benefit of everyone.

Figure 1.14 shows how surplus electricity can be converted into hydrogen, then stored in the required quantity, allowing for the production of methanol in continuously operated chemical synthesis plants.

References

1. G.M. Woodwell, E.V. Pecan, in *Carbon and the Biosphere, 24th Brookhaven Symposium in Biology*, Upton N.Y., 16–18 May 1972
2. J.M. Holländer, M. Simmons, *Annual review of Energy*, vol. I (Annual Reviews Publishers, Palo Alto, 1976)
3. M. Bertau, CO_2-ein Rohstoff mit großer Zukunft, in *Energie und Rohstoffe*, ed. by P. Kausch, M. Bertau, J. Gutzmer, J. Matschullat (Spektrum Akademischer Verlag, Heidelberg, 2011), pp. 135–149
4. http://wiki.bildungsserver.de/klimawandel/index.php/Terrestrischer_Kohlenstoffkreislauf (05 May 2013)
5. https://www.vci.de/Downloads/Top-Thema/DF_Rohstoffbasis.pdf. Accessed 10 Jan 2014
6. BP Statistical Review of World Energy. http://www.bp.com/statisticalreview, 2012
7. Arbeitsgruppe Energierohstoffe, BMWi, Arbeitsgruppe 3, Verfügbarkeit und Versorgung mit Energierohstoffen, (2006)
8. D. Meadows, D.H. Meadows, E. Zahn, *The Limits to Growth* (Universe Books, New York, 1972)
9. P. Levi, *Il sistemaperiodico* (Einaudi, Turin, 1975)
10. F. Asinger, *Methanol - Chemie- und Energierohstoff* (Springer-Verlag, Heidelberg, 1986)
11. http://www.ise.fraunhofer.de/de/downloads/pdf-files/aktuelles/stromproduktion-aus-solar-und-windenergie-2012.pdf (05 May 2013)
12. M. Bertau, F.X. Effenberger, W. Keim, G. Menges, H. Offermanns, Chem. Ing. Techn. **82**, 2055–2058 (2010)
13. Anonymous, Wer ist's? Friedrich Asinger, Nachr. Chem. Tech. Lab.1977, 408–409
14. W. Keim, H. Offermanns, Angew. Chem. **46**, 2–7 (2007)
15. F. Asinger, Über eine einfache Synthese von Thiazolinen (3,4), Vortrag GDCH – Jahrestagung, Angew. Chem. **68**, 377 (1956)
16. F. Asinger, M. Thiel, Angew. Chem. **70**, 67–683 (1958)
17. F. Asinger, H. Offermanns, Angew. Chem. **79**, 953–965 (1967)
18. F. Asinger, W. Leuchtenberger, H. Offermanns, Chem. -Ztg. **87**, 372–376 (1975)
19. F. Asinger, *Chemie und Technologie der Paraffinkohlenwasserstoffe* (Akademie Verlag, Berlin, 1956)
20. F. Asinger, *Paraffins: Chemistry and Technology* (Pergamon Press, Oxford, 1967)
21. F. Asinger, *Chemie und Technologie der Monoolefine* (Akademie Verlag, Berlin, 1956)
22. F. Asinger, *Monoolefins: Chemistry and Technology* (Pergamon Press, Oxford, 1968)
23. F. Asinger, *Einführung in die Petrolchemie* (Akademie Verlag, Berlin, 1959)
24. F. Asinger, *Die Petrolchemische Industrie I und II* (Akademie Verlag, Berlin, 1971)
25. F. Asinger, *Methanol: Chemie- und Energierohstoff* (Springer-Verlag, Heidelberg, 1986)
26. W. Keim, H. Offermanns, Nachr. Chem. **58**, 34 (2010)
27. G.A. Olah, A. Goeppert, G.K. Surya Prakash, *Beyond Oil and Gas: The Methanol Economy* (Wiley-VCH Verlag, Weinheim, 2006)
28. H. Schenzinger, *Bei IG-Farben: Roman der chemischen Großtechnik und Anilin: Roman eines deutschen Farbstoffes* (Bertelsmann, Gütersloh, 1956)
29. W. Teltschik, *Geschichte der deutschen Großchemie* (Entwicklung und Einfluß in Staat und Gesellschaft, Wiley-VCH, Weinheim, 1992)
30. G. Plumpe, Die I.G. Farbenindustrie AG. Wirtschaft, Technik und Politik 1904–1945, Duncker & Humblot, Berlin, (1990)
31. D. Jeffreys, *Hell's Cartel: IG Farben and the Making of Hitler's War Machine* (Bloomsbury, London, 2009)
32. P. Hayes, *From Cooperation to Complicity: Degussa in the Third Reich* (Cambrigde University Press, Cambridge, 2007)
33. F. Aftalion, *A History of the International Chemical Industry* (University of Pennsylvania Press, Philadelphia, 1989)

34. Degussa AG, Im Zeichen von Sonne und Mond: Von der Frankfurter Münzscheiderei zum Weltunternehmen Degussa AG; Degussa AG, Frankfurt, (1993)
35. H.-G. Brocksiepe, in *Ullmann's Encyclopedia of Industrial Chemistry*, vol. 8, 6. ed. (Wiley-VCH-Verlag, Weinheim, 2002), p. 93–98
36. F. Flügge, Die Entwicklung der Holzverkohlungs—Industrie in Deutschland, Technische Berichte, herausgegeben zum achtzigjährigen Bestehen der Deutschen Gold- und Silberscheideanstalt vormals Roessler, (1953)
37. H.J. Derdulla, K. Wellner, Nachr. Chem. Tech. Lab. **39**, 508 (1991)
38. Photo: Air Liquid E&C Global Solutions
39. DeWitt Bitts—Global Methanol Supply & Demand Estimates, (2011)
40. D. Johnson, Global Methanol Market Review, June 2012
41. Status and impact of MTBE bans, Department of Energy, www.eia.doe.gov, 2003
42. C.-J. Yang, R.B. Jackson, Energ. Policy **41**, 878–884 (2011)
43. J.Q. Chen, A. Bozzano, B. Glover, T. Fuglerud, S. Kvisle, Catal. Today **106**, 103–107 (2005)
44. Methanex Corp
45. M. Masih, M. Mansur, K. Albinali, M. DeMello, Energ. Policy **38**, 1372–1378 (2010)
46. L. Bromberg, W.K. Cheng, *Methanol as an alternative transportation fuel in the US: Options for sustainable and/or energy-secure transportation* (Massachusetts Institute of Technology, Cambridge USA, 2010)
47. H. Hariharan, China's methanol economy, ww.icis.com, July 2011
48. A. Tremel, M. Walz, M. in *Baldauf, Usecase analysis for CO2-based Renewable Fuels*. 3rd International Conference on Energy Process Engineering, Frankfurt, Germany, 4–6 June 2013

Chapter 2
Fossil Feedstocks–What Comes After?

Willi Keim

2.1 Fossil Raw Materials for Energy and Chemical Feedstocks

The abundant availability of fossil raw materials such as crude oil, natural gas, brown coal (lignite) and coal has given rise to our enormous prosperity. Fossil raw materials satisfy our energy needs and they provide a wide spectrum of chemicals that enrich our lives. This success is mainly based on the availability of fossil raw materials in vast amounts, energy density and transportability via pipelines. The so-called polymer age would have been impossible without the inexpensive wealth of oil and gas. Fossil raw materials make up approximately 80 % of world's energy supply (crude oil: 37 %, coal: 25 %, natural gas: 23 %). By 2035, the International Energy Agency expects a decline for fossil raw materials to 75 % while renewables increase, from today's 13 to 18 % of the world's energy supply [1]. China will be the world's largest energy consumer.

The worldwide material use for chemicals is approximately 10 %. To better understand the relationships and mutual dependences within the fossil raw material industry, a differentiation between use for energy and use for materials (chemicals) is helpful. For instance, naphtha produced in fuel refineries is used by the chemical industry for the manufacture of C_2–C_4 olefins and aromatics, which are the basic chemicals for mass polymers such as polyethylene, polypropylene and polystyrene. However, they are also used to save heating energy in houses via insulation, thus reducing energy consumption.

Approximately one-third of fossil raw materials for energy are used for transportation, one third for generation of electricity, and one-third for heating purposes. In the United States, 97 % of all air, sea and land transportation systems are crude oil-based. It is obvious that the availability and price of chemical feedstocks

W. Keim (✉)
RWTH Aachen, Institute of Chemical Technology and Macromolecular Chemistry, Worringerweg 1, 52056 Aachen, Germany
e-mail: Keim@itmc.rwth-aachen.de

M. Bertau et al. (eds.), *Methanol: The Basic Chemical and Energy Feedstock of the Future*, DOI: 10.1007/978-3-642-39709-7_2,

for organic materials, using only 10 %, will be dictated by the crude oil manufacturing industry.

The rapidly growing world population, the increasing per capita consumption by industrialised countries, and the thriving economies of countries such as China and India give rise to concern and worry regarding the future availability of fossil raw materials. The biggest impact on future availability comes from the world population growth. The population grows every year by 80 million people, which is close to the population of Germany. If China, with its population of 1.3 billion people, begins to consume the same amount of crude oil as Germany (93 Mio tonnes in 2010), China alone would use more than half of the world's crude oil production. This raises some questions: Will we be in a position to cover all future demand? Where in the future will we obtain our fossil raw materials to meet world's energy and material need? Do we have alternatives to fossil raw materials?

In addition, the burning of fossil fuels to carbon dioxide is assumed to contribute significantly towards climate change, causing massive environmental problems (the greenhouse effect). The majority of experts agree that there are still sufficient fossil reserves and resources to satisfy the demand in the next decades. Oil companies have provided many energy scenarios, which easily can be found in internet or ordered directly [2, 3].

2.1.1 Availability of Crude Oil, Natural Gas and Coal

About 90 % of the crude oil reserves and 85 % of the natural gas reserves are state owned. A few producers, mainly in the Middle East, control more than 50 % of the oil and gas. Considering the recent unrest in Arabian countries, there is reason for concern regarding a secure supply. In addition, prices fluctuate and are volatile. Firm predictable prices and reliable supply form the basic conditions for planning and investment.

To attach a timeframe to the availability of fossil raw materials, experts refer to the depletion point, which is the number of years obtained by dividing the global reserves by global consumption [4]: crude oil: 42 years, natural gas: 63 years, hard coal: 159 years, and lignite: 227 years. The depletion points are based on reserves and not resources, which are much bigger but less reliable. Nevertheless, the fossil raw material reserves—formed by nature over eons and therefore not renewable in our timeframe—are finite at a time in the not-too-distant future.

There is growing understanding that we have to economise our energy consumption, search for alternatives and move toward energy conservation, such as the following:

- Better utilisation of energy: Improve efficiency, which could come from different areas, such as material science, bionics, engineering, biotechnology and natural sciences

- Improved technologies for using energy and exploitation of fossil raw materials
- Changes in mobility (going electric) and search for better/other transportation means (fuel cells, biofuels, hydrogen economy, methanol economy)
- Better transport and storage of energy (smart grids, smart houses and cities)
- Search for new energy resources, including nuclear
- Use of microbes, which produce underground methane
- CO_2 avoidance, storage and utilisation.

All of these items will change our lifestyles. Politicians, scientists, industry and citizens are challenged to make this change possible. Politicians must forward policies that are targeted at specific technologies, which often involve heavy initial subsidising. Many countries look at Germany, which has introduced an ambitious programme that moves away from nuclear energy to 35 % renewable electric energy by 2020.

Due to the vast complexity and scale (there are limits to the rate at which new technologies can be developed), there is no quick solution to move away from fossil raw materials and carbon energy [5]. If renewable electricity generated by the sun can be implemented soon, the depletion points for fossil raw materials will be extended. Most likely, however, we will have to deal with an energy mix for a long time to come.

The depletion point for crude oil is given as 42 years. How reliable is this number? Great uncertainties surround this question. We can hope to discover new oil fields (deep water, arctic). The recovery rate can be increased by improved recovery methods. Up from 20 to 30 % half a century ago, many fields are now targeting a 50 % recovery rate, with the best surpassing 70 %. More sophisticated enhanced oil recovery technologies will be developed and applied, such as seismic modelling, fracturing and stimulation of the reservoir. There are also vast amounts of unconventional oils, such as heavy oil (Venezuela), oil sand (Canada) and oil shale. The worldwide reserves, which by definition are exploitable with today's production technologies, are estimated to be 164 Gigatonnes. Adding the reserves of unconventional oil (66 Gigatonnes) means that the oil reserves are 230 Gigatonnes. The current annual global consumption amounts to approximately 4 Gigatonnes, suggesting a depletion point of 58 years [6].

Natural gas is found as pure gas, together with petroleum, as coal bed methane, as shale gas methane and as methane hydrates. Natural gas is mainly used as energy for heating buildings and for combustion in power plants. A small part is used directly as motor fuel. The worldwide chemical industry consumes about 8 % for material use. Natural gas, due to its hydrogen content, emits less CO_2 and therefore is considered to be an environmentally friendly energy source. The depletion point is said to be 63 years. Again, one has to consider reserves (6,954 exajoule or $183 \times 1{,}012$ m^3) and resources. The resources embracing unconventional gas such as shale gas, coal bed methane and methane hydrates amount to 58,250 exajoule or $1{,}533 \times 1{,}012$ m^3 [6]. Methane hydrates, present under the continental shelves of the seas and in the Siberian and Canadian tundra,

are thought to be the biggest source of unconventional gas. Currently, there are no technologies available to recover gas hydrates. Shale gas and coal bed methane can be freed from coal and shale by hydraulic fracturing using extremely high pressure and the addition of chemicals. Currently, the U.S. shale gas production amounts to 5–6 % of the consumption and is estimated to be 20 % by 2020 [7].

However, there is concern about the potential environmental impacts of hydraulic fracturing, including the contamination of groundwater by the chemicals added, as well as the migration of gases and hydraulic fracturing chemicals to the surface. For these reasons, hydraulic fracturing has come under scrutiny, with some countries suspending or banning it [8]. Many research efforts and developments are underway to carry out hydraulic fracturing without the use of chemicals.

When discussing the availability of methane gas, one must mention the biogas derived by the methanogenesis of biomass. Numerous plants worldwide are producing biogas, which mainly is used to produce electricity or heat; to a minor degree, it is used as transportation fuel. To avoid competition with food production, research and development are focusing on the use of "non-food-biomass".

Historically, coal was the principal fossil raw material mined for heating purposes and for the production of coke for the steel industry. Coal was also the raw material used for establishing the chemical industry. Coal was supplanted by crude oil and natural gas. In 2004, the world's coal production amounted to 5.5 billion tonnes. Its share of the total world primary energy market was 24 % (oil: 35 %, gas: 21 %, nuclear: 7 %, hydroelectric: 2 %, renewable: 11 %). Reserves are estimated at 1 trillion tonnes and resources at 6.2 trillion tonnes [6]. Coal is geographically widely dispersed, but five countries possess about 80 % of it.

Political and market forces favour the development of coal as a widely available, low-cost energy option. National security, shortage of foreign currency and local sources of employment are driving forces. Coal is mainly used for the generation of electricity in power plants and for heating. The chemical use is small and varies from country to country. In China, coal is gasified on a large scale to produce ammonia and methanol. Also, coal-based acetylene is still used by the Chinese Chemical Industry. In Germany, the material use of coal has shrunk to 2 %.

Based on its reserves, coal is generally seen as a major fossil fuel source for the longer term. However, the anthropogenic emission of CO_2 gives rise to great concern regarding climate change and ways to store CO_2 or use it are under consideration and development. There is also much room to improve the efficiency of coal-burning power plants, thus minimising CO_2 emissions. Many experts believe that the sequential supply responses to the increasing energy demand will start with coal, then move to biofuels, followed by renewable energy.

Figure 2.1 elucidates the techniques for producing energy (fuel) and chemicals from coal.

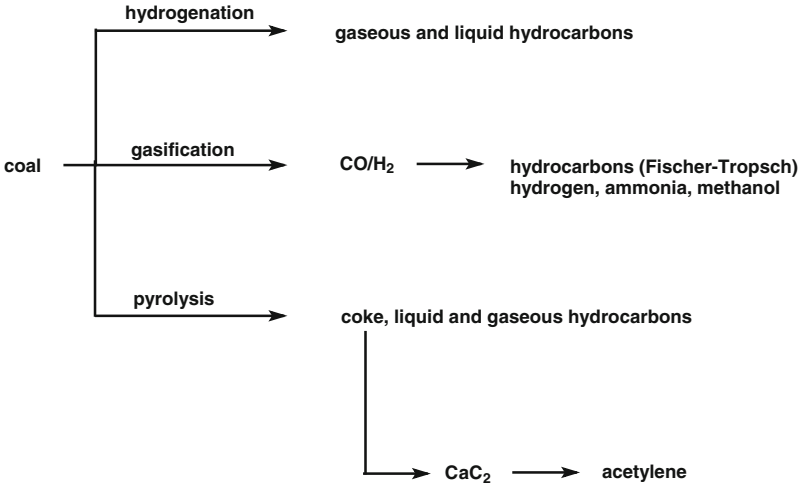

Fig. 2.1 Conversion technologies of coal for yielding energy (fuels) and chemicals

2.2 Alternatives for Replacing Fossil Raw Materials

The decline of fossil raw materials can entail serious economic and social implications. In addition to the concern about the future availability of raw materials for energy and material use, there is the threat of global warming caused by CO_2 emissions. Several options are available to mitigate dwindling fossil resources and global warming:

Solar resources wind, hydropower, thermal, photovoltaic, biomass
Biomass energy and chemicals
Planet movements ocean tides, waves, currents
Geothermal energy
Nuclear energy fusion and fission
Carbon dioxide hydrogenation to hydrocarbons and oxygenates

2.2.1 Solar Resources-Biomass

Wind, hydropower, thermal, photovoltaic and biomass can be used to generate electricity, thus replacing and substituting oil, gas and coal in conventional power plants [9]. The electricity can be used for driving cars, heating homes, and fueling the industry, which are major customers for fossil raw materials.

Figure 2.2 outlines various approaches for using sunlight to replace fossil raw materials.

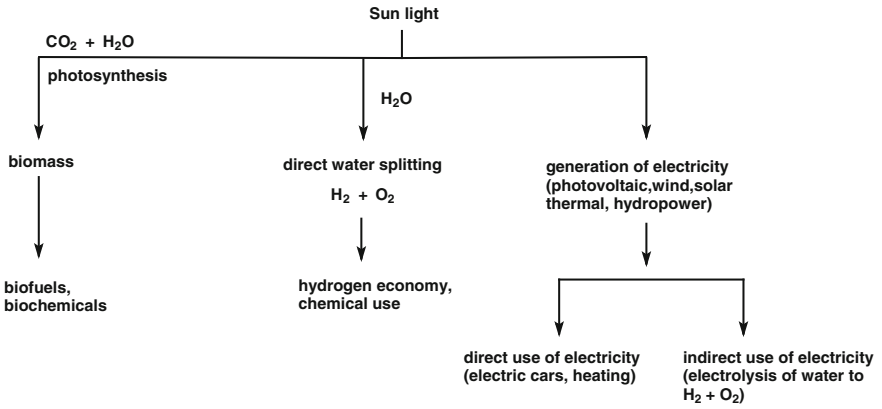

Fig. 2.2 Using sun light in replacing fossil raw materials

There are many options available to use the sun rays hitting the earth daily. The energy of the sun comes to us free of costs and represents a nearly unlimited resource, which we must learn to harvest to secure mankind's long-time survival. Numerous research and development efforts are underway worldwide to use sun's energy [10, 11].

As Fig. 2.2 shows, water or other liquids, when heated by the sun, can be used directly or via heat pumps. The direct use in solar power plants heats water via mirrors. The heated (400 °C) water can generate electricity via turbines and electrical generators. The electric energy can enter into existing or new electric grid structures and can be used for electric cars, heating of homes and industry uses.

Great potential exists for photovoltaics. Solar energy can be converted directly to electricity on the order of 20 % with silicon photovoltaic cells. By 2030, the European Photovoltaic Industry Association expects photovoltaics to have a 9 % share of world electricity consumption. However, photovoltaics are expensive and many doubts surround this expectation [12, 13].

Figure 2.2 also shows various other approaches that are under investigation, including direct water splitting to hydrogen and oxygen, thus enabling a hydrogen economy [14]. The hydrogen produced could also be used by the chemical industry, which is short of hydrogen and produces it from water and fossil carbon monoxide.

The most advanced method is the use of sun-derived wind energy, both onshore and offshore. Huge wind farms are in operation or are under construction. They are currently the best available technology for harvesting sunlight for electricity generation.

The direct storage of sun energy in reservoirs has been of interest for a long time [15]. Sun-derived renewable forms of energy, outside of biomass, involve mainly electric energy. It is very difficult to store electric energy as strategic reserve or for seasonal storage. When the sun is brightly shining or the wind is

powerfully blowing, more electricity is generated than the electric power grid can absorb. Various storage routes are under discussion: hydrogen, methane, liquid hydrocarbons, methanol and ethanol [16]. For sustainability, there are three requirements: accessibility, availability and acceptability. Methane meets all three requirements. With the availability of inexpensive hydrogen derived by water splitting through the sun (Fig. 2.2), CO_2 could be hydrogenated to methane. This route would provide an "eternal" feedstock, and at the same time would mitigate our CO_2 pollution problem. Methane can be stored and distributed safely within our existing, well-proven methane storage and distribution system. Another option is the hydrogenation of CO_2 to methanol (see later).

Biomass is an energy-rich carbon source derived by photosynthesis from CO_2, water and sunlight. In principle, biomass is inexhaustible and renewable. Biomass can substitute or replace fossil raw materials for many needs:

- ***Bioenergy***
  Heat (direct burning), electricity, fuels (bioethanol, biodiesel), biomethane
- ***Materials***
  Chemicals, biomaterials (biopolymers)

Biomass is widely used to provide energy. This can be achieved via direct burning, by wood-fired power plants yielding electricity, or by biofuels and biomethane. By 2035, the International Energy Agency expects the world's primary energy consumption to be composed of 29 % coal, 28 % oil, 22 % gas, 6 % nuclear, 2 % hydroelectric, 10 % biomass and waste and 3 % other [12].

The chemical industry is using biorenewable feedstocks such as plant oils, fats, sugar and starch for a wide spectrum of products (white biotechnology). Worldwide, this share amounts to about 8 % and is increasing constantly. "Green polymers" such as polylactid and biopolyethylene are also rapidly increasing their market shares [6].

For bioenergy disposal on a large scale, which is an essential condition to replace fossil raw materials, vast areas of arable land are needed—land that often also can be used for food and animal feed production. In Germany, about 18 % of arable land is used for biofuels. Many consider it irresponsible to convert food into fuel and chemicals. Therefore, the first generation of biofuels, namely bioethanol and biodiesel, is discussed very controversially. In addition, the risks of excessive fertiliser use, costs, loss of carbon sinks, net energy use, high tax subsidies and the destruction of rainforests to cultivate sugar cane and palm oil are further objections [17]. Therefore, great hopes rest with the second generation of biomass—namely "non-food-biomass," which will use lignocellulose derived from wood, agricultural and forestry remains. Non-food-biomass can be grown in areas that are unsuited to cultivate crops. Most Organisation for Economic Co-operation and Development countries, being in temperate regions, favour and support economic routes to second-generation biofuels and biochemicals [18], such as:

- Cellulosic ethanol (demonstration plants)
- Biomass conversion to synthetic gas (syngas) for biodiesel (demonstration plants)
- Biodiesel from microalgae and sugar-based hydrocarbons (research and development)
- Others, including methanol (commercial), biobutanol, dimethyl ether, pyrolysis-based fuels (demonstration plants) and novel fuels such as 2-methyltetrahydrofuran (research and development) [19]

In principle, there are three routes under investigation to convert non-food-biomass into energy and chemicals, as shown in Fig. 2.3: thermo-chemical-conversion, pyrolysis and biochemical conversion.

The biochemical conversion is based on a breakdown of lignocellulose into lignin, hemicellulose, cellulose and residues. The residues can be used for syngas or biogas manufacture. The intermediates lignin, hemicellulose and cellulose are further broken down by chemical or enzymatic processing techniques into chemicals such as furfurals, icatonic acid and levulinic acid (which are also called platform chemicals), thus opening up product routes to novel chemical feedstocks for the chemical industry and for novel fuels [20]. For instance, cellulosic ethanol can be converted to bioethene, which could replace or substitute fossil oil-derived ethylene.

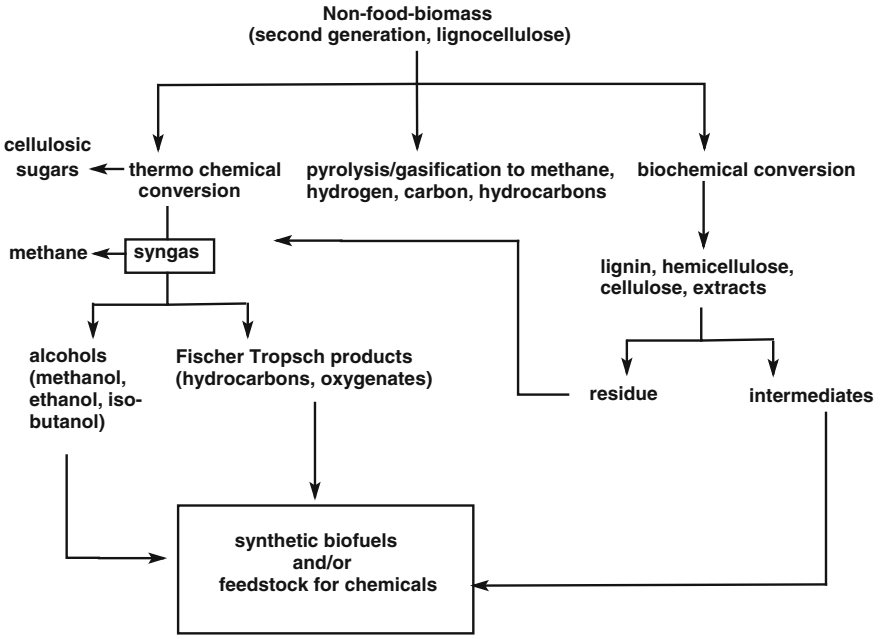

Fig. 2.3 Thermo- and biochemical conversion of non-food-biomass (lignocellulose)

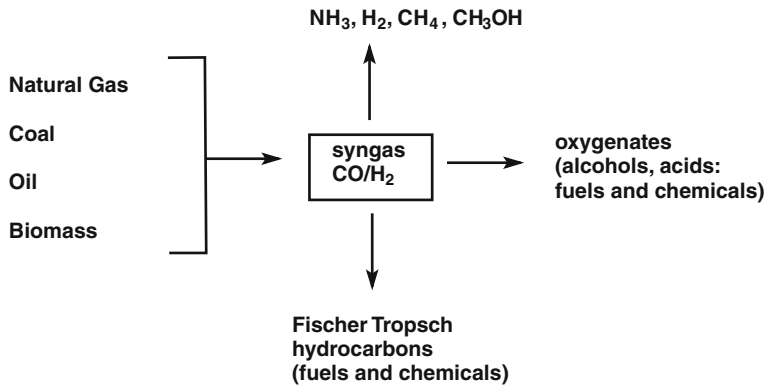

Fig. 2.4 Syngas C_1-chemistry

The thermo-chemical-conversion can follow two pathways: hydrolysis by water to sugars and conversion to syngas. The use of supercritical water (the Plantrose process by the company Remmatix) yields cellulosic sugars. Feedstock is wood or straw. Also, the use of acids and ionic liquids has been reported [21, 22].

The syngas route shown in Figs. 2.3 and 2.4, based on fossil raw materials gas, is a very old technology going back to the early 20th century that is still practiced today in many plants, such as coal (South Africa, China) and natural gas (Persian Gulf). This chemistry became known as the term C_1-chemistry [23, 24]. The synthesis of the oxygenate methanol and the Fischer–Tropsch process are state of the art. The application of biomass (Fig. 2.4) would integrate well into the existing fuel and chemical industry.

Biomass can also be pyrolised/gasified to gas (methane, hydrogen), oil and residue/carbon (Fig. 2.4). The gasification/pyrolysis is still in the developmental stages [25, 26]. The Carbo-V-Process by Choren is an example of a semicommercial plant, although it was recently closed down.

The lignocellulose pathway in Fig. 2.3 embraces the concept of a biorefinery [27], which represents the key to an integrated production of energy and chemicals. A biorefinery, analogous to today‘s petroleum refinery, integrates biomass conversion processes to produce biofuels and biochemicals.

One chemical with great potential to substitute fossil raw materials is biomethane. Enzymes and microorganisms can convert biomass very efficiently into biogas—a mixture of methane and CO_2. With 10,000 L biogas, based on 1 hectare of arable land, biomethane ranks before biomass-to-liquid diesel (3,101 L), bioethanol (1,450 L) and biodiesel (1,183 L), respectively. Therefore, numerous economical biogas plants are in operation. In addition, biomethane can also be derived from synthesis gas (Fig. 2.4) via hydrogenation of carbon monoxide.

When discussing the availability and substitution potential of biomass, one must also consider the impacts of the “green revolution” based on plant breeding, genetic engineering and proper selection of plants. For instance, Jatropha seeds are

rich in oil (35 %) and are drought resistant. The oil can be used for biodiesel and represents a viable feedstock for the chemical industry.

2.2.2 Nuclear Power/Energy

The energy stemming from nuclear fission substitutes for fossil raw materials on a large scale. Also nuclear fusion, which is still in its infancy, represents a potential carbon-free energy source that is also free of CO_2 emissions. However, accidents in nuclear power plants and problems with storing the nuclear waste have made nuclear energy to a very controversial energy source, with many advantages and disadvantages. Although Germany has decided to abandon nuclear power, other countries continue. At a recent meeting, B. Bigot, chairman and chief executive officer of the French Alternative Energies and Atomic Commissions, stated [28]: "There is real need to develop sustainable low-carbon safe, environmentally benign and economically competitive technologies as nuclear and renewable energies to build a flexible energy mix adapted to the specific needs of each country."

There is concern that biomass and solar energy cannot satisfy future energy demands. It is always dangerous to place all eggs in one basket. Therefore, the author of this chapter strongly believes that, at a minimum, research and development of nuclear power must continue to keep options open for nuclear energy (fission and fusion).

2.2.3 Carbon Dioxide

Carbon dioxide attracts many research efforts [6, 29–32]. The conversion of CO_2 into useful organic matter is pursued for two reasons: feedstock for fuels and chemicals [25, 33] and mitigation of CO_2 emission, which is held responsible for global warming. Here, it must be emphasised that there is a quantity problem. Even if we would base all chemicals on CO_2 as feedstock, the emissions of CO_2 would only be reduced by about 1 %. Application for fuels is 10 times greater.

Carbon dioxide is available in nearly unlimited amounts. It is the end product from all combustion processes using fossil raw materials. It is available as CO_2 gas in earth drilling operations, and it is present in carbonate rocks. One can expect unlimited reserves, as well as a secure and regional supply at stable prices.

To make use of the carbon atom in CO_2 for energy or chemicals, reduction routes are required in which one partner must contribute the necessary energy to overcome the thermodynamic and kinetic stability of CO_2. Quantitatively, great potential rests with the following reactions: hydrogenation to synthesis gas (Eq. 1),

hydrogenation to methanol (Eq. 2.2), reforming with methane (Eq. 2.3), photocatalytic/electrocatalytic reduction (Eq. 2.4) and hydrogenation to methane (Eq. 2.5):

$$CO_2 + H_2 \rightleftharpoons CO + H_2O \tag{2.1}$$

$$CO_2 + 3H_2 \rightleftharpoons CH_3OH + H_2O \tag{2.2}$$

$$CO_2 + CH_4 \rightleftharpoons 2CO + 2H_2 \tag{2.3}$$

$$CO_2 + H_2O \overset{h\cdot\gamma}{\rightleftharpoons} CO + H_2 + O_2 \tag{2.4}$$

$$CO_2 + 4H_2 \rightleftharpoons CH_4 + 2H_2O \tag{2.5}$$

$$CO_2 + H_2O \rightleftharpoons -CH_2- + 1.5O_2 \tag{2.6}$$

These "dream reactions," to be economical, require that the hydrogen or the energy come from inexpensive renewable energy resources that are sun derived (e.g. splitting of water) or based on nuclear energy. The dry reforming of methane with CO_2 (Eq. 2.3) needs high temperatures. The photocatalytic/electrocatalytic pathway (Eq. 2.4) is of great interest, but it is still in the stages of fundamental research and will not be a technically feasible option for the foreseeable future. The reaction of Eq. 2.6 can be regarded as technical photosynthesis and relates also to the Fischer–Tropsch synthesis [29].

2.3 Methanol Economy [34, 35]

Among all the discussions regarding the future availability of fossil raw materials and pollution by carbon dioxide, one of the oldest and versatile options—namely, a methanol economy—is not discussed with the same enthusiasm as a hydrogen economy or a ethanol economy [36]. However, methanol could fulfil nearly all requirements needed for raw materials, as is shown in Fig. 2.5.

The technical routes to methanol are based on synthesis gas, which can be produced from any carbon-containing source, such as fossil raw materials, CO_2, or biomass. Today, mainly natural gas is used, followed by coal. Generally, the use of biomass as raw material feedstock for fuels and for the chemical industry is hampered by a lack of selectivities and yields in processing, because biomass consists of a wide range of organic compounds similar to crude oil and coal. Therefore, for crude oil and coal, a breakdown to basic chemicals is practiced. Will biomass, via its conversion to synthesis gas, parallel the development of crude oil and coal gas by creating one universal building block, namely synthesis gas?

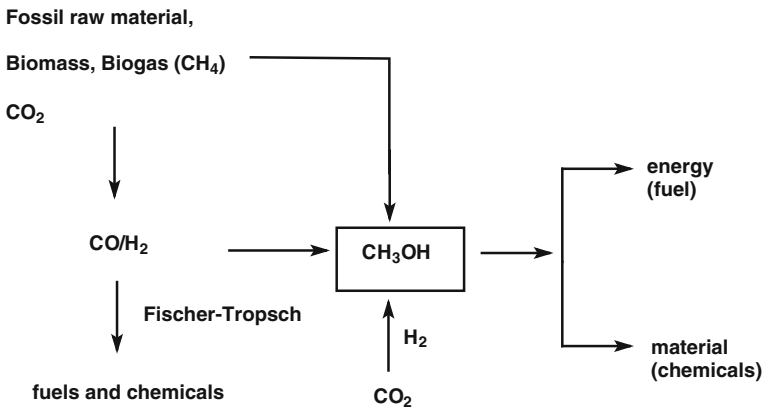

Fig. 2.5 A methanol economy

The old name for methanol is wood alcohol, pointing to its historical background. Enzymatic routes from biomass to methanol exist, but they are in their infancy for industrial usage. In this context, the missing link for a methanol economy, which is built on methane, is the direct chemical conversion of methane (e.g. biogas) into methanol—a reaction that is a great challenge for researchers.

Many gas fields exist, although they cannot be exploited due to their size. Portable methanol production units, which just appeared on the market, can be used for these stranded gas reserves. Also the transportation of coal out of arctic areas could be achieved applying methanol-coal slurry pipelines [37]. A part of the coal can be converted into methanol, which then together with coal can be pumped through a combined pipeline. Many concepts for a biorefinery also invoke methanol as one intermediate [26].

A fascinating alternative to fossil raw materials would be the direct conversion of CO_2 to methanol (Eq. 2.2). This would provide an "eternal" feedstock and at the same time would mitigate the CO_2 pollution problem. Nature uses photosynthesis from CO_2 and water to create biomass. Can we alter this process by converting CO_2 to methanol, whereby the hydrogen is derived from the sun or wind (electricity) (Eq. 2.7)?

$$\begin{array}{r} 3H_2O + h \cdot \gamma^* \rightarrow 3H_2 + 1.5O_2 \\ CO_2 + 3H_2 \rightarrow CH_3OH + H_2O \\ \hline CO_2 + 2H_2O + h \cdot \gamma^* \rightarrow CH_3OH + 1.5O_2 \\ *\text{sun, or wind (electricity)} \end{array} \tag{2.7}$$

Today, methanol is mainly used in single chemical applications, but methanol has the potential to provide the basic chemicals, C_2–C_4 olefins, and aromatics by proven technologies. This is exemplified by the 500,000 t plant recently built in China to convert methanol into olefins (see Sect. 6.4.3).

Methanol can also be a feedstock to generate energy via fuel cells (see Sect. 6.5.2) or internal combustion and compression ignition engines (see Sect. 6.3.1). Here, proper performance has been established. Also, methanol derivatives such as dimethyl ether, dimethyl carbonate and methyl-tert-butyl ether are of interest in fuel applications (see Sect. 6.3.2). Methanol fuel cells are already in commercial use, especially for generating portable electric power used in mobile phones and laptop computers. Nearly every major electronic manufacturer is involved in the application of methanol fuel cells.

Methanol can be used to produce single-cell proteins for animal feed. The apocalyptic prophecies that mankind in the near future will suffer from a lack of energy, global warming and food shortages may turn out to have a solution via a methanol economy. Finally, the energy storage problem could be solved via a methanol economy, in which methanol is the storage molecule (see Chap. 8).

2.4 Conclusion

Presently, there is no practical and economical energy source available to replace fossil raw materials. In the past, the availability of huge fossil raw material reserves created the illusion of unlimited supply. However, increasing demands from population growth and per capita energy consumption made us aware that fossil raw materials are finite. The burning of fossil fuel also causes a climate problem that must be addressed. History teaches that human beings react to an important problem only when a crisis is already upon them. The energy system of the future will be very different from that of today.

Fossil raw materials will not run out overnight. We have many options available, such as energy conservation, a hydrogen economy, a biofuel economy, nuclear energy, sun-derived energy and a methanol economy—to name a few. In theory, there are many solutions and “dream pathways”; however, many will be unrealistic and will not be practical for reasons of economy, ecology, size of the market and so on. It will be a great challenge to find the most economical and ecological solution in an extremely complex system. There is a great deal of inertia present in developing alternatives to fossil raw materials considering the size of the market. Decades may pass before we are able to make these changes. There will be no easy path, but we must react now to have the technology available when it is needed. Governments and politicians will be asked to fund approaches; however, one should remember that in the 1970s the government advocated for an energy mix of 50 % fossil and 50 % nuclear, which today seems outdated. A methanol economy is one option with many advantages and disadvantages. Methanol, in which CO_2 is hydrogenated by sun-derived hydrogen from water splitting, looks enticing from a standpoint of energy and CO_2 avoidance. Methanol can help to integrate fossil raw materials and biomass value chains.

References

1. IEA's World Energy Outlook. Oil Gas Eur. Mag. **4**, 170 (2011)
2. Shell International BV, Shell Energy Scenarios to 2050, 4th edn. VMS The Hague, 2009
3. BP Statistical Review of World Energy 2011, online unter: http://www.bp.com/assets/bp_internet/globalbp/globalbp_uk_english/reports_and_publications/statistical_energy_review_2011/STAGING/local_assets/pdf/statistical_review_of_world_energy_full_report_2011.pdf. 22 May 2013
4. Reserves, Resources and Availability of Energy Resources, Bundesanstalt für Geowissenschaften und Rohstoffe (BGR), Hannover, 2010
5. G.J. Kramer, M. Haigh, Nature **462**, 568–569 (2009)
6. Position paper of German scientific Organization DECHEMA, GDCh, DBG, DGMK, VDI-GVC, VCI, Change in the Raw Material Base, 2010
7. http://en.wikipedia.org/wiki/Natural_gas#Shale_gas. 22 May 2013
8. K.M. Reinicke, Erdöl Erdgas Kohle **127**, 340–342 (2011)
9. N. Armaroli, V. Balzani, *Energy for a Sustainable World: From the Oil Age to a Sun-Powered Future,* (Wiley-VCH Verlag, Weinheim, 2011); N. Armaloni, V. Balzani and N. Serpone, *Powering Planet Earth: Energy Solutions for the Future*, (Wiley-VCH Verlag, Weinheim, 2013)
10. R.B. Laughlin, *Powering the Future: How We (eventually) Solve the Energy Crisis and Fuel the Civilization of Tomorrow* (Basic Books, New York, 2011)
11. D.B. Botkin, *Powering the Future: A Scientist's Guide to Energy Independence* (F.T. Press Science, Upper Saddle River, 2010)
12. http://en.wikipedia.org/wiki/World_Energy_Outlook. 22 May 2013
13. International Energy Agency (IEA), World Energy Outlook. (2012)
14. S.K. Ritter, Chem. Eng. News **89**(48), 36–37 (2011)
15. A. Behr, W. Keim, G. Thelen, H.-D. Scharf, J. Chem. Tech. Biotechnol. **32**, 627–630 (1982)
16. F. Schüth, Chem. Ing. Techn. **83**, 1984–1993 (2011)
17. J. Johnson, Chem. Eng. News **89**(41), 12 (2011)
18. C. Somerville, H. Youngs, C. Taylor, S.C. Davis, S.P. Long, Science **329**, 790–792 (2010)
19. A. Janssen, M. Jakob, M. Müther, S. Pischinger, J. Klankermayer, W. Leitner, MTZ Worldwide, **71** (12), 54–60 (2010)
20. F.M.A. Geilen, B. Engendahl, A. Harwardt, W. Marquardt, J. Klankermayer, W. Leitner, Angew. Chem. **122**, 5642–5646 (2010)
21. R. Rinaldi, R. Palkovits, F. Schüth, Angew. Chem. Int. Ed. **47**, 8047–8050 (2008)
22. T. vom Stein, P. Grande, F. Sibilla, U. Commandeur, R. Fischer, W. Leitner, Green Chem. **12**, 1844–1849 (2010)
23. W. Keim, Methanol: Building Block for Chemicals, in *Catalysis in C1 Chemistry, D*, ed. by W. Keim (Reidel Publishing Company, Dordrecht, 1983). (Boston/Lancaster)
24. W. Keim, Pure Appl. Chem. **58**, 825–832 (1986)
25. M. Goderer, H. Spliethoff, Chem. Ing. Techn. **83**, 1897–1911 (2011)
26. N. Dahmen, E. Dinjus, Chem. Ing. Techn. **82**, 1147–1152 (2010)
27. B. Kamm, P.R. Gruber, M. Kamm, *Biorefineries—Industrial Processes and Products* (Wiley-VCH Verlag, Weinheim, 2006)
28. 23rd Annual Conference Academia European, Chemistry, Sciences, Culture and Society in the making of Europa, UNESCO Paris, 2011 Sept 20–22, 22
29. A. Jess, P. Kaiser, C. Kern, R.B. Unde, C. von Olshausen, Chem. Ing. Techn. **83**, 1777–1791 (2011)
30. M. Peters, B. Köhler, W. Kuckshinrichs, W. Leitner, P. Markewitz, T. E. Müller, Chem. Sus. Chem. 4 (9), 1177–1323 (2011)
31. W. Kuckshinrichs, W. Leitner et al., *Weltweite Innovationen bei der Entwicklung von CCS-Technologien und Möglichkeiten der Nutzung und des Recyclings von CO_2* (Studie/Endbericht, Forschungszentrum, Zentralbibliothek, Jülich, 2010)

32. A. Behr, *Carbon Dioxide Activation by Metal Complexes* (Wiley-VCH Verlag, Weinheim, 1988)
33. M. Aresta, *Carbon Dioxide as Chemical Feedstock* (Wiley-VCH Verlag, Weinheim, 2010)
34. F. Asinger, *Methanol - Chemie- und Energierohstoff* (Springer, Berlin, 1986)
35. G.A. Olah, A. Geoppert, G. Prakash, *Beyond Oil and Gas: The Methanol Economy* (Wiley-VCH Verlag, Weinheim, 2009)
36. M. Bertau, F.X. Effenberg, W. Keim, G. Menges, H. Offermanns, Chem. Ing. Techn. **82**, 2055–2057 (2010)
37. A. Bayer, K. Gruber, K. Hentschel und W. Keim, Erdöl und Kohle, Erdgas, Petrochem. **75**, 474–476 (1982)

Chapter 3
Vision: "Technical Photosynthesis"

Franz Xaver Effenberger

3.1 Introduction

In his book Methanol - Chemie- und Energierohstoff [1], published in 1986, Friedrich Asinger already expressed his concern for the excessive exploitation of the valuable raw materials of crude oil and natural gas. He saw a "methanol economy" as the only visionary way out of this situation: "If hydrogen were cheaply available, this readily obtainable pure, sulphur-free carbonic acid could easily serve as the starting point for the synthesis of methanol." And "If fossil raw material sources one day become increasingly short in supply and more expensive, or even totally exhausted... there remains apart from biomass only carbonic acid as the source of raw material for the organic chemical industry". In methanol, Asinger saw a chemical raw material that could spare the limited crude oil and natural gas resources. Apart from its importance as a chemical raw material, however, methanol could be of greatest importance as an energy carrier. Methanol itself or hydrocarbon derivatives thereof (fuels, olefins, etc.) could serve as a source of energy that can be easily stored and transported. At that time, Asinger evidently saw no danger of a shortage of carbon as a raw material.

Since the middle of the 1990s, George A. Olah and his coworkers at the Loker Hydrocarbon Research Institute (University of Southern California) have been intensively studying methanol and its potential as a raw material for energy and the chemical industry. They summed up and reported their findings in detail in 2009 [2].

Both Asinger and Olah consider methanol to be of equal importance as a source of energy and raw material for the chemical industry. However, in view of the dimension of a future "methanol economy," the amount of methanol needed for the energy sector would greatly exceed the amount that could be produced in the chemical industry. One can assume that the quantitative relationships for material and energy-oriented use would be similar to those for the use of crude oil today.

F. X. Effenberger (✉)
University of Stuttgart, Stuttgart, Germany
e-mail: franz.effenberger@oc.uni-stuttgart.de

M. Bertau et al. (eds.), *Methanol: The Basic Chemical and Energy Feedstock of the Future*,
DOI: 10.1007/978-3-642-39709-7_3, © Springer-Verlag Berlin Heidelberg 2014

Until a few years ago, the hydration of carbon dioxide for the production of methanol was generally not viewed as a viable option for a solution to the CO_2 issue. If this had been the case, we would not have been so intensively occupied with carbon capture storage technology—that is, the "burial" of the CO_2 from gaseous emissions. More recently, however, using CO_2 as a "carbon source" and, for instance, producing methanol via hydrogenation as a source of energy or for purposes of the chemical industry have received increasingly more attention. In 2010, for example, the US Department of Energy approved a research project titled "Artificial Photosynthesis." A number of universities and research institutes in California are participating in the project, which received $122 million in funding, for which the prerequisites for "artificial photosynthesis" are to be elaborated over a period of five years [3].

It is neither possible nor reasonable to quote all information and references in the literature on the subject of the carbon cycle. The main matter of concern of this chapter is to identify and discuss a carbon cycle on the basis of currently existing and industrially proven technologies that can be realised on a large scale and under the primacy of economical feasibility [4, 5].

3.2 The Natural Material Cycles of the Elements Carbon, Hydrogen, Nitrogen and Oxygen [6]

The natural material cycles are primarily determined by the three biopolymers: carbohydrates, proteins and nucleic acids. These three biopolymers essentially contain only the elements carbon, hydrogen, oxygen and nitrogen. The functioning cycles of these elements must be guaranteed in order to sustain life in its present form on earth. Cycles of other elements, such as sulphur in proteins or phosphorus in nucleic acids, are not yet considered to be problematic.

3.2.1 The Oxygen, Hydrogen and Nitrogen Cycles

From today's viewpoint, oxygen and hydrogen cycles are not viewed as challenging. Oxygen in its free form constitutes approximately 20 % of the atmosphere. When chemically bound in water or inorganic oxides, for instance, it is available in enormous amounts. Oxygen is continuously regenerated by way of photosynthesis and, because it is a rather heavy gas, it does not escape from the atmosphere of the earth. Hydrogen, as the lightest gas, would have diffused into space following the formation of our planetary system. However, due to its reaction with oxygen (presumably on dust particles) to form water, hydrogen has remained present on earth. Water became the basis for chemical and biological evolution, leading to the great diversity of life on Earth.

Before the onset of industrialisation at the beginning of the nineteenth century, the nitrogen cycle was largely in balance. With increasing population, however, the natural cycle was extended to its limits as a result of fertilising with manure and the cultivation of leguminous plants that are capable of binding nitrogen and converting this to nitrogen compounds used by the plants. From the middle of the nineteenth century, poorer harvests and increasing populations led to famines in Europe, eventually resulting in mass emigrations. The introduction of nitrate-based fertilisation (Chile saltpeter) by Justus von Liebig (around 1840) resulted in significantly higher harvest yields and was consequently a decisive factor in solving the famine problem in Europe. The breakthrough to a long-term technically secure nitrogen cycle was achieved by Fritz Haber and Carl Bosch in 1910 with the process named after them, using the hydrogenation of airborne nitrogen with hydrogen (synthesis gas) to ammonia at high temperature and high pressure:

$$N_2 + 3H_2 \xrightarrow[\text{[catalyst]}]{\text{550 °C, 250 bar}} 2NH_3 \qquad \Delta H = -92\ \text{kJ/mol}$$

Haber-Bosch process

The annual production of ammonia was 136 million tonnes in 2011. Without a technical solution for the nitrogen cycle, an increase in global population to today's level would never have been possible.

3.2.2 The Carbon Cycle

Before the onset of the industrial age (before 1830), the carbon cycle was completely in balance. In fact, this was still largely true until the middle of the twentieth century. However, the ongoing dramatic growth of global population, increasing from around 2.4 billion in 1950 to 7 billion in 2011 has drastically altered this situation. The burden on the carbon cycle by the population's basic needs (food, etc.) accounts for only a third of usage. The mobility sector (transportation) as well as higher life expectancies and desires for better quality of life (heating, cooling, etc.) are fuelling the rest of the demand for energy-rich carbon compounds (crude oil, coal, wood, etc.).

The basis of the natural carbon cycle is photosynthesis—that is, in a reaction mediated by chlorophyll, carbon dioxide and water produce glucose and oxygen using solar energy as an energy source:

$$6CO_2 + 6H_2O \xrightarrow[\text{[chloroplasts]}]{\text{solar energy}} C_6H_{12}O_6 + 6O_2$$

Photosynthesis

Through the action of photosynthesis in terrestrial vegetation, there is an annual fixation of approximately 120 billion tonnes of C (where "C" stands for carbon

not bound to other elements) in the form of glucose [6]. The latter is basis for the natural synthesis of numerous carbon compounds. Above all, however, it is the basis for the synthesis of starch and cellulose. These two biopolymers store solar energy in the form of chemical energy and are therefore available in large amounts, both as a stable and transportable source of energy and as a raw material.

Human beings and animals depend on these energy and carbon sources in order to sustain vital processes. In a sort of biological combustion, they convert carbohydrates back to carbon dioxide and water with the purpose of recovering energy. This process closes the carbon cycle, which began with photosynthesis.

Besides the terrestrial carbon cycle, there is also a significant maritime carbon cycle through the action of plankton fixing another approximately 90 billion tonnes of C per year [6]. Compared with the nitrogen cycle, which fixes approximately 160 million tonnes of nitrogen per year, the carbon cycle exceeds the nitrogen cycle by three orders of magnitude [6].

As already mentioned, until around 1950 the carbon cycle was largely in balance. However, since then, the situation has dramatically changed. In 2008, the combustion of fossil carbon sources (natural gas, crude oil and coal) released approximately 6.2 billion tonnes of C for which there was no capacity for elimination by photosynthesis. Although up to now a part of the CO_2 excess quantity has been absorbed by the CO_2 sinks of soil and sea water, there is an annual amount of approximately 3.5 billion tonnes of C remaining in the atmosphere, giving rise to a considerable increase in atmospheric CO_2 with all the consequences in discussion (global warming, acidification of the oceans, etc.).

If, as mentioned in this section, approximately two thirds of the carbon cycle is dominated by energy requirements rather than related to nutrition, there is an irrefutable obligation for covering the increasing demand for both energy C and chemical raw material C by other means than the combustion of fossil fuels—the future availability of which is largely regarded as decreasing.

3.3 Renewable Energy Sources

By definition, renewable energy is to be understood in terms of the sum of all energy sources sourcing in solar energy—all forms of water power, biomass, wind energy and solar thermal technology, as well as photovoltaic plants. At present, only a small fraction of solar irradiation is usable in practice. Therefore, the long-term energy supply of mankind will require optimisation of the technical exploitation of solar energy. Because the usability of renewable energy sources may vary substantially depending on their location (i.e. there is a direct outcome related to geographic conditions), the location issue is determined by economic considerations.

3.3.1 Water Power and Biomass

For thousands of years, man has made use of both water power and biomass (e.g. in the form of wood) as renewable sources of energy. Until the end of the eighteenth century, these were essentially the only available energy sources. It was not before early nineteenth century when coal became the dominant source of energy. With industrialisation, coal became an important raw material for the chemical industry, too. At the start of the twentieth century, natural gas and oil experienced growing economic impacts, both as energy and chemistry raw materials, which was complemented by nuclear energy in the 1950s.

Water power is a carbon–neutral energy source, as no CO_2 is produced through its use. However, today the technical and economic potential of harnessing water-power resources has been largely exhausted in Europe. For that reason, any further expansion of water power in that region appears to be economically unviable.

As already described in Sect. 3.2.2, biomass is produced photosynthetically from carbon dioxide and water in plants under irradiation of solar energy. Because plants need sufficient living space and, above all, water, biomass production on our planet is necessarily limited and can be further increased only at the expense of considerable ecological disadvantages. Moreover, the increasing global population significantly increases the pressure to utilise biomass, preferably in foodstuffs production rather than as a raw material (the latter should account for only a small portion of use). Biomass is in fact neutral with regard to the carbon cycle, because the carbon dioxide produced by biomass combustion is reintegrated through photosynthesis. However, a significant increase in biomass production is not feasible for the reasons outlined here (e.g. cultivation areas, water).

3.3.2 Direct Utilisation of Sunlight: Solar Thermal Energy, Photovoltaics

For the purpose of energy recovery on a global scale, solar thermal plants are assumed to gain great significance, provided the location is optimal. In India, China and the United States, solar thermal plants with a capacity of 2,000–3,000 MW are currently under construction. For comparison, typical nuclear power plant capacities range between 1,000 and 1,500 MW. Thus, solar thermal plants are essentially suitable substitutes for nuclear power plants. As a consequence, this would also affect energy recovery from carbon-based raw materials—the use of the latter would decrease in favour of rather reasonable uses, such as foodstuff production or synthesis of chemical and pharmaceutical products.

3.3.3 Wind Energy

When compared with other regions on earth, Germany and Europe in general are more suitable sites for wind energy recovery than for photovoltaic and solar thermal energy. This holds particularly true for the North Sea and Baltic Sea coastal regions, as well as the Atlantic coast. The current contribution of wind energy to energy recovery from renewable sources in Germany currently exceeds that of photovoltaic production by a factor of ten. In particular, installation and extension of off-shore wind parks are planned on a large scale. At the middle of 2013, the total installed wind energy park capacity in Germany alone amounted to more than 32,500 MW [7].

As a matter of course, wind power station efficiencies are less than 100 %. Only a few years ago, it was assumed that seven to eight times the corresponding base load energy was required for wind power stations. However, in practice, off-shore wind parks in England, the United States and China have shown that only 2.2–2.5 times the base load energy is required. Wind energy therefore also contributes to saving and more reasonably using valuable carbon-based input materials.

3.4 Hydrogen as a Source of Energy

Current developments indicate that enormous amounts of electricity could be generated in the foreseeable future by solar thermal plants in the "sun belt" of the Earth, as well as by off-shore wind parks in wind-rich regions. Nevertheless, as a rule, these would find no use on the spot. Major problems are associated with the storage and transport of the quantities of electricity produced between sun and wind. For example, there are large-scale solar thermal plants planned within the Desertec Project [8] in North Africa. The so-called Sahara power could supply enormous amounts of electricity. However, its transport to consumers in the industrial centres of Europe would require a gigantic power line network to be installed. Apart from the tremendous costs and the installation time for this electric power network, companies should expect to face massive protests by the population affected. To a lesser extent, due to shorter distances, this holds true also for the off-shore wind parks in the North and the Baltic Sea.

One solution is to convert the electric energy generated in solar thermal plants and wind parks to chemical energy, which can be easily stored and transported. Possible courses of action include the production of hydrogen and, using CO_2, the production of methane—in particular methanol, which as liquid has the advantage of easily being transported and stored. Especially recently, a number of investigations have been conducted toward the development of catalysts that allow for the direct photocatalytic cleavage of water into hydrogen and oxygen [9]. Even though promising results have been reported, it is unrealistic to assume that large-scale hydrogen production using this process will be realistic in the short to medium term.

One of the oldest and most important processes for the production of hydrogen is water electrolysis:

$$2H_2O \xrightarrow[\text{[catalyst]}]{\text{electric energy}} 2H_2\,(\text{cathode}) + O_2\,(\text{anode})$$

Electrolysis

For large-scale applications of water electrolysis, it is necessary to have high efficiencies and the option to run the processes discontinuously in order to have them function as a "buffer system." Particularly for wind parks, this concept is of utmost importance because the production of wind energy is subject to huge fluctuations, while the production of electricity needs synchronisation with consumer demand. For economic reasons, surplus electricity that cannot be supplied to the network at normal costs should preferably be used for electrolysis.

Water electrolysis is an established and widely used technology for the production of hydrogen. The electrolytic process is typically conducted in an acidic medium. Worldwide, there are research initiatives intensively investigating the possibilities for optimising water electrolysis. In Germany, this is done within the special research area "Hydrogen as an Energy Source" [10] or the HYSOLAR Project (Solar Hydrogen Energy) at the German Aerospace Centre. Particular attention was paid to applications of this technique in connection with renewable energy sources. Three particularly promising process variants were identified, which differ in their levels of development and their development potentials (Personal communication by Horst Friedrich, DLR, Stuttgart):

1. **Alkaline electrolysis (AEL)** is a fully developed technology that has been implemented in large-scale installations up to 156 MW power (Aswan dam). Useful operating lives of more than 20 years have been demonstrated.
2. **Polymer electrolysis (PEMEL)** is less advanced in its development, but it allows higher-power densities and is characterised by its overload capability.
3. **High-temperature electrolysis** with oxide ceramic technology **(HTEL)** is the least developed of the three process variants, but it shows the highest efficiencies.

In consideration of the constraints imposed by the timeframe for replacing nuclear energy by renewable sources of energy, the fully developed and well-tested AEL will undoubtedly play a special role in this context. Intensive work towards optimising the AEL process is in progress, aiming for instance at a significant improvement in the power density from 600 to 800 mA/cm^2. For these purposes, the catalytic properties of the electrode and the designs of electrode and separators are under investigation, as are the impact of higher pressures and temperatures. Under optimised conditions, a voltage efficiency of up to 87 % can be achieved with AEL. The Faraday efficiency of AEL is assumed to be in the range of 95–98 % [11].

Consequently an important initial step in the transformation of electric energy to chemical energy by the electrolysis of water could be implemented, virtually in the short term and on a large scale. Hydrogen contains a high level of energy, is chemically stable, and may therefore be stored for an indefinite period. As with natural gas, it can be transported via gas pipelines or in appropriate vehicles. Contrary to widespread opinion, the explosion behaviour of hydrogen (oxyhydrogen reaction) is far less dangerous than that of natural gas (mine gas explosion). The primary goal is the direct utilisation of hydrogen as a physical energy source. However, an extensive discussion of hydrogen recovery from nonfossil sources is beyond the scope of this chapter; see Sects. 4.5.2 and 4.5.3.

3.5 Hydrogenation of Carbon Dioxide [2, 12]

Coming from Asinger's introductory quote, according to which only the hydrogen price renders methanol synthesis by hydrogenation of carbon dioxide economically unattractive, the situation today is entirely opposite that of 1986. Independently performed calculations indicate a price of less than 3 EUR/kg for wind hydrogen, whereas the current price for fossil hydrogen is approximately 8–9 EUR/kg. This change in the price situation for hydrogen is owed to the availability of wind energy. However, evidently so little awareness exists that there is virtually no technical application using wind hydrogen (e.g. for CO_2 hydrogenation) that has been conceived for the general public. One step in this direction, which is currently being realised on a pilot scale, is the solar fuel concept, in which CO_2 is hydrogenated to give methane [12].

Depending on the degree of hydrogenation of CO_2, a distinction is made between three process types: (1) complete hydrogenation producing methane; (2) partial hydrogenation to methanol, including the direct utilisation of which and further conversion to other hydrocarbons, particularly fuels and olefins (see Chap. 6 and Sect. 6.4); and (3) a combination of hydrogenation and C–C linkage to fuels (Fischer–Tropsch synthesis) [13, 14].

Until the beginning of the twentieth century, methanol was primarily produced by dry distillation of wood. In the 1920s, BASF developed the industrial production of methanol on the basis of a synthesis gas (CO and H_2) derived from coal. In the 1950s, natural gas increasingly replaced coal in synthesis gas production because the energy expenditure was more favourable and the product gas was less contaminated. Section 4.3.1. deals with this subject in more detail.

In addition, the direct catalytic hydrogenation of CO_2 to methanol has been known for more than 80 years and has been used, for instance, for purposes of eliminating CO_2 from product mixtures in chemical processes. More recent developments primarily aim to use CO_2 as a carbon source, for which reason efforts to optimise the catalyst system are being undertaken (see Sect. 4.8).

3.6 Prospects for a "Technical Photosynthesis"

People may have expectations about the outcome of global warming, as experienced in recent decades by life on Earth, that are different and less pessimistic than the scenarios given by climate researchers and media. However, climate changes have taken place during the last millennium. There have always been principal climatic fluctuations on the Earth, leading to both ice age and tropical climate in central Europe. For example, the warm period of the early middle ages was followed by a relatively short ice age in the sixteenth and seventeenth centuries. An attribution of these changes to solar cycles alone cannot be excluded. However, what has considerably changed on Earth, irrespective of climate change discussions, is the balance of the carbon cycle.

There has been a dramatic increase in global population during recent decade. As a result, increasing demands of mankind in terms of energy consumption for heating, air conditioning and mobility cannot be satisfied by natural resources (water power, renewable resources). Since the middle of the 19th century, the fossil carbon reserves formed on Earth during millions of years (coal, crude oil and natural gas) are being increasingly consumed. The enormous amounts of carbon dioxide released from combustion processes can be compensated only in part by photosynthesis within the scope of the carbon cycle. Every year, the atmosphere and the oceans are confronted with more than 20 billion tonnes of CO_2 that can no longer be fully processed by the natural carbon cycle. Apart from global warming, the increased CO_2 concentration will inevitably affect floral development, for which CO_2 serves as most important carbon source.

In the long run, however, the global depletion of carbon reserves appears to be a more serious issue of concern than increasing CO_2 concentration. Mankind's thirst for energy continues to grow steadily, with the consequence of coal, crude oil and natural gas deposits being depleted faster than one can imagine today. In the short term, factors such as increasing CO_2 concentrations and the dramatic depletion of global carbon reserves urgently require technical solutions in order to counteract these developments and correct the carbon cycle.

With existing technologies that have been proven and tested on the large scale, it would be possible to realise a "technical photosynthesis" that is capable of correcting the imbalance of the carbon cycle, thus complementing natural photosynthesis. Climate-effective carbon dioxide would be consumed and energy-rich organic compounds, such as methanol, would be obtained.

The "technical photosynthesis" concept

$$6H_2O + \text{electric energy (wind, solar energy)} \xrightarrow{\text{electrolysis}} 2H_2\ (\text{cathode}) + O_2\ (\text{anode})$$

$$6CO_2 + 6H_2 \xrightarrow[\text{"wind hydrogen"}]{\text{hydrogenation}} 2CH_3OH + 2H_2O$$

$$6CO_2 + 4H_2O + \text{electric energy} \longrightarrow 2CH_3OH + O_2$$

Similar to photosynthesis in plants where carbohydrates and oxygen are produced, a technical photosynthesis would furnish methanol and oxygen as products from adding energy to CO_2 and water. The concept is easily conceivable by the summation of both partial steps. The crucial difference compared with "natural" photosynthesis is that energy-rich hydrogen (not water) reacts with CO_2 in technical photosynthesis. In natural photosynthesis, electron transfer reactions make water splitting reactions redundant. Instead, water directly serves as the hydrogen source. Currently, in a number of research institutes around the world, another variant is being investigated: "artificial photosynthesis"—that is, photocatalytic cleavage of water into hydrogen and oxygen with solar energy over suitable catalysts [9]. In fact, if attempts to conduct photocatalytic water cleavage in the presence of CO_2 would succeed in an in situ hydrogenation of CO_2, one would justifiably speak of "artificial photosynthesis."

For technical photosynthesis, a renewable form of energy (wind, solar thermal energy, photovoltaics, etc.) will be used for the production of hydrogen by means of electrolysis in the first step. In a subsequent second step, this hydrogen is used for the hydrogenation of carbon dioxide. Whether future attempts for a direct electrochemical reduction of carbon dioxide in the presence of water with electricity produced from a renewable energy source will prove successful is unclear [2]. This option would be closer to natural photosynthesis, but it would use a primary source of electrical energy as in conventional electrolysis.

It is not difficult to foresee that the energy issue will be governing future political and economic developments and decisions. Competition for energy resources will intensify and be reflected in rising costs for energy. Global differences between regions that are rich in energy resources and those that are less fortunate will soon make themselves felt economically. For instance, Europe is not a region that is blessed with abundant sources of energy; therefore, the development of technologies based on renewable energy sources on an industrial scale is a vital concern.

Photovoltaics will not be capable of significantly contributing to solving the energy problem in Central Europe. Nevertheless, photovoltaics can considerably

contribute to curbing energy demand in decentralised energy supplies (air conditioning, electromobility, etc.).

In Central and Northern Europe, by far the most significant contribution to regenerative energy supply will be made by wind turbines. Apart from the necessary expansion of the power grids, storage of the electrical energy form of chemical energy (as done with hydrogen, methane, or methanol) is indispensable. "Technical photosynthesis" is of particular importance here because this concept can convert electrical energy from wind turbines into methanol, dimethyl ether, or other hydrocarbons—that is, liquids suitable for use in combustion engines (power to liquid). Because methanol can also be employed both for the synthesis of innumerable major chemical products and for the production of fuels, it is an ideal chemical storage medium for electrical energy from wind turbines, photovoltaics and solar thermal energy.

The vision of technical photosynthesis could be realised using existing technologies tested and proven for large-scale applications. The existing and planned wind turbines and wind farms will be capable of delivering sufficient amounts of electricity. Excess electricity that is not fed into the grids is recommended to be used near to the energy production sites (decentralised solution) for the electrolytic synthesis of hydrogen. Because hydrogen is stable, storable and transportable, it can be distributed by gas pipelines (or by other known means) to those power plants, where sufficient carbon dioxide is generated. In these locations, carbon dioxide is eventually converted with hydrogen to give methanol, methane, or fuels.

Methanol is the most versatile product for the conversion of CO_2 with hydrogen. As a hazard-free liquid, it can be handled without any difficulty. It can directly be used as fuel for combustion engines and fuel cells and can easily be made available in existing filling station networks. Dimethyl ether, which is easily obtained from methanol, is becoming increasingly important as a diesel fuel. Last but not least, methanol can be utilised in lieu of synthesis gas for the production of fuels or fuel additives according to the processes described in Sects. 6.2 and 6.3. The visionary methanol economy proposed by Friedrich Asinger and George A. Olah could soon become reality, making a most significant contribution toward correcting the imbalanced carbon cycle.

References

1. F. Asinger, *Methanol - Chemie- und Energierohstoff* (Springer Verlag, Heidelberg, 1986)
2. G.A. Olah, A. Goeppert, G.K. Surya Prakasch, J. Org. Chem. **74**, 487–498 (2009)
3. C. Schmidt, The fate of spilled oil in the gulf rests with the hydrocarbon-digesting microorganisms colonizing underwatewr plumes. Chem.Eng.News **88**(31), 32 (2010)
4. F.X. Effenberger, *Der Kohlenstoffkreislauf*, Commemorative Colloquium, University of Stuttgart, 23 April 2010
5. M. Bertau, F.X. Effenberger, W. Keim, G. Menges, H. Offermanns, Chem. Ing. Tech. **82**, 2055–2057 (2010)
6. W. Fritsche, Biologie in unserer Zeit (BiUZ) **38**, 390–399 (2008)

7. Frankfurter Allgemeine Zeitung, 29 December 2013
8. Frankfurter Allgemeine Zeitung, 21 June 2009
9. T.S. Teets, D.G. Nocera, Chem. Comm. **47**, 9268–9274 (2011)
10. Final report of Special Research Project 270, *Hydrogen as a Source of Energy*, University of Stuttgart, **1998**
11. K. A. Friedrich, Personal communication
12. http://www.solar-fuel.net/. 22 May 2013
13. R. Schlögl, Angew. Chem. **123**, 6550–6553 (2011)
14. R. Schlögl, Angew. Chem. Ed. Engl. **50**, 6424–6426 (2011)

Chapter 4
Methanol Generation

Hans-Jürgen Wernicke, Ludolf Plass and Friedrich Schmidt

Introduction

Hans-Jürgen Wernicke

Methanol can be generated from a wide range of carbon and hydrogen sources. Currently, large-scale production is dominated by the conversion of fossil resources, mainly natural gas and coal, to carbon monoxide and hydrogen (synthesis gas) as the intermediate for catalytic methanol synthesis. Although they are not yet economically competitive, more ecologically friendly processes have been attempted using regenerative carbon and hydrogen sources such as biomass, (recycled) CO_2 and hydrogen from electrolysis using regenerative power sources.

Almost 60 million tonnes of methanol are presently being produced. Methanol today is the most important single building block for chemicals and fuel components. To promote and gradually realise the vision of a "methanol economy" as proposed by Olah (1994 Nobel laureate in Chemistry) [1] and his coworkers, novel process routes to produce methanol are indispensable to stepwise replace the use of conventional and unconventional fossil raw materials by regenerative sources.

Sections 4.2–4.8 discuss state-of-the art industrial processes. Some examples of unconventional routes to methanol are mentioned here, with reference to more detailed literature. However, the boundary conditions of most of these examples concerning yields, selectivity, reaction conditions and in some cases

H.-J. Wernicke (✉)
Kardinal-Wendel-Straße 75 a, 82515 Wolfratshausen, Germany
e-mail: h.j.wernicke@t-online.de

L. Plass
Parkstraße 11, 61476 Kronberg, Germany
e-mail: dr.ludolf.plass@t-online.de

F. Schmidt
Angerbachstrasse 28 83024 Rosenheim, Germany
e-mail: fs-ro@gmx.de

M. Bertau et al. (eds.), *Methanol: The Basic Chemical and Energy Feedstock of the Future*,
DOI: 10.1007/978-3-642-39709-7_4,

environmental constraints have not (yet) led to a scale up to economically feasible industrial processes:

(a) Selective oxidation of methane in gas or liquid phase [2]:

$$CH_4 + {}^1\!/_2 O_2 \rightarrow CH_3OH$$

- Via halogenation:

$$CH_4 + Br_2 \rightarrow CH_3Br + HBr$$

$$CH_3Br + H_2O \rightarrow CH_3OH + HBr$$

$$\underline{2HBr + {}^1\!/_2 O_2 \rightarrow Br_2 + H_2O}$$

$$CH_4 + {}^1\!/_2 O_2 \rightarrow CH_3OH$$

- Via methyl bisulphate in the presence of homogeneous catalysts (dissolved Hg- and other salts) [3]:

$$CH_4 + 2H_2SO_4 \rightarrow CH_3OSO_3H + 2H_2O + SO_2$$

$$CH_3OSO_3H + H_2O \rightarrow CH_3OH + H_2SO_4$$

$$\underline{SO_2 + {}^1\!/_2 O_2 + H_2O \rightarrow H_2SO_4}$$

$$CH_4 + {}^1\!/_2 O_2 \rightarrow CH_3OH$$

- As above, but in the presence of a solid Pt-covalent triazine framework (CTF) catalyst [4]

(b) From methane by high-temperature pyrolysis to hydrogen [5–8] followed by CO_2 hydrogenation:

$$3CH_4 \rightarrow 3C + 6H_2$$

$$\underline{2CO_2 + 6H_2 \rightarrow 2CH_3OH + 2H_2O}$$

$$3CH_4 + 2CO_2 \rightarrow 2CH_3OH + 2H_2O + 3C$$

(c) Enzymatically from methane by methane-monooxygenase [9, 10]:

$$NADH + CH_4 + O_2 \rightarrow NAD^+ + CH_3OH + H_2O$$

(d) From synthesis gas generated by the "Hynol" process [11]:
Hydropyrolysis of a carbonaceous feedstock (biomass) into

- A methane-rich synthesis gas followed by
- Methane steam reforming and methanol synthesis with
- Recycling of excess hydrogen to the hydropyrolysis stage

(e) By co-electrolysis of CO_2 and water into synthesis gas [12,13]
(f) By steam reforming [14, 15] or direct hydrogenation [16, 17] of glycerol (as biodiesel byproduct)

Sections 4.2–4.8 concentrate on the dominating process sequence for generating synthesis gas from various carbon sources (and water), its conditioning and conversion into methanol. The carbon sources to produce methanol can be manifold. If fossil raw materials, they usually are natural gas, crude residual oil (crude resid), coal, or "unconventional" hydrocarbons such as shale gas or synthetic crude oil (syncrude). Gasification processes also allow the use of biomass, such as wood, straw, or waste and sludge. A special case is the separation and hydrogenation of CO_2 to methanol with hydrogen from nonfossil sources.

Section 4.1 provides an overview of the types and availability of raw materials from fossil and nonfossil sources. Sections 4.3 and 4.4 contain the various schemes to generate and condition synthesis gas via steam reforming, partial oxidation (POX) and gasification. Section 4.5 describes special situations of CO_2 separation (e.g. from flue gases) and hydrogenation to methanol. This is only meaningful if hydrogen from regenerative or any other source of nonpurpose hydrogen production is being used. Section 4.5 also summarises all potential sources of hydrogen and focuses on water-splitting technologies that use regenerative power. Section 4.6 deals with the general principles of methanol catalysis. The properties and application of industrial methanol catalysts are described in Sect. 4.7, including the various large-scale methanol production processes based on synthesis gas. Section 4.8 deals with the special case of CO_2 hydrogenation to methanol.

4.1 Raw Materials for Methanol Production

Hans Jürgen Wernicke[1], Ludolf Plass[2] and Wladimir Reschetilowski[3]

[1]*Kardinal-Wendel-Straße 75 a, 82515 Wolfratshausen, Germany*
[2]*Parkstraße 11, 61476 Kronberg, Germany*
[3]*Institute of Chemical Technology, Dresden University of Technology, 01062 Dresden, Germany*

Economical methanol synthesis requires cheap synthesis gas, which can be produced from a variety of feedstocks such as coal, lignite, natural gas, shale gas, oil, oil refinery residues (vacuum residues or petroleum coke), as well as from renewable resources such as wood, wood and agricultural residues, biogas and waste (see Sects. 4.1.1 and 4.1.2). When CO_2 is used, the required hydrogen can be produced by a variety of technologies (see Sects. 4.5.2 and 4.5.3).

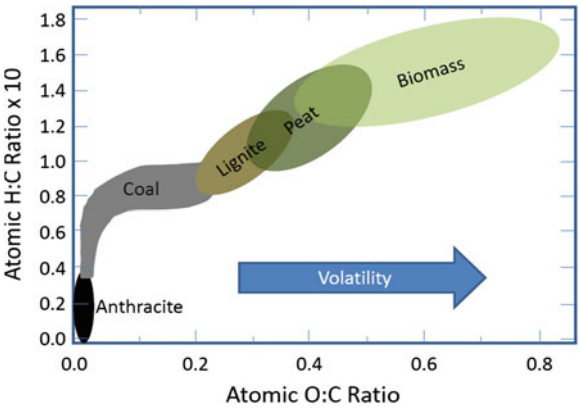

Fig. 4.1 Atomic ratio of solid fossil fuels against the oxygen content

The costs of these different feedstocks vary substantially according to quality, availability, cost of mining/preparation and transport. In addition, taxation issues according to different CO_2 production rates in the synthesis gas (syngas) process as well as government regulations for the use of renewable resources can—depending on the location of the plant—play an important role for the economics of the methanol production.

Chapter 7 describes the different influences of plant size, plant location and cost of feedstock in more detail. The different syngas generation processes vary according to the different feedstocks, and the requirements of the reforming or gasification technologies as will be outlined in more detail in Sects. 4.3 and 4.4. As illustrated in Fig. 4.1, the hydrogen and the oxygen contents of solid fossil fuels play an important role for the selection of feedstock preparation and gasification technology. Per tonne of methanol, approximately 1.5 t of bituminous coal (29,300 kJ/kg), 5.4 t of lignite (8,000 kJ/kg), 3 t of wood (15,500 kJ/kg) or 1,120 Nm^3 of natural gas (31,600 kJ/Nm^3) are required in terms of higher heating value (HHV).

"Associated gas" from crude oil production is used for methanol and chemical production in the Middle East. Plans to do the same in Russia (also from depleted oil and gas wells) have so far not materialised. The use of mixtures of coal and waste for methanol and power production has been demonstrated at the Sekundär-Rohstoff-Verwertungszentrum in Germany (see Sect. 4.4). Developments to place a MegaMethanol plant (see Sect. 4.7.3) on a ship to make use of associated gases from oil drilling platforms had been far advanced in the pre-engineering stage but was stopped because of the economic crisis in 2008.

The production of methanol and other chemicals from biomass has been especially studied at different places and plants that are in operation or under construction in Brazil [18] and Sweden. A methanol plant in the Netherlands was built in the 1970s and was originally based on natural gas. It shut down in 2005 but was reopened in 2008 by the Company BioMCM, Delfzijl/NL and converted to use raw glycerine as feedstock to produce "green methanol," essentially as a green blending component to gasoline. The "double counting" for biofuels of the second

generation makes it economically attractive to switch—at least partially—to renewable feedstocks.

Looking into the future, it seems that the combination of different feedstocks will play an increasingly important role for the production of fuel, chemicals and energy.

4.1.1 Fossil Raw Materials

Conventional raw materials for the production of methanol range from natural gas to coal. However, there is a major evolution towards the increased use of non-conventional and renewable sources of hydrocarbons. This chapter puts major emphasis on the techniques and scenarios to produce and use nonconventional and renewable sources.

Concerning the future availability of hydrocarbon feedstocks, one has to differentiate between the following:

- The initial *reserves* as the sum of cumulated production and proven reserves
- Potential availability of proven and assumed reserves as future potential *resources*.

Specifically, the resources of unconventional hydrocarbons compared to reserves and resources of conventional hydrocarbons are not definitely established; only rough estimates exist. It appears that these resources could easily exceed known reserves of conventional feedstocks (see Table 4.1) [19].

Natural Gas/Nonconventional Gas

Apart from dominating energy use, natural gas is the second most important feedstock (next to crude oil) for major chemical building blocks such as methanol, ammonia, hydrogen and their derivatives. Other industrial uses are in pulp and paper, iron and steel, ceramics and food processing.

In recent years, the production and use of natural gas has been more and more supplemented by increasing exploration and use of unconventional gas and other unconventional hydrocarbons, specifically of shale gas, tight gas, coal-bed methane, "deep deposits" of natural gas and also oil shales. Figure 4.2 schematically shows the sourcing of conventional and unconventional natural gas, which—apart from its energy use—is the hydrogen-richest and easiest-to-process raw material for methanol and other chemical building blocks.

Natural Gas

The reserves-to-production (R/P) ratio of natural gas worldwide is estimated at about 64 years, with the Middle East and Eurasian regions having the largest known reserves. The statistics also show a decline of R/P ratio over the last 30 years, which has not (yet) been compensated for by the increased exploration and production of nonconventional reserves and resources. Over the years, the known absolute reserves have increased substantially through explorations and

Table 4.1 Reserves and resources of conventional and nonconventional fuels concerning conventional and nonconventional gas production, reserves and resources [19]

Fuel	Units	Reserves (cf. left column)	EJ	Resources (cf. left column)	EJ
Conventional Crude Oil	Gt	168	7,014	159	6,637
Conventional Natural Gas	Tcm	191	7,240	307	11,671
Conventional Hydrocarbons [Total]	Gtoe	341	14,254	438	18,308
Oil Sand	Gt	27	1,120	63	2,613
Extra Heavy Oil	Gt	21	886	61	2,541
Tight-/Shale Oil	Gt	< 0.5	11	87	3,636
Oil Shale	Gt	–	–	97	4,068
Non-Conventional Oil [Total]	Gtoe	*48*	*2,018*	308	12,858
Shale Gas	Tcm	2.8 [5]	105 [5]	157	5,984
Tight Gas	Tcm	– [6]	– [6]	63	2,397
Coalbed Methane	Tcm	1.8	70	50	1,886
Aquifer Gas	Tcm	–	–	24	912
Gas Hydrates	Tcm	–	–	184	6,992
Non-Conventional Gas [Total]	Tcm	4.6	175	478	18,171
Non-Conventional Hydrocarbons [Total]	Gtoe	52	2,193	742	31,029
Hydrocarbons [Total]	Gtoe	393	16,446	1,180	49,337
Hard Coal	Gtce	638	18,692	14,486	424,553
Lignite	Gtce	111	3,260	1,684	49,340
Coal [Total]	Gtce	749	21,952	16,169	473,893
Fossil Fuels [Total]	-	-	38,398	-	523,230
Uranium [1]	Mt	2.1 [2]	1,061 [2]	13 [3]	6,254 [3]
Thorium [4]	Mt	–	–	5.2	2,606
Nuclear Fuels [Total]	–	–	1,061	–	8,860
Non-Renewable Fuels [Total]	–	–	39,459	–	532,090

– no reserves or resources

1) 1 t U = 14 000 – 23 000 toe, lower value used or 1 t U = 0.5 x 10^{15} J
2) RAR recoverable up to USD80/kg U
3) Total from RAR exploitable from 80-260 USD/kg U, and IR and undiscovered <260 USD/kg U
4) 1 t Thorium assumed to have the same toe-value as for 1 t U
5) only United States (Status: 2010)
6) included in conventional natural gas reserves

reassessment of new gas fields, responding to the heavy increase of world gas consumption (see Figs. 4.3, 4.4) [21].

Nonconventional Gas

The exploration and use of nonconventional gas is most advanced in the United States. Projections in Fig. 4.5 show a steep increase of shale and other unconventional gas production in the coming years, which has already overtaken the production of conventional gas.

The most important nonconventional natural gases are shale gas, tight gas and coal-bed methane. *Shale gas* is contained in a grained sedimentary rock, which is broken up to release the gas from its pores by so-called fracturing. This is done by

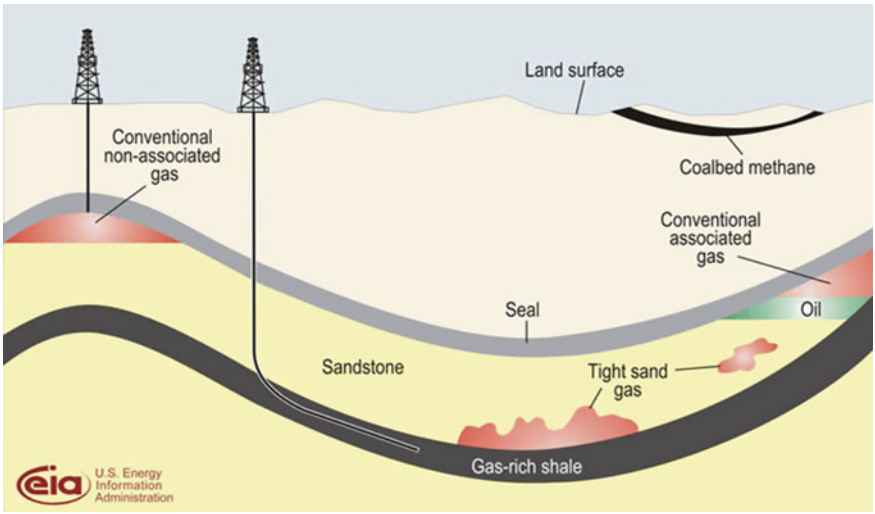

Fig. 4.2 Schematic geology of natural gas resources [20]

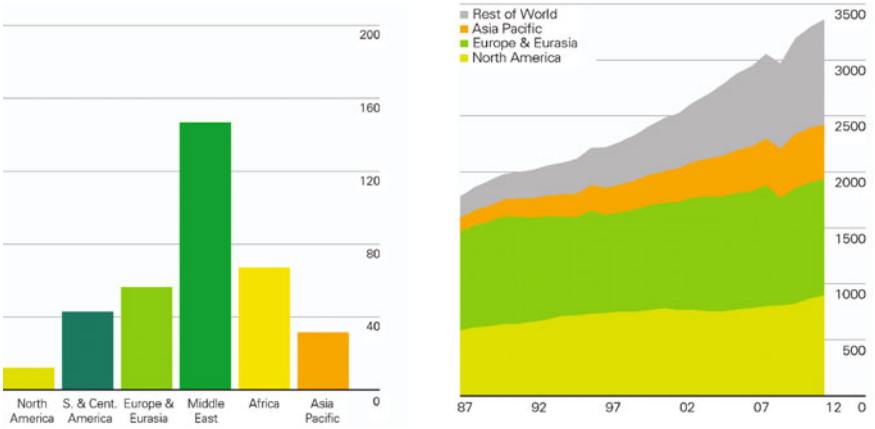

Fig. 4.3 Static Gas Reserves-to-Production (R/P) Ratios 2012 (years) and Gas Production (billion cubic metres) 1987–2012 by region [21]

injection of a mix of water, certain chemicals and sand as a spacer to keep the gas-releasing fissures open. The principle of hydraulic fracturing is shown in Fig. 4.6.

The reserves and potential resources of shale gas (and oil) are spread over 48 U.S. states, as shown in Fig. 4.7 [24]. This has led to oversupply situations in the recent years, with a reorientation from imports to even future exports accompanied

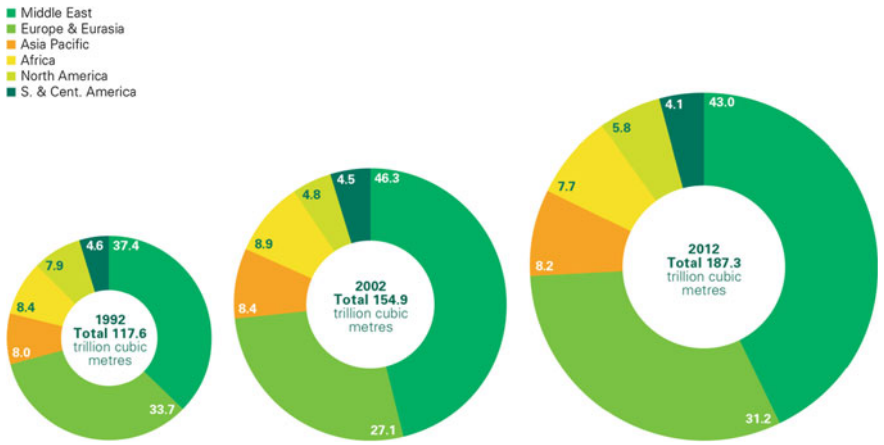

Fig. 4.4 Increase and geographical distribution of proven natural gas reserves (in %) [21]

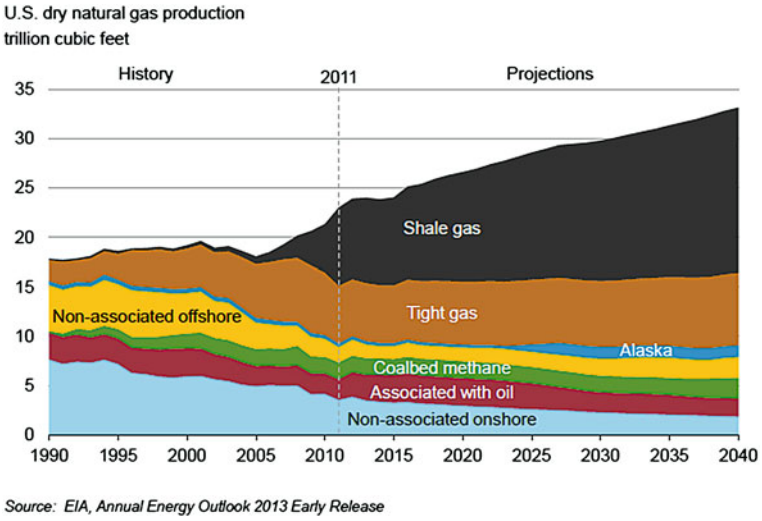

Fig. 4.5 Gas production in the United States [22]

by a significant decline of gas prices in the United States compared to other world regions (see Fig. 4.8).

So-called *tight gas* is natural gas that is contained in less permeable, nonporous hard rock, limestone, or sandstone formations. As with shale gas, several

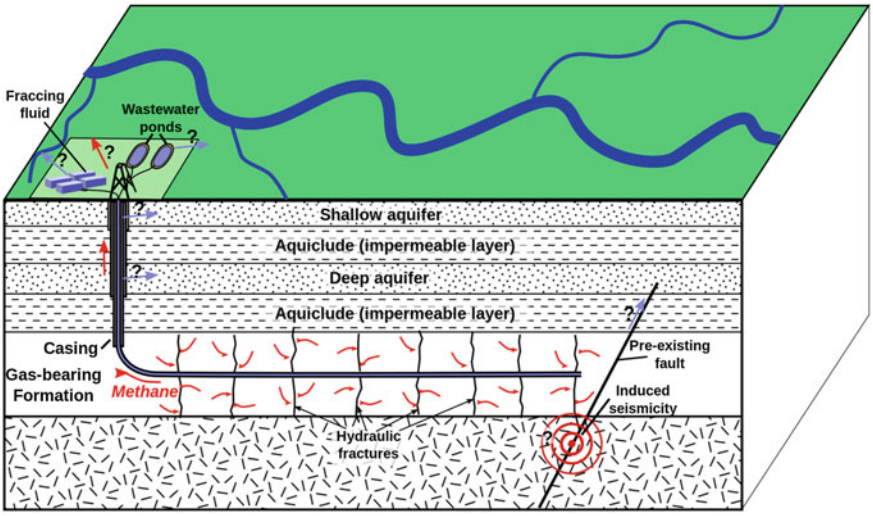

Fig. 4.6 Principle of gas fracturing [23]

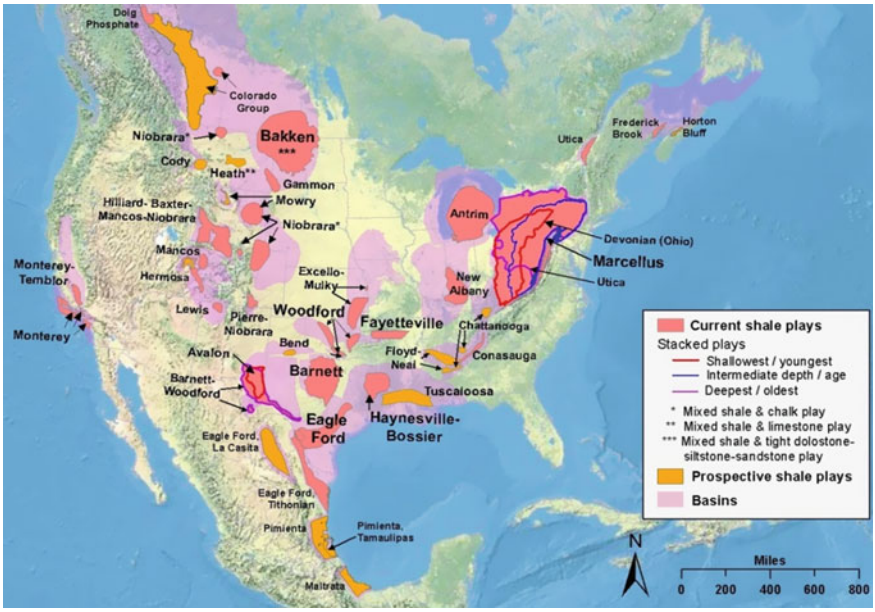

Fig. 4.7 Shale oil and shale gas distribution in North America [24]

techniques to extract tight gas from rock can be applied, such as fracturing and the use of rock-dissolving chemicals. Many of these techniques are under debate concerning long-term environmental impacts.

Fig. 4.8 Development of natural gas prices by region in US-$/MMBtu (until 2012) [25]

In connection with coal mining, *coal-bed methane* so far has been an unwanted byproduct and safety thread. Instead of releasing it to the atmosphere, the collection of coal bed methane has become a significant contributor to the gas network in the United States and other coal mining regions.

Compared with conventional natural gas, the composition of nonconventional gas varies. The content of C_{2+} hydrocarbons, sulphur and other components besides the main component methane are wide ranging. The use of unconventional gas as chemical feedstock requires the same cleaning and conversion steps as used for conventional "dry" and "wet" (i.e., higher hydrocarbon-containing) natural gas, as discussed in Sect. 4.3.

The low gas prices and often high content of C_{2+} hydrocarbons will initiate new capacities in the coming years for conversion into synthesis gas by steam reforming or POX, as well as the use of the C_{2+} fraction for olefins production by steamcracking. According to the International Energy Agency (IEA) [26], the United States will have the largest reserves worldwide and become the largest hydrocarbon-producing country in the world in 2017, pushing Saudi Arabia into the second position. By 2015, the United States will be ahead of Russia and also become the largest natural/shale gas producer worldwide; it will become independent from any fossil energy imports by 2035. According to the IEA, these reserves can provide energy independence for the United States for the next 100 years.

Despite all environmental concerns in connection with climate change and with the production techniques used to collect unconventional gas, its generation and use will expand from North America mainly into the Asian regions, where vast resources are assumed.

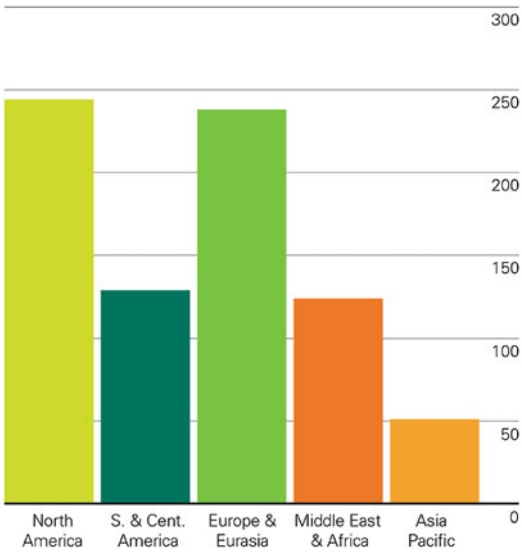

Fig. 4.9 Reserves-to-production ratio of coal by region in years (2012) [27]

Coal

Increasing crude oil prices, geopolitical aspects and large regional, easily accessible reserves will not only lead to more use of natural gas but also to a renaissance of coal conversion processes to produce chemical building blocks. The biggest growth of coal production and consumption for fuels and chemicals took place first in South Africa and then in China, where in 2009 more than 75 % of about 40 million tonnes of methanol was based on coal.

Coal reserves are more evenly distributed over the globe, with a proven R/P ratio of 109 years on average in 2012 (see Fig. 4.9). Production is increasing mostly in Asia, particularly in China (see Fig. 4.10).

As already explained in the introduction, coal can only play a substantial role for the production of methanol either (a) if natural gas is scarce or very expensive or (b) if the coal is cheap and available in large quantities. This means in practical terms that only run-of-mine coal or lignite without or with minimum transport and upgrading costs is suitable as feedstock. Typical examples for such mine-mouth-based chemical plants are the Sasol plants in South Africa, the ANG plant in North Dakota, and large-scale chemical complexes in China. Because the composition and nature of coals are rather complex, the syngas production processes have to be precisely adapted to the characteristics of the coal, as outlined in Sect. 4.4.

High-quality coal, which is traded on a worldwide basis, is today priced in the range of $60–80 per tonne. Therefore, at current methanol prices, it is not

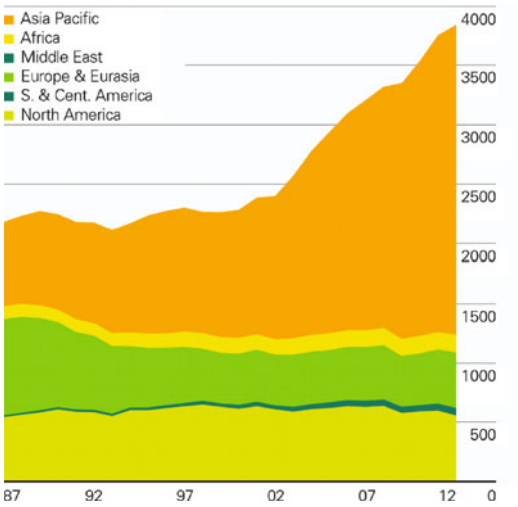

Fig. 4.10 Production of Coal 1987–2012 by region (Mio tonnes of oil equivalent) [27]

competitive if methanol is the only product. However, if the overall process scheme integrates syngas production with downstream production of power and chemicals such as methanol, then the economics are different and may also allow for the use of high-quality coal.

Heavy Oil and Oil Residues

High conversion rates in modern refineries generate substantial amounts of residues, such as vacuum residues and petroleum coke. The use of petroleum coke in power stations is becoming more and more difficult, especially because of the typically high sulphur contents in the coke. An alternative is the use as feedstock for chemicals via entrained flow (EF) gasification. More than 95 % of liquid material gasified consists of refinery residues [28]. POX at high temperatures (1,350–1,400 °C) and high pressures (30–80 bars) with O_2 produce a CO/H_2 syngas stream containing both gases with approximately the same volumetric quantities.

The noncatalytic process can accept a relatively broad spectrum of liquid feed. However, every feedstock needs to be evaluated carefully to meet the expected syngas requirements. EF-slagging gasifiers, designed for pulverised coal, have been successfully converted to petroleum coke. Because of the lower reactivity of the petroleum coke against coal, either the gasification temperature must be increased or the residence time prolonged (see Sect. 4.4). Also, ash must be added to produce enough liquid slag to protect cooled membrane wall reactors or to ensure a liquid slag in case of refractory-lined reactors.

4.1.2 Renewable Raw Materials

General aspects

Currently, mostly fossil raw materials are used for the production of methanol because the most important criteria are the cost of feedstock and its processing costs. For example, the synthesis gas production accounts for a large part (up to 60 %) of the investment of a methanol plant [29]. In the longer term, an increasing amount of methanol can be made from renewable and sustainable resources, including every kind of biomass, biogas, agricultural and timber waste, solid municipal waste and other feedstocks.

In principle, methanol can be produced from biomass in two different ways. "Dry" biomass (e.g. waste wood) can be gasified, producing a gas mixture that has to be conditioned in order to obtain a parent gas suitable for methanol synthesis [30]. A biogas that is rich in methane can be produced from "wet" biomass (e.g. biodegradable waste) by means of fermentation. Both gases have to be cleaned and conditioned before being suitable for methanol synthesis [31]. Pathways for the production of methanol from biomass are illustrated in Fig. 4.11.

The gasification of "dry" biomass produces a gas mixture mainly consisting of CO, CO_2, H_2, H_2O, CH_4 and higher hydrocarbons, as well as condensable aromatic compounds (tar). Such tar can condense at a temperature below 300–400 °C and will negatively affect the downstream processes. Furthermore, the obtained raw gas contains small amounts of contaminants such as dust, sulphur compounds, ammonia and halogens—some of which are poisonous to the methanol catalyst. In principle, the contaminants are the same as those found in the raw gas of coal gasifiers (see Sect. 4.4). A H_2/CO ratio slightly above 2 is desired for methanol synthesis, which requires further adjustment of the gas composition by means of scrubbing and shift conversion (see Sect. 4.4.8). Another possibility to adjust the H_2/CO ratio is the addition of hydrogen from other sources, such as water electrolysis (see Fig. 4.12).

This leads to a rough balance of a biomass input of 2 t/h (waste wood) and an energy input of approximately 5 MW_{el} to produce approximately 1.2 t/h of methanol [32]. The necessary separation of a large part of the CO_2 (more than 60 %), however, reduces the conversion of the biomass carbon into methanol further to approximately 45 %. The correlation between the rates of CO, CO_2 and hydrogen in the biomass-based synthesis gas and the methanol yield and selectivity was examined and described in detail by Yin et al. [33].

As described for natural gas feedstocks in Sect. 4.3, the production of methanol on the basis of biogas consisting mainly of methane, carbon dioxide, as well as some undesired components requires a complex purification and subsequent reforming and potential water gas shift conversion of the biogas. An undesired side reaction in the raw gas processing is the methanisation of CO_2, which consumes part of the generated hydrogen (Sabatier reaction):

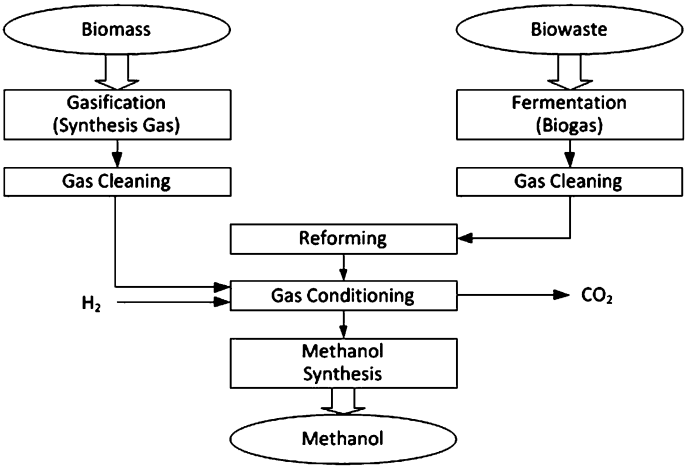

Fig. 4.11 Simplified schematic illustrating methanol production from biomass-based feedstocks

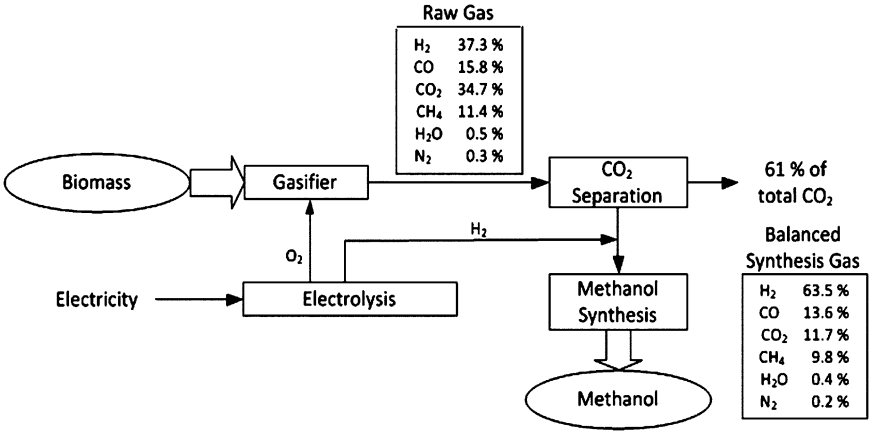

Fig. 4.12 Flow diagram for methanol synthesis from biomass, including hydrogen generation by electrolysis. Because there is still a hydrogen deficit, carbon dioxide has to be removed from the raw gas [32]

$$CH_4 + H_2O \leftrightarrows CO + 3H_2 \qquad \Delta_R H = 206\,\text{kJ/mol}$$

$$CO + H_2O \leftrightarrows CO_2 + H_2 \qquad \Delta_R H = -41\,\text{kJ/mol}$$

$$CO + H_2O \leftrightarrows CO_2 + H_2 \qquad \Delta_R H = -41\,\text{kJ/mol}$$

Excess CO_2 contents in the reformed biogas can be removed by scrubbing or by pressure swing adsorption (PSA). Lack of hydrogen in the synthesis gas may be corrected by hydrogen addition from external (regenerative) sources. Details of the methanol synthesis itself are described in Sects. 4.6 and 4.7.

Without any additional hydrogen and assuming a carbon dioxide separation efficiency of 95 %, the overall carbon-to-methanol conversion drops to about 20 %, with a methanol production of only 0.6 t/h based on a wood input of 2 t/h as a feedstock [34]. According to other reports, this procedure can produce 2 t of methanol (96 % pure) from 1,500 m^3 of biogas generated from 100 t of liquid sludge per day [35].

In newer facilities that use renewables for the production of methanol, the synthesis gas or biogas is mainly generated from organic residues. Such facilities also function as waste disposal facilities in that they fulfil an ecological task as well, which also changes the economic perspective [29].

Increasing production of methanol based on biological resources seems to be feasible, particularly because the individual process steps are for the most part known. Sound cost-benefit calculations for large industrial facilities are available as well.

Wood

Of all the types of biomass, wood appears to be attractive as a renewable raw material for chemicals, as in methanol production [36]. In 2005, the total volume of the accumulated wood from all forests in the entire world was estimated at 422 Gt by the Food and Agriculture Organization of the United Nations (FAO) [37]. Distribution of the world's forests is illustrated in Fig. 4.13. Every year, 3.2 billion m^3 of raw wood are cut—almost half of it in countries in the tropics. But with 2.3 m^3/ha, Western Europe presents the highest annual cutting rate. Almost 50 % of the global timber is used as firewood, particularly in countries in the tropics. However, power generation still remains the most important type of utilisation of wood. In Western Europe, firewood only accounts for almost a fifth of the wood cut. Wood is considered a renewable source of raw material and energy, provided that the volume used does not exceed the volume regrown. The fact that it is simple to process and accordingly requires little energy for production. However, logistics and processing of wood constitute other important factors in its ecologic assessment.

The wall of lignocellulosic plant cells typically consists of cellulosis (40–50 wt%), hemicellulosis (25–40 wt%), lignin (20–30 wt%), small amounts of so-called extractives (2–10 wt%) and some inorganic compounds (0.2–0.8 wt%) forming ash during combustion [38]. Fresh biomass contains up to 60–70 % water and must be dehumidified prior to gasification to reduce the water content to approximately 15 %. In order to constitute an economically attractive feedstock, it should cost only half as much as coal, calculated on the basis of the same heating value.

Table 4.2 indicates the composition and heating values of wood in comparison to hard and brown coal as well as peat on a dry, ash-free basis.

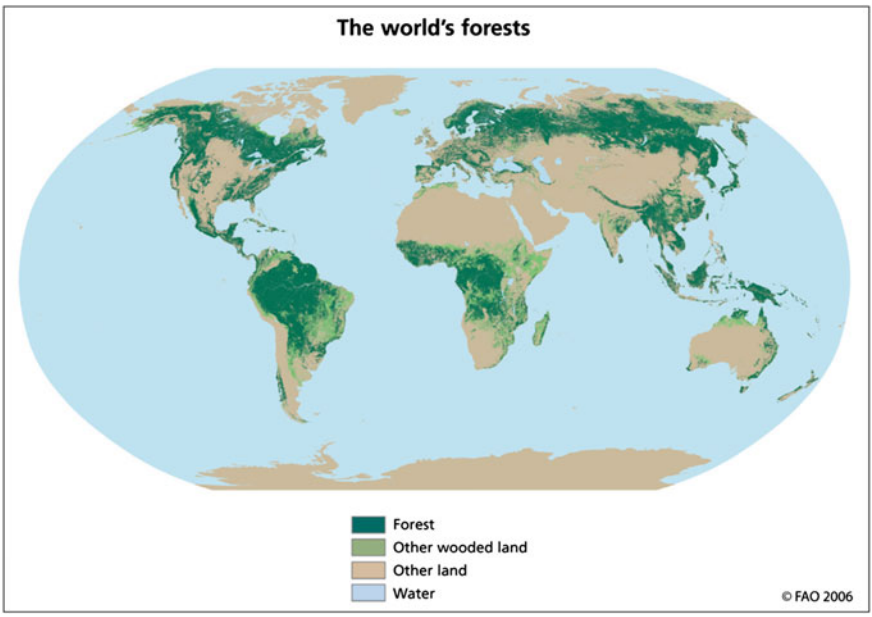

Fig. 4.13 Distribution of the world's forests, recorded by the Food and Agriculture Organization, 2006 [39]

Table 4.2 Comparison of the composition of completely dry hard coal, brown coal, peat and wood on an ash-free basis

Elemental composition, %	Hard coal	Brown coal	Peat	Wood
Carbon	79.5	66.6	56.9	49.5
Hydrogen	4.7	4.9	5.7	6.1
Oxygen	12.7	26.9	35.9	44.1
Nitrogen	1.4	1.2	1.3	0.3
Sulphur	1.7	0.4	0.2	0.02
Lower heating value, kJ/kg	31,100	25,500	21,800	18,400
Higher heating value, kJ/kg	32,100	26,600	23,000	19,700

Although coal mining and oil production hardly take up any surface area, the production of all kinds of biomass requires large areas and a suitable climate. This limits the use of such raw materials to those countries with a very large surface space and lack of oil, gas and coal resources.

Among all potential regenerative raw materials, methanol production based on wood is the most cost-efficient method. It is superior to every other process in terms of the total calorific efficiency, the expense for cultivation and harvesting, and the net yield per hectare. Wood is planted every 10–30 years, can be harvested and used throughout the entire year, and does not cause any environmental problems. Wood ash from the gasification process is conveniently returned to the

soil. This is possible due to its high melting point, so that it does not form slag in the gasifier (see Sect. 4.4).

Wood gasification and gasification of organic residues for the purpose of producing synthesis gas or gaseous fuels for heat and power generation has recently led to a growing number of research and demonstration projects. Wood from forests as well as agricultural lignocellulosic biomass is particularly suitable as feedstock. Lignocellulosic biomass primarily includes stalk material such as crop and corn straw as well as other residues from the agricultural cultivation of crops. In the future, this might be complemented by energy crops such as *Miscanthus giganteus* as well as poplar and willow wood cultivated on short-rotation plantations [40]. Compared to biomass containing starch or sugar, such as wheat, corn, sugar beets and sugar cane, the net yield of wood-based methanol is 1.5–2 times higher based on the same heating value.

Gasification of biomass has been tested up to the industrial scale in various reactors, but its use today in long-term operations is limited. The preparation and input of the feedstock as well as the monitoring of the ash behaviour constitute the greatest challenges. There is a great number of different versions in terms of the reaction engineering concerning gasification temperature, the type of biomass used, and its pretreatment. The various gasifier types are explained in detail in Sect. 4.4.

Examples of overall processes using biomass with high-temperature gasification in an entrained-flow reactor are Bioliq [41] and Chemrec [42]; examples of methods with gasification in a fluidised bed (FB) include allothermal gasification with a solid heat transfer medium in biomass power plant Güssing [43] and bubbling bed from Uhde, a ThyssenKrupp company [44]. Uhde has been selected as technology supplier and engineering partner by Värmlans Methanol for a biomass-to-methanol (BtM) plant with an annual production of 100,000 t of fuel-grade methanol from biomass (forest residue). The world's first full-scale BtM plant will be strategically located in the forest-rich province of Värmland, in Hagfors, Sweden. Fixed-bed reactors are not suitable for synthesis gas production due to the high amounts of byproducts formed and the critical scale-up. Several companies are working on the development of adapted syntheses for methanol or dimethyl ether, including Bioliq [45], BioDME [46] and TIGAS [47].

Particularly in the United States, work on the chemical processing of wood is stimulated by the fact that waste wood with a volume of more than 500 million tonnes (dry product) is generated every year. With regard to Brazil and the United States, many people believe that the global demand for fuel can be met with biomass, primarily wood. A number of companies have built or are building plants to prove biomass for methanol production technology. For example, Range Fuels (USA) is currently building a plant in Georgia to convert wood waste into syngas and then into a mixture of methanol and ethanol. Chemrec (USA) plans to build a plant in Michigan to convert black liquor into methanol and dimethyl ether. Methanex (Canada) has a joint development agreement with a Brazilian company to evaluate the conversion of sugar cane bagasse, tops and leaves into methanol [48].

This is certainly not applicable for Europe. The countries with the greatest percentage of forest in Europe are Finland, Slovenia, Sweden and, some distance

behind, Austria. The largest forest surface areas (absolute values) are located in Sweden (approximately 28 million hectares), Finland, Spain, France and Germany. Switzerland, Austria, the Czech Republic, Slovakia and Slovenia have the largest average resources of wood per hectare at their disposal, whereas Germany has the largest overall wood resources in Europe, with more than 3.4 billion solid cubic metres (followed by Sweden, France and Finland) [49].

In Germany, the amount of wood cut increases continuously. A new all-time high was reached in 2007, with 76.7 million solid cubic metres [50]. This value includes trunk wood (46.8 million solid cubic metres) and pulp wood (29.9 million solid cubic metres). At 21.2 million solid cubic metres, Bavaria's portion of cut wood is the largest. Nevertheless, the chances of the construction of 1,000 tonnes per day (tpd) plant for wood-based methanol in Europe are considered to be very small because the wood production surface area required for this purpose would be 1,500 km^2.

In summary, wood regained importance as a raw and work material at the beginning of the twenty first century because it can be produced in an almost CO_2-neutral manner, it is compatible with an ecological and sustainable economy, it can be processed with little energy, and it is recyclable in its entirety.

Biogas

Biogas as feedstock for the production of methanol can be produced by the fermentation of biomass in biogas plants [51]. Suitable basic materials for the technical production of biogas foremost include the following biological resources:

- Fermentable, biomass-containing residues such as biological waste, food residues, or sludge
- Farm fertiliser ([liquid] manure)
- Unused plants and plant parts (e.g. catch crops, plant residues)
- Energy plants cultivated for this purpose (regenerative feedstocks).

A large part of the feedstocks mentioned above—in particular, farm fertiliser, plant residues and energy plants—is produced in agriculture. Therefore, this sector has the greatest potential for biogas production.

Biogas is generated through the natural process of anoxic microbial decomposition of organic material. In this process, micro-organisms convert the carbohydrates, proteins and fats contained in the material into the primary products methane and carbon dioxide. The process consists of several steps, each of which is accomplished by micro-organisms with various types of metabolisms. Polymeric components of the biomass, such as cellulose, lignin, or proteins, are first converted into monomeric substances (of low molecular weight) through microbial exoenzymes. Substances of low molecular weight are degraded to alcohols, organic acids, carbon dioxide and hydrogen through fermenting micro-organisms. The alcohols and organic acids are converted into acetic acid and hydrogen through acetogens. In the last step, methanogenic archaea convert carbon dioxide, hydrogen and acetic acid into two final products: methane and water.

Table 4.3 Comparison of biogas feedstocks [52]

Feedstock	Biogas yield per tonne fresh mass, m^3	Average methane content, %
Maize silage	202	52
Grass silage	172	54
Whole-plant rye silage	163	52
Fodder beet	111	51
Biological waste	100	61
Poultry manure	80	60
Sugar beet chips	67	72
Pig manure	60	60
Cattle manure	45	60
Distillers' grains	40	61
Liquid pig manure	28	65
Liquid cattle manure	25	60

The gas mixture, which is saturated with water, is composed mainly of methane (45–70 %) and carbon dioxide (25–55 %). Traces of nitrogen (0.01–5 %), oxygen (0.01–2 %), hydrogen (0–1 %), hydrogen sulphide (10–30,000 mg/m^3) and ammonia (0.01–2.5 mg/m^3) are usually present in the mixture as well. As indicated in Table 4.3, different feedstocks produce different yields of biogas and, according to their respective composition, gas mixtures with varying methane content.

Prior to its utilisation (feeding into the natural gas network) or processing (production of synthesis gas), the raw biogas has to be subjected to a complex conditioning process. In addition to the removal of water, hydrogen sulphide, and carbon dioxide from the biogas, its heating value must be adjusted to that of the natural gas in the respective gas network (conditioning). Due to the high technical effort, the conditioning process is currently profitable for only very large biogas plants.

In the period from 1999 to 2010, the number of biogas plants in Germany increased from approximately 700 to 5,905, and they generate approximately 11 % of the power from renewable energy sources. By the end of 2011, this number was estimated to be 7,000 plants [53]. Due to the tendency to build larger plants, the installed capacity increased at a higher rate and reached 1,270 MW in 2007. The approximately 9 billion kWh of power generated in 2007 accounted for 10 % of all power generated from renewable energy sources and 1.5 % of the total power demand in Germany. It is expected that the production of biogas will increase to 12 billion m^3 of biomethane per year by 2020. This corresponds to a fivefold increase of the capacities in 2007 [54].

Parallel to the utilisation of conditioned biogas in the energy sector as discussed, the interest in biomethane as feedstock for the production of methanol has also continued to grow [33, 55]. The feedstock can be very different in quality due to the different biogas pathways and depending on various influencing factors (e.g. substrate used, biogas conditioning procedure used, reforming conditions), which are of significance for the economic and ecologic evaluation of the product methanol.

According to the current state of the art, two concepts for the generation of biomethane from biogas prevail. Both concepts are divided into two stages: (1) raw biogas production and (2) biogas conditioning. Raw biogas production comprises the preliminary treatment (including ensilage, storage and substrate treatment), the fermentation (wet fermenter with secondary fermenter), the gas reservoir, a condensing boiler for heating the fermenter, and the processing of the fermentation residues. The biogas conditioning stage comprises the drying, the desulphurisation, the methane enrichment and the pressure adjustment.

The substrate used in both types of plants is composed of different amounts of liquid manure, regenerative feedstocks and residues. Liquid manure in this case means liquid cattle manure; the regenerative feedstocks used consist of an established mixture of maize silage, whole-plant silage and grains. Both concepts reflect the current state of biomethane production and produce 250 Nm^3 of biomethane per hour. They differ in respect to the fermentation substrate and the methane enrichment method. For the first concept, liquid manure and regenerative feedstocks are used in equal amounts. The methane enrichment in this concept is carried out by means of pressure swing adsorption (PSA)—the procedure that has been used most often in Germany so far.

As a second concept for the production of biomethane, a typical plant for the utilisation of regenerative feedstocks (as they were built frequently in the past years) was examined. This plant was supplied with a mixture of 90 % regenerative feedstocks and 10 % liquid cattle manure. The altered composition of the substrate in this concept results in a higher specific power demand (with reference to the amount of substrate input) due to the more complex loading process. On the other hand, the demand for thermal energy for preheating the substrate decreases due to the higher energy density of the regenerative feedstocks. Preheating the substrate is necessary in order to avoid disturbing the sensitive fermenter environment (37 °C).

This concept uses pressurised water scrubbing instead of PSA for methane enrichment. This technology has been used in Europe for a long time, and it is mainly employed in large new plants. The biomethane produced in this way and purified to the quality level of natural gas is fed into the natural gas network or used for the production of methanol. The material flows required for economic and ecologic evaluation were accounted for on the basis of the method and data used by Althaus et al. [55]. Figure 4.14 illustrates the schematic flow diagram of the demonstration plant for methanol production from biogas as designed and operated by the Center for Solar Energy and Hydrogen Research (ZSW) in Stuttgart [32].

By means of anaerobic fermentation of sludge, biogas containing approximately 65 % methane and 35 % carbon dioxide is produced and used as fuel gas in a combined heat and power plant. For methanol production, a part of the biogas is channeled off, cleaned in a gas filter, and heated and desulphurised. The water vapour required for the reforming process is injected into the biogas flow before it enters the reformer. In the reformer, a synthesis gas is produced, which contains a high proportion of carbon dioxide in addition to hydrogen and carbon monoxide. After the water is condensed out of the product gas and separated, the synthesis gas is converted into raw methanol under 5–8 MPa pressure and a temperature of 250–280 °C.

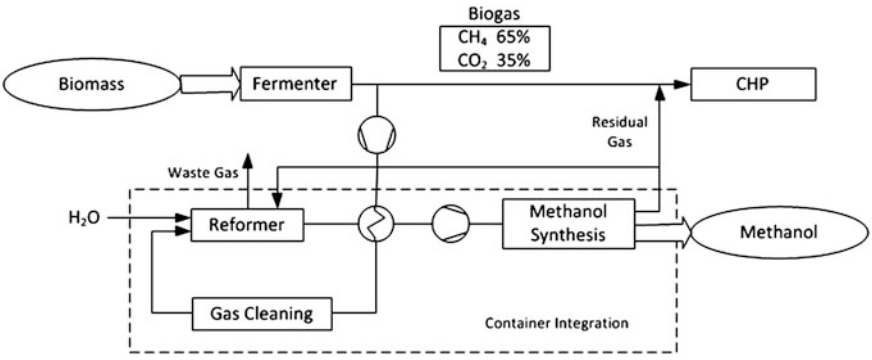

Fig. 4.14 Schematic flow diagram of methanol production from biogas based on the "once-through" concept without carbon dioxide separation

As the synthesis gas produced from biogas is not suitable for the recycle loop without a separation of CO_2, the facility is designed according to the "once-through" concept, which is simpler in terms of processes. For example, the synthesis gas can be used within the process for the operation of the reformer or in the power plant.

Waste and Sludge

Thus far, waste and sludge have not been used for the production of synthesis gas, although the volume of this kind of waste material is very large. Of the 455 kg of waste per capita produced in German households in 2009, 199 kg were household waste and bulky waste, 143 kg were recyclable materials, and approximately 111 kg were biological waste [56]. In the European Union, the amount of biological waste produced per year totals 118–138 million tonnes. This amount is expected to increase by 10 % until the year 2020, reaching an annual amount of approximately 680 kg per European citizen [57].

In Germany, sludge amounted to approximately 2.2 million tonnes (dry mass) with a calorific value of 10,470–18,840 kJ/kg in the past years. This corresponds to an energy equivalent of approximately 1 million tonnes of hard coal. Depending on its subsequent utilisation, the sludge has to be pretreated in different ways. Several sequential procedures have to be carried out: drainage, thickening, conditioning, and drying.

Sludge that is not used as fertiliser (because of its content of nutrients such as phosphate and nitrate) is used in thermal processes (combustion, gasification, or carbonisation) [57–59]. A sufficient heating value can be achieved by prior drying, which, however, requires a high amount of energy. To improve the energy balance for the energetic utilisation of sludge, only cofiring in power plants or waste incineration plants fuelled with solid materials is possible. Waste and sludge can also be used together with light agglomerating hard coal or brown coal as fuel. For example, sludge and municipal waste are briquetted together with light agglomerating coal and then gasified in the traditional way (see Sect. 4.4.6).

4.2 Synthesis Gas Generation—General Aspects

Ludolf Plass[1], Hans Jürgen Wernicke[2] and Friedrich Schmidt[3]

[1]*Parkstraße 11, 61476 Kronberg, Germany*

[2]*Kardinal-Wendel-Straße 75 a, 82515 Wolfratshausen, Germany*

[3]*Angerbachstrasse 28, 83024 Rosenheim, Germany*

As shown in Fig. 4.15, syngas can be produced from many different feedstocks and using a variety of different syngas-generating technologies. Section 4.3 deals with the production of syngas from gaseous feedstocks such as natural gas, refinery off-gases and biogas. Also, naphtha and liquefied petroleum gas (LPG) fall under this heading because they can be vapourised before being converted to syngas.

More than 60 % of the worldwide production of synthesis gases is used for the production of ammonia (51 %) and methanol (8 %), whereas approximately 35 % goes into refining for hydrodesulphurisation, hydrotreating and hydrocracking [60] of mineral oils [61]. Hydrogen is mainly produced from fossil fuels such as natural gas (48 %), liquid hydrocarbons (30 %) and coal (18 %). The production from water electrolysis amounts only to approximately 4 %, used preferably when very high hydrogen purity is needed. The current production of hydrogen for commercial use worldwide is approximately 50 million tonnes per year [62], representing approximately 140 million tonnes of oil equivalent, less than 2 % of the world primary energy demand. In more than 50 smaller hydrogen plants (capacities $< 2.000\ Nm^3/h$) methanol is used as a feedstock for hydrogen (see Sect. 6.5.1).

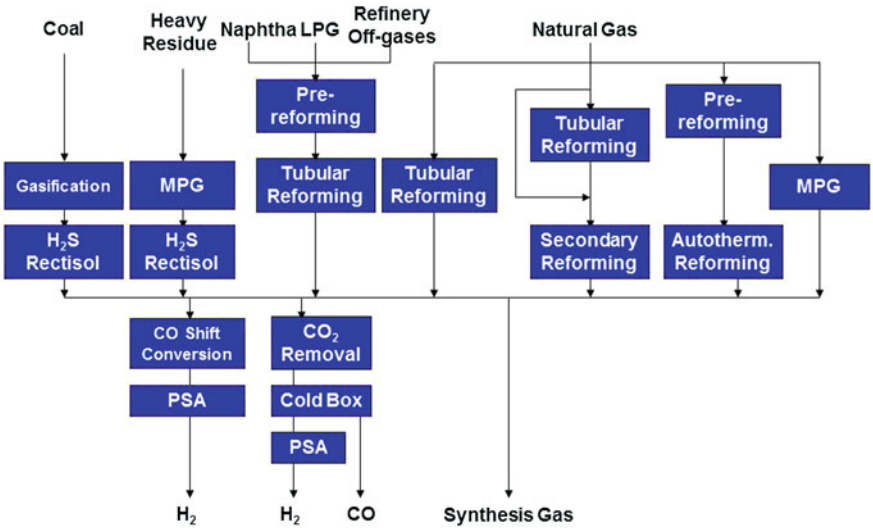

Fig. 4.15 Routes to synthesis gas. (Courtesy of Air Liquide Global E&C Solutions) [60]

Table 4.4 Various reforming reactions

• *Steam reforming*	
$CH_4 + H_2O \leftrightarrows CO + 3H_2$	Equation 4.1
$C_mH_n + m\ H_2O \leftrightarrows m\ CO + (m + n/2)\ H_2$	Equation 4.2
$CH_3OH + H_2O \leftrightarrows CO_2 + 3H_2$	Equation 4.3
• *Partial oxidation*	
$CH_4 + 1/2O_2 \leftrightarrows CO + 2H_2$	Equation 4.4
$C_mH_n + m/2O_2 \leftrightarrows m\ CO + n/2H_2$	Equation 4.5
$CH_3OH + 1/2\ O_2 \leftrightarrows CO_2 + 2H_2$	Equation 4.6
$CH_3OH \leftrightarrows CO + 2H_2$	Equation 4.7
• *Autothermal reforming or oxidative steam reforming*	
$CH_4 + 1/2H_2O + 1/2O_2 \leftrightarrows CO + 5/2H_2$	Equation 4.8
$C_mH_n + m/2H_2O + m/4O_2 \leftrightarrows m\ CO + (m/2 + n/2)H_2$	Equation 4.9
$CH_3OH + 1/2H_2O + 1/4O_2 \leftrightarrows CO_2 + 2.5H_2$	Equation 4.10
• *Gasification of carbon (coal, coke)*	
$C + H_2O \leftrightarrows CO + H_2$	Equation 4.11
$C + O_2 \leftrightarrows CO_2$	Equation 4.12
$C + 0.5O_2 \leftrightarrows CO$	Equation 4.13
$C + CO_2 \leftrightarrows 2CO$	Equation 4.14
• *Carbon formation*	
$CH_4 \leftrightarrows C + 2H_2$	Equation 4.15
$C_mH_n \leftrightarrows x\ C + C_{m-x}H_{n-2x} + x\ H_2$	Equation 4.16
$2CO \leftrightarrows C + CO_2$ (Boudouard)	Equation 4.17
$CO + H_2 \leftrightarrows C + H_2O$	Equation 4.18
• *Water–gas shift*	
$CO + H_2O \leftrightarrows CO_2 + H_2$	Equation 4.19
$CO_2 + H_2 \leftrightarrows CO + H_2O$ (reverse water–gas shift)	Equation 4.20
• *Selective CO oxidation*	
$CO + O_2 \leftrightarrows CO_2$	Equation 4.21
$H_2 + O_2 \leftrightarrows H_2O$	Equation 4.22

In a first step the feedstock has to be converted in the synthesis gas section into hydrogen and carbon oxides. Furthermore, a gas composition well suited for the subsequent synthesis has to be adapted, ranging from a 3:1 mixture of hydrogen and nitrogen used for the ammonia production, a mixture of 2:1 of hydrogen and carbon monoxide for the production of methanol to a mixture of 1:1 of hydrogen and carbon monoxide for the production of dimethyl ether. The components harmful to the downstream synthesis catalyst must be removed. The selection of process technologies for synthesis gas production and purification depends on the feedstock as well as on the local requirements.

The equations in Table 4.4 represent the possible reactions in different processing steps involving four representative fuels: natural gas (CH_4) and LPG for stationary applications, liquid hydrocarbon fuels (C_mH_n) and methanol (MeOH)

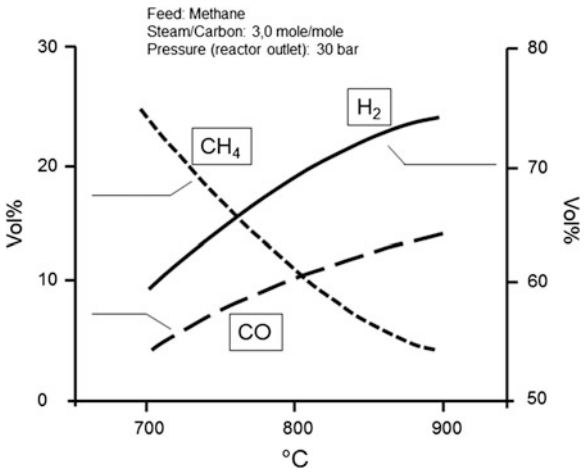

Fig. 4.16 Temperature dependence of steam reforming reaction

and other alcohols for mobile applications, and coal gasification for large-scale industrial applications for syngas and hydrogen production. Most reactions (Eqs. 4.1–4.14 and 4.19–4.21) require (or can be promoted by) specific catalysts and process conditions. Some reactions (Eqs. 4.15–4.18, 4.22) are undesirable but may occur under certain conditions [63].

Reforming or gasification produces syngas whose H_2/CO ratio depends on the feedstock and process conditions, such as feed steam/carbon ratio and reaction temperature and pressure.

Figure 4.16 shows that with increasing outlet temperature, methane conversion is increasing, resulting in higher concentrations of H_2 and CO.

4.3 Reforming and Partial Oxidation of Hydrocarbons

Ludolf Plass[1], Friedrich Schmidt[2], Hans Jürgen Wernicke[3] and Thomas Wurzel[4]

[1]*Parkstraße 11, 61476 Kronberg, Germany*

[2]*Angerbachstrasse 28, 83024 Rosenheim, Germany*

[3]*Kardinal-Wendel-Straße 75 a, 82515 Wolfratshausen, Germany*

[4]*Air Liquide Global E&C Solutions, c/o Lurgi GmbH, Lurgiallee 5, 60439 Frankfurt, Germany*

Table 4.5 Typical specification of different feed gases [64]

	Natural gas		Associated gas	
	Lean	Heavy	Lean	Heavy
N_2, vol%	3.97	3.66	0.83	0.79
CO_2, vol%	–	–	1.61	1.50
CH_4, vol%	95.70	87.86	89.64	84.84
C_2H_6, vol%	0.33	5.26	7.27	6.64
C_3, vol%	–	3.22	0.65	6.23
Maximum total sulphur, ppmv	20	20	4	4
Hydrogen sulphide, ppmv (typical)	4	4	3	3
Carbonyl sulphide, ppmv (typical)	2	2	n.a.	n.a.
Mercaptans, ppmv (typical)	14	14	1	1

4.3.1 Synthesis Gas Generation Processes and Feedstocks

For the production of synthesis gas from natural gas, oil-associated gas, coal-bed methane, or shale gas, the following technologies are well proven:

- Steam reforming
- Autothermal catalytic reforming
- Combined reforming
- Noncatalytic POX.

The most appropriate processes for the generation of synthesis gas for methanol production depend on a variety of parameters, as outlined later in this chapter. A summary of selection criteria is available in Sect. 4.3.6. A detailed review of catalysts and catalytic processes for the generation of synthesis gas from natural gas was published elsewhere by Aasberg et al. [64].

Table 4.5 shows a typical specification of different feed gases. Of special importance is the total content of sulphur, as well as small concentrations of other catalyst poisons such as carbonyl sulphide (COS) and mercaptans in the feed gas.

4.3.2 Steam Reforming

4.3.2.1 Principles and Introduction

Steam reforming of hydrocarbons converts hydrocarbon substances with an excess of steam into a product gas consisting of hydrogen, carbon monoxide, and carbon dioxide, with some slip of unconverted hydrocarbon from which hydrogen can be separated in high purity. The steam reforming process is endothermic, so that reactor concepts are allothermic with heat flux into the reactor. In the case of

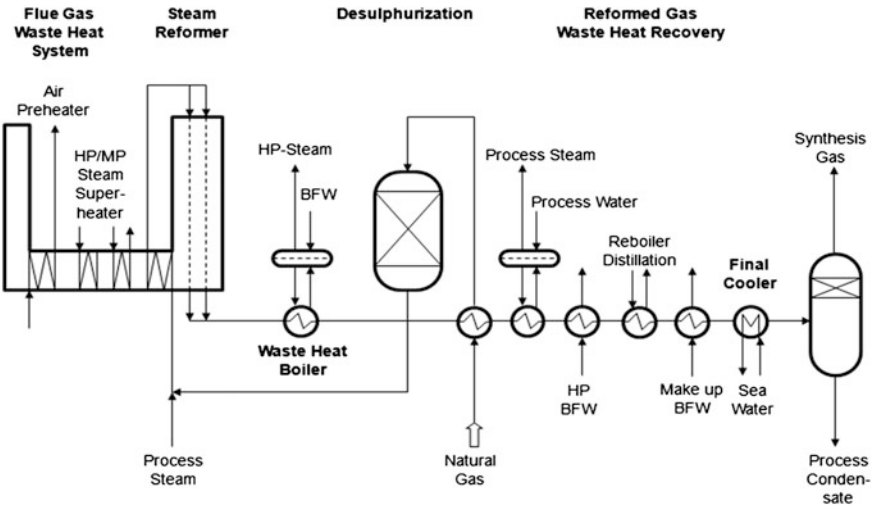

Fig. 4.17 Process scheme of a typical steam methane reformer (SMR) plant (*Source* Air Liquide Global E&C Solutions [65])

methane as hydrocarbon feed, the process is sometimes called steam methane reforming (SMR).

Modern steam reformer plants convert methane feed into syngas in a mature process. A typical design of a steam reformer is shown in Fig. 4.17. It provides a continuous product stream of syngas with a high reliability exceeding 8,600 operating hours per year. As a feedstock preparation step, sulphur-containing compounds are removed from the natural gas feed by a catalytic hydrogenation of sulphur followed by H_2S absorption guard bed (ZnO; see Fig. 4.19 in 4.3.2.2). Therefore, a minor stream of hydrogen is added into the natural gas, taken from the product hydrogen stream via a small hydrogen membrane compressor, followed by preheating in a feed-effluent heat exchanger. Sometimes, depending on the feedstock, a pre-reformer catalyst is placed in front of the hot steam reforming step, operating at a lower temperature to convert higher hydrocarbons into methane and carbon oxides and to avoid coking (see Sect. 4.3.2.5 and Fig. 4.28). Depending on the optimisation criteria, a high and variable amount of superheated steam is added into the feedstock gas to have an appropriate carbon/steam ratio and thereby avoiding coking on the catalyst. The mixture is preheated in a flue gas/feedstock heat exchanger from 520 to 650 °C. Reforming of hydrocarbons happens in the reactor, which is a reaction tube (up to 14 m length) installed in an oven that provides the heat. Modern large-scale reformers have up to 1,000 tubes. At the outlet of the reformer, chemical equilibrium between formed hydrogen, carbon monoxide and residue methane is almost reached and 85–90 % of methane is converted. Product gas with between 780 and 950 °C reformer outlet temperature is cooled in a process gas boiler while producing steam used for the process and as

Table 4.6 Typical conversion rates of a methane steam reformer. Feedstock: natural gas. (Adapted from [66])

	Feed	Before desulphurisation	Reformer inlet	Reformer outlet
H_2, vol%	0	4.8	1.1	51.9
N_2, vol%	1	1	0.3	0.2
CO, vol%	0	0	0	10.7
CO_2, vol%	0.5	0.5	0.1	5.1
CH_4, vol%	95	90.4	26.1	3.8
C_2, vol%	3.5	3.3	1	0
H_2O, vol%	0	0	71.4	28.3
Quantity, m^3(STP)/h	2,160	2,070	7,160	10,450
Temperature, °C	20	390	520	850
Pressure, MPa	2	1.9	1.9	1.7

export steam (if required in the chemical complex). The product stream is cooled via a series of heat exchangers as the feed preheater, boiler feedwater preheater and preheater for demineralised water. After passing through an air cooler and a water cooler, the syngas is ready for further processing, such as methanol synthesis.

Typical conversion rates for natural gas in the methane steam reformer can be seen from Table 4.6.

Feed flow can be downflow or upflow through the tubes. Improvements in tube metallurgy allow operation of steam reformers at pressures up to 40 bar and tube wall temperatures of up to 1,000 °C. The average heat flux is reported to be as high as 95,000 W/m^2 for top fired reformers.

Hydrocarbon Feeds

Hydrocarbon feeds can be:

- Natural gas
- LPG
- Refinery off gases
- Petrochemical off gas
- Naphtha.

Target Product Gases

Synthesis gas produced by steam reforming of hydrocarbons is used to manufacture the following:

- Ammonia synthesis gas
- Methanol synthesis gas
- Hydrogen
- Oxo synthesis gas
- H_2/CO reducing gas
- Pure CO.

Given the variability of primary reformer configurations and design, hydrocarbon feedstock and product gas requirements, a case-by-case consideration of suitable catalysts is necessary for every application.

The steam-to-carbon (S/C) ratio has an impact on the overall reaction as well. With increasing S/C, more reforming will take place and at the same time CO shift conversion will be increased. Beyond pure operational aspects, catalyst performance is most critical to the entire process.

Special attention has to be given to the following:

- Catalyst activity: nickel content and catalyst shapes
- Pressure drop: catalyst shapes
- Physical strength: catalyst carrier
- Suppression of coking: catalyst carrier promoter.

4.3.2.2 Conditioning of Gaseous Feedstocks for Steam Reforming

All commercially applied steam reforming catalysts are based on nickel as the catalytically active component. Catalyst poisons are therefore all substances that can react with nickel, especially the following:

- Sulphur
- Halogens
- Arsenic
- Heavy metals

Poisoning leads to a more or less drastic reduction of the catalyst activity, yielding undesired high tube wall temperatures (see Fig. 4.18), carbon formation, and increase of pressure drop in the steam reformer section.

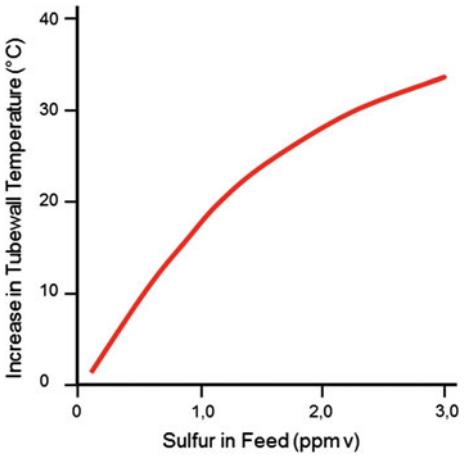

Fig. 4.18 Effect of sulphur on the tube wall temperature [67]

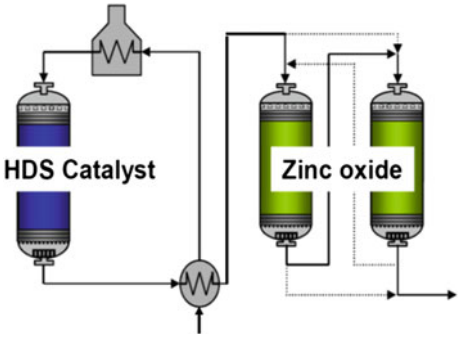

Fig. 4.19 Hydrodesulphurisation and sulphur removal set-up [67]

(A) **Sulphur**

Sulphur is a particular deactivator of nickel-reforming catalysts and it should be removed from any hydrocarbon feed to a level of less than 0.1 ppmv.

The sulphur reacts with nickel according to

$$\mathrm{Ni} + \mathrm{H_2S} \leftrightharpoons \mathrm{NiS} + \mathrm{H_2} \tag{4.23}$$

The equilibrium condition of this reaction shows that sulphur is not a permanent poison. Hence, the activity of the steam reforming catalyst can be mostly restored when the feedstock becomes sulphur-free. Also, steaming to remove sulphur and re-reduction of the steam reforming catalyst is a way to recover reforming activity. The presence of sulphur, however, increases the probability of carbon formation on the catalyst, leading to permanent deactivation or even catalyst breakage (due to carbon buildup). Sulphur poisoning must be avoided under all circumstances because it decreases the reforming activity of Ni-based catalysts so that the maximum tube wall temperatures increase (see Fig. 4.18) at the expense of lifetime.

Sulphur Removal

The typical process for desulphurisation of natural gas or similar feedstocks is a one- or two-step process based on hydrogenation of organic sulphur (HDS) and conversion to H_2S and subsequent adsorption/absorption of H_2S by zinc oxide beds. This process concept has been used industrially for decades and is well documented in the literature [67, 68], in which a description of technologies for sulphur removal from different raw materials, including both natural gas and heavier hydrocarbon streams is given. The hydrogen required for the hydrogenation reaction is typically provided as purge gas from the synthesis loop.

For the conversion of organic sulphur compounds, a Co/Mo- or Ni/Mo-hydrotreating catalyst in the sulphide form is used. The conversion and maintenance of the oxidic catalyst into its active, sulphidic form is normally achieved through the feed sulphur components. Figure 4.19 shows a process concept for the sulphur removal. If the heat balance requires, a "fired heater" (as shown in the figure) can be added.

The following principal chemical reactions take place in the dusulphurisation reactors:

(a) Hydrodesulphurisation

$$RSH + H_2 \rightarrow RH + H_2S \tag{4.24}$$

$$RSR + 2H_2 \rightarrow 2RH + H_2S \tag{4.25}$$

$$RSSR + 3H_2 \rightarrow 2RH + 2H_2S \tag{4.26}$$

$$COS + H_2 \rightarrow CO + H_2S \tag{4.27}$$

(b) Absorption by zinc oxide:

$$ZnO + H_2S \rightarrow ZnS + H_2O \tag{4.28}$$

The reaction of H_2S absorption to form zinc sulphide is exothermic ($\Delta H_o = -76.7$ kJ/mol, $\Delta S_o = -3$ J/molK, referring to formation of the most stable form of β-ZnS—sphalerite) [69]. The reaction is thermodynamically strongly favoured with the equilibrium constants as shown in Fig. 4.20 as a function of temperature.

Typical operating conditions for desulphurisation are as follows:

- For the hydrodesulphurisation stage, typically 4,000–6,000 $m^3/(m^3h)$ at 330–380 °C, 3–5 vol% hydrogen is added to the feed gas, which, for example, may be taken from the purge gas stream of the methanol reactor.

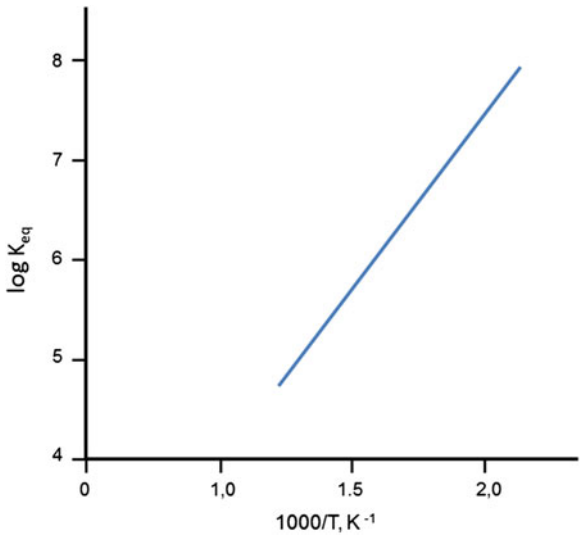

Fig. 4.20 Equilibrium constant for reaction according to Eq. 4.28 [70]

- The zinc oxide stage typically uses 1,000–2,000 $m^3/(m^3h)$ at 330–400 °C with an optimum around 370 °C.
- The ZnO absorbent will also catalyse the hydrolysis reaction of COS to form CO_2 and H_2S, the latter being absorbed.
- A typical commercial ZnO absorbent will consist of more than 90 wt% ZnO (plus a binder material) in the form of extrudates with a bulk density of about 1.1–1.3 kg/l. It will have a sulphur pickup capacity before sulphur breakthrough in the region of up to 32 wt% sulphur (lead bed of a two-reactor design), whereas the "saturation" pickup of the ZnO absorbent itself may reach even up to 39.6 wt% sulphur.

The two-reactor design of the ZnO reactors (see Fig. 4.19) allows a lead/lag operation, with the first reactor tolerating a sulphur slip as to maximise the sulphur pickup and with the second reactor for achieving the required outlet purity of less 0.1 ppmv sulphur. More recent process schemes allow the combination of hydrodesulphurisation and sulphur absorption in one step. In this case, the catalyst consists of a combination of ZnO absorbent, which at the same time serves as a carrier for the hydrodesulphurisation catalyst. A typical composition of the catalyst/absorbent is 1.5 wt% Co, 3.5 wt% Mo, with the balance as ZnO. Even if the absorption capacity of the zinc oxide (in the first reactor) is spent, the hydrodesulphurisation activity is maintained.

A setup that operates with only two instead of three reactors can typically handle feedstocks with 1–15 ppmv sulphur and is operated at about 330–400 °C, with pressures up to 60 bar and a space velocity of up to 5,500 $m^3/(m^3h)$. Especially for feed gases with lower sulphur contents below approximately 20 ppmv total sulphur, the simpler design and operation of the combined purification leads to substantial cost savings.

Product Gas Sulphur Content

The resulting residual sulphur content of the exit gas from a hydrodesulphurisation and absorption system is in the region of 0.1 ppmv or less, which is tolerable for the downstream reforming units.

In case of very high water contents in the feed gas, the equilibrium H_2S content will increase, causing higher H_2S leakage to the downstream units. For example, a 0.3 steam/hydrocarbon ration in the feed gas at 340 °C would increase the outlet sulphur content from about 0.1 to 0.4 ppmv.

The effect of high CO_2 contents in the feed gas will only have a negligible effect on the sulphur leakage in the product gas. Even 100 % CO_2 as feed gas at 340 °C would only cause 0.1–0.2 ppmv additional sulphur leakage by means of shifting the equilibrium for COS formation from ZnS.

(B) **Chlorine**

The effect of chlorine and other halogens on the steam reforming catalyst is not as severe as the effect of sulphur but halogens still reduce its activity. Chlorine

poisoning is partially reversible. An overview on the deactivation effects is given by Richardson et al. [71].

Entrained HCl reacts with Ni according to the following equilibrium reaction:

$$Ni + 2HCl \leftrightharpoons NiCl_2 + H_2 \tag{4.29}$$

Under typical operating conditions of primary reforming, the equilibrium will be on the side of the reduced and active nickel. Chlorine poisoning might also lead to higher tube wall temperatures and is a cause for shorter tube life and can destroy other downstream catalysts and equipment.

Chlorine migration into downstream sections containing copper-based catalysts [low temperature shifts (LTSs), methanol synthesis] leads to rapid sintering of the active phase and thus rapid deactivation of these catalysts. Their feedgas should have a chlorine content not exceeding approximately 5 ppbv [72].

Chlorine Removal in Reformer Feed-gas

In some cases, installation of a chloride guard—usually between the hydrodesulphurisation stage and the zinc oxide absorbers—is required. In the hydrogenation reactor chlorine, compounds will be converted into HCl, which can then be removed either by activated alumina or alkali (mostly potassium)-promoted alumina before entering the zinc oxide reactors. The alkali promoted alumina serves as an HCl scavenger:

$$4HCl + 2K_2O/Al_2O_3 \rightarrow 4KCl + Al_2O_3 + 2H_2O \tag{4.30}$$

Alkali-promoted aluminas have an absorption capacity of up to 15–20 wt% and work under the same conditions as the desulphurisation stages.

The chloride guard bed can be either installed as a separate reactor or as top-up of the zinc oxide beds (Fig. 4.21). For both versions, this setup avoids formation of zinc chloride by entrained HCl, which would reduce the sulphur pickup capacity of the zinc oxide beds and could sublime as a poison into the downstream reformer reactors.

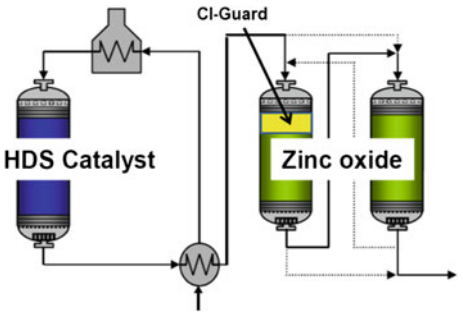

Fig. 4.21 Chlorine guard on top of desulphurisation bed [67]

(C) **Arsenic**

Arsenic traces will accumulate and poison the desulphurisation catalysts as well as the steam reforming catalysts. The buildup of arsenic on steam reforming catalysts will affect its operation when exceeding levels of approximately 50 ppmw [73]. The poisoning is irreversible due to alloy formation with the active nickel.

A content of maximum 5 ppbw in the reformer feedstock is seen as an upper tolerable limit. It normally is present as arsine (AsH_3) or organic derivatives. The desulphurisation catalysts can act as a trap, which in this case asks for a corresponding increase of the catalyst bed [73]. An alternative is the removal by an upstream absorbent bed.

(D) **Other Contaminants**

Removal of contaminants such as mercury and phosphorous is described in connection with the product gas from solid fuel gasification (see Sect. 4.4.8).

4.3.2.3 Carbon Formation/Coking

In the case of heavier feedstocks, carbon formation becomes an issue. Carbon can be formed by thermal cracking of hydrocarbons (see also equations in Table 4.4):

$$C_mH_n \leftrightarrows mC + n/2H_2 \tag{4.31}$$

$$CH_4 \leftrightarrows C + 2H_2 \qquad \Delta H = 90\,\text{kJ/mol} \tag{4.32}$$

It can also be formed by CO disproportionation (Boudouard reaction):

$$2CO \leftrightarrows C + CO_2 \text{ (Boudouard)} \qquad \Delta H = -85\,\text{kJ/mol} \tag{4.33}$$

Another possible reaction is a water–gas shift (WGS) type reaction, leading to elemental carbon:

$$CO + H_2 \leftrightarrows C + H_2O \tag{4.34}$$

The Boudouard reaction is favoured at high CO partial pressures and low temperatures.

Cracking reactions can occur at the acidic sites of the carrier. They are thermodynamically favoured at high temperature and are the main cause for carbon formation in fired reformers. Heavier hydrocarbons in the feed will crack first. As this occurs, the active sites of the catalyst are masked, resulting in less reforming and hence hotter gas and tube wall temperatures and increased cracking (see Fig. 4.22).

The thermodynamic boundaries of coking reactions can best be summarised in the triangular diagrams shown in Fig. 4.23 for a pressure of 15 bar [74]. In Fig. 4.23, the grey "carbon + gas" regime shows the equilibrium of carbon with

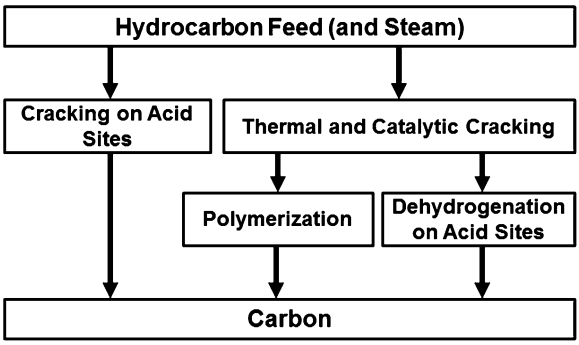

Fig. 4.22 Routes to carbon [67]

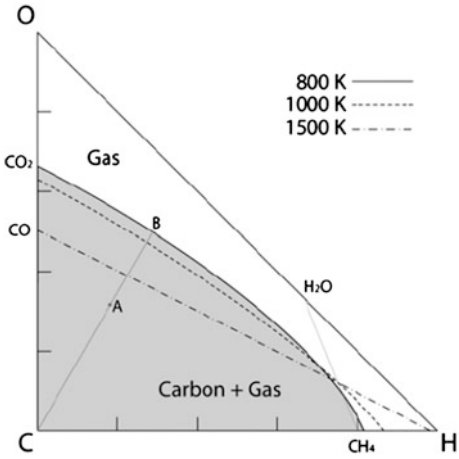

Fig. 4.23 The thermodynamic boundaries of coking reactions for a pressure of 15 bar [74]

the gas phase for different temperatures. In the "gas" region, carbon would not be formed.

The coking limits will change depending on the gas phase composition, as shown for a system steam–methane–carbon dioxide at 30 bar in Fig. 4.24, and different CO_2 concentrations and steam to (methane + CO_2) ratios.

At high temperatures (>1,000 K), higher CO_2 concentrations reduce the equilibrium carbon regime. Below 1,000 K, higher CO_2 concentrations extend the equilibrium carbon regime. The higher the operating pressure, the more favourable the carbon formation.

Steam/carbon ratios used in practice should be sufficiently high to be distant from equilibrium curves for carbon formation. CO_2 can also suppress carbon formation, but the effect is approximately only half compared to the one of steam. Figure 4.25 shows the minimum required S/C ratio as a function of the operating pressure (including the effect of CO_2).

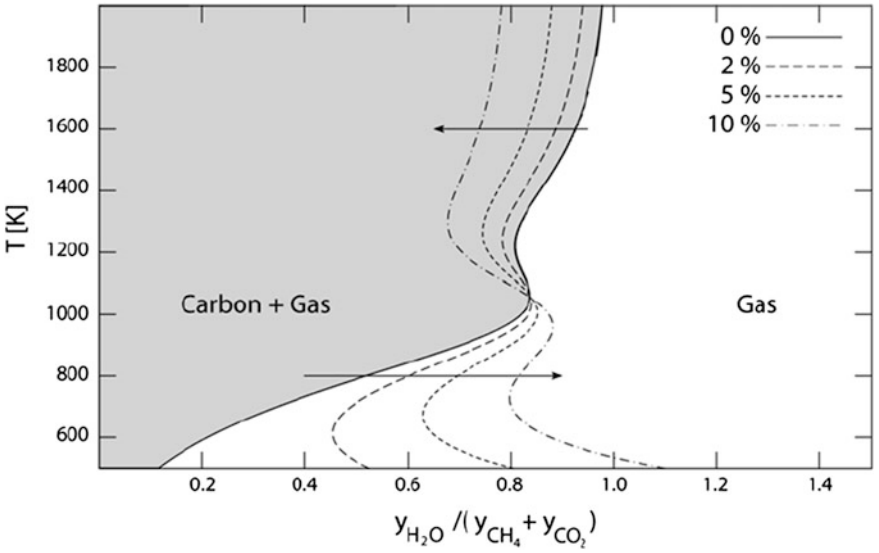

Fig. 4.24 Coking limits depending on the gas phase composition for a system steam-methane-carbon dioxide at 30 bar in and different CO_2 concentrations and steam to (methane + CO_2) ratios [75]

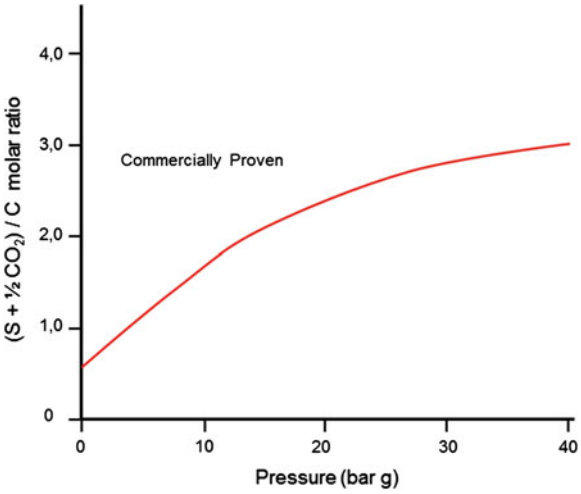

Fig. 4.25 Minimum required steam-to-carbon (S/C) ratio as a function of the operating pressure (including the effect of CO_2, without pre-reformer) [67, 68]

4.3.2.4 Catalysts for Steam Reforming

Aasberg et al. [64] reviewed the scientific aspects of the catalysts used for steam reforming.

(A) **General Aspects, Requirements**

The heart of the reforming process is the tubular primary reformer where the hydrocarbon feed reacts catalytically with steam. The main reactions in the primary reformer are the following:

- Steam reforming of higher hydrocarbons (see Table 4.4, Eq. 4.2)
- Steam reforming of methane (see Table 4.4, Eq. 4.1)
- WGS reaction (see Table 4.4, Eq. 4.19)

The reforming reaction is an equilibrium reaction and depends on several operational parameters:

- Outlet pressure
- Outlet temperature
- Inlet S/C ratio
- Feedgas composition.

Pressure levels have to be discussed in an overall pressure concept of a plant and the influence on the equilibrium within a few bar is insignificant.

Primary reforming catalysts have to satisfy several basic requirements in service:

- High activity
- Low pressure drop
- High physical strength
- Resistance against carbon formation
- Long life
- Cost efficiency.

For other reforming processes, one or the other additional items is also of great importance. The activity of a catalyst is only one out of several properties that are required to produce synthesis gas from light hydrocarbons. However, for primary reforming processes, it is the most critical issue.

Metal Component

It has been found that transition metals from group VIII are active in steam reforming of hydrocarbons [76–85]. Several parameters such as dispersion of the metal, accessibility of the active site, metal-support interaction and others also affect the activity. Because the most active metals of Pt, Ir, Rh and Ru are too expensive, the preferred large-scale industrial steam reforming catalysts are based on nickel, which has good steam reforming activity and a reasonable price. Precious metal-based catalysts play a major role in fuel processor applications for fuel cells, which currently is still a niche market.

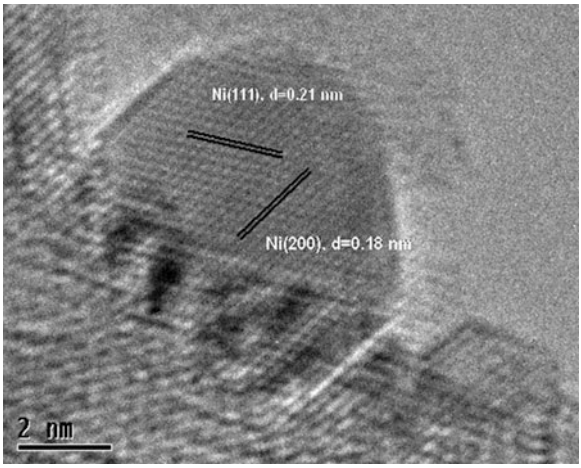

Fig. 4.26 Nickel supported on an $MgAl_2O_4$ spinel carrier. Recorded at 550 °C and 7 mbar of hydrogen using the in situ electron microscope at Haldor Topsøe A/S [64]

Usually, catalysts are supplied with nickel in the oxide form. Therefore, the catalyst needs to be reduced in order to become active. The commercial catalysts are easy to reduce in the plant using common proven procedures. At a low reformer inlet temperature, reduction of the catalyst may not be complete. For these rare cases, the catalysts can be supplied in the pre-reduced form. The pre-reduced material is only required in the inlet 1–2 m of the reformer tube [86].

Nickel is always supported on an oxidic carrier, typically Al_2O_3, ZrO_2, $MgAl_2O_4$, $CaO(Al_2O_3)_n$, MgO and mixtures thereof in order to maximise the dispersion of the active component (Fig. 4.26). For certain applications, the carrier is promoted with alkali to reduce coke formation while operating with heavier feedstock and, as the case may be, with some stabiliser component. For some rare applications, a noble metal spiking can be helpful to initiate the hydrocarbon reforming reaction.

Catalyst Carrier

The suppression of carbon formation reactions is accomplished by decreasing the acidity of the catalyst by incorporating alkaline earth metals into the carrier and by further promoting with an alkali metal. The most common commercial combinations used today are potassium-promoted calcium aluminate and potassium-promoted Mg-aluminate. The combination retards the formation of carbon and also accelerates the carbon gasification reaction once it has been formed.

The acidity of the carriers of commercially available reforming catalysts (see Table 4.7) is ranked from least to greatest: K-promoted Ca-aluminate < Ca-aluminate < Mg-aluminate < α-Al_2O_3. K-promoted Ca-aluminate (the carrier in ReforMax 210) or Mg-aluminate (the carrier for R-67-7H) are less acidic oxides than pure α-Al_2O_3. The alkaline nature of the appropriate commercial carriers is sufficient to ensure carbon-free operation when operating on light feedstocks.

Activity

In a tubular primary reformer, the SMR reaction is highly mass transfer limited (diffusion limited; effectiveness factor is less than 10 %). Approximately 90 % of the reaction takes place on the outer surface (geometric surface) of the catalyst. Thus, the effective activity of any catalyst formulation can be enhanced by using a catalyst that exposes more geometric surface area and hence more pore openings to the gas. Besides the geometric surface area, the catalyst activity is also influenced by the nickel content of the catalyst and the respective nickel dispersion on the catalyst surface.

Nickel Content

Nickel is the catalytically active component of any commercially available steam reforming catalyst. Catalytic activity increases to a certain extent with increasing content of nickel. The catalyst is loaded with nickel by dipping the catalyst carrier in an aqueous nickel salt solution followed by calcination to convert the respective nickel species into NiO. During startup of the steam reformer catalyst, NiO is reduced to elemental Ni, which is the active component. It is important that the nickel crystallites are well dispersed throughout the catalyst. Nickel surface area increases with increasing nickel content; nickel dispersion, however, decreases at the same time.

The catalyst carrier and the amount of potassium also influence the catalyst activity. Practical experience has shown that the maximum activity for the Ca-aluminate based ReforMax 330 (see Table 4.7) low differential pressure (LDP) is achieved with approx. 11 wt% Ni. The potassium promoted ReforMax 210 LDP catalyst for instance requires approximately 14.5 wt% Ni to reach the same level of activity. The optimised balance between coking resistance and activity has been reached in almost all commercial catalysts.

Sintering

Sintering of Ni particles on a $MgAl_2O_4$ support was particularly studied under simulated pre-reforming conditions and was assigned to migration and coalescence of nickel particles on the spinel carrier surface [87, 88]. Under these specific conditions, the sintering of the Ni particles is found to be initially fast and to slow down as the Ni particles grow in size. High partial pressures of steam were found to enhance the sintering. An increase in the sintering rate in H_2O/H_2 atmospheres is seen at temperatures above 600 °C. Furthermore, it is not unexpected that the dependence of H_2 partial pressure is found to be even stronger. The authors interpreted this finding as a change in sintering mechanism from particle migration and coalescence to Ostwald ripening via atom migration at the support. They concluded that for tubular reformers the sintering mechanism in the main part of the reactor will be governed by Ostwald ripening, whereas the migration and coalescence mechanism dominates under pre-reforming conditions

Fig. 4.27 Low differential pressure—a premium shape for low pressure drop. Courtesy of Clariant [89]

Geometric Surface Area

The simplest and most effective way to maximise catalytic activity at a given Ni loading is by using catalyst particles with maximised external geometric surface area. The geometry of a carrier, however, also determines the pressure drop of the respective catalyst. Sophisticated shapes have been developed to combine maximum geometric surface area with low differential pressure drop.

Pressure Drop

Everything related to pressure drop is most critical in the operation of the tubular reformer. Both the initial pressure drop and the evolution of the pressure drop with time on stream have to be considered. The initial pressure drop over the catalyst bed is determined by the catalyst shape and to a certain extent by the loading method. Evolution of the pressure drop is influenced by catalyst carrier material, catalyst shape and, of course, by the mode of operation.

Initial Pressure Drop

The catalyst development for reforming catalysts was always motivated by increasing catalyst activity and decreasing pressure drop. Recent developments include the LDP shape, see Fig. 4.27. With its high geometric surface area, high activity for the steam reforming reaction is provided. The most striking feature of the LDP shape, however, is the combination of high activity with extremely low pressure drop.

Loading the reformer catalysts with a particular designed shape allows operation at up to a 15 % higher throughput rate without having a corresponding higher pressure drop [89].

Physical Strength and Pressure Drop Development

A catalyst loaded in reformer tubes is subject to extreme physical stress due to the expansion and compression of the tubes during startup, shutdown and upset

conditions. The carriers for primary reforming catalysts are tailored for the respective feeds and operating conditions. For instance, the carrier of ReforMax 330 catalysts comprises hibonite, which is the only irreversibly formed phase in the CaO/Al_2O_3 phase diagram. This material is the basis for the extreme stability of the ReforMax 330 catalyst under physical and thermal stress, due to the higher ductility compared to the other carriers.

According to Haldor Topsøe, "The combination of two or even three sizes is chosen to minimise pressure drop and to provide the desired activity, where required. Particles of a relatively larger size are often used in the lower part of the tubes, as a larger part of the pressure drop is generated in the bottom half" [90].

Potassium Promotion

Feed gases for primary reformers become increasingly heavier, so the need for coking-resistant primary reforming catalysts has become very important. To minimise the formation of carbon in the primary reformer, promoted catalysts have been developed specifically for this application. The heavier the hydrocarbon feedstock and/or the lower the S/C ratio, the more likely carbon is formed on the catalyst. It is well understood that the acidic sites of the catalyst carrier promote carbon formation.

By using a more alkaline carrier, carbon formation is suppressed very well. With heavier feeds like LPG and light naphtha, however, the catalyst must be even more alkaline to suppress carbon formation. The various catalyst suppliers recommend related catalyst loading arrangements. For instance, ReforMax 210 LDP contains only 1.5 % K_2O, which is however chemically incorporated into the catalyst carrier. With this formulation, potassium is available in the necessary concentration to suppress carbon formation without depleting from the catalyst prematurely. ReforMax 210 LDP is typically used with heavy natural gas or LPG. A typical setup comprises 30–50 % of the top layer of the tube with ReforMax 210 LDP and a respective bottom layer of ReforMax 330 LDP. In many cases, naphtha reforming requires an even higher level of potassium promotion. This is achieved by adding more than 5 wt% K_2O to a carrier based on basic refractory oxide. These catalysts are usually loaded in the top 50 % of the tubes, with a respective bottom layer of a conventional methane steam reforming catalyst.

Effect of promoters

The influence of alkaline earth and alkali metals on the coking rate can be determined by measuring the thermal decomposition of various hydrocarbons over promoted conventional catalysts. The effect of the promoters to suppress carbon formation can be ranked as: $K > Ca > Mg > Al$. The most effective promoters that decrease coking are potassium and calcium. The catalyst incorporating one or a combination of these elements will decrease the rate of carbon formation but the method of incorporation is critical.

The addition of potassium increases the rate of carbon gasification as the adsorption of water and carbon dioxide at the catalyst surface is increased. The overall accumulation is determined by the difference in the rate of carbon

formation and the rate of carbon gasification. The carbon gasification reactions are as follows:

$$C + 2H_2O \rightarrow CO_2 + 2H_2 \tag{4.35}$$

$$C + CO_2 \rightarrow 2CO \tag{4.36}$$

$$2C + 2H_2O \leftrightarrows 2CO + 2H_2 \tag{4.37}$$

Potassium must be mobile to be effective, but it is widely known that mobile potassium significantly reduces the steam reforming activity. Soluble potassium is more effective in reducing carbon formation, but a great loss of catalytic activity comes along. Soluble potassium leaches quickly from the catalyst during normal operation so that coking resistance will be lost during operation. In extreme cases, condensation during shutdown or startup will easily wash the potassium from the catalyst. Potassium that is bound too tightly to the carrier will not reduce the reforming activity but will also not decrease the suppression of carbon formation.

Properly formulated catalysts are characterised by the following:

- Suppression of carbon formation
- High carbon gasification rate
- High activity
- High physical strength
- Little rate of "leaching".

The carrier for potassium-promoted catalysts is tailored to suppress coking effectively without reducing the reforming activity, as in the case of high alkali version, RK-212 and RK-202 or ReforMax 210 LDP. As a result, some of the potassium-promoted catalysts such as ReforMax 210 LDP contain a potassium reserve that can release potassium in the reformer environment at a controlled rate over its lifetime. The concentration of potassium in the wet reformed gas is typically less than 10 ppbv. The high-alkali catalysts with more than 1 % potassium oxide are capable of handling naphthas with final boiling point (FBP) up to 200 °C (392 °F) and aromatic contents up to 20 % [91].

The overall economics of a plant with a fired reformer depends significantly on the cost of tubes. It is good practice to operate the reformer with the tube wall temperatures as low as possible—consistent, of course, with satisfactory quality of the reformed gas. Even a slight increase in the tube wall temperatures will have a drastic impact on the tube lifetime. Increasing the maximum tube wall by only 10 °C above its design value may result in a shortened lifetime of the reformer tubes of up to 30 %.

(B) **Commercial steam reforming catalysts for various feedstocks**

A broad variety of catalysts is offered on the market to satisfy the needs of the particular reforming task. At first, the catalysts are selected with respect to the reforming technology, such as pre-reforming, secondary reforming, or combinations thereof. Subsequently, the catalysts are selected on the basis of the operating

Table 4.7 Selected commercial steam reforming catalysts

Catalyst	Supplier	Typical feedstock
ReforMax 330 LDP	Clariant	Natural gas, low steam
ReforMax 210 LDP on top of ReforMax 330 LDP	Clariant	Heavy natural gas, LPG
ReforMax 250 on top of ReforMax 330 LDP	Clariant	Naphtha, mixed feeds with high C_{5+} content
KATALCOJM 23-series	KATALCO$_{JM}$	High methane content gas, design plant rates
KATALCOJM 57-series	KATALCO$_{JM}$	High methane content gas, design plant rates
A combination of 25-series with 57/23-series	KATALCO$_{JM}$	Low steam-to-carbon ratio, high methane content gas
		High methane content gas, design plant rates
		Feedstock with significant levels of higher hydrocarbons
Topsøe's R-67-7H	Haldor Topsøe	Reforming of light feedstocks, such as natural gas
Topsøe's R-67-7H is combined with Topsøe's series of alkali promoted catalysts	Haldor Topsøe	In high heat flux top-fired steam reformers and on feedstocks ranging from heavy natural gas to naphtha
Topsøe's RK-211/RK-201 and RK-212/RK-202	Haldor Topsøe	The reforming of heavy natural gas and off-gases from refineries or LPG only requires the lightly alkali-promoted RK-211 and RK-201 (top layer) in combination with the traditional gas reforming catalyst, R-67-7H

conditions of the different reforming steps and on the plant capacity, type of feedstock, product specifications, desired steam production, etc.

Catalysts for Tubular Reformers

A high heat transfer coefficient minimises the tube wall temperature, thereby reducing the required wall thickness. The pellet size for primary steam reforming catalysts is much larger than for the pre-reforming catalyst, and the shape is optimised for low pressure drop and high heat transfer. Hydrocarbon feeds can be as previously outlined. Table 4.7 summarises typical catalyst types from various suppliers.

Johnson Matthey Catalysts manufactures three main catalysts for use in steam reformers using lighter hydrocarbon feedstocks ranging from refinery off-gas and natural gas to lighter LPG. The KATALCO$_{JM}$ 23-series is nickel oxide on an α-Al_2O_3 support. The KATALCO$_{JM}$ 57-series is based on nickel oxide on a Ca-aluminate support. The KATALCO$_{JM}$ 25-series is based on a slightly alkalised nickel oxide catalyst on a Ca-aluminate support [92]. All catalysts are made in a range of sizes, allowing optimum reformer loading for each individual plant. The

active metal of Haldor Topsøe's R-67-7H is nickel. Less than 10 wt% nickel is supported on an Mg-aluminate carrier.

A pre-reduced catalyst R-67R-7H is available to load the top 10–15 % in the tubes in order to support initiation of the reforming process immediately. Particles of a relatively larger size are often used in the lower part of the tubes to compensate for the pressure drop that usually is generated in the bottom half [90].

Haldor Topsøe's RK-200-series features alkali-promoted reforming catalysts. The RK-200 series uses nickel-containing catalysts based on a ceramic calcium magnesium aluminate carrier promoted with potassium oxide. The ceramic carrier does not contain any free magnesium oxide; therefore, there is no possibility of hydration of the catalyst during startup or during operation. The RK-200 series offers two types of alkali-promoted reforming catalysts:

- Low-alkali version, RK-211 and RK-201
- High-alkali version, RK-212 and RK-202

Catalysts for Naphtha Reforming

The steam reforming of naphtha requires a catalyst for primary reforming with even higher cooking resistance and hence a higher amount of potassium promoter. For this severe service, a nickel-containing naphtha steam reforming catalyst is on the market. The refractory support of ReforMax 250 is promoted with potassium and comprises oxides of calcium, magnesia and alumina. The concept of ReforMax 250 is similar to that of ReforMax 210 LDP. The potassium is mainly incorporated in the carrier and is released as needed on the catalyst surface.

Naphtha feeds can contain significant amounts of aromatics so that the risk of carbon formation increases dramatically. ReforMax 250 is optimised for processing naphtha feeds. Its high amount of potassium suppresses carbon formation throughout the catalyst life and the high amount of 18 % Ni on the catalyst balances cooking resistance and catalyst activity. The naphtha reforming activity of ReforMax 250 is very high and leaves no naphtha or heavy hydrocarbons as feed in the bottom part of the reformer part. Standard loadings are therefore mixed loadings with ReforMax 250 in the top (40–60 % of the tube) followed by a layer of ReforMax 330 LDP. Potassium migrates with time on stream to a certain extent down the tube and leads finally to waste heat boiler (WHB) fouling. The potassium concentration in the wet reformed gas at the exit of the reformer tubes is typically about 1,000 ppb.

ReforMax 250 can be applied for steam reforming of almost any type of naphtha. The primary reformer processing of naphtha is normally designed for pressures of 30–35 bar and outlet temperatures of 800–830 °C. The recommended S/C ratio under these conditions can be as low as 3.0 mol/mol.

The formation and accumulation of carbon on the catalyst is controlled by reaction kinetics. During normal operation, the rate of carbon removal is much greater than the rate of carbon formation. Therefore, carbon accumulation is unlikely. The rate of carbon formation, however, increases with the following:

- Heavier feedstocks
- Lower S/C ratios
- Higher gas temperatures.

Accumulation of carbon on the catalyst occurs when the rate of carbon formation exceeds the rate of removal. In such cases, catalytic activity and void fraction will be reduced, resulting in the following:

- Poor conversion
- Increased tube wall temperatures
- Catalyst breakage
- Increased pressure drop.

Process upsets that lead to cracking reactions include the following:

- Loss of steam
- Temperature drifts
- Feed composition changes
- Catalyst poisoning.

Other Application Aspects

Catalyst Compounding

The catalyst is prepared by mixing hydrated alumina, Ca-aluminate and colloidal-dispersed titanium compound with water, molding the mixture, pre-calcining and calcining the moldings to form the support, and coating the resulting support moldings with nickel. This type of calcium-promoted, alumina-supported, nickel-reforming catalyst stabilised with titanium is particularly useful for reforming reactions in feed streams containing significant quantities of CO and CO_2, low quantities of steam (the feed stream having a H_2O/CH_4 of less than 0.8 and a CO_2/CH_4 of greater than 0.5), and relatively high quantities of sulphur compounds (up to about 20 ppm) [93].

Reactors

Several types of reactors are used for steam reforming—that is, the conversion of hydrocarbons with steam into carbon oxides, hydrogen, and methane. The main types are

- Tubular reformers
- Adiabatic reformers
- Heat exchange reformers (HER).

In a conventional steam reforming process, hydrocarbons and steam are catalytically converted into hydrogen and carbon oxides. Because the overall reaction is a highly endothermic reaction, heat has to be provided externally. Because the methane level in the reformed gas should be at a minimum, the temperature at the

reformer outlet has to be as high as possible. However, the outer wall temperature and the wall thickness of the reformer tubes are limited—that is, the higher the reformer temperature, the lower the pressure to be specified. Because a low reformer pressure requires higher compression energy, an optimum has to be achieved between reformer temperature (methane slip) and reformer pressure (compression energy).

The composition of the reformed gas is characterised by the stoichiometric number (SN) and should be 2.0 or slightly above for the methanol synthesis.

$$\mathrm{SN} = (\mathrm{mol\ H_2} - \mathrm{mol\ CO_2})/(\mathrm{mol\ CO} + \mathrm{mol\ CO_2}) \tag{4.38}$$

If a natural gas with a high methane content is used as feedstock and no CO_2 is available, a SN of 2.8–3.0 is attained in the product gas.

The preheated reformer feed—a mixture of natural gas and process steam—is distributed via a header in the steam reformer upper section into parallel manifolds and then through an inlet pigtail system to each individual reformer tube. The tubes filled with catalyst are arranged in rows, with each having a fired length from 2.5 to 14 m. The tube diameter varies between approximately 6 and 20 cm and the wall thickness is between approximately 1 and 2 cm. The lifetime for the tubes is designed for >100,000 h.

The reforming reactions take place in a temperature range from approximately 600 °C at the inlet to the catalyst bed to approximately 950 °C at the outlet, requiring high alloy, Ni-based, centrifugally cast and inside machined tubes to withstand the combination of high pressure and temperatures, oxidising atmosphere on the outside and reducing atmosphere on the inside.

Because the main reaction is highly endothermic, heat to the catalyst tubes has to be supplied by external firing. During normal operation, a mixture of purge gas from the synthesis unit, off-gas from the distillation unit and natural gas is used for firing the reformer. For startup purposes and during upset conditions, only natural gas is used as fuel. The reformed gas consisting of H_2, CO, CO_2, inerts, non-converted CH_4 and steam leaves the reformer tubes and is passed to the outlet manifold into the reformed gas waste heat section.

Steam/Carbon Ratio

For trouble-free operation of a catalyst as for example ReforMax 210 LDP, it needs to be operated at certain minimum S/C ratios depending on the carbon number of the feed (see Table 4.8). It has been demonstrated in many commercial plants that the use of promoted catalysts can allow operation of the primary

Table 4.8 Typical steam-to-carbon (S/C) ratios (p = 30 barg) [94]

Feed	S/C Ratio (mol/mol)
Natural gas	2.6
Ethane (C_3 < 3 vol%)	2.8
Propane (C_4 < 30 vol%)	3.3
Butane	3.5
Hexane (C_7 < 1 vol%)	4.5

reformer with heavy feed gases without any significant operational changes. Problems due to carbon formation can be eliminated.

CO_2 as Additional Feedstock

If CO_2 is available for the methanol production, the carbon yield can be increased considerably. Especially for CO-rich syngas (e.g. MeOH, OXO), the process economics can be significantly improved (offsetting the additional investment for the CO_2 removal section including CO_2 compression).

Tube Wall Temperature

The effect of the catalyst activity on the tube wall temperature depends significantly on furnace design and operation. It is thus necessary to have a deeper understanding for the relationship between activity and heat transfer.

Heat transfer is represented by the equation:

$$\mathrm{Q/A} = U(T_{OW} - T_G) \tag{4.39}$$

where U is the overall heat transfer coefficient. Approximately 70 % of the heat flux (Q/A) is used in the reforming reaction and approximately 30 % is used for the sensible heat. The driving force for getting heat into the tube is the temperature difference between the outer tube wall (T_{OW}) and the gas inside the tube (T_G). In sections of the tube where the reaction is far away from reforming equilibrium, a more active catalyst can achieve more endothermic reforming and will hence consume a larger part of the incoming heat. This will result in a lower gas temperature in that region and allow the same amount of heat input starting with a cooler outer tube wall temperature.

However, in regions of the tube where the gas is already close to the reforming equilibrium, a more active catalyst cannot achieve additional reforming. In this case, there will be little effect on the temperature of the gas and of the outer tube wall in that section.

Thermal Shock Resistance

The catalysts need to have high mechanical and thermal stability as well as high thermal shock resistance at temperatures greater than 800 °C, particularly at more than 850 °C, and at pressures up to 30 bar in an environment consisting essentially of steam, hydrogen and carbon dioxide. Furthermore, the catalyst has to withstand abrupt temperature changes (e.g. during plant trips) and the resulting high thermal stresses. If the thermal stresses at a certain point within the catalyst particle exceed a critical value, then cracks occur at this point, which can sometimes lead to the complete breakage of the particle.

Certain efforts have been made to increase the thermoshock resistance of the catalyst pellets by using additives to the conventional alumina-based nickel catalysts, such as rare earth components [95], or a variety of earth alkali oxides, such as those disclosed in DE000002431983C2, which describes a catalyst for the steam reforming of hydrocarbons that contains a refractory nickel-containing Ca-

aluminate catalyst (carrier: 10–60 wt% of calcium oxide, 0–30 wt% beryllium oxide, magnesium oxide, and/or strontium oxide, 30–90 wt% alumina, and less than 0.2 wt% silica). The increase in crush strength is mainly ascribed to the use of Ca-aluminate with low silica content. This type of catalyst can be further improved by including in the alumina/calcium aluminate support approximately 0.2–10 wt% (preferably approximately 0.8–5 wt%) of titanium dioxide, related to the total weight of the support. The titanium dioxide apparently causes a conversion of the calcium so that the latter is at least partially in the form of a hibonite [$CaO(Al_2O_3)_6$] phase in an α-Al_2O_3 matrix as defined by X-ray diffractometry. The catalyst contains approximately 7–15 wt% of nickel (relative to the weight of the support). In addition to the nickel, the catalyst can also contain minor quantities of cobalt, according to the patent. The support is preferably a bulk material in the form of spheres, cylinders, rings, or other moldings [96].

4.3.2.5 Pre-reforming of Heavier Feedstocks

If the feedstock contains fractions of higher hydrocarbons including aromatic compounds or consists of naphtha, the tubular reformer catalyst under normal steam-methane reforming conditions is prone to carbon deposits due to cracking reactions. For these feedstock materials, pre-reforming is the technology of choice. The pre-reformer usually is a fixed-bed adiabatic reactor installed upstream of a tubular primary reformer or in combination with an autothermal reformer (ATR) (see Sect. 4.3.3) [97]. The adiabatic pre-reformer converts the higher hydrocarbons by steam reforming into a mixture of methane, hydrogen and carbon oxides.

The purpose of installing a pre-reformer is to convert higher hydrocarbons before reaching the main reformer stage to increase the capacity of the reformers, to stabilise and reduce the load to the downstream main reformer, to reduce overall steam consumption (and in the case of downstream autothermal reforming (ATR), oxygen consumption). Last but not least, the potential of coking with the use of higher than methane hydrocarbon feedstocks is minimised. A pre-reformer principally operates at lower temperatures than normal steam reforming and applies the principle of the "equilibrated gas". In some cases, a combined catalyst bed design with a layer of pre-reforming catalyst at the inlet bed of tubular reformers is used instead of a separate pre-reforming reactor. The feedstock is converted in the pre-reformer over a high nickel-containing catalyst into a mixture, mainly consisting of CO, hydrogen and methane (Fig. 4.28).

The principle reactions are as follows (see also equations in Table 4.4):

$$C_mH_n + mH_2O \leftrightarrows mCO + (m + n/2)H_2 \tag{4.40}$$

$$CH_4 + H_2O \leftrightarrows CO + 3H_2 \tag{4.41}$$

as well as the water gas shift (WGS) reaction:

$$CO + H_2O \leftrightarrows CO_2 + H_2 \tag{4.42}$$

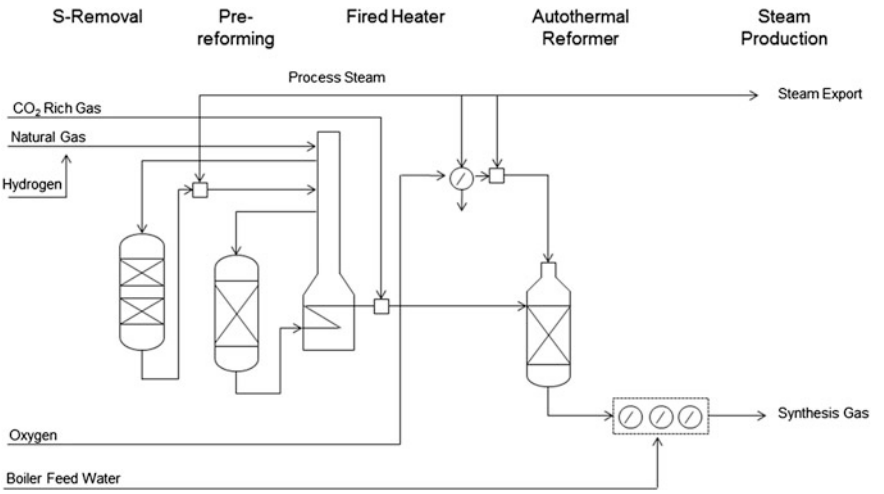

Fig. 4.28 Process design for syngas production by adiabatic pre-reforming and an autothermal reformer [64]

Although the reforming reactions are endothermic, the WGS reaction is exothermic. In the case of methane reforming, the overall heat of reaction would be endothermic; it can become exothermic for heavy feedstocks (naphtha).

The typical operating temperature of a pre-reformer is in the range of 400–500 °C, which is lower than in a primary reformer. Typical gas space velocities are 2,000–4,000 $m^3/(m^3h)$ or, on a wet basis, 10,000–14,000 $m^3/(m^3h)$, with a S/C ratio in the range of 1.0–3.5 depending on feedstock composition (where an aromatics content of up to 3.0 % can be tolerated). With increasing operating temperatures, the exothermic formation of methane is thermodynamically favoured at the expense of reforming reactions. This can be compensated for by a higher inlet S/C ratio through the higher heat capacity of the total feed and moderation of the methanisation equilibrium.

All poisons in the feedgas, specifically sulphur leakages from the upstream desulphurisation stage, must be removed in order to protect the pre-reformer catalyst.

Commercial Pre-Reforming Catalysts

General

The pre-reforming process was developed initially for the production of methane-rich gases for use as town gas and synthetic natural gas (SNG). Today, the technology is used as the first step in steam reforming of heavier feedstock, including

Table 4.9 Selected commercial pre-reforming catalysts for pre-reforming of heavy feedstock (open literature only) [105]

Supplier	Commercial name	Feedstock/ application	Active metal, wt%	Promoter, wt%	Carrier
Haldor Topsøe [106, 107]	RKNGR	Natural gas, LPG, naphtha; aromatics up to 30 wt%	NiO: 25	–	MgO, Al_2O_3
Johnson Matthey/ Katalco	46-3Q	Naphtha	NiO: 23	K_2O: 7 Na_2O: <0.5	$CaAl_2O_4$, ZrO_2, SiO_2
Abbott and McKenna [75], Shekawat [107]	46-5Q	Light hydrocarbon and naphtha	NiO: 20	K_2O: 1.8	$CaAl_2O_4$, SiO_2 $CaAl_2O_4$
Clariant [107], Süd-Chemie (2005)	ReforMax 100	Natural gas: naphtha/ adiabatic reactors	NiO: 56	–	Balance
Clariant [107], Süd-Chemie (2005)	ReforMax 250 (C11-NK)	Naphtha/top of bed in tubular reformers, fired by outside burners	NiO: 25	K_2O: 8.5	$CaAl_2O_4$

naphtha, which now has gained universal acceptance as a means of improving the efficiency and solving problems associated with the conventional tubular steam reforming process.

The pre-reforming catalyst converts higher hydrocarbons that are present in the natural gas feedstock into a mixture of methane, carbon dioxide, carbon monoxide, and hydrogen. Moreover, the pre-reforming catalyst can adsorb any slip of sulphur from the desulphurisation section. Because the pre-reforming catalyst is more expensive than the SMR catalyst, reliable upstream desulphurisation is recommendable. The catalyst life depends on the operating conditions and feed composition. A number of factors influence the deactivation such as sintering, poisoning and carbon formation [88, 98–104].

For a pre-reforming catalyst, a high nickel surface area is essential due to the low temperature of operation in adiabatic reactors with moderate reactor size. The catalyst crush strength, thermal shock resistance and pressure drop are less important than in other applications. This allows the use of catalyst pellets of moderate size to be used in pre-reforming reactors. Pre-reforming catalysts have been reviewed by Boon and van Dijk [105] (Table 4.9).

In addition, a naphtha steam pre-reforming catalyst YS-Z501 has been described. This catalyst, with more than 50 wt% nickel, has an active component and multipore complex substance as carrier [108]. The operating temperature is reported to be in the range of approximately 360–560 °C and the operating

pressure is recommended to be between atmospheric and 6.0 MPa. The optimum steam/carbon ratio is approximately 1.5–3.0 and the carbon space velocity is approximately 1,000–3,000 h^{-1}.

All these catalysts feature the following:

- Excellent reforming activities and stability, especially high activity at low temperature
- Ability to converting all C_{2+} hydrocarbons to methane-rich gas
- Suitability for pre-reforming under high space velocity
- Excellent reducibility; able to be reduced in pre-reformer
- Stability for long service life
- Suitability for a wide range of feedstocks.

Selected Commercial Pre-reforming Catalysts

Catalco JM (Johnson Matthey Catalyst) pre-reforming catalysts include CRG-LH, CRG-LHR, CRG-LHC and CRG-LHCR (CRG stands for 'catalytic rich gas'). The CRG LH is a precipitated catalyst based on nickel (45–50 wt% nickel as NiO) as the active component and on a carrier composed of magnesium, silicon, potassium, chromium, calcium, and alumina as Al_2O_3. This type is compared with CRG F (75–81 wt% nickel as NiO) on alumina containing 0.2 wt% silicon as SiO_2 and 0.35 wt% potassium [109]. The catalyst is supplied pre-reduced and stabilised: the oxidised form is available as a special order.

Haldor Topsøe's pre-reforming portfolio includes the RKNGR and AR-301 catalysts, as well as a new generation of pre-reduced pre-reforming catalysts, designated AR-401, with 35 wt% Ni on activated $MgAl_2O_4$.

4.3.2.6 Steam Reformer Designs

Economically, the steam reforming process is driven by optimum product and heat integration. Because hydrogen purification usually is done with PSA, there is a residue of tail gas from the PSA plant. This contains unconverted methane, carbon monoxide, carbon dioxide, residue water and hydrogen. The tail gas is used as the main heat source of the steam reformer furnace and contributes approximately 85–90 % of the heating value to the furnace. Additionally, this is a very economical and environmentally benign way to make use of byproducts and residues from steam reforming by using their heating value and destroying them to water and carbon dioxide. Natural gas only contributes 10–15 % of energy to the furnace in regular operations, and of course the heat demand during startup of the plant.

Besides the reliability of this mature process, the energy integration is a major success factor for steam reformer plants. Because the steam reforming reaction occurs at temperature of 800–950 °C, the temperature of the furnace is even hotter (approximately 1,100–1,200 °C), while the educts and products have ambient temperatures and the flue gas is released just slightly above the dew point with roughly 130 °C. Hence, exergy optimisation by heat exchange is the key driver of

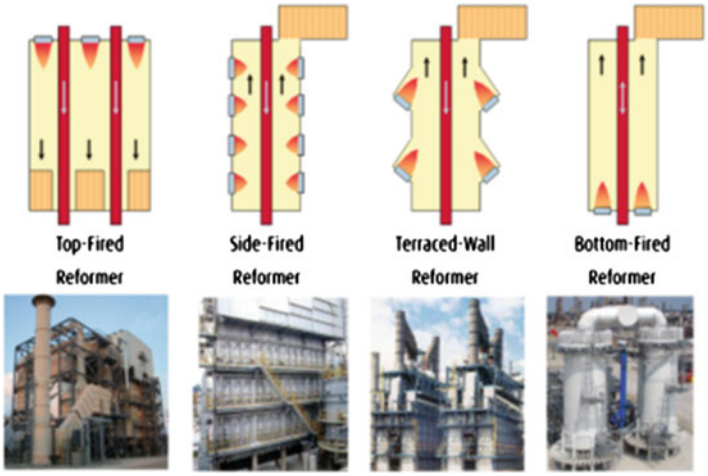

Fig. 4.29 Steam reforming technologies with tubular reformer types [110]

the process economy. Hence, the process makes use of flue gas temperatures in four different heat exchangers and utilises the heat flux in the product stream, as well as in four main heat exchangers. Only low-temperature heat has to be removed without further use in one air cooler and one water cooler.

Steam reformer designs exist as top-fired, side-fired, so-called terraced-wall,and bottom-fired reformers in the market (Fig. 4.29). Designs are proprietary to each technology company and are also a result of the design requirements for a certain capacity class of reformers.

The reactions taking place under the steam reforming process are given in Table 4.10 along with the enthalpy of reaction and the equilibrium constant [64]. Reactions 1 and 2 in Table 4.10 are the steam and CO_2 reforming reactions for methane and reaction 3 is the WGS reaction, which takes place simultaneously. The WGS reaction is fast and is generally considered in equilibrium. Reaction 4 is the steam reforming reaction of higher hydrocarbons. The enthalpy and equilibrium constant of reaction 4 is given for steam reforming of n-heptane.

Table 4.10 Key reactions in steam reforming [64]

	Standard enthalpy of reaction ΔH_{298K} (kJ/mol)	Equilibrium constant $\ln K_p = A + B/T$	
		A	B
1. $CH_4 + H_2O \leftrightarrows CO + 3H_2$	−206	30.420	−27.106
2. $CH_4 + CO_2 \leftrightarrows 2CO + 2H_2$	−247	34.218	−31.266
3. $CO + H_2O \leftrightarrows CO_2 + H_2$	41	3.798	4,160
4. $C_nH_m + n\ H_2O \leftrightarrows n\ CO + (n + m/2)\ H_2$ for H_2n-C_7H_{16}	−1,175	21.053	−41.717

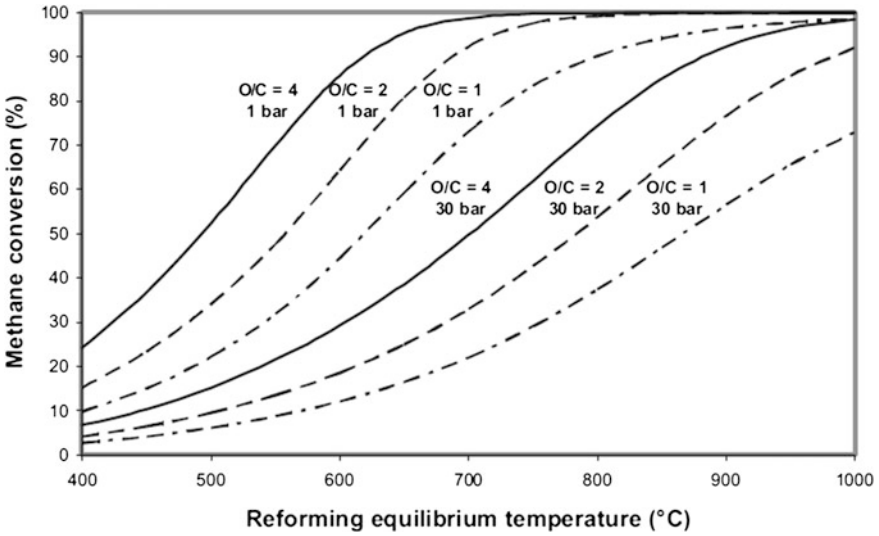

Fig. 4.30 Steam reforming and methane conversion. O/C: ratio of steam to methane in the feed gas [70]

The steam reforming reactions are strongly endothermic and lead to gas expansion. This means that reaction 1 is favoured at low pressure and high temperature, as illustrated in Fig. 4.30, where the equilibrium conversion is shown as a function of temperature and pressure. However, for industrial applications, the optimum window of operation conditions needs to be determined in view of supply pressure, steam host and total cost of ownership. The heat required for converting a 1:2 mixture of methane and steam from 600 °C to equilibrium at 900 °C is 214 kJ/mol CH_4 at 30 bar.

One has to distinguish between fired heaters, in which the heat is provided mainly via radiation through burners on the outside of the tubes, and HER, in which the heat is provided via convection from flue gas or process gas.

(A) **Fired Heaters**

The general furnace classifications according to firing patterns are described in the following [111].

Top-fired

A top-fired furnace is characterised by having the burners in the top and firing down. The tubes are often installed in parallel rows, with the burners firing down between each row. The principal radial temperature profile of the tubes is shown in Fig. 4.31. Examples include the furnaces by Kellogg/KBR, Davy Process Technologies, Humphreys & Glasgow, Technip/KTI, UHDE and Lurgi. A top-fired furnace sometimes is called a roof-fired furnace (see Figs. 4.32, 4.33, right.).

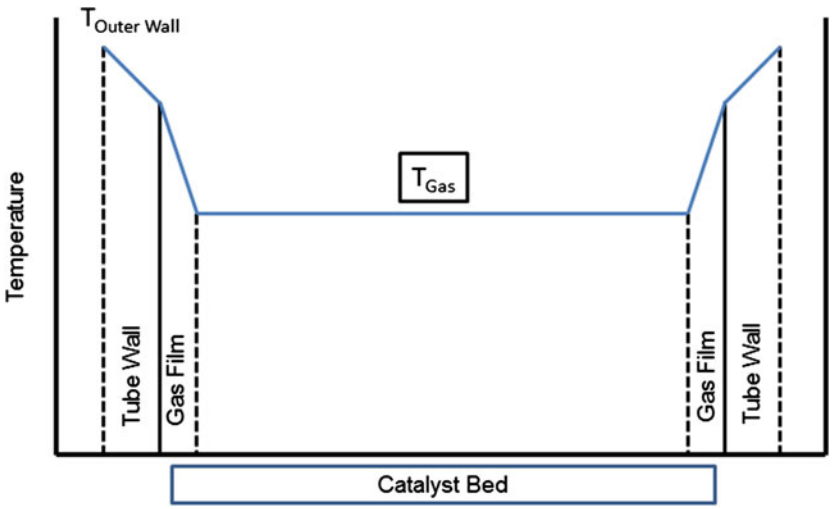

Fig. 4.31 Radial temperature profile for a top-fired furnace (40 % down from the top end of the pipe) [112]

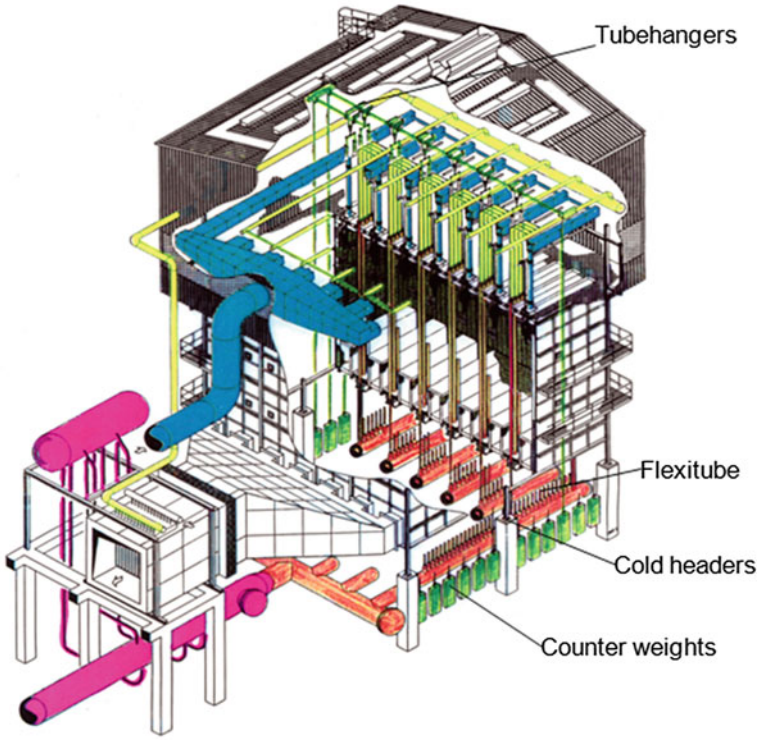

Fig. 4.32 Arrangement of top-fired reformer. (Courtesy of Air Liquide Global E&C Solutions)

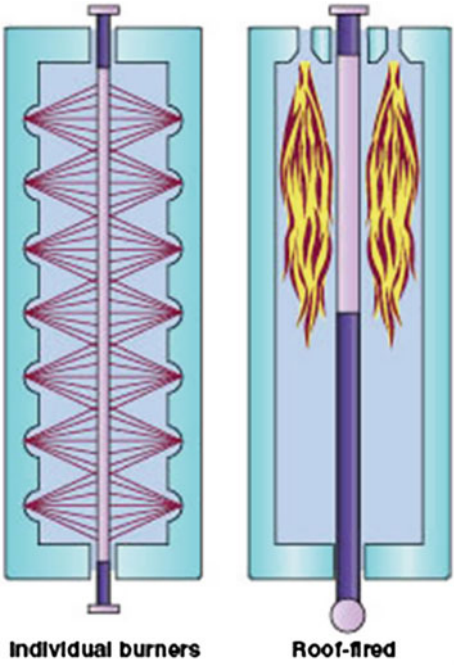

Fig. 4.33 Side-fired (*left*) and top-fired (*right*) burner. Maintaining a tube wall temperature that is hot enough for the reforming reaction is a critical factor in reformer heater design. © 2011 Chemical Engineering Processing, 29 May 2010 [115]

In top-fired reformers with very high heat flux (typically 75,000–95,000 W/m^2), the maximum tube wall temperatures are usually 30–40 % from the top, where the reaction can be significantly away from equilibrium (see Fig. 4.34). Thus, large reductions of the maximum tube wall temperature (typically 25–50 °C) can be achieved. The temperature differences cause significant variations in the methane reaction rate along the radial position, whereby the catalyst close to the reforming tube centre is poorly used [113].

As a typical example of a top-fired heater, the Lurgi reformer is described in the following (see Fig. 4.32). The reformer features an inlet pigtail design, which allows an inlet temperature of up to 650 °C, thus enabling one to achieve high radiant efficiencies with a reduced number of reformer tubes, a more uniform tube wall temperature, and reduced fuel requirement combined with lower NO and CO_2 emissions. The internal insulation at the top of the reformer catalyst tube avoids the damage of outside insulation by the tube movement. The flange bolts remain relatively cool, even at inlet temperatures of 650 °C, so that no periodic retightening is necessary. The insulation inserts are designed with a diffuser outlet. This diffuser ensures a gradual temperature profile at the tube inlet and optimally recovers the pressure drop.

The counterweight tube support system provides for upward expansion from the furnace outlet header. The system provides real constant load support for the tube over the whole range of movement, in contrast to the only approximate characteristic of spring or so-called constant-load hangers. The tubes remain straight without any necessity for routine readjustment.

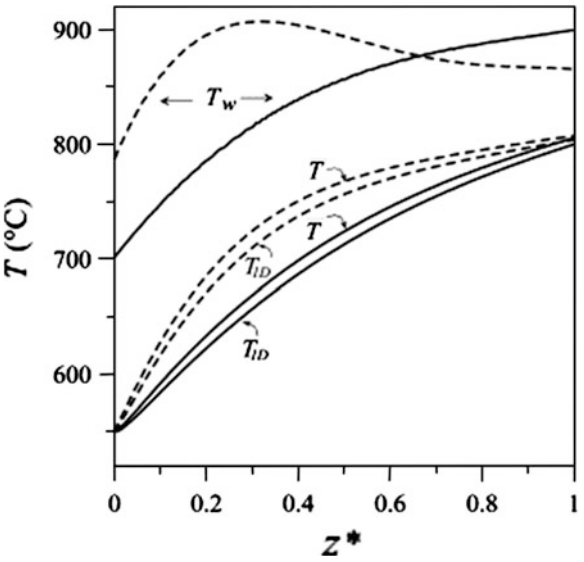

Fig. 4.34 Tube skin temperature (T_w), radial mean temperature (T) and temperature predictions given by the one-dimensional model (T_{1D}) as a function of the dimensionless reactor length for top-fired (*dashed lines*) and side-fired (*solid lines*) reformers [116]

The outlet system uses a "straight pigtail," which is welded to the cold header nipple. The cold header ensures minimum expansion of the header and the straight pigtail provides a flexibility that is not possible with a direct welded reformer tube. The external insulation around the pigtail is enclosed in a flexible stainless steel bellows-type casing, which is gasket-seated and clamped, both with the header nipple and the reformer box floor. By using this design for a large furnace, one can exploit the full capability of the reformer tube without other restrictions, be it pigtail or header length. Furthermore, the outlet system allows "tube nipping" during operation.

The design incorporates an additional feature that protects the tube-to-header transition from metal dusting at high outlet partial pressures of CO. Because the reformer tube is at approximately 800–950 °C and the header at approximately 200 °C, inevitably at some point or other in the transmission from tube to header the material is in the metal dusting range. The design provides for the introduction of a burner gas at the critical point, thus ensuring that materials are not exposed to a metal dusting gas atmosphere.

Side-fired (Tier)

Side-fired furnaces are characterised by having multiple-level burners firing backwards on heat-resistant refractory. The tubes are heated by the resulting radiation (see Fig. 4.33, left). Examples include furnaces by Haldor Topsøe and Selas [114].

In a side-fired reformer with medium to low heat flux (typically <70,000 W/m^2), the maximum tube wall temperatures are usually towards the bottom of the tube in a region where the reforming reaction is very close to equilibrium (see Fig. 4.34).

There, a more active catalyst may not be able to reduce the maximum tube wall temperature. However, activity reserves will allow these tube wall temperature levels to be maintained for a longer time on stream.

In side-fired furnaces, a reduction of the maximum tube wall temperature is possible if the furnace firing can be adjusted to put more heat into the top half of the tube, where the tube skin temperatures are cooler. This reduces the amount of heat required in the bottom zone below and hence lowers the maximum tube wall temperature.

Side-fired (Terrace)

Side-fired (terrace) furnaces are characterised by having one to three terraces with the burners firing up the side walls. The tubes can be in one straight row or two offset rows (staggered). Examples include furnaces by Foster Wheeler and Alcorn.

Bottom-fired (Box)

A bottom fired (box) furnace is characterised by having the burners in the bottom firing up between the tube rows.

Bottom-fired (Cylindrical)

A bottom-fired (cylindrical) furnace is characterised by having the burners in the bottom firing up between the tube rows. The tube rows run radially from the centre of the furnace to the outer wall.

The different types of reformers, including their burner arrangements, result in different heat fluxes and temperature profiles over the tube length. Adapting the different catalyst types to the heat flux profile optimises the reformer efficiency and allows for substantial part load operation for some reformer types (down to 30 %).

Compact Reformer

The fundamental processes taking place within the compact reformer are the same as those in a conventional steam reformer. Fresh feed mixed with steam enters the reformer tubes, where it passes over the reforming catalyst. Heat for the reforming reaction is provided by firing on the shell side of the reformer.

In the compact reformer, three of the main process steps involved in conventional steam reforming are incorporated into a single unit: reforming of process gas, reformed gas cooling and preheating of combustion air and fuel. The reformer can be divided into three sections (see Fig. 4.35). In the ‘feed preheat’ section, combustion on the shell side is complete and the combustion gases are relatively cool. Enhanced heat transfer is used to maximise the heat recovery from the flue gases into the process, which is also relatively cool at this stage.

The majority of the reforming reaction takes place in the ‘combustion zone’, where combustion is taking place and the temperature of the combustion gases is much higher. The catalyst bed ends at the top of the combustion zone. The reformed gas then enters the ‘air/fuel preheat’ zone, where it is cooled by counter-current heat exchange with cold combustion air. The combustion air in turn

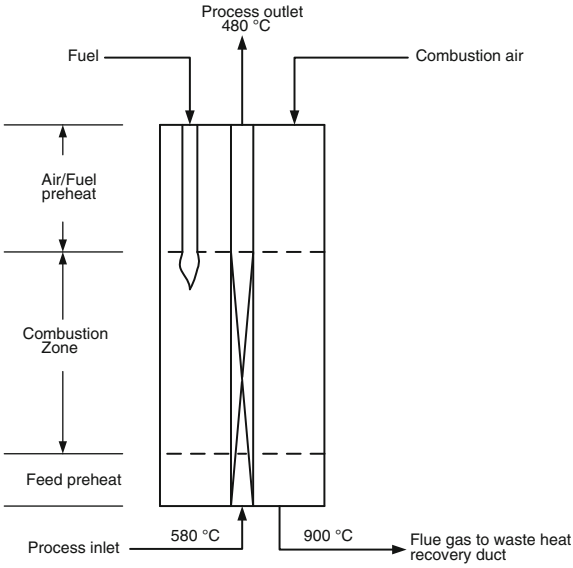

Fig. 4.35 Process principle of a compact reformer [117]

transfers heat to the fuel. Finally, the cooled reformed gas is collected in a header and leaves the device.

The incorporation of the air/fuel preheat zone means that the reformed gas is relatively cool when it leaves the reformer. This eliminates the need for a costly reformed gas boiler and steam system. Any steam or power required on the plant can then be provided by the most appropriate means (e.g. package boiler, gas turbine).

The compact reformer is designed to maximise the rate of heat transfer between the flue gas and the process gas. This results in an improved thermal efficiency compared to a conventional reformer and is achieved using a combination of methods:

- The firing is counter current to the process gas flow inside the tubes.
- Much smaller tubes are used than in a conventional reformer, giving a large surface area to volume ratio.

This is achieved by the following methods:

- The process tubes are much more tightly packed than in a conventional reformer
- Enhanced heat transfer is used where possible to maximise heat transfer rates and ensure the maximum amount of heat is recovered from the flue gas into the process.

In the early 1990s, this concept was tested in single tubes; a 0.3 million standard cubic feet (SCF) per day natural gas pilot unit was built and subsequently operated. This unit provided firm evidence of the potential for low-cost reformer

Fig. 4.36 DPT compact reformer [117]

technology with enhanced thermal efficiency, but it was realised that a new design approach was required. Figure 4.36 illustrates this pilot unit.

In a conventional reformer, the dominant heat transfer mechanism is radiation with convective heat transfer from the hot flue gases, accounting for less than 5 % of the total heat transferred to the tubes. In the compact reformer, this situation is reversed. The small, closely packed tubes are designed to promote convective heat transfer and the relatively small volume of flue gas reduces the potential for radiate heat transfer from the gas. Hence, about 90 % of the total heat transfer is by convection.

The compact reformer is conceived as a modular device. Scaling to various capacities from relatively small hydrogen plants to world-scale plants can then be achieved by installing the required number of standard modules. The construction of the modules is relatively simple and opens up the possibility for mass manufacture in a factory before transporting to the site for installation. Transportation is relatively straightforward; a single module will fit inside a standard shipping container. On an equal capacity basis, a compact reformer-based system occupies about 25 % of the plot area of a conventional steam reformer, with a corresponding reduction in weight [117].

(B) **Heat Exchange Reformers (HER)**

To reduce the capital cost of syngas-based processes and to decrease exergy losses, the heat-exchanger reforming system was developed. In HER, sometimes also called convective reformers, hydrocarbon gas together with steam is exposed to convective heat that is supplied by process gas or flue gas. The design is comparable to conventional tube heat exchangers. Examples are shown in Figs. 4.37 and 4.38. The catalyst is either filled inside tubes or in the space between tubes.

The amount of heat transferred to process gas may increase from approximately 50 % to approximately 80 % by using heat exchange devices [118]. However, because the heat exchange occurs dominantly by convection, heat fluxes are lower,

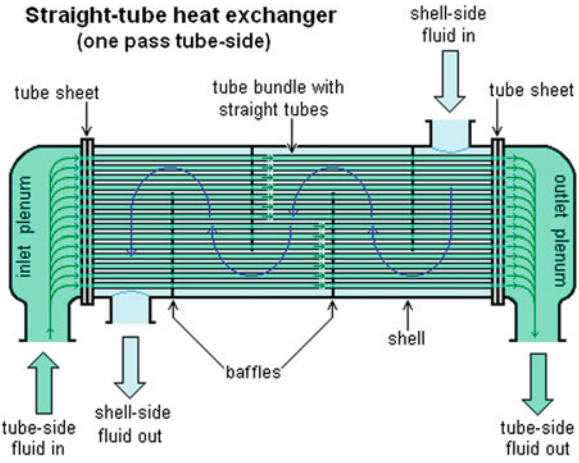

Fig. 4.37 Conventional straight-tube heat exchanger [119]

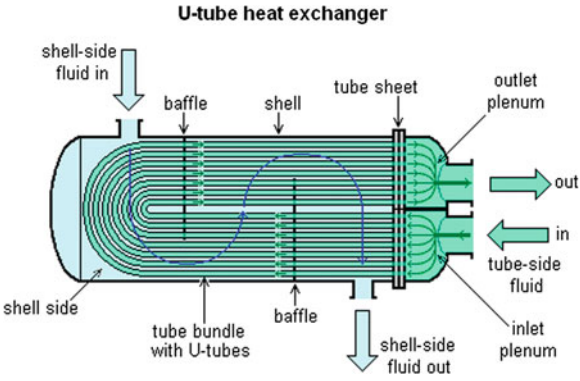

Fig. 4.38 Conventional U-tube heat exchanger [120]

resulting in bigger equipment than in tubular reformers with radiant heat transfer. Therefore, for large plants, this type of reformer cannot be a stand-alone solution but is operated in conjunction with another reformer.

Several types of HER have been developed, which can be grouped into three categories: (a) flue gas heated reformers (straight through), (b) flue gas heated reformers (bayonet tube concept), and (c) process gas heated reformers (gas-heated reformers, GHR), as shown in Fig. 4.39.

As mentioned, HER heated by process gas, which are called GHR, usually are fitted to another reformer, such as a fired tubular reformer, an air or O_2-blown secondary reformer, or an ATR.

In 1994, ICI (now part of Johnson Matthey Catalysts) extended the GHR concept into methanol production as part of the leading concept methanol technology. In the meantime, several design improvements (simplification of the fabrication, reliability, optimisation of the materials of construction) resulted in the

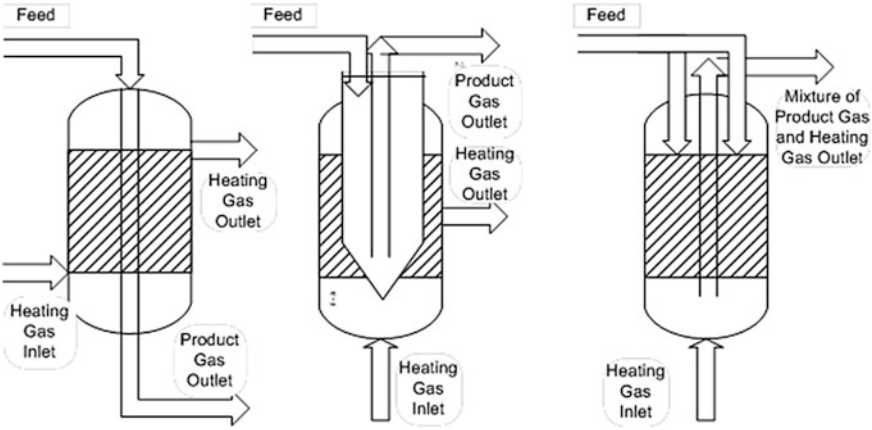

Fig. 4.39 Types of heat exchange reformers. Adapted from Aasberg [64]

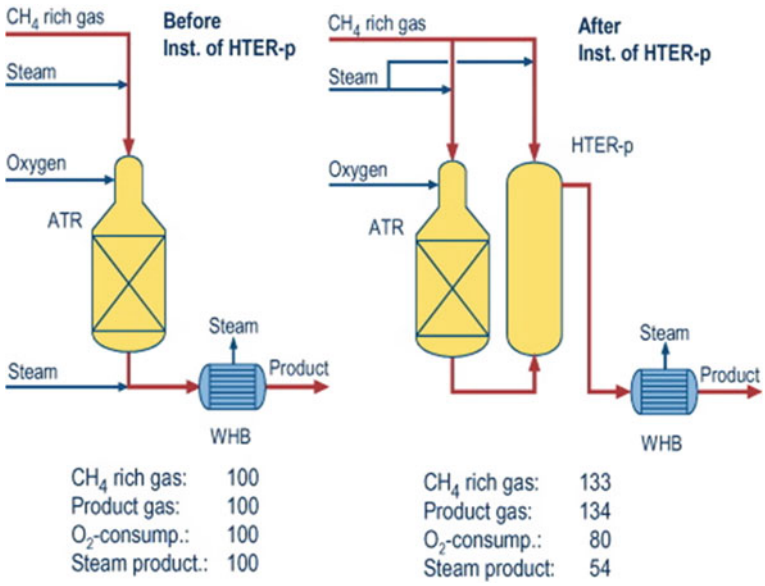

Fig. 4.40 Gas-heated reformer (*HTER*) in combination with autothermal reforming [122]. Adding the HTER to an ATR of the same size allows to increase the product gas production by 34 %, whilst reducing the O_2 consumption by 20 % and the steam production by nearly 50 %. (Numbers are in percentages)

advanced gas-heated reformer (AGHR). The AGHR concept is based upon the proven GHR and is optimally linked with an ATR, as presented in Fig. 4.40, in which the advantages are also summarised.

Topics to be mentioned are:

1. Metal dusting for HT reformers with a low S/C ratio (S/C < 2)
2. GIAP (now part of Clariant) design for ammonia plants can operate because they use a high S/C ratio (S/C > 2)

Further details on various heat exchanging reformers are discussed by Aasberg et al. [64].

4.3.3 Autothermal Reforming

The required heat for the endothermic reforming reactions is supplied by an autothermal catalytic reforming step, whereby internally partial and/or total combustion of part of the feed with oxygen or air provides the heat according to the following equations:

$$C_mH_n + (m + n/4)\ O_2 \rightarrow m\ CO_2 + n/2H_2O \tag{4.43}$$

$$CH_4 + 2O_2 \rightarrow CO_2 + 2H_2O \tag{4.44}$$

Compared these with the following equation:

$$C_mH_n + m/2O_2 \leftrightarrows mCO + n/2H_2 \tag{4.45}$$

In principle, the process can be executed by two different options: (a) ATR (with flame), which is common practice for today's large-scale syngas plants or (b) flameless ATR using catalytic partial oxidation (CPO), which is subject to current scientific work.

4.3.3.1 Characteristics of the Autothermal Reforming Process

The principal facts characterising the autothermal catalytic reforming process are described here. ATR produces high volumes of carbon-free synthesis gas with a low H_2/CO ratio for large-scale applications for methanol or Fischer–Tropsch. In these cases, there is a significant economic advantage compared to tubular reforming processes. In cases where cheap oxygen is available, ATR technology can also be used for the production of smaller syngas volumes, such as for CO production or Oxo-syngas. The process offers a wide range of operating flexibility, with a given installation being able to produce gas with a H_2/CO ratio varying from 1.7 to 4.7. Turndown ratios of approximately 65 % are readily achievable (Fig. 4.41).

The process is available for a wide range of operating conditions, which can be optimised for the specific application. Reformer outlet temperatures are typically in the range of 800–1,000 °C. Temperatures inside the combustion chamber are in

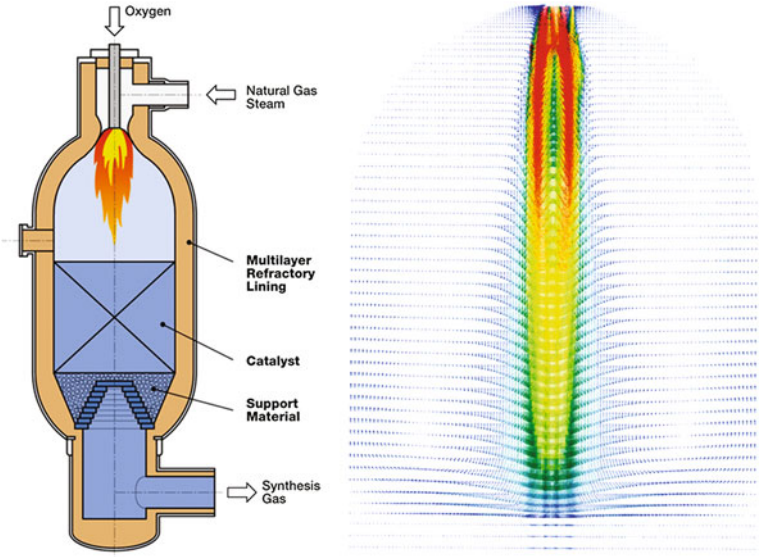

Fig. 4.41 Autothermal reactor and CFD simulation [125]

the range of 1,100–1,300 °C directly above the catalyst bed and up to 2,500 °C or more in the flame core (see Fig. 4.41). Commercial experience exists for pressures up to about 40 bar. A design for 60 bar has been incorporated into the Giga-Methanol process design (see Sect. 4.7.3).

Steam/carbon ratios can vary between 1.0 and 3.5. Operation at a steam/carbon ratio of 0.6 has been demonstrated in the Lurgi POX in Freiberg and on an industrial scale [121] (see also Sect. 4.3.3). A broad range of reactor sizes is available, with capacities running from 200,000 to 13 million m^3/day. The reactor design includes a special mixing burner so as to achieve optimal conditions for the catalyst. The reformed gas at the exit of the autothermal reactor contains H_2, CO, CO_2, N_2, Ar and nonconverted CH_4. Typically, the exit gas does not contain any soot.

The stoichiometric ratio for the methanol synthesis achieved by catalytic ATR normally is slightly less than 2. To adjust the H_2, CO and CO_2 balance, hydrogen is added from an outside source if available or generated from methanol synthesis purge gas in a PSA unit. When natural gas or oil-associated gas with high content of lighter hydrocarbons is used as feedstock, a partial removal of CO_2 from the reformed gas may be preferred. Figure 4.42 shows a typical scheme of ATR for methanol synthesis gas.

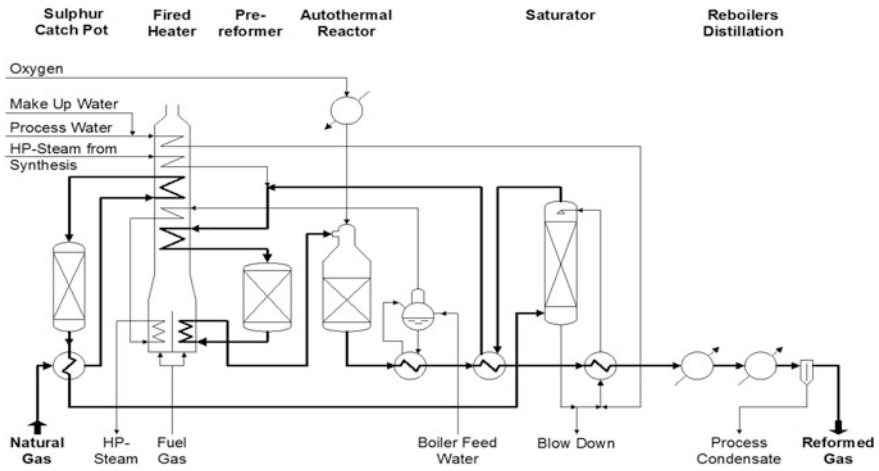

Fig. 4.42 Autothermal reformer. (Courtesy of Air Liquide Global E&C Solutions)

4.3.3.2 Commercial Catalysts for Secondary and Autothermal Reformers

In methanol plants, the secondary reformer is an oxygen-fired reformer that operates downstream the tubular reformer, "while in some synthesis gas (H_2/CO) plants, natural gas is heated in a fired heater, mixed with steam and oxygen or enriched air, and reformed in a reactor similar to a secondary reformer (ATR)" [123].

Catalysts for application in secondary and ATRs are strongly affected by diffusion limitations. The key aspect for this type of catalyst is a strong and stable catalyst carrier that can withstand the high temperatures applied in these processes. Haldor Topsøes's RKS-2-7H catalyst is based on a magnesia alumina spinel (ceramic-type) carrier with a fusion point in excess of 2,000 °C, well beyond the highest temperatures typically observed in the catalyst bed of secondary reformers. The nickel content generally is 9 wt%, except RKS2P-7H, which has only 0.5–1 wt% of nickel.

Clariant (formerly Süd-Chemie) offers two types of heat shield catalysts: ReforMax 400 GG (formerly C14-4 GG, with 12 wt% NiO on α-Al_2O_3 six-hole) and ReforMax 420 (formerly G-31 E). Active heat shield catalysts are placed as the top-bed catalyst layer while a reforming catalyst, as the main bed, is at the bottom. The fraction of heat shield layer ranges from 10 to 20 vol% of total catalyst. It is usual to protect the catalysts from direct firing by placing a heat shield on the top layer. ReforMax 410 LDP (12 wt% NiO on $CaAl_{12}O_{19}$ 10-hole)

is the bulk of catalyst loading for secondary reforming reaction. It is placed beneath an active heat shield. The fraction of this catalyst layer ranges from 80 to 90 %. The original name is C14 LDP.

Oxygen-rich ATR requires a mix of catalysts, including an active thermal shield and a reformer catalyst of excellent physical/thermal stability. The catalysts must also be resistant to thermal shocks through the flame. The standard mix is made up of a layer of 5–10 % of the catalyst to the catalyst ReforMax 420 (8 wt% NiO on α-Al_2O_3 extrudates) and ReforMax 330 LDP (12–15 wt% NiO on $CaAl_{12}O_{19}$ 10-hole).

In addition, there are other catalyst manufacturers, although with a less strong reference list. The SSR-202 (5 wt% NiO) by Sun Chemical Technology is a protection catalyst that can tolerate high temperatures at the top of the reactor. The catalyst support consists of $MgAl_2O_4$ spinel and nickel oxide. SSR-202B reveals a higher Ni content of 14 wt% NiO. Usually SSR-202 is loaded on the top layer of the reactor to protect under catalyst SSR-202B. The normal distribution is 25 % SSR-202 on the top and 75 % SSR-202B on the bottom section [124].

4.3.3.3 Autothermal Reactor Design

The ATR is a refractory-lined vertical vessel. The mixture of reformed gas from the steam reformer enters the ATR at the top. In a special mixer, the feed gas is mixed with the oxygen. At an operating temperature of about 960 °C and a pressure of about 31 bar, methanol synthesis gas with a low methane slip is produced. The synthesis gas leaves the ATR at the lower end through a special catalyst support.

Figure 4.43 shows a simplified flow sheet of the POX demonstration plant in Freiberg. Figure 4.44 gives an impression of the plant in Freiberg.

4.3.4 Combined Reforming

Combined reforming is a combination of a conventional steam reformer and an ATR. In the conventional process, natural gas is reformed with steam in a tubular reformer. The heat required for reforming is supplied by heating the reformer tubes from the outside. With the given C/H ratio of the natural gas and the hydrogen added by steam decomposition, the hydrogen surplus is such that the stoichiometric number $SN = (\text{mol } H_2 - \text{mol } CO_2)/(\text{mol CO} + \text{mol } CO_2)$ is too high for an optional methanol production. The surplus of hydrogen has to be compressed and behaves as a ballast gas in the synthesis loop; that is, it increases the size of the equipment in the loop and has to be discharged with the purge gas. Thus, it can only be used for firing the tubular reformer. In order to keep the methane level in the synthesis gas to a minimum, the outlet temperature at the reformer has to be as high as possible. However, because the outer wall temperature of the reformer tubes is limited, the wall thickness is limited as well; therefore, the higher the

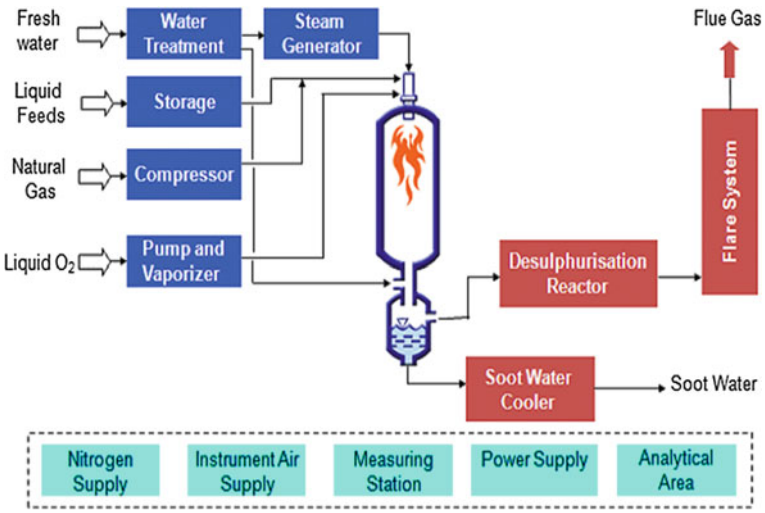

Fig. 4.43 Block flow diagram of a high-pressure partial oxidation demonstration plant in Freiberg Saxonia. (Courtesy of Air Liquide Global E&C Solutions)

Fig. 4.44 High-pressure partial oxidation demonstration plant in Freiberg, Germany. (Courtesy of Air Liquide Global E&C Solutions)

reformer temperature, the lower the pressure to be specified. Because a reformer pressure that is too low requires higher compression energy, an optimum has to be achieved between reformer temperature (inert content) and reformer pressure (compression energy).

In a conventional steam reformer, approximately 82 % of the hydrocarbons are reformed by external heating, so the fuel demand of the tubular reformer is very

high. The economy of the overall plant is very largely determined by waste heat recovery from the flue gas. In the catalytic autothermal process, the heat required for reforming is generated by partially combusting gas in the autothermal reactor. Because the autothermal reactor is a pressure vessel with inner lining, its limitations in regard to pressure and temperature are much less stringent. The temperature is limited alone by the thermal stability of the reforming catalyst and of the interior lining.

If only ATR would be applied, the heat required for reforming would largely be generated by free oxygen and the resulting synthesis gas would exhibit an understoichiometric ratio. In such cases, the SN can be adjusted by either removing CO_2, adding hydrogen from an external source, or recirculating hydrogen recovered from the purge gas. The ATR operates at low S/C ratios, thus reducing the gas flow through the plant to a minimum.

The reforming reactions may be described by the following equations:

$$CH_4 + H_2O \leftrightarrows CO + 3H_2 \tag{4.46}$$

$$CH_4 + 1/2O_2 \leftrightarrows CO + 2H_2 \tag{4.47}$$

In both cases, the WGS equilibrium is adjusted according to the outlet temperature:

$$CO + H_2O \leftrightarrows CO_2 + H_2 \tag{4.48}$$

Therefore, the two processes are combined in such a way that only the amount of natural gas that is required to generate a synthesis gas with a stoichiometric ratio of approximately 2 is routed through the tubular reformer. Thus, the synthesis gas

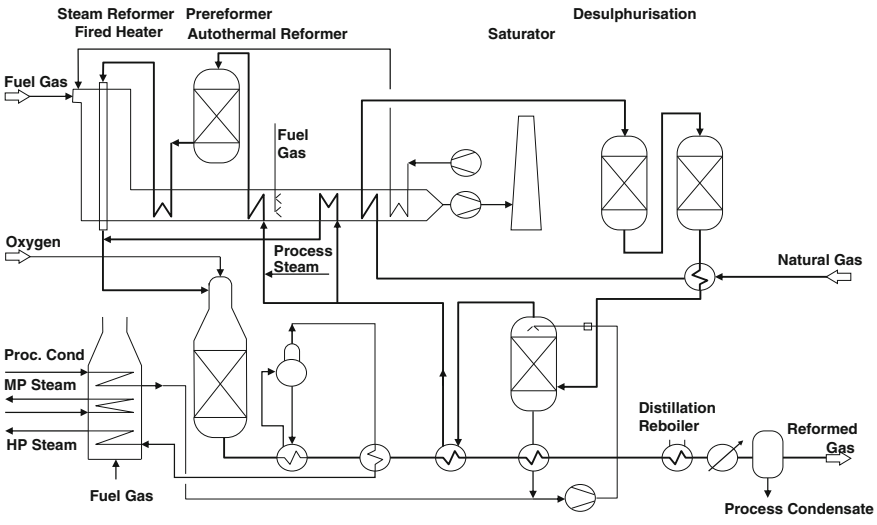

Fig. 4.45 Combined reforming (*Source* Air Liquide Global E&C Solutions)

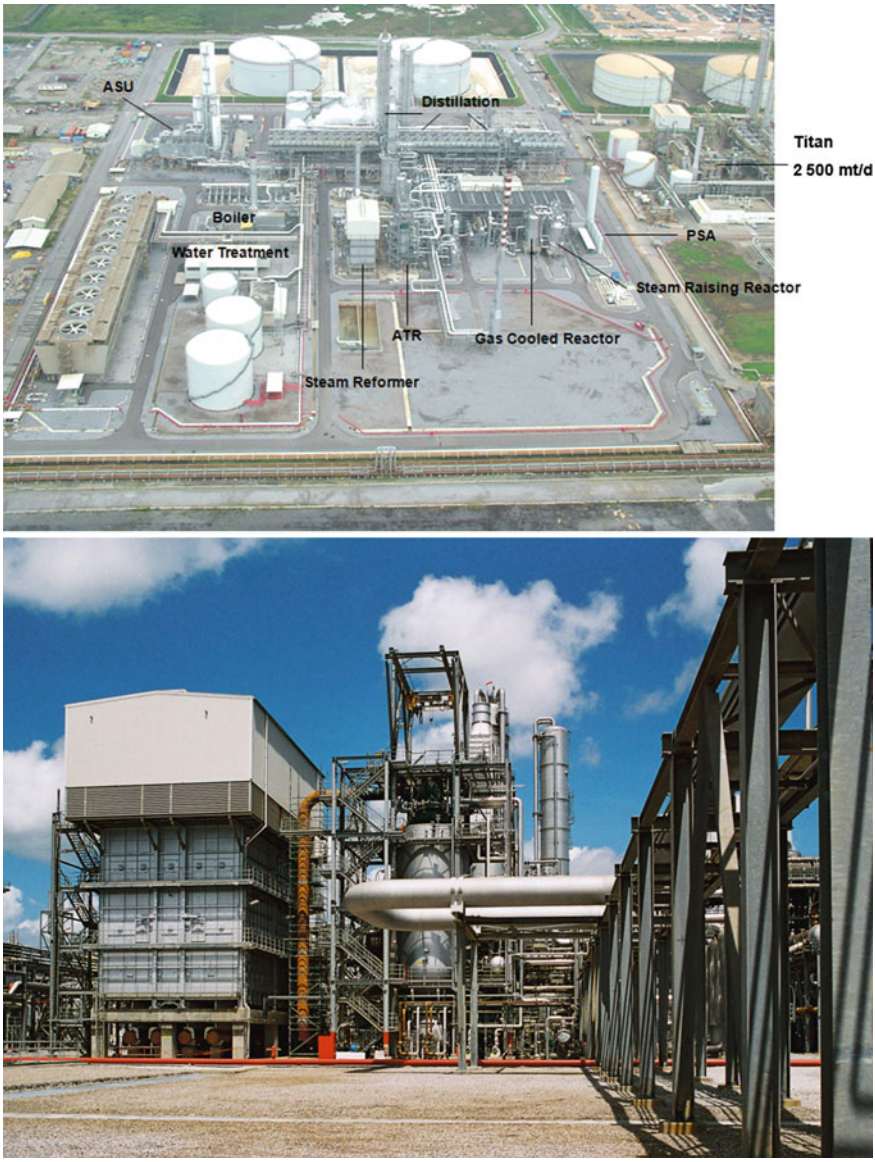

Fig. 4.46 Combined reformer at the Atlas methanol plant (capacity 5,000 tonnes/day). (Courtesy of Air Liquide Global E&C Solutions)

flow is reduced considerably (in the case of methanol, by approximately 25 %). Depending upon the composition of the natural gas, only 30 % of the hydrocarbons are converted in the tubular reformer; therefore, the tubular reformer in the

combined process is only about one quarter the size of a reformer in the conventional process. This means considerable savings in cost and energy.

As the reformed gas leaves the tubular reformer with a high methane slip, it is further reformed in the autothermal reactor together with the natural gas routed through the bypass. Due to higher suction pressure, the compression energy is only about 50 % compared to the compression energy for syngas of a conventional steam reforming. A further important advantage for reducing the plant cost and the energy requirement is the very low process steam requirement, resulting in a low S/C ratio. Because only about half the natural gas is reformed in the steam reformer, the necessary total S/C ratio drops to almost half. The compression of synthesis gas is possible in a single casing compressor. To keep the methane level low at high pressure, the catalytic autothermal reactor is operated at an outlet temperature of about 960 °C. Figure 4.45 shows a typical scheme of combined reforming [126].

The difference in size of the steam reformer and the ATR demonstrate that large-scale synthesis plants will use combined reforming, at least for capacities in the range of 1,500–6,000 tpd of methanol. Because the capital cost for the air separation unit (ASU), which is producing oxygen, is lower in comparison to savings due to economy of scale for the synthesis gas production, synthesis gas compression and methanol synthesis in large plants, the total cost of the combined reforming using oxygen provides the best economics (see Chap. 7) (Fig. 4.46).

4.3.5 Partial Oxidation

4.3.5.1 Introduction

A niche variant to ATR is POX. Only a limited number of plants for methanol production are in operation. The POX process can convert difficult feedstocks into clean synthesis gas with minimal environmental impact. Many of the undesirable components in crude oil (sulphur and heavy metals) are concentrated in residual fuel oil. Increasingly stringent environmental legislation dictates a reduction in sulphur content and/or the application of expensive flue gas treatment techniques when burning such residual fuels. POX makes these measures dispensable.

The declining demand for residual fuel oil and increasing demand for distillates are pushing refineries to look for alternative conversion processes of the heavy residues. POX is such an alternative. It will digest not only the traditional heavy refinery residues but also all kinds of other liquid and even solid-containing residues and combinations, apart from the gaseous feeds discussed here. POX is an attractive option with respect to the sustained trend toward closed-loop production, as byproducts of many chemical processes can be used as feedstock for POX. The process enables the manufacture of a wide range of products such as hydrogen, carbon monoxide, oxo-alcohols and fuel gas. When cheap oxygen is available, the production of ammonia and methanol is also economically feasible. The integration

of efficient POX with a combined cycle (integrated gasification combined cycle, or IGCC) represents an option for generating clean power from residual fuels.

4.3.5.2 Partial Oxidation Process Description

POX is a noncatalytic POX process that can convert gaseous feeds also containing liquid components (apart from wide variety of liquid/even solids containing hydrocarbon feedstocks) to clean synthesis gas, consisting mainly of hydrogen and carbon monoxide. Compared to the combustion of residue feedstock, which involves SO_2 removal, POX allows virtually complete removal (over 99 %) of the gaseous sulphides, with marketable sulphur produced. The metal salts in the feedstocks are separated from the product gas as a solid filter cake, which can serve as a raw material for metal recovery. State-of-the-art water treating techniques ensure clean effluents.

A gasification unit usually consists of the gasification reactor itself, where the feedstock reacts with oxygen to raw synthesis gas (a hydrogen–carbon monoxide mixture), a synthesis gas cooling section and a carbon handling system. The gasification is autothermal and is described by the following reaction:

$$2C_mH_n + m/2O_2 \leftrightharpoons 2m\ CO\ +\ n\ H_2 \tag{4.49}$$

Depending on the composition of the feedstock and the oxidant as well as the actual gasification temperature (1,200–1,450 °C), the raw syngas contains quantities of H_2O (to be condensed), CO_2, residual CH_4, H_2S, COS, N_2 and Ar. In addition, a small amount of unconverted carbon (soot) is present, approximately 0.5 wt% for liquid hydrocarbons. Gasification pressure may range from 1 to 100 bar, but is normally between 30 bar (preferred for some IGCC) and 70 bar (preferred for H_2 production). Metal ash (slag) is removed together with the soot or, at high concentrations, as molten slag via quench and slag hopper.

4.3.5.3 Partial Gasification: Quench Configuration

Reactor System

The noncatalytic POX of hydrocarbons by POX occurs in an empty, refractory-lined reactor (see Fig. 4.47). The refractory is selected as a function of the ash/slag load: the dry 'dusty' ash in most refinery applications results in less stringent specifications than molten slag. The feedstocks enter the reactor by a top-mounted, specially designed burner. This extremely robust burner—together with the quench—is the main reason for the high feedstock flexibility of POX. Feed and oxidant are preheated to minimise oxygen consumption. The oxidant (air, enriched air, O_2) is mixed with steam as moderator prior to feeding to the burner. Burner and reactor are tuned by fluid-dynamic simulation to achieve mixing of the oxidant with the feedstock at the smallest possible volume. Thus, the reactor space is

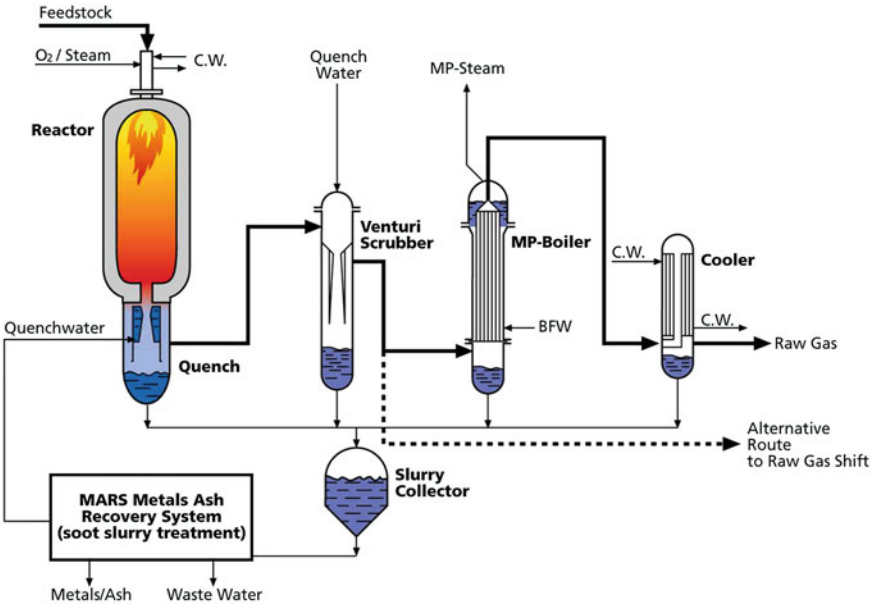

Fig. 4.47 POX flow diagram for quench configuration. (Courtesy of Air Liquide Global E&C solutions)

optimally used for complete conversion. The central bottom outlet leads directly into the water quench ring.

For liquid feed, the soot slurry from the gasification (in both quench and boiler mode) is flashed to atmospheric pressure in a slurry tank. The slurry is filtered, leaving a filter cake and a clear water filtrate, which is partly recycled as quench or scrubbing water. The filter cake is subjected to a controlled incineration process in a multiple hearth furnace, which allows, due to the combustion conditions, a recovery of the metals. The process is autothermal in principle, with the heat of combustion being sufficient to evaporate the moisture content of the filter cake.

The surplus of water from the metal ash recovery system (MARS; i.e., the overall net water produced in the gasification step) is routed to a sour water stripper (SWS) to remove traces of ammonia (NH_3), hydrogen cyanide (HCN), and hydrogen sulphide (H_2S). The off-gas is normally routed to a Claus/TGT unit.

Syngas Cooling

The hot raw gas from the reactor is shock-cooled ("quenched") by water from the soot removal section, which is injected into a quench ring optimised for large variations in gas and solids (slag) load. The gas is cooled almost instantly to the gas saturation temperature and leaves through the side of the quench separator. The soot slurry resulting from the quench is drawn off for low-ash (refinery) cases and routed to the MARS. When processing high-ash feedstock, molten slag forms and flows down the refractory wall into the quench ring where it is blast-cooled into glassy

spheres (1–2 mm diameter). This nonleachable glassy slag is collected and can be easily disposed of (e.g. as aggregate for road construction). The overflow water carries fine particles and soot to the MARS unit, where it is treated to allow partial recycling of process water and collection of soot and particles for further treatment in the rotary furnace. Final gas cooling occurs in a medium-pressure steam boiler, which produces steam for use in the complex. After passing through the final water cooler, the gas is routed to the acid gas removal unit.

4.3.5.4 Partial Gasification: Boiler Configuration

The burner and reactor are essentially the same as in the quench configuration described previously, only that the hot raw gas now leaves from the bottom side of the reactor to enter directly into a heat recovery boiler, which raises valuable high-pressure steam.

Syngas Cooling

The boiler configuration is designed for recovery of sensible heat at the highest possible temperatures. Primary heat recovery takes place in a WHB generating high-pressure (i.e., 100–140 bar) saturated steam in which the raw gas is cooled to approximatley 340 °C (see Fig. 4.48) This WHB is specifically designed for the high gas inlet temperatures and the particulate-charged gas at high velocities. A small part of the steam thus generated is used for feedstock and oxidant pre-heating; the bulk is superheated and can also be used in steam turbine drives or in an IGCC. Lower-level heat is recovered in a boiler feedwater economiser directly

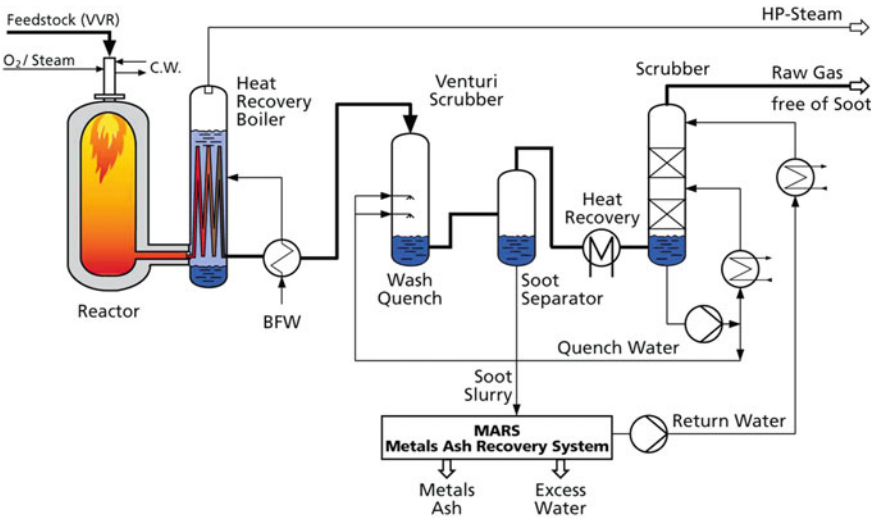

Fig. 4.48 Boiler configuration for partial gasification of partial oxidation. (Courtesy of Air Liquide Global E&C Solutions)

downstream of the WHB. Ash from the feedstock and soot particles are carried with the raw gas. They are removed from the gas in a wash quench and scrubber column. The soot slurry is collected and sent to the MARS.

4.3.6 Process Selection Criteria for Methanol Generation

4.3.6.1 General Aspects

As described previously, various reforming technologies are applicable for the conversion of natural gas, oil-associated gas and other gaseous feedstocks to (methanol) synthesis gas. Although most of the plants worldwide use conventional

Table 4.11 H_2/CO ratios and stoichiometric numbers (SN) for reforming technologies

Process	H_2/CO	SN
Steam reforming by means of CO_2 recycle, H_2/CO approaches SN	4–6 with CO_2 3:1	2.7–3.0
Autothermal reforming	2.7–3.3	1.5–1.6
Lurgi Multi Purpose Gasification (MPG)	1.7–1.8	1.5–1.6

Table 4.12 Single-train reformer capacities

Type of reformer	Single-train capacities, Nm^3/h dry syngas hour[a]
Steam reformers	1,000–200,000
Autothermal reformer	10,000–900,000
Multi Purpose Gasification (MPG) partial oxidation	5,000–100,000

[a] For a 5,000 tpd methanol unit, the syngas production rate is about 530,000 Nm^3/h

Table 4.13 Typical syngas compositions[a]

Feed	Natural gas	Natural gas and CO_2	Natural gas combined reforming	Naphtha C/H = 6	Vacuum residue or coal
CO_2 vol%	6.98	12.25	7.74	8.43	3.22
CO	16.42	15.48	21.79	20.37	28.24
H_2	73.52	69.36	67.53	67.22	68.05
CH_4	3.08	2.91	2.86	3.98	0.49
N_2 + Ar	–	–	0.08	–	–
Synthesis gas (Nm^3/t) CH_3OH	3,120	2,680[b]	2,546	2,590	2,300
Stoichiometric number = $(H_2–CO_2)/(CO–CO_2)$	2.84	2.06	2.03	2.04	2.06

[a] See Sect. 4.4

[b] Includes 151 Nm^3 CO_2

steam reforming, it is important to consider other proven technologies when the most economical methanol plant concept should be the objective.

The most important parameters are outlined and described in this section. As described previously, the right selection of the SN has an important influence on the overall cost. Table 4.11 shows a comparison of the SNs and ranges for the different reforming technologies. The reforming processes have different ranges for syngas production, as can be seen from Table 4.12.

Typical resulting syngas compositions are shown in Table 4.13 [127].

4.3.6.2 Specific Selection Criteria

A more specific guideline for the process selection is described here. There are no absolute limits for the application of the different reforming technologies, but there are certain preferences.

Conventional Steam Reforming

Convention steam reforming is preferred for the following:

- Plant capacities up to approximately 2,000 tpd [128] when no oxygen is available across the fence
- Combined plants for methanol and ammonia and methanol and hydrogen
- Plants having CO_2 available
- Low feedstock cost
- Low capital cost.

Autothermal Catalytic Reforming

Autothermal catalytic reforming is preferred for the following:

- All sizes, when oxygen is available across the fence
- Large-size stand-alone plant (greater than 6,000 tpd methanol) [97]
- Low feedstock cost.

Combined Reforming

Combined reforming is preferred for the following:

- All sizes, when oxygen is available across the fence
- Sizes greater than 1,500–6,000 tpd methanol [97]
- High feedstock cost
- High capital cost
- Conversion of NH_3 plants to methanol plants
- Debottlenecking of methanol plants using conventional steam reforming.

Noncatalytic POX

Noncatalytic POX is applied for special feedstocks, such as methanol plants where there is cheap oxygen and/or a combination of oxo-alcohol plants or acetic acid plants.

4.3.6.3 General selection criteria

Apart from the above-described process criteria, the decision for a reforming process is mainly dependent on the following:

- Capacity of the synthesis plant
- Feedstock properties
- Cost of feedstock
- Cost for investment capital
- Stand-alone or integrated synthesis plant
- Plant location
- Available infrastructure
- Available utilities.

4.4 Synthesis Gas from Gasification Processes

Ludolf Plass[1], Osman Turna[2], Hans Jürgen Wernicke[3] and Robert Pardemann[4]

[1]*Parkstraße 11, 61476 Kronberg, Germany*

[2]*Air Liquide Global E&C Solutions c/o Lurgi GmbH, Lurgiallee 5, 60439 Frankfurt, Germany*

[3]*Kardinal-Wendel-Straße 75 a, 82515 Wolfratshausen, Germany*

[4]*Institute of Energy Process Engineering and Chemical Engineering, Freiberg University of Mining and Technology, Fuchsmühlenweg 9, 09599 Freiberg, Germany*

4.4.1 Introduction

Gasification usually is a large-scale technology that is only economical for large-scale units. Although steam reformers are built with a capacity of 1,000–100,000 Nm^3/h syngas, gasification reactors usually start in a range of >100,000 Nm^3/h dry syngas ($CO + H_2$). Large gasification sites, such as for Fischer–Tropsch gasification and downstream installations, have dimensions up to 20 km^2 (see also Sect. 4.4.6).

The dimensions of a gasification reactor itself show the scale of this technology. An EF gasification unit easily has a height of 50–80 m; some designs reach over 100 m (see Figs. 4.61 and 4.62 in Sect. 4.4.6.6).

4.4.2 Development of Gasification Worldwide

A variety of gasification technologies exist and many developments are underway. A recent publication from the U.S. Department of Energy shows a sharp increase in worldwide syngas production, from approximately 70,000 MWth in 2010 from 144 operating plants with a total of 412 gasifiers to more than 120,000 MWth in 2016 (>72 % increase), with an expected 193 plants with 505 gasifiers in operation (Table 4.14). The majority of the additional plants (40 out of 48) will use coal as feedstock [129].

4.4.2.1 Industry Changes

Current industry syngas output has increased by 50 % since 2004. Seven plants are under construction in China, in addition to several plants for SNG production from coal (of which six convert coal to chemicals). Another 10 gasification plants are

Table 4.14 Worldwide gasification capacity and planned growth: summary [129]

Feedstock		Operating in 2010	Under construction in 2010	Planned for 2011–2016	Total
Coal	Syngas capacity (MW_{th})	36,315	10,857	28,376	75,548
	Gasifiers	201	17	58	276
	Plants	53	11	29	93
Petroleum	Syngas capacity (MW_{th})	17,938			17,938
	Gasifiers				138
	Plants	56			56
Gas	Syngas capacity (MW_{th})	15,281			15,281
	Gasifiers	59			59
	Plants	23			23
Petroleum coke	Syngas capacity (MW_{th})	911		12,027	12,938
	Gasifiers	5		16	21
	Plants	3		6	9
Biomass/ Waste	Syngas capacity (MW_{th})	373		29	402
	Gasifiers	9		2	11
	Plants	9		2	11
Total syngas capacity (MW_{th})		70,817	10,875	40,432	122,106
Total gasifiers		412	17	76	505
Total plats		144	11	37	192

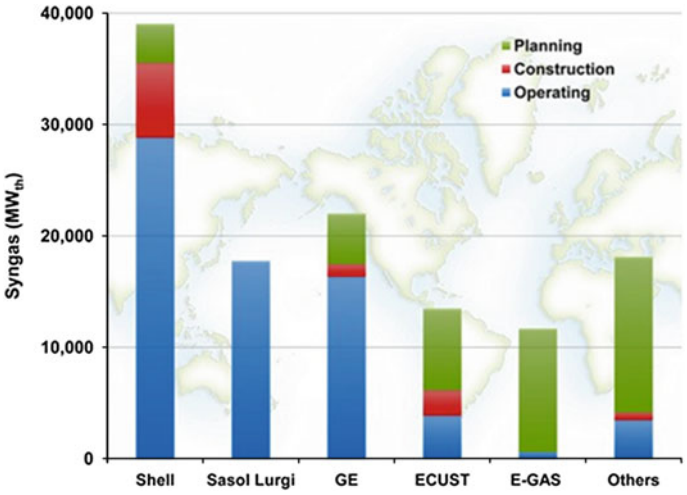

Fig. 4.49 Worldwide gasification capacity and growth by technology distribution [129]

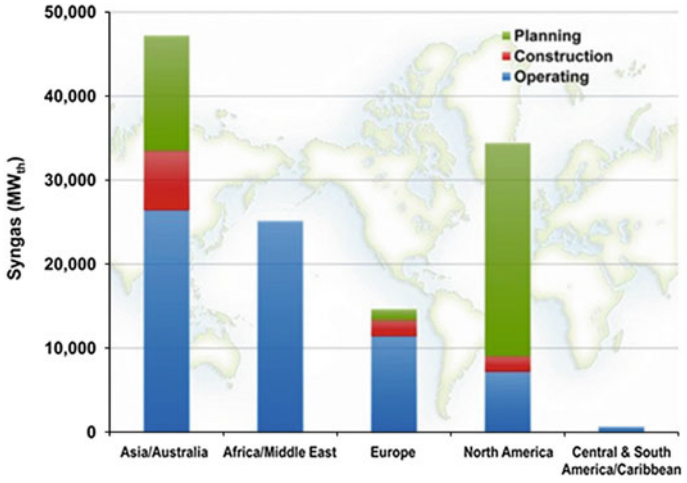

Fig. 4.50 Worldwide capacity and planned growth by region [129]

planned for 2016 (of which eight will convert coal to chemicals). Two IGCC plants are under construction in the United States, with 16 further projects planned through 2016 [135, 137]. As indicated in Fig. 4.50, this overall increase will result in a capacity growth of 47 % for U.S. power production, 23 % for gaseous fuels, 18 % for liquid fuels and 12 % for chemical plants. A total of 13 more plants are planned worldwide, 11 of which will use coal and 2 of which will use biomass/waste [134].

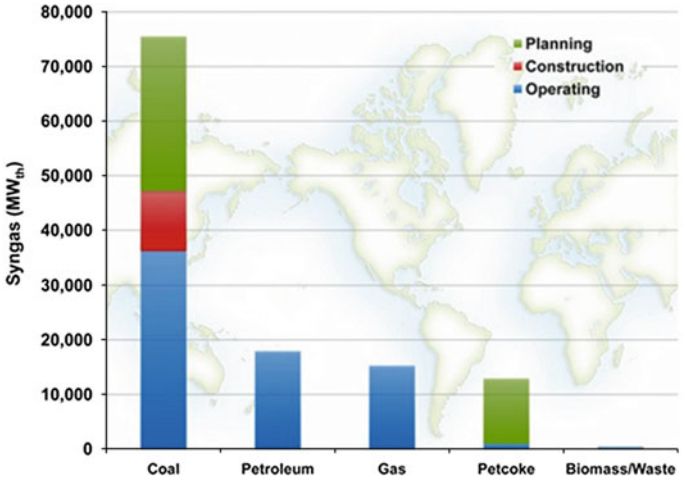

Fig. 4.51 Feedstock distribution [129]

4.4.2.2 Technology Development

Figure 4.49 demonstrates that the Shell entrained-flow process is currently the leading technology (also in terms of future growth), followed by Sasol Lurgi. The indicated growth of zero is not fully correct. The Jindal Steel and Power DRI project [seven fixed-bed dry-bottom (FBDB) gasifiers [138] and Sasol Synfuels extension of four FBDB gasifiers] is in addition to approximately 100 copies of FBDB gasifiers in China. However, the opposed multiple burners (OMBs) technology by East China University of Science and Technology in Shanghai shows the highest growth rate for a single technology.

As shown in Fig. 4.50, Asia/Australia has 37 % of the overall capacity. The second-place position of Africa/Middle East is mainly due to the gas-to-liquid (GTL) plants of Sasol and Shell in Qatar. Approximately 63 % of planned growth will be in the United States, followed by 34 % in Asia/Australia with China as the leader.

4.4.2.3 Feedstock Distribution

As can be seen from Fig. 4.51, coal is by far the preferred feedstock today (51 %) [136], with the 22 % of natural gas resulting from the Pearl GTL plant in Qatar. The capacity increase of more than 70 % is based on coal; the remaining 30 % is based on petroleum coke.

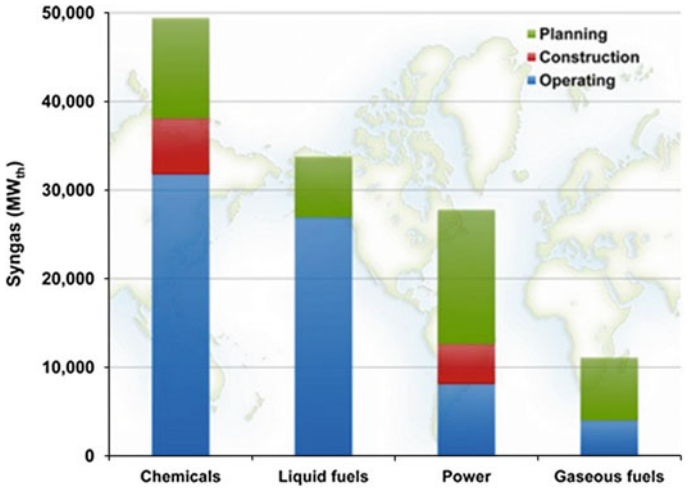

Fig. 4.52 Worldwide gasification capacity and planned growth by Product [129]

4.4.2.4 Product Distribution

Figure 4.52 shows that chemicals are currently and will also be in future the main product from syngas, followed by liquid fuels and power. The strongest increase on a percentage basis, however, will be for gaseous fuels and power (IGCC).

4.4.3 General Principles of Gasification Processes

Essentially, gasification means the conversion of a solid or liquid fuel to produce a gas that is suitable for combustion for energy generation or a syngas for the production of chemicals and fuels. Historically, the development of gasification started in the nineteenth century to produce town gas for illumination and heating purposes, using coal as fuel. The actual focus of gasification technology development and application is the generation of electricity (via IGCC technology) and the production (or coproduction) of electricity, chemicals and fuels based on a variety of fuels, such as coal, refinery residues, natural gas, biomass and waste (see Chap. 7). Important goals for these developments are to comply with stringent international environmental standards, maximise efficiency and allow for fuel flexibility as much as possible.

Gasification is the reaction of solid, liquid or gaseous fuels under partial combustion conditions with air or oxygen, steam, CO_2 or a mixture of these gases at temperatures greater than 700 °C to produce a gas, which can be used for the generation of energy or as source for the production of chemicals and fuels. When coal is heated under the absence of oxygen or under partial combustion conditions,

it first undergoes a pyrolysis step at temperatures greater than 250–500 °C, depending on the composition and rank of the coal. Pyrolysis products are a hydrogen-rich volatile stream together with condensable tars, oils, phenols, and noncondensable hydrocarbon gases (CH_4, C_nH_m) plus CO_2, H_2, CO, etc. The generation of pyrolysis products as a function of temperature is dependent on the rank of coal and pyrolysis conditions (heatup rate, pressure, purge gas composition). CH_4 and C_nH_m increase significantly with pressure. The release of volatile matter tails off between 600 and 900 °C.

With increasing temperatures, the gasification of residual char takes place, releasing CO, H_2, CH_4 gases, CO_2 from the combustion and a CO shift conversion taking place in the reactor. Solid residues (ash) will leave the combustion zone. For more details, see Refs. [130, 133, 140, 141, 142, 149].

4.4.4 Chemical Reactions of Gasification

The main chemical reactions forming the gasification can be described as follows (for more details, see also Refs. [131, 132, 156, 157, 165]. All gasification reactions with carbon from the solid phase and a gas phase agent (air/oxygen, H_2O steam, CO_2) are referred to as heterogeneous reactions. All gas/gas phase reactions are called homogeneous reactions.

Complete combustion with oxygen:

$$C + O_2 \rightarrow CO_2 \qquad \Delta_r H^\circ = -393.5\,\text{kJ/mol} \tag{4.50}$$

Most of the energy from the above exothermic reaction is needed to dry and heat the coal for the following endothermic gasification reactions.

Gasification with oxygen or air (partial combustion):

$$C + 1/2O_2 \rightarrow CO \qquad \Delta_r H^\circ = -110.5\,\text{kJ/mol} \tag{4.51}$$

Gasification with carbon dioxide (Boudouard reaction):

$$C + CO_2 \rightarrow 2CO \qquad \Delta_r H^\circ = +170\,\text{kJ/mol} \tag{4.52}$$

The Boudouard reaction is highly endothermic and much slower than the combustion reaction at the same temperature in the absence of catalyst.

Gasification with steam (water–gas reaction):

$$C + H_2O \rightarrow CO + H_2 \qquad \Delta_r H^\circ = +131.5\,\text{kJ/mol} \tag{4.53}$$

The water gas reaction is also endothermic. It increases with rising temperatures and reduced pressures, but it is very slow below 900 °C in the absence of a catalyst.

The water–gas shift reaction:

$$CO + H_2O \rightarrow H_2 + CO_2 \qquad \Delta_r H^\circ = -40.9\,\mathrm{kJ/mol} \tag{4.54}$$

The gas-phase WGS reaction takes place simultaneously with the above heterogeneous gasification reactions, determining the final crude gas quality. Thus, the WGS reaction plays an important role in adjusting the CO/H_2 ratio to the levels required for the production of H_2 and certain chemicals and fuels. Note that a second catalytic CO shift conversion step will be required downstream of the gasification should the H_2/CO ratio for gasification be too low (see Sect. 4.4.8). Note the heterogeneous gasification reactions (4.51) and (4.52) are implicit in the homogeneous water gas shift reaction (4.54), which is often used to simply describe the gasification process, although heterogeneous reactions take place in parallel.

With regard to the formation of methane, two principle reactions are considered:

– Gasification with hydrogen (hydrogasification reaction):

$$C + 2H_2 \rightarrow CH_4 \qquad \Delta_r H^\circ = -74.9\,\mathrm{kJ/mol} \tag{4.55}$$

Hydrogasification needs very high pressures to become effective.

– The gas-phase methanation reaction:

$$CO + 3H_2 \rightarrow CH_4 + H_2O \qquad \Delta_r H^\circ = -206.4\,\mathrm{kJ/mol} \tag{4.56}$$

The reaction requires high temperatures and catalytic conditions to become effective.

More details regarding the gasification reactions and the related kinetics can be found in Refs. [132, 144, 159, 161–164, 166, 167, 168–173, 175].

Depending on the gasification process conditions, the following different types of syngas can be produced [131]:

1. Low heating value gas (3.8–7.6 MJ/m^3), predominantly used as fuel gas in gas turbines or as reducing gas in steel production processes, is not suitable for chemical reactions due to the high content of nitrogen gas.
2. Medium heating value gas (10.5–16 MJ/m^3) is suitable for IGCC applications but also as feedstock for chemical reactions. Depending on the CO/H_2 ratio, catalytic adjustments via a shift reaction are necessary to adjust this ratio accordingly to produce methanol and other chemicals such as ammonia and Fischer–Tropsch products.

The composition and nature of the syngas is influenced by a variety of parameters. Their respective influence may vary substantially and in a complex manner, depending on the reactor type and configuration, pressure and temperature, residence time, type of fuel, fuel preparation and feeding, geometry, superficial gas velocity and particle size of the gasified fuel [132] (see Fig. 4.53).

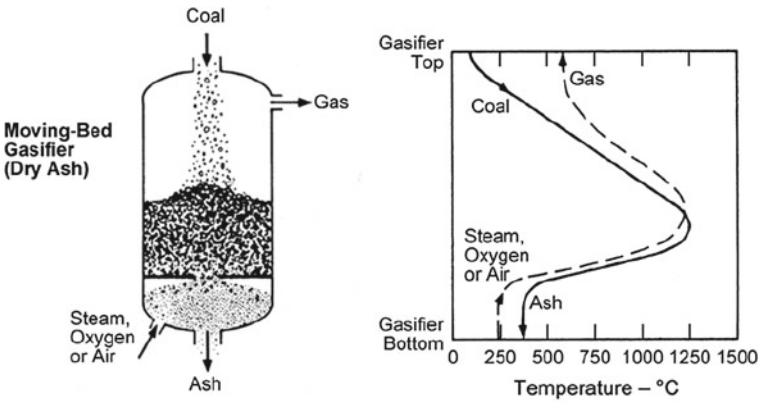

1. Moving-Bed Gasifier (Dry Ash)

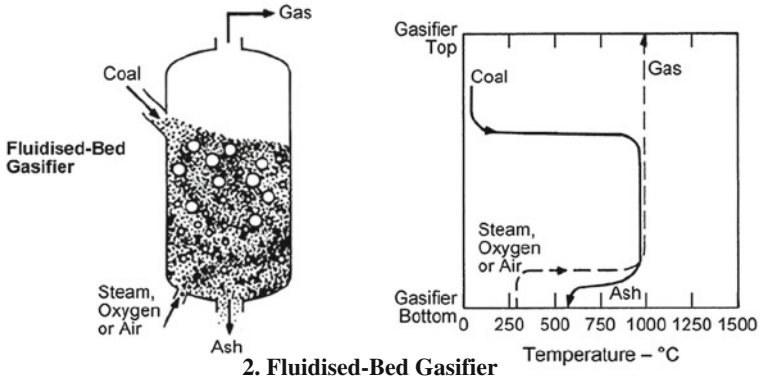

2. Fluidised-Bed Gasifier

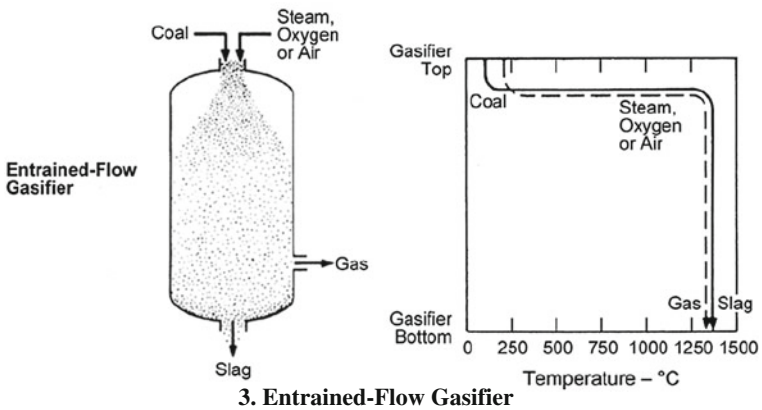

3. Entrained-Flow Gasifier

Fig. 4.53 General principles of gasification technologies [132, 195]

4.4.5 Commercial Processes

The principal differences between the technologies as per Fig. 4.53 are explained here.

4.4.5.1 Moving Bed (Fixed-Bed Dry Bottom) Gasifier

In this gasifier, a fixed bed of lumpy coal (approximately 5–60 mm) is formed, where coal is fed from the top of the reactor and the ash is extracted at the bottom. Gas flows through this fixed bed in countercurrent mode. The gas velocity is limited to prevent excessive carryover of fines to the next process step. Some reactor configurations have a co-current gas flow. Ash melting must be avoided for an FBDB gasifier, but coarse ash with some mild clinkering is preferred for better agent distribution. Worldwide, the majority of syngas from coal gasification is produced in FBDB gasifiers. As a further development of the fixed-bed gasifier is the British Gas/Lurgi (BGL) slagging gasifier, which features a liquid ash extraction system operating at temperatures above the ash melting temperature assisted by fluxing. For more details, see reviews in Refs. [143–148].

4.4.5.2 Fluidised Bed Gasifier

A fluid bed of relatively fine coal particles (typically in the 0.1–5 mm range) is formed, keeping the particles in suspension in the upward gas flow while they undergo the gasification reactions. In contrast to the moving bed system, the gasification temperature is constant in the overall FB reactor system. The gasification temperature is typically in the range of 800–1,050 °C, depending on the ash softening and sticking behaviour of the solid fuel. Ash softening/melting must be avoided.

A further development is the circulating fluid bed (CFB) gasifier. The combination of particle size and (substantially higher) gas velocity cause a high particle concentration in the gas stream leaving the reactor. The particles are separated in a downstream recycle cyclone and fed back to the reactor. The relative velocity between the particles and the gas maximises in these CFB gasifiers, favouring high heat and mass transfer rates [174]. Apart from coal, biomass is the preferred feed material for FB/CFB/transport gasifiers.

4.4.5.3 Entrained Flow Gasifiers

Pulverised coal and gases flow co-currently at high speeds in an EF. The reaction takes place at temperatures well above the ash melting point. Ash is extracted in a liquid form. This technology is actually the most employed for the production of H_2 and chemicals from coal. Modifications of this EF technology, including so-called two-stage reactors, are used for other solid fuels (e.g. petroleum coke), liquid or gaseous feed, or biomass.

Other gasification technologies, such as molten bath, rotary kilns, or in situ gasification, are not reviewed here because there are no commercial references available. Figure 4.54 shows a principal decision matrix for the selection of adequate technology for the gasification of different coals.

4.4.5.4 Prinicpal Technology Decision Matrix

The selection of the "best" gasification technology for a specific application depends on the correct selection of a variety of parameters and is therefore difficult [131, 132]. Parameters that must be considered include the following:

- Coal quality and properties, ash content and melting behaviour, minor/corrosive components, salts/cost of coal
- Further use of syngas and final product
- Capacity per gasifier
- Heating value/composition of gas
- Turndown ratio, operational features, reliability, availability
- Gas purity, cleanliness, gasification byproducts
- Environmental constraints.

In the case of coal as feed, the coal choice is typically the least flexible factor (geographical, economical, political, environmental factors), which means that the gasification process has to be adapted to the base coal to be processed.

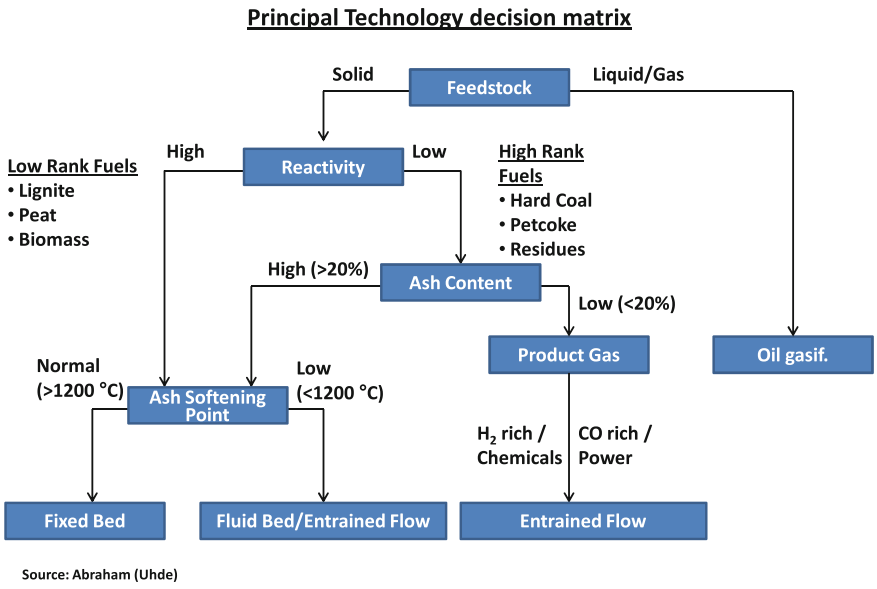

Fig. 4.54 Principal technology decision matrix (modified from Uhde) [191]

4.4.6 Examples of Commercial Gasification Processes

4.4.6.1 Moving Bed Gasification (FBDB Gasification)

The Lurgi FBDB gasifier is explained in more detail here as the typical and industrially most used moving-bed gasifier. A schematic representation of the Lurgi FBDB gasifier is depicted in Fig. 4.55.

In the gasifier, coal with particle size of preferably 5–50 mm is loaded from the bunker into an isolated coal lock, which is then pressurised with raw synthesis gas and opened to the gasifier. The coal is loaded into the gasifier in a batch mode. Almost all the gas used to pressurise the coal lock is recovered during depressurisation by lock gas recompression of the coal lock before loading it with coal from the bunker. The gasifier itself is a double-walled vessel. The boiler feed water (BFW) level is maintained between the outer shell and inner wall (jacket) to protect the outer pressure-bearing shell from high temperatures. At the same time, saturated steam is generated in the jacket at a pressure similar to the gasification pressure from the heat transferred through the reactor inner wall. This steam is added to the high-pressure superheated steam used in the gasification process.

Coal from the coal lock is charged to the cross-sectional area of the gasifier and descends slowly through the bed. The gasification agent, steam and oxygen, is distributed into the gasifier via the rotating grate located at the bottom of the gasifier. Heat recovery occurs between the hot ash bed consisting of course to fine particles and the ascending gasification agent (fed to the gasifier at steam–oxygen mixing

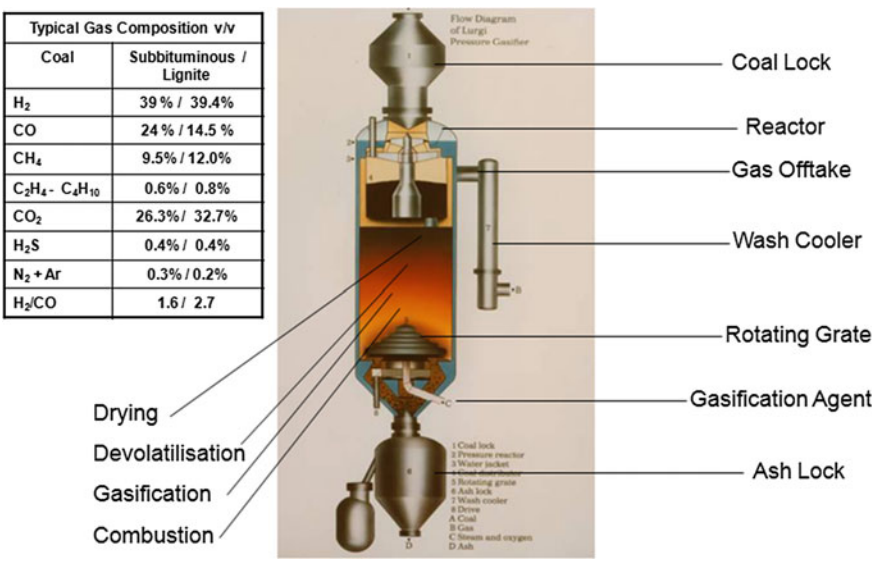

Fig. 4.55 Lurgi FBDB gasifier [187]

temperatures between 300 and 400 °C). The hot ash at 20–30 °C above the agent temperature is then discharged into the ash lock and subsequently to the deashing system (ash sluiceways are commonly in use but other deashing systems had been also used).

The ash produced has a residual carbon content typically in the range of 2.5–5 %, depending on the rank/reactivity of coal and operation. The grate is automatically speed controlled to remove ash from the bottom of the gasifier and fix the fire zone at a certain height above the rotating grate, thus protecting the grate. The temperature of the combustion zone is adjusted by using steam or CO_2 as a moderator to prevent excessive clinker formation by ash melting and to allow for an undisturbed removal of ash.

The combustion zone characterised by the reaction of O_2 with the carbon from char is the hottest zone of the gasifier (with temperatures between 1,250 up to 1,500 °C, depending on the ash fusion properties of the coal) and hence provides heat for the upper gasification/reduction zone. CO_2 and steam form the reactants for the endothermic gasification reactions that take place next. CO is preferably formed due to the equilibrium at high temperatures. H_2 is being produced by the steam carbon reaction. As the hot gases ascend up the gasifier bed, they cool down by exchanging heat with the descending coal/char; some of the CH_4 is formed at temperatures where the gasification reactions tail off. The value of this reaction end temperature for the gasification is very dependent on the rank/reactivity of the char being produced in the pyrolysis zone above. The low temperatures for reactive char favour the formation of CH_4 and C_nH_m, of which a certain fraction will be produced in the gasification zone; however, the major part will come from the pyrolysis taking place upstream in the gasifier bed.

The homogeneous WGS equilibrium is also defined by the gasification "reaction end temperature," which eventually determines the gas composition (H_2/CO ratio, CO_2) of the synthesis gas that is generated. For more literature regarding kinetics and simulation, see Refs. [150–155, 158, 176–180].

Most of the synthesis gas is being produced in this zone (see Fig. 4.56 for reference). It is worth noting that some of the CO shift conversion takes place already in the FBDB gasifier, resulting in H_2/CO ratios of 1.5–1.7 for bituminous coals and up to 2.8 (v/v) for lignites. EF gasifiers typically have a H_2/CO ratio of 0.5 v/v, which requires additional steam if the syngas has to be H_2 rich depending on the final product. It can be easily seen that the FBDB favours SNG production due to the high H_2/CO ratio and CH_4 from gasification plus pyrolysis. Note that up to 40 % of the syngas calorific value can be provided by CH_4, which makes the FBDB process quite efficient. Reaction kinetics are fast at high temperatures of the shown profile and will naturally slow down, which is different than a co- or cross-current process such as a FB, which operates at a fixed temperature and with finer grain size.

The gasification takes place between 1,250 and 1,500 °C, depending on the ash fusion temperature/steam–oxygen ratio, with a T_R of 700 °C for lignites and 1,100 °C for anthracite. These temperatures are quite different from the slagging operation described in Sect. 4.4.6.2. As the gases continue to move upwards in the gasifier, the volatile components are released in the pyrolysis zone and the syngas

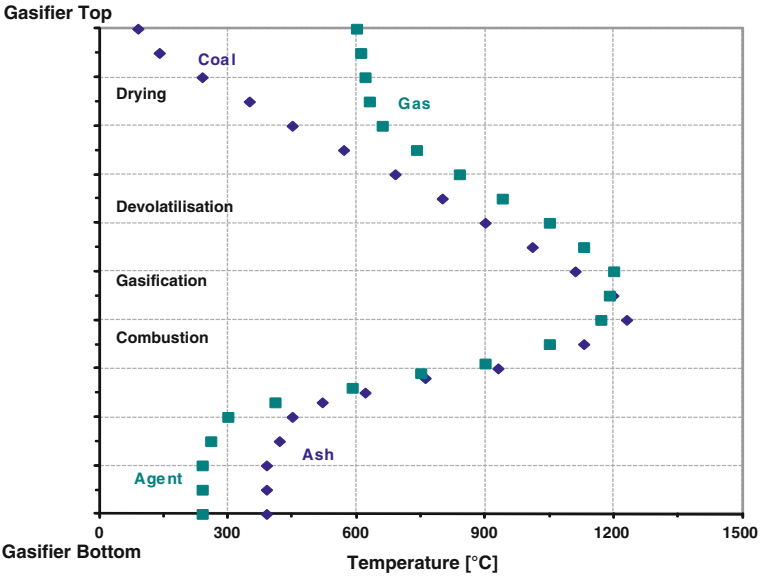

Fig. 4.56 Lurgi FBDB gasification process temperature profiles [193]

is further cooled down in the upper part of the gasifier where the coal is preheated and dried. The gas then exits the gasifier at temperatures of 230 °C for moist lignite, 450–550 °C for sub-/bituminous coals and 550–600 °C for relatively dry anthracite. The process will also accept high-moisture coals due to its in situ drying. The FBDB process combines gasification, CO-shift conversion, pyrolysis and drying in one reactor.

The composition is ultimately a result of plant operation and coal composition [160]. Also present in the raw gas are the volatiles from the coal in the form of heavy and light oils, phenolic compounds, ammonia, and sulphur compounds in the form of H_2S, COS and mercaptanes.

The produced gas leaving the gasifier is immediately quenched with gas liquor. The water-saturated gas is then further cooled in a WHB. Condensation from cooling is routed to the gas liquor separation unit. The H_2O-saturated crude gas saves steam in a downstream sour gas shift (SGS) system in the presence of H_2S.

Currently, two embodiments of the Lurgi FBDB gasification process are commercially available in the form of the Mark 4 (Mk4, "The Present") and Mark Plus (Mk+, "The Next Generation") gasifiers (see Table 4.15).

Continuous improvements that incorporate the operating experience from many large-scale plants have led to the latest Lurgi FBDB Mk4 design of 40 bar, which is used at the Jindal Steel and Power project in India. The Lurgi FBDB Mk+ gasifier is the next-generation gasifier (see Fig. 4.57). Conditions of the gasification at higher operating pressure have been fully validated against test results at the Lurgi pilot plant.

Table 4.15 FBDB gasifier capacities [193]

Name	Mk4 (Mark 4)	Mk+ (Mark Plus)
Raw gas loading (Nm^3/h) dry basis	Up to 60,000	Up to 120,000
Outside diameter (m)	4.13	5.05
Overall height (m)	12.5	17
Design pressure (bar)	40	60

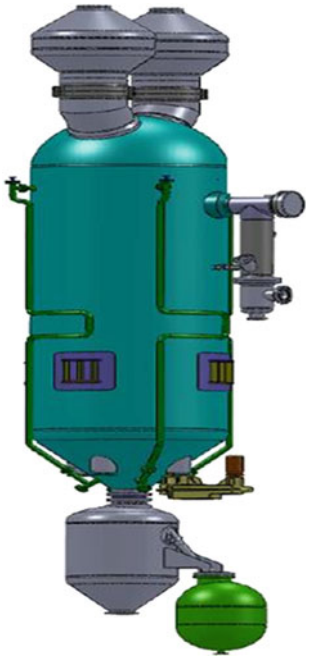

Fig. 4.57 LURGI FBDB Mark plus gasifier outline with double coal locks [193]

The Lurgi FBDB Mk+ gasifier doubles the dry raw gas production capacity, increases the methane yield in raw gas by 21 %, and decreases the byproduct of liquid higher hydrocarbons. The steam and oxygen consumption are reduced by 12 % and there is a 17 % decrease in gas liquor flow requiring treatment. Those gains will vary depending on coal properties.

The Lurgi FBDB Mk+ gasifier was developed using proven design features and components of Lurgi FBDB Mk4 gasification technology currently in operation worldwide. A Lurgi FBDB Mk5 prototype with a larger diameter has been successfully in operation for many years. The Mk+ was designed for elevated pressure, using double locks and improving gasification-related features, which resulted in the length of the reactor (see Table 4.15 and Fig. 4.57). The twin coal lock concept maintains the reliable lock design of the standard size while saving on pressuring gas.

System upgrades, improvements in operation and controls, and preventative maintenance strategies have resulted in high reliability, great availability and foreshortened inspection intervals. Economies of scale benefit from less FBDB Mk+ units being required to meet the gas demand. The increase in efficiency, raw gas heating value and operating pressure allows the downstream units to be reduced in size (i.e., gas cooling, gas cleaning units). Further benefits of the Lurgi FBDB Mk+ gasifier include benefits for downstream processes, with improvements in CO_2 absorption in Rectisol and the elimination or reduction in size of complex re-compression systems and their associated operating and maintenance costs.

For the gasification of wood, most fixed-bed gasifiers use the downdraft mode. The advantage is that the product gases pass the combustion zone before leaving the reactor, which cracks most of the condensable pyrolysis products due to the high temperatures. Typically, such wood-fired downdraft gasifiers are suited for small-scale operation (less than 200 kg/h of wood) [185].

More than 200 gasifiers using the Mark 4 concept are operating worldwide—most of them in South Africa and China. Robust operation and high reliability are key features of the technology.

FB gasifiers have the advantage of being able to process high-ash coals (up to 45 wt% ash). Because of the countercurrent flow, the thermal efficiency is high, resulting in a substantially lower oxygen consumption against EF gasification (e.g. a factor of 2.0–2.4 lower, depending on the reactivity of the coal) [139]. The carbon conversion efficiency is high. The steam demand for the gasification as such is significantly higher, especially for coals with low ash melting temperatures. For example it can be as high as a factor of 18 (FBDB versus EF-based on coal) or 16 (based on GJ syngas) [139]. However, steam is saved in the FBDB case when CO from syngas needs to be converted into H_2 by using the gas moisture, rather than by adding steam in the raw gas CO shift conversion process when using an EF process with heat recovery. When using EF technology with quench, steam for the CO shift is provided by the saturation level of steam in the raw gas, but then there is no heat recovery from the gasification. The best case for the FBDB is to sell the CH_4 as valuable byproduct, especially in a scenario of energy storage (see Chap. 8) [139]. Condensable hydrocarbons (tars, oils and naphtha) can be of advantage for Fischer–Tropsch production or represent otherwise an unwanted byproduct. Low gas outlet temperatures do not require a sophisticated heat recovery to use the sensible heat of the raw gas. The FBDB technology produces large quantities of process liquor containing tars and phenols, which are recovered; the remainder requires an elaborate effluent treatment.

4.4.6.2 Moving-Bed (British Gas/Lurgi) Gasification Process

The British Gas/Lurgi (BGL) slagging gasifier was originally developed on the basis of the Lurgi FBDB gasifier. Large-scale demonstration units were converted from a FBDB town gas plant in Westfield, Scotland. The initial goal was to

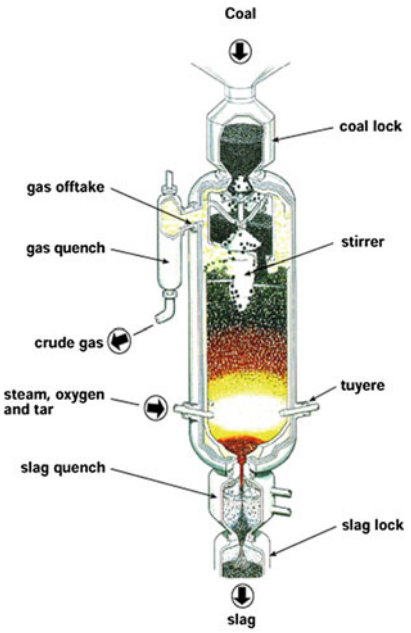

Extended Slagging Gasifier (ESG), 2.5 MPa Westfield, Scotland, 1984 -1990

Typical gas composition v/v for various coals	
H_2	25 -30 %
CO	55 -59 %
CH_4	6.5 – 8.0%
C_2H_4-C_4H_{10}	0.5 – 0.8%
CO_2	2.5 – 4.5%
H_2S	0.4 – 1.0%
N_2+Ar	2.6 – 3.0%
H_2/CO	0.45 – 0.55

Development of BGL Technology:

- **Pilot Slagging Gasifier, Holten/Solihull**
- **6' Slagging Gasifier , 2.5 MPa, Westfield, Scotland, 1975 –1983**
- **Experimental Slagging Gasifier (EG), 7 MPa, Westfield, Scotland, 1991**

Fig. 4.58 British Gas/Lurgi moving bed gasifier [187]

produce SNG from coal. However, in the later years of demonstration, the focus shifted to IGCC applications. A schematic is shown in Fig. 4.58.

The BGL gasifier in principle has the same design configuration in the top part of the reactor as the FBDB gasifier. When many bituminous coals are heated, they soften and form a plastic mass that swells and resolidifies into a porous solid. Coals that exhibit such behaviour are called "caking coals". The original BGL slagger was developed for U.K. and U.S. "caking coals," which required the installation of a modified coal distributor and stirring device at the gasifier top [172]. For noncaking coals, it could be equipped with an annular internal gas outlet arrangement replacing the rotating coal distributor and stirrer. Most of the Lurgi FBDB gasifiers in operation run with such an arrangement. The third configuration built was a modified top for the gasification for refuse-derived fuel (RDF). However, the bottom part of the reactor does not have a grate system for dry ash removal as does the FBDB.

This function is effected by a system of tuyeres (water-cooled injection nozzles similar to a blast furnace but extruding deeper into the bed) located just above the level of the molten slag bath. These tuyeres are also capable of introducing additional fuels, such as pyrolysis products from the raw gas (dusty tar, heavy and light oils) and/or fines as dry pulverised fuel (PF) or as slurry. Moving-bed processes do not accept many fine particles fed to the top because this would lead to bed instabilities. The ash leaves the bottom part of the BGL reactor in a liquid form through a slag tap into a slag quench chamber, where it is quenched with

water, solidified, and extracted via a slag lock. The BGL slagger comes in two designs: one is fully refractory lined with a water-cooled double-shell arrangement, whereas the other has a bare metal top similar to the FBDB but with a refractory-lined bottom.

Key drivers for the development were the following [144]:

- Suitability for coals with low ash melting point
- Improving cost effectiveness when using such coals
- Solving the fine particle problem.

For the first time, the BGL process was industrially applied in SVZ Schwarze Pumpe for the commercial gasification of waste in combination with coal. Various pelletised fuel combinations were run in a 3.6-m diameter reactor at 25 bars of pressure, containing 20–25 % brown and hard coal, up to 45 % RDF pellets, 10–40 % plastic waste, 5–15 % contaminated wood, and 10 % tar sludge pellets and other waste components. Because of the vitrified nature, the slag as such was nonleachable according to German standards [192].

The SVZ BGL gasifier (one unit) in combination with existing FBDB gasifiers and an entrained-flow Gas Kombinat Schwarze Pump (GSP, formerly GDR) gasifier for refuse oil and dusty tar provided syngas for methanol production. Purge and waste gases were routed to a combined gas turbine cycle to produce high-pressure steam and electrical power. The operation was stopped in the year 2007, and the BGL gasifier was dismantled and sold to India (Shriram). The FBDB and GSP gasifiers were scrapped.

In summary, the steam consumption is substantially lower compared to the FBDB. Oxygen consumption is higher for reactive coals and equal to the FBDB for nonreactive coals. The pyrolysis products such as tars and phenols are reduced if not consumed by injection to the tuyeres. CH_4 is about two-thirds of the FBDB value due to a higher reaction end temperature; C_nH_m is also reduced. The gas contains small amounts of CO_2 but high CO concentrations, resulting in a low H_2/CO ratio of about 0.5 v/v. The CO requires shift conversion depending on the required H_2/CO ratio in the downstream synthesis process. This requires more additional steam compared to the FBDB process.

4.4.6.3 Fluidised-bed Gasification Processes: High-temperature Winkler

The Winkler process is closely linked to the gasification of solid fuels since its first application in the 1920s for producing fuels and syngas from coal. Crushed coal (<9 mm) is fed via variable-speed screw feeders into the bottom part of a so-called dense phase or stationary FB. In a stationary FB, the particle size and the fluidising velocity in the reactor are selected in such a way that the particles can move freely in the bed, but they are not entrained into the freeboard area above the FB. Steam and oxygen are fed to the reactor via nozzles located at various levels in the FB.

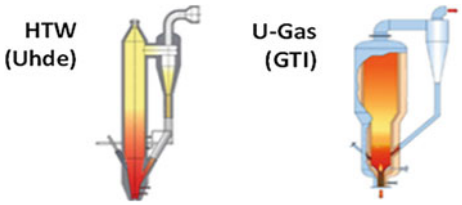

Fig. 4.59 Fluidised bed processes for high-temperature Winkler (HTW) and U-Gas [188]

The FB covers only approximately one-third of the reactor. It has a distinct surface from the freeboard area above. Secondary steam and oxygen are injected into the freeboard area to gasify unconverted carbon, tars and hydrocarbons. Ash is discharged at the bottom of the reactor. Smaller particles are entrained with the gas stream. Carbon conversion is limited by feedstock reactivity and by the continuous loss of carbon in the ash.

A further development in the Winkler generator has been the high-temperature Winkler (HTW) process, operating at elevated pressure (up to 30 bar) and slightly increased temperature by adding limestone or dolomite to increase the ash-softening temperature. The demonstration plant at Berrenrath (capacity of 600 tpd of dried lignite, operating pressure of 10 bar) was built and operated by Rheinbraun, producing syngas for the commercial production of methanol over a period of 12 years between 1986 and 1997. A further plant was built in Oulu (Finland), gasifying what is essentially peat at a pressure of 13.5 bar to produce ammonia. A 140 tpd pilot plant with a maximum thermal capacity of 36 MW was started up in 1989 at Wesseling, operating at higher pressure (25 bar) with an airblown and oxygen-blown gasifier, to demonstrate the behaviour of different types of coal and to study IGCC applications [131].

Fluid beds can take a very wide variety of coal qualities: hard coals with ash contents up to 40 %, lignite with high salt, sulphur content >5, and 1 % chlorine were successfully tested. Figure 4.59 shows an outline of the FBs according to HTW (Uhde) and U-Gas (Gas Technology Institute, GTI).

All three plants mentioned are no more in operation. The application of the HTW process was studied for a 300-MW_e IGCC power plant ("Kombikraftwerk Braunkohle"), which was never built. The replacement of 26 fixed-bed gasifiers by Lurgi at Vresova (Czech Republic) via two HTW units, resulting in a 400-MW_e IGCC, is under consideration. Also, the application of HTW technology for an IGCC with carbon capture is being studied by RWE in Germany [186].

HTW Biomass Gasification Process

A BtM plant is under development at Hagfors in the province of Värmland in Sweden with a capacity of 100,000 tonnes/year of methanol. It will use forest residues based on Uhde's HTW gasification. The plant is intended to start operation at the end of 2013.

4.4.6.4 Circulating Fluid Bed (CFB) Coal Gasification Processes

CFB systems operate at much higher superficial gas velocities (5–8 m/s). This results in much higher heat transfer and mass transfer between the gas and the particles due to their high differential velocities, resulting in a much reduced tar content in the raw gas. Due to the high gas velocity, the majority of the fluid bed material is entrained from the reactor top. A high-efficiency recycle cyclone is therefore an integrated part of the overall process. The entrained particles from the recycle cyclone are fed back to the bottom part of the fluid bed via a seal pot, thus increasing the carbon utilisation significantly. The CFB technology is less sensitive to particle size and form of the feed material, which favours it for the use of biomass

CFB technology was originally developed by Lurgi for alumina calcinations and was later adapted for the combustion and gasification of solid fuels. The technology is today offered by Envirotherm. A competing CFB technology was developed by the Ahlstrom of Finland for CFB combustion and gasification; this is now owned by Foster Wheeler.

In this section, CFB technologies that use oxygen for gasification and produce syngas suitable for methanol production are described. Air-blown gasification technologies are only mentioned briefly.

Kellog Brown and Root (KBR) have developed a transport reactor system operating at gas velocities of 11–18 m/s to further increase throughput, mixing, and heat transfer. A demonstration plant (2–3 tpd coal throughput) was operated initially as combustor, then as air-blown gasifier and finally (for more than 7,000 h until 2007) in the oxygen gasification mode in Wilsonville, Alabama. The gasification takes place at 900–1,000 °C and 11–18 bar pressure. Predominantly low-rank coals were used, resulting in carbon conversion rates of 95 %, with some results up to 98 %. According to various sources, economics favour the air-blown IGCC application. A 285-MW_e demonstration plant is undergoing detailed engineering studies and will be built in Stanton, Florida. To increase the carbon conversion further and to produce a nonleachable, low-carbon agglomerated ash, two developments were undertaken (somewhat similarly to the BGL development) to create an agglomerated ash in the bottom part of the CFB reactor, while maintaining fluid bed conditions without slagging or softening of the particles above the agglomerating bottom part.

The Kellog Rust Westinghouse (KRW) IGCC plant (rated at 100 MW_e), built near Reno, Nevada, did not achieve successful startup operation until 2002, according to the U.S. Department of Energy, mainly because of hot gas filtering difficulties.

The U-Gas technology was developed by the GTI, applied for various commercial plants using gasification of coal or biomass with air or oxygen under low- and high-pressure conditions. The process is now licensed by Synthesis Energy Systems (see Fig. 4.59). Further developments have been made in Finland, using biomass, as discussed later.

Bharat Heavy Electricals (India) have developed an air-blown CFB gasifier (6.2 MW_e, 168 tpd coal capacity), which is especially adapted to the high ash (approximately 42 % ash) coals of India. Operating ranges are pressure between 3 and 10 bar, temperatures between 980 to 1,050 °C. A 125-MW_e IGCC project is under development.

Another air-blown CFB gasification process was developed especially for the high-moisture containing lignites (up to 60 % moisture) of Victoria in Australia. The initial development phase was under the State Electricity Commission of Victoria, later on taken over by HRL Limited (1989–1998). The process is called integrated drying gasification combined cycle (IDGCC). Hot pressurised gas (25 bar/900 °C) and particles leaving the recycle cyclone are used to pre-dry the wet coal in a liftpipe dryer. The dried lignite particles (5–10 % residual moisture) and the syngas are separated in another cyclone at approximately 250 °C. The syngas is cleaned and routed to the combustion chamber; the lignite is fed to the CFB gasifier.

4.4.6.5 Circulating Fluid Bed Biomass Gasification

Biomass is very diverse, depending on the nature of the biomass source (wood, wood waste, agricultural residues, waste, sludge, etc.). Each type of biomass needs a special pretreatment before it can be fed to a specific gasifier technology. Drying from >40 to <15 % moisture is costly. Crushing to grain sizes that are suitable for the specific gasification technology is in many cases complicated and costly as well [181]. EF reactors need especially fine material (<200 μm). So far, dry feed of very fine grained biomass (such as sawsdust) was only possible in combination with pulverised coal and only at approximately 20 % (Buggenum). These problems can only be overcome if the biomass is converted into a "biosyncrude" using the Bioliq process [182, 189] or via torrefaction of the biomass. Both technologies are under development (see also Sect. 4.1.2).

When using lumpy wood-type biomass or pellets in a fixed-bed gasifier, then the upflowing gases contain very high loadings of tar and hydrocarbons, making downstream tar-removing units difficult. Downdraft Fixbed reactors overcome that tar problem, but they are very much limited in capacity. Therefore, fluid bed systems offer the best process conditions for biomass gasification. In addition, the high reactivity of biomass and the typically low ash contents result in high carbon conversion rates, unlike when using coal as feedstock.

However, tar conversion units are mandatory behind fluid bed gasifiers to achieve syngas quality. Also, the feeding of biomass against elevated pressure requires very specific lock hopper and/or screw feeding systems to achieve the necessary sealing against the environment, while securing adequate dosing performance.

Foster Wheeler developed an air-blown CFB under pressure, which operates at 20 bar with a capacity of 18 MWth for an IGCC application (Värnamo, Sweden). Their plant operated over 8,500 h, but it shut down due to lack of commercial

success in 1999. It is now being converted to operate with oxygen and steam to produce syngas for a biomass-to liquids plant.

The Carbona process was originally developed by GTI in the United States (see Fig. 4.59), testing a wide variety of biomass and other feedstocks in a 20-MWth pilot plant at gasification pressures up to 30 bar. A commercial air-blown plant is operating at Skive, Denmark for power generation and district heating, using approximately 110 t/h of wood pellets. An oxygen-blown version of this technology is being developed in cooperation with the GTI for biomass-to-liquid (Fischer–Tropsch) projects.

Fast internal-circulating fluid bed (FICFB) technology was developed at the Vienna University of Technology in Austria. A plant with a capacity of 42 t/h of wood chips was built at Güssing, Austria. This plant uses an allothermal process, whereby the heat for the gasification is provided by the combustion of char in a separate CFB combustor and circulation of the hot sand bed material, the ash and residual char to the gasifier reactor, which is fluidised with steam. The predried biomass is fed to the gasifier and the raw syngas leaves the gasifier at approximately 850 °C, is cleaned, and then is routed to a gas motor. Projects for the production of chemicals from the syngas by adding additional process steps are underway.

In summary, because of the lower gasification temperatures and the carbon in the fly ash (and to a lesser degree, also in the bed ash), fluid beds have a lower cold gas efficiency than fixed-bed and entrained-flow gasifiers. Potential disposal problems with the ash because of the carbon content can be solved by postcombustion in separate boilers. Low melting components in the mineral matter of the coal (e.g. alkali minerals) can cause the formation of agglomerates and subsequent plugging of the fluid bed. The addition of sulphur absorbents such as limestone can reduce sulphur emissions effectively (up to 90 %), thus favouring the use of high-sulphur coals. In addition, fluid-bed systems can gasify a broad particle size distribution and are therefore favoured for the gasification of biomass.

4.4.6.6 Entrained-flow Gasification Processes: General Principles

Entrained-flow gasification is applied for coal/water slurries (e.g. see the reactors in Figs. 4.65 and 4.66), for liquid hydrocarbon residues, and for dry coal dust (Figs. 4.63 and 4.64). The pressurised feedstock is fluidised and injected into a reaction chamber together with water steam and oxygen. Under extreme thermal conditions of flame temperatures >2,000 °C and equilibrium temperatures of 1,200–1,600 °C, carbon reacts with water steam in an endothermic, so-called heterogeneous water steam reaction to a thermodynamic equilibrium of hydrogen, carbon monoxide and carbon dioxide. Pressure is usually in a range of 30–80 bar, depending on the design and downstream processes. Reaction heat necessary for the heterogeneous water–gas reaction is delivered by a POX of carbon with oxygen. Coupled in one reactor, the positive and negative heat duties of both the oxidation and water–gas reaction have to be balanced carefully to result in an

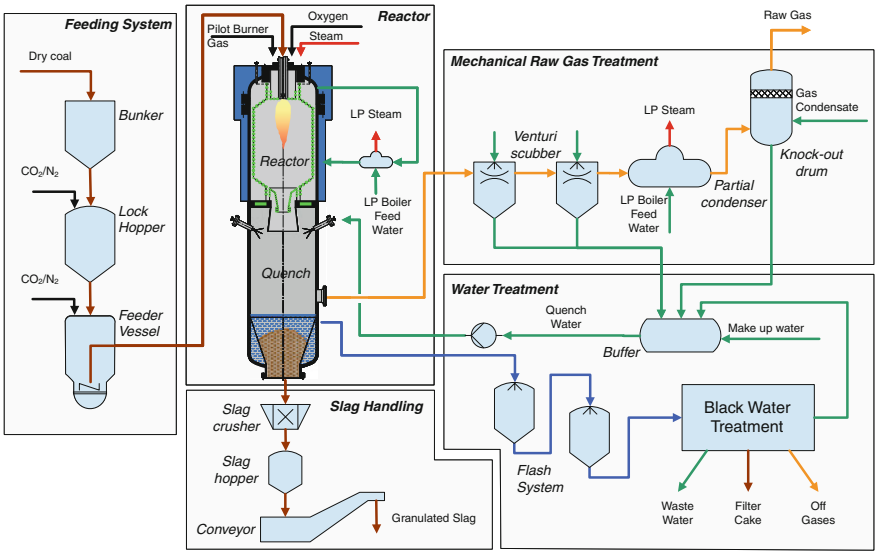

Fig. 4.60 Entrained-flow dry coal dust gasification system [194]

autothermal reaction. Inorganic material contained in the fuel, such as ash in the coal, melts under these conditions to an inorganic glass-like material containing the slag builders alumina, calcium oxide and silicon oxide. Depending on the design, the slag may cover a water-cooled basket (cooling screen reactor; see Figs. 4.63 and 4.64) and protect it against the hot atmosphere, while the pressure vessel stays comparably cool at temperatures <280 °C. Other designs make use of the heat in radiation coolers to generate high-pressure steam but carefully treat the slag. For fuel with a low content of slag builders, a refractory-lined reaction chamber is used.

For water quench systems, as shown in Fig. 4.60, the hot stream from the reactor is cooled down with a spray of water. In this process, additional hydrogen is formed from a homogenous WGS equilibrium. Further, the molten slag solidifies and can be taken out as granulate via a lock hopper system. Gas leaves the quencher downstream via some dust removal and condensation units to further reduce the dust content of the gas. Quench water containing soot, slag particles, and some soluble salts is brought into a filtration and treatment section and recycled.

Figure 4.61 shows the impressive dimensions of a GSP gasifier with a capacity of 500 MWth in the workshop. The reactor is 80 m long and has a total weight of 220 t [194].

Figure 4.62 shows the overall arrangement of the five GSP gasifiers, which produce the raw syngas for the downstream Rectisol gas cleaning plant, followed by the methanol-to-propylene process (see Sect. 6.4.3 and Figs. 6.84 and 6.85).

Fig. 4.61 A 500 MWth GSP gasification reactor

Fig. 4.62 Entrained-flow (EF) gasification plant with 5 × 500 MWth GSP EF gasifiers. (Shenhua Ningxia Coal Group) [194]

4.4.6.7 Dry-feed Entrained-flow Gasification Processes

EF gasifiers can take solid, liquid and gaseous fuels. They operate at temperatures well above ash melting points, have a very high carbon conversion and produce a syngas free of tar and phenols. For these reasons, they are regarded as the most flexible gasification systems. EF gasifiers typically operate under pressure of

20–80 bar, with the majority at approximately 25 bar, and in a temperature range between 1,200 and 1,600 °C [131].

In comparison to moving bed gasifiers, their steam consumption can be much lower (by a factor of 10–18 depending on the type of coal). It must be recognised, however, that typically additional steam (more than for FBDB) has to be added to the syngas from the EF gasifiers before entering the shift stage to adjust the H_2/CO ratio for the downstream synthesis. This can at least partly compensate the higher steam consumption of the FDBD technology (see above). However, a drawback is the significantly higher oxygen consumption of the EF technologies because of the operation in the ash fluid temperature ranges. (Typically FB gasifiers need only approximately 30–50 % of the O_2 consumption of an EF gasifier.)

Coal needs to be very fine (<1 mm). The degree of fineness and the particle size distribution depend strongly on the type of coal its ash content, and the mineral composition of the ash. Fluxes such as limestone can be added to reduce the ash melting temperature. Technically, the maximum ash content accepted by EF systems is around 40 %; however, there is an economical limit at approximately 20 % ash because the O_2 consumption for the melting of the ash becomes prohibitive. The fine coal can be brought into the reactor as dry feed (using steam or CO_2 as a transport medium for the dense phase flow) or pumped in via a coal slurry.

Reactor configurations differ according to the entry point of the fuel:

1. Top-fired gasifiers show a gas flow vertically from the top to the bottom of the reactor, together with the molten slag.
2. The gasifier may be horizontally fired from the side, resulting in an upward flow of the raw gas, while the slag particles flow downwards along the reactor walls. Some designs, based on slurry feed, use raw gas recycling to increase the retention time of the particles.

The very high reaction temperatures (1,200–1,600 °C) require expensive materials for the burners, the refractory or membrane wall and the downstream syngas coolers. The major existing EF processes are described in the following sections, and an outline on potential future dry EF processes is given.

Siemens GSP EF Process

The Gaskombinat Schwarze Pumpe (GSP) process was originally developed by Deutsches Brennstoff Institut in Freiberg, Germany and was first employed on the industrial scale in 1984. The gasifier had a thermal capacity of 200 MWth. The technology was bought by the Noell Group and subsequently by Babkock Borsig, Future Energy, and finally by Siemens AG Power Generation in 2006.

The Siemens GSP process is a downflow (feed and agent in same direction as the GE/Texaco technology), high-temperature, entrained-flow gasifier technology. The GSP technology is characterised by its proprietary cooling screen in the reactor (see Fig. 4.63). The cooling screen provides a relatively simple design and construction, enabling very short startup and shutdown sequences; as such, it is a significant improvement over the refractory-lined reactors offered by competing technologies. The lifetime of the screen is claimed to be about 10 years, compared

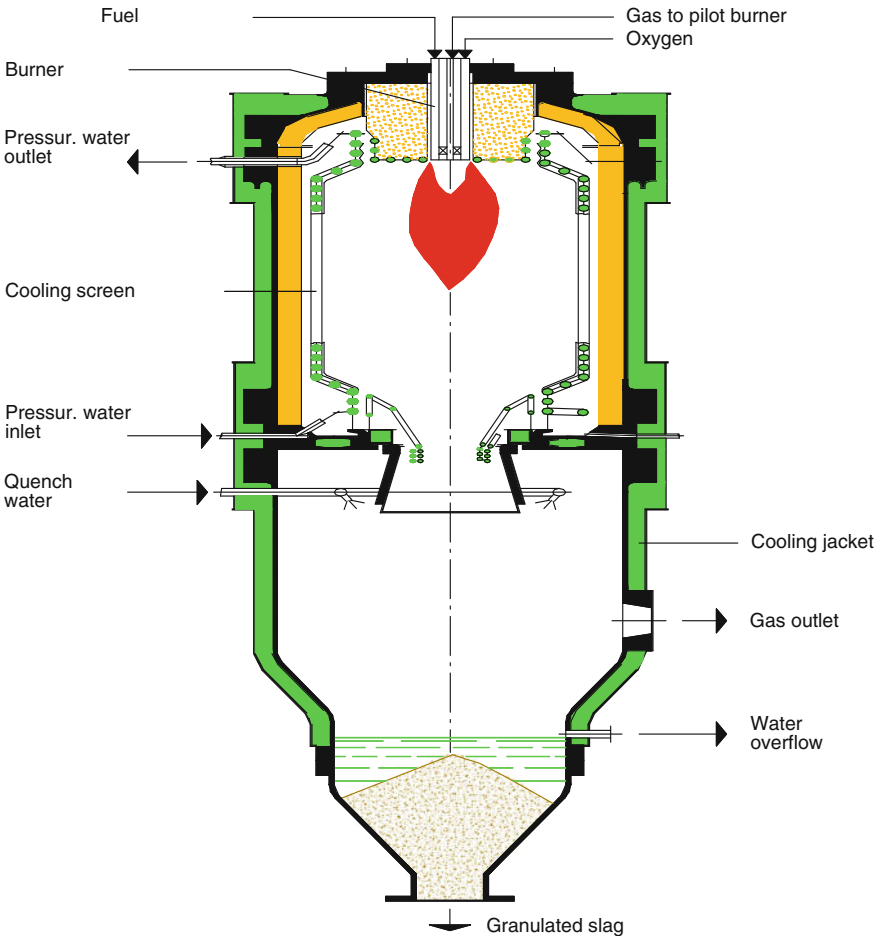

Fig. 4.63 The Siemens GSP process [132]

to 1–2 years for refractory-lined systems. For low-ash applications, the reactor can also be offered with refractory.

A layer of solidified and molten ash is formed on the cooling screen, providing thermal insulation and keeping the tube surface of the cooling screen at temperatures below 230 °C. To secure the ash layer on the wall, coals must have ash contents of at least 5 %, or else the addition of flux material or recycled fly ash is necessary. Approximately 2–3 % of the total heat produced is removed by the cooling screen and generates low-pressure steam.

The raw gas leaves the gasification chamber at the bottom of the cooling screen and is quenched with water sprays. The process water in the raw gas, condensed during further cooling, is recycled to the quench sprays. The water from the quench camber is cleaned of heavy metals, sulphur, and nitrogen components,

which are dissolved during the quench process. The molten slag is solidified, extracted from the reactor in a granulated form. A variety of coals have been tested, resulting essentially in the following parameters:

- Ash content should be below 15 %; if coals have higher ash contents, they should be blended with other low ash fuels (e.g. petroleum coke).
- Gasifier operating temperature should be adjusted to 100–200 °C above the melting point of the ash.
- Coals with very high ash melting points (>1,500 °C) should be blended with fluxes such as limestone.
- Low-reactivity coals (e.g. anthracite or petroleum coke) will be ground to smaller particle sizes, compared to higher reactivity coals.

Shell EF Process

The origin of the Shell EF process goes back to the Koppers–Totzek process. Shell and Koppers jointly developed the pressurised reactor technology and built a demonstration plant (150 t/h coal feed) at Harburg, Germany in 1978. Later on, Shell and Koppers separated their developments because Koppers was more interested in a better syngas, whereas Shell was more interested in the downstream production of Fischer–Tropsch products based on coal.

The Shell coal gasification process is a high-temperature entrained-flow process. The configuration of the gasifier is a bottom-up flow principle (see Fig. 4.64). The gasifier is fed with a dry, pulverised coal. The coal is very fine, with typically

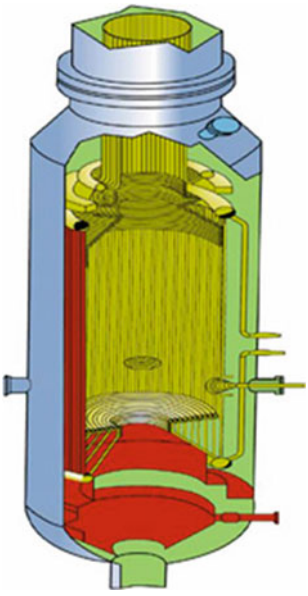

Fig. 4.64 Shell gasification reactor [195]

90 % being <90 μm. It is pressurised in lock hoppers, transported as a dense phase using nitrogen or CO_2 and injected as a mixture of coal, oxygen and steam. The burners and feed systems are located at the bottom of a gasification chamber enclosed by a nonrefractory membrane wall. The reaction is very fast, yielding a carbon conversion that is greater than 99 % within a residence time between 0.5 and 4 s. The raw gas flows upwards to the gas outlet. It contains approximately 66 % CO, 33 % H_2 and 1–2.5 % CO_2 and is free of any tar and phenols. Evaporating water circulates through the membrane wall tubes, controlling the membrane wall temperature and raising steam. The gasifier operates typically at 20–40 bar and temperatures of 1,500 °C and above. A gas quench via recycled raw syngas is used to reduce the raw synthesis gas to approximately 900 °C prior to a high temperature waste heat recovery boiler. Shell has recently introduced a water quench as an alternative to the syngas cooler, which has advantages, especially in cases where a CO shift is needed to trim the syngas composition for the downstream chemical production.

The process can gasify almost any coal that can be milled and pneumatically transported. However, certain adjustments regarding grain size, steam injection, oxygen-to-coal ratio must be made to secure optimum operation. Ash contents less than 8 % require ash recirculation to avoid reduction of the liquid slag layer, which would cause to high heat losses through the membrane wall, resulting in a reduced thermal efficiency. Ash contents greater than 15 % increase the operating cost (essentially causing higher oxygen consumption). Technically, the system can process coals with up to 40 % ash content, but obviously at a very much increased operating cost.

Shell has licensed more than 50 reactors of sizes between 900 and 4,000 tpd capacity, with more than half of them operating in China. The plants produce syngas for ammonia/urea production or H_2 for other chemical plants (methanol, oxo-synthesis).

Koppers–Totzek EF Process

This process was developed and used by Koppers from 1941 on, using oxygen gasification at atmospheric pressure. A total of 77 reactors were built through 1988.

Prenfo EF Process

Prenflo (pressurised EF) is the continued development of the atmospheric pressure operated Koppers–Totzek process. Because the Prenflo and the Shell process resulted from a joint development in the Harburg gasification plant, they are to a great extent similar. This gasifier structure is different from the Shell design because it incorporates both the gasifier and the syngas cooler in the same pressure vessel, which is refractory lined. Coal, oxygen and steam are fed through four horizontal burners in the lower part of the reactor.

The gasification temperature is approximately 1,600 °C. The gas flows upwards, is quenched by recycled gas to approximately 800 °C, flows downwards

through evaporator sections, leaves the gasifier at approximately 380 °C, and is thereafter dedusted and cleaned.

A Prenflo pilot plant (48 tpd) was successfully operated in Fürstenhausen (Germany) with a variety of coal with ash contents up to 40 % as well as low-volatile coals to demonstrate the flexibility of the process [190]. The Puertollano IGCC plant in Spain is so far the only commercial plant that uses the Prenflo process. However, with a capacity of 320 MW_e, it is one of the largest gasification units using solid fuel.

EF Gasification Process Developed in Japan

Mitsubishi Heavy Industries EF Process

This technology was initially developed by Mitsubishi Heavy Industries (MHI) and Clean Coal Power (CCP) research and development. It was demonstrated in a 200 tpd pressurised pilot plant in Nakoso in Japan using enriched air as an oxidant, but pure oxygen also can be used. The reactor is divided in two sections. Coal and enriched air are introduced into the bottom section from the side. The coal is burnt under combustion conditions. The hot flue gas flows upwards into the upper reactor (reductor) section, where additional fine coal is added to generate the reducing atmosphere for gasification. A follow-up project is the 250-MW IGCC demonstration plant, also at Nakosa, which started operation in 2007. Another project is under development in Australia (ZeroGen Project), which will be ready for startup in 2015.

EAGLE (Hitachi) EF Process

This technology is under development by the Electric Power Development Company in Japan. A 150 tpd oxygen-blown, pressurised pilot plant with an IGCC concept started up in 2002 [183]. The process also has a two-stage reactor. The first stage operates in oxygen-rich mode, with temperatures around 1,600 °C. The second stage is oxygen lean, using coal and recycled gas to reduce the temperature to approximately 1,150 °C. Tangential firing prolongs the residence time. Substantial test work has been performed since then under the Department of the New Energy and Industrial Technology Development Organization clean coal strategy programme in Japan.

EF Technologies Developed in China

Initially, gasification technology was imported to China (essentially Lurgi FBDB and Texaco). These technologies were further developed in China (see Fig. 4.65). Special developments, based on entrained-flow process principles, have been made by the Institute of Clean Coal Technology) at the East China University of Science and Technology in Shanghai. One process uses OMBs fed by coal/water slurry in a downflow reactor, operating at 65 bar. The first industrial plant was started up in 2004 (750 tpd) and was followed by two more units (1,150 tpd) coal feed in Yankuang in 2005. More than 15 units have been put into operation/development since 2005. Further developments include dry feeding and a membrane wall reactor design.

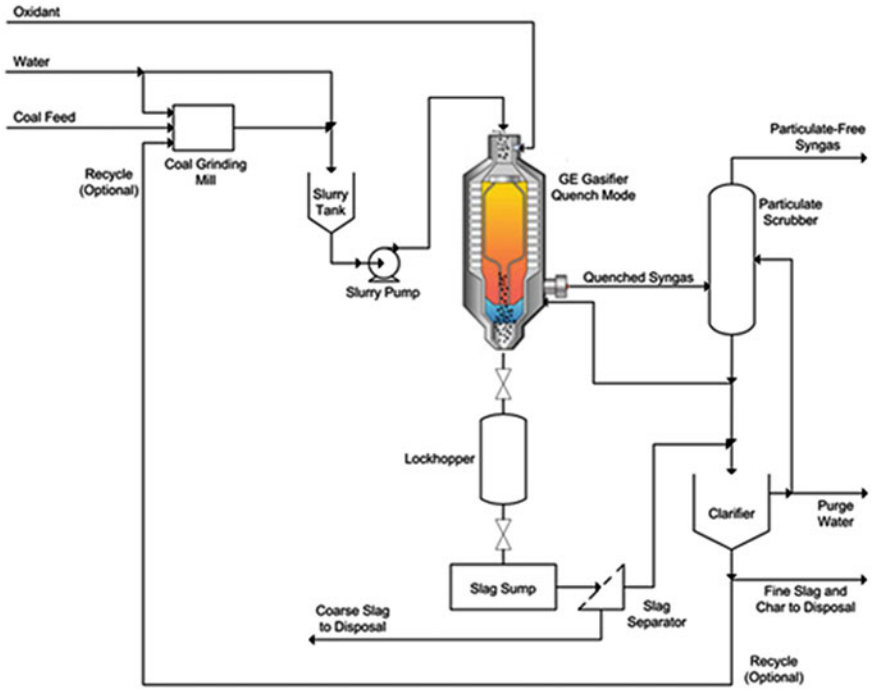

Fig. 4.65 GE/Texaco entrained-flow gasifier [195]

4.4.6.8 Slurry Feed EF Gasification Processes

General Electric/Texaco Entrained-flow Gasification

The General Electric (GE) Texaco process is a high-temperature entrained-flow process (see Fig. 4.65). There are two characteristic features of the process: The gasifier is a pressure vessel with a refractory lining, which operates at temperatures in the range of 1,250–1,450 °C and pressure of 30 bar for power generation, up to 60–80 bar for H_2 and chemical synthesis [184]. It has a topdown configuration and the feed is in slurry form. The feedstocks, oxygen and steam are introduced through burners at the top of the gasifier. The water content in the coal/water slurry replaces most of the steam, which is otherwise injected into the system. Although this makes the feeding system appear somewhat simpler in comparison to dry-feed systems, the operating cost impact of additional oxygen significantly outweighs the benefit of the feed system in many instances. The raw gas can be cleaned and cooled either by water quench or by a radiant syngas cooler (1,400–700 °C). The technically preferred option is the water quench for availability and reliability reasons, such as corrosion and fouling of the syngas cooler, despite the somewhat lower thermal efficiency.

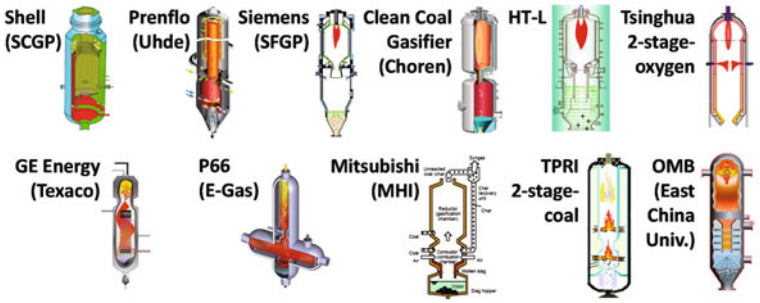

Fig. 4.66 Summary of entrained-flow processes [188]

A power plant using Texaco technology is operated in China for the production of power and town gas. Several projects for combined IGCC and chemical/fuel production are under consideration or development in the United States [131].

The Texaco technology is used for a variety of chemical plants in China. Approximately 25 chemical plants have been in operation since 1993. Eastman Chemicals operates two Texaco quench gasifiers in Kingsport, Tennessee, at 70 bar and 1,400 °C (one is in operation, one is in hot standby), using high-sulphur coal and petroleum coke as fuel to produce acetic acid and acetic anhydride. Part of the syngas is further processed to separate CO and H_2 prior to a methanol synthesis.

E-Gas EF Gasifier (Conoco Phillips)

This gasifier is a two-stage refractory-lined pressure shell (30 bar) (see Fig. 4.66). The coal slurry is preheated and introduced into the reactor in horizontally arranged burners at two levels. Approximately 80 % of the coal is introduced together with oxygen at the lower level, with the remaining 20 % at the upper level. The gasification temperature at the lower level is approximately 1,350–1,400 °C, falling to approximately 1,050 °C at the exit of the reactor head. The raw gas is cooled in a fire tube syngas cooler generating saturated steam. The advantage of the two-stage system is a HHV of the gas. According to Ref. [131], the fire tube cooler is considerably cheaper in comparison to other syngas coolers (Shell, Texaco and Prenflo).

The only plant in operation is the Wabash River plant in the United States. Three more projects are in the development, planning, or front-end engineering design phase in the United States. Startup is foreseen in 2012 or 2013.

Figure 4.66 shows a summary of EF processes that have been developed and commercialised in recent years. Clearly, there is an increasing number of EF processes from China, due to China's strong development towards coal-based chemical and fuel production technologies.

4.4.6.9 Evaluation and Decision Criteria for the Selection of the Best-suited Gasification Process for Methanol Production

Fixed-Bed Processes

As outlined above, the type, quality and the price of the coal have the most important influence on the selection of the gasification technology, as shown in Fig. 4.54 and in Chap. 7. The FB processes have their special advantage of being able to gasify coal with very high ash content (>25 % ash), and high fusion temperatures (>1,200 °C). These coals are typically run-of-mine coals or waste coals and therefore are inexpensive. The cost of coal preparation is comparatively low. The mechanical design is robust, and oxygen consumption is up to 60 % less compared to EF gasifiers. However, the steam consumption can be substantially (up to 3–4 times) higher than EF gasifiers, depending on the fusion temperature of the coal. Challenges include more complex gas cleaning, tar and phenol treatment, and the scaleup of reactor dimensions. The use of biomass as fuel is limited.

EF Processes

Important advantages of the EF processes are that several commercial designs are available, the gasifier has no moving parts and is simpler in geometry than fluid bed and FB processes, and it has the highest capacity per unit of volume. Large-scale units (up to 500 MWth) are in operation and scale up to 1,000 MWth per gasifier seams feasible, thus reducing the investments for future large-scale chemical complexes. Nearly every type of coal can be used, as long as it can be dried and milled to the necessary grain size. Ash contents up to 45 % have been tested in pilot operation [194], although at the expense of very high coal preparation and oxygen costs, which puts the economic limit at about 20–25 % ash. The EF processes produce a syngas free of tar and phenols, and the slag is very low in carbon, is virtually inert, and is therefore easy to dispose or is suitable for further use. Biomass can be used; it requires preparation, such as via pyrolysis or torrefaction, but it offers a longer time potential to switch from fossil to renewable feedstock.

Against these advantages, there are essentially the following challenges or limitations. The very small inventory and the very short retention time for the gasification reaction require advanced and sophisticated controls to ensure a safe and reliable operation. The very high temperatures necessitate high-quality and therefore expensive construction materials. Burners and heat recovery sections are critical design areas because of molten slag and the oxygen consumption is high in comparison to other gasification technologies.

Fluid-bed Processes

Regarding ash content and fusion temperature, similar limitations exist as for the EF processes. Operating under higher pressures is more difficult, carbon conversion is lower for coal gasification, the syngas also needs more complex gas cleaning because of tars and phenols, and scaleup is limited. Fluid-bed processes are well positioned for the gasification of biomass to methanol. The plant sizes are smaller, biomass preparation is simple and no pyrolysis or torrefaction necessary.

Conclusion

Taking into account the above-mentioned aspects, the most likely process for future methanol production from coal are the EF processes. Tables 4.16, 4.17, 4.18 and 4.19 summarise the essential facts to compare the gasification processes.

Table 4.16 Summary of gasification systems

Preferred feed coal characteristics	Fixed bed	Fluidised bed	Entrained flow
Particle size	6–50 mm	<6 mm	<0.1 mm
Preparation	Screening	Crushing	Milling and drying
Caking/swelling	Yes (with modifications)	Noncaking	Any
Ash melting temperature	>1,200 °C	>1,100 °C	<1,300 °C
Ash removed as	Ash	Ash and fly ash	Slag and fly slag
Rank	Low to high	Low to high	Low to high
Ash content	<50 % (ash + moisture)	No limitation	<25 %

Table 4.17 Characterisation of gasification technologies and operating principles

Typical operating characteristics	Fixed bed (FBDB)	Fluidised bed (HTW)	Entrained flow
Gasifier offtake temperature	400–600 °C	900–1,100 °C	1,200–1,900 °C
Oxidant requirement, kg O_2/kg moisture- and ash-free coal (maf)	0.3–0.5	0.5–0.7	0.9–1.1
H_2/CO ratio	1.5–2.5	0.9	0.4–0.5
Steam consumption split	Gasifier high CO shift zero–low	Gasifier low CO shift high	Gasifier zero–low CO shift high
Methane content in raw gas %	9–12	2–3	<0.1
Carbon conversion %	96–98	90–95	>99.5
Cold gas efficiency %	85–90	63–80	77–82
Fuel retention time	1 h (large inventory)	Minutes	Seconds

Table 4.18 Key distinguishing characteristics

	Fixed bed	Fluidised bed	Entrained flow
Key distinguishing characteristics	Hydrocarbon liquids in the raw gas	Large char recycle (carbon content)	Large amount of sensible heat in the hot raw gas
Key technical issues	Utilisation of hydrocarbons	Carbon conversion	Raw gas cooling
	Gasification/saleable byproduct	Combustion	Steam production
Experience in synthetic natural gas (SNG) Production	Dakota Gasification Company started up in 1984 at 160,000 Nm^3/h SNG		

Table 4.19 Summary comparison of gasification processes for methanol production

Gasification process	Fixed bed	Entrained flow	Fluidised bed
Gas composition for synthetic natural gas	++	–	n.a.
Operation pressure	+	++	Limited
Gas composition for methanol	+	++	Biomass only
Production efficiency	++	++	–
Capital expenditure	+	++	–
Operational expenditure	+	+	–
Coal: high ash (>25 %) high fusion temperature (>1,200 °C)	++	–	+
Coal: low ash (<20 %) low fusion temperature (<1,000 °C)	–	++	+
Coal preparation cost	++	–	–
Biomass as feed	–	++[a]	++
Scale-up potential	+	++	Limited

[a] Biomass can be fed after preparation as slurry (after pyrolysis) or as coke (after torrefaction)

4.4.7 *Raw Syngas from Different Gasifier Technologies: Quench and Particulates Removal*

Different gasification processes and different fuels result in different raw syngas compositions. Further cleaning and conditioning can be done by different process steps, as will be further outlined here. Figure 4.67 shows as an example a simplified scheme of the Shell EF process, where the raw gas from the gasifier is first cooled in a syngas cooler. A dry ash removal step and a subsequent water wash are

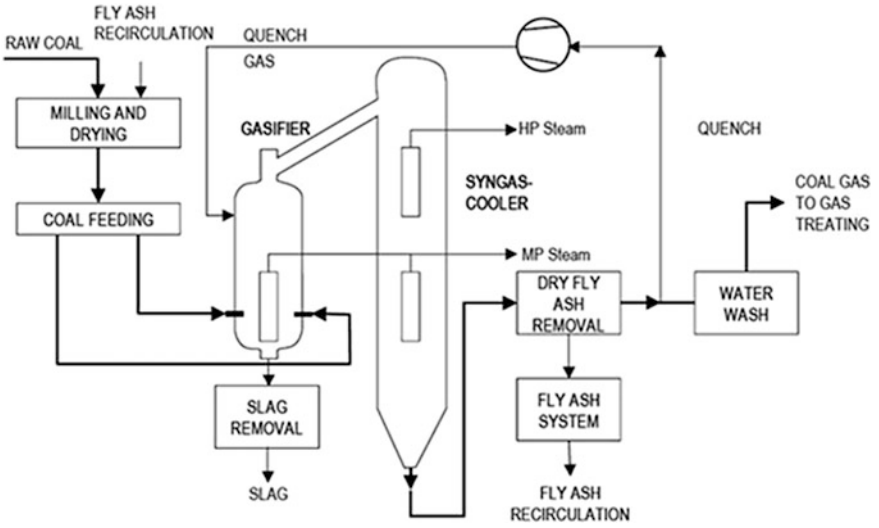

Fig. 4.67 Simplified Shell process scheme (including dry ash removal and water wash) [195]

Table 4.20 Range of syngas compositions across different gasifier types, and feedstock produced by the gasification of Coal feedstock [206]

Gasifier	E-Gas [197]	Kellog Rust Westinghouse [198, 200]	Oxygen blown–transport [199, 201]	E-Gas [202]	General Electric [197, 203] (oxygen blown)	Prenflo [204]	Lurgi FBDB	British Gas/Lurgi [205]
Facility	Wabash	Pinon-Pine Power-Project	–	Wabash	–	Puertollano	Various	SVZ
Coal	Several	Several	Several	Several	Unknown	Coal/petroleum coke	Illinois no 6	Illinois no. 6
CO	42.2–46.7	23.91	4–14	45.3	39.09–43.44	59.9	29.5	45.8
H_2	32.31–34.40	14.58	8–16	34.4	28.94–32.91	21.7	52.2	26.4
CO_2	14.89–17.13	5.45	12–14	15.8	9.32–13.53	2.9	5.6	2.9
H_2O	–	5.45	17–40	–	13.11–19.91	–	5.1	16.3
CH_4	1.04–2.29	1.35	2–5	1.9	0.02–0.03	< 0.1	4.4	3.8
Ar	–	0.56		0.6	0.06	14.4	1.0	1.5
N_2	–	48.68	30–55	1.9	0.41–0.45		0.6	1.8
H_2S	17.28–107.2 ppm	–	2,000–3,000 ppm	68 ppm	0.58–0.64	1.1	900 ppmv	1,000 ppmv
COS	9.03–162.13 ppm	–	–	–	0.03–0.04		40 ppmv	100 ppmv
Others	–	0.02	–	–	–	–	500 ppmv NH_3 + HCN	200 ppmv NH_3 + HCN

Table 4.21 Key parameters of syngas for the production of methanol and other fuels [196]

Product	Synthetic fuels Fischer–Tropsch gasoline	Methanol	Hydrogen	Fuel gas Boiler	Turbine
H_2/CO	0.6[a]	~2.0	High	Unimportant	Unimportant
CO_2	Low	Low[c]	Not important[b]	Not critical	Not critical
Hydrocarbons	Low[d]	Low[d]	Low[d]	High	High
N_2	Low	Low	Low	Note[e]	Note[e]
H_2O	Low	Low	High[f]	Low	Not[g]
Contaminants	<1 ppm sulphur, low particulates	<1 ppm sulphur, low particulates	<1 ppm sulphur, low particulates	Note[k]	Low particulates, low metals
Heating value	Unimportant[h]	Unimportant[h]	Unimportant[h]	High[i]	High[i]
Pressure, bar	~20-30	~50 (liquid phase) ~140 (vapour phase)	~28	Low	~400
Temperature, °C	200–300[j] 300–400	100–200	100–200	250	500–600

[a] Depends on catalyst type. For iron catalyst, the value shown is satisfactory; for cobalt catalyst, a value of approximately 2.0 should be used

[b] Water–gas shift will have to be used to convert CO to H_2; CO_2 in syngas can be removed at same time as CO_2 generated by the water–gas shift reaction

[c] Some CO_2 can be tolerated if the H_2/CO ratio is greater than 2.0 (as can occur with steam reforming of natural gas); if excess H_2 is available, the CO_2 will be converted to methanol

[d] Methane and heavier hydrocarbons need to be recycled for conversion to syngas and represent system inefficiency

[e] N_2 lowers the heating value, but the level is unimportant as long as syngas can be burned with a stable flame

[f] Water is required for the water shift reaction

[g] Can tolerate relatively high water levels; steam is sometimes added to moderate combustion temperature to control NO_x

[h] As long as H_2/CO and impurities levels are met, heating value is not critical

[i] Efficiency improves as heating value increases

[j] Depends on catalyst type; iron catalysts typically operate at higher temperatures than cobalt catalysts

[k] Small amounts of contaminants can be tolerated

used to remove essentially all particulate matter, before the coal gas is routed to the gas treating section.

Table 4.20 outlines the raw syngas compositions for the variety of gasification processes described previously. Before the conditioning and treatment via further process steps, as will be outlined in the following chapters, the raw gas from the gasification processes has to be cooled and cleaned from particulates, before being fed to further processing to a suitable methanol synthesis gas. As described

previously, this can be done in a dry fly ash removal step, as shown in Fig. 4.67. Thereafter, the remaining particles are finally removed via a water wash. As an alternative to a syngas cooler, the hot raw gas is directly quenched with water at the exit of the gasifier to cool it and clean it from particulate matter before entering the syngas conditioning section.

Table 4.20 outlines a range of raw gas compositions across different gasification processes, as described previously. In addition, Table 4.21 describes additional requirements for syngas for the different downstream processes, including methanol production.

4.4.8 Conditioning and Purification of Crude Synthesis Gas after Gasification

4.4.8.1 General

The raw gas from the gasification stage will have to be adjusted for its composition for further processing (e.g. methanol synthesis). To protect the downstream processing steps, the raw gas needs to be further treated to remove fine particulates and contaminants such as sulphur, arsenic, mercury and other traces. This includes conversion of COS, which often is formed in the gasification process. COS is converted to H_2S, which can then be totally removed in the acid gas scrubbers (see Sects. 4.4.8.6 and 4.4.9).

Usually, the raw gas from the gasifier is quenched and treated in filters/cyclones and a water scrubber. The scrubbed gas is then further treated in several catalytic, adsorption and finally acid scrubbing to meet the requirements of methanol synthesis feedstock.

The core parts include the following:

- WGS reactors, which in the case of methanol synthesis are normally operated with a partial stream to adjust the desired H_2/CO ratio in the combined stream
- COS hydrolysis and other fine-cleaning steps, depending on the case
- Sulphur and CO_2 recovery (see Sect. 4.4.9).

4.4.8.2 Adjustment of CO/H_2 Stochiometry for Methanol Synthesis

The various reactions of carbon and hydrocarbons with water and oxygen to form a mixture of hydrogen and CO ("water gas") lead to very different H_2/CO ratios. All are endothermic reactions with the exception of methane oxidation. Due to the low H/C ratios of gasifier feed stocks such as coal and crude residues, product gases are hydrogen deficient with H_2/CO molar ratios far below 2 although a stoichiometric number SN of slightly above 2 is needed for the methanol synthesis (see Fig. 4.68 and equation 4.38 in Sect. 4.3.2.4).

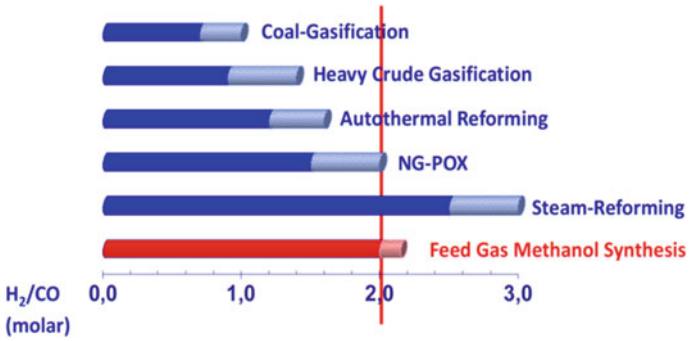

Fig. 4.68 H_2/CO ratios from different syngas-generating processes

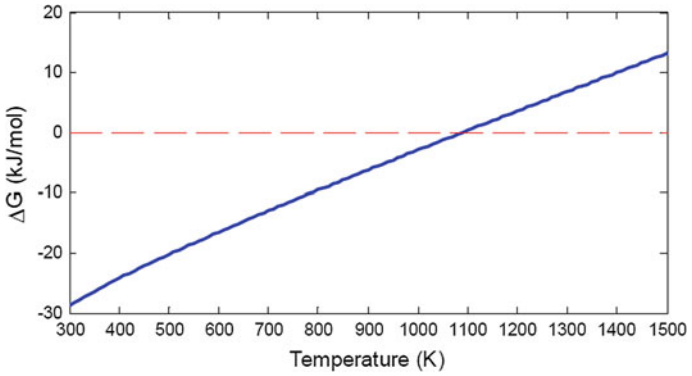

Fig. 4.69 Free enthalpy of the water–gas shift reaction

Although POX and steam reforming of hydrogen-rich hydrocarbons (e.g. methane) generate H_2/CO ratios of 2 or more, hydrogen-deficient raw gases from heavy feedstock gasification have to be converted (after conditioning to protect the conversion catalyst) into a hydrogen-richer gas. The WGS reaction of CO with water should be carried out in a split stream to achieve the desired hydrogen concentration in the combined feed gas to the methanol synthesis. The split depends on raw gas composition and conversion rates in the WGS reactor.

The principal reaction is as follows:

$$H_2O + CO \rightleftarrows CO_2 + H_2 \quad (\Delta H^\circ = -41.2\,\mathrm{kJ/mol})$$

The reaction is almost pressure independent, slightly exothermic and reversible. Higher temperatures thermodynamically lead to lower H_2/CO ratios, as can be seen from the temperature curve of the free enthalpy (Fig. 4.69) and the equilibrium constant (Fig. 4.70) [207].

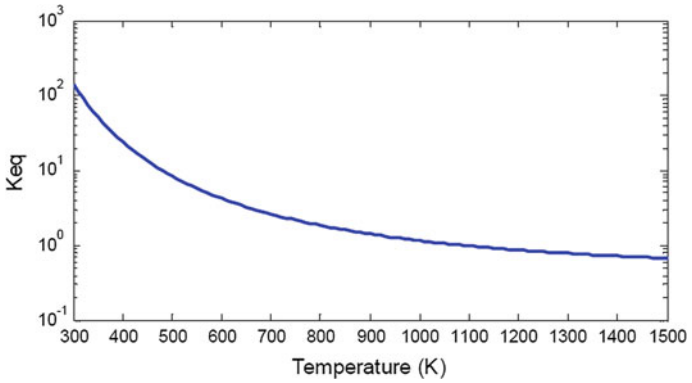

Fig. 4.70 Equilibrium constant of the water–gas shift reaction

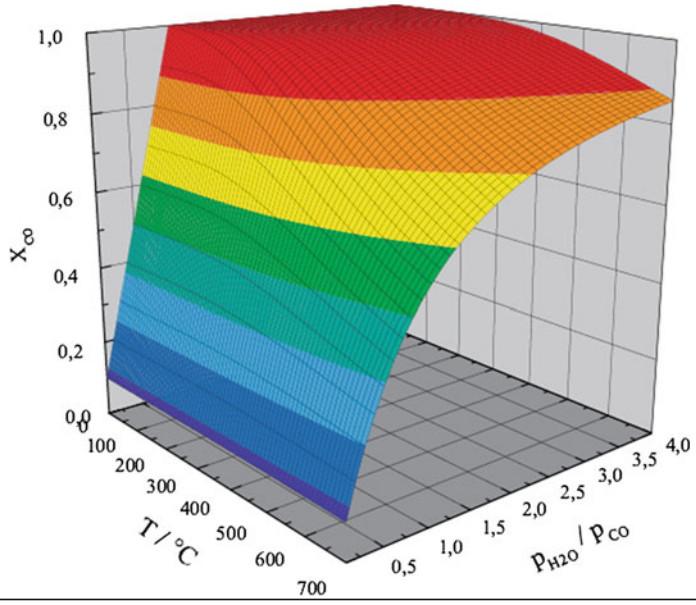

Equilibrium conversion of the water gas shift reaction at various p_{H2O}/p_{CO} and T for p_{total} = 1 bar (p_{CO} = 0.1, p_{H2O} = 0.05 … 0.4 bar, balance nitrogen). Calculation using Aspen 2006.3 with equilibrium constants from Laine et al.

Fig. 4.71 Equilibrium conversion of the water–gas shift reaction as a function of H_2O/CO ratio and temperature [209]

Table 4.22 Redox and formate mechanisms of the water–gas shift reaction

Redox mechanism	Formate mechanism
$CO + \theta \rightleftarrows CO^*$	$CO + \theta \rightleftarrows CO^*$
$H_2O + \theta \rightleftarrows H_2O^*$	$H_2O + \theta \rightleftarrows H_2O^*$
$H_2O^* + \theta \rightarrow H^* + OH^*$	$H_2O^* + \theta \rightarrow H^* + OH^*$
$OH^* + \theta \rightarrow O^* + H^*$	$CO^* + OH^* \rightleftarrows COOH^* + \theta$
$OH^* + OH^* \rightarrow H_2O^* + O^*$	$COOH^* + \theta \rightleftarrows CO_2^* + H^*$
$CO^* + O^* \rightarrow CO_2^* + \theta$	$COOH^* + OH^* \rightarrow CO_2^* + H_2O^*$
$CO_2^* \rightleftarrows CO_2 + \theta$	$CO_2^* \rightleftarrows CO_2 + \theta$
$H^* + H^* \rightarrow H_2 + 2\theta$	$H^* + H^* \rightarrow H_2 + 2\theta$

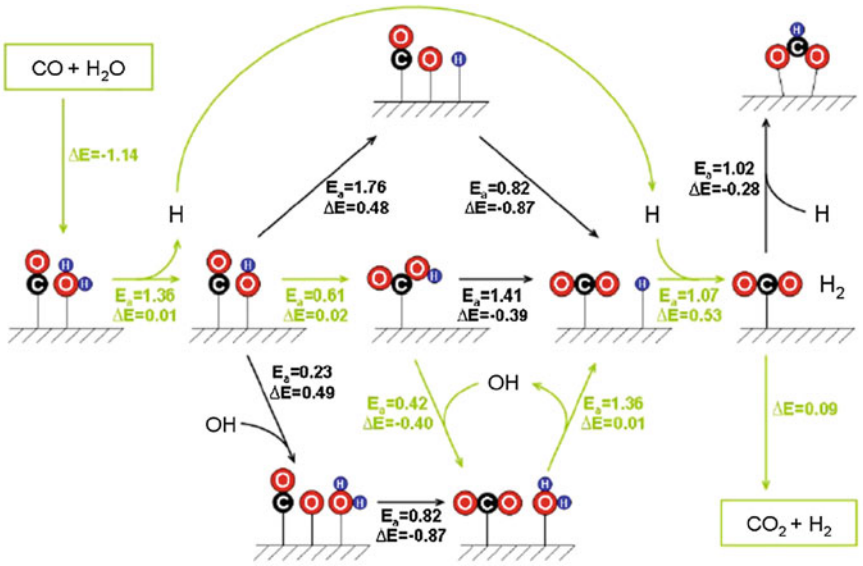

Fig. 4.72 Reaction mechanism of water–gas shift reaction (minimum energy path in green as eV), according to Brenna [210]

To calculate the equilibrium constant, according to Choi and Stenger, the following equation applies [208]:

$$K_{eq} = \exp\left(\frac{4,577.8}{T} - 4.33\right)$$

The strong temperature dependence means that the equilibrium content of CO changes by a factor of 20 in a temperature range of 200–400 °C and by a factor of 80 in the range of 200–600 °C. Figure 4.71 shows the equilibrium CO conversions as a function of temperature and steam-to-CO ratio [209].

The mechanism of the WGS reaction is widely discussed in literature based on two prevailing basic models, the redox mechanism and the formate mechanism (see Table 4.22).

The minimum energy path (given as eV) is shown in Fig. 4.72.

4.4.8.3 Application of Water–Gas Shift in the Methanol Process Scheme

To achieve the desired product H_2/CO ratio, the raw gas from gasifiers is quenched and scrubbed with water. The scrubbed raw gas is characterised by high amounts of sour gases (H_2S and CO_2) as well as contaminants such as metal carbonyls, mercury, arsenic, cyanides, COS, halogens and heavy metals species, which need to be removed for further processing. They would finally poison the shift conversion and methanol synthesis catalysts and might also damage downstream equipment.

To adjust the required stoichiometric ratio of H_2/CO for methanol synthesis and to protect the methanol synthesis catalyst, various process schemes provide a combination of WGS and purification of the synthesis gas in different sequences and by means of a combination of catalytic, absorptive and scrubbing steps.

In the WGS stage, CO and water react to hydrogen and CO_2. The CO conversion will approach close to equilibrium and be lower than desired for a methanol synthesis gas. For example, the CO contents in the product gas of a high temperature shift (HTS) reactor at equilibrium are shown in Fig. 4.73 on the basis of a POX of fuel oil [211].

Therefore, the shift reactors will usually be operated as a split stream because the shift conversion will "overshoot" the desired H_2/CO molar ratio of 2. This allows smaller reactors for the WGS with corresponding investment and operational cost savings to achieve the desired molar ratio in the combined stream.

Two main schemes are used to integrate WGS conversion and purification of the synthesis gas in the syngas stream from the gasifier (see Fig. 4.74):

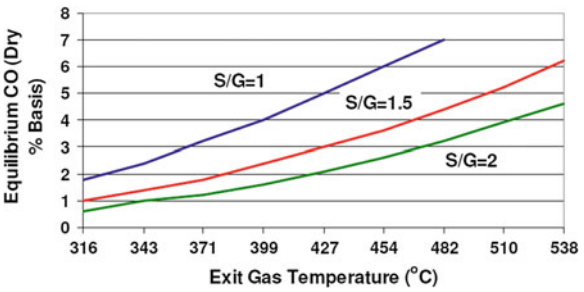

Fig. 4.73 Equilibrium CO concentrations in a high temperature shift reactor at various steam to gas ratios based on partial oxidation of fuel oil [211]

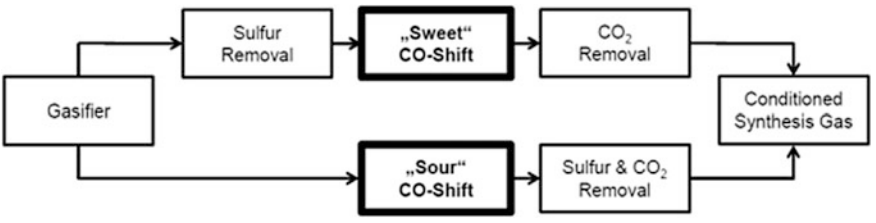

Fig. 4.74 Shift conversion options

- After raw gas filtering/water scrubbing *and* desulphurisation of the raw gas over conventional shift catalysts followed by CO_2 scrubbing ("sweet CO shift")
- In the presence of the "sour gas" (CO_2 and H_2S) conversion over a sulphur-tolerant shift catalyst followed by $H_2S + CO_2$ scrubbing ("sour CO shift")

4.4.8.4 Sweet CO Shift

The feed to the sweet gas shift system needs to be first desulphurised to levels that are tolerable for a HTS stage. The desulphurisation scrubber requires cooling of the gasifier raw gas from the water quench of the gasifier. After removing the condensate, the gas then enters a single-stage H_2S scrubber (e.g. a Selexol scrubber; see Sect. 4.4.9) and is afterwards reheated for shift conversion. After steam injection to adjust the required steam/CO ratio, the desulphurised gas enters the HTS reactor to achieve the desired H_2/CO ratio in the product gas. A sufficient S/C is necessary to avoid side reactions, such as coking or methanation. Depending on desired CO conversion, a single HTS reactor or a two-reactor system with intercooling is used.

WGS reactor designs for maximum hydrogen output, such as for ammonia plants, consist of a subsequent LTS stage for almost complete CO conversion. The LTS stage uses copper-zinc based catalysts, which are extremely sensitive to irreversible sulphur poisoning and require deep desulphurisation upstream from the HTS reactors.

The shift reaction over an iron-based catalyst operates in a 300–500 °C temperature range. Depending on feed gas composition typical conditions are a molar steam to carbon ratio at about 1–2, a space velocity of 2,000–4,000 Vol/Vol h (on a dry gas basis) and inlet temperatures of 340–380 °C.

In the case of partial CO conversion to produce a methanol synthesis gas, a HTS stage with iron-based catalyst is usually sufficient. The higher sulphur tolerance of the iron catalyst allows saving on a deep desulphurisation of the feed gas. The iron-based catalysts are fairly stable to entrained sulphur and undergo the reversible reaction with an equilibrium constant of $Kp = p_{H_2} p_{H_2S}^3 / p_{H_2O}^4$ in the range of 3 to 45 $\times$ 10^{-10} at 300–450 °C [211].

$$Fe_3O_4 + 3H_2S + H_2 \rightleftarrows 3FeS + 4H_2O \quad (\Delta H = -75.0\,\text{kJ/mol})$$

Feed gas sulphur contents can be even some 100 ppm. The sulphur will mostly slip through the HTS stage. Presence of sulphur, however, reduces the activity of the HTS catalyst, so the extra volume of catalyst has to be taken into account in the reactor design for compensation. These catalysts will not hydrolyse COS in the feed gas. This may require an extra COS hydrolysis step downstream of the HTS system.

The temperature dependence of the HTS reaction of CO is illustrated in Fig 4.75 [211]. From the WGS equilibrium, there should be no influence of

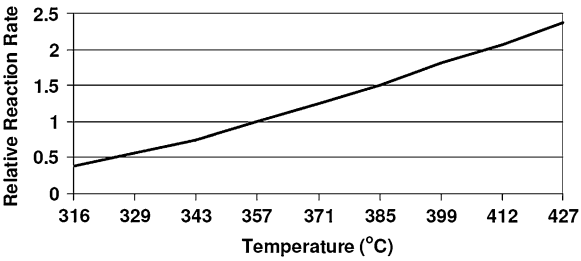

Fig. 4.75 High temperature shift reaction rate as a function of temperature

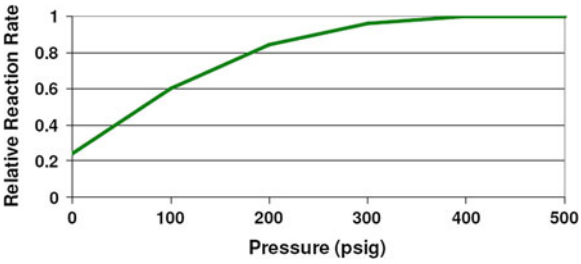

Fig. 4.76 Pressure influence on high temperature shift reaction rate

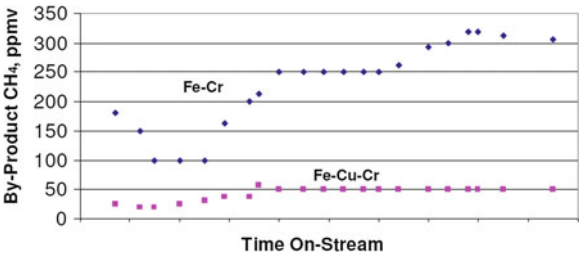

Fig. 4.77 Methane byproduct formation across high temperature shift catalysts

pressure, but in practice a slight dependence is observed from pore diffusion effects (see Fig. 4.76) [211].

Commercial HTS catalysts typically consist of >80 wt% Fe_2O_3 promoted with 8–10 wt% Cr_2O_3 for stabilisation and a small amount of copper for activation and selectivity enhancement. The addition of approximately 2 % copper allows lower overall steam-to-gas ratios in the feed gas, thus saving steam costs without negative effects from iron carbide formation and higher hydrocarbon byproduct formation through methanation and Fischer–Tropsch-type side reactions (Figs. 4.77, 4.78) [211].

Because the feed gas for a sweet shift system is usually desulphurised in a wet scrubbing system, reheating and steam addition to the feed gas are required. The "removal" of water by condensing it in the scrubber makes a sweet gas shift

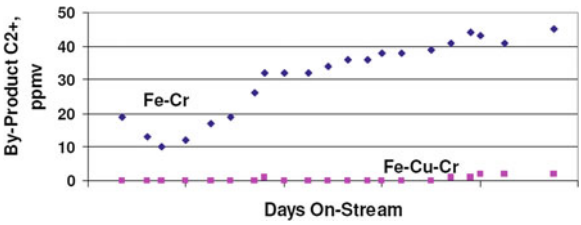

Fig. 4.78 C_{2+}-hydrocarbon formation across high temperature shift catalysts

system less attractive in the case of syngas taken from a slurry-fed gasifier or a high temperature water quench at gasifier outlet providing water-rich shift inlet gas at almost the required temperature levels. For any gasifier types that produce low-moisture gas needing steam addition, according to Grol and Yang the sweet water gas shift may be an option [212].

4.4.8.5 Sour CO Shift

Use of iron-based HTS catalysts in a high-CO, high-sulphur environment is principally possible. However, the active catalyst would convert into a sulphided state, thus leading to much lower shift activity and requiring higher steam-to-CO ratios in the feed gas to the shift reactor and larger catalyst beds [211]. Their operating temperatures of typically 350–450 °C are thermodynamically less favourable than the 50–100 °C lower operating temperatures of sulphided Co-Mo-catalysts, which are commonly used for SGS. An additional advantage is that the sulphur-tolerable Co-Mo-based shift catalysts will also hydrolyse COS to H_2S and hydrogenate HCN, which is not the case for iron-based shift catalysts.

Therefore, sulphided Co-Mo shift catalysts in synthesis gas streams from gasification of high-sulphur coal or residues are the preferred option, despite higher catalyst costs compared to rugged iron-based HTS catalysts. The sulphur handling around a sour CO shift system is less complex as intercooling and sulphur scrubbing of the raw gas from the gasifier is saved. All acid gases (CO_2 and H_2S) are finally removed in one scrubbing system at the outlet of the shift reactors.

Adjustment of the inlet steam-to-CO ratio for a sour water gas shift is easier because the water-saturated gas from the upstream gasifier does not have to be cooled down to operate a wet H_2S scrubber. It can be fed directly to the shift reactors with a temperature trim above water saturation temperatures and, depending on the gasifier type, some steam injection to adjust the overall inlet steam-to-CO ratio.

The SGS catalysts are composed of approximately 12–15 wt% MoO_3 and 3–4 wt% CO on alumina. Many SGS catalysts are alkalised with small amounts of alkali or earth alkali promoters as activity enhancers. Co-Mo-based SGS catalysts

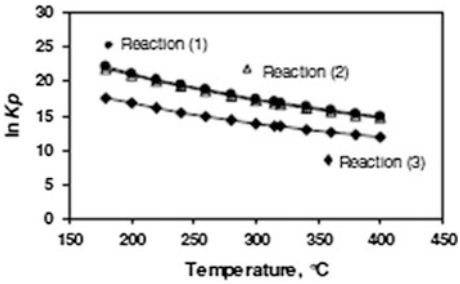

Fig. 4.79 Equilibrium constants of sulphiding reactions of a Co–Mo sour gas shift catalyst [213]

have a high sulphur tolerance and operate in the sulphided state under reaction conditions. Typical operating conditions for these catalysts are 230–350 °C, pressure ambient to 40 bar and gas space velocities of 2,000–3,000 h^{-1}. The steam/gas molar ratio is about 0.5–1.0.

The SGS catalyst requires less steam than HTS catalysts to maintain its active (sulphided) form and has fewer tendencies toward side reactions generating methane or higher hydrocarbons. Although the catalyst is not affected by low concentrations of ammonia or HCN (approximately <0.5 % [133]), chloride traces of even 1–2 ppb are a major, irreversible poison [211].

The activation of Co-Mo-catalysts used in SGS requires a presulphidation and certain sulphur content in the feed stream for maintaining the active sulphided form. The sulphidation can be described along the following chemical reactions and equilibrium conditions, as shown in Fig. 4.79 [213].

$$MoO_2 + 2H_2S \rightleftarrows MoS_2 + 2H_2O \tag{4.57}$$

$$CoO + H_2S \rightleftarrows COS + H_2O \tag{4.58}$$

$$Co_3O_4 + 8/3H_2S + 4/3H_2 \rightleftarrows 1/3Co_9S_8 + 4H_2O \tag{4.59}$$

Because the nonsulphided (oxide) form of Co-Mo-catalysts would have almost no shift activity, a certain sulphur level in the feed gas—ideally in the order of about 300 ppm or above—has to be maintained to keep the catalyst sulphided. In the case of low inlet sulphur levels, the catalyst can alternatively be presulphided before being put into operation. This allows use of the catalyst with feeds that contain H_2S-concentrations as low as 35 ppm [211].

SGS reactors usually consist of two to three reactors in series, depending on the CO inlet concentration and desired conversion. A typical setup of a SGS conversion over a Co-Mo SGS catalyst downstream of a Texaco POX of residual oil is shown in Table 4.23 [211]. In this example, the three-bed adiabatic system with 0.25 % sulphur in the inlet gas aims at maximum H_2 output, converting the inlet CO content of 46 to 1 % at outlet of the third reactor.

Table 4.23 Sour gas shift gas compositions over a three bed system (raw gas from a residual oil Texaco partial oxidation) [211]

Inlet feed composition (mol %)	Bed 1	Bed 2	Bed 3
CO	46	16	3.1
CO_2	6.9	26	34.2
H_2	47	57.9	62.6
CH_4	0.1	0.1	0.1
Sulphur	0.25	–	–
Inlet steam/gas (molar ratio)	0.96	0.7	0.61
Pressure (bar)	35	34	33
Inlet temperature (°C)	266	288	278
Outlet temperature (°C)	411	367	292
Space velocity (h^{-1})	2,940	2,220	1,785
Outlet CO (mol %)	16	3.1	1

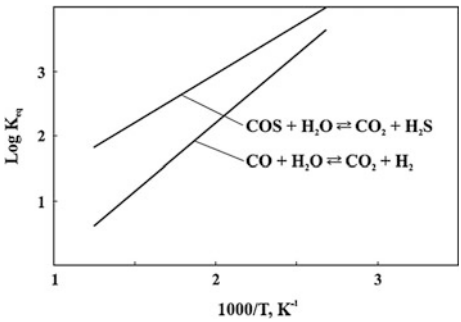

Fig. 4.80 Equilibrium constants for COS hydrolysis and water gas shift [214]

4.4.8.6 Conversion of COS (and HCN)

Co-Mo-based SGS catalysts will also promote the reaction of H_2S and CO in the feed gas to either form or hydrolyse undesired COS. The COS content at the outlet of the shift reactors will be almost at equilibrium according to reaction conditions:

$$COS + H_2O \rightarrow H_2S + CO_2$$

The equilibrium of the COS-related reaction is shown in Fig. 4.80 [214].

At high steam partial pressures (and operating pressures, although the reaction is equal molar) an outlet COS content of less than 0.1 ppmv can be reached in a SGS system [211].

Also, HCN traces will be converted in the SGS system to form traces of formic acid and ammonia, which will be contained in the condensate after cooling of the synthesis gas [214].

$$HCN + H_2O \rightleftarrows HCONH_2$$

$$HCONH_2 + H_2O \rightleftarrows HCOOH + NH_3$$

In some cases, depending on feed gas, reaction conditions and a flow scheme—especially when bypassing part of the synthesis gas around the shift reactors—a COS hydrolysis stage may have to be added in the bypass stream, which does not enter the shift reactors. The hydrolysis is catalysed with an activated alumina operating at approximately 200–250 °C. The hydrolysis activity of alumina can be increased by alkali or earth alkali promoters [215].

At high CO concentrations and in presence of metal carbonyls and HCN from the raw gas or upstream conversion stages, a combination of an 11 % Cr_2O_3/6 % K_2O catalyst on alumina to hydrolyse COS and HCN in combination with an inlet alumosilicate scavenger bed for carbonyl decomposition has been proposed [216].

4.4.8.7 Contaminants (Other than COS, HCN, Carbonyles, Chloride)

Other contaminants slipping through from the gasifier to the inlet of the acid gas scrubber section could be traces of arsine, mercury and metal carbonyl compounds. Entrainment into the methanol synthesis section will severely poison the methanol synthesis catalyst, even at levels in the ppb range.

The effects of poisoning by arsine and its absorption by a Cu/active carbon absorber has been described by Quinn et al. [217]. Also, copper or copper zinc on alumina [218] and copper/manganese absorbents have been offered for arsine scavenging.

Mercury can be removed by sulphur-containing active carbon absorbers ahead of the acid gas scrubbers. The absorbents contain about 10–15 % sulphur to bind the mercury.

Overviews of potential methanol catalyst poisons generated from fossil and biomass gasification have been compiled by Cornelissen and Clevers [219], Bartholomew [220], and Forzatti and Lietti [221].

4.4.9 Acid Gas Removal

Downstream from the syngas cooling, the next gas purification step comprises the removal of so-called acid gas components, such as H_2S and CO_2. The term "acid gas" originates from the sour pH value if the gases are dissociated in water. Besides the removal of catalyst poisoning gas components (mainly sulphur), CO_2 removal for the adjustment of the syngas quality is the second aim.

As previously described, there exist different CO-shift concepts to control the gas composition to meet the synthesis requirements. In the case of a sour shift, all acid gas components are typically removed after the CO-shift unit. In contrast, for a sweet shift system, the sulphur components are removed before entering the CO-shift reactor while CO_2 is removed subsequently. The following section introduces the fundamental principles of acid gas removal, then provides an overview of common scrubbing processes.

4.4.9.1 Fundamentals

Today's common acid gas removal processes are based on liquid scrubbing agents contacting the raw gas, thereby absorbing different gas components. Despite the existence of adsorptive processes that apply solid sorbent materials or membrane separation technologies, only absorption processes are addressed here because of their greater importance for large-scale industrial applications. In this context, chemical and physical absorption are distinguished dependent on the underlying mechanism.

Physical Absorption in Liquids

Physical absorption in liquids has been described by Kohl and Mielsen [222] and by Hiller et al. [223]. This adsorption is based on the dissolution of gases in liquids according to Henry's law:

$$p_i = x_i \times \mathrm{H}_i$$

Thereby, the gas is dissolved without condensing out and the molar amount of dissolved gas (x_i) is determined by the partial pressure of the gas component (p_i) in the gas phase and the Henry coefficient (H_i). The Henry coefficient describes the solubility of gases in liquids. It is specific for each gas component and solvent and it strongly depends on the temperature. The unit of the Henry coefficient is given as bar×mol (solvent)/mol (absorbed gas). Typically, the solubility of gases in liquids decreases with increasing temperature.

The Henry coefficient is available for a large number of gas–liquid systems in property data books. Most software packages for the simulation of chemical processes include internal databases with temperature-dependent functions for the description of vapour–liquid systems. High partial pressures are advantageous because the amount of dissolved gas increases with increasing partial pressure. The partial pressure results from the system pressure and the molar fraction of the component in the gas. It needs to be noted that Henry's law is an ideal law that is valid for dissolved, noncondensed gases in ideally and indefinitely diluted solutions. Henry's law also does not reflect multicomponent dissolution.

In real gas–liquid systems with multiple gas components in the gas phase, there will be dissolution of more than one component in the solvent, including not only acid gas components but also other gases such as CH_4, H_2 or CO. For most applications, the coabsorption of syngas components as well as methane is an undesired effect. Also, the joint absorption of multiple acid gas components may be unfavourable depending on the subsequent acid gas recovery process and the solvent regeneration process. Typical solvents for physical absorption are single component agents consisting of either organic substances or water. Physical absorption processes are slightly exothermic.

Chemical Absorption

Chemical absorption in liquids is also described by Kohl and Mielsen [222] and by Hiller et al. [223]. In contrast to physical gas absorption based on Henry's law, the activity of chemical solvents goes back to chemical reactions of the gas, with the solvent following the law of mass action. The amount of dissolved gas is determined by the chemical equilibrium constant of the chemical reaction being a function of the temperature. Higher partial pressure of the component being removed may be advantageous, but it is not necessary.

Today, there are two working principles for chemical solvents: neutralisation or oxidation. Although neutralising solvents are suitable for the removal of H_2S and CO_2, oxidising solvents are only applicable to oxidizable gas compounds. Consequently, oxidising solvents are 100 % selective towards H_2S. However, neutralising solvents are more relevant to today's industrial applications. In both types of chemical absorption processes, the acid gas needs to be dissolved and dissociated before reacting with the chemically active part of the solvent.

For this purpose, solvents for chemical absorption are at least two component liquids consisting of water and a chemically active liquid, often an organic substance such as alkanolamines. Less important but also available on the market are other basic solvents, such as aqueous NaOH solutions.

In every case, first water is needed to physically dissolve the acid gas component. In a second step, the gas component dissociates in the aqueous solution in one or more steps before it is available for the chemical reaction with the organic part of the solvent. Because of the different nature of CO_2 (Lewis acid) and H_2S (Brønstedt acid), the dissociation of H_2S is faster than for CO_2. In contrast, the neutralisation reaction enthalpy for CO_2 is higher compared to H_2S, indicating a higher affinity to neutralisation for the CO_2. Resulting from this, neutralisation scrubbing processes are kinetically selective towards H_2S but favour CO_2 neutralisation considering the chemical equilibrium. Hence, there will be coabsorption of H_2S and CO_2 for most solvents, with the H_2S being preferably absorbed at short residence times and CO_2 being increasingly absorbed at longer residence times. Thereby, the already absorbed H_2S is released to the gas phase again.

An exception from this is given for so-called primary alkanolamines. Those amines are capable of directly reacting with CO_2 without coabsorbing H_2S. Also, some other solvents, such as aqueous K_2CO_3, are selective towards CO_2 if additives are added. Because neutralisation and oxidation are exothermic processes, there will be heat released during the gas scrubbing process, requiring a sufficiently high heat capacity of the solvent to avoid solvent evaporation losses.

The absorption capacity in chemical scrubbing processes is limited by the availability of reactive agent components, resulting in saturation of the solvent, especially at higher partial pressures. After reaching this state, further acid gas removal can only be achieved by increasing the amount of scrubbing agent. In contrast, the absorption capacity of physical solvents increases with the partial pressure. Consequently, chemical solvents are preferably applied at lower partial

Table 4.24 Comparison of chemical and physical solvents [222, 223, 225]

	Physical absorption	Chemical absorption
Principle	Dissolution of gases according to the phase equilibrium (Henry's Law)	Reaction of dissolved acid gases with the solvent following the law of mass action
Binding strength	Weak	Intermediate to high
Cleaning effect	Good at high partial pressures	Very good at low partial pressures
Selectivity	Limited because of coabsorption of other syngas components	Highly dependent on selectivity of chemical reaction and residence time
Applicability	High partial pressures/high concentrations of the removed gas components	Low partial pressures/low partial concentrations
Solvent	Organic substances, water	Mixtures of water and dissociated chemically active (organic) substances
Regeneration	Simple by flashing and stripping	Complex because of thermal regeneration

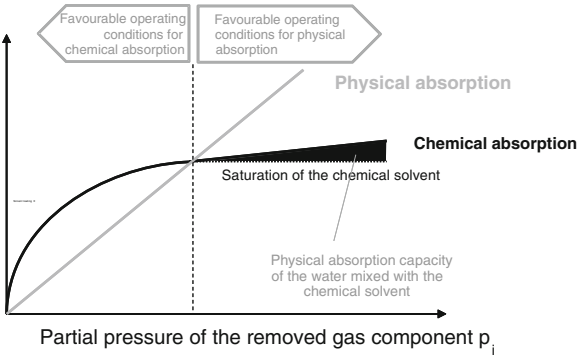

Fig. 4.81 Absorption isotherms of chemical and physical solvents [227]

pressures, whereas physical solvents are superior at high system pressure and high acid gas component concentrations.

A summarising comparison of chemical and physical solvents is given in Table 4.24 and Fig. 4.81, which shows typical absorption isotherms of chemical and physical scrubbing agents, illustrating the preferable conditions of operation.

Independent from the absorption mechanism, the majority of scrubbing processes are executed in column absorbers equipped with trays or column packing, aiming for the maximum surface area for heat and mass transfer between gas and liquid phases [222, 223, 225]. The solvent is introduced at the top and flows downwards through the column counter, currently to the raw gas flowing upwards. The loaded solvent leaves the absorber column at the bottom while the clean gas exits the process at the top. Depending on the volatility of the solvent, there may be condenser stages at the top to minimise solvent losses by recovering solvent

vapours by condensation and recirculation into the column. In contrast to distillation columns, absorbers are not equipped with a reboiler.

The loaded solvent is externally regenerated and recirculated to the absorber. Although physical solvents are regenerated mainly by flashing, chemical solvents need to be reboiled, thereby providing at least the heat of reaction that was released during the absorption process. In some cases, physical solvents are reboiled to minimise the residual solvent loading after regeneration to reduce the total amount of circulated solvent.

Columns are applied for regeneration, too. The regenerator column layout resembles typical rectification columns. If the scrubbing agent is thermally regenerated, the solvent vapour exiting the regenerator at the top will be recovered by condensation as reflux to the desorber. Reboiling and flashing processes can be supported by stripping, aiming for a dilution of the gas phase to enhance the gas component desorption caused by a reduced partial pressure. The lower the residual loading of the solvent is after regeneration, the less solvent is pumped around between absorber and regenerator, thereby reducing the pumping power demand. However, the effort for the regeneration process will increase with decreasing remaining concentration, in particular either the thermic power demand of the reboiler or the power demand for recompression after flashing.

Because coabsorbed syngas components are typically less strongly bound to the solvent than the acid gases, they can be recovered in most cases by staged decompression. Traces of acid gas that may be released during this process can be reabsorbed by scrubbing with the solvent again. The syngas components are either recycled into the raw gas or clean gas or they are used as fuel gas. Most regeneration processes aim for a selective recovery of the acid gas components with a H_2S-enriched gas stream for the sulphur recovery unit and a CO_2 stream being as pure as possible for venting to atmosphere, chemical utilisation, or sequestration. Further means aiming for an increase of the overall efficiency include the recovery of decompression energy by the application of turbines and the reduction of the heating demand by introducing heat exchangers between absorber and regeneration sections.

Special effort is necessary to avoid solvent degradation by irreversible chemical reactions with dissolved components. In particular, alkanolamines are sensitive towards the formation of salts. The intolerance of physical and chemical solvents towards certain gas components will be discussed in Sects. 4.4.9.2 and 4.4.9.3. Typical requirements to scrubbing agents are summarised in Table 4.25. Obviously, some of the requirements are conflicting, resulting in a tradeoff between different issues.

4.4.9.2 Physical Scrubbing Processes

A summary of commercial acid gas removal processes is provided in Table 4.26. Most of the named processes were developed for the sweetening of natural gas, but they also can be applied to syngas.

Table 4.25 Requirements for solvents [222, 223, 225]

Parameter	Requirement
Solubility (absorption capacity)	High for the gas component, which will be separated from the raw gas
Selectivity	Must be sufficiently high, such that maximum selectivity of physical solvents is 5:1 for H_2S/syngas components (coabsorption of 20 % syngas components) and 10:1 for H_2S versus CO_2 (Purisol process)
Regenerability	Simple regenerability for chemical scrubbing agents with no azeotopes, no irreversible chemical reactions with the absorbed gas component, sufficient boiling point difference between scrubbing agent and absorbed gas component
Vapour pressure	Low vapour pressure at absorption conditions (minimisation of scrubbing agent vapour losses)
Boiling temperature	Not too high to reduce the heating energy demand for thermic regeneration
Heat capacity	Sufficiently high to allow for removal of absorption heat from the system at low temperature increases
Viscosity	Low for improved mass transfer and reduced pumping energy requirement
Physical and chemical stability	High to avoid solvent degradation
Flammability	Low or inflammable
Economics	Cheap and high market availability
Safety	Low or nonflammable, nontoxic, environmentally safe

Table 4.26 Commercial chemical and physical scrubbing processes [222, 223, 225]

Physical processes	Chemical processes	
	Neutralisation	Oxidation (H_2S removal)
(Pressurised) water scrubbing	Alkanolamine processes	Stretford process
Rectisol process	Alkacid process	
Purisol process	Potash processes	
Fluor-Solvent process	H_2S/NH_3 process	
Selexol process	Inorganic basic processes	
Genosorb process		
Morphysorb process		

As mentioned previously, most physical scrubbing processes are operated preferably at high pressures. Although a high selectivity of absorption is favourable with respect to the acid gas recovery processes, the most important criterion is the removal of poisoning gas components down to a level demanded by the synthesis catalyst. An overview about common physical washing processes is given in Table 4.26. Contaminants such as alkalis, NH_3, HCl, dust, or tar are often already removed by upstream gas cleaning processes, such as dust filters or water scrubbers. Hence, the major task of the scrubbing process is the cleaning of the raw gas from sulphur-containing components to less than 1 ppmv and a sufficient

Table 4.27 Characteristics and operating conditions of physical scrubbing processes [222, 225, 227]

Process	Solvent	Boiling temperature (K)	Vapour pressure at 323 K (in mbar)	Molar mass (g/mol)	Ratio of component solubility	
					H_2S/CH_4	CO_2/CH_4
Purisol	*N*-methyl-pyrrolidone	475	2.2	99	133	13.3
Fluor-Solvent	Propylene carbonate/ Glycerine acetate	513	–	102	40	8.7
Sepasolv MPE	Oligo-ethylene glycol methyl ether	593	0.006	316	59	9.1
Selexol	Polyethylene glycol-dimethyl ether	553	0.02	Dependent on water content	100	15.3
Genosorb	Polyethylene glycol dimethyl ether/ Polyethylene glycol-dibutyl ether	503–553	0.005	>250	105	15.5
Morphysorb	*N*-formyl morpholine and *N*-acetyl morpholine	513–518.5	–	115–129	305.5	11.3

reduction of the CO_2 content. Although the latter issue is well fulfilled for all processes (typical CO_2 concentration for a methanol synthesis gas ranges between 2.0 and 4.0 mol %), most physical processes cannot achieve a sufficient low sulphur level. Furthermore, only a few of the named scrubbing processes are capable of handling the full range of organic and inorganic gaseous sulphur components. Consequently, most processes require a subsequent ZnO adsorption stage to capture traces of H_2S and prevent poisoning of the synthesis catalyst. Solvents incapable of capturing COS will need a prestage for COS hydrolysis. Common commercial processes listed in Tables 4.27 and 4.28 include the Purisol process, the Selexol and the Genosorb process.

The Rectisol Process

In contrast to the summary of physical solvents, the most important physical acid gas removal process—the Rectisol process—is not included in the table [223, 225, 228]. The Rectisol process is based on methanol as solvent. Although methanol is not a superior agent compared to Purisol and Selexol, it is possible to obtain the lowest clean gas sulphur concentrations and highest selectivity for the absorption of H_2S versus CO_2 by taking advantage of its strongly temperature-dependent absorption capabilities. In addition, the Rectisol process is capable of capturing all sulphur components efficiently and of removing other contaminants at lower operating temperatures as well.

Table 4.28 Selectivity and achievable clean gas purity of physical scrubbing processes [222, 225, 227]

Process	Selectivity (H_2S:CO_2)	Typical clean gas concentration (ppmv)		Absorption temperature (K)	Remarks
		H_2S	CO_2		
Purisol	10:1	1	2	293–298	Partial capture of COS and CS_2; capture of thiophenes, mercaptanes, NH_3 and HCN
Fluor-Solvent	4…5:1	1	2	Approx. 293	Especially designed for high CO_2/H_2S ratios in the raw gas; capture of mercaptanes and syngas components
Sepasolv MPE	6…7:1	1	20,000 for natural gas	Approx. 293	High selectivity for sulphur components including COS and mercaptanes
Selexol	7:1	1	20,000 for natural gas	273–313	Insufficient capture of COS
Genosorb	7:1	4	50	273–313	Capture of HCN, CS_2, COS, mercaptanes and NH_3
Morphysorb	High	4	50	298	Designed for natural gas

Today's typical Rectisol process scheme is the so-called selective process. The basis is the absorption of hydrocarbons (if contained in the gas) in a prewash stage at about 293 K, the separate absorption of H_2S in a second stage at approximately 273 K, and the removal of CO_2 in a third stage at a temperature that can be as low as 200 K. The prewash stage uses only a small amount of methanol to remove higher hydrocarbons (especially phenols and benzyls) and to dry the gas. The H_2S absorber is typically fed with preloaded methanol from the CO_2 absorber. Because of the higher selectivity for H_2S absorption at higher temperatures, the captured CO_2 is released to the gas again while the H_2S is dissolved in the agent. The sulphur-free but CO_2-containing raw gas finally enters the low-temperature CO_2 absorber, where it is contacted with thermally regenerated methanol. The CO_2 content of the clean gas is determined by the absorption temperature. It can be reduced to a low level (<10 ppmv). Because of the typically lower total H_2S amount in the gas, only a fraction of methanol from CO_2 absorber is needed for the H_2S removal.

Although the methanol from the prewash and drying stage is recovered by phase separation and distillation processes, the H_2S-enriched methanol is first gradually decompressed to recover syngas components before it is flashed at ambient pressure followed by thermal regeneration using low-pressure steam. H_2S desorption is supported by N_2 stripping. The CO_2-rich methanol is gradually decompressed and, if required, also thermally regenerated. Special effort is necessary to avoid methanol vapour losses. The CO_2 is obtained at different pressure

Table 4.29 Residual contaminant concentrations in clean gas at the end of the Rectisol process [225, 228]

Component	Concentration (ppmv)
CO_2	2
H_2S	0.1 (total sulphur)
COS	(0.1)*
Mercaptanes	(<0.01)*
NH_3	1
C_nH_m, HCN, resins, carbonyls	≈0
H_2S	60 (dew point at 223 K)

*Estimates, private communication by Lurgi.

levels (typically low and intermediate pressure) with high purity. The H_2S-rich acid gas contains significant amounts of CO_2 and N_2 besides the H_2S and organic sulphur gas components. The concentration of sulphur compounds in the clean gas is less than 1 ppmv, allowing for direct feeding to the synthesis without the need for an extra ZnO guard bed.

Resulting from the low temperature of the CO_2 removal stage, no additional clean gas drying is required after the Rectisol process. Absorption in the Rectisol process can be either carried out in one absorber column consisting of edificial separated absorption zones or in multiple absorber columns with each being operated at different temperatures. The big advantage of low residual contaminant concentrations is paid back by high electric auxiliary power consumption for the low-temperature cooling by compression-cooling machines and the consumption of low-pressure steam for regeneration. The resulting high costs for operation and investment (caused by low-temperature and corrosion-resistant construction materials and the complex, highly integrated process layout) make the Rectisol process attractive only for large synthesis plants with high restrictions for the sulphur and CO_2 content in the syngas. Typical residual concentrations of contaminants being achievable with the Rectisol process are presented in Table 4.29. The Rectisol process is licensed by Lurgi/Air Liquide and Linde.

4.4.9.3 Chemical Scrubbing Processes

The discussion of chemical solvents will be limited to alkanolamines and the Benfield process, applying potash dissolved in water. In contrast to physical solvents, which are mainly applied as pure solvents, chemical agents are mixtures of water with a chemically reactive component forming basic aqueous solutions. The majority of agents are corrosive towards common construction materials, thus requiring the addition of corrosion inhibitors and the use of higher alloyed steels for construction.

Alkanolamines can be distinguished into primary, secondary and tertiary amines depending on the number of hydrogen atoms substituted in amine group. Basicity increases in following the sequence: secondary > primary > tertiary [222, 223].

Table 4.30 Characteristics of commercially available amines [222, 225]

Solvent	Type of amine	Molar mass (g/mol)	Boiling temperature (K)	Vapour pressure at 293 K (bar)	Evaporation enthalpy at 1 bar (kJ/kg)	Concentration in water (wt%)
Monoethanolamine (MEA)	Primary	61	444	0.48	827	15–20
Diethanolamine (DEA)	Secondary	105	Degraded	0.013	671	25–30
Triethanolamine (TEA)	Tertiary	149	633	0.013	536	29.5
Methyldiethanol-amine (MDEA)	Tertiary	119	520	0.013	519	24–50
Diisopropanol-amine (DIPA)	Secondary	113	522	0.01	430	27–54
Diglycolamine (DGA)	Primary	105	494	0.013	510	21.0

Table 4.31 Performance of commercially available amines [222, 225]

Solvent	Absorption	H_2S selectivity	Clean gas concentration (ppmv)		Remarks
			H_2S	CO_2	
Monoethanolamine	CO_2, H_2S fast	None	4	20	COS is disadvantageous
Diethanolamine and diisopropanol-amine	CO_2 slow, H_2S fast	Low (short-time scrubbing)	16	200	Absorption of COS, CS_2 and mercaptanes
Triethanolamine (TEA)	CO_2 very slow, H_2S fast	High (short-time scrubbing)	16	200	Highly dissociated solvent → elongated isotherm
Methyldiethanol-amine (MDEA)	Equal to TEA	Very high (short-time scrubbing	3	1,000	Selective adsorption of COS and H_2S, even at high CO_2 concentration
aMDEA	CO_2, H_2S fast	None	3	5	Designed for CO_2 removal after H_2S scrubbing

Tables 4.30 and 4.31 indicate the characteristics and achievable residual contaminant concentrations of commercially available amines. Obviously, none of the available amines is capable of reducing the H_2S concentration to the required level, and some of them are sensitive towards organically bound sulphur. However, they are superior to the Rectisol process concerning the CO_2 absorption at moderate operating temperatures. For this reason, the preferable fields of application may be

the removal of CO_2 from flue gas (low partial CO_2 pressure) and sweetening of fuel gas in IGCC power plants (with low or intermediate partial pressures of CO_2 and H_2S).

One major disadvantage of alkanolamine-based solvents is the limited selectivity of absorption of H_2S and CO_2, resulting in a mixed acid gas after regeneration. Although there are highly selective alkanolamines for CO_2 absorption based on the so-called carbamate formation mechanism, recent development aim for "designer alkanolamines," which are sterically hindered and promising for a more selective adsorption of acid gas components. A typical example for such new amines is the activated methyl diethanolamine (aMDEA), which is commercially offered by BASF.

An alternative to alkanolamine solvents that was traditionally applied for natural gas-based synthesis plants is the Benfield process, which uses aqueous potash as a chemical solvent. The advantage of natural gas (in most cases) is the low sulphur content due to the natural gas treatment at the production field. By applying appropriate natural gas conversion technologies, it is also possible to adjust the $(H_2 - CO_2)/(CO + CO_2)$ ratio, which is close to the requirement of the synthesis. Hence, effort for acid gas removal can be reduced.

For this purpose, the Benfield process was developed. It applies K_2CO_3 (25–30 % in water) as the chemically active component. Although it is possible to selectively remove H_2S, it was originally designed for CO_2 separation from the syngas. Minimum concentrations in the clean gas are 1 ppmv for H_2S and 0.5 mol % for CO_2. Although there exist a number of process variations today, the Benfield process is characterised by the addition of amines diethanolamine (DEA) to accelerate the chemical reaction and by the addition of vanadium oxide (V_2O_5) as corrosion inhibiting component. Typical operating conditions for the absorption process are a pressure of 5–30 bar and a temperature of 293–303 K. The solvent is regenerated at 378–393 K.

4.4.9.4 Acid Gas Recovery

Significant effort has been made to provide highly concentrated acid gases from the solvent regeneration for further processing by acid gas recovery processes. In many cases, part of the CO_2 is used internally, such as for syngas production from natural gas or as inert gas for different purposes, but the largest fraction is simply vented to the atmosphere. Only for plants with subsequent syntheses using CO_2 as reactant is an option for the utilisation of larger amounts of CO_2. However, with upcoming emission trading systems in Europe and elsewhere and in accordance with CO_2 emission reduction targets, there is an increased activity in the field of CO_2 utilisation and storage. Although storage includes disposal in geological (mostly saline aquifer) formations and its use for enhanced oil recovery (EOR), the

chemical utilisation aims for the replacement of CO by CO_2 in syntheses, such as production of methane by integrating renewable hydrogen (power-to-gas), and the production of niche products compared to the overall amount of CO_2 being produced from syngas plants, such as carbonates. Nonetheless, significant amounts of CO_2 are already chemically processed each year, such as by the synthesis of urea. All applications require highest CO_2 purities.

Because of generally stricter environmental regulations for H_2S and other sulphur emissions, which often depend on the total sulphur capacity of the plant, there exist a number of processes to convert the H_2S into saleable products. They range from combustion with adjacent scrubbing of the flue gas for the production of gypsum to the synthesis of sulphuric acid based on the contact process or the conversion of H_2S to elemental sulphur in Claus plants. All processes have a long history and are commercially proven. In particular, the production of sulphuric acid and Claus plants are typical sulphur recovery processes in syngas plants. The choice for one process depends on local market and infrastructural conditions.

The Claus process is a multistage process, with an air- or oxygen-blown combustion furnace (1,073–1,673 K) as the first stage and a number of subsequent catalytic contact beds (Al_2O_3-based) operated above the sulphur condensation temperature (493–573 K). The principle is based on the adjustment of a stoichiometric H_2S/SO_2 ratio for simultaneous and subsequent sulphur-yielding reactions. The amount of undesired byproducts and the occurrence of side reactions are strongly dependent on the purity of the acid gas. Elemental sulphur is recovered by condensation between the reaction steps by intermediate cooling in specially equipped drums. Sulphur recovery rates of the Claus process without tail gas treatment may be as high as 97 % [224].

Further processing of the tail gas from the first section of the Claus plant may be required, depending on the regulations regarding the sulphur recovery rate. Multiple options exist for the tail gas treatment. A common configuration includes the recirculation of the tail to the inlet of the acid gas removal process after passing intermediate COS hydrolysis or hydrogenation reactors and intermediate gas scrubbing processes (e.g. the SCOT process). Alternatively, the tail gas can be processed in a number of low-temperature catalytic reactors with various catalysts (e.g. Al_2O_3 or activated carbon), which are often operated below the sulphur condensation temperature. In this way, it is possible to achieve sulphur recovery rates of more than 99.99 %, depending on the tail gas process (e.g. Sulfreen, Hydro-Sulfreen, Carbo-Sulfreen). Another option includes the combustion of the tail gas with adjacent flue gas cleaning. Overviews of commercially available technologies and special applications are provided in Refs. [224, 226].

In addition, wastewater management, reduction of the makeup solvent requirement, energetic optimisation and dealing with gaseous emissions caused by flaring are major issues in acid gas removal plant design, but they will not be discussed here.

4.5 CO_2 and H_2 for Methanol Production

Hans Jürgen Wernicke[1] and Wladimir Reschetilowski[2]

[1]*Kardinal-Wendel-Straße 75 a, 82515 Wolfratshausen, Germany*
e-mail: h.j.wernicke@t-online.de

[2]*Institute of Chemical Technology, Dresden University of Technology, 01062 Dresden, Germany*
e-mail: wladimir.reschetilowski@chemie.tu-dresden.de

Introduction

This chapter deals with various ways to use CO_2 as raw material for methanol generation that leads to carbon recycling schemes. The use of CO_2 for methanol is only meaningful in combination with hydrogen, which is produced by processes using regenerable energies. In special situations, also the use of "waste" or "byproduct" hydrogen can be meaningful. Methanol production from CO_2 is described in Sect. 4.8.

Table 4.32 Hydrogen production capacities in the United States [229]

Capacity type	Production capacity (1,000 metric tonnes per year)	
	2003	2006
On-purpose captive[a]		
Oil refinery	2,070	2,723
Ammonia	2,592	2,271
Methanol	393	189
Other	18	19
On-purpose merchant[a]		
Off-site refinery	976	1,264
Non-refinery compressed gas (cylinder and bulk)	2	2
Compressed gas (pipeline)	201	313
Liquid hydrogen	43	58
Small reformers and electrolysers	<1	<1
Total on-purpose[a]	**7,095**	**6,839**
Byproduct		
Catalytic reforming at oil refineries	2,977	2,977
Other off gas recovery[b]	462	478
Chlor-alkali processes	NA	389
Total byproduct	**3,439**	**3,844**
Total hydrogen production capacity	**10,534**	**10,683**

[a] On-purpose are those units where hydrogen is the main product, as opposed to "byproduct" units where hydrogen is produced as a result of processes dedicate to producing other products
[b] From membrane, cryogenic and pressure swing adsorption (PSA) units at refineries and other process plants
Sources The EIA-820 Refinery Survey, The Census Bureau MA28C and MQ325C Industrial Gas Surveys, SRI Consulting, The Innovation Group. Air Products and Chemicals, Bilge Yildiz and Argonne National Laboratory (Report # ANL 05/30, July 2005), and EIA analysis

Hydrogen

Table 4.32 shows hydrogen production capacities in the United States by the categories *on-purpose captive, on-purpose merchant* and *byproduct* [229]. Byproduct hydrogen quantities in the United States are substantial—approximately 43 billion m^3 in 2006, amounting to approximately one-third of total production capacities. In additional, European sources of byproduct hydrogen total 23 billion m^3.

Surplus hydrogen sources include crude oil refineries that operate thermal or catalytic crackers and catalytic reformers. The excess part of hydrogen is the amount that is not needed in the captive processes, such as for hydroprocessing and energy generation. Depending on the individual refinery structure, it may be a net hydrogen producer or have a need for additional hydrogen, which often is produced by steam reforming of the refinery light fractions.

An important surplus hydrogen source is the electrolytic production of chlorine (see Sect. 4.5.3):

$$NaCl + H_2O \rightarrow 1/2Cl_2 + NaOH + 1/2H_2$$

Other sources include the production of lower olefins by steam cracking, the production of acetylene by POX of methane, and the dehydrogenation of ethylbenzene to styrene monomer.

Section 4.5.3 describes the distribution networks for hydrogen by means of pipelines and grids in the area of chemical and refinery industry clusters. Europe has a hydrogen pipeline network of approximately 1,600 km and the United States has approximately 800 km (see overviews in Refs. [230, 231]).

Carbon Dioxide

Carbon dioxide is a natural component of the air; its current average concentration is 0.039 vol% (390 ppm). At the same time, it is an important part of the global carbon cycle. Carbon dioxide is produced both inside living organisms as a byproduct of cellular respiration and during the combustion of carbon-containing substances with sufficient supply of oxygen. Plants, certain bacteria and archaea reconvert carbon dioxide into biomass through fixation.

Carbon dioxide exists in the atmosphere, the hydrosphere, the lithosphere and the biosphere and ensures an intense exchange of carbon between these geospheres. Figure 4.82 illustrates the average global tropospheric carbon dioxide distribution. The atmosphere contains approximately 700 Gt of carbon in the form of gaseous carbon dioxide. The hydrosphere contains approximately 38,000 Gt of carbon in the form of dissolved carbon dioxide as well as dissolved hydrogen carbonates and carbonates. The lithosphere contains by far the largest portion of chemically bound carbon dioxide. Carbonate rock, such as calcite and dolomite, contains between 20,000,000 and 60,000,000 Gt of carbon [232].

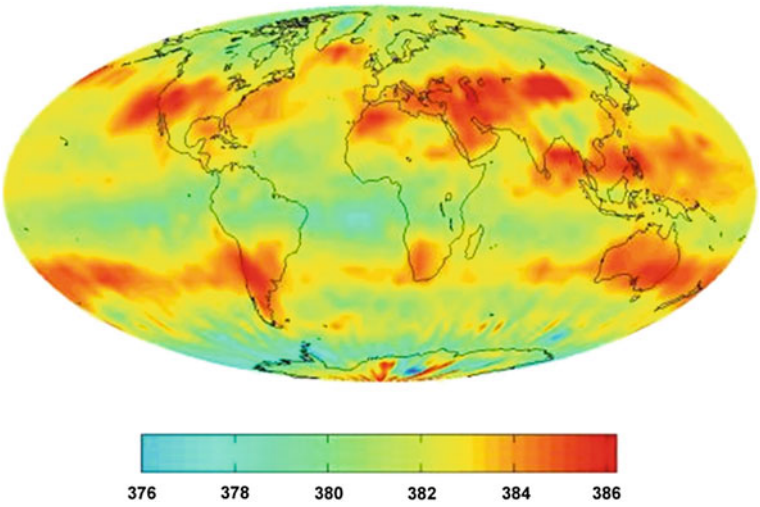

Fig. 4.82 Global carbon dioxide distribution in the troposphere, recorded by the National Aeronautics and Space Administration's Atmospheric Infrared Sounder (AIRS) in July 2008 [234]. Dark blue corresponds to a concentration of 368.2 parts per million and dark red corresponds to a concentration of 386.2 parts per million (ppmv)

Anthropogenic carbon dioxide emissions (i.e., those caused by mankind) amount to approximately 36.3 Gt per year and constitute only a small part of the total carbon dioxide produced from mostly natural sources, which is approximately 550 Gt per year [233]. Approximately half of the additional carbon dioxide is absorbed by the biosphere and the oceans. The other half of the emitted carbon dioxide remains in the atmosphere, resulting in a measurable increase of the concentration.

Carbon dioxide is a component of many natural gases and has to be extracted, usually prior to gas transport. For example, Alaskan gas contains approximately 20 % CO_2, and in some offshore gases the content is even higher. CO_2 is produced in any combustion process, but its extraction (e.g. from power plant flue gases) as a raw material for chemical utilisation is limited from a technical point of view and is only meaningful in combination with other value-adding conversion steps.

Extractable high CO_2 contents are found in flue gases of any combustion process of organic matter, but also in the off-gases of gasification and POX of hydrocarbons for the production of synthesis gas. CO_2 is generated in the gasification, reforming, or POX itself and additionally in the shift conversion in the case of maximum hydrogen output. In the production of SNG, the volume of CO_2 is even twice as high with reference to the amount of methane used.

Interest in the use of CO_2 in chemical processes has increased in connection with higher feedstock costs, concern about limited resources, and climate change discussions. Multiple attempts aim to utilise CO_2 as a carbon-containing building block for chemicals and fuels [235]. The high thermodynamic stability of the CO_2, with a free enthalpy of -393 kJ/mol, requires a high-energy input to reverse the formation of CO_2 as an end product of any combustion process.

Chemical processes that consume CO_2 as a building block are well known and have been applied on a large scale, including the production of urea from ammonia and CO_2 in vast amounts (in 2010, 155.6 million tonnes worldwide [236]), the production of certain polycarbonate polymers, and salicylic acid from phenol. Other routes to activate CO_2 as a chemical building block either need very reactive reducing components, such as hydrogen, or energy input by means of electrical energy or photolysis in combination with catalysts to transform the very stable C=O bond.

Apart from the many biochemical processes based on photosynthesis or other enzymatic conversion of CO_2 to products such as alcohols or organic acids, examples of chemical CO_2 activations with hydrogen or methane as reducing agents are:

Dry CO_2-reforming of methane	$CO_2 + CH_4 \rightarrow 2CO + 2H_2O$
Methanisation with hydrogen	$CO_2 + 4H_2 \rightarrow CH_4 + 2H_2O$
Reverse water–gas shift	$CO_2 + H_2 \rightarrow CO + H_2O$
Hydrogenation to formic acid	$CO_2 + H_2 \rightarrow HCOOH$
Hydrogenation to oxalic acid	$2CO_2 + H_2 \rightarrow (COOH)_2$

A combination of dry and wet reforming to generate a methanol synthesis gas ("metgas") with the desired 1:2 CO/H_2 stöchiometry has been proposed by Olah et al. [237, 238]. It combines both reactions either in two separate conventional steps to achieve the gas composition or in one step over a nickel catalyst at 800–1,000 °C and 5–40 bar of pressure:

$$3CH_4 + CO_2 + 2H_2O \rightarrow 4CO + 8H_2 \rightarrow 4CH_3OH$$

The process, called "bi-reforming," has been proposed for all kinds of natural or even shale gas. These source gases often already contain CO_2 and only require an additional adjustment of the necessary methane/CO_2 ratio, normally by addition of CO_2 from other sources.

A further evolution of bi-reforming is "tri-reforming," which in one step combines methane steam reforming with methane CO_2 reforming (both endothermic) and methane POX (exothermic):

$$3CH_4 + CO_2 + H_2O + 1/2O_2 \rightarrow 4CO + 7H_2$$

However, the SN of 2 (SN defined as (mol H_2 − mol CO_2)/(mol CO + mol CO_2)) for methanol feedgas is not achieved under adiabatic conditions (see overview in Ref. [239]).

CO_2 can directly be hydrogenated to methanol over copper zinc catalysts, which have been adapted to cope with high CO_2 contents in the feed gas (see Sect. 4.8). This only makes sense if hydrogen is available from excess byproduct hydrogen and from nonfossil sources, such as electrolysis using regenerative power (see Sects. 4.5.2 and 4.5.3).

Two projects in pilot and demonstration phases are testing a route of CO_2 to methanol with the use of hydrogen from water electrolysis. In 2008, Mitsui

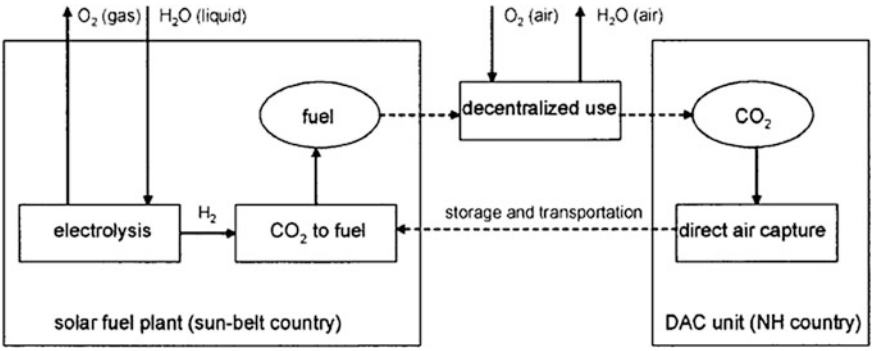

Fig. 4.83 Concept of decentralised use of solar energy in combination with CO_2 extraction from air [244]

Chemical built a 100 tonne/year methanol pilot unit in Osaka [240]. In November 2011, a semi-commercial methanol plant was commissioned in Grindavik, Iceland, using CO_2 from a nearby geothermal power station and electrolytically produced hydrogen. The emission-to-liquid plant has an energy input of about 5 megawatts for the production of 4,500 t methanol per annum [241, 242].

Future developments based on CO_2 and nonfossil hydrogen use formic acid as an intermediate (or hydrogen reservoir [243, 244]) via methylformiate reduction with hydrogen:

$$CO_2 + H_2 \rightarrow HCOOH$$

$$HCOOH + CH_3OH \rightarrow HCOOCH_3 + H_2O$$

$$HCOOCH_3 + 2H_2 \rightarrow 2CH_3OH$$

Another development is the electrocatalytic reduction of CO_2 to CO with gold catalysts followed by the bi-reforming reaction described above.

Various concepts to implement a closed-carbon cycle (i.e., a long-term carbon dioxide cycle with broad use of regenerative solar energy) were described in a 2011 review by Möller [245]. The review also proposes decentralised units that require CO_2 capture from the atmosphere (direct air capture) to use solar energy for conversions at any locations (see Fig. 4.83) [244].

A principal scheme to combine solar energy for hydrogen manufacture, CO_2 capture and conversion to hydrocarbons (which can be methane, but also any other hydrocarbon including methanol) is shown in Fig. 4.84.

The starting point of any use of CO_2 is the extraction from the various gas streams by means of regenerative scrubbing, absorption or adsorption processes, and subsequent conditioning as described in Sect. 4.5.1. Section 4.5.2 gives an overview of

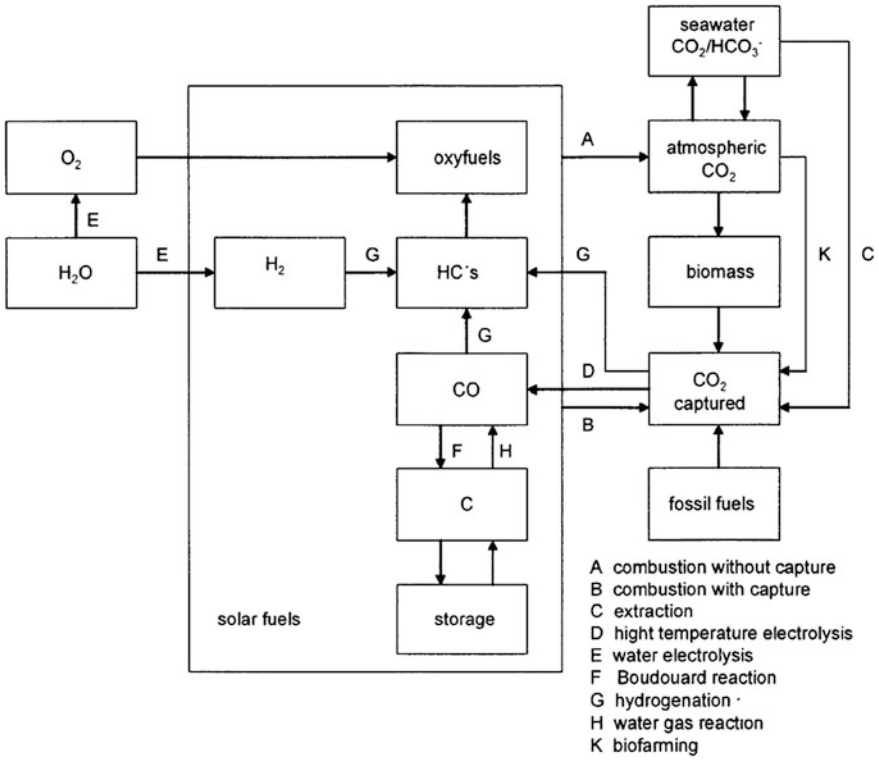

Fig. 4.84 Processes and carbon compounds in a closed-carbon cycle [240]

the many ways to generate hydrogen, whereas Sect. 4.5.3 concentrates on nonfossil hydrogen manufacturing as a basis to use byproduct or excess hydrogen in the conversion of CO_2 into chemicals and fuels, specifically into methanol.

4.5.1 CO_2 Separation from Natural Gas, Syngas, and Flue Gas

Matthias Seiler and Jörn Rolker

Evonik Industries AG Hanau, Rodenbacher Chaussee 4, 63457 Hanau-Wolfgang, Germany
e-mail: Matthias.Seiler@evonik.com; e-mail: Joern.rolker@evonik.com

When fossil fuels or any carbon-containing natural or synthetic product are combusted, CO_2 and water are produced. The great future challenge is to reverse this process towards an efficient and economic production of fuels, synthetic hydrocarbons and other materials from CO_2 and water [246, 247].

Table 4.33 CO_2 sources [252]

Source	CO_2 partial pressure
CO_2 fraction from acid gas scrubbing in ammonia or other synthesis gas plants or H_2-generation plants	1.0–1.2 bar
CO_2-containing off-gas from fermentation plants (e.g. breweries)	0.9–0.95 bar
CO_2 from underground deposits (also in mixtures with hydrocarbons)	1–30 bar
Natural gas purification plants, so-called sweetening plants	1.0–1.2 bar
Ethylene oxide plants	0.8–0.95 bar
Acid neutralisation plants	~1 bar
Lime and cement furnaces	0.2–0.5 bar
Flue gas	0.09–0.11 bar

To date, a large number of research projects have focused on methodologies that use CO_2 as building block for the synthesis of sustainable products [248–252]. In this context, the supply and recovery of CO_2 is an important topic. Prominent CO_2 sources, where CO_2 separation processes are often applied, are listed in Table 4.33.

Depending on the composition, temperature and pressure of the CO_2-containing gas streams, different kinds of unit operations, such as absorption, adsorption and membranes, can be applied to separate CO_2 fur further use. This chapter focuses on CO_2 separation by means of absorption. After a brief state-of-the-art summary, new industrial results are presented describing the performance of novel high-performance absorbents [253] for acid gas removal.

4.5.1.1 Introduction

This section focuses on the use of amine systems for separating CO_2 from various gas streams, such as those typical for natural gas and synthesis gas purification or the field of carbon capture and storage (CCS). Generic amines such as triethanolamine (TEA), diethanolamine (DEA), diisopropanolamine (DIPA), mono-ethanolamine (MEA) and methyldiethanolamine (MDEA) have been used for acid gas removal for decades. The utilised systems were constantly improved over the years to show a better performance in terms of stability, kinetics, or corrosion behaviour as well as the energy input for regeneration [254]. Although in the early years more or less pure aqueous amine systems were used, formulated solvents with special additives (specialty amines) such as corrosion inhibitors, defoaming agents, and kinetic activators evolved and were customised for special applications (e.g. selective removal of components, partial or bulk removal).

In recent years, the focus of absorption process optimisation has been on energy-efficient processes, and solvents were used to realise drastic savings in regeneration energy. The immense research and development programmes for climate protection and CCS pointed out the need for optimised solvents and contributed to worldwide activities in the field of economical absorbents for postcombustion CO_2 removal from flue gases [255–260]. A broad range of

different kind of amines were suggested for gas sweetening applications, such as primary amines with low loadings but fast kinetics and high enthalpies of absorption, as well as sterically hindered or tertiary amines with slower kinetics, high cyclic capacities, and moderate enthalpies of absorption. Each class offers advantages and disadvantages. In the end, an optimal solvent needs to be specified for each application; the treated gas stream has individual characteristics (e.g. CO_2 and/or H_2S partial pressure, side components) and requirements (specifications).

In the following sections, we discuss the requirements and challenges for the use of new amine systems for sour gas removal. After presenting a brief state-of-the-art summary including a description of the most relevant industrial challenges, we will describe the industrial progress in developing new absorbents.

4.5.1.2 Acid Gas Removal

State-of-the-Art Absorbents

Currently, CO_2 absorption is back on the agenda. The identification of CO_2 as a greenhouse gas as well as demand for sustainability in the chemical industry have sparked enormous, often publicly funded research and development activities to identify energy-efficient solvents for CCS applications in the field of postcombustion flue gas treating [253]. Recently, several newly developed solvent formulations, mostly based on amine compounds, were introduced to gas-treating applications. However, so far in the CCS research no breakthrough has been achieved; even in the classical fields of operation such as gas sweetening of syngas and natural gas feeds, the demand for energy-efficient technologies calls for improvements.

There are numerous different CO_2 removal processes available on the market. A proper decision about which is best suited should consider various criteria, such as the kind of treated gas stream (natural gas, syngas, flue gas), the partial pressure of carbon dioxide and the desired clean gas specifications.

Figure 4.85 shows a basic process scheme for CO_2 separation by absorption. It consists of an absorber column where the sour gas is contacted with the lean absorbent in counter-current flow and the acid gases dissolve into the liquid phase. At the bottom of the absorber, the loaded solution (rich solution) is introduced to various flash vessels where the pressure is decreased and co-absorbed gas components are predominantly released (high-pressure flash), with a second flash at lower pressure to release a part of the acid gases (low-pressure flash). The vast amount of acid gases is drawn from the stripper, which is equipped with a reboiler to generate stripping steam and provide the regeneration energy for desorption of the acid gases. Finally, the regenerated lean absorbent is fed back to the absorber.

There are different process technologies that make use of physical solvents, chemical solvents, or hybrid solvents (mixture of physical and chemical solvent). For each application, the proper choice of the solvent determines whether the separation process is economically feasible. In Table 4.34, different product specifications are listed. Together with additional information about the feed

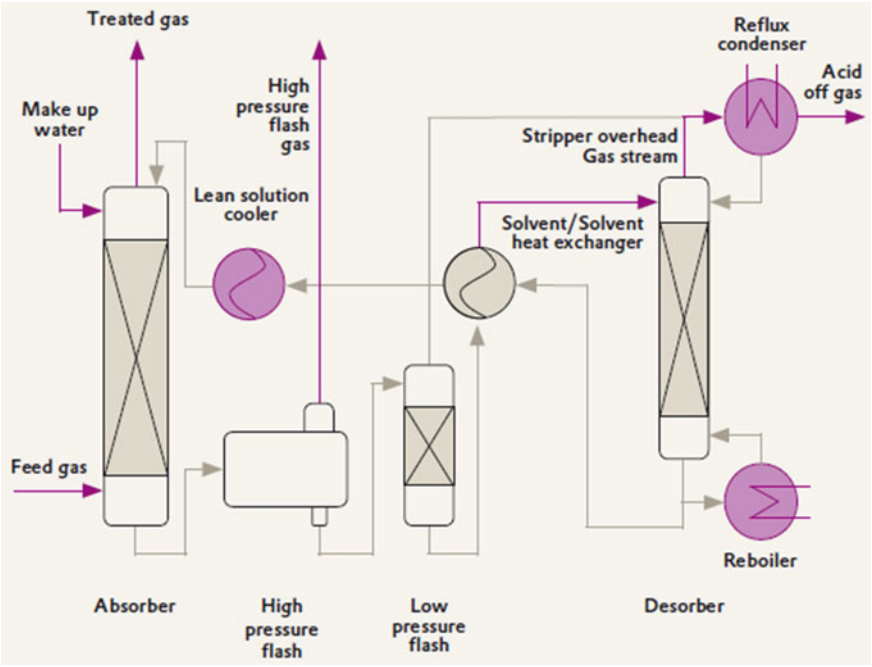

Fig. 4.85 Typical process scheme for acid gas removal with chemical absorbents

Table 4.34 Typical CO_2 specifications for various applications [254, 261]

Gas stream	CO_2 spec	CO_2 partial pressure/kPa	Additional impurities
Natural gas	2–3 % (v/v)	50–700	Hydrocarbons, H_2S
Liquefied natural gas	<50 ppmv		
Syngas (oxo)	10–100 ppmv	200–2,900	O_2, SO_2, HCN, H_2S, COS, C_mH_n
Syngas (ammonia)	<500 ppmv		
Flue gas	85–95 % removal	4–12	NO_x, SO_2, O_2

composition and the CO_2 partial pressure, it is possible to make a preselection of the process technology for the separation.

Processes with physical solvents are only applicable at higher CO_2 partial pressures. In comparison to chemical absorbents, lower solvent flow rates can be realised due to the higher solubility at high partial pressure of the sour gas. Therefore, equipment size is reduced (pumps, absorber, flash, piping), leading to lower capital expenditure (CAPEX) if additional equipment, such as for chilling the absorbent, is not needed. Nevertheless, the solubility of hydrocarbons in these kinds of solvents can be quite high [254]. Selectivity, such as between CO_2 and H_2S, results from the different solubilities of the gases and is realised in processes such as Rectisol or Selexol, as shown in Table 4.35.

Table 4.35 Some state-of-the-art processes with physical solvents and hybrid solvents [254, 261]

Process	Solvent	Solubility of hydrocarbons		
Physical solvents		C_1/CO_2	C_2/CO_2	C_4/CO_2
Rectisol	Methanol	0.12	0.56	4.14
Purisol	*N*-methyl-2-pyrrolidone	0.07	0.38	3.47
Fluor solvent	Propylene carbonate	0.04	0.17	1.75
Selexol	Dimethyl ether of polyethylene glycol	0.07	0.42	2.33
Hybrid solvents				
Sulfinol	Sulfolane + DIPA or MDEA	–	–	–
Amisol	Methanol + secondary alkylamine	–	–	–
Solubilities @ 1 bar, 25 °C				

C_1 = methane, C_2 = ethane, C_4 = butane

Due to the low enthalpy of absorption of CO_2, the solvent regeneration requires less energy input. A thermal regeneration step is only implemented in the case of tight product specifications. Due to the lower binding forces of the CO_2, one or more flash stages with a simple pressure decrease are often sufficient (see Table 4.35 for different processes with physical solvents). Tennyson and Schaaf specify a CO_2 partial pressure of >690 kPa in the feed gas as a typical set point for physical solvents. In the off-gas, purities of 14 kPa CO_2 partial pressure can be obtained [262]. Chemical solvents can meet much tighter product gas specifications and are always top on the list when lower CO_2 partial pressures are present in the feed gas. In the off-gas, the CO_2 content can be reduced to very low partial pressures (<1 kPa) [262]. However, this comes along with reasonable operational expenditure (OPEX) for the thermal solvent regeneration. Three contributions account for the total amount of heat that is supplied in the reboiler:

1. Generation of water vapour as stripping steam
2. Desorption of the CO_2 from the solvent
3. Temperature increase of the entering liquid streams (rich solution, reflux) to boiling point conditions.

The impact of these contributions on regeneration energy strongly depends on the kind of solvent [263, 264]. The influence of the solvent (high or low absorption enthalpy) on the total regeneration energy according to Rochelle is depicted in Table 4.36. A straightforward approach for a low reboiler duty would ask for a low enthalpy of absorption to minimise the regeneration energy. However, in terms of an overall process optimisation approach (e.g. if additional CO_2 compression is required), a solvent with a high absorption enthalpy allowing for a high temperature and high pressure regeneration might be beneficial because the expensive gas compression at lower pressures is not needed. An interesting study was undertaken by the Rochelle group, but so far, there are little results available that take into account the performance of the power plant and the impact of the steam extraction on a higher exergetic level on the efficiency of the power plant [264–266].

Table 4.36 Qualitative comparison of stripper steam requirement for different kinds of chemical solvents [266]

5 M amine	Primary amine (%)	Sterically hindered or tertiary amine (%)
Cyclic capacity	100	167
Enthalpy of absorption	100	60
Stripping vapour (A)	100	183
Desorption of CO_2 (B)	100	68
Temperature increase (C)	100	36
Total regeneration energy	100	78

It is not astonishing that this kind of optimisation approach is discussed in the field of CO_2 removal from flue gases at power plants; in this special application, a further scale-up of the existing absorption process technology is necessary. Several technical challenges come along the way and special attention has to be given to the interaction between the absorption process and power plant.

The proper choice of the solvent is a powerful tool for process optimisation. Absorbents such as sterically hindered or tertiary amines have higher cyclic capacities than primary amines due to the different reaction mechanisms.

The cyclic capacity of the solvent accounts for the difference in CO_2 loadings after the absorber and the stripper and determines the solvent flow rate in the separation process. Large cyclic capacities allow for lower solvent flow rates, thus reducing the regeneration energy in the stripper and keeping the equipment sizes small.

The simplified overall reaction mechanism is given below. It indicates that primary amines are limited to loadings of 0.5 mol CO_2/mol amine, while sterically hindered amines and tertiary amines absorb 1 mol CO_2/mol amine if one amine group is present. This mechanism leads to lower solvent flow rates and hence smaller equipment sizes. More detailed descriptions of the reaction phenomena can be found elsewhere [254, 267].

Primary Amines:

$$2R_1 - NH_2 + CO_2 \leftrightarrows R_1 - NH_3^+ + R_1 - NHCOO^-$$

Sterically Hindered and Tertiary Amines:

$$R_1R_2R_3 - N + CO_2 + H_2O \leftrightarrows R_1R_2R_3 - NH^+ + HCO_3^-$$

If the carbon dioxide is trapped as a carbamate as in primary amines, this stronger fixation needs more heat in the reboiler to break up the weaker bonding in the bicarbonate, as can be seen in Table 4.36. The effect in terms of process optimisation was impressively realised in syngas application by revamping older monoethanolamine systems with the activated methyldiethanolamine and reducing

Table 4.37 State-of-the-art chemical absorbents [261]

Solvent	Absorption enthalpy (kJ/mol)	Regeneration energy	Absorption rates
MEA/primary amine	85	High	Fast
AEE/primary amine	–	High	Fast
DIPA/secondary amine	–	Moderate	Moderate
DEA/secondary amine	70	Moderate	Moderate
MDEA/tertiary amine	60	Low	Slow

AEE Aminoethoxyethanol

the heat requirements in the reboiler by a factor of 3.8 [268]. In a similar way, sterically hindered amines might benefit from the absorption process, as pointed out by Sartori and Savage [269]. In Table 4.36, the tertiary amine solution in the desorber consumes more stripping vapour in relation to the primary amine, but the overall energy requirement is far less for sterically hindered or tertiary amines than for primary amines. In this estimation, kinetics are not covered and it is not considered that tertiary amines have much slower absorption rates and need to be activated, but it is obvious that the specified chemical solvent plays a major role for process economics because the aforementioned contributions can be optimised [253].

From Table 4.37, it can be depicted that the amine formulations offer quite different features. It seems that it is nearly impossible to get an overall optimum solvent with fast kinetics, low regeneration energy and minimum solvent flow rate to meet the customer's needs in terms of both low OPEX and low CAPEX. Subsequently, lots of different processes and technologies are available (see Ref. [254]) that are very often specially designed for certain applications, such as individual gas feeds (the content of sulphur compounds) or desired separation tasks (selective H_2S or nonselective sour gas removal) [254], and often use special solvent formulations.

A further chemical absorption process that can be used to remove CO_2 and H_2S is called the Benfield (Benson and Field) process. It was introduced by Benson in 1952 and is licensed by Universal Oil Products (UOP) as an effective method to separate acid gases with widely available low-cost chemicals (i.e., potassium carbonate along with a corrosion inhibitor) [254, 296].

The basic process chemistry is based on the following reactions:

$$K_2CO_3 + CO_2 + H_2O \leftrightarrows 2KHCO_3$$

$$K_2CO_3 + H_2S \leftrightarrows KHS + KHCO_3$$

The basic process equipment is similar to amine processes and consists of an absorber and desorber, but the absorber is operated at higher temperatures compared to amine processes (i.e., >90 °C), which helps to increase the rate of absorption. Because the CO_2-loaded solution enters the desorber at nearly desorption temperature, no steam is required to heat the solution to the stripping temperature and no additional heat exchangers are needed. In addition, the

enthalpy of absorption of CO_2 with K_2CO_3 is much lower compared to the reaction of CO_2 with standard amines such as monoethanolamine, which leads to a lower overall heat demand [254].

Since 1971, the usage of DEA as an activator has significantly improved the reaction kinetics and reduced the CAPEX [254]. In 2000, over 700 units worldwide were using the Benfield process to separate acid gases [297]. According to UOP, the Benfield process is best suited for CO_2 partial pressures of over 5 bar in feeds that need a high degree of purity [297].

In a typical Benfield process, a portion of the lean solution from the regenerator is cooled and fed into the top of the absorber, while the major portion is added hot at a point some distance below the top. This simple modification improves the purity of the product gas by decreasing the equilibrium vapour pressure of CO_2 over the portion of solution last contacted by the gas. A somewhat more complex scheme termed "two-stage'' has also been used for applications in which more complete CO_2 removal is required. In this modification, the main solution-stream is withdrawn from the stripping column at a point above the reboiler so that only a portion of the solution passes down through the bottom of the stripping column to the reboiler. Because this portion of the solution is regenerated by the total steam supply to the stripping column, it is thoroughly regenerated and is capable of reducing the CO_2 content of the gas to a low value. The main solution stream is fed into the midpoint of the absorber, while the more completely regenerated portion is fed at the top [254]. The aqueous potassium carbonate solution is very corrosive and therefore only runs safely in presence of V_2O_5 as corrosion inhibitor using up to 35 wt% K_2CO_3.

In the end, the best performance conditions of the process technology are obtained as a tradeoff between customer needs and featured solvent properties. Furthermore, there are other requirements concerning the targeted favourable solvent properties such as low corrosion rates, low viscosity, no foaming, high thermal and chemical stability (degradation), low price, high selectivity for CO_2, low vapour pressure, no toxicity and low environmental impact. All the listed solvent properties have to match with the application and contribute to a proper solvent selection [253].

4.5.1.3 Requirements and Challenges

There are different routes for process optimisation to achieve a more energy-efficient and more economical technology. Heat integration plays an important role (use of latent heat from the reflux condenser, internal heat integration). However, the right choice of solvent is crucial for OPEX because the key process parameters are determined by the utilised solvent.

Thermodynamics and Kinetics

High loadings at absorber temperature are a prerequisite and many solvents offer a high solubility for CO_2. However, at the same time, low loadings at stripper temperature are requested for a high cyclic capacity. It is the solvent flow rate that contributes first to the CAPEX when all sizes and geometries in the plant are fixed and second to the OPEX in terms of electricity demand for pumps and energy input for solvent regeneration. As discussed earlier, these needs favour tertiary or sterically hindered amines. At the same time, the higher molar masses of these compounds might limit the higher cyclic capacity on a molar basis. This issue leaves room for molecular optimisation/functionalisation of the targeted molecules to reach the best achievable ratio between CO_2-active groups and the bulk structure of the molecule. Another tradeoff is found for sufficient absorptions rates together with high cyclic capacities. Tertiary amines have a high cyclic capacity but very slow absorption rates. New solvent formulations will have to offer both a high cyclic capacity and sufficient absorption rates.

Regeneration Energy

As discussed earlier, the regeneration energy for absorption fluids is influenced by different contributions that are related more or less to the solvent's properties. The enthalpy of absorption is one important contribution; it has to be kept low. In amine systems, therefore, components should not directly react with CO_2 to form carbamates, but solve CO_2 as bicarbonates because these reaction mechanisms lead to lower regeneration energy demands [270, 271].

Makeup and Corrosion Behaviour

Absorption plants with standard amines, such as MEA or DEA, suffer from a remarkable makeup demand because of solvent losses due to volatility and unwanted side reactions with CO_2 or oxygen (formation of heat stable salts) [272]. A strong tendency to react with side components also affords the reclaiming of the solvent with additional apparatuses and energy demand; hence, this should be minimised. Optimised systems with a high chemical stability, which are often found with tertiary and hindered amines, are advantageous [254].

4.5.1.4 Materials and Methods Used for this Contribution

All experimental data were measured according to standard methods described elsewhere in the literature and will be only discussed briefly here [253]. Solubility measurements were carried out in stirred gas–liquid equilibrium autoclaves (stainless steel, 0.5 dm^3, 0–2,000 kPa and a Büchi glass reactor, 0.5 dm^3,

0–450 kPa). The method was already described by Shen and Li [273], and Dawodu and Meisen [274].

The solution (250 ml) was introduced to the evacuated cell and CO_2 was added with a flow metre until a specified pressure was reached. When the pressure was constant for 1 h, equilibrium was assumed and liquid samples (1.5 ml) were taken and analysed by the titration method described in Ref. [275]. The partial pressure of CO_2 was calculated by subtraction of the total pressure from the partial pressure of the aqueous amine solution. In case of subatmospheric pressure, the concentration of CO_2 in the liquid phase was calculated by means of the readout of the flow metre, taking into account the gas phase correction (amount of CO_2 in the gas phase when the total volume of the cell and the liquid volume are known). Absorption rates were determined by purging unloaded solution with a defined volume of CO_2 while the liquid and the gas phase were stirred at low stirrer speeds. By comparing the slope of the curve from the continuously recorded pressure loss versus time, a qualitative absorption rate is obtained [253].

All experimental procedures were tested with standard systems, such as monoethanolamine and methyldiethanolamine solutions. The enthalpy of absorption was measured in a calorimeter as described in Ref. [276]. Corrosion rates have been measured by using the standard test method for conducting potentiodynamic polarisation resistance measurements as described in ASTM G59-97e1. Steel (1.0402) was used as material in the corrosion tests.

The foaming behaviour was measured in terms of the Bikerman index (Σ = foam volume/volumetric gas flow [s]). The test cell setup was already described in Ref. [277]. The same amount of every unloaded solvent (700 ml) was used in the test cell and a water saturated nitrogen stream was bubbled through the liquid holdup using a frit for equal distribution of the gas in the liquid. The resulting height of the foam in the test cell was measured for different gas flows. Before a higher gas flow was specified, the system was allowed to reach a steady state in terms of height of the foam, which took 10–30 min.

The materials employed were CO_2 (Air Liquide, 0.9998 purity in mole fraction) and deionised distilled water. The used amine compounds were introduced in Refs. [253, 278–283] and were utilised in the experiments as aqueous solutions.

4.5.1.5 Results

In this section, selected experimental data for a novel and highly competitive solvent system are discussed, which can overcome several limitations of the aforementioned state-of-the-art systems. Table 4.38 shows experimental solubility data for a new Evonik absorbent formulation [253] and compared to state-of-the-art solvents, such as aqueous solutions of MEA and MDEA. The Evonik absorbent offers a cyclic capacity that is twice as high as for MEA. Therefore, the solvent flow rate in the Evonik system can be drastically reduced.

At the same time, other sour gases such as H_2S show significant high loadings in the Evonik absorbent, especially compared to state-of-the-art absorbents such as

Table 4.38 Results for cyclic capacities of state-of-the-art and new Evonik absorbents

Absorbent	Cyclic capacity/mol CO_2/kg absorbent	Source
MEA	1.2	[275]
Promoted MDEA	2.3	Pitzer model
Evonik absorbent 1	2.4	[253]
Evonik absorbent 2	2.6	

The cyclic capacity is given for isotherms between 40 and 120 °C at 1 bar. MEA = 30 wt% aqueous solution, Promoted MDEA = 3 wt% piperazine and 37 wt% MDEA, Evonik absorbents = 30 wt% aqueous solution

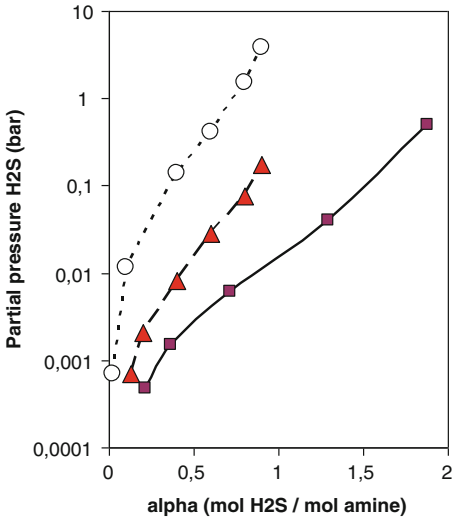

Fig. 4.86 Absorption isotherms of H_2S in different absorbents at 40 °C. The data of the Evonik absorbent 2 (*filled square*) is given for 30 wt% solution in water. MDEA (o) and Flexsorb SE^{TM} (*filled triangle*) are taken from [285] (2.5 molar amine solution)

MDEA or Flexsorb SE, as depicted in Fig. 4.86. Even at low partial pressures of H_2S, the Evonik absorbent will achieve remarkably high loadings up to 10 times higher than those of MDEA. It is well known that the acid–base reaction between H_2S and an amine is much faster than reactions of CO_2 with amines (either carbamate formation or the acid–base reaction). Therefore, it is expected that the absorbent formulation will also be of great interest to selectively remove H_2S with a high CO_2 slip and supply enriched sour gases to sulphur recovery units. Further field test investigations on absorption rates and the obtainable CO_2 slip are ongoing.

As in absorption processes, the solvent in the absorber never reaches equilibrium conditions, which is why the processes are kinetically limited. Therefore, absorption rates play a significant role and also have to be considered. As mentioned previously, for example, MDEA can not compete with MEA without further activation. Because of the slower absorption rates, inactivated MDEA would not reach the high loadings in the absorber and could not use its high cyclic capacity [286, 287].

Table 4.39 Results of the enthalpy of absorption for CO_2 in different absorbents at 40 °C

Solvent	Enthalpy of absorption (kJ/mol)	Source
MEA (30 wt%)	−85	[288]
MDEA (50 wt%)	−65	[284]
Evonik absorbent 1 (30 wt%)	−30	[253]
Evonik absorbent 2 (30 wt%)	–	

Table 4.40 Corrosion test results from the potentiodynamic polarisation resistance measurements with CO_2-saturated solutions at 25 °C for typical carbon steel (1.0402) [253]

Solvent	Corrosion rate (mm/year)
MEA (30 wt%)	1.99
MDEA (27.9 wt%) + piperazine (2.1 wt%)	0.99
MDEA (37.2 wt%) + piperazine (2.8 wt%)	1.18
Evonik absorbent 1	0.21
Evonik absorbent 2	0.29

As can be seen from the absorption results and the kinetic performance, the Evonik absorbent offers a unique opportunity to combine good kinetics with superior cyclic capacity. The lower enthalpy of absorption is one major advantage of MDEA that helped to replace MEA in many gas sweetening applications. The heat of reaction, the physical enthalpy of solution and the excess enthalpy of mixing contribute to the enthalpy of absorption. As discussed previously, this represents a major part of the regeneration energy that has to be supplied in the stripper. From Table 4.39, it can be seen that the Evonik absorbent has a considerably lower enthalpy of absorption compared to state-of-the-art solvents. This results in further energy savings in the regeneration of the solvent and makes the Evonik absorbent a highly energy-efficient and highly economically attractive alternative to state-of-the-art solvents such as MEA and MDEA.

The solvent has to fulfil additional requirements, as outlined previously, in order to lower the OPEX of a separation plant. In this context, one important point is corrosion, which is still a serious issue for absorption plants. The corrosion potential of the Evonik absorbents is much lower compared to uninhibited MEA (by a factor of 7) or piperazine and MDEA mixtures (by a factor of 3.4; see Table 4.40). As a result, additional degrees of freedom from the choice of different materials for constructing the plant and the chosen corrosion inhibitor allow for a reduction in both capital and OPEXs [253].

To determine the tendency of foaming of the new absorbent formulation, the Bikerman index was calculated according to the experimental procedure described previously. The lower the number of the Bikerman index, the less is the foaming height of the system and hence the foaming tendency. Figure 4.87 plots the Bikerman index for a promoted MDEA (10 wt% Evonik promoter and 20 wt% MDEA) and the Evonik absorbent 2 versus the gas flow rate. It can be concluded that even at higher gas flow rates the Evonik absorbent 2 did not show any

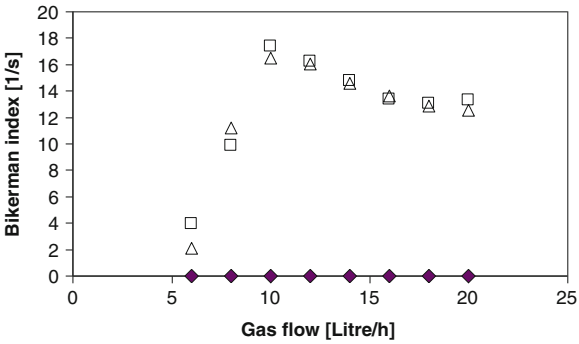

Fig. 4.87 Foaming tendency of a promoted MDEA solution (10 wt% Evonik promoter and 20 wt% MDEA) (*square, triangle*) and of Evonik absorbent 2 () without antifoaming agent. The Bikerman index is plotted versus the gas flow rate for different test runs at 40 °C

tendency to foam, which results in a Bikerman index of zero. MDEA is known to cause frequent foaming problems in gas sweetening plants and thus has a high number on the Bikerman index (approximately 14.5). From various reports in the literature, it is well known that the solution tends to foam, especially at high concentrations of MDEA [254, 289, 290].

Recent field trials confirmed that the Evonik absorbent shows no foaming tendency, whereas promoted and pure MDEA solutions tended to foam and needed an antifoaming agent [253, 293, 294]. Although foaming is a complex matter and is basically influenced by various solution contaminants (water-soluble surfactants, liquid hydrocarbons, particles, heat-stable salts and a host of others), these encouraging results indicate that a common problem of gas-treating units might become less of an issue with these new high-performance absorbents.

Here, results from an estimated process performance of the Evonik absorbent are derived based on the approach recently introduced by Hasse et al. [291]. By means of a modified Kremser equation, the absorber and the desorber are described and calculated on a simplified equilibrium-stage model that uses isotherms at absorber and desorber temperature and caloric data (heat capacity, absorption enthalpy). The model predicts the minimum reboiler energy at an optimum solvent flow rate for given boundary conditions. The kinetics of absorption are not considered and a sufficient number of equilibrium stages is assumed. The calculation is based on a simplified absorber/desorber flow sheet without a flash but with an internal heat exchanger, as illustrated by Fig. 4.88.

The feed gas enters the absorber at the bottom, and the lean solvent is fed at the top of the absorber, where the treated gas leaves the column with its CO_2 content reduced. The rich absorbent at absorber bottom is internally preheated and enters the desorber at the top. The reboiler at the bottom supplies the necessary heat for regeneration, which consists of parts for desorption enthalpy, stripping steam, heating of the solvent and heating of the condensate reflux. The boundary conditions for the calculations are given in Table 4.41. Table 4.42 depicts the necessary caloric data. Calculations were performed for a natural gas and a syngas

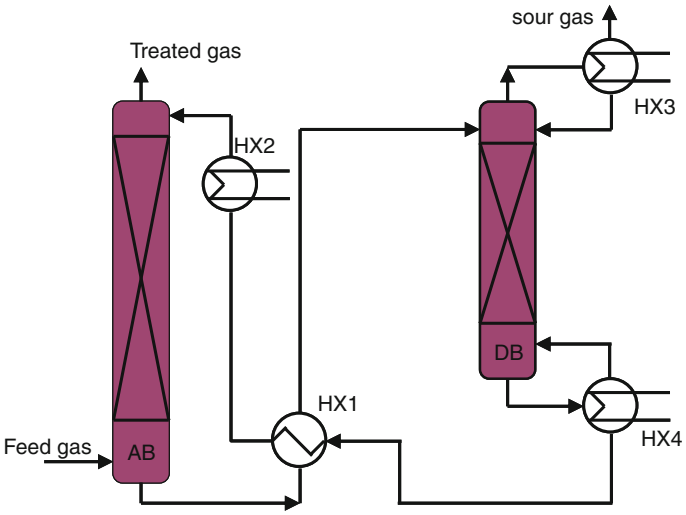

Fig. 4.88 Simplified process scheme for sour gas absorption used for the Kremser method (*AB* Absorber, *DB* Desorber, *HX1* Internal heat exchanger, *HX2* Absorbent cooler, *HX3* Condenser, *HX4* Reboiler)

Table 4.41 Boundary conditions for the calculation

Parameter	Value
CO_2 separation degree	90 %
Absorber inlet temperature	40 °C
Desorber inlet temperature	110 °C
Desorber pressure	2 bar
Desorber bottom temperature	120 °C
Equilibrium stages absorber	10
Equilibrium stages desorber	15

Table 4.42 Caloric data for the calculations for the 10 wt% piperazine and 30 wt% MDEA mixture and the 30 wt% Evonik absorbent

Caloric data	Value
Enthalpy of evaporation of water	2,210.6 kJ/kg
Heat capacity of water	4.197 kJ/kg K[a]
Absorption enthalpy of 10 wt% piperazine and 30 wt% MDEA at 110 °C	2,236 kJ/kg[b]
Absorption enthalpy of 30 wt% Evonik absorbent 1 at 110 °C	811.2 kJ/kg
Absorption enthalpy of 30 wt% Evonik absorbent 2 at 110 °C	1,817.5 kJ/kg
Heat capacity of all absorbents	4.048 kJ/kg K[a]

[a]Because no heat capacity data was available for either the piperazine/MDEA mixture or the Evonik absorbent, the estimated data from Ref. [291] was applied
[b]The value was taken from Ref. [292] and estimated for 110 °C [253]

Table 4.43 Natural gas and syngas feed used in the calculations [253]

Natural gas feed	Syngas feed
15 mol % CO_2	17 mol % CO_2
1 mol % H_2O	0.3 mol % CO
5 mol % N_2	60 mol % H_2
79 mol % CH_4	22 mol % N_2
	0.5 mol % CH_4
	0.2 mol % Ar
Total pressure = 10 bar	Total pressure = 36 bar

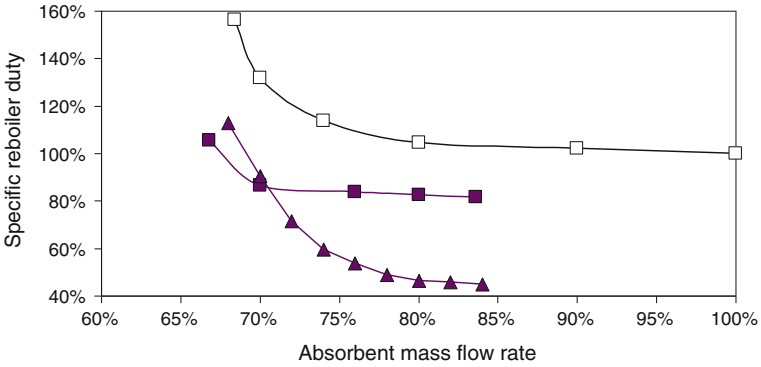

Fig. 4.89 Results from calculation of modified Kremser equations for a 90 % CO_2 separation from a natural gas feed. The specific reboiler duty is plotted against the solvent flow rate for a mixture of piperazine (10 wt%) and MDEA (30 wt%) (*square*) and Evonik absorbent 1 (30 wt%) (*filled triangle*) and for the Evonik absorbent 2 (30 wt%) (*filled square*). 100 % equals 2.68 GJ/t CO_2

feed (see Table 4.43). As reference system, a mixture of piperazine (10 wt%) and MDEA (30 wt%) was chosen for a comparison with the Evonik absorbent (30 wt%). In both cases, for natural and for syngas purification, 90 % CO_2 removal was specified to obtain an energetic comparison between the two absorbent systems in terms of specific reboiler duty.

In Figs. 4.89 and 4.90, the specific reboiler duty (GJ/t CO_2 separated) is plotted against the corresponding absorbent flow rate to achieve 90 % CO_2 separation. It can be concluded that in the case of the Evonik absorbent 2, the flow rate can be reduced to 74 % (syngas) and 84 % (natural gas) compared to the reference system [253, 293, 294]. The specific reboiler duty even decreases to 80 % (both cases) for the Evonik absorbent 2, achieving remarkable savings in the reboiler's steam consumption, which directly translates into lower OPEXs. For the calculation of the natural gas purification, the Evonik absorbent 1 also offers a 16 % reduction in absorbent flow rate and a drastic decrease of the specific reboiler duty, which amounts to 55 % compared to the reference absorbent. For all calculations, the superior thermodynamic properties, such as large cyclic capacities and lower

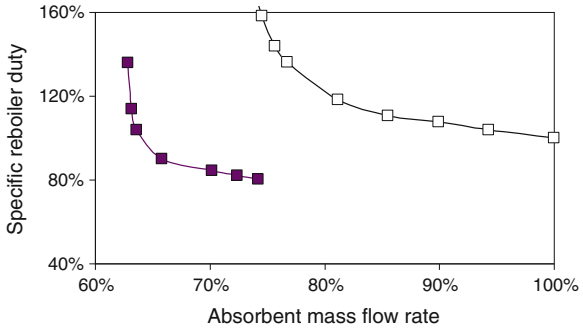

Fig. 4.90 Results from calculation of modified Kremser equations for a 90 % CO_2 separation from a syngas feed. The specific reboiler duty is plotted against the solvent flow rate for a mixture of piperazine (10 wt%) and MDEA (30 wt%) (*square*) and for Evonik absorbent 2 (30 wt%) (*filled square*). 100 % equals 2.60 GJ/tCO_2

enthalpies of absorption, allow for distinctive improvements in terms of energy efficiency.

In absorption processes, the absorbent never reaches equilibrium and therefore the processes are kinetically limited. This means that absorption rates play a significant role, too, and have to be considered. MDEA, for example, cannot compete with MEA in terms of absorption rate without further activation to accelerate the mass transfer. An inactivated MDEA solution would not reach high loadings in the absorber and could not use its high cyclic capacity due to the slower absorption rates.

In Fig. 4.91, the pressure decrease curves for various absorbents at 40 °C are shown. Based on these experimental results, one can calculate volumetric absorption rates as described by Vaidya and Kenig [295]:

$$R_A \cdot a = \frac{V_G}{V_L R' T} \frac{\mathrm{d}p_A}{\mathrm{d}t}$$

The volumetric absorption rate ($R_A a$) can be determined by the volume of the gas phase (V_G), the volume of the liquid phase (V_L), the gas constant (R'), the temperature (T) and the slope of the pressure curve. When all other parameters are kept constant, the kinetics of absorption are determined mainly by the slope in Fig. 4.91. MDEA is a tertiary amine and has the slowest absorption rate. At low activator concentrations, the absorption rates of the Evonik absorbent are in between the curves for a promoted MDEA solution.

It can be summarised that energy-efficient absorbent formulations for separating carbon dioxide from gas streams such as natural gas, syngas, or flue gas are important for a number of industrial applications. In many cases, a substantial share of their costs is driven by the OPEX of the CO_2 separation unit. One possible strategy for reducing OPEX is the improvement of the absorbent performance. Although a number of absorbents for the separation of CO_2 from gas streams exist,

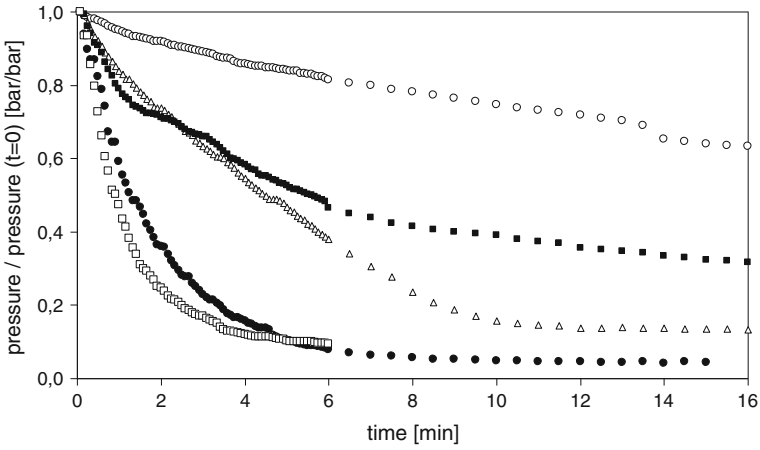

Fig. 4.91 Pressure decrease curves for various absorbents at 40 °C. (*circle*) 40 wt% MDEA, (*triangle*) 30 wt% MEA, (*filled square*) 37 wt% MDEA/3 wt% piperazine, (*filled circle*) 30 wt% activated new absorbent; (*square*) 33 wt% MDEA/7 wt% piperazine

there is still a need to develop CO_2 absorbents with an improved absorption performance, less corrosion and foaming, no nitrosamine formation, lower energy requirements, and therefore less OPEX. A comparison of selected, recent industrial absorbent developments to state-of-the-art systems was introduced and discussed in this contribution.

4.5.1.6 Summary

In recent decades, there has been a shift from the formerly most widely used amines, such as MEA and DEA, to more energy-efficient absorbent formulations based on MDEA. This significant development started in the 1970s with BASF absorbents based on a proprietary mixture of MDEA and an activator to boost the kinetics of CO_2 absorption and meet tight specifications in the ppm range for CO_2 and H_2S. Meanwhile, a lot of other absorption technologies based on MDEA became available from companies such as Dow (Ucarsol), Ineos (Gas/Spec), Shell (ADIP X), Huntsman (Jefftreat) and Prosernat (AdvAmine). Furthermore, there are several proven technologies based on physical absorbents that have not been discussed in this chapter but can be found in various applications, such as acid gas removal from coal-based synthesis gas (Rectisol process from Lurgi and Linde using cold methanol). In the future, an advanced absorption technology will have to make use of an optimised absorbent chemistry (as indicated in this contribution) as well as further optimised processes to obtain suitable customised process solutions for more challenging removal tasks (e.g. higher sour gas content).

4.5.2 Hydrogen Generation: Overview

Christoph Kiener

Untergasse 2, 09599 Freiberg, Germany
e-mail: christoph.kiener@gmx.de

Hydrogen is the lightest atom and the most abundant element in the universe. On Earth, it is commonly found in compounds with other elements. As an isolated element, it exists as hydrogen gas, H_2. Every chemistry textbook gives plenty of information on hydrogen properties, its formation, reactions, and use [298]. This chapter on hydrogen production methods focuses on some basic principles and the current state-of-the-art production technologies. It complements Sect. 4.4.1 (generation of CO/H_2 = synthesis gas) and Chap. 8.

In its chemical compounds, hydrogen can take different formal oxidation states: oxidised as +1, neutral as an H_2 molecule and −1 as hydride. The thermodynamically stable oxidation state depends on the environment where hydrogen is found. In all compounds in the biosphere, in the presence of oxygen, the oxidation state always is +1. Therefore, it always takes energy to generate molecular hydrogen H_2 or a hydride H^- in an environment as we are used to on our planet. In other environments, such as the atmosphere on the planets Jupiter and Saturn, which consist of liquid hydrogen, the energetic situation would be completely different. In this case, only molecular or hydridic hydrogen might be used as an energy carrier in biosphere conditions to release energy by oxidation. Despite this obvious fact, it is sometimes neglected in public debates about future energy concepts that claim liquid water is an abundant source of hydrogen on earth, which do not take into account the atom availability or the energy needed to convert it.

To generate hydrogen from liquid water, it takes at least a formation enthalpy of 285.9 kJ/mol (15.87 MJ/kg H_2O; 12.76 MJ/m^3 standard temperature and pressure [STP] H_2), equal to 3.55 kWh/m^3 STP H_2. For comparison, industrial water electrolysis usually consumes electrical energy of approximately 4.5–5.0 kWh_e/m^3 STP H_2 due to overvoltage and resistance loss. Also, for any other hydrogen production pathway, the energy input to make hydrogen is always higher than the energy return when using it as a fuel, which implies that production routes should be selected carefully. Nevertheless, hydrogen is attractive as an energy carrier due to its concentrated energy content.

From a redox chemistry point of view, in all chemical reactions molecular and hydridic hydrogen always act as reduction agents, regardless of whether they are used as an energy carrier or a chemical reaction partner. Conversely, production of H_2 needs either a reduction agent that is being oxidised while releasing energy during the formation of H_2 or it needs other forms of energy (thermal, photo, electrical).

Table 4.44 shows a set of reactions that are currently used in industrial processes and are well known as hydrogen generating reactions. Energy sources can either be the hydrogen-containing compound itself (methane POX), the energy

Table 4.44 Current and classical production methods for hydrogen H_2 generation

Process/reaction	Hydrogen source	Redox partner	Energy source
Hydrocarbon Steam Reforming $CH_4 + H_2O \rightarrow CO + 3H_2$	C_xH_y/H_2O	C_xH_y	C_xH_y/heat
Partial oxidation $CH_4 + O_2 \rightarrow CO_2 + 2H_2$	CH_4	O_2	CH_4/heat
Gasification of carbon feedstock $C + 0.5O_2 + H_2O \rightarrow CO_2 + H_2$	H_2O	C/O_2	$C^{(0)}$
Kvaerner process $CH_4 \rightarrow C + 2H_2$	CH_4	CH_4	Electric arc
Electrolysis $H_2O \rightarrow H_2 + 0.5O_2$	H_2O	H_2O	Electric potential
Historic *Kipp* gas generator $Zn + 2HCl\ (aq) \rightarrow H_2 + 2ZnCl_2\ (aq)$	HCl acid	Zn	$Zn^{(0)}$
Metal water reaction (solar concept) $Fe + H_2O\ (g) \rightarrow H_2 + FeO$	H_2O (g)	Fe	$Fe^{(0)}$/heat
Metal water reaction (solar concept) $Zn + H_2O\ (g) \rightarrow H_2 + ZnO$	H_2O (g)	Zn	$Zn^{(0)}$/heat
Metal water reaction (e.g. nuclear accident) $Zr + H_2O\ (g) \rightarrow H_2 + ZrO$	H_2O	Zr	$Zr^{(0)}$/heat
Photolysis $H_2O \rightarrow H_2 + 0.5O_2$	H_2O	H_2O	X-ray, visible ultraviolet light
Thermolysis $H_2O \rightarrow H_2 + 0.5O_2$	H_2O	H_2O	Heat > 2,000 K

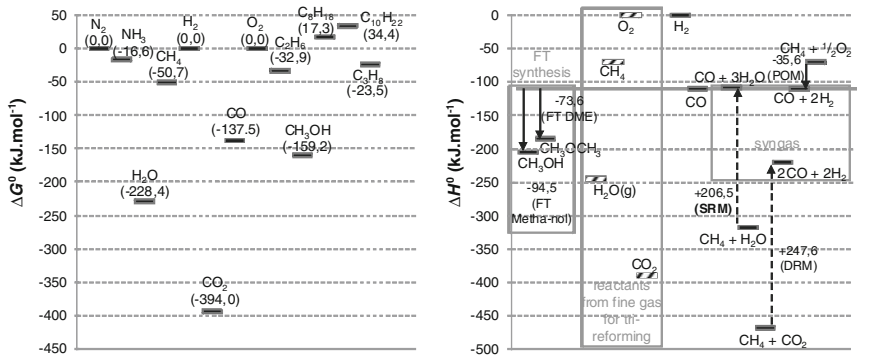

Fig. 4.92 Gibbs free energies of formation of selected compounds (*left*) and reaction enthalpies for hydrogen-related (production as well consumption) reactions (*right*) [299]

carrier (carbon/coal gasification), a reduced metal that is oxidised (Kipp gas generator; zinc/steam high temperature reaction), or an external source (heat, radiation, electric arc).

In Fig. 4.92, Jiang et al. show the Gibbs free energy of formation for hydrogen and several chemical compounds related to hydrogen production and synthesis gas

reaction [299]. With the exception of some long-chain hydrocarbons, most other chemical compounds are thermodynamically more stable than molecular hydrogen (Fig. 4.92, left). This means that additional energy is needed to convert these compounds into molecular hydrogen.

Any chemical reaction (conversion) is driven by the difference in the Gibbs free energy between the reactants and products of a chemical reaction under certain conditions, as shown by the Gibbs–Helmholtz relationship:

$$\Delta G^0 = \Delta H^0 - T\Delta S^0 \tag{4.60}$$

Hence, as shown in Fig. 4.92 (right), a large number of industrial-scale chemical manufacturing processes to produce hydrogen are operated on the basis of strongly endothermic chemical reactions. The steam reforming of hydrocarbons to yield synthesis gas (and hydrogen) is a prominent example:

$$CH_4 + H_2O \rightarrow CO + 3H_2 \quad \Delta H^0 = +206.3\,\mathrm{kJ\,mol^{-1}} \tag{4.61}$$

On the other hand, reactions using hydrogen or synthesis gas for production of Fischer–Tropsch fuels, ammonia, or methanol are exothermic, which means that the product contains less energy than the educts used.

Hydrogen (H_2) production in the environment of our planet is a process with three premises: (1) the source of hydrogen, (2) the need for energy input and (3) the need for a reduction equivalent. From an energy point of view, the use of a feedstock for hydrogen production will always be in competition with other energy application as fuel for mobility, heat, power generation or power storage, or production of chemical products, materials and food. The use of hydrogen in a hydrogen-energy economy always should be designed along a cradle-to-cradle lifecycle analysis as to determine the most efficient process routes.

Production Methods for Hydrogen

Hydrogen production methods are well described in major technical reviews [300]. Regarding the nature of the energy source, hydrogen production processes in technical applications may be grouped into different fields (see Table 4.45).

Currently, established industrial processes mostly use fossil sources for hydrogen generation. Catalytic reforming in steam reformers and ATRs is the most common installed technology. Gasification of hydrocarbon residues as petroleum coke, heavy residues and coal is growing, especially in Asia due to limited access to natural gas. A minor source of hydrogen is yielded as byproduct from chlorine electrolysis plants. In the 1970s, there were also some plants for water electrolysis in areas with cheap and abundant electricity. With the development of a natural gas distribution system, this technology became more expensive; however, it might again become more interesting in future.

Comparison of Current Hydrogen Production Methods

Regarding their technical advances, hydrogen production technologies (Table 4.46) experienced some movement over the last decade [301]. Natural

Table 4.45 Energy sources for hydrogen production

Energy source for hydrogen production	Applied industrial processes
Energy from oxidation of coal and hydrocarbons	Separation from coke oven gas
	Noncatalytic gasification of coal and liquid or gaseous hydrocarbons
	Catalytic reforming of hydrocarbons in allothermal or autothermal processes
	Separation from refinery process streams
	Separation from petrochemical process streams
Electrical energy/electrolysis	Conventional water electrolysis
	Byproduct from other electrolysis processes
Energy from high energy sources: radiolysis, photolysis, thermolysis	Thermochemical water cleavage
	Thermochemical methane cleavage
	Photochemical or photoelectrical water cleavage
	Hydrogen formation in biological systems
	Other methods for the cleavage of water
	Thermolytic and radiolytic processes
Energy from heat and the oxidation of metals	Hydrogen from conversion of metals
Energy from oxidation of other chemical carriers	Hydrogen from ammonia
	Hydrogen from methanol
	Hydrogen from hydrogen sulphide
	Hydrogen as byproduct

gas–based technologies have reached a high degree of maturity. Recent developments only improve details or extend the technology to more "difficult" feed stocks and other applications (e.g. dry reforming of methane with CO_2). Coal gasification also is a mature and stable process, but it still offers potential for improvement regarding an increase of operability and reliability of the plant, as well as further increase in efficient use of fuel and utilities. Electrolysis processes for water electrolysis are in development to cover the needs of a highly dynamic load as well as of cost reduction for this technology. In a methanol manufacturing

Table 4.46 Degree of development of hydrogen production technologies [301]

Production process	Status
Steam reforming of natural gas	Mature
Catalytic decomposition of natural gas	Mature
Partial oxidation of heavy oil	Mature
Coal gasification	Mature/R&D
Steam-iron coal gasification	R&D
Static water electrolysis	Mature
Dynamic water electrolysis	R&D
Thermochemical cycles (pure)	R&D
Thermochemical cycles (hybrid)	R&D
Photochemical processes	Early R&D
Photoelectrochemical processes	Early R&D
Photobiological processes	Early R&D

R&D research and development

Table 4.47 Current fields of large-scale hydrogen applications

Reaction	Reaction partner	Product	Equation
Ammonia synthesis	N_2	NH_3	$3H_2 + N_2 \rightarrow 2NH_3$
Methanol synthesis	CO	CH_3OH	$CO + 2H_2 \rightarrow CH_3OH$
Fischer–Tropsch synthesis	CO	$-(CH_2)-$	$CO + 2H_2 \rightarrow -(CH_2)- + H_2O$
Hydrodesulphurisation	R–S–R′	R–H, R′–H, H_2S	R–S–R′ + $2H_2$ → R–H + R′–H + H_2S
Hydrocracking	R–CH_2–R′	R–CH_3 + H–R′	R–CH_2–R′ + H_2 → R–CH_3 + H–R′
Hydrogenation	R–CH=CH–R′	R–CH_2–CH_2–R’	R–CH=CH–R′ + H_2 → R–CH_2–CH_2–R′
Reduction	R–(C=O)–R′	R–(HCOH)–R′	R–(C=O)–R′ + H_2 → R–(HCOH)–R′
Reduction	R–NO_2	R–NH_2	R-NO_2 + $3H_2$ → R-NH_2 + $2H_2O$
Hydroformylation	R–C=CH_2, CO	R–CH_2–CH_2–CHO	R–C=CH_2 + CO + H_2 → R–CH_2–CH_2–CHO
Fuel cell	O_2	Electricity	$2H_2 + O_2 \rightarrow 2H_2O$
Welding torch	O_2	Heat	$2H_2 + O_2 \rightarrow 2H_2O$
Metal surface protection	MEO_x (ME = Metal)	ME	$MEO_x + x/2H_2 \rightarrow ME + H_2O$
Direct reduction of iron	Fe_2O_3	Fe	$Fe_2O_3 + 3H_2 \rightarrow 2Fe + 3H_2O$
Internal combustion engine	O_2	Mechanical energy	$2H_2 + O_2 \rightarrow 2H_2O$
Hydrogen gas turbine	O_2	Mechanical energy	$2H_2 + O_2 \rightarrow 2H_2O$

chain, the majority of the hydrogen or synthesis gas manufacturing processes determine the overall investment costs, requiring strong focus on their reduction.

Markets and Applications

Close to 50 % of the global demand for hydrogen is currently generated via steam reforming of natural gas—about 30 % from oil/naphtha reforming from refinery/chemical industrial off gases, 18 % from coal gasification, 3.9 % from water electrolysis and 0.1 % from other sources [301, 302]. Depending on customers' needs and feedstock supply situations, small units are also being installed. Ammonia dissociation (the catalytic breaking of ammonia into hydrogen and nitrogen) and cleavage of methanol by low-temperature steam reforming are methods for remote locations without connection to the natural gas grid. Further, the supply from liquefied hydrogen by evaporation is a possibility to supply highest purity hydrogen in comparably small amounts [303].

Hydrogen is widely used in important industrial-scale chemical reactions (Table 4.47). For a long time, the main use was its reduction potential. In recent decades, hydrogen has also been discussed as an energy carrier for mobile applications (Fig. 4.93).

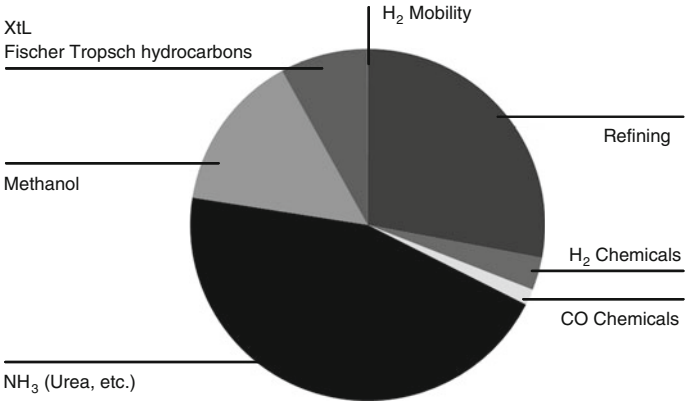

Fig. 4.93 Hydrogen and synthesis gas-based market distribution for business segments in 2012 [304]

Hydrogen finds use in diverse applications covering many industries, including crude oil refining, manufacture of fertilisers and steel treatment. Ammonia synthesis is the major consumer of hydrogen. Often, there is a downstream process, such as ammonia being an intermediate to manufacture urea. Urea as a solid product can be transported more easily and is used as fertiliser or starting material for melamine polymer production. Other uses are for production of nitric acid and ammonium nitrate, and, of course, in chemical production sites for many different reactions. Crude oil refineries use hydrogen to enhance gasoline and diesel output and quality through hydroprocessing. Removal of contaminants, mainly sulphur, helps refiners to meet Clean Air Act requirements.

The third major hydrogen consumer is the production of methanol, which increased in the last decade from 35 to 45 million tonnes/year. For methanol production, synthesis gas is used, which contains carbon monoxide as reaction partner with the required stoichiometric amount. Besides its classical applications (fuel additive methyl *tert*-butyl ether, formaldehyde, biodiesel methyl ester), methanol gains more use for production of dimethyl ether (heating gas; propellant, liquefied natural gas substitute), and as feedstock for condensation reactions to hydrocarbons (methanol-to-olefins, methanol-to-gasoline; see Sect. 6.4).

Apart from these large-scale consumers, there are broad applications for hydrogen in different branches, making use of different properties of hydrogen. The food business uses hydrogen to hydrogenate liquid oils (e.g. soybean, fish, cottonseed and corn oils), converting them to semisolid materials such as shortenings margarine, and peanut butter. In metal production and fabrication hydrogen, is used to serve as a protective atmosphere in high-temperature operations, such as stainless steel manufacturing. In aerospace, liquid hydrogen fuels space crafts, but it also powers life-support systems and computers, yielding potable water as a byproduct.

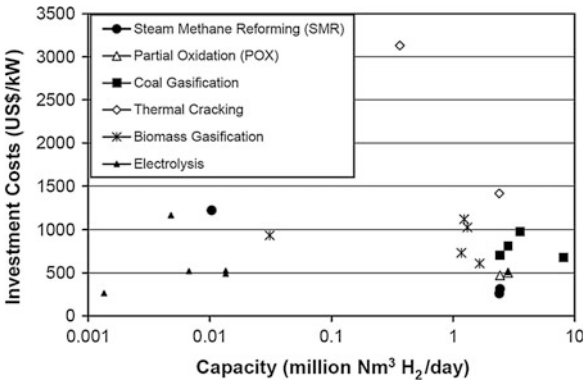

Fig. 4.94 Investment costs for hydrogen plants by capacity [306, 307]

In electronics production, hydrogen creates specially controlled atmospheres in the production of semiconductor circuits. In power generation, hydrogen serves as a heat transfer medium for cooling high-speed turbine generators. In fuel cells, hydrogen is used as a fuel to power fuel cell generators that create electricity through an electrochemical process in combination with oxygen (see Sect. 6.5.2) [305].

Hydrogen Plants and Markets

An economic study released in 2003, calculated using the U.S. dollar of 1990, shows the comparison of different hydrogen production technologies regarding scale and investment cost (see Fig. 4.94). Regarding CAPEXs, SMR is the cheapest method for large-scale applications; gasification units are two to four times higher in installation cost. However, feedstock for gasification is much cheaper and easier to transport than natural gas, especially for remote or less developed areas where no supply system for natural gas is installed. For very small production units, electrolysis is competitive by means of investment but suffers from high operating/electricity costs.

As described by Armor, the 2003 global H_2 production was 480 billion m^3 STP (17.0 trillion SCF) with a growth of approximately 10 % per year [308].

The market can be split into on-purpose/captive, on-purpose/merchant and byproduct market segments. U.S. demand for merchant H_2 in 2003 was 14 billion m^3 STP (502 billion SCF) [309, 310], which was 67 % of the global merchant H_2 sales or approximately 16 % of total U.S. H_2 production. The merchant H_2 market does not include the H_2 produced by a number of captive production operations, such as within methanol plants (9 % of global H_2 consumption), for the production of NH_3 (57 % of global H_2 consumption), or used internally (such as for hydrodesulphurisation in refinery processes). It is estimated that it would take 600 million tonnes/year (6.6 trillion m^3 STP, 233 trillion SCF of H_2/year) to satisfy a global energy market based only on H_2, which is about 14 times more than the total amount of H_2 produced at present globally [311]. Such a large gap in H_2 production capacity can only be filled by uncommitted H_2 (the merchant sales), new plants and/or a totally new production process.

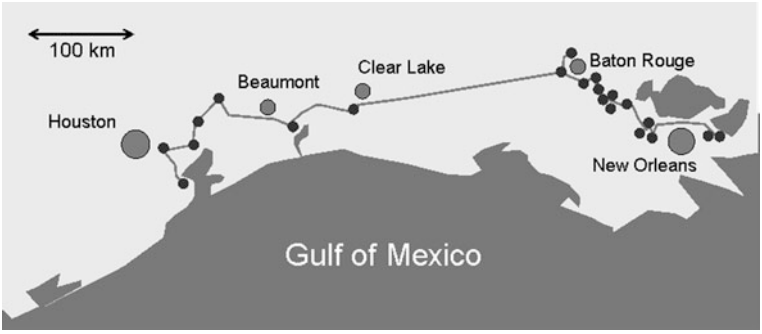

Fig. 4.95 The world's largest hydrogen grid in the Gulf of Mexico. Feed-in hydrogen plants are marked as small dots

Currently, hydrogen represents a market of roughly US$50 billion for about 40 million tonnes of annual production. Prospects of future population increase with the consequence of an increased requirement for food; various commodities will also increase the requirements for hydrogen [312].

Driven by aspects of a reliable and continuously available hydrogen supply, some highly industrialised areas developed hydrogen pipeline supply systems that connect numerous consumers with several feed-in production facilities. In the United States, the world's biggest supply system connects the Houston petrochemical area in Texas with the Baton Rouge and New Orleans chemical sites in Louisiana. In 2012, a new 180-mile long pipeline connector became operational to connect these two grids. This hydrogen pipeline supply network stretches from the Houston Ship Channel in Texas to New Orleans. This integrated pipeline system unites over 20 hydrogen plants and over 600 miles of pipelines. It supplies the Louisiana and Texas refinery and petrochemical industries with over 1.2 billion cubic feet of hydrogen per day [313].

Furthermore, in the Texas area between Houston and Beaumont, the world's only commercial hydrogen storage facility is being operated. Located in Liberty County, Texas, the facility will use an underground storage cavern. The underground hydrogen storage cavern, surrounded by a salt dome, is integrated into a 310-mile Gulf Coast hydrogen pipeline system. The hydrogen storage cavern system is designed to meet refiners' planned and unplanned hydrogen demand by providing online, backup supply [314]. Such peak-shaving systems significantly increase the on-demand availability of hydrogen during periods of peak demand. The Gulf Coast pipeline network will then be able to supply 700 million cubic feet per day of hydrogen on a steady-state basis, with peaking capacity of 800 million cubic feet per day (Fig. 4.95).

As shown in Table 4.48 similar hydrogen supply systems can be found in Europe, mainly in the Benelux/Rhine Ruhr area, northern France and around the Leipzig/Halle chemical complexes. In combination with an already existing refurbished pipeline with some new connectors, a hydrogen pipeline grid could be built that is more than 1,000 km in length.

Table 4.48 European hydrogen pipeline networks and their operators [315]

Operator	Network name	Length (km)	Transit countries	Length (km)
Air liquide	North Europe	949	Netherlands	187
			Belgium	613
	Dunkerque	14	France	303
	France East	37		
	France Centre East	57		
	France South East	42		
	Le Havre	4		
	Ruhr	240	Germany	240
	Monthey	2	Switzerland	2
	Priolo	6	Italy	6
	Sub total	**1,351**	**Sub total**	**1,351**
Linde (BOC)	Leuna-Bitterfeld	135	Germany	135
	Teesside	35	United Kingdom	35
	Sub total	**170**	**Sub total**	**170**
Air products (Sapio)	Rozenburg	50	Netherlands	50
	Teesside	5	United Kingdom	5
	Porto Marghera	2	Italy	2
	Sub total	**57**	**Sub total**	**57**
Others	Stenungsund	18	Sweden	18
TOTAL		**1,596**		**1,596**

4.5.3 Hydrogen Production: Water-Splitting Technologies with Renewable Energy

Eric Weingart and Martin Bertau

Institute of Chemical Technology, Freiberg University of Mining and Technology, Leipziger Straße 29, 09599 Freiberg, Germany
e-mail: martin.bertau@chemie.tu-freiberg.de

Hydrogen is, besides carbon dioxide, the basic resource for methanol production in the carbon capture and utilisation (CCU) process and therefore has to be producible at low cost. Today, hydrogen is chiefly obtained by dehydrogenating fossil resources or producing synthesis gas from the latter. The simplest available resource for hydrogen is water, which can be split into hydrogen and oxygen:

$$2H_2O \rightarrow 2H_2 + O_2 \qquad \Delta_R H = 572 \text{ kJ/mol} \tag{4.62}$$

By using renewable energy, various technologies of water splitting can be applied, which are summarised in Table 4.49. Hybrid technologies such as high temperature electrolysis (HTEL) are also possible. Furthermore, biological approaches with or without sunlight are still the subject of current studies. Because methanol can be produced directly from biomass via synthesis gas or fermentation, hydrogen generation of from biomass will not be discussed here.

Table 4.49 Water-splitting technologies with renewable energy

Technology	Geothermal	Solar	Water power	Wind power
Electrochemical	x[a]	x	x	x
Photochemical	–	x	–	–
Photoelectrochemical	–	x	–	–
Piezoelectrochemical[b]	x	x	x	x
Pyroelectrochemical	x	x	–	–
Thermochemical	x	x	–	–

[a] Via power from steam turbines
[b] Additional contribution by using vibration energy from versatile plant sections

4.5.3.1 Electrochemical

Water splitting by electrolysis is the most common technology for hydrogen generation from water and is the only one operating on an industrial scale. In 2009, 4 % of the worldwide production of hydrogen was realised by water electrolysis [316].

By means of electric power, water is split into the elements hydrogen and oxygen, which are co-deposited at cathode and anode, respectively:

$$\text{Cathode:} \quad 2H_2O + 2e^- \rightarrow H_2 + 2OH^- \tag{4.63}$$

$$\text{Anode:} \quad 2H_2O \rightarrow O_2 + 4H^+ + 4e^- \tag{4.64}$$

Depending on the technology, water is used as liquid or as steam. For the different electrolysis technologies, a distinction is made between low-temperature electrolysis (LTEL) and HTEL. Only the former is common, and it is further distinguished between alkaline electrolysis (AEL) and proton-exchange membrane electrolysis (PEMEL). Research is currently examining HTEL to decrease the decomposition voltage by substituting a part of the electric power by heat.

Additional research with the aim of decreasing electric power uptake for water splitting has been undertaken in combination with photo-electrochemically active electrodes. Under the influence of sunlight, they build up an electrochemical potential to another electrode, which can be standard equipment. Another possibility is the conversion of waste kinetic or thermal energy into power by piezoelectrochemical and pyroelectrochemical active substances to produce an additional amount of hydrogen by electrolysis [317]. Attention should be paid to the crystalline direction of the substances in order to produce spatially divided hydrogen and oxygen. However, exploratory studies at the Institute of Chemical Technology at Freiberg University of Mining and Technology have unambiguously proven hydrogen formation to occur in an alternating thermal field [318].

Alkaline Electrolysis

AEL is the oldest known electrolysis technology and is usually conducted in an aqueous solution of 30 % KOH at 80–90 °C. During the process, hydroxide ions migrate through the diaphragm from cathode to anode:

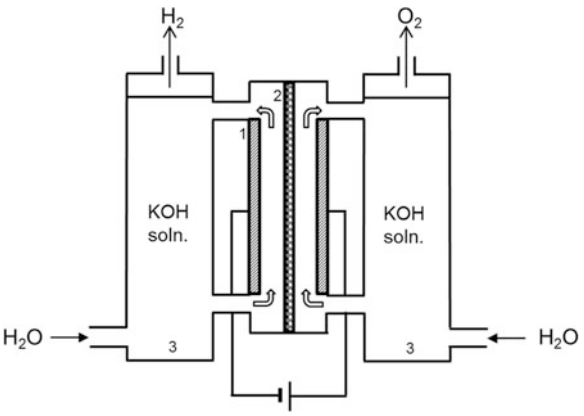

Fig. 4.96 General setup of alkaline electrolysis. *1*—electrodes, *2*—diaphragm, *3*—gas-fluid-separator [319]

$$\text{Cathode:} \quad 2H_2O\ (I) + 2e^- \rightarrow H_2 + 2OH^- \tag{4.65}$$

$$\text{Anode:} \quad 4OH^- \rightarrow O_2 + 2H_2O + 4e^- \tag{4.66}$$

The electrodes are usually nickel based due to its resistance against corrosion in this environment. Thus, neither expensive special alloys nor noble metals have to be used. The electrolysis cell itself has low investment costs and a long lifetime. Disadvantages arise from the liquid electrolyte, which is very corrosive against other parts of the installation and negatively affects the reaction kinetics of gas formation. In addition, the concentration of the electrolyte has to be controlled and adjusted constantly, hence requiring a more complex plant setup. The major drawback for its use with fluctuating renewable energy, such as wind power, is the poor partial load properties and the lag time for startup and shutdown of the electrolysis plant (Fig. 4.96).

Recent developments in the field of advanced AEL comprise augmentations of the active electrode surfaces by using porous electrodes, better catalyst systems that support the redox reactions at the electrodes, higher temperatures to decrease the decomposition voltage, less complex plants to decrease investment costs, and the usage of anion exchange membranes (in comparison with PEMEL) instead of liquid electrolyte solutions [320, 321].

Proton-exchange Membrane Electrolysis

Acidic electrolysis requires a proton exchange membrane, allowing for protons to migrate from anode to cathode (Fig. 4.97):

$$\text{Cathode:} \quad 4H^+ + 4e^- \rightarrow 2H_2 \tag{4.67}$$

$$\text{Anode:} \quad 2H_2O(I) \rightarrow O_2 + 4H^+ + 4e^- \tag{4.68}$$

The advantages of PEMEL compared to AEL include the compact setup, higher power efficiency and higher power density, which result in higher production rates

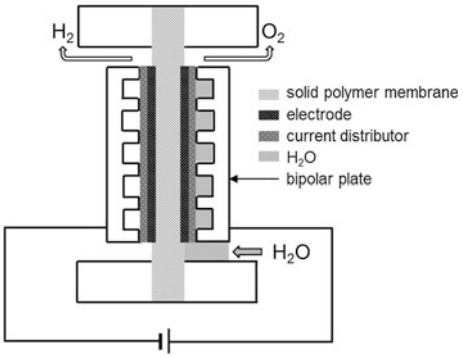

Fig. 4.97 General setup of proton-exchange membrane electrolysis [321]

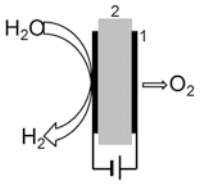

Fig. 4.98 General setup of solid-oxide electrolysis cells. *1*—electrodes, *2*—solid oxide electrolyte [324]

for hydrogen per cell. Moreover, the partial load properties are better, so the plant is suitable for fluctuating power from renewable resources. However, the applied membranes are expensive and therefore imply higher investment costs and limited long-term stability [321, 322].

High-temperature Electrolysis

Under high temperatures, decomposition voltage of water and overvoltage at the electrodes decrease while ion conductivity increases, which has made HTEL the focus of current research [323]. The electrolysis works at >800 °C in solid-oxide electrolysis cells (SOECs), where oxide ions migrate from cathode to anode (Fig. 4.98):

$$\text{Cathode:} \quad 2H_2O(g) + 4e^- \rightarrow 2H_2 + 2O^{2-} \tag{4.69}$$

$$\text{Anode:} \quad 2O^{2-} \rightarrow O_2 + 4e^- \tag{4.70}$$

To obtain pure hydrogen, it is necessary to separate it from steam. This could be avoided if proton conductors were used (e.g. PEMEL). However, it was shown that they conduct oxide ions at high temperatures as well, which so far cannot be sufficiently suppressed [325].

To generate heat and electricity for SOECs from renewable resources at the same time, concentrated sunlight could be used. For these purposes, sunlight is concentrated by reflectors and is guided through a ray separator, which reflects heat radiation and allows visible light to pass. The heat radiation is concentrated in

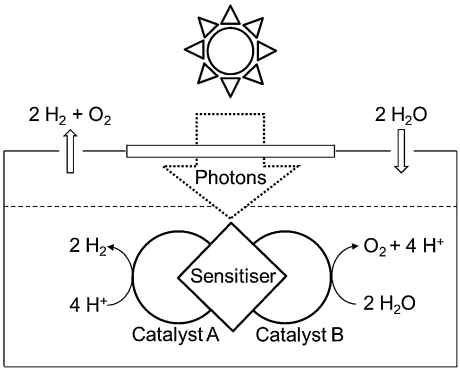

Fig. 4.99 Photochemical hydrogen production. *Sensitiser* activate electrons with photons, *Catalyst A* donating electrons for proton reduction, *Catalyst B* collecting electrons for water oxidation [326]

a steam generator for a SOEC, while the electricity is provided from photovoltaic (PV) cells, which are located behind the separator and convert the visible light. With this technology, conversion rates up to 40 % for solar-to-hydrogen appear within reach in the near-term future [326].

4.5.3.2 Photochemical

As an alternative to electrochemical methods, it is possible to split water with sunlight only. The advantage is the direct use of sunlight without the roundabout way of electrolysis. However, supporting reagents are required to supply the electrons generated by photons for H^+ reduction as well as to absorb electrons from O^2 oxidation. A photochemical system consists of a sensitiser for photon absorption and two catalysts for the redox reaction (Fig. 4.99). Nevertheless, hydrogen and oxygen are not produced separately and conversion rates range below 1 % [326].

4.5.3.3 Thermochemical

Thermal water splitting into its elements could be realised with geothermal heat (<600 °C) and solar thermal heat (<3,000 °C) with different technologies (Fig. 4.100).

Direct thermal water splitting is not practicable due to the required temperatures of >2,500 °C and simultaneous generation of hydrogen and oxygen. Therefore, more than 300 thermochemical and hybrid electrochemical-thermochemical processes via supporting reagents have been developed up to now. In the centre of interest are (1) the hybrid Cu-Cl cycle process (Fig. 4.101) for geothermal plants [327], (2) the S–I cycle process (Fig. 4.102) and (3) the hybrid sulphur cycle (HyS) process for solar thermal plants. The HyS process generates hydrogen via electrolysis of an aqueous solution of sulphur dioxide (SO_2). The produced sulphuric

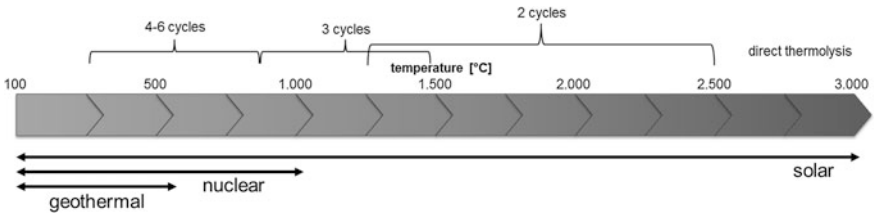

Fig. 4.100 Number of thermochemical cycles required for 100 % water splitting, depending on temperature [327]

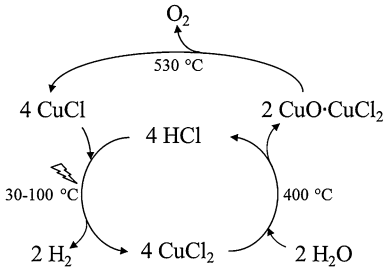

Fig. 4.101 Hybrid Cu–Cl cycle with electrochemical step and drying step at 100–200 °C

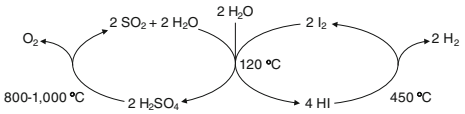

Fig. 4.102 Thermochemical S–I cycle

acid is decomposed at 800–1,000 °C to give sulphur dioxide, thus closing the loop [326].

Currently, there is no process that is working on an industrial scale, but promising technologies are being developed, such as the Hydrosol-3D (based on MeO_x cycle) or HycycleS (based on S–I and HyS cycle projects). The main advantage of solar thermal water splitting technologies is their superior use of solar energy with a conversion rate of up to 45 % in comparison to 16 % for electrolysis combined with PVs ($\eta = 20$ % for PV and 80 % for electrolysis) [326].

4.5.3.4 Biological

There are three major concepts for producing hydrogen with biological/biochemical methods:

1. Biological WGS reaction with purple bacteria
2. Fermentation with bacteria like *Enterobacter aerogenses*
3. Photosynthesis with cyanobacteria or green algae.

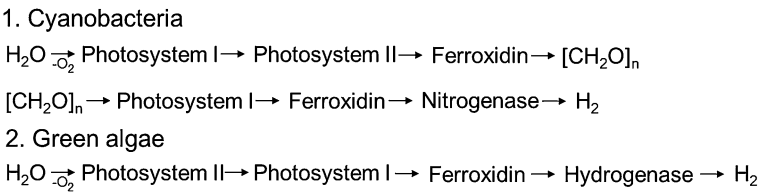

Fig. 4.103 Hydrogen generation mechanism of cyanobacteria and green algae

A disadvantage of bacteria-based technologies is the substrate required for consumption, which competes with the direct biomass gasification to methanol. Additionally, it is possible to use bacteria that produce methanol directly.

"Water–Gas Shift" Reaction

It is a well-known fact that purple bacteria produce hydrogen under anaerobic conditions. In 1976, Uffen cultivated bacteria called *Rodopseudomonas sp.* that produce hydrogen and CO_2 from CO and water in darkness using complex organic media [328]. Later, *Rubirivivax gelatinosus* was discovered to not require complex media and be applicable in hollow-fibre batch reactors. The generated hydrogen is CO-free and could be used in fuel cells directly [329]. The CO for this reaction can be produced by methanogenic bacteria, by which the methane is photocatalytically oxidised to CO [330]. However, methane is directly used or for methanol synthesis (steam reforming), so this process will only be adopted in niche applications where CO is formed as an exhaust gas.

Fermentation

Some bacteria produce hydrogen with organic substrates in anaerobic environment:

$$[CH_2O]_n \rightarrow \text{ferredoxin} \rightarrow \text{hydrogenase} \rightarrow H_2 \tag{4.71}$$

This is a generally well-known process by which the fermentation to hydrogen can also be transferred on existing facilities. Compared to purple bacteria, the hydrogen is generated from an organic substrate, which is in competition with the direct methanol fermentation.

Photosynthesis

The usage of cyanobacteria or green algae for hydrogen generation is a promising objective because it is the biological variant of the photochemical pathway (see Sect. 4.5.3.2). Depending on the microorganism, there are two different reaction schemes (Fig. 4.103):

Because cyanobacteria need a lot of energy to fix nitrogen where hydrogen is only produced as a byproduct, it is necessary to keep down the nitrogen concentration. Green algae only produce hydrogen for a short time in an anaerobic environment because their hydrogenase is very sensitive to oxygen [329].

Table 4.50 Summary of the discussed technologies for water splitting by renewable energy

Technology	Pro	Contra
Alkaline electrolysis	High conversion efficiency, long lifetime, easy setup, universally usable, proven technology, available for large plants	Insufficient partial load behaviour
Proton-exchange membrane electrolysis	High conversion efficiency, good partial load behaviour, universally usable	High investment costs, only available for small plants, low lifetime
High-temperature electrolysis	Decrease of electricity with usage of heat	High requirements for materials, still under research
Photochemical	Easy setup	Separation of hydrogen and oxygen needed, low conversion efficiency (<1 %) and lifetime [326], still under research
Thermochemical	Usable as a hybrid technology with electrolysis, high conversion efficiency of sunlight	Still under research
Piezo/	pyroelectrochemical	Use of vibration and waste heat
Still under research		
Biological	Easy setup	Low production rates, high need for research, concurrence with biomass gasification and methanol fermentation

4.5.3.5 Conclusion

The advantages and drawbacks of the technologies discussed in this chapter are summarised in Table 4.50. Because recent research in LTEL technologies resulted in rather low optimisation steps, thermochemical and thermoelectrochemical technologies appear to be highly promising for further developments.

4.6 The Catalysis of Methanol Synthesis

Friedrich Schmidt[1], Norbert Ringer[2] and Ludolf Plass[3]

[1]*Angerbachstrasse 28, 83024 Rosenheim, Germany*

[2]*Clariant Products Germany GmbH, Ottostraße 3, 80333 Munich, Germany*

[3]*Parkstraße 11, 61476 Kronberg, Germany*

4.6.1 Catalysts for the Synthesis of Methanol

Basically, there are three requirements for catalyst performance:

- Activity
- Selectivity
- Stability.

Numerous variables in the production of methanol synthesis catalysts influence the performance.

Catalysts for High-pressure Methanol Synthesis

Since the beginning of the industrial methanol synthesis in the 1920s, methanol was produced from synthesis gas by operating at 25–35 MPa and 300–450 °C using a catalyst system consisting of zinc oxide stabilised by chromium oxide although a more active Cu-based catalyst was known already at that time [331, 332]. The reason was that the zinc oxide/chromium oxide catalyst was much more stable for the sulphur and chlorine compounds present in synthesis gas at that time [333–337] than was the copper catalyst. In the 1950s, synthesis gas with higher purity was available, so the production of methanol using zinc oxide/chromium oxide catalysts in a high-pressure process was replaced by a new generation of copper-containing catalysts with higher activity, better selectivity and hence better economy. For a detailed discussion of high-pressure methanol synthesis catalysts, see Hoppener et al. [336].

Catalysts for Low-pressure Methanol Synthesis

All catalysts for low-temperature methanol synthesis are based on copper composites, mainly copper, zinc and aluminium phases. Alternative Cu-based catalyst systems can be obtained by Al leaching from Cu/Al alloys, yielding Raney-Cu catalysts with high surface areas [338–343]. Other catalyst systems, which were developed starting in the 1980s, are based on noble metals [344]. Already in 1928, the first catalyst for methanol synthesis based on palladium was claimed [345]. However, until today, none of the new noble metal combinations published gained industrial attention. Due to the significantly higher catalyst costs without improvements in the overall performance, the use of these catalyst systems in commercial methanol production plants is unattractive.

Experimental and theoretical studies on model catalysts of both single-crystal and polycrystalline Cu have demonstrated methanol synthesis over pure Cu using CO_2 and H_2 as reagents (see Ref. [346] and references therein), but the relevance of model studies for the performance of commercial catalysts is limited. Supported noble metal, in particular Pd-based catalysts, have also been developed. Yet, a completely different family of catalysts based on alkali metal-promoted MoS_2 was found to be active for methanol synthesis, although their selectivity for other alcohols is substantial. Their application for the synthesis of higher alcohols is as attractive as alkali-promoted copper/zinc systems.

The low-pressure catalysts for industrial production of methanol from synthesis gas were pioneered by ICI in 1966, who discovered a method of preparing sufficiently stable Cu catalysts. This copper oxide/zinc oxide catalyst was thermally stabilised with alumina. It was used to convert synthesis gas to methanol [347].

For the application of this catalyst, the synthesis gas has to be essentially free of sulphur and chlorine compounds ($H_2S < 0.1$ ppm). Besides the performance and thereby commercial benefits of the new catalyst system, the breakthrough for the use of this catalyst system was induced by the new purification systems and the new reforming technologies that were developed at the same time and fulfilled the required feed purity.

The methanol synthesis using this extremely active catalyst system could be carried out at 220–230 °C and 5 MPa, thus avoiding aging caused by sintering of copper at high reaction temperatures. The high selectivity of the new catalyst provided a methanol purity of >99.5 %. In addition, due to the low operating temperature of the new process, the formation of byproducts (e.g. dimethyl ether, higher alcohols, carbonyl compounds and methane) was significantly reduced.

Production of Catalysts for the Low-pressure Synthesis of Methanol

Industrial Cu/ZnO-based catalysts used in low-pressure methanol (LPM) synthesis plants are prepared by a co-precipitation method with Cu-rich molar compositions of Cu/Zn near 70/30 [348]. Copper-zinc-aluminium phases are obtained as metal hydroxycarbonates or nitrates by coprecipitation of aqueous metal salt solutions (e.g. nitrates), usually at constant pH, with an alkaline solution containing sodium carbonate and/or aluminate. During the precipitation process at constant p_H, temperature is controlled. This is followed by a controlled aging procedure. In the case of binary Cu/ZnO catalysts, this procedure has a strong impact on the activity of the resulting Cu/ZnO catalysts [349–352]. The superior activity of Cu/ZnO catalysts obtained from precipitates aged for more than 30 min was shown to correlate with the increasing microstrain in the copper nanoparticles [353]. The microstain could also be observed in the ternary system.

The quality of the final ternary Cu/ZnO/Al catalyst is determined by the optimum composition of the metal components, the precipitation temperature, the pH used for precipitation, aging time, aging temperature and the sequence of metal salt additions.

The precipitated and aged catalyst precursors (largely metal hydroxycarbonates) are filtered off from the mother liquor, washed free of troubling ions (e.g. sodium) and dried at approximately 120 °C. Examples of such hydroxycarbonates are malachite ($Cu_2CO_3(OH)_2$), rosasite ($(Cu,Zn)_2CO_3(OH)_2$ with a copper to zinc ratio of 3:2) [354–356], hydrozincite ($Zn_5(CO_3)_2(OH)_6$) and aurichalcite ($(Zn,Cu)_5(CO_3)_2(OH)_6$)). There are many different preparation procedures [357]. A typical preparation procedure was described by Ladebeck et al. in U.S. Patent 4,535,071, and another procedure was described by Yamagishi et al. [358] After tableting, the basic carbonates are transformed into oxides by endothermic calcination processes [359, 360]. The decomposition temperatures of the precursors range from approximately 250–475 °C [334, 336, 349, 361–363]. After a conventional reduction, porous aggregates of Cu and ZnO nanoparticles (NPs) are formed, plus low amounts of alumina as structural promoter.

Table 4.51 Commercial catalysts for methanol synthesis

Company	Catalyst	Country
Clariant/Süd-Chemie	Megamax 700 and Megamax 800 and Megamax NJ-1	Germany
Johnson Matthey	Katalco Apico 51-9	United Kingdom
Haldor Topsøe	MK 121 and MK 151 Fence	Denmark
Mitsubishi Gas	M5-5, M6	Japan

This type of catalyst is characterised by a high Cu-to-Zn ratio, with >50 mol % Cu (metal base), approximately spherical Cu NPs of a size around 10 nm, and ZnO NPs that are arranged in an alternating fashion to form porous aggregates [364]. These aggregates expose a large Cu surface area of up to approximately 40 $m^2\ g^{-1}$.

Properties

All currently used low-pressure catalysts comprise copper oxide and zinc oxide with one or more stabilising additives (Table 4.51).

Most of today's commercial catalysts are based on the Cu–Zn-Al system and prepared by coprecipitation, with a Cu:Zn atomic ratio in the 2–3 range and minor alumina amounts [365]. In the unreduced form, the MK-121 catalyst from Topsøe contains >55 wt% CuO; 21–25 wt% ZnO, 8–10 wt% Al_2O_3 in the fresh catalyst, graphite, carbonates and moisture balance [366]. Also the Clariant (formerly Süd-Chemie) Megamax series catalysts are reported to be constituted of CuO/ZnO/Al_2O_3 [367]. The most frequently used composition is as defined in U.S. Patent 4,535,071 [368], in which the atomic ratio of copper to zinc lies between 2.8:1 and 3.8:1. Uneven distribution of copper and zinc is claimed, for instance, in WO03053575, in which the Cu/Zn-atomic ratio for the entire catalyst is about 2.3, but in the interior part of the catalyst particle the atomic ratio is 0–2.8 and in the external is 2.9–3.5 [369].

The commercial catalysts usually are shaped into tablets of 6 × 4 mm (e.g. MEGAMAX-800 and MK-121) or alternatively 5.3 × 5.1 mm (Katalco 51-9). The bulk density (i.e., the catalyst mass per volume of oxidic catalyst) is of the order of 1,200 kg/l, but it may also be up to 1,300 kg/l (Katalco 51-9). Before use, the oxidic catalyst has to be reduced (generally after loading) by conventional methods.

The increasing diversity of converter types, feedstock and operating conditions of today's methanol production industry has caused the need for tailor-made catalysts. However, due to the high commercial risk of the megascale of methanol production, tailor-made catalysts are still in the development stage.

The Active Site

The question of why catalysts containing copper, zinc and aluminium ions are superior to other compositions has been answered but is still very controversial. Also, the nature of the active site on Cu/ZnO-based catalysts is still not comprehensively understood. A review of literature, written mostly by authors from

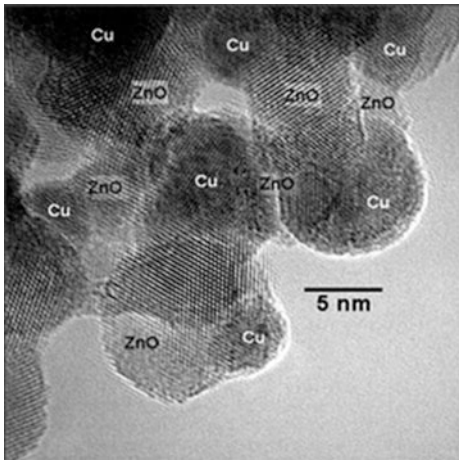

Fig. 4.104 High-resolution transmission electron microscope image of a conventionally prepared Cu/Zn/Al catalyst

Denmark or Japan, has been given by Hansen and Højlund Nielsen [370]. Other articles are cited in a publication by Behrens et al. [371]. The authors have shown how to identify the crucial atomic structure motif for the industrial $Cu/ZnO/Al_2O_3$ methanol synthesis catalyst by using a combination of experimental evidence from bulk, surface-sensitive and imaging methods collected on real high-performance catalytic systems in combination with density functional theory calculations. Figure 4.104 shows a high-resolution transmission electron micrograph of a selected area of a conventional catalyst analysed by the Behrens group. According to the team of authors, the active site consists of Cu steps decorated with Zn atoms, all stabilised by a series of well-defined bulk defects and surface species that need to be present jointly for the system to work.

The chemistry of the Cu/ZnO catalyst previously studied in simple model systems, such as in the form of accurately gauged copper islands on a completely flat surface of zinc oxide, is completely different from a catalyst used in chemical reactors in industry. The industrial catalyst presents a sponge-like conglomeration of innumerable beads that are just 10-nm in size, which sometimes consist of copper and zinc with a small amount of alumina. Until a few years ago, the state of knowledge was that the actual reaction takes place exclusively on copper. In addition, chemists assumed that they need to only give the copper a great surface to increase its activity. The zinc oxide was believed for to play only the role of a spacer that prevents the copper particles under reaction conditions to agglomerate into larger spheres with relatively small surface areas.

With a high-resolution transmission electron microscope, individual copper and zinc atoms could be detected inside a small section of the conglomerate. It is known that the catalyst works properly only when containing lattice defects. Small defects in the crystal lattice of the copper particles manifest themselves as kinks on the surface, valleys and peaks. Just these defects bind the reactants and the intermediates of the methanol synthesis in an optimal way to finally yield

methanol. However, an analysis of the individual atoms of the copper–zinc oxide sponge confirmed an assumption that was occasionally published: the zinc oxide is not only located in nanoparticles of the stabiliser phase, which separated the copper particles from each other, but it also crawls on top of some of the copper particles, forming a disordered deposit of a few atomic layers. Individual zinc atoms may even migrate into the copper lattice. As the calculations have shown, the oxygen-containing intermediates of the reaction to methanol are bound on the zinc atoms better than on the copper atoms. Because of this higher stability of the intermediates, they are formed more frequently. Hence, the catalyst performs better, because the energetic hurdle from the intermediate products back to the starting molecules has become higher than to the final product.

All catalysts containing copper, zinc and alumina phases differ only slightly in terms of overall technical performance. However, in megamethanol plants, minor differences in terms of technical performance translate into multimillion differences in terms of value.

4.6.2 Methanol from Synthesis Gas

4.6.2.1 Chemistry of Methanol Synthesis

Stoichiometry

The reactions that are involved in the production of methanol from various synthesis gases are as follows:

$$CO + 2H_2 \rightleftharpoons CH_3OH \qquad \Delta H_{R(298K,50bar)} = -90.7\,\text{kJ/mol} \qquad (4.72)$$

$$CO_2 + 3H_2 \rightleftharpoons CH_3OH + H_2O \qquad \Delta H_{R(298K,50bar)} = -40.9\,\text{kJ/mol} \qquad (4.73)$$

The synthesis of methanol from carbon monoxide and carbon dioxide are tied through the WGS reaction:

$$CO + H_2O \rightleftharpoons CO_2 + H_2 \qquad \Delta H_{R(298K,50bar)} = -42\,\text{kJ/mol} \qquad (4.74)$$

The reaction enthalpy $\Delta H_{R(298k,\ 50bar)}$ [372] refers to 298 K and 50 bar, whereas the standard enthalpy of reaction (denoted $\Delta_R H^-$) is the enthalpy change that occurs in a system when 1 mol of matter is transformed by a chemical reaction under standard conditions. Reactions 4.72 and 4.73 are exothermic and are accompanied by a decrease in volume. Reaction 4.74 in its forward direction is mildly exothermic. In principle, the methanol formation is therefore favoured by increasing pressure and decreasing temperature, with the maximum conversion being determined by the equilibrium composition.

Component Balance

$$\Delta n_{\mathrm{MeOH}} = -\Delta n_{\mathrm{CO}} - \Delta n_{\mathrm{CO_2}} \tag{4.75}$$

$$\Delta n_{\mathrm{H_2O}} = -\Delta n_{\mathrm{CO_2}} \tag{4.76}$$

$$\Delta n_{\mathrm{H_2}} = 2\Delta n_{\mathrm{CO}} + 3\Delta n_{\mathrm{CO_2}} \tag{4.77}$$

$$\Delta n_{\mathrm{Inerts}} = 0 \tag{4.78}$$

$$\mathrm{X_{CO}} = \Delta n_{\mathrm{CO}}/n_{\mathrm{CO},0} \Rightarrow \Delta n_{\mathrm{CO}} = \mathrm{X_{CO}} \cdot n_{\mathrm{CO},0} \tag{4.79}$$

$$\mathrm{X_{CO_2}} = \Delta n_{\mathrm{CO_2}}/n_{\mathrm{CO_2},0} \Rightarrow \Delta n_{\mathrm{CO_2}} = \mathrm{X_{CO_2}} \cdot n_{\mathrm{CO_2},0} \tag{4.80}$$

$$\Rightarrow \Delta \mathrm{n_{H_2}} = 2\mathrm{X_{CO}} \cdot \mathrm{n_{CO,0}} + 3\mathrm{X_{CO_2}} \cdot \mathrm{n_{CO_2,0}} \tag{4.81}$$

Real feeds do not contain only CO and H_2. One way to account for the WGS reaction in Eq. 4.74 is to define a stoichiometric number SN as

$$\mathrm{SN} = (\mathrm{mol\ H_2} - \mathrm{mol\ CO_2})/(\mathrm{mol\ CO} + \mathrm{mol\ CO_2}) \tag{4.82}$$

The stoichiometric number (SN) of the synthesis gas required for methanol synthesis should be 2.0, which is different from the molar ratio H_2/CO. However, a small increment in hydrogen that increases the SN to 2.05 and even to 2.08 has been found to improve catalytic performance, leading to more efficient production of methanol [373] (see also Sects. 4.3.2.4 and 4.3.6.1). Generally, the syngas produced from different sources covers an array of feed gas compositions (CO-free, CO-rich, or hydrogen-rich syngas), and consequently the stoichiometric value has to be adjusted by the WGS reaction. The synthesis gas from gasification (e.g. of coal) is rich in CO. The optimum syngas composition can be reached by a partial conversion of CO by high-temperature WGS followed by the removal of CO_2 or by addition of H_2 from synthesis purge gas. Because the rate of the methanol synthesis reaction can be improved by additional CO_2 in the synthesis gas, the balancing of the stoichiometry of the makeup gas (MUG) can improve the performance of the methanol production and selectivity.

Thermodynamics

Equilibrium Constant

If Eqs. (4.72) and (4.74) are regarded as independent reaction routes, the conversion of carbon dioxide to methanol (Eq. 4.73) is the overall result of Eqs. (4.72) and (4.74). Then the equilibrium constant K_2 can be described as $K_2 = K_1 \cdot K_3$. Furthermore, when the nonideal behaviour of gases under reaction conditions is taken into account, the equilibrium constants may be recorded as follows:

$$K_1 = \left[\frac{f_{\mathrm{CH_3OH}}}{f_{\mathrm{CO}} f_{\mathrm{H_2}}^2}\right] = \left[\frac{\varphi_{\mathrm{CH_3OH}}}{\varphi_{\mathrm{CO}} \varphi_{\mathrm{H_2}}^2}\right] \left[\frac{p_{\mathrm{CH_3OH}}}{p_{\mathrm{CO}} p_{\mathrm{H_2}}^2}\right] = K_{\varphi 1} \cdot K_{p1} \tag{4.83}$$

$$K_3 = \left[\frac{f_{CO} f_{H_2O}}{f_{CO_2} f_{H_2}}\right] = \left[\frac{\varphi_{CO} \varphi_{H_2O}}{\varphi_{CO_2} \varphi_{H_2}}\right] \left[\frac{p_{CO} p_{H_2O}}{p_{CO_2} p_{H_2}}\right] = K_{\varphi 3} \cdot K_{p3} \tag{4.84}$$

where f_i is the fugacity, φ_i the fugacity coefficient and p_i the partial pressure of the ith component.

Influence of Temperature

Many numerical formulations have been applied for calculating the temperature-dependent equilibrium constants K_1 and K_3. In general, the results do not match. Hansen and Højlund Nielsen [370] summarised the state of the discussion. For high temperatures, the equilibrium of the methanol formation reactions is restrictive and the reverse water–gas shift (RWGS) reaction is governing the product distribution, indicated by a net CO formation from CO_2.

For ideal gas behaviour, the temperature dependence of the equilibrium constants can be calculated by the following correlations [374]:

$$K_1(T) = 9.740 \times 10^{-5} \cdot \exp\left(21.225 + \frac{9{,}143.6}{T} - 7.492 \cdot \ln(T) + 4.076 \times 10^{-3} \cdot T - 7{,}161 \times 10^{-8} \cdot T^2\right) \tag{4.85}$$

for the reaction $CO + 2H_2 \rightleftharpoons CH_3OH$ and

$$K_3(T) = \exp\left(-13.148 - \frac{5{,}639.5}{T} - 1.077 \cdot \ln(T) + 5.44 \times 10^{-4} \cdot T + 1{,}125 \times 10^{-7} \cdot T^2 + \frac{49{,}170}{T^2}\right) \tag{4.86}$$

for the reaction $CO + H_2O \rightleftharpoons CO_2 + H_2$ with: T [K]; p [Pa].

For real gases (gas phase reactions at a reaction pressure over 10 bar), the above-mentioned correlations must be corrected by the means of fugacity coefficients of each individual component. The fugacity coefficients can be obtained by different approaches [375–377].

For the calculation of the equilibrium conversions, the equation of state model of Soave–Redlich–Kwong (SRK) frequently is used [376, 378], where also the interaction of the components in the gas mixture is taken into consideration (mixing rules).

A number of numerical formulations exist for calculating the temperature-dependent equilibrium constants K_1 [379–386] and K_3, [384, 385, 387]; their results differ widely [379]. A standard model widely used for process simulations was given by Graaf et al. in [384].

$$\log K_1 = \left(\frac{5{,}139}{T}\right) - 12{,}621 \tag{4.87}$$

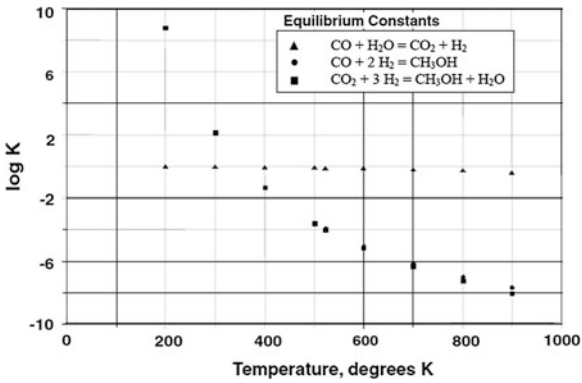

Fig. 4.105 Temperature dependence of equilibrium constants for principal reactions [388]

$$\log K_1 = \left(\frac{3{,}066}{T}\right) - 10{,}592 \tag{4.88}$$

$$\log K_1 = \left(\frac{-2{,}073}{T}\right) + 2{,}020 \tag{4.89}$$

As previously mentioned, the reactions 4.72 and 4.73 are exothermic and accompanied by a decrease in volume. Methanol formation is therefore favoured by increasing pressure and decreasing temperature. However, at lower temperatures the rates of the reactions are lower, which requires relatively high temperatures. Unfortunately, this leads to even higher pressure requirements. However, operating at higher pressure involves higher capital investment, greater energy demands, and more severe operational conditions. Additionally, at higher temperatures the catalyst requires higher thermal stability towards deactivation. For all these reasons, the once-through conversion (or single-pass conversion) of the synthesis reaction is kept low. Therefore, the recycle ratio needs to be higher. By recycling the unconverted syngas back to the methanol converter, the overall conversion and hence the process economics can be improved. Typical commercial operating conditions are 220–270 °C and 50–100 bar, which is close to critical point of pure methanol (i.e., approximately 240 °C and 80 atm).

The temperature dependence of equilibrium constants for principal reactions is shown in Fig. 4.105 [388].

The WGS reaction (Eq. 4.74) plays an important role in all processes in which a synthesis gas is involved. This is partly due to the fact that the equilibrium of the WGS reaction in the range of 20–1,000 °C, compared to the other synthesis gas reactions, is only slightly dependent on the temperature. Moreover, because the values of equilibrium constants in the large temperature range considered are relatively low, the reaction can easily proceed in the reverse direction by only small changes in the composition or partial pressure of the species involved. Furthermore, because typical WGS reaction catalysts have a very similar composition to the methanol synthesis catalysts, the latter also catalyse the WGS

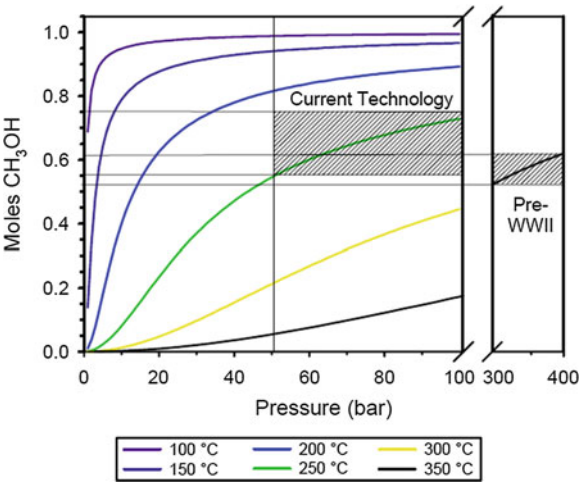

Fig. 4.106 Thermodynamic equilibria for methanol synthesis from syngas $2H_2 + CO = CH_3OH$. © Sandia [392]

reaction. The WGS equilibrium "can be very easily reversed in terms of its direction by the concentration of water in the reactor feed stream. Even 5 mol % of water in the feed syngas stream of $H_2/CO = 3{:}1$ is more than sufficient to affect the direction of WGS reaction at 250 °C and 75 atm. Under this specific circumstance, the WGS reaction proceeds in the forward direction. In the case of H_2O-free feed, otherwise under nominally the same condition, the WGS reaction proceeds in the reverse direction [388]." Because of the reversibility of the WGS reaction (RWGS) over a wide range of process conditions and hence the impact of the WGS on the resulting product compositions, the WGS reaction equilibrium is an important problem in designing steam reformer, methanol reformer, as well as methanol synthesis reactors and reactors for the formation of dimethyl ether (DME) from synthesis gas or from methanol [388].

In practice, per-pass conversions for methanol from syngas are significantly less than theoretical. Reported conversions range anywhere from only 15–25 % [389] to as high as 40 % [390] or 50 % (with advanced catalysts) [391]. One limiting factor is the exothermicity of the reaction, which drives a temperature increase. The temperature increase suppresses the potential conversion, but conversion may also be intentionally limited to minimise the increase.

Influence of Pressure

From Eq. 4.74, it can be concluded that if the pressure of the reaction is increased, the conversion of CO also increases; however, the increase is not very substantial above a pressure of 80 atm. For instance, in Fig. 4.105, the equilibrium yields from 2:1 H_2:CO mixtures are shown as a function of temperature and pressure. As indicated in the figure, operating conditions for the current technology are pressures of 50–100 bar and temperatures of approximately 250 °C. These conditions can theoretically result in per-pass methanol yields in the range of 55–75 % [393] (Fig. 4.106).

Kinetics

As discussed by Lim et al. [393] and literature cited therein, it is still unknown whether methanol formation generally proceeds via CO hydrogenation or via CO_2 hydrogenation. Experiments reveal that the presence of CO_2 in high concentrations does not necessarily lead to a lower activity (see Sect. 4.8).

Under industrial process conditions, the reaction is only slightly influenced by internal mass transport. According to Seyfert et al., the effectivity factor is between 1 and 0.65 for 538–518 °K at 80 bar [394]. Lommerts et al. showed that the rather simple Thiele modulus approach is sufficient to estimate the influence of mass transport on the overall reaction rate [395].

Graaf et al. [396, 397] developed a kinetic model considering both CO and CO_2 hydrogenation as well as the WGS reaction (Eqs. 4.72–4.74). This model is based on the Langmuir–Hinshelwood-mechanism and the kinetic equations of the elementary steps of each reaction. They ended up with 48 possible reaction schemes. By this model, a wide range of experimental conditions can predict the methanol process performance with sufficient accuracy.

Space–Time Yield

The space–time yield (STY) of a reaction vessel (reactor) is the amount of a product formed in a reactor of a certain volume (space) and in a particular time, expressed for example in *t* of product per cubic metre per year or kilograms per litre per second (1 metric tonne = 2,204.6 lb). The expression is used only in terms of continuous reactors. In heterogeneously catalysed reactions, the term STY is either based on the volume (STY) of a catalyst or on the mass of a catalyst (weight-time yield), such as kilogram of product formed per kilogram of catalyst per hour [398].

Space–Time Yield

$$\mathrm{STY} = \frac{m[t]\text{product}}{V[m^3]\text{catalyst} \cdot t[h]\text{time on stream}} = \frac{\dot{m}_p[t \cdot h^{-1}]}{V_{\mathrm{cat}}} = \frac{\dot{n}_p M_p}{V_{\mathrm{cat}}} \tag{4.90}$$

$$\mathrm{SV} = \frac{\dot{V}_N}{V_{\mathrm{cat}}} = \frac{\text{reactorinlet gas } [\mathrm{Nm}^3 \times \mathrm{h}^{-1}]}{V \text{ catalyst } [\mathrm{m}^3]} \tag{4.91}$$

$$\dot{n}_p = \dot{n}_{\mathrm{MeOH}} = \Delta\dot{n}_{\mathrm{CO}} + \Delta\dot{n}_{\mathrm{CO_2}} mit \cdot \dot{n}_{\mathrm{MeOH},0} = 0 \tag{4.92}$$

MeOH Space–Time Yield

$$\mathrm{STY}_{\mathrm{MeOH}} = \frac{1}{V_{\mathrm{cat}}} \cdot \left(X_{\mathrm{CO}} \dot{n}_{\mathrm{CO},0} + X_{\mathrm{CO_2}} \dot{n}_{\mathrm{CO_2},0}\right) \cdot M_{\mathrm{MeOH}} \tag{4.93}$$

$$\mathrm{STY_{MeOH}} = \frac{p_N \cdot \dot{V}_N \cdot M_{\mathrm{MeOH}}}{RT_N} \cdot \frac{1}{V_{\mathrm{cat}}} \cdot \left(X_{\mathrm{CO}} y_{\mathrm{CO},0} + X_{\mathrm{CO_2}} y_{\mathrm{CO_2},0}\right) \tag{4.94}$$

with:

M_{MeOH}	32.042×10^3 kg/mol
p_N	1.013×10^5 Pa
T_N	273.13 K
R	8.314 J/mol K

$$\mathrm{STY_{MeOH}} = 1.429 \cdot 10^{-3} \cdot \mathrm{SV} \cdot \left(X_{\mathrm{CO}} y_{\mathrm{CO},0} + X_{\mathrm{CO_2}} y_{\mathrm{CO_2},0}\right) \tag{4.95}$$

In laboratory experiments, the volume of the catalyst V_{Kat} is usually determined from the measured mass by means of the bulk density, with both referring to the oxidic material. The commercial catalysts are supplied by volume; however, depending on the specific catalyst supplied, the catalyst may exhibit different bulk densities—also but not only due to different tablet sizes. When comparing different catalysts with respect to their performance, the volume of the working catalyst has to be considered, particularly when prereduced and oxidic material is compared. Due to the shrinking during the reduction of the oxidic catalyst prior to be contacted to synthesis gas, the volume of the operating catalyst differs from the volume of the oxidic catalyst. Normalisation to weight-time yield is necessary to compare different catalysts with respect to their performance. In this case, the calculated weight of the water formed upon reduction can be taken into account. An even more meaningful normalisation is to relate the performance to the number of moles of copper present in the reactor.

4.6.2.2 Byproduct Formation

With all commercially available $Cu/ZnO/Al_2O_3$ catalysts for LPM synthesis, methanol is produced with selectivity (referred to the CO_x in the feed), typically above 99 %. According to the possible direct CO hydrogenation reactions [399] shown in Table 4.52, traces of several byproducts cannot be avoided. This is remarkable because all of the byproducts normally found, except formaldehyde and formic acid, are thermodynamically much more favoured products than methanol. This fact elucidates the importance of the particular physical, chemical and topological catalyst properties. All of the previously described reactions are of an exothermic nature and are equilibrium reactions. The direct hydrogenation reactions have different values of the rate-limiting free energy of activation, resulting in different reaction rates at the same temperature and pressure. Because catalysts influence the free energy of activation, it is obvious that the preferred reaction path can be influenced by choosing the right catalyst.

Other byproducts are ethers (mainly DME) [400, 401] and ketones [402]. Dimethyl ether formation is greatly inhibited by the presence of water. Ketones are present in very small amounts in crude methanol. Catalyst impurities such as alkali

Table 4.52 Byproducts through direct CO hydrogenation reactions

	Ratio of CO:H_2	Loss (%) as H_2O
$CO + 2H_2 \rightarrow$ methanol	1:2	–
$2CO + 2H_2 \rightarrow$ acetic acid	1:1	–
$2CO + 2H_2 \rightarrow$ methyl formate	1: 1	–
$2CO + 4H_2 \rightarrow$ ethanol	1:2	28
$3CO + 6H_2 \rightarrow$ propanol	1:2	38
$2CO + 3H_2 \rightarrow$ ethylene glycol	2:3	–
$4CO + 8H_2 \rightarrow$ isobutanol	1:2	50
$2CO + 4H_2 \rightarrow$ ethylene	1:2	56
$16CO + 33H_2 \rightarrow$ n-hexadecane, representative for Fischer–Tropsch	1:1.2	56

(higher alcohols), iron, cobalt and nickel (via typical Fischer–Tropsch reactions) can boost the byproduct formation. If the alumina component of the catalyst is too acidic, methanol can further react to form DME. Furthermore, because all commercial catalysts contain minor residual amounts of alkali, the formation of higher alcohol is possible. According to Hansen [403], when using conventional catalysts for the synthesis of methanol, higher alcohols are formed, preferably in CO-rich synthesis gas compared to CO_2-rich synthesis gas: 1,200–1,400 ppm ethanol versus 150–300 ppm ethanol in CO_2-rich syngases [403].

According to Eq. 4.4.14-16, the methanation is another possible reaction, but it needs a completely different catalyst. Methane is not a byproduct.

$$CO + 3H_2 \rightleftharpoons CH_4 + H_2O \qquad \Delta H^\circ = -205\,\text{kJ/mol} \tag{4.96}$$

4.6.2.3 Catalyst Deactivation

All structural properties of methanol synthesis catalysts, particularly the physical and chemical environment of the active sites, are crucial for the performance of the catalyst during the entire catalyst service life. However, these structural properties are significantly influenced and changed by the process conditions [404–406].

Poisoning

The primary deactivation mechanism for methanol synthesis catalyst is poisoning by trace levels of sulphur and chlorides in the feed gas because all methanol synthesis catalysts are copper based. Any constituent in the feed gas that reacts with copper acts as a poison. Sections 4.3 and 4.4 described how to avoid poisoning of a copper catalyst. Here, only a brief summary is given.

The sulphur content in the synthesis gas (or nitrogen circulation) should be less than 0.05 ppmv as H_2S. Sulphur that exceeds 0.8 wt% on the catalyst deactivates the catalyst completely. Chlorine in any form, such as Cl_2, HCl, or R-Cl, is a

strong poison to the methanol synthesis catalyst. Copper chloride sinters quickly, which reduces active copper surface area of the catalyst. Chlorine should be excluded completely from the system. The chlorine content in the synthesis gas should be at a nondetectable level. Chlorides that are more than 500 ppmw on the catalyst deactivate the catalyst completely.

In addition, solid particles, such as dust in the feed and trace metals physically block the catalyst surface and lead to premature deactivation of the catalyst. If iron in the form of iron carbonyls is carried onto the methanol synthesis catalyst, this catalyses the Fischer–Tropsch reaction and consequently byproduct formation increases. Iron and other heavy metals also block the active sites of the catalyst, thus reducing activity. Nickel has a similar deleterious effect on the catalyst performance. Any carryover of lubricating oil should be avoided because it is well known that these heavy hydrocarbons have a deactivating effect on methanol synthesis catalysts.

Steaming of methanol synthesis catalyst must be avoided because it leads to an accelerated growth of copper crystals and deactivates the catalyst prematurely. In CO_2-rich synthesis gases, the deactivation is caused by water, formed via the reversed WGS reaction. The higher water partial pressure destroys the matrix of the catalyst, which allows the copper crystallites to sinter more rapidly.

Oxygen can also be considered as poison because contact of oxygen with the reduced catalyst leads to partial re-oxidation followed by subsequent reduction by the process gas. These redox reactions affect the structure of the catalyst and lead to premature loss in crushing strength and rapid increase in pressure drop. This can also lead to thermal sintering, with the consequence of loss in active copper surface area.

Thermal Damage

To a lesser extent, the catalyst is also deactivated by changes in the copper crystals caused by thermal stress. Sintering results in the formation of larger copper crystallites. Even in the absence of poisons, methanol synthesis catalysts undergo relatively fast deactivation. More than one-third of the activity is lost during the first 1,000 h of operation [403, 405]. In particular, the high temperature sensitivity of the catalyst requires controlled conditions during reduction as well as during operation in order to avoid changes of the active site or accelerated sintering of the copper particles. The sintering process has been reviewed by Hansen and Højlund Nielsen [370]. The overall catalyst lifetime of an industrial catalyst for the methanol synthesis is found in practice to be at least 4 years, but was claimed to approach even 8 years [407]. The catalyst lifetime considerably influences the operational costs of a methanol plant.

Deactivation studies of a methanol synthesis catalyst under industrial conditions were published by Løvik [408] and by Rahimpour et al. [409].

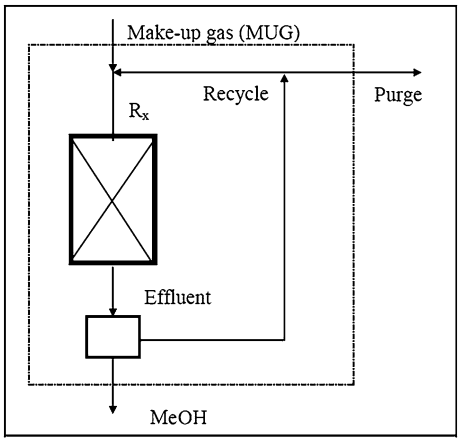

Fig. 4.107 Methanol loop [411]

4.6.3 Makeup Gas

In commercial processes, the unconverted syngas is recycled back to the methanol converter for enhancing the overall conversion, thereby improving the process economics [410]. The synthesis loop for the methanol synthesis is shown in Fig. 4.107.

The loop balance is given by the following with MUG being makeup gas:

$$\text{Recycle ratio: } \Phi = \frac{\text{recycle}}{\text{MUG}}$$

$$R_x = MUG + \text{recycle} \rightarrow \text{recycle} = R_x - MUG$$

$$\text{Flows: } \Phi = \frac{R_x - \text{MUG}}{\text{MUG}} = \frac{R_x}{\text{MUG}} - 1$$

$$\text{or: } \Phi + 1 = \frac{R_x}{\text{MUG}}$$

The concentrations for component i can be described as follows, demonstrating concentrations of component i in the MUG:

$$R_x \cdot y_{R_x} = \text{MUG} \cdot y_{\text{MUG}} + \text{recycle} \cdot y_{\text{purge}} \qquad \text{with: } y_{\text{recycle}} = y_{\text{purge}}$$

$$\frac{R_x}{\text{MUG}} \cdot y_{R_x} = 1 \cdot y_{\text{MUG}} + \Phi \cdot y_{i,\text{purge}}$$

$$\rightarrow \Phi_i = \frac{y_{i,\text{MUG}} - y_{i,R_x}}{y_{i,R_x} - y_{i,\text{purge}}} \qquad \text{respectively } y_{i,R_x} = \frac{y_{i,\text{MUG}} + \Phi \cdot y_{i,\text{purge}}}{\Phi + 1}$$

Table 4.53 Specific makeup gas consumption for different synthesis gas processes

Process	Makeup gas consumption (kmol/10^6 t)
Gasification (residual oil)	95–105
Combined reforming	110–120
Steam reforming with CO_2 addition	120–130
Steam reforming without CO_2 addition	140–150

The MUG analysis composition depends on the synthesis gas generation technology. MUG can be characterised by its stoichiometry number SN, which is defined as $(H_2 - CO_2)/(CO + CO_2)$.

Most of the worldwide methanol production is based on synthesis gas generated from steam reforming of natural gas or naphtha. Depending on the reforming process, there is a wide variety of MUG compositions with varying stoichiometric numbers (SN's). To adjust the SN of a steam-reforming process gas, CO_2 can be added. The addition of CO_2 decreases the byproduct formation across the catalyst and the amount of MUG needed per tonne of production due to a better SN (see Sect. 4.3).

The addition of carbon dioxide can reduce the SN of the MUG gas to the optimum level of 2.04–2.06, resulting in significantly more methanol production for each unit of MUG fed to the loop. A disadvantage of this type of operation is the additional amount of water that is produced. This water can have an effect on the methanol synthesis catalyst. The distillation system has to be able to handle the additional water if carbon dioxide is added to the reformer effluent. Development of newer methanol synthesis catalysts, such as Süd-Chemie's C79-5GL and Clariant's (formerly Süd-Chemie AG) Megamax series, has minimised the effect of the additional water on catalyst performance. A source of carbon dioxide also has to be available. The quantity needed in a large methanol plant usually means that the plant has to be located adjacent to or near one or more large ammonia plants [410, 412]. The MUG produced by the Lurgi combined reforming process (tubular steam methane reformer combined with oxygen-blown ATR) results directly in the optimum SN of 2.05. Typical synthesis gas compositions from steam reforming are shown in Table 4.53.

POX of natural gas, heavy residual oil, or coal results in an MUG that is very rich in CO but contains little CO_2 and inert gases. It is necessary to treat such a process gas with CO shift conversion followed by CO_2 removal and a sophisticated cleanup system to adjust the SN and to remove the relatively high amounts of sulphur and heavy metals in the feedstock (see Sects. 4.3 and 4.4). Independent of the loop design, the MUG composition determines the specific MUG consumption. MUG is a measure of the plant efficiency and also affects byproduct formation in the loop.

Specific MUG consumption is defined as the kilomole (kmole) of MUG per metric tonne of methanol in the crude methanol. The lowest specific MUG consumption is obtained with the optimum SN of 2.05 and the lowest inert level in the synthesis gas (i.e., using gasification gas). The highest specific MUG consumption usually results in the case of steam reforming of natural gas without CO_2 addition. Such a synthesis gas is hydrogen rich with a SN close to 3.0, which is quite high for efficient methanol production.

4.7 Commercial Methanol Synthesis from Syngas

Veronika Gronemann[1], Ludolf Plass[2] and Friedrich Schmidt[3]

[1]*Air Liquide Global E&C Solutions c/o Lurgi GmbH, Lurgiallee 5, 60439 Frankfurt, Germany*
[2]*Parkstraße 11, 61476 Kronberg, Germany*
[3]*Angerbachstrasse 28, 83024 Rosenheim, Germany*

4.7.1 Introduction

Imperial Chemical Industries (ICI) first introduced the LPM (low pressure methanol) process in 1966. The LPM Process revolutionised the industrial methanol production process. As a result, the worldwide size of commercial methanol plants increased rapidly over the succeeding 30–35 years, and the capacities are still going up.

This chapter discusses the following topics:

(a) Conventional commercial processes for LPM synthesis, typically less than 3,000 tpd methanol generation capacity
(b) Large-scale plant designs, including mega- and giga-methanol plants, exceeding 5,000 tpd methanol generation capacity
(c) Reactor systems for large-scale plants
(d) Methanol distillation
(e) Unconventional methanol synthesis on a semicommercial scale.

In topics (a) to (c), syngas generation and the methanol synthesis loop are discussed together because they are integrated systems.

Methanol plants based on natural gas as feedstock consist essentially of three process sections:

- Synthesis gas generation
- Methanol synthesis
- Methanol distillation.

It is not the intention of this chapter to discuss all methanol generation processes. Methanol technology licensors typically have varying designs; here, the best known

and most important in commercial use have been selected. The methanol synthesis reaction itself is described in Sect. 4.6. If fossil and renewable feedstocks need special syngas preparation processes, these are explained in Sects. 4.3 and 4.4.

When using natural gas as the feedstock, synthesis gas production including compression and the ASU (air separation unit) typically accounts for about 60 % of the investment. The reforming section consumes most of the energy. Considering the significant investment in large-scale plants of 5,000 tpd and more, there is substantial motivation to maximise single-line capacity, thereby utilising fully the economies of scale (i.e., increasing the economics of a facility with the capacity of the plant built).

As already explained in Sect. 4.6, the SN (which is the ratio $(H_2 - CO_2)/(CO + CO_2)$ and not the molar ratio H_2/CO) of the synthesis gas required for methanol synthesis should be 2.0 to 2.05. The CO-to-CO_2 ratio and the concentration of inerts are other important properties of the synthesis gas. A high CO-to-CO_2 ratio promotes the reaction rate and boosts the achievable per pass conversion [412]. If there are high CO-to-CO_2 ratios in the synthesis gas used for methanol production, the formation of water also will decrease.

The principal synthesis reactions are given in Sect. 4.6. These reactions are highly exothermic and the heat of reaction must instantaneously be removed from the catalyst bed. As the reaction approaches equilibrium conversion, the overall reaction rate is becoming zero (no more net methanol is formed but undesired byproducts are). Therefore, the hot equilibrium reaction gas has to be cooled and partly recycled in order to regain reasonable conversions. This can be accomplished efficiently and economically by different designs of methanol synthesis reactors and recycle loops. The methanol loops of the different technology licensors vary in reactor design and heat integration, resulting in different MUG recycle ratios, typically in the range of 7–9. If a water-cooled reactor (WCR) is used, the recycle rate can be reduced to 3–4 because of the higher heat removal rate. The consequences of changing methanol reaction conditions have been described by Supp [413].

Commercial reactor designs operate according to the following principals:

- Quench reactors (typically adiabatic multibed quench systems)
- Adiabatic reactors in series (typically indirect cooling)
- Boiling water reactors (BWR)
- Gas-cooled reactors (GCR).

A variety of different designs are used in commercial methanol plants (all based on loop designs), as will be more in detail described in Sect. 4.7.2.

Market Share by Methanol Process Technologies

The information in the literature regarding the number of plants licensed by the different technology owners vary substantially. The actual market share is approximately as follows:

The major part of the operating plants is licensed by Lurgi (27 %), Johnson Matthey (JM)/Davy (25 %), Topsøe (16 %) followed by Mitsubishi Gas Chemical Company (MGC), JM/Uhde, JM/Jacobs, JM/Others, JM/Toyo. All technologies are based on highly integrated technology concepts including all steps from gasification and gas cleaning to synthesis and workup. Thus, high energy and carbon efficiencies up to 67 and 83 %, respectively, can be reached (calculated from literature [414]).

JM owns the process and catalyst technology developed by ICI and Synetix [415]. The methanol capacity licensed by JM (formerly ICI) and Davy Process Technology (DPT; for a certain period of time, Kvaerner) amount overall to nearly 70 plants. Since 2004, JM and DPT have combined and boosted the development of their syngas and methanol technologies on an exclusive basis.

4.7.2 Conventional Commercial Methanol Synthesis Processes

Conventional commercial methanol synthesis processes from syngas are those that have a capacity of up to 3,000 tpd of methanol production. With respect to methanol technology, a broad variety of converter designs are offered by various contractors and licensors as described in the following chapters. Different tradeoffs between capitals, capacity, operability, yields and energy consumption are claimed.

4.7.2.1 The Johnson Matthey/Davy Process Technology Low-pressure Methanol Process Design

Figure 4.108 shows a schematic of the JM/DPT process, which was developed from the original LPM process first introduced by ICI in 1966. Methanol plants consist of three principal sections: (1) syngas generation, (2) methanol synthesis and (3) methanol purification. In the first step a hydrocarbon is converted to a mixture of hydrogen, carbon monoxide, and carbon dioxide called syngas by reaction with steam and/or oxygen. It can be generated from natural gas or naphtha via a reforming step or by the gasification of coal, coke, or biomass. The reforming step, also available from this licensor, may be conventional SMR (steam methane reformin), ATR (autothermal reforming) using oxygen, combined reforming (SMR and ATR in series), gas-heated reforming (GHR; more precisely, GHR and ATR in series), or compact reforming (SMR for offshore or remote applications). The methanol synthesis reaction takes place within a recycle loop to achieve high conversions. There is a choice of either axial- or radial-flow steam-raising reactors and GCR (originally direct quench reactors, now superseded by indirect tube cooled reactors). Purification is performed in conventional distillation columns. The flowsheet choices depend on a number of factors, such as the feedstock type and plant capacity.

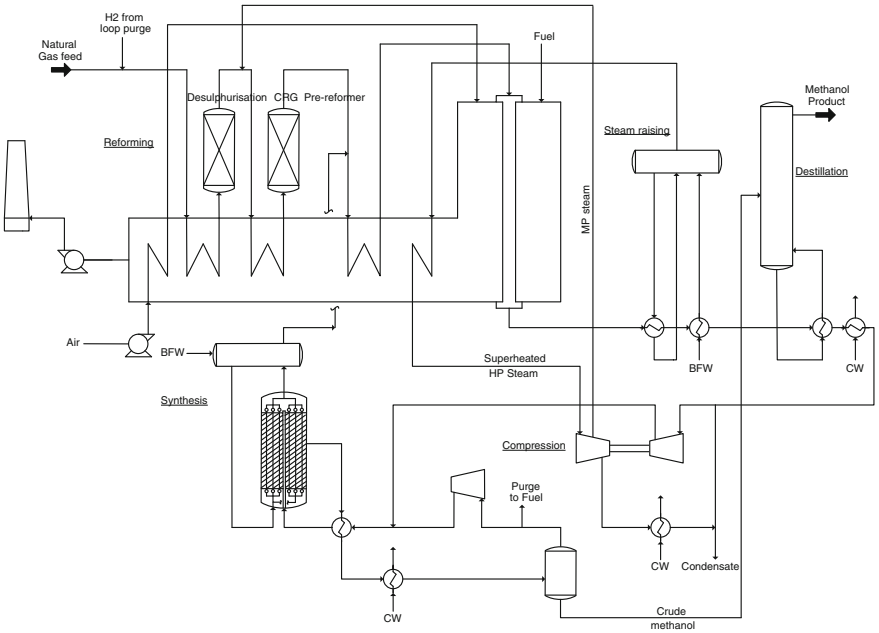

Fig. 4.108 A scheme of the Johnson Matthey/Davy Process Technology low-pressure methanol process [416]

The following description is based on the SMR option. Gas feedstock is compressed (if required), desulphurised, and sent to the optional saturator, where most of the process steam is generated. The saturator is used where maximum water recovery is important and it also has the benefit of recycling some byproducts. Further process steam is added, and the mixture is preheated and sent to the optional prereformer, using the CRG (catalytic rich-gas) process. Steam raised in the methanol converter is added, along with available carbon dioxide, and the partially reformed mixture is preheated and sent to the reformer. High-grade heat in the reformed gas is recovered as high-pressure steam, boiler feedwater preheat and for reboil heat in the distillation system. The high-pressure steam is used to drive the main compressors in the plant. After final cooling, the synthesis gas is compressed and sent to the synthesis loop. The loop can operate at pressures between 50 and 100 bar, typically between 70 and 80 bar.

The converter design does impact the loop pressure. Different designs are available, essentially depending on the capacity of the plant. The earlier and the smaller plants have used the LPM quench reactor. A radial-flow steam-raising converter developed for large-capacity plants is shown in the loop in Fig. 4.108. The synthesis loop comprises a circulator and the converter operates at approximately 220–280 °C. Low loop pressure reduces the total energy requirements for the process. Reaction heat from the loop is recovered as steam and saturator water and is used directly as process steam for the reformer. A purge is taken from the

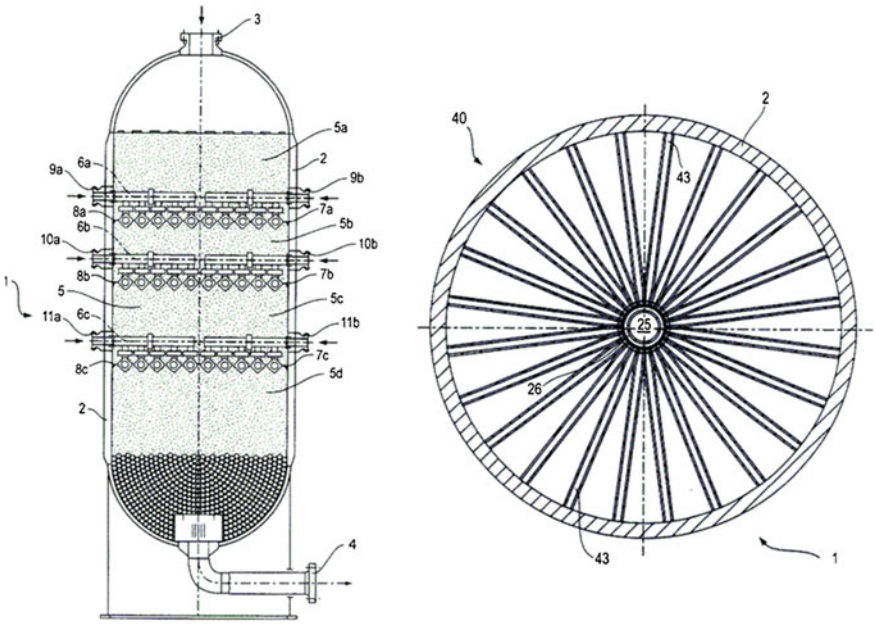

Fig. 4.109 Low-pressure methanol quench reactor (Lozenge reactor) [417]

synthesis loop to remove inerts (nitrogen, methane), as well as surplus hydrogen associated with nonstoichiometric operation. Also, the purge is used as fuel for the reformer. Crude methanol from the separator contains water as well as traces of ethanol and other compounds. These impurities are removed in a two-column distillation system (not shown in Fig. 4.108). The first column removes light ends such as ethers, esters, acetone, and dissolved noncondensable gases. The second column removes water, higher alcohols and similar organic heavy ends [416].

As already mentioned, for smaller capacities, a quench reactor was originally developed as shown in Fig. 4.109. A portion of the mixed synthesis and recycle gas bypasses the loop interchanger, which provides the quench fractions for the intermediate catalyst beds. The temperature is controlled by quenching the synthesis reaction by adding a cooled mixture of fresh and recycled syngas between the catalyst beds. The injection of the quench gas cools the reactant mixture and adds more reactants prior to entering the next bed.

Traditionally, reactors reveal an axial flow design. This permits a simple design, but it may become a problem for pressure drop as this can lead to large-diameter vessels. Increasing the diameter of the reactor results in thicker walls and restricts the number of suppliers. Therefore, Johnson Matthey has radial flow reactors, which have a much lower pressure drop and are less susceptible to fouling. The vessels have more complex and hence more expensive internals but the vessel diameter is reduced. Contraflow designs can be retrofitted into existing flow designs.

In axial flow, an uninterrupted catalyst bed is divided by lozenge distributors for quench gas addition. The gas is injected at appropriate depths within the reactor through spargers called lozenges. There are horizontal layers of these lozenges that run across the converter from side to side. Each has an outer surface covered with wire mesh and a central pipe that delivers the cold gas. ICI has an improved version of the Casale design lozenge reactor known as an axial-radial converter (ARC). The main technical difference is that instead of a single continuous catalyst bed, the bed is separated by distribution plates to form multiple consecutive catalyst domains.

The total energy consumption for a self-contained plant is typically around 32.6 GJ/t [425]. The figure depends on the type of feedstock used. Typical capacities are less than 3,000 tpd of methanol production.

4.7.2.2 The Lurgi Conventional Process Design

Syngas can be produced via different methods, as is described in Sects. 4.3 and 4.4. In the 1970s, Lurgi developed a quasi-isothermal process. The Lurgi conventional design involves the same basic steps as the original ICI LPM synthesis processes. The two processes differ mainly in their reactor designs and the way in which the produced heat is removed. The key component of the Lurgi process design is a multitubular reactor comparable to a heat exchanger but with the catalyst in the tubes and steam on the shell-side. It uses the exothermic nature of the reaction to generate high-pressure steam to drive the MUG compressor, recycle compressor, or to export high pressure steam. These process conditions result in a recycle/syngas ratio of 3.5 for the Lurgi process, compared to a substantially higher ratio of 6.0 for other designs such as ICI and consequently higher power consumption.

Owing to the isothermal operation of the reactor, the average catalyst bed reaction temperature is lower than that of the adiabatic converter. Therefore, the byproduct formation is lower and the lifetime of the catalyst across the isothermal reactor is longer. Also, the efficiency, expressed as the methanol STY (space time yield), is higher. Therefore, for a certain methanol production rate, less catalyst volume is required, compared to the methanol formation in an adiabatic quench converter. This process was developed to produce methanol from natural gas or oil-associated gas in a single-train plant with capacities up to 3,000 tpd. Figure 4.110 shows a schematic of this process.

The synthesis gas is converted to methanol in a catalytic-induced reaction in two parallel water-cooled methanol reactors (see Fig. 4.111).

The loop design can cope with all different types of syngas obtained from steam reforming, combined reforming, pure ATR, or gasification. For methanol plants with capacities as high as 3,000 tpd, oxygen-based syngas generation is normally applied by Lurgi to reduce the effective syngas volume flow. The pressure in this syngas outlet section (approximately 35 bar) is significantly higher than in a conventional reformer and reduces the syngas compression power substantially. The high-pressure steam and the medium-pressure steam generated from the process heat of the methanol plant are used as life steam for the steam turbine drives.

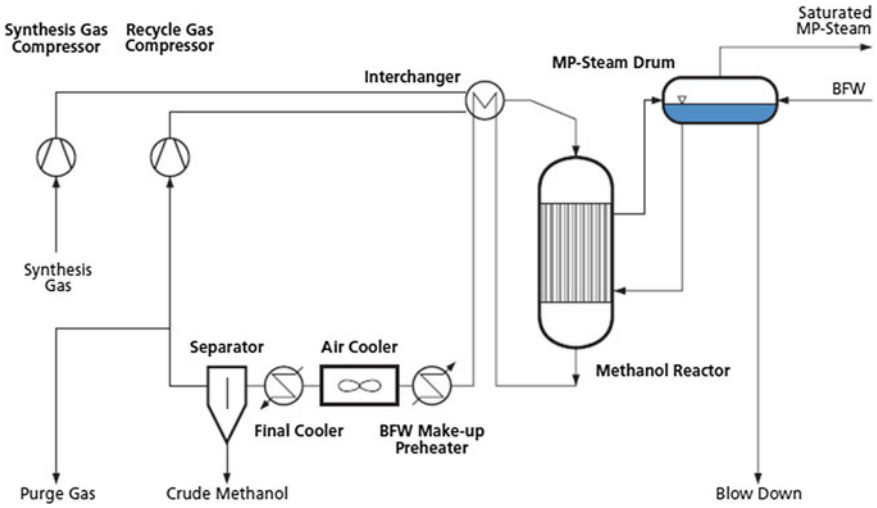

Fig. 4.110 Lurgi conventional methanol synthesis process. (Courtesy of Air Liquide Global E&C Solutions)

Fig. 4.111 Lurgi reactor system with two parallel water-cooled reactors. (Courtesy of Air Liquide Global E&C Solutions)

The reformed gas from the final separator is compressed by the synthesis gas compressor to the required pressure of the methanol synthesis loop. To protect the compressor from surging during startup and under partial load conditions of the

plant, an antisurge bypass is installed. The circulation in the methanol synthesis loop is achieved by the recycle gas compressor integrated in the synthesis gas compression. The synthesis gas compressor and the recycle gas compressor are driven by an extraction/condensation steam turbine using superheated high-pressure steam. The synthesis and recycle gas is preheated in a gas/gas interchanger to heat up the MUG to 220 °C before entering the water-cooled methanol reactors.

Apart from the methanol and water vapour produced, the reactor outlet gas contains nonreacted H_2, CO and CO_2; inerts such as CH_4 and N_2; and some reaction byproducts (ppm). This gas needs to be cooled from the reactor outlet temperature to about 40 °C in order to separate CH_3OH and H_2O from the gases. The gas is cooled in the synthesis air cooler and in the final cooler by sweet water. Apart from methanol and water, condensed crude methanol contains dissolved gases and impurities (reaction byproducts).

Separation of crude methanol from nonreacted gases takes place in the methanol separator. Crude methanol leaves the vessel on a level control for distillation, where pure methanol is separated from water and other impurities. The major part of gas is recycled back to the synthesis reactors via the recycle gas compressor in order to achieve a high overall conversion. A small amount is withdrawn on pressure control as purge gas to avoid unnecessary accumulation of inerts in the loop.

Most of the purge gas is sent to the syngas generation process. A small amount of purge gas is used for hydrogenation of the natural gas for desulphurisation. During startup and shutdown, the purge gas is routed to the flare. Crude methanol is routed to the distillation to produce pure methanol (see Sect. 4.7.5).

Reactor Startup System

To heat up the methanol reactor system from ambient temperature to operating temperature, start-up ejectors are used. Each WCR is equipped with two ejectors. The ejector suction nozzles are connected to the top of the reactor shell, whereas the discharge nozzles are connected to the bottom distribution header. Saturated medium-pressure steam from the header is used as a propellant for the ejectors and the circulating water is heated up by the condensed steam.

4.7.2.3 The Haldor Topsøe Process Design

Haldor Topsøe (HTAS) also has developed different syngas generation processes, as described in Sects. 4.2–4.4. A typical design of a two-stage reformer with HP methanol synthesis is shown in Fig. 4.112. The following description will concentrate on the synthesis loop.

Similar to the Lurgi MegaMethanol process (see Sect. 4.7.3), the Haldor Topsøe process is designed to produce methanol from natural or associated gas feedstocks, using a two-step reforming process to generate feed syngas mixture for the methanol synthesis. Associated gas is natural gas produced along with crude oil from the same reservoir.

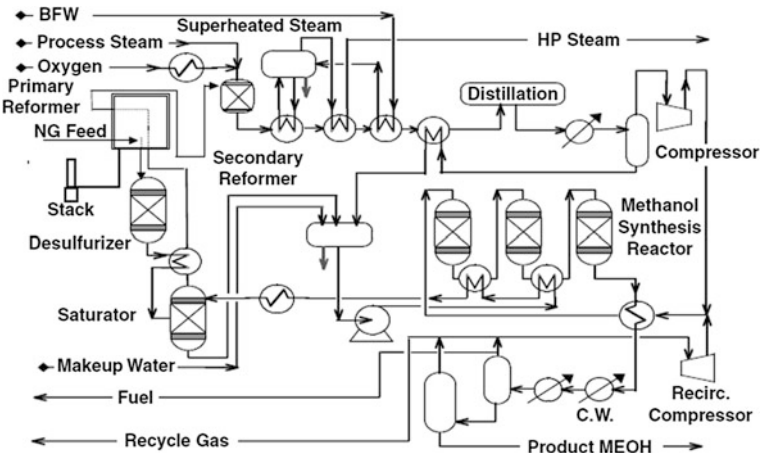

Fig. 4.112 A simplified process flow diagram of Haldor Topsøe A/S methanol synthesis process via two-step reforming. *BFW* boiling feed water, *NG* natural gas, *HP* high pressure. ©'Taylor Francis [412]

The key of the Topsøe process is a synthesis section with three adiabatic reactors possessing heat exchangers between the reactors, whereby the exothermic heat of reaction is recovered and used for heating saturator water. The arrangement is shown in Fig. 4.112.

Other Haldor Topsøe designs include an adiabatic catalyst bed installed on top of the upper tube sheet before the cooled part of the BWR to rapidly increase the inlet temperature to the boiling water part. This ensures optimum use of this relatively expensive unit, as the tubes are now used only for removal of reaction heat, not for preheat of the feed gas [412]. Topsøe claims that the installation of the adiabatic top layer in the BWR has a cost advantage compared to their reactor without the top layer.

Second energy integration is obtained by cooling the effluent from the last reactor to preheating the feed to the first reactor. For revamps of adiabatic ICI reactors, Topsøe offers a Casale ARC, using the collect-mix-distribute (CMD) concept. Vertical support beams separate catalyst beds. The gas inlet at the bottom of the reactor provides fresh syngas that flows radially up through the first catalyst bed. At the top of the reactor, this first pass through gas is mixed with quench gas and distributed evenly so that it flows radially down through the second catalyst bed [418]. The claimed benefit of this design is an increase in per-pass conversion. The total energy consumption for the process is said to be about 29.26 GJ/t of product methanol, including oxygen production. The process technology is reported to be suitable for smaller as well as very large methanol plants up to 10,000 tpd.

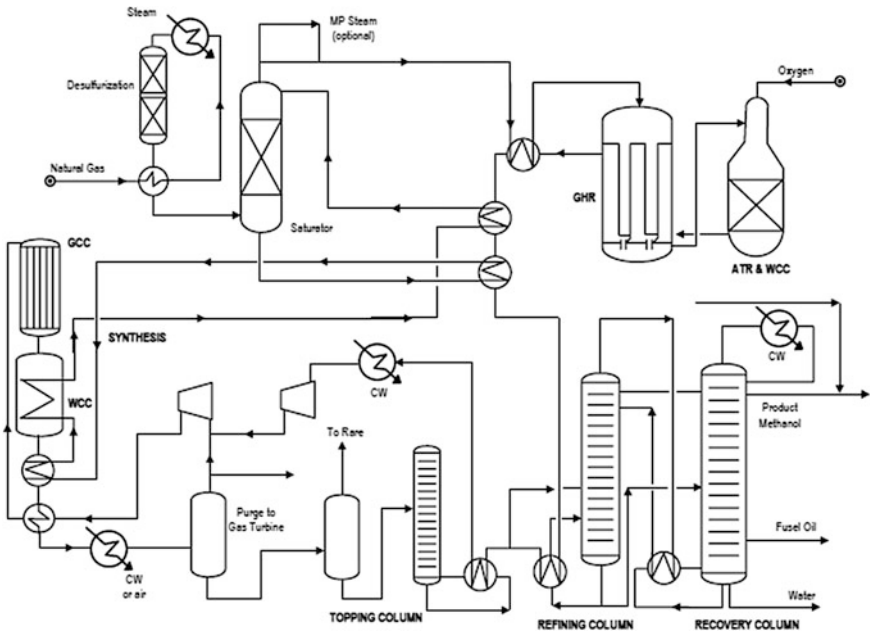

Fig. 4.113 Johnson Matthey leading concept methanol technology flowsheet. *ATR* autothermal reforming, *GHR* gas-heating reforming. Courtesy of Johnson Matthey

4.7.2.4 The Johnson Matthey Process Design and Davy Process Technology

In 1994, ICI introduced the leading concept methanol process, schematically [419] shown in Fig. 4.113. The design is developed around the advanced gas heat reformer (AGHR), which is a compact tubular reformer. More details are given in the PERP Report [420]. Two features are important: the saturator circuit and the AGHR. The arrangement of a saturator circuit can provide between 90 and 100 % of the process steam adding. Additional steam can be added to obtain the required S/C.

The concept features integration of the AGHR. In the AGHR unit, the gas is heated using the effluent of the secondary reformer and is fed to a small bed of reforming catalyst, which converts approximately 25 % of the natural gas. Then the gas mixture is directed to an oxygen-blown secondary reformer where the conversion is completed. The temperature of the effluent from the secondary reformer is approximately 975 °C and contains approximately 0.5 % methane. This hot stream is used to heat the mixed natural gas and steam in the AGHR.

The advantage of this design becomes particularly apparent in case of a feedstock for a steam reforming–based methanol plant containing already up to approximately 25 % CO_2 because this is almost the ideal composition. In contrast, oxygen-based methanol plants would need to substantially remove the CO_2 before

it could be processed. The GHR overcomes the capacity limit, beyond which ATR would be the technology of choice. From the stoichiometry, oxygen consumption needs to be at approximately 0.5 t of oxygen per tonne of methanol for an ATR-based process to work properly, but pure ATR consumes far too much oxygen.

4.7.2.5 The Mitsubishi Heavy Industry Process Design

With the cooperation of MGC, Mitsubishi Heavy Industry (MHI) has developed a methanol process (see Fig. 4.114) that is said to be characterised by high efficiency in the reaction and energy saving for the methanol synthesis (see Fig. 4.114). The process uses a new type of isothermal reactor known as the MGC/MHI super-converter [421]. This reactor design uses double-walled tubes that are filled with catalyst in the annular space between the inner and outer tubes. The feed syngas enters the inner tubes and is heated as it progresses through the tube. The gas then passes downward through the catalyst bed in the annular space. Heat is removed on both sides of the catalyst bed by the boiling water surrounding the tubes as well as by the feed gas introduced into the inner tube [422].

The temperature profile of the catalyst in the superconverter is different to that of a quasi-isothermal reactor. The catalyst bed temperature is higher near the inlet (up to 260 °C) but gradually lowers toward the outlet (down to 210 °C) by heat exchange with the feed gas. This means that the gas proceeds along the maximum reaction rate line (when methanol concentration is plotted against temperature) at least some of the time, giving a high one-pass conversion rate. A high conversion rate (about 14 % methanol in the reactor outlet) is cited for this reactor [423], but actually the value is assumed to be much lower. No experience has been reported to date to indicate that the higher bed temperature at the inlet harms the catalyst life.

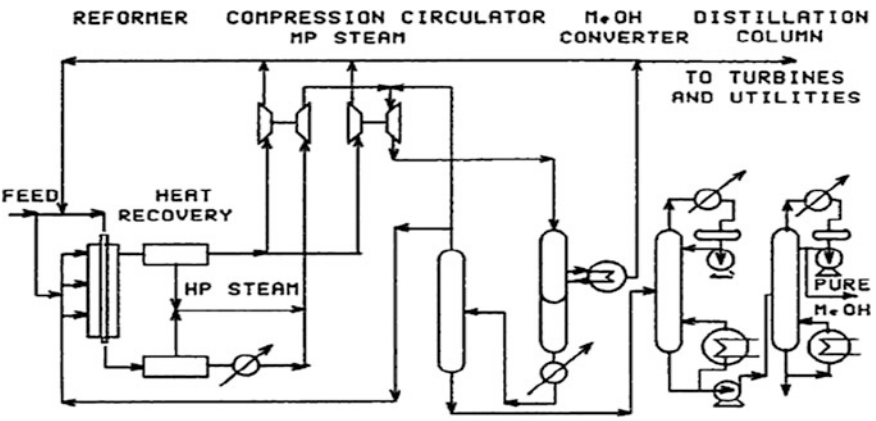

Fig. 4.114 Mitsubishi Gas Chemical low-pressure methanol synthesis process [425]

MHI has received three contracts for methanol plants in Saudi Arabia (5,000 tpd for Sabic, with the syngas generation process licensed by HTAS using the MHI superconverter), Venezuela, and Brunei [424].

4.7.3 Large-Scale Methanol Plant Process Designs

Large-scale methanol plants are defined as operations of 5,000 tpd or more. World demand for methanol has been growing steadily in recent years, and this trend is expected to continue, especially in light of the new applications for methanol in the fuels, chemicals and energy market. Cost-efficient methanol production is the key to stay competitive (see Chap. 7). The two main drivers are economies of scale and cheap feedstock.

Especially in remote areas, methanol is discussed as a well-transportable liquid energy carrier (see Chap. 8). To exceed equipment, piping and valve dimensions, the amount of gas flowing through the loop has to be minimised (i.e., the conversion per pass has to be increased).

For plants exceeding 3,000 tpd, just doubling the reactors would not work; the pipework, valves and equipment sizes make it impractical, and the necessary economy of scale would not be achieved. The solution was to design methanol loops with substantially reduced recycle rates that kept high conversion efficiency. In addition, the equilibrium temperature at the exit of the reactor systems has to be low, as the reaction is limited by equilibrium. High methanol content at the reactor exit combined with low CO levels to keep high efficiencies requires exit temperatures to be as low as possible.

As a typical example, Lurgi Combined Converter Methanol Synthesis (Fig. 4.115), which is part of the MegaMethanol process, is described in Sect. 4.7.3.1. Other designs, including their special features and reactors, are also discussed.

4.7.3.1 The Lurgi MegaMethanol Process Design [414]

The synthesis gas from battery limits is mixed with hydrogen from a PSA unit and compressed in the synthesis gas compressor. The outlet pressure of the compressor is at approximately 75–80 bar.

The circulation in the methanol synthesis loop is achieved by a one-stage recycle gas compressor and without any intercooling. The synthesis gas compressor and recycle gas compressor are driven by a steam turbine using superheated high-pressure steam. After this step, the gas is routed together with the recycle gas to the tube side of the GCR to be preheated by the heat of reaction coming from the shell side.

The preheated gas enters the tube side of the WCR, where it is partially converted to methanol on the copper-zinc catalyst contained in the tubes. The heat of reaction is removed by boiling water on the shell side. Medium-pressure steam is

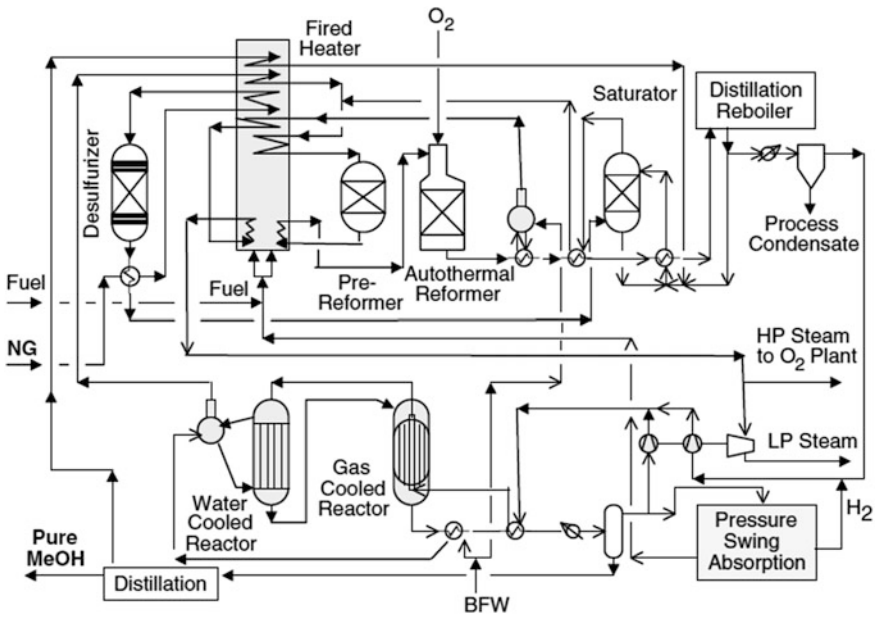

Fig. 4.115 Process scheme for the Lurgi MegaMethanol Synthesis Process [426]. MP = medium pressure; LP = low pressure; HP = high pressure

generated, collected in associated steam drum and exported to the plant network. To start up the reactors, injectors are needed, which are driven by medium-pressure steam.

Downstream of the WCR, the gas is cooled down in the interchanger, thereby transferring the heat to the feed gas heading to the GCR. Final cooling and condensation of methanol is achieved in the intermediate air cooler with the liquid methanol being separated from the gas stream in the intermediate methanol separator. The liquid methanol is cooled down further in the crude methanol cooler by the means of cooling water.

The remaining gas with low methanol content is reheated in the interchanger and sent to the shell side of the GCR for a second reaction step on copper-zinc catalyst at a lower temperature level compared to the WCR. The hot reactor outlet gas is used to preheat BFW for the steam drum in the medium-pressure boiling feed water (BFW) preheater and for the high-pressure steam drum in the high-pressure BFW preheater. Downstream of the BFW preheaters, the waste heat is used for reheating cold recycle gas coming from the recycle gas compressor in the trim heater. Temperature control for the GCR is achieved by partially bypassing this trim heater and by a cold gas bypass around the GCR tube side, which is mainly utilised during startup and shutdown of the unit.

The methanol produced in the GCR is being condensed in the air cooler and at low temperature in the water-cooled final coolers before the liquid product is separated in the methanol separator. The remaining nonreacted gas is being compressed by a recycle gas compressor, partially heated in a trim heater, and

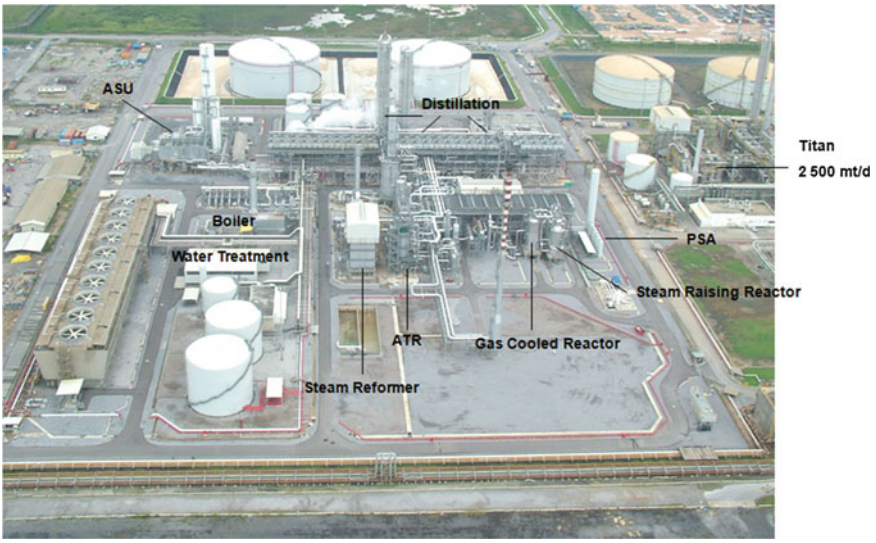

Fig. 4.116 The Atlas methanol plant (5.000 tpd) is based on the MegaMethanol technology (gas-cooled reactor and steam-raising reactor), which was developed and supplied by Germany-based engineering contractor Air Liquide Global E&C Solutions [426]

mixed with the fresh MUG from the synthesis gas compressor before entering the tube side of the GCR. A small amount of the recycle gas is removed from the system and sent as required to a PSA (pressure swing adsorption) unit to recover the hydrogen, which is used for adjustment of the SN of the feed gas. This crude methanol is processed further in the methanol distillation section.

4.7.3.2 The Lurgi GigaMethanol Process Design

(A) The GigaMethanol plant concept

Low natural gas and/or shale gas prices in the United States and the tendency to use methanol as a building block for fuels and as chemical storage for renewable electricity favour the development of even larger capacities beyond 5,000 tpd of methanol. Such capacities (10,000 tpd and even higher) have to be built as single-line plants to take advantage of the economies of scale. The scaleup to higher capacities, however, is limited because certain critical equipment, such as valves and some other special equipment, are not available beyond certain sizes. The only choice was to increase the operating pressure and thus to decrease the syngas volume. Having this in mind, Lurgi built a pilot plant in Freiberg (Germany) and tested catalytic and noncatalytic ATR operation with natural gas of different types as well as liquid hydrocarbons and oxygen (see Sect. 4.3).

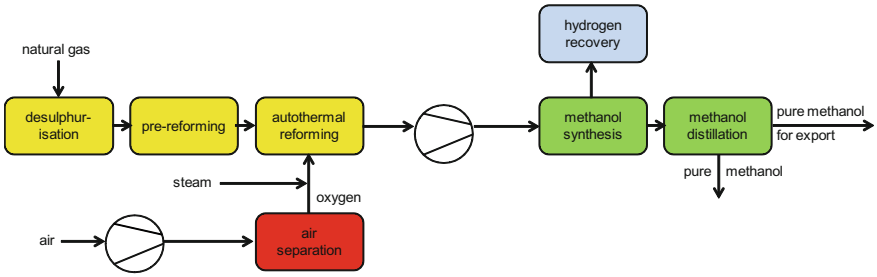

Fig. 4.117 Lurgi GigaMethanol concept

The most important parameters were the following:

- Pressures up to 100 bar
- Temperatures exceeding 1,000 °C at the ATR exit
- Catalytic(different types) and noncatalytic performance
- S/C for soot formation
- Ignition behaviour.

The results of the test work were included in simulation programmes to be able to design and simulate the behaviour of large plants. In addition, engineering studies confirmed that all equipment could be purchased/manufactured within the existing reference frame for capacities up to 10,000 tpd methanol.

The main benefits of the selected GigaMethanol technology compared to the conventional combined reforming concept are as follows:

- Large single-train capacity utilising cost benefits due to economies of scale
- Advanced, proven, safe and reliable technology
- Optimised energy efficiency
- Low environmental impact.

The use of an oxygen-blown ATR is the basis for this efficient methanol plant. The optimum syngas composition required for the downstream methanol synthesis section will be achieved by an enlarged PSA unit (see Fig. 4.117).

Apart from economic considerations, equipment manufacturing and transportation limitations are decisive for the selection of the maximum single-train capacity. Therefore, the main objective of the conceptual design of the GigaMethanol technology was to increase the capacity of the plant by not exceeding the mechanical possible dimensions of the individual items. The GigaMethanol concept follows these requirements by maximum reduction of the effective gas flows.

In contrast, a large-scale conventional combined reforming based plant needs technical scaleups and will include equipment and/or bulks outside the commercially proven range of size. To avoid critical configurations in the production stream, the parallel equipment and/or bulk installations are necessary consequences (e.g. steam reformer, syngas compressor, control valves). For

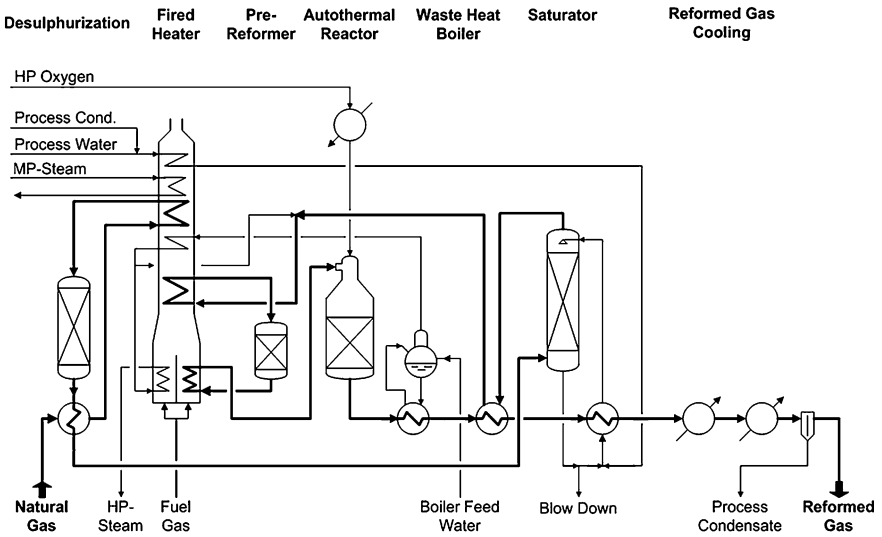

Fig. 4.118 Catalytic autothermal reforming for a 10,000 tpd methanol plant (simplified flowsheet) [415]. *HP* high pressure, *MP* medium pressure

GigaMethanol, the only main parallel installations will be the reformed gas WHBs (waste heat boilers) and the water-cooled methanol reactors.

The plant has the following processing units:

- Reforming unit
- Steam and condensate system
- Methanol synthesis
- PSA unit
- Methanol distillation.

ATR generates syngas with a SN lower than optimum for the downstream methanol synthesis (see Fig. 4.118). As a consequence, the syngas is short on hydrogen. The additionally required hydrogen will be produced in a PSA unit and mixed with the syngas stream (see Fig. 4.119).

Conventional steam reforming of natural gas generates a syngas with hydrogen in excess and at low pressures. The excess hydrogen is to be routed through the syngas production unit, has to be compressed, and is finally part of the purge gas from the synthesis unit, which is used as fuel. In the GigaMethanol concept, the natural gas is routed directly to the ATR, where the operating pressure is not anymore limited by the operating pressure of the steam reformer as it is for conventional and for combined reforming.

Reformed gas is produced, which can be adjusted to the optimum composition by adding hydrogen separated from the purge gas of the methanol synthesis loop. This concept together with the high pressure of the system reduces the effective reformed gas flow to the most favourable figure and allows comparably smaller

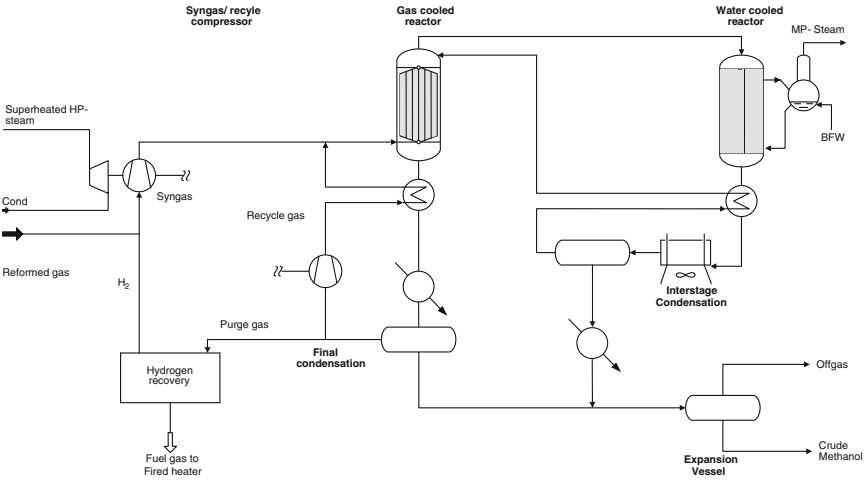

Fig. 4.119 Simplified process flow diagram of GigaMethanol synthesis. (Courtesy of Air Liquide Global E&C Solutions)

sized equipment and pipe/valve sizes, particularly in the main plant process sections. A SN number of 2.03 is achieved via ATR and recycle of purge gas, according to Fig. 4.119.

The steam utilised in the GigaMethanol plant during normal operation is generated by process WHBs and by auxiliary boilers. The pressure levels are 100 bar high-pressure/69 bar and 35 bar medium-pressure/4.8 bar low-pressure steam.

(B) **Methanol Synthesis in the GigaMethanol Process**

Based on these proven building blocks of the MegaMethanol process, Lurgi has improved the process further, pursuing the track towards a process that is even more optimised for CAPEX (capital expenses) and OPEX (operating expenses). The improvement features a condensation step between the water- and gas-cooled methanol reactor, removing the methanol produced in the first stage before entering the second reaction stage. The removal of methanol from the system results in a higher driving force for the reaction towards methanol in the GCR Reactor, such that the catalyst volume required and the reactor size are drastically reduced.

About 50 % of the methanol produced (depending on the aging status of the catalyst) is withdrawn in between the stages; the methanol content at the GCR outlet and the resulting dew point are therefore significantly lowered. Still, the combined per pass conversion is even higher than before, although the recycle rate has been lowered from 2.2 to about 1.7 with much less gas volume being circulated in the loop, resulting in a remarkable reduction of scale-up.

The condensation step comprises an interchanger to cool down the WCR outlet and reheat the gas before entering the GCR, an air cooler to condense the methanol, and a methanol separator. The size of the GCR and the downstream condensation section is reduced accordingly. The control of the cooling gas amount, as well as the control of the cooling gas temperature (via the trim heater), will allow for flexibility due to load changes or end-of-run conditions (Fig. 4.119).

(C) **Pressure Swing Adsorption (PSA) in the GigaMethanol Process**

For the purpose of adjusting the SN of the synthesis gas, hydrogen must be added to the reformed gas. Purge gas from the methanol is used as feedstock for the PSA. The off-gas from the PSA is compressed and used as fuel in the fired heater and in the auxiliary boiler. The hydrogen product is added to the reformed gas upstream of the synthesis gas compressor. The PSA unit works on the principle that the adsorbent attracts and retains the impurities at higher pressure and releases them at lower pressure (thus the expression *PSA*).

4.7.3.3 Other Large-Scale Methanol Processes

(A) **The Haldor Topsøe Process Design**

In the Haldor Topsøe process design, the feed gas is routed together with the recycle gas to an adiabatic top catalyst bed in the upper part of the WCR to be preheated by the heat of reaction. Then the preheated gas enters the cooled part of the catalyst bed in the tube of the WCR, where it is partially converted to methanol on the copper-zinc catalyst contained in the tubes. The adiabatic catalyst bed installed before the cooled part of the WCR has the effect of rapidly increasing the inlet temperature to the boiling water part. This ensures optimum use of this relatively expensive unit, as the tubes are now used only for removal of reaction heat, not for preheat of the feed gas.

According to Topsøe, the BWR with the installation of the adiabatic top layer in the WCR reduces the total catalyst volume and the cost of the synthesis reactor by approximately 15–25 %. The maximum capacity of one reactor may increase by approximately 20 % [412]. The two-step reforming scheme is claimed to be suitable for capacities between 1,500 and 7,000 tpd and S/C ratios of 1.5–1.8. Using ATR, capacity ranges of 5,000–10,000 tpd with an S/C ratio of 0.6–0.8 can be achieved. Topsøe claims that a natural gas–based plant using the two-step reforming has proven energy consumption as low as 28.76 GJ/t methanol [415].

(B) **The Davy Process Design**

A second example is the series loop technology of Davy Process Technology for exothermic synthesis gas compositions [415] (Fig. 4.120).

As was already shown in the case of Lurgi and HTAS designs for larger-scale plants, higher capacities (beyond approximately 3,000 tpd) increasingly use combined reforming for the syngas preparation. This has a strong impact on the

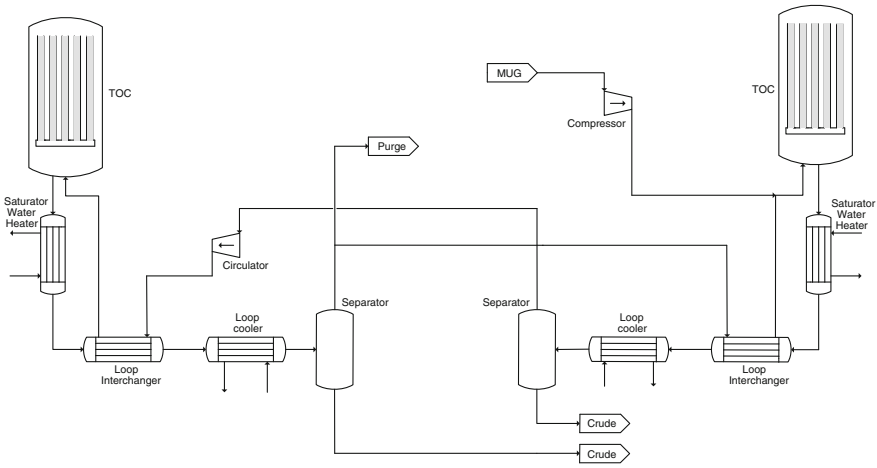

Fig. 4.120 Process scheme for the Davy Process Technology Series Loop [416] methanol process. (Courtesy of Nexant Inc.)

loop design and the selection of the reactor, as the more reactive gas leads to smaller catalyst volumes. The net heat of reaction per volume of catalyst is more than double that produced by SMR-based technology only. Simple loop arrangements would simply no longer be able to cope with the increased heat release, leading to impractical sizes of the loop and the related pipework. The large-scale loop design is also based on the principles of LPM synthesis. Instead of arranging two reactors in parallel, the reactors are arranged in series where the same circulation gas is used twice, first in the high-pressure reactor and secondly in the low-pressure reactor. The driving force for the reaction is maintained by condensing the methanol between the two reactors.

(C) The Improved Low-Pressure Methanol Process

The improved low-pressure methanol (ILPM) technology is based on a CRG prereformer, steam reformer and the Davy Process Technology (DPT) Steam Raising Converter (SRC). This combination of proven process units allows single-stream methanol plants of capacities in excess of 5,000 tpd, while only using one steam raising reactor (see Sect. 4.7.4). The specific feature of this design is that it does not need an oxygen plant. Figure 4.121 shows a simplified process flow diagram of the ILPM Process, which is based on a SRC and incorporates a CRG prereformer upstream of the primary reformer.

The DPT radial SRC design features a radial gas flow from the centre of the converter, passing over the methanol synthesis catalyst (see Sect. 4.7.4). Depending on the plant capacity, a two-stage methanol synthesis also may be

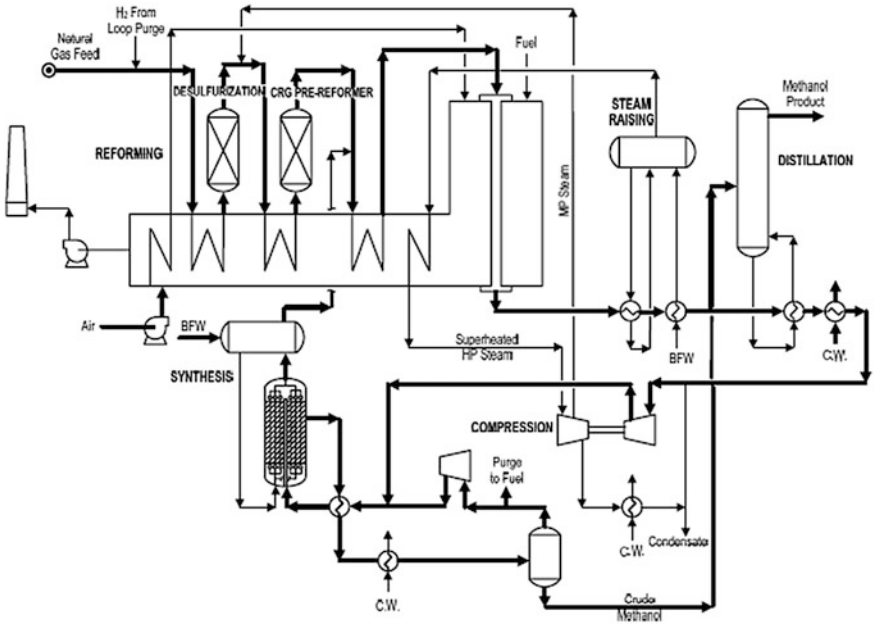

Fig. 4.121 Improved low-pressure methanol process [415]. *BFW* boiling feed water, *CRG* catalytic-rich converter, *MP* medium pressure, *HP* high pressure

incorporated, using for instance the DPT tube-cooled converter (TCC) as the main reactor, followed by a WCR as an additional process step [417].

(D) **The Toyo Process Design**

For plants with a capacity up to 5,000 tpd, Toyo proposed a design that incorporates only steam reforming for the syngas generation, and thus without the use of oxygen. This process is called JumboMethanol. For capacities beyond 5,000 tpd and up to 10,000 tpd, Toyo offers combined reforming with oxygen for the ATR [427]. The S/C ratio is kept at approximately 2.2–2.5 to maintain high efficiency and reasonable CAPEX, while keeping enough security against metal dusting. For plant capacities of 10,000 tpd and beyond, Toyo has developed a highly integrated scheme, incorporating an improved combined reforming process for syngas generation, called TAF-X. A primary reformer and the TAF-X reactor are installed in parallel; the S/C ratio is kept the same as before. The methanol production process is on a new radial-flow methanol converter called MRF-Z (see Sect. 4.7.4). For a 10,000 tpd plant, Toyo plans two parallel trains for the methanol synthesis loop and the downstream distillation.

(E) **The Methanol Casale Process Design**

For conventional methanol plants (less than 3,000 mtpd), Casale uses its standard process. For capacities up to 7,000–10,000 tpd, Casale designs their plants

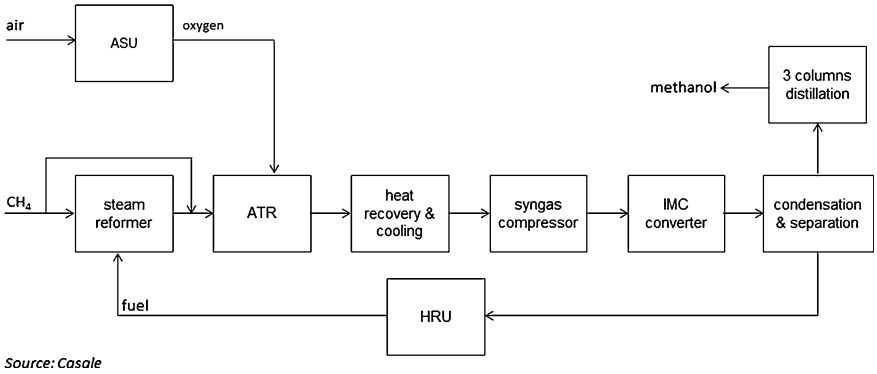

Fig. 4.122 Methanol Casale large-scale methanol process [431]

according to the advanced methanol process, as shown in Fig. 4.122. The process features a combined reforming step, consisting of SMR followed by ATR. The syngas ratio is adjusted via a bypass of a fraction of the natural gas around the SMR. The key feature of the Casale design is the proprietary methanol synthesis converter, which is described in Sect. 4.7.4.

4.7.4 Reactor Systems for Large-scale Plants

4.7.4.1 Reactor Design Principles

With increasing capacities the conventional methanol loop reactors are reaching their limits regarding gas flow, reactor size and fabrication and transport possibilities. In principal, other methanol reactors that are further discussed can be characterised as follows:

(A) **Isothermal boiling water/steam-raising reactor designs**

Isothermal boiling water/steam-raising reactor designs include the following:

- Lurgi tubular steam-raising reactor with the catalyst in the tubes and boiling water on the shell side, in which the heat of reaction is used to produce process steam.
- Linde steam-raising spiral reactor with the catalyst on the shell side and steam produced inside the coils, which are built in spirals through the catalyst bed
- ICI TCC with the catalyst on the shell side and straight cooling tubes inside the catalyst bed
- TOYO MRF-Z steam-raising reactor with radial process gas flow mode
- Casale Isothermal Methanol Converter (IMC) converter

- MHI superconverter
- HTAS tube-cooled reactor (for larger-scale plants, a combination of an adiabatic reactor followed by a tube-cooled BWR is used).

Normally the BWR is used due to its efficiency and ease of temperature control, but adiabatic reactors in series or combinations of BWR and adiabatic reactors may also be considered. The BWR is in principle a shell and tube heat exchanger with catalyst on the tube side. Cooling of the reactor is provided by circulating boiling water on the shell side. By controlling the pressure of the circulating boiling water, the reaction temperature is controlled and optimised. The steam produced may be used as process steam, either directly or via a falling film saturator.

The isothermal nature of the BWR gives a high conversion compared to the amount of catalyst installed. However, to ensure a proper reaction rate, the reactor will operate at intermediate temperatures (e.g. 240–260 °C). Consequently, the recycle ratio may still be significant. The BWR exhibits higher capital investment. The maximum size of the reactors is limited.

An adiabatic catalyst bed may be installed before the cooled part of the BWR either in a separate vessel, as in the case of the Lurgi design, or on top of the upper tube sheet, as in the case of the Topsøe design (see below). One effect of the adiabatic catalyst bed is to rapidly increase the inlet temperature to the boiling water part. This ensures optimum use of this relatively expensive unit because the tubes are now used only for removal of reaction heat, not for preheat of the feed gas.

(B) **Adiabatic reactor designs**

Adiabatic reactor designs include the following:

- Multibed quench (direct cooling) design (lozenge, ARC, CMD - collect-mix-distribute).
- Multibed with interstage heat exchange (indirect cooling).

A number of adiabatic catalyst beds installed in series inside one pressure shell are called a quench reactor. In practice, up to five catalyst beds have been used. The reactor feed is split into several fractions and distributed to the synthesis reactor between the individual catalyst beds. The quench reactor is not suitable for large-capacity plants.

In contrast to a quench reactor, in an adiabatic reactor a number (2–4) of separated fixed-bed reactors with separate pressure shells are placed in series with cooling between the reactors. The cooling may be by preheat of high-pressure BFW, generation of medium-pressure steam and/or by preheat of feed to the first reactor. The adiabatic reactor system features good economies of scale. Mechanical simplicity contributes to low investment cost. The design can be scaled up to single-line capacities of 10,000 tpd or more.

An optimum quench gas distribution can improve the performance of the SynLoop. In an adiabatic multistage quench converter, the quench gas distribution

directly influences the inlet temperatures and therefore the approach to equilibrium (ATE) of the individual catalyst beds. Optimum ATE is 10–20 °C for maximum reaction rates.

(C) **Tube (gas)-cooled reactor designs**

Tube (gas)-cooled reactor designs include the following:

- Casale gas-cooled reactor
- Lurgi gas-cooled reactor
- Davy Process technology TCC.

The gas/gas heat exchange allows very good temperature control close to equilibrium temperatures (Lurgi system) and a very good controlled heat removal from different parts of the catalytic bed for the Casale reactor.

Presently, nine major types of commercial methanol synthesis converters are on the market:

- Quench cooled
- Multiple adiabatic beds
- Tube cooled
- Tubular packed bed
- Multistage radial flow
- The superconverter
- Collect-mix-distribute
- Axial-radial converter
- Isothermal.

These reactor types are discussed in the following sections. The quench-cooled and tubular-packed bed types are the most common technologies. These two designs, besides the multiple adiabatic beds, have the largest capacity of the conventional methanol processes.

(D) **Lurgi Water-Cooled Reactor System (WCR)**

The Lurgi WCR is a tubular reactor. The tubes are filled with catalyst and surrounded by boiling water circulating between the reactor shell side and the steam drum mounted on top of the reactors. The reactions of H_2 with CO and CO_2 take place in the catalyst-filled tubes and the heat of reaction is removed by the boiling water outside the tubes. Hence, a quasi-isothermal condition is maintained in the system, which ensures a high conversion and eliminates the danger of catalyst overheating.

Boiler water from the steam drum enters the reactor shell side at the bottom through a distributor and rises up to the outlet at the top due to the thermosiphoning effect. The steam/water mixture from the reactor shell side is separated in the steam drum. Saturated medium-pressure steam at approximately 40 bar is discharged via a pressure control valve and water circulates back to the reactor.

The makeup water is supplied from the BFW pump on a level control. The pressure control at the steam outlet controls the pressure in the shell side of the

reactor and thereby the boiling point of the water, which in turn controls the reaction temperature. As consequence, the reaction temperature is well controlled by the boiling water rector design.

Main advantages of the WCR are the following:

- A quasi-isothermal operation in which byproducts are kept to a minimum
- Extremely quick transfer of reaction heat
- A methanol yield of up to 1.8 kg methanol/L catalyst
- Long catalyst lifetime; under adequate running conditions, most plants require catalyst replacement only after 4–5 years, or even later
- Approximately 80 % of the reaction heat was converted to HP steam; this means 1–1.4 t of steam per tonne of methanol, which is primarily used for driving turbines, thus minimising electric power consumption
- Overheating of catalyst is impossible
- Easy startup by direct steam heating,
- Fast load changes are possible, as is easy and fast load/discharge of catalyst.

4.7.4.2 Large Scale Reactor Designs

(A) **Lurgi Combined Reactor System Design**

For large-scale plants (above approximately 3,000 tpd methanol), the reaction is split into two conversion steps (see Fig. 4.123). As in LPM syntheses, the gas is compressed to the selected pressure (5–10 MPa) by a synthesis gas compressor and preheated to the required inlet temperature of the first methanol converter. This reactor is a quasi-isothermal boiling water reactor (WCR) with catalyst in the tubes to ensure the most efficient heat removal; the reaction gas entering this reactor is very reactive and overheating of the catalyst has to be avoided (see Fig. 4.124). In a second converter, the preconverted reaction gas is fed to a gas cooled reactor.

The preconverted gas is routed to the shell side of the GCR, which is filled with catalyst at the shell side, and the final conversion to methanol is achieved at continuously reduced operating temperatures along the reaction route. The decreasing reaction temperature provides a permanent driving force for conversion to methanol. The heat of reaction is used to preheat the reactor inlet gas inside the tubes for the first methanol converter. The reactor outlet gas is cooled; crude methanol is separated and routed for purification to the distillation section. Unreacted gas is compressed and recycled. Part of the unreacted gas is purged out of the loop to avoid accumulation of inerts in the loop [414].

The main advantage of the combined converter system is that the substantial reduction of the syngas volume via combined reforming, together with the reduction of the recycle ratio to about 2, was possible by introducing a second reaction step with the GCR, thus providing thermodynamically optimised reaction conditions in the GCR (see Fig. 4.125). In the WCR, the isothermal reactor, a partial conversion of the syngas to methanol is achieved at higher space velocities and higher temperatures compared to single-stage synthesis reactors. These steps

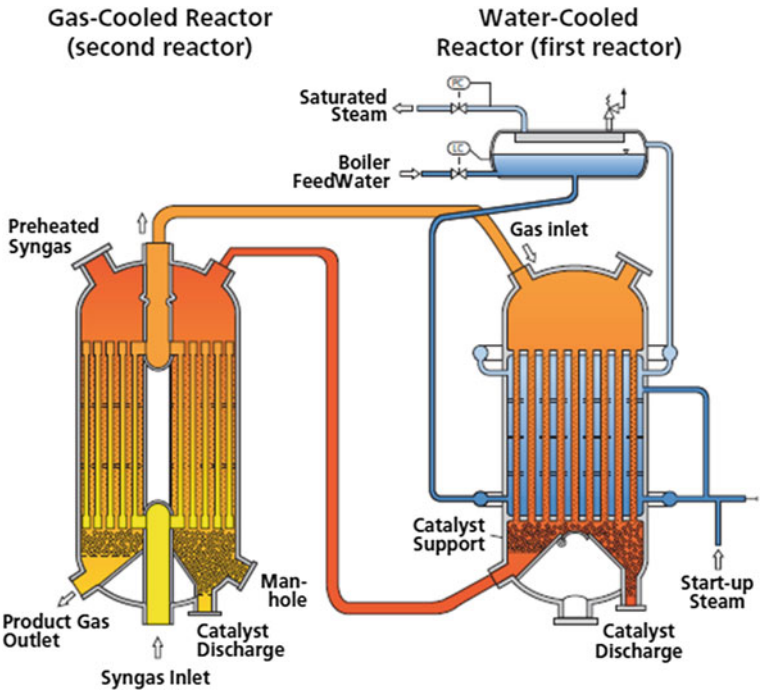

Fig. 4.123 Lurgi combined reactor system [429]

result in a significant size reduction of the WCR compared to conventional processes, while the steam raised is available at a higher pressure. As can be seen from Fig. 4.123, the methanol-containing gas is routed from the WCR outlet without any cooling to the downstream GCR.

In this reactor, cold feedgas for the WCR is routed through tubes in a countercurrent flow with the reacting gas. Thus, the reaction temperature is continuously reduced over the reaction path in the GCR (see Fig. 4.125), and the equilibrium driving force for the methanol synthesis maintained over the entire catalyst bed. The large inlet gas preheater normally required for the synthesis by a single WCR is replaced by a relatively small trim heater.

Because fresh synthesis gas is only fed to the WCR, no catalyst poisons can reach the GCR. In combination with the low operating temperatures, this results in a very long catalyst service life. In addition, if the methanol yield in the WCR is reduced as a result of declining catalyst activity, the temperature in the inlet section of the GCR will rise as a result of improved reaction kinetics and hence an increased yield in the GCR.

The main advantages of the combined reactor system are as follows:

- High syngas conversion efficiency: At the same conversion efficiency, the recycle rate is about half of the ratio in a single-stage WCR reactor.

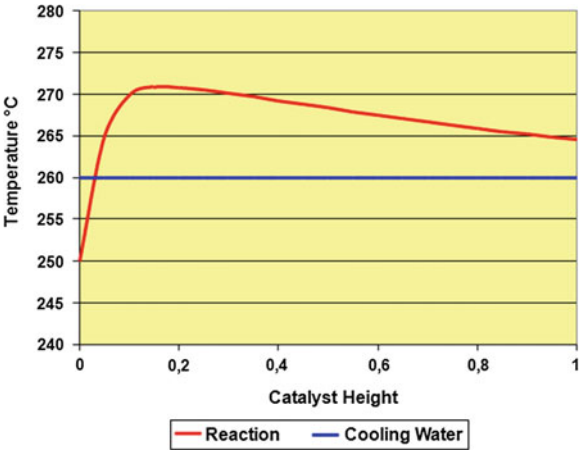

Fig. 4.124 Temperature profile of the water-cooled reactor [430]

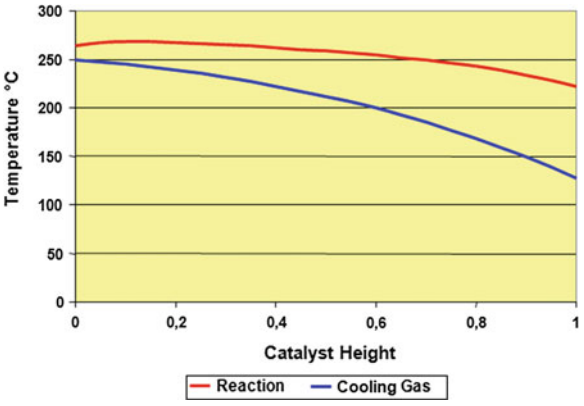

Fig. 4.125 Temperature profile of the gas-cooled reactor [415]

- High energy efficiency: About 0.8 t of 50–60 bar steam per tonne of methanol can be generated in the WCR reactor. In addition, a substantial part of the sensible heat can be recovered at the GCR reactor outlet.
- Low investment cost: The reduction of the catalyst volume for the WCR reactor, the omission of the large feedgas preheater, and savings resulting from other equipment due to the much lower recycle ratio result in approximately 40 % cost savings for the synthesis loop.
- High single-train capacities: The process improvements explained above have paved the way to large methanol plants, such as MegaMethanol and GigaMethanol.

The reaction temperature, as can be seen in Fig. 4.124, is well controlled by the boiling water rector design.

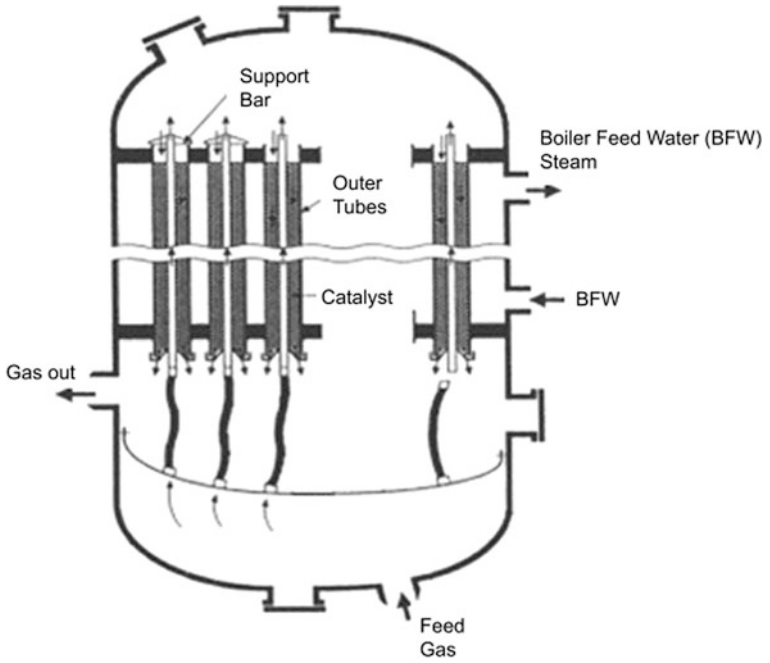

Fig. 4.126 Mitsubishi Heavy Industries Superconverter [415]

Main advantages of the gas-cooled reactor (see Fig. 4.125) are as follows:

– Extended catalyst lifetime,
– Possibility of very large single-train capacities
– Low investment cost.

(B) **MHI Reactor System**

The Superconverter, jointly developed by MGC and MHI, has been described elsewhere. It is a simple double tubular heat exchanger for methanol synthesis (see Fig. 4.126). The methanol synthesis catalyst is packed in the annular space between the inner and outer tubes. The feed gas enters the inner tube, through the flexible tubes connected to the bottom dome, and is further heated by passing through the inner tubes. The gas then is introduced downwards into the catalyst bed in the annular space. The catalyst bed is cooled by boiler water outside the double tube and feed gas from the inner tubes. Methanol and the unreacted gas exit through a bottom outlet. The temperature profile of the co-catalyst in the super-converter is different than that of a quasi-isothermal reactor.

The catalyst bed temperature is higher near the inlet but gradually lowers toward the outlet by heat exchange with the feed gas. This means that the gas proceeds along the maximum reaction rate line (when methanol concentration is plotted against temperature) at least some of the time, giving a high one-pass

conversion rate. MGC states that the superconverter's other advantages include safe operation and a high level of mechanical stability.

Mitsubishi has reported successful operation of the first commercial-scale (520 tpd) plant using the Superconverter at Niigatas Japans. The Superconverter has been incorporated in a 5,000 tpd plant for Sabic in Saudi Arabia.

(C) **Methanol Casale Reactor System Design**

Methanol Casale (Lugano-Besso, Switzerland) improved the so-called lozenge or ICI-type methanol reactor that consists of a single catalyst bed in which "lozenge-shaped" distributors for the cooling gases have been inserted. The single-bed version was replaced by a catalyst beds superimposed and in mutually spaced relationship. The ICM converter is basically a pseudo isothermal converter, in which the heat transfer surfaces are plates instead of tubes, and the catalyst is outside the cooling plates. A combination of different cooling fluids is also possible. The converter allows very effective quench mixing [415, 431] as the temperature spread at the inlet of the next bed is only a few degrees. This eliminates hot spots inside the bed and allows operation of the beds at very low inlet temperatures (Fig. 4.127).

According to Casale, the new design has the following main features:

- Heat removal from the catalytic bed can be controlled independently in different sections of the bed. Thus, it is possible to operate the reactor at a temperature profile in accordance with the highest reaction rate.
- No tube sheets are needed. The heat can be removed directly from the catalyst bed.
- The axial-radial gas flow through the converter results in very low pressure drop.
- The cooling fluid flowing inside the plates can be fresh converter feed gas, water, or another heat transfer fluid.

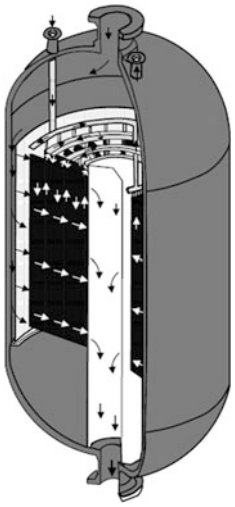

Fig. 4.127 Methanol Casale IMC (axial/radial reactor) ©PERP Nexant [415]

Fig. 4.128 Linde Reactor System. Courtesy of Linde [432]

– Casale claims that energy consumption is only about 29.3 GJ/mt methanol.
– Very high single vessel capacities can be realised.

(D) **Toyo Reactor System Design**

Toyo Engineering Corporation has designed a new version of a multistage radial flow methanol converter (MRF-Z) that uses bayonet boiler tubes for intermediate cooling. The tubes divide the catalyst into concentric beds. The indirect cooling system allows the temperature to be kept very close to the path of the maximum reaction rate curve, achieving maximum conversion per pass and reducing the catalyst requirement by 30 % compared to quench reactors of the same size.

The use of bayonet tubes avoids problems with thermal expansion stresses and allows for free draining. The pressure drop over the reactor system is low, allowing a scale-up to very large sizes (10,000 tpd) by simply enlarging the tube length.

(E) **Linde Reactor System Design**

The synthesis gas is converted to methanol in the Linde isothermal reactor shown in Fig. 4.128. The Linde isothermal reactor has the advantages of a tubular reactor, but the thermal stress problems of a straight tube bundle reactor are avoided. The reaction heat is flowing to a spiral-wound cooling tube, which is embedded in the catalyst bed. Thereby, the process can be operated at optimum temperature. The temperature is controlled by the vapour pressure. The very high heat transfer coefficients on the catalyst side, which are obtained by the cross-flow technology, reduce the cooling area required. Due to the flexible arrangement of the tubes in

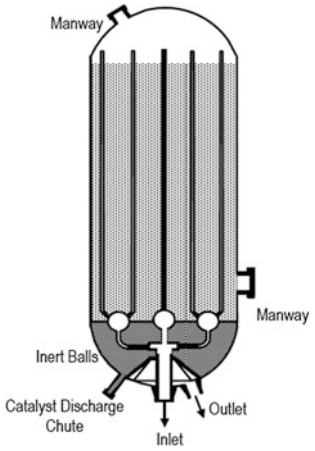

Fig. 4.129 Davy Process Technology tube converter cooler [415]

the bundle, high spatial and temporal temperature gradients can be tolerated, whereby fast startup and shutdown are possible. During loading, the physical damage of the catalyst is reduced to a minimum because the tube spiral-wounded bundle limits the free fall of the catalyst.

The Linde isothermal reactor exhibits the largest amount of catalyst per reactor volume of all the isothermal reactors. In case of the methanol synthesis, depending on process conditions, a capacity up to 4,000 tpd can be achieved. The Linde isothermal reactor is presently used in eight methanol plants.

(F) **DPT Tube-Cooled Converter**

Depending on the plant capacity, DPT uses a variety of methanol synthesis converters, such as the following:

- Axial steam-raising converter (up to 1,500 tpd per converter)
- Radial-flow steam-raising converter (up to 2,500–3,000 tpd per converter)
- TCC (up to 2,000 tpd per converter) (Fig. 4.129).

4.7.5 Methanol Distillation

4.7.5.1 The Principles

The raw methanol produced in the methanol synthesis contains water, dissolved gases and a quantity of undesired but unavoidable byproducts, which have either lower or higher boiling points than methanol. The purpose of the distillation unit is to remove those impurities in order to achieve the desired methanol purity specification. This is accomplished in the three following process steps.

First, dissolved gases (e.g. CO, CO_2, H_2, CH_4) are driven out of the raw methanol by simply flashing it at a low pressure into the expansion gas vessel. Removal of the light ends (e.g. ethers, formiates. aldehydes, ketones) and remaining dissolved gases is carried out in a pre-run column. Finally, the methanol is separated from the heavy ends (ethanol, higher alcohols and water) in a pure methanol distillation section consisting of one or two columns.

Lurgi offers two basic distillation concepts, which are both incorporated in a large number of methanol plants: an investment cost-saving two-column distillation and an energy-saving three-column distillation. Methanol purity remains unaffected, whereas pure methanol yield and consumption of steam depends upon the distillation concept.

4.7.5.2 Equipment and Process Description

(A) Cost-Saving Distillation

The two-column distillation is designed to reduce investment cost while accepting a higher energy requirement. This design is recommended for plain steam reforming (no use of CO_2 is required) or if steam import for column reboilers is possible. A process flow diagram of a typical two-column distillation is shown in Fig. 4.130.

Raw methanol withdrawn from the synthesis loop is flashed into the expansion gas vessel. The dissolved gases escape and are discharged via pressure control into the expansion gas line. Raw methanol is then fed to the pre-run column, where low

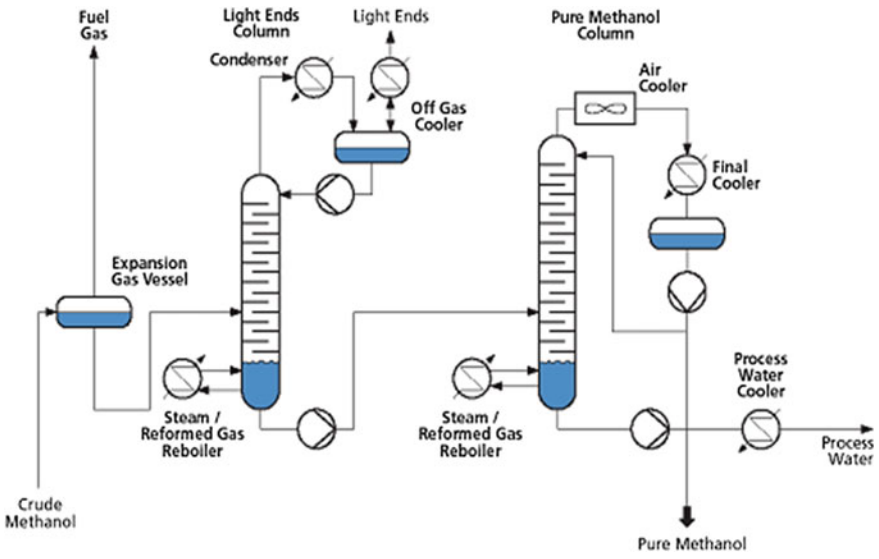

Fig. 4.130 Two-column distillation. (Courtesy of Air Liquide Global E&C Solutions)

boiling byproducts are removed. Light ends are taken overhead with a large volume of methanol vapours. The overhead vapours are passed to the pre-run column condenser, where condensation of the methanol vapours is accomplished, and further sent to the reflex vessel. Uncondensed light ends are vented off the top of the vessel to the off-gas cooler, which serves to condense residual methanol vapours out of the vent gases. Condensed methanol runs back into the reflux vessel while light ends are withdrawn. Light ends together with expansion gas, both saturated with water and methanol, are routed off and can be used as fuel gas. Methanol reflux is removed from the vessel and routed by way of the reflux pump back to the upper tray of the pre-run column. The column is heated from the bottom by thermosyphon and reboilers, utilising low-pressure steam and reformed gas.

The final product, stabilised methanol, is fed to the pure methanol column. The purpose of the pure methanol column is to remove the methanol from water and other heavier components. The column overhead stream is pure methanol, while process water containing traces of ethanol and higher alcohols is discharged from the bottom of the column via a pump and cooler.

The overhead methanol vapours are condensed in an air cooler, further cooled against cooling water, and then collected in the reflux vessel. Part of the methanol is pumped back as reflux to the top of the column, whereas the rest is routed to the pure methanol storage facilities.

(B) **Energy-Saving Distillation**

The energy-saving three-column distillation is recommended when insufficient reformed gas waste heat is generated (e.g. with use of CO_2) or if large plant capacities are considered. A typical process flow diagram of a three-column distillation is illustrated in Fig. 4.131. The distillation principle remains unaffected,

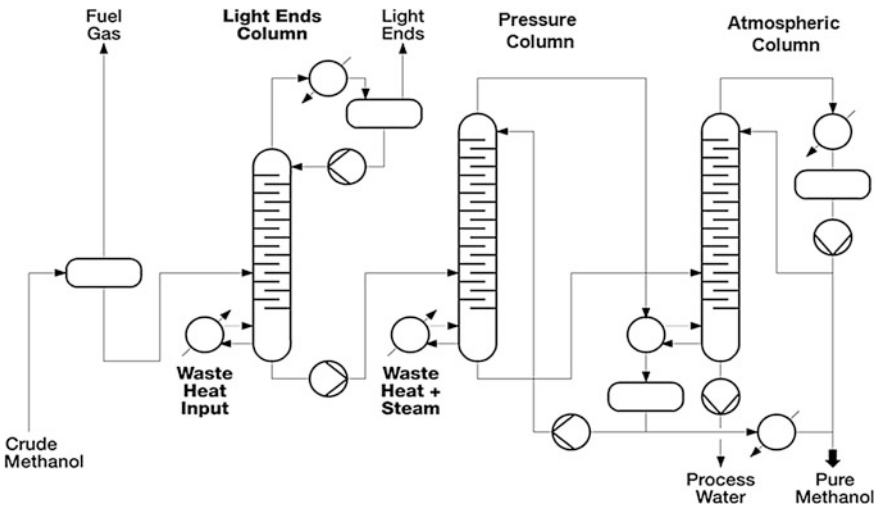

Fig. 4.131 Three column distillation. (Courtesy of Air Liquide Global E&C Solutions)

but the pure methanol column is divided into two separate columns, with one running at elevated pressure and the other at ambient pressure.

Pure methanol is discharged overhead in both columns, each refining between 40–60 % of the product. The ambient pressure column reboiler uses the heat of the pressure column overhead vapours, which are condensed simultaneously. This reduces the energy demand for heating the pure methanol column considerably by approximately 35 %.

4.7.6 Unconventional Methanol Synthesis on Semicommercial Scale

The LPMETHANOL liquid phase methanol synthesis process from Air Products and Chemicals offers superior reaction temperature control compared to fixed-bed technologies and higher conversion. The process is based on a bubble slurry reactor. An inert mineral oil/powdered catalyst slurry is used as a reaction medium and heat sink. The mineral oil transports the reaction heat to an internal tubular boiler, where the heat is removed by generating steam. The LPMETHANOL reactor is able to operate at isothermal (constant temperature) conditions by dampening large and rapid process changes, and when handling CO-rich (in excess of 50 %) syngas with wide compositional variations. Due to the ability to handle CO-rich syngas, an upstream WGS unit to increase the syngas H_2/CO ratio is not needed for partial methanol production up to full utlilisation of feed H_2. Therefore, the LPMETHANOL process can operate either base load or in IGCC co-production mode [433].

4.8 Methanol Production from CO_2

Tom Lorenz[1], Martin Bertau[1], Friedrich Schmidt[2] and Ludolf Plass[3]

[1]*Institute of Chemical Technology, Freiberg University of Mining and Technology, Leipziger Straße 29, 09599 Freiberg, Germany*

[2]*Angerbachstrasse 28, 83024 Rosenheim, Germany*

[3]*Parkstraße 11, 61476 Kronberg, Germany*

4.8.1 Introduction

Methanol synthesis by CO_2 hydrogenation is one of the most promising steps toward a future based on sustainability and responsible use of fossil materials. Shortages of fossil fuels and decreasing crude oil qualities will be great challenges in the coming decades. Methanol production from CO_2 and H_2 provides a possible solution for both problems at the same time.

Hydrogenation of CO_2 is not a recent invention. In order to adjust the CO/H_2 ratio of synthesis gas used for conventional methanol synthesis, scientists discovered during the early 1960s that small amounts of CO_2 added to the feed will enhance the yield of methanol [434]. The catalysts used in LPM synthesis (e.g. the GL-104 developed by Lurgi and Girdler, which is today a part of Clariant) mostly consist of copper, zinc oxide, and alumina. Using these catalysts, many scientists tried to investigate the optimal composition of catalysts for producing CO_2-based methanol. Particularly in the 1980s and 1990s, a large number of scientific articles dealing with this topic were published.

World wide first demonstration of converting the green house gas CO_2 to methanol as a useful chemical was reported by Lurgi at the 207th national meeting of the American Chemical Society in March 94. Another pilot plant was built in 1996 by the National Institute for Resources and Environment (NIRE, Japan) and the Research Institute of Innovative Technology for the Earth (RITE, Japan) [435–438]. Today, companies like Lurgi and Mitsui Chemicals run pilot plants to investigate the feasibility and problems of industrial-scale production [439]. In Iceland, another plant has been in operation since 2012 producing methanol from geogenic CO_2 [440].

CO_2-based methanol has another advantage besides the active reduction of CO_2 emissions. Methanol synthesis from CO_2 leads to a wide-ranging independence from fossil fuels if H_2 is produced by water electrolysis, employing electric power supplied from renewable energy sources. Further investments in renewable energy sources will promote methanol synthesis from CO_2 and H_2 as the missing link of a closed-carbon cycle. In addition, chemical CO_2 fixation will provide new options for storing renewable energy (see Chaps. 7 and 8).

Every year, approximately 35 billion tonnes of CO_2 are produced by industry, transportation and households. In view of the enormous efforts nature has invested over the last 4 billion years in establishing a highly efficient carbon cycle on earth, questions about whether we can afford to dispose of the raw material carbon in the atmosphere remain unanswered so far. Consequently, chemists are looking for way to recycle carbon (i.e., closing the carbon cycle by reintegrating CO_2). In other words, CO_2 is increasingly being viewed as a raw material rather than a waste product. As a result of CO_2-based chemistry on an industrial scale, fossil carbon resources will be replaceable by CO_2-derived base chemicals, particularly methanol (see Chap. 8). The approach described in this chapter is the chemical monetisation of CO_2 by its conversion into methanol according to the reactions outlined in Sect. 4.5. In fact, CO_2 hydrogenation very much resembles classic methanol production from synthesis gas:

$$CO + 2H_2 \rightleftharpoons CH_3OH \qquad \Delta_R H_{(298K,50bar)} = -90.7 \text{ kJ/mol} \qquad (4.97)$$

$$CO_2 + 3H_2 \rightleftharpoons CH_3OH + H_2O \qquad \Delta H_{R(298K,50bar)} = -40.9 \text{ kJ/mol} \qquad (4.98)$$

The syntheses of methanol from carbon CO and CO_2 are tied through the WGS reaction:

$$CO + H_2O \rightleftharpoons CO_2 + H_2 \qquad \Delta H_{R(298K,50bar)} = -42 \text{ kJ/mol} \qquad (4.99)$$

As previously mentioned, Eqs. 4.97–4.99 are equilibrium reactions. The reaction enthalpy ΔH_R refers to 298 K and 50 bar, whereas the standard enthalpy of reaction (denoted $\Delta_R H^-$) is the enthalpy change that occurs in a system when 1 mol of matter is transformed by a chemical reaction under standard conditions. Reactions 4.97 and 4.98 are exothermic and accompanied by a volume decrease. Reaction 4.99 in its forward direction is mildly exothermic. In principle, methanol formation is therefore favoured by increasing pressure and decreasing temperature, with the maximum conversion being determined by the equilibrium composition. If hydrogen is obtained from renewable or CO_2 neutral sources, such as biomass, solar, wind, or nuclear power, a potentially CO_2 neutral cycle is possible.

CO_2 separation technologies are discussed in Sect. 4.5.1, such as CO_2 capture from integrated gasification combined cycle plants through selective gas treatment in a Rectisol process. Also, there are several options for H_2 production, both sustainable (i.e., nonfossil, such as PVs or gasification of renewable feedstock) and conventional but nonfossil (e.g. nuclear power) [437, 441–446]. CO_2 capture from industrial emissions and the conversion of CO_2 into methanol for the transportation sector are also referred to as clean renewable methanol fuel. RM can be blended with different grades of gasoline for existing automobiles and hybrid flexible vehicles. RM is a drop-in fuel for existing automobiles and hybrid flexible vehicles and can be purchased at existing gasoline stations. The production of RM is feasible in many locations in the world with geothermal, wind and solar energy sources [447].

Because the RWGS is a reversible reaction (Eq. 4.99), catalysts active in the direct WGS reaction are also active in the reverse reaction. Copper-based catalysts have been studied for the WGS reaction and methanol synthesis from synthesis gas, most frequently modified by alumina and less frequently modified by zirconia, titania and/or silica. Although some CO_2 is accelerating the reaction rate of methanol synthesis from synthesis gas, typically up to a maximum of approximately 3 % CO_2 in the feed, the use of pure CO_2 results in lower reaction rates. As can be deduced from Eqs. 4.97–4.99, the reason is related to the formation of water, which is in favour of the reverse methanol synthesis reaction.

The stoichiometric number SN (see Sect. 4.3.2.4) of a synthesis gas required for methanol synthesis should be 2.0 or slightly above. The CO-to-CO_2 ratio as well as the concentration of inerts are other important properties of the synthesis gas. A high CO-to-CO_2 ratio will increase the reaction rate and the achievable per pass conversion. With high CO-to-CO_2 ratios, the formation of water will also decrease, thus reducing the catalyst deactivation rate. Both conditions are unfavourable for the formation of methanol from CO_2. However, for particular H_2/CO ratios, the addition of CO_2 can reduce the SN of the MUG to the optimum level of 2.04–2.06, which results in significantly higher methanol production for each unit of MUG fed to the loop. A disadvantage of this type of operation is the additional amount of water that is produced. This water can have an effect on the methanol synthesis catalyst. The distillation system has to be capable of handling the additional water if CO_2 is added to the reformer effluent, which conversely requires a source of CO_2 to be available. The quantities effectively needed in large methanol plants usually

mean that the plants should be located adjacent or near one or more large-scale ammonia plants [449].

For these reasons, it was believed that pure CO_2 created as waste from coal-fired power plants cannot efficiently enough be transformed into methanol. However, Lurgi researchers succeeded in producing methanol from almost pure CO_2 by using a Süd-Chemie (today Clariant) catalyst, which is manufactured commercially today [452]. Nevertheless, even thereafter researchers reported a significant deactivation of the catalyst. This is caused by the water produced in the course of CO_2 hydrogenation, which reduces the rate of methanol formation and affects ZnO crystallisation, thus rendering the process unfeasible in the long term [451, 454].

4.8.2 The Lurgi Process with a Cu/Zn/Al-Catalyst

Early studies on CO_2-based methanol synthesis were carried out in the early 1990s by Lurgi, who in 1994 unveiled the "worldwide first demonstration of converting the greenhouse gas CO_2 to methanol as a useful chemical" [452]. At that time, the key to the process was a new copper-zinc oxide catalyst developed by Süd-Chemie (now Clariant) with an economical service life of about the same as a commercial catalyst in a conventional methanol plant that has high CO in its feed gas. This new technology was attractive for producers with access to pure CO_2 and excess H_2, such as methyl tertiary butyl ether makers with dehydrogenation units, thus making the process as cost-effective as conventional methods. This approach may also be attractive in cases where H_2 is available through electrolysis of water by using energy from wind or solar sources (see Chap. 8) [450, 453].

4.8.2.1 Selection of Catalyst and Process Parameters

As mentioned previously, Cu-based catalysts are the by far most commonly used active catalysts for methanol synthesis from synthesis gas, due to their high activity, selectivity and long-term stability. As shown in Table 4.54, in particular, those catalysts developed by Süd-Chemie (now Clariant) display very high activities for methanol production. Because of the similarities between more CO_2-based and more CO-based methanol synthesis, it is possible to apply these catalysts for both pathways of methanol synthesis.

Therefore, a commercial Süd-Chemie (now Clariant) $Cu/ZnO/Al_2O_3$ catalyst was subjected to tests at Lurgi's research and development centre (now Air Liquide Research and Development) with synthesis gases composed of CO_2 and H_2 in different stoichiometric ratios with various proportions of inert gases. Catalyst activity proved to be excellent at a pressure of 60 bar and a space velocity of 22,000 h^{-1}, and methanol production exhibited a broad peak at temperatures between 260 and 270 °C.

Table 4.54 Overview of some catalysts used for methanol synthesis from synthesis gas, including methanol yields and reaction conditions

Process	Catalyst composition (wt%)	Reaction conditions	Space–time yield (kg_{MeOH}/kg_{cat} h) or (kg_{MeOH}/l_{cat} h)	Y_{MeOH} (%)	Reference/ patent filing date
Shell International Research	Cu-Zn-M 40:18:4[b]	300 °C, 53 bar, 10,900 h^{-1}	– 1.01	–	[454] (1971)
Mitsubishi Gas Chemical Company	Cu-Zn-Al 62:31.5:6.5[c]	240 °C, 88 bar, 30,000 h^{-1}	– –	–	[455] (2010)
Ammonia Casale	Cu-Zn-Cr–Al 30:50:16:3	250 °C, 100 bar, 12,500 h^{-1}	– 1.00	–	[456] (1982)
Süd-Chemie AG	Cu-Zn-Al 65.2:23.8:11	300 °C, 100 bar, 4,000 h^{-1}	– 0.82	–	[457] (1984)
Süd-Chemie AG	Cu-Zn-Al 63:27:10	250 °C, 60 bar, 22,000 h^{-1}	1.144 1.190	–	[458] (2001)
Lonza AG	Cu-Zn-Zr 40:20:40	250 °C, 50 bar, 8,000 l/kg h^{-1}	0.54 –	12.7	[459] (1996)
AIST, RITE[a]	Cu-Zn-Al-Zr-Si 45.2:27.1:4.5:22.6:0.6	250 °C, 50 bar, 10,000 h^{-1}	– 0.72	–	[460] (1998)
Mitsubishi Gas Chemical Company	Cu-Zn-Al-Zr[d] 57.6:29.5:9.2:3.7	250 °C, 49 bar, 4,000 h^{-1}	– –	34.7	[461] (1973)
YYK Corp[a]	Cu-Zn-Al 76.3:11:12.7	250 °C, 50 bar, 1.7 g/h mol	1.548 –	–	[462] (1998)
Fujimoto et al.	Cu-Mg–Na-Pd x:y:18.7:0.025	160 °C, 50 bar, batch	– –	–	[463] (2010)
Kang et al.	Cu-Zn-Al-Zr 60.5:30.1:7.6:1.8	250 °C, 50 bar, 4,000 h^{-1}	– –	–	[464] (2009)

M = Mixture of two or more rare earth elements (except Ce) in their natural ratio
a = The full list of all proprietors is published in the patent
b = Weight portion of the metal oxides
c = Molar ratio
d = A Ce/Zr-oxide support was used with a catalyst/support weight ratio of 5:1

4.8.2.2 Activity and Stability of the Commercial Catalyst System

Catalytic production processes of commodities on an industrial scale are mainly dependent on selectivity and stability of the catalyst system in use. Low conversions are acceptable as long as unconverted substrate can be recycled with an acceptable effort. Therefore, these aspects were in the focus of catalyst characterisation tests in a setup with recycling of unconverted synthesis gas. The catalyst showed a good performance and furnished almost complete conversion of CO_2. The CO_2 per-pass conversions were in the range of 35–45 % and showed a slight decrease over time-on-stream (TOS).

4.8.2.3 Selectivity of the Methanol Formation Reaction from CO_2

In general, the methanol synthesis reaction based on synthesis gas is already very selective. The crude product obtained from the low-pressure flash has normally a purity of approximately 90 % if the common synthesis gas is used as a feed (Table 4.55). The predominant byproduct is water with a content of 10–12 wt%. Water is a byproduct of the CO_2 hydrogenation, too, and can be converted in situ with CO to give CO_2 and H_2 (WGS reaction).

If CO_2-based feed gas is used, both primary reactions (i.e., the CO_2 hydrogenation to methanol and the RWGS reaction to CO) are accompanied by formation of water. Therefore, the crude methanol from the CO_2-based process contains approximately 30–40 % water. In both cases, the water content strongly depends on the CO_2 fraction in the synthesis gas and additionally on the activity of the catalyst towards the (reverse) WGS.

Apart from water as an inevitable byproduct, other byproducts from parallel or consecutive reactions are present in significantly lower amounts. For CO-based synthesis gas, the content of byproducts is in the range of 2,000 ppm (Fig. 4.132). The CO_2-based process yields methanol in higher purity with five times lower byproduct contents. This can be partly explained by the high temperature sensitivity of the byproduct formation reactions. These components are mainly formed at higher temperatures. Because the resulting catalyst bed temperature is higher when CO is present in the feed gas, byproduct formation is faster, too. However, in addition to this effect, CO_2 conversion seems to proceed with an inherently higher

Table 4.55 Purity of the crude methanol product from a pilot plant [464]

Synthesis gas basis/ process conditions	Overall selectivity for methanol (%)	Water content (wt%)	Content of other byproducts (ppmw)
CO 70 bar, 250 °C	87.0 (99.82)[a]	12.8	1,800
CO_2 80 bar, 250 °C	63.5 (99.96)	36.1	390

[a] Excluding water and only taking the other byproducts into account

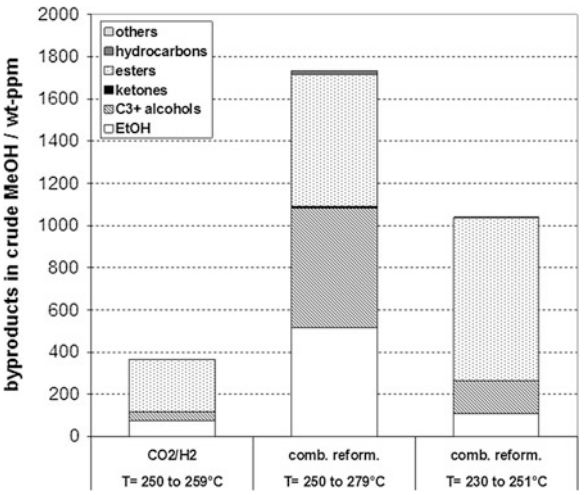

Fig. 4.132 Comparison of the byproducts in crude methanol for various feed gases using a standard catalyst under standard conditions compositions [490]. (Courtesy of Air Liquide Global E&C Solutions) 'comb. reform.' stands for 'combined reforming'

selectivity. The data show that, even at comparable peak temperature levels of the reaction, byproduct formation is significantly reduced for CO_2-based synthesis gas compared to CO-based synthesis gas.

Under similar process conditions, CO_2 conversion is slower than CO hydrogenation but more selective, which is owed to lower peak temperatures. However, productivity of the overall process always depends on the space velocity, recycle ratio and temperature, among other factors. In all cases, the producer must decide what the main aims of the process are. CO_2 may not lead to comparable productivities as CO, but it offers many other potential benefits and advantages.

4.8.2.4 Lurgi Process Technology for CO_2 Hydrogenation to Methanol

The high activity of a CO_2-to-methanol catalyst permits high loads and correspondingly good STYs. The low equilibrium conversion affects carbon and hydrogen use in the synthesis gas, rendering it slightly lower than that in a CO-based methanol synthesis. Lurgi has developed a concept for the synthesis of methanol from CO_2 and H_2 that almost offsets the drawbacks of the lower equilibrium conversion rate by subdividing the reaction system into WGS and methanol synthesis as two separate reaction units (Fig. 4.133) [465].

In this process, the conventional setup of adding the MUG to the recycle gas is supplemented by contacting the MUG with the catalyst in a fixed-bed prereactor in a once-through operation. This can be realised without overheating the catalyst even at high pressure because for the two reactions, CO_2 hydrogenation and

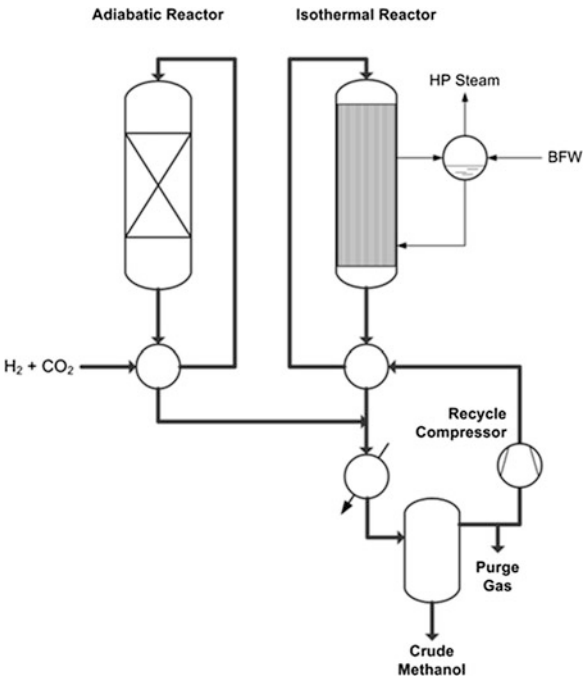

Fig. 4.133 Setup for methanol synthesis based on CO_2 and H_2. (Courtesy of Air Liquide Global E&C Solutions) [439]

RWGS reaction, the exothermic effect is only slightly higher than the endothermic effect. Under these conditions, the occurring reaction rates for the two reactions leads to only a marginal temperature increase.

The product gas from the prereactor is cooled and fed into a synthesis loop incorporating a conventional water-cooled methanol reactor. The exothermic reaction, which is clearly dominant during the recycle operation, can be conveniently controlled by the water-cooling reactor system. This well-proven reactor concept is perfectly suitable to accurately adjust the narrow temperature range where both kinetic and thermodynamic conditions reach their optima. The WCR requires only approximately 80 % of the volume that would be necessary if the MUG was fed directly into the methanol synthesis loop. Consequently, all equipment and piping within the loop is also reduced by the same percentage [465].

In both the adiabatic and the isothermal reactor, the same catalyst is used, which is composed of 67.4 wt% CuO, 21.4 wt% ZnO and 11.1 wt% Al_2O_3, sum is only 99.9 wt%. Prior to synthesis, the catalyst material is reduced in a conventional manner. The adiabatic reactor, which is operated at 80 bar and 240–280 °C, is loaded with 200 kg catalyst, whereas 800 kg is filling the tubular reactor, which is run at approximately 78 bar and 270 °C. Synthesis gas (according to the composition given in Table 4.56) is supplied to the adiabatic reactor at a rate of 11,000 Nm^3 per hour per m^3 of catalyst. The isothermal reactor is fed at a rate of 12,000 Nm^3/m^3 h.

Table 4.56 Typical gas compositions for methanol production from CO_2 according to the Lurgi process

Gas	Adiabatic reactor feed (mol%)	Isothermal reactor feed (mol %)	Isothermal reactor product (mol %)
CO_2	18.5	14.0	11.3
CO	3.6	3.0	2.5
H_2	64.5	69.1	62.0
CH_4	1.3	8.4	9.3
N_2	0.8	5.1	5.6
CH_3OH	4.0	0.3	5.2
H_2O	7.3	0.1	4.1

The amounts of CH_4, CH_3OH, and H_2O in the adiabatic reactor feed results from the process run as a loop process, in which the isothermal reactor product gas is mixed with makeup gas [465]

Cooling results in the formation of steam at 48 bar. From this process, a water-containing product mixture with 63.9 wt% methanol becomes available. For the production of 1,000 kg of that product mixture, 142 kg mol of synthesis gas having the composition stated in Table 4.56 are supplied to the adiabatic reactor. The feeds of both reactors have the SN of 2.066.

4.8.3 The Korean Institute of Science and Technology CAMERE Process

CAMERE stands for carbon dioxide hydrogenation to form methanol via reverse-water-gas-shift-reaction. The process, which has the status of a pilot plant, is a joint development of Korean Pohang Iron and Steel Company and the Korea Electric Power Research Institute funded by the Korean government. The setup consists of a RWGS reactor and a methanol formation reactor [466]. Both reactors are serially connected to remove water in the first reactor and synthesise methanol in the second one. Production capacity of the plant is 100 kg methanol per day. Methanol production yield in the CAMERE process exceeds that of the direct CO_2 hydrogenation without a RWGS reaction by a factor of >2. The pilot plant for methanol synthesis from CO_2 was combined with a pilot plant for the separation of CO_2 discharged from a power plant [467, 468].

In the CAMERE process, CO_2 is converted to CO and H_2O through the RWGS reaction, whereupon the product gas ($CO/CO_2/H_2/H_2O$) is freed from water and fed into the methanol reactor. Each reactor has a recycle stream to increase CO_2 conversion to CO and CO_2 to methanol, respectively. Water produced from the methanol reactor, which is fed back to the RWGS reactor via the recycling gas, is chemically eliminated through a WGS reaction with MUG ($CO/CO_2/H_2$), thus increasing CO_2 conversion to methanol and decreasing the recycle gas amount from the methanol reactor. Methanol productivity of the CAMERE process depends on the CO concentration in the methanol reactor feed, which depends on

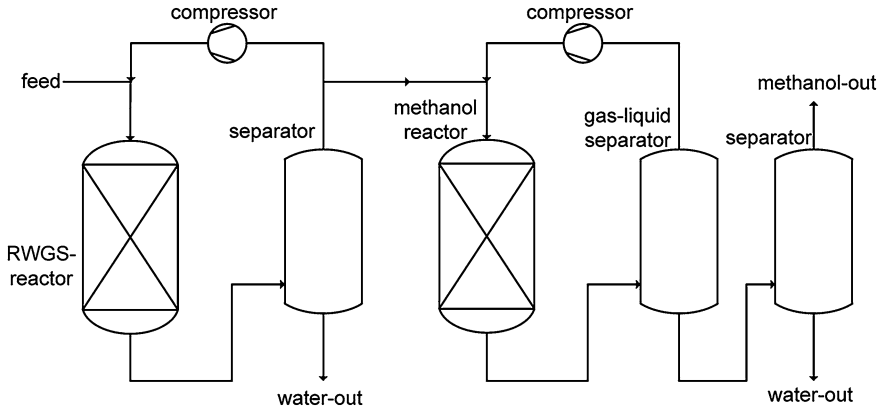

Fig. 4.134 Setup of the CAMERE process [461]

the RWGS reaction conditions (particularly temperature). Figure 4.134 illustrates the setup of the process.

The RWGS reaction is one of the most promising processes for a technically viable CO_2 recycling. In this process, a fraction of the CO_2 feed is converted to CO in a RWGS reactor (Eqs. 4.97–4.99). Thus, the CAMERE process benefits from chemical removal of water produced in the course of methanol synthesis via a WGS. Water is regarded detrimental for methanol synthesis because it deactivates the catalyst. However, because catalyst deactivation goes along with selectivity increase, it depends on the individual process conditions for which degree water removal prior to methanol synthesis is beneficial.

4.8.4 Mitsui's Process for Producing Methanol from CO_2

Another pilot-scale project is operated by Mitsui Chemicals in the Osaka manufacturing complex. Mitsui's catalytic process for producing methanol from CO_2 is based on their proprietary greenhouse gases-to-chemical resources (GTR) technology and that of Carbon Recycling International (CRI). The pilot plant at Osaka has a capacity to produce 100 tonnes/year of methanol and it has been operational since March 2009. An oxidised copper, zinc, aluminium, zirconium and silicon catalyst is used, which was developed within a joint research project with the Kyoto-based RITE. RITE developed several highly active Cu-based, multicomponent catalysts during the early 1990s, which have been tested in the first pilot plant built in 1996; they are capable of producing 50 kg methanol per day from a CO_2/H_2 feed. CO_2 and H_2 are also the major feedstocks used by the Mitsui plant. The hydrogen supplied to the plant stems from waste gases of an ethylene oxide (EO) unit operated by a nearby ethylene manufacturing facility [469].

Despite two patents having been published for the Mitsui approach, there is meager information available on the overall process. The core component is a copper-containing catalyst for the production of methanol. The process is reported to be characterised by including a step in which H_2 and CO_2 are supplied from the upstream side of the catalyst bed of the reactor and a reaction mixture containing methanol, which is obtained from the downstream side of the catalyst bed [470, 471].

4.8.5 The CRI Iceland Demonstration Plant

CRI is an Iceland-based company that produces methanol from CO_2 with the aim of converting it into clean RM fuel. In their Svartsengi plant named after George A. Olah the "George A. Olah Renewable Methanol Plant" and which was completed at the end of 2011, geogenic CO_2 and geothermal heat are used to produce methanol through water electrolysis and CO_2 hydrogenation. Initially, 2 million litres of methanol were intended to be produced per year. CRI planned to expand the plant to produce more than 5 million litres per year by 2012, which in terms of RM fuel corresponds to approximately 2 % of Icelandic gasoline consumption. CRI reports that RM is blendable with established gasoline qualities [472–474].

4.8.6 Catalysts

4.8.6.1 Catalytic Mechanism

In general, the overall mechanism of CO_2-based methanol synthesis can be summarised by reactions in Eqs. 4.97 and 4.99, the latter of which is also known as the RWGS reaction (the most important side reaction). In both reactions, water and CO occur together as the main byproducts, what may impair catalyst performance. Water is able to decrease catalyst activity by blocking coordinatively unsaturated binding sites, [440, 441] whereas CO chemisorbs strongly on Pd catalysts [475–477]. Further byproducts such as dimethyl ether, methyl formate, methane, or higher alcohols are also found, but in most cases with a total selectivity of less than 0.1 %. To improve selectivity for methanol synthesis from CO_2, a thorough understanding of the mechanism behind the reaction is a crucial prerequisite. Today, the so-called formate route (Fig. 4.135) is the most preferred reaction pathway to describe the mechanism, but nevertheless there is still controversy about the formed intermediates during methanol synthesis; in addition, the catalytic mechanism has not entirely been elucidated yet [478–483]. The most important steps of the formate route are described here.

As shown in Fig. 4.135, the reaction begins with the adsorption of hydrogen onto the Cu surface followed by a homogenous splitting (a), which provides atomic hydrogen by spillover (b). Conner et al. described the hydrogen spillover as

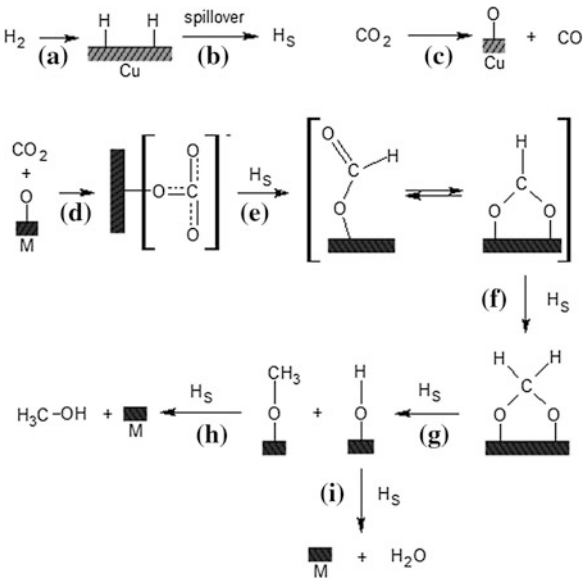

Fig. 4.135 Mechanism of methanol synthesis. (Adapted from [480])

wandering of H atoms over the Cu surface by establishing new bonds to neighbouring Cu atoms [484]. This wandering continues until the H atoms pass the Cu/metal oxide boundary. Beyond the boundary, the H atoms are available for CO_2 reduction. Simultaneously, CO_2 adsorbs onto the catalyst surface, giving way to two competitive reactions. The dissociative adsorption (c) represents one part of the RWGS reaction, leading to CO and adsorbed oxygen. Alternatively, CO_2 adsorbs onto the catalyst surface, where it reacts with adsorbed oxygen to form a carbonate-like transition state (d). Considering the fact that CO_2 also adsorbs on metal oxides such as ZnO, ZrO_2, or Ga_2O_3 for instance, subsequently *M* will be used as a placeholder instead of particular chemical entities.

In the next step, hydrogen supplied by spillover reduces the transition state (d), yielding formate being bound in two different ways to the catalyst surface (e). Of these entities, only the bidentate formate reacts with atomic hydrogen (f). The resulting methylenediol species undergoes a further reduction to yield a catalyst-bound methoxy and hydroxy species each (g). The methoxy species undergoes a final reaction with hydrogen to give methanol, which desorbs as methanol in subsequent course (h). In a consecutive reaction, the remaining hydroxy species is converted to water (i). The rate-determining step of the mechanism is the reduction of the bidentate methyl formate.

In addition to Cu-based catalysts, gallia (Ga_2O_3) supported Pd catalysts show a similar reaction pathway, yet with a few differences [477, 485, 486]. The entire CO_2 hydrogenation takes place on the gallia surface, while the atomic hydrogen is supplied by spillover from Pd [485]. The latter is indispensable, although a dissociative adsorption of hydrogen may take place on the gallia surface alone. However, the subsequent reduction steps only yield methoxy species, and no

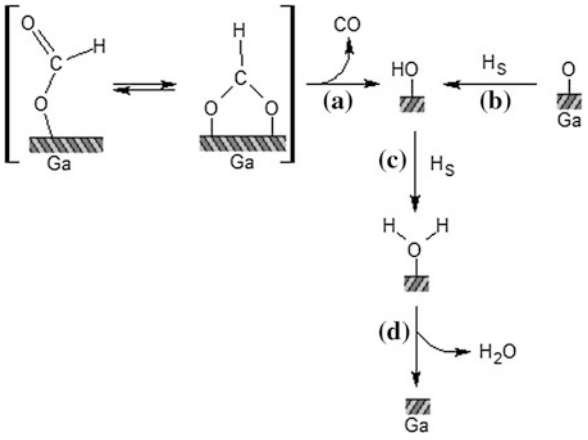

Fig. 4.136 Reverse water-gas shift reaction on a Pd-Ga_2O_3 catalyst. (Adapted from [477])

methanol is formed. Pd is required for the supply of atomic hydrogen on Pd-Ga_2O_3 catalyst surfaces, thus allowing for CO_2 to be reduced to methanol. Considering the rate-limiting step of formate reduction, it is the monodentate formate rather than the bidentate form that reacts with hydrogen to form methoxy species. In fact, the contribution of each individual pathway (mono- and bidentate) to the overall process has not been finally elucidated so far after literature [485, 486]. Another difference compared to Cu-catalysts concerns the RWGS reaction, which takes place on gallia as shown in Fig. 4.136.

First of all, no dissociative adsorption of CO_2 could be observed on gallia-supported Pd-catalysts. Instead of dissociative adsorption, CO is produced by decomposition of monodentate and bidentate formate (a). Similarly to the case of formate decomposition, the reaction of surface-bound oxygen with hydrogen supplied by spillover leads to hydroxyl species (b), from which water is formed in consecutive reactions (c, d) [471].

4.8.6.2 Catalyst Compositions

Due to similar mechanisms, reaction conditions and the fact that minor amounts of CO_2 in the synthesis gas mixture increase the methanol yield, most of the catalyst compositions used for methanol generation from synthesis gas equal those for CO_2 hydrogenation. Particularly in recent decades, a large quantity of catalysts has been examined in terms of selectivity, long-term stability and activity with regard to methanol synthesis [453, 455–461, 487, 488]. Table 4.54 gives a short overview of representative catalysts used in methanol synthesis from synthesis gas.

As mentioned, conventional Cu catalysts were the basis for further catalyst improvements and research. Most of the catalyst systems consist of a noble metal component such as Cu, Re, Pt, Pd, Ag, or Au (hydrogen activation) and some less noble metal oxides, such as ZnO, ZrO_2, Ga_2O_3, or Al_2O_3 (carbon oxide activation). Depending on the fabrication technique, SiO_2, metal oxides, or more recently

Table 4.57 Changes in catalyst properties caused by metal oxides [493]

Catalyst (molar ratio)	X_{CO2} (%)	S_{MeOH} (%)	S_{CO} (%)	Y_{MeOH} (%)
Cu/ZnO (50/50)	27.3	31.9	68.1	8.7
Cu/ZnO/MgO (47/47/6)	19.1	57.0	43.0	9.0
Cu/ZnO/Al_2O_3 (47/47/6)	35.3	64.7	35.3	22.8

Reaction conditions $H_2/CO_2 = 3$, temperature = 493 K, pressure = 13 bar, space velocity = 3,600 h^{-1}

carbon structures such as carbon nanotubes [479] are used as catalyst support. Despite the huge variety of metal–metal oxide combinations, Cu catalysts are still by far the most commonly used catalysts. Aside from catalyst composition, fabrication technique and catalyst pretreatment also have a substantial influence on catalyst properties. Therefore, the size of the catalytic surface is a very important factor because this has a direct outcome on catalytic activity. For more detailed information, see Sect. 4.7.

CO_2-to-methanol hydrogenation catalysts are mostly like those in use for synthesis gas to methanol conversions. After all, it was in the early 1960s when the usefulness of cofeeding CO_2 in methanol production from synthesis gas was discovered [434]. Consequently, catalyst compositions and preparation techniques are the same or at least greatly resemble those used for synthesis gas conversion catalysts. However, hydrogenation of pure CO_2 has some peculiarities that require these protocols to be individually adapted. The major difference between the two starting materials for methanol synthesis, CO_2/H_2, and synthesis gas consists in the production of water in stoichiometric amounts occurring in the course of CO_2 hydrogenation. This side-product formation is generally thought to impair catalyst activity by blocking unsaturated bonding sites [475, 485, 490]. In this context, the catalysts converting CO_2/H_2 have to become more stable and more active to keep up with those catalysing methanol synthesis from synthesis gas. Therefore, changes in catalyst composition are expected to be helpful. Many metal oxides are able to improve the catalytic properties, for which reason using more than one metal oxide is generally regarded as favourable. Table 4.57 shows how catalyst properties can be improved by moving from a binary to a ternary system.

Most metal oxides examined as catalyst promoters are alkali metals, alkaline earth metals, rare earth metals, transition metals, or main group III metals of the boron group. However, not all of them are suitable as catalyst components. Some metal oxides impair catalyst properties and some metal oxides (e.g. most of the rare earth oxides) are simply far too expensive. The most commonly used metal oxides are ZnO, ZrO_2, Al_2O_3 and Ga_2O_3.

ZnO is found in most of the Cu catalysts, where it effectuates an enhanced dispersion of Cu particles, thus increasing catalytic surface area [438, 477, 494, 495]. As described earlier, ZnO also participates in the catalytic mechanism, which renders ZnO as an essential catalyst component. Furthermore, ZnO is capable of retaining small amounts of sulphides, which may contribute to prevent catalyst deactivation [495, 496].

Al_2O_3 represents another often used metal oxide. In particular, the combination of ZnO and Al_2O_3 showed a synergetic effect, resulting in delaying the unavoidable sintering of Cu particles during long-term operation [438, 495, 496]. Al_2O_3 also promotes Cu particle dispersion. However, this effect is not observable with Re or Pd catalysts, for which addition of Al_2O_3 causes massive impairment both of selectivity and activity of the catalysts [493, 497, 498].

Sometimes **ZrO_2** is used instead of Al_2O_3 in ternary catalyst systems. It became apparent that catalysts containing ZrO_2 show a less intensive adsorption of water onto the catalyst surface than those containing Al_2O_3 [477, 498]. Like the latter, ZrO_2 is capable of enhancing Cu particle dispersion, too [438, 500], although this effect is slightly less pronounced than with ZnO [495].

Ga_2O_3 in the form of monoclinic β-Ga_2O_3 is often used in combination with Pd as noble metal component, where it is required for CO_2 adsorption [478, 479, 501]. As an additive of Cu catalysts, Ga_2O_3 prevents the latter from sintering [477]. Furthermore, Ga_2O_3 interacts with Cu in the course of methanol formation and regulates the Cu^0/Cu^+-ratio [438, 502]. Both oxidation states are part of the catalytic mechanism.

Many other metal oxides, such as K_2O [503], B_2O_3 [477], MgO [493], MnO [475], TiO_2 [498], CeO_2, [438] and Cr_2O_3, [493, 504] have also been used as catalyst promoters, although with small effects on methanol synthesis from CO_2 and H_2 only.

4.8.6.3 Catalyst Preparation Techniques

The following section refers mainly to scientific literature. The easiest and most commonly used fabrication technique is to coprecipitate. However, as a matter of course, for the purpose of research there are also other techniques that use impregnation, decomposition of citrate complexes, or gels for catalyst preparation, for instance. Each method affects catalyst activity and long-time stability. Therefore, it is necessary to pay attention to every single step of preparation. In order to basically illustrate catalyst preparation and the influence each preparation step has on the catalytic properties, coprecipitation of a catalyst is exemplified here. For more detailed information on the respective techniques as well as peculiarities of individual catalyst preparation steps, the reader is kindly referred to the original literature cited.

Catalyst preparation commences with dissolving the nitrate salts of the chosen metal components (e.g. $Cu(NO_3)_2/Zn(NO_3)_2/Al(NO_3)_3$) in demineralised water under vigorous stirring according to the desired catalyst composition. During the next step, a Na_2CO_3 solution is added dropwise to precipitate the respective metals, thus furnishing a mesoporous, needle-shaped zincian malachite, $(Cu, Zn)_2(OH)_2CO_3$, which serves as catalyst precursor [505, 506]. Because of the different precipitation pH values of Cu^{2+} and Zn^{2+}/Al^{3+} ions of approximately 3 and 5, respectively, pH has to be kept at 7.

Table 4.58 Influence of aging time [476]

Aging time (h)	Sodium content (wt%)	BET surface (m^2/g)	X_{CO2} (%)	S_{MeOH} (%)	Y_{MeOH} (%)
0.5	3.4	42	7.7	14.9	1.15
12	1.3	74	19.6	23.8	4.66
24	0.8	99	19.4	29.3	5.68

Reaction conditions temperature = 523 K, pressure = 30 bar, $H_2/CO_2 = 3$, $\dot{V} = 50\,\text{mol/min}$
Catalyst $Cu/ZnO/ZrO_2$ (average molar ratio: 48/45/7)

In some experiments to improve the catalyst precursor formation, use of the respective metals' formate salts are claimed to be superior to nitrates. The formate ion can serve as ligand and buffer during the precipitation procedure, thus leading to catalysts with higher activities in methanol synthesis [507]. Precipitation temperature is another important parameter. For instance, $Cu/ZnO/ZrO_2/Al_2O_3/Ga_2O_3$ catalyst activity was observed to decrease by 7 % upon raising precipitation temperature from 0 to 60 °C [508]. Before filtering, the precipitate is aged in its solution under continuous stirring for a certain period of time. This is an essential process step because—among other consequences—aging time has an effect on sodium content of the catalyst, and sodium remainders in the catalyst impair the development of fine catalyst structures, thus reducing catalytic surface and activity. According to Chiavassa et al. a long aging time is favoured to decrease sodium content stepwise, while at the same time activity, selectivity and methanol yield benefit from this measure (Table 4.58).

After filtering, the filter cake is extensively washed with distilled water and dried at 120 °C. The dry filter cake is then calcined at 350 °C for a several hours, causing the mesoporous catalyst precursor to decompose to the corresponding nano-structured metal oxides and CO_2. In laboratory experiments, the sieved catalyst is now ready for the reduction step. For these purposes, in the laboratory a mixture of H_2 and a noble gas such as helium or argon is used to reduce CuO slowly to Cu^0. This reduction process is an exothermic reaction that may cause the Cu particles to sinter on the catalyst surface. This undesired effect can be avoided by keeping hydrogen at <10 vol%. It is important to note, however, that not all CuO is reduced. In fact, both species, Cu^0 and Cu^+, are involved in the catalytic mechanism. After finishing the reduction step, the catalyst is ready for use.

Apart from coprecipitation of carbonates, water-insoluble metal citrate complexes were also examined [477]. For these purposes, a solution of citric acid is added slowly to the dissolved nitrates to precipitate the metal citrate complexes. From this step on, the procedure follows the one described above.

A special technique, so-called oxalate gel coprecipitation, works with metal nitrates and oxalic acid separately dissolved in absolute ethanol [509, 510]. Precipitation is conducted by mixing the two solutions at ambient temperature under vigorous stirring. The centrifuged precipitate consisting of isomorphic substituted oxalates exhibits the consistence of a gel, which during drying shrinks to one-fifth of the former volume. Compared to catalysts prepared by the carbonate and

Table 4.59 Comparison of fabrication techniques [478]

Method	X_{CO2} (%)	S_{MeOH} (%)	Y_{MeOH} (%)
Carbonate coprecipitation	15.8	22.8	3.6
Oxalate coprecipitation	19.3	22.3	4.3
Gel oxalate coprecipitation	19.3	36.3	7.0

$Cu/ZnO/Al_2O_3$-catalyst (molar ratio: 45/45/10)
Reaction conditions temperature = 513 K, pressure = 20 bar, $H_2/CO_2 = 3$, space velocity = 3,600 h^{-1}

oxalate coprecipitation method, respectively, catalysts prepared by the latter method gave a much higher methanol yield (Table 4.59).

During calcination release of CO formed from oxalate, decomposition emerged as detrimental. CO is very reactive under calcination conditions and reduces CuO and ZnO to the corresponding metals [487]. The heat released during the exothermic reduction may cause Cu particles to agglomerate, thus impairing catalyst activity. This can be avoided by choosing a moderate temperature increase rate under the addition of fresh air in order to oxidise CO to CO_2.

The impregnation method may be used, particularly for catalysts with expensive components such as platinum group metals. This method allows for synthesising the catalysts with a very low amount of the expensive metallic component. For example, a Pd/β-Ga_2O_3-catalyst (1 wt% Pd) was produced by impregnating a β-Ga_2O_3-surface with a solution of palladium(II)-acetate in acetone. After drying, calcination and reduction in the H_2/Ar stream, the catalyst is ready for methanol synthesis from CO_2 [485].

4.8.7 Alternative Approaches

Because catalysts are inhibited by reaction water, as alternatives to the previously described prereactor membranes were examined. For these purposes, the membrane is used to remove water and/or methanol in situ from the reactor system. In this regard, a Nafion membrane from DuPont [509–511] and a special silica/alumina-membrane [512–514] were found to be suitable for removing water and methanol faster than the gaseous components. Due to the shift of the equilibrium towards the side of the products, membrane reactors were supposed to achieve higher methanol yields. In fact, both membranes were capable of increasing methanol yield by 50 % compared to a fixed-bed reactor operating at the same reaction conditions. The results are summarised in Table 4.60.

However, membranes suffer from an insufficient stability, for which reason temperature and pressure have to be lower than what is usually applied for fixed-bed reactors. As a result, the catalysts will not be operable at optimal conditions. Even worse in this context, there are opposing membrane characteristics. Nafion membranes, for instance, can be operated up to 200 °C, while their selectivity for

Table 4.60 Results of the examined membrane reactors [485, 488]

Membrane	Nafion	Silica/Alumina
Flow mode	Countercurrent	Parallel flow
Pressure (bar)	4.3	3
Temperature (°C)	200	200
H_2/CO_2 ratio	3:1	3:1
GHSV (h^{-1})	1,000	3,000
Catalyst	Cu/ZnO	Cu/ZnO
Methanol yield (%)	3.6	3.4
Fixed-bed reactor[a] (%)	2.4	2.3

[a] Methanol yield of the comparable fixed-bed reactors, working under the same conditions

methanol and water are optimal at far higher temperature levels. In fact, methanol and water selectivity are rather meager within the operating range of organic membranes. Inorganic membranes, such as the silica/alumina-membrane, which were once regarded as a loophole, display the same characteristics. This is the background for the relatively low methanol yields of membrane reactors, which range between 3.4 and 3.6 %.

Another process design addresses the heat released during methanol synthesis, which promotes slow sintering of Cu particles on the catalyst surface. To improve heat removal, methanol synthesis is conducted in an inert liquid. This so-called LPMeOH process (from liquid-phase methanol) was initially developed for conventional methanol synthesis from synthesis gas by Chem Systems in 1975 (see Sect. 4.6). In the 1990s, research eventually was directed to investigating catalysts applicable in liquid-phase CO_2-based methanol synthesis [515–517]. Apart from improved heat removal, liquid-phase methanol synthesis also benefits from the option to recover product methanol through extraction of the solvent–water mixture leaving the reactor [515]. On the other hand, solvent molecules may also adsorb on the catalyst surface, thus impairing catalyst activity [518]. However, although this concept proved successful, it has never left laboratory status. Indeed, one has to bear in mind that methanol synthesis from CO_2/H_2 releases only half of the heat produced in conventional methanol synthesis from synthesis. In conclusion, fixed-bed reactors are much easier to handle compared to LPMeOH reactors—the shortcomings of which cannot be compensated for in CO_2 hydrogenation.

Another approach considers hydrogenation of CO_2 bubbled through an alkaline suspension of a photocatalyst by irradiating with visible light/ultraviolet radiation at the same time. The STYs of such photocatalysts are still more than three orders of magnitude lower than those of conventional catalysts. At present, experiments with photocatalysts applied for methanol synthesis are constrained to laboratory use only [519–521].

Homogeneously catalysed CO_2 hydrogenation using metal organic catalysts, such as ruthenium triphos complexes dissolved in anhydrous THF, offer another option for producing methanol under mild reactions conditions, but with comparatively low TON [522]. Also, this approach is far from being applicable on a pilot scale.

4.8.8 Conclusion

Today, the CO_2-to-methanol technology is (at least in principle) state of the art, allowing for an active reduction of CO_2 emissions by simultaneously exploiting CO_2 as a basic commodity for industrial methanol production. Improvements of process and catalyst systems are desirable but not mandatory. The two severe impediments for commercialisation of this technology are (1) the commercially feasible production of renewable hydrogen from various energy sources and (2) the economically feasible production of clean CO_2 from waste gas streams. The various technologies require individual investments, which depend on the geographical, geological and climatic conditions of the specific location for the realisation of the particular approach.

References to Chapter 4

1. G.A. Olah, A. Goeppert, G.K. Surya Prakash, *Beyond Oil and Gas: The Methanol Economy* (Wiley-VCH, Weinheim, 2006)
2. Q. Zhang, D. He, Q. Zhu, J. Natural Gas Chemistry **12**, 81–89 (2003)
3. R.A. Periana, G. Bhalla, W. Tenn, K. Young, X.Y. Liu, O. Mironov, J. Cj, J. Mol. Catalysis A: Chemical **220**(1), 7–25 (2004)
4. R. Palkovits, M. Antonietti, P. Kuhn, A. Thomas, F. Schüth, Angew. Chem. Int. **48**, 6909–6912 (2009)
5. T.V. Choudary, D.W. Goodman, Catalysis **19**, 164–183 (2006)
6. H.F. Abbas, W.M.A. Wan Daud, Int. J. Hydrogen Energy **35**, 1160–1190 (2010)
7. N. Muradov, Int. J. Hydrogen Energy **26**, 1165–1175 (2001)
8. N. Muradov, T.N. Veziroglu, Int. J. Hydrogen Energy **30**, 225–237 (2005)
9. M. Merkx, D. Kopp, M. Sazinsky, J. Blazyk, J. Müller, S.J. Lippard, Angew. Chem. **113**, 2860–2888 (2001)
10. S.I. Chan, Y.-J. Lu, P. Nagababu, S. Maji, M.-C. Hung, M.M. Lee, I.-J. Hsu, P.D. Minh, J.C.-H. Lai, K.Y. Ng et al., Angew. Chem. Int. Ed. **52**, 3731–3735 (2013)
11. Y. Dongi, S. Meyer, Int. J. Hydrogen Energy **22**, 971–977 (1997)
12. G.A. Olah, G.K.S. Prakash, US 7704369, 2010
13. L.J. Frost, J. Hartvigsen, S. Elangovan, *Formation of Synthesis Gas Using Solar Concentrator Photovoltaics (SCPV) and High Temperature Co-electrolysis (HTCE) of CO2 and H2O*, OTC-20408-PP 2010 Offshore Technology Conference held in Houston, May 2010
14. J.G. van Bennekom, R.H. Venderbosch, H.J. Heeres in *Biodiesel—Feedstocks, Production and Applications* ed. by Z. Fang (InTech, 2012)
15. P.D. Vaidya, A.E. Rodrigues, Chem. Eng. Technol. **32**, 1463–1469 (2009)
16. W.O. Oduru, D.J. Redman, S.C.E. Tsang, EP 2279160 A1, 2011
17. www.isis-innovation.com, 22 May 2013

References to Section 4.1

18. J. Schulte, Process **5**, 8–10 (2011)
19. DERA-German Minerals Resources Agency, Annual Report, (2012), p.12

20. http://commons.wikimedia.org/wiki/File:HydroFrac_de.svg. 17 July 2013
21. BP, *Statistical Review of World Energy* (2013), p. 21
22. EIA Annual Energy Outlook 2013, AEO 2013 Early Release Presentation Washington, 5 Dec 2012
23. http://commons.wikimedia.org/wiki/File:HydroFrac_de.svg, 17 July 2013
24. US Energy Information Administration, 09 May 2011
25. BP, *Statistical Review of World Energy* (2013), p. 27
26. International Energy Agency (IEA), *World Energy Outlook* (2012)
27. BP, *Statistical Review of World Energy* (2013), pp. 31–34
28. C. Higman, M. van der Burgt, *Gasification* (GPP Gulf Professional Publishing, Elsevier, Amsterdam [etc.], 2008)
29. R. Dittmeyer, W. Keim, G. Kreysa, A. Oberholz (eds), Winnacker-Küchler: Chemische Technik—Prozesse und Produkte, 5th edn, vol. 4 (Wiley-VCH, Weinheim, 2006), p. 807
30. A. Bandi, M. Specht, *Gewinnung von Methanol aus Biomasse, Expertise im Auftrag der Union zur Förderung von Oel- und Proteinpflanzen e.V. (UFOP)*, Zentrum für Sonnenenergie und Wasserstoff-Forschung Baden-Württemberg (ZSW), Stuttgart, 2004
31. M. Mittelbach, Methanolgewinnung aus Biogas, Machbarkeitsstudie im Auftrag von Ökostrom Mureck GmbH, Land Steiermark, Graz, 2005
32. M. Specht, A. Bandi, *The Methanol-Cycle—Sustainable Supply of Liquid Fuels*, Center for Solar Energy and Hydrogen Research (ZSW), Themes 98/99 (Stuttgart, 1999) pp. 59–65
33. X. Yin, D.Y.C. Leung, J. Chang, J. Wang, Y. Fa, C. Wu, Energy Fuels **19**, 305–310 (2005)
34. M. Specht, A. Bandi, F. Baumgart, C.N. Murray, J. Greetz, in *Greenhouse Gas Control Technologies*, ed. by B. Eliasson, P.W.F. Riemer, A. Wokann (Pergamon, Amsterdam, 1999)
35. K.N. Wyatt, *Catalytic Production of Methanol from Biogas*. GB 2,375,353, 2002
36. F. Asinger, *Methanol- Chemie- und Energierohstoff* (Akademie, Berlin, 1987) pp. 17–19
37. Food and Agriculture Organization of the United Nations, *Global Forest Ressources Assessment—Progress towards sustainable forest management*, *FAO Foresty Paper 147*, Rome, 2005
38. F. Behrend, Y. Neubauer, M. Oevermann, B. Wilmes, N. Zobel, Chem. Eng. Technol. **31**(5), 667–677 (2008)
39. http://foris.fao.org/static/data/fra2005/maps/2.2.jpg, 30 May 2013
40. M. Kaltschmitt, H. Hartmann, H. Hofbauer, H. (eds), *Energie aus Biomasse: Grundlage, Techniken und Verfahren* (Springer, Berlin Heidelberg, 2009), p. 377 ff
41. N. Dahmen, E. Dinjus, Chem. Ing. Tech. **82**(8), 1147–1152 (2010)
42. Chemrec—Company Presentation, *Transformative Biorefinery Technology for Forest, Biofuels and Power Industries*, 2010
43. R. Rauch, Advanced biofuels by gasification—Status of R&D work in Güssing, Conference Highlights aus der Bioenergieforschung V, Wieselburg, 2011
44. Uhde Company Profile, online: www.uhde.eu, 25 Dec 2011
45. http://www.bioliq.de/, 30 May 2013
46. http://www.biodme.eu/, 30 May 2013
47. T. Rostrup-Nielsen, P.E. Højlund, F. Jøensen, J. Madsen, *Polygeneration—integration of gasoline synthesis and IGCC power production using Topsøe's TIGAS Process*, in Risø International Energy Conference (Roskilde, 2007) pp. 56–68
48. http://www.methanol.org/, 30 Dec 2011
49. State of Europe's Forest, *The MCPFE Report on Sustainable Forest Management in Europe*, Warsaw, 2007, p. 182
50. ZMP GmbH, Bonn, www.zmp.de, 23 June 2008
51. http://www.biogasportal.info/, 26 Dec 2011
52. Fachagentur Nachwachsender Rohstoffe e.V. Biogas Basisdaten Deutschland, 2008
53. Fachagentur Nachwachsender Rohstoffe e.V. Bestandsentwicklung der Biogasanlagen in Deutschland, 2011
54. Broschüre des Fachverbandes Biogas Multitalent Biogas, Berlin, 2008

55. S. Majer, A. Gröngröft, Ökologische und ökonomische Bewertung der Produktion von Biomethanol für die Biodieselherstellung, DBFZ-Studie, Leipzig, 2010
56. Statistisches Bundesamt Deutschland, Pressemitteilung Nr. 050 vom 08.02.2011
57. R. Rölle, *Stoffliche Verwertung von Klärschlamm durch Vergasung*, Tagungsband der 6 (AWL-Tech, Sinsheim, 2002)
58. S. Lechtenböhmer, S. Nanning, B. Hillebrand, H.-G. Buttermann, *Einsatz von Sekundärbrennstoffen* (Umweltbundesamt, Dessau, 2006). Texte 07/06
59. H. Charisius, Technol. Rev. **1**, 38 (2010)

References to Section 4.2

60. T. Wurzel, Lurgi MegaMethanol® technology-Delivering the building blocks for the future fuel and monomer demand. Oil Gas Eur. Mag. **2**, 92–96 (2007)
61. C. Higman, M. van der Burgt, *Gasification* (GPR, 2006)
62. G.A. Olah, A. Goeppert, G.K. Surya Prakash, *Beyond Oil and Gas: The Methanol Economy*, 2nd edn (Wiley-VCH, Weinheim, 2009)
63. C. Sing, K. Liu, C. Song, V. Subramani (eds.), *Hydrogen and Syngas Production and Purification Technologies* (AIChE, Wiley, Copyright 2010 by American Institute of Chemical Engineers)

References to Section 4.3

64. K. Aasberg-Petersen, I. Dybkjær, C.V. Ovesen, N.C. Schjødt, J. Sehested, S.G. Thomsen, J. Nat. Gas Sci. Eng. **3**, 423–459 (2011)
65. W. Hilsebein, "*Gas to Methanol*", Lurgi Presentation (2006)
66. P. Häussinger, R. Lohmüller, A. Watson, *Ullmann's Encyclopedia of Industrial Chemistry* (Wiley-VCH, Weinheim, 2003)
67. N. Ringer, JJ&A Methanol Forum, Houston, 2010
68. J.J. Philipson, *Catalyst Handbook* (Wolfe Scientific Books, London, 1970), p. 46
69. C. Ratnasamy, J.P. Wagner, Catal. Rev. **51**, 325–440 (2009)
70. K. Aasberg-Petersen, T.S. Christensen, I. Dybkjaer, J. Sehested, M. Ostberg, R.M. Coertzen, M.J. Keyser, A.P. Steynberg, *Studies in Surface Science and Catalysis. Fischer-Tropsch Technology* (Elsevier, Amsterdam, 2004), pp. 258–405
71. J.T. Richardson, J.D. Ortego, N. Coute, M.V. Twigg, Catal. Lett. **41**, 17–20 (1996)
72. P. Broadhurst, in *Hydrocarbon Processing*, Mar 2006
73. P. Broadhurst, Hydrocarbon Eng. **11**(71–72), 74–75 (2006)
74. M.C. Annesini, V. Piemonte, L. Turchetti, *Chemical Engineering Transactions* (2007), pp. 21–26
75. P.E.J. Abbott, M. McKenna, GB2407818, 2005
76. G. Jones, J.G. Jakobsen, S.S. Shim, J. Kleis, M.P. Andersson, J. Rossmeisl, F. Abild-Pedersen, T. Bligaard, S. Helveg, B. Hinnemann et al., J. Catal. **259**, 147–160 (2008)
77. A. Yamaguchi, E. Iglesia, J. Catal. **274**, 52–63 (2010)
78. J. Wei, E. Iglesia, Angew. Chem. Int. Ed. **43**, 3685–3688 (2004)
79. J. Wei, E. Iglesia, Phys. Chem. Chem. Phys. **6**, 3754–3759 (2004)
80. J. Wei, E. Iglesia, J. Catal. **225**, 116–127 (2004)
81. J. Wei, E. Iglesia, J. Catal. **224**, 370–383 (2004)
82. J. Wei, E. Iglesia, J. Phys. Chem. B **108**, 7253–7262 (2004)
83. J. Wei, E. Iglesia, J. Phys. Chem. B **108**, 4094–4103 (2004)
84. J. Rostrup-Nielsen, J. Catal. **144**, 38–49 (1993)
85. D. Qin, J. Lapszewicz, Catal. Today **21**, 551–560 (1994)

86. S. Helveg, C. López-Cartes, J. Sehested, P.L. Hansen, B.S. Clausen, J.R. Rostrup-Nielsen, F. Abild-Pedersen, J.K. Nørskov, Nature **427**, 426–429 (2004)
87. F.B. Rasmussen, J. Sehested, H.T. Teunissen, A.M. Molenbroek, B.S. Clausen, Appl. Catal. A **267**, 165–173 (2004)
88. J. Sehested, A. Carlsson, T.V.W. Janssens, P.L. Hansen, A.K. Datye, J. Catal. **197**, 200–209 (2001)
89. Catalyst Brochure Clariant Deutschland GmbH http://www.catalysts.clariant.com/bu/catalysis/internet.nsf/023cfbb98594ad5bc12564e400555162/2345da075fc114efc1257ad0002d2c00?OpenDocument
90. Haldor Topsøe A/S, R-67-7H, can be found under http://www.topsoe.com/business_areas/ammonia/processes/~/media/PDF%20files/Steam_reforming/Topsoe_steam_reforming_cat_r%2067%207h.ashx
91. Haldor Topsøe A/S, RK-200 Series, can be found under http://www.topsoe.com/business_areas/ammonia/processes/~/media/PDF%20files/Steam_reforming/Topsoe_steam_reforming_cat_rk%20200_series.ashx
92. Johnson Matthey Group, Katalco. Steam reforming catalysts Natural gas, associated gas and LPG, can be found under http://www.jmcatalysts.com/ptd/pdfs-uploaded/Steam%20Reforming%20Feb%2007.pdf
93. S. Zhao, Y. Cai, J. Ladebeck, US7378369, 2008
94. Private Communication Clariant Deutschland GmbH
95. H. Yamashita, A. Kato, S. Uno, M. Mizumoto, S. Matsuda, EP0130835, 1984
96. G. Burgfels, K. Kochloefl, US4906603, 1990
97. K. Aasberg-Petersen, C.H. Christensen, C.S. Nielsen, I. Dybkjær, Fuel Chem. Div. Prepr. **47**, 96–97 (2002)
98. J.R. Rostrup-Nielsen in *Catalysis, Science and Technology* ed. by J.R. Anderson, M. Boidart (Springer, Berlin, 1984), p. 1
99. C.H. Bartholomew, Appl. Catal. A **212**, 17–60 (2001)
100. F.B. Rasmussen, J. Sehested, H.T. Teunissen, A.M. Molenbroek, B.S. Clausen, Appl. Catal. A **267**, 165–173 (2004)
101. J. Sehested, Catal. Today **111**, 103–110 (2006)
102. J. Sehested, J. Catal. **223**, 432–443 (2004)
103. J. Sehested, J. Catal. **217**, 417–426 (2003)
104. J.R. Rostrup-Nielsen, J. Sehested, J.K. Nørskov, J. Catal. **217**, 65–139 (2003)
105. J. Boon, E. van Dijk, Adiabatic Diesel Pre-reforming. Literature Survey, can be found under http://www.ecn.nl/docs/library/report/2008/e08046.pdf
106. Haldor Topsøe A/S, RKNGR: Topsøe RKNGR Prereforming Leaflet (2001), can be found under http://www.topsoe.com
107. D. Shekhawat, D.A. Berry, T.H. Gardner, J.J. Spivey, Catal. Rev. **19**, 184–254 (2006)
108. Shanghai YOSO Chem&Tech Co., Ltd., Naphtha Steam Pre-reforming Catalyst (ys-z501), can be found under http://yosochem.en.busytrade.com/selling_leads/info/2256262/Naphtha-Steam-Pre-reforming-Catalyst-ys-z501-.html
109. Johnson Matthey Group, Katalco. Delivering world-class methanol plant performance, can be found under http://www.jmcatalysts.com/ptd/pdfs-uploaded/Methanol%20Top%20level%20Feb%2007.pdf
110. S. Muschelknautz, P. Fritz, *Syngas and Hydrogen Production for Chemical and Refinery Applications based on Natural Gas and other Feedstocks*, ACHEMA, 2012
111. Süd-Chemie (now Clariant AG), *Syngas Technical Manual* (2006)
112. Süd-Chemie (now Clariant AG), *Catalyst Brochure, ReforMax Catalysts for Primary Reforming*, Product Bulletin (2011)
113. M.N. Pedernera, J. Piña, D.O. Borio, V. Bucalá, Chem. Eng. J. **94**, 29–40 (2003)
114. B. Hartvigsen, *Haldor Topsøe A/S Steam Reforming Technology User Conference*, 2007
115. R. Elshout, *Energy, Systems Engineering. Hydrogen Production by Steam Reforming*, posted in Chemical Engineering Processing 2010
116. M.N. Pedernera, J. Piña, D.O. Borio, V. Bucalá, Chem. Eng. J. **94**, 29–40 (2003)

117. Nexant PERP Study, 2008
118. J.R. Rostrup-Nielsen in *Handbook of Heterogeneous Catalysis* ed. by G. Ertl, H. Knözinger, F. Schüth, J. Weitkamp (Wiley-VCH, Weinheim, 2008)
119. http://commons.wikimedia.org/wiki/File:Straight-tube_heat_exchanger_1-pass.PNG. Last modified 28 May 2006
120. http://en.wikipedia.org/wiki/Heat_exchanger. Page was last modified on 6 June 2013
121. T. Wurzel, Oil Gas Eur. Mag. 92 (2007)
122. P.K. Bakkerud, Catal. Today **106**, 30–33 (2005)
123. Haldor Topsøe A/S, RKS-2-7H Secondary reforming catalyst, can be found under http://www.topsoe.com/business_areas/ammonia/~/media/PDF%20files/Steam_reforming/Secondary_reforming_catalyst_RKS%202%207H.ashx
124. Made-in-China.com, Secondary Reforming Catalyst (SPR-202), can be found under http://www.made-in-china.com/showroom/suncatalysts/product-detailJqNxAhnVvEcK/China-Secondary-Reforming-Catalyst-SPR-202-.html
125. H. Göhna, Nitrogen **224**, 31–38 (1996)
126. J. Wagner, *MegaMethanol Technology, most economical and reliable technology for the new generation of Methanol plants*. Süd-Chemie Conference "Defing the Future", Bahrein, 2004
127. H. Schlichting, Update on lurgi syngas technologies. Gasification Technologies, San Francisco, 2003
128. Anon, *Nitrogen + Syngas*, **316**, 50–61 (2012)

References to Section 4.4

129. DOE, US department of Energy, *Gasification* 2010, worldwide database
130. T. Kolb, Brennstoffe 2, Karlsruhe, Karlsruher Institut für Technologie, Engler-Bunte-Institut, Chemische Energieträger und Brennstofftechnologie, Vorlesungsscript (2011)
131. A.-G. Collot, *Matching gasifiers to coals* (International Energy Agency, 2002)
132. C. Higman, *Gasification* (Elsevier, Burlington, 2003)
133. D.W. van Krevelen, *Coal: Typology, Physics, Chemistry, Constitution* (Elsevier, Delft, 1993)
134. A. Faaij, Modern biomass conversion technologies. Mitig. Adapt. Strat. Glob. Change **11**, 335–367 (2006)
135. G. Schaub, *Brennstoffe 1—Grundlagen, flüssige Brennstoffe, Erdölverarbeitung, BioBrennstoffe*, Karlsruhe, Karlsruher Institut für Technologie, Engler-Bunte-Institut, Chemische Energieträger und Brennstofftechnologie, Vorlesungsscript, 2011
136. American Coal Foundation, *Coal's Past, Present, and Future* (Online), http://teachcoal.org/. Accessed 2011
137. Gasification Technology Council, *Gasification—An investment in our future* (Online), www.gasification.org. Accessed 2010
138. R. Cheeley, Coal Gasification for DRI Production—An Indian Solution. Steel Times Int. (2010)
139. O. Turna, Lurgi GmbH, personal communication (based on process calculations)
140. H.J. Mühlen, F. Sowa, K.H. van Heek, Comparison of the gasification behavior of a West and East German brown coal. Fuel Process. Technol. **36**, 185–191 (1993)
141. R.F. Probstein, R.E. Hicks, *Synthetic fuels* (McGraw-Hill Book, New York, 1990)
142. SFA-Pacific, *Gasification: Worldwide Use and Acceptance*, US Department of Energy, Office of Fossil Energy, National Energy Technology Laboratory, Gasification Technology council, 2000
143. O. Turna, Utilization of Sasol-Lurgi fixed bed bottom gasifcation for syngas production, Sasol Technology, R&D division, 2000
144. E. Supp, *How to produce methanol from coal* (Springer-Verlag, 1989)

145. G. Baron, Entwicklungsprobleme bei der technischen Vergasung fester Brennstoffe unter erhöhtem Druck nach dem Lurgi-Verfahren für die Erzeugung von normgerechtem Stadtgas, Universität (TH) Karlsruhe, Dissertation, 1963
146. D.E. Woodmansee, Modeling of fixed bed gas producer performance. Energy Commun. **2**, 13–44 (1976)
147. M. Hobbs, *Modeling Countercurrent Fixed-bed Coal Gasification.* Brigham Young University, PhD, Brigham, 1990
148. P.R. Desai, C.Y. Wen, *Computer Modeling of the MERC Fixed Bed Gasifier* (U.S. Department of Energy, Morgantown, West Virginia, 1978)
149. N.R. Amundson, L.E. Arri, Char Gasification in a Countercurrent Reactor. AIChE J. **24**, 87 (1978)
150. R. Stillman, Simulation of a Moving Bed Gasifier for a Western Coal. IBM J. Res. Dev. **240**(s.1) 23 (1979)
151. H. Yoon, *Modeling and Analysis of Moving Bed Coal Gasifiers*, Universtiy of Delaware, Newark, PhD, 1978
152. Y.S. Cho, B. Joseph, Heterogeneous model for moving-bed coal gasification reactor. Ind. Eng. Chem. Process Des. Dev. **20**, 314 (1981)
153. M. Kim, B. Joseph, Dynamic behavior of moving-bed coal gasifiers. Ind. Chem. Process Des. Dev. **22**, 212 (1983)
154. W. Yu, M. Denn, Radial effects in moving-bed coal gasifiers. Chem. Eng. Sci. **38**, 1467 (1983)
155. J.R. Bunt, F.B. Waanders, An understanding of lump coal physical property behaviour (density and particle size effects) impacting on a commercial-scale Sasol-Lurgi FBDB^{TM} gasifier. Fuel **87**, 2856–2865 (2008)
156. H.-P. Schilling, B. Bonn, U. Krauss, *Coal gasification: existing processes and new developments* (Graham & Trotman, London, 1981)
157. F. Rodriguez-Reinoso, *Controlled gasification of carbon and pore structure development.* NATO advanced study institute, Cadarache (Kluwer Academic Publishers, France, 1990)
158. K.J. Daniel, *Transist Model of a Fixed-Bed Gasifier*, presented at AIChE, 88th National meeting, 1980
159. K. Hedden, Die Bedeutung der Reaktionsfähigkeit des Brennstoffs für koksbeheizte Schachtöfen. Chem. Eng. Sci. **14**, 317–330 (1961)
160. A. Kristiansen, *Understanding coal gasification* (IEA Coal Research, London, 1996)
161. M.F. Ifran, M.R. Usman, K. Kusakabe, Coal gasification in CO_2 atmosphere and its kinetics since 1948: a brief review. Energy **36**, 12–40 (2011)
162. C.Y. Wen, *Coal Conversion Technology* (Addisoon-Wesley Publishing, Reading, Massachusetts, 1979)
163. N.M. Laurendeau, Heterogeneous kinetics of coal cahr gasification and combustion. Prog. Energy Combust. Sci. **4**, 221–270 (1978)
164. J.L. Johnson, Kinetics of bitumious coal char gasification with gases containing steam and hydrogen, *Kinetics of coal gasification* (Wiley, New York, 1979)
165. S. Kajitani, N. Suzuki, M. Ashizawa, S. Hara, CO_2 gasification rate analysis of coal char in entrained flow gasifier. Fuel **85**, 162–169 (2006)
166. H. Marsh, *Introducing in Coal Science* (Butterwoth, London, 1989)
167. C. Natterman, Research on the pressurised gasification of coal with steam and carbon dioxide, *Erdöl und Kohle. Erdgas, Petrochemie vereinigt mit Brennstoff*-Chemie, **47**, 287–295 (1994)
168. R. Kandiyoti, A. Herod, K. Bartle, *Solid Fuels and Heavy Hydrocarbon Liquids* (Elsevier, Oxford, UK, 2006)
169. F. Kapteijn, J.A. Moulijn, Kinetics of catalysed and uncatalysed coal gasification, in *Carbon and Coal Gasification–Science and Technology*, Alvor, Portugal, 20–31 May 1985
170. Z. Ma, A study on the intrinsic kinetics of steam gasification of Jincheng coal char. Fuel Process. Technol. **31**, 69–76 (1992)

171. G. Liu, Mathematical modeling of coal char reactivity with CO_2 at high pressures and temperatures. Fuel **79**, 1145–1154 (2000)
172. Q. Xu, S. Pang, T. Levi, Reaction kinetics and producer gas compositions of steam gasification of coal and biomass blend chars, part 2: mathematical modelling and model validation. s.l. Chem. Eng. Sci. **10**, 2232–2240 (2011)
173. M. Weeda, H.H. Abcouwer, F. Kapteijin, J.A. Moulijn, Steam gasification kinetics and burn-off behaviour for a bituminous coal derived char in the presence of H_2. Fuel Process. Technol. **36**, 235–242 (1993)
174. A. Megaritis, Y. Zhuo, R. Messenböck, Pyrolysis and gasification in a bench-scale high-pressure fluidised-bed reactor. Energy Fuels **12**, 144–151 (1998)
175. J.R. Arthur, Reactions between Carbon and Oxygen. Chem. Soc. J. Faraday Trans. **47**, 164–178 (1951)
176. G. Schaub, Experimentelle und Mathematische Simulation der Kohlevergasung in Festbettreaktoren, Frankfurt a. M., Interner Bericht, Lurgi GmbH (1986)
177. C.P.P. Singh, D.N. Saraf, Simulation of high-temperature water-gas shift reactors. Ind. Eng. Chem. Process Des. Dev. **16**(3), 313–319 (1977)
178. O. Levenspiel, Chemical reaction engineering, 3rd edn (Wiley, New York, 1999)
179. M. Bearns, *Chemische Technik* (Wiley-VCH, Weinheim, 2006)
180. G. Schaub, Gas production from coal, wood and other solid feedstocks, in *Ullmann's Encycloedia of Industrial Chemistry* (VCH Verlagsgesellschaft, Weinheim, 1989)
181. E. Supp, *How to produce methanol from coal* Berlin, Springer, 1990
182. A. Guenther, Gasification of biomass for 2nd generation fuels, Achema presentation, 2012
183. M. Taijma, J. Tsunoda, Status of the EaGLE gasification pilotplant. Paper presented at the Gasification technologies conference San Francisco, 2002
184. Z. Yu, G. Yu, Opposed multiburner gasification technology, seven new projects in China. Paper presented at the gasification technology conference San Francisco, 2007
185. H. Hiller, Gasproduction (Wiley-VCH, Weinheim, 2007)
186. W. Renzenbrink, K.J. Wolf, J. Ewers, RWE's Cero-CO_2 IGCC power plant: first steps towards commercial implementation. Paper presented at the 2nd International Freiberg conference on IGCC and XTL technologies, 2007
187. O. Turna, *Moving Bed gasification of coal and substitutes,* Dechema Kolloqium, Frankfurt, 4 April 2008
188. R. Pardemann, B. Meyer, Stand und Perspekiven der Kohlenutzung in Kraftwerken mit Vergasung. CIT **11**, 1805–1819 (2011)
189. L. Plass, M. Wagner, *Production of Synthetic Biofuels for the Bure Project in France*, 4th BTL Conference, Berlin, 1/2 Dec 2010
190. Prenflo Krupp-Koppers, *Clean Power Generation from Coal* (Essen, Krupp-Koppers, 1996)
191. R. Abraham, *Kohlevergasung: Stand und Ausblick*, DGMK, 75. Sitzung, Arbeitskreis Kohle, Hamburg, 27.10.2011
192. Siedlungsabfall, Technische Anleitung zur Verwertung, Behandlung und sonstigen Entsorgung von Siedlungsabfällen, (Dritte Allgemeine Verwaltungsvorschrift zum Abfallgesetz) vom 14. Mai 1993, (BAnz. Nr. 99a vom 29.05.1993)
193. S. Schwinghammer, *Mark+: The next Generation of Lurgi's FBDB^{TM} Gasifier*, Coal Asia Conference, New Delhi, 27–28. Feb 2012
194. Siemens gasification and IGCC update, Gasification Technologies conference, 2 Nov 2010
195. http://www.netl.doe.gov/technologies/coalpower/gasification/gasifipedia/4-gasifiers/4-1-2-3_shell.html. Accessed 2013
196. J. Ciferno, J. Marano, Benchmarking Biomass Gasification technologies for fuels, Chemicals and Hydrogen Production, National Energy Technology Laboratory (2002)
197. O. Maurstad, *An Overview of Coal based Integrated Gasification Combined Cycle (IGCC) Technology* (MIT, 2005)
198. T. Giampaolo, *The Gas Turbine Handbook: Principles and Practices*, 2nd edn (The Faimont Press, Inc., 2003)

199. X. Guan et al., *Demonstration of Hot Gas Filtration in Advanced Coal Gasification System*, Power Systems Development Facility, Southern Company Services, 2007
200. P. Spath et al., *Technoeconomic analysis of hydrogen production from western coal augmented with CO_2sequestration and coalbed methane recovery* (National Renewable Energy Laboratory, 1999)
201. G. Raggio et al., *Coal gasification pilot plant for hydrogen production. Part B: syngas conversion and hydrogen separation*, in prepared for the Second International Conference on Clean Coal Technologies for our Future, 2005
202. T.A. Lynch, *Operating Experience at the Wabash River Coal Gasification Repowering Project*, in Dynergy Power Corp., prepared for the Gasification Technologies Conference, 1998
203. M.S. Naijar, D.Y. Jung, High Temperature Desulfurization of Synthesis Gas with Iron Compounds (Texaco Inc., 1993)
204. Uhde Press Release, No. 02, 2008
205. Allied Syngas Marketing Document
206. http://www.netl.doe.gov/technologies/coalpower/gasification/gasifipedia/4-gasifiers/4-3_syngas-detail.html. Accessed 2013
207. C.A. Callaghan, Worcester Polytechnic Inst., PhD (2006), p. 40
208. Y. Choi, H.G. Stenger, J. Power Sources **124**, 432 (2003)
209. S. Werner, Friedrich-Alexander-Universität Erlangen, PhD, 2011
210. G. Brenna, University of Bologna, PhD (2010), p. 40
211. C. Ratnasamy, J.P. Wagner, Catal. Rev. Sci. Eng **51**(3), 325–440 (2009)
212. E. Grol, W.C. Yang, *DOE/NETL Report 401/080509*, 2009
213. J. Wang, J. Spencer, J. Butler, Y. Cai, in *21st North American Catal. Society Meeting*, San Francisco, 2009, P-W-88
214. K. Aasberg-Petersen, I. Dybkjær, C.V. Ovesen, N.C. Schjødt, J. Sehested, S.G. Thomsen, J. Nat. Gas. Sci. Eng. **3**, 423 (2011)
215. H. Huang, N. Young, P. Williams, S. Taylor, G. Hutchings, Catal. Lett. **110**, 243 (2006)
216. Clariant, Actisorb 300 series brochure, 2011
217. R. Quinn, T. Mebrahtu, T.A. Dahl, F.A. Lucrezi, B.A. Toseland, Appl. Catal. **264**, 103 (2004)
218. Clariant, Actisorb 400/410 series brochure, 2011
219. R.L. Cornelissen, S. Clevers, CCS, Chrisgas project, 6th EU framework program, Report Chrisgas, 2009, WP3_D14
220. C.H. Bartholomew, Appl. Catal. **212**, 17–60 (2001)
221. P. Forzatti, L. Lietti, Catal. Today **52**, 165–181 (1999)
222. L. Kohl, R.B. Mielsen, *Gas Purification*, 5th edn. (Gulf Publishing Company, Houston, 1997)
223. H. Hiller, R. Reimert, F. Marschner, H.-J. Renner, W. Broll, E. Supp, M. Brejc, W. Liebner, G. Schaub et al., Gas Production. Ullmanns Enzyklopädie der technischen Chemie, 6. Auflage, Electronic CD-ROM version (Wiley-VCH, Weinheim, 2002)
224. R. Dittmeyer, W. Keim, G. Kreysa, A. Obernholz, *Winnacker-Küchler, Chemische Technik, Prozesse und Produkte*, Band 3: Anorganische Grundstoffe, Zwischenprodukte, 5. Auflage (Wiley-VCH, Weinheim, 2005)
225. S.A. Newmann, *Acid and Sour Gas Treating Processes* (Gulf Publishing Company, Houston, 1985)
226. B. Schreiner, Der Claus-Prozess. Chem. Unserer Zeit **42**, 378–392 (Wiley-VCH, Weinheim, 2008)
227. R. Pardemann, B. Meyer, Status and Perspectives of coal utilization in power plants with coal gasification (German article). *Chemie Ingenieur Technik* **82**(11), 1805–1819 (2011)
228. Lurgi/Air Liquide, The Rectisol Process–Lurgi's leading technology for purification and conditioning of synthesis gas, Process information sheet 308e/01.11/10, 2012

References to Section 4.5

229. US Hydrogen Production Capacity, EIA report SR-01AF-CNEAF/2008-04
230. G. Maisonnier, J. Perrin, R. Steigenberger-Wilckens, S.C. Trümper, *European Hydrogen Infrastructure Atlas, Industrial Excess Hydrogen Analysis Part II: Industrial Surplus Hydrogen Markets and Production*, Roads2HyCom, Document R2H20006PU.1, 7 Mar 2007
231. J. Perrin, R. Steigenberger-Wickens, S.C. Trümper, *European Hydrogen Infrastructure Atlas, Part III: Industrial Distribution Infrastructure*, Roads2HyCom, Document R2H2007PU.1, 3 July 2007
232. M. Kappas, *Klimatologie Klimaforschung im 21. Jahrhundert—Herausforderung für Natur- und Sozialwissenschaften* (Spektrum Akademischer, Heidelberg, 2009), p. 159 ff
233. J.G. Canadell, C. Le Quéré, M.R. Raupach, C.B. Field, E.T. Buitenhuis, P. Ciais, T.J. Conway, N.P. Gillett, R.A. Houghton, G. Marland, PNAS **104**(47), 18866–18870 (2007)
234. Global Carbon Dioxide Transport from AIRS Data, July 2008, online: http://photojournal.jpl.nasa.gov/catalog/PIA11194, 31 May 2013
235. F. Ausfelder, A. Bazzanella, *Position Paper on CO2 Utilizaiton and Storage*, DECHEMA, Oct 2008
236. M. Prud'homme, in *International Fertilizer Association Annual Meeting*, Paris, 2010
237. G.A. Olah, A. Goeppert, K. Surya Prakash, J. Org. Chem. **74**(2), 487–498 (2009)
238. G.A. Olah, Angew. Chem. Int. Ed., **52**, 104–107 (2013) plus references cited therein
239. J. Strautmann, D. Wolf, T. Riethmann, A. Kather, M. Klostermann, M. Blug, A. Schraven, D. Kruse, Green Chem., **15**, (2013) submitted
240. Press Release, Mitsui Chemicals, Tokyo, 25 Aug 2008
241. K.C. Tran, *Carbon Recycling International*, presentation to World Energy Council, 2009
242. http://www.carbonrecycling.is, 30 May 2013
243. A. Boddien, M. Beller et al., Science **333**, 1733 (2011)
244. M. Czaun, A. Goeppert, R. May, R. Haiges, G.K.S. Prakash, G.A. Olah, ChemSusChem **4**, 1241–1248 (2011)
245. D. Möller, LIFIS ONLINE, 15 Aug 2011. ISSN: 1864-6972

References to Section 4.5.1

246. G.A. Olah, A. Goeppert, G.K. Surya Prakash, *Beyond Oil and Gas: The Methanol Economy* (Wiley-VCH, Weinheim, 2009). 2nd Updated and enlarged Edition
247. F. Asinger, *Methanol: Chemie- und Energierohstoff* (Springer, Berlin Heidelberg, 1986)
248. J. Leclaire, G. Husson, N. Devaux, V. Delorme, L. Charles, F. Ziarelli, P. Desbois, A. Chaumonnot, M. Jacquin, F. Fotiadu, G. Buono, J. Am. Chem. Soc. **132**(10), 582–3593 (2010)
249. J.-L. Wang, C.-X. Miao, X.-Y. Dou, J. Gao, L.-N. He, Curr. Org. Chem. **15**(5), 621–646 (2011)
250. S.N. Riduan, Y. Zhang, Dalton Trans. **39**, 3347–3357 (2010)
251. A. Bar-Evena, E. Noora, N.E. Lewisbc, R. Milo, Design and analysis of synthetic carbon fixation pathways. PNAS **107**(19), 8889–8894, 11 May 2010
252. H.-W. Häring, *Industrial Gases Processing* (Wiley-VCH, Weinheim, 2008)
253. J. Rolker, M. Seiler, Adv. Chem. Eng. Sci. **1**, 280–288 (2011)
254. A.L. Kohl, R.B. Nielsen, *Gas Purification*, 4th edn. (Gulf Publishing, Houston, 1997)
255. C.M. White, B.R. Strazisar, E.J. Granite, J.S. Hoffman, H.W. Pennline, J. Air Waste Manag. Assoc. **53**(6), 645–715 (2003)

256. M. Ramezan, N. Nsakala, G.N. Liljedahl, L.E. Gearhart, R. Hestermann, B. Rederstorff, *Carbon Dioxide Capture from Existing Coal Fired Power Plants*, DOE/NETL-401/120106 (National Energy Technology Laboratory, 2006). doi:10.1081/SS-200042244
257. D. Aaron, C. Tsouris, Sep. Sci. Technol. **40**(1), 321 (2005)
258. O. Davidson, H.C. de Coninck, M. Loos, L.A. Meyer (eds.) *IPCC Special Report on Carbon Dioxide Capture and Storage* (Cambridge University Working Group III of the Intergovernmental Panel on Climate Change Press, Cambridge, New York, 2005)
259. J. Van Straelen, F. Geuzebroek, N. Goodchild, G. Proto-papas, L. Mahony, Int. J. Greenhouse Gas Control **4**(1), 316–320 (2010). doi:10.1016/j.ijggc.2009.09.022
260. J.D. Figueroa, T. Fout, S. Plasynski, H. McIlvried, R.D. Srivastava, Int. J. Greenhouse Gas Control **2**(1), 9–20 (2008). doi:10.1016/S1750-5836(07)00094-1
261. J. Seagraves, M. Quinlan, J. Corley, *Fundamentals of Gas Treating*, in Laurance Reid Gas Conditioning Conference (LRGCC), 2010
262. R.N. Tennyson, R.P. Schaaf, Oil Gas J. **10**(1), 78–86 (1977)
263. B.T. Oyenekan, G.T. Rochelle, Ind. Eng. Chem. Res. **45**(1), 2457–2464 (2006). doi:10.1021/ie050548k
264. J. Oexmann, A. Kather, Int. J. Greenhouse Gas Control **4**(1), 36–43 (2010). doi:10.1016/j.ijggc.2009.09.010
265. B.A. Oyenekan, G.T. Rochelle, AIChE J. **53**(1), 3144–3154 (2007). doi:10.1002/aic.11316
266. G.T. Rochelle, *CO2 capture by aqueous absorption/stripping opportunities for better technology*, in Workshop on Carbon Sequestration Science, Washington, D.C., 2001
267. P.V. Danckwerts, *Gas-Liquid Reactions* (McGraw-Hill, New York, 1970)
268. Wiley-VCH and LASTWiley-VCH, *Ullmann's Agrochemicals*, vol. 1 (Wiley-VCH, Weinheim, 2007)
269. G. Sartori, D.W. Savage, Ind. Eng. Chem. Fundam. **22**(1), 239–249 (1983). doi:10.1021/i100010a016
270. J.-Y. Park, S.J. Yoon, H. Lee, Environ. Sci. Technol. **37**(1), 1670–1675 (2003). doi:10.1021/es0260519
271. F. Bougie, M.C. Iliuta, Chem. Eng. Sci. **65**(1), 4746–4750 (2010). doi:10.1016/j.ces.2010.05.021
272. R.G.F. Albry, M.S. DuPart, *Amine Plant Trouble-Shooting and Optimization* (Gulf Publishing Co., Houston, 1995), pp. 3–11
273. K.P. Shen, M.-H. Li, J. Chem. Eng. Data **37**(1), 96–100 (1992). doi:10.1021/je00005a025
274. O.F. Dawodu, A. Meisen, J. Chem. Eng. Data **39**(1), 548–552 (1994). doi:10.1021/je00015a034
275. F.-Y. Jou, A.E. Mather, F.E. Otto, Can. J. Chem. Eng. **73**(1), 140–145 (1995). doi:10.1002/cjce.5450730116
276. J. Gmehling, J. Chem. Eng. Data **38**(1), 143–146 (1993). doi:10.1021/je00009a036
277. G. Senger, G. Wozny, Chem. Ing. Tech. **83**(4), 503–510 (2011). doi:10.1002/cite.201000210
278. M. Seiler, J. Rolker, PCT/EP 2010/051083, 2010
279. M. Seiler, J. Rolker, DE 102010043838.3, 2010
280. M. Seiler, T. Pott, WO 2006/048182, 2006
281. M. Seiler, J. Rolker, R. Schneider, A. Kobus, J. Reich, W. Benesch, H. Brüggemann, WO 2010/139616, 2010
282. M. Seiler, J. Rolker, R. Schneider, A. Kobus, D. Witthaut, M. Neumann, M. Keup, D. Dembkowski, W. Benesch, H. Winkler, J. Reich, T. Riethmann, EP 2258460, 2010
283. M. Seiler, J. Rolker, R. Schneider, B. Glöckler, A. Kobus, J. Reich, W. Benesch, H. Brüggemann, T. Riethmann, H. Winkler, WO 2010/089257, 2010
284. F.-Y. Jou, A.E. Mather, F.E. Otto, Ind. Eng. Chem. Process Des. Dev. **21**(1), 539–544 (1982). doi:10.1021/i200019a001
285. T.R. Aikins, L.E. Parks, J.N. Iyengar, R.B. Fedich, D. Perry, *Sterically hindered amines-thirty years of gas treating practice*, in Annual Laurance Reid Gas Conditioning Conference, Norman, 20–23 Feb 2011

286. G.W. Xu, C.-F. Zhang, S.-J. Qin, Y.-W. Wang, Ind. Eng. Chem. Res. **31**(1), 921–927 (1992). doi:10.1021/ie00003a038
287. P.W.J. Derks, *Carbon dioxide absorption in piperazine activated N-methyldiethanolamine*, Ph.D. Thesis, University of Twente, Nederland, 2006
288. F.-Y. Jou, F.-E. Otto, A.E. Mather, Ind. Eng. Chem. Res. **33**(1), 2002–2005 (1994). doi:10.1021/ie00032a016
289. J. Seagraves, R.H. Weiland, Treating high CO_2 gases with MDEA. Petrol. Technol. Quart. GAS 103–109 (2009)
290. J.A. Bullin, J.C. Polasek, S.T. Donnelly, *The Use of MDEA and Mixtures of Amines for Bulk CO2 Removal* (Bryan Research & Engineering, Inc., 2006). http://www.bre.com
291. R. Notz, I. Tönnies, H.P. Mangalapally, S. Hoch, H. Hasse, Int. J. Greenhouse Gas Control **5**(3), 413–421 (2010). doi:10.1016/j.ijggc.2010.03.008
292. B. Schäfer, A.E. Mather, K.N. Marsh, Fluid Phase Equilib. **194–197**, 929–935 (2002). doi:10.1016/S0378-3812(01)00722-1
293. J. Rolker, M. Seiler, Elements 37. Quaterly Sci. Newsl. Evonik Ind. AG **4**, 2011
294. J. Rolker, T. Lenormant, M. Seiler, Chem. Ing. Tech. **84**(6), 849–858 (2012)
295. P.D. Vaidya, E.Y. Kenig, Chem. Eng. Commun. **194**(12), 1543–1565 (2007)
296. H.E. Benson, J.H. Field, R.M. Jimeson, Chem. Eng. Prog. **50**, 356–364 (1954)
297. Overview of UOP Gas Processing Technologies and Applications, Presentation, 2009. http://www.uop.com/wp-content/uploads/2011/02/UOP-Overview-of-Gas-Processing-Technologies-and-Applications-tech-presentation.pdf

References to Section 4.5.2

298. A. Earnshaw, N.N. Greenwood, *Chemistry of the Elements* (Butterworth-Heinemann, Oxford, 1997)
299. Z. Jiang, T. Xiao, V.L. Kuznetsov, P.P. Edwards, Phil. Trans. R. Soc. A **368**, 3343–3364 (2010)
300. P. Häussinger, R. Lohmüller, A.M. Watson *Ullmann's Encyclopedia of Industrial Chemistry* (Wiley-VCH Verlag GmbH & Co. KGaA, Weinheim, Germany, 2000)
301. M.A. Rosen, D.S. Scott, in *Proceedings of the Ninth World Hydrogen Energy Conference*, (Paris, France, 1992), p. 457
302. N.Z. Muradov, T.N. Veziroglu, Int. J. Hydrogen Energy **30**, 225–237 (2005)
303. http://www.praxair.com/gases/buy-compressed-hydrogen-gas-or-liquid-hydrogen
304. S. Muschelknautz, P. Fritz, *Syngas and hydrogen production for chemical and refinery applications based on natural gas and other feedstocks*, in ACHEMA Congress, Frankfurt/Main, Germany, 2012
305. http://www.praxair.com/praxair.nsf/AllContent/7E8A75E1CC87FA998525655E000B40DA?OpenDocument&URLMenuBranch=88FFF0AAE2BDB4948525706F00587825 nicht auffindbar
306. L. Barreto, Int. J. Hydrogen Energy **28**, 267–284 (2003)
307. L. Barreto, A. Makihira, K. Riahi, *Medium and Long-term Demand and Supply Prospects for Fuel Cells: The Hydrogen Economy and Perspectives for the 21st Century*, Laxenburg, Austria, 2002
308. J.N. Armor, Catal. Lett. **101**, 131–135 (2005)
309. G. Parkinson, Chem. Eng. **108**(10), 29–37 (2001)
310. B. Suresh, S. Schlag, Y. Inoguchi, *Hydrogen Market Report*, document 743.5000 A, SRI (Consulting, Menlo Park, USA, 2004), p. 6
311. C. Petit, US News World Rep. **135**(22), 54 (2003)
312. I. Dincer, Int. J. Hydrogen Energy **37**, 1954–1971 (2012)
313. Press Release, *Air Products'Gulf Coast Pipeline Fills Additional Hydrogen Requirement* (Air Products & Chemicals, Inc., Lehigh Valley, 2011), can be found under http://

www.airproducts.com/company/news-center/2011/08/0809-air-products-gulf-coast-pipeline-fills-additional-hydrogen-requirement.aspx
314. Brochure, *Increase Hydrogen Supply Availability with Cavern Storage*, Praxair Information 10/06 P-9808 (Praxair Technology, Inc., Danbury, 2006) can be found under http://www.praxair.pt/praxair.nsf/0/3A0AB529A089B473852571F0006398A3/$file/027847_PRAX_RefinSpec_4_low_res.pdf
315. J. Perrin, R. Steinberger-Wilckens, S.C. Trümper, *European Hydrogen Infrastructure Atlas, Part III Industrial distribution infrastructure*, document R2H2007PU.1, 2007, can be found under http://www.roads2hy.com/wp2.html

References to Section 4.5.3

316. IHS Chemical, *CEH Marketing Research Report Hydrogen. Abstract*, 2010, can be found under http://www.ihs.com/products/chemical/planning/ceh/hydrogen.aspx
317. M. Bertau, C. Pätzold, D. Meyer, unpublished results
318. C. Lange, Bachelor Thesis, Freiberg University of Mining and Technology, 2011
319. T. Smolinka, M. Günther, J. Garche, *Stand und Entwicklungspotenzial der Wasserelektrolyse zur Herstellung vonWasserstoff aus regernativen Energien*, Berlin, 2010
320. S. Marini, P. Salvi, P. Nelli, R. Pesenti, M. Villa, M. Berrettoni, G. Zangari, Y. Kiros, Electrochim. Acta **82**, 384–391 (2012)
321. K.E. Ayers, E.B. Anderson, C. Capuano, B. Carter, L. Dalton, G. Hanlon, J. Manco, M. Niedzwiecki, *ECS Transactions* (ECS, 2010)
322. A. Goñi-Urtiaga, D. Presvytes, K. Scott, Int. J. Hydrogen Energy **37**, 3358–3372 (2012)
323. M. Laguna-Bercero, J. Power Sources **203**, 4–16 (2012)
324. T. Ishihara, T. Kannou, S. Hiura, N. Yamamoto, T. Yamada, *Steam Electrolysis Cell Stack using LaGaO3-Based Electrolyte*, Karlsruhe, 2009
325. W. Suksami, I. Metcalfe, Solid State Ionics **178**, 627–634 (2007)
326. Z. Wang, R. Roberts, G. Naterer, K. Gabriel, Int. J. Hydrogen Energy **37**, 16287–16301 (2012)
327. M.T. Balta, I. Dincer, A. Hepbasli, Int. J. Energy Res. **34**, 757–775 (2010)
328. R.L. Uffen, Proc. Natl. Acad. Sci. U.S.A. **73**, 3298–3302 (1976)
329. S.A. Markov, Energy Procedia **29**, 394–400 (2012)
330. R.L. Uffen, Enzyme Microb. Technol. **3**, 197–206 (1981)

References to Section 4.6

331. R.W. Joyner, F. King, M.A. Thomas, G. Roberts, Catal. Today **10**, 417 (1991)
332. G. Petrini, F. Mortino, A. Bossi, F. Garbassi, Preparation of Catalysts III, in *Studies in Surface Science and Catalysis,* ed. by P. Grange, P.A. Jacobs, G. Poncelet, vol. 16 (1983) p. 735
333. Y. Zhang, Q. Sun, J. Deng, D. Wu, S. Chen, Appl. Catal. A. 158, 105 (1997)
334. P. Gherardi, O. Ruggeri, F. Trifiro, A. Vaccari, G. Del Piero, G. Manara, B. Notari. Preparation of Catalysts III, in *Studies in Surface Science and Catalysis,* ed. by P. Grange, P.A. Jacobs, G. Poncelet, vol. 16 (1983), p. 723
335. Y. Zhang, Q. Sun, J. Deng, D. Wu, S. Chen, Appl. Catal. A **158**, 105 (1997)
336. R.H. Hoppener, E.B.M. Doesburg, J.J.F. Scholten, Appl. Catal. **25**, 109 (1986)
337. Y. Okamoto, K. Fukino, T. Imanaka, S. Teranishi, J. Phys. Chem. **87**, 3747 (1983)
338. W.L. Marsden, M.S. Wainwright, J.B. Friedrich, Ind. Eng. Chem. Prod. Res. Dev. **19**, 551 (1980)
339. M.S. Wainwright, W.L. Marsden, J.B. Friedrich, GB 066 856, 1981

340. H.E. Curry-Hyde, D.J. Young, M.S. Wainwright, Appl. Catal. **29**, 31–41 (1987)
341. H.E. Curry-Hyde, M.S. Wainwright, D.J. Young, *Methane Conversion.* s.l (Elsevier, Amsterdam, 1988), p. 239
342. W.G. Baglin, G.B. Atkinson, L.J. Nicks, Ind. Eng. Chem. Prod. Res. Dev. **20**, 87 (1981)
343. J.B. Friedrich, M.S. Wainwright, D.J. Young, J. Catal. 14 (1983)
344. F. Fajula, R.G. Anthony, J.H. Lunsford., J. Catal., 237–256 (1982)
345. Storch, H., US 1.681.753 A 1, 1928
346. J. Yoshihara, S.C. Parker, A. Schafer, C.T. Campbell, Catal. Lett. **31**, 313 (1995)
347. J. Gallagher, Y. H. Kiold, GB 1 159 035, 1965
348. J. Ladebek, J. Koy, T. Regula, US 2005.080.148
349. D. Waller, D. Stirling, F.S. Stone, M.S. Spencer, Faraday Discuss. **87**, 107 (1989)
350. S.H. Taylor, G.J. Hutchings, A.A. Mirzaei., Chem. Commun. 1373 (1999)
351. D.M. Whittle, A.A. Mirzaei, J.S.J. Hargreaves, R.W. Joyner, C.J. Kiely, S.H. Taylor, G.J. Hutchings, Phys. Chem. Chem. Phys. **4**, 5915 (2002)
352. B. Bems, M. Schur, A. Dassenoy, H. Junkes, D. Herein, R. Schlögl, Chem. Eur. J. **9**, 2039 (2003)
353. B.L. Kniep, T. Ressler, A. Rabis, F. Girgsdies, M. Baenitz, F. Steglich, R. Schlögl, Angew. Chem. Int. Ed. **43**, 112 (2004)
354. M. Behrens, F. Girgsdies, A. Trunschke, R. Schlögl, Minerals as model compounds for Cu/ZnO catalyst precursors: Structural and thermal properties and IR spectra of mineral and synthetic (zincian) malachite, rosasite and aurichalcite and a catalyst precursor mixture. Eur. J. Inorg. Chem. 1347–1357 (2009)
355. M. Behrens, F. Girgsdies, Structural effects of Cu/Zn substitution in the Malachite–Rosasite system. Zeitschrift für Anorganische und Allgemeine Chemie **636**, 919–927 (2010)
356. B. Kniep, Technical University of Berlin, Microstructural modifications of copper Zinc Oxide, PhD Thesis, 2005. opus.kobv.de/tuberlin/…/kniep_benjamin.pdf
357. C. Baltes, S. Vukojevic, F. Schüth, J. Catal. **258**, 334–344 (2008)
358. K. Yamagishi, Y. Obata, Y. Sugano, Mitsubishi Gas Chemical. ss for manufacturing methanol and process for manufacturing catalyst for methanol synthesis. EP19960106327 (1996)
359. J.C.J. Bart, R.P.A. Sneeden, Catal. Today **2**, 122 (1987)
360. G.C. Chinchen, P.J. Denny, J.R. Jennings, M.S. Spencer, K.C. Waugh, Appl. Catal. **36**, 1 (1988)
361. S. Gusi, F. Pizzoli, F. Trifiro, A. Vaccari, G.D. Piero, Preparation of Catalysts IV, in *Studies in Surface Science and Catalysis,* ed. by P. Grange, P.A. Jacbos, G. Poncelet, B. Delmon, vol. 31 (1987)
362. M. Minelli, G. Moretti, J. Catal. **109**, 367 (1988)
363. G. Sengupta, D.P. Das, M.L. Kundu, S. Dutta, S.K. Roy, R.N. Sahay, K.K. Mishra, Appl. Catal. **55**, 165 (1989)
364. I. Kasatkin, P. Kurr, B. Kniep, A. Trunschke, R. Schlögl, Angew. Chem. Int. Ed. **46**, 7324–7327 (2007)
365. L. Ma, T. Tran, M.S. Wainwright, Top. Catal. **22**, 295–304 (2003)
366. H. Topsoe, online: http://www.topsoe.com/business_areas/methanol/~/media/PDF%20files/Methanol/Topsoe_methanol_mk%20121.ashx
367. Süd Chemie, General Catalyst Catalogue, online: www.clariant.com. www.sudchemie.com]
368. M. Schneider, K. Kochloefl, J. Ladebeck, US Patent 4,535,071
369. J. Koy, F. Schmidt, J. Ladebeck, WO03053575
370. J.B. Hansen, P.E. Højlund Nielsen, in *Handbook of Heterogeneous Catalysis,* 2nd edn, ed. by H. Knözinger, F. Schüth, J. Weitkamp, G. Ertl (Wiley–VCH, Weinheim, 2008), pp. 2920–2949
371. M. Behrens, F. Studt, I. Kasatkin, S. Kühl, M. Hävecker, F. Abild-Pedersen, S. Zander, F. Girgsdies, P. Kurr, B.-L. Kniep, M.l Tovar, R.W. Fischer, J.K. Nørskov, R. Schlögl, Sci. online, 18 May 2012

372. C.Kittel, H. Kroemer (eds.) *Thermal Physics* (S.R Furphy and Company, New York, 1980), p. 246
373. W. Liebner, E. Supp. Combined reforming: a most economical way from natural gas to alcohols and synfuels, in *VIII International Symposium on Alcohol Fuels*, 1988
374. H.F. Rase, Handbook of commercial catalysts: heterogeneous catalysts (CRC Press LLC, 2000), p. 430
375. O.A. Hougen, K.M. Watson, R.A. Ragatz, Chemical Process Principles, vol. part 2 (1959)
376. G. Soave, Chem. Eng. Sci. **27**, 1197 (1972)
377. D.Y. Peng, D.B. Robinson, Ind. Eng. Chem. Fundam. **15**, 59 (1976)
378. Y. Lwin, Int. J. Eng. Ed. **16**(4), 335–339 (2000)
379. W.J. Thomas, S. Portalski, Ind. Eng. Chem. **50**, 967 (1958)
380. R.H. Newton, B.F. Dodge, J. Am. Chem. Soc. **56**, 1287 (1934)
381. R.M. Ewell, Ind. Eng. Chem 149 (1940)
382. V.M. Cherednichenko, Ph. D. Thesis, Korpova, Physico-Chemical Institute, Moscow, 1953
383. T. Chang, R.W. Rousseau, P.K. Kilpatrick, Ind. Eng. Chem. Process Des. Dev. **25**, 477 (1986)
384. G.H. Graaf, P.J.J.M. Sijtsema, E.J. Stamhuis, G.E.H. Joosten, Chem. Eng. Sci. **11**, 2883 (1986)
385. W. Kotowski, Przem. Chem. **44**, 66 (1965)
386. Kirk-Othmer, *Encyclopedia of Chemical Technology*, vol. 15. (Wiley, 2005), pp. 398–415
387. L. Bisset, Chem. Eng. (N.Y.) 21, 155 (1977)
388. S. Lee, in *Handbook of alternative fuel technologies,* ed. by J.G. Speight, S.K. Loyalka, S. Lee. s.l. (CRC Press, Taylor & Francis Group, LLC, 2007)
389. X.-M. Liu, G.Q. Lu, Z.-F. Yan, J. Beltramini, Recent advances in catalysts for methanol synthesis via hydrogenation of CO and CO2. Ind. Eng. Chem. Res. **42**, 6518 (2003)
390. Sinor Synthetic Fuels Report, vol. 6, p. 126 (1999)
391. P.J.M. Tijm, F.J. Waller, D.M. Brown, Methanol technology developments for the new millenium. Appl. Catal. A **221**, 275 (2001)
392. J.E. Miller, Sandia Report, SAND2007-8012, 2007
393. H.-W. Lim, M.-J. Park, S.-H. Kang, H.-J. Chae, J.W. Bae, K.-W. Jun, Ind. Eng. Chem. Res. **48**, 10448–10455 (2009)
394. W. Seyfert, G. Luft, Chem. Ing. Tech. **57**, 482 (1985)
395. B.J. Lommerts, G.H. Graaf, A.A.C.M. Beenackers, Chem. Eng. Sci. **55**, 5589–559 (2000)
396. G.H. Graaf, E.J. Stamhuis, A.A.C.M. Beenackers, Kinetics of low-pressure methanol synthesis. Chem. Eng. Sci. **43**(12), 3185–3195 (1988)
397. G.H. Graaf, H. Scholtens, E.J. Stamhuis, A.A.C.M. Beenackers, Chem. Eng. Sci. **45**, 773–783 (1990)
398. A. Brehm, Kinetik homogener Reaktionen—Formalkinetik. *gmehling.chemie.uni-oldenburg.de.* (Online)
399. W. Keim, Pure Appl. Chem. **58**(6), 825–832 (1986)
400. E. Ramaroson, R. Kieffer, A. Kiennermann, Appl. Catal. **4**, 281 (1982)
401. E.R.A. Matulewicz, Ph. D. Thesis. s.l. (University of Amsterdam, 1984)
402. D.J. Elliott, F. Pennella, J. Catal. **119**, 359 (1989)
403. J.B. Hansen, in *AIChE National Meeting, Conference Proceedings* (1990), p. 109
404. G.C. Chinchen, Appl. Catal. **36**, 1–65 (1988)
405. J.C.J. Bart, R.C.P. Sneeden, Catal. Today **2**, 1–124 (1987)
406. M.V. Twigg (ed.), *Catalyst Handbook*, 2nd edn (1989), pp. 441–468
407. JM, Katalco-51 Apico
408. I. Løvik, Modelling, estimation and optimizazion of the methanol synthesis with catalyst deactivation, Doctoral Thesis Norwegian University of Science and Technology, 2001
409. M.R. Rahimpour, J. Fathikalajahi, A. Jahanmiri, Can. J. Chem. Eng. **76**, 753–761 (1998)
410. J. Richardson, Nitrogen Methanol. (1999)
411. N Ringer, Clariant Produkte Deutschland GmbH. Nitrogen Methanol (2004)

References to Section 4.7

412. K. Aasberg-Petersen, C.S. Nielsen, I. Dybkjær, J. Perregaard, Large scale methanol production from natural gas, 2013, found at: http://www.topsoe.com/business_areas/methanol/~/media/PDF%20files/Methanol/Topsoe_large_scale_methanol_prod_paper.ashx
413. E. Supp, *How to produce methanol from coal* (Springer, New York, 1990)
414. J. Ott, V. Gronemann, F. Pontzen, E. Fiedler, G. Grossmann, B. Kersebohm, G. Weiss, C. Witte, *Ullmann's Encyclopedia of Technical Chemistry*, 7th edn. (Wiley-VCH Verlag GmbH & Co. KGaA, Weinheim, 2013)
415. Chemsystems PERP Program, 'Methanol', Nexant Report 07/08-2, Nov 2008
416. Adapted from a private communication of Davy Process Technology
417. U. Zardi, G. Pagani, US Patent 5756048, 1998
418. I. Dybkjaer, Chem. Econ. Eng. Rev. **13**(6), 17–25 (1981)
419. JM/DPT private communication
420. ChemSystems, Prospectus 2009/10, Methanol Strategic Business Report, Nexant Inc
421. I. Takase, K. Niwa, Chem. Econ. Eng. Rev. **17**(5), 24–30 (1985)
422. P.J.A. Tijm, F. Waller, D.M. Brown, Appl. Catal. A, **221**, 275–282 (2001)
423. E. Fiedler, G. Grossmann, D. Kersebohm, G. Weiss, C. Witte, "Methanol." Ullmann's Encyclopedia of Industrial Chemistry Release 2003, 6th edn (Wiley-VCH Verlag GmbH & Co.KGaA, Weinheim, 2003)
424. T. Wurzel, in *World Methanol Conference*, Houston, 15 Mar 2012
425. S. Lee, *Methanol Synthesis from Syngas*. In: S. Lee, James G. Speight, Sudarshan K. Loyalka (eds.) Handbook of Alternative Fuel Technologies (CRC Press, 2007), © 2007 by Taylor & Francis Group, LLC
426. W. Hilsebein, J. Blaurock, in *Constructing a MegaMethanol® Plant—Start to finish*, Methanol Forum Houston, 14 Oct 2004
427. Methanol Technologies: Methanol plants keep getting bigger, Nitrogen + Syngas, 316, 2012
428. L. Connock, Nitrogen + Syngas, **297**, 40–55 (2009)
429. T. Wurzel, Lurgi MegaMethanol® Technology-Delivering the Building Blocks for the Future. Fuel and Monomer demand. Oil Gas Eur. Mag., **2**, 92–96 (2007)
430. B. Höhlein, T. Grube, P. Biedermann, H. Bielawa, G. Erdmann, L. Schlecht, G. Isenberg, R. Edinger, Methanol als Energieträger, Forschungszentrum Jülich (2003)
431. U. Zardi, G. Pagani, EP-A-O 359 952
432. Linde, 2013 http://www.linde-engineering.com./de/footer/termsofuse.htmlAccessed. Referenz ist OK
433. PERP Report, Nexant ChemSystems, 2013 http://www.netl.doe.gov/technologies/coalpower/gasification/gasifipedia/pdfs/lpmeoh-oct2001.pdf

References to Section 4.8

434. P. Davies, F. Forster Snowdon, G.W. Bridger, D.O. Hughes, P.W. Young, DE 1241429 B, 1963
435. M. Saito, M. Takeuchi, T. Fujitani, J. Toyir, S. Luo, J. Wu, H. Mabuse, K. Ushikoshi, K. Mori, T. Watanabe, Appl. Organomet. Chem. **14**, 763–772 (2000)
436. K. Ushikoshi, K. Mori, T. Kubota, T. Watanabe, M. Saito, Appl. Organomet. Chem. **14**, 819–825 (2000)
437. J. Toyir, R. Miloua, N.E. Elkadri, M. Nawdali, H. Toufik, F. Miloua, M. Saito, Phys. Proc. **2**, 1075–1079 (2009)
438. M. Saito, Catal. Surv. Jpn. **2**, 175–184 (1998)

439. V. Gronemann, W. Liebner, P. di Zanno, F. Pontzen, M. Rothaemel, Nitrogen+Syngas, **308**, 36–39 (2010)
440. First Commercial Plant for methanol production (Carbon Recycling International), download from http://www.carbonrecycling.is/index.php?option=com_content&view=article&id=14&Itemid=8&lang=en, 25 March 2013
441. G.A. Olah, A. Goeppert, G.K.S. Prakash, J. Org. Chem. **74**, 487–498 (2009)
442. Mitsui CSR Report 2010 (Mitsui Chemicals Inc.) 2010, download from http://www.mitsuichem.com/csr/report/ebook/2010/index.htm, 9 Dec 2011
443. V. Gronemann, W. Liebner, P. DiZanno, F. Pontzen, M. Rothaemel, Nitrogen + Syngas, **308**, 36–39 (2010)
444. Bayer Sustainable Development report 2010 (Bayer AG), 2010, download from http://www.sustainability2010.bayer.com/en/sustainable-development-report-2010.pdfx, 12 Dec 2011
445. Y. Zhang, J. Fei, Y. Yu, X. Zheng, Energy Conv. Mgmt. **47**, 3360–3367 (2006)
446. G. Centi, S. Perathoner, Greenhouse Gases: Sci. Technol. **1**(1), 21–35 (2011)
447. Research and Development of WVCoal (West Virginia Coal Association) 2013, download from http://www.wvcoal.com/Research-Development/iceland-recycles-even-more-co2.html, 25 March 2013
448. J. Richardson, Nitrogen Methanol, **238**, 29ff (1999)
449. H. Göhna, P. König, Chem. Technol. **24**, 36–39 (1994)
450. J. Wu, S. Luo, J. Toyir, M. Saito, M. Takeuchi, T. Watanabe, Catal. Today **45**, 215–220 (1998)
451. M. Saito, T. Fujitani, M. Takeuchi, T. Watanabe, Appl. Catal. A **138**, 311–318 (1996)
452. D. Rotman, Chem. Week **154**(11), 14 (1994)
453. E. F. Magoon, L. H. Slaugh (Shell Int. Res. Maatschappij B.V.), DE 2154074 B2, 1971
454. H. Yamada, T. Watanabe (Mitsubishi Gas Chemical Co.), EP 2492008 A1, 2010
455. A. Passariello (Ammonia Casale S.A.), DE 3238845 A1, 1982
456. M. Schneider, K. Kochloefl, O. Bock (Süd-Chemie AG), DE 3403491 A1, 1984
457. J. Koy, F. Schmidt, J. Ladebeck (Süd-Chemie AG), WO 2003053575 A1, 2002
458. E. Armbruster, O. Frei et al. (Lonza AG), WO 199703937, 1996
459. M. Takeuchi, H. Mabuse et al., EP 0864380 B1, 1998
460. S. Asano, T. Nakamura (Mitsubishi Gas Chemical Co.), DE 2365001 A1, 1973
461. H. Fukui, M. Kobayashi et al. (Direktor General of Agency of Ind. Sci. and Techn., YKK Corp.), DE 69808983 T2, 1998
462. K. Fujimoto, K. Fujimoto, N. Yamane, US 20100234649 A1, 2007
463. S.-H. Kang, J.W. Bae et al., US 20110118367 A1, 2009
464. Data provided by Lurgi AG. Reproduction with kind permission
465. H. Göhna, P. König et al. (Metallgesellschaft AG), US 5,631,302, 1997
466. O.-S. Joo, K.-D. Jung, Y. Jung, Carbon Dioxide utilization for global sustainability, in *Proceedings of the 7th International Conference on Carbon Dioxide Utilization*, 2007
467. O.-S. Joo, K.-D. Jung, Y. Jung, Stud. Surf. Sci. Catal. **153**, 67–72 (2004)
468. O.-S. Joo, CAMERE Process for carbon dioxide hydrogenation to form methanol, 2013, download from http://web.anl.gov/PCS/acsfuel/preprint%20archive/Files/45_4_WASHINGTON%20DC_08-00_0686.pdf, 25 March 2013
469. Mitsui Seeks Partners for CO_2-Based Methanol Plant IHS Chemical Week (1 March 2010), 2010
470. T. Matsushita, T. Haganuma, D. Fujita (Mitsui Chemicals Inc.), US 20130237618 A1, 2011
471. T. Matsushita, T. Haganuma, D. Fujita (Mitsui Chemicals Inc.), WO 2011136345 A1, 2011
472. G. Olah, S. Prakash (The University of Southern California), US 7,608,743, 2009
473. A. Shulenberger, F. Jonsson, O. Ingolfsson, K.-C. Tran, US 20070244208, 2007
474. http://www.chemicals-technology.com/projects/george-olah-renewable-methanol-plant-iceland/
475. J. Słoczyński, R. Grabowski, P. Olszewski, A. Kozłowska, J. Stoch, M. Lachowska, J. Skrzypek, Appl. Catal. A. **310**, 127–137 (2006)

476. D.L. Chiavassa, J. Barrandeguy, A.L. Bonivardi, M.A. Baltanás, Catal. Today **133–135**, 780–786 (2008)
477. D.L. Chiavassa, S.E. Collins, A.L. Bonivardi, M.A. Baltanás, Chem. Eng. J. **150**, 204–212 (2009)
478. G.J. Millar, C.H. Rochester, K.C. Waugh, Catal. Lett. **14**, 289–295 (1992)
479. M. Muhler, E. Törnqvist, L.P. Nielsen, B.S. Clausen, H. Topsøe, Catal. Lett. **25**, 1–10 (1994)
480. Q. Sun, C.-W. Liu, W. Pan, Q.-M. Zhu, J.-F. Deng, Appl. Catal. A **171**, 301–308 (1998)
481. M.S. Spencer, Catal. Lett. **60**, 45–49 (1999)
482. K.-D. Jung, A.T. Bell, J. Catal. **193**, 207–223 (2000)
483. T. Kubota, I. Hayakawa, H. Mabuse, K. Mori, K. Ushikoshi, T. Watanabe, M. Saito, Appl. Organomet. Chem. **15**, 121–126 (2001)
484. W. Curtis Conner, J.L. Falconer, Chem. Rev. **95**, 759–788 (1995)
485. S.E. Collins, M.A. Baltanás, A.L. Bonivardi, J. Catal. **226**, 410–421 (2004)
486. S.E. Collins, M.A. Baltanás, A.L. Bonivardi, Langmuir **21**, 962–970 (2005)
487. S.-H. Kang, J.W. Bae, K.W. Jun, K.-S. Min, S.-L. Song, S.-H. Jeong, EP 2305379 A2, 2009
488. A. Barber Stiles, DE 2320192 A, 1972
489. X. Dong, H.-B. Zhang, G.-D. Lin, Y.-Z. Yuan, K.R. Tsai, Catal. Lett. **85**, 237–246 (2003)
490. F. Pontzen, W. Liebner, V. Gronemann, M. Rothaemel, B. Ahlers, Catal. Today **171**, 242–250 (2011)
491. Z. Xu, Z. Qian, L. Mao, K. Tanabe, H. Hattori, Bull. Chem. Soc. Jpn. **64**, 1658–1663 (1991)
492. Y. Nitta, O. Suwata, Y. Ikeda, Y. Okamoto, T. Imanaka, Catal. Lett. **26**, 345–354 (1994)
493. X.-M. Liu, G.Q. Lu, Z.-F. Yan, J. Beltramini, Ind. Eng. Chem. Res. **42**, 6518–6530 (2003)
494. J. Ladebeck, J. Koy, T. Regula, DE 10160486 A1, 2001
495. A. Erdohelyi, M. Pasztor, F. Solymosi, J. Catal. **98**, 166 (1986)
496. N. Tsubaki, K. Fujimoto, Top. Catal. **22**(3–4), 325–335 (2003)
497. J. Słoczyński, R. Grabowski, A. Kozłowska, M. Lachowska, J. Skrzypek, Pol. J. Chem. **75**, 733–742 (2001)
498. T.C. Schilke, I.A. Fisher, A.T. Bell, J. Catal. **184**, 144–156 (1999)
499. S.E. Collins, D.L. Chiavassa, A.L. Bonivardi, M.A. Baltanás, Catal. Lett. **103**, 83–88 (2005)
500. J. Toyira, P.R. de la Piscina, J.L.G. Fierro, N. Homs, Appl. Catal. B **29**, 207–215 (2001)
501. N. Nomura, T. Tagawa, S. Goto, Appl. Catal. A **166**, 321–326 (1998)
502. M. Saito, T. Fujitani, M. Takeuchi, T. Watanabe, Appl. Catal. A **138**, 311–318 (1996)
503. M. Behrens, J. Catal. **267**, 24–29 (2009)
504. M. Behrens et al., Chem. Commun. **47**, 1701–1703 (2011)
505. M. Behrens et al. App. Catal., A. **392**, 93–102 (2011)
506. M. Saito, M. Takeuchi, T. Watanabe, J. Toyir, S. Luo, J. Wu, Energy Convers. Mgmt. **38**, 403–408 (1997)
507. J. Deng, Q. Sun, Y. Zhang, S. Chen, D. Wu, Appl. Catal. A **139**, 75–85 (1996)
508. Q. Sun, Y.-L. Zhang, H.-Y. Chen, J.-F. Deng, D. Wu, S.-Y. Chen, J. Catal. **167**, 92–105 (1997)
509. R.P.W.J. Struis, S. Stucki, M. Wiedorn, J. Membr. Sci. **113**, 93–100 (1996)
510. R.P.W.J. Struis, M. Quintilii, S. Stucki, J. Membr. Sci. **177**, 215–223 (2000)
511. R.P.W.J. Struis, S. Stucki, Appl. Catal. A **216**, 117–129 (2001)
512. B. Sea, K.-H. Lee, React. Kinet. Catal. Lett. **80**, 33–38 (2003)
513. B. Sea, K.-H. Lee, J. Ind. Eng. Chem. **7**, 417–423 (2001)
514. B. Sea, K.-H. Lee, Bull. Korean Chem. Soc. **22**, 1400–1402 (2001)
515. K. Hagihara, H. Mabuse, T. Watanabe, M. Kawai, M. Saito, Engery Convers. Mgmt. **36**, 581–584 (1995)
516. K. Hagihara, H. Mabuse, T. Watanabe, M. Saito, Catal. Today **36**, 33–37 (1997)
517. H. Mabuse, K. Hagihara, T. Watanabe, M. Saito, Energy Convers. Mgmt. **38**, 437–442 (1997)
518. G.P. van der Laan, A.A.C.M. Beenackers, B. Ding, J.C. Strikwerda, Catal. Today **48**, 93–100 (1999)

519. Q.D. Truong, J.-Y. Liu, C.-C. Chung, Y.-C. Ling, Catal. Commun. **19**, 85–89 (2012)
520. J. Mao, T. Peng, X. Zhang, K. Li, L. Zan, Catal. Commun. **28**, 38–41 (2012)
521. P.L. Richardson, M.L.N. Perdigoto, W. Wang, R.J.G. Lopes, App. Catal. B **126**, 200–207 (2012)
522. S. Wesselbaum, T. vom Stein, J. Klankenmeyer, W. Leitner, Angew. Chem. **124**, 7617–7620 (2012)

Chapter 5
Substance Properties of Methanol

Heribert Offermanns, Katja Schulz, Elisabeth Brandes and Thomas Schendler

5.1 Physical Properties of Pure Methanol

Heribert Offermanns

Methanol (also known as CH_3OH, methyl alcohol, hydroxymethane, wood alcohol, or carbinol) is a widely used basic raw material. It is a colourless neutral polar liquid that can be mixed with water and most other organic solvents in any ratio. It acts, owed to its polarity, as a solvent for many inorganic salts. The flammability of methanol (flash point 12.2 °C, ignition temperature 470 °C) can cause safety problems. For this reason, there exist many international guidelines for safe handling, explosion protection and electrical equipment to handle methanol. Methanol also is a substance of high toxicity that is rapidly and almost completely adsorbed orally (via the gastrointestinal tract), by inhalation, or through the skin.

H. Offermanns (✉)
Grünaustraße 2, 63457 Hanau, Germany
e-mail: heppoff@gmx.de

K. Schulz
Institute of Legal Medicine, Medical Faculty Carl Gustav Carus, Dresden University of Technology, Fetscherstraße 74, 01307 Dresden, Germany
e-mail: katja.schulz@tu-dresden.de

E. Brandes
Physikalisch-Technische Bundesanstalt (PTB), AG 3.41, Bundesallee 100, 38116 Braunschweig, Germany
e-mail: elisabeth.brandes@ptb.de

T. Schendler
Chemical Safety Engineering, Federal Institute for Materials Research and Testing, Unter den Eichen 87, 12205 Berlin, Germany
e-mail: thomas.schendler@bam.de

M. Bertau et al. (eds.), *Methanol: The Basic Chemical and Energy Feedstock of the Future*, 303
DOI: 10.1007/978-3-642-39709-7_5,

Table 5.1 Physical properties of pure methanol

Molecular weight	32.04 g mol^{-1}
Critical temperature	512.5 K (239 °C; 463 °F)
Critical pressure	8.084 MPa
Critical density	0.2715 g cm^{-3}
Critical compressibility factor	0.224
Specific gravity	
Liquid	
(25°/4 °C)	0.7866
(20°/4 °C)	0.7915
(15°/4 °C)	0.7960
Vapour	1.11
Vapour pressure	
20 °C (68 °F)	12.8 kPa (1.856 psia) (96 mm Hg)
25 °C (77 °F)	16.96 kPa (2.459 psia) (127.2 mm Hg)
Latent heat of vapourisation	
25 °C (77 °F)	37.43 kJ mol^{-1} (279.0 cal g^{-1})
64.6 °C (148.3 °F)	35.21 kJ mol^{-1} (262.5 cal g^{-1})
Heat capacity at constant pressure	
25 °C (77 °F) (101.3 kPa)	
Liquid	81.08 $Jmol^{-1}$ K^{-1} (0.604 $calg^{-1}$ K^{-1}) (0.604 Btu lb^{-1} $°F^{-1}$)
Vapour	44.06 J mol^{-1} K^{-1} [1] (0.328 $calg^{-1}$ K^{-1}) (0.328 Btu lb^{-1} $°F^{-1}$)
Coefficient of cubic thermal expansion	
20 °C	0.00149 per °C
40 °C	0.00159 per °C
Boiling point	
760 mm Hg (101.3 kPa)	64.6 °C (148 °F)
Freezing point	−97.6 °C (−143.7 °F)
Reid vapour pressure	32 kPa
Flash point	
Closed vessel	12 °C (54 °F)
Open vessel	15.6 °C (60.1 °F)
Auto ignition temperature	470 °C (878 °F)
Viscosity	
Liquid	

(continued)

Table 5.1 (continued)

−25 °C (−13 °F)	1.258 mPa·s
0 °C (32 °F)	0.793 mPa·s
25 °C (77 °F)	0.544 mPa·s
Vapour	
25 °C (77 °F)	9.68 μPa·s
127 °C (261 °F)	13.2 μPa·s
Surface tension	
20 °C (68 °F)	22.6 mNm^{-1}
25 °C (77 °F)	22.07 mNm^{-1}
Refractive index	
15 °C (59 °F)	1.33066
20 °C (68 °F)	1.32840
25 °C (77 °F)	1.32652
Thermal conductivity	
Liquid	
0 °C (32 °F)	207 mWm^{-1} K^{-1}
25 °C (77 °F)	200 mWm^{-1} K^{-1}
Vapour	
100 °C (212 °F)	14.07 mWm^{-1} K^{-1}
127 °C (261 °F)	26.2 mWm^{-1} K^{-1}
Heat of Combustion	
Higher heating value	726.1 $kJmol^{-1}$
(25 °C, 101.325 kPa)	(22.7 kJg^{-1})
Lower heating value	638.1 $kJmol^{-1}$ [calc]
(25 °C, 101.325 kPa)	(19.9 kJg^{-1})
Flammable limits (in air)	Lower 6.0 (v/v) %
	Upper 36.5 (v/v) %

With its boiling point of 65 °C and melting point of −96 °C, methanol can be stored in tanks, distributed via pipelines, and transported by tank cars. The miscibility of methanol with water is a great advantage in case of a methanol accident (fire or spilled liquid).

The physical properties of pure methanol are summarised in Table 5.1 [1].

5.2 Toxicology

Katja Schulz

5.2.1 Occurrence of Methanol

In free form, methanol occurs in nature in just a few plants (cotton plants, some grasses and heracleum fruit). In conjugated form, as ester and ether, methanol occurs in the pectin of fruit as a supporting substance and in the lignin as the

lignified part of the plant cell wall. The enzymatic degradation of pectin and lignin leads to the production of methanol.

Alcoholic beverages contain methanol in varying concentrations. It originates from the pectin of the fruit or fruit skins that were used for the production of alcoholic beverages. The highest concentrations of methanol can therefore be found in fruit spirits. Due to its toxicity, maximum amounts of methanol have been stipulated for spirits. Depending on the fruit used, these maximum amounts are between 1,000 and 1,500 g per hectolitre of pure alcohol [2].

Contrary to fusel alcohol, methanol is not a byproduct of alcoholic fermentation. Nonfermented soft drinks, such as fruit juices, also contain methanol if fruit or fruit skins have been used for production. Pectin-rich natural fruit juices contain 24–230 mg of methanol per litre [3]. The fruit as such contains harmless amounts of methanol [4].

Tobacco smoke has a low concentration of methanol, derived from the pyrolytic cleavage of the lignin-containing part of the tobacco. Contrary to many other substances contained in tobacco, methanol is not of toxicological concern.

A large part of the methanol that can be found in the atmosphere stems from plant emission [5, 6]. The atmospheric methanol has an estimated lifetime of about 12 days by reaction with OH radical [7]. It is oxidise to carbon dioxide and water.

Up until the beginning of the twentieth century, methanol was produced by using dry wood for distillation. The wood was heated to approximately 500 °C, and the contained lignin was thermally decomposed. Among other substances, the distillate contains methanol. The name "wood alcohol" for methanol is derived from the occurrence of alcohol in wood. Another historical name for methanol is carbinol. The production of methanol by isolation from natural occurrences is long forgotten. For about 80 years now, methanol has been produced on a large scale by catalysing carbon monoxide and hydrogen. For details, see Chaps. 3 and 4 of this book.

5.2.2 Use of Methanol

With an annual production of several million tonnes worldwide, methanol is one of the most common chemicals. Above all, methanol is used as a base material in the chemical industry, such as in the production of formaldehyde, acetic acid and methyl tert-butyl ether. Methanol is also used as a fuel additive. According to the European norm for petrol fuels, it is permitted to add 3 vol% of methanol to gasoline. Experiments with higher contents of methanol in gasoline (regular and diesel) have been carried out, and they are feasible without any problems if the automobile has been technically modified. Pure methanol can also be used as fuel in adapted motors. Due to its toxicity and above all its physicochemical properties (easily flammable, relatively low boiling point, burning with a hardly visible flame), additional safety measures are required.

Methanol is also used in the industry as a technical solvent or as an ingredient of solvent mixtures. Because methanol is known to be toxic, it is no longer allowed

in household chemicals or do-it-yourself supplies in Germany, except in a few cases. The Federal Institute for Risk Assessment decided on these measures because numerous accidents caused by confusion (some of which also involved children) were registered. Exceptions are made for gasoline for model aircraft with high methanol levels (e.g. helicopters) and generators in small motorboats as well as for fuels used in (Belgian) fireplaces in the living area that were installed in Germany [8].

Methanol is no longer used in motor coolants or windshield defrosters. During World War II, methanol was employed because there was a lack of other conventional defrosters (glycerin and glycol). At that time, many accidents happened because people confused it with ethanol [3]. Today, the key defroster is isopropanol and not methanol. In the past, denaturated alcohol was produced by adulteration ethanol with methanol [9–12]. Today, methanol is no longer used as denaturant.

As described in detail in this book, another major field of application for methanol is its application as an energy source.

5.2.3 Biological Effects of Methanol

Toxicokinetics

The topic of toxicokinetics comprises all processes concerning the fate of a toxic substance in the body. They are subdivided into resorption, distribution, metabolism, storage and excretion. Metabolism, storage and excretion are also brought together under elimination, as the concentration of the substance and usually its effect are reduced.

Resorption

Methanol is rapidly and almost completely absorbed orally (via the gastrointestinal tract) or by inhalation (via the lungs). Maximum blood levels are reached after 30–90 min upon oral absorption. Methanol can also be absorbed dermally (via the skin).

Methanol is usually uptaken when ethanol is confused with methanol or with adulterated alcoholic beverages. In the past, when ethanol was denatured with methanol, there were cases of intoxication due to the consumption of these spirits. Today, denaturated alcohol is produced by adulteration with methyl ethylketone and denatonium benzoate. Denatonium benzoate is one of the bitterest substances known and therefore has a warning effect. Methanol, however, tastes nearly the same as ethanol, so its taste does not keep people from drinking it accidentally.

When homemade spirits made with poorly separated forerun are consumed, they can rarely lead to methanol intoxication because the antidote ethanol is always contained in it, too.

Methanol is a relatively volatile substance, so that it can also be inhaled, such as when working with solvents containing methanol in the industry or when extracting substances with methanol in laboratories.

Distribution

Methanol, like ethanol, is distributed uniformly to body water content because it is very well soluble in water. The approximate value of this body water content is 0.7 times the body weight of men and 0.6 times the body weight of women.

Metabolism

The liver oxidatively metabolises methanol. First, its metabolism goes through the same steps as ethanol metabolism. With the help of the enzyme alcohol dehydrogenase (ADH), an enzymatic oxidation of methanol to formaldehyde takes place. Compared with ethanol, the chemical reaction of methanol takes much longer if caused by ADH. In rats, the oxidation rate for methanol is 25 mg/kg/h, whereas for ethanol it is 175 mg/kg/h [4, 13–15]. Even if other metabolic pathways come to the fore with rats (catalase/peroxidase), the rate of elimination is comparable with humans [16].

In a second reaction, the aldehyde dehydrogenase (AIDH) enzyme immediately oxidises formaldehyde to formic acid. In monkeys, the biological half-life of formaldehyde in blood is 1.5 min [16]. Only a minor amount of the developed formate is eliminated via the kidneys (less than 5 % of the methanol uptake).

The metabolism of formic acid (or of the formate) produces CO_2 very slowly. This is done in two ways: There is a metabolism depending on catalase and a C_1-metabolism depending on tetrahydrofolic acid in the liver and the retina [17, 18]. The mechanism depending on tetrahydrofolic acid is of greater importance [19]. This oxidation step depends on the supply of active folic acid. Thus, folic acid can be used to increase formic acid elimination in cases of intoxication [20]. The metabolism of methanol in humans is shown in Fig. 5.1.

Due to the very slow metabolism and the poor elimination of the formate, there is an accumulation of formic acid leading to a reduction of the hydrogen carbonate concentration with a subsequent acidosis. With methanol intoxications, acidose is a typical and life-threatening pathology that can last several days. In extreme cases, it can reduce the blood pH from normal values between 7.35 and 7.45 to less than 7.0. In addition, there is an extensive acid-base imbalance.

Formic acid inhibits an enzyme of the respiratory chain, mitochondrial cytochrome oxidase, by bonding the sixth coordination area of Fe^{3+} in the heme molecule [21, 22]. The more severe the acidose, the more inhibited the cellular respiration. The inhibition of cellular respiration leads to the production of lactic acid, which makes the acidosis worse [16, 17, 22–24]. This cycle is called circulus hypoxicus. The cause of death with methanol intoxications is usually respiratory paralysis.

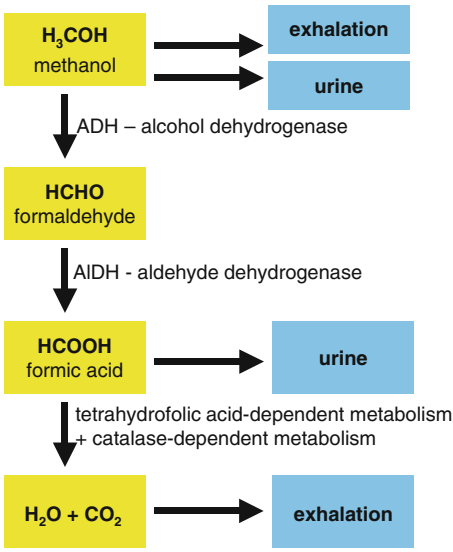

Fig. 5.1 Metabolism of methanol in humans

Storage

Methanol is not stored in the human body. Because it is eliminated only slowly, there is a risk of accumulation if taken repeatedly.

Excretion

Due to the slow ADH oxidation compared with ethanol, methanol is exhaled to a high degree (30–60 %) via the lungs non-metabolised [16]. To a low degree (<5 %), it is also eliminated non-metabolised via the kidneys.

Most of the methanol is oxidatively metabolised in the liver. A small amount of the metabolic intermediate formic acid (<5 %) is eliminated via urine. Formaldehyde is virtually undetectable due to its rapid metabolic pathway to formic acid. Formic acid is then metabolised to CO_2 and H_2O.

5.2.4 Toxicodynamics

Toxicodynamics characterise the kind and strength of the effect of poisons on the organism. Methanol toxicity in humans and higher mammals such as monkeys is characterised by a latent period of many hours followed by metabolic acidosis and ocular toxicity. Methanol competes with ethanol for the ADH enzyme; this is called competitive antagonism. Due to ethanol's higher affinity for ADH, methanol can be displaced. This property is used advantageously on treatment of methanol intoxication. To date, the mechanism causing damage to the optic nerve as a result of methanol intoxication has not yet been discovered.

Acute Toxicity

The difficulty in identifying methanol intoxication is mainly due to methanol being a classic latent poison, which implies that symptoms occur several hours or days after ingestion of the toxic agent. The temporary development of methanol intoxication is shown in Fig. 5.2. In addition, methanol is sensorily hardly ever distinguishable from ethanol and primarily shows a less pronounced inebriation than ethanol.

An excellent review article describes the toxicity of methanol [25]. Here, the author classified the methanol poisoning in humans into four stages:

1. A central nervous system depression of short duration, but milder than that seen following ethanol ingestion
2. An asymptomatic latent period of 12–24 h following ingestion of methanol, where no signs or symptoms are noted
3. After the latent period, severe metabolic acidosis occurs
4. Complaints that are characteristic of ocular toxicity are described, followed by blindness, coma, other central nervous system signs, and death

The acute toxicity of methanol after ingestion is shown primarily by narcotic effects, much like inebriation from ethanol but milder. At small but toxic dosages, drowsiness might not occur. After an asymptomatic latent period, symptoms such as respiratory failure, circulation failure and renal insufficiency are the consequence of metabolic acidosis. This acidosis may persist for several days. In this stage, laboratory investigations show a severe anion gap acidosis. At this time, methanol itself is completely metabolised and therefore not detectable in blood and urine.

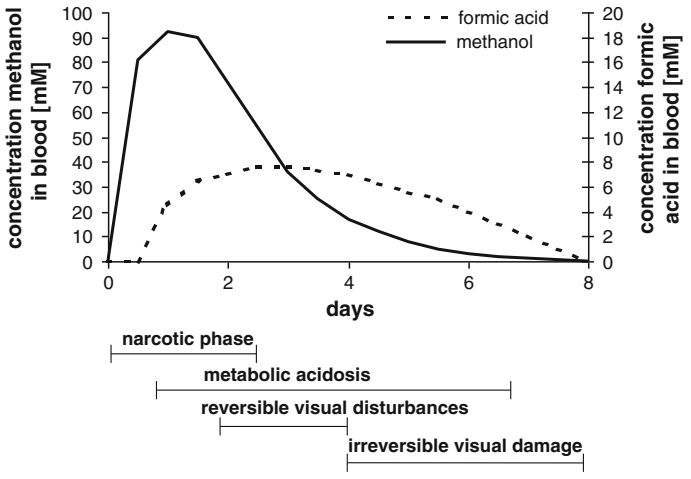

Fig. 5.2 Temporary development of acute methanol intoxication [16]

With methanol intoxications, pathological changes of the central nervous system (a toxic neuropathy) are observed. The optic nerve appears to be particularly sensitive. Also, the acoustic nerve may be concerned. After a latent period of approximately 2 days, methanol causes typical visual disturbances with retina edema. This stage may be reversible. If the edema persists for a substantial period of time and the damage is sufficiently severe, optic nerve atrophy including permanent blindness will ultimately result.

These observations at the optic nerve and the optic system can be detected on autopsy in fatal cases of methanol intoxications with longer survival times [22, 26–30]. The intoxication mechanism of ocular toxicity has not been definitely clarified. Probably, the combination of metabolic acidosis and formic acid inhibition of cytochrome c oxidase in the optic nerve results in histotoxic hypoxia, which is responsible for the ocular and central nervous system toxicity of methanol [17, 18, 31, 32].

The sensitivity to ocular toxicity of methanol is individually different. About half of the survivors of intoxications suffer from visual disturbances and approximately one in four suffers from permanent visual damage. There is a risk of blindness with a dosage of only 5–15 mL in adults [13, 33]. Blindness may occur even if the metabolic acidosis is treated. In cases of methanol-induced toxic optic neuropathy, high-dose corticosteroids are assumed to prevent the irreversible degeneration of the optic nerve in the early stages of intoxication [32].

Death occurs as a result of the metabolic acidosis, mostly in the form of respiratory paralysis. The lethal dosage of methanol in adults is approximately 30–100 mL [13, 33]. Children are more sensitive to the risk of blindness and more likely to die from an intoxication. The lethal dosage depends on the amount of simultaneously consumed ethanol with an antidotal effect, the filling of the stomach and the individual susceptibility.

Chronic Toxicity

Chronic intoxication can occur through repeated ingestion of small but not acutely toxic amounts, such as in the form of fumes between industry and commerce. This can lead to toxic neuropathies, alterations in vegetative area with headache, dizziness, or painful digestive disorders, and even a degeneration of the visual and auditory nerves leading to functional limitations and possibly to blindness and deafness [16, 34].

Toxicity tests for teratogenicity in experimental animals (rats) led to malformations due to high methanol concentrations. For humans, methanol is classified in the gestational group C, meaning there is no need to fear embryonal and fetal impairment with compliance of the maximal allowable concentration (MAC) and biological exposure limit (BEL) values [35].

5.2.5 Treatment of Methanol Intoxication

The treatment of methanol poisoning depends on the amount of ingested methanol, the concentration of methanol determined in the blood, and the occurring symptoms. Mostly, the amount of incorporated methanol is unknown. If it can be estimated, there is usually no need for treatment up to an ingestion of 0.1 g/kg body weight (BW) with adults [33]. Methanol dose levels of 1 g/kg BW or higher are required for severe intoxication leading to death [25]; consequently, the intensive-medical treatment is necessary.

The determination of methanol in the blood/serum is absolutely essential, particularly for the assessment of the severity of the poisoning. Serum-methanol concentrations are toxic from 200 mg/L and life threatening from 500 mg/L [33] or 900 mg/L [36–38]. Especially in the earliest stage of poisoning, when there is no recognisable pathology as is usual with latent poisons; the poisoning can only be identified and treated effectively if the analyte methanol is detected in the blood. If the typical symptoms of methanol poisoning (visual disturbances and metabolic acidosis) occur, the treatment and the progress of the poisoning become much more difficult than at the stage without severe symptoms.

If methanol was recently ingested, the primary decontamination is the gastric lavage, in which case the patient must be conscious. An antidote treatment should follow with ethanol or 4-methyl-pyrazol (Fomepizole), which is supposed to prevent methanol metabolism to the toxic metabolites formaldehyde and formic acid. The application of ethanol competitively inhibits the metabolism of methanol at the ADH enzyme due to its approximately 10 times higher substrate specificity compared with ethanol. An ethanol treatment with a blood alcohol concentration of about 1 per million [20, 33, 34] lasting several hours to days is desirable. The pharmaceutical agent 4-methyl-pyrazol is an inhibitor for the ADH enzyme. It binds to ADH and thereby also inhibits the metabolism of methanol. 4-Methyl-pyrazole has long been known as an inhibitor of ADH [39], but it has only been used as such for the last 10 years [40–44]. Both cases of antidote treatment reduce the action of ADH on methanol by competitive inhibition, and more methanol can be exhaled or excreted non-metabolised by the kidneys.

Metabolic acidosis is treated with a sodium bicarbonate solution or Tris buffer containing the agent trometamol, possibly for several days. In addition, a high dose of folic acid is recommended [16, 33, 34]. It increases the metabolism of the toxic formic acid in the blood through the folate cycle. With methanol poisoning, the human folic acid deposits are not sufficient for proper metabolisation of the toxic metabolite formic acid.

In severe or expectedly severe cases (from an intake of about 25 mL of methanol with a serum methanol concentration from about 500 mg/L or severe acidosis), hemodialysis should be carried out as well [33]. In this way, the concentrations of methanol, formaldehyde and formic acid in the blood are substantially reduced.

The measures described here serve to prevent or to treat life-threatening metabolic acidosis. Against methanol-induced toxic optic neuropathy, these measures

are not certainly effective. Tephly [25] wrote: "Death may occur if patients are not treated for metabolic acidosis, and blindness may result even if treatment for metabolic acidosis is performed". Therefore, high-dose corticosteroids are assumed to prevent the irreversible degeneration of the optic nerve in early states of intoxication [32].

5.2.6 Risks and Dangers by Exposition of Methanol

Until quite recently, the most frequent source of methanol intoxication has been the confusion with ethanol by people who are unaware of the danger. Today, methanol is not used in household chemicals in higher concentrations in Germany, with the exception of the few applications mentioned above. In other countries, these regulations may not be in place, so there household chemicals containing methanol may be an important source of intoxication. Also, methanol individual and mass poisonings from illegal spirits have occurred in countries with a poor ethanol supply or adulterated alcoholic beverages.

In the chemical industry, methanol is a commonly employed organic solvent and reactant in organic synthesis procedures. In the more recent literature, there are no reports of poisonings due to the use of methanol in laboratories or as an industrial chemical. Because methanol is very volatile (boiling point = 65 °C), vapours may form by exposure with methanol or methanol-containing mixtures. If these vapours are inhaled, they can cause toxic effects. People with occupational exposure are likely to be exposed to methanol by inhalation or resorption via the skin.

For protection of human health, threshold values concerning the handling of chemicals have been stipulated. These values are based on toxicological aspects. The MAC is the maximum permissible average concentration of an agent in the form of gas, vapour, or suspended matter in the air at the workplace that does not normally harm (based on present knowledge) most of the people exposed to it for a long time (8 h/day, 5 days/week, all of their working life). The MAC values are, however, not reliable limits for separating the dangerous from the harmless zone. MAC values exist for more than 600 substances, including methanol. The MAC for methanol is 200 mL/m^3 (ppm) and 270 mg/m^3, respectively [35]. The odour threshold for methanol, however, is 2,000 ppm [45]. It is many times higher than the MAC value. Consequently, there is no warning effect for humans.

The BEL is the highest quantity of an agent or of its metabolites allowed in humans (blood or urine) or the subsequent variation of a biological indicator that usually does not harm the workforce, even if exposed repeatedly and for a long time. The BEL values apply to healthy people under the same work time conditions as with MAC values. The values are not applicable to the general population. The BEL value for methanol is 30 mg/L in urine [35].

The MAC and BEL values are prepared, checked and updated every year by the Senate Commission for the control of health hazards of the German Research

Foundation. Even if the values cannot be applied to the general population, they help to estimate the potential risk and the toxicity.

Exposure to methanol during its production or processing is not the only risk leading to poisoning, except for poisoning through ingestion due to a confusion with ethanol. If pure methanol is used as a fuel for vehicles, additional sources of exposure need to be taken into account. However, this excludes the well-established addition of methanol to fuel.

A powerful argument that speaks for the use of methanol as a fuel for vehicles is its reduced environmental impact compared to the gasoline and diesel emissions. In contrast to currently used fuels, methanol completely combusts to carbon dioxide and water. Pollutants such as particulate matter, oxides of nitrogen and ozone are reduced through the usage of methanol as automotive fuel [46, 47]. On the other hand, the concentrations of two gaseous pollutants are expected to increase: formaldehyde and methanol [48, 49]. Formaldehyde is a byproduct resulting from the incomplete combustion of methanol.

Besides the continuous emission of methanol while driving, it may also be emitted when the motor is ignited, as uncombusted material in the exhaust, from its evaporation during refuelling, through the daily heating of the fuel tank, and in special cases such as engine malfunctions. In personal garages and service stations, the estimated methanol concentrations represent the highest exposure levels; in parking garages and roadway tunnels, concentrations are lower [50]. Even at the highest estimated exposure levels, the concentrations are below the MAC threshold limit value of 270 mg/m^3. Back in 1987, the Environmental Protection Agency identified the importance of technically evaluating the relevant health issues with the two pollutants methanol and formaldehyde [51]. The conclusion of this study was that methanol-powered motor vehicles are applicable to these situations as well.

However, it is necessary to consider all special cases, such as accidents or leaking fuel lines, for methanol-powered vehicles. The latter situation can cause dangerously high methanol concentrations, not only in the interior of the vehicle but also in personal garages and service stations. The MAC value is then assumed to be exceeded. In such cases, the immediate main risk lies in the ignition of the methanol fuel. Such cases can be found in literature [52].

In the beginning of the twentieth century, methanol was a widely spread substance on the consumer goods market, as a pure substance, an additive to several products, and an often-used chemical at the workplace. At that time, the documented number of methanol poisonings was extremely high [50, 53–59]. In most cases, methanol was taken in orally. Many poisonings resulted from methanol as an adulterant in alcoholic beverages [60–64]. Other cases occurred due to the extensive presence of methanol at the workplace in combination with a lack of work safety measures and ignorance towards the corresponding dangers. The results of a survey carried out in the United States in 1904 showed that about 2 million people worked in jobs where they had to use methanol. The most common professions were painters, glaziers, varnishers, launderers, boot and shoemakers, painters and lithographers [50, 55]. In this context, literary sources

also give proof of accidents caused by inhalation or percutaneous uptake of lethal amounts of methanol [39, 56, 58, 65]. Today, these accidents are basically a thing of the past and hardly ever take place in industrialised countries.

However, if methanol is introduced as a fuel for motor vehicles, larger quantities of methanol would have to be stored and transported. Occasionally, the media report about accidents involving trucks or freight cars that transported pure methanol or methanol blends [66, 67]. These accidents conflict with the equally dangerous accidents with regular or diesel fuels.

5.2.7 Mass Poisoning and Accidents Caused by Methanol

In the past, besides single methanol poisonings, there were also some mass poisonings and incidents that concerned larger groups of people. For example, mass poisonings occurred in Estonia in September 2001 from the consumption of illegal spirits containing 50–100 % of methanol. Consequently, 154 people were poisoned and 68 of them died [68]. In March 2009, three students from Lübeck died in Turkey during a class trip, where they drank alcohol adulterated with methanol [69, 70]. In Bali in May 2009, 25 people died after drinking methylated rice wine [73]. In textbooks, there is evidence of historic mass poisonings from methanol [71].

As mentioned, one cannot rule out the possibility that accidents with tankers or freight cars carrying methanol will continue to happen at greater frequency. There is a serious risk of inhalation exposure to pure methanol vapour for emergency responders and the people involved in the accident, in addition to the risk of the methanol igniting. However, methanol fires can extinguished with plain water, in contrast to petroleum fires. In 1981, an accident occurred with a methanol-powered racing car at the Indianapolis Motor Speedway, where methanol ignited when the car was being filled [52]. Burning methanol has an invisible flame. The racecar driver and a member of the pit team were burning without any visible flames. Injecting water to the opening of the tank now prevents this kind of accident from happening while the car is filled. Since 2007, all vehicles in the Indianapolis race have run with ethanol.

In the literature, there are reports on numerous Swedish cases that have taken place between 1980 and 1983 involving accidental burns with domestic fire-lighting fluids containing methanol as an igniting fluid [72]. These accidents occurred while using this fluid for lighting barbecues or filling lamps and stoves, caused by negligence or inadequate knowledge of the dangers of methanol used for igniting.

5.2.8 Environmental Toxicology of Methanol

Methanol is completely miscible with water. It exhibits relatively high mobility if introduced into an aqueous environment. Methanol is readily biodegradable and shows no bioaccumulation. Methanol does also not persist in the environment [45]. Regular and diesel fuels, in contrast to methanol, are not readily biodegradable and show an appreciable potential for bioaccumulation. Furthermore, in contrast to methanol, regular and diesel fuel may cause cancer by long-term exposure [74, 75].

Despite the recognised human toxicity by direct (oral) ingestion of methanol, the properties related to environmental behaviour indicate only a marginal possibility of human exposure to methanol concentrations via consumption of contaminated water or food or contact with contaminated water or soil [76].

5.2.9 Conclusion

The toxicology of methanol has been discussed. The highest risk of intoxication exists for an accidental oral intake of methanol when it is confused with ethanol. Through governmental regulations to not allow methanol-containing chemicals in household or do-it-yourself products, the risk of methanol intoxication is reduced.

In contrast, the handling of methanol as base material for chemical industry, automotive fuel and industrial processes is easily technological realisable. Using qualified persons and safety measures, the risk of intoxication from methanol exposure likely is decreased.

5.3 Transport, Storage and Safety Handling

Elisabeth Brandes and Thomas Schendler

Because of its properties, methanol is subject to classification as dangerous good for transport and as a dangerous substance for handling, use and storage. Transport, handling and use classifications are based on European or international regulations [77–80], whereas storage instructions are based on national regulations, such as those in Germany (the *Betriebssicherheitsverordnung* [81] and the *Gefahrstoffverordnung* [82] and the respective downstream regulations *Technische Regeln für Betriebssicherheit* [TRBS] or *Technische Regeln für Gefahrstoffe* [TRGS]). Furthermore, the European Directives 94/9/EC [83], 1999/92/EC [84], and 98/24/EC [85] apply when methanol is produced or used in industrial processes.

5.3.1 Transport

Methanol is classified as a class 3 flammable liquid in packing group II, with a subsidiary risk of being toxic for transport on roads according to the ADR [86], on rail according to the RID [87], on inland waterways according to the ADN [88], for sea transport according to IMDG Code [89], and for air transport [90]. ADR, RID, ADN and IMDG are the European implementations of the Recommendations on the Transport of Dangerous Goods [91] elaborated and developed further by the United Nations.

Within these transport regulations, the classification as a class 3 flammable liquid is based on the substance's flashpoint. The class 3 designation includes substances meeting the following criteria:

- Liquid
- Vapours pressure of not more than 300 kPa (3 bar) at 50 °C
- Not completely gaseous at 20 °C and at standard pressure of 101.3 kPa
- Flashpoint of not more than 60 °C [86–90]

The class 3 flammable liquid designation is further divided into three packing groups that reflect the degree of danger associated with the substance/article and the requirements of the packaging and—in combination with toxicological and environmental dangers—of stowage (see Table 5.2).

Table 5.2 Classification of dangerous goods with class 3 flammable liquid designation

Packing group	Flash point (closed cup)	Initial boiling point (°C)
I	–	≤35 °C
II	<23 °C	>35 °C
III	≥23 °C and ≤60 °C	>35 °C

Furthermore, "the heading of Class 6.1 covers substances of which it is known by experience or regarding which it is presumed from experiments on animals that in relatively small quantities they are able by a single action or by action of short duration to cause damage to human health, or death, by inhalation, by cutaneous absorption or by ingestion [86–90]". This dangerous goods class 6.1 toxic substances designation is furthermore divided into three packaging groups, which reflect the degree of danger associated with the substance/article and the requirements of the packaging and—in combination with toxicological and environmental dangers—of stowage (see Table 5.3).

For many dangerous goods, a specific identification number is given. Together with its name and classification code, it listed in the respective regulations. For methanol, the following transport classification is valid: UN 1230 Methanol, 3 (6.1) II. It is based on its boiling point of 65 °C, its flash point of 9 °C and its classification as toxic (see Sect. 5.2) corresponding to the major hazard on the basis of the order of precedence [86–90].

Table 5.3 Classification of dangerous goods with class 6.1 toxic substances designation

	Packing group	Oral toxicity LD_{50} (mg/kg)	Dermal toxicity LD_{50} (mg/kg)	Inhalation toxicity by dusts and mists LC_{50} (mg/L)
Highly toxic	I	≤5	≤50	≤0.2
Toxic	II	>5 and ≤50	>50 and ≤200	>0.2 and ≤2
Slightly toxic	III	>50 and ≤300	>200 and ≤1,000	>2 and ≤4

LD_{50} median lethal dose, LC_{50} median lethal concentration

For sea transport, special stowage requirements apply [89], namely "clear of living quarters." Depending on the number of passengers on board, stowage is allowed on deck only. Special regulations concerning the amount of shipped methanol apply for transport by air [88]. For passenger aircraft the maximum amount of the packaging is 1 L; for cargo aircraft, the maximum amount of the packaging is 60 L.

5.3.2 Handling and Use

With respect to handling, methanol is classified as a flammable liquid (category 2), with acute inhalation toxicity, acute dermal toxicity, acute oral toxicity (category 3) and specific target organ toxicity for single exposure (category 1), according to Regulation (EC) No 1272/2008 on the classification, labelling and packaging of substances and mixtures (CLP regulation) [80]. The CLP regulation is the EU implementation of the Globally Harmonised System for the Classification and Labelling of Chemicals [92], elaborated and developed further by the United Nations. This CLP regulation replaced the former Council Directive 67/548/EEC in 2010 [93]. Within this CLP regulation, a flammable liquid is defined as a liquid with a flash point of not more than 60 °C. The criteria in Table 5.4 apply for the respective categories in Regulation (EC) No 1272/2008.

In the CLP regulation, acute toxicity is defined as "adverse effects occurring following oral or dermal administration of a single dose of a substance or a mixture, or multiple doses given within 24 h, or an inhalation exposure of 4 h." The hazard classes of acute toxicity are differentiated into acute oral toxicity, acute dermal toxicity and acute inhalation toxicity. The limiting values for these categories are given in Table 5.5.

Table 5.4 Criteria for the respective categories

Category	Criteria
1	Flash point <23 °C and initial boiling point ≤35 °C
2	Flash point <23 °C and initial boiling point >35 °C
3	Flash point ≥23 °C and ≤60 °C

Table 5.5 Limiting values for the categories of acute toxicity

Exposure route	Category 1	Category 2	Category 3	Category 4
Oral (mg/kg body weight)	ATE $\leq$ 5	5 < ATE $\leq$ 50	50 < ATE $\leq$ 300	300 < ATE $\leq$ 2,000
Dermal (mg/kg body weight)	ATE $\leq$ 50	50 < ATE $\leq$ 200	200 < ATE $\leq$ 1,000	1,000 < ATE $\leq$ 2,000
Inhalation vapours (mg/L)	ATE $\leq$ 0.5	0.5 < ATE $\leq$ 2.0	2.0 < ATE $\leq$ 10.0	10.0 < ATE $\leq$ 20.0

ATE: acute toxicity equivalence, which equals the mean lethal dose (LD_{50})/mean lethal concentration (LC_{50}) where available or as calculated from range test results or classification categories.

The criteria for the classification and the limiting values for the categories according to the CLP regulation are identical to those of the transport regulations, except that category 4 is of no relevance for transport classification. However, the principle precedence of hazard is only an aspect within the transport classification. This means that, for handling and use, each hazard assigned to a substance/mixture is of similar significance.

5.3.3 Storage

Currently, no European or international storage regulations exist. The German regulation on flammable liquids, which has regulated the storage conditions in nonportable vessels for flammable liquids, came out of force in 2002. The related downstream regulation (*Technische Regel brennbare Flüssigkeiten* 01) [94], however, is still valid until the new storage regulations that are being developed at the moment come into force. This is foreseen for the end of 2012. The requirements for the storage of methanol in nonportable vessels have been and will be based on its hazards of flammability and acute toxicity (see above). For the storage in portable vessels, TRGS 510 applies [95].

5.3.4 Safe Handling in Industrial Processes

According to Council Directives 89/391/EEC [96] and 98/24/EC [97] on the introduction of measures to encourage improvements in the safety and health of workers at work, the employer is supposed to take measures with respect to the safety and health of the workers. If hazards caused by potentially explosive atmospheres may arise during industrial processes, Directive 1999/92/EC on the minimum requirements for improving the safety and health protection of workers who are potentially at risk from explosive atmospheres [84] has to be applied. This

Table 5.6 Safety characteristic data of methanol [100, 101]

Safety characteristic	Ambient (20 °C[a], 1 bar)	Temperature dependence	Pressure dependence
Flash point	9 °C	Only existing at ambient conditions	
Lower explosion point	8 °C	–	Exponential increase
Lower explosion limit	6.0 vol%	Relative linear decrease −12.5 % per 100 K	More or less independent
Upper explosion limit at 50 °C	50.0 vol%	Relative linear increase ≈ + 10.0 % per 100 K up to ≈ 400 °C	Linear increase up to 30 bar
Limiting oxygen concentration, N_2	8.1 vol%	Linear decay up to ≈ 400 °C	Linear decay up to 30 bar
Automobile ignition temperature	440 °C	–	Exponential decay
Maximum experimental safe gap (MESG)	0.92 mm	Linear decay ≈ −15.5 % per 100 K	$\sim 1/p$
Minimum ignition energy	0.2 mJ	Linear decay	$\sim 1/p^2$
Maximum explosion pressure (p_{max})	850 kPa	$\sim T_0/T$; T in K	$\sim p/p_0$

[a] Unless other information is given in column 1

European Directive contains the minimum requirements that can be extended by the EU member states when transferred to national legislation. For Germany, this is done by the *Betriebsicherheitsverordnung* [85] and the *Gefahrstoffverordnung*. Accordingly, an explosion risk assessment has to be conducted. Depending on its result, an explosion protection document has to be prepared where specific measures have to be laid down to ensure a safe working environment and appropriate surveillance during the presence of workers. The Guide of Good Practice for implementing Directive 1999/92/EC [98] helps to fulfil this requirement. The specific measures are based on the individual safety characteristic data of the respective substance/mixture.

Because of its flashpoint, methanol is able to form an explosive atmosphere at ambient conditions, as well as during processes that are run at elevated pressure or temperatures. An explosion risk assessment for methanol would, therefore, result in "formation of explosive atmosphere possible". The explosion protection document should then list possible measures to handle the associated hazards. Such a measure based on the safety characteristic data of methanol (see Table 5.6) might include the following:

- Prevention of the formation of hazardous explosive methanol/air
  This can be done by keeping the concentration of the methanol/air mixture below the lower explosion limit, either by dilution with air/inert gas or by using process temperatures that are below the flashpoint/lower explosion point, because then the concentration of the methanol is expected to be below the lower explosion limit. TRBS 2152 [99] part 2 recommends a safety distance of

−3 to −5 K from the flashpoint and 1–2 K from the lower explosion point. Another measure is to stay below the limiting oxygen concentration by dilution with an inert gas (e.g. nitrogen).
If it is not possible to reliably prevent the formation of a hazardous explosive atmosphere, hazardous areas have to be assigned (zoning), taking into account the likelihood of the formation of explosive atmospheres.

- Avoidance of the ignition of explosive atmospheres
The most widespread ignition sources are hot surfaces (related safety characteristic: automobile ignition temperature [AIT]; see Table 5.6), electrical sparks (related safety characteristic: MIC; see Table 5.6), flames (related safety characteristic: maximum experimental safe gap [MESG]; see Table 5.6), and electrostatic discharges (related safety characteristic: minimum ignition energy [MIE]; see Table 5.6). Only explosion-protected equipment fulfilling the requirements of Directive 1994/9/EC [83] is allowed within the respective zones.
- Mitigation of the detrimental effects of an explosion
If the ignition of hazardous explosive atmospheres cannot be excluded, the detrimental effects of an explosion have to be mitigated. This can be done by limiting the effects of an explosion to an acceptable extent, such as by explosion-resistant design, explosion relief based on the safety characteristic p_{max}, or the prevention of flame and explosion propagation through gaps designed on the basis of MESG.

If process conditions other than ambient apply, it has to be taken into account that safety characteristic data are temperature and pressure dependent. The lower explosion limit (LEL) decreases with increasing temperature; the influence of pressure is negligible. The upper explosion limit (UEL) increases with increasing temperature and pressure. The limiting oxygen concentration, MESG and MIE decrease with increasing pressure and temperature. The AIT decreases with increasing pressure, whereas the LEP increases with increasing pressure. The pressure and temperature dependence are not constant; they vary from substance to substance and from safety characteristic to safety characteristic. Therefore, the use of individual data is recommended.

Reference to Section 5.1

1. www.methanex.com/products/MSDS/European_SDS_German.pdf; www.methanol.org/Health-And-Safety/Safety-Resources/Health—Safety/Methanex-TISH-Guide.aspx

References to Section 5.2

2. Europäische Gemeinschaft (EG) (2008) Verordnung Nr. 110/2008 des Europäischen Parlaments und des Rates vom 15. Januar 2008 zur Begriffsbestimmung, Bezeichnung, Aufmachung und Etikettierung von Spirituosen sowie zum Schutz geographischer Angaben

für Spirituosen und zur Aufhebung der Verordnung (EWG) Nr. 1576/89. Amtsbl Eur Union, **2008**, L39: 16
3. H. Marquardt, S.G. Schäfer, *Lehrbuch der Toxikologie* (Mannheim, Leipzig, Wien, Zürich, BI Wissenschafts-Verlag, 1994), p. 759
4. F.-X. Reichl, *Taschenatlas der Toxikologie* (Georg Thieme Verlag, Stuttgart, New York, 1997), p. 88
5. T. Stavrakou, A. Guenther, A. Razavi, L. Clarisse, C. Clerbaux, P.F. Coheur, D. Hurtmans, F. Karagulian, M. De Maziere, C. Vigouroux, C. Amelynck, N. Schoon, Q. Laffineur, B. Heinesch, M. Aubinet, C. Rinsland, J.F. Müller, Atmos. Chem. Phys. **11**, 4873 (2011)
6. D.B. Millet, D.J. Jacob, T.G. Custer, J.A. de Gouw, A.H. Goldstein, T. Karl, H.B. Singh, B.C. Sive, R.W. Talbot, C. Warneke, J. Williams, Atmos. Chem. Phys. **8**, 6887 (2008)
7. C.N. Hewitt, T. Karl, B. Langford, S.M. Owen, M. Possell, TRAC **30**, 937 (2011)
8. A. Hahn, Federal Institute for Risk Assessment, Berlin, Germany, personal communication, **2011**
9. H. Hager, *Handbuch der pharmazeutischen Praxis* (Springer, Berlin, 1938)
10. S. Moeschlin, *Klinik und Therapie der Vergiftungen*, 6th edn. (Georg Thieme Verlag, Stuttgart, New York, 1980), p. 259
11. H. Orthner, *Die Methylalkohol-Vergiftung* (Springer Berlin Göttingen Heidelberg, 1950)
12. H. Orthner, Arch. Exp. Path. Pharmakol. **218**, 67 (1953)
13. R.K. Müller, K. Lohs, *Toxikologie*, 2nd edn. (Gustav Fischer Verlag, Stuttgart, Jena, 1992), p. 117
14. J.C. Mani, R. Pietruszko, H. Theorell, Arch. Biochem. Biophys. **140**, 52 (1970)
15. R. Pietruszko, Non ethanol substrates of alcohol dehydrogenase, (Plenum Press, New York, 1979), p. 87–106
16. G. Eisenbrand, M. Metzler, *Toxikologie für Chemiker* (Georg Thieme Verlag, Stuttgart, New York, 1994), p. 201
17. J. Liesivuori, H. Savolainen, Pharmacol. Toxicol. **69**, 157 (1991)
18. M.K. Martinasevic, M.D. Green, J. Baron, T.R. Tephly, Appl. Pharmacol. **141**, 373 (1996)
19. R. Kavet, K.M. Nauss, Crit. Rev. Toxicol. **21**, 21 (1990)
20. T. Karow, R. Lang, *Allgemeine und spezielle Pharmakologie und Toxikologie*, 8th edn. (Bergisch-Gladbach, Druckerei F. Hansen, 2000), p. 677
21. P. Nicholls, Biochim. Biophys. Acta **430**, 13 (1976)
22. O. Roe, Acta Ophthalm. **4**, 169 (1949)
23. M.T. Seme, P. Summerfelt, J. Neitz, J.T. Eells, M.M. Henry, Invest. Ophthalmol. Vis. Sci. **242**, 834 (2001)
24. J.T. Eells, M.M. Salzmann, M.F. Lewandowski, T.G. Murray, Toxicol. Appl. Pharmacol. **140**, 58 (1996)
25. T.R. Tephly, Life Sci. **1991**, 48 (1031)
26. W.H. Fink, Am. J. Ophthalm. **26**, 649 (1943)
27. R. Menne, Arch. Pathol. **26**, 77 (1938)
28. L. Pick, M. Bielschowsky, Berlin. Klin. Wochenschr. **49**, 888 (1912)
29. D.J. Tonning, N.S. Med, Bull. **24**, 1 (1945)
30. H. Andresen, H. Schmoldt, J. Matschke, F.A. Flachskampf, E.E. Turk, Forensic Sci. Int. **179**, 206 (2008)
31. M.S. Hayreh, S.S. Hayreh, G.L. Baumbach, P. Cancilla, G. Martin-Amat, T.R. Tephly, K.E. McMartin, A.B. Makar, Arch. Ophthalmol. **1977**, 95 (1851)
32. M. Abrishami, M. Khalifeh, M. Shoayb, M. Abrishami, J. Ocul. Pharmacol. Th. **27**, 261 (2011)
33. R. Ludewig, *Akute Vergiftungen*, 9th edn. (Wissenschaftliche Verlagsgesellschaft mbH Stuttgart, 1999), p. 422
34. C.J. Estler, *Pharmakologie und Toxikologie*, 3rd edn. (Schattauer Verlag, Stuttgart, New York, 1992), p. 614
35. Senatskommission für gesundheitsschädliche Arbeitsstoffe der DFG, 2010
36. R.J. Flanagan, Ann. Clin. Biochem. **35**, 261 (1998)

37. R. Regenthal, M. Krüger, C. Köppel, R. Preiß, Anästhesiol. Intensivmed. **40**, 129 (1999)
38. D.R.A. Uges "Therapeutic and toxic drug concentration list" to be found under www.tiaft.org/members 'or' www.gtfch.org/intern, (2002)
39. R. Pietruszko, Biochem. Pharmacol. **24**, 1603 (1975)
40. H.E. Zimmermann, K.K. Burkhart, J.W. Donovan, P.A. Hershey, J. Emerg. Nurs. **25**, 116 (1999)
41. J. Brent, K. McMartin, S. Phillips, C. Aaron, K. Kulig, N. Engl, J. Med. **340**, 832 (2001)
42. B. Megarbane, S.W. Borron, F.J. Baud, Intens. Care Med. **31**, 189 (2005)
43. M.B. Mycyk, J.B. Leikin, Am. J. Ther. **10**, 68 (2003)
44. R. Green, Am. J. Emerg. Med. **25**, 799 (2007)
45. Kommission der Europäischen Gemeinschaften, Sicherheitsdatenblatt Methanol, Richtlinie 2001/58/EG, (2007)
46. M.D. Gold, *Abstract.* Paper presented at 78th Annual Meeting of the Air Pollution Control Association (Detroit, MI, 1985), p. 31
47. Report of the Three-Agency Methanol Task Force, *California Energy Communication and South Coast Air Quality Management District*, 1986
48. C.A. Harvey, P.M. Carey, J.H. Somers, R.J. Garbe, *AE Technical Paper Series* 1984, #841357, (Baltimore, MD, 1984)
49. M.D. Gold, C.E. Moulis, *Abstract.* Paper presented at *18th Annual Meeting of the Air Pollution Control Association* (Detroit, MI, 1988), p. 449
50. R. Kavet, K.M. Nauss, Crit. Rev. Toxicol. **21**, 21 (1990)
51. Health Effects Institute, R*eport of the Institute's Health Res. Comm.* (1987)
52. C. Lewalter, "Unsichtbares Feuer" to be found under http://www.fwnetz.de, (2013)
53. S.E. Jelliffe, Med. News **86**, 387 (1905)
54. C.A. Wood, Int. Clin. **16**, 68 (1906)
55. H.H. Tyson, M.J. Schoenberg, JAMA **63**, 915 (1914)
56. C.A. Wood, F. Buller, JAMA **43**, 972 (1904)
57. C.A. Wood, JAMA **1912**, 59 (1962)
58. S.L. Ziegler, JAMA **77**, 1160 (1921)
59. H.H. Tyson, Arch. Ophthalmol. **16**, 459 (1912)
60. W.B. Chew, E.H. Berger, O.A. Brines, M.J. Capron, JAMA **130**, 61 (1946)
61. W.D. Province, R.A. Kritzler, F.P. Calhoun, Bull. US Army Med. Dept. **5**, 114 (1946)
62. I.L. Bennett, F.H. Cary, G.L. Mitchell, M.L. Cooper, Medicine **32**, 431 (1953)
63. R.L. Kane, W. Talbert, J. Harlan, G. Sizemore, S. Cataland, Arch. Environ. Health **17**, 119 (1968)
64. R. Dethlefs, S. Naraqi, Med. J. Aust. **2**, 483 (1978)
65. E.R. Gimenez, N.E. Vallejo, E. Roy, M. Lis, Clin. Toxicol. **1**, 39 (1968)
66. "Deutschland: Schwerer Unfall mit 24 Tonnen Methanol beladenen Lkw" available from http://www.fireworld.at/cms/printer.php?id=32123. (2013)
67. Methanol-Güterzug stand in Flammen, available from http://www.fireworld.at/cms/printer.php?id=307. (2013)
68. R. Paasma, K.E. Hodva, A. Tikkerberi, D. Jacobsen, Clin. Toxicol. **45**, 152 (2007)
69. E.-M. Meester, Rätseln um den Tod der drei Lübecker Schüler, available from http://www.zeit.de/online/2009/15/luebeck-alkohol/komplettansicht. (2013)
70. Getränkehändler in der Türkei festgenommen, available from http://www.zeit.de/online/2009/15/methanol-turkei-festnahmen/komplettansicht. (2013)
71. W. Huckenbeck, W. Bonte in Handbuch gerichtliche Medizin (Eds.: B. Madea, B. Brinkmann) Springer-Verlag, Berlin, Heidelberg, New York, Hongkong, London, Mailand, Paris, Tokio, p. 523, (2003)
72. G. Jurell, J. Kjartansson, M. Malm, B. Nylen, Scand. J. Plast. Reconstr. Surg. **18**, 155 (1984)
73. 25 Tote durch gepanschten Alkohol, available from http://www.sueddeutsche.de/panorama/2.220/bali-tote-durch-gepanschten-alkohol-1.446679. (2013)
74. Safety data sheet gasoline, 1272/2008/EC and EEC Commission Regulation 1907/2006/EC (REACH), (2011)

75. Safety data sheet fuel, 1272/2008/EC and EEC Commission Regulation 1907/2006/EC (REACH), (2010)
76. P.T. Katsumata, W.E. Kastenberg, Hazard. Waste Cons. **13**, 485 (1996)

References to Section 5.3

77. Directive 2008/68/EC of the European Parliament and of the Council of 24 September 2008 on the inland transport of dangerous goods
78. Directive 2002/84/EC of the European Parliament and of the Council of 5 November 2002 amending the Directives on maritime safety and the prevention of pollution from ships
79. Convention for the Unification of Certain Rules for International Carriage by Air-Montreal Convention (1999). Rules for International carriage by air
80. Regulation (EC) No 1272/2008 of the European parliament and of the council of 16 December 2008 on classification, labelling and packaging of substances and mixtures, amending and repealing Directives 67/548/EEC and 1999/45/EC, and amending Regulation (EC) No 1907/2006
81. Verordnung über Sicherheit und Gesundheitsschutz bei der Bereitstellung von Arbeitsmitteln und deren Benutzung bei der Arbeit, über Sicherheit beim Betrieb überwachungsbedürftiger Anlagen und über die Organisation des betrieblichen Arbeitsschutzes (Betriebssicherheitsver-ordnung-BetrSichV), 2002, Zuletzt geändert durch Art. 5 G v. 8.11.2011 I 2178
82. Verordnung zum Schutz vor Gefahrstoffen (Gefahrstoffverordnung - GefStoffV)
83. Directive 94/9/EC of the European Parliament and the Council of 23 March 1994 on the approximation of the laws of the Member States concerning equipment and protective systems intended for use in potentially explosive atmospheres
84. Directive 1999/92/EC of the European Parliament and of the Council of 16 December 1999 on minimum requirements for improving the safety and health protection of workers potentially at risk from explosive atmospheres
85. Council Directive 98/24/EC of 7 April 1998 on the protection of the health and safety of workers from the risks related to chemical agents at work (fourteenth individual Directive within the meaning of Article 16(1) of Directive 89/391/EEC)
86. European Agreement Concerning the International Carriage of Dangerous Goods by Road (ADR)
87. Convention concerning International Carriage by Rail (RID)
88. European Agreement concerning the International Carriage of Dangerous Goods by Inland Waterways (ADN)
89. International Maritime Code for Dangerous Goods (IMDG Code)
90. Technical instructions for the safe transport of dangerous good by air (ICAO-TI), (IATA DGR)
91. Recommendations on the Transport of Dangerous Goods, Model Regulations
92. Globally Harmonized System for the Classification and Labelling of Chemicals (GHS) Council
93. Directive 67/548/EEC of 27 June 1967 on the approximation of laws, regulations and administrative provisions relating to the classification, packaging and labelling of dangerous substances
94. Technische Regel brennbare Flüssigkeiten (TrbF) 01 “Allgemeines, Aufbau und Anwendung der TRbF” (Hinweise des BMA). BArbBl. 7-8/2002 S. 143
95. TRGS 510 “Lagerung von Gefahrstoffen in ortsbeweglichen Behältern”. GMBl. 2010, Nr. 81-83, S. 1693-1721
96. Council Directive of 12 June 1989 on the introduction of measures to encourage improvements in the safety and health of workers at work (89/391/EEC)

97. Council Directive 98/24/EC of 7 April 1998 on the protection of the health and safety of workers from the risks related to chemical agents at work (fourteenth individual Directive within the meaning of Article 16(1) of Directive 89/391/EEC
98. Guide of good practice for implementing Directive 1999/92/EC of the European Parliament and of the Council on minimum requirements for improving the safety and health protection of workers potentially at risk from explosive atmospheres
99. Technische Regel für Betriebssicherheit TRBS 2152 Teil2 – Technische Regel für Gefahrstoffe TRGS 722: Vermeidung oder Einschränkung gefährlicher explosionsfähiger Atmosphäre, 2006
100. Chemsafe: Database for rated safety characteristic data, DECHEMA, online: http://www.dechema.de/chemsafe
101. E. Brandes, W. Möller, *Safety Characteristic Data*, vol. 1 (Wirtschaftsverlag-NW, Bremerhaven, 2008)

Chapter 6
Methanol Utilisation Technologies

Martin Bertau, Hans Jürgen Wernicke and Friedrich Schmidt

6.1 Introduction

Martin Bertau, Hans Jürgen Wernicke and Friedrich Schmidt

Oil and gas are raw materials the availability of which is prognosticated to run short in the near future [1]. The peak oil discussion is an example generally perceived as proof of this development to come [2]. Other reports appear to calm these fears, stating that oil and gas production will even increase until 2050 [3–6]. Whether or not these forecasts hold true, shale gas exploitation will bring relief in supplying the chemical industry with fossil carbon.

Nevertheless, crude oil qualities will still be constantly declining. Crude oil compositions will move towards higher fractions of heavy hydrocarbons, while the fraction of lower-boiling hydrocarbon decreases, rendering low qualities more expensive [7]. Together with a growing demand for oil and gas in emerging economies (Brazil, Russia, India, Indonesia, China and South Africa), a severe shortage in oil and gas supply at economically reasonable prices will expectedly affect the chemical industry in the short to medium term.

It is therefore critical to have synthetic products on hand that can easily substitute for classic petrochemicals. To achieve this without impairing national economies, a substitute is required that can be used in lieu of oil and gas without the need for further investments in both national infrastructure and petrochemical plants. This central

M. Bertau (✉)
Institute of Chemical Technology, Freiberg University of Mining and Technology,
Leipziger Straße 29, 09599 Freiberg, Germany
e-mail: martin.bertau@chemie.tu-freiberg.de

H. J. Wernicke
Kardinal–Wendel-Straße 75 a, 82515 Wolfratshausen, Germany
e-mail: h.j.wernicke@t-online.de

F. Schmidt
Angerbachstrasse 28, 83024 Rosenheim, Germany
e-mail: fs-ro@gmx.de

M. Bertau et al. (eds.), *Methanol: The Basic Chemical and Energy Feedstock of the Future*, 327
DOI: 10.1007/978-3-642-39709-7_6,

requirement, the strict fulfilment of which is the only way to escape from problems with the supply and quality of fossil raw materials, is solely met by methanol. Any such approach will primarily run on synthesis gas, the main product of which is methanol.

Methanol use as an energy raw material has been extensively reviewed in this book so far; in this chapter, methanol's potential as chemistry raw material is explored. A series of technical processes to several intermediates that are accessible from methanol will be described, with the purpose of illustrating how important petrochemical products can be substituted by C_1-based chemistry. However, other approaches to the described compounds are beyond the scope of this book, so the reader is kindly referred to elsewhere to learn more about C_{2+}-based approaches.

Figure 6.1 gives examples of common processing methods of synthesis gas and methanol and how they can easily be interconverted. Table 6.1 shows the weight percent of synthesis gas that is eventually included in the final product.

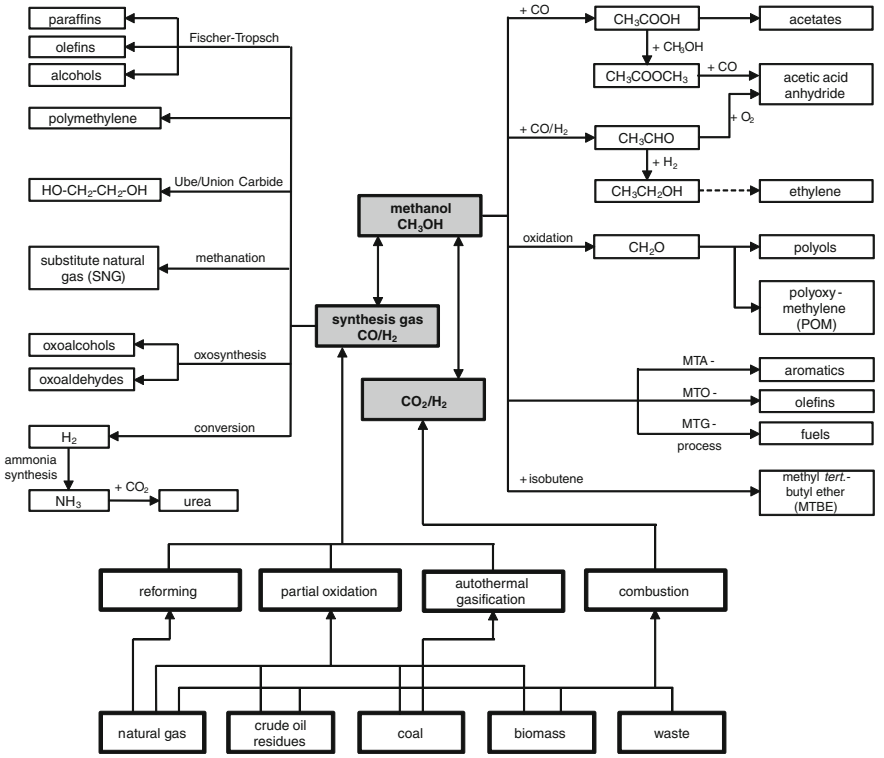

Fig. 6.1 Common processing and interconversion of synthesis gas and methanol. MTBE, methyl tert-butyl ether; MTG, methanol-to-gasoline

In Sects. 6.3 and 6.4, it becomes apparent how difficult it can be to draw a clear line between methanol use as a chemistry raw material or as an energy raw material when the latter application is as a fueling agent. As described extensively

Table 6.1 Consumption of synthesis gas for different products of C_1-chemistry

Synthesis gas product	Ratio CO:H_2	Wt% of synthesis gas in the product
Methanol	1:2	100
Acetic acid	1:1 (1:2 + 1 CO for carbonylation)	100
Ethylene glycol (direct synthesis)	1:1.5	100
Acetic acid anhydride (via methyl acetate)	1:1	85
Vinyl acetate (via methyl acetate)	1:1.25	71
Ethanol (Homologation)	1:2	72
Acetaldehyde	1:1.5	71
Ethylene and higher olefins (Mobil process)	1:2	44
Aromatics (Mobil process)	1:1.5	42
Gasoline (MTG, Mobil process)	1:2	44

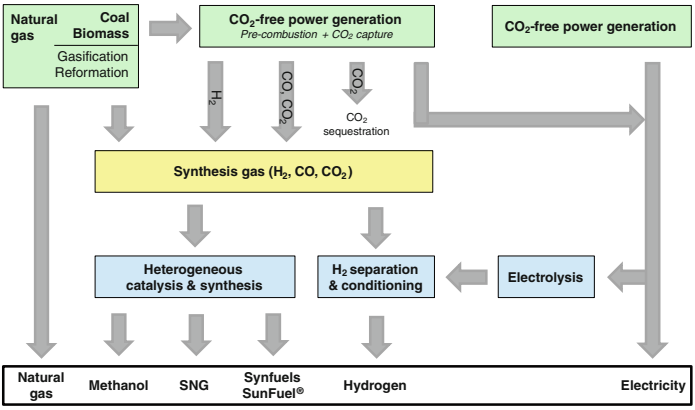

Fig. 6.2 Schematic pathways for syngas-based alternative fuels from fossil and renewable sources. SNG, synthetic natural gas. (Adapted from [8])

reviews by Höhlein et al. [8] and Olah et al. [9] and as schematically illustrated in Fig. 6.2, methanol is expected to play an increasingly important role as a substitute transport fuel or blending stock to conventional fuels. Also, derivatives of methanol such as dimethyl ether (DME) or fatty acid methyl esters (FAME) serve as alternatives to conventional crude oil-based fuels, which are readily available from fossil raw materials, as well as from biomass and organic waste.

Methanol-containing fuels for transportation have been investigated for many decades, with the purpose of using the alcohol both in ignition and in diesel engines [10, 11 and Sect. 6.3.1]. Methanol itself is mostly used as a blending stock, such as M15 (15 % methanol in gasoline), M85 (85 % methanol, 15 % gasoline) or even M100. It can be mixed in any ratio with gasoline and ethanol, has a high

octane number (RON 160) and is biodegradable. An addition of 15 vol% methanol to a 90-octane RON gasoline increases the octane number by 6–7 points [12]. The disadvantage (of any added oxygenate) is the lower heating value of methanol and a somewhat increased emission of formaldehyde in the exhaust gas.

In general, methanol fuel is toxic. In relation to conventional gasoline fuels, it is less toxic and not classified to be carcinogenic or chronically toxic. The short-term exposure limit of methanol is 250 ppm by inhalation. Small amounts of methanol taken up orally can be fatal. Symptoms are systemic acidosis, optic nerve damage, and central nervous system damage (see Sect. 5.2).

For geopolitical reasons, China is presently the most advanced country in the general use of (mostly coal-based) methanol in transportation fuels. The blending of methanol is presently exercised in 26 of 31 provinces. China's coal industry hub, the Shanxi province, is taking the lead, with more than 1,200 fuel stations offering methanol blends. All grades (M5–M100) are sold, depending on province or town. Most common in China is the use of M15, but large-fleet tests with taxis and other light duty vehicles have increasingly targeted the use of M85 and M100 fuel. In China, the estimated methanol consumption for fuel varies between 4.5 and 7.0 million tonnes (2010), representing about 5 % of China's fuel pool or a third of China's total methanol consumption of approximately 22 million tonnes in 2010 [13]. Outside China, the only major fleet test with a M85 fuel blend was started in Israel in 2012 with the purpose of investigating effects on cars and fuel pumps as well as to prepare broader introduction in the forthcoming years.

Cars with high compression engines (e.g. race cars) are often run with pure methanol for performance reasons, as well as for safety reasons because methanol fires are extinguishable with water [14]. Because of the low cetane number of methanol, there is no self-ignition in diesel engines—an issue which eventually has been overcome by adding incandescent devices or using pilot injections of conventional diesel fuel.

Increasing environmental concern about maritime transport emissions has led to new concepts for ship fuel used in special emission control areas (SECAs). In Europe, a SECA extends over the total area of the Baltic Sea, North Sea and the British Channel, restricting use of marine fuels to sulphur contents not exceeding 1 wt%—an amount that has to be reduced to 0.1 wt% sulphur by 2015. For marine diesel fuels, the limit is already 0.1 wt%. EU regulations require vessels to use 0.1 wt% sulphur fuel if remaining in port for more than 2 h. One option to meet those regulations is using the concept of alcohol/spirits and ethers as marine fuel (SPIRETH), which (temporarily) uses on-board methanol as a clean fuel. A pilot project started on a Swedish vessel in 2012 feeds a methanol/dimethyl ether (DME) mixture to an auxiliary diesel engine. DME is produced on-board by dehydration of methanol in the on-board alcohol-to-ether process (OBATE) [15].

Methyl tert-butyl ether (MTBE) produced from isobutylene and methanol is widely used as an octane enhancer to replace formerly used environmentally problematic metal-organic additives, such as tetraethyl lead. Before the broad introduction and usage of MTBE as a blending stock and octane enhancer for gasoline, processes and catalysts had been developed with the purpose of converting synthesis gas into a mix of methanol with higher alcohols through homologation reactions (Eqs. 6.1 and 6.2).

$$CH_3OH + CO + 2H_2 \rightarrow CH_3CH_2OH + H_2O \quad (6.1)$$

$$C_nH_{(2n+1)}OH + CO + 2H_2 \rightarrow CH_3(CH_2)_nOH + H_2O \quad (6.2)$$

Besides octane enhancement and replacement of lead-containing antiknock additives, the application of mixed alcohols improves methanol solubility in gasoline, increases water tolerance of the blend, and reduces Reid vapour pressure. Catalysts such as those used in Lurgi's Octamix process are copper-zinc based and contain promoters displaying certain Fischer–Tropsch activity, which enables them to generate higher carbon chain lengths in the alcohol product. Other catalysts are based on promoted MoS_2. A detailed review is given in Ref. [16].

DME made from methanol dehydration is the simplest ether molecule, with properties similar to liquid petroleum gas (LPG, Eq. 6.3).

$$2CH_3OH \rightarrow CH_3OCH_3 + H_2O \quad (6.3)$$

Apart from being used as a propellant, DME can be used in diesel engines with the advantage of high efficiency, a high cetane number, and low exhaust emissions (no particulates, no sulphur, and low NO_x). A first demonstration unit to produce bio-DME was started in 2010 in Piteå, Sweden, in which black liquor from a paper mill is gasified and converted into DME. The product is used to fuel a truck fleet [17]. DME blends with propane can also be used in gasoline engines adapted to be run with LPG.

Synthetic hydrocarbon mixtures suitable as gasoline or even diesel fuel and lubricants are accessible through methanol conversion over shape-selective (zeolite) catalysts, such as the methanol-to-gasoline (MTG) process (Eq. 6.4).

$$2n\ CH_3OH \rightarrow n\ CH_3OCH_3 + n\ H_2O \rightarrow \text{“}(CH_2)_n\text{”} + n\ H_2O \quad (6.4)$$

This process and other uses of methanol as precursor of petrochemicals are described in detail in Sect. 6.4.

Biodiesel is produced by transesterification of fats and oils. The triacyl glycerides are transformed into FAME, with glycerine as a byproduct (Sect. 6.2.20). Rape seed or palm oil, for example, can serve as feedstock, as can waste fats. The transesterification reaction to the methyl esters is run in the presence of approximately 10 vol% of methanol and an alkaline catalyst such as caustic soda or sodium methylate.

Usually, biodiesel is blended into conventional diesel in the amount of several volume percent; in Germany, this is 7 vol% (B7) [18]. In 2011, global biodiesel production amounted to approximately 18.7 million tonnes, with Europe representing 39 % of world output. The United States and Germany are the world's largest producers (3.2 million tonnes/year), followed by Argentina (2.8 million tonnes/year) and Brazil (2.7 million tonnes/year) [19].

Methanol properties for use as transportation fuel in cars and various related engine concepts are discussed in Sects. 6.3 and 6.3.2 addresses production and use of the most important fuel additive MTBE (and the corresponding amyl ether, TAME) in methanol-to-gasoline technology (MTG).

Synthesis gas is the key platform for the production of non-oil-based chemicals. Fuels, gasoline, jet fuel and middle distillates can be produced by Fischer–Tropsch synthesis or by methanol based processes such as MTG. Hydrogen, ammonia, and methanol are the most important chemicals that are also produced from synthesis gas. The paramount importance of methanol is that it can be converted into a plurality of other major bulk chemicals, as well as into fuel and fuel additives.

The supreme advantage of the methanol route versus the Fischer–Tropsch route is the flexibility of the methanol path with respect to the market. Depending on the market demand, methanol can either be sold as such or in form of its primary or secondary derivatives.

Most of the processes to convert methanol to hydrocarbons are based on zeolites of the pentasil type. These catalysts and the chemistry of the corresponding methanol conversion are discussed in Sect. 6.4. Sections 6.4.1 and 6.4.2 are devoted to the methanol-to-gasoline process and the methanol-to-olefin process, respectively. Special attention is given in Sect. 6.4.3 to the methanol-to-propylene process due to the paramount importance of polypropylene. Finally, a short review of the production of other methanol derivatives is given in Sect. 6.4.4.

In particular, when methanol conversion to gasoline and olefins is discussed, it becomes clear that the boundary between both uses is slim. The message of both sections, however, is obvious: Oil substitution by methanol is technically feasible and can be realised in an economically viable manner while maintaining our living standards (see also Chap. 7).

Parallel to the efforts deployed for the substitution of oil and gas as chemistry raw materials, new technologies were developed with the purpose of not only substituting oil but also the combustion engine itself. This development culminated in the development of fuel cells using a variety of concepts. Sect. 6.5 would not be complete without discussing the green hydrogen issue. Hydrogen generation from methanol as a clean hydrogen source in lieu of natural gas and applications of methanol in biotechnology are described, from which the enormous potential of methanol becomes intriguingly evident.

6.2 Methanol-Derived Chemicals: Methanol as a C_1-Base

Martin Bertau[1], Konstantin Räuchle[1], Nicola Ballarini[2] and Matthias S. Wiehn[3]

[1]*Institute of Chemical Technology, Freiberg University of Mining and Technology, Leipziger Straße 29, 09599 Freiberg, Germany*

[2]*Clariant Catalysis Italia, Via G. Fauser, 36/B, 28100 Novara, Italy*

[3]*Evonik Industries AG Luelsdorf, Feldmühlestraße 3, 53859 Niederkassel-Luelsdorf, Germany*

Methanol is of particular interest for the chemical industry because it can easily be interconverted as a chemistry or energy raw material. A series of chemical syntheses can be operated on the basis of methanol instead of classic petrochemicals. As can be seen in this chapter, attempts to switch to the use of methanol as a raw

material in classic refinery processes have to be regarded with the same restraint as for every facile change in complex matters. The reader will see that some processes, such as acetic acid synthesis, have always been methanol based, whereas others are new processes in industrial chemistry. Indeed, the great majority of established petrochemical products are achievable using both crude oil and methanol as a raw material base.

6.2.1 Acetic Acid Anhydride

Acetic anhydride mostly serves as an acetylation reagent, such as in the production of acetyl cellulose, pharmaceuticals (e.g. acetyl salicylic acid), acetanilide and other intermediates.

6.2.1.1 Acetic Acid Anhydride Through Carbonylation of Methyl Acetate

Acetanhydride was the first large-scale product based on synthesis gas produced using the process by Halcon SD and Tennessee Eastman (a division of Eastman Kodak), who combined their technical knowledge, through catalytic carbonylation of methyl acetate according to the following reaction:

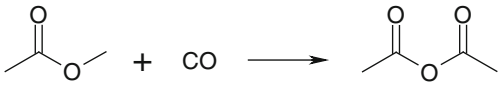

Converting 2 mol of methyl acetate with 2 mol of CO gives 2 mol of acetic anhydride. Of these 1 mol is removed as the final product, while the other 1 mol is converted with methanol to give 2 mol of methyl acetate, which are re-used for the reaction. Proceeding this way, acetic anhydride synthesis requires nothing else but methanol and CO. The latter is recovered from synthesis gas; hydrogen is used for the synthesis of methanol. When acetic anhydride is used for the production of cellulose acetate, the acetic acid being released from the acetylation reaction can be recovered and used for the esterification of methanol, which increases the amount of acetanhydride produced in a plant. The first large-scale plant based on coal with a capacity of about 230,000 t/a of anhydride was put into operation in Kingsport, Tennessee in 1983. Since then, its capacity has been increased to 300,000 t/a [20, 21]. In theory, only synthesis gas is needed as a starting material: once converted into methanol, once used for CO supply. To start up the system, however, methyl acetate is required.

The most developed route to acetanhydride on a technical scale is the carbonylation of methyl acetate, which preferably is realised at 150–200 °C and 25–75 bar in the presence of rhodium catalysts, such as $[RhI_2(CO)_2]$ (Monsanto catalyst; see Sect. 6.2.8), methyl iodide and an inorganic iodide or hexacarbonylchromium/picoline, for instance, as promoters.

To start the reaction, methyl acetate is required, which is produced from acid catalysed esterification of acetic acid with methanol. In Fig. 6.3, the rhodium-catalysed reaction (a) corresponds to acetic acid synthesis according to the Monsanto process. Without addition of inorganic iodide, the reaction proceeds according to the acid cycle (Fig. 6.3, left), where CH_3I is generated from a reaction of methyl formate and HI (b). Acetyl iodide and acetic acid react in an equilibrium reaction to give acetic acid anhydride and HI (c).

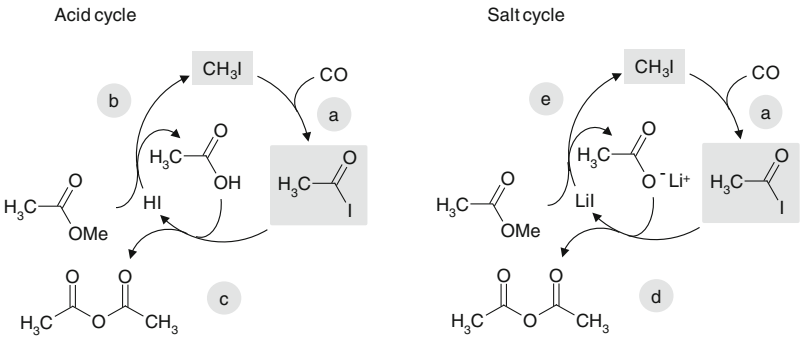

Fig. 6.3 Iodide cycles in acetic anhydride production without promoter (acid cycle, left) and with LiI as promoter (salt cycle, right). Starting material and product of the rhodium-catalysed cycles are marked in grey. (After [22])

In contrast to the Monsanto process, the reaction system is free of water, what leads to a long induction period; furthermore, the reaction proceeds rather slowly. It was therefore necessary to optimise the process. The induction period is due to the fact that there is no suitable reducing agent for the catalyst formation ($Rh^{III} \rightarrow Rh^{I}$). The addition of H_2 does not only shorten the induction phase, inactive Rh^{III} complexes that have been formed in the course of the reaction are subject to reduction, too.

Upon addition of inorganic iodides (LiI, $(NR_4)I$ or $(PR_4)I$) as promoters, the reaction proceeds according to the salt cycle (Fig. 6.3, right). Here, it is the inorganic iodide instead of HI from which CH_3I is regenerated from the reaction with methyl acetate (e). The resulting lithium acetate reacts with acetyl iodide to give acetic acid anhydride (d), with the advantage of the equilibrium of this reaction (in contrast to the analogous reaction (c) in the salt cycle) being far on the right side.

The individual steps can be summarised as follows:

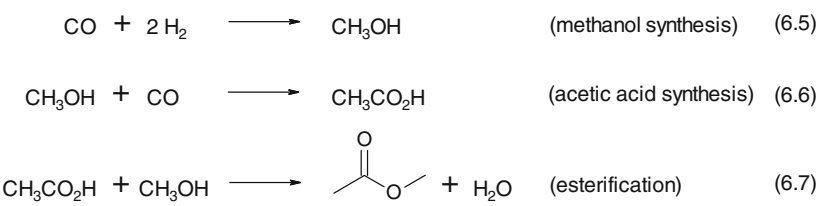

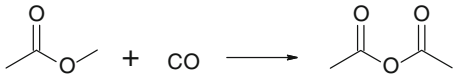

Besides methanol synthesis (6.5), reactions (6.6) and (6.7) are continuously operated reactions. Reaction (6.8) and (6.9) need to be conducted only once. The net gas reaction is

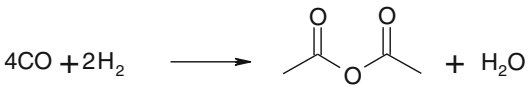

The methyl acetate process is the dominant synthetic route to acetanhydride in the United States. In Europe, approximately 50 % is produced via the addition of ketene to acetic acid (see Sect. 6.2.1.2); in Japan, this is the sole industrially realised process.

Follow-up approaches by Halcon and Hoechst pursue the homogeneously catalysed carbonylation of dimethyl ether (DME) and methyl acetate [23, 24]. Other approaches work with glacial acetic acid as the solvent. The reaction proceeds via intermediary formed methyl acetate. With nickel acting as a catalyst, the reaction furnishes methyl acetate only [23, 25, 26].

6.2.1.2 Wacker Process

The Wacker process uses acetic acid that is dehydrated to give ketene in the presence of triethyl phosphate at reduced pressure and 700–750 °C. The H_3PO_4 that is formed in the course of the reaction is neutralised with NH_3 or pyridine and the fission gas is cooled down rapidly in order to freeze the reaction. After purification, ketene is funnelled in glacial acetic acid, where it reacts at 0.05–0.2 bar to acetic acid anhydride.

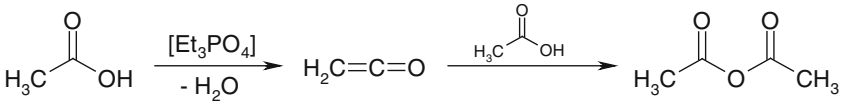

The Wacker process benefits from the availability of ketene, which can be isolated as reactive intermediate. Starting from acetic acid is economically favourable because the starting material can be produced cost-effectively by methanol carbonylation (see Sect. 6.2.8). Moreover, acetic acid recovered from acetylation reactions can be reintegrated into the process, thus creating a cheap raw material base.

6.2.1.3 Other Processes

Alternatively, acetic acid anhydride can be obtained from dimethyl carbonate carbonylation, where CO inserts in the O–CH_3 bond:

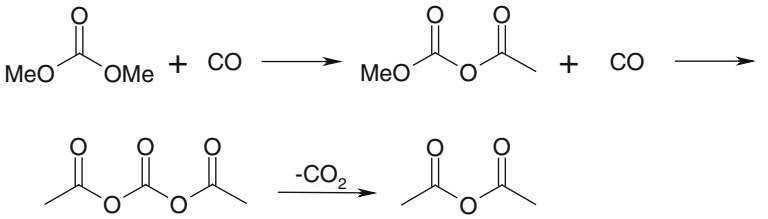

Also, DME has been used, where methyl acetate is formed as an intermediate:

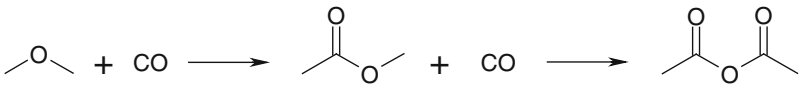

Whatever process is chosen, industrial acetic acid anhydride production can be realised exclusively on the basis of synthesis gas or on coal or gas (i.e., a cost-effective C-base).

6.2.2 Production of Vinyl Acetate Monomer on the Basis of Synthesis Gas

In 2005, vinyl acetate production capacity amounted to approximately 5.5 million tonnes. Its synthetic use consists solely of its reactive vinyl group, which has been used for homo- and co-polymer production, with polyvinyl acetate (PVA) as its most important product. The world's largest manufacturer of vinyl acetate monomer (VAM) is Celanese (22 %) with a capacity of $\sim$1.2 million t/a.

For VAM production, there exist four major routes:

1. Addition of acetic acid to acetylene
2. Conversion of acetaldehyde with acetanhydride via ethylidene diacetate
3. Hydrocarbonylation of methyl acetate via ethylidene diacetate
4. Acetoxylation of ethylene

Among these, routes 1–3 are generally economically unfeasible. The predominant process delivers VAM through acetoxylation of ethylene. All processes can be realised on the basis of synthesis gas with acetic acid as starting material on the one hand and methanol-derived ethylene and its derivatives acetaldehyde and acetylene on the other.

6.2.2.1 VAM Through Acetoxylation of Ethylene

Modern catalytic production processes for VAM from acetic acid and ethylene are based on an observation by Moiseev and co-workers (1960) who found that ethylene oxypalladation (using the Wacker process to acetaldehyde) can be extended to nonaqueous solvents. These act themselves as nucleophiles instead of water, what is the reason why they are found in the final product. Conversion in acetic acid/sodium acetate delivers VAM via intermediary-formed acetoxyethyl palladate(II). It was this discovery that allowed for a rapid access to VAM starting from ethylene and acetic acid (Fig. 6.4).

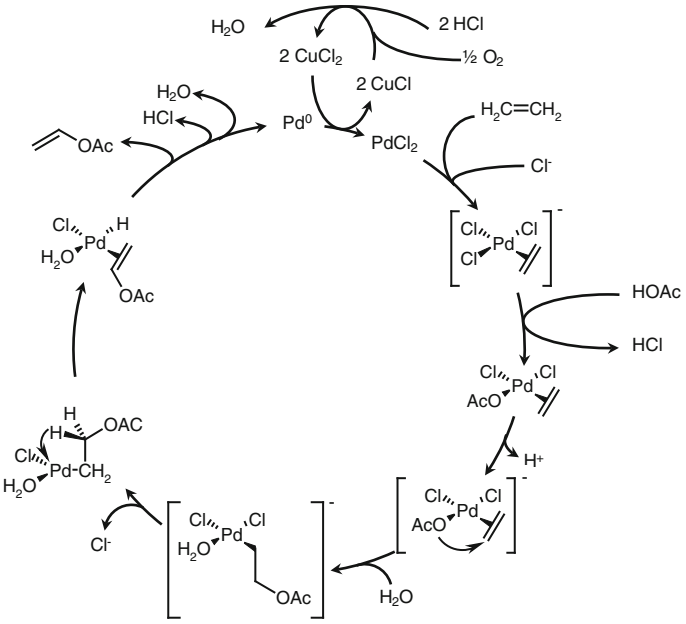

Fig. 6.4 Palladium catalysed acetoxylation of ethylene. (Modified from [21, 27])

The process is similar to classic ethylene oxidation to acetaldehyde. However, because an acidic hydrogen is missing in the vinyl acetate ligand, there is no reductive elimination leading to the vinyl compound. It is the hydrido complex that decomposes to release VAM.

Although it was the elucidation of a homogeneously catalysed reaction that led to a commercial process, on a technical scale the reaction is conducted as heterogeneous process:

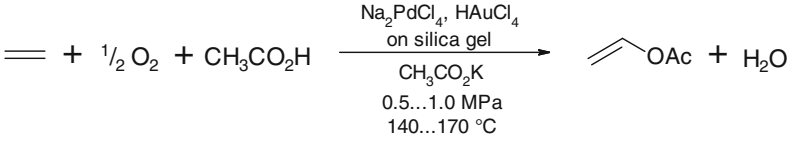

6.2.2.2 VAM Through Hydrocarbonylation of Methyl Acetate via Ethylidene Diacetate

The hydrocarbonylation route was developed by Tennessee-Eastman with the purpose of directly integrating coal as a carbon source into the production of VAM. The required synthesis gas is provided by coal gasification according to a modified Texaco/Ruhrchemie/Ruhrkohle gasification process. An integrated gasification/VAM plant has a production capacity of 220,000 t/a from 1.8 million tonnes of lignite.

As shown above (Sect. 6.2.1.1), carbonylation of methyl acetate yields acetic anhydride. If, however, the reaction is conducted with the same or similar catalysts, such as $RhCl_3$ + CH_3I + picoline or triphenylphosphine, but with synthesis gas instead of pure CO at 150 °C and 40–70 bar, acetic acid and ethylidene diacetate are formed as summarised in Fig. 6.5:

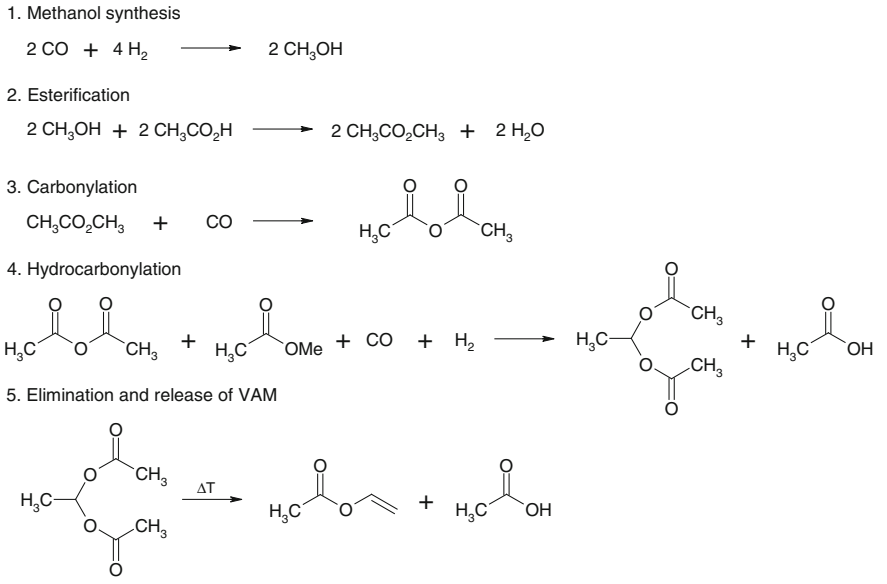

Fig. 6.5 Vinyl acetate monomer formation from synthesis gas via methyl acetate and ethylidene diacetate

At 170 °C, in the presence of benzene sulphonic acid in the liquid phase, accompanied by elimination of acetic acid, ethylidene diacetate can be converted into vinyl acetate (Fig. 6.5). The central process in this reaction sequence is the concerted conversion of acetic anhydride and methyl acetate with carbon monoxide and hydrogen—the hydrocarbonylation step—in the course of which acetic

acid and ethylidene diacetate are being formed (reaction 6.8). In the presence of CO alone, the reaction does not proceed further than the formation of acetic anhydride. Only in the presence of hydrogen (from the synthesis gas) are consecutive reactions initiated. This reaction does not proceed in the absence of halogen sources. Instead of methyl iodide, acetyl chloride and other methyl halogenide come into use.

Both processes are characterised by extraordinarily corrosive reaction conditions, which require the devices to be made from tantalum, titanium, zirconium, or Hastelloy steels. In addition, chlorinated byproducts are formed, thus necessitating sumptuous removal processes.

6.2.3 Ethylene Glycol

6.2.3.1 Ethylene Glycol on Basis of Synthesis Gas

Currently, the production of ethylene glycol is based on ethylene oxide. In fact, it is the largest derived product from ethylene oxide, and the majority of glycol processes are based on ethylene. However, with C_1-chemistry gaining increasing importance in industrial chemistry, the use of synthesis gas as a starting material is of growing interest [20].

There are two major fields of application for ethylene glycol: antifreezing agents (in which glycol is contained in up to 95 %) and diol for polyester synthesis. Polyethylene terephthalate (PET), which is the most important product, is used for the production of fibres, one-way beverage containments, foils, and resins. Further applications exist in surfactant synthesis. Polyethylene glycol is used as brake and hydraulic fluid, as plasticiser and an antifriction agent (Fig. 6.6).

By the end of the 1940s, DuPont demonstrated the suitability of synthesis gas for ethylene glycol production by hydrogenating CO in aqueous cobalt salt solution. In the 1970s, Union Carbide investigated synthesis gas conversion in homogeneous rhodium carbonate systems using various different promoters and Lewis acids containing nitrogen. In a high-pressure reaction at 1,400–3,400 bar and 125–350 °C, a mixture of ethylene glycol, 1,2-propanediol and glycerine is obtained with a selectivity sum of $\leq$70 %. It is apparent that these extreme reaction conditions coupled with the insufficient catalytic effectivity stand against realisation on a technical scale. This is in line with a series of investigations undertaken by other companies, mostly focusing on rhodium, palladium, copper and ruthenium, for which no significant progress was made either. Figure 6.7 provides an overview of ethylene glycol synthesis starting from synthesis gas.

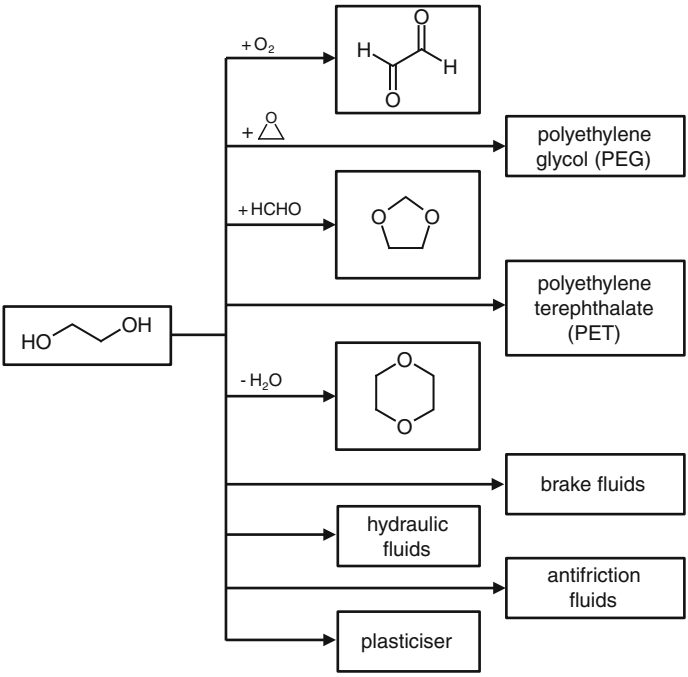

Fig. 6.6 Utilisation of ethylene glycol

1. Methanol synthesis

$$CO + H_2 \longrightarrow CH_3OH$$

2. Dehydrogenation to formaldehyde

$$CH_3OH \longrightarrow H_2C{=}O + H_2$$

3. Glycolic acid synthesis

$$H_2C{=}O + CO + H_2O \xrightarrow{H_2SO_4} HO{-}CH_2{-}COOH$$

4. Esterification

$$HO{-}CH_2{-}COOH + CH_3OH \longrightarrow HO{-}CH_2{-}COOMe + H_2O$$

5. Hydrogenation of glycolic acid methyl ester and release of ethylene glycol

$$HO{-}CH_2{-}COOMe + H_2 \xrightarrow{\Delta T} HO{-}CH_2{-}CH_2{-}OH + CH_3OH$$

Fig. 6.7 Ethylene glycol synthesis on the basis of synthesis gas. [28]

For these reasons, the direct conversion of synthesis gas was not further pursued in favour of indirect routes starting from the synthesis gas products methanol or formaldehyde instead. Here, the strategy is to subject the latter to hydroformylation, oxidative carbonylation, or carbonylation to intermediates (the hydrogenation of which delivers ethylene glycol). In this context, the Ube process (1978) has attracted the most economic interest, in particular through further developments in the second process step by Union Carbide (UCC), who is currently undertaking test runs. On this basis, among the synthesis gas routes to ethylene glycol, the Ube/UCC process has the best chance of being commercially realised. The Ube/UCC approach consists of an oxidative carbonylation of methanol to dimethyl oxalate followed by hydrogenolysis to ethylene glycol and methanol:

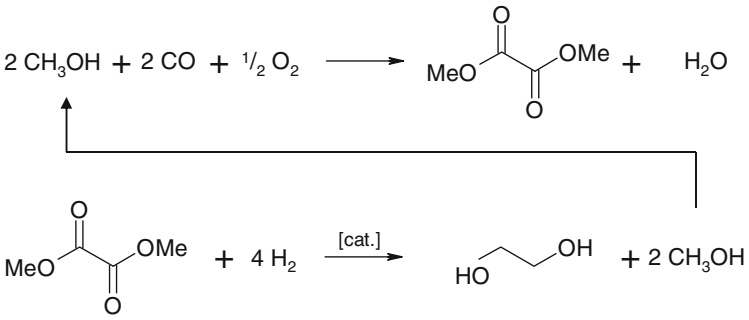

The first process step is conducted at 90 bar and 110 °C with 97 % yield in the presence of a palladium catalyst in 70 % HNO_3. Nitric acid is needed to convert methanol into methyl nitrite as a reactive intermediate. The second hydrogenation step proceeds with ruthenium oxide, for instance, in ~90 % yield under reformation of methanol. Instead of methanol, other alcohols such as *n*-butanol can be used. In fact, through the use of methanol as a synthesis gas-derived substrate and both CO and H_2, it is synthesis gas on which this process is based [29].

DuPont developed a three-step synthesis starting with formaldehyde from a hydrating carbonylation with sulphuric acid as catalyst at 500–700 bar and 200–250 °C, which is followed by esterification of intermediary glycolic acid with methanol (Fig. 6.8).

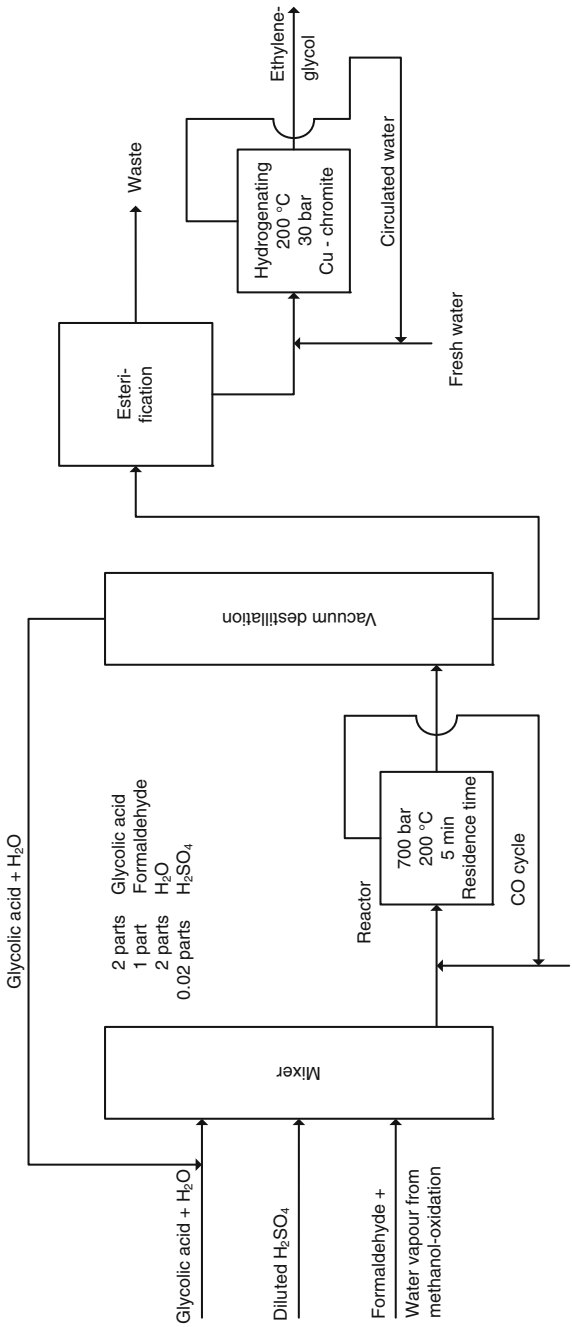

Fig. 6.8 DuPont's ethylene glycol process. (Adapted from [20])

Finally, the methyl ester is hydrogenated to give ethylene glycol:

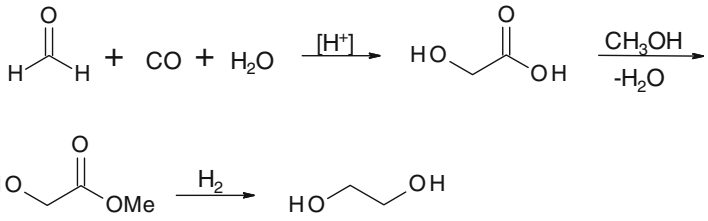

Glycol production using this process ceased by end of the 1960s, but plants were kept in operation for glycolic acid production (≤60,000 t/a). With growing interest in C_1-chemistry, several companies have developed alternative approaches, although none of which have yet come to realisation on a technical scale.

Glycolic acid serves as cleaning agent for boiler plants and conduits or as chelating agent for Ca and Fe ions in boiler feed water. It is used in textile, leather, and paper processing and the esters serve as solvents for varnishes.

6.2.3.2 Ethylene Glycol from Transesterification of Dimethyl Carbonate

See Sect. 6.2.10.2.

6.2.4 Methyl Formate and its Role as Synthetic Building Block in C_1-Chemistry

Methyl formate is produced from CO and methanol. As such, it is a useful synthetic C_1 building block. The compound can be used as chemical storage for both CO and CH_3OH, from which the latter can be released in the course of a reaction. Because of this property, methyl formate has attracted increased interest for synthetics in recent decades [20].

6.2.4.1 Methyl Formate Production Through Methanol Carbonylation

As early as in 1925, methyl formate was manufactured by BASF by reacting carbon monoxide with methanol. The reaction proceeds exothermically under pressure in the presence of sodium methylate (see Sect. 6.2.20) as a catalyst with approximately 29.3 kJ/mol (Fig. 6.9).

The methanol carbonylation to methyl formate resembles the process leading to acetic acid. Which product is formed depends on the catalyst used and the locus of CO insertion. If it is the carbinolic O–H bond (Fig. 6.9a), methyl formate is produced; if CO is inserted into the C–O bond (Fig. 6.9b), acetic acid is formed.

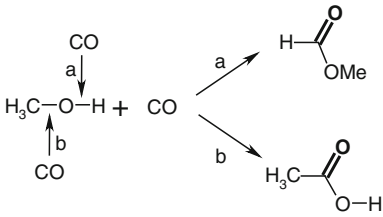

Fig. 6.9 Methanol carbonylation products methyl formate and acetic acid are produced according to regioselectivity of the catalytic reaction. **a** Insertion into the O–H bond furnishes methyl formate. **b** Insertion into the C–O bond furnishes acetic acid

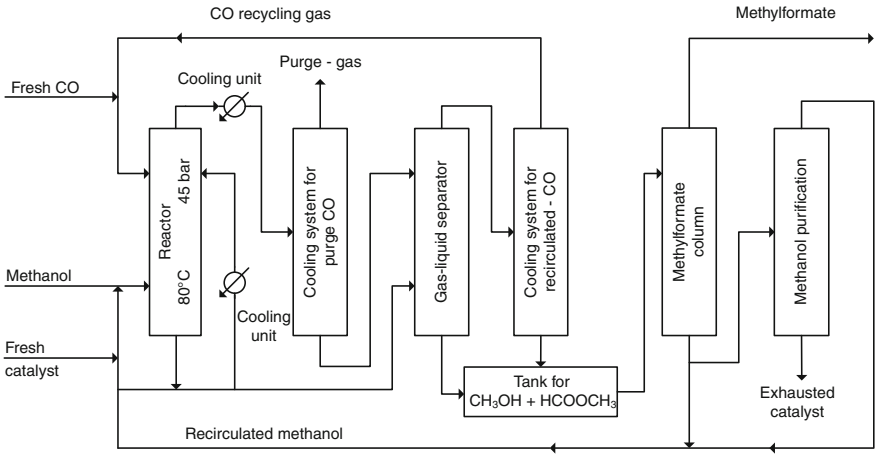

Fig. 6.10 The carbon monoxide from the top of the reactor is passed through a cooler in a cooling system in order to remove entrained product and methanol, which are fed into a gas–liquid separator. Impure CO (purge gas)is utilised as fuel gas. At the reactor bottom, the mixture of methanol and methyl formate is removed. One portion of the mixture is recycled via a cooler as a cycle product for reactor temperature maintenance. Together with the methanol/methyl formate mixture from the cooling system (purge gas separation), the remainder is separated from cycled CO in a gas–liquid separator. In a second cooling system, the cycle-CO is liberated from entrained liquids before it is fed to the reactor together with fresh CO. The product streams are combined and introduced into the methyl formate column. Pure methyl formate is taken overhead. Methanol still contains some catalyst, for which reason it is cycled back to the reactor from the bottom of the column, thereby adding some fresh catalyst. In another column, a portion of backcycled methanol is liberated from heavy fractions and spent catalyst. The purified methanol is funnelled into the back-methanol stream. (Adapted from [30])

Figure 6.10 shows the principle of a methyl formate production plant. In backward-feed operation, methanol and carbon monoxide are brought into reaction in a continuously operated reactor at 45 bar and about 80 °C in the presence of 2 % sodium methylate in methanol. All reagents and devices must be completely

free of water; otherwise, sodium formate will be formed, which precipitates and can clog the pipes. CO_2, H_2S and O_2 must be removed, too, but methane and hydrogen do not interfere. One can use for these purposes highly CO-enriched gases from second-generation coal gasification plants, which can contain up to 75 % CO and allow for less complex conversion into pure CO. CO conversion is 95 %, whereas methanol conversion is 30 %. The yield in terms of CO and methanol conversion is 99 %. Per hour and litre of reaction space, 800 g of methyl formate (b.p. = 31.8 °C) are formed.

6.2.4.2 Methyl Formate Production Through Methanol Dehydrogenation

A more recent approach to methyl formate was developed by Mitsubishi. Under yet unpublished copper-catalysed reaction conditions, methanol is dehydrogenated in the gas phase:

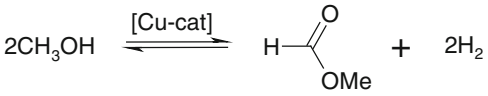

As a byproduct, formic acid is formed, mostly in undesirable nonselective oxidative degradation reactions. The amounts are rather small and in most cases do not sum up to economically viable concentrations. However, the formic acid impurities account for the greater process effort because the corrosive byproduct requires titanium columns for distillative separation. Yet, HCO_2H-formation was reported to reach up to 18 % in the product. Under these conditions, the additional process effort is overcompensated by formic acid separation, and the bycomponent even contributes to overall process economy.

The Mitsubishi process has roots in early activities by Industrial Alcohol Co. in the 1920s, who were the first to report on the dehydrogenative variant to methyl formate [31, 32]. As catalyst copper was used, however, conversions and yields were unsatisfactory. In the late 1970s, Japanese companies regained interest in this approach. Particularly with Cu-Zr-Zn- and Cu-Zr-Zn-Al catalysts, $\leq$50 % conversion with methyl formate selectivity (up to 90 %) were obtained [33–36]. Based on these catalysts, Mitsubishi Gas Chemical erected a plant on the semi-technical scale in 1979. The catalysts displayed long run times, and space-time yields up to 3,000 kg m^{-3} h^{-1}were obtained. Figure 6.11 provides a simplified scheme of a methanol dehydrogenation plant [30].

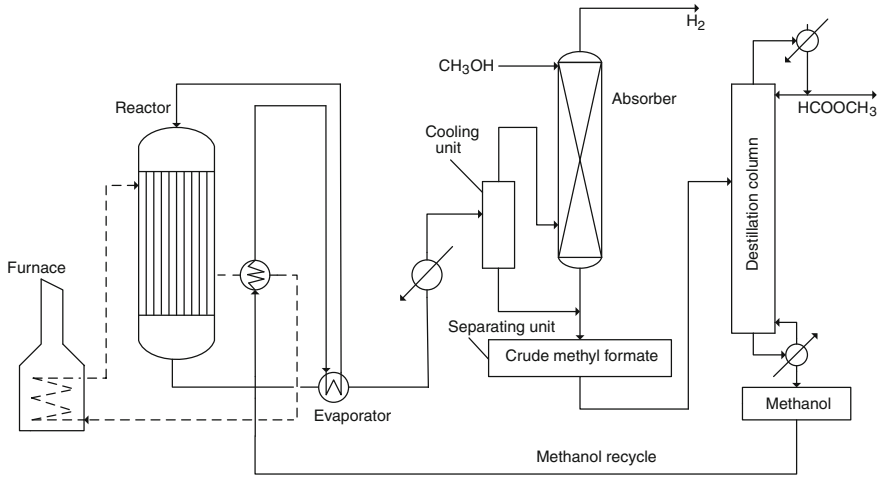

Fig. 6.11 Methyl formate production by dehydrogenation of methanol. (Adapted from [37])

Although current dehydrogenation catalysts consist of copper, several compositions have been tested since, particularly those containing Ti, Zr or rare earth metals. However, none provided the productivity of copper [38].

6.2.4.3 Methyl Formate Production catalysed by Potassium Methylate

Novel approaches pursue methyl formate production through nucleophilic attack of methoxide at CO under H_2 atmosphere with $Mo(CO)_6$ as a co-catalyst [39]:

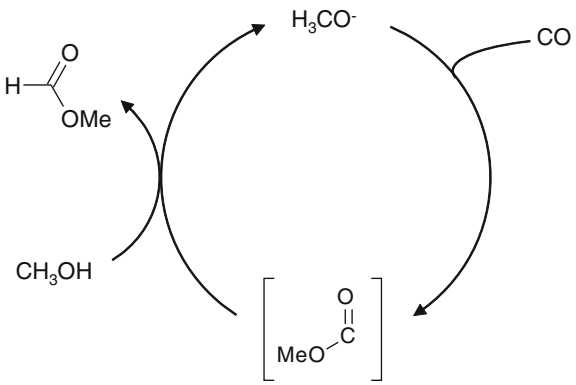

6.2.4.4 Methyl Formate as a Synthetic Building Block

Because its production is based exclusively on synthesis gas, as well as the fact that it is a versatile starting material for a series of chemical processes, methyl formate has great synthetic potential in industrial C_1-chemistry [20, 40].

Hydrolysis to Formic Acid

See Sect. 6.2.5.2.

Glycolic Acid Methyl Ester and Ethylene Glycol

Reacting methyl formate with formaldehyde in presence of Brønsted (e.g. H_2SO_4 or organic sulphonic acids) or Lewis acids at ambient pressure and 70–200 °C leads rapidly to glycolic acid methyl ester, which can be converted to ethylene glycol by copper-catalysed hydrogenation:

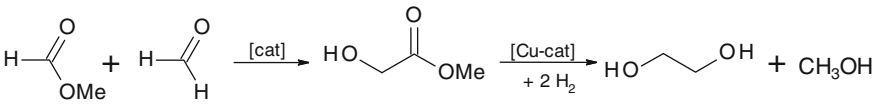

Alternatively to formaldehyde, paraformaldehyde or trioxane can be used. This reaction resembles hydrating carbonylation of formaldehyde, which along similar reaction parameters yields ethylene glycol as well (see Sect. 6.2.3), thus constituting an alternative to the DuPont process to glycolic acid, with the difference of methyl glycolate being produced directly. Solid Lewis acids are also suitable but require higher reaction temperatures (6 bar and 110 °C).

The follow-up chemistry of methyl glycolate is manifold. Reaction with CO delivers malonate ester, an important intermediate in fine chemistry, such as in the production of pharmaceuticals or pesticides:

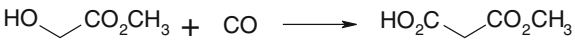

When reacted with ammonia, glycine, the simplest amino acid is formed:

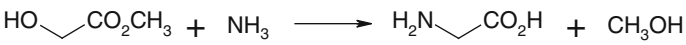

Hydrolysis to glycolic acid and methanol allows the former to undergo self-condensation to polyglycolate, which is of particular interest as a surgical suture because it is easily hydrolysed in vivo:

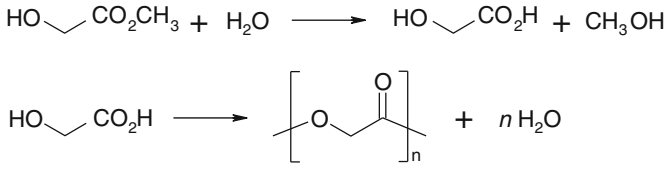

Methyl Propionate

In polar solvents in the presence of Ru or Ir complexes, methyl formate and ethylene react at 190–200 °C to give methyl propionate:

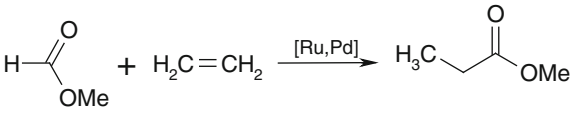

When the reaction takes place in the presence of iodide at 80 bar and 180 °C in N-methyl pyrrolidone (NMP), methyl ethyl ketone (MEK) is the major product, with up to 50 % selectivity [41]:

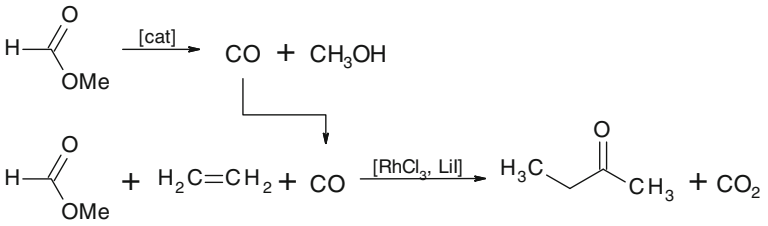

However, if the reaction is conducted with LiBr present, methyl formate has been observed to be subject to a disproportionation reaction. As the outcome of this reaction, gaseous CH_4 and CO_2 are formed as the sole products [41]:

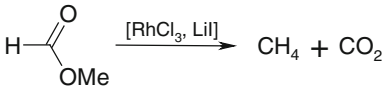

Isomerisation to Acetic Acid

Upon heating at 300 bar with CO in the presence of iodine and metal salts such as cobalt, iron, nickel or mercury, acetic acid is formed at 220 °C from methyl formate within one hour in 94 % yield [42]. The reaction proceeds particularly smoothly with rhodium methyl iodide and CO. Acetic acid is formed with 98 % yield at 100 °C, with the reaction being very much like methanol carbonylation according to the Monsanto process.

Mechanistically, methyl formate isomerisation to acetic acid can be regarded as a sequence of backward reaction to methanol and CO followed by methanol carbonylation:

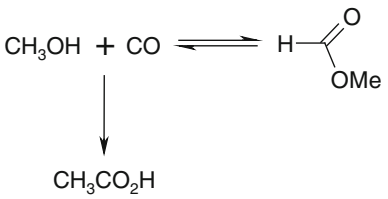

Formally, methyl formate can be regarded as a reservoir for methanol and CO, from which the final product acetic acid is produced. In terms of process economy, a reaction sequence via two differently catalysed single steps will hardly be able to compete with a direct route. Indeed, because of the superiority of the Monsanto and Cativa processes, this reaction has no technical relevance.

Hydroisomerisation over Ir or Rh Catalysts to Acetaldehyde

Comparable to acetic acid formation from methyl formate either a reductive carbonylation of methyl formate into acetaldehyde or its homologation into methyl acetate takes place under CO pressure in an Rh/RhI_2 catalysed reaction. Acetaldehyde formation occurs selectively only in dipolar aprotic solvents, such as NMP (or related solvents) with high Rh/I^- ratio, low methyl formate concentration, and high CO pressure. Methyl acetate is formed at a lower Rh/I^- ratio, higher methyl formate concentration, and under lower CO pressure [43, 44].

Oxidative Conversion with Methanol at Se Catalysts to Dimethyl Carbonate

The conversion of methyl formate and methanol over Se catalysts produces dimethyl carbonate (DMC; see Sect. 6.2.10) in the presence of oxygen [45]:

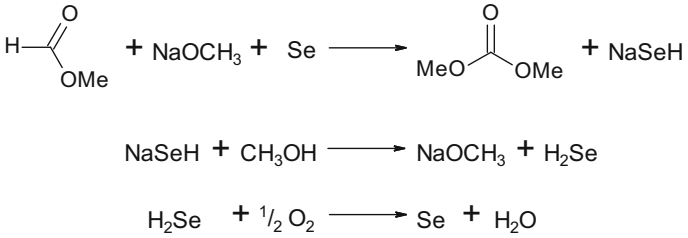

The reaction suffers from methyl formate decarbonylation to methanol as a competing reaction. In addition, selenium displays poor catalytic selectivity.

Synthesis of Formamide and its *N*-methyl Derivatives

Formamide and its *N*-methyl derivatives are technically versatile compounds. For their polar properties, they are highly useful selective solvents and extractants. Dimethyl formamide (DMF) is one of the few solvents that are suited for fibre production. DMF worldwide production is estimated to 220,000 t/a, with the largest manufacturer being BASF. Analogous to methyl formate ammonolysis to formic acid, both *N*-methyl and *N*,*N*-dimethyl formamide are obtained by reactions with methyl and dimethyl amine, respectively:

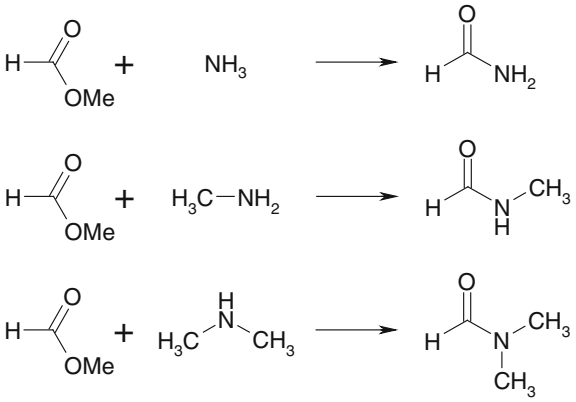

Alternatively, formamide as well as *N*-methyl and *N*,*N*-dimethyl formamide are accessible directly through reacting CO and NH_3 in methanol at 20–100 bar and 80–100 °C in the presence of sodium methanolate:

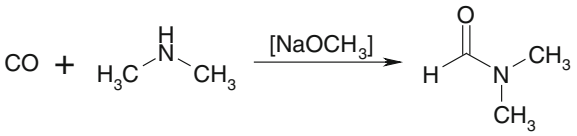

Here too, the synthetic basis for all reactants and solvents is synthesis gas. Using the latter approach, DMF yield can reach up to 95 %. On a technical scale, this process is operated in several plants, such as in the Leonard process.

Palladium Catalysed Oxidative Carbonylation of Olefins

Oxidative carbonylation of olefins makes use of the property of methyl formate to form an equilibrium with CO and CH_3OH in the presence of methylate anions; thus, it serves as a CO reservoir, avoiding direct use of CO.

Key steps of the process are methyl formate decarbonylation and formation of the methoxy-carbonyl complex, followed by insertion of the olefin and ß-elimination, furnishing the olefinic ester and Pd^0 (Fig. 6.12). Consequently, the reaction requires catalyst regeneration, which is best accomplished by $CuCl/CuCl_2$. Therefore, it very much resembles the Wacker process (see Sect. 6.2.1.2). Alternatively, $FeCl_2/FeCl_3$ are also suited, but to the detriment of selectivity favouring benzaldehyde byproduct formation [46]. Further improvements can be achieved by conducting the reaction in the presence of one aliquot of triethyl amine, thus allowing for very mild reaction conditions (1.0 bar, 30 °C) [47].

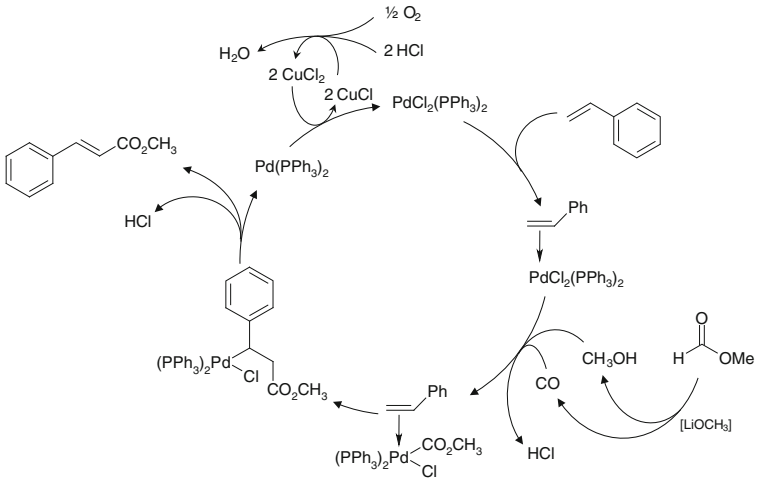

Fig. 6.12 Palladium catalysed oxidative carbonylation of styrene to methyl cinnamate. (Adapted from [46])

The oxidative carbonylation is suited for olefins other than styrene, too. It has to be taken into account that mild reaction conditions favour this reaction; however, with harsher conditions, aldehyde and polymerisation occur in disfavour of carbonylation.

Methanol Synthesis

As an alternative to classic methanol production, synthesis gas conversion to the C_1-carbinol can be carried out in the liquid phase, too. The two-step process consists of an alkali metal alkoxide (typically sodium methoxide)–catalysed carbonylation of methanol to methyl formate, which here acts as an intermediate rather than starting point for follow-up synthetic procedures. Hydrogenolysis over a copper-chromite type catalyst then delivers 2 mol of methanol per mole of methyl formate. However, because one mole of methanol is required for subsequent carbonylation in order to keep the cycle upright, the net output is 1 mol of methanol (Fig. 6.13). The process can be run also with higher alcohols.

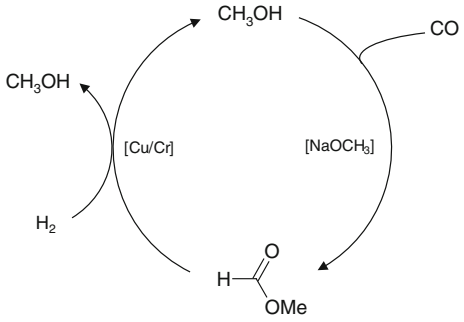

Fig. 6.13 Methanol synthesis through intermediate formation of methyl formate. (Adapted from [40])

The mild reaction conditions and the favourable thermodynamic equilibrium for product formation make this route interesting. However, the process is highly sensitive towards the presence of CO_2, for which reason a rigorous removal of CO_2 has to be ensured. The reaction is conducted at 1.0 bar and 140 °C with a selectivity >90 % and methyl formate conversion of 70–80 %. Higher H_2 pressures are in favour of this process [40].

Halogenation

Monochlorination and complete chlorination of methyl formate deliver methyl chloroformate and trichloromethyl chloroformate, respectively:

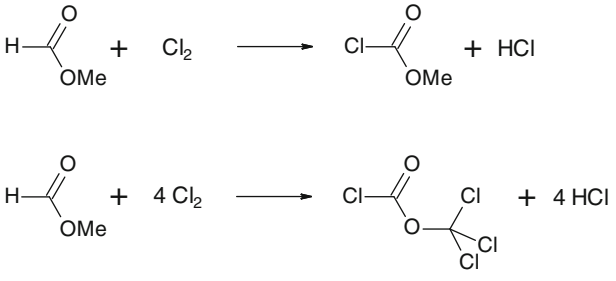

Methyl chloroformate is used for the synthesis of methoxy carbonyl compounds. Trichloromethyl chloroformate is also known as *diphosgene*. It is more convenient to transport and handle than phosgene and serves as a synthetic reagent in fine chemical synthesis where substitution of the latter is required. It is produced under ultraviolet irradiation in the presence of PCl_3 as a catalyst. Diphosgene is converted into phosgene when brought into contact with activated carbon or iron oxide [40].

An overview of the synthetic spectrum of methyl formate is given in Fig. 6.14.

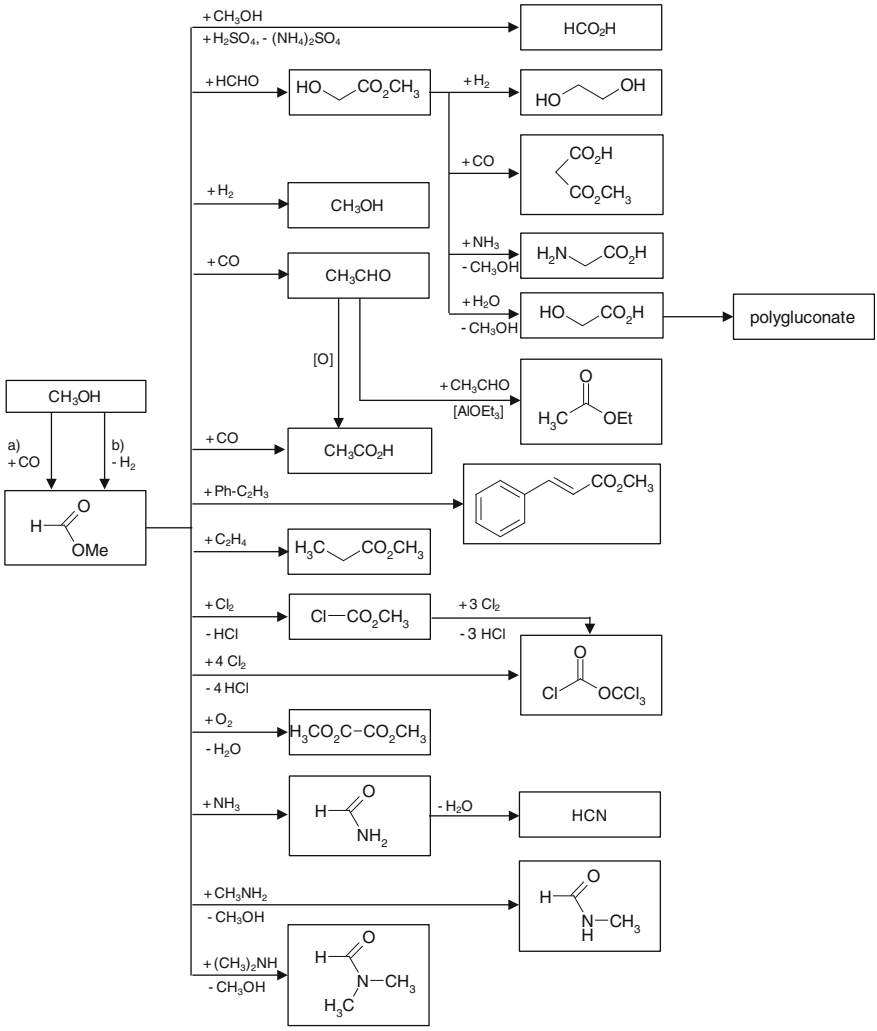

Fig. 6.14 Products derivable from methyl formate as a C_1-building block

Others

Because of its empirical formula, $C_2O_2H_4$, methyl formate can be understood in terms of $(CO)_2H_4$—that is, a condensed phase storage for oxo gas ($CO/H_2 = 1:1$), which can be obtained from methyl formate pyrolysis:

The same reaction, but under mild conditions (1.0 bar and 30 °C), can be carried out with alkali metal alkoxides, where an equilibrium between methyl formate, CO and H_2 is established. Removal of synthesis gas forces the equilibrium to furnish the latter until methyl formate is consumed completely [40, 48].

Synthesis Gas Production Through Methanol Dehydrogenation to Methyl Formate and its Pyrolysis

As outlined previously, methyl formate can be regarded as a storage for CO and methanol. It can also serve as storage for synthesis gas, thus constituting an alternative to methanol reforming to CO and H_2. Figure 6.15 illustrates a process for producing methyl formate from methanol through dehydrogenation. The hydrogen formed in the course of this reaction is drawn off and methyl formate is subjected to pyrolysis over activated carbon, zeolites, or alkaline earth oxides, yielding CO in 98 % purity and methanol, which can be recycled in the process.

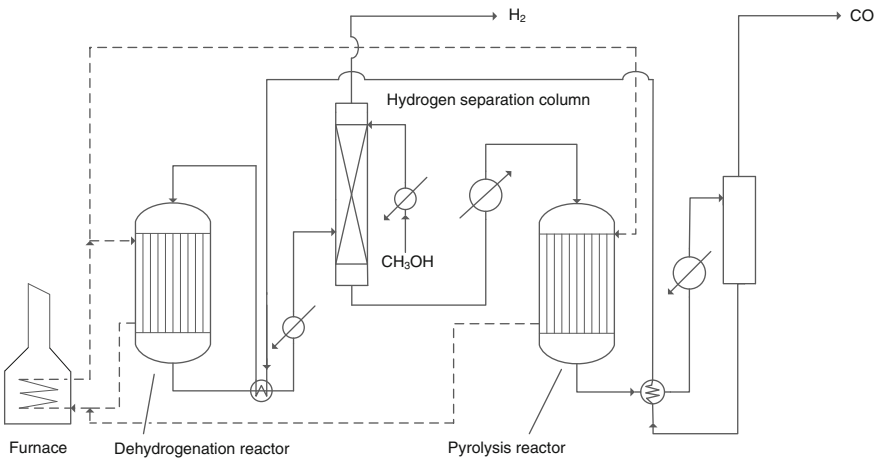

Fig. 6.15 Process for methanol dehydrogenation to H_2 and methylformat and the subsequent pyrolysis to methanol and CO. (Adapted from [30])

6.2.5 Formic Acid

Formic acid is the simplest organic acid. Its technical meaning is based upon its properties as carbonic acid and, because it is formally conceivable as hydroxyl formaldehyde, also as a reducing agent. Production capacity in 2009 was 720,000 tonnes, with BASF, Feicheng Acid Chemicals and Kemira as world's largest producers. It is commercially available in solutions of various concentrations between 85 and 99 w/w% at prices ranging from 650 EUR/tonne in Western Europe to 915 EUR/tonne (1,250 USD/tonne) in the United States.

A major use of formic acid is as a preservative and antibacterial agent in livestock feed. In Europe, it is applied on silage (including fresh hay) to promote the fermentation of lactic acid and to suppress the formation of butyric acid. Formic acid arrests certain decay processes and causes feeding stuff to retain its nutritive value longer, so it is widely used to preserve winter feed for cattle. In the poultry industry, it is sometimes added to feeding stuff to kill *E. coli* bacteria. Use as a preservative for silage and animal feed constituted 30 % of the global consumption in 2009. Formic acid is also significantly used in the production of leather (23 %) and in the dying and finishing of textiles (9 %). Use as a coagulant in the production of rubber constituted 6 % of the global consumption in 2009. Formic acid is also used in place of mineral acids for various cleaning products, such as limescale remover and toilet bowl cleaner. Some formate esters are ingredients of artificial flavourings or perfumes. Beekeepers use formic acid as a miticide against the tracheal mite (*Acarapis woodi*) and the *Varroa* mite. Before the (direct) methanol fuel cell, formic acid was discussed as hydrogen source for fuel cells [49, 50]. Formic acid is stable for years, such as methanol; however, upon contact with a platinum-group metal (PGM), such as platinum or rhodium, it decays readily at room temperature to CO_2 and H_2:

$$HCO_2H \xrightarrow{[PGM]} CO_2 + H_2$$

Because only a very simple device is needed for hydrogen mobilisation, formic acid appears to be an ideal hydrogen storage. A disadvantage, however, is that 1 kg of formic acid provide only about 500 L of H_2 gas, whereas both methanol ($CH_3OH + H_2O \rightarrow CO_2 + 3H_2$) and ammonia ($2NH_3 \rightarrow N_2 + 3H_2$) yield about 2,100 L of H_2 per kg.

Methanol requires reforming at elevated temperatures in the presence of a catalyst; likewise, liquid ammonia is transferred at higher temperatures in ammonia splitting gas. The technical effort is therefore greater, while e.g. 1 % palladium on activated carbon formic acid catalyses immediate hydrogen supply at ambient temperature.

Formic acid is a raw material for silage and is used in the textile industry (dying, finishing, carpet dying, leather tanning, rubber industry, chemical synthesis, etc.). It is also an important reducing agent for the reduction of enamines

and inorganic compounds. In addition, it replaces zinc in dithionite production from sulphite and allows for reducing nitrate to nitrite [51]. The free acid is also used for pickling of steel.

Because each mole of formic acid contains 38.5 kJ (9.2 kcal) more energy than the fission gases $CO_2 + H_2$, one would expect spontaneous decomposition to occur. In fact, this takes place only in the presence of a catalyst, such as 1 % Pd on activated carbon. Because in the oxidation to water 1 mol H_2 yields 238 kJ, as much as 86 % of the energy content of formic acid can be recovered.

Historically, formic acid was obtained by the reaction of sulphuric acid with sodium formate in concentrations ≤85 %. Sulphuric acid concentration and temperature must not be too high; otherwise, carbon dioxide is produced [52]. Alternatively, formic acid can be obtained from formal formic acid nitrile, i.e. hydrogen cyanide (HCN), or by hydrolysis of orthoformic acid trichloride, chloroform ($CHCl_3$) with KOH.

Commercially, the acid can be derived from targeted production or is obtained as a byproduct, such as in methyl formate production through methanol dehydrogenation (see Sect. 6.2.4.2) [20].

In general, two approaches exist:

1. Direct synthesis: reaction of CO with water.
2. Indirect synthesis: reaction of CO with an alcohol followed by hydrolysis:

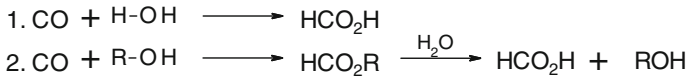

6.2.5.1 Direct Synthesis

CO can be conceived as a chemically inactive acid anhydride of formic acid—the hydration of which leads to the latter. The reaction benefits from bases present, such as NaOH or $Ca(OH)_2$, as well as pressure. Typical process conditions are 8–30 bar and 115–150 °C. Instead of pure CO, synthesis gas may be used. The free acid is obtained through acidification and extraction, such as with diisopropyl ether or by distillation. The direct synthesis is operated in a 40,000 t/a plant in Russia.

6.2.5.2 Formic Acid Through Methyl Formate Hydrolysis

Conversion of CO with alcohols, preferably with methanol, is the first step of the most important production process for formic acid. Formally a CO insertion into the O–H bond of methanol, this reaction is different from methanol carbonylation to acetic acid (Fig. 6.9). The process is conducted with catalytic amounts of sodium methylate at 2–200 bar and 70 °C. With an excess of methanol, CO conversion reaches ≤95 %.

Current methyl formate hydrolysis processes with technical significance have been developed by BASF, Halcon SD and Leonard. They are very similar in their carbonylation conditions and mainly differ in the process engineering concepts for the autocatalytic hydrolysis to formic acid at 3–18 bar and 80–140 °C, where cycle methanol needs to be prevented from competing re-esterification. The molar HCO_2CH_3/water ratio typically ranges between 2:1 and 4:1. Alternatively, excess water is used, which requires instant distillative methanol removal (i.e., minimal contact time between formic acid and methanol).

For this reason, an indirect route via formamide formation with NH_3 at 4–6 bar and 80–100 °C and follow-up hydrolysis is often favoured. Formamide saponification proceeds continuously above 85 °C with 70 % H_2SO_4 to formic acid and ammonia sulphate:

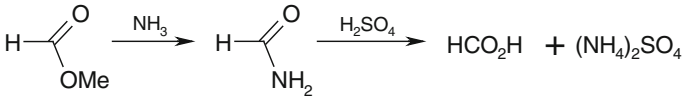

Workup of the reaction product is realised in a rotary kiln. The obtained acid is purified in a column made from V4A or polypropylene with a cooler made from silver or graphite. A technical process of this kind had been developed by BASF and was in operation until 1982, when it was substituted by direct hydrolysis.

Figure 6.16 illustrates the Leonard process to formic acid in a simplified flow scheme [53]. Methanol is being converted at a CO pressure of 42 bar in the presence of a catalyst. The resulting mixture of methanol and methyl formate is funnelled into a degassing column where it is freed from residual CO gas. From there,

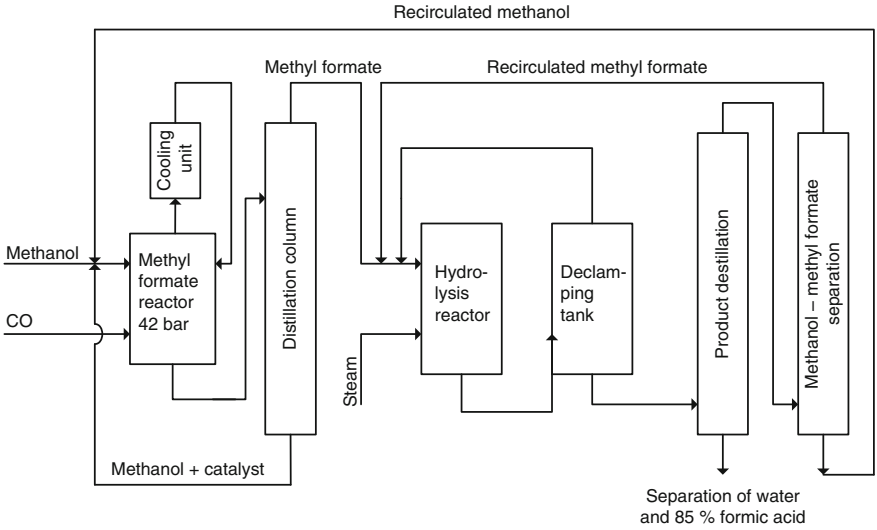

Fig. 6.16 Leonard process for the indirect synthesis of formic acid via methyl formate. (Adapted from [53])

the mixture is fed into the hydrolysis column without prior separation of methyl formate from methanol. The hydrolysate, which has been obtained at mild temperatures in the presence of water vapour, is continuously fed into a distillation column, where methyl formate and unreacted methanol are removed overhead and then separated by distillation. Methyl formate is recycled to hydrolysis, with methanol in the reactor. Eventually, formic acid is separated from water by distillation and the product is obtained as a maximum-boiling azeotrope with a content of 85 %. Alternatively, methyl formate separation from unreacted methanol can be realised prior to the hydrolysis step, thereby entering pure ester into hydrolysis.

6.2.5.3 Formic Acid from Carbon Monoxide

Alternatively, formic acid preparation can be accomplished according to the Marcellin Berthelot method from 1855, which is a two-step synthesis starting with the reaction of NaOH with CO at 6–8 bar and 130 °C. The resulting sodium formate can be marketed directly or is reacted with sulphuric acid to formic acid and sodium sulphate:

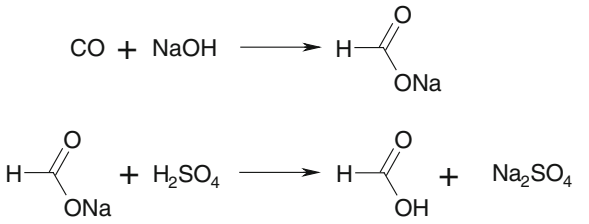

6.2.6 Carbon Monoxide for Organic Syntheses

Because methanol can easily be reformed to synthesis gas, the alcohol not only stores hydrogen but also CO. The latter is separated from synthesis gas (directly or obtained by reforming methanol) by low-temperature separation or absorption in aqueous copper salt solutions.

6.2.6.1 Carbon Monoxide from Low-Temperature Separation of Synthesis Gas

Prior to low-temperature separation of synthesis gas (e.g. according to the Linde process or the Air Liquide process), the crude gas is freed from CO_2 by ethanol amine wash until the content does not exceed 50 ppm. In molecular sieve adsorbers, water and residual CO_2 are removed. Both components would cause clogging through freeze-out. In addition the synthesis gas must be free from N_2

since for vapour pressures being too similar N_2-separation would cause uneconomically high process effort.

The actual low-temperature separation is realised as a two-step process, starting with partial condensation of CO at 40 bar and −180 °C. When synthesis gas has been produced from sources other than methanol in a subsequent step, an expansion into a CO/CH_4 separation column follows. CO is removed overhead with less than 0.1 vol% CH_4. The process is characterised by a highly effective gas recirculation, allowing for recovery of most of the cold energy.

6.2.6.2 Carbon Monoxide Separation from Synthesis Gas by Absorption in Aqueous Copper Salt Solutions

CO absorption in hydrochloric CuCl solution, ammoniacal Cu_2CO_3, or Cu formate solution is conducted under pressure up to 300 bar. CO desorption is realised under reduced pressure at 40–50 °C. The Uhde process binds CO in the form of $[Cu(CO)]^+$ with copper salts in NH_3–H_2O [54]. Process parameters may differ greatly depending on whether CO is to be recovered from gas mixtures or whether gas mixtures are to be freed from CO traces.

The Cosorb process by Tenneco Chemicals uses a solution of CuCl and anhydrous $AlCl_3$ in toluene. It makes use of the temperature dependence of CO-forming complexes with $Cu[AlCl_4]$. The Cu(I)-CO complex is formed at ≤20 bar and about 25 °C and releases CO at 1–4 bar and 100–110 °C. Water (hydrolysis of $AlCl_3$) and acetylene (acetylide formation) must be removed prior to CO separation. The Cosorb process has been in use worldwide after its introduction in 1976.

6.2.6.3 CO Separation Using Membrane Technology

Novel approaches enrich CO from gas mixtures using semipermeable membranes.

6.2.6.4 CO use in Synthetic Organic Chemistry

CO is a starting material for a multitude of reactions. Pure CO is used rather rarely, however. Typically, the pure gas is used for metal carbonyl or phosgene synthesis from the reaction of CO with Cl_2 (starting material for isocyanates; e.g. toluylene diisocyanate for polyurethane production). Other processes comprise methanol carbonylation reactions to methyl formate (Sect. 6.2.4) or acetic acid.

On a technical scale, CO use in combination with H_2 is of much greater significance. Apart from classical synthesis, gas chemistry to methanol, and Fischer–Tropsch synthesis, hydroformylation reactions (oxo aldehydes, oxo alcohols) are commercially important. In combination with a nucleophilic partner such as water

or alcohols, the Reppe carbonylation reaction to acrylic acid (acetylene), propionic acid (ethylene), and their esters is of technical importance, as well as the Koch reaction to branched carbonic acids (Fig. 6.17).

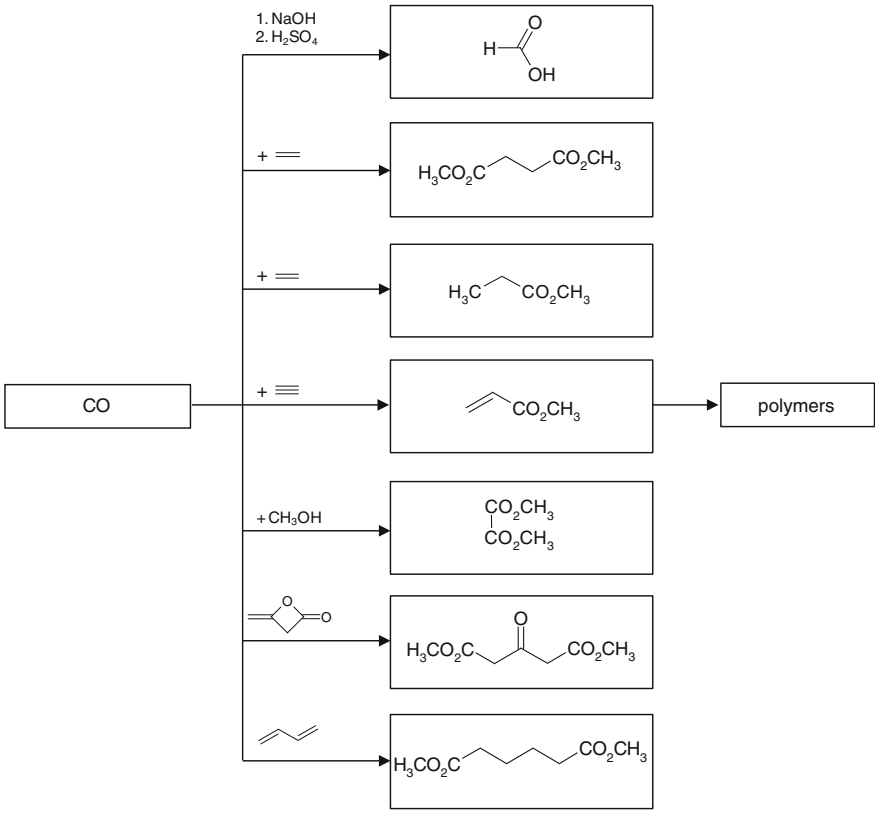

Fig. 6.17 Use of carbon monoxide in synthetic chemistry

6.2.7 Methanol Homologation to Ethanol

The direct coupling of classic petrochemical ethanol production to ethylene prices makes alternative routes to ethanol economically more interesting. Novel developments therefore preferably focus on synthesis gas. One possible route is the so-called methanol homologation to ethanol, which was discovered by BASF in 1941. In this reaction, methanol is converted in the gas or fluid phase with CO/H_2 in the presence of Rh- or Co-containing multicomponent catalysts:

$$CH_3OH + CO + 2H_2 \rightarrow C_2H_5OH + H_2O$$

Depending on reaction conditions, this reaction can be used to produce either ethanol or acetaldehyde from methanol.

In the original experiment at 200 bar and 160–170 °C, $CO/H_2 = 1{:}1$ was reacted with methanol in the presence of cobalt carbonyl, leading to a complex mixture containing ethanol, acetaldehyde, acetic acid and other compounds [55]. With CO alone instead of synthesis gas, acetic acid methyl ester is obtained [56, 57]. Because of the potential of this reaction, it is clear why it was investigated in detail in Europe and the United States. It can be used for the synthesis of ethanol, acetaldehyde, acetaldehyde dimethyl acetal and acetic acid methyl ester:

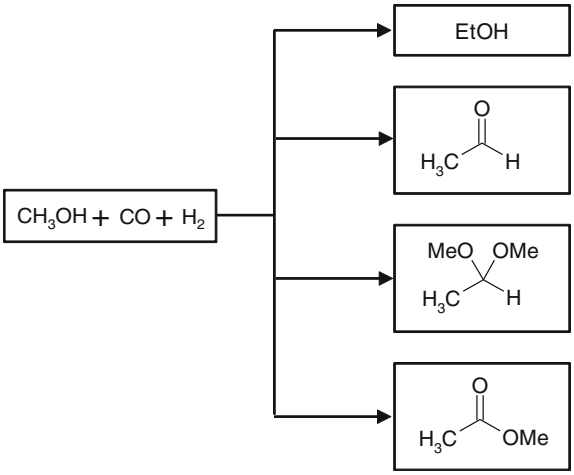

Although the process has been elucidated and understood in detail with catalysts having been optimised, no technical application currently exists.

6.2.8 Acetic Acid

Acetic acid is among the most important aliphatic intermediates. It is also the carbonic acid that has been in use for the longest time. Worldwide production capacity was 11.5 million tonnes in 2012. Consequently there are a number of processes for generating acetic acid through oxidative fermentation of ethanol. Alternatively, there are processes for its production from wood coking (pyroligneous acid) or from sugar cane molasses.

For decades, acetic acid was chiefly produced from acetaldehyde. At the beginning of the 20th century, Hoechst, Wacker and Shawinigan operated oxidation processes on a technical scale. Consequently, acetic acid production was closely linked to acetaldehyde availability. At the same time, the raw material base for acetic acid changed from acetylene to ethylene. For reasons of process economy, the necessity to use light paraffins caused oxidation routes to be developed in

the United States, Germany and England by Celanese, British Distillers, Hüls and Union Carbide. Bayer and Hüls were also active in using C_4 olefins.

In the 1920s, methanol carbonylation came into play. First introduced by BASF on a technical scale (Co-catalysis), this process was replaced by the Rh-catalysed Monsanto process, which in turn was surpassed by the Cativa process that uses an Ir-catalyst. Consequently, acetaldehyde oxidation lost its dominating role in favour of more economical methanol carbonylation. In 1979, approximately 62 % of acetic acid production was based on acetaldehyde; it was less than 28 % in 1995 and has continued to decrease since [20]. Figure 6.18 provides an overview on the intermediates and products that are derived from acetic acid in industrial chemistry.

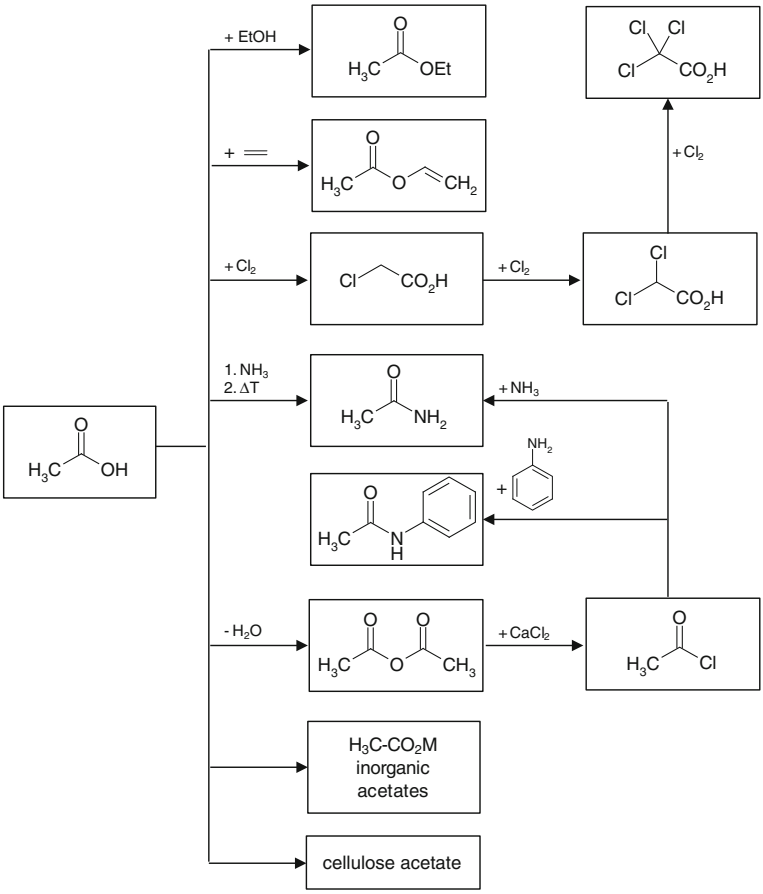

Fig. 6.18 Products derived from acetic acid

6.2.8.1 Acetic Acid Through Acetaldehyde Oxidation

For the sake of completeness and in order to understand the quantum leap methanol carbonylation entailed, acetaldehyde oxidation is discussed here briefly. The reaction proceeds as a radical reaction with air or oxygen via peracetic acid as an intermediate:

1. Acetyl radical formation is initiated by the action of a transition metal, such as Mn^{3+}

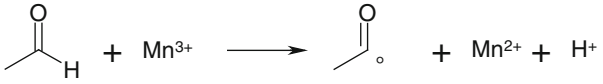

2. Oxidation

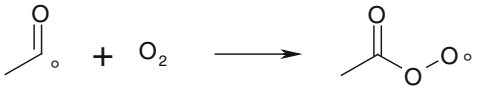

3. Peracetic acid formation and chain propagation

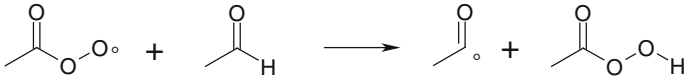

4. Acetic acid formation via hydroxyethyl peracetate

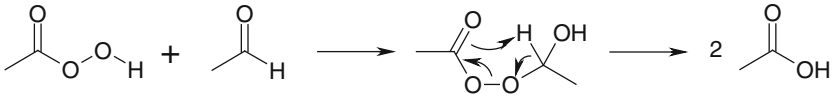

This process is still technically important because it allows peracetic acid to be easily derived as major product under mild conditions. The reaction is conducted without the need of a catalyst in ethyl acetate at 25–40 bar and −15 to +40 °C with air. Commercial plants in which this process is run are operated by British Celanese, Daicel and UCC.

6.2.8.2 Acetic Acid Through Methanol Carbonylation

The discovery that methanol is susceptible for carbonylation to acetic acid by BASF dates back to 1913. The reaction had little importance until the early 1920s, when methanol became available in considerable amounts on a technical scale at reasonable prices. This was the impetus for other companies, such as British Celanese, to adapt the process in 1925. From the very beginning, the process suffered from corrosion, what was overcome in the 1960s when a smaller plant was put into operation by BASF using Hastelloy as a reactor material.

BASF Process

Methanol alone or as a mixture with DME and little water is converted with CO in the presence of CoI_2 in the liquid phase at 680 bar and 250 °C. The process makes use of CoI_2 for in situ generation of $[Co_2(CO)_8]$ and HI:

$$2CoI_2 + 2H_2O + 10CO \rightarrow [Co_2(CO)_8] + 4HI + 2CO_2$$

Under these reaction conditions, $[Co_2(CO)_8]$ reacts in terms of a CO conversion:

$$CO + H_2O \rightarrow CO_2 + H_2$$

As a result, cobalt tetracarbonyl hydrogen, $[CoH(CO)_4]$, is produced in the hydrogenous atmosphere:

$$[Co_2(CO)_8] + H_2O + CO \rightarrow 2[CoH(CO)_4] + CO_2$$

After deprotonation, the cobalt complex is catalytically active. At the same time, methanol reacts with HI to methyl iodide:

$$CH_3OH + HI \rightarrow CH_3I + H_2O$$

Cobalt tetracarbonyl hydrogen and methyl iodide form methyl cobalt tetracarbonyl, which after CO insertion is hydrolysed to acetic acid, with cobalt tetracarbonyl hydrogen being regenerated:

1. $CH_3I + [CoH(CO)_4] \rightarrow CH_3Co(CO)_4 + HI$
2. $CH_3Co(CO)_4 + CO \rightarrow CH_3COCo(CO)_4$
3. $CH_3COCo(CO)_4 + H_2O \rightarrow CH_3CO_2H + [CoH(CO)_4]$

On a technical scale, Co and I_2 can be fully recovered. The selectivity for acetic acid is 90 % (CH_3OH) and 70 % (CO). Per tonne of product, ~40 kg of byproduct are formed, consisting of a complex mixture of different chemical entities. After distillation, the product is obtained in 98.3 % purity.

Monsanto Process

In 1968, Monsanto Co. (St. Louis, Missouri, USA) used a rhodium-catalysed process after it had been discovered that Rh in combination with I_2 constitutes a more active catalytic system than CoI_2. It works at considerably milder reaction conditions at 30–60 bar and 150–200 °C. In addition, it exhibits a far higher selectivity of ~99 % (CH_3OH) and 90 % (CO). From then on, the BASF process was no longer competitive, and today it is of historical interest only. In 1970, in Texas City, Texas, USA, the first technical plant was put into operation with a capacity of 150,000 t/a.

Mechanistically the Rh-catalysed reaction is completely different from the CoI_2 process, even though rhodium is directly placed under cobalt in the periodic chart. In the Monsanto process, the catalytic system consists of RhI_3 and an iodine containing co-catalyst, such as HI/H_2O. Under reaction conditions, a precatalyst is

formed, which is a tetragonal-planar diiodo dicarbonyl rhodate(I) complex and, secondly, methyl iodide from the reaction of methanol with HI:

1. $RhI_3 + 3CO + H_2O \rightarrow [RhI_2(CO)_2]^- + I^- + 2H^+ + CO_2$
2. $MeOH + HI \rightarrow CH_3I + H_2O$

From a mechanistic point of view, two cycles have to be differentiated:

- The rhodium cycle, which is the actual metal complex catalysed reaction.
- The iodide cycle, at the basis of which there are no metal catalysed reactions.

The active species is $[CH_3\text{-}Rh(CO)_2I_3]^-$. After insertion of CO into the CH_3–Rh bond, an acetyl rhodium complex is formed, which decomposes under formation of acetic acid and regeneration of $[Rh(CO)_2I_2]^-$ (Fig. 6.19).

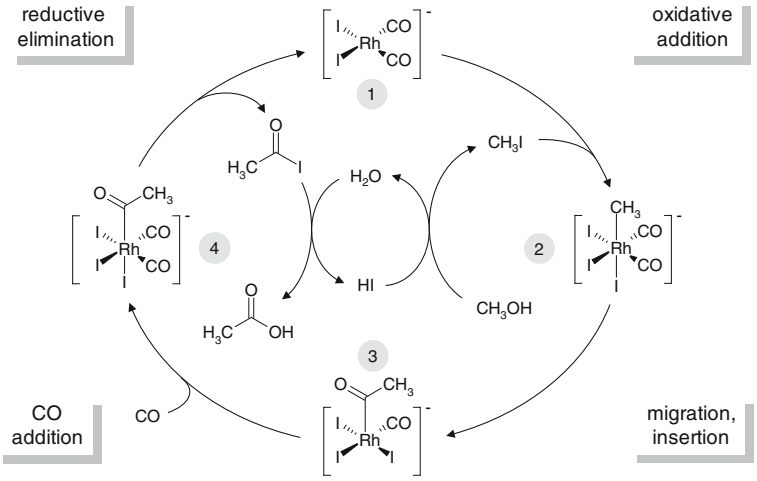

Fig. 6.19 The Monsanto process. (Modified from [22, 27])

The reaction profile obtained from kinetic data of oxidative addition of CH_3I (1 → 2) and subsequent migratory CO insertion (2 → 3) shows that the oxidative addition is the rate-determining step. The methyl rhodate(III) complex is instable with regard to reductive elimination (2 → 1) and migratory CO insertion (2 → 3). As a consequence, equilibrium concentrations of (2) are very low. Nevertheless, (2) was identified by infrared and nuclear magnetic resonance spectroscopy in reaction mixtures of $[RhI_2(CO)_2]^-$ and CH_3I.

Like the BASF process, the Monsanto process is conducted in polar solvents (acetic acid/water). Owing to the highly corrosive action of the acidic iodine-containing reaction media, there are high demands on the reactor material.

One drawback of the process is the capability of rhodium complexes to catalyse CO conversion as well:

$$CO + H_2O \rightleftharpoons H_2 + CO_2$$

$[RhI_2(CO)_2]^-$ (1) which is the active complex in methanol carbonylation catalyses establishing of the water gas equilibrium, too, thus causing a decreased CO-selectivity. There are two complex reactions on which CO conversion is based (Fig. 6.20):

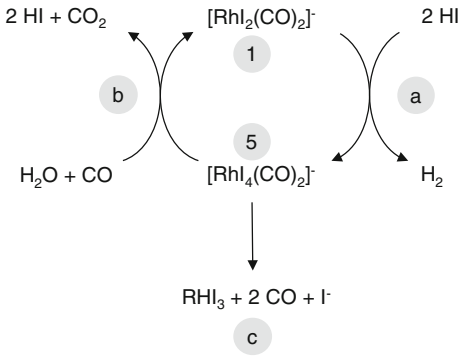

Fig. 6.20 Mechanism of CO conversion as catalysed by $[RhI_2(CO)_2]^-$ (1). Thus, the same complex that catalyses methanol carbonylation in the Monsanto process is the species by which competing CO conversion is catalysed. This latter process is responsible for reduced CO selectivity. The higher nucleophilicity of the respective Ir catalyst (see Fig. 6.21) causes shorter lifetimes of the $[MI_2(CO)_2]^-$ (M = Rh, Ir) complex, which finds its expression in higher CO selectivity. (Adapted from [22])

(a) Reduction of $H^+ \rightarrow H_2$ and formation of a dicarbonyl tetraiodorhodate(III) (5).
(b) Oxidation of $CO \rightarrow CO_2$, upon which (1) is regenerated.
(c) In addition, the Rh^{III} complex $[RhI_4(CO)_2]^-$ (5) tends to decompose under deposition of RhI_3.

As a result, H_2 and CO_2 are produced as major byproducts from CO conversion. Fully automated process control and full catalyst recovery are crucial for process economy.

In a novel process that is in use by BP in a plant based in England, methanol and methyl acetate are used as starting materials, allowing for the generation of acetic acid/acetic acid anhydride mixtures in a ratio of 40:60–60:40 (for acetic acid anhydride production from methyl acetate, see Sect. 6.2.1 and the Hoechst-Celanese process in this section).

Cativa Process

A significant optimisation of the Monsanto process is the Cativa process, which was introduced in 1995–1996 by BP Chemicals (Hull, England). The process uses an iridium complex (Fig. 6.21).

The fundamental steps of the rhodium- and iridium-catalysed reactions are similar but differ in their relative rates. This has significant consequences for the whole catalytic process with the oxidative addition of CH_3I at $[MI_2(CO)_2]^-$ (M = Rh, Ir) playing a key role. Kinetic investigations and quantum chemical calculations have shown that this reaction step proceeds under formation of methyl

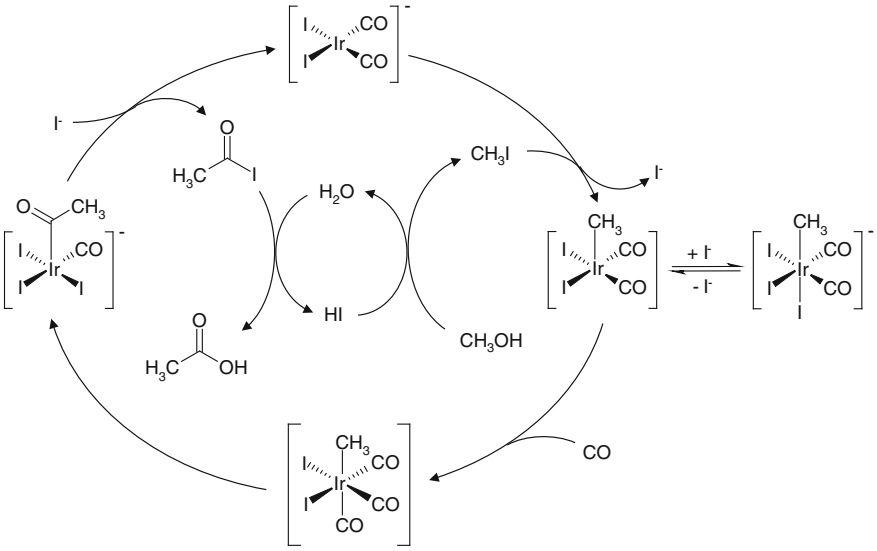

Fig. 6.21 The Cativa process. The iodide cycle is identical to that in Fig. 6.19 and is therefore not shown. (Adapted from [22])

metal(III) complex according to the S_N2 mechanism (Fig. 6.22). As the nucleophilic agent, the tetragonal-planar complex $[MI_2(CO)_2]^-$ (1) was identified in which the doubly occupied dz^2 orbital is the centre of nucleophilicity.

In the transition state (2), the M-C bond has been formed while the C–I bond has been broken. Thus, the energy required for C–I bond fission is partially compensated by M–C bond formation. For the binding energies of the complexes, Ir–C was found to exceed that of Rh–C. Hence, the activation barrier of the Ir complex is lower than for the Rh complex. For the same reason, rhodium complex formation is endergonic whereas iridium complex formation is exergonic (Fig. 6.22).

In fact, CH_3I is added to the iridium complex $[IrI_2(CO)_2]^-$ approximately 150 times faster than to the analogous rhodium complex. For this reason, the oxidative addition of CH_3I is no longer rate-determining in iridium-catalysed methanol carbonylation. However, for complexes that are constitutionally the same, migratory CO insertion (3 → 4) is several orders of magnitude slower in aprotic solvents for M = Ir than for M = Rh.

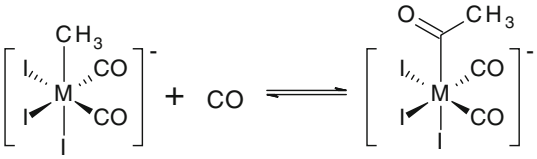

Therefore, a reaction is observed to be accelerated in protic solvents such as methanol, in which a dissociative substitution of I^- by CO (1 → A → B) is

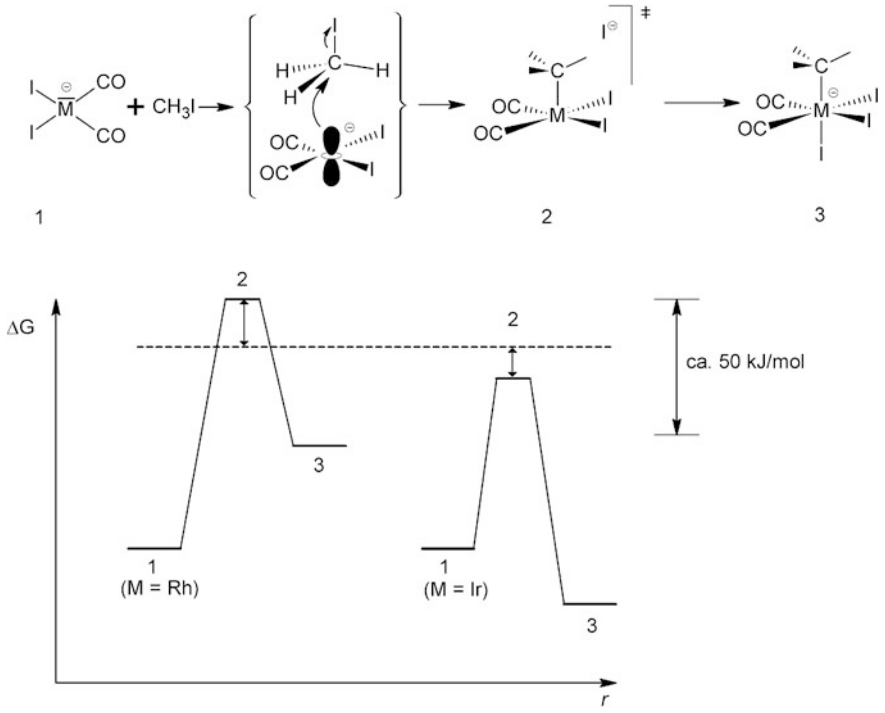

Fig. 6.22 Disparities in nucleophilic addition behaviour favour octahedral oxidative addition to octahedral complex 3 for iridium complexes, while the same is disfavoured for rhodium species. (Adapted from [22])

considerably faster. Complex B is subject to a substantially faster CO insertion than complex 1.

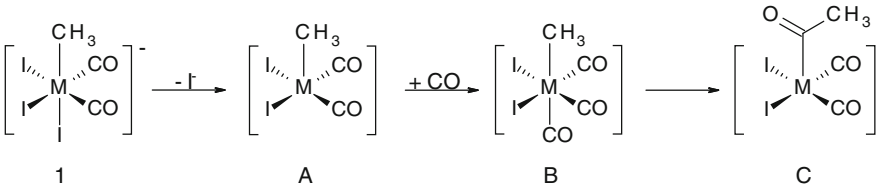

Table 6.2 summarises similarities and differences between the three processes. It is obvious how a higher CO selectivity reduces byproduct formation.

Hoechst-Celanese Process

A reduction of water content of the reaction mixture considerably affects the iodide cycle of the Monsanto process. As a consequence of a higher methanol ratio, acetyl iodide is preferably converted with methanol instead of water. This reaction furnishes methyl acetate, which can be saponified with HI to give CH_3I

Table 6.2 Comparison of technical methanol carbonylation processes. (Adapted from [22])

	Co	Rh	Ir
Technical introduction	1960 BASF	1970 Monsanto	1995 BP Chemicals
Process	BASF	Monsanto	Cativa
Temperature (in °C)	250	150-200	180
Pressure (in bar)	600-700	30-60	30-40
Selectivity			
MeOH (%)	90	99	99.5
CO (%)	70	90	>94
Major by-products	CH_4, CO_2, EtOH, CH_3CHO, EtCOOH	CH_4, CO_2, H_2, EtCOOH	Very few

and acetic acid. Acetic acid anhydride formation from methyl acetate was described in Sect. 6.2.1. In addition, methyl acetate is formed through an acidic catalysed reaction of methanol with acetic acid.

At high methyl acetate concentration, HI concentration is low, what decreases the hydrogen formation rate within the competing CO conversion (Fig. 6.20, reaction a). This results in lower CO release from (5) and consequently in a considerably higher CO selectivity. The lower HI concentration, however, would favour precipitation of insoluble RhI_3, which is avoided by adding soluble iodides such as LiI, $(NR_4)I$, or $(PR_4)I$.

Figure 6.23 shows the different iodine cycles of the Monsanto and the Hoechst-Celanese processes.

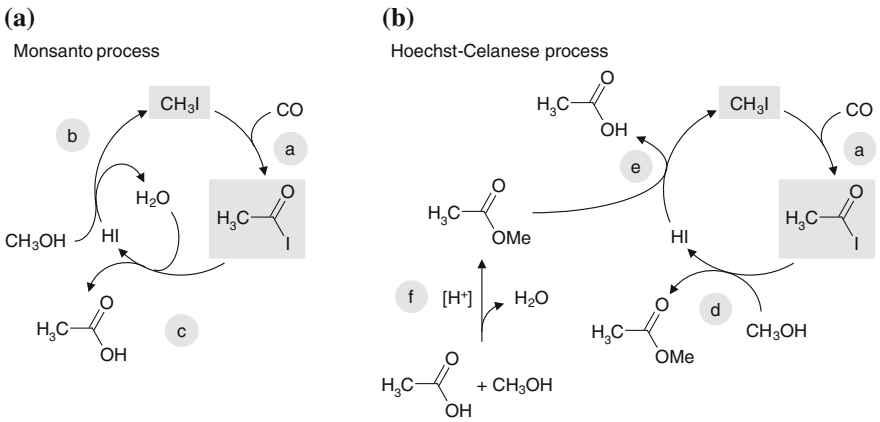

Fig. 6.23 Iodide cycles of the Monsanto (a) and Hoechst-Celanese process (b). Starting material and product of the rhodium-catalysed cycles are marked in grey. (Adapted from [22])

The centrepiece of the Monsanto process is a rhodium-catalysed formation of acetyl iodide from CO and CH_3I (a). The latter is formed from CH_3OH and HI (b), which in turn is regenerated from acetyl iodide hydrolysis (c). If sufficient water is present in the reaction mixture, methyl acetate formation from acetyl iodide and

CH_3OH (d), as well as methyl acetate conversion with HI to CH_3I and acetic acid (e), play only a minor role.

By understanding the reasons behind methyl acetate formation, it becomes evident how propionic acid (Table 6.2) emerges from methanol carbonylation. At the same time, it is obvious that acetaldehyde is formed through rhodium-catalysed acetic acid reduction with H_2 formed from CO conversion (vide supra). Follow-up reduction of acetaldehyde delivers ethanol [20, 22].

Other Processes

The isomerisation of methyl formate is one additional route to acetic acid (see Sect. 6.2.4.4). Acetic acid can also be produced from DME by hydrating carbonylation technology according to the Monsanto-process [58]:

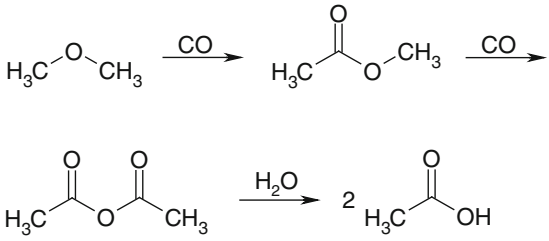

6.2.9 Formaldehyde

Formaldehyde (CH_2O) is an important molecule for global chemical economy; due to its reactivity, it is used in a whole range of industry: construction, textiles, carpeting, wood processing and chemical. At ambient temperature, formaldehyde is a colourless gas that tends to polymerise rapidly in the presence of small amounts of impurities. For this reason, three commercial forms have been established [20]:

1. Aqueous 35...55 % solution, with 37 % being the most widely used grade which may also contain 0–15 % methanol and a polymerisation inhibitor. In solution formaldehyde is present as hydrate or as a mixture of oligooxymethylene glycols.

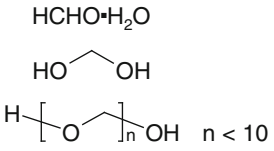

2. Trioxane, the cyclic, trimeric form that is obtained by acid-catalysed conversion of formaldehyde.

3. Paraformaldehyde, the polymeric form of formaldehyde which is produced upon boiling-down of aqueous formaldehyde solutions. The latter can be regenerated through heating or addition of acid.

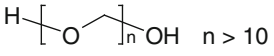

Since the first commercial production of formaldehyde in Germany in 1888 through methanol dehydrogenation, its synthesis has changed from radical oxidation of propane and butane or DME oxidation, respectively, to the two main routes starting from methanol that are in use today: (1) oxidation-dehydrogenation over a silver catalyst and (2) direct oxidation of methanol to formaldehyde using metal oxide catalysts (Formox process). Up to 50 % of methanol production is consumed for formaldehyde synthesis. In 2012, worldwide formaldehyde production amounted to 40.9 million tonnes, what is an increase of 77 % compared to 23 million tonnes in 2003. Globally leading manufacturers are Borden and BASF [59].

Formaldehyde is usually produced close to the point of consumption because it is fairly easy to make but cannot be shipped easily over long distances. It can develop stability-associated problems during transport. As a result, world trade in formaldehyde is minimal. Consumption of formaldehyde depends mainly on the construction, automotive and furniture markets. The main downstream demand for formaldehyde around the world is in the production of thermosetting resins. The largest group is the amino resins produced by condensing either urea or melamine with formaldehyde (Table 6.3) [60].

6.2.9.1 Formaldehyde Production from Methanol

Formaldehyde is produced industrially from methanol by the following three processes based on two different catalytic technologies, as described here.

1. Oxidative dehydrogenation

In this method, formaldehyde is formed by dehydrogenation of methanol. Vapourised methanol and air are passed over a thin bed of silver-crystal catalyst at 600–720 °C:

$$CH_3OH \rightarrow HCHO + H_2$$

Because of the high decomposition rate of formaldehyde, residence time must be kept below 0.01 s, which is accomplished through high-flow velocity and rapid cooling after passing the catalyst bed. The heat required for the endothermic reaction is obtained by burning the off-gas (N_2, H_2, H_2O, CO, CO_2, CH_3OH, HCHO) produced from the dehydrogenation reaction. Formaldehyde is isolated from the reaction gases by absorption in water and is obtained as a 37–44 % solution (formalin).

In the chemical industry, there are two different modes of operation:

(1a) *Single pass*

Using partial oxidation and dehydrogenation, the feed is composed of methanol, air and steam in the presence of silver crystals at 680–720 °C with an excess of methanol being used. In the BASF process, methanol conversion is 97–98 %.

Table 6.3 Commercial use of formaldehyde [60]

Product	Use	Remarks
Formaldehyde	• Disinfectant • Conservation • Chemicals	Commercial forms: • Formaldehyde hydrate • Trioxane • Paraformaldehyde
Urea formaldehyde resins	• Binders in nonstructural wood-based panels for particle board and medium-density fibreboard	Largest sector
Melamine formaldehyde resins	• Adhesives • Binders • Clear coats for automobile industry • Paper-impregnating resins • Surfacing of panels	
Phenolic formaldehyde resins	• Composites • Durable binders and adhesives in structural wood panels • Binders in mineral wool insulation • Insulation foams • Brake linings • Foundry binders • Oil well productivity enhancers in oil industry	Water resistant, high thermal stability
Polyoxymethylene	• Tough engineering thermoplastics replacing metals in electrical, electronic, automotive and consumer applications	Second largest use for formaldehyde
Methyl di-*p*-phenylene isocyanate	• Polyurethane foam • Polyurethane elastomers • Adhesives • Binders • Sealants	Fastest growing of the formaldehyde derivative markets
Butanediol	• Polyester thermoplastic resins used in textile fibres	
Pentaerythritol	• Alkyd resins • Lubricants • Tall oil esters	Produced from alkaline condensation of formaldehyde with acetaldehyde; demand for pentaerythritol is falling around the world
Trimethylol propane	• Textile and leather impregnation	

(1b) *With recycle*

Partial oxidation and dehydrogenation with air and steam in the presence of crystalline silver (or silver gauze) at 600–650 °C with an excess of methanol yields a primary conversion of methanol between 77 and 87 %. The conversion is completed by distilling the product and recycling the unreacted methanol in the main feed.

2. Methanol oxidation

The second technology involves pressureless methanol oxidation by an excess of atmospheric oxygen over a catalyst of molybdenum and iron oxide with $Fe_2(MoO_4)$ as the actual active component at approximately 350 °C. With a modified iron-molybdenum-vanadium oxide catalyst, the process is run at 250–400 °C. The reaction is conducted in catalyst-packed reactor tubes where the metal oxides act as an oxygen carrier on to hydrogen to be cleaved off the methanol. The reduced catalyst is simultaneously reoxidised by atmospheric oxygen:

$$CH_3OH + {}^1/_2O_2 \rightarrow HCHO + H_2O$$

The reaction is highly exothermic, for which reason it is realised in a multitube fixed-bed reactor and generates heat to provide steam for turbines and process heating. Methanol conversion is 98–99 %.

Crude aqueous methanol obtained by high-, medium-, or low-pressure synthesis contains low concentrations of inorganic impurities and limited amounts of other organic compounds (byproducts). The methanol for this process must first be subjected to purification processes and preliminary distillation to remove undesired contaminants (as low-boiling components) because most of the byproducts act as catalyst poisons or they favour side reactions over the catalyst in the process, thus resulting in less pure formaldehyde.

Yields from the oxidation process are around 90–92 %. The oxidation route has a lower reaction temperature and the metal catalyst is more cost-effective than silver. Nevertheless, the oxidative dehydrogenation route is still the most prevalent.

In the following sections, both approaches—oxidative dehydrogenation and methanol oxidation—are described in detail.

Oxidative Dehydrogenation

General aspects

This route is the classical method for the industrial production of formaldehyde. The two main reactions governed by this process are dehydrogenation and partial oxidation. The silver catalyst processes are generally carried out at atmospheric pressure and 600–720 °C using a feed with an excess of methanol. The reaction temperature depends on the excess of methanol present in the methanol/air mixture. The composition of the mixture must be outside the explosive limits. The amount of air in the feed is determined by the catalytic quality of the silver surface. The main reactions occurring during methanol conversion to formaldehyde are the following:

1. $CH_3OH \rightleftarrows CH_2O + H_2$ $\Delta H = +84\,kJ/mol$
2. $H_2 + {}^1/_2O_2 \rightarrow H_2O$ $\Delta H = -243\,kJ/mol$
3. $CH_3OH + {}^1/_2O_2 \rightarrow CH_2O + H_2O$ $\Delta H = -159\,kJ/mol$

Process parameters determine the extent to which each of these three reactions occur. Byproducts result from secondary reactions:

4. $CH_2O \rightarrow CO + H_2$ $\Delta H = +12.5\,kJ/mol$
5. $CH_3OH + {}^3/_2O_2 \rightarrow CO_2 + 2H_2O$ $\Delta H = -674\,kJ/mol$
6. $CH_2O + O_2 \rightarrow CO_2 + H_2O$ $\Delta H = -519\,kJ/mol$

Other important byproducts are methyl formate, methane and formic acid, with all of them not only being formed in the reactor but also in the absorption column.

The endothermic dehydrogenation reaction (1) is highly temperature-dependent. Conversion increases from 50 % at 400 °C to 90 % at 500 °C and to 99 % at 700 °C. Kinetic studies with supported silver show that reaction (1) is a first-order reaction [61]. Therefore, the rate of formaldehyde formation is a function of the available oxygen partial pressure (concentration) and the oxygen residence time on the catalyst surface. However, for the reaction of methanol to formaldehyde over a silver catalyst surface, no complete reaction mechanism has been proposed so far. Some authors postulate a change in mechanism occurring at approximately 650 °C [62]. New insight into the reaction mechanism is available from recent spectroscopic investigations that demonstrate the influence of different atomic oxygen species on reaction pathway and selectivity [63–65]. Formaldehyde synthesis over a silver catalyst is carried out under strictly adiabatic conditions. The reaction is very fast and only few millimetres lie in between sites with high methanol concentration and sites with high formaldehyde concentration.

The oxygen in the process is shared between the exothermic reactions, which is primarily reaction (2) and, to a lesser extent depending on the process used, the secondary reactions (5) and (6). Thus, oxygen concentration in the feed determines the desired reaction temperature as well as the extent of conversion of the endothermic reactions (1) and (4). Another important factor affecting the yield of formaldehyde and the conversion of methanol, apart from catalyst temperature, is the addition of inert material to the reactants. Water is added to reactor feed and nitrogen is added to air feed, as well as air/off-gas mixtures that are recycled to dilute the CH_3OH/O_2 reaction mixture. The throughput per unit of catalyst area provides another way of improving the yield and affecting side reactions. [66, 67].

Silver Catalyst Process with Complete Methanol Conversion (BASF Process)

The BASF process for the complete conversion of methanol to formaldehyde is illustrated in Fig. 6.24.

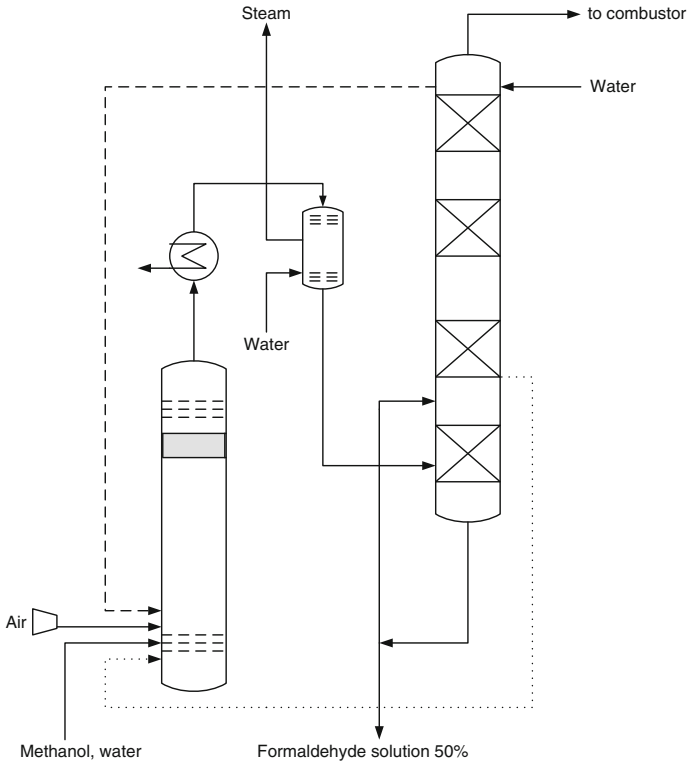

Fig. 6.24 BASF process for formaldehyde production from methanol. (Redrawn from [59])

In this process, a mixture of methanol and water is fed into the evaporating column. Fresh air and, if necessary, recycled off-gas from the last stage of the absorption column enter the column separately [68]. A gaseous mixture of methanol and oxygen is thus formed, in which an inert gas content (N_2, H_2O or CO_2) is fed in order to prevent the upper explosive limit from being reached.

Methanol and gas are mixed in a molar ratio of 60 parts of methanol to 40 parts of water, with or without inert gases. The packed evaporator constitutes part of the stripping cycle. The heat required to evaporate the methanol and water is provided by a heat exchanger, which is linked to the first absorption stage of the absorption column [69]. After passing through a demister, the gaseous mixture is superheated with steam and fed to the reactor, where it flows through a 25–30 mm thick bed of silver crystals. The crystals have a defined range of particle sizes, from 0.4 mm in the first layer to 2 mm in the last [70]. They rest on a perforated tray covered with a fine corrugated gauze, thus permitting optimum reaction at the surface.

The bed is positioned immediately above a water boiler (cooler), which produces superheated steam and simultaneously cools the hot reaction gases to a temperature of 150 °C corresponding to that of the pressurised steam (5 bar). The

almost dry gas from the gas cooler passes to the first stage of a four-stage packed absorption column, where the gas is cooled and condensed. Formaldehyde is eluted countercurrent to water or to the circulating formaldehyde solutions, the concentrations of which increase from stage to stage.

The product circulating in the first stage may contain 50 wt% formaldehyde if the temperature of the gas leaving this stage is kept at approximately 75 °C; this temperature provides sufficient evaporation energy for the feed stream in the heat exchanger. The final product contains 40–55 wt% formaldehyde, as desired, with an average of 1.3 wt% methanol and 0.01 wt% formic acid. Formaldehyde yield of the process is 89.5–90.5 mol %.

Some of the off-gas is removed at the end of the fourth stage of the column [63] and is recycled (Fig. 6.24, route indicated by dashed lines). The residual off-gas has a net calorific value of 1,970 kJ/m^3 and is fed to a steam generator, where it is combusted [71]. Prior to combustion the gas contains approximately 4.8 vol% CO_2, 0.3 vol% CO and 18.0 vol% H_2 as well as nitrogen, water, methanol and formaldehyde. The combusted off-gas contains no environmentally harmful substances. The total steam equivalent of the process is 3 tonnes per tonne of 100 wt% formaldehyde.

In an alternative procedure to the off-gas recycling process (Fig. 6.24, dotted line), the formaldehyde solution from the third or fourth stage of the absorption tower is recycled to the evaporator, and a certain amount of steam is used in the evaporation cycle. The resulting vapour is combined with the feed stream to the reactor for the purpose of obtaining an optimal methanol/water ratio. [72] In this case, the temperature of the second stage of the absorption column is approximately 65 °C. The yields of the two processes are similar and depend on the formaldehyde content of the recycled streams.

Catalyst lifetime depends strongly on reaction temperatures, throughput rates, and impurities. Upon exposure to excessively high reaction temperatures and high throughput rates, the silver crystals get matted, thus causing increased pressure across the catalyst bed. This effect is irreversible and requires the catalyst bed to be changed after 3–4 months. The catalyst is regenerated via electrolytic processes. Impurities such as inorganic salts in the air and methanol feed may lead to catalyst inactivation. Some impurities cause poisoning effects that are reversible within few days, yet with catalytic properties that are not fully restorable compared to the initial situation. Because formaldehyde solutions corrode carbon steel, all parts of the manufacturing equipment exposed to formaldehyde solutions must be made of a corrosion-resistant alloy, such as certain types of stainless steel.

If throughput and reaction temperature have been optimised, the capacity of a formaldehyde plant increases in proportion to the diameter of the reactor. One of largest known reactor appears to be that of BASF in Germany, which has an overall diameter of 3.2 m and a production capacity of 72,000 t/a (calculated as 100 wt% formaldehyde).

Incomplete Conversion and Distillative Recovery of Methanol

Another approach to industrial formaldehyde production is that of partial oxidation and distillative recovery of methanol. This process is used by numerous companies (e.g. ICI, Borden and Degussa) and is based on recent developments (Fig. 6.25) [73–78].

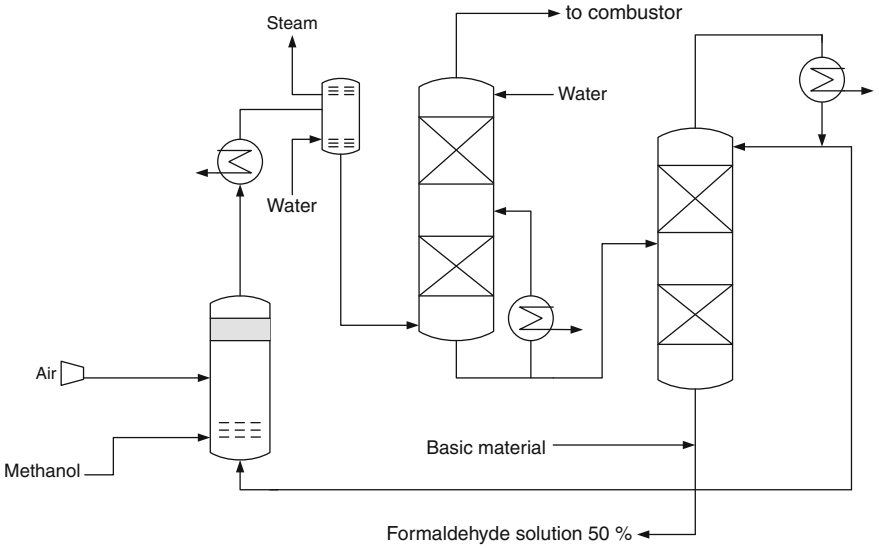

Fig. 6.25 Formaldehyde production through incomplete conversion and distillative recovery of methanol

A feed mixture of pure methanol vapour and freshly blown-in air is generated in an evaporator. The resulting vapour is mixed with steam and then fed into the reactor. The reaction mixture contains excess methanol and steam and is very similar to that used in the BASF process.

The vapour passes through a shallow catalyst bed made from silver crystals or layers of silver gauze. Conversion is incomplete and the reaction takes place at temperatures between 590–650 °C. A low temperature compared to the BASF process minimises undesirable secondary reactions. For these purposes, reaction gases are cooled indirectly with water immediately after leaving the catalyst bed, thereby generating steam. The remaining heat of reaction is then removed from the gas in a cooler and is fed to the bottom of a formaldehyde absorption column. At the top of the column, all condensable portions of the remaining formaldehyde and methanol are washed out from the tail gas by countercurrent contact with process water.

A 42 wt% formaldehyde solution from the bottom of the absorption column is fed to a second column for distillation, which is equipped with a steam-based heat exchanger and a reflux condenser. Methanol is recovered at the top of the column and is recycled to the bottom of the evaporator. From the bottom of the distillation

column, a solution containing up to 55 wt% formaldehyde and less than 1 wt% formic acid is taken, which is funnelled into an anion-exchange unit to remove formic acid to the specified level of typically <50 mg/kg.

Formaldehyde concentration in the final solution is adjusted by process conditions and in particular distillation conditions:

- 50–55 wt% formaldehyde with ≤1.5 wt% formic acid is obtained if steam addition is restricted and a larger excess of methanol is employed. The ratio of distilled recycled methanol to fresh methanol ranges between 0.25 and 0.5.
- 40–44 wt% formaldehyde is produced by applying an energy-intensive distillation protocol for methanol removal, saving steam and electrical power as well as capital costs. In this case, the off-gas from the absorption column has a similar composition to that described for the BASF process.

The off-gas is combusted to generate steam, thus avoiding environmental problems caused by residual formaldehyde. Alternatively, the tail gas from the top of the absorber can be recycled to the reactor. This inert gas is introduced with additional steam in the feed, thus reducing excess methanol in the reactor feed, with the consequence of providing a more concentrated product with less expenditure on distillation. The yield of the process is 91–92 mol %.

A process variation to increase yields of the incomplete conversion of methanol process employs two-stage oxidation systems [79–82]. First, methanol is partially converted into formaldehyde using a silver catalyst at a comparably low reaction temperature of 600 °C, for instance. The reaction gases are subsequently cooled and excess air is added in order to convert remaining methanol in a second stage, employing either a metal oxide (Formox Process) or another silver bed as a catalyst.

Formox Process

In the Formox process, a metal oxide (e.g. iron, molybdenum, vanadium oxide) is used as a catalyst for the conversion of methanol to formaldehyde (Fig. 6.26). Many such processes have been patented since 1921 [83–86]. The oxide mixture usually has an Mo:Fe atomic ratio between 1.5 and 2.5, and small amounts of V_2O_5, CuO, Cr_2O_3, CoO and P_2O_5 serve as promoters [87–90].

The Formox process has been described as a two-step oxidation reaction in the gaseous state, which involves an oxidised (Cat_{ox}) and a reduced (Cat_{red}) catalyst site [91–94]:

1. $CH_3OH(g) + Cat_{ox} \rightarrow CH_2O(g) + H_2O(g) + Cat_{red}$
2. $Cat_{red} + {}^1/_2O_2(g) \rightarrow Cat_{ox} \qquad \Delta H = -159\ \text{kJ/mol}$

Formaldehyde production works fine in the temperature range of 270–400 °C. Conversion at atmospheric pressure is virtually complete as a function of residence time. However, conversion is temperature dependent, too. At a temperature >470 °C, the formaldehyde oxidation side reaction increases considerably:

3. $CH_2O + {}^1/_2O_2 \rightarrow CO + H_2O \qquad \Delta H = -215\ \text{kJ/mol}$

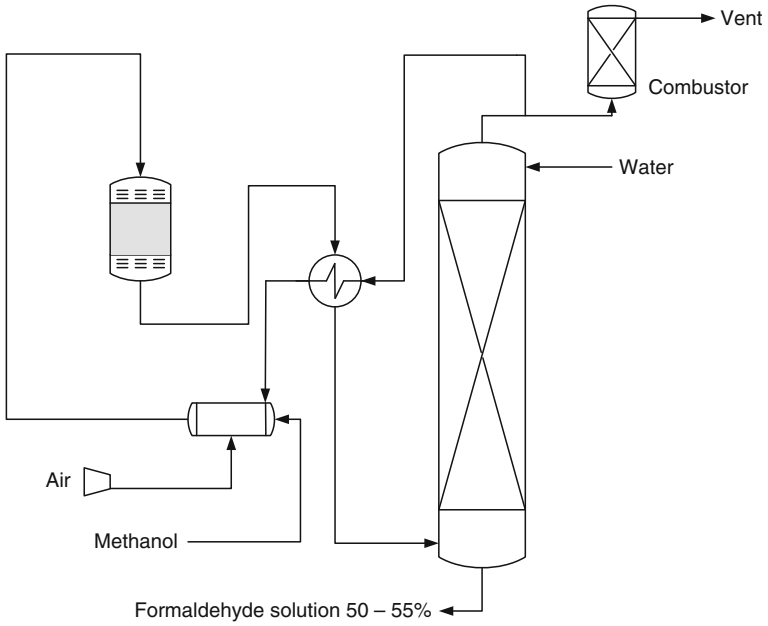

Fig. 6.26 Formox process

Methanol oxidation is inhibited by steam and very pure methanol is required to obtain high conversion. Kinetic studies on the reaction rate of formaldehyde formation indicated that the rate is independent of the formaldehyde partial pressure.

As shown in Fig. 6.26, methanol feed is passed to a steam-heated evaporator. Fresh air blown in and recycled off-gas from the absorption column are mixed and, if necessary, preheated through the product stream in a heat exchanger before being fed into the evaporator. The gaseous feed passes through catalyst-filled tubes in a heat-exchanging reactor. A typical reactor for this process has a shell with a diameter of approximately 2.5 m, which contains between 10,000 and 18,000 tubes that are 1.0–1.5 m in length. A high-boiling heat-transfer oil (or molten salt mixture) circulates outside the tubes and removes the heat of reaction generated from the catalytic reaction inside the tubes.

The process employs excess air and temperature is controlled isothermally to a value of approximately 300–340 °C. Steam is simultaneously generated in a boiler and is used to generate electric power. The air/methanol feed is a flammable mixture. To prevent it from spontaneous combustion, the oxygen content is reduced to approximately 10 mol % by mixing introduced air with tail gas from the absorption tower, whereas the methanol content in the feed can be increased without generating an explosive mixture [95, 96].

After leaving the reactor, the gases are cooled to 110–125 °C in a heat-exchange unit and are passed to the bottom of an absorber column. The formaldehyde concentration is regulated by controlling the amount of process water

added at the top of the column and the temperature in the top of column. The product is removed from the water-cooled circulation system at the bottom of the absorption column and, if necessary, is fed through an anion-exchange unit to reduce the formic acid content.

The final product contains up to 55 wt% formaldehyde and 0.5–1.5 wt% methanol, the resulting conversion of which ranges from 95 to 99 mol %. Formaldehyde yield depends on selectivity, activity and spot temperature of the catalyst, with the latter being effected by the heat transfer rate and the throughput rate. The overall plant yield is generally 90–93 mol %.

Well-known processes using the Formox method have been developed by Perstorp/Reichhold (Sweden, United States, Great Britain) [97, 98], Lummus (United States) [99, 100], Montecatini (Italy) [101], Hiag/Lurgi (Austria) [102], and DB Western (United States).

6.2.9.2 Polyoxymethylene

Polyoxymethylene (POM; also known as acetal, polyacetal and polyformaldehyde) is a semicrystalline engineering thermoplastic formed by polymerisation of formaldehyde. It mainly consists of unbranched oxymethylene units, $–[OCH_2]_n–$ [103]. Based on basic research of Hermann Staudinger in the 1920s, the first homopolymer polyoxymethylene was developed and marketed by DuPont in 1959. In 1962, the first copolymer polyoxymethylene was introduced onto the market by Celanese, who raised their market share to >75 % of all produced polyoxymethylenes today. POM shows a high mechanical resistance and stability against common solvents, for which reason it is a favoured engineering plastic to form metal-free technical precision parts [105–111].

POM is characterised by low water uptake, high stiffness and a high elastic recovery. The long-term heat resistance temperature is 110 °C for glass fibre–reinforced POM. These excellent properties are the outcome of the high crystallinity of POM, which is approximately 75 % for homopolymers and 65 % for a copolymer with 3 % co-monomers. The notched impact is low. Disadvantageous characteristics of POM are its flammability and inconsistency against acids. The main differences between homopolymeric and copolymeric POM lies in lower stiffness and toughness of the homopolymer compared to the copolymer. On the other hand, the copolymer exhibits higher thermal and chemical stability (Table 6.4).

POM is mainly used without further modifications. For special applications, several modified variants of POM have been developed and are still under development. Impact-modified products can be realised by blending of POM with thermoplastic polyurethane. Improved stiffness and structural strength is the result of a modification with glass fibres. Those mineral-reinforced products are destined to build low-distortion components. The high abrasion and wear resistance of POM can further be improved by additives such as polytetrafluoroethylene, MoS_2, silicon oil, or graphite. Main application branches for POM products are the

Table 6.4 Properties of polyoxymethylene homopolymer and copolymers. [104]

	Homopolymer Delrin 500 (Du Pont)	Copolymer ultraform N2320 (BASF/ Degussa)	Copolymer celcon M90 (Celanese-Ticona)
Melting point (°C)	177	165	165
Glass temperature (°C)	-60	-60	
Water uptake (°C) (23 °C/50 % relative humidity)	0.2	0.3	0.2
Elastic modulus (N/mm^2)	3,200	2,800	2,760
Yield strength (N/mm^2)	72	65	66
Yield strain (%)	8	8	10
Notched impact (N/mm^2)	9	7	6
Long-term heat resistance (°C)	110[a]	110[a]	101

[a] With 25 % glass fibre

automotive and electronics industries, in which polymer resistance against fuels and high dimensional stability are of particular interest. The good sliding friction behaviour of POM often leads to applications in ball bearing or transport chain construction.

Homopolymeric Polyoxymethylene

Evaporating aqueous formaldehyde solutions lead to the formation of oligomeric polyoxymethylenediols, also known as paraformaldehydes. However, the resulting gelatinous material with polymerisation grades up to 100 does not show high thermal stability. Due to its hemiacetal end groups, these low-molecular polymers depolymerise at the chain ends in a zip-type reaction:

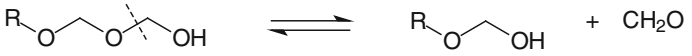

This depolymerisation reaction can be avoided by transforming the terminal hemiacetal moieties into thermally stable ones by acetylation with acetic anhydride:

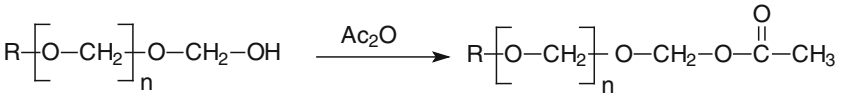

In addition to this preferred method, alternative transformations into ester, ether and urethane end groups have been developed.

There exist further decomposition mechanisms of polyoxymethylenes. Autoxidative cracking processes take place below the melting point of about 160 °C, even in those cases where end groups had been transformed. The presence of acids accelerates degradation processes. In this respect, formaldehyde released as a fission product can be oxidised by air to formic acid, thus causing an auto-catalytic decomposition process.

High-Molecular Polyoxymethylene

The synthesis of high-molecular POM can be performed by cationic or anionic polymerisation of purified formaldehyde at low temperatures (−80 °C) using boron triflouride or trimethyl amine as a catalyst. Even though the absence of water leads to high-molecular products, traces of water as well as acids and bases catalyse polymerisation, too. Without further end group modification, the resulting polyoxymethylene is thermostable until approximately 150 °C.

Polymerisation of Trioxane

The cationic polymerisation of molten trioxane, the cyclic trimer of formaldehyde, is easier to handle than the conversion of gaseous formaldehyde, which is owed to a lower polymerisation rate compared to formaldehyde. Trioxane can easily be obtained by trimerisation of formaldehyde in the presence of strong acids. The polymerisation process has thoroughly been investigated for the system trioxane/methylene chloride/boron triflouride. After a ring-opening step induced by Lewis-acidic BF_3, the resulting cationic species is starting point for further trioxane insertions:

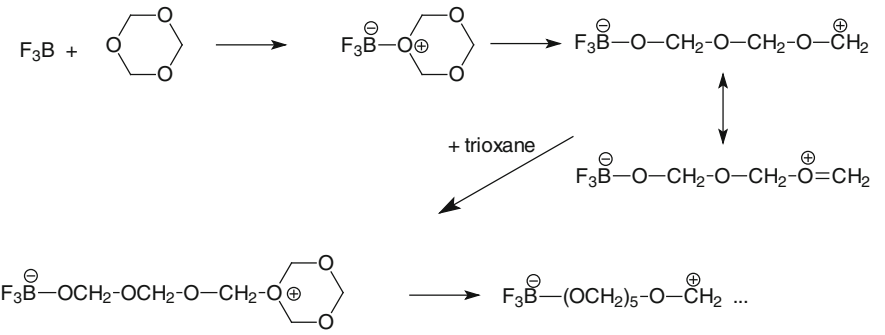

Technological Implementation of Polyoxymethylene Synthesis

Highly pure formaldehyde is the basis for high-molecular polyoxymethylene synthesis. A process for the manufacture of high-purity formaldehyde is the thermal decomposition of semiformals [112, 113]. Undesired byproducts are extracted from the reaction mixture. The resulting formaldehyde, with a residual water content <0.1 wt%, is being polymerised in suspension in the presence of an inert organic solvent [114]. Mass polymerisation cannot be handled due to the high reaction rate and generated heat. In general, two alternative methods are being used for that reason:

(a) Dry gaseous formaldehyde is added together with nitrogen at 30 °C to an inert solvent containing a starter reagent.
(b) The starter reagent is being added to a water-free solution of formaldehyde at −60 °C.

In both cases, a high-grade polymer is being realised by fast polymerisation rates under continuous stirring. Typical solvents are *n*-heptane, cyclohexane, benzene, toluene, xylene, decaline and ether, but also chlorinated hydrocarbons such as methylene chloride. Though formaldehyde starts polymerisation at −80 °C and an addition of a starter reagent is not mandatory, its presence improves the handling of the polymerisation process (Table 6.5).

The mechanical properties of the resulting polymers are a direct outcome of their molar masses. POM polymers with masses in the area of 30,000–50,000 u are well suited for injection molding applications and show improved mechanical stability. Molecular mass distribution can be controlled by selectively using additives such as water, methanol, formic acid, acetic acid anhydride, or ethyl acetate during the polymerisation process with the aim to interrupt chain propagation. As already mentioned, a transformation of thermally unstable hemi-acetal end groups into stable ones is mandatory. Commercially, this is done by acetylation [116].

The lower reactivity of trioxane, compared to its monomer formaldehyde, brings about the option for trioxane mass polymerisation under adiabatic conditions [117]. Though progressing conversion rates increase reaction mass temperature up to 130–140 °C, thereby exceeding the trioxane boiling point of 115 °C, polymerisation can be controlled well because the majority of the trioxane remains polymerised and the evaporated trioxane can be recovered adsorptively in a scrubbing column. Nevertheless, reaction and crystallisation heat removal is a major challenge in synthesising polyoxymethylene under continuous conditions.

Typically, the polymerisation process is carried out below the melting point of POM. As a result, the reaction mass changes fast from the liquid to the solid state at higher conversion rates. To deal with this problem, the reaction is performed in specially designed reactors. Hoechst and Celanese developed a polymerisation process using a kneading stirrer. Degussa developed a band-polymerisation process where the monomer and starter is filled into a PE tube [118]. The welded tube is rolled to flat band of about 2 cm thickness, which is dragged through a bath of water at 70–80 °C to initiate polymerisation and to remove generated reaction heat.

Thermally Stable Polyoxymethylene by Copolymerisation of Trioxane

Another strategy to obtain thermally stable polyoxymethylene is the copolymerisation of trioxane with small amounts of suitable co-monomers, in particular oxocyclic compounds such as 1,3-dioxane, 1,3-dioxolane, or ethylene oxide [119–121]:

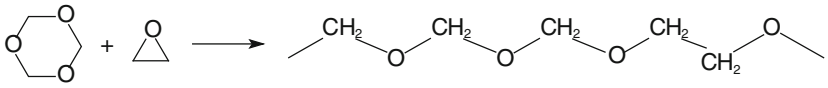

Primarily, the resulting trioxane copolymers are thermally unstable. Chain degradation starts as already mentioned at the terminal hemi-acetal moieties, but it will be interrupted by C–C bonding in the chain that origins from co-polymer integration. By optimising the minimum necessary amount of co-monomers, POMs can be obtained. They show initial thermal degradation of approximately

Table 6.5 Typical classes of starters for the polymerisation of formaldehyde to polyoxymethylene. [115]

Class of starters	Typical amount based on formaldehyde [wt%]	Typical starters	Remarks
Tertiary amines	~0.2	Tris-*n*-butylamine, octadecyl dimethylamine, diphenylamine, morpholine, or hydrazine	Building of high-molecular products
Phosphine, arsine, stibnine	~0.05	Triphenylphosphine, tributylphosphine, trinaphthylarsine, triethylstibnine	Triphenylphosphine shows a higher reactivity than triphenylamine or other amines
Metal carbonyls	~0.005	Carbonyls of Fe, Co, Ni	–
Organometallics R_nM with M = main group or transition metals and R = alkyl, aryl, alkoxyl, acyl	~0.05	Phenyllithium, sodium decanolate, methyl magnesiumiodide, calcium hydride, aluminium triisopropylate, dimethylcadmium, triphenylbismuth, diphenylmercury, diphenyltin	Diphenyltin leads to the highest molar weights

1–2 wt%, after which they are thermally stable, comparable with acetylated homopolymeric polyoxymethylenes.

A summary of the two discussed synthesis routes to get thermally stable polyoxymethylene is given in Fig. 6.27.

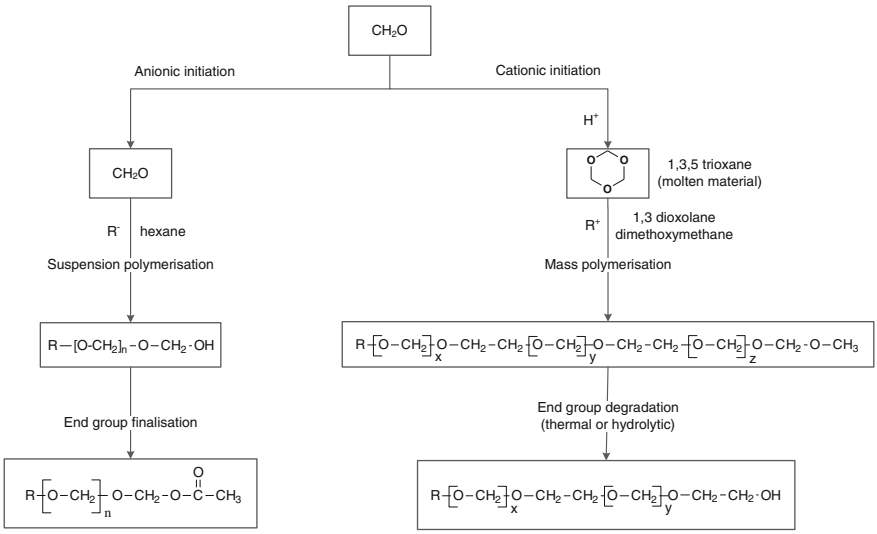

Fig. 6.27 Synthesis routes of thermally stable polyoxymethylene by postfinalisation of homopolymeric POM or copolymerisation of trioxane. (Adapted from [104])

6.2.10 Dimethyl Carbonate

Carbonic acid dimethyl ester, dimethyl carbonate (DMC), is a chemical that is being produced in rapidly increasing amounts. In 1990 global production amounted to 45,000 t/a, in 1997 it was 62,000 t/a and in 2009 overall production totalled approx. 370,000 t/a with China as the world's largest producer, but based on transesterification processes only. Enichem, who developed the methanol oxycarbonylation process (Fig. 6.29), produced 70,000 t/a in 2001 [122, 123].

About half of DMC production is used for the production of coatings and adhesives, where it is mainly used to replace solvents such as toluene, ethyl acetate, butyl acetate, acetone, or methyl ethyl ketone. Another large amount goes to pesticide and pharmaceuticals production, where it is mostly used as a methylation agent to replace dimethyl sulphate.

Phosgene, $COCl_2$, is a highly reactive and highly toxic carbonylation reagent for the synthesis of isocyanates, diisocyanates, polycarbonates and others. However, phosgene is a hazardous chemical, compared to which DMC is about 1,000

times less toxic and, in addition, considered to be environmentally benign. It is highly reactive towards nucleophiles, making it a valuable reactant for carbonylation reactions. In methylation reactions, DMC can replace dimethyl sulphate (see Sect. 6.2.15.4) and methyl halides (see Sect. 6.2.14), which themselves through their strong methylation potential are highly toxic as well [124].

6.2.10.1 Dimethyl Carbonate Production Through Phosgenation

Until the 1980s, like alkyl carbonates in general, DMC was produced by reacting methanol with phosgene. This manufacturing process was chiefly pursued by Bayer (Germany) and the Societé Nationale des Poudres et Explosifs (France). The base-catalysed two-step process involves methyl chloroformate as an intermediate:

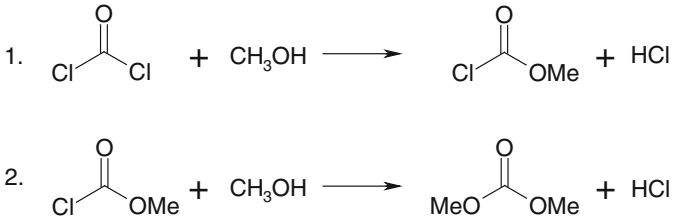

This process benefits from high yields of 82–85 %, yet it suffers from the need to neutralise large amounts of the base used (pyridine or NaOH) and to dispose of the salts [125–128].

6.2.10.2 Dimethyl Carbonate Production Through Transesterification

The vast majority of global DMC production is obtained from transesterification of ethylene or propylene carbonate with methanol. Although it is most important in industrial chemistry, transesterification processes as industrialised by Texaco, Shell and Shenghua Chemical Group (China) suffer from ethylene and propylene carbonate being expensive raw materials. The reaction is conducted in batch operations at 80 bar and 100–150 °C over a tetravalent Lewis acidic catalyst such as $ZrCl_4$, or $Ti(acac)_2$, with 98 % selectivity for methanol [129].

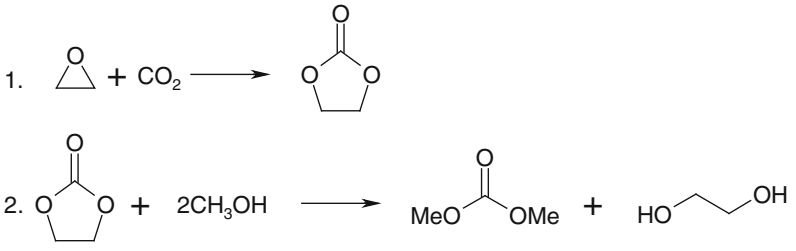

Formally, the process can be realised as a pure C_1 route if oxirane is obtained from methanol derived ethylene. However, DMC production suffers from the reaction equilibrium being in strong favour of the reactants, which leads to separation problems for the product/reactant mixture because DMC and methanol form an azeotrope.

In fact product separation and purification accounts for about 25 % of the total production costs of DMC. Additionally, the cost-effectiveness of DMC production processes via the transesterification route is ruled by the marketability of ethylene (propylene) glycol co-product, a situation that is aggravated by the market, demanding pharmaceutical-grade glycol qualities preferably. With biological routes to propylene glycol (PG) emerging, thus causing PG prices to drop and rendering co-product marketing economically less attractive, processes have been switched to ethylene glycol (EG) as a raw material.

As an alternative, ethylene carbonate can by regenerated from ethylene (propylene) glycol by conversion with urea:

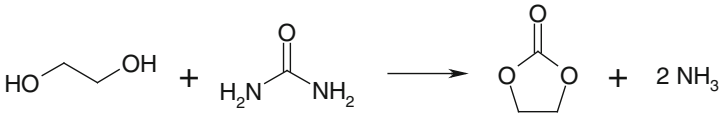

Urea can directly be used as carbonyl source for DMC production, too. The process again suffers from the equilibrium lying far on the left; however, it avoids separation problems because no azeotropic mixture is formed with DMC. The first step yielding methyl carbamate is done at approximately 100 °C over Al(*i*Bu)$_2$H as a Lewis acidic catalyst. Full conversion to DMC is achieved upon heating up to 180–190 °C over a Lewis base such as PPh_3.

There are two other commercial processes in operation: Enichem's oxycarbonylation of methanol and Ube's methyl nitrite process, for which a first plant for selective gas phase carbonylation of methanol has been put into operation. Daicel and Sekka pursued the same reaction in the liquid phase [130].

6.2.10.3 Dimethyl Carbonate from Methanol Oxycarbonylation

The oxidative carbonylation of methanol is a catalytic route to produce DMC from CH_3OH, CO and O_2. Oxygen is required in order to oxidise the carbonyl carbon from oxidation state II to oxidation state IV (carbonic acid).

In 1983, Enichem (Italy) industrialised this process, which makes use of the catalytic properties of copper, i.e. the ability to switch between Cu^I and Cu^{II} [131, 132]. The oxidative carbonylation of methanol is conducted in the liquid phase in a slurry reactor, which is continuously fed with CO, O_2 and CH_3OH (Fig. 6.28).

The reaction is strongly exothermic, thus furnishing gaseous products that can easily be removed from the slurry together with excess unreacted reactants. Like the transesterification variants, a methanol/DMC azeotrope is obtained, from which DMC is separated and CH_3OH is funnelled back into the reactor. The sole byproducts are CO_2 and water. Although CO_2 can be recycled to produce CO, water

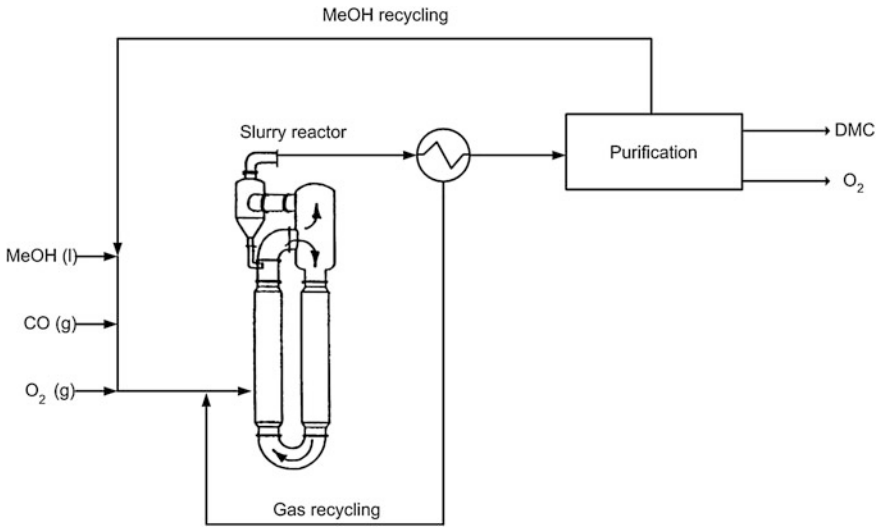

Fig. 6.28 Conceptual scheme of Enichem's dimethyl carbonate (DMC) process. (Adapted from [124])

formation is critical. The reason is competing formation of $CuCl_x(OH)_y \cdot n\ H_2O$-like phases, which are less reactive for DMC production [45]. Secondly, water allows CuCl be reduced to metallic copper in the presence of CO, causing catalyst inactivation and formation of HCl. Last but not least, the latter either reacts with methanol to give $CHCl_3$ or DME formation is catalysed. For that reason, water content was found to be optimal at 3 wt%, with the overall reaction taking place in excess methanol.

Typical reaction conditions are 20–40 bar and 120–140 °C. In any case, oxygen remains the limiting reaction in order to avoid explosive risks, which occur upon oxygen contents exceeding 4 mol % in zones where CO is the main component [45, 125, 133].

Figure 6.29 shows the current model of methanol oxycarbonylation. Although it remains contradictory in some respects, it is the generally accepted mechanism for this process.

The ENI plant was originally designed for 5,000 t/a and was expanded in 1993 to 12,000 t/a [134].

6.2.10.4 Dimethyl Carbonate from Methyl Nitrite Carbonylation

Another approach to DMC is Ube's methyl nitrite process, which is a two-step synthesis. It starts with methyl nitrite formation (I) from CH_3OH, NO and O_2 in reactor I:

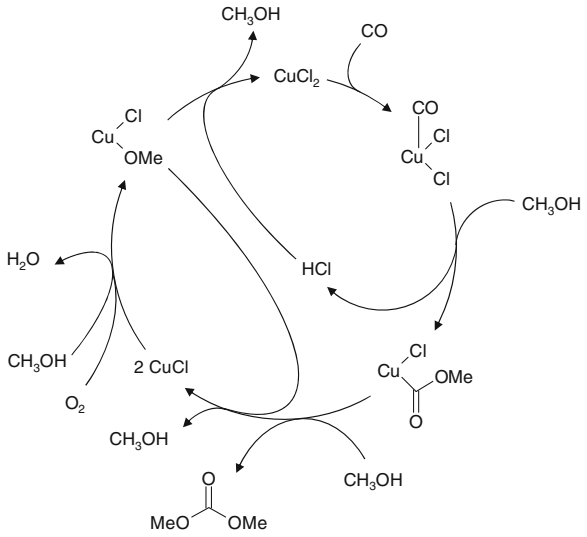

Fig. 6.29 Catalytic cycle of copper-catalysed methanol oxycarbonylation to dimethyl carbonate. (Modified from [131])

$$1.\ 2\,NO + {}^{1}/_{2}\,O_2 \longrightarrow N_2O_3$$

$$2.\ 2\,CH_3OH + N_2O_3 \longrightarrow 2\,H_3C{-}ONO + H_2O$$

$$2\,CH_3OH + 2\,NO + {}^{1}/_{2}\,O_2 \longrightarrow 2\,H_3C{-}ONO + H_2O$$

This reaction is performed in the liquid phase at 60 °C with a residence time of 0.5–2 s and does not require a catalyst. Product water must be removed in order to maintain catalyst activity in the second step.

Methyl nitrite is brought to reaction with CO in the gas phase (both reactants are approximately 5–30 vol%) in reactor II over an activated charcoal-supported $PdCl_2$ catalyst in a fixed-bed reactor with small amounts of chloride compounds diluted in an inert gas present. The catalytic reaction takes place with a contact time of approximately 0.5–5 s at 5–10 bar and 100–120 °C:

$$2H_3C{-}ONO + CO \xrightarrow{[PdCl_2]} \underset{MeO}{\overset{O}{\underset{}{}}}\!\!\overset{}{\underset{}{}}\!\!\underset{OMe}{} + 2NO$$

The outlet stream of reactor II contains DMC and unreacted reactants. As co-products, dimethyl oxalate, methyl formate and dimethoxymethane (methylal) are obtained. Over an adsorption column, CO, NO and methyl nitrite are separated from the product mixture with the purpose of reinjecting them in reactor I. This procedure avoids contact between water, DMC and methanol, thus circumventing the separation problems caused by azeotrope formation between these compounds. Figure 6.30 shows methyl nitrite formation (I) and the catalytic cycle (II) of Ube's methyl nitrite process.

Among the above mentioned byproducts dimethyl oxalate is the only significant one obtained by the Ube process. It is formed as a result of the decomposition of

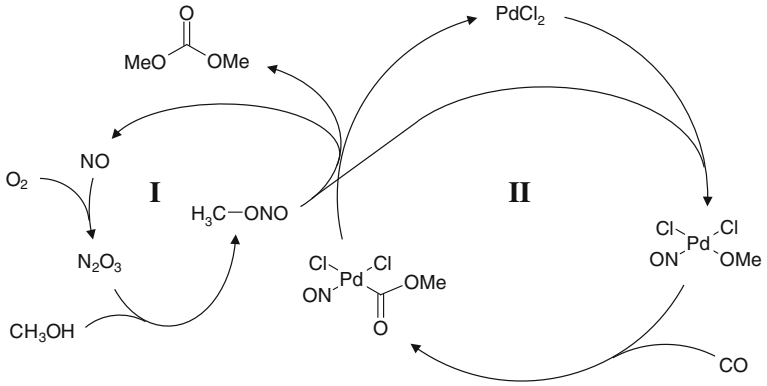

Fig. 6.30 Catalytic cycle of methyl nitrite carbonylation to DMC. With NO being regenerated, CH_3OH, CO and O_2 are the actual raw materials of the process. Oxygen is required to formally oxidise CO to C^{IV}. (Modified from [130])

the intermediate $[Pd(CO_2CH_3)(NO)Cl_2]$ complex into methyl chloroformate, NO and metallic palladium. The latter reacts with methyl chloroformate under regeneration of $PdCl_2$, thereby producing dimethyl oxalate:

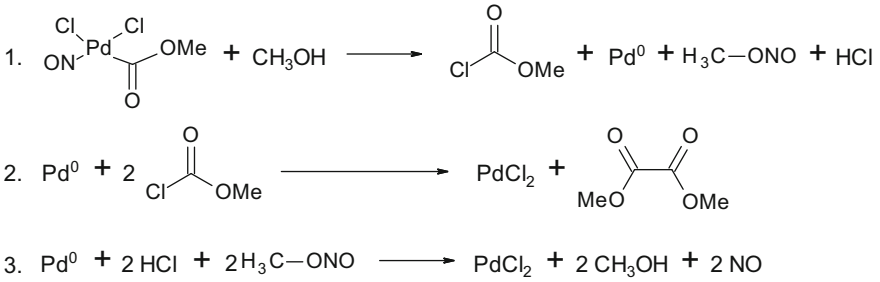

Hence, methyl nitrite plays a double role in the Ube process. It acts as a reactant for the synthesis of DMC and also as an oxidising agent for keeping palladium in the $PdCl_2$ form (i.e. regenerating the catalyst).

6.2.10.5 Dimethyl Carbonate from Methyl Formate

See Sect. 6.2.4.4.

6.2.10.6 Direct Synthesis from CO_2

Direct DMC synthesis starting from CO_2 appears compelling because it is a true C_1 route.

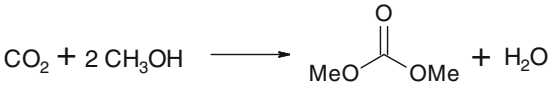

In fact, a multitude of approaches have been tested, although with no noticeable commercial significance so far. Comparable to transesterification variants, direct synthesis requires catalysts and suffers from unfavourable positions of equilibrium as well as the need for continuous product removal from azeotrope mixtures. Typical yields range between 1 and 4 % [125]. Details of the numerous approaches are beyond the scope of this chapter, though.

Like with classical catalysts, DMC is accessible by enzymatic methods. However, conversions <4 % do not surpass classical approaches and necessitate recirculation processes with continuous product removal. Enzymatic DMC synthesis is done in water using hydrolases as a biocatalyst. It is inspired by the high productivity of carbonic anhydrase, which catalyses the reaction:

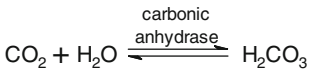

The enzymatic conversion was found to succeed with methanol instead of water as a nucleophile [135]:

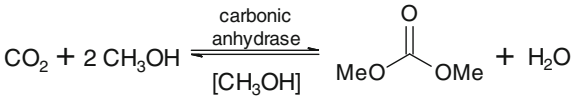

6.2.11 Hydrogen Cyanide

Hydrogen cyanide is an important synthetic building block (Fig. 6.31) for which two synthetic routes exist:

1. Dehydration of formamide.
2. Ammonoxidation of Methane
3. Ammondehydrogenation

In addition, HCN is formed as a byproduct in acrylonitrile production through ammoxidation of propylene.

Being the formal C_1-approach starting from methanol, formamide dehydration (see Sect. 6.2.4.3) is conducted under reduced pressure at 480–530 °C in iron made tube reactors filled with $FePO_4$ or $AlPO_4$ using Mg, Ca, Zn, or Mn as promoters with an HCN selectivity of 92–95 %:

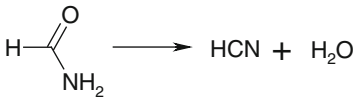

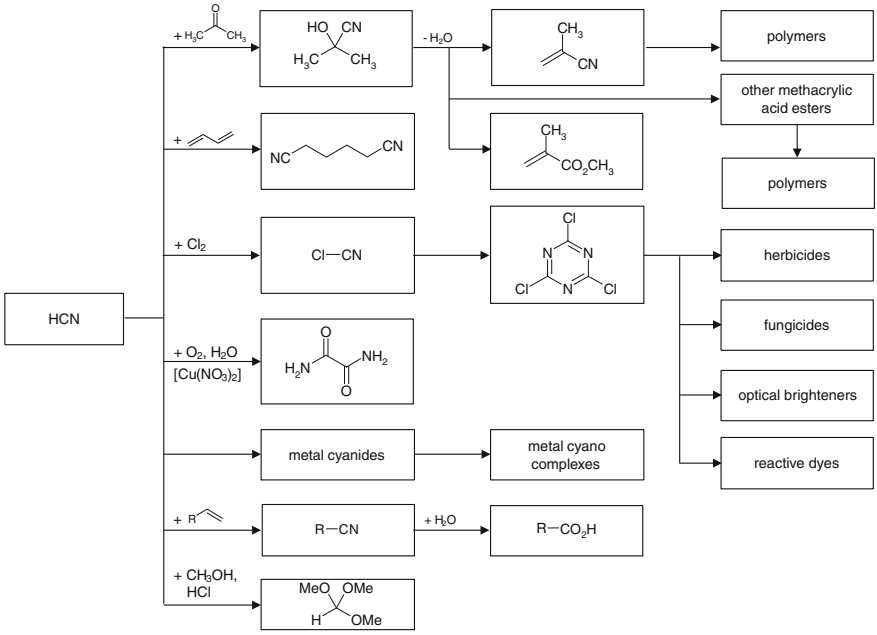

Fig. 6.31 Products derived from hydrogen cyanide

The product gas is rich in HCN (60–70 %), for which reason it is suitable for direct liquefaction. The process (developed by BASF, Degussa and Knapsack) is no longer economically significant, however. It has been replaced by oxidative or dehydrogenating conversions of hydrocarbons with ammonia, where preferably methane is used according to the Andrussow or BMA process, respectively.

6.2.12 Methyl Methacrylate

Methyl methacrylate (MMA) is starting material for the production of Polymethyl methacrylate (PMMA), which is commonly known as Plexiglas®, a highly transparent and bright polymer. In addition MMA finds application in the production of oil additives (e.g. Viscoflex®), film coatings of pharmaceutical preparations Pharma (Eudragite®) and dental products. Further, MMA is used as wettener as well as thickener for emulsion paints. MMA production has experienced steady growth over the last years. In 2007, 3.15 million tonnes were produced on a global scale. In 2009, Evonik installed another MMA plant in Shanghai, China with approximately another 100,000 tonnes of production capacity, which equals an increase of 33 % in global MMA production within only 6 years [136, 137].

There are 9 different processes industrialised for MMA production among which the direct oxidation process and the direct oxidation esterification process deserve more detailed description within the scope of this book. Till present however saponification of acetone cyanhydrine (ACH) through concentrated H_2SO_4 with subsequent acid recycling is the dominating process. Recent improvements have been achieved by introducing Evonik's Aveneer® catalyst.

6.2.12.1 Direct Oxidation Process

The isobutylene direct oxidation process has been in operation for more than 25 years now. As pointed out in Sect. 6.2.16, this process profits from methyl tert-butyl ether (MTBE) and tert-butyl alcohol (TBA) being cheap and easily transportable vehicles for isobutylene. In particular, MTBE has an economic advantage because MMA production consumes both isobutylene and methanol recovered from catalytic MTBE decomposition.

MMA production commences with either using isobutylene as a starting material (Sumitomo Chemical, Nippon Shokubai), TBA (Mitsubishi Rayon, Kururai, Mitsui Chemicals) or MTBE (Evonik). TBA and MTBE are used as starting materials because they are easily decomposed to give isobutylene and water or methanol, respectively. For TBA, the endothermic reaction is carried out at an elevated temperature over inexpensive alumina as decomposition catalyst. For MTBE, silica impregnated with metal sulphate or an aqueous heteropolyacid solution is used (Fig. 6.32).

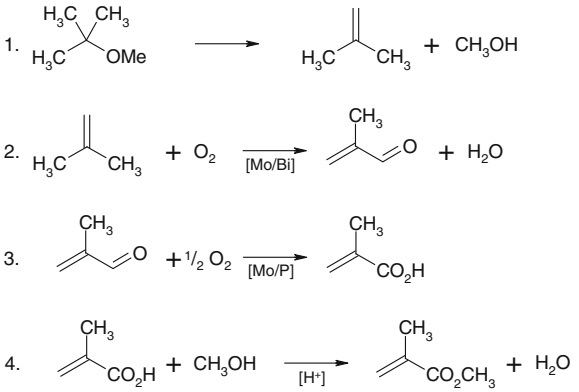

Fig. 6.32 Methylmethacrylate production according to the direct oxidation process starting from methyl tert-butyl ether

Isobutylene oxidation is divided into two steps, with the first delivering methacroleine and the second only furnishing methacrylic acid. The first oxidation step is conducted over a Mo-Bi–Fe-Co/Ni-A (A: alkali metal, alkaline earth, Tl) composite oxide catalyst in the gas phase. Although the catalyst is similar to that used for propylene oxidation, the catalyst for the latter purpose would be far too active, always bearing the risk of total oxidation. In the second step, a catalyst of

molybdophosphoric acid, $H_3PMo_{12}O_{40}$, is used. The acid catalyst must be anhydrous and present in the Keggin structure, under which conditions uniform Brønstedt acidic properties are provided due to protons sharing oxygen centres. The hydrated species is not quite as active and exerts detrimental effects on the reaction for being thermally not sufficiently stable. Another benefit of using molybdophosphoric acid results from its molybdenum centres, which promote the reaction through their ability of switching between oxidation states. Nevertheless, second-step catalyst performance is not yet satisfactory, for which reason catalyst optimisation is a major issue in MMA industry.

Esterification of methacrylic acid—the final product obtained from isobutylene oxidation—is carried out with methanol under acidic conditions. Production routes starting from MTBE benefit from using the methanol obtained from MTBE decomposition. [136, 137]

6.2.12.2 Direct Oxidation Esterification Process

As depicted in Fig. 6.33, a modification of the direct oxidation process was developed by Asahi. It shortens the process to three reaction steps by realising the second oxidation step in methanolic solution over a Pd-Pb catalyst. Under these conditions, once methacrylic acid is formed, it is instantly converted into its methyl ester.

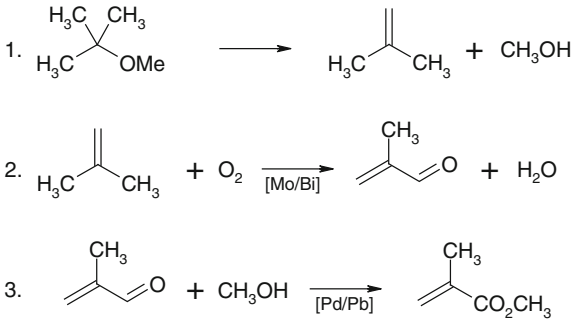

Fig. 6.33 Methylmethacrylate production according to the direct oxidation esterification process

The reaction proceeds with maximum 95 % selectivity. Although the economic attractiveness is obvious, there are still problems to be solved, such as heat flux reintegration. Nevertheless, this method has great potential for replacing the four-step route. [136]

6.2.13 Methyl Amines

All three methyl amines are important intermediates in the synthesis of solvents, insecticides, herbicides, pharmaceuticals and detergents. The demand for each

species is rather different, with dimethyl amines being the most important product as they are required for the synthesis of *N*,*N*-dimethyl formamide (DMF) (see Sect. 6.2.4.4). Monomethyl amine, which is used for the production of methyl urea, NMP and methyl taurine (used in CO_2 scrubbing or as washing agent ingredient) is also important. Trimethyl amine has less importance but is used in choline chloride synthesis (Fig. 6.34).

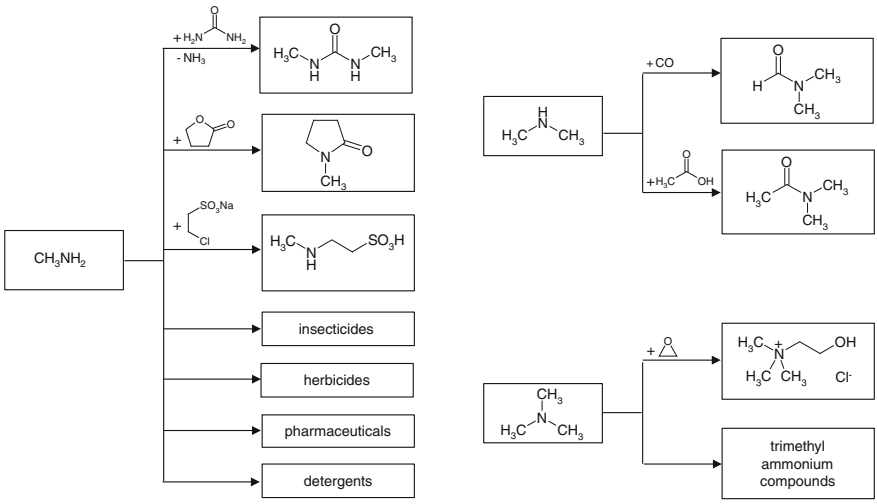

Fig. 6.34 Products derived from methyl amines

Regarding methanol consumption, methyl amines are in the fifth position among the methanol derivatives with approximately 3–5 % methanol consumption, after formaldehyde, acetic acid, methyl halogenides and MTBE. Large-scale producers are BASF, Montedison, DuPont and Air Products.

For commercial production, CH_3OH and NH_3 are converted at 15–30 bar and 350–500 °C in the presence of aluminium oxide, silicate, or phosphate:

$$CH_3OH + NH_3 \xrightarrow{[cat]} CH_3NH_2 + H_2O$$

Because pressure exerts a rather insignificant effect on the course of reaction, amine synthesis is done mostly at 20 bar. The alkylation does not stop at the stage of monomethyl amine; the reaction simultaneously furnishes all three possible amines. Excess NH_3 and addition of H_2O favour mono- and dimethyl amine formation. At 500 °C and with a NH_3/CH_3OH-ratio of 2.4:1, 54 % monomethyl amine, 26 % dimethyl amine and 20 % trimethyl amine are obtained. Byproducts are CO, CO_2, CH_4, H_2 and N_2. The overall selectivity for methyl amines is approximately 94 %. For the reason of azeotropes being formed, the reaction products are separated by a set of pressure distillations and extractive distillation.

Alternatively to aluminium salts, acidic zeolite catalysts can be used, which shift the product composition. The Nitto process furnishes ≤86 % dimethyl amine and 7 % monomethyl amine and trimethyl amine. This variant is of importance when dimethyl amine is the most desired product, such as for DMF synthesis [20].

6.2.14 Methyl Halogenide Production from Methanol

Chloromethanes are typically produced through chlorination of methane at 440 °C:

$$CH_4 + Cl_2 \longrightarrow \underset{37}{CH_3Cl} + \underset{41}{CH_2Cl_2} + \underset{19}{CHCl_3} + \underset{3}{CCl_4}$$

6.2.14.1 Chloromethane (Methyl Chloride)

Methyl chloride also can be obtained by reacting CH_3OH with HCl in the liquid phase at 100–150 °C at elevated pressure. The reaction can be accomplished without a catalyst or in the presence of a Lewis acid, such as $ZnCl_2$ or $FeCl_3$. CH_3Cl production succeeds in the gas phase as well, at 3–6 bar and 300–380 °C over $ZnCl_2$ or $CuCl_2$. Alternatively, H_3PO_4 on SiO_2 can be used:

$$CH_3OH + HCl \rightarrow CH_3Cl + H_2O$$

The conversion is highly selective (98 % for CH_3OH). Only small amounts of DME are formed as a byproduct (see Sect. 6.2.19). Today, this methanol hydrochlorination process is the preferred access to CH_3Cl. This approach has growing importance, with increasing methanol availability at reasonable prices.

Further contributions resulted from development of the Tokuyama Soda process, according to which higher chloromethanes are produced by follow-up chlorination of CH_3Cl at 100 °C. The off-product, "chlorination hydrochloric acid" finds re-use in esterification processes for methanol. In this way, methanol is the raw material base for all chloromethanes, too [20].

6.2.14.2 Methanol-Based Methyl Chloride Recovery in the Müller-Rochow Direct Process

Prior to polydimethylsiloxane (silicone) production, silicon was required to be converted into dimethyldichlorosilane according to the Müller-Rochow process by converting Si with CH_3Cl. In classic silicone synthesis, dimethyldichlorosilane is hydrolysed whereupon HCl is produced, which in turn serves to regenerate CH_3Cl from methanol:

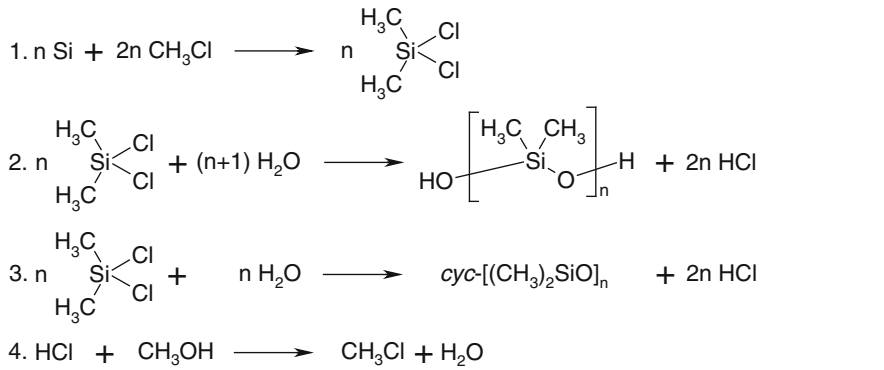

CH_3Cl regeneration is conducted both in the liquid and the gas phase.

Contemporary approaches shortcut CH_3Cl regeneration by using methanol as an OH source instead (direct process). Again chloromethane is recycled from the process, yet from methanolysis in lieu of two-step hydrolysis/HCl conversion:

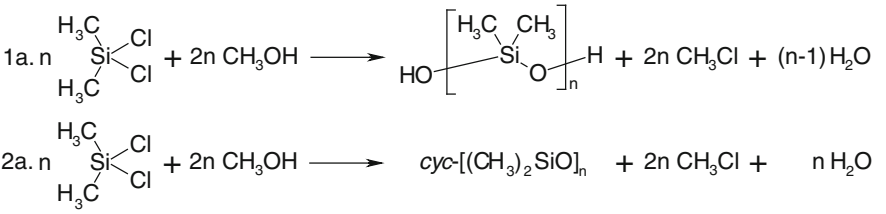

Continuous methanolysis is performed in the gas phase. Depending on the reaction conditions, cyclic or linear siloxanes are retrievable in line with the classical approach. Linear siloxanes are preferably obtained if cyclic siloxanes, which can be distilled, are funnelled back into the process. DME (see Sect. 6.2.19) is a possible byproduct [138–141].

6.2.15 Sulphur Compounds Derived from Methanol

6.2.15.1 Methanethiol

Methanethiol (methyl mercaptane) has a persistent unpleasant odour. For this reason, it is added as an odouriser to natural gas or propane in order to draw attention to leaks. Synthetically, it is chiefly used to produce methionine, an animal feedstuff additive in poultry and animal feed. Methanethiol is also used as a precursor in the manufacture of pharmaceuticals, pesticides and other agricultural chemicals (Fig. 6.35) [142–145]. Evonik produced approximately 200,000 tonnes in 2012 with about 190,000 tonnes for methionine production compared to

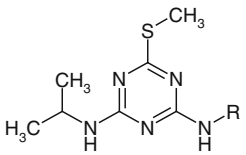

R	Commercial product
-*i*-Pr	Semeron
-$(CH_2)_3$-O-CH_3	Gesaran
-Et	Ingran

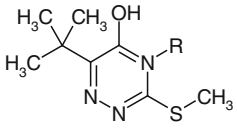

R	Commercial product
-NH_2	Sencor
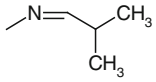	Tantizon

Fig. 6.35 Examples of herbicides derived from methanethiol. (From [149])

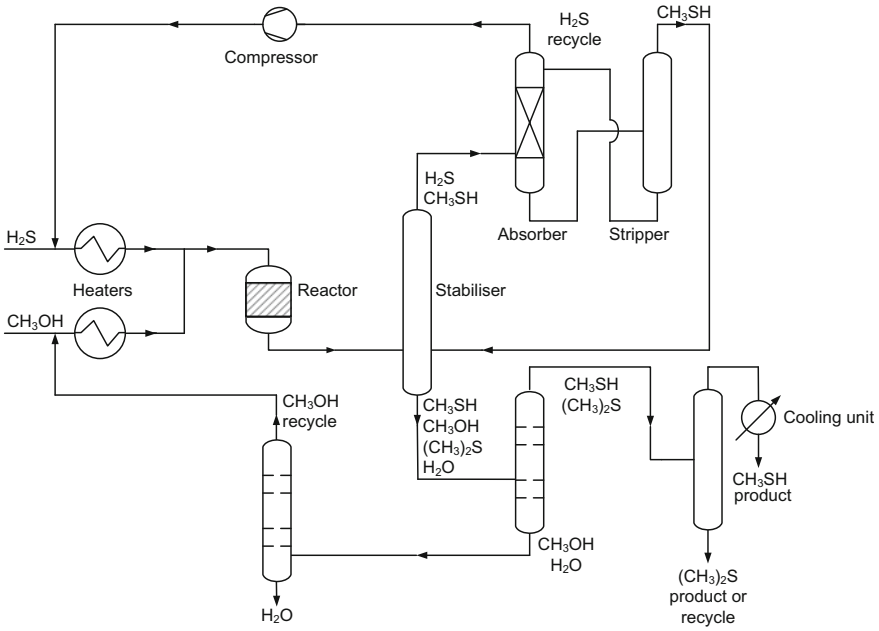

Fig. 6.36 Methyl mercaptane production process. (From [150])

~50,000 tonnes in 2003 [146]. In addition, methanethiol is released as a byproduct of wood pulping [147–149].

Methyl mercaptane is produced in a gas phase reaction from methanol and hydrogen sulphide over basic Al_2O_3 as the dehydration catalyst at ≥300 °C:

$$CH_3OH + H_2S \rightarrow CH_3SH + H_2O$$

Figure 6.36 illustrates a methyl mercaptane production process. As can be seen there, dimethyl sulphide (see Sect. 6.2.15.2) is also obtained as a byproduct, which can be understood in terms of the similar reaction conditions for the synthesis of each species.

Alternatively, methyl mercaptane can be obtained from the reaction of methyl iodide with thiourea [147].

6.2.15.2 Dimethyl Sulphide

Commercially, dimethyl sulphide (DMS) is used in petroleum refining and petrochemical production processes to control formation of coke and CO. Another use is dust control in steel rolling mills. DMS serves as a reagent in a variety of organic syntheses. In the food industry, DMS is employed as a flavouring component. Oxidation furnishes dimethyl sulphoxide (DMSO), which is an important industrial solvent.

DMS is obtained from reacting methanol in an acidic medium [150]:

$$2CH_3OH + H_2S \rightarrow (CH_3)_2S + H_2O$$

6.2.15.3 Dimethyl Sulphoxide

In technical applications, DMSO is mainly used as a solvent. Therapeutically, it has antiphlogistic and analgetic properties, for which reason it is applied percutaneously for the local treatment of pain, and it serves as percutaneous absorption promoter. DMSO itself has a low toxicity, yet concentrated DMSO is reported to be neurotoxic at levels >0.3 mL/kg. [151–153]

DMSO is commercially produced by oxidation of dimethyl sulphide with O_2 and/or N_2O:

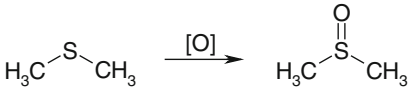

6.2.15.4 Dimethyl Sulphate

As a strong methylating agent, dimethyl sulphate is used for the production of methyl esters, ethers and quaternary amines in the synthesis of dyestuffs, pharmaceuticals, perfumes, pesticides, or phenol derivatives. It is highly toxic and carcinogenic.

Dimethyl sulphate is produced from converting DME with liquid SO_3 which is continuously funnelled under cooling into a reactor made from stainless steel or aluminium filled with dimethyl sulphate as the reaction medium:

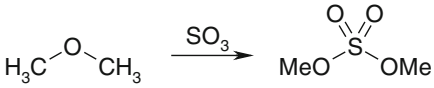

6.2.16 Methyl Tert-Butyl Ether and Tert-Butanol from Isobutylene

Isobutylene constitutes the major component of raffinate I (44–49 %) in the workup of the C_4 fraction. In steam cracker gases, it is removed from the gas mixture by acid-catalysed conversion with methanol to give MTBE. The addition of water leads to tert-butanol.

These processes make use of isobutylene being the most reactive component, meaning a tert-butyl carbenium ion is easily formed under acid catalysis. Similarly, in the backward reaction, isobutylene is released from either of these species. The benefit of these operations is the rapid and easy separation of isobutylene from gas mixtures. In addition, MTBE and tert-butanol serve as transport vehicles for isobutylene. Being liquids, there is no further effort required to compress and safely store and transport gaseous isobutylene. Using MTBE is doubly beneficial because two chemicals are available in one process: methanol and isobutylene.

6.2.16.1 Tert-Butyl Alcohol

Tert-Butanol (tert-butyl alcohol, TBA) is used as a solvent and as an intermediate in the synthesis of methyl tert-butyl ether (MTBE) and/or ethyl tert-butyl ether (ETBE), where these two latter are not obtained directly from gaseous resources. Together with H_2O_2, tert-butyl hydroperoxide is obtained. In fuel chemistry, it serves as an octane booster for gasoline, i.e. as an oxygenate gasoline additive. In final product formulations, it is found in paint removers, flavours and perfumes.

In the presence of diluted mineral acid or an acidic ion exchanger, isobutylene is converted to tert-butanol in a reversible reaction. Most companies use 50–60 % H_2SO_4. HCl is in use by Nippon Oil, and the Hüls process works with ion exchanger.

Isobutylene is extracted in a countercurrent flow from C_4-raffinate I at 10–20 °C. After dilution with water, tert-butanol is isolated by distillation. In the Nippon Oil process, which uses HCl, a mixture of tert-butanol and tert-butyl chloride is obtained, from which isobutylene and HCl are regenerated:

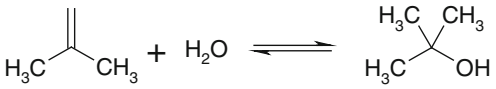

The reverse reaction, tert-butanol fission to isobutylene, is accomplished according to a process by Arco. Isobutylene regeneration is in as much favourable, as tert-butanol is obtained as a co-product; for instance from the oxirane process in propylene oxide production, it can be recovered and used as an isobutylene raw material.

The fission process is realised in the gas phase at 14 bar and 260–370 °C over a high-surface alumina catalyst. tert-Butanol conversion is $\leq$98 % with high selectivity for isobutylene. Other processes work in the liquid phase below 150 °C in the presence of heterogeneous catalysts [20].

6.2.16.2 Methyl Tert-Butyl Ether

Apart from its use as a component in fuel for gasoline engines (see Sect. 6.3.1), MTBE is used as solvent. Its use as a vehicle for isobutylene has been discussed above. For its use as a solvent, MTBE possesses one distinct advantage over most ethers: it does not form dangerous hydroperoxides for a methylene group in α-position to the ether oxygen is missing (Fig. 6.37):

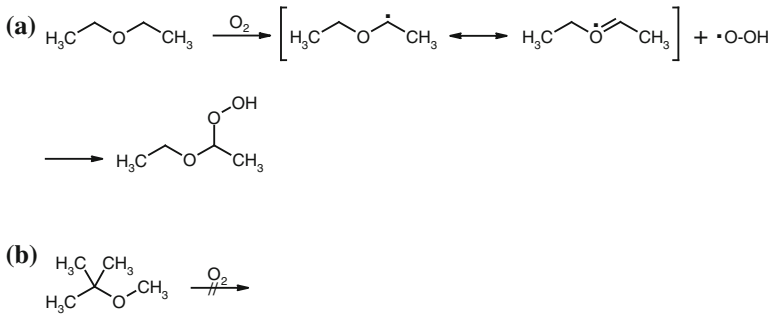

Fig. 6.37 Hydroperoxide formation in ethers. a) When a secondary carbon is present adjacent to ether oxygen, hydroperoxide formation is considerably facilitated through resonance stabilisation of the intermediary radical. Recombination of the ether radical and hydroperoxide radical furnishes ether peroxides highly liable for detonative decomposition. b) With a primary and a tertiary carbon neighbouring oxygen, hydroperoxide formation is substantially disfavoured

MTBE is raising environmental concerns because it can render large quantities of groundwater nonpotable. One source of MTBE release into water-supply aquifers are leaking underground storage tanks (UST) at gasoline stations or gasoline containing MTBE that is spilled onto the ground. The higher water solubility and persistence of MTBE cause it to travel faster and farther than many other components of gasoline when released into an aquifer. A further discussion of this issue is beyond the scope of this book. For reasons of objectification, however, it has to be emphasised that any chemical entity, including table salt, has to be kept off water-supply aquifers. It is no distinctive property of MTBE to spoil drinking water. When discussing the banning of a chemical compound, advantages and disadvantages need to be evaluated carefully in terms of a holistic view. The actual reason why MTBE has been recommended phasing out as an additive to gasoline by the US Environmental Protection Agency (EPA) were reports on probable occurrence of cancerous tumours in laboratory rats which had been injected with it [154].

Production of MTBE from isobutylene and methanol proceeds at slight overpressure and 30–100 °C in the liquid phase over acidic ion exchangers. The process is realised either in one or two reactors or in a two-stage tower-reactor in order to achieve complete isobutylene conversion (>99 %).

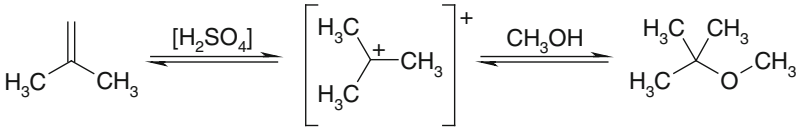

The pressure-dependent azeotrope formation between methanol and MTBE necessitates a multistage pressure distillation. Alternatively, methanol can be removed by adsorption to adsorber resins (Bayer and Erdölchemie). Contemporary approaches pursue methanol removal by means of hydrophilic pervaporation, such as over polyvinyl alcohol membranes [20].

6.2.17 Tert Amyl Methyl Ether

Tert Amyl Methyl Ether (TAME) is chiefly used as an oxygenate to gasoline (cf. Sect. 6.3.1) in order to increase octane enhancement and to raise the oxygen content in gasoline. TAME in fuel reduces exhaust emissions of volatile organic compounds (VOC).

Conversion of methanol with isopentene from C_5 fractions is accomplished similarly to MTBE production (see Sect. 6.2.16.2) over an acidic ion exchanger. The reaction profits doubly from an intermediary isoamyl cation being formed. In this way, not only is methanol addition facilitated, but carbenium ion formation also allows for unifying 2-methyl-1-butene and 2-methyl-2-butene into one common product, TAME:

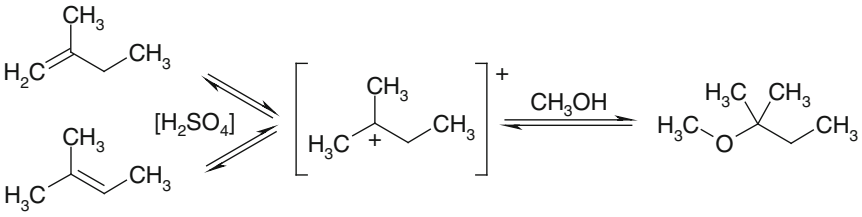

Novel developments by Erdölchemie allow for the reaction to be realised over bifunctional catalysts. The first TAME plant was established in the United Kingdom in 1987. TAME production was 1.26 million tonnes in 1999 compared to 12.25 million tonnes of MTBE [20].

6.2.18 Dimethyl Terephthalic Acid

Predominant use of dimethyl terephthalate (DMT) is polymer synthesis with polyethylene terephthalate as the most important plastic material. DMT is produced according to a series of different liquid-phase oxidation processes starting from *p*-xylene. The process developed by Chemische Werke Willen consists of

p-xylene oxidation at 6 bar and 150–170 °C in liquid medium in the presence of Co and Mn salts as a first step, which takes place in an oxidation reactor and furnishes *p*-toluic acid. The latter is reacted with methanol in a second reactor, the esterification reactor. The reaction is conducted at 20 bar and 250–260 °C and requires no further catalyst addition.

Upon distillation of the reaction mixture, *p*-toluic acid is recovered overhead and refunnelled into the oxidation reactor, where it is subjected to another oxidation step at the unreacted methyl group. This reaction takes place parallel to *p*-xylene oxidation in the same reaction medium. Likewise, the second esterification step is conducted parallel to *p*-toluic methyl ester synthesis, yet with the difference of DMT being poorly volatile and as such accumulating in the bottom product, from where it is recovered through recrystallisation from methanol. Further purification may be achieved by distillation (Fig. 6.38) [155].

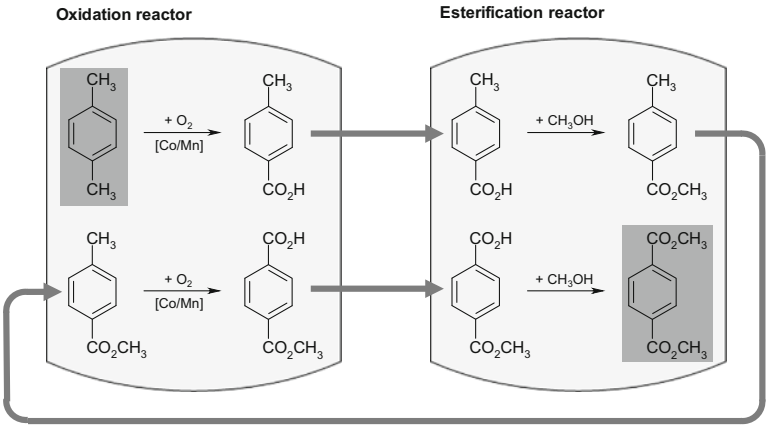

Fig. 6.38 Dimethyl terephthalate (DMT) synthesis starts with the Co/Mn-catalysed oxidation of *p*-xylene to *p*-toluic acid, which in the esterification reactor is transformed into the respective methyl ester. The latter is refunnelled into the oxidation reactor, where the second methyl group is oxidised. Terephthalic acid monoester is once again transferred into the esterification reactor, where the final esterification step to the diester DMT takes place. Thus, both the oxidation and the esterification reaction steps are passed through two times each. For reasons of process economy, *p*-xylene together with *p*-toluic acid methyl ester and *p*-toluic acid together with *p*-toluic acid monoester, respectively, are converted in one reaction step. (Modified from [155])

Figure 6.39 illustrates a DMT production unit.

Other variants accomplish *p*-xylene oxidation and methyl ester formation at 10 bar and 150 °C in the presence of Co salts in the same reaction medium.

6.2.19 Dimethyl Ether

Technical-quality DME is an alternative to liquefied petroleum gas (LPG). It has excellent combustion characteristics due to a low autoignition temperature.

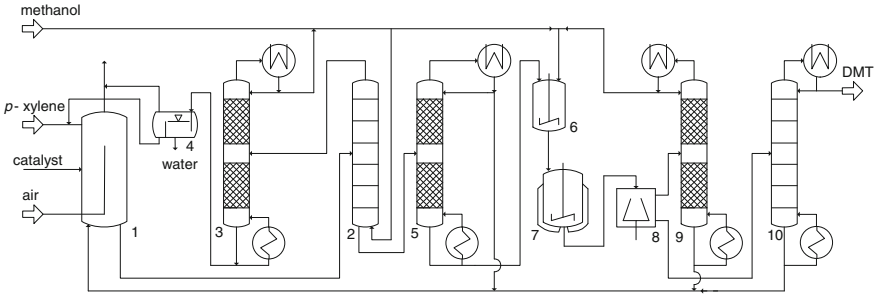

Fig. 6.39 Dimethyl terephthalate production through *p*-xylene oxidation. 1 – oxidation reactor; 2 – esterification reactor; 3 – methanol column; 4 – separation vessel; 5 – ester column; 6 – solvent container; 7 – crystallsation; 8 – centrifuge; 9 – centrifugate distillation; 10 – DMT column. (Adapted from [155])

As oxygenated fuel additive it promotes establishing a favourable fuel/air-mixture and consequently prevents soot formation and reduces NO_x production.

Ultrapure DME is commonly applied as an aerosol propellant. Another large fraction of DME production (15,000 t/a) in Western Europe is converted with SO_3 to dimethyl sulphate, $(CH_3O)_2SO_2$ (see Sect. 6.2.15.4). World total production volume was 11.3 million tonnes in 2012. DME carbonylation gives acetic acid (see Sect. 6.2.8) or acetic acid anhydride (see Sect. 6.2.1) via methyl acetate. It is also an intermediate in the synthesis of olefins, such as ethylene or propylene from methanol (methanol-to-olefins (MTO); see Sects. 6.4.2 and 6.4.3, Fig. 6.40). Refrigerant R723 is an azeotropic mixture of DME and NH_3 [156].

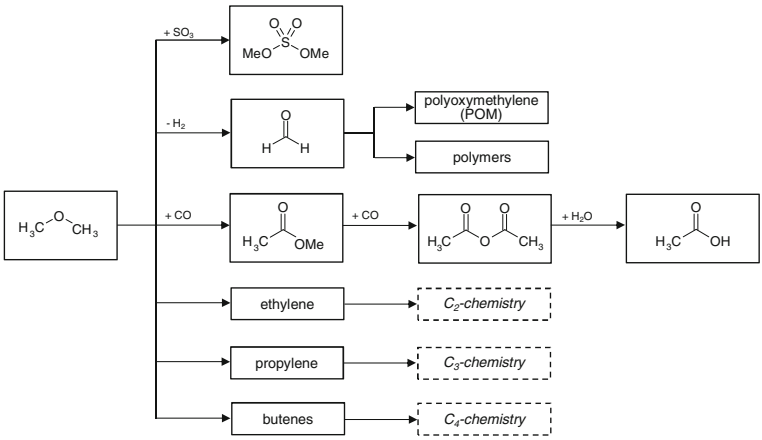

Fig. 6.40 Dimethyl ether use in synthetic chemistry

With a cetane number of 55–60, DME can be used as a substitute for diesel fuel in a diesel engine. Only slight modifications to the engine are needed. DME in

diesel engines burns clean without soot (see Sect. 6.3.1). According to the biofuels directive 2003-30-EC, DME counts as biofuel if it is "produced from biomass and intended for use as a biofuel". In the long term, DME is intended to replace LPG [157]. As a raw material for the production of synthesis gas, black liquor from the paper and pulp industry is envisaged [158].

DME was obtained as a byproduct in the high-pressure synthesis of methanol until about 1975. In this process, 3–5 wt% were contained in the product mixture, from which it was obtained by distillation. The low-pressure methanol processes developed by and ICI mostly avoided DME byproduct formation and replaced almost all high-pressure plants by 1980 (see Sect. 4.4). For that reason, catalytic processes for the synthesis of DME had to be developed.

DME synthesis is a two-stage process. In the first step, methanol production is catalysed over $CuO/ZnO/Al_2O_3$ at 50–100 bar and 270 °C. In a second step, CH_3OH is dehydrated in the presence of a Brønstedt or Lewis acidic catalyst, such as Al_2O_3, ZSM-5 or else (see Sect. 6.4) [58, 159, 160]:

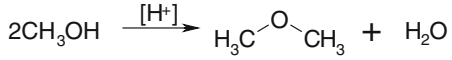

As raw-material base for DME the synthesis of which intermediarily typically involves synthesis gas, in particular coal and natural gas are used. Also biogas and biomass are of interest. DME is directly accessible from synthesis gas, too [161]. Figure 6.41 illustrates Lurgi's MegaDME® production process.

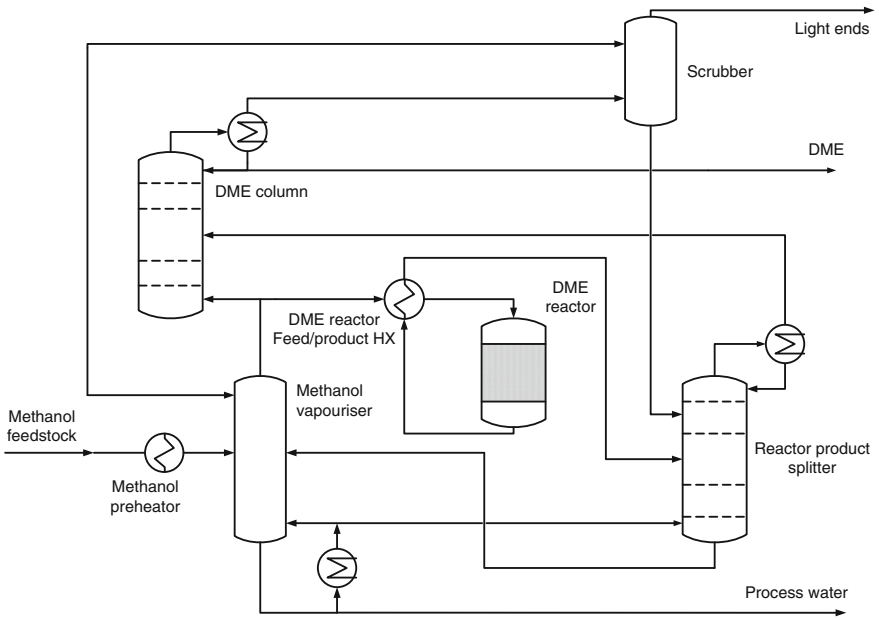

Fig. 6.41 Lurgi's MegaDME process. (Adapted from [159])

6.2.20 Sodium Methylate

Sodium methylate (also sodium methanolate or sodium methoxide) is a colourless, combustible and caustic solid. It self-ignites at 70 °C when exposed to air. There is no defined melting point and decomposition of the substance begins at 280 °C. It is used either in powder form or as methanolic solution. Like all alcoholates of highly electropositive metals, it is a very basic compound of ionic nature. The hygroscopic solid reacts heavily with water to give sodium hydroxide and methanol. Contact of both powder and methanolic solution with air must be avoided as carbon dioxide is absorbed and soda, Na_2CO_3, is formed through CO_2 uptake. Sodium methanolate is soluble in alcohols such as methanol and ethanol but insoluble in hydrocarbons [162]. The maximum solubility in methanol is 32 % at 20 °C.

$NaOCH_3$ is a standard reagent in organic chemistry. It is widely used in a series of pharmaceutical and agrochemical processes, e.g. vitamin A synthesis. It serves as a strong base (the pKa of methanol is 15.5) in various alkylation/elimination reactions, such as dehydrohalogenations, or condensation reactions, like the Aldol, Claisen and Knoevenagel types. Due to the high nucleophilicity of the methanolate ion, it is also used in substitution reactions like Williamson ether synthesis or nucleophilic aromatic substitution. Moreover, the methyl esters of inorganic acids like boronic, silicic, sulphuric and phosphoric acid are produced from sodium methanolate and the corresponding chlorides [163, 164].

Based on the total volume, one of the biggest sales markets for sodium methanolate is the biodiesel industry. Biodiesel consists of fatty acid methyl esters (FAME). In 2010, approximately 17 million tonnes of biodiesel [165] have been produced from vegetable oils, in which sodium methanolate is involved as a catalyst in the majority of the processes. The main feedstock for biodiesel production is rapeseed, soybean and palm oil as well as animal fats. The catalyst is used for triglyceride transesterification with methanol to give the corresponding fatty acid methyl esters (FAME) (Fig. 6.42).

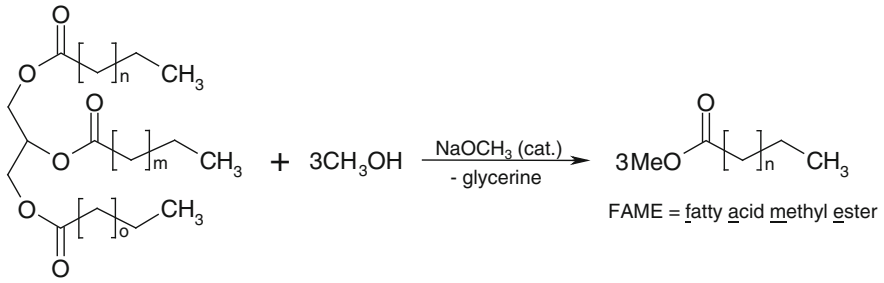

Fig. 6.42 Transesterification of vegetable oils or animal fats to give biodiesel (fatty acid methyl ester, FAME) using NaOMe as catalyst

Depending on the process, 0.5–0.6 % of the catalyst related to the amount of oil is used. Compared to the corresponding hydroxide catalysts, which in principle can

also be used for transesterification, $NaOCH_3$ and its potassium analogue do not show undesired saponification as a side reaction. With the reaction completed, the catalyst is hydrolysed to give sodium hydroxide and methanol.

Another industrial application of sodium methylate is its use as an initiator for anionic polymerisation reactions. Nucleophilic attack of methanolate at formaldehyde produces POM, for instance (see Sect. 6.2.9.2), and its reaction with ethylene oxide produces polyethylene glycol, also known as polyethylene oxide:

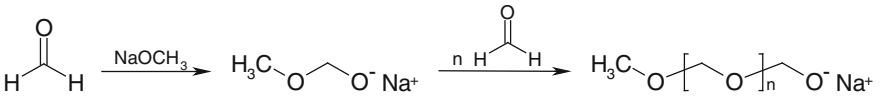

Sodium methylate is industrially produced via three different routes:

1. Reaction of methanol with sodium metal:

$$2Na + 2CH_3OH \rightarrow 2NaOCH_3 + H_2$$

The reaction is very exothermic. Molten sodium is slowly added at a metred rate to an excess of methanol in a stirred vessel or the molten sodium, as well as methanol, is added to a solution of $NaOCH_3$ in methanol. Temperature is maintained at 80–86 °C. The reaction can be carried out batchwise or in a continuous process [166, 167].

2. Reaction of methanol with sodium amalgam:

$$2NaHg_x + 2CH_3OH \rightarrow 2NaOCH_3 + H_2 + 2x\ Hg$$

Figure 6.43 illustrates the amalgam process, which is initiated by the production of sodium amalgam, $NaHg_x$, at the cathode of a sodium chloride electrolysis (a). The amalgam is then transferred into a separate reactor, the decomposer (b), where it reacts with methanol over a catalyst like activated carbon or iron catalysts to give $NaOCH_3$ solution and hydrogen [168–170]. Alternatively, lumpy anthracite covered with nickel and molybdenum oxide is used as a catalyst [171]. The alcoholate solution is purified and concentrated to give the methanolic solution or (after complete drying) $NaOCH_3$ powder. The sodium-depleted mercury, $NaHg_y$, is fully converted with water in a second decomposer (c) and then recycled into the electrolysis process.

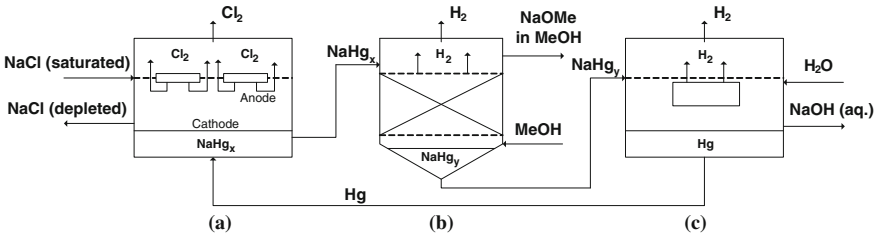

Fig. 6.43 Sodium methylate amalgam process: a) electrolyser, b) decomposer I, c) decomposer II. (Courtesy of Evonik Industries AG)

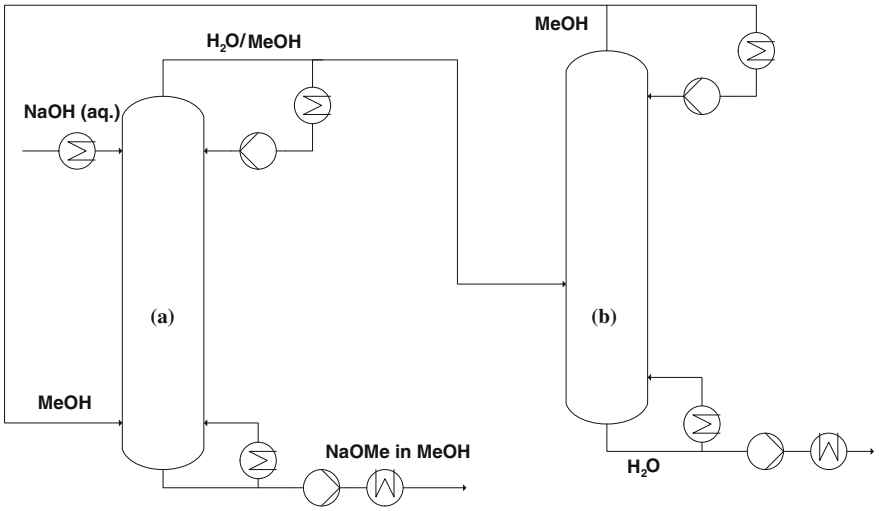

Fig. 6.44 Evonik's sodium methylate reactive distillation process: a) reaction column, b) H_2O/CH_3OH separation column. (Adapted from [172])

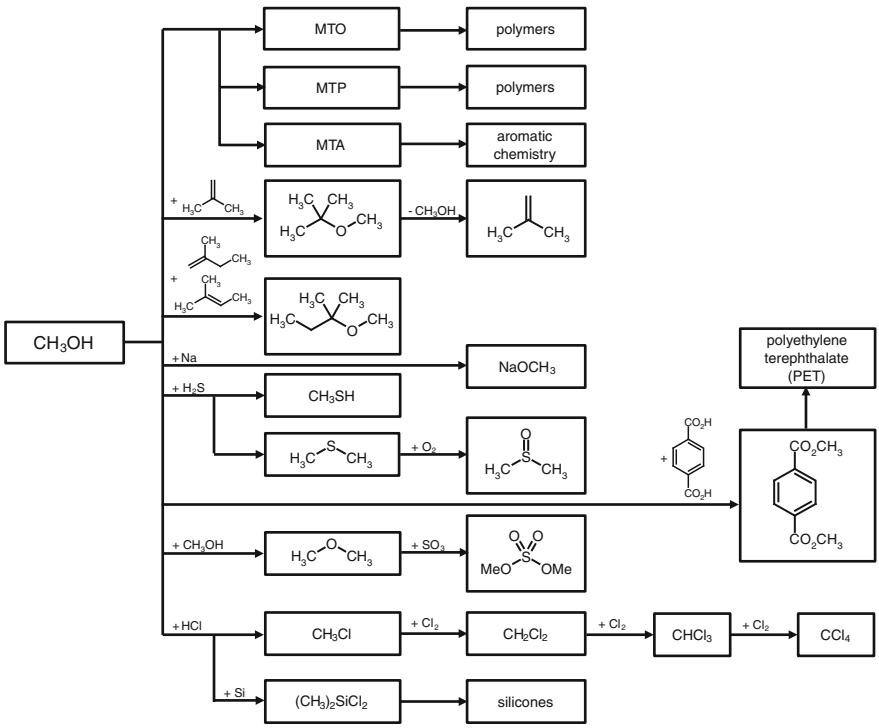

Fig. 6.45 Methanol-derived products

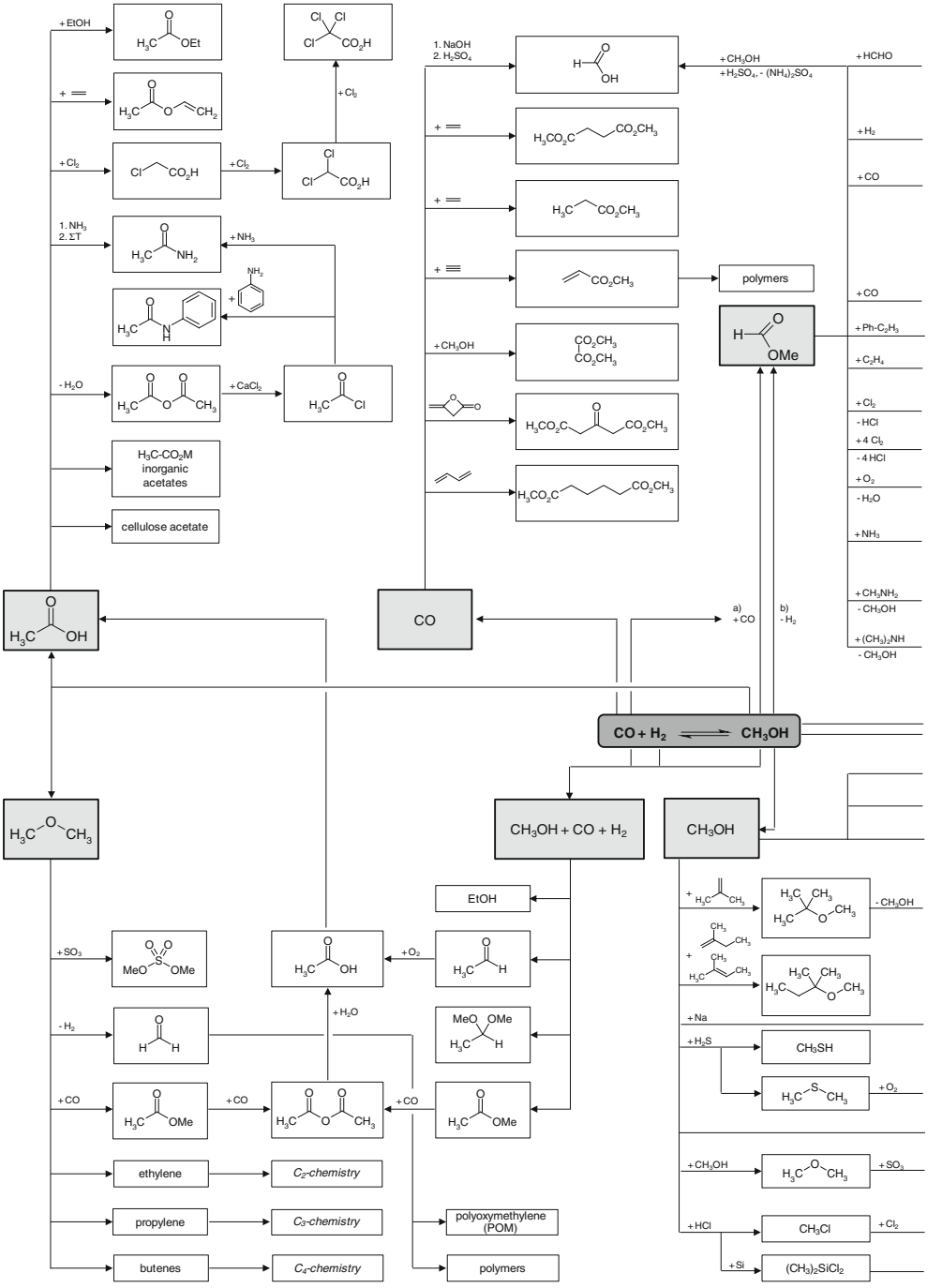

Fig. 6.46 General overview of methanol chemistry

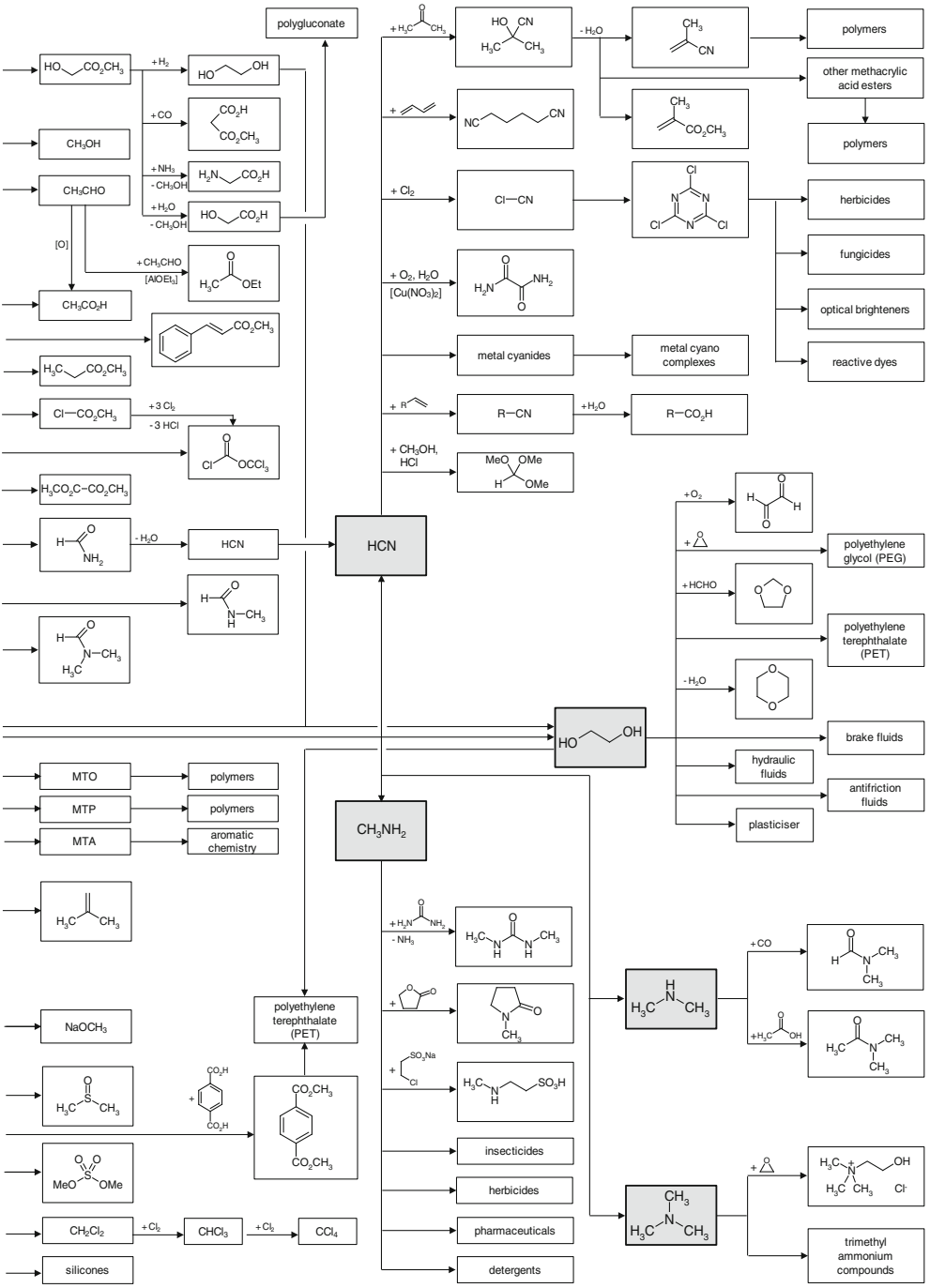

Fig. 6.46 continued

3. Reactive distillation of methanol with aqueous sodium hydroxide:

$$NaOH + CH_3OH \rightleftarrows NaOCH_3 + H_2O$$

In a continuous process, sodium hydroxide solution is fed in the top and methanol is fed in the bottom of the countercurrent reaction column (Fig. 6.44a). The reaction equilibrium is shifted to the product by removing water with the distillate using an excess of methanol. The water/methanol distillate is then transferred to a second column (b), where the organic solvent is separated from the water and recycled to the reaction column. $NaOCH_3$ in methanol is continuously taken as product stream from the sump. Afterwards, it is either directly filled as methanolic solution or separated from the solvent and dried to give sodium methanolate powder.

6.2.21 Miscellaneous

The different products resulting from methanol (the synthetic routes to which have been discussed in Sects. 6.2.14–6.2.20) are graphically summarised in Fig. 6.45.

A general overview of all products derivable from methanol is given in Fig. 6.46. As can be seen there, a large number of established petrochemicals are accessible via methanol. It is also obvious that from C_1-chemistry there is a link to C_2-chemistry, as well as to C_3- and C_4-chemistry. Via the established protocols of MTO, MTP and MTA (see Sects. 6.4–6.4.3) higher C-numbers as well as aromatics can be obtained from this alternative chemical feedstock. Whether or not substitution of classical petrochemical routes by methanol chemistry is economically viable is beyond the scope of this chapter. Additional information on this issue is given in Chap. 7.

It has to be emphasised that a large quantity of chemical entities are already produced starting from methanol as feedstock. Likewise, synthetic protocols that appear to be secondary choices now may become more economically attractive as a result of straightforward research and development efforts. However, no one expects the chemical industry to switch immediately to C_1-chemistry simply for the reason of its existence as a powerful alternative. The raw material markets will decide on the feedstock. Be it oil or methanol, the road ahead is clear.

6.3 Methanol as Fuel

6.3.1 Methanol Fuel in Combustion Engines

Ulrich-Dieter Standt and Frank Seyfried

Volkswagen Group Research, Volkswagen AG, Berliner Ring 2, 38436 Wolfsburg, Germany

Since the early 1970s, many studies have attempted to find alternative fuels that are not derived from fossil sources. Because of their relatively simple production

pathways, alcohols such as methanol and ethanol have been considered as substitutes for conventional fuels. Because alcohols are quite miscible with gasoline, gasoline-alcohol-fuel blends were the focus of early investigations. Later, an increasing shortage of diesel fuel induced considerable efforts to establish diesel-alcohol-fuel blends [173] (Fig. 6.47).

Fig. 6.47 Methanol structure

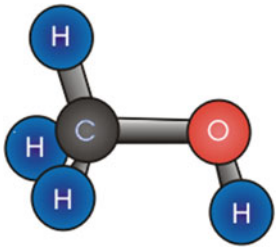

Development Results in the Literature

Basic work on methanol-fueled engines has been performed by Menrad et al. [174], who pointed out the advantages of a passenger car powered by a spark-ignition engine with a carburetor:

- Lower energy consumption.
- Better thermodynamic efficiency at an increased compression ratio.

Because the engine in this study was equipped with an outdated fuel preparation system, their engine modifications for methanol are not as applicable for today's engines, which are designed with respect to emission regulations.

A project group of the former German Federal Department for Research and Technology (BMFT; now the Federal Department for Education and Research) has stated the conditions for methanol fuel introduction:

- Up to 3 vol% methanol content: no materials have to be changed.
- More than 3 vol% methanol content: the materials that have contact with the fuel have to be altered; phase separation has to be avoided; drive and cold-start ability and engine knock have to be regarded.
- More than 89 vol%: a hydrocarbon component such as isopentane has to be added to improve starting and warm-up ability; the compression ratio can be adjusted to higher values in order to improve the level of thermodynamic efficiency [175].

Low blending rates of methanol (up to 2.5 vol%) have shown no adverse effects, such as material wear. The acceptable limit of methanol content in gasoline, however, could not be exactly stated. A 15 vol% methanol blend (M15) has been shown to cause material problems in unmodified cars [176].

Volkswagen (VW) performed a fleet test with methanol- and ethanol–diesel fuel mixtures in diesel passenger cars of the German Post Company. For this, the

standard VW 1.6 L (40 kW) diesel-engine with a swirl chamber and a compression ratio of 23 was used in the VW Golf. The methanol fuel consisted of 15 vol% methanol, 15 vol% solubiliser, 1 vol% cetane improver and 69 vol% diesel fuel. This mixture exhibited a density of 0.820 g/mL (lower limit of the DIN/EN 590 standard: 0.815) and a kinematic viscosity of 3.5 mm^2/s. The cetane number of the mixture was 37 without the cetane improver and 45 with the cetane improver. The fuel did not unmix at prolonged storage tests.

The following engine parts had to be modified for the methanol-fuel mixture: the distributor fuel injection pump, the injector mounting, the fuel filter, the glow plugs and the glow plug control. The cars have been driven between 3,000 and 21,000 km. During the test period, a slight wear of the distributor fuel injection pumps was found. The injectors did not exhibit wear, however. The test cycle emissions of NO_x and particulate matter were reduced, whereas emissions of hydrocarbons and carbon monoxide were increased. With respect to nonregulated emissions, polycyclic aromatic hydrocarbons were reduced and aldehydes increased. During the summer, some hot start problems (vapour bubble formation) were reported [177, 178].

Volkswagen performed a methanol fleet test with eight Santana models in China in 1987 and 1988. The fuel was methanol with 10 vol% of a low boiling gasoline fraction or 15 vol% of ordinary gasoline, respectively [179]. The vehicles were equipped with a carburetor engine; the carburetor was a special design for methanol use from Pierburg. The displacement of the engine was 1.8 L and the rated power output was 66 kW. As the engine lube oil, special oil from Shell (LA 1060) was used. Mileage was between 34,000 and 83,000 km per car, with a total mileage of 449,000 km for the whole fleet. Emission reductions were found for hydrocarbons, carbon monoxide and NO_x; an emission increase was found for formaldehyde. In cold periods, a slightly worse acceleration was reported. The reliability of the methanol vehicles was comparable to that of the conventional gasoline type. The fleet test was supported by the German BMFT and the State Science and Technology Commission of China [180, 181].

A heavy-duty compression-ignition (CI) engine constructed for methanol was designed by Hino Motors. The resulting low exhaust-gas temperatures had to be compensated for by an electric heater for the catalyst in order to accelerate the start of its conversion [182].

Volkswagen developed a port-injection spark-ignition (PISI) methanol flex-fuel engine with a compression ratio of 10 for passenger cars. Full flexibility of the methanol content was given using an alcohol sensor, based on the dielectric constant, conductivity and temperature of the fuel. The sensor signal was processed by the engine control unit (ECU), which at that time was a Volkswagen in-house development called Digifant. The ECUI adapted the injection timing and fuel mass to the alcohol content of the fuel. The cars took part in a demonstration fleet programme in California from 1990 to 1992. All materials used in the fuel system were modified for the methanol operation, as well as for ethanol operation.

Special multigrade engine oil, altered with respect to its viscosity index improvers, was used. The regulated emissions (HC, CO and NO_x) were lower than of corresponding gasoline usage. For some of the nonlimited emissions, such as reactive hydrocarbon components as precursors for ozone, distinctly lower values were found. Only formaldehyde was found to be significantly higher than for gasoline fuel [183]. This flexible fuel sensor was originally invented by FEV Motorentechnik and was supplied and further developed for broader applications by Siemens Automotive [184–186] (Fig. 6.48).

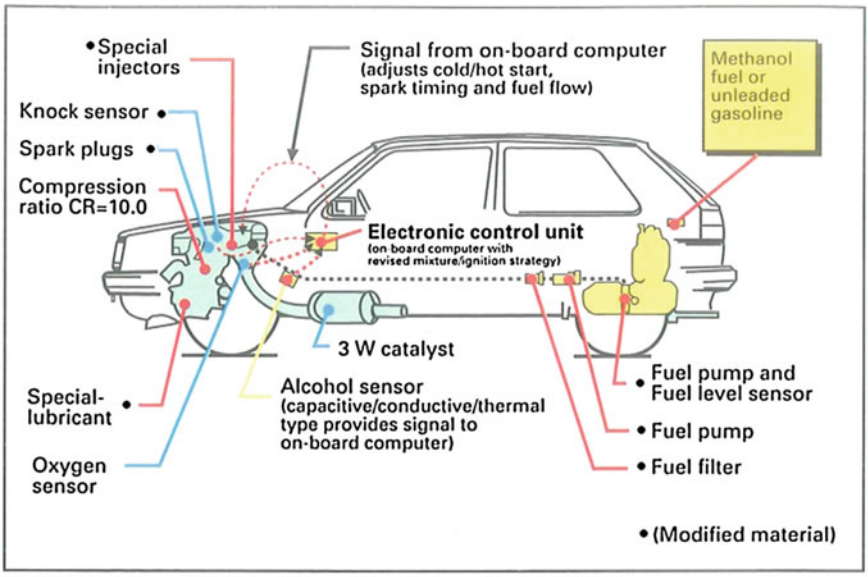

Fig. 6.48 Multifuel concept car

TNO developed a similar flexible fuel engine for methanol-gasoline mixtures in co-operation with Volvo Car Corporation and Robert Bosch GmbH. The compression ratio was altered to 12.5. The ECU was a Bosch Motronic M2.1. For the fuel sensor, an optical device (NTK TFF 8510) was used. Practical field usage up to some 80,000 km was reported. Due to the higher compression ratio, better fuel consumption for methanol was found. The baseline engine for gasoline use had a compression ratio of 9.8 [187].

At the same time, Mercedes-Benz reported that technical solutions for flexible methanol-gasoline engines should include the following:

- Use methanol-resistant electromagnetic fuel injection valves, tanks and fuel pumps.
- Apply a suitable fuel sensor for detecting the methanol content in gasoline-methanol-mixtures.

- Reduce the exhaust emissions, especially formaldehyde.
- Take into consideration driving at low temperatures, cold start and exhaust cloud formation.
- Apply a special engine lube oil without viscosity-index improvers.

As a fuel sensor, Mercedes-Benz tested an optical sensor and a capacitive sensor measuring the dielectric constant. Because the optical sensor exhibited a deviation, when coloured gasoline-methanol mixtures were used, the capacitive sensor was determined to be the better solution [188].

Hyundai reported that methanol use caused severe corrosion of engine parts such as crankshafts, camshafts and cylinder liners in their durability tests. They stated that acid formation at lower temperatures caused wear. The oil viscosity is higher when methanol is used as a fuel. Gasoline mixes with the lube oil, whereas methanol forms emulsions with it, causing a higher viscosity. Furthermore, preignition of methanol is described, which can be avoided by special spark plugs [189].

Honda reported that their methanol engines exhibited substantial wear of valve trains, cylinder liners and piston rings at low-temperature operation. The valve seats and valve guides of the fuel injector wore more rapidly with methanol due to a lack of lubricity of methanol. Deposits of polymer components from the lube oil were detected at those parts. An additional fuel additive for methanol fuels had to be added to avoid these deposits. Honda has formulated special lube oil for methanol as a fuel, which exhibited better results in the camshaft wear test. An optical sensor exhibited a cross-sensitivity to aromatics; therefore, they have decided to select a capacitor-type sensor. Methanol fuel caused increased fuel tank pressures; in order to avoid damages, fuel lines, fuel vapour lines and the fuel vapour canister had to be enlarged [190].

Toyota identified cold starting ability as a problem using pure methanol (M100), so they adopted a dual fuel system using gasoline assistance at low temperatures to enable the engine start. Further technical problems included injector clogging, fuel pump malfunction, poor driving ability at elevated temperatures, wear and corrosion of engine moving parts. In tests with M85 fuel, Toyota used an altered fuel injector with a ball-type valve to prevent injector clogging, an in-tank fuel pump with a brushless drive and special lube oil with a higher calcium ash content in order to neutralise formic acid. Because of the higher octane number of methanol-gasoline mixtures, it was possible to raise the compression ratio from 9.5 to 11.

For methanol CI engines, Toyota developed a dual fuel system to obtain stable ignition and combustion of methanol under various operating conditions. A small quantity of diesel fuel is predelivered at the nozzle tip by the fuel loader, before the injection pump supplies methanol to the injector. Methanol and diesel are injected in an unmixed state, and methanol penetrates the diesel fuel plume. The

compression ratio is 21. Increased formaldehyde formation has been reported as a problem of the CI and the PISI engines [191].

Mitsubishi established that some changes in materials have to be made due to the corrosive nature of methanol and its combustion products. Several materials in the fuel supply system and the powertrain components have to be modified or subjected to surface treatment in order to avoid excessive wear:

- The tank has to be constructed using stainless steel.
- The fuel tubes have to be plated with nickel.
- A brushless in-tank fuel pump was adopted.
- All elastomers which have contact to the fuel have been replaced by fluorocarbon elastomers (FKM).

In addition, specially formulated engine oil has to be used and an optical fuel sensor was applied. For the cold and hot starting abilities, additional measures have been taken [192]. Automotive suppliers have pointed out that methanol-gasoline mixtures are the worst case for many materials in the engine. Even ordinary FKM O-rings swelled significantly. They proposed a special-grade FKM for methanol engines [193].

Research Work

Pre-ignition and engine knock may be undesirable effects when alcohol-containing fuel blends are used. Methanol-gasoline blends have been investigated with respect to its knock properties and pre-ignition at higher loads. It has been described that pre-ignition of methanol blends often do not correspond to standard knock measures, such as RON or MON, at higher speed. Methanol has been described to be the fuel that is most susceptible to self-ignition. The admixture of isopentane or other suitable fuel additives reduce pre-ignition tendencies. Air–fuel ratios in the range of 5–10 vol% rich, compared to the stoichiometric air-to-fuel ratio, favour pre-ignition [194].

The pre-ignition properties of various alcohol-gasoline blends, including methanol, have been investigated with various gasoline engines of the MPI and DI type. It has been shown that the type of fuel mixture preparation, the evaporation behaviour, and the combustion process have shown occasionally opposite effects on their full load potential. Methanol-gasoline mixtures containing 10, 25 and 50 vol% have been evaluated as splash blends. The methanol blends showed the lowest air efficiencies of all alcohol-gasoline fuels, relative to conventional gasoline. The methanol blend M50 showed the highest increase of torque, measured at equal centres of combustion in a turbocharged direct-injection engine [195].

Pischinger et al. investigated methanol-diesel fuel mixtures with a single-cylinder test engine with a compression ratio of 23 using the Volkswagen swirl-chamber combustion system. Mixtures of 65 or 20 vol% methanol, respectively,

and 15 vol% solubiliser were used; in a second test series, a mixture of pure methanol and an ignition improver (c-hexyl nitrate, 12 vol%) was investigated. An alcohol-resistant fuel pump was used. The partial fuel substitution enables a reduction of particulate matter combined with an increase of NO_x emissions at a reasonable level of fuel consumption. The mixture of pure methanol with the ignition improver enables a higher diesel fuel substitution degree at higher loads and no particulate matter emissions but high NO_x emissions. The higher burning rate and shorter burning period with methanol fuel causes higher NO_x and lower particulate matter emissions [196].

In an early attempt to construct a DI methanol engine with compression ignition, Volkswagen developed a turbocharged and intercooled prototype engine for methanol as a fuel, demonstrating the favourable efficiency of a state-of-the-art diesel engine with very low NO_x and particulate emissions, using an oxidation catalyst for conversion of HC and aldehyde emissions. The concept engine combined a high compression ratio with a turbocharger, an electronically controlled EGR and electronically controlled glow plugs [182].

A direct-injection methanol engine has been constructed by FEV Motorentechnik (Pischinger et al.). The 1.9 L engine has been described with 66 kW power at a declared engine speed of 4,000 rpm and a maximum torque of 186 Nm (at 2,500 rpm). It had a turbocharger and a charge air cooler. The ignition of the methanol was assisted by a glow plug. The potential to minimise the relatively high NO_x emissions is given by variation of injection timings and exhaust gas recirculation. The engine does not produce particulate matter emissions. The exhaust gas has been treated by an oxidation catalyst [197, 198].

Nakamura et al. [199] pointed out that methanol causes a significantly higher formation of calcium sulphate in the engine oil. They have given evidence that it is formed by the reaction between intermediately formed calcium formate, $Ca(HCOO)_2$ (from basic calcium compounds such as $CaCO_3$), and zincdithiophosphate, which is degraded.

Wang et al. [200] investigated methanol for dual-fuel applications, based on a diesel engine with a compression ratio of 18. With respect to methanol, the engine has a port injection; the diesel fuel, however, is directly injected for pilot use. The high methanol content reduces smoke and NO_x emission. At lower loads, the heat release is bimodal; at higher loads, the heat release changes to an unimodal type, indicating a better fuel economy.

A problem encountered in methanol-gasoline mixtures is the separation of phases at higher methanol contents and at higher water contents. Phase separation can be avoided by the addition of ethanol to increase the possible methanol content. Care has to be taken to prevent swelling of the elastomers [201]. The compatibility of elastomers was the subject of a development by Freudenberg. The company reports of an elastomer that is fit for use in engines driven with alternative fuels, such as FAME, triglycerides and methanol [202].

A Chinese working group has reported that China favours methanol as the most promising alternative fuel when it is blended to gasoline. Measurements with two cars fulfilling the Euro III and Euro IV emission limits are presented. To avoid phase separation of the blends, mixtures were made just before the experiments were carried out, additionally using automatic and manual blenders. Methanol contents were set from 10 to 30 vol%. Experimental data of the conversion of the catalyst have been presented only up to 15 vol% methanol. For the higher methanol contents, which are expected to cause deviations of the air/fuel sensor, no conversion efficiency data have been reported. The Euro IV limits were fulfilled [203].

Volkswagen investigated a series of gasoline alcohol blends at an engine dynamometer using a single cylinder engine of 0.35 L displacement. The engine was constructed with respect to optimal reproducibility of the thermodynamic properties. As the reference fuel, European standard fuel for EU IV legislation was used because this fuel did not contain alcohols, below fuel labelled with M0. At the time, the European standard DIN/EN 228 limited the methanol content of gasoline to 3 vol%; therefore, a mixture of gasoline with 3 vol% methanol is used as the second fuel. The upper limit for the ethanol content is limited to 10 vol%, corresponding to a mixture of gasoline with about 7 vol% methanol containing the same oxygen content; therefore, these two blends were chosen as additional fuels. The third fuel containing 7 vol% methanol does not match the limits of the DIN/EN 228 standard (see Table 6.6).

Table 6.6 Methanol fuel blend matrix

Feature	M0	M0 + 3 vol% Methanol	M0 + 7 vol% Methanol	M0 + 10 vol% Ethanol
RON	101	101	101	101
Antiknock index	95	95	95	95
Density at 15 °C (kg/m^3)	753	755	756	757
Energy density (MJ/L)	32.21	31.54	30.97	30.89
Air/fuel ratio	14.55	14.34	14.05	13.97
Content C/H/O (% m/m)	86.9/13.1/< 0.1	84.7/14.0/1.3	82.8/13.7/3.5	82.7/13.8/3.5

The blends differ from each other mainly in their boiling properties (see Fig. 6.49). Adding methanol-to-gasoline does not affect the initial and the final boiling point, but it affects the distillation centre. The changes in volumetric fuel consumption of the methanol/ethanol blends, relative to M0, are in good accordance with their volumetric energy content.

Methanol and ethanol exhibit lower knock sensitivities than gasoline. An earlier centre of combustion, however, was not detected for the observed blends (see Fig. 6.50). The observed changes in combustion differ in the range of about 1 %, which is the limit of detection for this type of measurement. If the base fuel, which

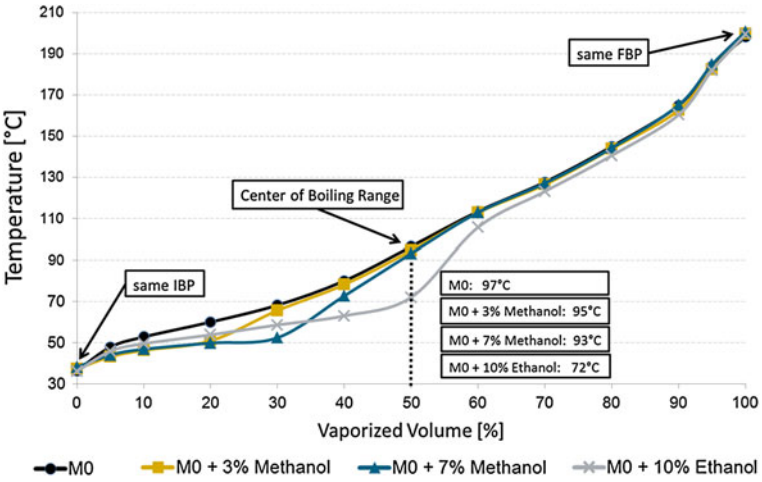

Fig. 6.49 Boiling properties of methanol/ethanol blends

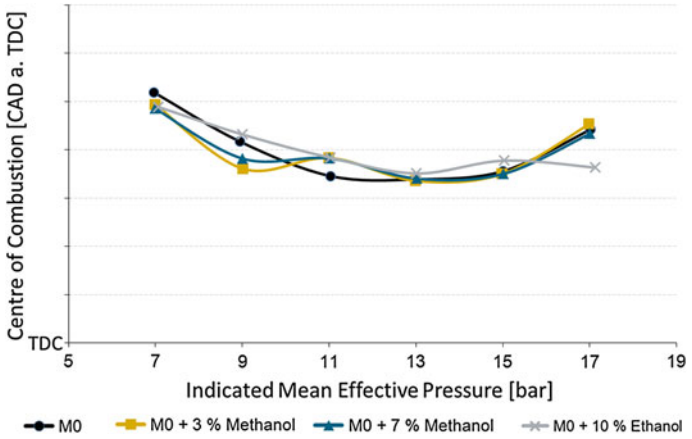

Fig. 6.50 Centre of combustion at 2,000 rpm

has been used for blending, had been of lower quality (i.e. lower RON), differences in RON and knock sensitivities should have been found between M0 and the methanol or ethanol blends, respectively.

Conclusions

The following conclusions can be made regarding the use of methanol fuel in combustion engines:

- Gasoline blends up to 3 vol% methanol fulfil the limits of the standard DIN/EN 228 and may be used without further technical changes. For higher methanol-containing blends, special care has to be taken.
- When using higher contents of methanol in gasoline, one has to prevent adverse effects such as corrosion of engine parts and swelling of elastomers, and the engine lube oil has to be adopted to methanol. Care must be taken for enabling cold starting ability; hot starting may cause vapour bubbles at certain mixture ratios with minimum boiling point.
- Phase separation has to be avoided using solubilisers.
- Methanol blends with diesel fuel are a technically more ambitious task: a solubiliser has to be used, care has to be taken to prevent oxidation and swelling of elastomers, and a special lube oil has to be used. For higher methanol contents, starting ability and cold driving ability have to be enabled using a cetane improver. Higher methanol contents can be applied using a dual fuel system.
- Further work has to be done to evaluate the degradation mechanism of viscosity improvers by methanol fuel mixtures and to the adaption of direct injection gasoline engines to methanol blends (Fig. 6.51).

Fig. 6.51 Volkswagen Golf I fleet test vehicle running an extended period with methanol

6.3.2 *Methanol-based Fuel Additives*

Stefan Buchholz[1], Gereon Busch[2] and Markus Winterberg[2]

[1]*Evonik Industries AG, Creavis Technologies and Innovation, Paul-Baumann-Straße 1, 45772 Marl, Germany*

[2]*Evonik Industries AG Luelsdorf, Feldmühlestraße 3, 53859 Niederkassel-Luelsdorf Germany*

Methyl tert-Butyl Ether

Methyl tert-butyl ether (MTBE) is produced by the reaction of methanol and isobutene on acidic ion exchange resins at mild temperatures.

$$(CH_3)_2C=CH_2 + CH_3OH \rightarrow (CH_3)_3COCH_3 \qquad \Delta_r H = 36.8\ \text{kJ/mol} \qquad (6.10)$$

MTBE is mainly used as blending component for gasoline fuels due to its high octane number. Therefore, the availability of MTBE enabled the phase-out of metal-containing anti-knock additives, such as tetraethyl lead or methylcyclopentadienyl manganese tricarbonyl; thus, it has been a prerequisite for the introduction of catalytic converters in passenger cars. Besides the application in fuels, MTBE is also used for the production of high-purity polymer-grade isobutene by catalytic cleavage into its starting materials.

MTBE is a colourless liquid with low viscosity and a characteristic terpene-like odour. Stoichiometrically, 360 kg methanol and 640 kg isobutene are required to make 1 tonne of MTBE. Table 6.7 summarises the most important physical and fuel-related properties of MTBE. MTBE has unlimited miscibility with all ordinary organic solvents and all hydrocarbons. At 20 °C, the solubility of MTBE in water is approximately 4 vol%, whereas water solubility in MTBE is 1.3 vol%. MTBE is stable under alkaline, neutral and weakly acidic conditions. In the presence of strong acids, MTBE is cleaved to methanol and isobutene.

Table 6.7 Selected properties of MTBE

Molecular weight	88.16 g/mol
Melting point	−108.6 °C
Boiling point	55.3 °C
Density (20 °C)	740.4 kg/m^3
Viscosity (20 °C)	0.36 mPa·s
Heat of vapourisation (at boiling point)	337 kJ/kg
Heat of combustion	−34.88 MJ/kg
Flash point (Abel-Pensky)	−28 °C
Ignition temperature	460 °C
Explosion limits in air	1.65–8.4 vol%
Research octane number	117
Motor octance number	101
Reid vapour pressure	550 hPa

At present, most of the isobutene used for MTBE production comes from C_4 containing streams in refineries or petrochemical production complexes. Raffinate 1 and fluid catalytic cracking units (FCC) C_4 (from refinery catalytic crackers) are the most important sources for the production of MTBE and provide isobutene for more than 50 % of world's total MTBE production [204]. Table 6.8 shows the composition of these C_4 streams.

These feedstocks can be used directly in MTBE synthesis. Other sources of isobutene are based on dedicated isobutene production processes, such as isobutane dehydrogenation, which is used to produce the feedstock for approximately 35 % of the MTBE production, and the dehydration of tert-butanol, which is a co-product of propylene oxide from the Halcon/Arco process, which is expected to decline in the future and is of minor importance already today. Production of

Table 6.8 Typical composition of raw material streams for MTBE production

Component	Raffinate 1 (wt%)	Fluid catalytic cracking (wt%)
Isobutene	44–49	10–25
Isobutane	2–3	20–35
1-Butene	24–28	10–20
2-Butene	19–21	20–35
n-Butane	6–8	5–15

MTBE is closely related to the availability of isobutene; consequently, the amounts produced depend on isobutene supply.

All MTBE processes have in common the reaction of isobutene with a certain molar excess of methanol on a macroporous acidic ion exchanger operating at 50–90 °C. In most industrial plants, isobutene conversion of 95–97 % is sufficient. Residual butenes are mainly used for the manufacture of alkylate gasoline or they are recycled to the cracker. If they are to be used for other chemical purposes, such as the production of polymer-grade 1-butene, the degree of isobutene conversion must be significantly increased. This high conversion can be obtained by using highly sulphonated acidic resins in the reaction section followed by an additional catalytic distillation column in the refining section.

Catalytic distillation (CD) or reactive distillation refers to a process, in which both catalytic reaction and distillation are carried out simultaneously in the debutaniser column. From the viewpoint of reaction engineering, this column acts as a two-phase countercurrent-flow, fixed-bed catalytic reactor. The most important advantage of using CD for MTBE synthesis lies in the elimination of equilibrium limitation of isobutene conversion as a result of continuous removal of the reaction product MTBE from the reaction mixture. The partly reacted mixture from the reaction section, which is usually in chemical equilibrium, enters the CD column below the catalyst packing zone to ensure the separation of the high-boiling component MTBE from the feed stream. The catalyst packing is installed in the upper mid-portion of the column with normal distillation sections above and below [205]. An example for this approach is the Evonik CD process, which has been developed by UOP and Hüls in 1992 and is commercialised as the Ethermax process (see Fig. 6.52).

Changes in legislation and complete or partial replacement of MTBE with ethanol or ethyl tert-butyl ether in gasoline blending in the European Union, North America and Japan have lowered the global MTBE demand. Therefore, the corresponding global production of more than 21 million tonnes in the early years of the 2000 decade declined to 14.4 million tonnes in 2009 [207]. In 2009, approximately 12 % of global methanol production were used to make MTBE [207, 208]. MTBE production in Europe amounted 1.8 million tonnes in 2009 [207]. By now, the transition away from MTBE in developed countries is nearing completion. The main underlying drivers for the future MTBE demand growth include a growing population and a higher standard of living in major emerging markets, along with the resulting increasing consumption of gasoline. In addition, demand for higher

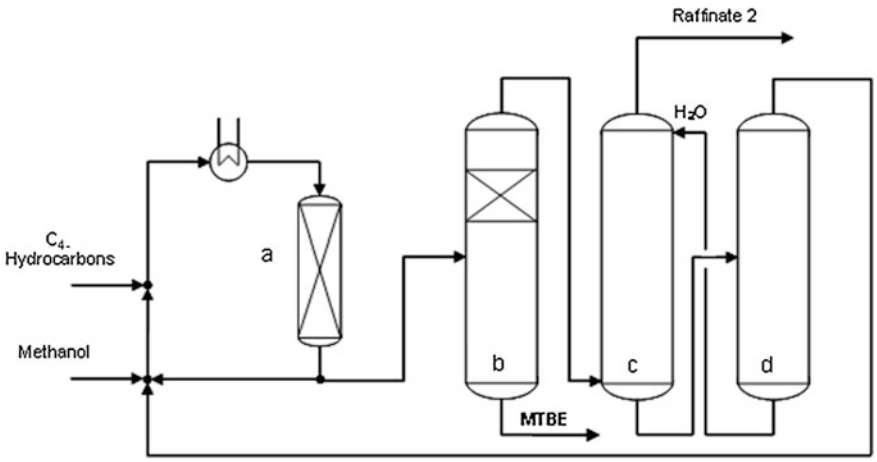

Fig. 6.52 Evonik catalytic distillation methyl tert-butyl ether (MTBE) process: a) Reactor, b) Catalytic distillation column, c) Methanol extraction, d) Methanol column [206]

octane and cleaner-burning gasoline in many developing countries is also supporting MTBE consumption.

Tertiary Amyl Methyl Ether

In addition to MTBE, tertiary amyl methyl ether (TAME) is made from methanol and an olefin—in this case, isoamylenes (C_5s). TAME can be made by etherification of the isoamylenes in a process analogous to the MTBE process. The primary feedstock comes from FCC and cokers and is thus readily available within refineries. Steam crackers are another source of C_5s. At present, most isoamylenes are blended directly into gasoline. Their etherification removes some of the highest vapour pressure olefins from gasoline [209]. The C_5s from an FCC are usually combined with the light naphtha as the bottom product from a debutaniser. The overhead stream from the debutaniser contains the isobutylene used to synthesise MTBE. The isoamylene component can be separated from the light naphtha by either adding a debutaniser or by revamping the debutaniser to act also as a debutaniser. In the former case, the isoamylenes can be converted in a separate TAME unit; in the latter case, a mixed C_4/C_5 stream can be used to manufacture a combination of MTBE and TAME.

Unlike a typical MTBE feedstream, the feed to a TAME unit must usually undergo a more complex pretreatment, involving selective hydrogenation, isomerisation, Merox treatment, or a combination of these processes. Selective hydrogenation is required for FCC C_5 in order to eliminate the diolefins, whereas the Merox treatment is used to remove sulphur-containing impurities. The TAME reaction occurs in the liquid phase and is exothermic. High temperatures, although favouring the reaction kinetics, decrease equilibrium to TAME. Compared to MTBE synthesis, the conversion of isoamylene to TAME is lower because of less

favourable reactivity and equilibrium. Similar to MTBE processes, two stages of etherification are commonly used, including catalytic distillation technology, which can boost the TAME yield to more than 90 %. TAME production is small compared to MTBE production and TAME is usually produced as a coproduct of MTBE. The estimated TAME production in Europe was approximately 170,000–250,000 tonnes in 2008 [210].

6.4 Catalysis of Methanol Conversion to Hydrocarbons

Friedrich Schmidt[1], Lydia Reichelt[2] and Carsten Pätzold[2]

[1]*Angerbachstrasse 28, 83024 Rosenheim, Germany*
[2]*Institute of Chemical Technology, Freiberg University of Mining and Technology, Leipziger Straße 29, 09599 Freiberg, Germany*

Introduction

The formation of hydrocarbons from methanol is catalysed by zeolites and was discovered by accident by the scientists at Mobil Oil in the 1970s. Many new process routes were developed after this discovery, including the methanol-to-gasoline (MTG), the methanol-to-olefins (MTO) and the methanol-to-aromatics (MTA) processes. This high product selectivity is caused by the catalyst used and by the reaction conditions.

Zeolites and Zeotype Materials

Zeolites are crystalline aluminosilicates whose special catalytic properties are determined by their structure of well-defined pore openings and channels. Due to these special structural properties, zeolites can also be used as molecular sieves. In addition to the zeolites (which are characterised by tetrahedral coordinated Si and Al atoms), molecular sieve materials include a variety of other microporous and mesoporous materials, for example carbon sieves, MCM-41, zeotypes, for example aluminophosphates (AlPO; with tetrahedral coordinated Al and P atoms) and silicon aluminium phosphates (SAPO; with tetrahedral coordinated Si, Al and P atoms), as well as metalloaluminates, silicates and metal silicates [211].

Structure and Related Properties

Zeolites and zeotype materials are distinguished by a three-letter code that is assigned to the different structure types (topologies), with a specific connectivity to characteristic topological properties. For example, the zeolite Zeolite Socony Mobil 5 (ZSM-5) belongs to the MFI structure type (having MFI topology), whereas the zeolite SSZ-13 and the zeotype SAPO-34 are members of the

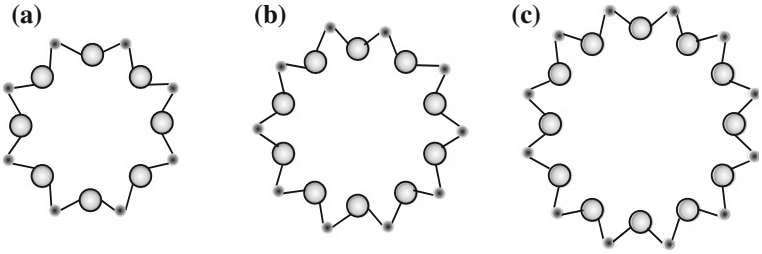

Fig. 6.53 Schematic channel profile of small pore (a), medium pore (b) and large pore (c) zeolites and zeotypes, with oxygen atoms (big) and silicon, aluminium, or equivalent atoms (small)

chabazite (CHA) structure type. Additional information about the various structures can be found in the *Atlas of Zeolite Framework Types* [212].

The zeolite framework consists of repeating structural units, the so-called secondary building units (SBUs) [213, 214], which leads to a uniform, highly ordered structure with channels and cavities of molecular dimension [215]. These channels form monolithic structures or three-dimensional intersecting networks that are permeable in one, two, or three dimensions of the crystal, depending on the type of zeolite. They are usually occupied by water molecules and exchangeable cations. The channels in the dehydrated zeolites are large enough to allow diffusion and adsorption of molecules. The dehydration can be achieved almost completely at temperatures around 400 °C and is almost completely reversible.

Regarding the channel diameters, zeolites and zeotype materials can be divided into three groups (see Fig. 6.53): those formed of eight corner-linked tetrahedra (small pores, for example SAPO-34), those with 10-membered rings (medium pores, such as ZSM-5), and those with large pores of 12 oxygen atoms. The pore diameter varies from 0.2 to 1.3 nm [211, 216, 217].

The differences in size of the pore openings as well as the channel diameters and structures result in a high shape selectivity of the diffusing molecules concerning molecular weight and structure. Additionally, the catalytically active sites are situated inside the crystal channels [218, 219]. Therefore, these structural constraints have a major influence on the formation of hydrocarbons in terms of the following: [215, 218, 220]

- *Reactant selectivity:* Only reactants that are small enough to fit into the channels can reach the catalytically active sites.
- *Transition state selectivity:* During the formation of hydrocarbons, only transition states that fit into the structure can occur.
- *Product selectivity:* Only products that are small enough to pass the channels can move to the surface of the catalyst and may leave it.

Bulkier hydrocarbons need to undergo cracking reactions before being able to leave the catalyst [221]. Therefore, focusing on the formation of hydrocarbons in the

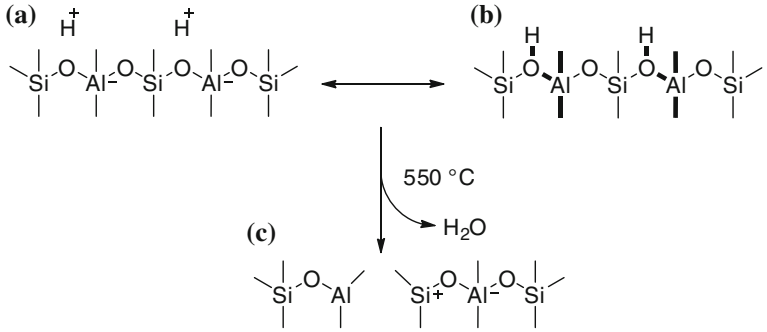

Fig. 6.54 Brønsted acidic sites (a, b) and their transformation into Lewis acidic sites (c) [220]

gasoline boiling range, only medium-pore zeolites such as ZSM-5 [215, 221, 222] and ZSM-11 [215] with channels of 10 oxygen atoms are suitable [215].

The crystal lattice is negatively charged due to the tetrahedral coordinated cations (usually aluminium and silicon atoms; see Fig. 6.54) within the specific network of corner-linked oxygen tetrahedra [215, 218, 220, 223].

In a mere silicate structure, all silicon atoms are topologically equivalent. The same applies for the pure aluminium phosphate structure, where all phosphorous atoms and all the aluminium atoms are topologically equivalent. It has been observed that there are no two adjacent aluminate tetrahedra in either natural or synthetic zeolites (Loewenstein rule), because the resulting electrostatic repulsion would destabilise the zeolite framework [224]. A small fraction of the aluminium atoms is situated on the outer surface of the zeolite or inside on nonlattice sites. The latter increases with progressing deactivation of the catalyst [218].

Tetrahedra corners that are not shared with adjacent tetrahedra may be saturated by (OH, F) groups [225, 226]. The crystal becomes neutral through exchangeable cations. Therefore, zeolites can be described by the following formula [215]:

$$M_{x/n}\left[(AlO_2)_x(SiO_2)_y\right] \cdot z\ H_2O$$

in which n stands for the charge of the cation, which is usually an alkali metal ion, an ammonium or alkylammonium ion, or, as in those materials that are important for catalysis, a proton. The proton forms a hydroxyl group with the lattice oxygen of Si-O-Al bonds of the bridged tetrahedra and builds up a strong Brønsted acidic site, like it is shown in Fig. 6.54a and b [215, 220, 227]. These sites are essential for the catalytic activity of the zeolite, whereupon the acidic site density and strength (in an aqueous system equivalent to the pK_a value) are crucial for the properties of each material. Therefore, with regard to the shape selectivity and catalytic applications, it is important whether catalytically active sites are situated on the outer surface of the crystals or inside the pores [228]. The number and thus the density of Brønsted acidic sites can be determined by proton nuclear magnetic resonance (^{1}H-NMR) spectroscopy and infrared spectroscopy. For pure H-zeolites,

it can be determined in a good approximation simply by back-titration with sodium or silver ions.

All such acidic sites exhibit a uniform acidic strength due to the high degree of crystalline order [229]. The Si/Al-ratio is generally ≥ 1 [215] and is indirectly proportional to the density of the acidic sites and directly proportional to the pH value because an ideal zeolite possesses only one cationic deficiency per aluminium atom, which in turn can form an acidic site [229–231]. A ZSM-5 catalyst with a Si/Al-ratio lower than approximately 80 is very active, but the high density of acidic sites causes a rapid further reaction of lower olefins to undesired byproducts if applied in the MTO process; a low Brønsted acidity favours the formation of olefins, especially if the conversion is not complete [231]. Even in the MTG reaction, a very high activity is not favoured because the aromatic fraction and coking increases [223]. Despite their relatively high octane number, aromatics have only limited desirability because of legal restrictions on the aromatic content in gasoline and the disproportionate increase in durene, which causes drivability problems at higher ratios.

With increasing Si/Al-ratios, the acid strength of the individual centre increases. Therefore, the Si/Al-ratio can be constrained to $5 < \mathrm{Si/Al} \leq \infty$ for the application of ZSM-5 and ZSM-11 in the MTG process [215], although aluminium atoms need to be present in order to maintain catalytic activity [221]. There is a correlation between the aluminium content of the zeolite and the catalytic activity, in the range of 10 to 10,000 ppm of aluminium [223].

An ideal zeolite does not have any Lewis acidic sites. They emerge from imperfections in the structure of the crystal, such as from coordinative unsaturated aluminium-containing species. Those structural defects occur after dealumination by steam contact or ion exchange (see Fig. 6.54c) [223, 229, 232]. Under certain circumstances, Lewis acidic sites can increase the strength of the neighbouring Brønsted centres (pK_a value), causing an indirect effect on the catalytic activity [217]. The distribution of the acidic site strength in zeolites is determined by using a temperature-programmed desorption of bases.

The acidity of the SAPOs depends on the (Al + P)/Si-ratio. With decreasing silicon content, and thus with increasing (Al + P)/Si-ratios, the acidic strength of the individual centre increases but the number of centres decreases, whereby the pH value increases. For zeolites and zeotype materials, the superposition of the two opposite effects, pK_a on the one side and pH on the other, leads to the formation of a maximum of total acidity.

Material with MFI Topology: ZSM-5

A reasonable conversion of methanol into gasoline with a commercially acceptable cycle length (controlled by the catalyst) was first discovered on ZSM-5 catalysts. ZSM-5 is a medium-pore synthetic aluminosilicate zeolite from the pentasil family of MFI structure type. It was first synthesised by Argauer and Landolt in 1972 [233]. Currently, it is the most commonly used zeolite for the commercial production of hydrocarbons from methanol.

ZSM-5 exhibits the common formula [215, 223, 229]

$$Na_zAl_zSi_{96-z}O_{192} \cdot H_2O \quad \text{with } z < 27 \text{ and typically } z \approx 3.$$

For application in methanol-to-hydrocarbon (MTHC) processes, sodium ions are substituted by protons whereby a solid acid arises, which is often called H-ZSM-5.

The crystal lattice of ZSM-5 is characterised by a channel structure (see Fig. 6.55) of straight channels running parallel to the [010] direction with an elliptical shape and appropriate free dimensions of 0.51 × 0.54 nm and sinusoidal channels running parallel to [100] direction with a nearly circular cross-section area of 0.54 × 0.56 nm [215, 221, 223]. At the crossings of the channels, an opening of 0.89 nm is formed [233, 234], which is ideal for the MTG process because there is enough space for cyclisation reactions and intermolecular hydride transfers [235] but not enough free volume for the formation or release of higher aromatics. As a result, using ZSM-5 a hydrocarbon product for MTG processes with a maximum chain length of C_{10} and mainly methyl substituted aromatics is accessible. Durene (1,2,4,5-tetramethylbenzene) is the bulkiest molecule built [215]. It is a very undesirable product, because it has a melting point of 79 °C and therefore leads to drivability problems if its content in gasoline exceeds 2–3 vol%.

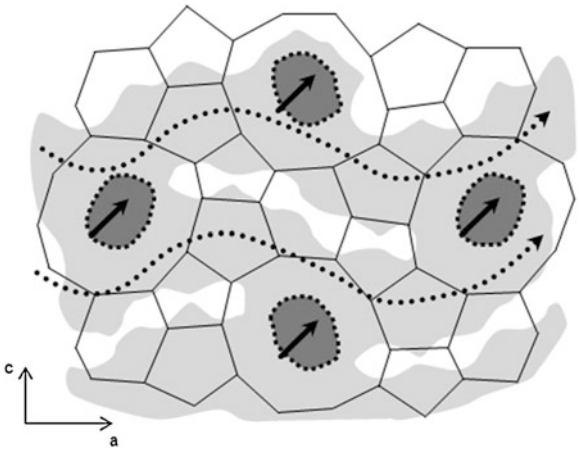

Fig. 6.55 Crystalline structure scheme of ZSM-5 with straight channels (into the plane, marked with bold arrows) and sinusoidal channels (marked with dotted arrows). Adapted from Ref. [211]

The highly branched channel network promotes the diffusion of reagents and causes a large inner surface. Additionally, the availability of two different channel types with intersections results in a higher transportation rate because reactants can use one system on their way to the catalytic active sites and the products are able to diffuse through the other channels out of the catalyst [223].

Materials with CHA Topology: SAPO-34 and SSZ-13

Materials with CHA topology are characterised by a cage structure, wherein relatively large pores are connected through small windows with a width of 0.38 nm (see Fig. 6.56) [235–239]. They possess the general formula

$$(Si_xAl_yP_z)O_z \quad \text{with } 0.01 \leq x \leq 0.98,\ 0.01 \leq y \leq 0.6,\ 0.01 \leq z \leq 0.52$$

The most commonly used zeotype material for MTHC reactions is SAPO-34, which has a channel system of cages. The cages can include a sphere of 0.737 nm [211] and are accessible through six 8-rings [211]. Because of this, the maximum diameter of a sphere that can diffuse along *a*, *b*, or *c* is 0.372 nm [211].

Because the catalytic active sites are situated inside the pores and channels, chemical reactions are limited to molecules that are small enough to enter and leave these positions. Also, large molecules cannot diffuse in or out of the crystal. This implies that large molecules, which may have been formed in the cages during the reaction, are encapsulated inside. As a consequence, SAPO-34 is in particular highly selective for the production of the desired linear olefins ethylene and propylene.

As H-SAPO-34 and H-SSZ-13 have the same topology, the only difference lies in the composition. H-SSZ-13 is a zeolite with an Si/Al-ratio of 11, corresponding to one aluminium ion per cage and its associated proton. For the comparable H-SAPO-34 with an (Al + P)/Si-ratio of 11, this proton is adjacent to a silicon ion. This leads to different acidities; thus the density of Brønsted acidic sites (in the aqueous system equivalent to the pH value) of H-SSZ-13 is the same as in SAPO-34, but the acidity value (equivalent to the pK_a value) of H-SAPO-34 is less than that of H-SSZ-13 [240].

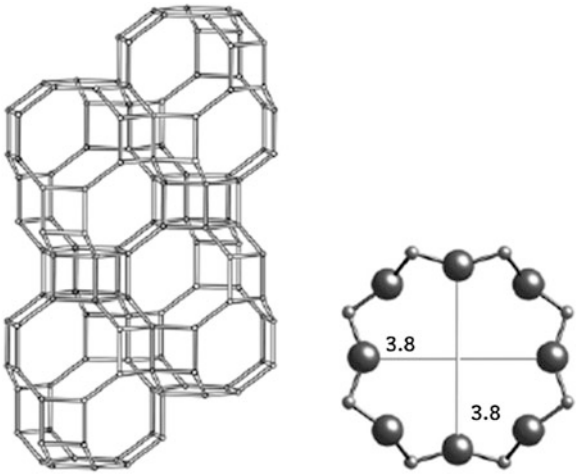

Fig. 6.56 Structure of SAPO-34 [211] and pore cross-section with central atoms (small) and oxygen atoms (big)

In a chabazite aluminosilicate, the substitution of a silicon atom with an aluminium atom results in four topologically distinct Brønsted acidic centres. Three centres belong to protons (or other cations), which are connected to oxygen ions in 8-rings and hence belong to two cages. The fourth acidic centre is adjacent to an oxygen ion in a 6-ring and thus lies only in one cage. Analogously in an aluminophosphate, a Brønsted acidic centre is created by replacing a phosphorous ion by a silicon ion.

Catalyst Synthesis

Zeolites are formed by a multilevel self-assembly process of dissolved silicate and aluminosilicate anions, in which the solvent and structure-directing agents (e.g. organic cations) interact with the silicate and aluminosilicate anions to build organic–inorganic composites. These composites assemble into ordered arrays. Subsequent condensation processes result in nucleation and finally in the growth of three-dimensional covalent crystalline networks [241].

The preparation of zeolite-based catalysts, such as ZSM-5 catalysts for MTHC reactions, includes the following steps: [242, 243]

- Contacting a silicon source with aluminium species, alkali and optionally a template in aqueous suspension to get a gel.
- Converting the gel into a crystallised aluminosilicate at elevated temperature and normal or elevated pressure.
- Separating the crystalline product from the suspension.
- Drying and calcination of the solid to remove the template.
- Substitution of the enclosed alkali ions by protons or proton-providing substances in aqueous medium.
- Drying and calcination.
- Milling the aluminosilicate to get small particles, which are mixed with a binder, such as finely divided hydrated alumina, alumina, silica or $AlPO_4$.
- Shaping the mixture and final calcination, for example at a relatively low temperature in the range of 470–650 °C for 5 h.

There are a lot of parameters that influence the production of a special catalyst, such as the sources of silicon, aluminium, and alkali. The used template has a major influence on the topology of the formed zeolite as well. Furthermore, there may be an influence of the sequence of the addition of the chemicals, the stirrer type and the stirring speed. The heating rate in the commercial synthesis and the synthesis time influence the catalyst properties as well as the synthesis temperature. During the calcination steps, the heating rate and temperature also play an important role, as does the type of furnace. Finally, during the shaping of the catalyst, the desired porosity is created, which is not only determined by the source of binder precursor but also by its physical properties, such as the grain size distribution, the alkali content, the kinetic of the solubility and the type of shaping aids.

The various parameters influence each for itself, as well as in combination with one another, the constitution of the catalyst and its catalytic properties, such as the

distribution of the aluminium ions in terms of a depletion of aluminium in the core or on the outer surface of the individual zeolite crystals [244]. Therefore, H-ZSM-5 crystals without any substantial concentration gradient can be obtained by crystallisation from inorganic gels, whereas all types of gradients can be created when organic templates are used [245].

Catalyst Modification

In addition to the targeted production of gradients of the acidic sites, the acidity of zeolites can be modified by treating the material with steam, which causes dealumination and thus an irreversible deactivation along with an increase of catalytic activity. Exposure of pure and binder-free zeolites with relatively low Si/Al-ratio to mild steaming causes the formation of aluminium pairs, with one aluminium ion of the pair being proposed as to be not tetrahedrally coordinated. This ion acts as a strong electron-pulling centre for the adjacent tetrahedral aluminium ion, creating a stronger Brønsted acidic centre [217]. This behaviour cannot be transferred straightforwardly to the technically interesting zeolites with relatively high Si/Al-ratios.

Leached aluminium atoms can also interact with bridging hydroxyl groups, which results in the formation of Lewis acidic centres [223]. These centres are also accessible by heating the material up to 550 °C, so that water gets lost (see Fig. 6.54) [220]. Moreover, dealumination processes occur during catalyst usage and regeneration. Another possibility of introducing Lewis acidity into zeolites is to contact the material with alkalines. Thus silicon atoms are removed by desilylation and free Al–OH groups are formed [232].

Dealumination methods can also be used in order to change the Si/Al-ratio in zeolites after synthesis. This is accompanied by a reduction of the number of acidic sites. Alternatively, all zeolites can be dealuminated by acid treatment, which means that aluminium ions are dissolved from the zeolite lattice and then remain inside the cavities as so-called extra-framework aluminium (EFAL) [246, 247]. On the other hand, aluminium can be incorporated into the zeolites by treatment with aluminium halides. Furthermore, to a limited extent, aluminium can be incorporated into the zeolite lattice by solid state reaction at high temperatures when aluminium oxide is used as a binder [246, 248–251].

For a ZSM-5 zeolite, specifically, the Si/Al-ratio in the product can be varied within a wide range by adjusting the Si/Al-ratio in the synthesis batch. A low-cost ZSM-5 with a low Si/Al-ratio can be prepared without expensive organic templates. Starting from such a strongly acidic material, the desired acidity can be adjusted by means of an on-purpose dealumination through steam treatment. However, for ZSM-5-based catalysts for MTHC processes, this method has drawbacks in practice. In addition to the change of acidity profile, selectivity and Si/Al-ratio, the leaching of aluminium from the lattice of ZSM-5 causes the hydrothermal stability of the zeolite to be promoted. Therefore, the on-purpose steam treatment is also used as a method to stabilise the catalyst prior to use.

The selectivity of SAPO catalysts for olefin formation can be enhanced by a reduction of acidity, higher Si/Al-ratios, or exchange of silicon atoms with

magnesium, zinc, iron, cobalt, nickel, manganese, or chromium [252–255]. For SAPO-34, a pretreatment, especially with ammonia, is discussed to increase the hydrothermal stability. As with ZSM-5, in SAPO-34 the selectivity to olefins is improved when the catalyst is exposed to a mild steam treatment. By an acidic treatment of SAPO-34, the selectivity to olefins, particularly to ethylene, is also improved.

Additionally, CHA framework components, which are grown together with an AFI type substance such as SAPO-5 or AlPO-5, possess a high selectivity for propylene production [256]. However, with nickel-containing SAPO-34, the ethylene selectivity can be raised up to 86 % at nearly complete methanol conversion and medium reaction temperatures of around 425 °C without significant deactivation [257].

Parameters for the Optimisation of Technical MTHC Catalysts

Mainly in the laboratories of Mobil Oil, Union Carbide and Exxon, favourite catalysts and reaction conditions for MTHC reactions have been developed on the basis of extensive laboratory experiments in the 1970s and 1980s. As a result of the attained insights, a model based on correlations of empirically determined parameters was evolved. The investigated factors influencing activity and selectivity of the MTHC reaction concern the most important process parameters of pressure, temperature and space velocity, as well as the main catalyst properties. The latter can be particularly easy shown by the example of ZSM-5.

The profile of the different acidic sites and the spatial distribution of acidic sites in the crystal are adjusted through the used synthesis conditions and latter modifications of the catalyst stated above. Besides the zeolite or zeotype material, the binder also plays a role. In the case of MTHC reactions, the binder is preferably made of an alumina precursor, which after calcination has acidic properties and thus also catalyses dehydration reactions, essentially the dehydration of methanol to DME (dimethyl ether). Ideally, about one-third of the total heat released in the dehydration of methanol is produced at the alumina contact (pre-reactor and binder).

The disadvantages in product composition caused by low Si/Al-ratios can be compensated within certain limits by an increased space velocity. However, the space velocity cannot be arbitrarily increased because it is important that the product distribution at the reactor outlet has closely reached equilibrium, which cannot be achieved at very high space velocities. Also, the application of small primary crystallites of less than 0.1 μm as precursor for the catalyst has an analog influence on product selectivity as the raised space velocity. However, primary crystallites of less than 0.1 μm also have distinct disadvantages. So, the gaps between the primary crystallites have a diameter of the same dimension as the pores and thus represent a certain diffusion barrier, which encourages undesirable secondary reactions. Additionally, such small crystallites are expensive to produce. A remedy can be found in either using a wide or a bimodal distribution of crystallites, in which small crystallites grow together into larger agglomerates or by adopting the so-called zeolite bound zeolite technique, where the zeolite in the binder is converted in a secondary synthesis into a microcrystalline ZSM-5.

Whereas the morphology of the entire catalyst, if it has a three-dimensional pore system, is of some importance for the selectivity, the morphology of the primary crystallites plays only a minor role.

Deactivation

Zeolites and zeotype materials deactivate in two ways: reversible deactivation due to coking and irreversible deactivation, which is mainly caused by dealumination and results in structural defects.

Reversible Deactivation

Reversible deactivation takes place when coke is formed. This happens during a reaction along the catalytic active zone, which migrates down the catalyst bed if a fixed-bed reactor is used [215, 221, 258–262]. Coking starts at the catalytic active sites inside the channels [227, 259, 263], with the formation of methyl substituted aromatics within the hydrocarbon pool mechanism [227, 264, 265] or on the active sites of adsorbed oxygenates [259]. These precursors are very mobile and able to migrate through the channels onto the surface, [223] although this process is still controversial [227]. Hence, coke can deposit on the surface, especially at strong coking, [227] as well as block the channels [227, 259, 263]. Additionally, external coke can be formed on the outside [263].

The rate of coking depends on the structure of the zeolite because it is a shape-selective reaction [215, 223, 260, 266–268]. Therefore, 8-membered-ring [215] and 12-membered-ring zeolites [215, 259] coke much faster than 10-membered-ring materials such as ZSM-5 [215, 223, 259] and ZSM-11 [259]. Additionally, three-dimensional channel systems coke slower than two-dimensional ones because blocked channels can be bypassed and the activity decreases only slowly. Therefore, H-ZSM-5 possesses special advantages in comparison to other zeolites, resulting in a much longer lifetime [259, 260]. Generally, zeolites with a high rate of methane formation deactivate very fast [221, 269].

Coking depends on the reaction temperature as well, with high temperatures supporting the formation of coke through higher rates of crack reactions. A minimum in coking can be observed at a reaction temperature of 400–450 °C [260, 270]. Below the temperature range of 270–300 °C, coke consists mainly of ethyltrimethylbenzenes, isopropyldimethylbenzenes and unsaturated compounds, which can be dealkylated at 475 °C to reactivate the catalyst. At higher temperatures, other coke molecules are formed slowly and can only be removed by burning. With elevated temperatures and particular pressures, more and more aromatics are formed and the C/H-ratio of the formed coke increases [260].

Longer contact times increase coking [259, 266–268]. Also the degree of conversion, the occurrence of special molecules and the actual activity of the zeolite have an impact on coking [263, 266–268]. Finally, the Si/Al-ratio also influences the kind of coke formed, [266–268, 271] with silicon-rich materials (e.g. H-ZSM-5) causing a hydrogen-rich coke, which can be burnt easily [259].

As coking progresses, the spectra of products formed changes because acidic sites become blocked. This change is very similar to a shortening of contact time or the decrease of active sites. Therefore, the rate of C_3 and C_4 paraffins decreases; formation of isoparaffins, naphthenes, olefins and nonaromatic C_{5+} compounds increases; and the amount of aromatics declines or stays unaffected [215, 221, 258, 260, 261, 272]. These changes can be modelled quite easily [263]. The formation of methane increases significantly. It is formed as a consequence of catalytic dehydrogenation of methanol getting in contact with external coke [260]. The highest yield of gasoline components is reached before methanol breakthrough, marking the total deactivation of the catalyst. Over the catalyst's lifetime, the octane number stays nearly constant [215, 221, 258, 261].

The catalyst can be reactivated by burning the coke. The achievable activity after reactivation depends on the activity in deactivated state and the length of reactivation [271]. Usually, reactivation is carried out with air or oxygen containing gases at 500–600 °C [259, 263, 271]. In this temperature range, permanent deactivation processes can occur. Therefore, normally it is not possible to reactivate a catalyst completely [263, 271].

Irreversible Deactivation

Dealumination causes irreversible deactivation. This process is supported by higher temperatures [221, 227, 258, 259, 263, 273] and pressure [274]. It takes place in the course of the catalytic cycle over several hundred hours if steam is present, [221, 227, 258, 259, 263, 273] especially during regeneration [227, 263, 271]. Hence, the reduction of steam production during hydrocarbon synthesis by the application of a dehydrogenated ether feedstock leads to an extended catalyst life due to a higher stability of the catalyst [255].

By losing crystalline-bound aluminium atoms, structural defects [263, 271] and aluminium atoms situated on nonlattice sites of the zeolite or zeotype material are generated. This causes a modification of the acidity profile resulting in a changed selectivity of the catalysts in hydrocarbon synthesis [218]. Therefore, crucial for the determination of a reliable correlation of the acidity profile and the selectivity is that both the acidity profile and selectivity remain constant for a significant period of several days—that is, a steady state has been reached.

In a process based on several reactor trains as well as a fluidised bed process with continuous regeneration, these fluctuations of the selectivity are compensated to a certain degree. However, in the MTG process with a fixed-bed arrangement, the gasoline yield after regeneration increases with each cycle, although the yield at the end of the cycle remains unchanged. In addition, the catalyst productivity increases, whereas at the same time changes in product distribution during each cycle decrease. This is due to permanent deactivation [258, 261, 275]. Also along the fixed bed, a permanent gradient of activity evolves as the different parts of the bed are subjected to varying partial pressures of steam and different temperatures. This permanent gradient is reflected in the broad product spectra observed in different

cycles [258, 261]. ZSM-5 exhibits a very low tendency for permanent deactivation with significant influences observed above 500–550 °C [259, 263, 273].

Reaction Mechanism

The formation of hydrocarbons is a process that is difficult to explore while all reactions take place inside the channels of the catalyst. In addition, primary products are hardly detectable because their formation is controlled by diffusion and secondary reactions have a higher reaction rate [230]. In general, it is assumed that methanol dehydrates first to form DME. This reaction reaches equilibrium, [218, 220, 221, 223, 235, 261, 276, 277] although during the reaction the equilibrium is moved towards the starting material methanol because water is formed as a byproduct in hydrocarbon synthesis [276]. This can be explained by DME having a higher reaction rate than methanol. DME reacts to C_2 to C_5 olefins, which form paraffins, aromatics and higher olefins in further reaction steps [215, 218, 223, 258, 261, 276, 278]. This general concept was the basis for several approaches to describe the overall reaction kinetics, as discussed by Keil [261].

The primary olefins that are built and the further reactions that take place depend on many parameters. Influencing parameters are the properties of the catalyst, especially:

- Acid strength.
- Density of acidic sites (decreasing density favouring heavier primary products)[230].
- Si/Al-ratio (silicon-rich materials support propene and butenes, whereas silicon-poor materials favour ethane [230]).
- The ratio of Brønsted and Lewis acidic sites (Lewis acidic sites are held responsible for catalysing reactions, leading to the formation of heavier products [232]).
- Catalyst topology [264].
- Crystallinity [264].

Furthermore, reaction conditions such as temperature, pressure and space velocity also affect the catalytic reactions [215, 218, 230, 235, 276]. At last, the present partial pressure of steam affects the product distribution and modifies the acidic strength of the catalytic active sites [221, 222].

Because of the above-mentioned difficulties in detecting primary products, there are a lot of experimental and theoretical approaches to describe the catalytic processes [215, 276, 279]. Initially, methanol reacts on the Brønsted acidic sites to DME [222, 230, 278, 279]. Using NMR technology, it is possible to follow the different reaction steps, initiated by methanol interacting with a bridging hydroxyl group, as shown in Fig. 6.57. As a function of methanol concentration, neutral complexes with hydrogen bonds or partly protonated clusters are formed, which dehydrate with elevated temperature to form methoxy groups. DME is generated along two reaction paths. The first path includes the reaction of a methoxy group with a methanol molecule followed by regeneration of the active site. The second

path describes the reaction of two adsorbed methanol molecules, which are bond side-on or end-on onto the surface [276] (Fig. 6.57).

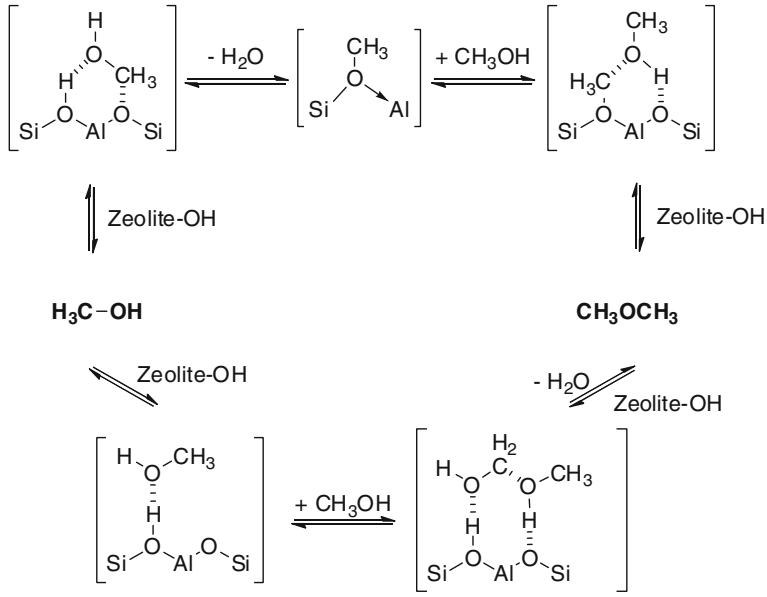

Fig. 6.57 Formation of dimethyl ether from methanol [276]

For the following reactions, regarding the formation of the first C-C-bond, more than 20 different mechanisms have been postulated, mostly excluding the induction period. These mechanisms can be categorised as oxonium ylide mechanisms, carbene mechanisms, carbocationic mechanisms, mechanisms with radicals and combinations of the different types [221, 277, 279]. Because of the insufficient acidity of the zeolites, the formation of carbenium ions can be excluded [276].

Today, the dual-cycle concept is used for the description of hydrocarbon production [264]. The first cycle is called the hydrocarbon pool mechanism and was first postulated during the 1990s [280–282]. It is based on the formation of aromatics on the acidic sites by hydrogen transfer [272]. The reaction is catalysed by aromatics (e.g. benzene, toluene, or *p*-xylene) [218, 283, 284] and proceeds autocatalytically [218, 276]. An increase in reaction temperature changes the product distribution, favouring smaller over larger olefins [218]. The catalytic active species consist of an organic–inorganic hybrid compound of the zeolite and active organic intermediates, which are situated inside the channels and intersections [235, 264, 265]. These intermediates are cyclic carbenium ions, such as 1,3-cyclopentenylcarbenium ions, which are in equilibrium with their neutral dienes, as well as methylbenzenes and polymethylnaphthalenes, which are not able to leave the catalyst because of their volume [221, 229, 235, 264, 265, 276, 285]. Cyclopentenylcarbenium ions are able to form methylbenzenes, which in turn

react with methanol to give polymethylbenzenium ions [276]. The occurrence of particular molecules depends on the zeolite type and the reaction conditions.

As the reaction proceeds, the organic intermediates react with methanol [264, 280–282] or DME [235, 264] and eliminate olefins, especially ethene and propene [221, 264, 265, 276]. Elimination is postulated to proceed through side-chain alkylation, which is characterised by the existence of an exocyclic double bond that adds methanol molecules [265, 283, 284]. A possible reaction scheme for the side-chain alkylation is shown in Fig. 6.58. Alternatively, the pairing mechanism occurs with growing alkyl side chains in consequence of ring-contraction and ring-expansion reactions (see Fig. 6.59) [229, 265]. Experimental results show that the side-chain alkylation dominates, although the pairing mechanism proceeds at least under certain circumstances [276].

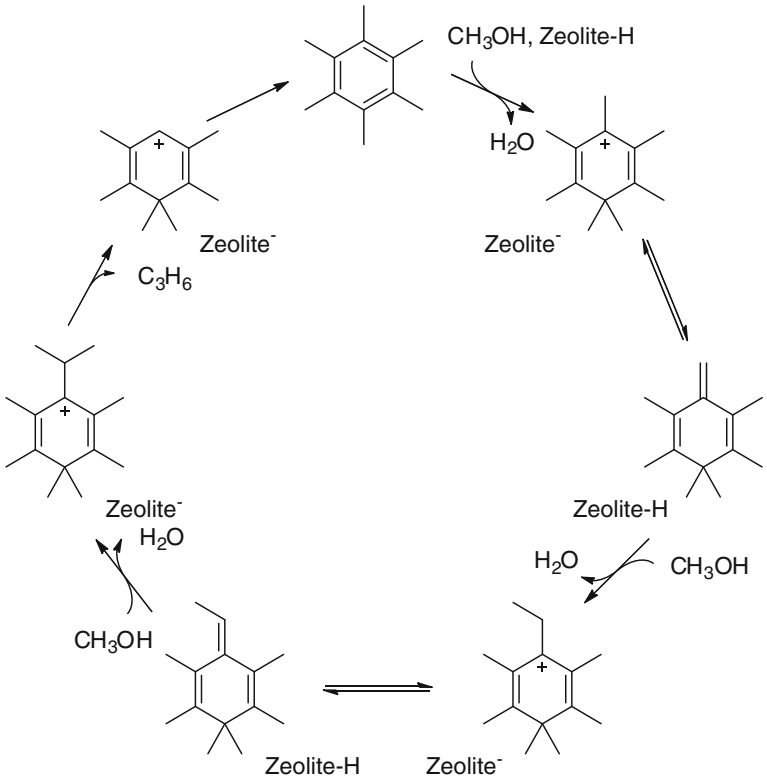

Fig. 6.58 Formation of propene using the side-chain mechanism [235]

The catalytic active species have to be formed as a first step; therefore, no hydrocarbons are released during the induction period [229, 269, 276]. These reactions proceed in the presence of radicals [221]. The induction period can

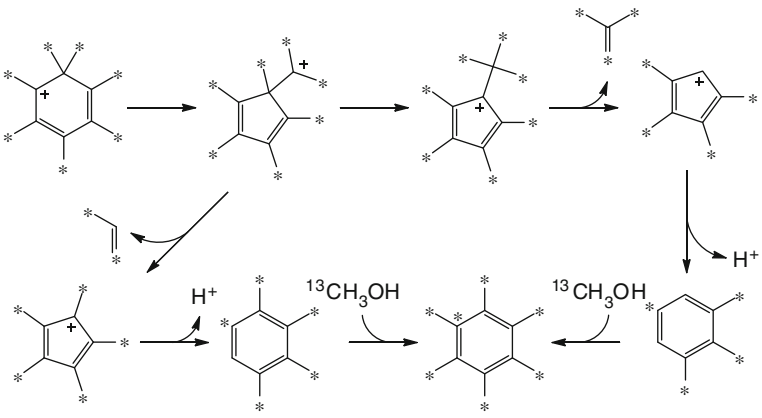

Fig. 6.59 Scheme of the pairing mechanism. Adapted from Ref. [286] (* denotes ^{13}C atoms)

be shortened by co-adsorption of water [287], co-injection of methylbenzenes [283, 284], propene or butene [269] and the application of contaminated reagents with organic substances [229, 285]. The induction period does not occur if cyclopentenylcarbenium ions are present.

In further steps of the hydrocarbon pool mechanism, it is necessary that aromatics are built through cyclisation reactions and hydride transfer of alkenes outside of this catalytic cycle [264].

This second cycle is called the Dessau mechanism, during which hydrocarbons are formed by methylation of alkenes with methanol molecules [218, 264]. Alkenes formed through this mechanism undergo cracking reactions, yielding products being able to oligomerise, become methylated by methanol, or desorb out of the catalyst. In this cycle, ethene is a secondary product in contrast to the higher alkenes, which are mainly formed therein [221, 264]. In contrast to the hydrocarbon pool mechanism, this cycle can proceed isolated, for instance in zeolites with two-dimensional channels as H-ZSM-22, which do not have enough free space for the formation of aromatics [264].

Commercial MTHC Catalysts

Often, hydrocarbon synthesis from methanol is done by a two-stage process. First, methanol is dehydrated to form DME, which is afterwards transformed into hydrocarbons. This procedure exhibits some advantages in terms of catalyst lifetime, process and heat control. As a result, catalysts that are important for MTHC processes include dehydration catalysts for DME synthesis, as well as zeolite and zeotype catalysts for hydrocarbon formation. Additionally, catalysts for olefin splitting are important for the refining of crude hydrocarbon products.

DME Catalysts for MTHC Processes

Methanol may be converted to gasoline in a two-stage operation. In the first step, methanol is partially dehydrated, whereupon an equilibrium mixture of DME, methanol and water is formed in a conventional dehydration reactor. The dehydration reactor has an equilibrium range of 75–80 %. Thus, a large portion of water is already created during this dehydration reaction, which can be optionally separated from the DME before hydrocarbon synthesis. The reaction is rapid, reversible and exothermic with liberation of approximately 30 % of the total reaction heat.

The dehydration of methanol to DME is catalysed by a number of solid acids, such as γ-Al_2O_3, H-ZSM-5, amorphous silica-alumina, or titanium-doped zirconium oxide. As early as 1928, Adkin published his research results on the dehydration of methanol over aluminium and zinc oxide [288]. For the MTP process, the commercially available catalysts DME-1 (Süd-Chemie) and its equivalent Girdler T126 catalyst [289] are used. Further suitable catalysts are Catapal carrier, T-4021 (Süd-Chemie) and DK-500 (Haldor Topsøe).

Catalysts for the Conversion of Methanol

Using methanol as raw material, a wide variety of hydrocarbon products are accessible. For the selective production of a special hydrocarbon fraction, the different catalyst providers developed special catalysts for the different products and processes. These processes are the MTG, MTO, MTA and MOGD processes by ExxonMobil, the TIGAS process, an advanced modification of the MTG process by Haldor Topsøe, as well as Lurgi's methanol-to-synfuel (MTS) process, with its major product being diesel fuel (Cetane Number $\sim$55) and approximately one-fifth being a gasoline boiling range product with a RON of 80 [290].

MTG Catalyst

The original MTG catalyst was developed based on the ZSM-5 zeolite, which was invented by Argauer and Landolt [233]. To date, no other material has proved to be as suitable for this application as ZSM-5. Clariant (formerly Süd-Chemie) produces the ZSM-5-based catalysts (the brand of this series of catalysts is CMG) for application in MTG processes. The preparation and some properties of this type of catalysts are discussed elsewhere [291]. In comparison to the MTP catalyst MTPROP-1, which is also a modified ZSM-5 catalyst offered by Clariant, they have a lower acidic site density; however, their acidity is higher than that of the COD-9 catalyst. As a result, the acidity of these catalysts in terms of acidic site density as well as with respect to the profile of acidic strength is designed for superior performance of the MTG process, which could be demonstrated on commercial plant scale.

MTO Catalysts

Argauer and Landolt [233] invented the original MTO catalyst, which was also based on ZSM-5 zeolite. Further research showed that the zeotype material SAPO-34 is more selective with respect to lower olefins compared to ZSM-5 for application in MTO processes. However, this occurs at the expense of converting approximately 10 mol% of the carbon in the methanol feed to coke, which is transferred to useless carbon dioxide upon regeneration [292].

SAPO-34

The UOP SAPO-34 based catalyst is especially designed to produce lower olefins [293]. This has been demonstrated on a pilot plant scale and will be applied in China by China's Wison (Nanjing) Clean Energy Company to convert methanol into building blocks for chemical products at an existing coal chemical complex [239].

ZSM-5

Clariant offers the ZSM-5 based MTO catalyst CMO-12 [291] with an acidic site density higher than that of the MTG catalyst CMG-1. On pilot plant scale, this catalyst has demonstrated exceptional performance for the Mt-Synfuel process. In general, the catalyst is ready for commercialisation. ZSM-5 or ZSM-11 catalysts are used by UOP in the UOP/Hydro MTO process using a raiser regenerator system for olefin synthesis. This process includes a downstream fixed-bed heavy olefin interconversion step (olefin cracking process) [294].

Catalysts for the Conversion of Olefins

The conversion of olefins to hydrocarbons is used in the MOGD process to get a gasoline boiling range product. Clariant offers for this and analog applications, like their COD process, the ZSM-5 based COD catalyst [291], with an acidic site density higher than that of the MTG catalyst CMG-1 [295]. The catalyst has been produced and used on a commercial scale for approximately 10 years [296].

Olefin-Splitting Catalysts

It is well known that the propylene yield of an MTP product stream could in principle be increased by a metathesis of ethene and 2-butene, if ethene and 2-butene would be present in the right ratio. Another possibility to increase the yield of propene is to re-equilibrate the C_{4+} or C_{5+} olefin fraction from the first MTP reactor in a succeeding second MTO unit, thus delivering additional propylene. This method is independent of the ethane-to-butene ratio after the first reactor.

The Clariant catalyst for this step recommended by Lurgi is a ZSM-5 based catalyst [291], with an acidic site density higher than the MTG catalyst. It is sensitive to dienes and similar potential oligomerisation precursors. The catalyst is

ready for commercialisation and has already demonstrated its exceptional performance for the MTP process on pilot plant scale.

Lyondell's Superflex process and Mobil's Olefin Interconversion (MOI) process are two new secondary olefin conversion technologies that crack C_4-C_8 olefins to predominately ethylene and propylene. Both technologies are based on a reactor/regenerator design similar to conventional fluid catalytic cracking. The catalyst applied in the Superflex process consists essentially of ZSM-5 [297], whereas the MOI process uses ZSM-5 or ZSM-11 as catalysts, which can be modified by metals such as gallium or phosphorus and have a high Si/Al-ratio [298]. The Superflex process is the only commercial olefin interconversion process; it was first applied at Sasol in the Republic of South Africa in 2006. It is used to convert a highly olefinic $C_{6/7}$ stream to propylene and ethylene, with a propylene production capacity of approximately 250 kt per year. JiHua is the second Superflex licensee, located in Jilin City, China.

6.4.1 Methanol-to-Gasoline Process

Lydia Reichelt[1] and Friedrich Schmidt[2]

[1]*Institute of Chemical Technology, Freiberg University of Mining and Technology, Leipziger Straße 29, 09599 Freiberg, Germany*

[2]*Angerbachstrasse 28, 83024 Rosenheim, Germany*

Introduction

In the early 1970s, researchers at Mobil Central Research discovered that methanol can be converted into higher hydrocarbons over Zeolithe Socony Mobil 5 (H-ZSM-5), a group of zeolites that was developed in the laboratories of Mobil Oil (*Socony* stands for "Standard Oil Company of New York") [299–301]. These hydrocarbons consist of a mixture of aromatic compounds, olefins and paraffins, with reaction conditions and the kind of catalyst determining the achieved predominant species. In contrast to the methanol-to-olefins (MTO) process and the methanol-to-aromatics (MTA) process, which aim for the production of olefins (MTO) and aromatics (MTA), the methanol-to-gasoline (MTG) process is capable of producing a high-quality gasoline.

The discovery of this MTG process was the biggest step in fuel synthesis since the development of the Fischer-Tropsch process in the 1920s; it led to intensive research, especially during the oil crises in the 1970s and 1980s. In consideration of the shrinking oil and gas resources as well as the ability to produce methanol from a wide variety of starting materials (e.g. coal, petroleum, natural gas, shale gas, pyrolysis oil from organic material, heavy fuel oil, biomass and organic waste), the so-found reactions are today of enormous societal significance again because they have the potential to secure and broaden the raw material base for mobility and the production of polymers, especially polyethylene and

polypropylene. The associated declining dependency on the availability of crude oil becomes increasingly attractive with each energy crisis.

Fuels from a MTHC technology completely satisfy the requirements for the usage as motor fuel in terms of octane number, cold-start behaviour, driveability, and emissions [302]. Compared to the application of pure methanol, they have the advantage of already existing worldwide safe distribution and storage networks as well as optimised engines for its usage. Furthermore, the development of alternative drive systems is presently taking place but has still not concluded. Therefore, the production and application of MTG-derived fuels can be seen as a transitory technology with a future in special areas in which alternative engines are inapplicable.

Therefore, MTHC processes, and especially processes for the production of fuels, receive high attention in scientific research and industrial applications. For instance, a new industrial facility using these technologies started up in 2009. This is remarkable because the first (and prior to that, unique) industrial plant for fuel synthesis from methanol—a fixed-bed MTG plant situated in Motunui, New Zealand—only operated from 1986 [302–307] until 1996 [308] due to too high methanol prices and low fuel prices.

The Catalytic Formation of Hydrocarbons

For the formation of hydrocarbons from methanol and related raw materials, a catalyst is generally required. The structure and properties of the catalytic active sites affect the obtainable products. The underlying chemical reactions are today mostly known. In contrast, the reactions during the induction period, until the catalyst reaches its complete activity and for the formation of the first C-C bond, are still part of the scientific discussion.

Catalysts and Raw Materials

Solid acids or immobilised mineral acids are known to be active for the catalysis of heteroatom elimination and the oligomerisation of olefins. If both processes are combined, hydrocarbons can be synthesised from compounds of type R_1-X-R_2, wherein R_1 is an alkyl, R_2 is an alkyl or a hydrogen atom, and X often is oxygen or sulphur, such as alcohols and ethers. For MTHC processes, methanol and DME are the most important raw materials; their conversion has been studied intensely during recent decades.

Zeolite H-ZSM-5 is the only known suitable catalyst for high-quality fuel synthesis from methanol. Zeolites are crystalline aluminosilicates with regularly ordered tetrahedral-coordinated Si and Al atoms. Thus, highly ordered structures with channels and cavities of molecular dimension [302] are formed, in which the catalytic active sites are situated. Because of this structure, strong constraints influence the catalytic reactions since the diameters of the channels and cavities determine the biggest molecules able to form and enter or leave the catalyst.

The H-ZSM-5 zeolite has MFI topology with a three-dimensional channel system with channel windows of 10, 6, 5 and 4 rings. In Fig. 6.60, the 10-ring is schematically shown. The maximum diameter of a sphere that can be included in

the channel crossing is 0.636 nm. The maximum diameter of a sphere that can diffuse along direction *a* is 0.470 nm and along *b* or *c* is 0.446 nm [309]. Further information on suitable catalysts for application in MTHC processes and their properties is given in Sect. 6.4 above.

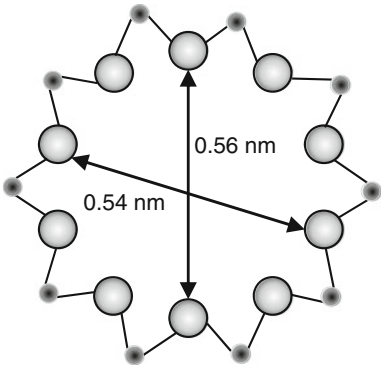

Fig. 6.60 Channel profile of ZSM-5 with Si or Al central atoms (small) and oxygen atoms (big)

Reaction Mechanism

The catalytic reactions of oxygenates to hydrocarbons take place inside the channels of the porous solid acid, especially zeolite H-ZSM-5. Using a fresh catalyst, until the induction period is passed, no hydrocarbons are set free. According to Mokrani et al., during this time methanol is completely converted in the presence of radicals [308] to give organic and aromatic substances. They add to the evolution of an inorganic–organic hybrid compound, which later acts as a catalyst for the formation of the hydrocarbon product. The question of which mechanism leads to the formation of the first C-C-bond is still not fully clarified, and thus it has led to numerous experimental and theoretical studies with more than 20 proposed mechanisms [310].

Generally, it is assumed that methanol dehydrates first to give an equilibrium mixture of DME and water [303, 308, 311–316]. DME is afterwards converted into C_2 to C_5 olefins, which form paraffins, aromatics and higher olefins: (Eq. 6.11) [302, 311, 312, 315–318].

$$CH_3OH \xrightarrow{-H_2O} CH_3OCH_3 \xrightarrow{-H_2O} C_2 \ldots C_5 \text{ olefins} \rightarrow \begin{matrix} \text{paraffins} \\ \text{aromatics} \\ \text{higher olefins} \end{matrix} \qquad (6.11)$$

The formation of hydrocarbons through hydrogen transfer, alkylation, elimination and polycondensation is shown in detail in Sect. 6.4 above. For 100 mass units of methanol, stoichiometric yields of approximately 44 wt% hydrocarbons and 56 wt% water are obtained [317]. The product spectrum comprises paraffins, olefins and mainly methyl-substituted aromatics with a maximum chain length of C_{10}. Durene (1,2,4,5-tetramethylbenzene) is the bulkiest molecule built, which is very undesirable because of its high melting point of 79 °C [302].

The thermal energy release of this reaction is approximately 1.74 MJ/($kg_{methanol}$), with approximately 15–30 % of this heat being set free during DME formation from methanol.

Deactivation

Zeolites can be reversible or irreversible deactivated. Reversible deactivation takes place when coke is formed. The rate of coke formation depends on the structure of the zeolite [302, 312, 319–322], the Si/Al-ratio [320–323], the reaction temperature, [319, 324] and the contact time [320–322, 325]. As reversible deactivation progresses, the spectra of the products formed change because acidic sites become blocked. Therefore, as the rate of C_3 and C_4 paraffins decreases, the formation of isoparaffins, naphthenes, olefins and nonaromatic C_{5+} compounds increases while the amount of aromatics declines or stays unaffected [302, 308, 315, 317, 319, 326].

In a fixed-bed reactor, a catalytic active reaction zone occurs, which moves during usage to the reactor outlet and is called band aging. When this zone reaches the outlet and the methanol content in the product rises to a certain value, the catalyst has to be regenerated [317, 327]. This is done by burning the coke with air or oxygen containing gases at 500–600 °C [323, 325, 328].

Irreversible deactivation appears when desalumination occurs and structural defects are generated [323, 328]. This process occurs at rising temperatures [308, 317, 325, 328–330] and pressure [331] if steam is present [308, 317, 325, 328–330] and takes place especially during regeneration [323, 328, 329].

Using a fixed-bed process, a permanent activity gradient along the catalyst bed evolves because of varying permanent deactivation due to different steam pressures and the S-shaped temperature profile, which is typical for adiabatic reactors.

ZSM-5 exhibits a very low tendency for reversible [319, 325] as well as irreversible deactivation, with significant influences of structural defects observed only above 500–550 °C [325, 328, 330]. The rate of overall aging decreases with increasing numbers of cycles [315].

Reaction Conditions and General Dependencies

The product selectivity and the activity profile strongly depend on the specific process parameters (temperature, pressure and contact time [302, 323]) and particular catalyst properties, whereupon the main influences are known from experimental work since the early development of MTHC processes. These experimental results can only partially be reproduced or simulated because of continuous changes in catalyst properties as a consequence of reversible and irreversible deactivation [302]. A steady state is mostly reached after several days. Additionally, the selectivity is often related only to the products at the exit of the catalytic reactor system; instead, the total carbon balance should be considered (i.e., to take the remaining coke on the catalyst into account).

When operating the MTG process at temperatures less than 300 °C, the conversion is not 100 % and DME is the main product [302, 308, 332]. Above this temperature range, conversion increases [308, 330] and hydrocarbons are formed

according to chemical equilibrium [325, 330]. Beyond 450 °C, secondary cracking reactions occur and result in a larger amount of methane and light olefins [302, 308, 330] and less C_{5+} hydrocarbons (naphtha), until above 500 °C more and more hydrogen and carbon monoxide are observed as a consequence of decomposition of methanol [302, 308]. Normally, MTG processes are performed at 300–450 °C with lower reaction temperatures leading to higher volumes of raw gasoline. However, the octane numbers decrease and the concentration of durene grows, as can be seen in Table 6.9 for the fluid-bed MTG process [333–335].

Table 6.9 Effect of temperature at constant pressure on yield and quality of total gasoline (naphtha and alkylate) from the fluid-bed methanol-to-gasoline demonstration plant. (Actual data were not disclosed) [335]

Temperature	*Low temperature*	*High temperature*
Gasoline yield	88.5 %	85.5 %
Research octane number	94.6	97.5
Motor octane number	85.3	87.4
Durene	6.5 %	3.0 %

Table 6.10 Effect of pressure at constant temperature on yield and quality of total gasoline (naphtha and alkylate) from the fluid-bed methanol-to-gasoline demonstration plant. (Corresponding temperature data were not disclosed) [335]

Pressure	1.7 *bar*	3.2 *bar*
Gasoline yield	87.5 %	89.5 %
Research octane number	96.3	95.6
Motor octane number	87.3	86.3
Durene	3.5 %	5.0 %

The operating pressure influences the relative rates of the formation of olefins and aromatics. Low pressure uncouples both processes, supporting the formation of olefins, as shown in Fig. 6.61, whereas a high pressure level results in an overlap with an increased selectivity for substituted aromatics (Fig. 6.62) [302, 308, 336]. With increasing pressure, the volume of raw gasoline increases although the research octane number (RON) and motor octane number (MON) decrease, whereupon especially the content of durene increases quickly with growing pressure (see Table 6.10) [302]. For this reason, the MTG process in several studies is performed at pressures of approximately 100 kPa [325].

The exothermic character of the conversion reaction (1.74 $MJ/kg_{methanol}$) results in an adiabatic temperature increase of about 670 °C for pure methanol feed. Therefore, careful management of the methanol feedrate in relation to the catalyst loading (e.g. as weight hourly space velocity (WHSV) or liquid hourly space velocity (LHSV)) is required. In general, the MTG process is carried out at contact times ranging from 0.01 to 0.1 h [325]. Based on the catalytic reaction pathway, a short contact time supports the formation of olefins [308, 315, 323, 337], as shown in Fig. 6.63, whereas even shorter contact times lead to the formation of DME [302]. Conversion increases with contact time [302].

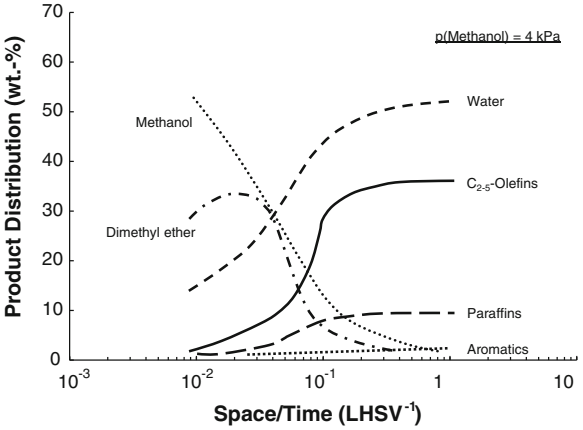

Fig. 6.61 Product distribution at low pressure [302]

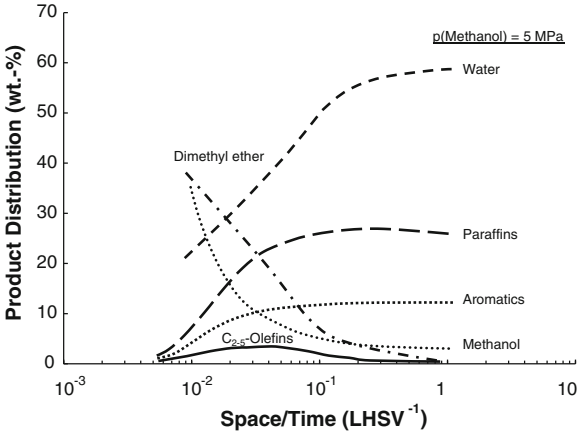

Fig. 6.62 Product distribution at high pressure [302]

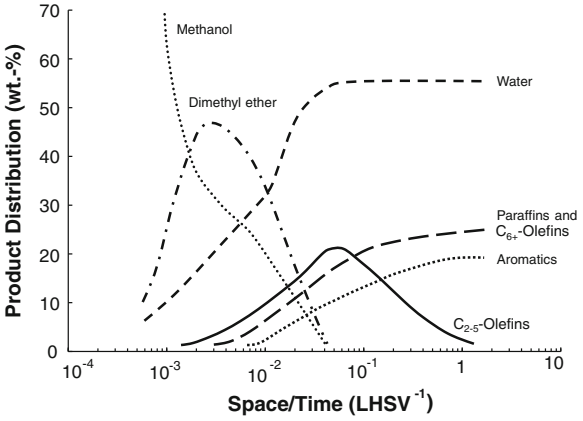

Fig. 6.63 Product distribution in dependency on contact time [302]

The production of gasoline boiling range hydrocarbons has an optimum at a certain space velocity. The maximum yield increases with increasing temperature and decreasing contact time [323]. MTHC processes are predominantly carried out at complete conversion of methanol. This way, the aqueous product can be used directly as process water and the disposal of excess water does not bear any problems regarding the toxicity of methanol. So, when methanol breaks through, the process cycle has to end and the catalyst needs to be regenerated.

Industrial Processes

Microporous crystalline solid acids have been widely used for several decades in the chemical and petrochemical industry as catalysts for the conversion of aromatics [338] and for the cracking of hydrocarbons [339, 340]. Their application in MTHC processes is mainly limited to the fixed- and fluid-bed processes by Mobil, although there are several other concepts of minor importance. Hence, today there are only a few industrial (MTG: Methanex, NZ [341, 342], dismantled in 2004; Jincheng Anthracite Mining Group, China [299–301, 343]; conversion of olefins to diesel, COD: RSA [344], similar to the second part of the MOGD process) and demonstration plants besides some projects (e.g. 15,000 barrel/day plant for DKRW's coal-to-liquids (CTL) project in Medicine Bow, Wyoming, USA, based on commercially proven ExxonMobil MTG [345]).

Fixed-bed MTG Process

The fixed-bed process was developed by Mobil Oil Corporation during the 1970s using a bench-scale reactor (4–8 L/d methanol) [317]. After successful tests in a pilot plant (640 L/d) and the discovery that upscaling has no negative but only positive effects [317, 346], the industrial plant at Motunui (New Zealand) was constructed [302, 304, 308, 315, 317, 346]. In 2009, JAMG started up yet another plant at Jincheng (China), using coal instead of natural gas as raw material for methanol synthesis.

Plant at Motunui

Due to the oil crises in 1973 and 1978, the government of New Zealand decided to become more independent from fuel imports in 1979 [303]. It aimed to use its own resources of natural gas to synthesise fuels. As a result of these considerations, it was planned to build an industrial MTG plant, with preference to the MTG process over the alternative Fischer-Tropsch process.

The construction of the plant at Motunui started in 1982. It was mechanically completed in 1985 and put into normal operation in 1986, [302–307] although the first synthetic fuel was synthesised in October 1985. The plant exhibited a capacity of 570,000 t/a gasoline [304, 305, 307, 308, 315, 317], which sufficed to satisfy one-third of New Zealand's demand for gasoline [303, 305, 306]. Until March 1987, about 739,000 t of gasoline had been produced [304, 305]. In 1996, [308]

the plant was shut down for economic reasons and sold to Methanex. Today, only the part producing methanol is still in operation [303, 308, 347]. The equipment for methanol conversion was dismantled in 2003–2004 [348].

Process

In general, the MTG plant consists of two parts. The first part is used to transform natural gas into methanol using the ICI low-pressure methanol process. In the second part, the MTG plant converts methanol to gasoline boiling range hydrocarbons, which is schematically shown in Fig. 6.64. Therefore, crude methanol, which includes about 17 wt% of water [304, 305, 315, 317], is heated up to 300–320 °C [302, 304, 305, 308, 315] and compressed to 2.6–2.7 MPa [305, 308, 315]. Then, it passes a first adiabatic fixed-bed reactor with an average space velocity of 1.6 h^{-1} (based on methanol) [302], where DME is formed on a catalyst consisting of γ-alumina. In this first step, approximately 15–30 % of the total heat of reaction (1.74 $MJ/kg_{methanol}$) is released, [302, 305, 308, 315, 317, 346] heating the reactor effluent up to 410–420 °C [302, 304, 305, 308, 315].

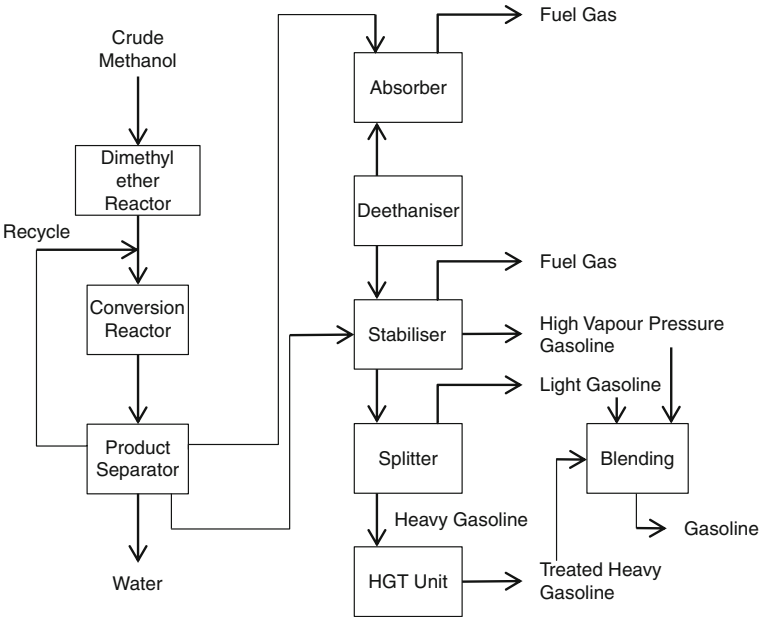

Fig. 6.64 Schematic flow diagram of the fixed-bed methanol-to-gasoline process. HGT, heavy gasoline treating

The product, in its chemical equilibrium, is mixed with a recycle gas, [304, 305, 308, 315, 346] which is needed to control temperature rise in the following adiabatic reactor from 350–370 °C [305, 308, 315] to 412–420 °C [302, 304, 308]. This reactor contains the ZSM-5 fixed bed and is used to form hydrocarbons at

1.9–2.3 MPa [305, 308, 315]. The hot product is used to preheat the recycle gas and crude methanol as well as to produce steam [304, 305, 315, 346]. Finally, the product can be separated into a recycle stream, water and hydrocarbons [304, 308, 315, 317] at 25–35 °C and 1.6 MPa [305, 315]. Afterwards, the hydrocarbon stream is split into a heavy gasoline, gasoline and liquid gas [304, 308, 315, 317].

C_3 and C_4 olefins are alkylated to increase the gasoline yield [302]. The heavy gasoline with a boiling point of ≥177 °C passes the heavy gasoline treating (HGT) unit, in which disproportionation, isomerisation, transalkylation, ring saturation, and dealkylation/cracking occur on a multifunctional catalyst at 220–270 °C and 3.1–4.1 MPa [305], resulting in reduction of the durene content from 5.5 to 2 wt% [304, 305, 308, 315, 317] without changing the octane number [305, 308, 317]. Product water is processed in a biological wastewater treatment unit to remove dissolved oxygenates (0.1–0.2 wt%) [305, 308, 315, 317].

In the continuos process at Motunui, the plant consisted of five parallel MTG reactors, with four reactors on stream and one in regeneration [305, 315, 323, 346]. This regeneration was necessary every 20–50 days [349, 350] (depending on the operating conditions and on the catalyst age [346, 351]) and the catalyst had to be changed after a certain number of cycles. The catalyst is reported to have a life of about 2 years [352]. From these data, an average cycle length of 35 days can be estimated. The average number of cycles can be expected to be approximately 20.

Products

In this process, methanol is converted to 43.4 % hydrocarbons, of which 85 % are hydrocarbons in the gasoline boiling range [302], 56 % is water and traces of carbon monoxide, carbon dioxide and coke (see Table 6.11) [302, 304]. The reaction is virtually complete and stoichiometric [302, 304, 305, 308, 315, 317, 346]. Only 5 % of the thermal energy of the methanol feed is liberated during reaction,

Table 6.11 Product distribution, based on wt% methanol charged, using the fixed-bed methanol-to-gasoline process [302]

Fixed-bed reactor		
Yields	Methanol + ether	0
	Hydrocarbons	43.4
	Water	56.0
	CO, CO_2	0.4
	Coke, other	0.2
Reactor effluent composition	Light gas	1.4
	Propane	5.5
	Propylene	0.2
	i-Butane	8.6
	n-Butane	3.3
	Butenes	1.1
	C_{5+} gasoline	79.9
Commercial hydrocarbon products	Gasoline	85
	Liquefied petroleum gas	13.6
	Fuel gas	1.4

but 95 % is preserved in the hydrocarbon product [342]. The resulting gasoline is fully compatible with conventional gasoline and has a RON of 92–95 [302, 304, 305, 308, 315, 317] and a MON of 82.6–83 [308, 315, 317].

The Mobil Shanxi Jincheng Anthracite Coal Mining Plant

In 2006, JAMG awarded a contract to Uhde for the engineering and supply of a coal-based MTG plant. It was planned to produce 100,000 t of gasoline annually starting in 2008 [353]. However, the plant was first put into service in 2009 [343]. The new MTG plant is part of a complex on a pilot-plant scale, which was constructed at Jincheng, Shanxi Province (approximately 600 km southwest of Beijing). This complex also includes a fluidised-bed hard-coal gasification plant and a methanol plant. From 1,000 t of methanol, the process produces 387 t of gasoline, 46 t of LPG, 7 t of fuel gas and 560 t of water, which is recycled as process water.

Fluid-bed MTG Process

Besides studies on the fixed-bed MTG process, Mobil developed an isothermal fluid-bed process. Therefore, at first a bench-scale reactor was used [315]. Afterwards, from 1982 to 1985, a demonstration plant was developed in Wesseling (Germany) with a capacity of 4,000 t/a [303, 306, 315], which was additionally used to carry out the MTO process. This plant had approximately 8,600 h on stream to investigate a variety of process conditions [308]. It was assembled and operated by Mobil Research and Engineering, Uhde GmbH and Union Rheinische Braunkohlen Kraftstoff AG in a joint project under sponsorship of the U.S. Department of Energy and the German BMFT. Thereafter, a commercial-scale study was carried out based on the results of that plant. However, no commercial fluid-bed MTG plants have yet been built.

Process

The fluid-bed MTG process operates at almost complete conversion and yields a high-quality gasoline in addition to LPG and fuel gas. Further information on yields and product composition are given in Table 6.12. The process uses distilled [307, 308] or crude methanol [308] as a starting material, which is vapourised and fed into the reactor. Within the reactor, immersed coils serve as a heat exchanger, which is advantageous for heat transfer through the fluid catalyst [307, 308, 315] and for producing a homogeneous temperature profile. Additionally, a part of the catalyst can be continuously externally or internally cooled in a heat exchanger [315].

Catalysis proceeds at 380–430 °C, 0.24–0.45 MPa, 500–1,050 kg/h methanol feed, 0.5–1.3 h^{-1} and 0.2–0.55 m/s gas superficial velocity [302, 307]. The catalyst is continuously withdrawn and regenerated by burning off the coke in a second reactor. The catalyst is separated from the gaseous product through cyclones. Afterwards, the product gas is cooled down and separated into a gas, liquid hydrocarbons and water using a three-phase separator. Additional separation steps are used to obtain product gasoline, C_3 and C_4 hydrocarbons, which are alkylated, and a recycle of light olefins (Fig. 6.65).

Table 6.12 Product distribution, based on wt% methanol charged, using the fluid-bed methanol-to-gasoline process [302]

Fluid-bed reactor		
Yields	Methanol + ether	0.2
	Hydrocarbons	43.5
	Water	56.0
	CO, CO_2	0.1
	Coke, other	0.2
Reactor effluent composition	Light gas	5.6
	Propane	5.9
	Propylene	5.0
	i-Butane	14.5
	n-Butane	1.7
	Butenes	7.3
	C_{5+} Gasoline	60.0
Hydrocarbon product composition	i-Paraffins	44.6
	n-Paraffins	9.2
	Olefins	16.5
	Naphthenes	5.0
	Aromatics	24.7
Commercial hydrocarbon products	Gasoline including alkylate	88.0
	Liquefied petroleum gas	6.4
	Fuel gas	5.6

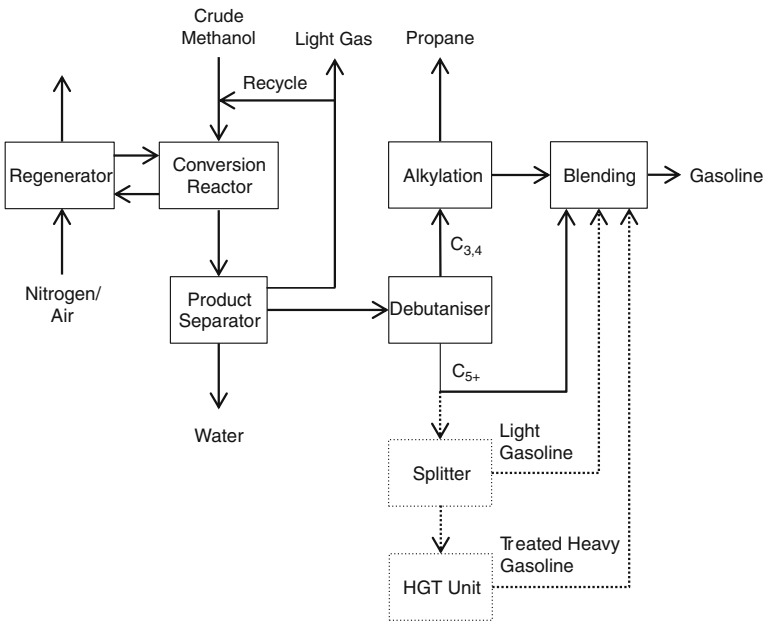

Fig. 6.65 Schematic flow diagram of the fluid-bed methanol-to-gasoline process

The alkylation of C_3 and C_4 hydrocarbons is very important to improve gasoline yield because the rate of alkylate petrol in total gasoline yield is approximately 25–30 %. However, the application of an HGT unit is not essentially needed, because the concentration of durene is less than in the fixed-bed process due to the lower pressure [307, 308, 315].

Products

The fluid-bed MTG process operates at almost complete conversion and yields a high-quality gasoline besides LPG and fuel gas. Further information on yields and product composition are given in Table 6.12.

Comparison with the fixed-bed process

The most important difference between the fluid-bed and the fixed-bed process is that the product distribution does not depend on time [308, 315]. The product contains an increased fraction of light olefins and fewer C_{5+} components, particularly less durene [302, 308], as can be seen in comparison of Tables 6.11 and 6.12.

By alkylating the light olefins with isobutene, the yield of gasoline can be improved, resulting in an about 7.5 % higher yield of gasoline than using the fixed-bed process [306, 307, 315]. Furthermore, the alkylated product gasoline possesses a similar RON of 95 but a higher MON of 85 [306, 307, 315].

In all, the fluid-bed MTG process proved to be more economical than the fixed-bed process because the heat of reaction is recovered as high-pressure steam, whereby this energy can be used more efficiently, causing a 10 % reduction in energy demand [308]. In addition, investment costs are lower, the specific throughput is higher and a liquid injection to tailor the steam balance is possible.

Other processes

Topsøe's Integrated Gasoline Synthesis

Topsøe's Integrated Gasoline Synthesis (TIGAS) process was the first process to use DME as an intermediate without isolation of methanol. The formation of DME instead of methanol has some advantages. The chemical equilibrium of methanol formation does not limit the yield of this first step and thus decreases the volume of the recycle stream and the pressure needed for synthesis. In addition, the permanent deactivation of the zeolite declines because less water is formed during hydrocarbon synthesis [331]. A fundamental benefit of the direct synthesis of DME is the possibility of using a synthesis gas with a H_2/CO-ratio of 1. This is very important for the production of synthesis gas from biomass or coal. The high vapour pressure of DME is crucial because separating DME from the product is expensive. However, in comparison to the MTG process, only two reactors are necessary, resulting in lower investment costs.

The TIGAS process was developed for application in remote areas, where natural gas is cheap but investment costs determine economic efficiency [306, 315, 331]. A pilot plant was tested from 1984 till 1987 in Houston, Texas, with a capacity of

1 t/d gasoline. Haldor Topsøe A/S developed the DME process (with a bifunctional catalyst) but used the knowledge gained from the MTG process for hydrocarbon synthesis [331]. The whole process is carried out in one train with only one recycle-stream from hydrocarbon separation back to the synthesis of DME [306, 315, 331]. A schematic flow diagram can be seen in Fig. 6.66. This necessitates the realisation of all reaction steps at one pressure level (2 MPa), which is not possible when methanol is isolated. Furthermore, the recycle stream passes the hydrogenation catalyst of the DME synthesis. The olefins included in that stream are hydrogenated, which results in a stable product with low olefin content but increases the consumption of hydrogen [306, 331]. However, unreacted hydrogen passes the zeolite, where durene formation and coking are decreased, thus regeneration is just required every 6 months [331]. Because of the slow formation of coke, the product distribution remains nearly unchanged over the cycle and the selectivity for the synthesis of C_{5+} hydrocarbons is approximately 80 % [331].

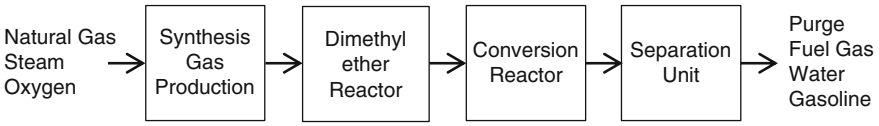

Fig. 6.66 Schematic flow diagram of the TIGAS process [331]

Although produced gasoline has a lower RON than the product from the MTG process [306, 331], its MON is nearly identical. This difference is caused by the decreased content of olefins and depends on the actual reaction conditions, especially the hydrogen content of the synthesis gas [331].

MtSynfuel and MOGD

Lurgi developed the MtSynfuel process as an alternative to the Mobil's olefin-to-gasoline and distillate (MOGD) process up to pilot plant scale [354]. The commercial MtSynfuel process would use a MegaMethanol plant for the production of methanol. The methanol is converted in a second step into DME and further into dominantly propene, using the MTP process [355] with a zeolite catalyst at temperatures between 300 and 550 °C and at pressures of 0.1–2 MPa. Afterwards, the olefins are oligomerised at 150–350 °C and 3.5–8.5 MPa using a zeolite as catalyst (COD) [356]. From the product, the C_{10+} fraction is separated by distillation and hydrogenated. Afterwards, the streams are blended to form a high-quality gasoline [357, 358] or diesel, which is even suitable for application in polar regions [359]. The overall efficiency of this process is according to Lurgi approximately the same as for the Fischer-Tropsch process, whereupon the MtSynfuel process yields a higher-quality gasoline but the Fischer-Tropsch process yields a higher cetane number of the distillate fraction.

The MOGD process [306] developed by Mobil is based on the MTO process, and it was tested in 1981 in a Mobil refinery. For the reaction, three reactors are operated in series with interstage cooling. The product consists mainly of C_5 to C_{20} i-olefins, with the C_{10} to C_{20}-fraction needing additional hydrogenation [315]. Additionally, MTO and MOGD processes can be combined to produce gasoline (RON $>$ 92) and diesel (cetane number $\approx$ 50), and an alkylation unit can be added to improve yield. This configuration results in high flexibility according to seasonal variations in fuel demand [360]. Because of the olefinic intermediates, both processes are explained in more detail in Sects. 6.4.2 and 6.4.3.

Others

The syngas-to-fuel (STF) process includes the formation of methanol and its further reaction to form a gasoline boiling range hydrocarbon product. It can be regarded as a successor of the MTG process and has been tested in a pilot plant in Freiberg, Germany. The STF process uses a new zeolite catalyst and a novel reactor concept, which abolishes the need for an HGT unit. First results are promising but final tests have yet to be carried out.

A demonstration plant for the so-called bioliq process was completed at the Karlsruher Institute for Technology. This process aims for gasification of biomass, especially using straw as feedstock for the synthesis gas production, which is converted into DME and finally into a hydrocarbon product.

The University of Akron and the Electric Power Research Institute developed the dimethyl ether-to-gasoline process. Synthesis gas reacts on a bifunctional catalyst of $Cu/ZnO/Al_2O_3$ and γ-alumina [315] at 250 °C [361] to DME. The synthesis of hydrocarbons occurs at 250–375 °C [361].

Summary

Synthetic fuels made of methanol have a high quality, whereupon methanol can be produced from a wide variety of feedstocks. These fuels are free of sulphur or nitrogen and match all legal restrictions. Using MTG technology, a high overall energy efficiency of 92–93 % (including processing energy) is possible, whereupon approximately 95 % of the thermal energy of the methanol feed is preserved in the hydrocarbon product [342]. Including the production of methanol from natural gas, the overall energy efficiency is within the range of 50–60 % [342], which is comparable to the production of diesel with the Fischer-Tropsch process (55–57 % [362]) without steam or energy export.

Although there are a lot of studies on MTG processes, only a few industrial MTG plants are at work or in the planning stage. In contrast, for the conversion of MTO or Fischer-Tropsch olefins to diesel, only few studies exist, but these technologies have already been industrially tested for approximately 20 years on zeolite catalysts, for example in South Africa.

6.4.2 Methanol-to-Olefins Processes

Friedrich Schmidt[1] and Carsten Pätzold[2]

[1]*Angerbachstrasse 28, 83024 Rosenheim, Germany*

[2]*Institute of Chemical Technology, Freiberg University of Mining and Technology, Leipziger Straße 29, 09599 Freiberg, Germany*

Introduction

The reactions of oxygenates, primary alcohols and more specifically methanol, to hydrocarbons have enormous societal significance because these reactions involve two of the most important areas of modern industrial society—namely, to secure and broaden the resource base (1) for mobility and (2) for the production of polymers (polyethylene and polypropylene for the production of consumer goods).

The worldwide outlook on light olefins seems to be positive for the years to come, with ethylene and propylene demand growing at 4–5 %, and 5–6 %, respectively, in 2009 [363]. The two primary propylene sources are steam crackers and refineries, as of 2003 represented 66 % and 32 % of the production share [364]. However, propylene production from steam crackers is expected to decline relative to ethylene production because of a growing share of ethane as cracker feedstock [365].

In the early 1970s, researchers at Mobil Central Research have discovered that methanol can be converted into higher hydrocarbons over the zeolite H-ZSM-5 [366–368]. More details about the catalyst are given in Sect. 6.4 above. The formed hydrocarbons consisted of a mixture of aromatic compounds, olefins and paraffins, delivering a gasoline of high quality. The process, named methanol-to-gasoline (MTG), is described in more detail in Sect. 6.4.1.

Efforts have been made to improve the selectivity of the MTG towards the production of dominantly lower olefins. MTO conversion is a very important process for the production of light olefins, such as ethene and propene, from alternative and abundant resources of natural gas or coal. Since this discovery, tremendous work has been devoted to the improvement of the catalyst and process performance [369, 370]. The first commercial MTO unit was the Mobil/Uhde fluid-bed MTO in Wesseling, Germany, which produced 100 barrels per day (BPD; corresponds to approximately 50 tonnes per year). Liu et al. reported on another commercial MTO unit with a production capacity of 600 tonnes of lower olefins per year, which proved to be completely successful in its first commissioning [371].

The MTO process provides an alternative route for increasing demand to light olefins, especially ethylene and propylene. These compounds are mainly manufactured by steam-cracking of naphtha. It is a thermal cracking process whereby the feedstocks (naphtha, but also lower paraffins) are mixed with steam (to reduce coke deposition) and then heated above 800 °C for pyrolysis [372]. Product

spectrum with C_2–C_5 compounds can only be changed in narrow margins; thus, additional routes (especially for propylene) are necessary [373].

Conversion of methanol to olefins has advantages compared to the steam-cracking of naphtha as well as to fluid catalytic cracking (FCC) and dehydrogenation of paraffins. Different raw materials as an alternative to oil can be used and processed to olefins with low energy consumption and CO_2 emissions. Moreover, olefins from a methanol-to-hydrocarbon route have the advantage compared to olefins from steam crackers, in that the olefins obtained via methanol are of polymer grade.

Some reviews have covered the MTHC topic from an academic viewpoint [374–376] and from a semitechnical viewpoint [367, 374]. A review by Stöcker covered the details of catalyst and reaction mechanisms of the MTHC processes, especially the MTG, MTO and Mobil's olefin-to-gasoline and distillate (MOGD) processes [377]. Keil presented a paper focusing on the technology of the MTG, MTO and MOGD processes but did not discuss those processes, which are presently operating commercially [367].

The Methanol-to-Hydrocarbon Reactions

The conversion of a number of organic compounds is catalysed by solid acids. An important group of such reactions is the elimination of heteroatoms, X, from compounds of type R_1–X–R_2 with the formation of hydrocarbons, wherein R_1 is an alkyl, R_2 is an alkyl or a hydrogen atom and X often is oxygen (rarely sulphur). Alcohols—predominantly methanol and ether, with DME in particular—are compounds of this type, whose conversion to hydrocarbons has been studied using solid acid catalysts. Another group of reactions that are catalysed by solid acids or immobilised mineral acids is the oligomerisation of light olefins to fuel. For several decades, both types of reactions on microporous crystalline solid acid catalysts have been the subject of intense scientific research. The work of the last three decades on MTHC concern, however, essentially only the MTO and MTG reactions, but not the conversion of MTO or Fischer–Tropsch olefins to diesel (COD), although the latter technology has already been industrially tested for about 20 years on zeolite catalysts. Reviews describe the state of scientific discussion until 1998 and by 2011, focusing primarily on the chemistry and mechanism of the MTO and MTG reaction, as well as to the appropriate catalysts for these reactions [377, 378]. The conversion of oxygenates was described in depth by Chang [379] and in U.S. Patents 3,931,349 to Kuo [380] and 4,404,414 to Penick et al. [381].

The reaction steps are given schematically as:

$$2CH_3OH \rightarrow CH_3OCH_3 + H_2O \rightarrow (CH_2)_2 + 2H_2O \tag{6.12}$$

In first step, methanol dehydrates to form DME. Further dehydration leads to olefins. Besides ethylene and propylene in high yields, small amounts of paraffins, higher olefins and aromatics are obtained.

Numerous studies on the MTO process have been carried out dealing with the effect of reaction conditions, influence of formed water, coke deposition, catalyst regeneration, or reactor design [382–389]. Kinetic models [390–397] were established and different catalysts such as silicoaluminophosphate SAPO-11 [385], SAPO-18 [398–401] or (H-)ZSM-X [402–405] (X stands here for various numbers, such as 5 or 22) instead of SAPO-34 were used for MTHC reactions. Objectives of these investigations were to find out advantageous conditions for methanol transformation into hydrocarbons with a high yield of desired olefins but also to derive the reaction mechanism. The temperature range was between 250 and 550 °C [390] in these studies.

The mechanism of the MTO reaction is still not clarified. More than 20 distinct mechanisms have been proposed concerning the first C–C bond formation for olefins starting from DME [377]. Union Carbide developed a process to convert methanol to olefins in 1986 using SAPO catalysts, which were invented by Union Carbide researchers [406]. The olefins yield exceeded 90 %, and they report that the process could be modified for high ethylene and propylene yield (about 60 %) [407–410].

Among the molecular sieves that have been investigated for use as oxygenate conversion catalysts, materials having the framework type of the zeolitic mineral chabazite (CHA) have shown particular promise. For example, SAPO-34 is a crystalline SAPO molecular sieve of the CHA framework type. It has been found to exhibit relatively high product selectivity to ethylene and propylene and low product selectivity to paraffins and olefins with four or more carbon atoms.

The preparation and characterisation of SAPO-34 have been reported in several publications [411–417]. In the early 1990s, UOP and Norsk Hydro carried out research activities for the MTO process. They used SAPO-34 as molecular sieve catalyst [418]. This catalyst showed an improvement in selectivity to carbon and light hydrocarbons up to 80 %, with dominantly light olefins at nearly complete methanol conversion compared to early Mobil pilot plant results on ZSM-5 catalyst.

The SAPO-34 catalyst is a microporous SAPO molecular sieve with CHA structure that has a pore size of only 3.8 Å [419–423]. Caused by the 8-membered ring of the SAPO-34, the chain length of the MTO product peaks at lower number compared to the 10-membered ring size of the ZSM-5 catalyst; however, along with this higher yield of lower olefins, a higher amount of C_1 as coke has to be accepted. Further information on the catalysts for MTO is found in Sect. 6.4 above.

Although microporous crystalline solid acids have been widely used for several decades in the chemical and petrochemical industry as catalysts for the conversion of aromatics [424] and the cracking of hydrocarbons [425], the industrial application of these types of catalysts for MTHC processes is still limited to few plants [426–431]. Due to the diversity of possible starting materials (e.g. coal, petroleum, natural gas, shale gas, pyrolysis oil from organic material, heavy fuel oil) and due to the relatively low dependence on the availability of crude oil, the method of synthesis gas to hydrocarbons via methanol becomes increasingly attractive with each energy crisis.

General Process Outline

General Process Description

In a review by Arné and Scheeline [432] on ethylene from synthesis gas, the economics of producing 1,000 million lb/yr of ethylene by direct Fischer–Tropsch synthesis from coal-derived synthesis gas was presented. The economics are compared with those of gas oil cracking and those of the conversion of methanol to olefins in all cases, a consistent set of feed and byproduct prices has been used. According to the authors, the economics for ethylene by direct synthesis are more favourable than that for the methanol route. These results must nonetheless be considered as speculative.

Process conditions and catalysts are selected accordingly so that the conversion of methanol or methanol equivalents to olefins is quantitatively accomplished. In addition to olefins and other hydrocarbons, water is a reaction byproduct.

It is expected that MTO processes will become the most important nonpetrochemical route for the production of light olefins from coal or natural gas—and in future, possibly from renewable carbon resources. A successful application of the MTO process requires a very high efficiency conversion of methanol to the desired products with very little by-product generation. The desired light olefins are dominantly propylene but also butylene and ethylene, all for the polymer industry. However, process variables must be carefully managed because the conversion of methanol to gasoline boiling components is a highly exothermic reaction.

The MTO reaction is strongly exothermic: Approximately 790 kJ (750 BTU) of heat per 450 g of methanol are released. This amount of heat release will result in an adiabatic temperature increase of about 649 °C (1,200 °F) for pure methanol feed. Therefore, two measures are taken to control the heat of reaction: (1) a two-step dehydration of methanol producing an equilibrium mix of methanol, DME, and water followed by a conversion of the mixture to olefins and (2) a suitable process concept, such as a multistage fixed-bed or fluidised-bed reactor.

In the first stage, methanol is catalytically converted to a mixture of methanol, DME and water to near-equilibrium. This mixture can then be processed, depending on catalyst and process conditions to either fuel (MTG) or olefins (MTO, methanol-to-propylene [MTP]), where $[CH_2]$ is the average composition of the hydrocarbon product, comprising olefins and aromatics plus paraffins according to Eq. 6.12. The light olefins react to paraffins, aromatics, naphthenes and higher olefins by hydrogen transfer, alkylation, and polycondensation. The above scheme is not a chemical reaction equation. It is still unclear whether the first product of all microporous solid acids is ethylene [433].

It is generally assumed that the first intermediate in the dehydration of methanol to DME (step 1 in Eq. 6.12) on solid acid catalysts is a protonated methoxy group on the surface. According to the previously cited review articles, a nucleophilic attack of methanol on the methoxy group is anticipated, but this assumption as well as the subsequent conversion to light olefins and further to paraffins, aromatics, naphthenes and higher olefins is not yet fully elucidated. For the first step (i.e., the

first C–C coupling), the following mechanisms are discussed: the oxonium ylide mechanism, the carbene mechanism, the mechanism of free radicals, the carbocation mechanism, the mechanism by consecutive addition of C_1-building blocks, and the so-called hydrocarbon pool mechanism.

With respect to the 8-membered ring molecular sieve catalysts for MTO, the ExxonMobil group of Xu and White were the first to determine the structure of the carbon pool that was active in the MTO reaction in 8-membered ring systems, such as H-SAPO-34, the first MTO catalyst system that was more precisely understood in view of the reaction mechanism. Their work, which began in 1998, resulted in the filing of two patents in early 2000, claiming for the first time that the hydrocarbon pool contains dominantly methyl-aromatic structures (e.g. toluene, xylenes, methylnaphthalenes) [434, 435].

The subsequent reactions of paraffins, aromatics, naphthenes and higher olefins are generally assumed to proceed in a known manner via a classical carbenium ion mechanism with simultaneous hydrogen transfer [436]. Although the mechanism of the first carbon–carbon bond formation has little relevance for the activity and selectivity of the dehydration of methanol or DME, there are numerous experimental and theoretical studies for the more than 20 proposed mechanisms [377]. None of these efforts, however, have so far led to a rational design for an improved catalyst and process. The reason is that the main influences on the dependence of the activity and selectivity on the process parameters are known from experimental work since the early development of MTHC processes, but the final products strongly depend on the specific process parameters and also depend on the particular catalyst properties. The detailed on-stream catalytic properties in the experiments of the various laboratories can only partially be reproduced or simulated.

As a consequence of the partially irreversible formation of byproducts such as coke and due to partially irreversible changes of the catalyst under reaction conditions (caused by the presence of steam at the high temperatures), the formation phase may take several days until a reasonably stable steady state is reached. When interpreting experimental results, it is therefore necessary to be sure that the results were obtained in a reasonable steady state. In addition, when experimental results are compared, it should be noted that the selectivity is often related only to the products at the exit of the catalytic reactor system; instead, consider the total carbon balance (i.e., take into account the remaining coke on the catalyst). For more details, see Sect. 6.4 above.

The exothermic character of the conversion reaction requires careful management of the methanol feed rate in terms of weight hourly space velocity (WHSV) based on catalyst loading. Methanol breakthrough—a term indicating the appearance of methanol in the aqueous product stream and, therefore, less than quantitative conversion—has generally been followed to signal the end of the process cycle and the need to regenerate catalyst. The number of methanol conversions at which the cycle limit is set depends on the particular design of the downstream workup equipment (i.e., the methanol and the DME recovery section). Usually, the cycle is finished if the conversion drops below 99 %.

How could the high level of MTHC technology be achieved? With respect to the catalysts, this is discussed in Sect. 6.4 above, taking the two most important representatives (i.e., ZSM-5 and SAPO-34) as examples.

The MTO Process

Today, two major designs for the MTO process are applied: the fixed-bed process and fluidised-bed process. The fixed-bed process operates on the basis of a protonated ZSM-5 catalyst. In the fluidised-bed process, H-ZSM-5 as well as H-SAPO-34 zeolite catalysts are applied.

Fluidised-Bed MTO

Mobil Pilot and Demonstration Plant

Mobil Oil developed a fluid bed process for methanol conversion initially for MTG (see Sect. 6.4.1) and later for MTO [437, 438]. For both processes, the Mobil ZSM-5 catalyst was used. The 100-BPD (approximately 11.56 m^3/day) fluid-bed MTG demonstration plant was constructed at the facilities of Union Rheinische Braunkohlen Kraftstoff AG in Wesseling, Germany [439]. The three industrial participants were Mobil Research and Development Corporation (MRDC), Uhde GmbH, and Union Rheinische Braunkohlen Kraftstoff AG.

The MTO process was developed by MRDC initially in laboratory scale and thereafter in a 4-BPD fluid-bed pilot plant. The latter was scaled-up to the existing 100-BPD MTG demonstration plant after converting the MTG mode to MTO by some modifications. This MTO programme included the following [437]:

- Pretests in MRDC's 4-BPD pilot plant to evaluate the preferred range of operating conditions set for the 100-BPD plant operation.
- Design and construction of plant modifications according to the new process conditions.
- Nine months of operation in the 100-BPD plant.

The simplified flow scheme is shown in Fig. 6.67. The reaction system contained two major vessels: the dense fluid-bed reactor (0.6 m internal diameter, 18 m in height), incorporating the cooling coils for reaction heat removal and the catalyst regenerator:

> The methanol was vaporised and fed to the reactor. The operating conditions were set so that a complete conversion is achieved. The catalyst was separated from the product gas and returned to the reactor. The product was cooled and separated downstream into gaseous hydrocarbons, C_{5+} hydrocarbons and water. The coke deposited on the catalyst in the reactor was burned off in the regenerator, with continuous catalyst circulation between the two vessels. [439]

The MTG process can be modified so that the hydrocarbon selectivity shifts towards olefin production MTO [440]. Gasoline and distillate can be co-produced

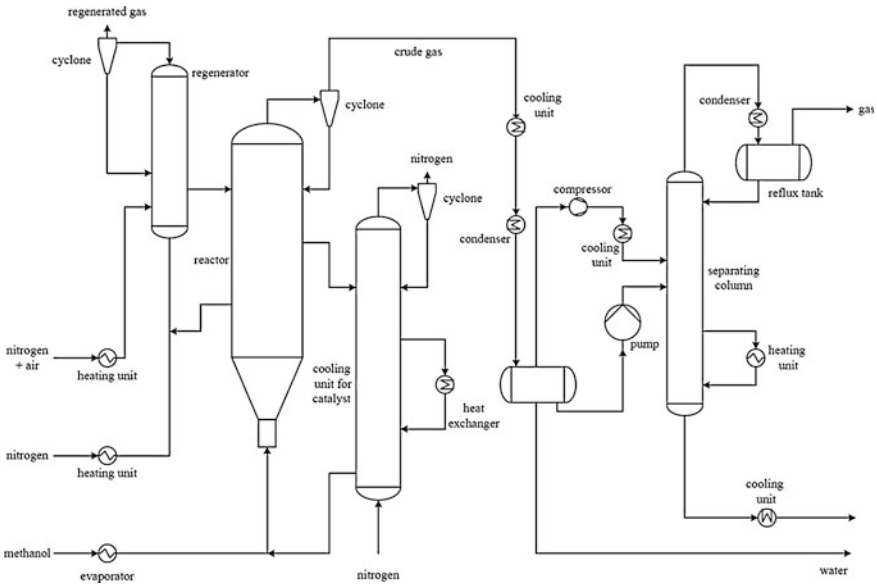

Fig. 6.67 Gasoline mode of the methanol-to-olefins gasoline plant at Wesseling, Germany (© Uhde, ExxonMobil)

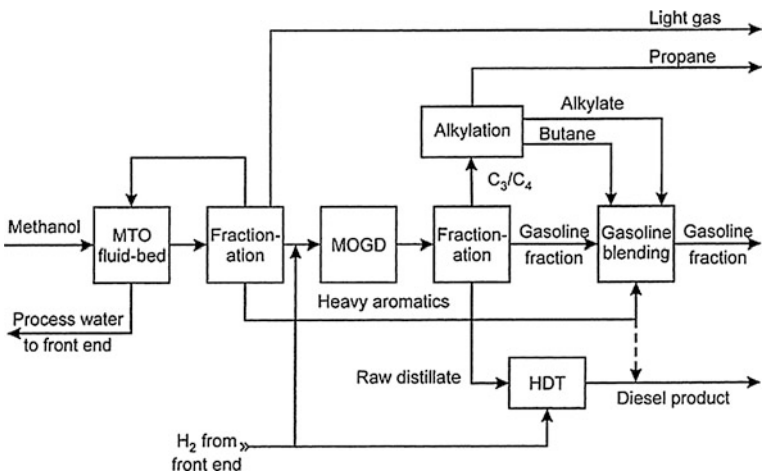

Fig. 6.68 The Mobil olefins-to-gasoline and distillate process (MOGD) flow scheme. MTO, methanol-to-olefins. (© Elsevier)

using an olefin oligomerisation step, such as MOGD [441, 442]. A scheme for the manufacture of gasoline and distillate from coal via Mobil processes is shown in Fig. 6.68.

Process Description

Pretest studies were conducted by MRDC in their 4-BPD fluid-bed unit to determine the effects of temperature, pressure and space velocity on MTO product selectivity. The results of these studies defined the preferred range of operating conditions for the 100-BPD unit. The 100-BPD MTO and MTG plant operating conditions are summarised in Table 6.13 [437].

Table 6.13 The 100-BPD methanol-to-olefins (MTO) and methanol-to-gasoline (MTG) process conditions

	MTG	MTO
Temperature, °C	380–430	470–515
Pressure, kPa	270–450	220–350
MeOH feed rate, kg/h	500–1,000	580–620
Hours on stream	8,600	3,600
On-stream factor, % Including scheduled shut-downs	65	57

The 100-BPD MTO plant was started up on February 22, 1985. According to Keim et al., "MTO operation started with a sensitivity study to determine the effect of reaction temperature on product selectivity (Fig. 6.69). This was followed by a pressure sensitivity study, and a steady state run was established in order to determine the fresh catalyst make-up requirements for continuous operation to compensate for chemical deactivation"[439] (Fig. 6.69).

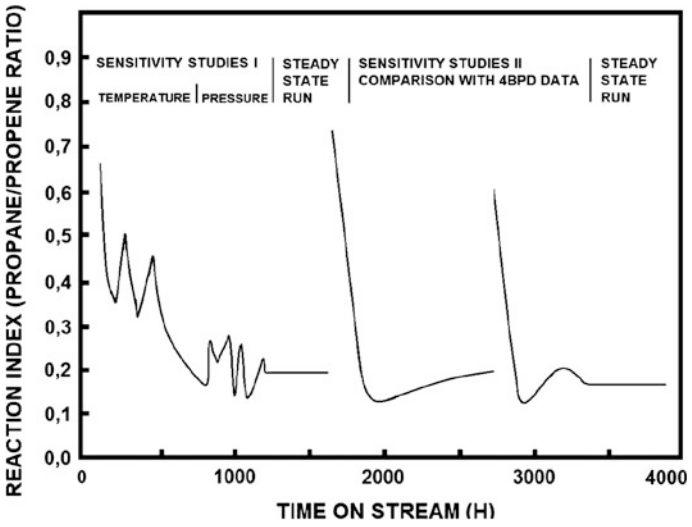

Fig. 6.69 Catalyst activity versus on stream hours [439]

A steady-state run at optimised MTO conditions, including ethene recycle simulation, could be demonstrated. The ethene recycle increases the process efficiency of the methanol-to-hydrocarbon reactions with respect to propylene because the product distribution of ethene conversion is very similar to that of methanol conversion.

The propane/propene ratio (also named reaction index, selectivity index, or R-factor) correlates with catalyst activity. With increasing cycle time, the R-factor decreases because the yield on olefins increases. The selectivity (particularly the yield) of light olefins increased by about 7 % when the reaction temperature was raised from 470 to 515 °C. Disadvantages of higher temperature are higher coke and light saturated hydrocarbons yields. Decreasing pressure allows the same conversion to be achieved at a lower reaction index, again increasing olefin yield.

The steady-state runs were performed at constant methanol conversion above 99.9 % and constant coke level on the catalyst. The catalyst makeup rate was lower than 0.5 wt% of catalyst inventory/day. This is equivalent to that observed at MTG conditions [437].

The MTO process allows remarkable shifts in olefin selectivity by adjustment of reaction conditions. This has a direct impact on the gasoline/distillate ratio in the combined MTO/MOGD processes.

The 100-BPD MTO plant had accumulated:

- 12,200 h of MTG/MTO operation, including 3,600 at MTO conditions.
- The actual MTO time on-stream factor was 57 %.
- 9,000 tonnes of methanol were processed, including 2,130 tonnes during MTO operation.

The scale-up of the fluid-bed MTO process has been successfully demonstrated in the 100-BPD plant. Results obtained in this unit are in close agreement with those obtained in the 4-BPD pilot plant under the same conditions: The total olefin yield for the 100-BPD demonstration plant was similar to that from the 4-BPD plant, and the methanol breakthrough occurred at approximately the same reaction index for both units. Lower pressure and higher temperatures were shown to increase olefin yields at constant methanol conversion [437].

UOP/Hydro Fluidised-Bed

The UOP/Hydro MTO process uses a fluidised-bed reactor system for both olefin synthesis and regeneration, like shown in Fig. 6.70. The raiser regenerator principle is known from the FCC process that is used in petroleum refining. Due to this catalyst management, a high stability and abrasion resistance of the catalyst is necessary, and resistance of the used catalyst towards frequent regeneration is essential.

The fluidised-bed system was chosen for two reasons: (1) due to the fact that MTO conversion is a strongly exothermic reaction, it is necessary to remove the high exothermic heat; and (2) the stronger coking tendency of the UOP catalyst compared to the Mobil ZSM-5 in the Mobil 100-BPD demonstration plant requires frequent regeneration of the catalyst.

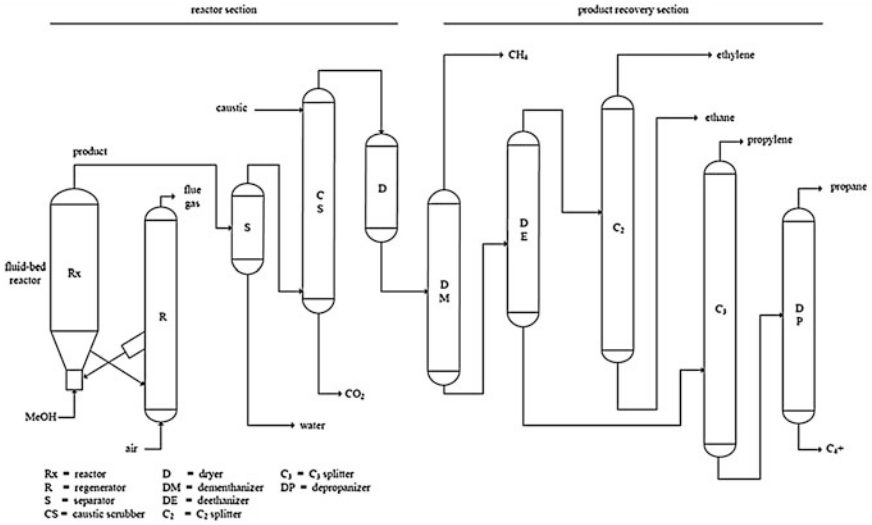

Fig. 6.70 UOP/Hydro methanol-to-olefins process [369]

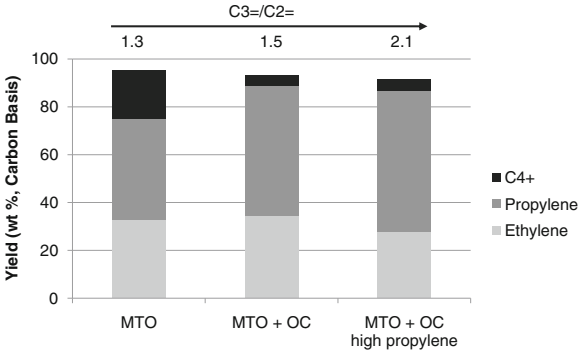

Fig. 6.71 Propylene/ethylene ratios: comparison of the methanol-to-olefins (MTO) and MTO/olefin cracking processes. OC, olefin cracking. (Adapted from [423])

Because the oxygenate impurities in the olefinic product are harmful for the downstream production of polyolefins, it is necessary to install additional equipment for removal of the major oxygenates from the product. A positive side effect of recycling these oxygenates back to the conversion reactor is the increase of the olefin yield.

The propylene/ethylene ratio can be adjusted in a wide range between 0.77 and 1.33, with a carbon-based total olefin yield of approximately 75–80 %. Process parameters are 350–600 °C and 1–6 bar [433]. At higher temperatures, more olefins are formed. However, because the SAPO-34 catalyst favours the

formation of light olefins, a higher yield of ethylene is perceived, which leads to an enhanced coke deposition and thereby in the end reduces the total olefin yield.

By an integration of the MTO process with the olefin cracking process developed by Total/UOP [423], a further boost of the propylene/ethylene ratio over 2.0 is possible. Thus, the selectivity to light olefins can be increased to about 85–90 % (Fig. 6.71).

The ExxonMobil Fluid-Bed MTO Process

In 1984, Mobil Oil filed a patent related to the conversion of alcohols and related oxygenates in a riser reactor and dense fluid catalyst bed comprising a ZSM-5-type catalyst circulated through a plurality of satellite stripping-cooling zones for temperature control [443]. Remarkably, they also claimed a partial regeneration to be advantageous for higher selectivity to olefins: their catalyst used 5–30 wt% coke for activity and selectivity control, promoting the formation of olefins and aromatics at temperatures below approximately 427 °C (Fig. 6.72).

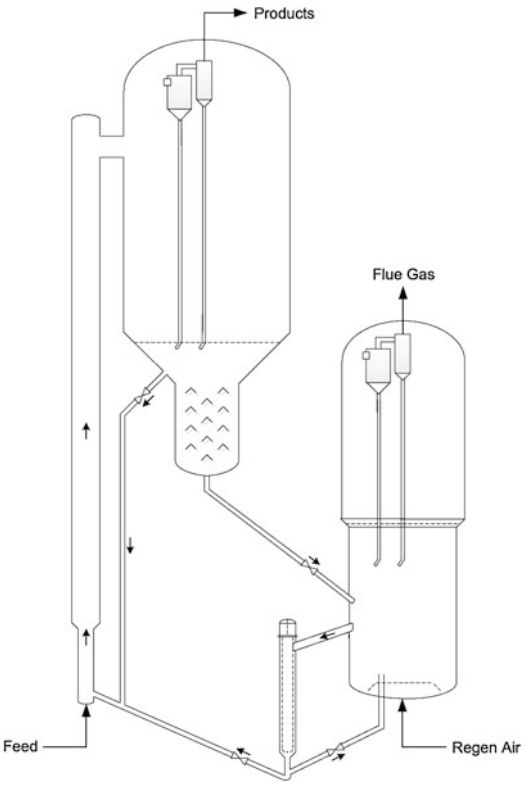

Fig. 6.72 ExxonMobil fluidised-bed methanol-to-olefins process. (Adapted from U.S. Patent 6,023,005 [444])

DMTO Technology

The DICP (Dalian Institute of Chemical Physics, Chinese Academy of Sciences) methanol-to-olefins (DMTO) technology converts methanol as the reactant to produce light olefins, such as ethylene and propylene for the further production of PE and PP. The first DMTO commercial unit in the world, with a production capacity of 600,000 tonnes of lower olefins per year, proved to be completely successful in its first commissioning operation in August 2011.

Chicago Bridge and Iron Company announced the process of converting syngas via DME to light olefins [445]. The syngas is produced by coal gasification. The gasification unit is one of the world's largest coal-to-olefins projects and started up successfully at the China Shenhua Coal to Liquid and Chemical Company's project in Baotou, Inner Mongolia (Shenhua Baotou Coal to Olefins project). The gasification unit uses advanced coal gasification technology provided by General Electric.

The plant combines the DMTO methanol-to-olefins technology of SYN Energy Technology with the Lummus Technology. Start-up was in Baotou, China. After the two commercial MTP plants in China (Shenhua Ningxia Coal Industry Group [446] in northwestern Ningxia province; see Sect. 6.4.3), this is the world's third MTO unit operating on a commercial scale. The plant is owned by China Shenhua Coal to Liquid and Chemical Company [447]. The technology enables licensees to produce olefins (ethylene and propylene) from methanol. The plant is designed to produce 600,000 tonnes per annum of olefins from methanol. On-spec ethylene and propylene product were achieved less than 72 h after methanol was introduced to the unit.

DICP developed the technology called DMTO consisting of coal gasification to obtain methanol, which is then converted to light olefins. The plant can convert 1.8 million tonnes of methanol per year into 600,000 tonnes per year of ethylene and propylene. This conversion takes place at a pressure slightly higher than the normal pressure, at a temperature between 400 and 550 °C. By variation of these operating conditions, the propylene/ethylene ratio changes between 0.8 and 1.2. A fluidised-bed catalytic reactor provides the ethylene and propylene, as well as butene, 1– 2 % coke and other light products and 55 % water [448].

Fixed-Bed MTO

The fixed-bed MTO is offered as a standalone process by Lurgi. Lurgi also offers the MTO technology as part of the Lurgi MtSynfuel process. Originally on behalf of the Central Energy Fund of South Africa in the late 1980s, Lurgi developed a fixed-bed MTO process aiming for 50 % olefins and 50 % gasoline. Using the economically highly attractive technologies of MegaMethanol and MTO, which compares to the MTP process with slightly different operating parameters, it was already proposed by Mobil [449] to combine the MTO technology with a conversion of olefins to diesel, with the latter being an industrially proven process. A gas-based synfuel plant using this process, then named COD, was developed and built by Lurgi for Mossgas (today PetroSA), RSA, in 1992 and has been performing well since its start-up in 1993. Remarkably, the industrial design was

based on a scale-up factor of 3,600 over the preceding demonstration plant. This basically was possible through the use of fixed-bed catalysis (on zeolite basis), which lends itself to easy scale-up. Other important process features are semi-continuous operation and a 98 % conversion of C_3- and C_4-olefins.

For the stand-alone fixed bed process, ethylene and propylene are the target products and gasoline is regarded as byproduct. In case of the MtSynfuel process, the ratio of olefin-based diesel to gasoline can be adjusted according to the market needs simply by adjusting the operating parameters. Compared to all other carbon valorisation, the MtSynfuel process has the highest flexibility. The Fischer–Tropsch technology is much less flexible. The MtSynfuel process allows the sale of DME, methanol, light olefins, gasoline, or diesel in optional ratios out of one single MegaMethanol plant. The plant has a capacity of more than 1 million metric tonnes per year, with the actual "standard" size being $1.7 \cdot 10^6$ t/a (equivalent to 5,000 t/d) (Fig. 6.73).

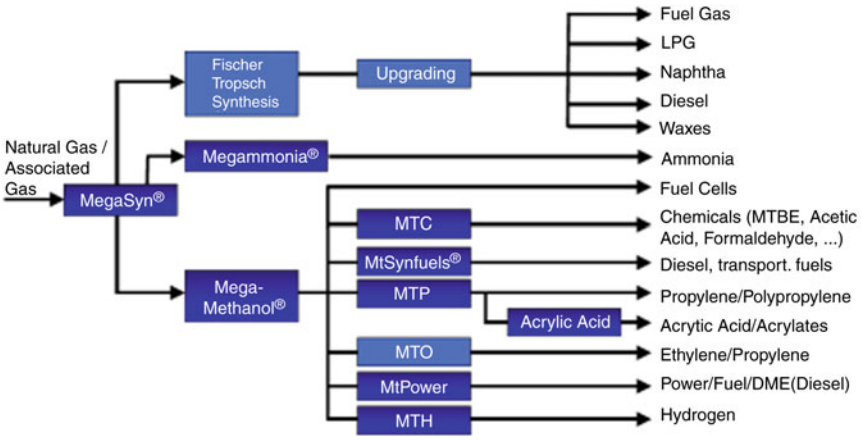

Fig. 6.73 Methanol to chemicals and fuels. DME, dimethyl ether; LPG, liquefied petroleum gas; MTO, methanol-to-olefins; MTP, methanol-to-propylene. (© Lurgi)

Boosting Olefin Yield: The Olefin Interconversion Processes

New propylene technologies, including propylene recovery from refineries, propane dehydrogenation (e.g. the Catofin or the Oleflex process), natural gas or coal conversion to light olefins via methanol (e.g. the Lurgi MTP process or the UOP/Hydro MTO process) and olefins to olefins conversion are gathering momentum. The latter includes ethylene-butene metathesis, as well as more recently developed olefins cracking technologies, such as the Lurgi Propylur process or the ATOFINA/UOP olefin cracking process (OCP) [450].

Olefin interconversion gets particular attention to boost the propylene yield from MTO or MTP plants by converting C_{3+} olefins to C_2–C_3 olefins. Olefin interconversion is offered for licensing by ExxonMobil/Washington (MOI),

Lyondell/Halliburton KBR (Superflex), ATOFINA/UOP olefin cracking process, and Lurgi/Linde (Propylur). These processes are based on thermodynamic equilibrium of olefins. Using a suitable catalyst, such as a modified ZSM-5 or other zeotype, higher olefins like C_4 and C_5 can be converted to lower olefins. Ethylene is not consumed. Propylene is the target product. Two types of technologies are offered on the market: fixed-bed and moving-bed technologies.

Fixed-Bed Process

Two fixed-bed processes are known: the Lurgi olefin conversion process [451] and the ATOFINA/UOP olefin cracking process.

The Lurgi Olefin Conversion Process

BP Köln (Cologne, Germany) demonstrated that for a C_4 cut, approximately 85 % of the C_4 olefins are converted. The Propylur plant was converting an olefin cut to propylene at yields of 60 %, with an additional 15 % yield of ethylene. A shape-selective heterogeneous ZSM-5 zeolite type catalyst, developed by Clariant (former Süd-Chemie), was used in a fixed-bed reactor operating at 500 °C and 1–2 bar. Steam was added to promote the selectivity of the reaction and reduce coking and polymer formation. The liquid C_4/C_5 feedstock is vapourised and mixed with the steam. However, dienes should be hydrogenated upstream of the unit to keep coking low.

The hydrocarbon/steam mixture is heated in a fired heater before entering the fixed-bed adiabatic reactor. By cooling the reactor effluent, the steam is condensed and separated, together with some gasoline byproducts. The remaining vapour is compressed to carry out the C_3/C_4 separation at reasonable temperatures. The C_4/C_5 stream from the depropaniser bottom is partially recycled to increase the overall propylene yield. A typical reactor product contains about 42 wt% propylene, 13 wt% ethylene and 31 wt% butenes. Due to the mild cracking conditions, the cycle length allowed the use of discontinuous in situ regeneration.

The ATOFINA/UOP Olefin Cracking Process

The Total Petrochemicals/UOP olefin cracking process converts C_4–C_8 olefins to propylene and ethylene at a high propylene/ethylene ratio. A demonstration unit was started up in 1998 at an industrial facility located at Antwerp, Belgium, which processes feed stocks from a commercial operating plant. The demonstration plant includes feed pretreatment, reactor section, catalyst regeneration facilities and internal recycle capabilities.

The ATOFINA/UOP olefin cracking process features fixed-bed technology, high space velocity, low reactor pressure (1–5 bar), 500–600 °C reactor temperature and a swing regeneration system. The process uses a proprietary zeolitic catalyst that yields 95 % propylene and ethylene in C_3 and C_2 fractions, while maintaining high olefin conversion. A key advantage of OCP is the absence of steam diluent, minimising the reactor size and saving on capital and utility costs. Unlike metathesis processes, the ATOFINA/UOP olefin cracking process does not consume valuable ethylene.

The chemistry of higher olefins cracking is more complex than it might appear at first glance. For example, butenes do not crack to $C_3 =$ or $C_2 =$ directly. Studies showed that butenes (and to some extent, higher olefins) oligomerise first; then, the oligomer species selectively crack to propylene and ethylene. The propylene/ethylene ratio is a function of the relative abundance of secondary and primary carbenium ions and therefore strongly depends on the temperature. C_5 and higher olefins can crack directly; therefore, higher ethylene yield is favoured if C_5-rich feed is used. Naphthene conversion under OCP conditions is negligible, whereas cyclo olefins tend to convert to aromatics. If C_6–C_8 aromatics are present in the feed, the toluene/benzene product ratio goes up, which can be important when the byproducts are blended into gasoline pools with limitations on benzene content.

An OCP unit can be integrated with an existing or grassroot plant that has olefinic products available, such as an FCC unit in a refinery, a steam cracker, or an MTO complex. An OCP unit has a very good potential for integration with an MTO unit. Because an MTO unit is designed primarily for stranded natural gas regions, the C_4–C_5 byproducts, which otherwise could be used, for example, as alkylation feed stocks, have very little value in such areas. Integration with an OCP unit increases overall light olefins production and can increase the propylene/ethylene weight ratio to as high as about 1.75:1. The improved utilisation in methanol for light olefin production can result in more than a 10 % reduction in methanol consumption for a fixed light olefin production [452].

Moving-Bed Process

An economical unit for processing large volumes of olefin-containing feedstocks to produce world-scale quantities of on-purpose propylene requires appropriate selection of a reaction system for the production, as well as downstream processing facilities for the recovery of the desired petrochemical products. A fluid solids reactor/regenerator configuration is well suited for such large-capacity units. Two moving bed processes are known: KBR Superflex and ExxonMobil MOI.

Superflex

In 2002, KBR (Houston, TX), the engineering and construction subsidiary of Halliburton, was building a 250,000 metric tonnes per year propylene and ethylene production facility for Sasol Technology's Synfuels Catalytic Cracker Project in Secunda, South Africa. KBR employed its Lyondell-licensed Superflex technology, which selectively converts light hydrocarbon streams to propylene and ethylene. JiHua is the second Superflex licensee, located in Jilin City, China. This unit, when commissioned, will have a design capacity of 200 kt/a of propylene production from C_4/C_5 feed.

The ExxonMobil PCCSM Process

ExxonMobil developed an on-purpose propylene technology based on catalytic naphtha cracking, called the ExxonMobil PCCSM Process. This process offers significant advantages over prior systems. The development of this technology was driven by the need for increased volumes of propylene to supplement supplies of

propylene currently produced as co-products in steam cracking and fluid catalytic cracking. The PCC process provides a possibility converting olefin molecules in naphtha streams to high value ethylene, propylene and (optionally) butylene. The process is also suitable to convert C_{4+} olefins from a MTP plant into C_2–C_3 olefins, thus boosting the yield of light olefins.

Advantages of a fluid-bed process include the following:

- No steam dilution (as in the case of Propylur)
- Continuous regeneration (i.e., no swing)

Disadvantages of a fluid-bed process include the following:

- High capital expenditure
- Operation has turned out to be not easy
- High scale-up efforts necessary

Summary

In Table 6.14 [453], a summary of natural gas-to-olefins routes is presented. All yields shown are maximum yields and are given as the mass weights of products divided by that of natural gas. Feedstock is natural gas to methanol via syngas.

Table 6.14 Summary

Technologies	UOP MTO[a]	ExxonMobil MTO[b]	Lurgi MTP[c]
	Via methanol and DME	Via methanol and DME	Via methanol and DME
Reactors	Fluidised-bed	Fixed-bed demonstration plant and fluidised-bed	Fixed-bed commercial plant
Catalysts	Silico-aluminophosphate (SAPO-34 or MTO-100)	MTO-100 ZSM-35, SAPO	ZSM-5
Temperature °C	350–525	350–500	450
WHSV			25
Ethylene yield	26 % with C_{4-5} upgrading	14 %	Negligible
Propylene yield	33 % with C_{4-5} upgrading	18 %	46 %
C_{4-5} yield	9 % (without upgrading)	Negligible	Negligible
Gasoline yield	Negligible	29 %	20
Fuel gas yield	2 %	0.1 %	6
Water yield	83 %	81 %	81 %
Total HVCs yield	62 %	45 % (61 % if gasoline is weighted 100 %)	57 % (65 % if gasoline weighted 100 %)

[a] UOP MTO data is based on Refs. [454, 455] Olefin upgrading data is based on Refs. [456, 457].
[b] ExxonMobil MTO data is based on Refs. [458, 459].
[c] MTP data is based on Refs. [460–462].
DME, dimethyl ether; MTO, methanol-to-olefins; MTP, methanol-to-propylene; WHSV, weight hourly space velocity.

Comparison of Fluidised-Bed (SAPO-34) and Fixed Bed (H-ZSM-5)

The striking differences in process design are simply a consequence of the different catalysts used. The SAPO-34 catalyst is more selective with respect to ethylene and propylene but suffers from severe coking, which requires very frequent regeneration. The ZSM-5 catalyst is less selective but much more stable due to a very low coking tendency.

The findings of Yingxu et al. [463] regarding an extensive and accurate investigation of the coke laydown in MTO reaction on CHA type zeolites are of utmost importance to underline the superiority of the MTP process compared to the UOP MTO process with respect to carbon efficiency. In case of the fluidised-bed process using SAPO-34 as catalyst, approximately 10 % of the carbon atoms in the methanol are burned to CO_2 upon regeneration. Moreover, apart from the environmental aspects, from a commercial point of view the fact that the Lurgi MTP process does not convert 10 mol% of the methanol feed to CO_2 upon regeneration translates into an economical advantage. Although the MTP process reveals also a small formation of carbon, there is still a clear benefit for the MTP process even if the loss caused by the lower value of the gasoline by product generated in the MTP process is compared to the higher propylene value in the case of the SAPO catalyst. It is assumed that the Dalian process uses the SAPO-34 catalyst. To date, there has been no confirmation of that assumption.

MTO/MTP Market

Details related to the global methanol market are discussed in Sect. 1.3. China has taken a leading role in the growth of the global methanol industry. The country already accounts for a little more than 40 % of demand, and its share is set to expand rapidly in the coming years. According to ICIS, China has become the main driver of global methanol markets. China has seen double-digit growth in methanol demand, with strong performances in the acetic acid sector, methanol blending in gasoline and the nontraditional sectors, which include MTO/MTP and DME. This production currently totals to about 10 million tonnes per year of methanol, which is about a third of China's total methanol consumption of about 30 million tonnes per year [464]. In the same source, it is reported that China will remain a driving force in the global methanol market.

Particularly in the area of feedstocks for the petrochemical industry, there has been considerable interest in MTO and MTP technologies, with pioneering projects in China because many producers are turning to coal-based methanol production. Coal-to-olefins project proponents in the country are looking for sites near coal mines where abundant coal can be sourced without having to incur transportation costs.

As for MTP economics, Lurgi estimated that the investment costs of starting up an MTP project in China would be much less than in the Arabian Gulf due to cheaper construction costs. However, because Chinese projects are mostly coal based, this would result in higher costs in the syngas production section. Hence, the overall investment and economics might be similar to that of a project in the Middle East.

Although Lurgi's technology is focused on propylene production, given the forecasts of a growing gap between supply and demand for this product, it can also deliver up to 8 % of ethylene, allowing the production of highly valuable high-impact polypropylene (see Sect. 6.4.3). The production of ethylene from MTO units will hardly be competitive to that from gas crackers in the Middle East. If necessary, an ethylene recycle increases the process efficiency of methanol-to-hydrocarbon reactions with respect to propylene, as was described here. However, the situation could be different in China, where ethylene production is mainly based on naphtha.

Ethylene will be produced cheaply from Middle East gas crackers; the MTO route based on natural gas or coal presently cannot beat this. For example, it will be more economical to import PE from the Middle East to China. As of 2005, it was expected that the production of propylene and PP from naphtha crackers and FCCs would be very competitive if only propylene (and PP + co-polymer) was produced [465]. The actual figures for 2013 are not yet available for various reasons (see Sect. 6.4.3). However, with China being the most important economy in Asia, it is pursuing MTO and MTP projects because of its huge reserves of coal, which in China is the most important raw material for methanol:

> Coal-produced methanol provides the country with a strong cost advantage over naphtha-based petrochemical production during times when oil prices are high. In China, sixteen MTO and methanol-to-propylene (MTP) projects spread across the country with a total capacity of around 10 million tonnes per year are due to come on stream from 2012 to 2015. By 2015, MTO/MTP is expected to account for more than 17 % of China's methanol demand, assuming all the other projects came on line as planned [466].

Four of the 16 MTO/MTP projects, with a combined capacity of 1.76 million tonnes/year, started production in 2012. Construction of the remaining 12 projects is expected to start soon.The existing MTO/MTP projects are listed in Table 6.15. MTO/MTP projects that are expected to be commissioned until 2015 are listed in Table 6.16.

Table 6.15 Existing methanol-to-olefins projects

Project	Location	Unit	Capacity	Status
Datang international power generation	Inner Mongolia	MTP	460,000 tonnes/year (1.68 million tonnes/year integrated methanol supply)	Operating
Shenhua group (Baotou)	Inner Mongolia	MTO	600,000 tonnes/year (integrated 1.8 million tonnes/year methanol unit)	Stable operation, unknown rates
Shenhua Ningxia coal industry group	Ningxia	MTP	500,000 tonnes/year (integrated 1.67 million tonnes/year methanol unit)	Operating
Sinopec Zhongyuan petrochemical	Henan	MTO	200,000 tonnes/year	80 %–90 %
Total			1,760,000	

MTO, methanol-to-olefins, MTP, methanol-to-propylene

Table 6.16 Upcoming approved methanol-to-olefins projects (planning projects excluded)

Project	Location	Unit	Capacity (tonnes/year)	Start date
Ningbo Heyuan (Skyford)	Zhejiang	MTP	600,000	November 2012
Zhejiang Xingxing new energy technology	Zhejiang	MTO	600,000	Pending; no exact startup date
Wison Nanjing Clean Energy	Jiangsu	MTO	300,000	2013
Zhengda (Changzhou) new material	Changzhou	MTO	1,000,000	2013
Shaanxi Pucheng clean energy chemical	Shaanxi	MTO	700,000 (300 kt/yr of ethylene, 400kt/yr of propylene; integrated methanol capacity 1.8 million tonnes/year)	2014
Ningxia coal industry	Ningxia	MTP	500,000	2014
Shanxi Coking	Shanxi	MTO	600,000 (existing methanol capacity 200,000)	End of 2014
Shenhua Shenmu chemical	Shaanxi	MTO	600,000	2014
Jiutai energy (Zhungeer)	Inner-Mongolia	MTO	600,000	2014
Sinochem (Zhonghua) YiYe	Shaanxi	MTO	800,000	2014
Shaaxi Yanchang (joint venture with Zhongmei)	Shaanxi	MTO	600,000	2014
Xinjiang Guanghui coal chemical industry	Xinjiang	MTO	1,000,000	2015
Total			7,900,000	

MTO, methanol-to-olefins, MTP, methanol-to-propylene

6.4.3 Methanol-to-Propylene Process

Sven Pohl[1], Ludolf Plass[2] and Friedrich Schmidt[3]

[1]*Air Liquide Global E&C Solutions, c/o Lurgi GmbH, Lurgiallee 5, 60439 Frankfurt, Germany*
[2]*Parkstraße 11, 61476 Kronberg, Germany*
[3]*Angerbachstrasse 28, 83024 Rosenheim, Germany*

Introduction

Methanol is currently one of the most important feedstocks for the chemical industry. Most of the nearly 60 million tonnes of methanol produced in 2012 are used for the production of a large variety of chemical products, such as

formaldehyde (approximately 30 %), acetic acid (approximately 9 %) and methyl tert-butyl ether/tert-amyl methyl ether (13 %). According to De Witt [467] approximately one-third of the production is consumed by the fuel sector.

In recent years, there has been a greatly growing interest in the conversion of coal-based synthesis gas or natural/associated gas via methanol to synthetic high-value petrochemical commodities and products that can be supplied to the consumer market. The driving forces to use coal-based or natural/associated gases include the following:

- Availability of abundant and competitive resources.
- Constant high crude prices.
- Advantageous spread between gas and crude oil pricing.
- Interest in diversifying the fuel supply.
- Minimised operating cost.

A strong growing demand comes from MTO and methanol-to-propylene (MTP) plants, which have recently started operation (approximately 4 million tonnes in 2012; see Sect. 6.4.2). Methanol-derived light olefins (ethylene and propylene) can replace such light olefins from cracker operation (in some applications), especially because of the growing price differences between oil and natural gas/coal (see Fig. 6.74).

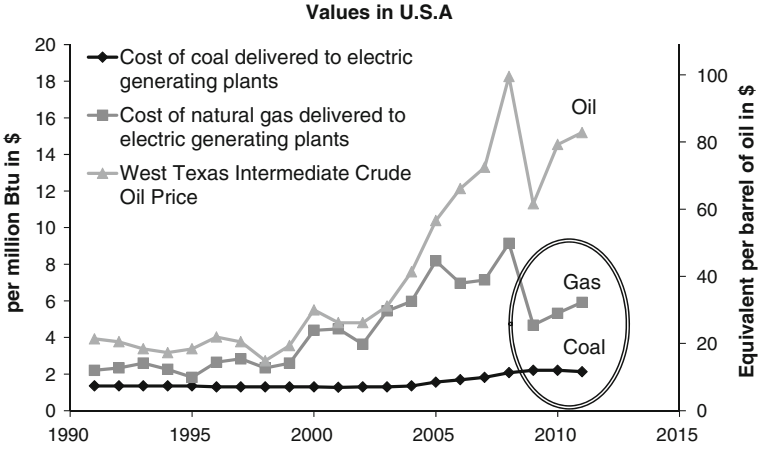

Fig. 6.74 Prices illustrate the growing advantage of using feedstocks derived from natural gas and coal[468]

Ethylene and propylene are by far the two largest volume chemicals produced by the chemical industry. Approximately 120 million tonnes of ethylene and 80 million tonnes of propylene were consumed worldwide in 2011 [467]. The demand for propylene is growing at a faster rate (approximately 4.5–5 % per year; in China 6 % per year) than that of ethylene (approximately 3–4 % per year). Because the majority of both chemicals is still produced by steam cracking and

fluid catalytic cracking, resulting in a given ratio of both chemicals, the increasing imbalance will need to be compensated by "on-purpose" production of propylene.

Technologies used for on-purpose production are mainly propane dehydrogenation (PDH), metathesis, olefin cracking and to a growing extent, MTO (see Sect. 6.4.2) and MTP. The common chemistry of MTO, MTP and MTG was described in Sect. 6.4. Figure 6.75 shows the projected strong increase of propylene from MTO/MTP plants through 2016 .

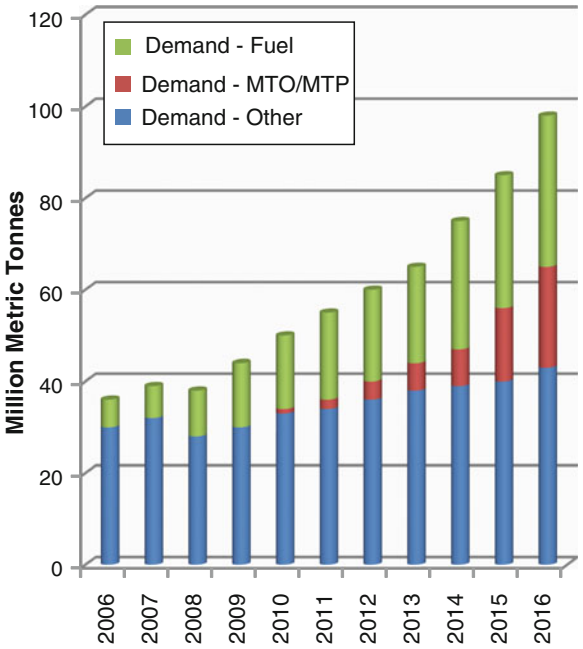

Fig. 6.75 Development of methanol-to-olefin (MTO) and methanol-to-propylene (MTP) demand through 2016 [469]. Fuel demand AAGR for 2006-2011: 9.2 %; MTO/MTP demand AAGR 2011–2016: 61.2 %; other demand AAGR 2011-2016: 4.6 %

The propylene demand is rising steadily, at an average of 6 % per year in the Chinese economy. Target production for propylene in China is an increase from approximately 13,500 kilotonnes (kt) per year in 2010 to 21,600 kt/year in 2015 [470]. To achieve this target, a large number (some sources mention up to 36) of coal-to-olefins projects are in the process of planning, erection, commissioning, and/or operation in China. Figure 6.76 shows a selected number of such projects in China, which are in operation or in the confirmed erection/planning phase.

Recent updates are given in Tables 6.17 and 6.18 below. The existing MTP projects with a combined capacity of 0.96 million tonnes per year have started production recently after a successful guaranty test with entire in-spec performance. However, according to ICIS [471], as of spring 2013 none of them could run at full capacity, partly due to poor petrochemical markets.

By 2015, MTO/MTP is expected to account for more than 17 % of China's methanol demand, assuming all the other projects come online as planned. Until 2015, about 1.8 million of the total 8.660 million tonnes per year of MTO/MTP is expected to be assigned to MTP technology [471].

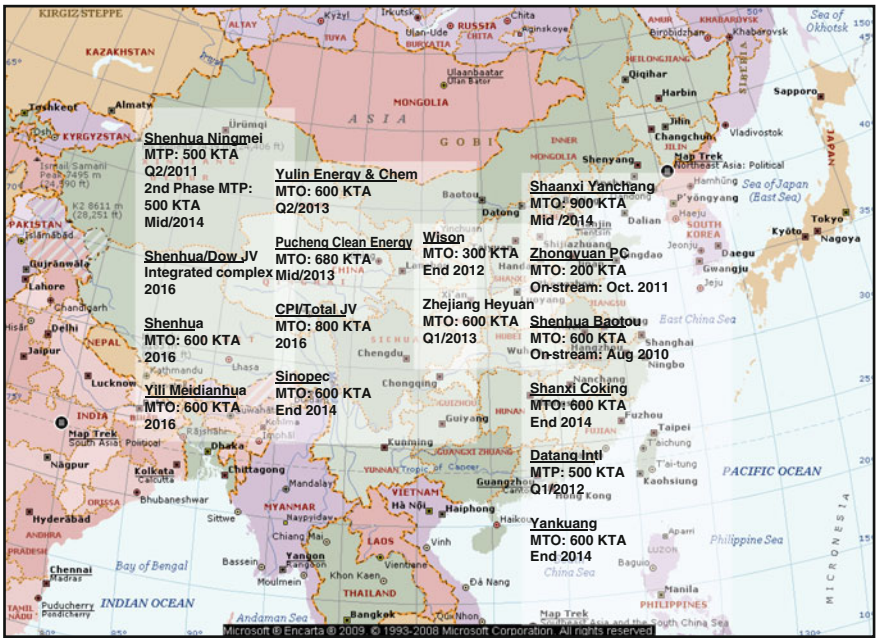

Fig. 6.76 Actual methanol-to-olefins (MTO) and methanol-to-propylene (MTP) projects in China

Table 6.17 China: Existing methanol-to-propylene projects[471]

Project	Location	Capacity in tonnes/year	Status
Datang international power generation	Inner Mongolia	460,000 (1.68 million t/a integrated methanol supply)	Operating
Shenhua Ningxia coal industry group	Ningxia	500,000 (integrated 1.67 million t/a methanol unit)	Operating
Total		960,000	

Table 6.18 China: Upcoming approved methanol-to-propylene projects (planning projects excluded)[471]

Project	Location	Capacity in tonnes/year	Start date
Ningbo Heyuan (Skyford)	Zhejiang	600,000	November 2012
Ningxia coal industry	Ningxia	500,000	2014
Total		1,100,000	

Due to the short time since commissioning, reliable figures for the economic efficiency of MTO/MTP processes in China are not yet available. Earlier studies, such as Nexant in 2003 [472], are based on data that are rather uncertain or have in the meantime been substantially modified. Additionally, a generalisation of the

economic performance of the present Chinese production of lower olefins via methanol is rather uncertain [472]. The cost of coal and other utilities, the installation cost and the operating cost are at the present time either not reported in actual studies or recorded only with relatively large uncertainty margins. The limitations of a generalisation are due to the fact that the presently installed capacity is based on coal-based methanol as feedstock, whereas in other areas natural gas or flared gas as raw materials may be the favourable feedstock for methanol.

As shown in Fig. 6.77, a large variety of chemicals and fuels can be produced efficiently based on a combination of methanol/MTP technology, going downstream to many other high-value products. In the early 1970s, researchers at Mobil Central Research discovered that methanol can be converted into higher hydrocarbons over the zeolite H-ZSM-5 [473–475]. These hydrocarbons consisted of a mixture of aromatic compounds, olefins and paraffins and delivered a gasoline of high quality.

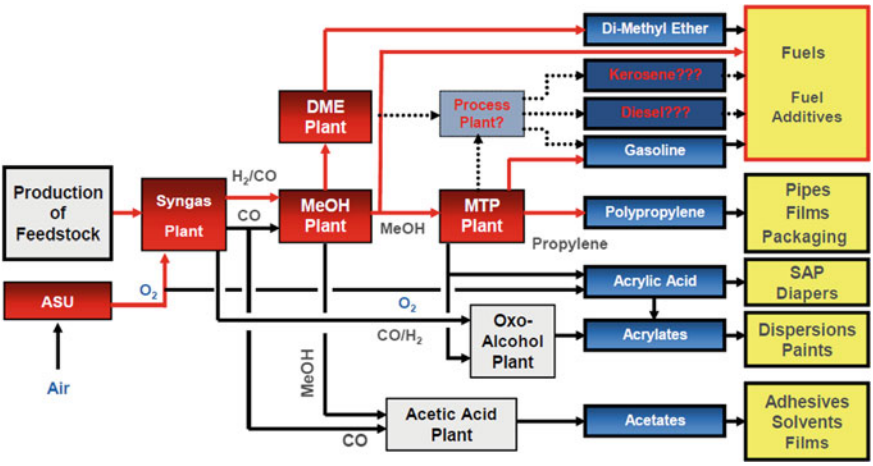

Fig. 6.77 Products based on methanol/methanol-to-propylene (MTP) technology. DME, dimethyl ether [476]

Olefins from a methanol-to-hydrocarbon (MTHC) route have an advantage compared to olefins from steam cracker: the olefins obtained via methanol are of polymer grade. The MTHC technology is reviewed in Sect. 6.4. The MTO technology chain provides the key to make almost everything from coal/biomass/natural gas that can be made out of crude oil [477].

In the view of an increasing demand for on-purpose propylene, Lurgi developed the MTP Process. The MTP technology—usually as part of a gas-/coal-to-propylene concept (GTP/CTP; see Fig. 6.78)—is characterised by its low operating cost and, hence, its reduced risk of exposure to fluctuations in propylene pricing. Furthermore, the feedstock price is decoupled from oil pricing; therefore, high oil prices provide an excellent environment for a successful GTP/CTP project (Fig. 6.78).

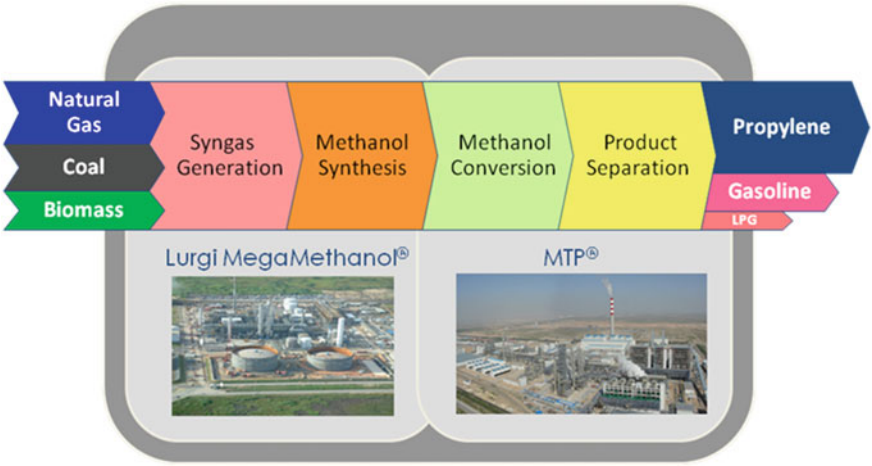

Fig. 6.78 Lurgi processes from alternative feedstock to propylene production (Air Liquide Global E&C Solutions). LPG, liquefied petroleum gas

Process Overview

Lurgi's MTP process is based on an efficient combination of the most suitable reactor system and a very selective and stable zeolite-based catalyst. Süd-Chemie AG (now part of the Clariant Group) manufactures the fixed-bed catalyst commercially. The catalyst provides maximum propylene selectivity and has a low coking tendency, a very low propane yield and also limited byproduct formation. In turn, this leads to a simplified purification scheme that requires only a reduced cold box system as compared to on-spec ethylene/propylene separation.

In Lurgi's MTP process, propylene is produced from methanol in two steps. First, methanol is converted into an almost equilibrium mixture of DME and methanol. This mixture is converted in a second step to dominantly propylene. This is the major common feature between the MTP and the MTO technology (see Sect. 6.4.2). The major differences between MTP and MTO technology lie in the process technology and in the catalyst used. Apart from the early MTO 100-BPD demonstration plant, which operated using an H-ZSM-5 catalyst with MFI topology, all other technical-scale MTO plants are based on catalysts with at least one zeotype component with chabazite (CHA) topology. The advantage of the CHA structure type in MTO reactions is that the carbon number of the product hydrocarbons peaks at lower values. However, the gain in C_2 and C_3 olefins compared to ZSM-5-based catalysts is obtained at the expense of a high C_1 formation, mainly coke. The coke formation requires frequent regeneration. This is the main reason for the necessity to apply fluid-bed technology in case of the state-of-the-art MTO processes. In contrast, Lurgi's MTP process is based on a catalyst with H-ZSM-5 as an active component that has a very low coking tendency. This in turn allows the application of a fixed-bed technology that is easy to scale-up with low capital expenditure.

A MTP plant with a feed of 5,000 t/d methanol produces typically 1,410 t/d propylene, 540 t/d MTP gasoline and 109 t/d MTP-liquefied petroleum gas (LPG). In addition, with an extension of the plant, 60 t/d of ethylene can be recovered from the purge gas, which is otherwise used as fuel. Approximately 2,800 t/d of process water is generated from the methanol.

Both the propylene and the ethylene are of polymer grade. MTP gasoline and MTP-LPG are produced as co-products, contributing additional value to the economy of the technology. The MTP gasoline has excellent characteristics as a blending stock because it is free of sulphur, has low benzene content and has a high octane number. Technology solutions are also available to process the MTP gasoline to pump-grade gasoline. The process can be described along the simplified process flow diagram given in Fig. 6.79.

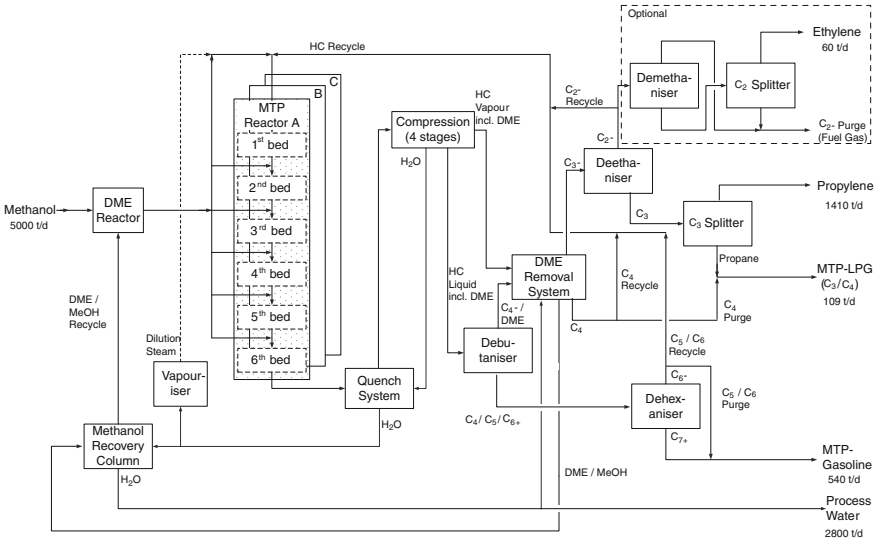

Fig. 6.79 Simplified block flow diagram: methanol-to-propylene (MTP) reaction section. DME, dimethyl ether; LPG, liquefied petroleum gas

The MTP Reactor Section

Methanol (MeOH) is used as feed to the MTP unit. The majority of the MeOH feed is vapourised, superheated and fed to the DME reactor (see also Sect. 6.4.4). A smaller part of the feed MeOH is used as solvent for oxygenate removal in the fractionation section of the MTP unit. The DME reactor is a single-stage adiabatic reactor where most of the MeOH vapour is converted to DME on an aluminium oxide catalyst according to the following equation:

$$2CH_3OH(MeOH) \rightleftharpoons CH_3OCH_3(DME) + H_2O$$

The catalyst features high activity and high selectivity, achieving an almost thermodynamic equilibrium. The reaction is exothermic and the reaction

equilibrium is nearly independent of the operating pressure. Unconverted MeOH is separated from the aqueous stream in the methanol recovery column and sent back as additional feed to the DME reactor.

The MTP synthesis features a 2 + 1 reactor concept (two reactors in operation and one reactor in regeneration mode or standby), which ensures regeneration as well as exchange of the catalyst at continued production. Each reactor represents 50 % of the plant capacity and comprises six adiabatic reactor stages for a better approach to isothermal conditions in order to achieve maximum propylene yield.

In the MTP reactor, the DME/MeOH mixture is converted to olefins on a ZSM-5 catalyst. The conversion of MeOH via a zeolite-based catalyst has been extensively investigated and discussed in past decades by various scientists. The reaction mechanism is elaborately described in Sect. 6.4. The selectivity of the MTP reaction is a result of the relative reactive rates of the reactive pool in combination with the shape selectivity of the zeolite catalyst, which through its pore structure influences the atomic structure of the produced molecules. The MTP catalyst is tailored for maximum propylene yield and maximum total olefin yield. Furthermore, coke formation of the MTP zeolite catalyst is less than 0.5 mol% (carbon conversion) depending on the lifetime of the catalyst. This low coking tendency results in excellent carbon efficiency of the MTP synthesis.

Almost 85 % of the carbon of the fresh feed (DME or MeOH) reacts in the MTP reactors to olefins in the range of C_2 to C_8 with the peak at propylene. Side products from the reactions in the MTP reactors are naphthenes, paraffins, aromatic components and light ends. The oxygen that is chemically bound in the methanol results in process water.

The product of the DME reactor is sent to the MTP reactor section and split to feed the reactor stages of each MTP reactor in operation. Before entering the first catalyst bed, the DME feed is mixed with a hydrocarbon recycle stream and dilution steam from the process steam vapouriser. The hydrocarbon conversion over the MTP catalyst bed is dominated by exothermic reactions, which results in an adiabatic temperature rise over each bed. The MTP process is designed in a way to control the temperature rise over each reactor bed while a high average operating temperature over the six reactor stages is maintained.

The intermediate reaction product from each catalyst bed is cooled and mixed with additional fresh DME/MeOH feed before entering the next catalyst bed. The quantity of fresh DME/MeOH feed to each catalyst bed is adjusted to guarantee similar reaction conditions and maximum overall propylene yield.

One result of the hydrocarbon conversion over the zeolite catalyst are also small amounts of heavy hydrocarbons, which partly block the pore structure and the active sites, which reduce the overall conversion over the catalyst. To minimise coke formation, process steam is added to the process. Steam serves as an inhibitor for coke formation and has also a role as a heat sink for the exothermic reaction, supporting temperature control over the catalyst bed.

The hydrocarbon recycle to the first MTP reaction stage increases the propylene yield by conversion of olefins other than propylene to the same product range as the DME feed. In addition, like the process steam, the hydrocarbons serve as a heat

sink for the exothermic reaction, supporting additional temperature control over the catalyst bed.

Nevertheless, the coke formation cannot be fully prevented and the catalyst has to be regenerated when the overall conversion falls below the economical limit. Typical operating cycles of one MTP reactor are approximately 600 h. The regeneration of the MTP reactor is performed in situ by controlled combustion of coke with an air/nitrogen mixture. The catalyst is regenerated at temperatures close to the normal operating temperature, thus keeping the possible thermal stress to a minimum.

Water Hydrocarbon Separation Section

The MTP reactor effluent is cooled in a heat recovery system and finally in the quench system, where the hydrocarbon product is separated from the bulk of the water. The hydrocarbons leave the quench system as overhead vapour, whereas the water is condensed and sent to the methanol recovery column. There, MeOH and DME are recovered and subsequently fed as unconverted fresh feed to the DME reactor. The stripped water containing traces of methanol is finally routed as process water to battery limits. This process water can be used as supplemental raw water for utilisation in the petrochemical complex or for irrigation after appropriate and inexpensive treatment.

Hydrocarbon Compression Section

The hydrocarbon vapour product from the quench system is compressed to approximately 2.5 MPa by a multistage centrifugal compressor. Between the compression stages, the product is cooled and partially condensed. Water and hydrocarbon liquid are separated from the vapour phase. The vapour phase is further compressed. The condensed water is recycled to the quench system, whereas hydrocarbon liquid and hydrocarbon vapour are sent to the purification section.

The hydrocarbon streams are dried by molecular sieves before the hydrocarbon liquid is fed to the debutaniser column and the hydrocarbon vapour is processed in the DME removal system.

Hydrocarbon Purification Section

The debutaniser column separates light boiling components C_{4-} and DME from C_{4+} hydrocarbons. The C_{4+} bottom product is fed to a dehexaniser distillation column, where aromatics and C_{7+} are separated from the C_{6-} stream. The major portion of this C_{6-} fraction is sent back to the MTP reaction. The remainder, along with the C_{7+} dehexaniser bottom product, form the MTP gasoline product. The compressed hydrocarbon vapours, including light olefins and DME, and the overhead C_{4+}/DME product from the debutaniser are fed to the DME removal system. Here, C_{3-} hydrocarbons are separated from C_{4+} hydrocarbons and oxygenates.

The methanol and DME-containing streams are routed to the methanol recovery column so that methanol and DME can be recycled to the DME reactor. The C_4 hydrocarbon fraction is recycled to the MTP reaction system for further propylene production. A smaller portion is purged out of the reaction loop, forming the C_4 component in the MTP-LPG product.

The C_{3-} product (including all C fractions below C_3), which is free from DME and any other oxygenates, is fed to the deethaniser. From the deethaniser, a C_{2-} stream (defined as above) is recovered as the top product. One part of the C_{2-} stream is recycled to the MTP reactor, whereas the rest is sent to the ethylene purification unit. The C_3 bottom product, containing propylene (~97 wt%) and propane (~3 wt%), but no unsaturated components such as methyl acetylene or propadiene, flow through a safeguard bed of activated alumina to the C_3 splitter. The C_3 splitter column separates propane from the polymer-grade propylene product. The propane forms the C_3 component in the MTP-LPG product.

Ethylene Purification Section

The ethylene purification is achieved in a two-column system, the demethaniser and the C_2 splitter column. The overhead vapours from the demethaniser contain C_1, hydrogen and inert material, whereas the bottom product C_2 (paraffinic and olefinic) is heated up and sent to the C_2 splitter. The C_2 stream is split and rectified to polymer-grade ethylene in the overhead system of the C_2 splitter. The ethane stream, which is drawn off from the bottom section of the splitter column, is mixed with the overhead stream of the demethaniser and is used internally as fuel gas for heater firing. If no polymer-grade ethylene is to be produced, the ethylene purification section is not needed; accordingly, the C_2 feed stream is used as internal fuel gas and minimises the fuel requirements of the MTP process plant.

Product Description Data

The products listed in Table 6.19 are based on a feed rate of 5,000 t/d methanol.

Wastes and Emissions

The catalyst of the DME reactor is an aluminium oxide catalyst with an expected lifetime of 10 years, whereas the catalyst of the MTP reactor is a ZSM-5 catalyst with an expected lifetime of more than 1 year. Both catalysts can be safely disposed in a landfill after use. The only emissions of note are the typical flue gases from gas-fired heaters/boilers and the catalyst regeneration gas, which basically consists of nitrogen-diluted air with a somewhat elevated CO_2 content.

From Laboratory Scale to Commercial Reference

Lurgi launched the MTP process development in 1999. During this time, the first tests of the MTP reaction with the Süd-Chemie catalyst (today Clariant) were performed at the Lurgi Research and Development centre. A catalyst test unit was used for tests under idealised conditions (polytropic and once-through operation) to allow optimisation studies of the reaction temperature, pressure and space velocity. The first tests showed very positive and promising results, which justified the construction of a larger-scale pilot plant to enable adiabatic test conditions and artificial recycle streams.

By means of the two test units, the basic process design data for the MTP process were derived from more than 9,000 operating hours. Parallel to the various tests, Lurgi decided to build a larger-scale demonstration unit to test the new

Table 6.19 Product description data

Product	Property
1,410 t/d propylene (polymer grade)	
Purity	>99.60 wt%
60 t/d ethylene (polymer grade)	
540 t/d gasoline	
Density at 15 °C	740–790 kg/m^3
Equivalent dry vapour pressure	35–70 kPa
Research Octane Number	90–95
Composition	
Paraffins	15–35 wt%
Olefins (increasing over run time of catalyst)	30–60 wt%
Aromatics (decreasing over run time of catalyst)	50–15 wt%
Benzene	< 1 wt%
Total sulphur components	< 0.1 wt/ppm
109 t/d liquefied petroleum gas	
Composition	
C_2 hydrocarbons	< 0.2 vol%
C_3 hydrocarbons	> 10 vol%
C_4 hydrocarbons	< 90 vol%
C_5 hydrocarbons	< 1.5 vol%
Total sulphur components, maximum	< 0.1 wt/ppm
2,800 t/d process water (either for use as raw water supplement, such as cooling water makeup, or for irrigation purposes after biological treatment)	

process in the site stream of a world-scale methanol plant, with continuous (24 h/day, 7 days/week) operation using real methanol feedstock. During the design of the pilot plant and demonstration unit, care was taken to optimise them for a possible scale-up of the MTP reactors. For example, the bed heights in the smaller units were chosen to be identical to their projected commercial-size counterparts. In this respect, the beds in the laboratory and demonstration plant can be seen as a cutout of the commercial MTP reactor. The laboratory plant was then also optimised to have an ideal adiabatic multistage operation like in the commercial plant so as to get a good prediction of the temperature profiles and the resulting propylene yields and byproducts (Fig. 6.80).

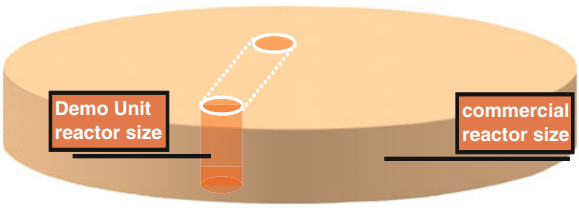

Fig. 6.80 Scale-up visualisation

After a cooperation agreement with Statoil ASA was signed in January 2001, the demonstration unit was assembled in Germany and transported to the Statoil methanol plant at Tjeldbergodden (Norway) in November 2001. Borealis joined the co-operation in 2002. The demonstration unit started continuous operation in January 2002.

In September 2003, the demonstration unit completed the scheduled 8,000 h lifecycle test. The 8,000 h test was an important milestone because the main purpose of the demonstration unit was achieved: to demonstrate that the catalyst lifetime meets the commercial target of 8,000 h on stream. Cycle lengths between regenerations were longer than expected. Deactivation rates of the methanol conversion reaction decreased with operation time. Propylene selectivity and yields were in the expected range for this unit, with only a partial recycle. Another important milestone was the successful polymerisation of the propylene from the MTP process into polypropylene in collaboration with Borealis, Norway (see Fig. 6.81). The polymerisation tests demonstrated that MTP propylene exhibits the same quality as regular, crude-oil based propylene and does not contain any new or harmful poisons for the very demanding polymerisation catalysts.

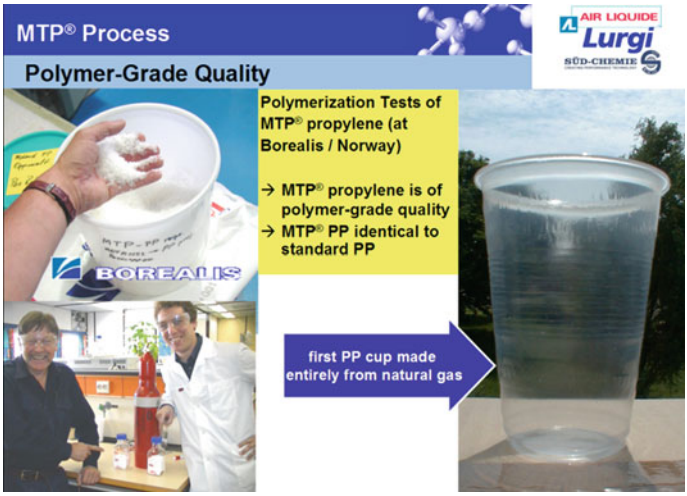

Fig. 6.81 The first polypropylene (PP) cup made from the Lurgi methanol-to-propylene (MTP) process

The demonstration tests also proved the high quality of the byproduct gasoline. After the 8,000 h test, the demonstration unit was operated for another 3,000 h with a second batch of catalyst to obtain verification and new results from variation of operating conditions. Thus, after successfully logging 11,000 h in an industrial environment, the demonstration unit was brought home to Lurgi's Research and Development centre. There, for further investigations and fine-tuning, a new process demonstration unit (PDU) was erected, which is a representation of a

commercial unit in all relevant process and recycle streams. Currently this PDU delivers continuously additional data for further developments of the process as well as support purposes for engineering. Today, the catalyst development has been completed and the supplier Clariant commercially manufactures the catalyst. Nevertheless, because there is always room for improvement, new studies have been initiated to possibly raise propylene yield and/or lifetime.

In September 2010, the Shenhua Ningxia Coal Industry (Shenhua Ningmei) Group started up its commercial coal-to-propylene complex. The gasification was licensed by Siemens GSP, producing 520,000 Nm^3/h raw syngas (see Sect. 4.4.6). The air separation unit was supplied by Air Liquide, producing 190,000 Nm^3/h of oxygen. The polypropylene technology was licensed by ABB (gaseous phase process). 6x460 t/h steam boilers and a 150 MW power plant complete the project. Only one month later, the MTP plant, as part of the coal-to-propylene complex, produced first-time on-spec propylene with a purity of 99.69 %. The commercial scale-up of the MTP process was realised based on research and development data only. A scale-up factor of more than 6,900 compared to the demonstration unit in Norway (based on feed rate) has been realised (Fig. 6.82).

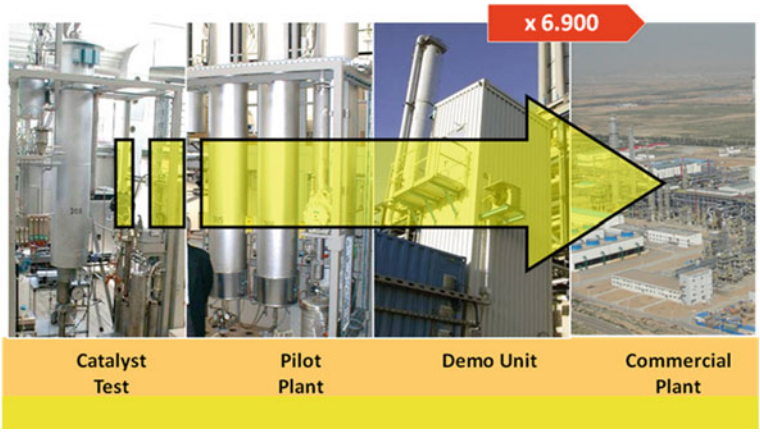

Fig. 6.82 Scale-up from pilot plant to commercial plant

The smooth commercial commissioning and operation of the first coal-to-propylene complex has been an outstanding success for the MTP development history. The comparison of performance data from the commercial MTP plant with the performance data of the process demonstration unit in the Research and Development (R&D) centre are in very good agreement. This comparison underpins the R&D capabilities for prediction of yields and even product properties of commercial MTP plants. Fig. 6.83 presents the good agreement of product slate of the commercial plant with results of the process demonstration unit operated in the R&D laboratories.

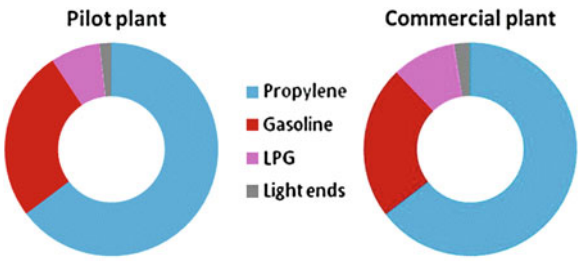

Fig. 6.83 Comparison between product slates in pilot plant versus commercial plant. LPG, liquefied petroleum gas

Operating Experience

The Shenhua Ningxia Coal Industry Group MTP plant started construction in April 2008. After mechanical completion in August 2010, commissioning started on September 6, 2010. The first on-spec propylene production was achieved on October 4, 2010, achieving a propylene purity of more than 99.69 wt%. Since then, the plant has been in smooth, stable operation. The production of propylene has been maximised through increased selectivity via reaction temperature optimisation. Ethylene is produced only in very small quantities, but enough to be able to produce valuable high-impact co-polymers based on propylene. No catalyst attrition has been observed. Regeneration of the catalyst is done in situ via an air/nitrogen mixture at about the same temperatures as the reaction, thus avoiding temperature imbalances during cycle changes. The carbon loss during coking is very low (<0.5 %). The cycle time is between 600 and 800 h. In comparison to the extensive laboratory tests (in total >60,000 h using essentially three pilot and one demonstration unit), the large-scale operation shows the same or even better results. The fixed-bed reactors are simple and easy to operate.

Commercial References

Today, Lurgi offers the MTP process on fully commercial terms. In 2005 and 2006, contracts were signed for two full-size MTP plants of 1,410 t/d propylene capacity in China. Both complexes are coal based and use third-party coal-gasification technology (Siemens GSP EF technology; see Fig. 6.84), Lurgi's licensed Rectisol syngas cleaning, Lurgi's MegaMethanol technology and Lurgi's MTP technology. In both plants, the produced propylene is converted into polypropylene by a third-party technology.

The Shenhua Ningxia Coal Industry (Shenhua Ningmei) Group started construction of their coal to propylene complex in April 2008. Mechanical completion was achieved in August 2010 and commissioning started in September 2010. The first propylene was produced in October 2010, which was the first propylene production at a world-scale MTP plant in commercial operation at that time. From the beginning of commercial operation, the operating experience was extremely satisfying because it was the first commercial MTP plant based on an upscaling factor of more than 6,900.

Fig. 6.84 Methanol-to-propylene plant at Shenhua Ningxia Coal Industry Site

No crucial issues appeared during start-up, which would have resulted in a substantial change of the plant concept. The six-stage MTP fixed-bed reactor design showed a stable and very reliable operating behaviour from the beginning. Ramp-up and fine-tuning of the MTP plant required some time, as expected for a first-of-its-kind plant. This was also influenced by the fact that upstream of the MTP plant a whole process chain, starting with coal gasification, went into commercial operation. Today, the plant is in smooth operation and produces on-spec propylene that is polymerised into polypropylene. The performance test run of the MTP plant was successfully executed in May 2012. All performance indicators have been achieved without any issues. All product description data, as listed in Table 6.19, were met or exceeded. As a result of this success story, Shenhua Ningxia Coal Industry Group has ordered a second MTP unit from Lurgi (Fig. 6.85).

In parallel to the coal-to-propylene complex for the Shenhua Ningxia Coal Industry Group, a second coal-to-propylene complex was built by Datang International Power Generation. The complex, which also uses third-party coal-gasification technology (Shell EF Gasification) and Lurgi's licensed Rectisol syngas cleaning, Lurgi's MegaMethanol technology and Lurgi's MTP technology, is producing propylene for the production of polypropylene. It represents the second MTP reference in commercial operation.

As of early 2013, five licenses have been sold worldwide. Currently, Lurgi (as an affiliate of Air Liquide global E&C Solutions) is involved in several further MTP projects with a total capacity of approximately 3,000,000 t/y. The projects, which are either in the study or project development phase, are based on gas, coal, and direct methanol feed.

Fig. 6.85 Shenhua Ningxia Coal Industry Group's coal-to-polypropylene complex (Ningdong, Province of Ningxia, China). See also Sect. 4.4.6. DME, dimethyl ether; MTP, methanol-to-propylene

Economy

With the implementation of Lurgi's MegaMethanol technology at the beginning of the twenty first century for single-train production of 5,000 t/d of methanol and more, methanol production costs have decreased significantly. The capability of low production price, the constant trend of increasing crude oil prices and increasing demand for high-value commodities such as propylene are some reasons why developments of methanol-based downstream technologies stepped into the focus of the petrochemical industry. Attention was also paid to the monetisation of stranded gas. Actual gas prices during the early twenty first century reached levels that forbade investments in gas conversion, which was incidentally one of the reasons why the first MTP plants are coal based.

Today, on a worldwide basis, the exploitation of large conventional and unconventional (shale gas in North America and Australia) natural gas reserves, coupled with the differential value between such reserves and benchmark crude oil, reflects the consideration of this feedstock for conversion to high-value petrochemical commodities. Using the specific example of the US Gulf Coast region, the increasing differential between natural gas and crude oil prices in the early twenty first century is illustrated in Fig. 6.86. This high differential is causing a variety of gas-based processes, including MTG and others, to be investigated for gasoline and chemical production in the USA.

Lurgi's MTP (or in a broader sense, gas-to-propylene [GTP]) process presents a simple, cost-effective and highly selective on-purpose propylene production technology. Both routes allow for the production of petrochemicals that then would be gas-based. In this section, the economics of a GTP complex are presented on the basis of an internal rate of return calculation. The GTP complex considers a syngas production section, a methanol synthesis for 5,000 t/d methanol production, MTP synthesis and relative off sites and utilities.

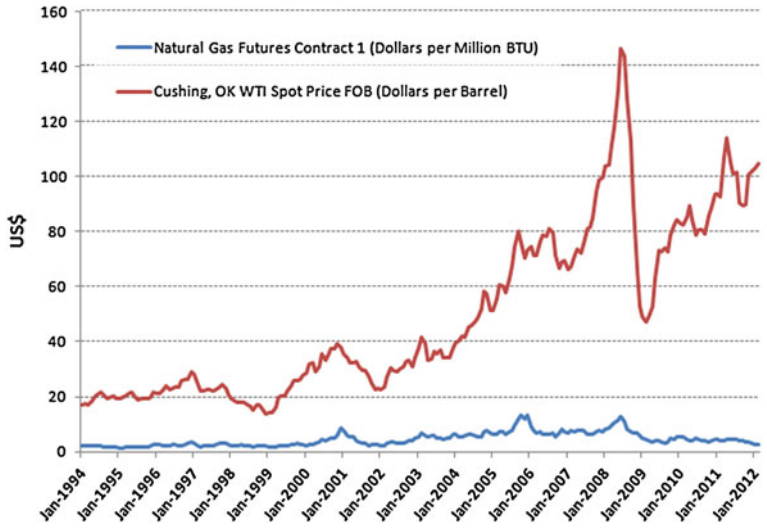

Fig. 6.86 Difference between natural gas and crude oil prices (US Gulf Coast Region)

The increasing attractiveness of the GTP technology stands in direct correlation with the increasing crude oil prices because MTP products are classic crude-based products, and product pricing is linked to crude oil economy. On the other hand, the attractiveness benefits from the feedstock costs. For GTP, the feedstock is natural gas, which remains at low and stable price levels.

Figure 6.87 presents the IRR of the GTP route as function of gas and crude oil pricing. It shows that the MTP technology stands for a stable feasibility already at

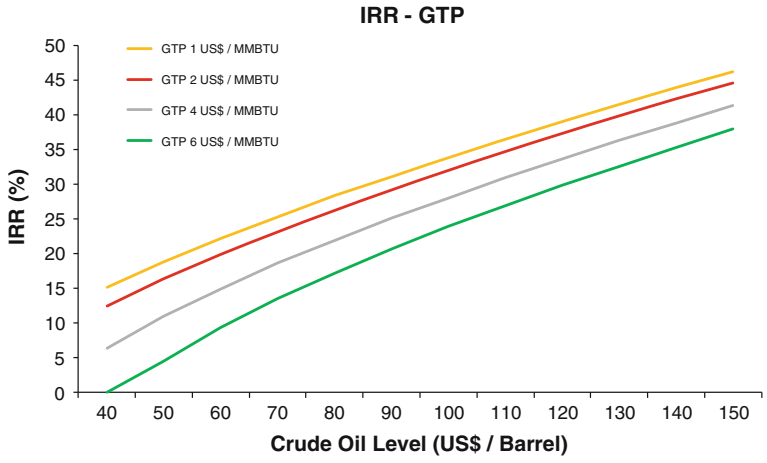

Fig. 6.87 IRR of a gas-to-propylene complex

low crude oil prices, taking up speed with increasing crude oil prices. As the spread between natural gas and crude oil prices increases, it contributes directly to the profit if the GTP route. Traditional propylene production technologies (Cracker, PDH) will not benefit from the spread because their feedstock cost and product prices rise with crude oil cost.

Another advantage of the GTP route is the robustness of the technology against fluctuations in feedstock cost. A doubling of natural gas price from 2 to 4 US$/MMBTU results in a IRR reduction in the range of approximately 3 % points, which is still very attractive, especially in today's crude oil price scenarios.

6.4.4 Other Methanol Derivatives

Friedrich Schmidt[1] and Ludolf Plass[2]

[1]*Angerbachstrasse 28, 83024 Rosenheim, Germany*
[2]*Parkstraße 11, 61476 Kronberg, Germany*

6.4.4.1 Introduction

The reactions of oxygenates (primarily alcohols and more specifically methanol) to hydrocarbons have enormous societal significance because these reactions involve two of the most important areas of modern industrial society—namely, to secure and broaden the resource base (1) for mobility and (2) for the production of polymers (aromatics, polyethylene and polypropylene for the production of consumer goods). In the early 1970s, researchers at Mobil Central Research discovered that methanol can be converted into higher hydrocarbons over the zeolite H-ZSM-5 [478–480]. These hydrocarbons consisted of a mixture of aromatic compounds, olefins and paraffins and delivered a gasoline of high quality.

Some reviews covered the MTHC topic from an academic viewpoint [481–483] and from a semi-technical viewpoint [480, 484]. A review by Stöcker covered the details of catalyst and reaction mechanisms of the MTHC processes, especially the methanol-to-gasoline (MTG), methanol-to-olefins (MTO) and Mobil's olefin-to-gasoline and distillate (MOGD) processes [485]. Keil presented a paper focusing on the technology of the MTG, MTO and MOGD processes but did not discuss those processes, which are presently operating commercially [484].

6.4.4.2 Dimethyl Ether

The Catalyst Group Resources [486] summarises the commercial situation for DME as follows:

In general, all companies that offer MegaMethanol technologies can modify their processes to produce DME instead. They will use the same reactor technology as they use for methanol production. All the current commercial plants use conventional methanol technology and then add a dehydration reaction to make DME. The only other plant design change is to modify the distillation sequence to recover DME instead of methanol.

JFE (formerly NKK) offers a direct DME process that uses a slurry phase reactor. The reactor technology was proven over a five year period in a 5 tpd pilot plant, starting in 1999, in Hokkaido, Japan. It was then proven in a 100 tpd plant, starting in 2002, at the same site. Toyo Engineering built the 110,000 tonnes per year (tpy) DME plant in Luzhou, China that started DME in the fuels market, and the 1,000,000 tpy plant in Inner Mongolia.

They used their own proprietary reactor technology for methanol dehydration. Air Products offers a process analogous to the liquid phase methanol synthesis process, LPMEOH, to make DME directly, and call it the Liquid Phase Dimethyl Ether Process (LPDME). Haldor-Topsøe provided the design basis for a 800,000 tpy DME plant in Assuluyah, Iran for Zagros Petrochemical Company—the first mega-scale DME project in the world. Startup has been delayed somewhat, originally projected for 2008. More recently, Haldor-Topsøe has been selected to supply DME technology for two plants in China [486].

DME has excellent diesel properties (cetane number 55–60, sulphur and aromatic content of zero) and thus represents a future alternative to conventional diesel fuel for mobile applications. DME is also regarded as an environmentally friendly alternative to diesel for power generation (MtPower [487]) because DME burns completely sootless. DME as fuel component reduces NO_x up to 90 %. The DME is completely free of sulphur. Due to the similarity of its physical properties with those of LPG, DME can easily add or replace LPG (especially for storage and transportation). For the concept of electricity with methanol and/or DME, methanol is produced using low-cost natural gas. The electricity is then carried out in places that have no gas supply pipelines or liquefied natural gas.

The synthesis of ethers with the aid of activated alumina as a catalyst has been known since 1928 through the work of Adkins and Perkins [488]. The promoting effect of using high-surface area γ-alumina for methanol dehydration has been widely studied and reported by many authors [489–494]. It is now well established that the activity of methanol dehydration is largely promoted by the number of free acidic sites. These sites are directly proportional to the specific surface area of the γ-alumina catalyst. The dehydration of methanol is a strongly exothermic reaction [495].

DME is one of the most promising diesel and LPG substitutes and has gained huge interest in research and industry [496]. In comparison to common fuels, the combustion of DME is soot-free and hardly emits any harmful particles [497]. DME can be produced by either dehydrating methanol over an acid catalyst (MT-DME) or in a single-step process from synthesis gas (syngas-to-dimethyl ether—STD) [498].

Currently, there are several licensors that offer technology for the production of DME based on a two-step process, including Haldor Topsøe, Lurgi, Mitsubishi Gas Chemical, Toyo Engineering Corporation and Uhde [499]. The existing DME plants in the world are based on the conventional methanol route; in most cases, their capacity is only of the order of 10–20 kt per year capacity. (Topsøe has supplied DME catalysts and technology for a number of plants in China, with capacities up to 400,000 tonnes per year.)

The conventional DME plants are producing DME for chemical use, such as solvents and spray propellant for cosmetics. Due to the limited size of these markets, the price of DME could stay at a very high level. However, if the objective is to produce DME for fuel market, the price of DME must be competitive in the existing fuels market. For this market, the size of a single DME plant should be at least 1–2 million tonnes/year capacity, which requires scale-up to a larger plant that is more than 100 times the size of existing conventional plants [500].

Direct DME Synthesis Reactions

Methanol synthesis is an equilibrium-restricted reaction. When the dehydration reaction takes place simultaneously, the syngas conversion rises dramatically. Figure 6.88 shows stoichiometric equilibrium syngas conversion of DME synthesis (a) and (b) at 5 MPa, and methanol synthesis (c) at 5 and 9 MPa. DME synthesis reaction (a) gives much higher syngas conversion in all temperature conditions than reaction (b).

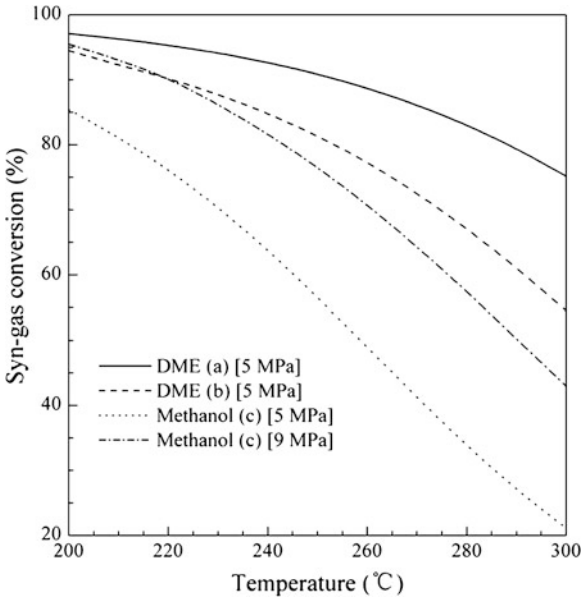

Fig. 6.88 Stoichiometric equilibrium conversion of dimethyl ether (DME) and methanol synthesis [501]

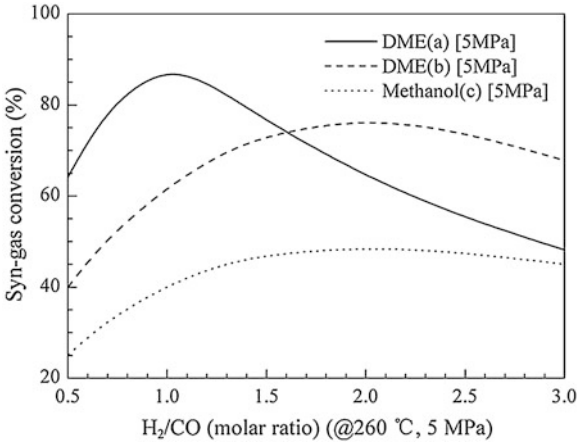

Fig. 6.89 Equilibrium conversion of synthesis gas versus H_2/CO ratio [501]. DME, dimethyl ether

Figure 6.89 shows syngas conversions of the two overall DME syntheses, (a) and (b), and the methanol synthesis (c), as a function of H_2/CO ratio of syngas. In each reaction, the equilibrium conversion reaches its maximum point when the H_2/CO ratio is equal to its stoichiometric number, which is 1.0 for (a) and 2.0 for both (b) and (c). The maximum equilibrium conversion of (a) is higher than (b) by more than 10 %.

MT-DME Two-Step Technology

The Production Process

To achieve an economic price, the production of DME needs to be on megascale. Traditionally, DME was a byproduct of high-pressure methanol synthesis. Since the development of the low-pressure methanol synthesis process, DME is produced from methanol by dehydration in the presence of a suitable catalyst. This process is carried out in fixed-bed reactors. The product is cooled and distilled to pure DME (Fig. 6.90).

A modification of the conventional methanol synthesis process would enable the production of DME in the methanol synthesis loop as a byproduct in higher yields (two-step process, below). This pathway, however, has two major drawbacks. During the dehydration of methanol, the water vapour content increases and thus reinforces the water–gas shift reaction. Through the conversion of CO to CO_2, the quality of the synthesis gas declines. The rate of the reaction of CO_2 and H_2 is slower than the rate of the reaction of CO and H_2. In order to compensate for this drawback, the volume of the synthesis catalyst and the circulating volume need to be increased. A further drawback is the low boiling point of DME, which requires a cryogenic separation of DME [502].

In the case of a combination of a DME unit with a MegaMethanol system, the methanol three-column distillation unit can be reduced to a single column, with corresponding savings. In the Lurgi DME process (MT-DME, methanol-to-DME,

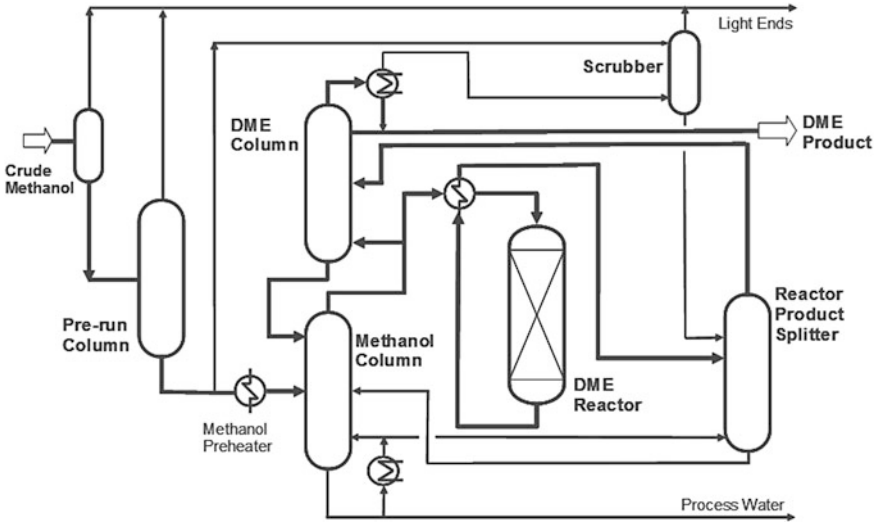

Fig. 6.90 Dehydrating methanol over an acid catalyst (MT-DME). DME, dimethyl ether

MTD, or MegaDME), all types and qualities of DME can be produced. The different requirements for fuels or to generate electricity (MtPower) or for DME as chemical can be achieved by varying the size and the design of the DME distillation columns.

Economic Evaluation

The economics of the Lurgi DME process are summarised in Table 6.20 [503].

The following assumptions were made:

- Natural gas consumption and product value are normalised to an equivalent of methanol (capacity: 7,500 t/d methanol).
- The DME product quality meets the specifications.
- The natural gas consumption figures include the energy required for an air separation plant and a power generation unit.

Table 6.20 Economy of dehydrating methanol over an acid catalyst (MT-DME)

Characteristics and costs	MegaMethanol and dehydration
DME capacity (t/d)	5,000
Specific MMBtu/$t_{Methanol}$	28.5
Consumption of natural gas (MMBtu/t_{DME})	40.2
Total fixed costs for EPC (US$)	415 million
DME production cost (US$/$t_{DME}$)	93

DME, dimethyl ether; EPC, engineering, procurement and construction

- The total fixed costs include an air separation unit, a power generation unit and the other components.
- The price of natural gas was assumed to be 0.50 US$/MMBtu.
- The depreciation of 10 % of the total fixed cost was recognised.
- The return on investment of 20 % of total fixed cost was fixed.
- Operating costs for operating personnel, plant overhead, upkeep/maintenance, and materials are included.

The budgeted costs are given with an accuracy of ±20 %. Specific location factors are not included in these figures.

When it is produced in large quantities, DME (as traditional methanol derivative) is therefore a promising complement to existing diesel fuel, LPG, electricity generation and also olefin production. The production of DME by dehydration of methanol is an economic way [495].

DME Direct from Syngas Competing with the Methanol Route

STD Direct Synthesis Route (Typical)

The production of DME from synthesis gas (STD) [504] is reported to be favourable if a biomass-derived synthesis gas is applied that is carbon monoxide-rich with typical H_2/CO-ratios of approximately 1 or lower. The STD process requires catalyst systems that comprise highly active sites for methanol synthesis and acid sites for methanol dehydration. The water–gas shift reaction is the third simultaneously proceeding reaction in the STD process. All three reactions are described in Table 6.21.

Table 6.21 Direct syngas-to-dimethyl ether (STD) reactions

	Reaction			Reaction heat in kJ/mol
MeOH	$CO + 2H_2$	$\rightleftharpoons$	CH_3OH	90.3
MeOH dehydration	$2CH_3OH$	$\rightleftharpoons$	$CH_3OCH_3 + H_2O$	23.4
Shift	$CO + H_2O$	$\rightleftharpoons$	$CO_2 + H_2$	40.9
Overall	$3CO + 3H_2$	$\rightleftharpoons$	$CH_3OCH_3 + CO_2$	245.7

Catalyst systems for the direct synthesis of DME are usually mechanically mixed systems containing a copper-based methanol catalyst ($CuO/ZnO/Al_2O_3$, CZA) and a solid acid, such as zeolites or γ-Al_2O_3. Recently, the preparation of bifunctional catalysts that combine both types of active sites in one compound have been prepared and investigated [505].

Ahmad et al. reported the synthesis of alumina- and zeolite-based bifunctional catalysts with various copper and zinc oxide loadings using different preparation methods, such as co-precipitation, impregnation, sol–gel, or hydrothermal processes. These catalyst systems yielded the same conversion and selectivity as an admixed reference system containing a commercially available CZA catalyst and γ-Al_2O_3 [506].

Toyo Jumbo DME

For the Toyo JFE Pilot Plant in Japan (100 t/d), no commercial performance experience has been reported [504].

Topsøe DME from Synthesis Gas

Haldor Topsøe developed a one-step process technology for large-scale production of DME via direct synthesis from natural gas, without having to first produce and purify methanol. An illustration is given in Fig. 6.91.

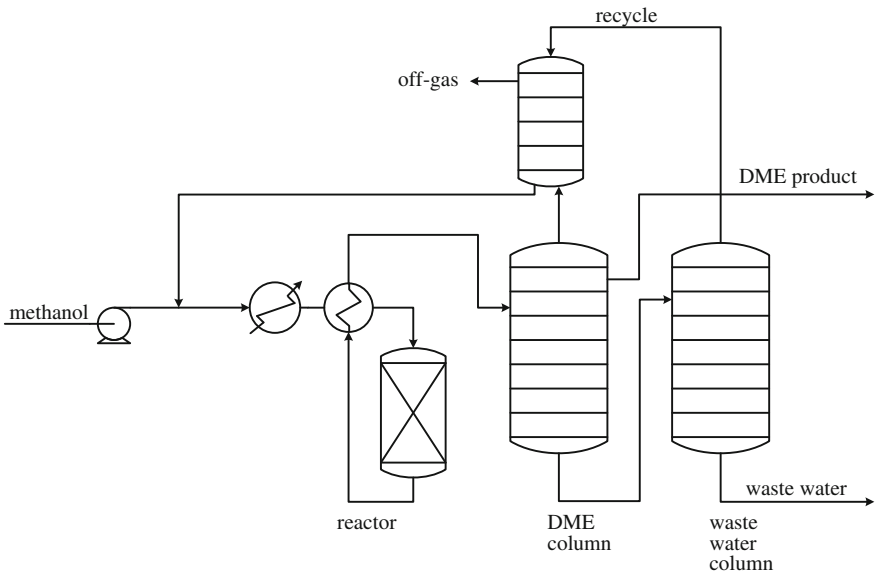

Fig. 6.91 Topsøe dimethyl ether (DME) Plant

6.4.4.3 Methanol-to-Aromatics

Methanol can be also used as synthesis feedstock for aromatics: "methanol-to-aromatics" or "Conversion of Methanol to Aromatics". The conversion of methanol to aromatics over H-ZSM-5 or H-gallosilicate (H-GaMFI) zeolite, with different Si/Ga ratios and degrees of H^+ exchange, which is calcined at different temperatures (600–1,100 °C), and pretreated hydrothermally at different temperatures and partial pressures of steam at 400 °C.

Clariant (formerly Süd-Chemie AG) offers the commercially proven catalysts for this process. The aromatisation activity and product distribution in the methanol-to-aromatics conversion are found to be influenced strongly by the above zeolite factors and calcination/pretreatment parameters. The aromatisation activity

of the zeolite shows a close relationship with its strong acidity (measured in terms of pyridine chemisorbed at 400 °C). H-GaMFI and H-ZSM-5 zeolites (having almost the same Si/(Ga + Al) ratio and degree of H^+ exchange and pretreated under similar conditions) and H-GaMFI show much higher aromatisation activity.

Applying advantageous conditions, high selectivity toward the desired aromatic product can be obtained. An example for this is the synthesis of *p*-xylene. It can be produced in great excess of the thermodynamic equilibrium distribution by using large H-ZSM-5 crystals and reaction parameters that reduce the degree of reactions taking place at the outer zeolite surface [507]. Under certain laboratory conditions, metal-doped ZSM-5 zeolites with Ag, Ni and Cu also show a higher selectivity to aromatics compared to unmodified ZSM-5 [508, 509]. Clariant (formerly Süd-Chemie AG) offers the commercial proven catalysts for this purpose.

Competition is represented by a process developed by BP, now licensed by UOP. Light alkane aromatisation over zeolite-based catalysts is well known [510–512]. The BP Cyclar process converts LPG directly into a liquid, aromatic product in a single processing step. The Cyclar process provides a route to upgrade low-value propane and butane, recovered from gas fields or petroleum refining operations, into a high-value, liquid aromatic concentrate that is ideal as feedstock in an aromatics complex.

The activity of Ga/ZSM-5 is consistently high (>95 % conversion) over the temperature range of 300–460 °C. The Ga-modified zeolite produced predominantly benzene, toluene and the xylenes and other heavier aromatics [513]. This difference in product distribution is consistent with the short-chain alkanes formed within the internal pore structure of the zeolite being intermediates in a Cyclar-type aromatisation mechanism. UOP also offers the commercially proven catalysts for this process. For converting paraffins to aromatics (CPA), Clariant (formerly Süd-Chemie AG) offers the commercial proven CPA-1 catalyst, which is a Ga-free H-ZSM-5.

6.4.4.4 Methanol-Derived Poly(oxymethylene) Dialkyl Ethers

Poly(oxymethylene) dialkyl ethers (also named polyethyleneglycol dialkyl ethers), particularly poly(oxymethylene) dimethyl ethers (POMDMEs), may serve as components of tailored diesel fuel [514].

The fuel blend comprises (1) fuel oil and (2) polyoxymethylene dialkyl ethers of the general formula R-O-$(CH_2O)_n$-R′, with the following meanings for R, R′ and n:

- R: methyl, ethyl, propyl, butyl, preferably methyl, ethyl, more preferably methyl,
- R′: methyl, ethyl, propyl, butyl, preferably methyl, ethyl, particularly preferably methyl,
- n: 2, 3, 4, 5, 6, 7, 8.

The oligomer POMDMEs of the general structure CH_3-O-$(CH_2$-$O)_n$-CH_3 open a new route for tailoring diesel fuels. POMDMEs belong to the group of oxygenates that reduce soot formation in the combustion when added to diesel fuels. POMDMEs can be produced on a large scale based on methanol.

POMDME produced from synthesis gas-based methanol results in an increase in the cetane number when added to diesel fuel, as well as in a clean burning of the diesel fuel, causing a reduced soot formation. The gas can come from geological sources, preferably those that are designated as "flared gas" or "stranded gas" or from those sources that are obtained as a byproduct of oil production. The methanol can also be equally of biological origin derived from biomass.

Hagen et al. reported on the preparation of POMDMEs by catalytic conversion of methanol-based DME with formaldehyde formed by oxidation of methanol [515]. In general, after the feedstream is passed over the catalyst, it will contain a mixture of organic oxygenates—at least one of which is of higher molecular weight than the starting DME. Effluent mixtures can be water, methanol, formaldehyde, DME, methylal and other POMDMEs having a structure represented by $CH_3O(CH_2O)_nCH_3$, in which n is a number ranging between 2 to approximately 7. Conditions of reaction include temperatures in a range from approximately 150–250 °C.

The stoichiometry of this condensation may be expressed by the following equations:

$$CH_3OCH_3 + n\ CH_2O \rightarrow CH_3O(CH_2O)_nCH_3 \tag{6.13}$$

$$2CH_3OH + m\ CH_2O \rightarrow CH_3O(CH_2O)_mCH_3 + H_2O \tag{6.14}$$

which may be combined as in the following equation when n is equal to m;

$$CH_3OCH_3 + 2CH_3OH + 2n\ CH_2O \rightarrow 2CH_3O(CH_2O)_nCH_3 + H_2O \tag{6.15}$$

As shown, the synthesis of methylal and higher POMDMEs from DME, methanol and formaldehyde is a reversible reaction that yields water as a co-product. Under certain conditions, at least a portion of the water may be consumed in a dehydrogenation reaction expressed by the following equations:

$$CH_3OCH_3 + CH_3OH + H_2O \rightarrow 3CH_2O + 3H_2 \tag{6.16}$$

and

$$CH_3OCH_3 + H_2O \rightarrow 2CH_3OH \tag{6.17}$$

Suitable DME sources may contain other oxygen-containing compounds, such as alkanol and/or water—preferably not more than approximately 15 % methanol and/or water by weight.

The ratio of formaldehyde to DME is between approximately 2:1 and 1:2 mol. Preferred temperatures are approximately 115–125 °C. Preferred pressures are approximately 15–25 bar. The reaction mixture feed gas flow rate, expressed as gas hourly space velocity, can be approximately 100–2,000 h^{-1}. Unconverted DME can be recovered from the mixture by well-known methods, including the use of distillation of the condensed product. The catalyst system is preferably a

crystalline borosilicate molecular sieve [515]. This type of process replaced the older, less benign and more expensive productions of polyethylene glycol dialkyl ethers, which are summarised by Arpe [516].

It has been known that POMDMEs can be prepared starting from methanol and paraformaldehyde at high temperatures. In the Dupont patent US 2,449,469, the polyformals are prepared starting from paraformaldehyde and dialkyl with sulphuric acid as the catalyst (acid concentrations of about 0.1–2 % by weight) [517–519].

> "A mixture of alkoxy-terminated poly-oxymethylenes, having a varied mixture of molecular weights, is blended with diesel fuel to form an improved fuel for autoignition engines. The base diesel fuel, when blended with the mixed alkoxy-terminated poly-oxymethylenes in a volume ratio of from about 2 to about 5 parts diesel fuel to 1 part mixed alkoxy-terminated poly-oxymethylenes, provides a higher quality fuel having significantly improved lubricity and reduced smoke formation, without degradation of the cetane number or smoke formation characteristics when compared with the base diesel fuel." From [520]

Such fuel blends on diesel base are described in US patient 5,746,785, WO 86/10351 and EP-A 1070755 [521]. Advantages of these blends are (1) a reduction of soot formation just for "heavy" diesel engines, which generally cannot be provided without loss of performance with particulate filters; (2) the preferred blends, due to their composition and their benefits, reduced freezing in storage, handling use and transport at low temperatures; and (3) an optimisation of the flash point.

Particularly preferred are polyoxymethylene with three or four oxymethylene units and mixtures thereof, especially tetra-oxymethylendimethylether ($n = 4$). The blending component contains a weight fraction of $H_3C–O–(CH_2O) \geq 4\text{-}CH_3$.

The BASF process for preparing POMDMEs, in particular of polyoxymethylene with $n = 3$ and 4 (trimer, tetramer) uses methylal ($n = 1$) or DME and trioxane. These components are preferably fed into a reactor and reacted in the presence of an acid catalyst, whereby the volume of water introduced into the reaction mixture of methylal/trioxane is less than 1 wt% of the reaction mixture. During the conversion of methylal with trioxane to polyoxymethylene, no water is formed as a byproduct. The reaction is generally conducted at a temperature of 90–150 °C and a pressure of 2–10 bar. The molar ratio of methylal to trioxane is generally from 0.5 to 5.

According to the BASF patent, the addition of 5 vol% tetraethylene to a diesel fuel reduced particulate emissions of a single-cylinder diesel engine up to 70 % at constant NO_x emission (according to EN 590), depending on the operating point. The reduction of the heating value of the fuel by the addition of tetraethylene is as low as 1.6 %. The oxygen content of the mixture is about 1.8 %. Polyethylene glycol dialkyl has good solvent properties. Therefore, necessary materials such as elastomers and plastics, as well as coatings that come into contact with polyethylene glycol dialkyl ethers, should be selected carefully [522].

The corresponding flash point of the mixture was measured according to DIN EN ISO 13 [736], and was 61 °C. The corresponding mixture had filterability (EN 116) of less than 54 °C. The cloud point (according to EN 23015) was −53 °C. The cetane number of the mixture was not determined in a MWM test engine. From the measurement of mixtures with 30/50/70 % kerosene, however, a borderline cetane number of 98.6 could be determined. The blends were prepared on a

static mixing system. A blend of glycol DME mixture (10 %) with diesel fuel (90 %) was prepared and tested in a DaimlerChrysler OM646 DE 22La engine in a dynamometer test. The result was a reduction of the soot emission compared to the operation of pure diesel fuel of up to 60 %.

MAN reported similar results [523]. A single-cylinder research engine had a capacity of 1.75 L, an engine power of 55 kW, a common rail injection system (rail pressure: 1,800 bar), a compression ratio of 20.5, and a start of injection before top of −8 °C a crank angle and an exhaust gas recirculation rate of 20 %. In this engine, a fuel mixture was tested consisting of 95 vol% diesel fuel according to EN 590 and 5 vol% oxymethylen-(dimethylglycol)ether (also known as bis(2-methoxyethoxy)methane; $C_7H_{16}O_4$; boiling point 197/205 °C; Alfa Aesar, Karlsruhe, Germany). For comparison, a diesel fuel without additive additions according to EN 590 was tested.

Diesel Fuel News reported on Snamprogetti's research results, referencing "cheap diesel fuel 'poly-oxy-methylenes'" that could cost less than ordinary diesel fuel, because it is basically a reaction of methanol with formaldehyde. Both of these products are considered to be relatively inexpensive feedstocks, especially if they are produced from low-cost remote gas [524]. According to Snamprogetti's preliminary process cost analysis on the basis of the year 2001, the oxy-diesel product could be produced at about US$130/tonne with gas feed at 50 cents/million BTU, or US$150/tonne with gas at US$1/MmBTU—cheaper than ordinary diesel fuel, even when crude trades around US$23/barrel. Snamprogetti's proposed process would use a cationic resin catalyst operating at 90–100 °C, with greater than 98 % product selectivity and greater than 95 % formaldehyde conversion. Catalyst life tests have not shown deactivation problems. Furthermore, the blend would not cause any product quality or environmental/health problems.

Snamprogretti's oxy-diesel was described as a "proprietary tailored mixture produced via proprietary process" with "3-6 [CH_2]-O units, no C–C bonds, high oxygen percentage and high cetane number." Although the product has fewer BTUs per gallon than diesel fuel, fuel consumption is "almost unchanged" at blend volume levels of 5–10 %. At the 10 % level, fuel oxygenate content is 4.5 wt%.

After synthesis of hundreds of litres for product testing, tests of the fuel properties showed a cetane number of 80–100. Blended diesel flash point was not affected and good cold-flow properties were realised. In vehicle tests on a modern Alfa-Romeo 156 1.9 TDI with common-rail injection, a 10 % blend of the oxy-diesel with 90 % baseline diesel (30 ppm sulphur) cut particulate matter emission by 15–20 %, carbon monoxide/hydrocarbon by 5–10 % and left nitrogen oxides almost unchanged. Only the best Euro diesel fuels (such as Swedish Class 1) were found to match the performance of the oxy/diesel blend, as reported by the company [525].

The oxy component biodegradability is similar to diesel fuel and 10 times more degradable than MTBE. A preliminary investigation on toxicology did not indicate any negative information. In addition, the product does not have any foul odour, which is a major advantage over many other fuel oxygenates. Still, social

acceptance research is not complete, as "toxicology, biodegradability, and all other health/safety/environmental impacts are to be severely checked" prior to any commercialisation effort.

The Snamprogetti polyoxymethylene product does not seem to have the market-killing volatility problems of DME and DMM, the huge cost (and taxpayer subsidy problems) of biodiesel, the flashpoint problems of ethanol–diesel and the water-pollution/odour problems that are typical of ether oxygenates.

6.5 Other Methanol Utilisation Technologies

6.5.1 Methanol Splitting and Reforming for Hydrogen-Rich Gases

Jürgen Roes[1], Michael Steffen[2] and Hans Jürgen Wernicke[3]

[1]*Institute of Energy and Environmental Process Engineering, University of Duisburg-Essen, Lotharstraße 1, 47048 Duisburg, Germany*

[2]*The fuel cell research centre ZBT GmbH, Carl-Benz Straße 201, 47057 Duisburg, Germany*

[3]*Kardinal–Wendel-Straße 75 a, 82515 Wolfratshausen, Germany*

Introduction

Methanol has many advantages as an energy carrier for mobile, portable and off-grid applications [526]. Compared to hydrogen stored as gas, liquid, or hydride, methanol requires a far lower volume for the same energy content. Methanol can easily be transported and stored on site; hence, compared to natural gas or LPG, it is an attractive hydrogen and energy carrier for decentralised supply.

in comparison to other alcohols and hydrocarbons, generating hydrogen or synthesis gas methanol is attractive, not only because of its low reforming temperature but because of the low steam-to-carbon (S/C) ratio that is required, its good solubility in water, and the usually very low sulphur content. Methanol is the only alcohol or hydrocarbon that can be reformed at temperatures as low as 180–300 °C to convert it into a hydrogen-rich gas mixture. The basic physical data of methanol are summarised in Sect. 5.1. Its toxicity and procedures for safe handling and transport are discussed in Sects. 5.2 and 5.3.

Methanol Production

Methanol is produced on an industrial scale from synthesis gas containing hydrogen, carbon monoxide and carbon dioxide and is based on fossil and regenerative raw materials (see Chap. 4). Methanol is used as feedstock for numerous synthesis reactions, such as to produce acetic acid, formaldehyde, or ethanol (see Sect. 6.2) or as a component in fuels (see Sects. 6.3 and 6.4). Conversely, methanol can be

decomposed into its starting products hydrogen, CO, and CO_2 by means of "dry" splitting or "wet" reforming in the presence of steam. This process is being used for specific purposes of hydrogen generation on a smaller scale or for generation of special gas mixtures, mainly for materials treatment.

Thermodynamics of Methanol Splitting and Reforming

When methanol is used to produce a synthesis gas containing carbon monoxide and hydrogen, the simplest process is the splitting of methanol (Eq. 6.18):

$$CH_3OH \rightarrow 2H_2 + CO \quad \Delta_R H^{\emptyset} = 128\ \text{kJ/mol} \tag{6.18}$$

Other possibilities are the partial exothermic oxidation into hydrogen and CO_2 (Eq. 6.19):

$$CH_3OH + 0,5O_2 \rightarrow 2\,H_2 + CO_2 \quad \Delta_R H^{\emptyset} = -155\ \text{kJ/mol} \tag{6.19}$$

In the presence of steam, methanol reforming, which is less endothermic than methanol splitting (as shown in Eq. 6.18) leads to maximum hydrogen output (Eq. 6.20):

$$CH_3OH + H_2O \rightarrow CO_2 + 3H_2 \quad \Delta_R H^{\emptyset} = 49\ \text{kJ/mol} \tag{6.20}$$

The combination of partial oxidation and steam reforming allows maximising hydrogen yield under autothermal conditions (Eq. 6.21):

$$2CH_3OH + H_2O + 0,5O_2 \rightarrow 5H_2 + 2CO_2 \quad \Delta_R H^{\emptyset} = \pm 0\ \text{kJ/mol} \tag{6.21}$$

The method that is most often applied in practice to produce a hydrogen-rich synthesis gas from methanol is the steam-reforming process (Eq. 6.20). Depending on process conditions and desired application of the product gas, it will lead to a mixture of hydrogen, carbon monoxide and carbon dioxide. The reaction usually takes place at 180–350 °C and is accelerated by catalysts typically based on copper/zinc or precious metals. The steam-reforming reactions are expressed as a series of reactions [527, 528]: first, the endothermic decomposition of methanol (Eq. 6.18) followed by the slightly exothermic water–gas shift reaction

$$CO + H_2O \rightleftharpoons CO_2 + H_2 \quad \Delta_R H^{\emptyset} = -41\ \text{kJ/mol} \tag{6.22}$$

To reach a high degree of conversion and high catalyst activities, high reaction temperatures are preferable. Figure 6.92 shows the composition of the product gas (on a dry basis) at thermodynamic equilibrium as a function of the temperature at a pressure of 0.5 MPa and an S/C ratio of 1.5 [529].

As temperatures increase, the equilibrium shifts towards higher carbon monoxide contents in the product gas (Fig. 6.93). The influence of temperature and S/C ratios on the equilibrium concentration of carbon monoxide is shown elsewhere.

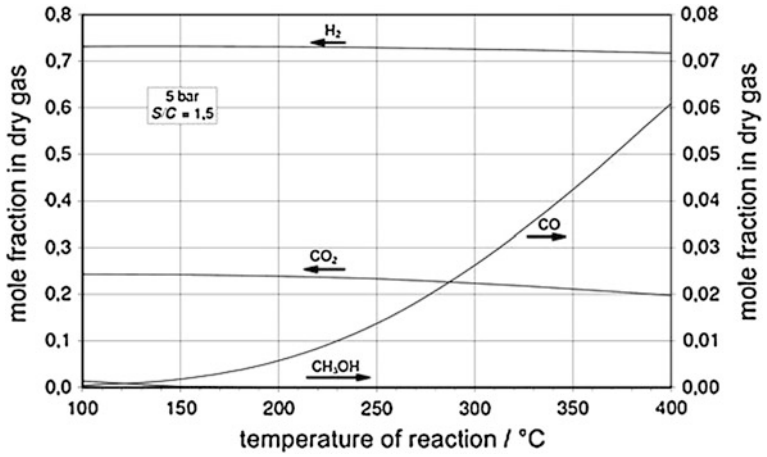

Fig. 6.92 Product gas composition in thermodynamic equilibrium for methanol steam reforming as a function of reaction temperature [529] S/C: steam-to-carbon ratio

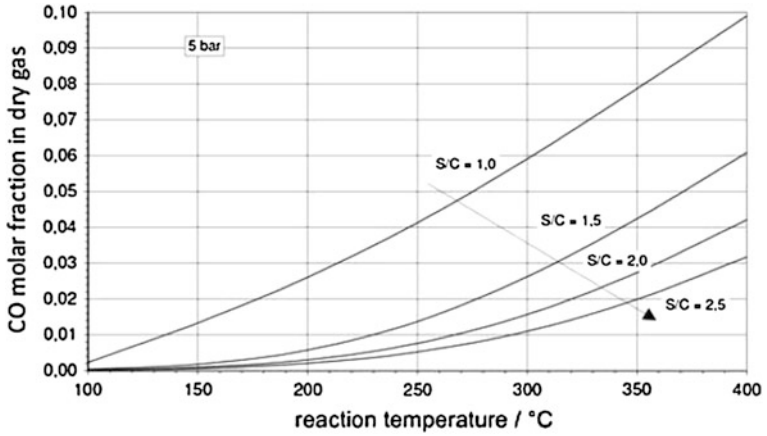

Fig. 6.93 Carbon monoxide fraction in the dry product gas in thermodynamic equilibrium for methanol steam reforming at 5 bar [529]

An increase of the S/C ratio increases the hydrogen yield and decreases the carbon monoxide yield in the product gas due to an increased CO conversion by the water–gas shift reaction. The correlation of the composition of the dry product gas as a function of the S/C ratio in the feed is shown in Fig. 6.94.

From the equilibrium calculations as shown in Figs. 6.92, 6.93, 6.94, optimal conditions for temperature and (costly) steam addition are in the range of 200–300 °C and S/C ratios are in the range of 1.1–1.5.

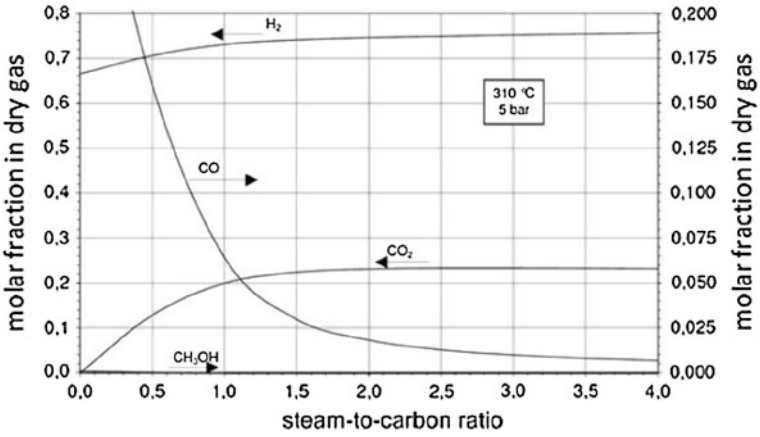

Fig. 6.94 Product gas composition in thermodynamic equilibrium for methanol steam reforming at 310 °C and 5 bar [529]

Reaction Mechanism of Methanol Steam Reforming

In addition to the desired reforming reaction of methanol, side reactions such as methanisation of products CO and CO_2 are possible (Eq. 6.23 and 6.24):

$$CO + 3H_2 \rightarrow CH_4 + H_2O \quad \Delta_R H^{\emptyset} = -206.1\,\text{kJ/mol} \tag{6.23}$$

$$CO_2 + 4H_2 \rightarrow CH_4 + 2H_2O \quad \Delta_R H^{\emptyset} = -164.94\,\text{kJ/mol} \tag{6.24}$$

Another side reaction is the formation of carbon by the Boudouard reaction (Eq. 6.25):

$$2CO \rightleftharpoons CO_2 + C \quad \Delta_R H^{\emptyset} = -172.45\,\text{kJ/mol} \tag{6.25}$$

Deposition of carbon on the catalyst results in a reduction of its activity as the carbon occupies the active sites of the catalyst and is blocking the catalyst pores [527, 530]. It will also contribute to an increased pressure drop of the reactor system. The formation of carbon by the Boudouard reaction is favoured by low reaction temperatures, high total pressures and low S/C ratios. Thermodynamic calculations were performed by Formanski [529] in order to determine the regime of potential carbon formation.

Two different models were considered, which differ in the consideration of methane as a product. Although model 1 (H_2, CO, CO_2, C(s)) disregards methane, model 2 (H_2, CO, CO_2, CH_4, C(s)) allows the formation of methane in the reaction mechanism. The equilibrium of the reactions for both models is iteratively calculated using mass balance and equilibrium approaches. For the calculation, pressures of 0.01, 0.1 and 1 MPa were assumed and the reaction temperature was varied between 300 and 800 K (27–527 °C).

Figure 6.95 illustrates the thermodynamic calculations under these conditions, which result in areas with and without potential carbon formation. For model 1 (methane formation disregarded), a temperature over 530 K (260 °C) would be necessary in order to prevent carbon deposition at S/C ratios above 1.3. For model 2 (methane formation included) and S/C ratios above 1.3, reaction temperatures above 450 K (177 °C) are sufficient to be outside the regime of potential carbon formation.

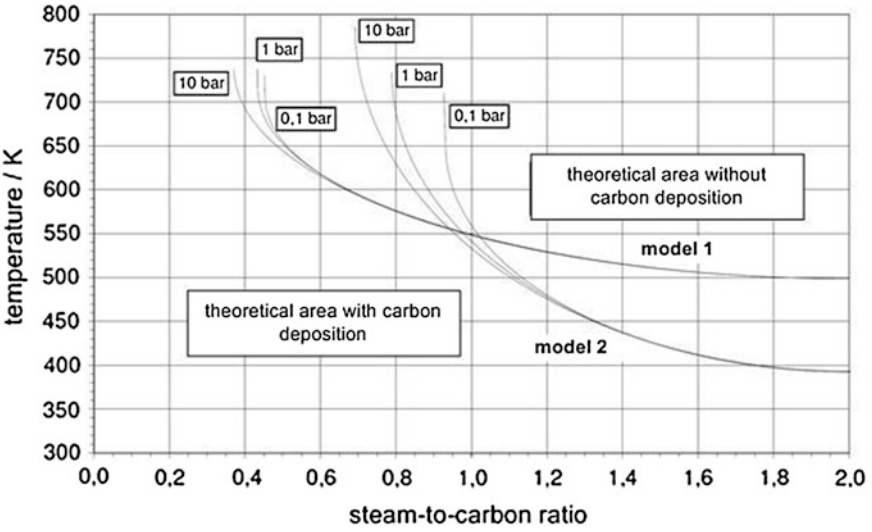

Fig. 6.95 Limiting conditions for the deposition of solid carbon for steam reforming of methanol [529]

Figure 6.96 shows the principal pathways of methanol steam reforming, including the formation of byproduct methane [527]. If the methane formation can be suppressed by a sufficiently selective catalyst, it results in a simplified reaction scheme, as shown in Fig. 6.97 [527]. Typical catalysts that minimise methanisation are copper/zinc catalysts, which are also applied for the water–gas shift conversion of carbon monoxide and for methanol synthesis. In this way, methanol reforming can simply be described as a combination of methanol decomposition (reverse synthesis) and water–gas shift reaction [527]. In addition to copper/zinc catalysts, chromium and iron-containing copper catalysts are more temperature stable. Mechanistic studies of the assumed combination of methanol decomposition followed by the water–gas shift reaction are contained in various sources [527, 528, 531].

If the reaction temperature is increased or the space velocity through the catalyst bed is increased, the concentration of carbon monoxide in the product gas is somewhat below the thermodynamic equilibrium, which can be seen in Fig. 6.98 [532].

The various effects of higher catalyst space velocities on the product yields, the approach to equilibria and the underlying potential reaction mechanisms are

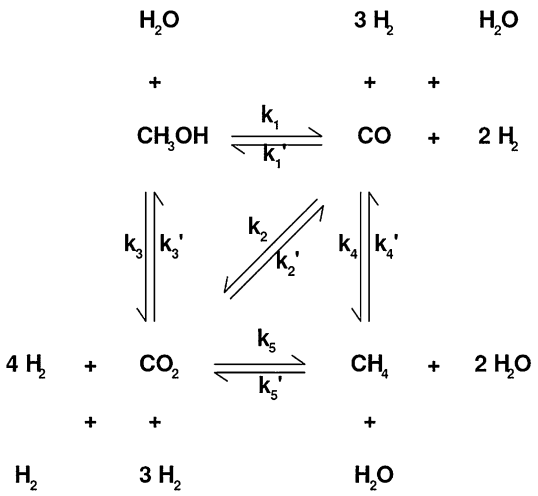

Fig. 6.96 General reaction scheme of methanol steam reforming [527]

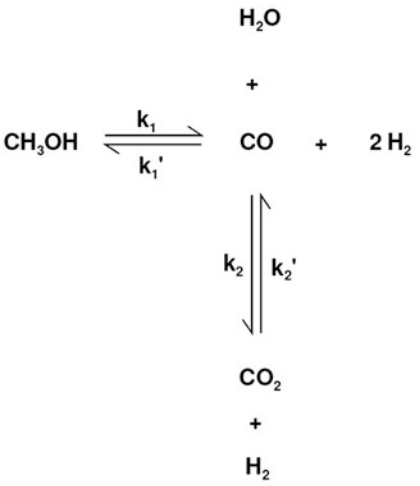

Fig. 6.97 Simplified reaction scheme of methanol steam reforming [527]

described in various sources [527, 533, 534]. Generally, nonnoble catalysts based on promoted CuO/ZnO are used for the steam reforming of methanol. The composition of these catalysts is very similar to catalysts used for the low-temperature water–gas shift reactions. CuO/ZnO catalysts are only used in a moderate temperature region because they tend to sinter on higher temperatures. They are pyrophorous in their active (reduced) form. They are also sensitive to entrained liquid water or condensing steam, as well as to poisons such as sulphur or chlorine compounds and nonsaturated hydrocarbons.

Noble metal-based catalysts that are used for methanol reforming (mostly promoted palladium or platinum on alumina carriers) are more robust by means of handling. Driven by mobile applications and small power generators based on

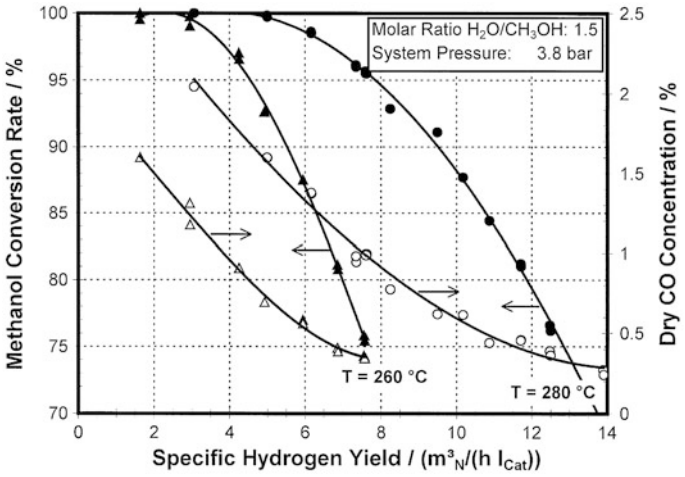

Fig. 6.98 Methanol conversion and carbon monoxide fraction as a function of catalyst load [532]

methanol fuel cells, more active noble metal catalysts have been developed, which are impregnated on wash-coated, low-pressure drop ceramic or metal substrates.

Methanol Decomposition in Absence of Steam

One option to produce hydrogen (and CO) is the endothermal splitting of methanol, carried out thermally or in presence of catalysts. The resulting reducing gas is used for protection of materials against oxidation or (with the presence of CO) for special heat treatments. Thermal decomposition is performed by injecting a mixture of nitrogen and methanol directly into the heat treatment furnace at temperatures over 750 °C. At these temperatures, methanol predominantly splits into carbon monoxide and hydrogen [538]. At temperatures below 640 °C, the methanol decomposition is thermodynamically favoured; exothermic side reactions lead to H_2O, CO_2 and CH_4.

The composition of the gas from methanol splitting (i.e., its carbon content) can be flexibly adjusted by varying the inlet feed methanol-to-nitrogen ratio as needed for the respective application. For the carburisation of materials, an inlet feed that has a high methanol-to-nitrogen ratio will be used. For the purpose of normalising, bright annealing, or sintering, a treatment gas richer in nitrogen is used. Sometimes, other gases are co-fed, such as propane or natural gas, to control carbon content or ammonia for nitriding. Companies offering such treatment systems are named in various sources [535–537].

To significantly reduce the operation temperature, the methanol splitting can be done with the use of catalysts, which are selective to generate CO and hydrogen and avoid undesired side reactions such as methanisation. Common catalysts for this “dry catalytic reforming” are based on promoted copper/zinc, which are also used for methanol synthesis or on precious metal, usually platinum or palladium

on a carrier [538]. In mobile applications, on-board methanol decomposition has been investigated to produce a CO/hydrogen fuel for internal-combustion engines or (with the addition of a water–gas shift reactor) to produce pure hydrogen for fuel cells [539, 540]. Methanol-based fuel cells are comprehensively described in Sect. 6.5.1.

Methanol Reforming with Steam

For hydrogen maximisation from methanol, reforming in the presence of steam is preferred. Although natural gas as a feedstock for hydrogen generation would be cheaper (also in smaller hydrogen plants), methanol steam reformers benefit from significantly lower investment costs due to the considerably lower reforming temperatures and a simpler process flow sheet. Using methanol avoids feed conditioning (sulphur removal) and high or low temperature shift conversion, which overall saves 20–30 % investment costs. Typical capacities for methanol steam reformer plants range from 50 to 3,000 Nm^3/h hydrogen.

The main feed streams for the process are methanol and demineralised water, which are premixed in a mixing tank. For the production of 1 Nm3 H_2 (compared to a thermal hydrogen output of 3 kW), approximately 0.65 kg methanol (compared to 20.3 mol CH_3OH or a thermal methanol output of 3.6 kW based on a lower heating value of 637.7 kJ/mol) is required. This leads to a very high thermal efficiency of approximately 83 % due to an internal heat recovery by preheating the feed against cooling the flue gas [542].

Figure 6.99 shows a simplified process flow sheet for methanol steam reforming. This process typically takes place at operating pressures of

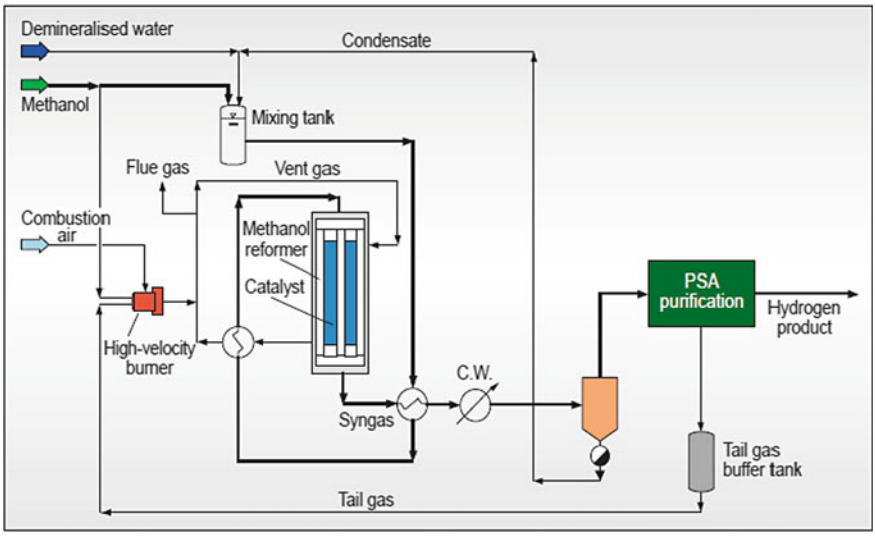

Fig. 6.99 Process scheme of a methanol steam reformer system (Caloric Anlagenbau, Gräfelfing, Germany) [541–543]. PSA, pressure swing adsorption

approximately 2–3 MPa and reforming temperatures between 250 and 300 °C given by the thermodynamic equilibrium (see Fig. 6.92) and the operating temperature range of the Cu/Zn catalyst, which is applied here.

All components of heat management are combined in a so-called hot box, including preheating of the feed, evaporation of the methanol water mixture, the steam-reforming reactor and the product gas cooling. A burner is heating the hot box with circulating flue gas by convective heat transmission. The large volume of circulating flue gas leads to an even heat distribution. The flue gas adjusts the reactor temperature to about 300 °C and is controlled to the optimum operation temperature of the catalyst for maximum yields and catalyst life. Figures 6.100 and 6.101 show a typical arrangement and a photograph of a complete methanol-to-hydrogen plant with reformer, gas purification (by pressure swing adsorption, PSA) and buffer tank setup by Caloric Anlagenbau. The hydrogen output of the shown plant is 750 Nm^3/h.

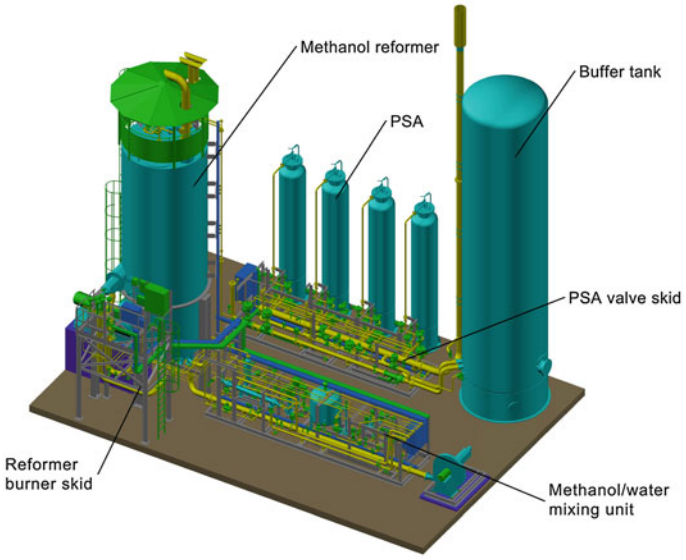

Fig. 6.100 Configuration of a 1,500 Nm^3/h methanol-to-hydrogen plant with reformer and pressure swing adsorption (PSA). (Caloric HM process) [541]

Another industrial example is the Hydroform-M plant by Mahler AGS [544], which has a hydrogen capacity from 100 to 3,000 Nm^3/h and a purity up to 99.999 %. A typical design pressure delivers hydrogen at 1.3 MPa at the exit of the PSA unit (alternatively at 2.6 MPa). The unit uses a thermo-oil cycle for heat management. As shown in Fig. 6.102, demineralised water and methanol from the battery limit are fed into the feed storage vessel (D 10). The feed mixture is pumped and heated up in the process gas heat exchanger (E 10) against the

Fig. 6.101 Caloric HM methanol steam reforming plant with a hydrogen capacity of 750 Nm^3/h [541]

reformed process gas coming from the methanol reformer reactor (R 10). Thereby, part of the feed is already vapourised. Complete vapourisation and a temperature of approximately 260 °C is achieved in a thermo-oil heat exchanger (E 20) before entering the reformer reactor (R 10).

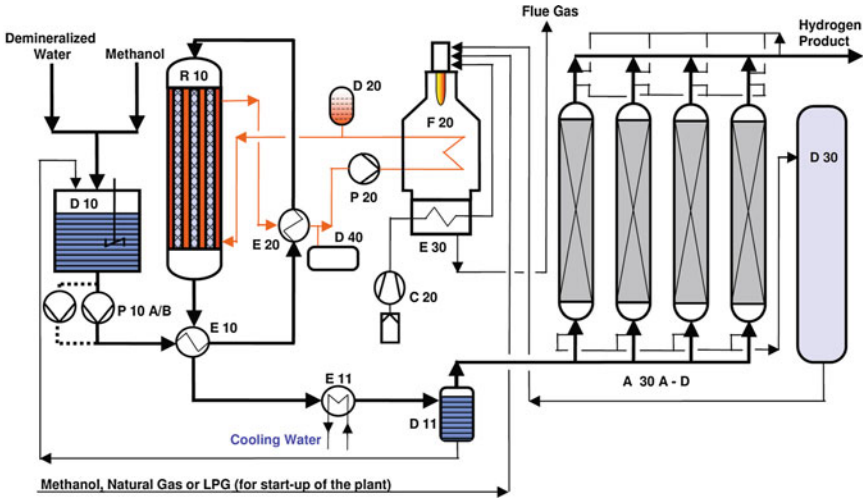

Fig. 6.102 Flow diagram of the Mahler Hydroform-M process [544]. A 30 = A-D pressure swing adsorption unit, C 20 = combustion air blower, D 10 = feed storage vessel, D 11 = knockout drum, D 20 = thermal oil expansion vessel, D 30 = pure gas puffer, D 40 = thermal oil drain tank, E 10 = feed preheater, E 11 = water cooler, E 20 = feed superheater, E 30 = combustion air preheater, F 20 = thermal oil heater, P 10 = feed pump, P 20 = thermal oil pump, R 10 = reactor

Reaction conditions are maintained by circulation of thermo-oil (pump P 20) through the reformer reactor, the thermo-oil heat exchanger (E 20), and the heater (F 20). The final cooling of the process gas to approximately 38 °C takes place against cooling water in a water cooler (E 11). Excess water vapour of the syngas is condensed and separated in a so-called knockout drum (D 11) and then sent back into the feed storage vessel (D 10).

The purification of the process gas is performed in a four-bed PSA unit. The hydrogen product downstream the PSA can achieve a purity of more than 99.999 vol%. Typically, the purge gas from the PSA is collected in buffer (D 30) and sent to the burner in the heater (F 20) and used as burner fuel. During normal operation, a small amount of additional methanol fuel is required; during start-up of the plant only, additional heat is generated by burning of methanol. The combustion air provided by the air blower (C 20) is preheated in the flue gas system of the thermal oil unit (E 30) in order to save fuel [544]. The thermal oil as the heat transfer medium helps to avoid temperature peaks and thereby protects the catalyst for the complete lifetime, as well as reduces the needed instrumentation for the process. A photograph of a Mahler Hydroform-M plant is shown in Fig. 6.103 [544].

Fig. 6.103 Mahler Hydroform-M plant [544]

The product gas from the methanol steam reformer usually has a maximum hydrogen content of 70–80 vol% (on dry basis) at elevated pressures and is usually treated in a PSA to further concentrate the hydrogen to more than 99.9 vol% (up to 99.999 vol%). The PSA process is a gas purification system using different adsorption capacities of solid adsorbent materials and pressure differences between adsorption and desorption steps. Typical adsorbents are activated carbon, zeolithic molecular sieves, silica gel and carbon molecular sieves. Such a PSA unit consists of at least two but mostly four adsorber towers, with several layers of different adsorbent materials in order to produce an almost continuous pure hydrogen flow from the alternating adsorption, desorption (depressurising), regeneration and re-pressurising steps. The principal arrangement of a unit with four single adsorbers is shown in Fig. 6.104 (Hydroswing, Mahler AGS) [545].

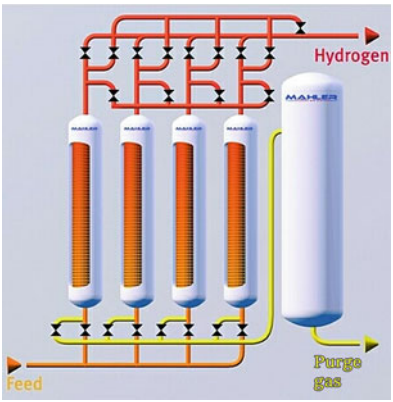

Fig. 6.104 Principal arrangement of a pressure swing adsorption unit for pure hydrogen production

For lower purity requirements, an enrichment of hydrogen from the product gas in a continuous process can be achieved by polymer membranes. Examples are the PRISM separator from Air Products [546] or the PolySep separator from UOP [547]. Very pure hydrogen (>99.9999 vol%) can be generated by application of selective membranes consisting of Pd–Ag or Pd/Cu alloys.

Major Applications of Methanol Reforming

In mobile applications, on-board reforming of methanol for hydrogen/CO driven ignition motors (see review [539]) has not yet found broader applications. However, the use of hydrogen in fuel cell systems may have some future applications (see Sect. 6.5.1). More important are stationary plants to generate hydrogen in locations where the demands falls in between a supply in cylinders or cylinder bundles and the larger hydrogen capacity of natural gas steam reformers. Limited, decentralised hydrogen demand can be found in specialty chemicals and pharmaceutical applications, in edible oil processing (fat hardening) and recycling, hydrofinishing of lubes and waxes and in the production of float glass.

The broadest application is the supply of protective gas against oxidation of materials during heat treatment. Various gas mixtures of methanol with other components are used for special treatment of materials, mostly of metal alloys to modify their physical and mechanical properties. An example for a variety of metallurgical treatments is the Tempron process by Westfalen AG [537]. An overview of such applications is given in Table 6.22.

Table 6.22 Heat treatment of metal alloys with various mixtures of inert gases with methanol, ammonia, hydrocarbons and oxygen [537]

Application	Steel (< 0, 3 % C)	High Carbon Steel (> 0, 3 % C)	Cr- and Mn- steel	Corrosion-, Acid- and Heat-resistant Steels	Casted Iron and Steel	Non-ferrous metals Silver, Nickel, Copper. Brass	aluminium and aluminium Alloys
Carburising	NM, NME, NMP, NMO	NME, NMP	NM, NMP				
Bright Annexing	NH, NM	NH, NM, NMP	NM, NH, NMP	NH, Ar	N	0NH, NM, H	NH. NM, N
Nitriding	NA	NA	NA				
Nitrocarburising	NMA, NCA	NMA, NCA, NWEA	NMA				
Dry-cyaniding	NMA, NPA	NMA, NMPA, NMEA, NPA	NMA, NMPA. NMEA, NPA				
Decarburising, Blueing	NO, NH + H20	NO, NH + H20	NO, N + H20	NH, H, AfH + H20	Air + H20		
Normalising	N, NM, NP	NM, NP, NMP	N, NM, NP, NMP	Af	NM NPO, NMP		
Sintering	NH, NM, NP	NH, NM, NP, NME, NMP	NH, ArH, H	NH. A(H, H		NH, NM	NH, NM
Oven soldering, Brazing	NH, MM	NH, NM, NP	NH, ArH	H, NftAfH		NH, NM	NH

Abbreviations: Ar = argon, N = nitrogen, H = hydrogen, ArH = argon + hydrogen, NH = nitrogen + hydrogen, NP = nitrogen + propane, NM = nitrogen + methanol, NME = nitrogen + methanol + ethanol, NMP = nitrogen + methanol + propane, NMO = nitrogen + methanol + oxygen, NMEA = nitrogen + methanol + ethanol + ammonia, NMPA = nitrogen + methanol + propane + ammonia, NMA = nitrogen + methanol + ammonia, NPA = nitrogen + propane + ammonia, NCA = nitrogen + CO_2 + ammonia, NA = nitrogen + ammonia, NO = nitrogen + oxygen

Summary

Methanol is widely available from fossil and regenerative sources, and as a liquid it can be easily transported and stored. In specific cases of decentralised supply with hydrogen or other gas mixtures, a stationary methanol splitting or reforming unit can be advantageous as a technically proven and economical alternative. Typical capacities of those units range from 50 to 3,000 Nm^3/hour. The broadest application of methanol and its decomposition products is the heat treatment of metals, either as a protective atmosphere or a functional treatment to change the metallurgical properties. Mobile applications by means of on-board methanol reforming to fuel ignition engines are still in experimental status, whereas on-board hydrogen generation for fuel cells may find broad applications in the future (see Sect. 6.5.2).

6.5.2 Methanol Fuel Cells

Gerd Sandstede[1] and Angelika Heinzel[2]

[1]*Esperantostraße 5, 50598 Frankfurt/M, Germany*

[2]*Institute of Energy and Environmental Process Engineering, University of Duisburg-Essen, Lotharstraße 1, 47048 Duisburg, Germany*

6.5.2.1 Introduction

Methanol is an energy carrier with several advantages compared to other fuels [548]. The properties of methanol are the subject of several other chapters of this book. In this chapter, the use of methanol as fuel for fuel cells is discussed. This includes the direct methanol fuel cell (DMFC), which is properly designed for methanol as fuel, as well as fuel cells connected to a methanol reformer, which generate electricity from hydrogen being contained in the reformate. In this introduction, the different types of fuel cells are described in some detail before special developments for the use of methanol as fuel are given. This includes basic thermodynamic information, material properties and electrochemical aspects. Finally, state-of-the-art developed systems and their properties are presented. Advantages and disadvantages are discussed, leading to the conclusion and vision for the future use and application of methanol as fuel for fuel cells.

6.5.2.2 Introduction of Fuel Cells

Reasons for the Application of Fuel Cells

The modern development of fuel cells started in the United States in the 1960s for application as an electricity generator during space missions. This initiated widespread research and development (R&D) efforts in the United States, as well as in Europe and Japan, leading to different types of fuel cells for various terrestrial applications, such as stationary combined heat and power supply and power supply for electric drives and portable devices as a battery replacement or range extender.

The increasing awareness of the environmental challenges connected to the use of fossil energy carriers and the need for cleaner and more efficient energy conversion processes gave a good reason to foster the development of fuel cell technology. One of the driving factors was the demand for reduction of traffic-related emissions in regional conurbations by introducing zero-emission vehicles. This request was at first formulated in the Californian Clean Air Act [549] and has led to significant efforts in realising electric vehicles. The various types of batteries—even the recently introduced high-energy–density lithium-ion battery—enable typical passenger cars for a limited driving range and require quite long charging (fueling) times; therefore, fuel cells have been considered to be an attractive option.

Some reasons for the use of fuel cells are

- High conversion efficiency, at least of hydrogen as fuel into electricity
- Low or even no emissions, except water from the electrochemical conversion process
- Good scalability due to the modular design of the fuel cell
- Independent choice of power (size of fuel cell) and energy (size of fuel tank)
- Suitability for combined heat and power supply
- Availability of different technologies for different operation temperatures and thus for different fields of application
- Electrochemical energy conversion that does not require moving parts and does not emit noise

In a fuel cell, chemical energy is directly converted in an electrochemical conversion process into electricity and heat. The theoretical maximum efficiency is determined by the ratio between the free Gibbs energy (free enthalpy) and the enthalpy of the reaction under consideration and is not limited by the Carnot factor, as it is the case for conventional thermal energy conversion processes as used in engines or in power plants. Depending on the fuel, a fuel cell might require a preceding fuel processing step, which generates a hydrogen-rich gas from the fuel (e.g. natural gas, methanol). The enthalpy and free enthalpy values of various combustion reactions under constant pressure are well known and can be taken from classical thermodynamic tables [550] in order to calculate the maximum of electrical energy and the theoretical limit for the efficiency that can be delivered by a certain fuel cell.

Some Thermodynamic Aspects

To understand the operation principle of fuel cells, energy conversion processes have to be considered. In contrast to conventional combustion reactions that are based on direct chemical reaction of a fuel with oxygen (in general, taken from the ambient air), fuel cells divide this reaction into two parts: the electrochemical oxidation of the fuel and the reduction of oxygen. For this purpose, separate fuel and oxygen (air) compartments or half cells are realised, being equipped with an electrocatalyst that is especially designed to catalyse the electrochemical reaction, even at relatively low reaction temperatures. Hydrogen is a fuel that is highly reactive, even at low temperatures (in the presence of a platinum catalyst). Equation 6.26 shows the exothermal chemical reaction.

$$2H_2 + O_2 \rightarrow 2H_2O \qquad \Delta_R H^0 = -285.8\,\text{kJ/mol} \tag{6.26}$$

The heat of reaction at normal conditions (0.101325 MPa, 273.15 K) and constant pressure $\Delta_r H^0$ is negative, meaning that heat is released from the system.

For methanol, the reaction with oxygen gives carbon dioxide and water.

$$2CH_3OH + 3O_2 \rightarrow 4H_2O + 2CO_2 \quad \Delta_R H^0 = -726\,\text{kJ/mol} \tag{6.27}$$

Both reactions are valid for the combustion process and the electrochemical process as well. For energy conversion devices, the efficiency of conversion is one of the most important criteria.

Characteristics of Fuel Cells

Electrochemical energy conversion devices differ significantly from those for chemical conversion. The latter usually scale with the volume, but electrochemical conversion is related to an area. The reason is easy to understand because the fuel and the oxygen have separately to be brought into contact with an electrode comprising the electrocatalyst and a current collector. On one side of the electrode, the chemical substances (educts and products) are circulating in the electrode compartment; electrons (electrical energy) are transported in the electrode itself and the adjacent current collectors. In the case of a fuel cell, continuous feeding of fuel and oxidant results in continuous energy release. The operation principle of a fuel cell is depicted in Fig. 6.105. Here, the simplest reaction is chosen, the conversion of hydrogen.

The electrodes and electrocatalysts are highly porous and therefore have a high specific surface area; the gas diffusion layers (GDLs) are also porous, but much less so because they serve as current collectors and for the distribution for the reactant gases. The electrolyte is gas tight but water can diffuse through it. Reviews in the literature about fuel cells give much more details [551–564].

Electrochemical Reactions

Electrochemical reactions are characterised by the local separation of the reduction reaction—here, for example, the reduction of oxygen molecules to oxygen ions

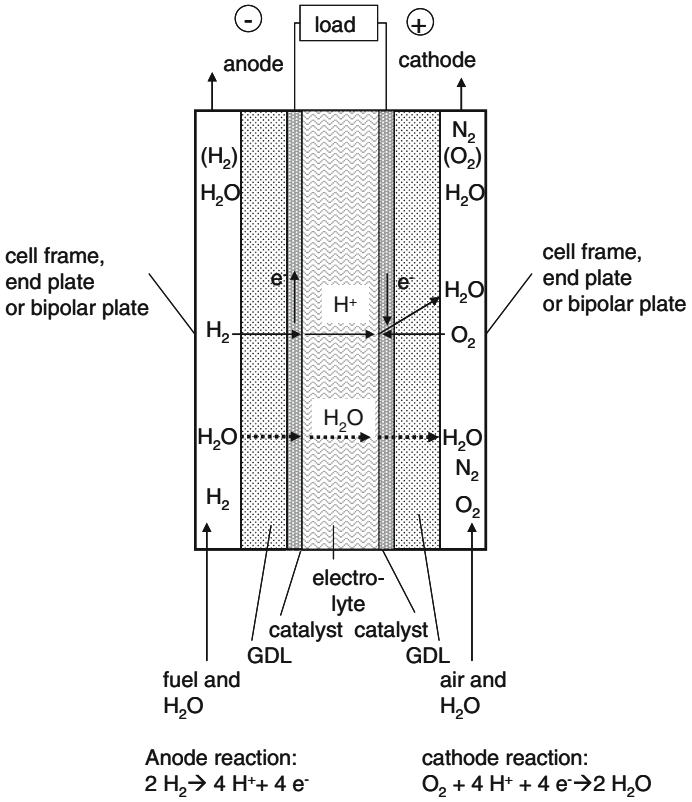

Fig. 6.105 Hydrogen fuel cell with proton conducting electrolyte. GDL, gas diffusion layer

and the oxidation reaction of hydrogen to protons (Eq. 6.28 and 6.29). Reduction reactions take place at the cathode; the anode serves for oxidation. The separate reactions occur at the electrodes, leading to a certain electrode potential. Due to this potential, the reaction stops as electrons cannot longer be transferred to or from the charged electrodes. A continuous reaction requires a closed electrical cycle. For this purpose, the cathode and the anode have to be connected to an electric load, allowing electrons to flow from the anode to the cathode. A second prerequisite is that hydrogen ions must reach the cathode compartment and must react with oxygen in order to form water as a product. This can be realised by an electrolyte that is proton conductive.

$$2H_2 \rightarrow 4H^+ + 4e^- \tag{6.28}$$

$$O_2 + 4H^+ + 4e^- \rightarrow 2H_2O \tag{6.29}$$

The ideal theoretical difference between the electrode potentials, the cell voltage, can be calculated from thermodynamic values. The basic equation is the

Gibbs equation, giving the relationship between the Gibbs free enthalpy at normal conditions $\Delta_r G^0$ and the enthalpy $\Delta_r H^0$ of a reaction (Eq. 6.30).

$$\Delta_R G^0 = \Delta_R H^0 - T\Delta_R S^0 \quad \Delta_R G^0 = -237.1\,\text{kJ/mol} \tag{6.30}$$

Although the free enthalpy of the reaction can be converted into electrical energy, the remaining part, $T\ \Delta_R S^0$, represents a heat. Conversion of 1 mol of hydrogen allows the calculation of U_{rev}, the reversible cell voltage:

$$U_{rev} zF = \Delta_R G^0 \quad \text{or} \quad U_{rev} = \Delta_R G^0 / zF = 1.229\,\text{V} \tag{6.31}$$

with

z Number of transferred electrons per mole of substance (2 for hydrogen) and
F Faraday constant = 96,485 C for 1 mol of electrons being transferred.

If the value of $\Delta_R H^0$ would be used to calculate the voltage, a value of U ($\Delta_R H^0$) = 1.48 V would result. This value cannot be achieved due to thermodynamic reasons.

Efficiency of the Fuel Cell

For the derivation of an equation for the theoretical efficiency of a fuel cell, again the Gibbs equation (Eq. 6.30) is used. The maximum thermodynamic efficiency of a fuel cell is defined by Eq. 6.32.

$$\eta_{theor} = \Delta_R G^0 / \Delta_R H^0 = U_{rev} / U\left(\Delta_R H^0\right) = 83\,\% \tag{6.32}$$

Here it should be mentioned that all values are related to the generation of liquid water; thus, the higher heating value is used as basis, leading to lower efficiency values. In a fuel cell, the operation temperature determines how much water in liquid and in gaseous form is generated.

So far, ideal thermodynamic considerations have been used to explain fuel cell behaviour. However, these ideal conditions typically cannot be achieved in technical devices. The open circuit voltage (no load connected to the fuel cell) is lower than the calculated, theoretical voltage U_{rev} and if a current is drawn from the cell, additional losses are observed. A typical current voltage dependence measured with a real fuel cell is depicted in Fig. 6.106.

At open circuit conditions, a voltage of 1 V or even a bit lower is measured. These losses of approximately 20 % are mainly caused by the oxygen reduction reaction. Because the oxygen molecule has to be split into atoms and four electrons have to be transferred, this reaction is complicated and side reactions are possible. The formation of hydrogen peroxide is a well-known side reaction, leading to the formation of a mixed potential, which is described in Sect. 6.5.2.5. Another factor is the permeability of the electrolyte for fuel and oxygen. Hydrogen at the cathode side (or vice versa, oxygen at the anode side) will lead to direct chemical reactions at the catalyst, not contributing to the electrical energy generation.

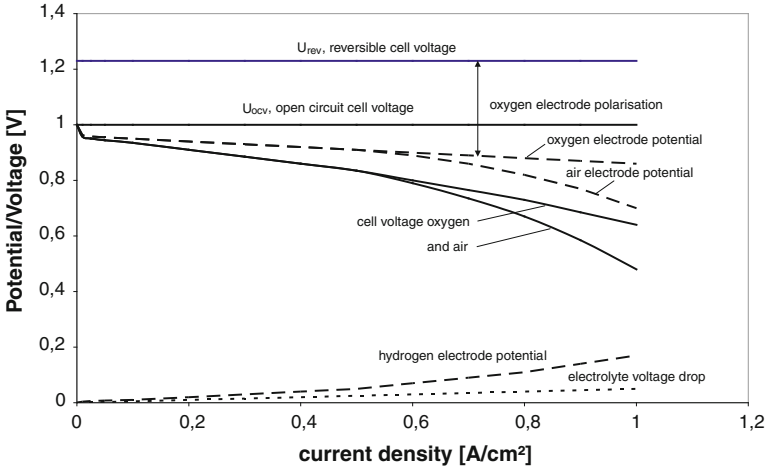

Fig. 6.106 Performance of a fuel cell; current–voltage/potential curves

The current–voltage characteristic of a fuel cell is of utmost technical interest, in addition to its technical construction principles. Both main properties determine the ratio of cost related to power. To better compare different types of cells, the current density is given as current divided by the active electrode area. For detailed electrochemical investigations, it might additionally be of interest to analyse the behaviour of one electrode of the cell separately without the influence of the second electrode. In that case, a third electrode—a reference electrode with constant potential—has to be introduced. The electrode potential versus current density curves gives detailed insight about occurring losses, namely overpotentials due to different temperatures, pressures, concentrations of the educts, side reactions, impurities and interactions between electrode and electrolyte and catalytic properties of the electrocatalyst, ohmic losses, as well as incomplete fuel usage (Coulomb or Faradaic efficiency η_{coul}). In systems, the consumption of electrical system components can significantly contribute to a reduction of efficiency. For example, a cell that is operated at 0.2 A/cm^2, according to Fig. 6.106, gives a cell voltage of 0.72 V. With these values, a voltage efficiency η_V of 49 % can be calculated.

6.5.2.3 Types of Fuel Cells with Respect to the use of Methanol

Operation of Different Fuel Cells with Methanol

In this chapter, the different types of fuel cells are shortly described because in principle they are suitable for operation with methanol. The different materials for electrodes and electrolytes being used for the construction of the cells determine

the operation temperature. The required operation temperature is dominated by the ionic conductivity of the electrolytes, and thus the type of electrolyte is chosen for the classification of the fuel cell. In Table 6.23, the types of fuel cells and some of their important properties are summarised.

For all types of fuel cells, it is valid that numerous single cells have to be connected electrically in series to reach a technically interesting operation voltage. In most cases, this is achieved by flat cell design for cell frames, which are manufactured from conducting materials. Thereby, it is possible to connect the anode of the first cell with the cathode of the second and so forth, leading to a bipolar design of the plate type cell frames, the bipolar plates. This design is shown in Fig. 6.107. Especially for the solid oxide fuel cell (SOFC), tubular designs have also been realised.

Another important question is the kind of fuel being used. Most fuel cells operate best with pure hydrogen. But here, the availability of the fuel is a major problem to be solved. The generation, storage and transport of hydrogen are complicated and are the subjects of different textbooks [553, 562, 563, 565]. However, almost any energy carrier can be converted to a reformate gas containing hydrogen, carbon dioxide and carbon monoxide with oxygen or steam as reaction partner [566]. The possible reaction equations are given for gaseous methanol:

$$CH_3OH + H_2O \rightleftharpoons CO_2 + 3H_2 \qquad \Delta_R H^0 = 49.3\,\text{kJ/mol} \tag{6.33}$$

$$CO_2 + H_2 \rightleftharpoons CO + H_2O \qquad \Delta_R H^0 = 41.0\,\text{kJ/mol} \tag{6.34}$$

The conversion of methanol is a fast reaction at Cu/Zn catalysts and is theoretically complete at temperatures of above 200 °C. Because the water–gas shift reaction (Eq. 6.34) is endothermic, the higher the temperature, the more CO is formed. The equilibrium concentration of CO at a temperature of 200 °C is about 0.5 vol%. All other fuels (e.g. natural gas, LPG, gasoline, diesel) require reforming temperatures exceeding 700 °C. Therefore, depending on CO tolerance of the fuel cell, catalytic CO removal is necessary. For this purpose, this reaction is used in reverse direction, which can be realised by cooling the reformat in the presence of a suitable catalyst. For the low-temperature fuel cells, where the electrocatalyst is especially sensitive to CO poisoning due to the adsorption and slow oxidation kinetics of CO, a fine purification is required. This final catalytic step is realised as selective oxidation in most cases. A small amount of air is mixed into the reformate stream. At a highly selective catalyst, more or less only the CO is oxidised to CO_2; the hydrogen should not react to a significant amount. These types of fuel processors have been developed for a variety of fuel cell applications.

Alkaline Fuel Cells

Due to the alkaline electrolyte, the electrode potentials of an alkaline fuel cell (AFC) are shifted to more negative values of approximately −400 mV for the hydrogen electrode and +830 mV for the oxygen electrode. This makes the use of

Table 6.23 Types of fuel cells, including the operation with methanol and reformate (e.g. from methanol)

Fuel cell	Abbreviation	Electrolyte	Operation temperature	Operation with methanol	Operation with reformate
Alkaline fuel cell	AFC	30 % KOH in H_2O	-20 to 90 °C	Yes (DMFC), but K_2CO_3 precipitation, consumes electrolyte	Yes, K_2CO_3 precipitation
Polymer electrolyte membrane fuel cell	PEMFC	Perflourinated, sulfonated polymer membrane	-20 to 90 °C	Yes, called DMFC	Yes, but CO removal is required
	HT-PEMFC	Polybenzimidazole/H_3PO_4	120–180 °C	Yes, called HT-DMFC	Yes
Phosphoric acid fuel cell	PAFC	Phosphoric acid	200 °C	Yes, called HT-DMFC	Yes
Molten carbonate fuel cell	MCFC	Eutectic mixture of Li_2CO_3 and K_2CO_3	650 °C	No	Yes
Solid oxide fuel cell	SOFC	Y dot. ZrO_2	900–1,000 °C	No	Yes

DMFC, direct methanol fuel cell; HT, high temperature

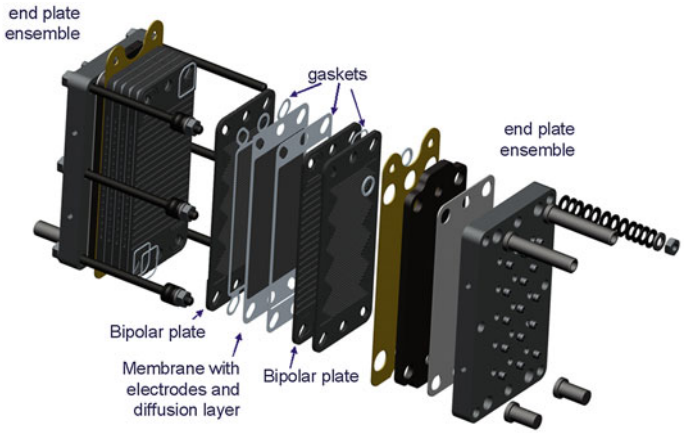

Fig. 6.107 Fuel cell stack with bipolar design

relatively cheap materials and electrocatalysts possible, such as Raney nickel or silver. The electrolyte is soaked in a porous separator, which forms a barrier between the reaction gases. Pressure differences between the fuel and oxygen sides should be avoided.

The main disadvantage of the AFC is the reaction of the electrolyte with CO_2, leading to the precipitation of solid K_2CO_3. Therefore, the operation with reformate gas is not feasible. Even if air is used as oxidant, CO_2 removal or frequent electrolyte regeneration is required. The development and use of AFCs were therefore more or less restricted to space applications. AFCs were used in Apollo and space shuttle missions and operated with pure hydrogen and oxygen.

Proton Electrolyte Membrane Fuel Cells

As already mentioned above, the polymer electrolyte has two functions: it is proton conducting and it safely separates the reaction gases. This approach to realise a safe fuel cell was first reported by Grubb and Niedrach 1958 [556], who proposed to sulphonated a polymer backbone in order to realise the proton conducting polymer electrolyte. The breakthrough was reached when Grot [567] used a perfluorinated polymer material for this purpose. At present, different chemical companies offer such membranes, even as assemblies with optimised electrode coatings for commercial products (called membrane electrode assemblies). Membrane thickness can vary between 20 and 120 μm. A good protonic conductivity is only achieved if liquid water is present. Therefore, the water management of a proton electrolyte membrane fuel cell (PEMFC) is crucial.

Because water is mainly transported from the anode to the cathode and the reaction water as well is formed at the cathode, strong humidity gradients can lead to significant differences in ionic conductivity from fuel and air inlet to outlet. Dry

conditions as well as very wet conditions lead to a reduction in power; therefore, drying out of the membrane as well as flooding of the electrocatalyst have to be avoided. To cope with these difficult requirements, gas diffusion media have been developed, with a gradient in pore structure and hydrophobic properties. A scanning electron microscopy picture of a cross-section of a GDL with a micro porous layer and catalyst layer on top of a membrane is shown in Fig. 6.108.

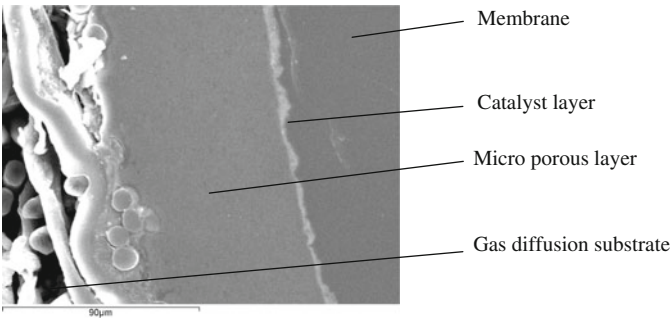

Fig. 6.108 Scanning electron microscopy image of a membrane electrode assembly with a gas diffusion layer from Freudenberg. (Courtesy of University of Duisburg-Essen)

Due to the acid electrolyte, air and CO_2-containing reformate gases can be used as fuels; even methanol can be supplied to the anode. At low operation temperatures, CO leads to severe poisoning of the catalyst. As mentioned above, a fine purification for CO removal has to be included in the fuel processor if the PEMFC will be operated with reformate gas. Additionally, special alloy catalysts have been developed, mainly on the basis of platinum and ruthenium for accelerated CO oxidation [568–570]. Similar problems occur during the direct electrochemical oxidation of methanol.

Phosphoric Acid Fuel Cells

As the name indicates, concentrated phosphoric acid is used as an electrolyte in phosphoric acid fuel cells (PAFCs). The acid is soaked in a porous SiC matrix, which is covered on both sides by a porous carbon electrode with platinum as an active catalyst in a fine dispersion at the interface. The concentrated H_3PO_4 allows operation temperatures up to 200 °C. The higher temperatures lead to a significant increase in tolerance of the catalyst with respect to CO poisoning. The tolerable CO content is approximately 1 vol%. These cells are typically operated with reformate gas being generated by a preceding fuel processing step using natural gas as fuel. The typical application is combined heat and power supply at industrial sites.

High-Temperature Polymer Electrolyte Membrane Fuel Cells

A fuel cell combining the properties of a PEMFC and a PAFC is the high-temperature polymer electrolyte membrane fuel cell (HT-PEMFC) [570, 571]. Here, a polymer with good temperature stability is used, such as polybenzimidazole (PBI). The porous polymer matrix with alkaline imid-groups (R_2N) are able to bind phosphoric acid quite tightly and maintain a good proton conductivity. The operation temperature of this type of fuel cell lies between 130 and 180 °C. The advantage of the more secure separation of fuel and oxidant in the cell compared to PAFC and the robustness towards CO poisoning comes with a longer startup phase compared to PEMFC and problems of electrolyte loss upon condensation, mainly occurring during start and stop procedures. The HT-PEMFC can be operated with 1 vol% CO in hydrogen without any loss in performance, as CO desorption is significantly accelerated at 160 °C compared to the 80 °C of the low-temperature PEMFC. An important drawback of the high temperature is the accelerated corrosion of carbon carrier materials, catalysts and construction materials.

Liquid-Fuel Fuel Cells

The DMFC is described in detail in Sect. 6.5.2.5. Various other liquid fuels have been investigated as possible option for direct electrochemical conversion. Ethanol is the most interesting one due to its environmental friendliness and biological source. However, because C–C bonds generally are difficult to split in electrochemical processes, only incomplete conversion is observed [572]. The higher alcohols, diols such as ethylene glycol and formic acid were the low-molecular C-, H- and O-containing species being investigated in R&D. Other options for compounds releasing hydrogen are hydrazine and alkali boron hydrides, but commercial use was not realised. Hydrazine is the most active compound, but unfortunately it is poisonous (carcinogenic). Some electrochemical data are summarised in Table 6.24.

Molten Carbonate Fuel Cells

The molten carbonate fuel cell (MCFC) was an earlier development, using a mixture of molten alkali carbonates as electrolyte. The eutectic mixture of Li_2CO_3 and K_2CO_3 performed best, with respect to corrosion and wettability of the electrodes. The operation temperature is well above the melting point at about 650 °C. The molten salts are sucked in a porous matrix consisting of $LiAlO_2$. The pores have to be finer than those of the adjacent electrodes in order to stabilise the electrolyte film for gas separation. In an MCFC, oxygen is reduced to oxygen ions, but the conduction path requires an additional molecule of CO_2. The formed carbonate ions are transported through the electrolyte to the anode compartment, where CO_2 is released again. Thus, the MCFC requires a CO_2 recycling path from

Table 6.24 Thermodynamic and electrochemical data of fuel reactions [550]

No.	Fuel	Reaction	z	$\Delta_R H^0$ (kJ/mol)	$\Delta_R G^0$ (kJ/mol)	U_{rev} (V)	η_{theor} (%)
1	Hydrogen	$H_2 + 0.5O_2 \rightarrow H_2O$	2	−286.0	−237.3	1.229	83.0
2	Carbon	$C + 0.5O_2 \rightarrow CO$	2	−110.6	−137.3	0.712	124.2
3	Carbon	$C + O_2 \rightarrow CO_2$	4	−393.7	−394.6	1.020	100.2
4	Carbon monoxide	$CO + 0.5O_2 \rightarrow CO_2$	2	−283.1	−257.2	1.066	90.9
5	Methane	$CH_4 + 2O_2 \rightarrow CO_2 + 2H_2O$	8	−890.8	−818.4	1.060	91.9
6	Methanol	$CH_3OH + 1.5O_2 \rightarrow CO_2 + 2H_2O$	6	−726.6	−702.5	1.214	96.7
7	Formaldehyde	$HCHO + O_2 \rightarrow CO_2 + H_2O$	4	−561.3	−522.0	1.350	93.0
8	Formic acid	$HCOOH + 0.5O_2 \rightarrow CO_2 + H_2O$	2	−270.3	−285.5	1.480	105.6
9	Ethanol	$C_2H_5OH + 3O_2 \rightarrow 2CO_2 + 3H_2O$	12	−1,367	−1,325	1.145	97
10	Dimethyl ether	$CH_3OCH_3 + 3O_2 \rightarrow 2CO_2 + 3H_2O$	12	−1,460[a]	−1,387[a]	1.20	95

[a] Calculated from U_{rev} and η_{theor}

the anode to the cathode. Therefore, the MCFC is the only fuel cell that cannot be operated with pure hydrogen.

The cathodic and anodic reaction are shown in Eqs. 6.35 and 6.36.

$$O_2 + 2CO_2 + 4e^- \rightarrow 2CO_3^{2-} \tag{6.35}$$

$$H_2 + CO_3^{2-} \rightarrow CO_2 + H_2O + 2e^- \tag{6.36}$$

Due to the high operation temperature, the electrochemical kinetics are fast. Noble metal catalysts are not required; typical electrode materials are nickel for the anode and nickel oxide for the cathode. Another advantage of the high temperature is the option for internal reforming.

One of the MTU MCFC systems was operated in Berlin at a BEWAG (the former electric utility of Berlin; today called Vattenfall) site with methanol as fuel. The adaptation from natural gas to methanol was easily done according to the communication of the owner and MTU.

Solid Oxide Fuel Cells

At even higher temperatures in the range of 800–1,000 °C, some ion-conducting ceramic electrolytes are known. The first modern investigations of laboratory cells were carried out by Weissbart and Ruka, Moebius, Sandstede et al., Tannenberger, and others in the early 1960s [556, 573]. The higher the temperature, the higher is the mobility of the ions in the lattice. Most interesting would be a solid proton conducting material, but R&D in the field did up to now not lead to suitable materials. However, oxygen conduction materials are well known, because Nernst used doped zirconium oxide as material for gas mantles. The mobility of oxygen ions originate from lattice defects, which are formed by doping the ZrO_2 with an

oxide with a three or two-valent material, such as yttrium oxide (Y_2O_3) or calcium oxide (CaO). For a long time, yttrium-doped ZrO_2 (YSZ) was used for SOFC, showing the maximum conductivity of 0.1 S cm^{-1} at a temperature of 1,000 °C at a composition of 8 mol % yttrium.

The operation principle can be explained using Fig. 6.105. However, because the electrolyte is oxygen ion-conducting, oxygen reduction at the cathode directly leads to the required conducting ions. Water vapour is formed at the anode by reaction, with the protons being formed by hydrogen oxidation at the anode.

As for the MCFC, the SOFC does not require highly active catalysts. More important are thermal expansion coefficients, as each startup procedure means also a heating process for the layers of the cell. At an operation temperature of 900 °C, the reversible cell voltage is 0.89 V at operation with hydrogen and oxygen. But typically, the SOFC is operated with natural gas and air. The reforming process can be carried out either external or internal of the fuel cell stack; the latter process gives the option of using the endothermic reforming reaction for cooling of the cell. There are detailed reviews about high-temperature fuel cells MCFC and SOFC [553, 562–564].

6.5.2.4 Gaseous and Liquid Fuels: Thermodynamic Data

Because fuel cells can be operated with synthesis gas, the combination of fuel cell systems with fuel processors in which the reforming of any fuel takes place are state of the art. In Sect. 6.5.2.6, the detailed description of methanol fuel processing for fuel cells is given. Possible fuels for fuel cell systems are briefly listed and their most important properties are summarised. Thus, methanol as a fuel can easily be ranked in comparison to other fuels.

The thermodynamic values of the electrochemical oxidation reactions determine the achievable cell voltage U_{rev} and can be calculated according to (6). From a theoretical point of view, the most interesting reaction would be the direct electrochemical conversion of coal. For the first partial combustion step leading to carbon monoxide, a theoretical reversible cell voltage U_{rev} of 0.71 V and a theoretical efficiency of 124 % can be calculated. This high-efficiency value of more than 100 % can be explained by the increase in entropy during the course of the reaction, which usually is the case for the generation of gaseous products from solid or liquid educts. The complete conversion to CO_2 would result in a reversible cell voltage of $U_{rev} = 1.02$ V as given in line 3 of Table 6.24. The third possibility is the electro-oxidation of CO to CO_2, leading to $U_{rev} = 1.066$ V.

The electro-oxidation of methanol (Table 6.24, line 6) leads to carbon dioxide if the oxidation reaction is complete. As intermediates, formaldehyde and formic acid can be formed. Both substances can be oxidised further; formic acid has even been used as fuel for a fuel cell in early experiments. DME can easily be synthesised from methanol and also be easily electro-oxidised according to the equation given in Table 6.24 (line 10).

6.5.2.5 Direct Methanol Fuel Cells

Basic Principle of a DMFC System

Usually, the DMFC is operated with liquid methanol as fuel. The construction principle (see Fig. 6.109) is the same as for a hydrogen consuming PEMFC. Some minor changes are required for liquid operation. Although the air side remains the same, the anodes need hydrophilic structures to facilitate access of liquid fuel to the electrode. During methanol oxidation, the generated CO_2 has to be removed from the cell (see Eq. 6.37). A second important difference is the significant diffusion of methanol through the polymer electrolyte. This can be understood because of the chemical similarity of the water molecule and the methanol molecule and the complete miscibility of the two substances. This permeation or crossover is highest under OCV conditions and diminishes upon increasing load, as methanol in the vicinity of the electrode is depleted. The permeated methanol is reacting at the cathode with oxygen, leading to a loss in cell voltage, a loss in fuel,

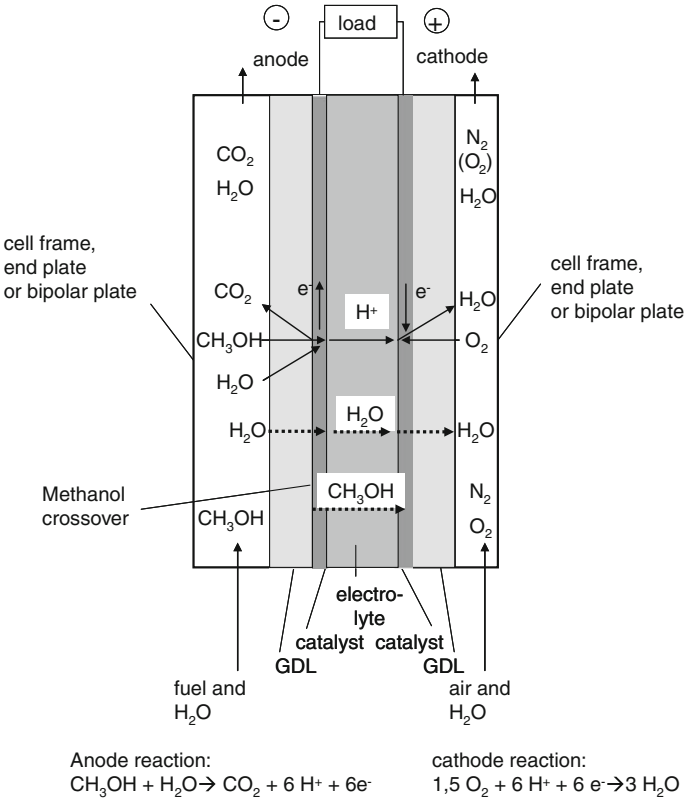

Fig. 6.109 Direct methanol fuel cell. GDL, gas diffusion layer

and thus resulting in a reduction of efficiency. Additionally, during the electro-oxidation of methanol, CO adsorbates are formed on the anode catalyst.

$$\text{Anodic reaction}: \quad CH_3OH + H_2O \rightarrow CO_2 + 6H^+ + 6e^- \tag{6.37}$$

$$\text{Cathodic reaction}: \quad 1.5O_2 + 6H^+ + 6e^- \rightarrow 3H_2O \tag{6.38}$$

The total cell reaction for methanol oxidation is as follows:

$$CH_3OH + 1.5O_2 \rightarrow CO_2 + 2H_2O \tag{6.39}$$

Thermodynamic and electrochemical values for the methanol fuel cell and further detailed information are given in Sect. 6.5.2.4.

Although methanol is one of the most reactive liquid fuels, it has some drawbacks compared to a hydrogen-fueled cell. The principle of electrochemical conversion of methanol is known since 1922. The cell was realised as alkaline fuel cell with a certain concentration of methanol in the liquid-fed anode chamber. These early cells were operating robustly but at low power density. The introduction of a technically mature product on the basis of this operation principle was never successful. However, new R&D efforts were undertaken, when proton-conducting membranes were available for PEMFC. In that architecture, a mixture of water and methanol could be used as fuel. For more historical details, see Sect. 6.5.2.3. Meanwhile, the first DMFC-based products became commercially available. Besides the advantage of methanol being a liquid fuel and therefore easily to carry, there is another favourable property—namely the fact that the specific energy content is quite high at 6.30 kWh/kg.

Besides the theoretical cell voltage of the methanol cell (1.214 V, Table 6.24), the reversible methanol electrode potential is of interest:

$$u_{revanode} = u_{revO2} - U_{revcell} = 1.229 - 1.214\,V = 0.015\,V \tag{6.40}$$

Theoretically, the difference between the methanol and the hydrogen electrode potential is small.

In principle, a DMFC system can be constructed quite simply, as depicted in Fig. 6.110. The fuel cell stack is connected to a methanol and water circuit, consisting of a tank and a pump. CO_2 is released in the tank. To supply air to the cathode, a fan can be used. But long-term stable operation requires some more controls; mainly, the water balance of the system has to be actively regulated. According to Eq. 6.37, water is consumed at the anode and released at the cathode. Additional water is transferred by the electro-osmotic drag and the total amount of water is released as liquid or as humidity with the excess of air. The ratio of liquid water and steam is strongly dependent on temperature and air flow.

A certain methanol/water mixture is used as fuel, but during operation the concentration relations change due to the reasons mentioned above. Therefore, a methanol sensor is frequently used for controlling the supply of fuel. If a methanol–water mixture has to be refuelled, the energy density of the fuel is significantly

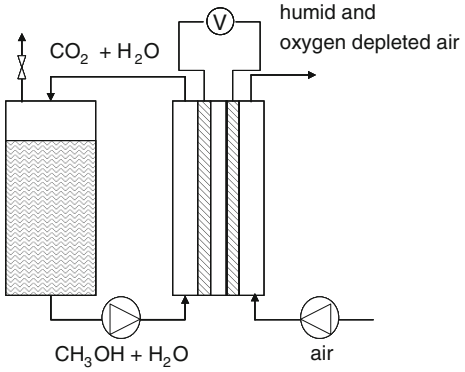

Fig. 6.110 Direct methanol fuel cell system

reduced compared to pure methanol. Therefore, much development effort was put into closing the water loop inside the system. The water being released at the cathode with the excess air has to be condensed and fed back to the anode side. The remaining task is the dosing of the correct amount of methanol to the fuel side of the cell.

Fundamentals of the Methanol Oxidation Reaction

It has been known that hydrogen oxidation can occur along two pathways. Because hydrogen also has to be oxidised during the process of methanol electro-oxidation, the basic principles are given. Immediately after adsorption of hydrogen molecules at the electrode surface, dissociation and electron transfer occurs.

$$2Pt + H_2 \rightarrow 2Pt - H \tag{6.41}$$

$$Pt - H \rightarrow Pt + H^+ + e- \tag{6.42}$$

The oxidation of methanol to CO_2 as product is the desired reaction, as six electrons are transferred and are available for power production. However, this total oxidation proceeds stepwise with numerous possible side products and intermediates. The reaction at the platinum surface can be formulated as follows:

$$2Pt + CH_3OH \rightarrow Pt - CH_2OH + Pt - H \tag{6.43}$$

$$2Pt + Pt - CH_2OH \rightarrow Pt_2 - CHOH + Pt - H \tag{6.44}$$

$$Pt + Pt_2 - CHOH \rightarrow Pt_2 - COH + Pt - H \tag{6.45}$$

Each Pt–H- site is reacting according to Eq. 6.42 to a proton and an electron. The COH adsorbate being formed according to Eq. 6.45 might even be triple bonded. Using (infrared) spectroscopy, adsorbed CO could finally be detected on the electrode surface.

$$(Pt) + Pt_2 - COH \rightarrow Pt - CO + Pt - H \tag{6.46}$$

For the further oxidation of this strongly adsorbed CO species, oxide species at the catalyst surface are required, such as Pt–OH. Adjacent CO and OH- species react according Eq. 6.48 and finally CO_2 is generated.

$$Pt + H_2O \rightarrow Pt - OH + H^+ + e^- \tag{6.47}$$

$$Pt - CO + Pt - OH \rightarrow Pt - COOH + Pt \tag{6.48}$$

$$Pt - COOH \rightarrow Pt - H + CO_2 \tag{6.49}$$

This mechanism was explained stepwise by many authors (including reviews) [555, 557, 568, 574–578]. If the electrode surface is brought into contact with a methanol-containing electrolyte, the adsorption takes place. In order to oxidise the adsorbate, the potential can be raised, for example, by means of a potentiostat by sweeping the potential and recording the current (see Fig. 6.111). From the charge being transferred during the oxidation current peak at 675 mV, it can be calculated that it amounts to 1.8 electrons per platinum atom. Consequently, the adsorbate consists to a large extent of Pt–CO. At higher potentials, oxidised platinum sites are abundantly available and the oxidation of methanol occurs.

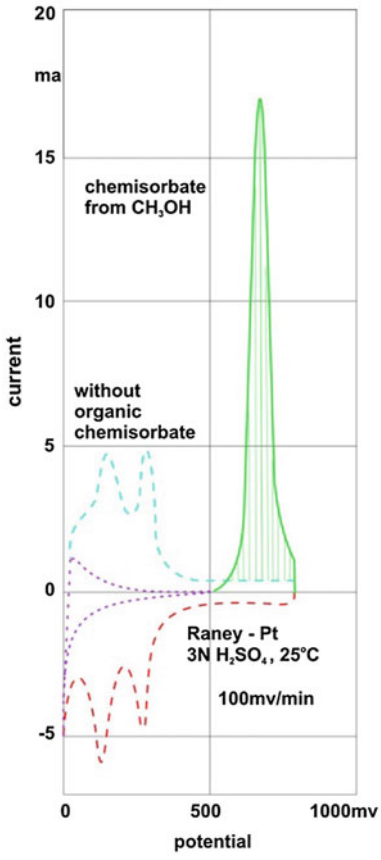

Fig. 6.111 Potentiodynamic current–voltage curve with Raney-Platin with methanol chemisorbate, which is removed by anodic oxidation

Because the potential loss in continuous fuel cell operation by these surface-blocking intermediates would be significant, much R&D effort was designated to this topic, in addition to the methods of surface analysis and the development of improved electrocatalysts compared to platinum. Formaldehyde and formic acid can also be formed under certain conditions, depending mainly on temperature and electrocatalysts.

Anode Electrocatalysts: Stability Against CO

As explained in Sect. 6.5.2.3, CO-like adsorbates block the anode electrocatalyst and prevent methanol oxidation at low potentials. For example, ruthenium is known to form Ru-oxide covered surfaces at much lower potential than platinum, so a Pt/Ru alloy or mixture was assumed to improve electrooxidation of methanol. The Ru–O surface species are able to transfer oxygen to the CO adsorbates on Pt, thus leading to a further oxidation at lower potentials of about 500 mV (see Fig. 6.112).

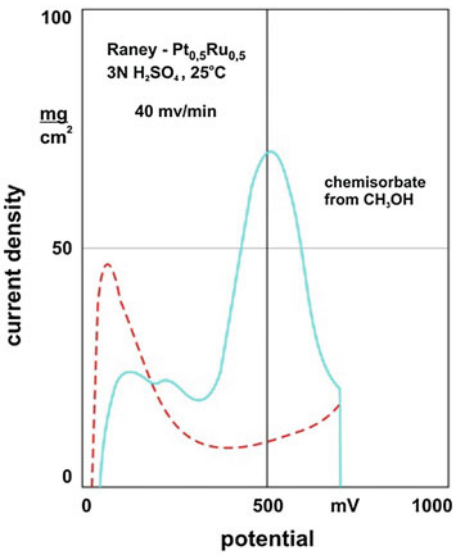

Fig. 6.112 Potentiodynamic current–voltage curve with Raney-Platin-Ruthenium with methanol chemisorbate, which is removed by anodic oxidation

The development of improved electrocatalysts proceeded approximately simultaneously with the research about the mechanism of the anodic oxidation of methanol. Besides ruthenium and other platinum metals, nonnoble metals also have been investigated. Thus, tin and molybdenum have been discovered as alloy components, which increase the activity of platinum. These results have been obtained by several research groups almost in parallel in the 1960s [555, 579–581]. Further groups are mentioned in later works [557, 562].

To demonstrate the activity increase of platinum, two figures from (8) are used. Galvanostatic anodic potential-current density curves of platinum black with molybdenum and other components are shown in Fig. 6.113. A significant improvement by using molybdenum/platinum instead of pure platinum black or addition of tungsten or lead is obvious from the measurements. Corresponding curves with Raney platinum alloyed with gold, iridium, osmium, palladium, rhodium and ruthenium are shown in Fig. 6.114; the activity increases in this order from platinum/gold alloy to platinum/ruthenium.

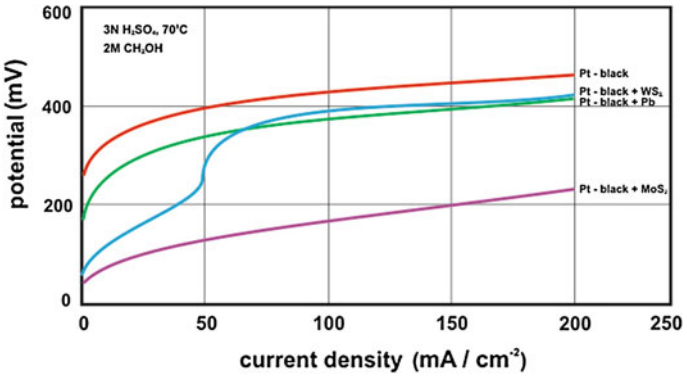

Fig. 6.113 Stationary current–voltage curves with platinum black and Mo, Pb, or W

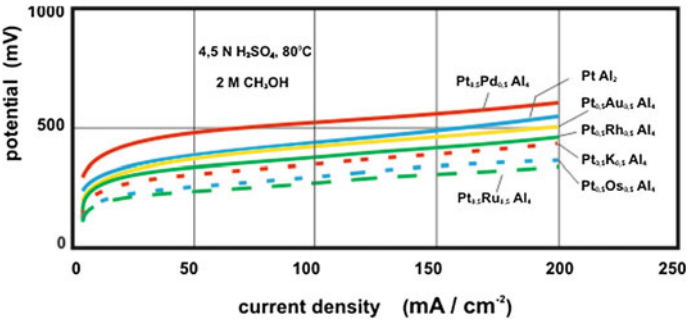

Fig. 6.114 Stationary current–voltage curves with Raney platinum alloys, especially $Pt_{0.5}Ru_{0.5}$

Furthermore, the activity increase depends on the percentage of the additional components in the platinum alloy. The dependence of the activity for the methanol oxidation (true current density) on the composition of the platinum-ruthenium alloy is displayed in Fig. 6.115. In this case, 30 % ruthenium gives the maximum effect.

Later on, even more active catalysts using ternary or even quaternary alloys with platinum as the basic catalyst alloyed with further noble and non-noble metals were investigated [562, 582–588]. Nevertheless, a quite high noble metal content of the electrode still is required in order to achieve stable operation at acceptable power density.

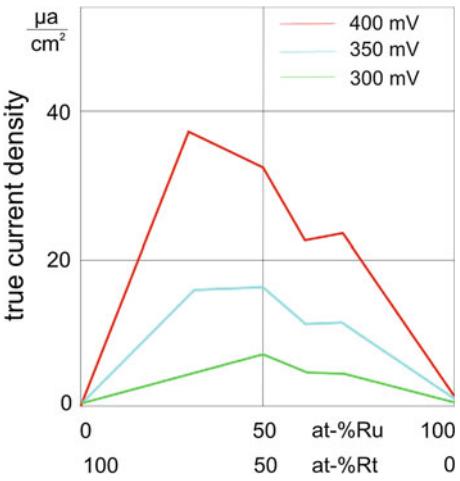

Fig. 6.115 True current density for methanol oxidation on Raney platinum-ruthenium at 70 °C, 3 N H_2SO_4 and 2 M CH_3OH

Cathode Electrocatalysts: Stability Against Methanol

Basically, the cathode side of the DMFC remains unchanged in comparison to a hydrogen-fueled cell. In the case of DMFCs, the anode is limiting the current density and even higher over voltages occur with methanol oxidation than with oxygen reduction, if the electrochemical reactions are carried out separately in so-called half-cell arrangements. Thus, the lessons learned by improving PEMFC with respect to cathode electrocatalyst were directly transferred to the DMFC.

A closer look analysing the surface of platinum as cathode catalyst shows that the surface is covered with oxide species at positive potentials. The mechanism of the oxygen reduction reaction representing a transfer of four electrons per oxygen molecule in order to form water directly has to be considered in detail. At first, two electrons are transferred to give hydrogen peroxide:

$$O_2 + 2H^+ + 2e^- \rightarrow H_2O_2 \tag{6.50}$$

The H_2O_2 will not electrochemically be reduced further to give water because the equilibrium potential according to Eq. 6.52 amounts to 1.77 V, which means that this reaction is very improbable. Therefore, the further reaction of H_2O_2 is the chemical disproportionation [552, 557].

$$H_2O_2 + 2H^+ + 2e^- \rightarrow 2H_2O \tag{6.51}$$

$$2H_2O_2 \rightarrow 2H_2O + O_2 \tag{6.52}$$

In acid electrolyte, the standard potential of the oxygen electrode is 1.23 V; the corresponding potential of the hydrogen peroxide formation is lower with 0.682 V. If both reactions can occur at the cathode during operation, the potential decreases to a value of a mixed potential (Fig. 6.106) and thus the efficiency of the cell also decreases. In addition, H_2O_2 accelerates corrosion processes.

The objective of the catalyst research is therefore to improve the surface properties in such a way that the adsorption of the oxygen molecule is stronger so that up to four electrons can be transferred and H_2O_2 formation be avoided. This can be achieved by alloying platinum with non-noble metals such as chromium and cobalt; ternary alloys are best. Such catalysts also have already been developed for the hydrogen/oxygen PEMFC.

As mentioned in Sect. 6.5.2.2 and shown in Fig. 6.106, methanol is being transferred through the membrane material, especially at low current density—a process that is called methanol cross over. Thus, methanol, air and catalyst are present in the cathode chamber. The electrocatalyst of the cathode, finely dispersed Pt on carbon, is active for direct chemical methanol oxidation, even at low temperatures. Thus, methanol is combusted and heat is released. If the combustion reaction is not fast enough, mixed potentials are formed, leading to a reduction in cell voltage. This effect could be avoided if the catalyst and thus the potential of the cathode were not influenced by the presence of methanol. Again, ruthenium was found to be an effective additional compound for improving the platinum catalyst. Thus, ruthenium is active for methanol oxidation at the anode; at the cathode, it is effective for the protection of the oxygen reduction against methanol. By now, there are more components and compositions known, such as sulphur compounds [589] and Chevrel phases [590–592]. Further information about this subject can be found in the literature [576, 585, 593–596].

In liquid alkaline electrolyte, the problem does not occur or is negligible. The best catalyst for the cathodic oxygen reduction is silver. However, also in alkaline electrolyte, the four-electron mechanism is not likely to occur. The reduction will also proceed via the peroxide step, namely forming of the peroxide ion (Eq. 6.53).

$$O_2 + H_2O + 2e^- \rightarrow HO_2^- + OH^- \tag{6.53}$$

Again, the further reaction of HO_2^- is a chemical disproportionation [552, 560]:

$$2HO_2^- \rightarrow 2OH^- + O_2 \tag{6.54}$$

Silver has a big advantage because it does not catalyse the methanol oxidation, which is of importance for the alkaline DMFC (see Sect. 6.5.2.5).

Cell Structures: Electrolytes

In principle, in addition to acid, alkaline electrolytes are also suitable for DMFC. The alkaline electrolyte is methanol in aqueous KOH solution; the acid electrolyte typically is a sulphonated polymer as proton exchange membrane. From the electrochemical reactions, it can be seen that the reaction mechanism is different. In alkaline solution (Eq. 6.55 and 6.56), hydroxyl ions are consumed at the anode and water

and CO_3^- is formed, with acid electrolyte gaseous CO_2 (see Eq. 6.37 and 6.39). For a liquid alkaline electrolyte, dilution occurs in the anode loop upon operation.

$$CH_3OH + 8OH^- \rightarrow CO_3^{2-} + 6H_2O + 6e^- \quad \text{anode reaction} \tag{6.55}$$

$$1.5O_2 + 3H_2O + 6e^- \rightarrow 6OH^- \quad \text{cathode reaction} \tag{6.56}$$

$$CH_3OH + 1.5O_2 + 2OH^- \rightarrow CO_3^{2-} + 3H_2O \quad \text{total reaction} \tag{6.57}$$

At the cathode, hydroxyl ions are formed (but less than are consumed at the anode), and water is consumed. Therefore, balancing measures are required: the removal of water from the (anode) electrolyte and the transfer of OH^--ions from cathode to anode and the removal of precipitated K_2CO_3. A porous separator is used in order to separate the reactant gases during operation, requiring accurate differential pressure control.

In acid mechanism, the protons are formed during methanol oxidation; they migrate to the cathode and there, product water is formed. CO_2 is released again in the anode chamber. In a DMFC with a solid membrane electrolyte, the water is partly evaporating and carried out of the cell with the cathode off-gas; water and methanol as well have to be fed to the anode of the acid DMFC. In acid DMFC, liquid is only present in the anode chamber; the cathode is a usual gas-consuming electrode.

If an acid DMFC with liquid electrolyte is used, a gas diffusion electrode is required for the cathode, separating the air from the liquid electrolyte but still enabling the electrochemical reaction. A hydrophobic electrode with fine pores has been developed for alkaline fuel cells, enabling transfer of oxygen and preventing the electrolyte from penetration. Sufficient current densities can only be achieved if a large surface area of the triple-phase boundary (electrode, electrolyte and gas) can be achieved. The possibility of using PTFE as binding material for the electrodes was discovered by many research groups in the 1960s, by Kordesch, Sandstede, Winsel and others [552, 560, 597, 598]. The latter developed a rolling process to fabricate suitable electrodes from PTFE mixed with silver catalyst powder. This process was the basis for air-breathing electrodes in the chlorine electrolysis.

Methanol Crossover

In DMFC with an acid electrolyte, protons with hydrate shells migrate from anode to cathode; in an alkaline cell, hydroxyl ions migrate from cathode to anode. This difference explains why methanol crossover is a more severe problem in acid electrolytes [599]. Because various power losses add up in a DMFC, R&D efforts were undertaken to determine the losses due to methanol crossover. Chemical analysis has been used to determine the transfer through the membrane during stand still, flushing the cathode with an inert gas. However, when a current is drawn from such a cell, the only possible electrochemical reaction at low cell

voltage is the oxidation of methanol. Thus, the methanol crossover could be determined in terms of a current density. A typical result [600] is depicted in Fig. 6.116. For many years, polymer scientists developed membrane materials with lower methanol crossover to diminish the losses [571, 591, 592, 601].

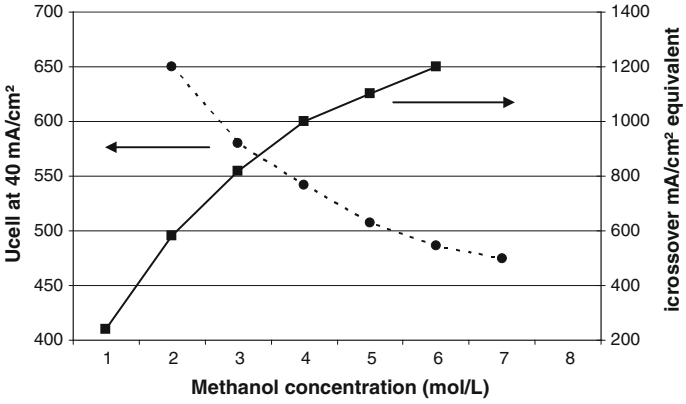

Fig. 6.116 Concentration dependence of cell voltage and methanol crossover at low current density of a liquid-fed direct methanol fuel cell. Nafion 105 temperature = 90 °C. Anode: Pt/Ru at 5.3 mg/cm^2, pa = 0.15 MPa, flow 4 mL/min. Cathode: Pt at 6.4 mg/cm^2 pc = 0.3 MPa, flow = 4 L/min

6.5.2.6 Types of DMFC

Dissolved Fuel Cells

As explained in Sect. 6.5.2.5, liquid methanol can be fed to the fuel cell in alkaline electrolyte or in a mixture with water (compare also Fig. 6.110). A high methanol concentration would be desirable to achieve a high current density and (for the purpose of fuel storage) a high energy density. The first goal proved not to be simply realizable because high methanol concentrations led to high methanol crossover and thus high fuel losses (see Fig. 6.116).

In the acid DMFC with proton exchange membrane, technical solutions were investigated. In principle, it should be possible to store pure methanol in the tank of the system, to close the water cycle in the cell by condensing humidity from the cathode gas stream, and to use a methanol sensor in order to keep the methanol concentration in the fuel in an optimal range. For several years, the development of methanol sensors was an important field for R&D and many different measuring principles have been patented: density, refractory index and infrared absorption, to name a few. This type of fuel cell was developed to first systems and marketable products (see Sect. 6.5.2.7).

Vapour-Fed DMFC

Instead of using a liquid methanol–water mixture as fuel, it is likewise possible to construct the fuel cell in such a way that the fuel mixture can be fed as vapour into the cell [602]. For this purpose, a vapourising device can be incorporated in the fuel cell system, by which a mixture of methanol and water vapour is produced. This fuel gas is introduced to the fuel compartment of the DMFC system (Fig. 6.110) and then distributed into the anode chambers of the stack. After the reaction of the methanol at the anodes to yield carbon dioxide, the remaining methanol water vapour mixture is condensed in a cooling unit to separate it from the carbon dioxide.

During the operation, the whole DMFC system has to be kept at a higher temperature (e.g. 150 °C). Of course, the materials (including the electrolyte membrane) have to be mechanically and chemically stable at this temperature. At a first glance, this concept poses a membrane material problem. Typical sulphonated membranes are known to swell as well in contact with methanol and water; the swelling becomes more pronounced at elevated temperatures. Thus, the gain in kinetics, resulting in higher current density at a given electrode potential, may be overcompensated by fuel losses by crossover through the swollen membrane. It should be stated that the methanol will not be reformed during the operation at the electrode catalyst. The higher performance would make the vapour-fed DMFC especially suitable for the drivetrain of a bus and truck. Therefore, research is continuing for the optimisation of this DMFC [562, 597]. The typical membrane materials being used in PEMFC and DMFC do not fulfil the stability requirements. Thus, vapour-fed DMFC has not yet been developed to marketable systems.

Alkaline Direct Methanol Fuel Cell

Typically, DMFC is called a fuel cell, which contains an acid electrolyte; this means that the gaseous carbon dioxide, being the oxidation product of methanol, will not be dissolved in the acid solution and thus is able to escape off the cell. Also, in a cell with a proton-conducting membrane, the membrane will reject the carbon dioxide. In contrast, carbon dioxide would not be formed because the complete oxidation of methanol would result in the formation of carbonate ions if an alkaline medium were present. The electrochemical reactions are given in Eqs. 6.50–6.52.

The alkaline methanol fuel cells were the first to have been developed because they had a big advantage. The electrocatalyst for the oxygen electrode was silver, which did not have any activity for the methanol oxidation. Thus, it was not necessary to separate anolyte and catholyte completely. Furthermore, the catalysts were cheaper than those for the acid electrolyte, which were derived from platinum.

Otherwise, a platinum metal catalyst would be necessary for the methanol oxidation in alkaline electrolyte, but here methanol is not so strongly bound to the catalyst surface as in acid electrolyte. Regarding the mechanism of the methanol oxidation in alkaline electrolyte, there are a lot of investigations [552, 554, 558, 560, 598, 603, 604]; some of these results are described in Sect. 6.5.2.9.

A few examples of the first alkaline DMFCs are cited here, which were developed in the early 1960s. Some of them were single cells with a performance of about 1 W [552, 603], whereas others consisted of stacks with a power of up to 100 W [552, 559]. The Battelle Institute in Frankfurt, Germany described an alkaline methanol cell in 1961; the electrodes had a size of 13 cm^2. A small stack of several cells with a total surface size of 60 cm^2 was subsequently presented in 1964 and a 30-watt methanol battery was exhibited in 1967. The single cell, shown in Fig. 6.117, served as a demonstration object for electrochemistry courses at DECHEMA (the German Society for Chemical Engineering and Biotechnology) for decades. The anodes of these cells were made from nickel together with a Raney-palladium catalyst, which was alloyed with further metals; the hydrophobic cathodes were produced from nickel, silver carbonate and polytetrafluoroethylene (PTFE) as well as some filler. The voltage-current density curves obtained with the Battelle methanol battery are shown in Fig. 6.118 [554, 605–607].

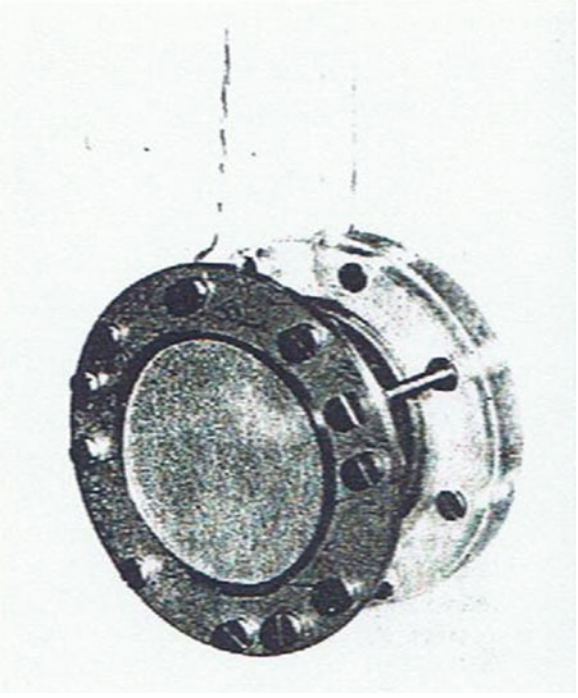

Fig. 6.117 Single alkaline DMFC with approximately 7-cm diameter (ACHEMA 1961)

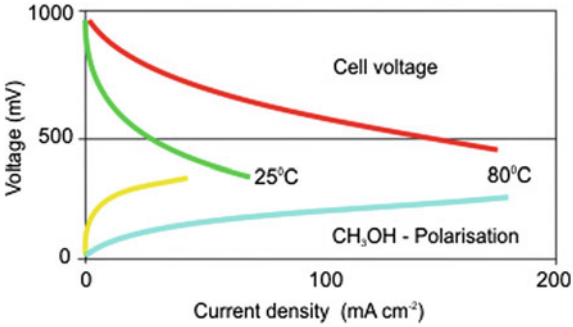

Fig. 6.118 Alkaline methanol cell voltage and polarisation versus current density

6.5.2.7 Indirect Methanol Fuel Cell Systems

Characteristics of the Indirect Systems

The importance of the indirect methanol fuel cell system (IMFC) is increasing because the technology practically is a PEMFC, which has meanwhile been developed to be a reliable and cost-effective product. On the other hand, the methanol reformer is also very advantageous, as has been described already. The IMFC is also called the reformed methanol fuel cell (RMFC) [608].

In Sect. 6.5.2.5, it was shown that methanol can be used as a fuel for practically all possible fuel cells; in Sect. 6.5.2.4, the properties of gaseous fuels are listed. Most fuels have to be converted before feeding them into the fuel cell. In this chapter, the technology of the methanol-reforming reactions are described. Because the limited power density of a DMFC could not be overcome yet, the combination of a methanol reformer with a PEMFC is an interesting concept. Of course, the additional weight and volume and efficiency loss of the reforming unit has to be compensated by the smaller, more efficient and cheaper fuel cell [561, 566, 609, 610].

Because there are several possibilities of conversion of methanol into a reformat that can be fed into a fuel cell, the basic reactions are described in this subchapter, before the different applications are explained in Sect. 6.5.2.8. The big advantage of methanol over other fuels, such as hydrocarbons, is the fact that its reforming takes place at relatively low temperatures; therefore, the technical apparatus can be extremely compact. The steps in the total fuel processing sequence are summarised in Fig. 6.119.

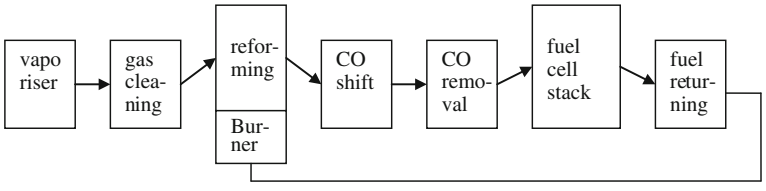

Fig. 6.119 Fuel processing of methanol and its conversion to heat and electricity (gas cleaning and CO shift are optional)

Because methanol is a synthetic product, it can be very clean. It does not contain any disturbing ingredients like products derived from crude oil, which often contain sulphur, which is a poison for the catalyst. However, if it stems from a reprocessing of used products, it may also contain sulphur. In that case, a gas cleaning apparatus, especially for sulphur removal, has to be introduced. After that, the conversion of methanol vapour to reformat can take place. It can be carried out in three different ways, which may comply with the application of the whole system. To discuss this situation, the three reaction equations are presented here and the thermodynamic enthalpies are given for all the substances in the gaseous state:

$$\text{Dissociation} \quad CH_3OH \rightarrow CO + 2H_2 \quad \Delta_R H = +90.9\,\text{kJ/mol} \tag{6.58}$$

$$\text{Reforming} \quad CH_3OH + H_2O \rightarrow CO_2 + 3H_2 \quad \Delta_R H = +49.3\,\text{kJ/mol} \tag{6.59}$$

$$\text{Partial oxidation} \quad CH_3OH + 0.5O_2 \rightarrow CO_2 + 2H_2 \quad \Delta_R H = -192.2\,\text{kJ/mol} \tag{6.60}$$

The dissociation is a kind of decomposition, which takes place at a relatively low temperature, namely 200–250 °C. Although it is a simple process, it is applied quite seldom because the carbon monoxide is harmful for the platinum catalyst of the fuel cell. The CO content of the reformate must be less than 10 ppm; this concentration is tolerated by the platinum electrocatalyst of the fuel cell. The higher the temperature in the reformer is, the more carbon monoxide can be formed according to reverse shift reaction (Eqs. 6.4.2-9). Also, nonhomogeneous concentration profiles may occur. Therefore, it is necessary to remove most of the rest of the CO in a further reactor (Fig. 6.119 and Sect. 6.5.2.6).

Furthermore, there is a method of influencing the CO concentration by the steam-to-methanol ratio, which can be seen in Fig. 6.120. That is why the process is typically run with an excess of steam. Although the stoichiometric ratio is 1, a ratio of 1.5 is often used for the feed.

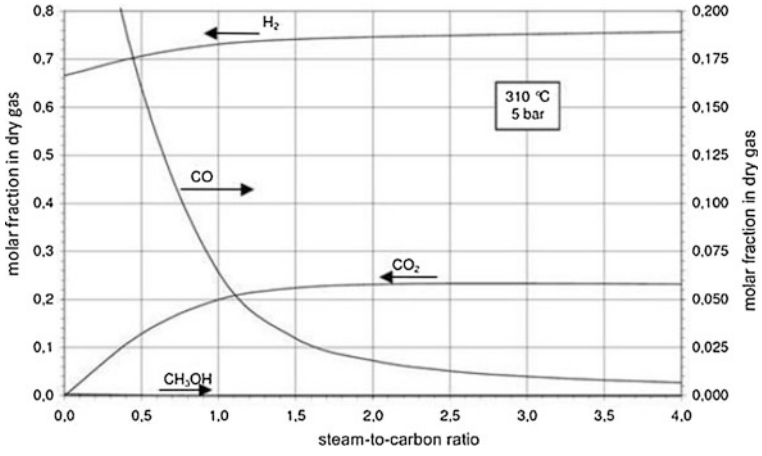

Fig. 6.120 Methanol reforming; gas composition versus steam-to-methanol ratio

The third way of generating hydrogen from methanol is not really a reforming reaction but a partial oxidation; however, for the sake of classification it is subsumed under reforming. This reaction is exothermic and does not need additional heating of the reformer, only initial heat for ignition (see Sect. 6.5.2.5). Depending on the conditions of reforming and the way the fuel consumption is controlled, there may be an anode off-gas, which can be returned and used in the burner of the reformer if necessary (see Fig. 6.119).

Historically, the development of reformers started in the 1960s. The Battelle Institute in Frankfurt developed a reformer that was used for the reforming as well as the splitting of methanol at approximately 250 °C with a Zn/Cu-catalyst from BASF. This reformer was connected to a fuel cell with an anode containing a tungsten carbide catalyst and a hydrophobic air cathode. The carbon monoxide being formed according to Eq. 6.58 was partly anodically oxidised and did not harm the catalyst. The electrodes of this laboratory assembly had a diameter of approximately 10 cm; it was demonstrated at the ACHEMA exhibition in Frankfurt/Germany in 1970 [611]. The device, shown in Fig. 6.121, was run for months without any loss in performance, which accounted for about 100 mA/cm^2 at room temperature.

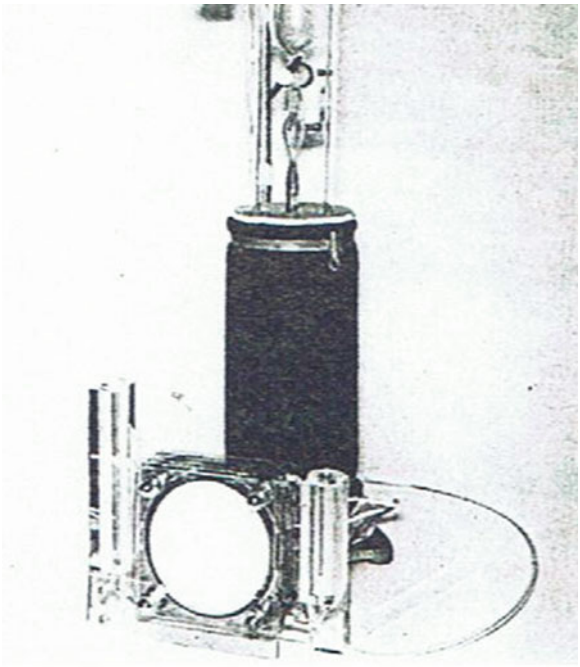

Fig. 6.121 Methanol reformer and reformat fuel cell (ACHEMA demonstration 1970)

Syngas Production from Methanol

According to thermodynamic data, methanol should be easy to reform and different reactions can be used to generate hydrogen from methanol. Besides steam reforming and partial oxidation, auto-thermal reforming has been developed as a combination of both of the processes. The first step of each reforming process is the vapourisation of the fuel and (if required) of the educt water. In any case, heat is required to operate a reforming reactor, which can be supplied by a burner or by using waste heat from any part of the process or a combination of both.

The steam reforming of methanol is kinetically inhibited; a significant reaction velocity even in presence of a suitable catalyst cannot be observed at temperatures below 150 °C. According to the thermodynamic equilibrium, methanol conversion should be complete at that temperature already and the highest possible yield of hydrogen will be achieved. As catalyst, Cu/ZnO on aluminium oxide has set the standard. In a temperature range between 250 and 300 °C, steam reforming leads to a gas with high hydrogen content. For the dry gas and complete conversion, 75 % would be the theoretical limit, with the remaining 25 % being CO_2. But at 300 °C, for example, when the reaction velocity is high, the shift reaction leads to a significant CO content in the product gas. The higher the temperature in the reforming reactor, the higher the CO concentration in the reformate will be, according to Eq. 6.4.2-9. The Cu/ZnO catalyst is active for this reaction as well.

The important thermodynamic data are

Steam reforming of liquid educts: $\Delta_R H^0 = +131.4\,\mathrm{kJ/mol}$

Steam reforming of gaseous educts: $\Delta_R H^0 = +49.3\,\mathrm{kJ/mol}$

Heat of evaporation for methanol: $\Delta_V H = +37.6\,\mathrm{kJ/mol}$

Heat of evaporation of water: $\Delta_V H = +44.0\,\mathrm{kJ/mol}$

It can be seen that a higher amount of heat is required to vapourise methanol and water than is required for the steam reforming of the gas mixture.

For partial oxidation, oxygen (air) is supplied to the reforming reactor and ignition is sufficient to start the exothermic reaction. Partial oxidation could even occur without any catalyst. Typically, however, a catalyst is used because the product water of the combustion reaction can be used for achieving higher hydrogen yields by CO conversion and methanol steam reforming. For partial oxidation of methanol, noble metal catalysts have mainly been investigated because they are active at low temperatures and much more stable than transition metal catalysts. If the stoichiometric ratio of educts is applied, the reaction of partial methanol oxidation releases $\Delta_R H^0 = -192.5$ kJ/mol.

The autothermal reaction is a combination of partial oxidation and steam reforming. The condition of net reaction enthalpy is reached with the following stoichiometry [612]:

$$CH_3OH + 0.1O_2(+0.4N_2) + 0.8H_2O \rightarrow CO_2 + 2.8H_2 + (0.4N_2) \qquad (6.61)$$

Without the dilution by nitrogen from air and with perfect selectivity of oxygen to react with the carbon atom, the hydrogen content could theoretically amount to nearly 74 %.

The product gas being generated by a methanol reformer can be fed directly to high- and medium-temperature fuel cells; even the HT-PEMFC is able to tolerate the typical CO levels of some vol% CO in the fuel. Only for PEMFC is a further CO removal required.

The possible CO removal processes being developed and applied in fuel cell systems in the past decades include the following:

- Shift reaction
- Selective oxidation
- Selective methanisation
- Membrane separation.

The shift reaction typically plays a minor role because the CO content of reformat from methanol already is quite low, and the best catalyst for low temperature shift reaction is Cu/ZnO.

The selective oxidation is carried out by feeding a small air stream into the reformate using a highly selective catalyst. Only special formulations of noble metals exhibit the required selectivity, avoiding significant hydrogen losses:

$$CO + 0.5O_2 \rightarrow CO_2 \quad \Delta_R H^0 = -284\,\text{kJ/mol} \tag{6.62}$$

The best selectivity of this exothermal reaction is typically only achieved in a narrow temperature window.

For methanisation, the reaction conditions also have carefully to be controlled because methanisation of CO and CO_2 can compete. Even if the selectivity of the catalyst is high, remarkable amounts of hydrogen are consumed.

$$CO + 3H_2 \rightarrow CH_4 + H_2O \quad \Delta_R H^0 = -206\,\text{kJ/mol} \tag{6.63}$$

Nevertheless, the methanisation might be interesting when the anode off-gas of the fuel cell is used in a burner. In addition, safety aspects are in favour of methanisation compared to selective oxidation because feeding air to a reformate gas stream implies some risks.

Palladium separation membranes for hydrogen purification are known from various applications. This technique also has been considered to be suitable for separation of hydrogen from reformate. To achieve good selectivity and sufficient hydrogen flux through the membrane, the membrane itself has to be adapted and a pressurised system concept has to be developed. Typically, a palladium-silver alloy for an operation temperature of about 300 °C is applied. Because this operation temperature of the membrane is quite close to that of a methanol steam reformer, the combination of these technologies has been successfully realised. The liquid educts water and methanol can be pressurised without much energy effort.

From a thermodynamic point of view, the efficiency of a methanol reformer can be calculated from the heating values of the product hydrogen (and CO) and of methanol:

$$\eta = \mathrm{LHV}(\mathrm{H_2})/\mathrm{LHV}\ (\mathrm{CH_3OH}) \tag{6.64}$$

For steam reforming, this simple calculation would lead to an efficiency value of 107 %, not taking into account the heat that is required to perform the process. If the heat of reaction has to be covered by combustion of methanol, the required amount of educt would increase and a maximum efficiency value of 75.8 % is the result.

6.5.2.8 Applications for DMFCs

Overview on Different Technologies for Applications

As described in section Sect. 6.5.2.5, DMFCs in general exhibit a quite low energy efficiency, require a higher amount of expensive noble metal loadings on the electrode catalysts, and also achieve limited current densities. Thus, for a required total system power, a DMFC is always much more expensive and also larger than a hydrogen-fueled fuel cell. Therefore, the DMFC so far has been developed for applications with limited power (about 100 W) and long run times [613–616]. Examples of such applications include the following:

- Remote sensors, such as fire detection in forests
- Military applications, such as power for soldiers
- Leisure applications, such as mobile homes
- Consumer electronics, such as grid-independent battery charging systems
- Light traction applications, such as scooters
- Forklift trucks or other material handling systems.

For all these applications, volume and weight are critical (except perhaps forklift trucks). Robust systems that are simple to operate are a basic requirement for commercialisation.

The first results of research and development towards higher power are described in here. An argument for using methanol as fuel instead of hydrogen is easy handling and refuelling by connecting a new methanol containing canister to the system. Various DMFC systems have been realised and tested. The first power generators are already commercially available, with some tens of thousands being already sold, mainly to the military sector but also to owners of mobile homes. The most important company to date is SFC Energy (Brunnthal, Germany).

Commercial DMFC System by SFC Energy

The SFC DMFC system is marketed under the brand name EFOY in a power range from 25 to 110 W. In the hybrid system, a battery is charged by the fuel cell.

The battery voltage is monitored and the fuel cell is automatically started if the voltage drops below a threshold value and also is automatically switched off as soon as the battery is fully charged. This results in reliable, continuous power, reduces the battery capacity needed and extends the lifetime as damaging deep discharge conditions can be avoided. In this hybrid system, the high power density of batteries is favourably combined with a high-energy density DMFC system. The DMFC is operated at constant power, as fluctuating demand is covered by the battery. Long-term autonomy is achieved for the application, as is long lifetime for the fuel cell (up to 5 years warranty is given).

In SFC's fuel cell systems, water recycling is realised, making the use of 100 % methanol as replacement fuel possible. Thus, including all efficiency losses, 31 kWh of electricity can be generated from a 22 kg fuel cartridge. Up to now, several thousand camping cars and mobile homes have been equipped with an EFOY fuel cell system, adapted to the 12 V onboard electricity systems. The industrial market is growing. Whenever small amounts of energy are needed in off-grid or rural areas such as along highways, coasts, or in the mountains, DMFC are a suitable power source. In many examples, a 1 km distance to the grid is worthwhile for a fuel cell installation because it will pay off within the first month. Examples for stationary applications are traffic management, environmental data acquisition, surveillance and security applications and even applications in the wind industry. SFC offers a portable fuel cell system JENNY 600S including a fuel cell and a Li-battery with a volume lower than 3.5 L and a weight less than 2 kg. This backpack system uses 350 ml methanol cartridges and can provide 25 W continuous for 16 h before a replacement cartridge is needed.

For military applications, SFC also provides a power managing device together with the portable fuel cell, which allows the user to set the output voltage for up to four different connected devices to the level needed. The SFC power manager also provides charging features for lithium batteries, and a solar cell or a vehicle power outlet can also be connected.

For on-board power supply in vehicles, DMFCs offer long autonomy and reduced weight. Because many specialised vehicles of authorities need a lot of electronic equipment to communicate, receive data and send data, cost and weight savings can be achieved by using such a fuel cell (Figs. 6.122, 6.123, 6.124).

Fig. 6.122 The EFOY Pro fuel cell on board a vehicle

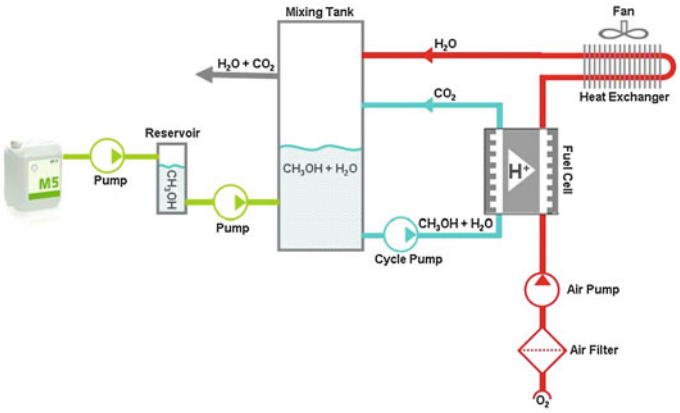

Fig. 6.123 Operation principle of the EFOY direct methanol fuel cell system

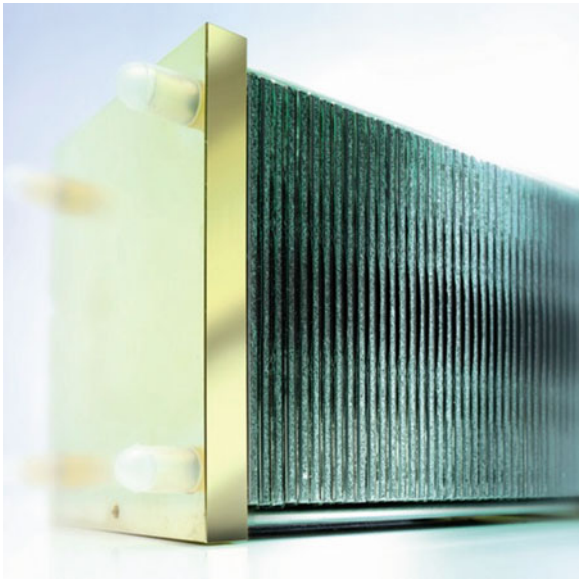

Fig. 6.124 Direct methanol fuel cell stack

Further Examples of Portable DMFC Devices

In the electronic sector, a charger for mobile phones was introduced in 2008 by Toshiba into the Japanese market. The first limited edition quickly sold out, but the improved capacity of Li-Ion accumulators seemed to hinder further commercialisation.

A number of chargers on the basis of a DMFC have been developed by research institutes [617, 618]. An effective technology was developed by Gottesfeld et al. of the Los Alamos Laboratory in 2000, and a 50 W system was applied by the Ball Aerospace Corporation. Another charging device with another technology was

developed by Jörissen of ZSW in Ulm and demonstrated in 2002, shown in Fig. 6.125. A dozen or so examples for portable DMFC devices can be found in literature [584]. There are a number of institutes in Germany (DLR, FZJ, HIAT, ICT, ISE, ZBT, ZSW) that continue research about methanol fuel cells. A further example is shown in Fig. 6.126, a micro-DMFC system of 100 W; it was developed in the frame of the Project Battext in cooperation with the DLR, University of Stuttgart ICVT and the companies Freudenberg FCCT, Staxon, and Kopf Solarschiff in 2010. This battery extender can be used in numerous portable, mobile and stationary applications. Meanwhile, a 1 kW system has been developed.

Fig. 6.125 Direct methanol fuel cell charging device by ZSW

Fig. 6.126 Micro-direct methanol fuel cell of 100 W, applied as support for the solar battery system, by DLR

Stringent miniaturisation might be a further chance for DMFC systems for future industrial application; robust power supplies to moving parts of robots and other systems in the factory automation might be another future chance. Passive air breathing stacks and systems have been demonstrated by various companies (e.g. Motorola, Toshiba, Sanyo, MTI micro fuel cells) and research institutions (Jet Propulsion Laboratory), but so far a breakthrough has not been achieved.

DMFC Applications for Light Traction

At the U.S. National Renewable Energy Laboratory, the development of DMFC for forklift trucks (pallet jacks) was pursued within a 2-year project (2011–2012). It is expected to achieve longer runtime and lower greenhouse gas emissions because methanol from renewable sources shall be used. For the battery in this designed hybrid energy system, a longer lifetime is expected as well. The project partner Oorja Protonics will have access to operational data from 75 pallet jacks being equipped with this DMFC system (OorjaPac). Within this project, methanol infrastructure is regarded as well. The outdoor storage and indoor dispenser for the methanol are not expected to be costly.

Pictures of the forklift trucks, including the methanol hybrid energy system, are shown in Figs. 6.127 and 6.128. The OorjaPac units act as an on-board battery charger, allowing grid independence. Battery change-out is eliminated by this construction. In addition, there is increased autonomy by quick refuelling with methanol and up to 14 h on single refuelling [619]. One big warehouse company said that they will initiate deployment of DMFC units at all sites.

The OorjaPac unit is a variant of a PEM fuel cell system that uses an anode catalyst to extract hydrogen from the methanol molecule; therefore, the anode catalyst for methanol is not much different from that for hydrogen. The specifications

Fig. 6.127 OorjaPac direct methanol fuel cell power pack

Fig. 6.128 OorjaPac direct methanol fuel cell power pack

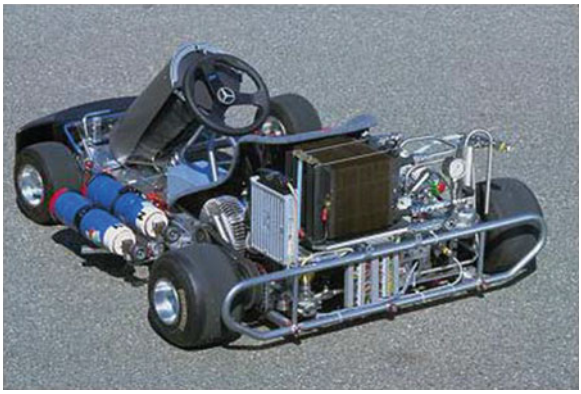

Fig. 6.129 Daimler-Go-Cart with direct methanol fuel cell technology

of the OorjaPac model 3 embrace a power output of 1.5 kW; an output voltage of 24, 36 and 48 V; a methanol tank volume of 12 L; and therefore an energy output of 20 kWh per tank.

In 2003, Daimler developed a drivetrain for a Go-Cart on the basis of DMFC technology [620], which is shown in Fig. 6.129. Net power of the DMFC system is approximately 2 kW [621]. Apparently, the amount of noble catalysts was too high for a commercial product. Daimler continued catalyst research, but so far no new results have become known.

FZJ researchers have been engaged for many years in the development of DMFC drive trains for light traction. The first DMFC system was put into operation in a conventional scooter in the year 2004 [622, 623]. Pictures of the scooter are shown in Figs. 6.130 and 6.131. The DMFC stack consists of 100 cells and has a nominal power of 1.3 kW and a peak power of 1.9 kW. As can be recognised from Fig. 6.131, the DMFC stack is a real drive train, which is exchanged for the battery inside the scooter for the operation of the electric motor. Thus, it is not a hybrid system.

A drive module for a forklift truck was also demonstrated by FZJ, which has been developed since 2007 [624]. This DMFC system, which is shown in Fig. 6.134, is a kind of hybrid system with a battery. The DMFC stack has a nominal power of 1.3 kW and the total system has a peak power of 7 kW, which

Fig. 6.130 Scooter with direct methanol fuel cell drive train, by FZJ

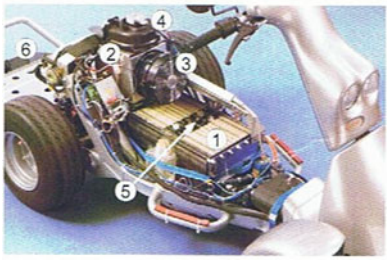

Fig. 6.131 Scooter with the FZJ direct methanol fuel cell (DFMC) drive train, showing a look inside

mainly stems from the battery. Because the nominal power is also the steady state power, the MEAs deliver a permanent power density of 75 mW/cm^2 at a voltage of 450 mV, which means a good success, but the noble metal loading is still a bit high (4.5 mg/cm^2) (Fig. 6.132).

Fig. 6.132 Direct methanol fuel cell battery hybrid system, by FZJ

6.5.2.9 Applications of the Indirect Methanol Fuel Cell Systems

Remarks About the Advantage of the IMFC Systems

The main differences between DMFC and PEMFC with a methanol reformer is the elevated temperature of the reformer (~300 °C). A laser welded compact ($90 \times 32 \times 100$ mm^3) integrated reformer and burner prototype has been developed by the Institut für Mikrotechnik, Mainz (Germany) for applications up to 100 W (see Fig. 6.133).

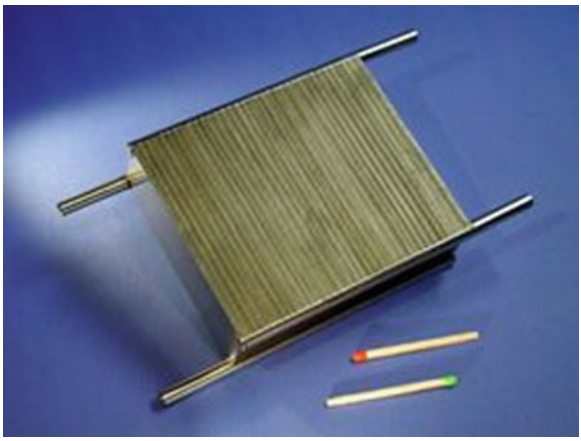

Fig. 6.133 Microstructured methanol reformer of Institut für Mikrotechnik Mainz

According to the data given in Sect. 6.5.2.3, the reformate gas contains about 1 vol% of CO. This reformat can be fed directly without further purification to every fuel cell except to low-temperature PEMFC. For PEMFC, a fine purification reactor for CO has to be included in the system. Although this two-staged fuel processor is more complicated, the first commercially available systems used this principle. At present, they directly compete with the DMFC as well, related to the target applications and also with respect to cost.

The company Ultracell (USA) is engaged in developing methanol reformer PEMFC systems. In 2007, the company announced that they participated in a contest being performed by the U.S. military. Additionally, the Danish company Serenergy is marketing a RMFC with a HT-PEMFC with a power output of 350 W, a volume of 27 L and a weight of 13.7 kg. As a new chance for an even simpler and more compact power generator for methanol as fuel, an integrated reformer/HT-PEMFC system (see Fig. 6.134) has been developed in several R&D projects. The waste heat of the HT-PEMFC being operated at temperatures up to 200 °C shall be used optimally for the vapourisation of the methanol–water mixture. Low-temperature reforming might be possible because the hydrogen being formed is consumed instantaneously upon formation, and thus a shift in equilibrium is possible.

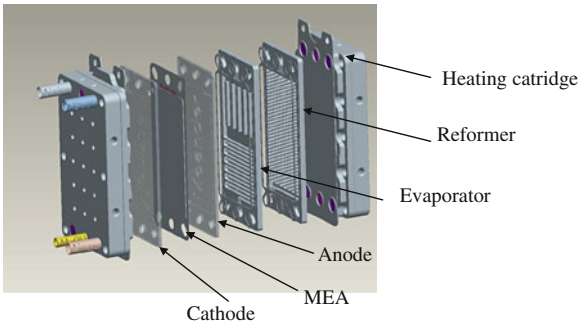

Fig. 6.134 Laboratory prototype of an integrated reformer/high-temperature proton electrolyte membrane fuel cell module (ZBT)

This approach combines a simple reformer with a hydrogen fuel cell with good power density. Due to good heat integration, the system might be the smallest in comparison with DMFC and reformer/low-temperature PEMFC. For startup, electrical heaters or (catalytic) methanol burners are required because neither the fuel cell nor the reformer can be started at room temperature. This leads to a somewhat extended startup period.

According to recent investigations, CO is not converted electrochemically at the HT-PEMFC anode. This means that the possible release of CO from the system has to be avoided by a postcombustion process, using the anode off-gas for delivering additional heat to the fuel processor (see Fig. 6.119).

At present, methanol as fuel is not state-of-the art for transportation or domestic use, so the possible applications will remain limited. The more renewable electrical power will be used, the more important is the generation of storable fuel. The first step will be the generation of hydrogen, but the second step could be the synthesis of methanol, thereby leading to more applications for methanol fuel cells.

Interim Development of Passenger Cars with IMFC Drive Train

The first research car with methanol reformer was developed by Daimler in 1997 (Figs. 6.135 and 6.136) [625], and 1 year later an Opel/GM-Zafira with methanol drive train was presented [626].

Around the year 2000, the car manufacturers did not yet know which fuel would be best for which fuel cell for driving a car. Therefore, they experimented with all possible fuels: gaseous hydrogen, liquid hydrogen, methanol, gasoline, diesel, sodium hydride, ethanol and others. LBST shows a complete compilation of all those experimental cars from the year 1807 until now in Wikipedia under the heading "Hydrogen and Fuel Cell Vehicles Worldwide". Cars with IMFC drivetrains have been listed from Daihatsu, Daimler, Ford, Georgetown University, Honda, Hyundai, Mazda, Mitsubishi, Nissan, Opel/GM, Subaru, Toyota and Volkswagen. All these automobile companies presented complete prototypes that could have been used for starting a model series.

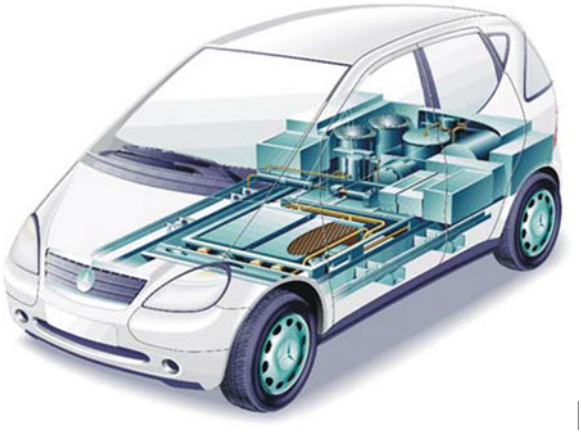

Fig. 6.135 NECAR III methanol reformer and fuel cell (1997)

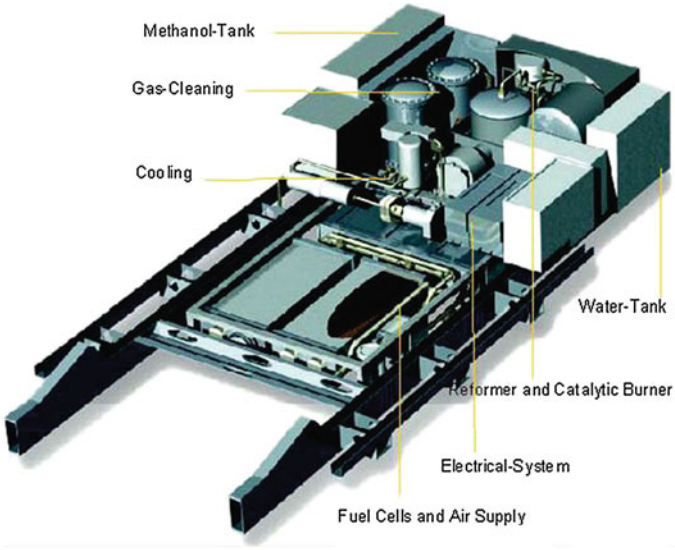

Fig. 6.136 NECAR III underfloor concept

The NECAR 3 by Daimler (NECAR = new electric car) got a successor, the NECAR 5, which was a comfortable car like other conventional cars. From Figs. 6.137 and 6.138, it can be seen that the volume for the complete reformer and fuel cell was limited to a sandwich floor of the car.

Not only the volume but also the weight was reduced drastically, altogether by more than 300 kg. The PEMFC from Ballard was improved to a great extent.

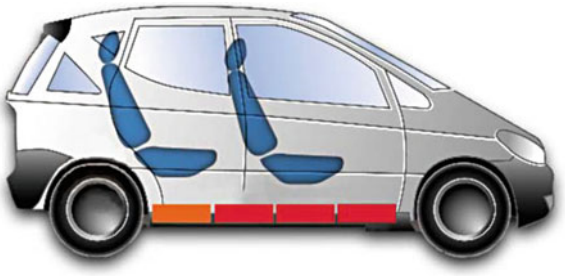

Fig. 6.137 NECAR 5 methanol tank (orange box), reformer and fuel cell (red boxes) in the sandwich floor (1998)

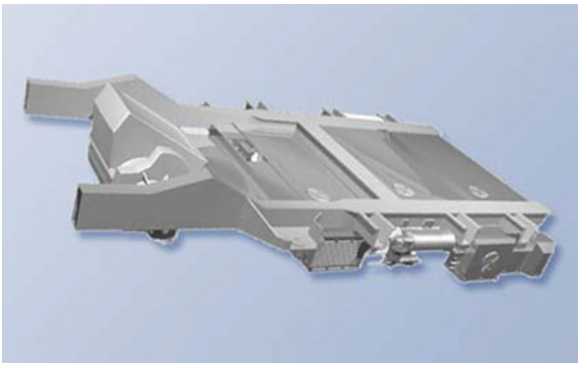

Fig. 6.138 NECAR 5 fuel cell system

Whereas NECAR 3 had two stacks with 150 single cells and a power of 50 kW in total, NECAR 5 was equipped with only one stack, whose nominal power amounted to 75 kW. The operational temperature was kept to 80 °C. The catalyst for the reforming was developed by BASF and was also improved. The tank volume amounted to 38 L, which covered a travelling distance of 300 km. The rated power of the electric motors amounted to 45 and 55 kW and the top speeds to 120 and 150 km/h for NECAR 3 and 5, respectively.

Although there was no cooperation between the two big automobile companies, their fuel cell cars had similar data. The first methanol car of Opel was presented a few months later. Its electric motor had a power of 50 kW, which was sufficient for a top speed of 120 km/h. The methanol tank capacity was approximately 54 L and the water tank was approximately 20 L.

Thus, the cruising range was somewhat higher. The curb mass was 1,850 kg. Figures 6.139 and 6.140 show the first prototype car by Opel, in which the methanol reformer system appears to be a small chemical plant on board the car.

Together, Daimler, Ballard, BASF, BP, Methanex and Statoil founded the Methanol Fuel Cell Alliance. They issued together a joint position document in 2002, in which they declared that their objective would be to go on the market very soon [621]. A few years later, most developments of methanol cars were stopped because the car manufacturers and oil companies changed their mind and decided

Fig. 6.139 Opel/GM-Zafira methanol concept car with reformer and fuel cell (1998)

Fig. 6.140 Opel/GM-Zafira methanol concept car with reformer and fuel cell in the rear

to continue on the basis of hydrogen. There is still some research going on, but it is unclear whether methanol will play a role in the general automobile market in the future. Despite this, special applications may still come out one day.

Special Applications of IMFCs

As was mentioned in Sect. 6.5.2.7 about the practical application of DMFC systems, there are likewise quite a number of examples for IMFC systems that could be described. In particular, two publications should be referred to when looking for demonstration of IMFCs, namely those by Garche, [612, 627] including the first book about IMFC, titled *Methanol Fuel Cell Systems: Advancing Towards Commercialization*. Among other companies, he mentioned IdaTech and Protonex Technology., which developed two IMFC systems called ElectraGen3 and ElectraGen5, rated with 3 and 5 kW respectively.

More recently, a new type of combination system was demonstrated. The company Wärtsilä started with the development of an ideal power source for special services, the power of which should be 10 or 50 kW or even more. They were the first to present an indirect fuel cell system using a SOFC. Early in 2011, they teamed up with Versa Power Systems (VPS), a developer of high-power SOFCs with headquarters in Littleton, Colorado, USA. Wärtsilä had developed reformers for an IMFC and an indirect hydrocarbon fuel cell, and they looked for a suitable fuel cell to combine with. Therefore, they presented the first IMFC system with a SOFC fuel cell. The target of the agreement with VPS was to develop commercial Wärtsilä fuel cell products that generate power and heat for various applications in the distributed energy, including marine markets. The demanding objective was to use the power source also on-board of a ship, which meant that it had to comply with outstanding environmental requirements. Figures 6.141, 6.142 and 6.143 show pictures of the transportation and installation of the WFC20 fuel cell unit on board the Swedish Wallenius Lines [628].

The WFC20 is a fuel cell system of a methanol reformer and a SOFC with a power of 20 kW. The development and installation has been carried out by the international METHAPU consortium, whose participants are Wärtsilä, Wallenius Marine, Lloyd's Register, Det Norske Veritas and the University of Genoa, who are active in the field of fuel cell system integration and environmental assessment in shipping.

Fig. 6.141 Wärtsilä's WFC20 fuel cell unit in operation

Fig. 6.142 Wärtsilä's fuel cell unit WFC20 started its journey in Finland

Fig. 6.143 Installation of the Wärtsilä WFC20 fuel cell unit on-board of the "Undine" of the Swedish Wallenius Lines

6.5.2.10 Conclusion

History of the Methanol Fuel Cell

A few steps were especially important for the development of the DMFC and the IMFC. The fuel cell effect was discovered with gaseous reactants as early as 1838 by Schönbein in Basel, who published it in the January 1839 edition of the (*British*) *Philosophical Magazine*. At the same time William Grove, who lived in London and who was a friend of Schönbein, carried out similar experiments (namely electrolysis of dilute sulphuric acid) and measured a voltage afterwards, while hydrogen and oxygen gases were present at the electrodes. He published it in the February 1839 edition of the same magazine. Whereas Schönbein investigated the effect further and discovered ozone, Grove recognised that he had invented a gaseous battery, as he called it; therefore, he knew that he had discovered an electricity generating device. The reason for his quick recognition was that he had invented several battery elements before [629, 630].

Therefore, the continuation of the research about the fuel cell effect lead to the investigation of a solid fuel, namely coal, which did not find success, even now. After all, one has to take into account that the designation "fuel cell" was used in 1889 (by Mond and Langer for the first time) and that the mode of operation of a fuel cell was recognised in 1894 by Wilhelm Ostwald, who got the Nobel Prize for his work on catalysis a few years later. Thus, the basis was laid for a target-oriented and purposeful research about fuel cells for technical applications. Despite these facts:

– it took a lot of time until the first investigation of a fuel cell with methanol as a dissolved fuel was carried out by Taitelbaum in 1910 [552].

– There were only few investigations about the electrochemical oxidation of methanol every now and then in the course of time. The next researcher was Müller 1922, and then Kordesch and Marko dealt with dissolved fuel cells and proposed the DMFC with alkaline electrolyte in 1951. It took a further 10 years or so for real DMFCs to be developed. All of a sudden, a number of groups presented cells or stacks during the 1960s—some with alkaline electrolyte and some with acid electrolyte or both. Among the first were Justi in Braunschweig and Vielstich in Bonn, along with their students, as well as the Battelle Institute in Frankfurt and the companies Allis Chalmers, Bosch (Fig. 6.144), Esso, Shell, Siemens and Varta (Fig. 6.145) [631].

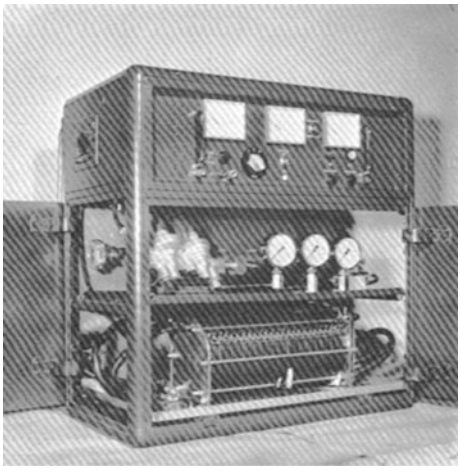

Fig. 6.144 Alkaline direct methanol fuel cell with a power of 100 W, developed in the 1960s by the Bosch company

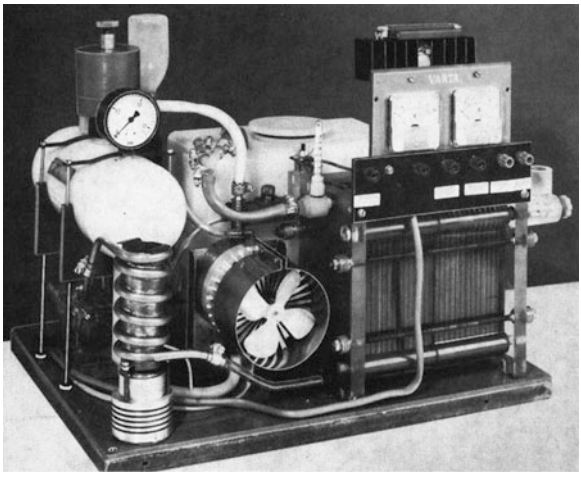

Fig. 6.145 Alkaline direct methanol fuel cell with a power of 140 W at 60 °C, developed in the 1960s by the Varta company

Fig. 6.146 Direct methanol fuel cell module of a power of 300 W with acid liquid electrolyte, developed in the 1960s by Shell Research

Shell and Esso tried to develop real prototypes of DMFC with acid electrolyte, but were not satisfied with the durability of the stacks. One example is shown in Fig. 6.146.

From the mid-1960s until the end of the 1990s, the progress was slow. However, many companies, especially small companies, tried to develop small portable DMFC units, as has been reported in Sects. 6.5.2.5 and 6.5.2.7. The DMFC was based on the same components as the PEMFC in the 1980s; after this, the hydrogen fuel cell type won great success in the 1990s. Two examples may be mentioned—the equipment of submarines with H_2/O_2-PEMFCs by Siemens and the development of the electrotraction of passenger cars and buses with compressed hydrogen/air-PEMFCs by many automobile companies all over the world, as a preparation of electromobility of the traffic for environmental reasons [630].

Also, Siemens developed a small DMFC of the PEMFC type, whose design data and performance results were already quite interesting. It was a three-cell stack for the purpose of demonstration; the operational area of the electrodes amounted to approximately 550 cm^2 and the working temperature was about 90 °C. The electrocatalyst of the anode consisted of supported platinum-ruthenium of an amount of 2.6 mg/cm^2 and the one of the cathode contained platinum, approximately 4 mg/cm^2; the methanol concentration (methanol/water mixture) amounted to 0.5 M. A current density of 0.1 A/cm^2 and a voltage of 0.5 V were measured. Thus, the little methanol battery delivered a power of 83 W at an efficiency of 42 % and of 113 W at maximum [632].

DMFC batteries in the kW range were also successful; they have been described in Sect. 6.5.2.7. They were useful for special applications; however, for a broad applications concerning passenger cars, the units are still too expensive, which mainly originates from the noble metal loading of the electrodes. Therefore, the automobile industry changed to the other type of methanol cells, the IMFC. The cars with drivetrains with IMFCs have been developed around the year 2000; they have been described in Sect. 6.5.2.9. The development of the IMFC drive

train systems was not yet completely finished when a decision about the future transportation fuel had to be made, which is known to have become hydrogen. As was described in Sect. 6.5.2.9, special applications of the IMFC are just in the process of entering the market.

Prospects of Methanol Fuel Cells

Reflecting about the prospects of methanol fuel cells, one has to investigate (in our opinion) the objectives of the existing developments of the various types of methanol cells. Furthermore, one has to find out whether these objectives can be extrapolated into the future, if this is desirable at all, and whether there are possibilities to change them (either to expand or to narrow them for whatever reason). In addition, the discussion has to deal with the technological goals as well as the commercial targets. To detect these indicated objectives, it is helpful to look into the history of the different methanol fuel cells so far developed (see Sect. 6.5.2.9 and elsewhere in this publication).

In addition, the description of the broad technological field of the fuel cells, which can use methanol as fuel, in the preceding chapters can be completely divided into two areas. All the very different modes and designs—be they of a microscale or a size up to megawatts-can be allotted to the DMFC type or to the indirect methanol fuel cell type (IMFC). If one considers the situation from the technological side and has observed the huge spectrum of possible kinds of methanol fuel cells, then there is certainly no loss of hope for a suitable new type of DMFC or IMFC in the future.

What has to be considered as a main goal for each new device is the target of an acceptable and appropriate cost and price situation. This situation depends either on the task you will substitute for or on the new task the fuel cell will attack to solve. There are two main functions for which the methanol fuel cell can be applied. First, it can be a powering device for any situation, to make electricity available at remote spots, and even to provide a backup facility. This may be a substitute for a battery, which has been used for this purpose up to now and which does not fulfil the requirement of being as reliable and durable as the new fuel cell. On the other hand, methanol fuel cells can be used as a charging device for a battery. Commercial examples have been described in Sect. 6.5.2.7. They are called “on-board battery charger” or “fuel cell battery hybrid system” and are in general powering devices.

The second group of methanol fuel cells are the IMFCs, which are practically a combination of a PEMFC and a reformer for methanol, which changes the methanol into hydrogen. Now, the importance of the indirect methanol fuel cell, which is also called reformed methanol fuel cell, is increasing because the hydrogen fuel cell has meanwhile been developed to a reliable and cost-effective product and the methanol reformer has also made good progress and can be developed to any size. Therefore, the IMFC is an ideal system and can also be applied as a drivetrain for all kinds of vehicles. Although the big automobile

manufacturers have decided to use the pure hydrogen system as fuel cell drive for passenger cars, there are enough future mobile applications for the methanol system.

The DMFC needs a bit longer for the introduction into the consumer market. However, this market is not satisfied with the accumulator technology for the time being and is expecting a portable power source of small sizes quite soon. At present, from the efficiency point of view, the DMFC may be a niche system for small power applications. After all, various DMFC systems have been realised and the first power generators are already commercially available, with some tens of thousands being already sold (mainly to the military sector but also to owners of mobile homes). Up to now, about 30 companies are involved in relevant fuel cell development. In addition, the state of the art of fundamental research shows that there is a big amount of basic knowledge still missing, which means that university and high school research is necessary and can support the education and training of very many students, who carry the progress of science and technology. It may be possible that fuel cells will change the telecommuting world by powering all kinds of digital handheld devices in the not-too-distant future. In addition, all other applications of methanol fuel cells will profit from the situation mentioned.

Methanol is a commercial fuel suitable for stationary, vehicle and military applications, but as at present, it is not the state of the art for transportation or domestic use. The more renewable electrical power will be used, the more important is the generation of storable fuel. The first step will be the generation of hydrogen, but the second step could be the synthesis of methanol, thereby giving more applications for methanol fuel cells a chance. In addition, we must not forget that approximately 50 % of the energy generated is not electricity but heat; thus, the heating of a mobile home or any other room or piece would save a large amount of energy.

The advantage of methanol fuel cells is that they are able to cope with a lot of demands and requirements, be they of legal or societal nature. Thus, DMFC devices can be used in airplanes, including the cartridges for the fuel, either as pure methanol or methanol–water mixtures. However, the demands for the methanol fuel cells are much broader and eclectic. They are to supply electrical energy in form of very clean energy so that the process of powering is not a burden for the environment and that everything operates sustainably. Raw material has to be preserved and the fuel efficiency must be as high as possible. Furthermore, two problems of mankind can be solved by methanol: Biomass can be easily changed into methanol and thus is available as energy source; and garbage can also be easily changed into methanol and thus removed from the surface, presenting clean energy in the process.

6.5.3 Methanol in Biotechnology

Sebastian Hippmann[1], Martin Bertau[1], Dirk Holtmann[2], Frank Sonntag[2], Thomas Veith[2] and Jens Schrader[2]

[1]*Institute of Chemical Technology, Freiberg University of Mining and Technology, Leipziger Straße 29, 09599 Freiberg, Germany*

[2]*DECHEMA Research Institute, Theodor-Heuss-Allee 25, 60486 Frankfurt/M., Germany*

Introduction

Methylotrophs play a key role in the global cycling of C_1 compounds and offer biotechnological opportunities for the production of commodity chemicals from methanol [633]. The major proportion of the annual plant-released methanol does not enter the atmosphere. The methanol is converted by methanol-oxidising prokaryotes. These methylotrophic bacteria belong to different classes including Proteobacteria, Verrucomicrobia, Firmicutes and Actinobacteria. The wide variety of bacteria (and also yeasts) are able to grow in inexpensive synthetic media with methanol as the sole or major source of carbon and energy. This is due to the presence of a few unique enzymes that enable these organisms to generate metabolic energy and synthesise cell constituents from this one-carbon substrate. As a feedstock for industrial fermentations, methanol is also attractive because of its low cost, ease of handling and abundant availability [634]. Furthermore, methanol is often used as a carbon source in biological wastewater treatment plants and as fuel in biofuel cells; it also can be produced by biological components.

6.5.3.1 Metabolism and Physiology

Metabolism of Methylotrophic Bacteria

Methylotrophy can be defined as the ability of (micro-)organisms "to grow at the expense of reduced carbon compounds containing one or more carbon atoms but containing no carbon–carbon bonds" [635]. Thus, besides methane and methanol, methanesulphonate and other methylated sulphur species, methylated amines, the halogenated hydrocarbons chloromethane, bromomethane and dichloromethane also can serve as sole carbon and energy source—either exclusively or in addition to methanol. Methylotrophy research dates back to 1906 with the discovery by Soehngen of a bacterium growing on methane or methanol, *Bacillus methanicus,* which was later renamed as *Methylomonas methanica*. Nowadays, numerous bacterial methylotrophs are known and several genomes have been published, including the smallest known genome of a (nonparasitic) free living cell to date: the marine methylotroph *Methylophilales bacterium* HTCC2181 [636]. Phylogenetically, bacterial methylotrophs mainly belong to the alpha, beta and gamma subclasses of Proteobacteria or the group of Gram-positive bacteria [637].

In a dissimilatory process, methylotrophic bacteria oxidise the reduced one carbon (C_1) source stepwise to CO_2. Thereby, adenosine triphosphate is generated due to the involvement of electron-transport-coupled phosphorylation. In this process, formaldehyde represents the key intermediate. It is the first intermediate after the oxidation of methanol. Besides its function in the dissimilatory pathway leading to CO_2, it also serves as input for C_1 assimilation pathways in methylotrophs (see below). The oxidation of methane to methanol is performed by a subgroup of methylotrophic bacteria, the methanotrophs. Two versions of the respective enzyme, methane monooxygenase (MMO), have been described: a soluble (s) cytoplasmic MMO and a particulate (p) membrane-bound MMO. Both enzymes are regulated due to the availability of copper. sMMO (a non-heme iron-containing enzyme) is expressed under low copper conditions, whereas pMMO (with a di-copper centre in the active site) is expressed under high copper conditions [638–640]. This biological methane oxidation is remarkable because the chemical methanol synthesis is a three-stage catalyst-requiring process, whereas the MMO reaction is carried out directly with di-oxygen [641]. Most attention has been focused on the iron-containing sMMO, especially from the species *Methylosinus trichosporium* and *Methylococcus capsulatus.* The ability of MMO to activate methane at room temperature and ambient pressure makes it an attractive target for research toward a potential enzymatic large-scale production of methanol [642].

After the uptake of methanol or its generation from methane in the case of methanotrophs, methanol is further converted by methanol dehydrogenase to formaldehyde. So far, periplasmic pyrroloquinolin quinone (PQQ)-dependent methanol dehydrogenases have been described for Gram-negative bacteria as well as nicotinamide adenine dinucleotide phosphate (NADP)-dependent enzymes in Gram-positive bacteria [643, 644]. The following conversion of toxic formaldehyde to CO_2 by methylotrophs can be achieved by several (linear or cyclic) pathways, of which some can occur in parallel within one organism [645]. Exemplarily, co-factor dependent linear pathways such as the tetrahydromethanopterine (H_4MPT) pathway, discovered in the alphaproteobacterium *Methylobacterium extorquens*, and glutathione (*Paracoccus denitrificans*) and mycothiol (Gram-positive methylotrophs) pathways, should be mentioned as well as the cyclic ribulose monophosphate (RuMP) pathway of Gram-negative Proteobacteria (e.g. *Methylobacillus flagellates*) [635, 646–648]. The latter is nearly identical to the assimilatory RuMP pathway mentioned afterwards (see Fig. 6.147) [635].

The assimilatory incorporation of C_1 compounds of bacterial methylotrophs can be roughly divided into two pathways, with both requiring the aforementioned formaldehyde as precursor (reviewed in Ref. [635]). Assimilation via the RuMP pathway uses all carbon needed from formaldehyde by catalysing the reaction from ribulose-5-phosphate to hexulose-6-phosphate by hexulose phosphate synthase (see Fig. 6.147). In contrast, the serine cycle for carbon assimilation of Alphaproteobacteria (e.g. *M. extorquens*) incorporates CO_2 additionally by carboxylation reactions besides formaldehyde assimilation via serine. This remarkable combination of pathways leads to accumulation of approximately 50 % biomass carbon

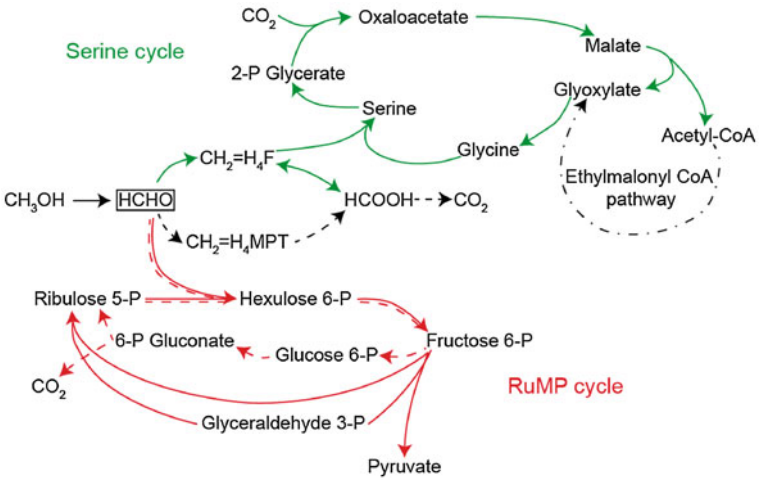

Fig. 6.147 Generalised scheme of methanol assimilation via the serine (green) and ribulose monophosphate (RuMP; red) cycles of methylotrophic bacteria. Note that formaldehyde plays a central role as branch point for all shown pathways (box). Dissimilatory processes are indicated by dashed arrows. The multistep conversion of acetyl-CoA to glyoxylate via the ethylmalonyl-CoA pathway is indicated by a dashed-dotted arrow

from CO_2 and thus to a refixation of CO_2 produced during the dissimilatory process described above [649, 650]. The fixation of CO_2 occurring within central pathways can be calculated from the difference between CO_2-utilising and CO_2-releasing fluxes [651]. Approximately 20 % of the formed CO_2 is recovered, which correlates to 16 % of the consumed methanol.

Although the general understanding of metabolism of methylotrophic bacteria is not as advanced as for model organisms such as *Escherichia coli* or baker's yeast, research on methylotrophy is advancing, especially considering *M. extorquens* is the probably best understood organism within methylotrophic bacteria. With the genome published [652] and a variety of genetic tools at hand, ubiquitous efforts have been made to study its (one carbon and multicarbon) metabolism, including proteome and transcriptome analyses as well as metabolite profiling (reviewed in Ref. [634]). Recently, the activities of all (postulated) enzymes required for methanol assimilation and their regulation in comparison to acetate and succinate grown cells, as well as metabolic adaptation processes occurring during the shift to C_1 carbon metabolism, were published [653, 654].

Physiology and Metabolism of Methylotrophic Yeasts

Contrary to prokaryotic cells, eukaryotic cells are substantially larger and possess membrane-surrounded compartments in which the reaction conditions for metabolic processes are ideally adjusted: short diffusion ways, the enrichment of the intermediates in sufficient concentrations, necessary enzymes and pH value. Thus, different reactions can take place at the same time in the cell without interacting [655].

The only known eukaryotes that can use methanol as carbon and energy source for growth belong to the yeasts (i.e., single-cell fungi). Yeasts are widely spread in nature and occur particularly in the ground and on plants. They have been in use by man for thousands of years in order to manufacture alcoholic beverages and bread. It was not until the nineteenth century that they were cultivated in larger quantities. Yeast cells are 5–10 μm large and they mostly belong to the group of the ascomycota. Their cell shape is predominantly round oval to cylindrical. Reproduction takes place either asexually via budding or sexually via formation of ascospores [656].

Yeasts using methanol for growth are called facultative methylotrophs; these were first mentioned in 1969 by Ogata [657]. "Facultative" means that they are not able to metabolise methane. However, they can use higher oxidised C_1-substrates, such as methanol, or substrates with C–C-bonds, such as glucose as a carbon and energy source [658]. Some important representatives of this group are shown in Table 6.25.

Table 6.25 Name of some methylotrophic yeast (year of renaming) [659]

Common Name	Scientific Name	Other Synonyms
Pichia angusta	*Ogataea angusta* (2010)	*Pichia angusta* (1984)
		Hansenula polymorpha (1959)
		Hansenula angusta (1961)
		Ogataea polymorpha (1994)
Pichia pastoris	*Komagataella pastoris* (1995)	*Pichia pastoris* (1956)
		Saccharomyces pastoris (1952)
		Zygowillia pastoris (1954)
		Zymopichia pastoris (1961)
Pichia guilliermondii	*Meyerozyma guilliermondii* (2010)	*Pichia guilliermondii* (1966)
		Yamadazyma guilliermondii (1989)
		Candida carpophila (2005)
Candida boidinii	*Candida boidinii* (1953)	*Candida methanolica* (1972)
		Candida methylica (1974)
		Candida queretana (1978)
		Hansenula alcolica (1975)
		Kloeckera boidinii (1975)

In nature, these yeasts can be found in spoiled fruits and vegetable products as well as in exudates and the bark of trees [660]. The existence of these eukaryotes in those habitats can be attributed to the fact that methanol becomes available by the degradation of the methoxy-moieties of lignin. Equally, most of the tested methylotrophic yeasts are able to grow on a medium with pectin-a polymer that is rich in methoxy-groups and is ubiquitous in fruit [661]. Unlike bacteria, yeasts are not equipped with methanol dehydrogenase to form formaldehyde. Instead, they possess specialised cell compartments, peroxisomes, in which methanol oxidation occurs. Peroxisomes are round organelles, approximately 0.5 μm large, surrounded by a membrane; they are located in the cytoplasm of eukaryotes. These vesicles proliferate if the cells are exposed to nutrients that require metabolism where peroxisomal

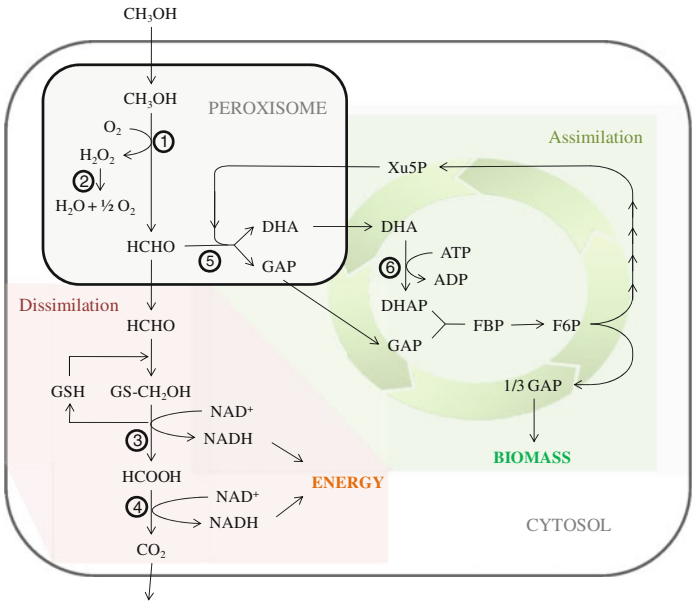

Fig. 6.148 Methanol metabolism pathway in methylotrophic yeasts[663] 1 – alcohol oxidase, 2 – catalase, 3 – formate dehydrogenase, 4 – formaldehyde dehydrogenase, 5 – dihydroxyacetone synthase, 6 – dihydroxyacetone kinase. GSH, glutathione; Xu5P, xylulose-5-phosphate; DHA, dihydroxyacetone; DHAP, dihydroxyacetone phosphate; GAP, glyceraldehyde-3-phosphate; FBP, fructose-1,6-bisphosphate; F6P, fructose-6-phosphate

functions and enzymes are involved. Therefore, in the presence of methanol, they account for up to 80 % of the total cell volume [662]. An overview of methanol metabolic pathways in methylotrophic yeasts is summarised in Fig. 6.148 [663].

Methanol metabolism is initiated by an alcohol oxidase mediated oxidation to formaldehyde, the key intermediate of methylotrophs, which takes place under oxygen consumption. This reaction goes along with hydrogen peroxide formation, upon which H_2O_2 degradation by catalase sets in. Therefore, compartmentalisation of this reaction is an elementary strategy to prevent cell damage caused by formaldehyde and hydrogen peroxide [664]. Subsequently, formaldehyde can be successively dissimilated to CO_2 and reduced nucleotides (energy). In detail, this process encompasses formaldehyde oxidation through the action of NAD^+ and glutathione-dependent formaldehyde dehydrogenase to form *S*-formyl-glutathione. This latter compound can now either be oxidised to CO_2 by formate dehydrogenase (NAD^+ dependent) or it can be hydrolysed by formylglutathione-hydrolase to formate, which is then oxidised to CO_2 by formate dehydrogenase. The assimilation of formaldehyde is accomplished through the xylulose monophosphate cycle. In this pathway, the C_1-entity formaldehyde reacts with C_5-building block xylulose-5-phosphate (Xu5P) to form two C_3-compounds: glyceraldehyde-3-phosphate (GAP) and dihydroxyacetone (DHA); the reaction is catalysed by

dihydroxyacetone synthase. Dihydroxyacetone kinase, the next enzyme involved, phosphorylates DHA to dihydroxyacetone phosphate, which in a next step reacts with glyceraldehyde-3-phosphate to form fructose-1,6-bisphosphate, a C_6-compound. Dephosphorylation leads to fructose-6-phosphate, which is further converted to GAP and Xu5P, thus rendering the pathway ready for the next cycle (Figs. 6.148 and 6.149). To produce one molecule of the C_3-body GAP, which is then funnelled into central metabolism to form biomass, the Xu5P-cycle has to be run three times.

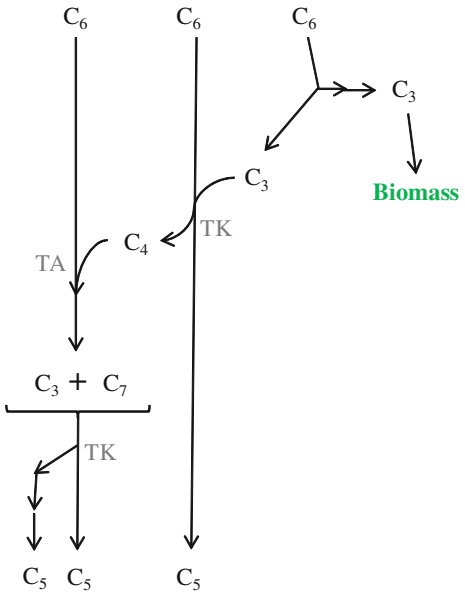

Fig. 6.149 Rearrangement reactions to convert three molecules fructose-6-phosphat (C_6) to three xylulose-5-phosphate (C_5) to keep Xu5P-cycle running [665]. C_3, glyceraldehyde-3-phosphate; C_4, erythrose-4-phosphate; C_7, sedoheptulose-7-phosphate; TK, transketolase; TA, transaldolase

Most yeasts, including the methylotrophic ones, possess "generally recognised as safe" status, for which reason they are used for a huge number of fermentations, as food additives, as a source of vitamins and also as "biofactories" for the production of various antibiotics, steroid hormones, homologous and heterologous proteins, as well as models for studying genetic regulation in eukaryotic cells [666].

6.5.3.2 Growth and Product Formation

Methylotrophic Bacteria

The key issues in the use of methylotrophic bacteria are productivity, carbon conversion efficiency and achievable product concentration. Various authors developed stoichiometric equations for biomass formation on methanol via the RuMP pathway the average values of which are shown in Eq. 6.65 [667–669].

$$1.63CH_3OH + 1.39O_2 + 0.23NH_3 + \text{nutrients} \rightarrow CH_{1.69}O_{0.38}N_{0.24}(\text{biomass}) + 0.63CO_2 + 2.76\ H_2O \quad \Delta H = -449.7\ \text{kJ/mol}_{MeOH} \tag{6.65}$$

The carbon balance shows that approximately 38 % of the methanol is dissimilated and 62 % is used for the formation of cellular mass. An amount of 0.85 g oxygen is required for the oxidation of 1 g of methanol and 0.52 g of carbon dioxide is produced. In Table 6.26, published data for biomass productivities and concentrations as well as yields are summarised. The table shows that high biomass productivities over 25 g biomass per litre an hour can be achieved. Surprisingly, the highest reported biomass concentration was 250 g/l [670]. This value has not been reproduced in the last 15 years. Optimum growth rates for biomass accumulation can be obtained by maintaining low and stable methanol concentrations. High methanol concentrations and sudden concentration shifts cause toxic effects on the bacteria due to the accumulation of formaldehyde [671, 672].

Table 6.26 Examples of growth parameters of microorganisms on methanol

Microorganisms	Pathway	Biomass productivity (g_{CDM} g/l)	Cell dry mass (g/l)	Cell yield (g_{CDM}/g_{MeOH})	Comment	Literature
Methylomonas methanolica	RuMP	25 (potential)	50	0.5	Industrial SCP process	[667]
Methylomonas sp.	RuMP	28.4	114	0.49	Continuous process ($\mu = 0.25\ h^{-1}$)	[673]
Methylobacterium organophilum	Serine	3.6	250	0.34	PHA process	[670]
Methylobacterium sp.	Serine	2	172		PHA process	[674]
Methylobacterium extorquens	Serine	1.2	56.1	0.28	GFP production, recombinant	[675]
Mixed culture		4.55	10.6	0.44	Continuous process	[676]

PHA, polyhydroxyalkanoates; RuMP, ribulose monophosphate; SCP, single-cell protein

Typical products of methylotrophic prokaryotes are polyhydroxyalkanoates (PHA) and amino acids. On the basis of known metabolic pathways, Leak compared predicted carbon conversion efficiencies for diverse products in different microorganisms either growing on methanol or glucose [677]. For extracellular polysaccharides, polyhydroxyalkanoates and glutamate, the predicted conversion efficiencies are similar. This indicates that, for high yielding organisms, methanol-based bioprocesses could be economically competitive. The higher oxygen demand of methylotrophs could be considered as a disadvantage. In the case of glutamate, the oxygen-based yield Y_{P/O_2} is predicted to be two- to threefold lower for the growth on methanol than for the growth on glucose. A comparison of the stoichiometric conversion of methanol to glutamate via either the RuMP or the

serine pathway indicates predicted yields of 0.76 and 0.92 g/g [677], respectively, whereas the theoretical yield for glutamate production of organisms growing on glucose is 0.82 g/g.

Comparison of lysine production by *Bacillus methanolicus* that starts from methanol with lysine production in *Corynebacterium glutamicum*, which employs glucose, shows that the yields were comparable [678]. The theoretical yields for both conversions of methanol to lysine with *B. methanolicus* were $Y_{P/S} = 0.82$ $g_{Lysin\text{-}HCl}/g_{methanol}$ and 0.71 $g_{Lysin\text{-}HCl}/g_{methanol}$, respectively. The highest productivity of PHA was described by Kim et al. [670]. The biomass and PHA formation rate reached 3.57 and 1.86 g h/l, respectively. The highest product yield was 0.2 g PHA per gramme of methanol. A recombinant *M. extorquens* strain produces PHA derivates. By cofeeding methanol and 5-hexenoic acid, functionalised PHA containing C–C double bonds were produced [679, 680].

A genetically modified strain of *Methylobacterium rhodesianum* was used for the production of the chiral compound *(R)*-3-hydroxybutyrate [681]. The product is formed during intracellular degradation of a PHA. In fed-batch cultivation, 2.8 g/l of *(R)*-3-hydroxybutyrate were produced. Wild-type strains of *B. methanolicus* can secrete more than 58 g/l of L-glutamate in fed-batch cultures [682] and mutants of *B. methanolicus* secreted 69 g/l of L-glutamate [683]. A further mutant of *B. methanolicus* produced L-Lysine up to 65 g/l [683]. Further products from the metabolism of methylotrophic microorganisms are polysaccharides [684, 685], indole-3-acetic acid[686], trans-zeatin [687, 688] as well as different proteins such as GFP [675, 689, 690], enterocin P [691], acylamide amidohydrolase [692], haloalkane dehalogenase [693] and an esterase [689, 694, 695]. Belanger et al. [675] carried out fermentation to produce the green fluorescent protein as a model protein to study the recombinant protein production. The maximum specific GFP production was 80 mg/g, representing approximately 16 % of the total cell protein.

Methylotrophic Yeasts

After discovering methylotrophic yeasts' ability to metabolise inexpensive substrates such as methanol, attempts were undertaken to use them for production of single-cell protein (SCP) and metabolites. Yeasts possess the advantages of a fast cell growth, the possibility of simple genetic engineering and simple process preparation due to their size [696].

Among the various yeast cultures studied, *Pichia pastoris* showed particularly high cell yield from methanol, high protein content and stable fermentation characteristics. Without optimisation, *P. pastoris* was slowly growing (doubling time: 5.5–6.0 h) [697]. The reason is that yeasts consume more metabolic energy for synthesis of one C_3-molecule compared to methylotrophic bacteria using the ribulose monophosphate cycle (RuMP cycle) for formaldehyde fixation. A stoichiometric equation with the average values for biomass formation on methanol via the Xu5P-cycle for the methylotrophic yeast *Kloeckera* sp. 2201 is shown in Eq. 6.66 [698].

$$2.06CH_3OH + 2.02O_2 + 0.15NH_3 + \text{nutrients} \rightarrow CH_{1.75}O_{0.5}N_{0.15}(\text{biomass}) + 1.06CO_2 + 3.47H_2O \quad \Delta H = -268.4\ \text{kJ/mol}_{MeOH} \tag{6.66}$$

The ratio of methanol and the formed biomass shows that approximately 49 % of the methanol is used to produce cellular mass and 51 % is dissimilated to gain energy. This is reflected in lower growth yields of yeasts (yeasts: 0.37–0.45 g/$g_{methanol}$; bacteria: 0.55 g/$g_{methanol}$) [699]. Additionally, yeasts have higher oxygen consumption when using methanol as carbon source. For example, for the oxidation of 1 g of methanol to 0.71 g of carbon dioxide by *Kloeckera* sp. 2201, an amount of 0.98 g of oxygen is required. This means this yeast needs 15 % more oxygen than bacteria (0.85 g O_2 per g methanol). Therefore, in order to use these microorganisms in biotechnological applications with methanol as sole carbon and energy source, a specific reactor design is needed (see Sect. 6.5.3.3).

The singular enzymes of methanol metabolism of methylotrophic yeasts offer special applications, which are discussed here. Formate dehydrogenase (FDH; EC 1.2.1.2), which can be obtained from the methylotrophic yeast *Candida boidinii,* catalyses the last step of methanol oxidation in methylotrophs and is located in the cytosol (Fig. 6.148). It consists of two identical subunits of approximately 36 kDa. FDH is moderately thermostable (30–60 °C), is insensitive against oxygen and is active along a broad pH range (pH 5–10) [700]. An important application of this enzyme is, in combination with formate, the in situ regeneration of NADPH or NADH in catalytic systems; the gaseous, volatile product CO_2 allows for easy shifting of the reaction equilibrium to the right (Fig. 6.150) [701, 702].

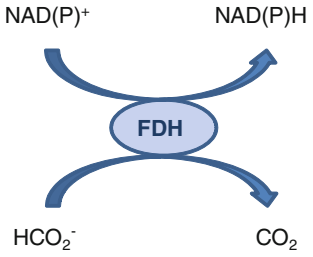

Fig. 6.150 In situ regeneration of NAD(P)H by formate dehydrogenase (FDH)

Because the concept proved successful and fields of applications are so broad, FDH is commercially available and used on an industrial scale in a large set of applications, such as production of tert-L-leucine [701–703]. Also, it was discovered that FDH selectively cleaves formic acid esters to the respective alcohol and carbon dioxide. FDH differentiates between formic acid esters and nonformic acid esters, contrary to hydrolases, which renders this enzyme particularly suitable for protective group chemistry. It was shown that even rather disubstituted esters, such as 1-acetoxy-4-formoxy butane, are a substrate for FDH, which catalysed the cleavage of the formate group while the acetate group remained unaffected [704].

Another enzyme belonging to the metabolism of methylotrophic yeasts is methanol oxidase or alcohol oxidase (AOX, EC 1.1.3.13), catalysing oxidation of

methanol in the peroxisomes to formaldehyde and hydrogen peroxide using oxygen as electron acceptor (Fig. 6.148). AOX consists of eight identical subunits (74 kDa [666]), and each one is noncovalently bound to one FAD as prosthetic group. The AOX has a large temperature and pH range, such as that of *P. pastoris* (temperature: 18–45 °C, pH: 6.5–8.3), under which conditions the enzyme displays at least 50 % of its original activity [705]. AOX oxidises most of the primary short chain alcohols to the corresponding aldehydes, for which reason it is used in combination with oxygen and hydrogen peroxide sensors for the determination of lower alcohols [666]. Additionally, it could be used as a potential catalyst for organic synthesis. It was found that AOX is able to oxidise 2-chloroethanol, 2-cyanoethanol and 2-methoxyethanol to their aldehydes, which are important intermediates in heterocycle synthesis [706]. Furthermore, AOX applications are the production of formaldehyde and hydrogen peroxide. Both were examined on a laboratory scale, obtaining 0.95 M formaldehyde by a mutant of *Candida boidinii* [707] and 10 mM H_2O_2 by chemically treated *Pichia pastoris* cells. The latter could be used for in situ bleaching, oxidising toxic organic compounds and disinfection [708].

Heterologous Gene Expression in Methylotrophic Yeasts

In methylotrophic yeasts, enzymes of the methanol metabolism can be produced in high quantities only by growing on methanol. This circumstance renders them very interesting targets for genetic engineering. A promoter that tightly regulates the AOX gene is responsible for the high expression of these proteins [709].

Methylotrophic yeasts, in particular *Pichia pastoris* and *Pichia angusta*, are used preferentially as expression systems for the production of heterologous proteins because of the easy handling, the inexpensive substrate and the strong methanol-induced promoter, which is missing in the model organism baker yeast (*Saccharomyces cerevisiae*). In addition, high protein yield, the possibility for high cell density approaches and the option for posttranslational modification of proteins render these methylotrophic yeasts attractive in industrial biotechnology. Thus far, more than 500 foreign proteins, including eukaryotic proteins, were successfully expressed, which were accessible in *E. coli* only as inactive inclusion bodies. Foreign proteins can be secreted into the medium, if behind the AOX promoter a secretion-signal sequence is cloned. In Table 6.27, some heterologous proteins are listed, which are produced by methylotrophic yeasts [710, 711].

6.5.3.3 Specific Bioprocess Characteristics

Compared to other microbiological cultivation techniques for the production of bulk chemicals, two important differences have to be considered. First of all, inexpensive, defined mineral media can be used because there is no need to supply the carbon source in a complex matrix, which is usually done to reduce costs in sugar-based fermentations. In addition, ammonia can be added as an inexpensive nitrogen source and costly vitamins or other organic molecules are not required.

Table 6.27 Selection of heterologous proteins expressed in *Pichia pastoris* (Pp), *Pichia angusta* (Pa), *Candida boidinii* (Cb) and *Pichia methanolica* (Pm) successfully

Protein	Mode	Host	Yield	Reference
Bacteria				
Pertussis pertactin protein (*Bordetella*)	C	Pp	3 g/l	[712]
Subtilisin inhibitor (*Streptomyces*)	S	Pp	0.5 g/l	[713]
Tetanus toxin C fragment (*Clostridium*)	C	Pp	12 g/l	[714]
Fungi				
1,2-Mannosyltransferase (*Saccharomyces*)	S	Pp	0.4 g/l	[715]
Adenylate kinase (*Saccharomyces*)	C	Cb	2 g/l	[716]
Alt a 1 allergen (*Alternaria*)	S	Pp		[717]
Catalase T (*Saccharomyces*)	C	Pa		[718]
Dipeptidyl-peptidase V (*Aspergillus*)	S	Pp		[719]
Glucoamylase (*Schwanniomyces*)	S	Pa	1.4 g/l	[720]
Glucose oxidase (*Aspergillus*)	S	Pa	0.9 g/l	[721]
Invertase (*Saccharomyces*)	S	Pa	1 g/l	[722]
Phytase (*Aspergillus*)	S	Pa	13.5 g/l	[723]
Plants				
Cyn d 1 allergen (Bermuda grass)	S	Pp		[724]
Glycolate oxidase (spinach)	C	Pp; Pa		[718, 725]
Malate dehydrogenase (water melon)	C	Pa		[726]
Phytochrome (oat)	C	Pa		[727]
Phytochromes A and B (potato)	C	Pp		[728]
Seed storage protein	C	Pa		[729]
Animal				
Aprotinin (bovine)	S	Pa	0.35 g/l	[730]
Bm86 antigen (tick)	C	Pp		[731]
Green fluorescent protein (jellyfish)	C	Pp		[732]
Hirudin	S	Pp; Pa	1.5 g/l	[733, 734]
Human				
μ-Opioid receptor	S	Pp		[735]
Haemoglobin	C	Pa		[737, 738]
Hepatitis B surface antigen	C	Pp; Pa	0.4 g/l	[738]
Human endostatin	S	Pp	0.02 g/l	[739]
Human glutamate decarboxylase	C	Pm	0.5 g/l	[740]
Human Lewis fucosyltransferase (Fuc-TIII)	S	Pp	0.03 g/l	[741]

Mode: C, cytosolic; S, secreted
Yield: g (protein)/l (medium)

This also significantly reduces downstream processing costs of products that are secreted to the medium. Furthermore, process instabilities caused by compositional variations in complex raw materials can be avoided.

The second important difference in sugar-based processes is the toxicity of the carbon source [671, 674, 742]. On the one hand, this tremendously reduces the risk of contaminations. On the other hand, toxicity has to be considered during the development of appropriate feeding strategies to maximise growth and product formation rates. Methanol has a higher reduction state than sugars; thus methanol

fermentations are characterised by higher oxygen demands. As heat evolution increases with oxygen consumption, the cooling requirements also rise for fermentations using methanol instead of sugar.

Bourque et al. [743]. developed high cell-density processes with *M. extorquens* for the production of PHA. Control algorithms were used to maintain both the methanol and the dissolved oxygen concentration at the desired setpoint value. Suzuki et al. [744]. also described a process for PHA production. Concentration of methanol was maintained automatically at 0.5 ± 0.2 g/l. Dissolved oxygen in the culture broth was controlled in the range of 2–3 mg/l. Kim et al. [670] carried out fed-batch cultures to avoid the inhibitory effect of methanol for cell growth in a 2.5 l fermenter equipped with standard control units and instrumentations. Schendel et al. [745]. carried out fed-batch cultivation of *Bacillus methanolicus* at 50 °C to produce the amino acid L-lysine. The higher fermentation temperature reduces the costs for cooling the reaction system.

The production of single-cell protein with methanol as substrate reached the industrial scale. The ICI process [669, 746–748] used a pressure airlift reactor with inner loop. The working volume was 1,500 m^3, capable of producing up to 50,000 tonnes per year. Under continuous fermentation conditions, runs in excess of 100 days without contaminations have been reported. To optimise the oxygen transfer, the reactor was driven with an overpressure of 0.3 MPa in the head of the reactor [749]. To avoid high, potentially toxic, local concentrations of methanol (>0.2 g/l), the carbon substrate was sparged via 3,000 outlets in the reactor [750].

The ICI process used the methylotrophic bacterium *Methylophilus methylotrophus.* At a maximum specific growth rate of approximately 0.55 h^{-1}, the continuous process was carried out at dilution rates of 0.16–0.19 h^{-1} [677]. Biomass concentration during fermentations reached 30 g/l and maximum cell yield was up to 0.5 g/g. The organism *Methylomonas clara* was used by Hoechst/Uhde, who employed 20 m^3 reactors to reach an annual production capacity up to 1,000 tonnes. The substrate concentration was controlled to a value of 0.005 %. The maximum growth rate was 0.5 h^{-1} and dilution rates of 0.3–0.5 h^{-1} were applied. Under these conditions, biomass production rates of 5 g h/l and a methanol-based biomass yield of 50 % were achieved.

In order to be able to run an industrial process economically, high biomass yields are required. Therefore, it is necessary to optimise medium component concentrations. It was observed that methanol concentration should be less than 6 vol%, to avoid toxic effects [751]. *P. pastoris* is able to grow at high cell density with a continuous mineral nutrient supply. Yeasts usually prefer temperatures of 25–35 °C and have a high oxygen demand when growing on methanol [752]. Consequently, the result of scale-up experiments showed that heat removal and oxygen transfer are the limiting factors on the large scale.

To minimise these limitations, reactors were modified or developed further, eventually leading to the Phillips/Provesta continuous high-cell density, direct-dry process [697]. Cell densities of 125–150 g/l dry cell weight were achieved at a pH of 3.5 and a temperature between 30 and 40 °C [753]. The reactor design allowed for an effective heat exchange and oxygen transfer up to 1 mol O_2/l h. The main

benefit of this particular process was the replacement of cell concentration steps by a direct drying of the culture broth through heat treatment. A 100 % recovery of yeast-soluble products was achieved, in combination with lower operating costs and easier processing [697]. Although SCP from methylotrophic yeasts are rich in essential amino acids and have a high protein content, all SCP production systems based on methylotrophic yeast were not produced any further because it was feared that the cells contain toxic residuals [754]. Additionally, the methanol price is not low enough in order to allow for fermentations being run economically compared to other commercial processes [755]. Yet, the advantages of the Phillips process led to the fermenter design being used for other yeast and bacteria, such as *Torula* yeast grown on sucrose to produce yeast products for human and animal food sector [756]. Today, SCP from nonmethylotrophic yeast is used in the form of yeast extract in small quantities as a flavour-enhancing component in food products or as meat substitutes [755].

6.5.3.4 Further Application of Methanol in Biotechnological Processes

Methanol as Carbon Source in Biological Wastewater Treatment

Denitrification is the biological reduction of nitrate to nitrogen gas by facultatively heterotrophic bacteria. Denitrification occurs when oxygen levels are depleted and nitrate becomes the primary oxygen source. The process is performed under anoxic conditions, when the dissolved oxygen concentration is less than 0.5 mg/l. For the denitrification process, the bacteria need a readily degradable carbon source such as methanol. The denitrification process can be described by Eq. 6.67.

$$6NO_3^- + 5CH_3OH \rightarrow 3N_2 + 5CO_2 + 7H_2O + 6OH^- \quad (6.67)$$

Methanol as a carbon source in denitrification has different advantages; it contains no solids and no additional nutrients, has a neutral pH, is inexpensive and contains 100 % readily degradable substrate [757]. The denitrification with methanol as carbon source is an established technique in municipal wastewater treatment plants [758–761]. Nevertheless, there are still some parameters to be optimised. A precise feeding of methanol is necessary. Low dosage rates can lead to an excess of NO_3^- in the effluent. If methanol is overfed, it may result in elevated effluent biochemical oxygen demand concentrations. The addition of methanol can also improve biological phosphorus removal by creating anaerobic conditions and increasing the availability of organic carbon in wastewater for polyphosphate accumulating organisms [759]. Unlike acetate, long-term application of methanol has no negative impact on the settling properties of the sludge.

Methanol Biofuel Cell

Biofuel cells are fuel cells that employ biocatalysts to convert chemical energy into electrical energy. The main types of biofuel cells are defined by the type of biocatalyst. Microbial biofuel cells employ living cells to catalyse the oxidation of

the fuel, whereas enzymatic biofuel cells use enzymes for this purpose [762]. There is growing interest in enzyme-based biofuel cells as a source of renewable and sustainable power [763]. They are attractive for special applications, such as implantable devices, sensors, drug delivery, microchips and portable power supplies. Several drawbacks, such as short lifetimes and low power density, limited enzyme-based biofuel cells from being used for practical applications.

Methanol oxidation sequentially follows the methylotrophic pathway to give formaldehyde, formate and carbon dioxide [764]. Each oxidation step releases two electrons, yielding six electrons per molecule of methanol. The cofactor nicotinamide adenine dinucleotide (NAD^+) is reduced in the enzyme-catalysed reactions and can be used as mediator to transport the electrons to an electrode. The formal redox potential of NAD^+/NADH is -0.56 V versus a standard calomel electrode [765]. However, the oxidation of NADH by electrodes has poor kinetics and requires large overpotentials. Mediators can be used to reduce the overpotentials and improve the electron transfer rates (Table 6.28). The first methanol biofuel cell used a diaphorase/benzyl viologen system as NADH oxidation catalyst [766]. Electropolymerised mediators such as methylene green, toluidine blue and neutral red can be used as stable catalysts with enhanced activity toward NADH oxidation [765, 767–770]. Often, the stability of the mediator restricts the performance of the biofuel cell [771]. By the addition of aluminium dioxide into the electrode paste, the mediator tetramethyl phenylenediamine can be stabilised.

Table 6.28 Characterisation of methanol biofuel cells

Catalyst	Mediator	Fuel cell characteristic	Literature
Alcohol dehydrogenase, aldehyde dehydrogenase and formate dehydrogenase	Benzyl viologen	Open-circuit voltage of the cell: 0.8 V, power output: 0.67 mW/cm^2 at 0.49 V	[766]
Methanol dehydrogenase from *Methylobacterium extorquens*	Tetra methyl phenylene diamine	Open-circuit voltage: 1.4 V, power density: 0.2 mW/cm^2, current density: 0.38 mA/cm^2 at 0.67 V	[771]
Alcohol dehydrogenase, aldehyde dehydrogenase and formate dehydrogenase	Poly(methylene green)	Power density: 0.26 mW/cm^2, current density: 0.85 mA/cm^{-2}	[769]

Miscellaneous

Enzymatic Reduction of CO_2 and Formaldehyde to Methanol

The NADH-mediated reduction of CO_2 for the production of methanol can be described as a multistep reaction process. The reaction consists of three reversible enzymatic steps: reduction of CO_2 to formate catalysed by formate dehydrogenase FDH reduction of formate to formaldehyde by formaldehyde dehydrogenase (Fald-DH) and reduction of formaldehyde to methanol by alcohol dehydrogenase (ADH) [772, 773]. Reduced nicotinamide adenine dinucleotide (NADH) acts as an electron donor for each dehydrogenase-catalysed reduction.

Thermodynamic studies have shown that the enzymatic conversion of carbon dioxide is highly sensitive to the pH value and ionic strength of the reaction solution [774]. It is possible to shift the metabolic reaction equilibrium constants by a factor of several orders of magnitude to favour the synthesis of methanol. Electrolysis of carbon dioxide-saturated buffer solution in the presence of the enzymes formate dehydrogenase and methanol dehydrogenase together with methylviologen or pyrroloquinoline quinone as an electron relay yielded formaldehyde and methanol as the reduction products [775, 776]. The combined photochemical and enzymatic synthesis of methanol from formaldehyde is possible by using alcohol dehydrogenase (ADH) from *Saccharomyces cerevisiae* and photoreduction of NAD^+ by zinc tetraphenylporphyrin tetrasulphonate (ZnTPPS) in the presence of methylviologen, diaphorase and triethanolamine [777]. In a similar approach, the synthesis of methanol from HCO_3^- using formate dehydrogenase, aldehyde dehydrogenase and alcohol dehydrogenase was shown [778].

Biotechnological Conversion of Methane to Methanol by P450 s

Besides methane mono-oxygenases, enzymes of the cytochrome P-450 family, with a less complicated structure than MMO, have been found to catalyse methane oxidation to methanol [779]. Cytochrome P450 enzymes are heme-dependent mono-oxygenases that catalyse the oxidation of formally nonactivated C–H bonds. The addition of chemically inert perfluoro carboxylic acids to P450 BM3 causes an activation of the enzyme for short-chain aliphatic substrates as a result of the conversion of the Fe/heme from a low-spin to a high-spin state, and the reduction of the binding-pocket size. Together, these effects allow otherwise inert substrates such as propane and even methane to be oxidised [779].

6.5.3.5 Conclusion and Outlook

The disadvantages associated with the conversion of food substrates into biofuels and bulk chemicals have stimulated the search for alternative raw materials. Methanol is an already important carbon feedstock in the chemical industries. As a feedstock for industrial fermentations, methanol is also attractive because of its similar costs compared with other raw materials and its abundant availability. Recent advances in understanding the physiology and biochemistry of methylotrophs made it possible to evaluate their potential in biotechnological processes.

Compared with chemical syntheses starting from methanol, biotechnological processes are particularly promising in cases where high selectivities are needed or complex products are desired, such as branched C_3 to C_6 metabolites. Furthermore, many metabolites of methylotrophic bacteria are not found in the metabolism of established microorganisms, such as *E. coli*. The special metabolites can be suitable building blocks for chemicals, such as for novel fuels and polymers [634, 679, 681, 780].

References

1. K.S. Deffeyes, *Hubbert's Peak: The Impending World Oil Shortage* (Princeton University Press, Princeton, 2011)
2. M.K. Hubbert, Drill. Prod. Prac. 7–25 (1956)
3. R.W. Bentley, Energ. Policy **30**, 189–205 (2002)
4. S. Sorrell, J. Speirs, R. Bentley, A. Brandt, R. Miller, Energ. Policy **38**, 5290–5295 (2010)
5. D. Zhu, S. Tao, R. Wang, H. Shen, Y. Huang, G. Shen, B. Wang, W. Li, Y. Zhang, H. Chen, Y. Chen, J. Liu, B. Li, X. Wang, W. Liu, Appl. Energ. **106**, 17–24 (2013)
6. New York Times, 13.11.2012
7. R. Bacon, S. Tordo, *Crude Oil Price Differentials and Differences in Oil Qualities: A Statistical Analysis* (Energy and Water Department, Washington, D.C., 2005). Can be found under http://www.esmap.org/sites/esmap.org/files/08105.TechnicalPaper_CrudeOilPriceDifferentialsandDifferencesinOilQualitiesAStatisticalAnalysis.pdf
8. B. Höhlein, P. Biedermann, T. Grube, *Methanol as an Energy Carrier*, Schriften des Forschungszentrums Jülich- Reihe Energietechnik/Energy Technology (2006)
9. G.A. Olah, A. Goeppert, G.K.S. Prakash, *Beyond Oil and Gas: The Methanol Economy* (Wiley-VCH, Weinheim, 2006)
10. A. Kuhlmann, H. May, F.G. Pischinger, *Methanol und Wasserstoff*: *Automobil-Kraftstoffe der Zukunft* (Verlag TÜV, Rheinland, 1976)
11. A. Kowalewicz, M. Wojtyniak, *Proc. Inst. Mech. Eng., Part D: J. Automobile Eng.***219**, 103–125 (2005)
12. Methanol Institute, *Methanol Gasoline Blends*: *Alternative Fuel For Today's Automobiles and Cleaner 'Burning Octane For Today's Oil Refinery*. Can be found under http://www.methanol.org/Energy/Transportation-Fuel/Fuel-Blending-Guidelines/Blenders-Product-Bulletin-(Final).aspx (2011)
13. L. Bromberg, W.K. Cheng, *Methanol as an Alternative Transportation Fuel in the US: Options for Sustainable and/or Energy-Secure Transportation* (2010), can be found under http://www.afdc.energy.gov/pdfs/mit_methanol_white_paper.pdf
14. Methanol Institute, *Methanol Transportation Fuel* (2011), can be found unter http://www.methanol.org/Energy/Transportation-Fuel.aspx
15. C. Duwig, P. Gabrielson, H. Nielsen, Haldor Topsøe A/S presentation at Marine Days, Gothenburg (2011)
16. P.L. Spath, D.C. Dayton, *Preliminary Screening*: *Technical and Economic Assessment of Synthesis Gas to Fuels and Chemicals with Emphasis on the Potential for Biomass-Derived Syngas* (2003), can be found under http://www.nrel.gov/docs/fy04osti/34929.pdf
17. A.B. Chemrec, Press release from 09.09.2010 (2010)
18. DIN EN 590, *Kraftstoffe für Kraftfahrzeuge—Dieselkraftstoff—Anforderungen und Prüfverfahren* (Beuth, 2011)
19. Statista GmbH, *Global biofuel production from 2000 to 2011* (2013), can be found under http://www.statista.com/statistics/198866/global-biofuel-production–production-in-oil-equivalent-since-2000/

References to Section 6.2

20. F. Asinger, *Methanol—Chemie- und Energierohstoff. Die Mobilisation der Kohle*, 1. Aufl. (Springer, Heidelberg, 1986)
21. H.J. Arpe, *Industrielle Organische Chemie: Bedeutende Vor- und Zwischenprodukte*, 6. Aufl. (Wiley-VCH, Weinheim, 2007)
22. D. Steinborn, *Grundlagen der metallorganischen Komplexkatalyse*, 2. Aufl. (Vieweg + Teubner, Wiesbaden, 2009)

23. N. Rizkalla (Halcon International), DE 2610036, 1976
24. R.V. Porcelli, V.S. Bhise (Halcon International), DE 3024353, 1981
25. G. Luft, G. Ritter, M. Schrod, Chem. Ing. Tech. **54**, 750–760 (1982)
26. C. Hewlett (Halcon International), DE 2441502, 1975
27. C. Elschenbroich, Organometallchemie, 6. Aufl. (Vieweg + Teubner, Wiesbaden, 2008)
28. D.L. King, J.A. Cusumano, R.L. Garten, Cat. Rev. Sci. Eng. **23**, 233–263 (1981)
29. S. Rebsdat, D. Mayer, Ethylene glycol. In: *Ullmann'sEncyclopedia of Industrial Chemistry*, 7th edn. (Wiley-VCH, Weinheim, 2012), pp. 531–546
30. T. Ikarashi, Chem. Econ. Eng. Rev. **12**, 31–34 (1980)
31. H.F. Willkie (US Industrial Alcohol Co.), US 1400195, 1921
32. Companie de Béthune, F.P. 673.051, 1929
33. Mitsubishi Gas Chemical Co., Japan. Pat. **15**, 3068–766 (1978)
34. Mitsubishi Gas Chemical Co., Japan. Pat. **15**, 3108–916 (1978)
35. Mitsubishi Gas Chemical Co., Japan. Pat. 46.821 (1978)
36. Mitsubishi Gas Chemical Co., GB 1546004, 1979
37. A. Aguilo, T. Horlenko, Hydrocarbon Process **142**, 120–130 (1980)
38. M. Ioneoka (Mitsubishi Gas Chemical Co.), DE 2716842, 1977
39. S. Jali, H.B. Friedrich, G.R. Julius, J. Mol. Catal. A: Chem. **348**, 63–69 (2011)
40. J.S. Lee, J.C. Kim, Y.G. Kim, Appl. Catal. **57**, 1–30 (1990)
41. F. Mathé, Y. Castenet, A. Mortreux, F. Petit, Tetrahedron Lett. **32**, 3989–3992 (1991)
42. Mitsubishi Gas Chemical Co., Japan. Pat. 30.253 (1973)
43. M. Fontaine, Y. Castanet, A. Mortreux, F. Petit, J. Catal. **167**, 324–336 (1997)
44. G. Jenner, Appl. Catal. A: Gen. **121**, 25–44 (1995)
45. K. Kondo, N. Sonoda, H. Sakurai, Tetrahedron Lett. **15**, 803–804 (1974)
46. P. Pennequin, M. Fontaine, Y. Castanet, A. Mortreux, F. Petit, Appl. Catal. A: Gen. **135**, 329–339 (1996)
47. S. Otsuka, A. Nakaruma, T. Yoshida, M. Namto, K. Atato, J. Am. Chem. Soc. **95**, 3180–3188 (1973)
48. G. Jemier, E.M. Nahmed, S. Libs-Konrath, J. Mol. Catal. **64**, 337–347 (1991)
49. http://en.wikipedia.org/wiki/Formic_acid
50. V.V. Gercev, J.J. Markov-Zemljanski, *J. Angew. Chem.* (*UdSSR*) **43**, 1633–1635 (1970)
51. Anonymous, Chem. Eng. News **48**(28), 24 (1970)
52. A.H. Hanson (A.B. Perstorp), SE 331990, 1971
53. L.J. Kaplan, *Chem. Eng*. 71–73 (1982)
54. J. Menzel (Uhde GmbH), EP 2010056154, 2010
55. G. Wietzel, K. Eder, A. Scheuermann (BASF AG), DRP 867.849, 1953
56. M. Jahrsdorfer, G. Schwerte (BASF AG), DE 7414, 1941
57. K. Pieroh (BASF AG), DRP Anm. J. 69072 (1941)
58. M. Müller, U. Hübsch, Dimethyl ether, in *Ullmann'sEncyclopedia of Industrial Chemistry*, vol. 11, 7th edn. (Wiley-VCH, Weinheim, 2011), pp. 305–308
59. G. Reuss, W. Disteldorf, A. O. Gamer, A. Hilt, Formaldehyde. In: *Ullmann'sEncyclopedia of Industrial Chemistry*, 7th edn., **2012**, Wiley-VCH, Weinheim, p. 735–768
60. http://www.icis.com/v2/chemicals/9076013/formaldehyde/uses.html, 2010
61. E. Jones, G.G. Fowlie, J. Appl. Chem. **3**, 206–213 (1953)
62. V.N. Gavrilin, B.I. Popov, *Kinet. Catal.* (*Engl. Transl.*) **6**, 799-803 (1965)
63. H. Schubert, U. Tegtmeyer, R. Schlögl, Catal. Lett. **28**, 383–395 (1994)
64. H. Schubert, U. Tegtmeyer, D. Herein, X. Bao, Muhler M, R. Schlögl, Catal. Lett. **33**, 305–319 (1995)
65. G.J. Millar, J.B. Metson, G.A. Bowmaker, R.P. Cooney, J. Chem. Soc., Faraday Trans. **91**, 4149–4159 (1995)
66. H. Sperber, Titel. Chem. Ing. Tech. **41**, 962–966 (1969)
67. H.B. Uhl, I.H. Cooper, *Heyden Chem. Corp.*, US 2465498, 1949
68. G. Halbritter et al. (BASF AG), DE 2442231, 1978

69. A. Aicher, G. Lehmann, N. Petri, W. Pitteroff, G. Reuss, H. Schreiber, R. Sebastian (BASF AG), EP 0150436 (1985)
70. A. Aicher, H. Haas, H. Sperber, H. Diem, G. Matthias, G. Lehmann (BASF AG), DE 2322757 (1974)
71. A. Aicher, H. Haas, H. Diem, C. Dudeck, F. Brunnmüller, G. Lehmann (BASF AG), DE 2655321 (1978)
72. H. Diem, A. Aicher, H. Haas, C. Dudeck, F. Finkbeiner (BASF AG), DE 2444586 (1976)
73. Anonymous, Chem. Week, **105**, 79 (1969)
74. D.G. Sleemann, *Chem. Eng. N.Y.*, **75**, 42–44 (1968)
75. M. Weimann, *Chem. Eng. N.Y.*, **77**, 102–104 (1970)
76. A. Chauvel, P. Courty, R. Maux, C. Petitpas, Hydrocarbon Process **135**, 179–184 (1973)
77. J.H. Marten, M.T. Butler, Oil Gas J. **72**, 71–72 (1974)
78. FR000001487093A (2013), download from: https://depatisnet.dpma.de/DepatisNet/depatisnet?action=pdf&docid=
79. W.A. Payne (Du Pont), US 2519788, 1950
80. E.S. Northeimer (Du Pont), US 3959383, 1976
81. G.L. Kiser, B.G. Hendricks (Du Pont), US 4 076 754, 1978
82. W.B. Meath (Allied Chemical and Dye Corp.), US 2462413, 1949
83. G.C. Bailey, A.E. Craver (Barrett Comp.), US 1383059, 1921
84. V.E. Meharg, H. Adkins (Bakelite Corp.), US 1913405, 1933
85. F. Traina (Montecatini), US 3198753, 1965
86. S.A. Bergstrand(Perstorp AB), GB 1 080 508, 1967
87. G.D. Kolovertnov, G.K. Boreskov, V.A. Dzisko, B.I. Popov,. D.V. Tarasova, G.C. Belugina, *Kinet. Catal./Engl.* (*Transl.*), **6**, 950–954 (1965)
88. G.D. Kolovertnov, G.K. Boreskov, L.M. Kefeli, L.M. Plyasova, L.G. Karakchiev, V.N. Mastikin, V.I. Popov, V.A. Dzisko, V.D. Tarasova, *Kinet. Catal./Engl.* (*Transl.*), **7**, 125–130 (1966)
89. T.S. Hodgins, F.J. Shelton (Reichhold Chemicals), US 2 973 326, 1961
90. J.J. Hukki, E.J. Honkanen (Laeaeketehdas Orion Oy), CH 392484, 1961
91. P. Jiru, B. Wichter1ova, J. Tichy, in *Proceedings of 3rd International Congress Catalysis*, Amsterdam, vol. 1, 1965, pp. 199–213
92. M. Dente, R. Poppi, I. Pasquon, *Chim. Ind.* (*Milan*) **46**, 1326–1336 (1964)
93. M. Dente, I. Pasquon, *Chim. Ind.* (*Milan*) **47**, 359–367 (1965)
94. M. Dente, A. Collina, *Chim. Ind.* (*Milan*) **47**, 821–829 (1965)
95. W.F. Brondyke, J.A. Monier (Du Pont), US 2 436 287, 1948
96. W.F. Brondyke, J.A. Monier (Du Pont) GB 589 292, 1947
97. Anonymus, *Chem. Eng. N.Y.***61**, 109-110 (1954)
98. Anonymus, *Chem. Process Eng.* (*London*) **51**, 100–111 (1970)
99. C.M. Sze (Lummus Comp.), US 3 277 179, 1966
100. A.W. Gessner (Lummus Comp.), US 3408309, 1968
101. G. Greco, U. Soldano, Chem. Ing. Tech. **31**, 761–765 (1959)
102. W. Exner, *Chem. Anlagen + Verfahren*, pp. 87–92 (1973)
103. G. Sextro, Polyoxymethylenes, in *Ullmann'sEncyclopedia of Industrial Chemistry*, vol. 29, 7th edn. (Wiley-VCH, Weinheim, 2011), pp. 367–379
104. M. Heym, Angew. Makromol. Chem. **244**, 67–92 (1997)
105. H. Staudinger, M. Lüthy, Helv. Chim. Acta **8**, 41–64 (1925)
106. H. Staudinger, H. Johner, R. Signer, G. Mie, J. Hengstenberg, Z. Phys. Chem. **126**, 425–448 (1927)
107. H. Staudinger, R. Signer, H. Johner, M. Lüthy, W. Kern, D. Rusidis, O. Schweitzer, Liebigs Ann. Chem. **474**, 145–275 (1929)
108. H. Staudinger, R. Sieger, Z. Kristallogr, Mineralog. Petrogr. A **70**, 193 (1929)
109. (Du Pont), FP 1082519, 1954
110. M.F. Bechtold, K. Square, R.N. Macdonald (Du Pont), BE 558693, 1957
111. R.N. Macdonald (Du Pont), DE 1037705, 1958

112. D.L. Funck, (Du Pont), DE 1057086, 1959
113. D.L. Funck, (Du Pont), DE 1090191, 1960
114. R.N. Macdonald, (DuPont), DE 1037705, 1958
115. W. Kern, H. Cherdron, V. Jaacks, Angew. Chem. **73**, 177–186 (1961)
116. S. Nogare, J.O. Punderson, S.H.J. Jun, F.C. Starr, W. Jun, G.S. Stamatoff, (Du Pont), DE 1223551, 1966
117. H. Amann, E. Baeder, (Degussa), DE 2003270, 1971
118. J. Hagimory, E. Kitajima, (Tsukamoto Sogyo Co. Ltd.), DE 1964527, 1970
119. W. Thomson, F. Brown, B.K. William, J. Polly, W. George, (Celanese Corp.), DE 1420283, 1969
120. W. Kern, V. Jaacks, (Degussa), DE 1194145, 1965
121. V. Jaaks, W. Kern, Makromol. Chem. **83**, 71–79 (1965)
122. M.A. Pacheco, C.L. Marshall, Energ. Fuels **11**, 2–29 (1997)
123. D. Delledonne, F. Rivetti, U. Romano, Appl. Catal. A: Gen. **221**, 241–251 (2001)
124. F. Rivetti, C.R. Acad. Sci. Paris, SerieIIc, Chem. **3**, 497–503 (2000)
125. N. Keller, G. Rebmann, V. Keller, J. Mol. Catal. A: Chem. **317**, 1–18 (2010)
126. H. Babab, A.G. Zeiler, Chem. Rev. **73**, 75–91 (1973)
127. M. Matzner, R.P. Kurkjy, R.J. Cotter, Chem. Rev. **64**, 645–656 (1964)
128. A. Shaikh, S. Sivaran, Chem. Rev. **96**, 951–976 (1996)
129. J. Knifton, (Texaco Inc.), US 4661609, 1987
130. L. Cassar, Chim. Ind. Milan **72**, 18–22 (1990)
131. U. Romano, R. Tesel, G. Cipriani, L. Micucci, (Anic S.p.a), US 4218391, 1980
132. U. Romano, F. Rivetti, (EnichemSintesi), EP 365083, 1988
133. H.-J. Buysch, Carbonic esters, in *Ullmann'sEncyclopedia of Industrial Chemistry*, vol. 7, 7th edn. (Wiley-VCH, Weinheim, 2011), pp. 45–71
134. F. Matsuda, K. Narita, H. Oikawa, Y. Okuda, T. Saito, Y. Takahashi, K. Ueno, K. Watanabe (Nippon Steel Corp.), EP 685453, 1995
135. M. Bertau, C. Pätzold, U. Singliar (TU Bergakademie Freiberg), DE 102007051072, 2007
136. K. Nagai, T. Ui, Sumitomo Kagaku (2), 1–12 (2004) (English translation)
137. Evonik Industries AG, Press release from 23.10.2009 (2009)
138. J. Burkhardt, in Symposium am 28 on Silicone Chemie und Technologie, April 1989 (Vulkan, Essen, 1989), pp. 23–27
139. H.-H. Moretto, M. Schulze, G. Wagner, Silicones, in *Ullmann's Encyclopedia of Industrial Chemistry*, vol. 32, 7th edn. (Wiley-VCH, Weinheim, 2011), pp. 675–679
140. W. Kalchauer, B. Pachaly, Müller-Rochow synthesis: the direct process to methylchlorosilanes, in *Ullmann'sEncyclopedia of Industrial Chemistry*, vol. 32, 7th edn. (Wiley-VCH, Weinheim, 2011), pp. 2635–2641
141. H. Brauer, *Handbuch des Umweltschutzes und der Umwelttechnik,* vol. 2*, Produktions- und produktintegrierter Umweltschutz*, 1. Aufl. (Springer, Heidelberg, 1996), pp. 467–468
142. H. Gysin, E. Knuesli, (Geigy AG), CH 337019, 1959
143. W. Draber, K. Dichore, Naturwissenschaften **55**, 446 (1968)
144. K. Westphal, W. Meiser, L. Fue, H. Hack, (Bayer AG), US 3671523, 1972
145. R. Schmidt, L. Eue, C. Metzger, K. Dickore, (Bayer AG), DE-OS 2407144, 1975
146. Degussa AG, Press release from 12.03.2003 (2003)
147. R. Dittmeyer, W. Keim, G. Kreysa, A. Oberholz (eds.) *Winnacker-Küchler: Chemische Technik*, vol. 5, 5th edn. (Wiley-VCH, Weinheim, 2006), p. 250
148. M. Fielding (Du Pont), US 3255075, 1966
149. K.-M. Roy, Thiols and organic sulfides, in *Ullmann'sEncyclopedia of Industrial Chemistry*, vol. 36, 7th edn. (Wiley-VCH, Weinheim, 2011), pp. 629–655
150. H.O. Folkins, E.L. Miller, Ind. Eng. Chem. Proc. Des. Dev. **1**, 271–276 (1962)
151. B.J. Aungst, N.J. Rogers, Int. J. Pharm. **53**, 227–235 (1989)
152. W. Qia, D. Dinga, R.J. Salvi, Hearing Res. **236**, 52–60 (2008)
153. G. Da Violante, N. Zerrouk, I. Richard, G. Provot, J.C. Chaumeil, P. Arnaud, Biol. Pharm. Bull. **25**, 1600–1603 (2002)

154. S.L. Moskowitz, Methanol, in Kirk-Othmer Concise Encyclopedia of Chemical Technology, vol. 2, 5th edn. (Wiley, New York, 2007), pp. 1006–1009
155. M. Liauw, T. Prinz, H.-M. Weber, A. Reitzmann, Aromatische Zwischenprodukte, in *Winnacker-Küchler, Chemische Technik*, eds. by R. Dittmeyer, W. Keim, G. Kreysa, A. Oberholz, vol. 5, 5th edn. (Wiley-VCH, Weinheim, 2005), pp. 374–375
156. T. Ren, M.K. Patel, K. Blok, Energy **33**, 817–833 (2008)
157. Directive 2003/30/EG of the European Parliament and Council from 8 May 2003 for the promotion of biofuels or other renewable fuels in traffic (2003)
158. P. Fairly, Taking pulp to the pump, download from: http://www.technologyreview.com/news/411363/taking-pulp-to-the-pump/?a=f, 2008
159. F. Pontzen, W. Liebner, V. Gronemann, M. Rothaemel, B. Ahlers, Catal. Today **171**, 242–250 (2011)
160. B. Ahlers, G. Birke, H. Kömpel, H. Bach, M. Rothaemel, W. Liebner, W. Boll, V. Gronemann, (Lurgi AG) WO2010/060566 A1, 2010
161. G. Pagani, (SnamProgetti), DE 2362944, 1974
162. GESTIS Data Base, Natriummethanolat
163. F.A. Carey, R.J. Sundberg, Organic Chemistry, 1. Aufl. (Wiley-VCH, Weinheim, 1995)
164. N. Wiberg, E. Wiberg, Lehrbuch der Anorganischen Chemie, 102. Aufl. (de Gruyter, Berlin, 2007)
165. P. Lamers, Market study biodiesel, Fuels of the Future, Berlin, 23.-24.01.2012 (2012)
166. S.W. Tse, US 1697 H 19971104
167. W. Shunkwok, US H001697, 1997
168. C.H. Hamann, P. Schmittinger, (Huels Chemische Werke AG), EP 0810193, 1997
169. H.-J. Sterzel, D. Schläfer, J. Guth, H. Friedrich, P. Zehner, (BASF AG), EP 1195369, 2002
170. A. Qwczarek (Inst. Tech. Elektronowej), PL 211292, 1979
171. R. Auschner, P. Schmittinger, S. Rudolf, (Dynamit Nobel AG), EP 0177768, 1986
172. J. Ruwwe, K.-M. Krüger, U. Knippenberg, V. Brehme, M. Neumann, (Evonik Degussa GmbH), EP 1997794, 2008

References to Section 6.3

173. K. Weidmann, *Alternative Kraftstoffe für Dieselmotoren*, Essen, 1985
174. H. Menrad, Wenpo Lee, W. Bernhardt, SAE-770790, 1977
175. B. Nierhauve, G. Seidel, H. Menrad, *BMFT-Study Voraussetzung für die Einführung von Alkoholkraftstoffen* (TÜV Rheinland, Köln, 1983)
176. H. Menrad, B. Nierhauve, SAE-831686, 1983
177. K. Weidmann, H.Menrad, SAE-841331, 1984
178. K. Weidmann, H. Menrad, MTZ **46**, 373 (1985)
179. G. Decker, Personal communication (2012)
180. P. Kuirun, Z. Hua, Y. Yun et al., in IX International symposium on alcohol fuels, Firenze, 1991, p. 768
181. U. Hilger, G. Jain, F. Pischinger et al., in IX International symposium on alcohol fuels, Firenze, 1991, p. 479
182. K. Hikino, T. Suzuki, S. Uematsu, in IX International symposium on alcohol fuels, Firenze, 1991, p. 485
183. G. Decker, H. Heinrich, U. Kammann, in IX International symposium on alcohol fuels, Firenze, 1991, p. 501
184. F. Pischinger, E. Scheid, U. Hilger, G. Schmitz (FEV Motorentechnik GmbH & Co. KG), DE 3843243 C2, 1988
185. L. Brabetz, M. Siedentop, G. Schmitz, in IX International symposium on alcohol fuels, Firenze, 1991, p. 552
186. Siemens Automotive Company, *Flexible Fuel Sensing Technology* (2006)

187. J. van der Weide, H.J. Dekker, A. de Voogd, in IX International symposium on alcohol fuels, Firenze, 1991, p. 509
188. K. Kollmann, J. Abthoff, D. Hüttebräucker, IX International symposium on alcohol fuels, Firenze, p. 518
189. Y-G. Shin, S.–S. Hwang, H-S. Lee, in IX International symposium on alcohol fuels, Firenze, 1991, p. 526
190. T. Suga, S. Kitajima, Y. Hamazaki, in IX International symposium on alcohol fuels, Firenze, 1991, p. 532
191. H. Nohira, S. Kudo, Y Tsukasaki et al., in IX International symposium on alcohol fuels, Firenze, 1991, p. 538
192. M. Namba, T. Yokohama, K. Iida et al., in IX International symposium on alcohol fuels, Firenze, 1991, p. 546
193. Research and Markets, Impact of Alternative Fuels: Fuel Lines, Seals and Injectors, Dublin (2011)
194. H. Menrad, M. Haselhorst, W. Erwig SAE-821210, 1982
195. P. Dedl, P.Hofmann, B. Geringer et al., 13th Symposium on the working process of the internal combustion engine, Graz, 2011
196. F. Pischinger, P. Burghardt, Cornelis Havenith, SAE-830552, 1983
197. F. Pischinger, U. Hilger, G. Jain et al. Wiener, Konzept eines 1,9 l DI-Methanolmotors für den Einsatz im Pkw, 11. Int. Wiener Motorensympos., Düsseldorf, 1990
198. U. Hilger, G. Jain, E. Scheid, SAE-901521, 1990
199. H. Nakamura, M. Oshima, M. Kido, in IX international symposium on alcohol fuels, Firenze 1991, p. 623
200. L.-J. Wang, R.-Z. Song, H.-B. Zhou et al., in *Proceedings of the Institution of Mechanical Engineering* Part D 222, 2008, p. 619
201. D.H. Qi, S.Q. Liu, J.C. Liu, C.H. Zhang, in *Proceedings of the Institution of Mechanical Engineering* Part D 219, 2005, p. 405
202. Fluid, **40**, p. 36 (2007)
203. F. Zhang, S. Shuai, J. Wang, Z. Wang, SAE-2009-01-1182, 2009

References to Section 6.3.1

204. K. D. Miller, 23rd Annual Dewitt Petrochemical Review, Houston (1998)
205. U. Peters et al., in B. Elvers (ed.) Handbook of Fuels (Wiley-VCH, 2008)
206. M. Winterberg, in Ullmann's Encyclopedia (Wiley-VCH, 2010)
207. CMAI, *World Butylenes Analysis* (2010)
208. CMAI, *World Methanol Analysis* (2012)
209. Chem. Systems, *Tertiary Amyl Methyl Ether* (1994)
210. CEH, *Gasoline Octane Improvers/Oxygenates* (2009)

References to Section 6.4

211. IZA Structure Commission, Database of Zeolite Structures, can be found under http://www.iza-structure.org/databases/
212. C. Baerlocher, D.H. Olson, L.B. McCusker, *Atlas of Zeolite Framework Types* (Elsevier, Amsterdam, 2007)
213. A. Dyer, *An introduction to zeolite molecular sieves* (Wiley, Chichester, New York, 1988)
214. E. Wiberg, N. Wiberg, *Lehrbuch der anorganischen Chemie* (Walter de Gruyter, Berlin, 1995)
215. C.D. Chang, Catal. Revs **25**, 1–118 (1983)

216. D.H. Everett, Pure Appl. Chem. **31**, 577–638 (1972)
217. R. Lago, W. Haag, R. Mikovsky, D. Olson, S. Hellring, K. Schmitt, G. Kerr in *Murakami (Hg.) 1986—New developments in zeolite science*
218. T. Mole in *Studies in Surface Science and Catalysis*, eds. by D.M. Bibby, C.D. Chang, R.F. Howe, S. Yurchak, vol 36 (Elsevier, Amsterdam, 1988)
219. K. Segawa, M. Sakaguchi, Y. Kurusu in *Studies in Surface Science and Catalysis,* eds. by D.M. Bibby, C.D. Chang, R.F. Howe, S. Yurchak, vol 36 (Elsevier, Amsterdam, 1988)
220. M. Stöcker, Microporous and mesoporous materials, **82** (2005)
221. T. Mokrani, M. Scurrell, Catal. Rev. Sci. Eng. **51**, 1–145 (2009)
222. S.R. Blaszkowski, R.A. van Santen, J. Am. Chem. Soc. **119**, 5020–5027 (1997)
223. G.F. Froment, W.J.H. Dehertog, A.J. Marchi in *Catalysis. A Review of Recent Literature*, ed. by J.J. Spivey. The Royal Society of Chemistry (Cambridge, England, 1992)
224. W. Loewenstein, *American Mineralogist*, pp. 92–96 (1954)
225. D.S. Coombs, A. Alberti, T. Armbruster, G. Artioli, C. Colella, E. Galli, J.D. Grice, F. Liebau, J.A. Mandarino, H. Minato et al., Can. Mineral. **35**, 1571–1606 (1997)
226. IZA Structure Commission
227. R.F. Howe in *Studies in Surface Science and Catalysis*, eds. by D.M. Bibby, C.D. Chang, R.F. Howe, S. Yurchak., vol 36 (Elsevier, Amsterdam, 1988)
228. J.A. Rabo, G.J. Gajda in Guidelines for mastering the properties of molecular sieves. Relationship between the physicochemical properties of zeolitic systems and their low dimensionality (Plenum Press, New York, 1990)
229. J.F. Haw, Phys. Chem. chem. Phys. pp. 5431–5441 (2002)
230. P.L. Benito, A.G. Gayubo, A.T. Aguayo, M. Olazar, J. Bilbao, J. Chem. Tech. Biotechnol. pp. 183–191 (1996)
231. C.D. Chang, Catal. Revs. **26**, 323–345 (1984)
232. M. Bjørgen, F. Joensen, M. Spangsberg Holm, U. Olsbye, K.-P. Lillerud, S. Svelle, Appl. Catal. A **345**, 43–50 (2008)
233. R.J. Argauer, G.R. Landolt, US 3702886, 1972
234. E.M. Flanigen, R.L. Patton, US 4073865, 1978
235. J.F. Haw, W. Song, D.M. Marcus, J.B. Nicholas, ChemInform **34** (2003)
236. Z.-M. Cui, Q. Liu, W.-G. Song, L.-J. Wan, Angew. Chem. Int. Ed **45**, 6512–6515 (2006)
237. C. Baerlocher, W.M. Meier, D. Olson, *Atlas of zeolite framework types* (Elsevier, Amsterdam, New York, 2001)
238. J.F. Haw, D.M. Marcus, Top. Catal. **34**, 41–48 (2005)
239. Honeywell International Inc., Honeywell UOP's Advanced Methanol-to-Olefins Technology Selected In China To Produce Chemical Products (2011), can be found under http://honeywell.com/News/Pages/Honeywell-UOP%E2%80%99s-Advanced-Methanol-To-Olefins-Technology-Selected-In-China-To-Produce-Chemical-Products.aspx
240. S. Bordiga, L. Regli, D. Cocina, C. Lamberti, M. Bjørgen, K.P. Lillerud, J. Phys. Chem. B **109**, 2779–2784 (2005)
241. J. Sefcik, E. Demiralp, T. Cagin, W.A. Goddard, III, Rational Design of Zeolites for catalysis and separation (1998)
242. G. Burgfels, S. Klingelhöfer, L. H. Ong, R. Olindo, J. Lercher, F. Schmidt, DE 102010005704, 2011
243. Y.-f. Chang, S.N. Vaughn, L.R.M. Martens, J.E. Baumgartner, S.L. Soled, K.R. Clem, US 2005/0137080, 2005
244. R. von Ballmoos, W.M. Meier, Nature **289**, 782–783 (1981)
245. A. Tissler, P. Polanek, U. Girrbach, U. Müller, K. Unger, pp. 399–408
246. V.S. Nayak, V.R. Choudhary, Appl. Catal. **10**, 137–145 (1984)
247. A. de Lucas, P. Canizares, A. Durán, A. Carrero, Appl. Catal. A **154**, 221–240 (1997)
248. G. H. Kühl in *Catalysis and zeolites. Fundamentals and applications*, eds. by J. Weitkamp, L. Puppe (Springer, New York, 1999)
249. V. Zholobenko, L. Kustov, V. Kazansky, E. Loeffler, U. Lohse, G. Oehlmann, Zeolites **11**, 132–134 (1991)

250. C.D. Chang, C.T.W. Chu, J.N. Miale, R.F. Bridger, R.B. Calvert, J. Am. Chem. Soc. **106**, 8143–8146 (1984)
251. D.S. Shibabi, W.E. Garwood, P. Chu, J.N. Miale, R.M. Lago, C.T.W. Chu, C.D. Chang, J. Catal. **93**, 471–474 (1985)
252. M. Kang, J. Mol. Catal. A: Chem. **160**, 437–444 (2000)
253. D.L. Obrzut, P.M. Adekkanattu, J. Thundimadathil, J. Liu, D.R. Dubois, J.A. Guin, React. Kinet. Catal. Lett. **80**, 113–121 (2003)
254. M. Salmasi, S. Fatemi, A. Taheri Najafabadi, J. Ind. Eng. Chem. **17**, 755–761 (2011)
255. T.L. Marker, C.D. Gosling, US 5817906, 1998
256. M.M. Mertens, M.J. Janssen, L.R.M. Martens, K.R. Clem, US 20060079397, 2006
257. T. Inui, M. Kang, Appl. Catal. A **164**, 211–223 (1997)
258. S. Yurchak in *Studies in Surface Science and Catalysis*, eds. by D.M. Bibby, C.D. Chang, R.F. Howe, S. Yurchak, vol 36 (Elsevier, Amsterdam, 1988)
259. P.L. Benito, A.G. Gayubo, A.T. Aguayo, M. Olazar, J. Bilbao, Ind. Eng. Chem. Res. 3991–3998 (1996)
260. H. Schulz, Catal. Today **154**, 183–194 (2010)
261. F.J. Keil, Microporous Mesoporous Mater. **29**, 49–66 (1999)
262. D.E. Krohn, M.G. Melconian in *Studies in Surface Science and Catalysis*, eds. by D.M. Bibby, C.D. Chang, R.F. Howe, S. Yurchak, vol 36 (Elsevier, Amsterdam, 1988)
263. T.V. Janssens, J. Catal. **264**, 130–137 (2009)
264. S. Teketel, U. Olsbye, K.-P. Lillerud, P. Beato, S. Svelle, Microporous Mesoporous Mater. **136**, 33–41 (2010)
265. U. Olsbye, M. Bjørgen, S. Svelle, K.-P. Lillerud, S. Kolboe, Catal. Today **106**, 108–111 (2005)
266. M. Guisnet, J. Mol. Catal. A: Chem. **182–183**, 367–382 (2002)
267. M. Guisnet, P. Magnoux, Appl. Catal. **54**, 1–27 (1989)
268. M. Guisnet, P. Magnoux, Appl. Catal. A **212**, 83–96 (2001)
269. S. Kolboe in *Studies in Surface Science and Catalysis*, eds. by D.M. Bibby, C.D. Chang, R.F. Howe, S. Yurchak, vol 36 (Elsevier, Amsterdam, 1988)
270. B.E. Langner, Appl. Catal. **2**, 289–302 (1982)
271. A.G. Gayubo, J.M. Ortega, A.T. Aguayo, J.M. Arandes, J. Bilbao, Chem. Eng. Sci. **55**, 3223–3235 (2000)
272. J. Li, Y. Tan, Q. Zhang, Y. Han, Fuel **89**, 3510–3516 (2010)
273. A.T. Aguayo, D. Mier, A.G. Gayubo, M. Gamero, J. Bilbao, Ind. Eng. Chem. Res. **49**, 12371–12378 (2010)
274. Topp-Jørgensen in *Studies in Surface Science and Catalysis*, eds. by D.M. Bibby, C.D. Chang, R.F. Howe, S. Yurchak, vol 36 (Elsevier, Amsterdam, 1988)
275. K.G. Allum, A.R. Williams in *Studies in Surface Science and Catalysis*, eds. by D.M. Bibby, C.D. Chang, R.F. Howe, S. Yurchak, vol 36 (Elsevier, Amsterdam, 1988)
276. I.I. Ivanova, Y.G. Kolyagin, Chem. Soc. Rev. 5018–5050 (2010)
277. C.D. Chang in *Studies in Surface Science and Catalysis*, eds. by D.M. Bibby, C.D. Chang, R.F. Howe, S. Yurchak, vol 36 (Elsevier, Amsterdam, 1988)
278. A.C. Gujar, V.K. Guda, M. Nolan, Q. Yan, H. Toghiani, M.G. White, Appl. Catal. A **363**, 115–121 (2009)
279. M. Stöcker, Microporous Mesoporous Mater. **29**, 3–48 (1999)
280. I.M. Dahl, S. Kolboe, Catal. Lett. 329–336 (1993)
281. I.M. Dahl, S. Kolboe, J. Catal. 458–464 (1994)
282. I.M. Dahl, S.Kolboe, J. Catal. 304–309 (1996)
283. T. Mole, G. Bett, D. Seddon, J. Catal. 435–445 (1983)
284. T. Mole, J.A. Whiteside, D. Seddon, J. Catal. 261–266 (1983)
285. W. Song, D.M. Marcus, H. Fu, J.O. Ehresmann, J.F. Haw, J. Am. Chem. Soc. **124**, 3844–3845 (2002)
286. M. Bjørgen, J. Catal. **221**, 1–10 (2004)
287. E.J. Munson, A.A. Kheir, N.D. Lazo, J.F. Haw, J. Phys. Chem. 7740–7746 (1996)

288. H. Adkins, P.D. Perkins, J. Phys. Chem. **32**, 221–224 (1928)
289. J.M. Parera, Ind. Eng. Chem. Prod. Res. Dev **15**, 234–241 (1976)
290. R. Abraham in DGMK Conference Future Feedstocks for Fuels and Chemicals, Berlin, Germany. Supplement to conference preprints, DGMK, Hamburg, Sept 29–Oct 1, 2008
291. G. Burgfels, K. Kochloefl, J. Ladebeck, F. Schmidt, M. Schneider, H.J. Wernicke, DE 3838710, 1990
292. Y. Wei, J. Li, S. Xu, S. Yuan, L. Xu, J. Chen, Y. Zhou, Y. Qi, Z. Liu, Complete prospect and carbon atom economy evaluation of methanol-to-olefins reaction. Abstract ICC 2012, can be found under http://events.dechema.de/events/en/Events/Materials+for+Energy+_+EnMat+II/Congress+Planer/Datei_Handler-tagung-564-file-7857-p-127866.htm
293. B.M. Lok, C.A. Messina, R.L. Patton, R.T. Gajek, T.R. Cannan, E.M. Flanigen, US 4440871, 1984
294. T.N. Kalnes, T.V. Voskoboynikov, US 7414167, 2008
295. E. Köhler, F. Schmidt, H.J. Wernicke, M. de Pontes, H.L. Roberts, Hydrocarbon technology international 37–40 (1995)
296. C. Knottenbelt, Catal. Today **71**, 437–445 (2002)
297. D.W. Leyshon, G.E. Cozzone, US 5043522, 1991
298. D.L. Johnson, K.E. Nariman, R.A. Ware, US 6222087, 2001

References to Section 6.4.1

299. R.J. Argauer, G.R. Landolt, US 3702886, 1972
300. C.D. Chang, A.J. Silvestri, J. Catal. 249–259 (1977)
301. C.D. Chang, A.J. Silvestri, ChemTech **17**, 624–631 (1987)
302. C.D. Chang, Catal. Revs. **25**, 1–118 (1983)
303. M. Stöcker, Microporous and Mesoporous Mater. 82 (2005)
304. C.J. Maiden in *Studies in Surface Science and Catalysis*, eds. by D.M. Bibby, C.D. Chang, R.F. Howe, S. Yurchak, vol 36 (Elsevier, Amsterdam, 1988)
305. K.G. Allum, A.R. Williams in *Studies in Surface Science and Catalysis*, eds. by D.M. Bibby, C.D. Chang, R.F. Howe, S. Yurchak, vol 36 (Elsevier, Amsterdam, 1988)
306. G.A. Mills, Fuel **73**, 1243–1279 (1994)
307. H.R. Grimmer, N. Thiagarajan, E. Nitschke in *Studies in Surface Science and Catalysis*, eds. by D.M. Bibby, C.D. Chang, R.F. Howe, S. Yurchak, vol 36 (Elsevier, Amsterdam, 1988)
308. T. Mokrani, M. Scurrell, Catal. Rev. Sci. Eng. **51**, 1–145 (2009)
309. Structure Commission of the International Zeolite Association (2008), can be found under http://izasc.ethz.ch/fmi/xsl/IZA-SC/ftc_fw.xsl?-db=Atlas_main&-lay=fw&-max=25&STC=MFI&-find
310. M. Stöcker, Microporous Mesoporous Mater. **29**, 3–48 (1999)
311. T. Mole in *Studies in Surface Science and Catalysis*, eds. by D.M. Bibby, C.D. Chang, R.F. Howe, S. Yurchak, vol 36 (Elsevier, Amsterdam, 1988)
312. G.F. Froment, W.J.H. Dehertog, A.J. Marchi in *Catalysis. A review of recent literature*, ed. by J.J. Spivey. The Royal Society of Chemistry (Cambridge, England, 1992)
313. J.F. Haw, W. Song, D.M. Marcus, J.B. Nicholas, ChemInform 34 (2003)
314. C.D. Chang in *Studies in Surface Science and Catalysis*, eds. by D.M. Bibby, C.D. Chang, R.F. Howe, S. Yurchak, vol 36 (Elsevier, Amsterdam, 1988)
315. F.J. Keil, Microporous Mesoporous Mater. **29**, 49–66 (1999)
316. I.I. Ivanova, Y.G. Kolyagin, Chem. Soc. Rev. 5018–5050 (2010)
317. S. Yurchak in *Studies in Surface Science and Catalysis*, eds. by D.M. Bibby, C.D. Chang, R.F. Howe, S. Yurchak, vol 36 (Elsevier, Amsterdam, 1988)
318. A.C. Gujar, V.K. Guda, M. Nolan, Q. Yan, H. Toghiani, M.G. White, Appl. Catal. A **363**, 115–121 (2009)
319. H. Schulz, Catal. Today **154**, 183–194 (2010)

320. M. Guisnet, J. Mol. Catal. A: Chem. **182–183**, 367–382 (2002)
321. M. Guisnet, P. Magnoux, Appl. Catal. **54**, 1–27 (1989)
322. M. Guisnet, P. Magnoux, Appl. Catal. A **212**, 83–96 (2001)
323. A.G. Gayubo, J.M. Ortega, A.T. Aguayo, J.M. Arandes, J. Bilbao, Chem. Eng. Sci. **55**, 3223–3235 (2000)
324. B.E. Langner, Appl. Catal. **2**, 289–302 (1982)
325. P.L. Benito, A.G. Gayubo, A.T. Aguayo, M. Olazar, J. Bilbao, Ind. Eng. Chem. Res. 3991–3998 (1996)
326. J. Li, Y. Tan, Q. Zhang, Y. Han, Fuel **89**, 3510–3516 (2010)
327. A.T. Aguayo, A.G. Gayubo, J. Ereña, R. Vivanco, J. Bilbao, Chem. Eng. J. **92**, 141–150 (2003)
328. T.V. Janssens, J. Catal. **264**, 130–137 (2009)
329. R.F. Howe in *Studies in Surface Science and Catalysis*, eds. by D.M. Bibby, C.D. Chang, R.F. Howe, S. Yurchak, vol 36 (Elsevier, Amsterdam, 1988)
330. A.T. Aguayo, D. Mier, A.G. Gayubo, M. Gamero, J. Bilbao, Ind. Eng. Chem. Res. **49**, 12371–12378 (2010)
331. Topp-Jørgensen in *Studies in Surface Science and Catalysis*, eds. by D.M. Bibby, C.D. Chang, R.F. Howe, S. Yurchak, vol 36 (Elsevier, Amsterdam, 1988)
332. S. Kolboe in *Studies in Surface Science and Catalysis*, eds. by D.M. Bibby, C.D. Chang, R.F. Howe, S. Yurchak, vol 36 (Elsevier, Amsterdam, 1988)
333. H.-H. Gierlich, W. Dolkemeyer, A. Avidan, N. Thiagarajan, *Umwandlung von Methanol zu Benzin nach dem Wirbelbett-Verfahren*, Innsbruck
334. K.H. Keim, J. Maziuk, A. Toennesmann, Erdöl and Kohle, Erdgas, Petrochemie **37**, 558–562 (1984)
335. K.H. Keim, F.J. Krambeck, J. Maziuk, A. Toennesmann, Erdöl, Erdgas, Kohle **103**, 82–85 (1987)
336. C.D. Chang, Catal. Revs. **26**, 323–345 (1984)
337. H.A. Zaidi, K.K. Pant, Ind. Eng. Chem. Res. **47**, 2970–2975 (2008)
338. I. Nexant, PERP Program: Developments in para-Xylene Technology, can be found under http://www.chemsystems.com/about/cs/news/items/PERP%200809S11_paraXylene.cfm
339. J. Scherzer, *Octane-enhancing, zeolitic FCC catalysts. Scientific and technical aspects* (M. Dekker, New York, 1990)
340. M.L. Occelli, P. O'Connor, *Fluid Cracking Catalysts* (M. Dekker, New York, 1998)
341. S. Tabak, ExxonMobil Methanol to Gasoline, can be found under http://www.uschinaogf.org/Forum7/7Topic23-SamuelTabak-ExxonMobil-English.pdf
342. J. Packer, The Production of Methanol and Gasoline, can be found under http://nzic.org.nz/ChemProcesses/energy/7D.pdf
343. J. Peckham, JAMG's Methanol-to-Gasoline Plant Starts-up, can be found under http://www.worldfuels.com/wfExtract/exports/Content/33fead92-fc2d-447d-bc2e-3e95a8ff6e12.html
344. M. Schneider, F. Schmidt, G. Burgfels, H. Buchold, F.-W. Möller, EP 0448000, 1991
345. ExxonMobil, ExxonMobil's Methanol to Gasoline (MTG) Techno logy Selected for DKRW Advanced Fuels' Coal to Liquids Project, can be found under http://www.dkrwaf.com/_filelib/FileCabinet/PDFs/Press_Releases/ExxonPressRelease.pdf?FileName=ExxonPressRelease.pdf
346. D.E. Krohn, M.G. Melconian in *Studies in Surface Science and Catalysis*, eds. by D.M. Bibby, C.D. Chang, R.F. Howe, S. Yurchak, vol 36 (Elsevier, Amsterdam, 1988)
347. M. Bjørgen, F. Joensen, M. Spangsberg Holm, U. Olsbye, K.-P. Lillerud, S. Svelle, Appl. Catal. A **345**, 43–50 (2008)
348. Methanex Corporation, Global Environmental Report 2005, can be found under http://www.methanex.com/environment/documents/2005_Environmental_Excellence_Report.pdf
349. S. Yurchak, US 4814536, 1989
350. J.H. Beech, Jr., F.P. Ragonese, US 5059738, 1991
351. W. Lee, S. Yurchak, N. Daviduk, J. Maziuk in Proceedings of the NPRA Annual Meeting, 1980

352. T. Sugiyama, Thesis, Massachusetts Institute of Technology, 1994
353. Green Car Congress, DKRW Selects ExxonMobil's Methanol-to-Gasoline (MTG) Technology for Coal-to-Liquids Project, can be found under http://www.greencarcongress.com/2007/12/dkrw-selects-ex.html
354. Lurgi GmbH, The R&D centre, can be found under http://www.gcg-es.com/PrincipalsProducts/18-Lurgi/Lurgi02-Researchcentre.pdf
355. M. Rothaemel, H.-D. Holtmann, Erdöl Erdgas Kohle 234–237 (2002)
356. G. Burgfels, K. Kochloefl, J. Ladebeck, F. Schmidt, M. Schneider, H.J. Wernicke, DE 3838710, 1990
357. H. Hartmann, Erdöl Erdgas Kohle **123**, 362–369 (2007)
358. W. Liebner, M. Wagner, Erdöl Erdgas Kohle 120 (2004)
359. PetroSA, COD Technology, can be found under http://www.petrosa.co.za/innovation_in_action/Pages/COD-Technology.aspx
360. S.A. Tabak, A.A. Avidan, F.J. Krambeck, Production of synthetic gasoline and diesel fuel from non-petroleum resources, can be found under http://web.anl.gov/PCS/acsfuel/preprint archive/Files/31_2_NEW YORK_04-86_0293.pdf
361. S. Lee, M. Gogate, C.J. Kulik, Fuel Sci. Technol. Int. **13**, 1039–1057 (1995)
362. M. Wang, GREET1.5a: Changes from GREET1.5 (2000), can be found under http://www.transportation.anl.gov/pdfs/TA/150.pdf

References to Section 6.4.2

363. Chemical Market Associates Inc. (CMAI), World Light Olefins Analysis (WLOA) (2009). http://www.ihs.com/products/chemical/index.aspx?pu=1&rd=cmai
364. D. Greer, M. Houdek, R. Pittmann, J. Woodcock, Erdöl Erdgas Kohle **118**(5), 242 (2002)
365. CMAI, World Light Olefins Analysis, Houston Texas 173–176 (2003)
366. R.J. Argauer, G.R. Landolt, US Patent 3,702,886
367. C.D. Chang, A.J. Silvestri, Catalysis **47**, 249–259 (1977)
368. C.D. Chang, A.J. Silvestri, ChemTech **10**, 624 (1987)
369. F.J. Keil, Microporous and Mesoporous Mater. **29,** 49–66 (1999) (Review Methanol-to-hydrocarbons: process technology)
370. Z.M. Liu, C.L. Sun, G.W. Wang, Q.X. Wang, G.Y. Cai, Fuel Process. Technol. **62**, 161–172 (2000)
371. J. Li, Y. Wei, G. Liu, Y. Qi, P. Tian, B. Li, Y. He, Z. Liu, Catal. Today **171,** 1 (2011)
372. T. Ren, M. Patel, K. Blok, Olefins from conventional and heavy feedstocks: Energy use in steam cracking and alternative processes. Energy **31**, 425–451 (2006)
373. T. Mokrani, M. Scurrell, Gas conversion to liquid fuels and chemicals: the methanol route-catalysis and processes development. Catal. Rev. **51**, 1–145 (2009)
374. C.D. Chang, in *Methanol to Hydrocarbons*, eds. by G. Ertl, H. Knözinger, Weitkamp. Handbook of Heterogeneous Catalysis, 1st edn, p. 1894
375. S. Kvisle, T. Fuglerud, S. Kolboe, U. Olsbye, K.P. Lillerud, B. Vora, in *Methanol-to-Hydrocarbons*. Handbook of Heterogeneous Catalysis, vol 2, p. 707
376. T.J. Gregor Remans, G. Jenzer, A. Hoek, *Gas-to-Liquids*. Handbook of Heterogeneous Catalysis, pp. 2994–3010 (2008)
377. Michael Stöcker, Methanol-to-hydrocarbons: catalytic materials and their behaviour. Microporous Mesoporous Mater. **29**(1–2), 3–48 (1999). doi:10.1016/S1387-1811(98)00319-9
378. J. Li, Y. Wei, G. Liu, Y. Qi, P. Tian, B. Li, Y. He, Z. Liu, Catal. Today **171**(1), 221–228 (2011)
379. C.D. Chang, Catal. Rev. Sci. Eng. **25**, 1(1983)
380. U.S. Pat. No. 3,931,349
381. U.S. Pat. No. 4,404,414

382. D. Chen, H.P. Rebo, K. Moljord, A. Holmen, Methanol Conversion to Light Olefins over SAPO-34. Sorption, Diffusion, and Catalytic Reaction. Ind. Eng. Chem. Res. **38**, 4241–4249 (1999)
383. A.G. Gayubo, A.T. Aguayo, M. Castilla, M. Olazar, J. Bilbao, Catalyst reactivation kinetics for methanol transformation into hydrocarbons. Expressions for designing reaction-regeneration cycles in isothermal and adiabatic fixed bed reactor. Chem. Eng. Sci. **56**, 5059–5071 (2001)
384. H. Hu, F. Cao, W. Ying, Q. Sun, D. Fang, Study of coke behaviour of catalyst during methanol-to-olefins process based on a special TGA reactor. Chem. Eng. J. **160**, 770–778 (2010)
385. A.J. Marchi, G.F. Froment, Catalytic conversion of methanol to light alkenes on SAPO molecular sieves.Appl. Catal. **71**, 139–152 (1991)
386. J. Luckner, Effect of process parameters on methanol-to-olefins reactions over SAPO catalysts. PhD Thesis, Auburn University, 2005
387. G. Qi, Z. Xie, W. Yang, S. Zhong, H. Liu, C. Zhang, Q. Chen, behaviours of coke deposition on SAPO-34 catalyst during methanol conversion to light olefins. Fuel Process
388. L. Travalloni, A.C.L. Gomes, A.B. Gaspar, M.A.P. da Silva, Methanol conversion over acid solid catalysts. Catal. Today 133–135, 406–412 (2008)
389. X. Wu, M.G. Abraha, R.G. Anthony, Methanol conversion on SAPO-34: reaction condition for fixed-bed reactor. Appl. Catal. A: Gen. **260**, 63–69 (2004)
390. A. T., Aguayo, D., Mier, A. G., Gayubo, M., Gamero, J. Bilbao, Kinetics of Methanol Transformation into Hydrocarbons on a HZSM-5 Zeolite Catalyst at High Temperature (400-550°C). Ind. Eng. Chem. Res.2010, 49, 12371–12378
391. S.M. Alwahabi, G.F. Froment, Single Event Kinetic Modeling of the Methanol-to-Olefins Process on SAPO-34. Ind. Eng. Chem. Res. **43**, 5098–5111 (2004)
392. D. Chen, H.P. Rebo, A. Grønvold, K. Moljord, A. Holmen, Methanol conversion to light olefins over SAPO-34: kinetic modeling of coke formation. Microporous Mesoporous Mater. 35–36, 121–135 (2000)
393. S.M. Al Wahabi, Conversion of methanol to light olefins on SAPO-34: Kinetic modeling and reactor design. PhD Thesis, Texas A&M University, 2003
394. N. Fatourehchi, M. Sohrabi, S.J. Royaee, S.M. Mirarefin, Application of a Fluidized bed reactor in the MTO (Methanol to Olefin) process: preparation of catalyst and presentation of a kinetic model. Petrol. Sci. Technol. **29**, 1578–1589 (2011)
395. A.G. Gayubo, A.T. Aguayo, A.E. Sánchez del Campo, A.M. Tarrío, J. Bilbao, Kinetic modeling of methanol transformation into olefins on a SAPO-34, Catalyst. Ind. Eng. Chem. Res. **39**, 292–300 (2000)
396. A.T. Najafabadi, S. Fatemi, M. Sohrabi, M. Salmasi, Kinetic modeling and optimization of the operating condition of MTO process on SAPO-34, Catalyst. J. Ind. Eng. Chem. **18**, 29–37 (2012)
397. S. Soundararajan, A.K. Dalai, F. Berruti, Modeling of methanol-to-olefins (MTO) process in a circulating fluidized bed reactor. Fuel **80**, 1187–1197 (2001)
398. A.T. Aguayo, A.G. Gayubo, R. Vivanco, A. Alonso, J. Bilbao, Initiation step and reactive intermediates in the transformation of methanol into olefinsover SAPO-18. Catal. Ind. Eng. Chem. Res. **44**, 7279–7286 (2005)
399. A.T. Aguayo, A.G. Gayubo, R. Vivanco, M. Olazar, J. Bilbao, Role of Acidity and microporous structure in alternative catalysts for the transformation of methanol into olefins. Appl. Catal. A: Gen. **283**, 197–207 (2005)
400. A.G. Gayubo, A.T. Aguayo, A. Alonso, J. Bilbao, Kinetic Modeling of the Methanol-to-Olefins Process on a Silicoaluminophosphate (SAPO-18) Catalyst by Considering Deactivation and the Formation of Individual Olefins. Ind. Eng. Chem. Res. **46**, 1981–1989 (2007)
401. A.G. Gayubo, A.T. Aguayo, A. Alonso, A. Atutxa, J. Bilbao, Reaction scheme and kinetic modeling for the MTO Process over a SAPO-18. Catal. Catal. Today **106**, 112–117 (2005)

402. Y. Kumita, J. Gascon, E. Stavitski, J.A. Moulijn, F. Kapteijn, Shape selective methanol-to-olefins over highly thermostable DDR catalysts. Appl. Catal. A: Gen. **391**, 234–243 (2011)
403. J. Li, Y. Wei, G. Liu, Y. Qi, P. Tian, B. Li, Y. He, Z. Liu, Comparative study of MTO conversion over SAPO-34, H-ZSM-5 and H-ZSM-22: Correlating catalytic performance and reaction mechanism to zeolite topology.Catal. Today **171**, 221–228 (2011)
404. D. Mores, J. Kornatowski, U. Olsbye, B.M. Weckhuysen, Coke Formation during the Methanol-to-Olefin Conversion: In Situ Microspectroscopy on Individual H-ZSM-5 Crystals with Different Brønsted Acidity. Chem. Eur. J. **17**, 2874–2884 (2011)
405. B. Valle, A. Alonso, A. Atutxa, A.G. Gayubo, J. Bilbao, Effect of nickel incorporation on the acidity and stability of HZSM-5 zeolite in the MTO process. Catal. Today **106**, 118–122 (2005)
406. E.M. Flanigen, B.M. Lok, R.L. Patton, S.T. Wilson1987 Aluminophosphate molecular sieves and the periodic table, in New Developments in Zeolite Science and Technology, in Proceedings of 7th international Zeolite Conference, Tokyo, eds. by Y. Murakami, A. Ijima, J.W. Ward (Elsevier, Amsterdam, 1986) pp. 103–112
407. S.W. Kaiser, US Patent 4 499 327, 1985
408. S.W. Kaiser, US Patent 4 524 234, 1985
409. S.W. Kaiser, Arab. J. Sci. Eng. **10**, 361 (1985)
410. G. Pop, G. Musca, D. Ivanescu, E. Pop, G. Maria, E. Chirila, O. Muntean, Chem. Ind. **46**, 443 (1992)
411. U.S. Pat. No. 4,440,871
412. J. Chen, P.A. Wright, S. Natarajan, J.M. Thomas in Studies in Surface Science and Catalysis **84**, 1731–1738 (1994)
413. U.S. Pat. No. 5,279,810
414. J. Chen, P.A. Wright, J.M. Thomas, S. Natarajan, L. Marchese, S.M. Bradley, G. Sankar, C.R.A. Catlow, P.L. Gai-Boyes **98**, 10216–10224 (1994)
415. J. Chen, J.M. Thomas, P.A. Wright, R.P. Townsend, Catal. Lett. **28**, 241–248 (1994)
416. A.M. Prakash, S. Unnikrishnan, J. Chem. Soc. Faraday Transactions, Royal Society of Chemistry, London, **90**, 2291 (1994)
417. Y. Xu et al. J. Chem. Soc., Faraday Transactions **86,** 2, 425–429 (1990)
418. E.M. Flanigen, B.M. Lok, R.L. Pattonand S.T.Wilson Aluminophosphatemolecular sieves and the periodictable, in New Developments in ZeoliteScience and Technology, in Proceedings 7th International Zeolite conference, Tokyo, 1986 eds. Y. Murakami, A. Ijima, J.W. Ward (Elsevier, Amsterdam,1987), pp. 103–112
419. Z.-M. Cui, Q. Liu, W.-G. Song, L.-J. Wan, Insights into the Mechanism of Methanol-to-Olefin Conversion at Zeolites with Systematically Selected Framework Structures. Angew. Chem. Int. Ed. **45**, 6512–6515 (2006)
420. C. Baerlocher, W.M. Meier, D.H. Olson, Atlas of Zeolite Framework Types, 5th edn. (2001)
421. J.F. Haw, W. Song, D.M. Marcus, J.B. Nicholas, The Mechanism of Methanol to Hydrocarbon Catalysis. Acc. Chem. Res. **36**, 317–326 (2003)
422. J.F. Haw, D.M. Marcus, Well-defined (supra)molecular structures in zeolite methanol-to-olefin catalysis. Topics Catal. **34**, 1–4, 41–48 (2005)
423. J.Q. Chen, A. Bozzano, B. Glover, T. Fuglerud, S. Kvisle, Recent advancements in ethylene and propylene production using the UOP/Hydro MTO process. Catal. Today **106**, 103–107 (2005)
424. PERP Program -Developments in para-Xylene Technology. http://www.chemsystems.com/about/cs/news/items/PERP%200809S11_paraXylene.cfm
425. J. Scherzer, Octane-enhancing, Zeolitic FCC Catalysts: Scientific and Technical Aspects (1990)
426. S. Tabak http://www.uschinaogf.org/Forum7/7Topic%2023-%20Samuel%20Tabak-%20Exxon Mobil-%20English.pdf, http://nzic.org.nz/ChemProcesses/energy/7D.pdf
427. http://www.worldfuels.com/wfExtract/exports/Content/33fead92-fc2d-447d-bc2e-3e95a8ff6e12.html

428. M. Schneider, F. Schmidt, G. Burgfels, H. Buchold, Friedrich-Wilhelm, Möller, Süd-Chemie AG, METALLGESELLSCHAFT AG, European Patent EP0448000
429. http://www.petrosa.co.za/cod_technology.php
430. Engineering and Construction: A New Lurgi-MTP® Unit for China 27/08/2011. http://www.cn.airliquide.com/en/news/local-news-and-events/engineering-construction-a-new-lurgi-mtp-unit-for-china.html
431. Coal Chemical Products (Methanol, PE, PP) http://www.shenhuagroup.com.cn/english/productsservices/product0introduction/coal0chemicals0products/index.shtml
432. M. Arné, H.W. Scheeline, PEP Report 146, Bulk Chemicals from Synthesis Gas, June 1982
433. S. Kvisle, T. Fuglerud, S. Kolboe, U. Olsbye, K.P. Lillerud, B.V. Vora, "Methanol-to-Hydrocarbons" in Handbook of Heterogeneous Catalysis, **2**, pp. 707
434. T. Xu, J.L. White, U. S. Patent 6,734,330, 2004, priority filingand PCT published Feb 2000
435. T. Xu, J.L. White, U. S. Patent 6,743,747, 2004, priority filingand PCT published Feb 2000
436. A. Dyer, *An Introduction to Zeolite Molecular Sieves* (Wiley, New York, 1988)
437. S.E. Volz, J.J. Wise, Development studies on conversion of methanol and related oxygenates to gasoline. Final Report ERDA Contract No. E(49-18)-1773 (1976)
438. A. Kam, W. Lee, Fluid-bed process studies of the conversion of methanol to high octane gasoline. Final Report Contract No. EX-76-C-01-2490 (1978)
439. K.-H. Keim, F.J. Krambeck, J. Maziuk, A. Tonnesmann, ERDÖL, ERDGAS, KOHLE, 103. Jahrgang, Heft 2, Feb 1987
440. C.D. Chang, C.T.-W. Chu, R.F. Socha, J. Catal. **86**, 289–296 (1984)
441. S.A. Tabak, F.J. Krambeck, Shaping Process makes Fuels. Hydrocarbon Process. **64**, 9, 72–74 (1985)
442. A.A. Avidan Gasoline and distillate fuels from methanol, in Methane conversion proceedings of a symposium on the production of fuels and chemicals from natural gas, ed. by D.M. Bibby, C.D. Chang, R.F. Howe, S. Yurchak, Studies in Surface Science and Catalysis, **36**, pp. 307–323 (1988)
443. N. Daviduk, J.H. Haddad; United States Patent4,431,856, Assignee: Mobil Oil Corporation (1984)
444. U.S. Pat. No. 6,023,005
445. http://www.syn.ac.cn/ennews/Technology/2009/6/09631633371761.html
446. Shenhua Ningxia Coal Industry Group Co is a joint venture between the Ningxia provincialgovernment and China's largest coal producer Shenhua Group Corp, with 49 and 51 % stake-holding, respectively
447. http://www.csclc.com.cn/ens/gsxx/gsjj/2010-12-15/238.shtml
448. http://publications.polymtl.ca/158/1/2009_MarineKeraron.pdf
449. E.N. Givens, C.J. Plank, Edward J.Rosinski; US Patent 3,960,978, 1976
450. D.Wei, T. Voskoboynikov*, M. Quick, UOP LLC, 50 East Algonquin Road, Des Plaines, IL 60017, USA, W. Vermeiren, ATOFINA Research, Zone Industrielle C, B-7181 Feluy, Belgium
451. DE000010233069C1 assigned to Lurgi AG, Frankfurt, DE, 19.07.2002
452. D.Wei, T.Voskoboynikov*, M.Quick, UOP LLC, 50 East Algonquin Road, Des Plaines, IL 60017, USA, W.Vermeiren, ATOFINA Research, Zone Industrielle C, B-7181 Feluy, Belgium
453. T. Ren, M.K. Patel, K. Blok, Energy **33**, 817–833 (2008)
454. Kvisle S, Nilsen HR, MTO: state of art and perspectives. In: DGMK conference: creating value from light olefins-production and conversion in Hamburg. Hamburg: German Society for Petroleum and Coal Science and Technology (2001)
455. US Patent Office. Methanol-to-olefin process with increased selectivity to ethylene and propylene (US Patent 6,534,692). UOP LLC, US Patent Office (2003)
456. J. Gregor Meeting the changing needs of the olefins market by UOP LLC. In: The 5th EMEA petrochemical technology conference in Paris. London: Euro Petroleum Consultancy Ltd. (2003)

457. J. Grootjans, V. Vanrysselberghe, W. Vermeiren, Integration of total petrochemicals: UOP olefins conversion process into a naphtha steam cracker facility. Catal. Today **106**(1–4), 57–61 (2005)
458. P. Keep, Comparison of remote gas conversion technologies (Synetix Inc., London, 1999). See also: www.synetix.com/methanol/pdfs/papers/imtof99-paper9(59w).pdfS
459. US Patent Office. Production of light olefins from oxygenate using framework gallium-containing medium pore molecular sieve (US Patent application 20030018231). ExxonMobil Inc., US Patent Office, 2003
460. W. Liebner, GTC-Gas to Chemicals Process Options for Venezuela by Lurgi Oel-Gas Chemie Engineering. In: PdVSA-EFO seminar. Caracas, Venezuela: Petro′leos de Venezuela S.A. (2002)
461. H. Koempel, W. Liebne, M. Wagner, MTP—an economic route to dedicated propylene. In: The 2nd ICIS-LOR world olefins conference (ICIS-LOR Inc., Amsterdam, 2003)
462. M. Rothaemel, H.D. Holtmann, MTP, Methanol-to-Propylene—Lurgi's way, in DGMK conference "creating value from light olefins—production and conversion" (German Society for Petroleum and Coal Science and Technology, Hamburg, 2001)
463. L. Yingxu Wei, J. Li, S. Xu, C. Yuan, L. Xu, J. Chen, Y. Zhou, Y. Qi, Z. Liu, 12th ICC, München 2012, Abstracts
464. http://www.icis.com/Articles/2007/11/05/9076035/methanol-uses-and-market-data.html, 12 Oct 2010
465. http://www.icis.com/Articles/2005/08/20/2009637/mtomtp-ready-to-takeoff.html
466. H. Hui, http://www.icis.com/Articles/2012/10/30/9604963/china-annual-methanol-demand-to-spike-on-mto-mtp-projects.html, 30 Oct 2012

References to Section 6.4.3

467. De Witt Bits 2011 Global Industry Overview, Methanol and Derivatives Service, 1st Feb 2012
468. R. Kempf, Advantages of Commercialization of the UOP Advanced MTO technology, 2011 Middle East Chemical Week Conference, 16–19 Oct 2011, Abu Dhabi National Exhibition centre
469. IHS INC, 2012
470. Propylene Feedstock Diversification Conference, Shanghai, 2012
471. H. Hui, 'China annual methanol demand to spike on MTO, MTP projects', ICIS news, Oct 2012, http://www.icis.com/Articles/2012/10/30/9604963/china-annual-methanol-demand-to-spike-on-mto-mtp-projects.html
472. ICIS 22nd Aug 2005 http://www.icis.com/Articles/2005/08/20/2009637/mtomtp-ready-to-takeoff.html (Source: ACN)
473. R.J Argauer, G.R., Landolt, US Patent 3,702,886
474. C.D. Chang, A.J. Silvestri, J. Catal., **47**, 249–259 (1977)
475. C.D. Chang, A.J. Silvestri, ChemTech **10**, 624 (1987)
476. P. Trabold, Sustainable Routes to Petrochemical Products, in 7th international petrochemical conference, Athene, 23th/24th June 2005
477. M. Stöcker, Microporous and Mesoporous Mater., 3–48 (1999)

References to Section 6.4.4

478. R.J. Argauer, G.R. Landolt, US Patent 3,702,886
479. C.D. Chang, A.J. Silvestri, J. Catal. **47**, 249–259 (1977)
480. C.D. Chang, A.J. Silvestri, ChemTech **10**, 624 (1987)

481. C.D. Chang, in *Methanol to Hydrocarbons*, Handbook of Heterogeneous Catalysis, Ertl, G., Knözinger, H. & Weitkamp, 1st edn., p. 1894
482. S. Kvisle, T. Fuglerud, S. Kolboe, U. Olsbye, K.P. Lillerud, B. Vora, in *Methanol-to-Hydrocarbons*. Handbook of Heterogeneous Catalysis, vol 2, p. 707
483. T.J. Gregor Remans, G. Jenzer, A. Hoek, Gas-to-Liquids. Handbook of heterogeneous catalysis, pp. 2994–3010 (2008)
484. F.J. Keil, Microporous Mesoporous Mater. **29**(1–2), 49–66 (1999)
485. M. Stöcker, Microporous and Mesoporous Mater. **29**(1–2), 3–48 (1999)
486. The Catalyst Group Resources, Inc., Volume 2: Syngas Conversion to Products Assessment, April 2007
487. Technologies of Lurgi Oel Gas Chemie, 302.e/02.03/40, Lurgi Oel Gas Chemie GmbH, 60295 Frankfurt/Main (2003)
488. Adkins, Perkins, J. Phys. Chem. **32**, 219 (1928)
489. H. Knözinger, Angew. Chem. Int. Ed. **7**, 791 (1968)
490. J.R. Jain, C.N. Pillai, J. Catal. **9**, 322 (1967)
491. H. Knozinger, R. Kohne, J. Catal. **5**, 264 (1966)
492. K.L. Ng, Ph.D. Thesis, Imperial College of Science, Medicine and Technology, London, **1999**
493. S.G. Hindin, S.W. Weller, J. Phys. Chem. **60**, 1501 (1956)
494. S.W. Weller, S.G. Hindin, J. Phys. Chem. **60**, 1506 (1956)
495. B. Höhlein, Th. Grube, P. Biedermann, H. Bielawa, G. Erdmann, L. Schlecht, G. Isenberg, R. Edinger, Methanol als Energieträger, Schriften des Forschungszentrums Jülich, Reihe Energietechnik/Energy Technology Band/Volume 28
496. T.H. Fleisch, A. Basu, M.J. Gradassi, J.G. Masin, Stud. Surf. Sci. Catal. **107**, 117–125 (1997)
497. T.A. Semelsberger, R.L. Borup, H.L. Greene, J. Power Sour. **156**, 497–511 (2006)
498. M. Stiefel, R. Ahmad, U. Arnold, M. Döring, Fuel Process. Technol. **92**, 1466–1474 (2011)
499. PERP Program: Dimethyl Ether Technology and Markets. http://www.chemsystems.com/about/cs/news/items/PERP%200708S3_DME.cfm, 6th June 2013
500. Hubert de Mestier du Bourg, 23rd World Gas Conference, Amsterdam 2006: http://www.igu.org/html/wgc2006/pdf/paper/add10696.pdf, 6th June 2013
501. T. Ogawa, N. Inoue, T. Shikada, Y. Ohno, J. Nat. Gas Chem. **12**, 219–227 (2003)
502. W. Balthasar, W. Hilsebein: Methanol as a Feedstock for Power, Fuel and Olefins, in 'Nitrogen & Methanol', p. 261, January/February, 2003
503. U. Wagner, W. Liebner, 'Gas To Chemicals: Advanced technologies for natural gas monetisation' in 12th International Oil, Gas and Petrochemical Congress, Iran 2007
504. http://www.syngasrefiner.com/dme/dmepres/HiroshiFukuyama_pres1.pdf, Toyo Engineering Corporation, 2005
505. G. Yang, N. Tsubaki, J. Shamoto, Y. Yoneyama, Y. Zhang, J. Am. Chem. Soc. **132**, 8129–8136 (2010)
506. R. Ahmad, U. Arnold, M. Döring, in Abstract 12th ICC 2012
507. E. Unneberg, S. Kolboe, Formation of p-Xylene from Methanol over H-ZSM-5, in *Methane Conversion*, ed. by D.M. Bibby, C.D. Chang, R.F. Howe, S. Yurchak (Elsevier Science Publishers B.V, Amsterdam, 1988)
508. M. Conte, J.A. Lopez-Sanchez, Q. He, D.J. Morgan, Y. Ryabenkova, J.K. Bartley, A.F. Carley, S.H. Taylor, C.J. Kiely, K. Khalid, G.J. Hutchings, Catal Sci. Technol. **2**, 105–112 (2012)
509. D. Zeng, J. Yang, J. Wang, J. Xu, Y. Yang, C. Ye, F. Deng, Microporous Mesoporous Mater. **98**, 214–219 (2007)
510. C.P. Nicolaides, N.P. Sincadu, M.S. Scurrell, Catal. Today **71**, 429 (2001)
511. J.A. Biscardi, E. Iglesia, J. Catal. **182**, 117 (1999)
512. C.D. Gosling, F.P. Wilcher, L. Sullivan, R.A. Mountford, Hydrocarb. Process. **69,** Dec 1991
513. S. Pradhan, R. Lloyd, J.K. Bartley, D. Bethell, S. Golunski, R.L. Jenkins, G.J. Hutchings, Chem. Sci. **3**, 2958–2964 (2012)

514. J. Burger, M. Siegert, E. Ströfer, M. Nilles, H. Hasse, AIChE Annual Meeting, 2011. http://www.aiche.org/cei/resources/chemeondemand/conference-presentations/polyoxymethylene-dimethyl-ethers-components-tailored-diesel-fuel-properties-synthesis-and, 6th June 2013
515. G.P. Hagen, M.J. Spangler, US Patent 6,166,266, 2000
516. H.-J Arpe, *Industrielle Organische Chemie*: *Bedeutende Vor- und Zwischenprodukte*, Wiley-VCH, Weinheim, 6. Vollständig überarbeitete Auflage, p. 176 (2007)
517. Helv. Chim. Acta 8, **64** (1925)
518. Ann. 474, 213, (1929)
519. Dupont patent US-2,449,469. Cited from EP1070755
520. D.S. Moulton, D.W. Naegeli, Southwest Research Institute, United States Patent, 5,746,785 May 5, 1998
521. R. Patrini, M. Marchionna, EP1070755, 2001
522. E. Stroefer, R. Sinnen, O. Schweers, J. Thiel, H. Hasse, WO/2008/074704
523. E. Jacob, WO/2011/012339
524. Diesel Fuel News, July 9, 2001 cited by Jack Peckham http://findarticles.com/p/articles/mi_m0CYH/is_14_5/ai_76908160/
525. D. Sanfilippo, R. Patrini, M. Marchionna, Patent US7,235,113

References to Section 6.5.1

526. G. Olah, A. Goeppert, S. Prakash, *Beyond Oil and Gas: The Methanol Economy* (Wiley-VCH, Weinheim, 2009)
527. J.C. Amphlett, M.J. Evans, R.A. Jones, R.F. Mann, R.D. Weir, Can. J. Chem. Eng. **63**, 605–611 (1985)
528. G. Colsmann, Dissertation, Berichte des Forschungszentrums Jülich, Jül-3127, Jülich 1995
529. V. Formanski, *dissertation, Fortschritt-Berichte VDI, Reihe 3 Verfahrenstechnik* (VDI Verlag GmbH, Düsseldorf, 2000)
530. J.C. Amphlett, M.J. Evans, R.A. Jones, R.F. Mann, R.D. Weir, Can. J. Chem. Eng. **59**(4), 720–727 (1981)
531. B. Ganser, Dissertation, Berichte des Forschungszentrums Jülich, Jül-2748, Jülich 1993
532. W. Wiese, B. Emonts, R. Peters, Int. J. Power Sour. **106**, 249–257 (1999)
533. M.S. Wainwright, C.J. Jiang, D.L. Trimm, N.W. Cant, Appl. Catal. **97**, 145–158 (1993)
534. M.S. Wainwright, C.J. Jiang, D.L. Trimm, N.W. Cant, Appl. Catal. **93**, 245–255 (1993)
535. Messer Group GmbH, *Variocarb-therm-process*, can be found under http://www.messergroup.com/de/Daten/Fachbroschueren/Metallurgie/Variocarb-therm.pdf, Krefeld, 2012
536. Air Liquide Deutschland GmbH, *Alnat C^{TM}-process*, can be found under http://www.airliquide.de/loesungen/business/metall/equipment/alnatc.html, Düsseldorf, 2013
537. Westfalen AG, *Tempron®-process*, can be found under http://www.westfalen-ag.de/fileadmin/user_uploads/Westfalen_AG/Technische_Gase/Allgemein/Prospekte_Technische_Gase/Perfekte_Atmos_Tempron.pdf, Münster, 2013
538. T. Weiss, Dissertation, Saarbrücken, 2008
539. L. Pettersson, K. Sjostrom, Combust. Sci. Technol. **80**, 265–303 (1991)
540. J.C. Brown, E. Gulari, Catal. Commu. **5**, 431–436 (2004)
541. Caloric Anlagenbau GmbH, *Caloric HM Plant for H_2Generation by Methanol Reforming*, can be found under http://www.caloric.com/en/produkte/h2-generation/methanol-reforming/methanol-reforming.html, Graefelfing, 2013
542. P. Neumann, F. von Linde, *inform*, *14*, 5, 313-315 (2003)
543. P. Neumann, F. von Linde, MPT. Metall. Plant Technol. Int. **2**, 72–75 (2003)
544. Mahler AGS GmbH, *Process description for Hydroform-M plant*, can be found under http://www.mahler-ags.com/hydrogen/hydroform-m.htm, Stuttgart, 2013

545. Mahler AGS GmbH, *Process description for Hydroform-M plant*, can be found under http://www.mahler-ags.com/hydrogen/hydroswing.htm, Stuttgart, 2013
546. Air Products and Chemicals, Inc., *Hydrogen Recovery and Purification*, http://www.airproducts.com/products/Gases/supply-options/prism-membrane-hydrogen-recovery-and-purification.aspx, Allentown, 2013
547. UOP LLC, *Hydrogen selection matrix*, www.uop.com/uop-hydrogen-selection-matrix, des Plaines, 2013

References to Section 6.5.2

548. F. Asinger, Methanol: Chemie- und Energierohstoff. Die Mobilisation der Kohle (Springer, Berlin, Germany 1986), p. 407
549. G.A. Olah, A. Goeppert, G.K.S. Prakash, *Beyond Oil and Gas: The Methanol Economy* (Wiley-VCH Verlag, Weinheim, Germany, 2006), p. 304
550. A.J. Appleby, F.R. Foulkes, *Fuel Cell Handbook* (Van Nostrand Reinhold Int. Co, New York, 1989), p. 763
551. E.W. Justi, A. Winsel, *Kalte Verbrennung, Fuel Cells* (Franz Steiner, Wiesbaden Germany, 1962), p. 414
552. W. Vielstich, Translated by Ives DJG. Fuel Cells (Wiley-VCH, Weinheim, Germany, 1965/70), p. 502
553. W. Vielstich, A. Lamm, H. Gasteiger (eds.), *Handbook of Fuel Cells* (Wiley, Chichester, UK, 2003), vol 1–4, p. 2606
554. G. Sandstede, Elektrochemische Brennstoffzellen, in Fortschritte der Chemischen Forschung (Springer, Berlin, Heidelberg, New York, 1967), pp. 171–221
555. G. Sandstede (ed.), *From Electrocatalysis to Fuel Cells* (University of Washington Press, Seattle and London, 1972), p. 415
556. H.A. Liebhafsky, E.J. Cairns, *Fuel Cells and Fuel Batteries* (Wiley, London, 1968), p. 692
557. J.O.M. Bockris, S. Srinivasan, *Fuel Cells: Their Electrochemistry* (McGraw-Hill Book Company, London, Sydney, Toronto, Mexico, 1969), p. 660
558. F. von Sturm, Elektrochemische Stromerzeugung (Verlag Chemie, Weinheim, Germany, 1969), p. 190
559. H.H. von Döhren, K.J. Euler, *Brennstoffelemente*, 6th edn., VARTA-Fachbuchreihe Bd 6, (VDI, Düsseldorf, Germany, 1971), p. 223
560. A.K. Kordesch, G. Simader, *Fuel Cells and their Applications* (VCH Verlagsgesellschaft Weinheim, Germany, 1996)
561. A. Heinzel, P. Beckhaus, Brennstoffzellen für portable Anwendungen: kleine Energiepakete (2006). GDCh-Wochenschau 32b: online: http://www.aktuelle-wochenschau.de/2006/woche32b/woche32b.html, p. 5
562. V.S. Bagotsky, Fuel cells: Problems and solutions (Wiley, New York, 2009), p. 322
563. J. Garche, Ch. Dyer, P. Moseley, Z. Ogumi, D. Rand, B. Scrosati (eds.), *Encyclopedia of Electrochemical Power Sources* (Elsevier, Amsterdam, 2009). (vol 1–5)
564. D. Stolten (ed.), *Hydrogen and Fuel Cells: Fundamentals, Technologies and Applications, Chapters* (Wiley-VCH Verlag, Weinheim, Germany, 2010), p. 878
565. D. Stolten (ed.), *Hydrogen Energy* (Wiley-VCH Weinheim, 2010)
566. G. Kolb, *Fuel processing for fuel cells* (Wiley-VCH, Weinheim Germany, 2008), p. 412
567. W. Grot, Perfluorinated cation exchange polymers, Chem. Ing. Tech. **47,** MS260/75, p. 617 (1975)
568. T. Iwasita, *Methanol and CO electrooxidation*, vol 2, eds. by W. Vielstich, A. Lamm, H. Gasteiger, Handbook of Fuel Cells (Wiley, Chichester, UK, 2003), pp. 603–624
569. A. Heinzel, Stand der Technik von Polymer-Elektrolyt-Membran-Brennstoffzellen—ein Überblick. CIT 81: 567–571 (Special Issue: Brennstoffzellen und Wasserstofftechnologie) (2009)

570. A. Heinzel, G. Bandlamudi, W. Lehnert, High Temperature PEMFCs, in *Encyclopedia of Electrochemical Power Sources*, ed. by J. Garche, Ch. Dyer, P. Moseley, Z. Ogumi, D. Rand, B. Scrosati (Elsevier, Amsterdam, 2009), pp. 951–957. (vol 2)
571. L. Gubler, D. Kramer, J. Belack, Ö. Ünsal, ThJ Schmidt, G.G. Scherer, A Polybenzimidazole-Based Membrane for the Direct Methanol Fuel Cell. J. Electrochem. Soc. **154**, B981–B987 (2007)
572. Q. Wang, G.Q. Sun, L.H. Jiang, Q. Xin, S.G. Sun, Y.X. Jiang, S.P. Chen, Z. Jusys, R.J. Behm, Adsorption and oxidation of ethanol on colloid-based Pt/C, PtRu/C and Pt3Sn/C catalysts: In situ FTIR spectroscopy and on-line DEMS Studies, Phys. Chem. Chem. Phys. **9**, pp. 2686–2696 (2007), www.rsc.org/pccp/altfuel
573. Tannenberger, in Sandstede G (ed) (1972) From Electrocatalysis to Fuel Cells, 415 pages, University of Washington Press, Seattle and London
574. A. Heinzel, R. Holze, C.H. Hamann, J.K. Blum, The electrooxidation of methanol and formaldehyde at a platinum electrode: A SEESR study of radical intermediates. Electrochim. Acta **34**, 657 (1989)
575. S. Wasmus, A. Küver, Methanol oxidation and direct methanol fuel cells_a selective review. J. Electroanal. Chem. **461**, 14–31 (1999)
576. V.S. Bagotsky, Y.S. Vassiliev, O.A. Khazova (1977) Generalized scheme of chemisorption, electrooxidation and electroreduction of simple organic compounds on platinum group metals, J. Electroanal. Chem. 81, 229
577. A. Hamnett (2003) Direct methanol fuel cells (DMFC). In: Vielstich W, Lamm A, Gasteiger H (eds) Handbook of Fuel Cells, Vol. 1: 305-322, Wiley, Chichester, UK
578. M. Neergat, D. Leveratto, U. Stimming, Catalysts for Direct Methanol Fuel Cells. Fuel Cells **2**(1), 25–30 (2002)
579. V.S. Bagotsky, Y.B Vassilyev (1964 and 67) Electrochimica Acta 9, 869 and 12, 1323
580. H. Binder, A. Köhling, G. Sandstede, The Anodic Oxidation of Methanol on Raney-Type Catalysts of Platinum Metals, in *Hydrocarbon Fuel Cell Technology*, ed. by B.S. Baker (Academic Press, New York and London, 1965), pp. 91–102
581. O.A. Petry, B.I. Podlovchenko, A.N. Frumkin, H. Lal, J. Electroanal. Chem. **10**, 253 (1965)
582. J.-F. Drillet, R. Dittmeyer, K. Jüttner, L. Li, K.-M. Mangold, New composite DMFC anode with PEDOT as a mixed conducter and catalyst support. Fuel Cells **6**(6), 432–438 (2006)
583. C. Cremers, M. Scholz, W. Seliger, A. Racz, W. Knechtel, J. Rittmayr, F. Grafwallner, H. Peller, U. Stimming, Developments for improved direct methanol fuel cell stacks for portable power. Fuel Cells **7**(1), 21–31 (2007)
584. A.S. Arico, V. Baglio, V. Antonucci (2009) Direct Methanol Fuel Cells: History, Status and Perspectives. In: Liu H, and Zhang J (eds) Electrocatalysis of Direct Methanol Fuel Cells:_From Fundamentals to Applications, Hardcover, Chapter 1: 1-78, Wiley, Chichester, UK, and Wiley Online Library, 582 pages: http://media.wiley.com/product_data/excerpt/75/35273237/3527323775.pdf
585. H. Liu, J. Zhang (2009) Electrocatalysis of Direct Methanol Fuel Cells: From Fundamentals to Applications, 606 pages, Wiley-VCH Verlag, Weinheim, Germany http://eu.wiley.com/WileyCDA/WileyTitle/productCd-3527323775.html
586. M. Watanabe, H. Uchida (2010) Catalysts for the electro-oxidation of small molecules, 18 pages, Wiley Online Library: http://onlinelibrary.wiley.com/doi/10.1002/9780470974001.f500007/full, http://onlinelibrary.wiley.com/doi/10.1002/9780470974001.f500007/pdf
587. J. Wu, F. Hu, P.K. Shen, C.M. Li, Z. Wei, One-step preparation of Pt on pretreated multiwalled carbon nanotubes for methanol electrooxidation. Fuel Cells **10**(1), 106–110 (2010)
588. C. Zhou, F. Peng, H. Wang, H. Yu, J. Yang, X. Fu, Facile preparation of an excellent Pt-RuO2-MnO2/CNTs nanocatalyst for anodes of direct methanol fuel cells. Fuel Cells **11**(2), 301–308 (2011)
589. H. Behret, H. Binder, G. Sandstede, Inorganic and Organic Non-Noble Metal Containing Electrocatalysts for Fuel Cells, in *Electrocatalysis*, ed. by M.W. Breiter (The Electrochemical Society Princeton, N.J, 1974), pp. 319–338

590. C. Fischer, A. Alonso-Vante, S. Fiechter, H. Tributsch, J. Appl. Chem. **25**, 1004 (1995)
591. T.S. Zhao, C. Xu, Direct Methanol Fuel Cell: Overview Performance and Operational Conditions, in *Encyclopedia of Electrochemical Power Sources, Vol 2: 381-389*, ed. by J. Garche, Ch. Dyer, P. Moseley, Z. Ogumi, D. Rand, B. Scrosati (Elsevier, Amsterdam, 2009)
592. T.S. Zhao, Z.X. Liang, J.B. Xu, Overview (Direct Alcohol Fuel Cells), in *Encyclopedia of Electrochemical Power Sources, Vol 2: 362–369*, ed. by J. Garche, Ch. Dyer, P. Moseley, Z. Ogumi, D. Rand, B. Scrosati (Elsevier, Amsterdam, 2009)
593. N.K. Beck, B. Steiger, G.G. Scherer, A. Wokaun, Methanol tolerant oxygen reduction catalysts derived from electrochemically pre-treated Bi2Pt2-yIryO7 pyrochlores. Fuel Cells **6**, 26–30 (2006)
594. A.M. Remona, K.L.N. Phani, Study of methanol-tolerant oxygen reduction reaction at Pt–Bi/C bimetallic nanostructured catalysts. Fuel Cells **11**(3), 385–393 (2011)
595. H. Wang, J. Liang, L. Zhu, F. Peng, H. Yu, J. Yang, High oxygen-reduction-activity and methanol-tolerance cathode catalyst Cu/PtFe/CNTs for direct methanol fuel cells. Fuel Cells **10**(1), 99–105 (2010)
596. J. Yang, C.H. Cheng, W. Zhou, J.Y. Lee, Z. Liu, Methanol-tolerant heterogeneous PdCo@PdPt/C electrocatalyst for the oxygen reduction reaction. Fuel Cells **10**(6), 907–913 (2010)
597. Ch. Hartnig, L. Jörissen, J. Kerres, W. Lehnert, J. Scholta, Polymer electrolyte membrane fuel cells, in *Materials for Fuel Cells*, ed. by M. Gasik (Woodhead Publisher Ltd, Cambridge, 2008), pp. 101–184
598. A. Winsel, Galvanische Elemente, Brennstoffzellen. In: Ullmanns Encyclopädie. Bd **12**, 113–136 (1974)
599. A. Heinzel, V.M. Barragán, A review of the state-of-the-art of methanol crossover in direct methanol fuel cells. J. Power Sources **84**, 70 (1999)
600. Jörissen L, and Gogel V (2009) Direct Methanol: Overview. In: Garche J, Dyer Ch, Moseley P, Ogumi Z, Rand D, and Scrosati B (eds) Encyclopedia of Electrochemical Power Sources, Vol 2: 370-380, Elsevier, Amsterdam
601. Ch. Hartnig, L. Jörissen, W. Lehnert, J. Scholta, Direct methanol fuel cells, in *Materials for Fuel Cells*, ed. by M. Gasik (Woodhead Publisher Ltd, Cambridge, 2008), pp. 185–208
602. N. Neergat, K.A. Friedrich, U. Stimming, New Materials for DMFC MEAs, in *Handbook of Fuel Cells, Vol 4: 856-877*, ed. by W. Vielstich, A. Lamm, H. Gasteiger (Wiley, Chichester, UK, 2003)
603. Justi, Winsel 1962
604. K. Scott, E. Yu (2009) Electrocatalysis in the Direct Methanol Alkaline Fuel Cell. In: Liu H, and Zhang J (eds) Electrocatalysis of Direct Methanol Fuel Cells:_From Fundamentals to Applications, Hardcover, Chapter 13: 487-525, Wiley, Chichester, UK, and Wiley Online Library, 582 pages: http://eu.wiley.com/WileyCDA/WileyTitle/productCd-3527323775.html
605. H. Binder, A. Köhling, W.H. Kuhn, W. Lindner, G. Sandstede, Hydrogen and methanol fuel cells with air electrodes in alkaline electrolyte, in *From Electrocatalysis to Fuel Cells*, ed. by G. Sandstede (University of Washington Press, Seattle and London, 1972), pp. 131–141
606. H. Binder, A. Köhling, G. Sandstede, Effect of alloying components on the catalytic activity of platinum in the case of carbonaceous fuels, in *From Electrocatalysis to Fuel Cells*, ed. by G. Sandstede (University of Washington Press, Seattle and London, 1972), pp. 43–58
607. H. Binder, A. Köhling, G. Sandstede, Platinum catalysts modified by adsorption or mixing with inorganic substances, in *From Electrocatalysis to Fuel Cells*, ed. by G. Sandstede (University of Washington Press, Seattle and London, 1972), pp. 59–80
608. Fuel Cell (2011) 31 pages, in: Wikipedia: http://en.wikipedia.org/wiki/Fuel_cell
609. J.B. Hansen (2003) Methanol reformer design considerations. In: Vielstich W, Lamm A, Gasteiger H (eds) Handbook of Fuel Cells, Vol. 3: 141-148, Wiley, Chichester, UK
610. C. Zhang, Z. Yuan, N. Liu, S. Wang, S. Wang, Study of Catalysts for Hydrogen Production by the High Temperature Steam Reforming of Methanol. Fuel Cells **6**(6), 466–471 (2006)

611. K. von Benda, H. Binder, A. Köhling, G. Sandstede, Electrochemical behaviour of tungsten carbide electrodes, in *From Electrocatalysis to Fuel Cells*, ed. by G. Sandstede (University of Washington Press, Seattle and London, 1972), pp. 87–100
612. D. Edlund, *Methanol Fuel Cell Systems: Advancing towards Commercialisation, 206 pages* (Pan Stanford Publishing Pte, Ltd, Singapure, 2011)
613. A. Heinzel (2001) Brennstoffzellen im kleinen Leistungsbereich – portable Anwendungen und Batterieersatz. In: Ledjeff-Hey K, Mahlendorf F, and Roes J (eds) Brennstoffzellen, Entwicklung Technologie Anwendung, 2. Ed.: 211-219, C.F.Müller Verlag, Heidelberg
614. A. Heinzel, C. Hebling, M. Müller, M. Zedda, C. Müller, Fuel cells for low power applications. J. Power Sources **105**, 250–255 (2002)
615. Heinzel A (2010) Brennstoffzellen - Mobil, stationär und portabel; Stand der Entwicklungen heute. GDCh-Wochenschau 33: 4 pages online: http://www.aktuelle-wochenschau.de/2010/w33/woche33.html
616. S.R. Narayanan, T.I. Valdez, Portable direct methanol fuel cell systems, in *Handbook of Fuel Cells, Vol 4: 1133-1141*, ed. by W. Vielstich, A. Lamm, H. Gasteiger (Wiley, Chichester, UK, 2003)
617. A. Heinzel, C. Hebling, Portable PEM Systems, in *Handbook of Fuel Cells, Vol 4: 1142-1151*, ed. by W. Vielstich, A. Lamm, H. Gasteiger (Wiley, Chichester, UK, 2003)
618. S.R. Narayanan, T.I. Valdez, N. Rohatgi (2003) DMFC system design for portable applications. In: Vielstich W, Lamm A, Gasteiger H (eds) Handbook of Fuel Cells, Vol. 4: 894-904, Wiley, Chichester, UK
619. T. Ramsden (2011) Direct methanol fuel cell material handling equipment demonstration, 21 pages, NREL National Renewable Energy Laboratory, US-DoE http://www.hydrogen.energy.gov/pdfs/review11/mt004_ramsden_2011_o.pdf
620. A. Lamm, J. Müller, System design for transport applications, in *Handbook of Fuel Cells, Vol 4: 878-893*, ed. by W. Vielstich, A. Lamm, H. Gasteiger (Wiley, Chichester, UK, 2003)
621. ballard, basf, bp, daimlerchrysler, methanex, statoil (2002) Methanol Fuel Cell Alliance, 236 pages: http://www.methanol.org/Energy/Resources/Fuel-Cells/MFCA-overall-document-from-09_06.aspx
622. H. Dohle, J. Mergel, D. Stolten, Heat and power management of a direct-methanol-fuel-cell (DMFC) system. J. of Power Sources **111**, 268–282 (2006)
623. J. Mergel, A. Glüsen, Ch. Wannek, Current Status of and Recent Developments in Direct Liquid Fuel Cells, in *Hydrogen and Fuel Cells: Fundamentals, Technologies and Applications, Chapter 3: 41–60*, ed. by D. Stolten (Wiley-VCH Verlag, Weinheim, Germany, 2010)
624. A. Glüsen, M. Müller, N. Kimiaie, I. Konradi, J. Mergel, D. Stolten (2010) Manufacturing Technologies for Direct Methanol Fuel Cells (DMFCs). In: 18th World Hydrogen Energy Conference - WHEC 2010 Proceedings, Parallel Sessions Book 1: 219-226, Stolten D, and Grube Th (Eds), Zentralbibliothek Forschungszentrum Jülich 2010, Schriften des Forschungszentrum Jülich, ISBN: 978-3-89336-658-4
625. H.-P. Schmid, J. Ebner, DaimlerChrysler fuel cell activities, in *Handbook of Fuel Cells, Vol 4: 1167-1171*, ed. by W. Vielstich, A. Lamm, H. Gasteiger (Wiley, Chichester, UK, 2003)
626. A. Rodrigues, M. Fronk, B. McCormick, General Motors/OPEL fuel cell activities – Driving towards a successful future, in *Handbook of Fuel Cells, Vol 4: 1172-1179*, ed. by W. Vielstich, A. Lamm, H. Gasteiger (Wiley, Chichester, UK, 2003)
627. Garche J (2010) Portable Applications and Light Traction. In: Stolten D (ed) Hydrogen and Fuel Cells: Fundamentals, Technologies and Applications, Chapter 35: 715-734, Wiley-VCH Verlag, Weinheim, Germany
628. Wärtsilä installs fuel cell unit on vessel (2010) http://www.wartsila.com/en/press-releases/newsrelease357
629. G. Sandstede, E.J. Cairns, V.S Bagotsky, K. Wiesener (2003) History of low temperature fuel cells. In: Vielstich W, Lamm A, Gasteiger H (eds) Handbook of Fuel Cells, Vol. 1: 145-218, Wiley, Chichester, UK

630. P. Kurzweil, History: Fuel Cells, in *Encyclopedia of Electrochemical Power Sources, Vol 3: 579–595*, ed. by J. Garche, Ch. Dyer, P. Moseley, Z. Ogumi, D. Rand, B. Scrosati (Elsevier, Amsterdam, 2009)
631. H. Hoogers (ed.), *Fuel Cell Technology Handbook, 360 pages* (CRC Press, Boca Raton, London, 2003)
632. A. Heinzel, F. Mahlendorf, J. Roes (eds.), *Brennstoffzellen Entwicklung-Technologie-Anwendung. 3rd. completly revised and extended Ed.* (C.F. Müller Verlag, Heidelberg, 2006)

References to Section 6.5.3

633. M. Madhaiyan, P. S. Chauhan, W. J. Yim, H. P. D. Boruah, T. M. Sa in *Bacteria in Agrobiology: Plant Growth Responses* (Ed.: D. K. Maheshwari), Springer Berlin Heidelberg, Berlin, Heidelberg, **2011**
634. J. Schrader, M. Schilling, D. Holtmann, D. Sell, M. Filho, A. Marx, J. Vorholt, Trends Biotechnol. **27**(2), 107–115 (2009)
635. C. Anthony, *The biochemistry of methylotrophs, Academic Press* (New York, London, 1982)
636. S.J. Giovannoni, D.H. Hayakawa, H.J. Tripp, U. Stingl, S.A. Givan, J.-C. Cho, H.-M. Oh, J.B. Kitner, K.L. Vergin, M.S. Rappé, Environ. Microbiol. **10**, 1771–1782 (2008)
637. M. E. Lidstrom in *The Prokaryotes* (Eds.: M. Dworkin, S. Falkow, E. Rosenberg, K.-H. Schleifer, E. Stackebrandt), Springer, New York, **2006**, 618
638. R. Balasubramanian, S.M. Smith, S. Rawat, L.A. Yatsunyk, T.L. Stemmler, A.C. Rosenzweig, Nature **465**, 115–119 (2010)
639. J.C. Murrell, B. Gilbert, I.R. McDonald, Arch. Microbiol. **173**, 325–332 (2000)
640. R.L. Lieberman, A.C. Rosenzweig, Crit. Rev. Biochem. Mol. Biol. **39**, 147–164 (2004)
641. H. Dalton, Philos. Trans. R. Soc. Lond. B Biol. Sci. **360**, 1207–1222 (2005)
642. G.A. Olah, A. Goeppert, G.K.S. Prakash, *Beyond oil and gas* (The methanol economy, Wiley-VCH, Weinheim, 2006)
643. C. Anthony, M. Ghosh, Prog. Biophys. Mol. Biol. **69**, 1–21 (1998)
644. P.W. van Ophem, J. van Beeumen, J.A. Duine, Eur. J. Biochem. **212**, 819–826 (1993)
645. L. Chistoserdova, L. Gomelsky, J. A. Vorholt, M. Gomelsky, Y. D. Tsygankov, M. E. Lidstrom, *Microbiology (Reading, Engl.)***2000**, *146 (Pt 1)*, 233-238
646. J.A. Vorholt, Arch. Microbiol. **178**, 239–249 (2002)
647. L. Chistoserdova, Science **281**, 99–102 (1998)
648. A.J. Beardsmore, P.N.G. Aperghis, J.R. Quayle, Microbiology **128**, 1423–1439 (1982)
649. P.J. Large, D. Peel, J.R. Quayle, Biochem. J. **81**, 470–480 (1961)
650. G.J. Crowther, G. Kosaly, M.E. Lidstrom, J. Bacteriol. **190**, 5057–5062 (2008)
651. R. Peyraud, K. Schneider, P. Kiefer, S. Massou, J.A. Vorholt, J.-C. Portais, BMC Syst. Biol. **5**, 189 (2011)
652. S. Vuilleumier, L. Chistoserdova, M.-C. Lee, F. Bringel, A. Lajus, Y. Zhou, B. Gourion, V. Barbe, J. Chang, S. Cruveiller et al., PLoS ONE **4**, e5584 (2009)
653. H. Šmejkalová, T.J. Erb, G. Fuchs, A. Herrera-Estrella, PLoS ONE **5**, e13001 (2010)
654. E. Skovran, G.J. Crowther, X. Guo, S. Yang, M.E. Lidstrom, R. Aramayo, PLoS ONE **5**, e14091 (2010)
655. K. Munk, *Biochemie - Zellbiologie* (Thieme Verlag, Stuttgart, 2008)
656. M. T. Madigan, J. M. Martinko, T. D. Brock, *Brock Mikrobiologie*, Pearson Studium, München [u.a.], **2006**
657. K. Ogata, H. Nishikawa, M. Ohsugi, Agric. Biol. Chem. **33**, 1519–1520 (1969)
658. A. Solà, P. Jouhten, H. Maaheimo, F. Sánchez-Ferrando, T. Szyperski, P. Ferrer, Microbiology **153**, 281–290 (2007)

659. F. Bisby, Y. Roskov, A. Culham, T. Orrell, D. Nicolson, L. Paglinawan, N. Bailly, W. Appeltans, P. Kirk, T. Bourgoin et al., "Species 2000 & ITIS Catalogue of Life, 3rd February 2012. *Saccharomycetes*", can be found under www.catalogueoflife.org/col/, **2012**
660. P. Kaszycki, M. Tyszka, P. Malec, H. Kołoczek, Biodegradation **12**, 169–177 (2001)
661. P. Blanco, C. Sieiro, T.G. Villa, FEMS Microbiol. Lett. **175**, 1–9 (1999)
662. M.A. Gleeson, P.E. Sudbery, Yeast **4**, 1–15 (1988)
663. G. Gellissen, G. Kunze, C. Gaillardin, J.M. Cregg, E. Berardi, M. Veenhuis, I. van der Klei, FEMS Yeast Res. **5**, 1079–1096 (2005)
664. H. Yurimoto, N. Kato, Y. Sakai, Chem. Record. **5**, 367–375 (2005)
665. R. Caspi, T. Altman, J.M. Dale, K. Dreher, C.A. Fulcher, F. Gilham, P. Kaipa, A.S. Karthikeyan, A. Kothari, M. Krummenacker et al., Nucleic Acids Res. **38**, D473–D479 (2009)
666. O. Negru, O. Csutak, I. Stoica, E. Rusu, T. Vassu, Rom. Biotechnol. Lett. **15**, 5369–5375 (2010)
667. H. Mogren, Process Biochem. **14**, 2–4 (1979)
668. U. Faust, P. Praeve, D.A. Sukatsch, J. Ferment. Technol. **55**(6), 609–614 (1977)
669. D. G. MacLennan, J. S. Gow, D. A. Stringer, *Proc. R. Aust. Chem. Inst.* **40**(3), (1973)
670. S. Kim, P. Kim, H. Lee, J. Kim, Biotechnol. Lett. **18**, 25–30 (1996)
671. J.H. Choi, J.H. Kim, M. Daniel, J.M. Lebeault, Kor. J. Appl. Microbiol. Biotechnol. **17**, 392–396 (1989)
672. S. B. Pluschkell, M. C. Flickinger, *Microbiology (Reading, Engl.)* **148**, 3223–3233 (2002)
673. L.K. Shay, H.R. Hunt, G.H. Wegner, J. Ind. Microbiol. **2**, 79–85 (1987)
674. P. Kim, J.-H. Kim, D.-K. Oh, World J. Microbiol. Biotechnol. **19**, 357–361 (2003)
675. L. Bélanger, M.M. Figueira, D. Bourque, L. Morel, M. Béland, L. Laramée, D. Groleau, C.B. Míguez, FEMS Microbiol. Lett. **231**, 197–204 (2004)
676. A. Crémieux, J. Chevalier, M. Combet, G. Dumenil, D. Parlouar, D. Ballerini, European. J. Appl. Microbiol. **4**, 1–9 (1977)
677. D. Leak in *Encyclopedia of Bioprocess Technology*, John Wiley & Sons, Inc, **2002**
678. T. Brautaset, Ø.M. Jakobsen, K.D. Josefsen, M.C. Flickinger, T.E. Ellingsen, Appl. Microbiol. Biotechnol. **74**, 22–34 (2007)
679. P. Höfer, Y.J. Choi, M.J. Osborne, C.B. Miguez, P. Vermette, D. Groleau, Microb. Cell Fact. **9**, 1–13 (2010)
680. P. Höfer, P. Vermette, D. Groleau, Biochem. Eng. J. **54**, 26–33 (2011)
681. T. Holscher, U. Breuer, L. Adrian, H. Harms, T. Maskow, Appl. Environ. Microbiol. **76**, 5585–5591 (2010)
682. F. J. Schendel, R. Dillingham, R. S. Hanson, K. Sano, K. Matsui, WO1999020785, **1997**
683. T. Brautaset, Ø.M. Jakobsen, K.F. Degnes, R. Netzer, I. Nærdal, A. Krog, R. Dillingham, M.C. Flickinger, T.E. Ellingsen, Appl. Microbiol. Biotechnol. **87**, 951–964 (2010)
684. D. I. Stirling (Celgene Corporation (Warren, NJ)),US 5071976, **1991**
685. D.K. Oh, J.H. Kim, T. Yoshida, Biotechnol. Bioeng. **54**, 115–121 (1997)
686. Z. Omer, R. Tombolini, A. Broberg, B. Gerhardson, Plant Growth Regul. **43**, 93–96 (2004)
687. M.E. Lidstrom, L. Chistoserdova, J. Bacteriol. **184**(7), 1818 (2002)
688. R.L. Koenig, R.O. Morris, J.C. Polacco, J. Bacteriol. **184**, 1832–1842 (2002)
689. C. B. Miguez, M. M. Figueira, L. Laramee, J. C. Murrell, WO2003046226, **2003**
690. M. M. Figueira, L. Laramee, J. C. Murrell, L. Belanger, D. Groleau, C. B. Miguez, US 20030104527, **2003**
691. J. Gutiérrez, D. Bourque, R. Criado, Y.J. Choi, L.M. Cintas, P.E. Hernández, C.B. Míguez, FEMS Microbiol. Lett. **248**, 125–131 (2005)
692. D. Byrom, M. Carver (Imperial chemical Industries PLC), US 5077212, **1991**
693. K.A. FitzGerald, M.E. Lidstrom, Biotechnol. Bioeng. **81**, 263–268 (2003)
694. Y.J. Choi, D. Bourque, L. Morel, D. Groleau, C.B. Míguez, Appl. Environ. Microbiol. **72**, 753–759 (2006)
695. Y.J. Choi, C.B. Miguez, B.H. Lee, Appl. Environ. Microbiol. **70**, 3213–3221 (2004)
696. C. Anthony, Adv. Microb. Physiol. **27**, 113–210 (1986)

697. G.H. Wegner, W. Harder, Antonie Van Leeuwenhoek **53**, 29–36 (1987)
698. T. Egli, N. Lindley, *J. Gen. Microbiol.* **130**, 3239–3249 (1984)
699. L. Dijkhuizen, T.A. Hansen, W. Harder, Trends Biotechnol. **3**, 262–267 (1985)
700. N. Kato, M. Kano, Y. Tani, K. Ogata, Agric. Biol. Chem. **38**, 111–116 (1974)
701. R. Wichmann, C. Wandrey, A.F. Bückmann, M.-R. Kula, Biotechnol. Bioeng. **23**, 2789–2802 (1981)
702. B. Bossow, C. Wandrey, Ann. N. Y. Acad. Sci. **506**, 325–336 (1987)
703. V.I. Tishkov, V.O. Popov, Biochemistry Mosc. **69**, 1252–1267 (2004)
704. P. Fröhlich, K. Albert, M. Bertau, Org. Biomol. Chem. **9**, 7941 (2011)
705. R. Couderc, J. Baratti, Agric. Biol. Chem. **44**, 2279–2289 (1980)
706. G. Dienys, S. Jarmalavičius, S. Budrien, D. Čitavičius, J. Sereikait, J. Mol. Catal. B Enzym. **21**, 47–49 (2003)
707. Y. Sakai, Y. TANI. Agric. Biol. Chem. **50**, 2615–2620 (1986)
708. M. Zhang, H.Y. Wang, Enzyme Microb. Technol. **16**, 10–17 (1994)
709. G. Gellissen, Appl. Microbiol. Biotechnol. **54**, 741–750 (2000)
710. G. Gellissen, C. P. Hollenberg in *Encyclopedia of Food Microbiology* (Ed.: Editor-in-Chief: Richard K. Robinson), Elsevier, Oxford, **1999**
711. K. Chitkala in *Encyclopedia of Food Microbiology* (Ed.: Editor-in-Chief: Richard K. Robinson), Elsevier, Oxford, **1999**
712. M.A. Romanos, J.J. Clare, K.M. Beesley, F.B. Rayment, S.P. Ballantine, A.J. Makoff, G. Dougan, N.F. Fairweather, I.G. Charles, Vaccine **9**, 901–906 (1991)
713. A. Markaryan, C.J. Beall, P.E. Kolattukudy, Biochem. Biophys. Res. Commun. **220**, 372–376 (1996)
714. J.J. Clare, F.B. Rayment, S.P. Ballantine, K. Sreekrishna, M.A. Romanos, Nat. Biotech. **9**, 455–460 (1991)
715. P.A. Romero, M. Lussier, A.M. Sdicu, H. Bussey, A. Herscovics, Biochem. J. **321**, 289–295 (1997)
716. Y. Sakai, T. Rogi, R. Takeuchi, N. Kato, Y. Tani, Appl. Microbiol. Biotechnol. **42**, 860–864 (1995)
717. M.W. de Vouge, A.J. Thaker, I.H. Curran, L. Zhang, G. Muradia, H. Rode, H.M. Vijay, Int. Arch. Allergy Immunol. **111**, 385–395 (1996)
718. G. Gellissen, M. Piontek, U. Dahlems, V. Jenzelewski, J.E. Gavagan, R. DiCosimo, D.L. Anton, Z.A. Janowicz, Appl. Microbiol. Biotechnol. **46**, 46–54 (1996)
719. A. Beauvais, M. Monod, J.-P. Debeaupuis, M. Diaquin, K. Hidemitsu, J.-P. Latgé, J. Biol. Chem. **272**, 6238–6244 (1997)
720. G. Gellissen, Z. A. Janowicz, A. Merckelbach, M. Piontek, P. Keup, U. Weydemann, C. P. Hollenberg, A. W. Strasser, *Biotechnology (N.Y.)* **9**, 291–295 (1991)
721. M. Hodgkins, P. Sudbery, D. Mead, D.J. Ballance, A. Goodey, Yeast **9**, 625–635 (1993)
722. R. Narciandi, L. Rodriguez, E. Rodriguez, R. Diaz, J. Delgado, L. Herrera, Biotechnol. Lett. **17**, 949–952 (1995)
723. A.F. Mayer, K. Hellmuth, H. Schlieker, R. Lopez-Ulibarri, S. Oertel, U. Dahlems, A.W.M. Strasser, A.P.G.M. van Loon, Biotechnol. Bioeng. **63**, 373–381 (1999)
724. P.M. Smith, C. Suphioglu, I.J. Griffith, K. Theriault, R.B. Knox, M.B. Singh, J. Allergy Clin, Immunol. **98**, 331–343 (1996)
725. M.S. Payne, K.L. Petrillo, J.E. Gavagan, L.W. Wagner, R. DiCosimo, D.L. Anton, Gene **167**, 215–219 (1995)
726. K. N. Faber, P. Haima, W. Harder, M. Veenhuis, G. AB, Curr. Genet. 1994, 25, 305-310
727. D. Mozley, A. Remberg, W. Gartner, Photochem. Photobiol. **66**, 710–715 (1997)
728. A. Ruddat, P. Schmidt, C. Gatz, S.E. Braslavsky, W. Gärtner, K. Schaffner, Biochemistry **36**, 103–111 (1997)
729. R.G. Buckholz, M.A.G. Gleeson, Nat. Biotech. **9**, 1067–1072 (1991)
730. C. Zurek, E. Kubis, P. Keup, D. Hörlein, J. Beunink, J. Thömmes, M.-R. Kula, C. P. Hollenberg, G. Gellissen, Process Biochem. 1996, 31, 679-689

731. M. Rodríguez, R. Rubiera, M. Penichet, R. Montesinos, J. Cremata, V. Falcón, G. Sánchez, R. Bringas, C. Cordovés, M. Valdés et al., J. Biotechnol. **33**, 135–146 (1994)
732. E.Z. Monosov, T.J. Wenzel, G.H. Lüers, J.A. Heyman, S. Subramani, J. Histochem. Cytochem. **44**, 581–589 (1996)
733. S.A. Rosenfeld, D. Nadeau, J. Tirado, G.F. Hollis, R.M. Knabb, S. Jia, Protein Expr. Purif. **8**, 476–482 (1996)
734. U. Weydemann, P. Keup, M. Piontek, A.W. Strasser, J. Schweden, G. Gellissen, Z.A. Janowicz, Appl. Microbiol. Biotechnol. **44**, 377–385 (1995)
735. F. Talmont, S. Sidobre, P. Demange, A. Milon, L.J. Emorine, FEBS Lett. **394**, 268–272 (1996)
736. S.C. Gilbert, H. van Urk, A.J. Greenfield, M.J. McAvoy, K.A. Denton, D. Coghlan, G.D. Jones, D.J. Mead, Yeast **10**, 1569–1580 (1994)
737. J.M. Cregg, J.F. Tschopp, C. Stillman, R. Siegel, M. Akong, W.S. Craig, R.G. Buckholz, K.R. Madden, P.A. Kellaris, G.R. Davis et al., Nat. Biotechnol. **5**, 479–485 (1987)
738. Z.A. Janowicz, K. Melber, A. Merckelbach, E. Jacobs, N. Harford, M. Comberbach, C.P. Hollenberg, Yeast **7**, 431–443 (1991)
739. T. Boehm, S. Pirie-Shepherd, L.-B. Trinh, J. Shiloach, J. Folkman, Yeast **15**, 563–572 (1999)
740. C.K. Raymond, T. Bukowski, S.D. Holderman, A.F.T. Ching, E. Vanaja, M.R. Stamm, Yeast **14**, 11–23 (1998)
741. P.F. Gallet, H. Vaujour, J.M. Petit, A. Maftah, A. Oulmouden, R. Oriol, C. Le Narvor, M. Guilloton, R. Julien, Glycobiology **8**, 919–925 (1998)
742. D. Bourque, B. Ouellette, G. André, D. Groleau, Appl. Microbiol. Biotechnol. **37**, 7–12 (1992)
743. D. Bourque, Y. Pomerleau, D. Groleau, Appl. Microbiol. Biotechnol. **44**, 367–376 (1995)
744. T. Suzuki, T. Yamane, S. Shimizu, Appl. Microbiol. Biotechnol. **23**, 322–329 (1986)
745. F.J. Schendel, C.E. Bremmon, M.C. Flickinger, M. Guettler, R.S. Hanson, Appl. Environ. Microbiol. **56**(4), 963–970 (1990)
746. R. Westlake, Chem. Ing. Technol. **58**, 934–937 (1986)
747. J.D. Windass, M.J. Worsey, E.M. Pioli, D. Pioli, P.T. Barth, K.T. Atherton, E.C. Dart, D. Byrom, K. Powell, P.J. Senior, Nature **287**, 396–401 (1980)
748. P.J. Senior, J. Windass, Biotechnol. Lett. **2**, 205–210 (1980)
749. K. Muttzall, *Einführung in die Fermentationstechnik* (Behr, Hamburg, 1993)
750. G.L. Solomons, CRC Crit. Rev. Biotechnol. **1**, 21–58 (1985)
751. E.W. Jwanny, M.M. Rashad, Acta Biotechnol. **7**, 31–38 (1987)
752. A.M. Henstra, J. Sipma, A. Rinzema, A.J.M. Stams, Curr. Opin. Biotechnol. **18**, 200–206 (2007)
753. E. H. Wegner, US 4414329, **1981**
754. R. Renneberg, *Biotechnologie für Einsteiger, Elsevier, Spektrum* (Akad. Verl, Heidelberg, 2006)
755. U. O. Ugalde, J. I. Castrillo in *Applied Mycology and Biotechnology : Agriculture and Food Production* (Ed.: George G. Khachatourians and Dilip K. Arora), Elsevier, **2002**
756. G.H. Wegner, FEMS Microbiol. Lett. **87**, 279–284 (1990)
757. A. Onnis-Hayden, A.Z. Gu, Proceedings of the Water Environment Federation **17**, 253–273 (2008)
758. I. Purtschert, H. Siegrist, W. Gujer, Water Sci. Technol. **33**(12), 117–126 (1996)
759. M. Ginige, J. Bowyer, L. Foley, J. Keller, Z. Yuan, Biodegradation **20**(2), 221–234 (2009)
760. H. Lee, J.A. Brereton, D.S. Mavinic, R.A. Fiorante, W.K. Oldham, J.K. Paisley, Environ. Technol. **22**(10), 1223–1235 (2001)
761. M. Komorowska-Kaufman, H. Majcherek, E. Klaczyński, Process Biochem. **41**(5), 1015–1021 (2006)
762. S.D. Minteer, B.Y. Liaw, M.J. Cooney, Curr. Opin. Biotechnol. **18**(3), 228–234 (2007)
763. J. Kim, H. Jia, P. Wang, Biotechnol. Adv. **24**(3), 296–308 (2006)
764. P.L. Yue, K. Lowther, Chem. Eng. J. **33**, B69–B77 (1986)

765. P. Kar, H. Wen, H. Li, S.D. Minteer, S.C. Barton, J. Electrochem. Soc. **158**(5), B580–B586 (2011)
766. G.T.R. Palmore, H. Bertschy, S.H. Bergens, G.M. Whitesides, J. Electroanal. Chem. **443**(1), 155–161 (1998)
767. A. A. Karyakin, in *Electropolymerization.* Wiley-VCH Verlag GmbH & Co. KGaA, **2010**, 93-110
768. A. A. Karyakin, E.E. Karyakina, W. Schuhmann, H.-L. Schmidt, S.D. Varfolomeyev, Electroanalysis **6**(10), 821–829 (1994)
769. P.K. Addo, R.L. Arechederra, S.D. Minteer, Electroanalysis **22**(7–8), 807–812 (2010)
770. R.A. Rincón, C. Lau, K.E. Garcia, P. Atanassov, Electrochim. Acta **56**(5), 2503–2509 (2011)
771. X.-C. Zhang, A. Ranta, A. Halme, Biosens. Bioelectron. **21**(11), 2052–2057 (2006)
772. R. Obert, B.C. Dave, J. Am. Chem. Soc. **121**, 12192–12193 (1999)
773. H. Wu, Z.Y. Jiang, S.W. Xu, S.F. Huang, Chin. Chem. Lett. **14**(4), 423–425 (2003)
774. F. Baskaya, X. Zhao, M. Flickinger, P. Wang, Appl. Biochem. Biotechnol. **162**(2), 391–398 (2010)
775. S. Kuwabata, R. Tsuda, K. Nishida, H. Yoneyama, Chem. Lett. **22**(9), 1631 (1993)
776. S. Kuwabata, R. Tsuda, H. Yoneyama, J. Am. Chem. Soc. **116**(12), 5437–5443 (1994)
777. Y. Amao, T. Watanabe, J. Mol. Catal. B Enzym. **44**(1), 27–31 (2007)
778. Y. Amao, T. Watanabe, *Appl. Catal., B* **86**(3-4), 109–113 (2009)
779. F. E. Zilly, J. P. Acevedo, W. Augustyniak, A. Deege, U. W. Häusig, M. T. Reetz, *Angew. Chem., Int. Ed.* **50**(12), 2720–2724 (2011)
780. B. Alber, Appl. Microbiol. Biotechnol. **89**(1), 17–25 (2011)

Chapter 7
Methanol Generation Economics

Matthias Blug, Jens Leker, Ludolf Plass and Armin Günther

7.1 Introduction

Methanol is one of the most important intermediates in the chemical industry. The applications of methanol are versatile, ranging from feedstock for the production of specialty chemicals, polymers, and pharmaceuticals to energy applications such as the production of fuel additives or direct fuel blending. Considering a market price of approximately $450 per tonne, methanol compares well with other liquid fuels, based on the costs per energy content. For comparison, the natural gas price as defined in Fig. 7.1 would be approximately 7 €/GJ.

In this chapter, an overview of different technologies and the related economical boundary conditions for the production of methanol from natural gas and coal are given. Furthermore, some insights about state-of-the art technologies for industrial methanol production as well as alternative technologies based on biomass and renewable electricity are provided.

M. Blug
Evonik Industries AG, Creavis Technologies & Innovation, Science-to-Business Center Eco, Essen, Germany
e-mail: matthias.blug@evonikindustries.com

J. Leker
WWU Münster, Institute of Business Administration at the Department of Chemistry and Pharmacy, Münster, Germany
e-mail: leker@uni-muenster.de

L. Plass (✉)
Parkstraße 11, 61476 Kronberg, Germany
e-mail: dr.ludolf.plass@t-online.de

A. Günther
Air Liquide Global E&C Solutions, c/o Lurgi GmbH, Frankfurt, Germany
e-mail: Dr.Armin.Guenther@Lurgi.com

M. Bertau et al. (eds.), *Methanol: The Basic Chemical and Energy Feedstock of the Future*, DOI: 10.1007/978-3-642-39709-7_7,

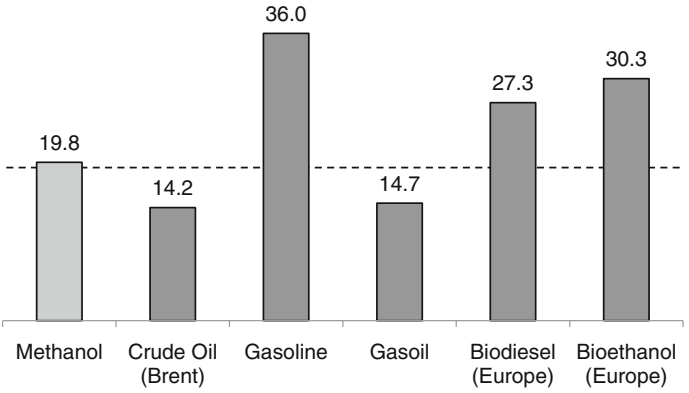

Fig. 7.1 Comparison of specific energy content (costs) of common liquid fuels (energy carriers) compared to methanol (€/GJ) as of February 2014

7.2 State-of-the-Art Technologies for Methanol Production

Currently, there are two major fossil feeds for the production of methanol: (1) natural gas, which accounts for about 90 % of the global methanol production, and (2) coal, which is used as a feedstock in regions where natural gas is scarce, the price of natural gas is prohibitive, and coal is available in large quantities at competitive rates for methanol production. The first commercial catalyst for this reaction was developed by BASF back in 1923; it required high process temperatures (360–380 °C) and pressures (250–300 bar) at low conversion rates of approximately 10 %. In the 1960s, Imperial Chemical Industries (ICI, now Johnson Matthey) has developed a copper-zinc catalyst that allowed for "low-pressure" conversion of synthesis gas to methanol—a process on which most current methanol production processes are based. This catalyst allowed for operating the methanol production process at pressures of 50–100 bar, which was significantly lower than the pressures required by the BASF process developed in the 1920s. As a result of the better performance using lower pressure, this process has become the only one that is applied for the synthesis of methanol [1].

Methanol from Natural Gas

The current industrial technologies for methanol production are based on three process steps:

- Synthesis gas production
- Methanol synthesis
- Distillation

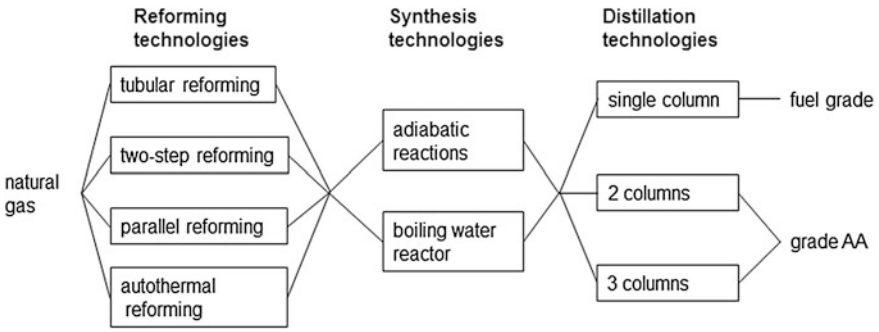

Fig. 7.2 Commercial methanol technologies based on natural gas [2]

The three different process technologies (Fig. 7.2) can be optimised largely independently and according to the specific needs of the project. Capital cost and efficiency are the normally the deciding factors for the selection of technology. They become even more important when the plants grow bigger, as the market development demonstrates. Of specific importance is the section of syngas production and compression, as it accounts for up to 60 % of the overall investment of the plant if natural gas is used as feedstock (see also Sect. 4.3). If coal is the feedstock, then the syngas preparation, the investment cost for the syngas preparation via gasification, and gas cleaning are even substantially higher (see also Sect. 4.4), as can be seen from Fig. 7.2.

Synthesis Gas Production

The most commonly used method for units producing less than 3000 tonnes per day (tpd) is steam reforming. The resulting synthesis gas is characterised by the so-called stoichiometric number see also Sect. 4.3.2.4:

$$SN = (\text{mol } H_2 - \text{mol } CO_2) / (\text{mol } CO + \text{mol } CO_2)$$

which in the case of an ideal synthesis gas for methanol production is in the range of 2.0–2.1.

Being an endothermic reaction, steam reforming requires the firing of large amounts of fuel near the reactor tubes to supply the heat of reaction. High temperatures (900 °C) and excess of steam are required for shifting the thermodynamic equilibrium to carbon monoxide and hydrogen formation (Scheme 7.1)

$$CH_4 + H_2O \longrightarrow CO + 3H_2 \quad \Delta H_{298K} = 206 \text{ kJ/mol} \quad \text{(Steam-Methane-Reforming)}$$

$$CO + H_2O \longleftrightarrow CO_2 + H_2 \quad \Delta H_{298K} = -41 \text{ kJ/mol} \quad \text{(Water-Gas-Shift-Reaction)}$$

$$CH_4 + 0.5\ O_2 \longrightarrow CO + 2H_2 \quad \Delta H_{298K} = -35 \text{ kJ/mol} \quad \text{(PartialOxidation)}$$

Scheme 7.1

Table 7.1 Comparison of energy consumption and investment cost for alternative syngas production technologies [2]

10 kt per day MeOH	Two-step reforming	Parallel reforming	Autothermal reforming
NG process feed	100	107	110
NG fuel	100	50	0
Steam export (additional to steam for ASU comp)	100	156	69
Electrical power consumption	100	104	142
Net energy consumption	100	100	100
Steam-to-carbon ratio	1.8	2.5/0.6	0.6
Specific O_2 consumption	100	104	142
CO/CO_2 ratio in syngas	2.7	4.7	6.3
H_2O in raw product	13	8	5
Investment cost	100	95	85

NG natural gas

The excess of steam also leads to the subsequent steam reforming of large amounts of CO to CO_2. The resulting synthesis gas is rich in H_2 and is characterised by a high stoichiometric number of 3. The need for fuel firing together with the heating and cooling of the gas and excess steam imply large heat transfer duty—and consequently, a large investment cost.

Although steam reforming is the most used and most efficient technology for methanol plants producing up to 3,000 t per day [3], very large steam reformers become progressively more expensive and thus show nearly no economy of scale, as they are difficult to operate beyond 1,000 tubes per reformer. Therefore, a methanol plant with a production capacity of 5,000 t per day would need five steam reformers, one steam reformer combined with an autothermal reformer, or an autothermal reformer alone. The cost advantage is obvious, even taking into account the cost of the air separation unit that is additionally needed for autothermal reforming.

A detailed comparison of energy consumption and investment cost for different syngas production technologies at the level of a 10,000 t/d methanol plant is available in Ref. [2] and is shown in Table 7.1.

Gas-Phase Methanol Synthesis

Synthesis gas to methanol conversion is a mature process. The reaction of carbon monoxide with hydrogen is the primary methanol synthesis reaction. In addition, a small amount of CO_2 in the feed (2–10 %) acts as a promoter of this reaction and helps to maintain catalyst activity [4]. Removing the large excess heat of reaction and overcoming the thermodynamic constraint are challenges to overcome in commercial methanol synthesis. The maximum per-pass conversion efficiency of synthesis gas to methanol is theoretically limited to about 25 % [5], whereas conversion rates from only 4–14 % are achieved under real conditions, resulting in the need for recycling large amounts of synthesis gas. Higher conversion

$$CO + 2H_2 \longrightarrow CH_3OH \qquad \Delta H_{298K} = -91\ kJ/mol$$
$$CO_2 + 3H_2 \longrightarrow CH_3OH + H_2O \qquad \Delta H_{298K} = -50\ kJ/mol$$

Scheme 7.2

efficiencies per-pass can be realised either at lower temperatures (where the methanol equilibrium is shifted towards products) or by removing the produced methanol from the equilibrium [6] (Scheme 7.2)

The synthesis process has been optimised to a point that modern methanol plants yield 1 t of methanol per m^3 of catalyst per hr with >99.5 % selectivity for methanol. Commercial methanol synthesis catalysts (see also Sect. 4.6) have lifetimes on the order of 3–5 years under normal operating conditions [6]. A prerequisite for the use of the highly active and selective copper-zinc catalyst is proper gas cleaning. Copper catalysts are extremely sensitive to poisons (see also Sects. 4.4.7 and 4.4.8) such as sulphur and chlorides [7]. Furthermore, it is important to control the reactor temperature to avoid sintering of small copper particles [6].

Distillation of Crude Methanol

Although selectivity of state-of-the-art catalysts is extremely high, distillation of crude methanol is necessary to obtain "AA" or chemical-grade methanol. Crude methanol usually contains up to 18 % water as well as trace amounts of higher alcohols and dissolved synthesis gas [6]. Distillation is usually carried out in a two-column or three-column configuration (see Sect. 4.7.5). Although the two-column configuration has the advantage of lower investment costs, the three-column configuration has a higher energy efficiency [8].

7.3 Economics of Methanol Synthesis from Natural Gas

Methanol is a commodity chemical. Therefore, it is vital to methanol producers to produce at a low cost. An overall production cost of 204 €/t is estimated for a 5,000 tpd plant (Fig. 7.3), with natural gas being the main cost component with approximately 47 %, followed by capital costs (22 %) and depreciation (15 %) [9].

As a matter of course, the relative share of natural gas cost on the production cost is related to the natural gas price. Furthermore, this analysis allows the correlation of the natural gas price with production cost of methanol, as the remaining cost will be independent from the price of natural gas. This correlation shows that the production cost for methanol in areas where natural gas is available at very low prices, such as in Saudi Arabia at $0.75/MMBTU (0.5–0.6 €/GJ) of natural gas, [10] the share of the investment costs for the methanol plant of the methanol production costs become more important and the production costs can be estimated approximately 130 € per tonne of methanol (Fig. 7.4). (Note that 1$/mmBTU = 0.76 €/GJ (based on 1 US$ = 0.769 € as of April 23, 2013.). These low methanol production

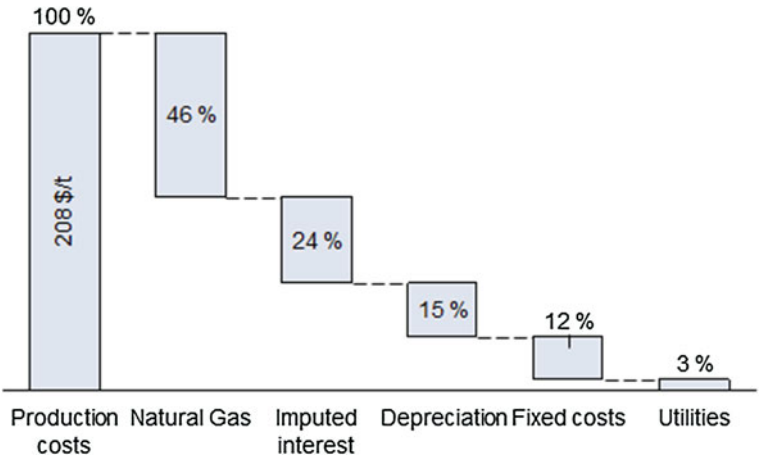

Fig. 7.3 Cost breakdown for methanol synthesis from natural gas in the U.S. Gulf Coast region. Production capacity: 5,000 tpd; natural gas price: $3/MMBTU [9]. Note that 1$/mmBTU = 0.76 €/GJ (based on 1 US$ = 0.769 € as of April 23, 2013)

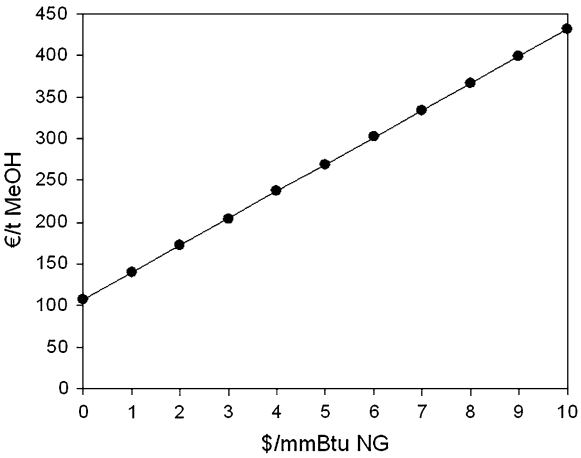

Fig. 7.4 Correlation of the methanol production cost to the natural gas feed price

costs are a premise for the commercialisation of emerging technologies, such as the methanol-to-olefins process and methanol-based fuel substitutes and blends.

7.4 Methanol from Coal

Aside from natural gas, coal has the potential to be a feedstock for large-scale production of methanol. Coal gasification is competitive with steam methane reforming in regions where natural gas is relatively expensive or scarce, as in

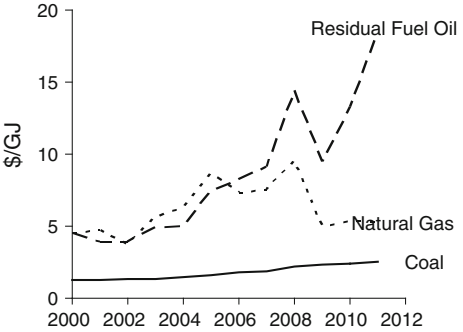

Fig. 7.5 Cost of fossil fuels in the United States (in 2005 dollars, including taxes, yearly averages, 7-month averages for 2011). *Data Source* U.S. Energy Information Administration

China or South Africa. As a special case, in addition to the coal gasification–based methanol production, an integrated gasification combined-cycle power plant in the United States, with additional production of hydrogen or chemicals, was assessed as an alternative to the conventional natural gas–based technology (Fig. 7.5).

Synthesis Gas from Coal

Coal is first gasified with oxygen and steam to produce a synthesis gas consisting mainly of carbon monoxide (CO) and hydrogen (H_2), with some CO_2, sulphur, particulates, and trace elements. Oxygen (O_2) is added in less than stoichiometric quantities so that complete combustion does not occur. This process is highly exothermic, with temperatures controlled by the addition of steam. The resulting synthesis gas has a low stoichiometric number of 0.5–0.7. Additionally, the steps of coal preparation and syngas cleaning (grinding, ash separation, and coal gas cleanup, with desulphurisation as a part of coal gas cleanup) contribute largely to investment costs for equipment and recurring costs of operation and maintenance, which overcompensate for the cost benefit of coal-based methanol production processes, as can be seen from Fig. 7.6.

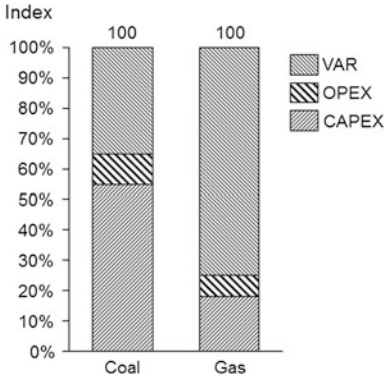

Fig. 7.6 Differences in coal- and gas-based syngas production cost for methanol production [11]. OPEX, operational expenditure; CAPEX, capital expenditure

Methanol Synthesis

As in the case of natural gas–based methanol production, gas-phase methanol synthesis is a commonly used technology for methanol synthesis from coal-derived syngas.

7.5 Economics of Methanol Synthesis from Coal

At a price of $60 per tonne, coal has the highest share in the methanol production costs. Nevertheless it should be noted that the relative share of raw materials is significantly smaller than for natural gas. The specific investment costs for a coal-based methanol plant are approximately 100 % higher than for a gas-based methanol plant on a western price level, whereas investment costs in China are 30 % lower. Therefore, capital costs and depreciation increase significantly, as can be seen from Fig. 7.7. Overall, this leads to a production for coal-based methanol in China that is approximately 20 % higher compared to current U.S. Gulf Coast natural gas–based methanol production costs and about 90 % higher than methanol production costs in Saudi Arabia, considering present raw material costs.

Figure 7.8 summarises the significant differences of average methanol production costs in 2011 due to the different feedstock costs in the various regions of the world.

In Fig. 7.9, the methanol production costs are plotted against the cumulative world capacity. The global demand was approximately 60.2 million tonnes in 2012 and is expected to reach 90 million tonnes in 2016. The methanol plants in regions with "advantaged gas" in the Middle East and South America demonstrate the cost

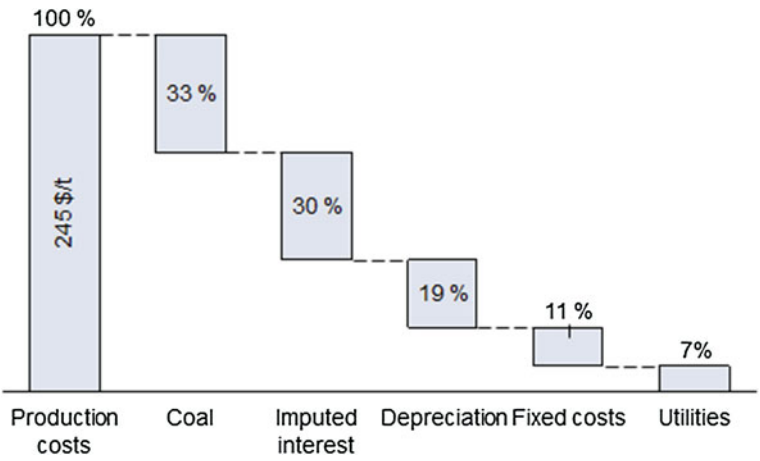

Fig. 7.7 Cost breakdown for methanol synthesis from coal in China (production capacity: 5,000 tpd; coal price: $60/t) [9]

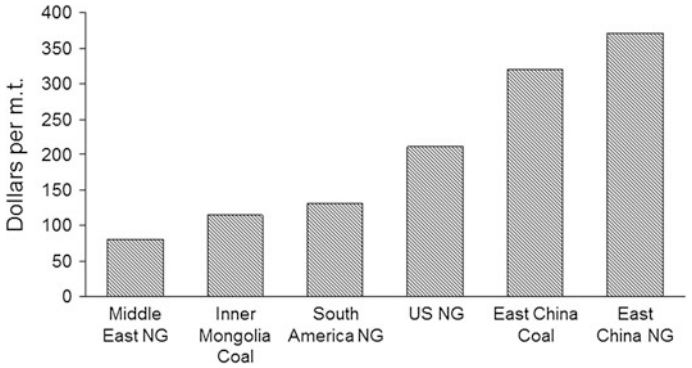

Fig. 7.8 2011 average methanol production costs. NG, natural gas (*Source* IHS) [12]

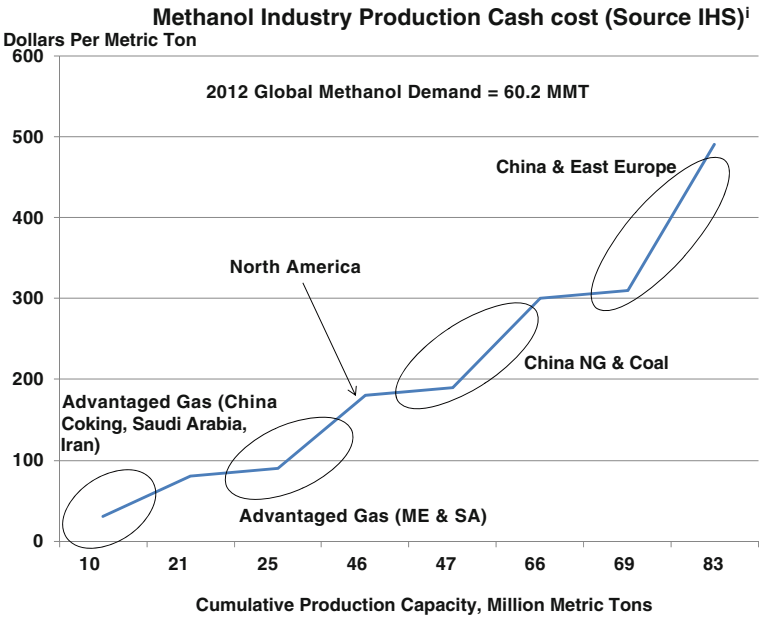

Fig. 7.9 2012 methanol industry production cash cost (*Source* IHS) [12]

advantage against plants in China and East Europe, where natural gas and coal are much more expensive.

Table 7.2 shows that the specific energy price for coal must be lower than for heavy oil, and the latter must be lower than for natural gas to be competitive.

Table 7.2 Comparison of 1,000-tpd ammonia and methanol plants for various feedstocks [13]

	Natural gas	Heavy oil	Coal
Ammonia plant			
Capital cost (%)	100	170	225
Energy requirements (%)	100	115	135
Methanol plant			
Capital cost (%)	90	150	200
Energy requirements (%)	95	105	125

N/A not available

7.6 Methanol from Renewable Energies

In light of global warming, the international community has agreed on substantially reducing greenhouse gas emissions in order to stabilise the global warming to a maximum of 2 °C [14, 15]. For example, in 2007, the European Council adopted very ambitious energy and climate change objectives for 2020: to reduce greenhouse gas emissions by 20 %, to increase the share of renewable energy to 20 %, and to make a 20 % improvement in energy efficiency [16]. Increasing the share of renewable energies on the energy production is thus of utmost importance. Given methanol's potential for the production of commercial goods and as an energy carrier, methanol produced from renewable energy sources could make a substantial contribution to these efforts.

Methanol from Biomass

An overall potential of 3,500 TWh/year of sustainably producible biomass for the primary energy supply of the European Union in 2030 was identified by the European Environmental Agency [17]. Considering this large potential, which equals about 25 % of Europe's primary energy consumption, [18] "bio-energy is seen as one of the key options to mitigate greenhouse gas emissions and substitute fossil fuels" [19] (see also Sect. 4.1.2).

The biomass that is available can be divided into three categories (Fig. 7.10):

- Wastes
- Crops
- Forestry residues

Wastes comprise residues, byproducts, and wastes of biological origin arising from agriculture, industry, and households, such as agricultural residues (e.g. cereal and rapeseed straw, green tops from potatoes and beets and manures) or municipal solid waste (e.g. kitchen and garden waste, paper and cardboard) and industrial residues (e.g. black liquor, wood processing waste wood, food processing wastes) [17]. Crops comprise "conventional" bio-energy crops such as starch crops (e.g. corn, sugar beets) or oil crops (e.g. rapeseed, sunflower), as well as perennial grasses or short rotation forests on agricultural land [17]. Forestry biomass is defined as residues from harvest operations that are normally left in the

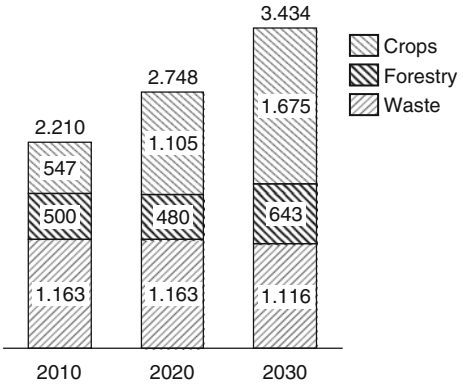

Fig. 7.10 Environmentally compatible primary bioenergy potential in the European Union in TWh [17]

forest after stem wood removal, such as stem top and stump, branches, foliage, and roots. Additional sources of forestry bioenergy potential are complementary fellings, which describe the difference between the maximum sustainable harvest level and the actual harvest needed to satisfy round wood demand [17].

Key driving factors for the increasing bioenergy potential were identified: an increase in the productivity as well as an assumed liberalisation in the agricultural sector, resulting in a larger area available for dedicated bioenergy farming. In contrast, the potential of bioenergy based on wastes and forestry residues that currently display the largest available potential are considered to remain more or less at the same level [17].

In general, there are two pathways that are conceivable for the conversion of biomass to methanol: (1) the anaerobic digestion of biomass to biogas, resulting in a 1:1 mixture of methane and carbon dioxide and (2) the gasification of biomass to biosynthesis gas. Digestion has a low overall electrical efficiency (roughly 10–15 %, strongly depending on the feedstock) and is particularly suited for wet biomass materials [19]. In contrast, gasification is more suited for dry biomass and provides high overall electrical efficiencies (70–80 %) [20].

7.7 Economics of Methanol Synthesis from Biomass

Economic data were reported for several demonstration plants that have been operating in recent years in Spremberg, Germany; Güssing, Austria; and Piteå, Sweden. These plants have produced methanol from various feedstocks at production costs of 150–400 €/t of methanol [20]. A summary is given in Table 7.3. Additionally, Bandi and Specht have assessed the production cost of methanol via anaerobic digestion of manures (220–276 €/t of methanol) and energy crops (476–516 €/t of methanol) [20].

In 2010, the first commercial-scale plant for methanol synthesis, based on biomass and natural gas as feedstocks, started operation in Delfzijl in the

Table 7.3 Biomass-to-methanol demonstration plants [20]

Location	Spremberg	Güssing	Piteå	Hagfors
Process	BGL	Fluid bed	Chemrec	Uhde
Feed	Waste + coal	Biomass	Black liquor	Forest residues
Capacity	120 kt/a	300 t/a	1,3 kt/a	100 kt/a
Availability (%)	85–95	90	90	N/A
Efficiency (%)	50	N/A	N/A	N/A
Production cost (€/t)	150–180	N/A	182	N/A

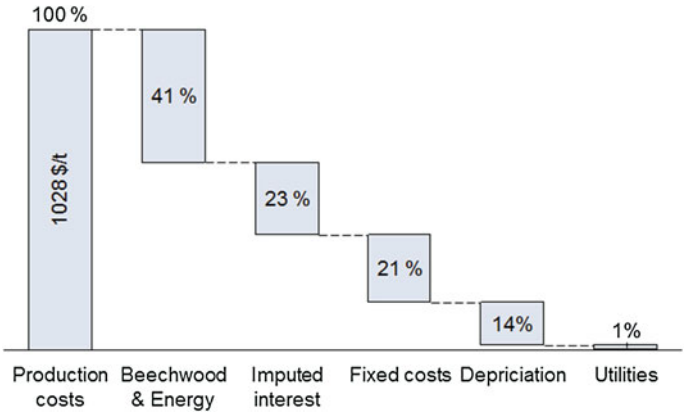

Fig. 7.11 Cost breakdown for methanol production (450,000 t/a) from biomass (wood cost assumed to be 75 €/t_{atro}) [21]

Netherlands. A total capacity of 200 kt per year of methanol is produced partly from crude glycerine, which is a residue of the biodiesel production. Due to the double-counting regulations for biofuels of the second generation, this is economically possible against the other feedstock natural gas (depending, however, on the price relation of the two feedstocks). In Sweden, a biomass-to-methanol plant with a capacity of 100,000 tpy methanol, based on gasification technology from Uhde (Prenflo, see Sect. 4.4.6.7), is scheduled to start up in 2013 (Fig. 7.11).

In summary, the production of methanol from manures or wastes (e.g. municipal solid waste) is possible at a 50–80 % higher production cost than methanol production, which is based on fossil fuels. In light of these results, it becomes clear that methanol based on bioenergy crops can hardly be economically attractive unless process improvements or lower feedstock prices allow the production at substantially lower total cost or subsidies and regulatory pressure change the economic preconditions.

When additional savings due to omitted costs for the disposal of wastes or potentially increasing feedstock costs for fossil fuel–based methanol are considered, the production of methanol from waste biomass may already be an economically attractive option. In contrast to the production of first-generation

$$CO_2 + 3H_2 \longrightarrow CH_3OH + H_2O \qquad \Delta H_{298K} = -50\,kJ/mol$$

Scheme 7.3

biofuels, such as ethanol from sugar- or starch-based feedstock, the production of methanol via gasification of wood or energy crops can decouple a linkage to a dependency of biofuels to food crops.

7.8 Recycling of Carbon Dioxide to Methanol

The vision of Friedrich Asinger that "carbon dioxide could become a valuable feedstock as soon as fossil fuel resources become scarce, expensive or even depleted" [22] has recently been rediscovered and refined by numerous scientists. For example, Nobel Laureate George Olah proposed "that it is reasonable to consider the methanol economy as a practical and sensible approach to eventually replace fossil fuels. It can provide a feasible and safe way to store energy, to make available a convenient liquid fuel, and assure mankind an unlimited source of hydrocarbons, while at the same time mitigating the dangers of global warming owing to the greenhouse effect of carbon dioxide" [23].

As mentioned before, methanol can be synthesised from carbon dioxide via hydrogenation (Scheme 7.3). If the conversion of carbon dioxide is considered in order to remove carbon dioxide from the atmosphere, the hydrogen that is used for the hydrogenation cannot be prepared via steam methane reforming or coal gasification. These processes emit even more carbon dioxide in the hydrogen generation than is consumed in the methanol synthesis.

A suitable alternative for the production of hydrogen is water electrolysis, which has a significantly lower carbon footprint than steam methane reforming and coal gasification, if the electricity that is used originates from renewable sources.

A few demonstration plants are currently in operation to study the conversion of carbon dioxide to methanol. For example, Mitsui Chemicals has inaugurated a pilot plant with an annual production capacity of 100 t of methanol in 2009 [24]. Additionally, Carbon Recycling International constructed the first commercially operating methanol plant using hydropower and carbon dioxide in Iceland, with an annual capacity of 40 kt; it will be operational by 2013 [25].

To date, little attention was paid to the assessment of the economical boundary conditions of methanol synthesis from carbon dioxide and renewably produced hydrogen. Therefore, a model for the synthesis of methanol from carbon dioxide and hydrogen from electrolysis was composed. A recent study by Smolinka and coworkers [26] dealing with the generation of hydrogen from renewable energies was used as a basis for estimating the hydrogen production costs. The authors have developed different scenarios that include improvements of electrolyser technology. In the following, two scenarios will be examined. In the first scenario, continuous operation of a state-of the art alkaline electrolyser is considered; it was estimated that

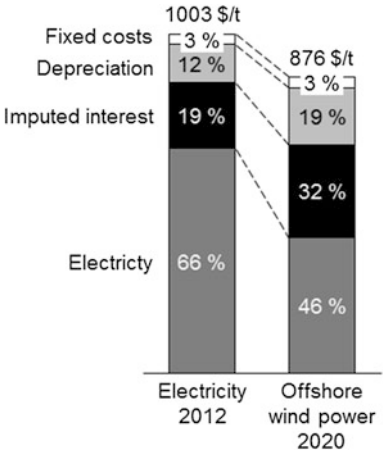

Fig. 7.12 Methanol generation cost from different renewable power scenarios

Table 7.4 Economic boundary conditions and estimated hydrogen production cost for electrolysis, according to Ref. [26]

Scenario	A	B
System efficiency (%)	78.7	82.3
Full load hours (h)	8,000	4,000
Investment costs (€/kW)	1,000	8,00
Interest rate (%)	10	10
Depreciation time (a)	15	15
Cost of electricity (€/kWh)	0.0625	0.03

electricity is available at $0.0625/kWh. Given the stoichiometry of the methanol synthesis from carbon dioxide and hydrogen, 187.5 kg of hydrogen is needed for the production of 1 tonne of methanol at full conversion efficiency (Fig. 7.12) (Table 7.4).

The second scenario includes an electrolyser with improved system efficiency and lower investment costs, which is likely to reflect the development level of alkaline electrolysers at the end of the present decade. For the second scenario, intermittent utilisation of offshore wind power with 4,000 full load hours was assumed, reflected by a lower capacity utilisation of only 46 %. Taking into account massive increase in offshore wind power capacity, lower electricity costs of only $0.0375/kWh were assumed.

The technology to convert hydrogen and carbon dioxide to methanol is comparable to that of a steam methane reformer. To extract the CO_2 from flue gas of a power plant, clean it, compress it, and transport it will add an additional charge of at least 40€/tonne of methanol to the raw material costs if one considers state of the art technology for a large-scale gas phase methanol synthesis plant excluding the cost of a steam reformer. Therefore, methanol synthesis from carbon dioxide will not be competitive with conventional methanol synthesis from fossil fuels or waste biomass at current cost levels.

Even if additional economic benefits, such as allowances for regulating energy and carbon credits are considered, significant improvements of electrolyser technology will be needed (both in terms of investments costs as well as in efficiency) to significantly lower the production cost of methanol via this technology. It must be recognised, however, that the horizon for this simulation goes until the year 2020, which implies that only technologies that are presently available and/or close to commercialisation can be used. In contrast, Chap. 8 deals with a timescale until 2050, allowing further new developments and cost reductions to be assumed.

Another situation may arise if methanol-blended fuels are adopted, such as in China or in the United States. When comparing the cost of methanol against gasoline as shown in Fig. 7.1, it becomes apparent that at the present (and the future expected) high oil prices (see Fig. 7.6) in the range of $100/barrel in 2013 and more, the combined production of methanol based on a feedstock combination of natural gas at approximately $5/mmBtu (3.8 €/GJ) and additional streams of hydrogen from renewable energy and waste CO_2 from power plants are competitive with traditional gasoline from fossil resources. For more details, see Chap. 8.

7.9 Conclusion

In this chapter, the production costs of methanol with various technologies was assessed. However, the production cost for each technology varies significantly with respect to raw materials, location, capacity, and process technology. At present, raw material prices and investment costs are in favour of gas-based technologies in the Americas and the Middle East, where so-called stranded gas and/or shale gas in resources are available. In contrast, coal-based technologies are more attractive in areas such as China.

Among the renewable-based technologies, the conversion of waste to synthesis gas via gasification is the most competitive technology, whereas methanol synthesis from carbon dioxide with hydrogen from water electrolysis suffers from the huge investment costs of the electrolyser. Therefore, the storage of renewably produced electricity as methanol, which could be used as a fuel for transportation or as chemical feedstock, will be an attractive option once investment costs of electrolysers can be significantly reduced and electricity from renewable sources is constantly available at low costs.

References

1. P.J.A. Tijm, F.J. Waller, D.M. Brown, Methanol technology developments for the new millennium. Appl. Cat. A **221**, 275–282 (2001)
2. Methanol plants keep getting bigger, Nitrogen + Syngas 316, March-April 2012, pp. 50–61
3. L. Connock; Grand designs, N + S 297, Jan–Feb 2009, pp. 40–55

4. R. Esquivel, Coal to methanol design report. San Diego, 2008, http://maecourses.uscd.edu/eng124/rpts/gp1_final.pdf
5. I. Wender, Reactions of synthesis gas. Fuel Process. Technol. **48**, 189–297 (1996)
6. P.L. Spath, D.C. Dayton, Preliminary screening—Technical and economic assessment of synthesis gas to fuels and chemicals with emphasis on the potential for biomass-derived syngas, Technical Report, 2003, NREL/TP-510-34929
7. M.V. Twigga, M.S. Spencer, Deactivation of copper metal catalysts for methanol decomposition, methanol steam reforming and methanol synthesis. Topics Catal. **22**(3–4), 191 (2003)
8. W. Hilsebein, J. Blaurock, Constructing a MegaMethanol® plant, Start to Finish, Houston, 14 October 2004
9. Nexant's ChemSystems PERP Report 07/08-2, Methanol, November 2008
10. Saudi Ministry of Petroleum
11. E. Schwarz, BASF SE, Coal to chemicals. Fachgespräch Kohle, BMBF, Berlin 18.11.2011
12. D. Johnson, Global methanol market review June 2012, IHS Inc http://www.ptq.pemex.com/productosyservicios/eventosdescargas/Documents/Foro%20PEMEX%20Petroqu%C3%ADmica/2012/PEMEX_DJohnson.pdf
13. J. Wagner, *Lurgi's MegaMethanol technology—most economical and reliable technology for the new generation of methanol plants*, presentation at Süd-Chemie's conference, Bahrain, 1st June 2004
14. Cancun Agreements to the United Nations Framework Convention on Climate Change, United Nations, Cancun, 2010
15. Kyoto Protocol to the United Nations Framework Convention on Climate Change, United Nations, Kyoto, 1997
16. EU action against climate change; Leading global action to 2020 and beyond, Eurpean Commision, 2009
17. How much bioenergy can Europe produce without harming the environment? EEA Report No 7/2006. European Environment Agency, Copenhagen, 2006
18. IEA, Key world energy statistics 2009, http://www.iea.org/statistics/
19. A.P.C. Faaij, Bio-energy in Europe: changing technology choices. Energy Pol. **34**, 322–342 (2006)
20. A. Bandi, M. Specht, Gewinnung von Methanol aus Biomasse, ZSW-Zentrum für Sonnenenergie- und Wasserstoff-Forschung Baden-Württemberg, 2004, Stuttgart
21. K. Wagemann, Roadmap biorerfineries, German Federal Government 2012
22. F. Asinger, *Methanol—Chemie—und Energierohstoff* (Springer, Heidelberg, 1986)
23. G. Olah, Beyond oil and gas: The methanol economy. Angew. Chem. Int. Ed. **44**, 2636–2639 (2005)
24. Pilot Project investigates new methanol synthesis route Mitsui chemicals; Chemical ICO2 Immobilistion project. Report in www.HydrocarbonProcessing.com
25. K. Tran, O.F. Sigurbjornsson, That's why we should all go to Iceland. Tce **840**, 28–31 (2011)
26. T. Smolinka, M. Günther, J. Garche, NOW-Studie "Stand und Entwicklungspotenzial der Wasserelektrolyse zur Herstellung von Wasserstoff aus regenerativen Energien" Kurzfassung des Abschlussberichts, Fraunhofer ISE, FCBAT 2011

Chapter 8
Methanol as a Hydrogen and Energy Carrier

Ludolf Plass, Martin Bertau, Matthias Linicus, Ringo Heyde and Eric Weingart

8.1 Introduction

Energy sources in the future are a widely discussed topic, and many statements have been published recently by scientific societies and organisations. However, in most cases, an overall view on the topics of energy, fuels, raw materials, and climate is missing and only little attention is paid to the recycling of CO_2 for use as a raw material (e.g. for the synthesis of methanol), whereas much more emphasis is placed on carbon capture and storage [1]. Future energy systems will rely more and more on renewable energy (RE), such as wind, solar power, and biomass (Fig. 8.1).

RE today has a share in the overall installed power production in Germany of 18 %. This value is projected to increase to 35 % in 2020, to 50 % in 2030, and to a target value of 80 % in 2050. As a consequence, CO_2 emissions related to power generation need to be reduced by 80 %. As can be seen from Fig. 8.1, in 2025 the share of wind and solar photovoltaic (PV; in GW) as percentage of the overall installed capacity is estimated to reach 44 % in Germany (89 GW) and Spain (57 GW), 34 % in the United Kingdom (39 GW), and 18 % in the United States (225 GW).

L. Plass (✉)
Parkstraße 11, 61476 Kronberg, Germany
e-mail: dr.ludolf.plass@t-online.de

M. Bertau · R. Heyde · E. Weingart
Institute of Chemical Technology, Freiberg University of Mining and Technology, Leipziger Straße 29, 09599 Freiberg, Germany
e-mail: martin.bertau@chemie.tu-freiberg.de

M. Linicus
Air Liquide Global E&C Solutions c/o Lurgi GmbH, Lurgiallee 5, 60439 Frankfurt, Germany

M. Bertau et al. (eds.), *Methanol: The Basic Chemical and Energy Feedstock of the Future*, DOI: 10.1007/978-3-642-39709-7_8, © Springer-Verlag Berlin Heidelberg 2014

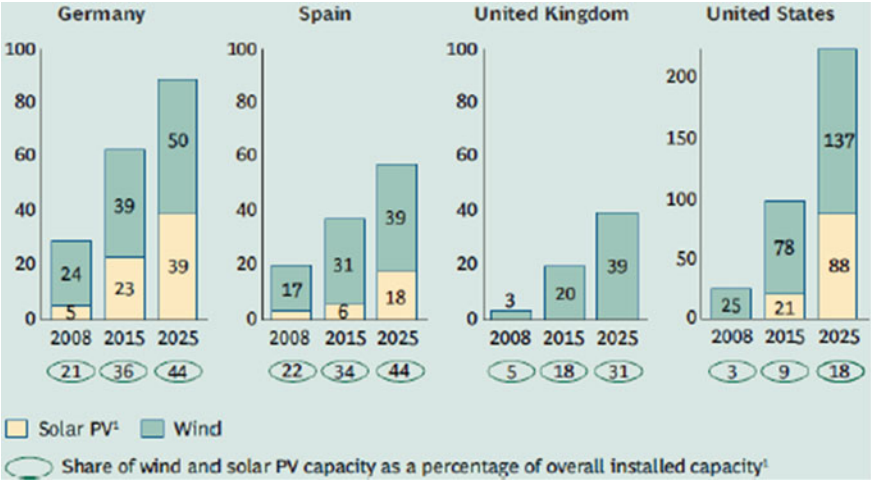

Fig. 8.1 Development of installed wind and PV power. (Courtesy of Boston Consulting Group [2])

In addition, the power consumption in Germany is intended to be reduced by 10 % until 2020 and by 25 % until 2050, while increasing power purchasing from abroad. As a consequence for Germany, this means a reduction in gross power production by 45 % until 2050.

The forecasts for power production and consumption in the period until 2050 differ considerably, however; the underlying assumptions vary strongly (e.g. different percentages of RE power, developments of the heat and mobility market, load management) and have a high degree of uncertainty. According to the different scenarios (see Fig. 8.20), the envisaged strong decrease of the gross power production by 45 % in Germany through 2050 may not be reached. Figure 8.2 shows the long-term perspective of the development of installed power and gross power production in Germany through 2050. The substantial differences between installed capacity and power production from the RE due to the high degree of unavailability are demonstrated.

The transition from a predominantly fossil fuel- and nuclear-based energy system to an RE-based energy system within the given timeframe of only 40 years presents tremendous technical, economic, and political challenges—particularly for the development of appropriate technologies. The RE power production from wind and sun is by nature highly volatile (see Figs. 8.3 and 8.4), but consumers need stable and precisely controlled power production. Therefore, one of the key challenges for safe and reliable power production from RE is to provide energy storage systems that can balance the fluctuations.

Grid simulations have shown that when the share of renewable power exceeds 35 %, storage systems are mandatory because conventional power stations can no longer balance these variations. According to an analysis by BCG [2], a compensation power in the range of 30–40 % of the average vertical grid load will be

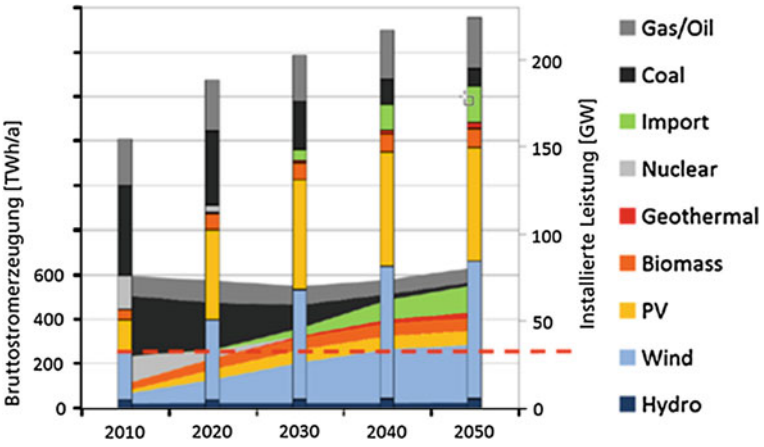

Fig. 8.2 Long-term prospective of installed power production (*Installierte Leistung*) and gross power production (*Bruttostromerzeugung*) in Germany. PV, photovoltaic. (Courtesy of the German Federal Ministry for the Environment, Nature Conservation and Nuclear Safety) [3]

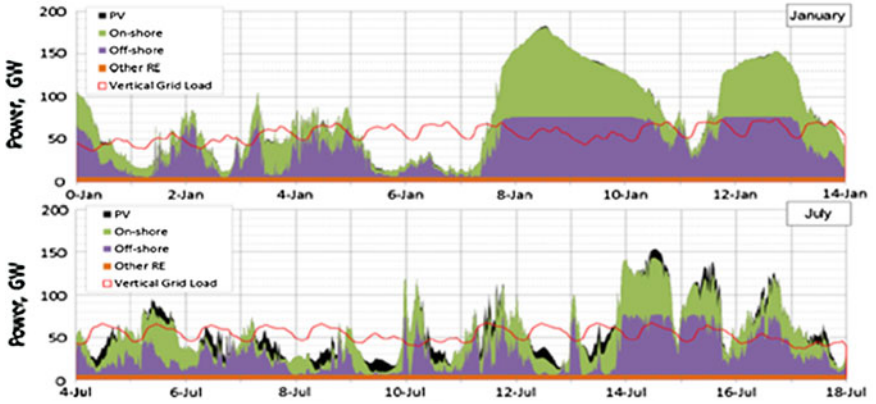

Fig. 8.3 RE production in scenario and vertical grid load (*red line*) for *January* and *July* in 2010 [4]

necessary to balance RE fluctuations, once the share of wind and PV power exceeds 20 % of the actual electricity generation. For the year 2025, the capacities required to compensate for fluctuating renewable resources are estimated to reach 39 GW in Germany (versus 22 GW in 2009), whereas Spain will need 30 GW, the United Kingdom 23 GW, and the United States 170 GW [2].

Figure 8.3 demonstrates the resulting high volatility of the vertical grid load as a consequence of the strong fluctuations of the RE power, as measured over 2 weeks in January and July 2010. Figure 8.4 visualises the resulting residual and surplus power production over the same time periods.

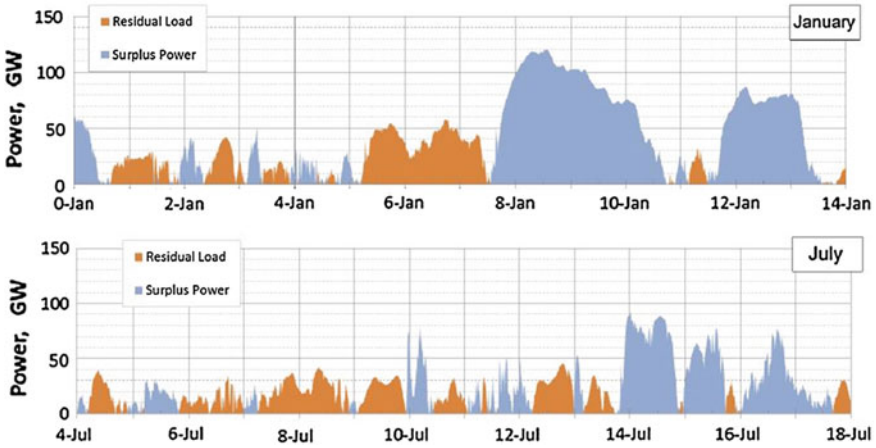

Fig. 8.4 Surplus power and residual power in winter and summer 2010 [4]

Because the technical, economic, and political boundary conditions can vary substantially within the next 40 years compared to today's strategy and planning, it is required that different development pathways and technologies for our future energy system are pursued, in order to provide options in cases of unforeseen changes or ruptures [5].

Some key figures illustrate the complexity and challenges of the energy system change. The overall installed capacity in Germany was 168 GW in 2010, of which 33 % was renewables. Power production was 621 TWh in total, of which RE was only 101 TWh (16 %). Wind power utilisation was only about 1,700 full load hours per year and solar was only 850 h/a, whereas consumption of nuclear power was 7,300 h/a, lignite power was 6,800 h/a, coal was 4,500 h/a, and natural gas (NG) was 3,200 h/a [7]. The nonavailability of RE was very high (75–94 %) compared to 10 % for conventional power plants. The percentage of wind power, which has baseload capability, is only 10–15 % in Germany. [8]

Current planning is to feed approximately 50 GW wind power and another 50 GW solar power into the grid by 2020 [9]. According to a study by Fraunhofer, by 2050 the installed capacity for wind will be approximately 80 and 65 GW for solar power (see Fig. 8.2) [10]. Such high and highly volatile power generation can only be integrated into a reliable overall energy system by coordinating several systems/components:

- Development of supraregional compensation capacity through interconnections of the grids of the European countries via international cooperation.
- Effective increase of demand-side management through smart grid development.

- Development of new flexible fossil power plants (preferably biomass- and/or gas-based combustion or IGCC) to manage peak demand and provide synthesis gas and CO_2 for methane and methanol synthesis plants.
- Efficient storage systems.

As outlined, fluctuating power generation constitutes the main challenge of RE sources, such as solar (see Fig. 8.5) and wind power. Therefore, energy storage technologies are necessary for periods with high power production and consumption. One established technology with high power efficiency (70–85 %) are the pumped hydro energy systems (PHES), but their capacities are limited. The storage capacity is approximately 40 GW [9], which represents approximately 2.3 % of the German average daily electrical power consumption—by far too low to meet the future challenges. Only Norway has a large PHES storage capacity (approximately 85 TWh), but the powerline capacity between Norway and Germany (approximately 1.4 GW) is by far too low against the 42–62 GW that will be required in 2050 [8]. As a consequence, wind power plants are shut down in times with surplus power production and fossil fuels have to be operated in times with power shortage, or even worse, surplus power is sold to other countries at negative prices. The estimated annual power export from Germany is 23 TWh in 2012, mainly PV power (see also Fig. 8.5) [11].

Figure 8.6 shows the development of different categories of necessary power generation in Germany through 2050. Due to the increasing RE power and the phasing out of nuclear power, the necessary base load capacity is more and more reduced and completely eliminated after 2040. The required capacities for medium load and peak load will increase strongly. After 2030, increasing amounts of strongly fluctuating surplus power of up to 40 GW in 2050 have to be managed, demonstrating the need for longer-term chemical storage systems.

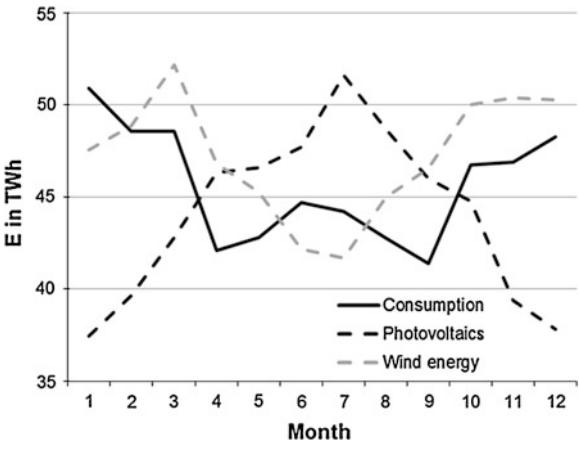

Fig. 8.5 Power consumption and production by PVs and wind (monthly data, Germany 2010). [6]

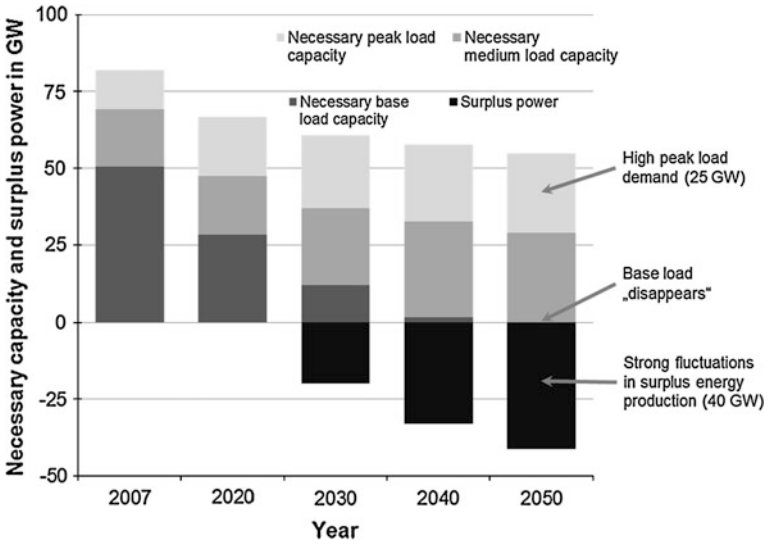

Fig. 8.6 Development of surplus power generation through 2050 [12]

An alternative could be provided by hydrogen generation from surplus electric power via electrolysis. Hydrogen would serve as chemical energy storage in this case:

$$2H_2O\ (l) \rightarrow\ 2H_2 + \ O_2 \qquad \Delta_R H^0 = +572\ \mathrm{kJ/mol}$$

This can only be the first step though, because hydrogen as a gas has a low volumetric energy density and is difficult to store. To avoid difficulties as mentioned before and outlined in more detail below, an alternative consists of further reacting the hydrogen in a consecutive reaction together with carbon dioxide to form methane or methanol:

$$CO_2 + 4H_2 \rightarrow CH_4 + 2H_2O\ (g) \qquad \Delta_R H^0 = -165\ \mathrm{kJ/mol}$$
$$CO_2 + 3H_2 \rightarrow CH_3OH\ (g) + H_2O\ (g) \qquad \Delta_R H^0 = -49\ \mathrm{kJ/mol}$$

This approach benefits from recycling CO_2 (carbon capture and utilisation) in contrast to final disposal (carbon capture and storage), particularly because methane and methanol exhibit significant higher volumetric energy densities than hydrogen. In the next sections, the different processes for chemically stored energy will be discussed and compared. All conversion efficiencies are based on the higher heating value (HHV).

Transforming the energy system to more renewable forms of energy implies that energy will predominantly be generated as electric energy, which is difficult to store directly on a large scale. High amounts of energy are most effectively stored in the form of chemical compounds, like all our fossil energy reserves of today are storing solar energy from millions of years ago. Figure 8.7 compares the weight-specific storage densities of different energy storage options in comparison to

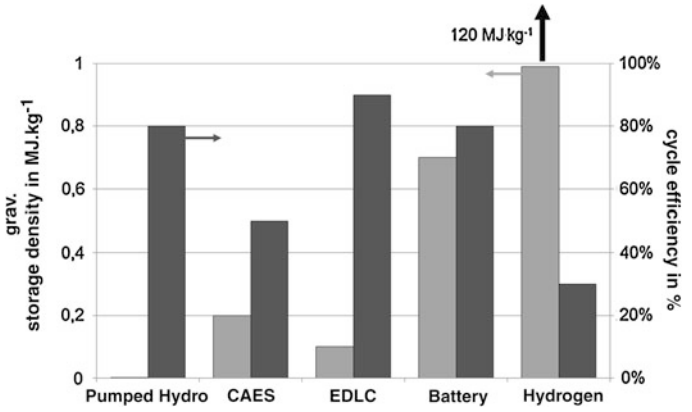

Fig. 8.7 Comparison of approximate gravimetric storage densities and cycle efficiencies of different energy storage technologies, using hydrogen as the example for chemical storage. *EDLC* Electrochemical double-layer capacitor; *CAES* Compressed air energy storage. Current CAES capacity in Germany is approximately 3.5 GW. There is some upward potential for CAES if the invested compression energy can be recovered; however, this has not been realised so far in present-day installations. Storage capacity of PHES depends on height differences (here 200 m). Values for batteries are referred to Li-ion batteries. Cycle efficiency of batteries depends on charging and discharging currents [13]

hydrogen as chemical storage. The main result from this graph is that, among all variants, the chemical bond allows for realisation of the highest energy storage density. It has to be taken into account, however, that according to Fig. 8.7 the unequalled high energy density of hydrogen only applies to cases in which it is present as a liquid. Yet, in practice hydrogen is typically handled and transported as a gas only. Consequently, any efficiency calculation merely relying on energy content, as given in Fig. 8.7, will necessarily ignore those additional energies required for compression (up to 300 bar) as needed for transport, storage, and decompression. In fact, a substantial amount of heat has to be invested in order to avoid freezing of the gas during decompression.

Owing to the high volatility and nonavailability, a power generation in Germany that is purely based on renewables would require a storage capacity of 20 TWh in 2040, assuming that 50 % of the surplus power has to be stored [6]. Another scenario estimates, based on the maximum residual power of 60 GW in 2009 for time spans of 14 and 21 days, a storage capacity of approximately 17 and 25 TWh_{el}, respectively [14]. However, for a longer-term storage (i.e., seasonal storage of energy over weeks or months), an even considerably higher storage capacity would be needed, which in Germany cannot be provided by conventional storage systems such as lakes. To visualise the dimensions, such a PHES system would need to comprise not less than the volume of the Lake of Constance at an altitude of 800 m [14]. In reality, there is negligible water storage capacity (40 GWh today) and negligible additional potential for expansion [15].

As outlined above, compressed air energy storage (CAES) (efficiency 50–60 %) could provide up to 3.5 TWh storage capacity in Germany [9]. To reach the higher efficiency of 60 %, the heats of compression and expansion need to be recovered. However, such technologies are in an early stage of development. Thus, this technology could only contribute, but not solely provide, a comprehensive solution for longer-term storage of energy.

The summarised German storage capacity is sufficient to maintain a base load of 60 GW for no longer than approximately 30 min [9]. As a consequence, there is no way of escaping the necessity of installing large chemical energy storage capacities, be they liquid and/or gaseous energy carriers.

Based on current technologies and cost figures, the DB study gives an estimate of the range of the costs for different storage options: [9]

PHES	3.3 €ct/kWh
CAES	4.1–5.2 €ct/kWh
Hydrogen storage	10 €ct/kWh
Methane	15 €ct/kWh

These costs deserve comparison with conventional electricity generation costs. In Germany, this is approximately 4.2 €ct/kWh at present. The average power generation cost in Germany from January 2008 to October 2012 was 4.9 €ct/kWh at the German power exchange. The European average for the same period was 5.3 €ct/kWh. The highest prices were paid in Italy (7.3 €ct/kWh), Great Britain and Switzerland (5.8 €ct/kWh), with the lowest in Norway (4.2 €ct/kWh and Spain (4.7 €ct/kWh) [4, 16].

Figure 8.8 shows the development of electricity prices for customers from industry over the past 6 years. It is easy to recognise that German energy prices

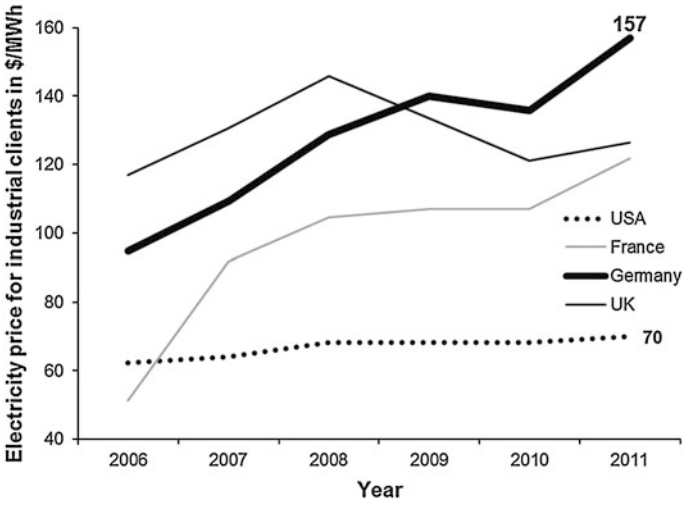

Fig. 8.8 Electricity prices for customers from industry (USD/MWh) [16, 17]

have brought the domestic industry into a conceivably unfavourable situation in global completion for markets. This is a clear argument for storage of regenerative energies as methane or methanol.

In Germany, the consumer has to pay additional 16 €ct/kWh for taxes and duties and the power suppliers add a profit margin of approximately 8–10 €ct/kWh [18]. Although this situation is completely adverse from that in other countries that do not add such high duties to pay for the turnaround in energy policy as in Germany, it is obvious from these figures that energy storage costs surmount energy generation costs by far. Thus, in the present situation among the conventional energy storage options only, PHES will be able to compete with conventional power generation. Among the RE power variants, there is no competitive solution at hand.

Nevertheless, it has to be noted that politically enforced implementation of costly energy storage solutions may provoke deindustrilisation as well as have socioeconomic implications. The same applies to artificially elevated market price levels, as in Germany. Whenever RE is intended to replace conventional energy generation, there is, for these reasons, no alternative to developing appropriate technical solutions providing stored energy at competitive prices. In other words, the energy storage issue has to be solved the day conventional power generation is switched off. In addition, the large-scale utilisation of shale gas in the United States has led to a considerable replacement of coal-fired power generation—emitting less CO_2, fewer pollutants at lower costs. Ultimately, this is the threshold that all concepts of RE generation will have to match. Hence, energy storage in form of methane or methanol is an important step into this direction because both compounds are easily combinable with fossil methane usage, either through the direct use of methane or via synthesis gas generation of methanol [19].

The overall costs for conventional storage capacities to be newly erected in Germany in the next 20 years are estimated to amount to 30 billion €. Because chemical storage systems will be needed on a much larger scale in the period following 2030 (see Fig. 8.6), electrochemical technologies are required to have made substantial progress regarding efficiency and cost reduction.

Figure 8.9 outlines the specific storage capacities and discharge times of various storage technologies:

- Storage capacity in Germany's existing NG grid is approximately 21 billion Nm^3 storage volume, equivalent to approximately 230 TWh_{el}; including present and future salt dome storage caverns, the capacity will be increased in the foreseeable future to 36 billion Nm^3, equivalent to 400 TWh_{el} [8].
- Long-term storage implies a storage time/capacity > 2 months.
- Energy density of CH_4: 33 MJ/Nm^3.
- Energy density of H_2: 10 MJ/Nm^3.
- Efficiency power–gas–power is approximately 30–40 % (Combined heat and power efficiency, see Fig. 8.17).
- Efficiency of water-power (PHES) is approximately 80 %

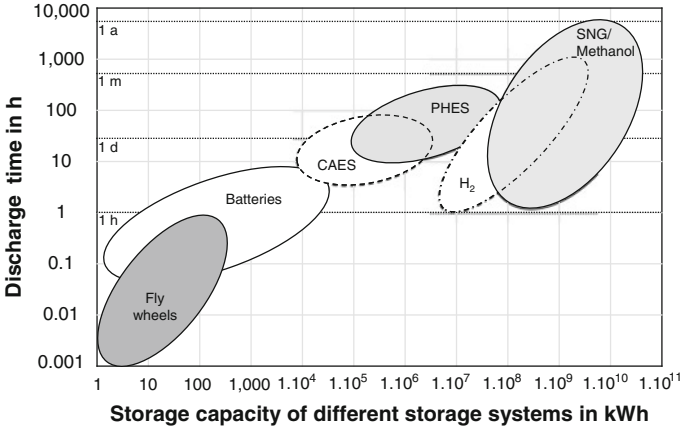

Fig. 8.9 Energy storage systems: Storage capacities and discharge time of different technologies [20]. *CAES* Compressed air energy storage; *PHES* Pumped hydro energy systems; *SNG* Synthetic natural gas

In summary, as shown in Fig. 8.9, only H_2 and CH_4 are suited for storage capacities in the TWh region. However, methanol also is a candidate for long-term storage, as will be further outlined below.

Table 8.1 gives a more detailed overview on energy densities and heat values of different energy storage media. For purposes of comparison, the table includes the values for established fuels.

Figure 8.10 shows a simplified roadmap of different pathways from RE sources to storage compounds as well as to electricity. The dashed arrows indicate

Table 8.1 Energy densities and heat values of several energy storage media and fuels [21]

Storage medium	Energy density (MJ/kg)	Lower heat value* (MJ/kg)	
Water power	0.0014		
Lead accumulator	0.11		
Lithium ion accumulator	0.5		
Wood	18.0–19.0	14.4–15.8	
Lignite	20.0–28.0	19.6–22.0	
Hard coal	29.0–32.7	27.0–32.7	
Methanol	22.7	19.9	
Ethanol	29.7	26.8	
Gasoline	42.7–44.2	40.1–41.8	
Diesel	45.4	42.5	
Methane (25 °C)	55.5	50.0	
Hydrogen	143.0	121.0	
		1 bar, 25 °C	143
		200 bar, 25 °C	93
		Hydride fuel tank	1
Nuclear power	3,801,600	./.	

* *LHV* Lower heat value $= w - \Delta_v H^0$ (H_2O) [45 kJ/mol (25 °C)]

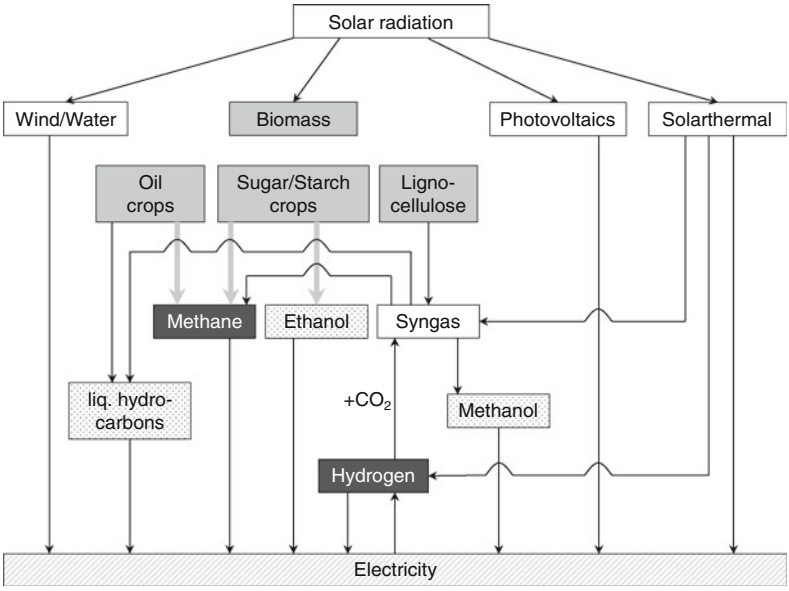

Fig. 8.10 Simplified schematic of different pathways from solar radiation to storage compounds and to electricity [13]

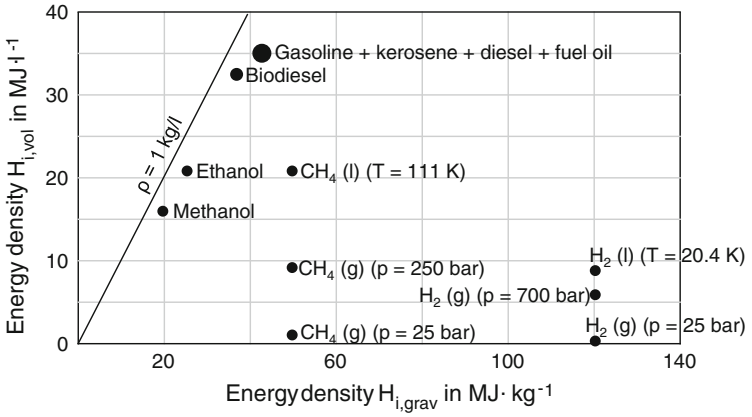

Fig. 8.11 Comparison of the energy densities of different chemical energy carriers on a volumetric and gravimetric scale [22]. The chart shows that the "conventional" energy carriers (gasoline/diesel/kerosene) have the advantage of a very high energy density by volume (and by weight), whereas those of ethanol and methanol merely amount to approximately 50 %. However, they have the advantage of being liquids, which are much easier to transport and store compared with gaseous energy carriers. Methane and hydrogen need very high pressure storage systems in order to make substantial amounts of energy available, such as for mobility applications

pathways for such compounds, which preferably may not be reused for power generation but rather directly combusted in engines in order to generate mechanical energy. However, it should be noted that also the combustion of methanol in gas turbines (MTPower) has been studied by leading gas turbine manufacturers together with Lurgi, with very positive results:

The high losses during conversion from renewable power to secondary energy carriers and repowering constitute a general disadvantage. In addition, there are a variety of other criteria, including the following:

1. Environmental criteria (pollution and climate gas generated during production and combustion).
2. Diversity and flexibility of the energy carrier during transport and use.
3. Economic aspects (depending on raw material availability and price, as well as necessary process cost of conversion).
4. Compatibility with existing infrastructure.

8.2 Production of Storage Molecules

8.2.1 Renewable Hydrogen Production

At present, the most important commercial source of hydrogen is NG, because its generation from electric power through electrolysis is too expensive. However, using RE during times with surplus power—which is otherwise sold at negative prices abroad—could provide an economically more attractive alternative.

At present, there are two major processes in operation (Fig. 8.12 and Table 8.2; see also Sect. 4.5.3).

- Alkaline electrolysis (AEL)
- Proton exchange membrane electrolysis (PEMEL)

The differences between the two processes lie primarily in the energy conversion efficiencies, partial load properties, and the investment costs per kWh. For fluctuating RE, the specific cost per kilowatt-hour is the most important factor: AEL has a conversion efficiency of about 80 % (due to liquid water as reagent), but its partial load flexibility is limited (>40 % load). The more expensive PEMEL has the same conversion efficiency but is much more flexible regarding partial load (>5 %) and overload (up to 300 % for approximately 1 h) [24]. Table 8.2 shows a comparison of key parameters of AEL and PEMEL technologies [8].

H_2 has the advantage of high gravimetric energy content but also the problem of very low volumetric energy content, which is only about one-third of that of methane. Mobile applications need H_2 storage under high pressure, typically at 700 bar (see Fig. 8.11). Consequently, the cylinders are heavy and often cause packaging problems. In addition, hydrogen compression consumes approximately

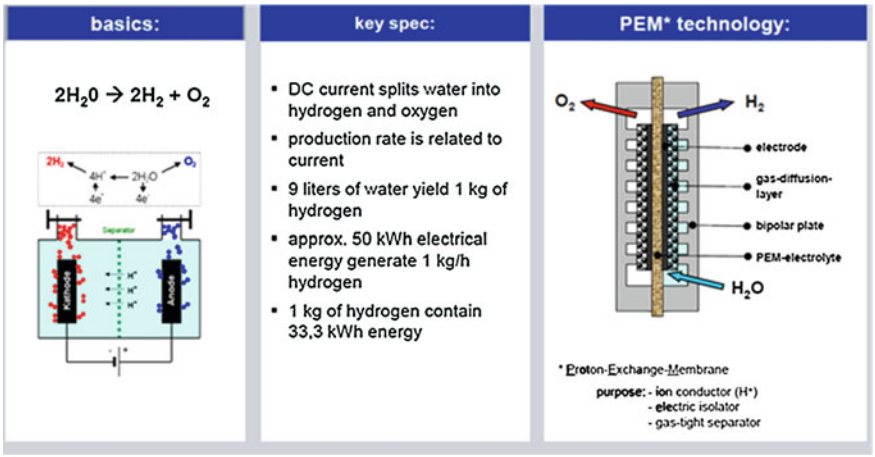

Fig. 8.12 Comparison of alkaline and PEMEL. (Courtesy of M. Waidhas, Siemens AG) [23]

Table 8.2 Comparison of AEL and PEMEL technology [8]

Technology	Alkaline	PEMEL
Maximum size/module in Nm^3/h	760	30
Pressure (bar)	<30*	<30*
Temperature (° C)	50–80	50–80
Efficiency (atmospheric pressure, in %)	~80	~80
Power consumption (atmospheric pressure, in kWh/m^3)	4.1–4.6	>4.3
Combing with RE	Limited	Highly flexible
Investment cost (€/kW, potential)	800–1,500 (500)	2,000–6,000 (800)
Overload potential	0	Up to 300 % for 1 h

* Higher pressures are possible in principal

15 % of its energy content. Higher pressures are not favourable because storage capacity increase is not linear with elevated pressure. H_2 burns clean, generates only water as a reaction product, and can be reused in gas turbines (although they have to be adopted for the specific combustion conditions of hydrogen and tested on a commercial basis, as well as the fuel cells, for variable power production). The overall cycle efficiency is approximately 30 %.

According to DVGW Arbeitsblatt G 262, up to 5 % H_2 can be added to the gas pipeline system immediately; in the midterm, a fraction 10–20 % was discussed, thus making use of existing storage capacity of the NG pipeline network [25]. However, the maximum concentration of hydrogen is 2 % for NG–fueled cars (DIN 51624). Research is presently underway to study the maximum admixing of hydrogen with respect to gas infrastructure and gas utilisation. The German network has a length of approximately 500,000 km, an overall storage capacity of 230 TWh_{el} NG, and a transport capacity of 1,000 TWh_{el}/a, allowing 3 TWh H_2 to be stored at any point of time—equaling 15 TWh_{el} that can be stored over a 1 year

period. The transport capacity of the network is comparably high: 18 GW for a pipeline with 1 m in diameter, whereas high-voltage lines do not exceed 3.6 GW transport capacity [26].

In Germany, four very strict and specific regulations regarding the quality/purity of the EE hydrogen have to be met. Also, the transport capacity of the pipeline at the feedpoint and the actual load (summer/winter) can limit the real storage capacity significantly—from the average value of 5 % to a more conservative average of 1.5 % [26]. To minimise the overall losses in the process chain, hydrogen should be added directly to the pipelines until the limit of admixing; any additional surplus power should be converted to methane or methanol.

Some significant disadvantages become effective when elementary hydrogen is used for energy storage and transport: [27]

- Hydrogen storage requires either very high pressure or very low temperature (−250 °C). Both options are technically viable, but the public is not prepared for handling challenges like these.
- Hydrogen compression consumes an energy equivalent to 15 % of the heat value, thus considerably reducing storage capacity while rendering hydrogen storage technically more complex and expensive.
- A longer storage time in salt caverns will saturate the hydrogen with water; also the salt content can cause pollution of the NG extracted from the caverns.
- There is no established H_2 infrastructure outside of the chemical industry.
- Hydrogen causes embrittlement of a manifold of metallic materials.
- Through its comparably high solubility in many metals, as well as its high diffusion coefficient in many materials, hydrogen transport and storage is necessarily accompanied by material losses.

For these reasons, gaseous hydrogen is hardly suited for medium- to long-term storage of electrical energy. However, a significant advantage of hydrogen is its property of being the only carbon-free energy carrier, for which reason there is no contribution to CO_2 emissions.

- If renewable electrical energy is intended to be stored in the medium- to longer-term (days to months), as envisaged by hydrogen production through electrolysis, then additional process steps have to be taken into consideration:
- Hydrogen storage on an energy-carrying material, from which the gas has to be released prior to use (research work is underway, but larger-scale industrial application is still far away).
- Hydrogen conversion to methane and/or methanol, for which purposes CO_2 as a carbon source is readily available worldwide.
- However, that these options require hydrogen to be partially consumed in order to fix the oxygen bound to carbon in the reverse water–gas shift reaction.

Stolten et al. [4] have simulated an energy change scenario to reduce CO_2 emissions in Germany by 2030 by 55 % while producing hydrogen from surplus RE as energy storage for times without renewable power production. The resulting

hydrogen production would be 5.4 Mt/a, equivalent to 257 TWh_{el}. This is an amount sufficient to feed 29 MegaMethanol plants producing 5,000 tpd.

For storage of substantial amounts of H_2, large-scale salt caverns are a matter of current discussion. For NG, this is an established technology. The existing NG storage capacity in Germany, for instance, is 21 billion Nm^3, which equals approximately 25 % of the yearly consumption of approximately 81.3 billion Nm^3 (895 billion kWh) [28]. Salt dome caverns with a capacity of 21 billion Nm^3 are in operation (8 billion Nm^3), planning, and construction (21 billion Nm^3). The costs for such a scenario (55 % CO_2 emission reduction) through the year 2030 were estimated at approximately 110–126 billion €. Assuming one wished to install a storage capacity for a 60 day reserve, this would require approximately 90 TWh_{el} of electricity for hydrogen generation (i.e., 16 MegaMethanol plants). In terms of storage capacity in salt domes, this would require not less than twice the existing caverns' capacity [6]. The feasibility of hydrogen storage on a large scale in salt domes has been demonstrated in refineries in the United States, however [29].

Today, 48 % of hydrogen production occurs via steam reforming of methane, 30 % is formed as a byproduct from refinery processes, and 18 % stems from coal gasification. Not more than 4 % is generated through water electrolysis. More recent approaches pursue the strategy to produce hydrogen via surplus power from renewable resources. An example is a pilot plant operated by Enertag in the Uckermark county in eastern Germany, which combines wind power, biogas, and electrolysis to produce 120 Nm^3/h of pure hydrogen [30]. However, a severe drawback for hydrogen production from RE is the high investment costs for electrolysers (see Table 8.2). In addition, current technology has to be further developed towards tolerating unstable, largely varying operating conditions. Thus, the overall hydrogen generation and storage economics are questionable, particularly under variable load conditions [31]. Alternative production routes study the direct thermal splitting of water, but there are still too many technical hurdles to overcome, particularly because of the extremely high reaction temperatures [32].

8.2.2 Renewable Methane Production

The reaction of H_2 and CO_2 to methane was discovered at the beginning of the 20th century by Sabatier and Senderens (the Sabatier process) [33]. This reaction is industrially applied in coal gasification processes, but it has not been employed commercially with H_2 from electrolysis and CO_2 from the atmosphere or flue gas until now. However, in view of both continuously increasing prices for NG and the overproduction of RE, research projects are in progress to store the latter in form of methane. A pilot plant for the production of synthetic natural gas (SNG: 90 % CH_4, 5 % H_2, 5 % CO_2) with H_2 from electrolysis and CO_2 from the air was put into operation in late 2012 in Stuttgart, Germany, with a power-to-methane-to-power (pmp) efficiency of 16 % [34]. The first semicommercial 6 MW plant will be erected 2013 in Werlte, Germany by Audi AG with a pmp efficiency of up to 21 % [35].

With respect to 78 % being the maximum energy conversion of hydrogen to methane, the overall conversion efficiency of the methanation process is expected to reach approximately 70 % [12, 36, 37].

The main advantage of methane is the existing infrastructure in many countries. The energy density is 3 times that of hydrogen and 26 times that of CAES. A severe drawback of this approach lies in the high loss of energy once stored in hydrogen, which amounts to approximately 25 % for the methanation reaction. Methane can be produced on different ways: (1) from fossil or renewable resources through gasification, (2) from CO or CO_2 via methanation, (3) from biomass by anaerobic microbial fermentation (see Sect. 4.5.3 in Chap. 4). It can readily be reused for power generation in gas turbines or fuel cells (SOFC).

In this context, a smooth transition from fossil to renewable infrastructure is matter of discussion. According to Sterner, the methanation concept offers a variety of advantages [38]. The German NG network has a substantial storage capacity of approximately 220 TWh_{el} at pressure levels between >130 bar for import lines and 70–80 bar for long-distance pipelines, 4–16 bar for regional distribution pipelines, and 0.5 bar in the cities [26]. Equaling a repowering efficiency (methane to electric power) of approximately 60 %, this results in approximately 132 TWh_{el} or a reach of 2 months at an unloading rate of 70 GW_{el}/month.

One has to bear in mind, however, that a pipeline system cannot be unloaded by 100 %. Corrected by the overall volume, the methane storage capacity of the German public pipeline system is 20 billion Nm^3 (i.e., 200 TWh_{chem}) [26]. Because of the characteristics of methane, displaying a much higher volumetric energy density in comparison to H_2, this storage form allows for establishing integrated methane utilisation concepts. The methane gas is not only suited for power generation but also for vehicle fuelling (transport) as well as heating of buildings. By means of steam reforming, it is a raw material for the chemical industry, too.

A major disadvantage of methane is its greenhouse potential, which is 25 times that of CO_2. Studies have shown that roughly 370,000 million m^3 of biomethane could be produced in the EU-27, compared to a NG consumption of approximately 81.3 billion Nm^3 in Germany [39]. Thus, a substantial fraction of the current European NG demand could be met by biomethane. Full lifecycle analysis studies have shown that biogas-to-electricity plants can achieve 60 % efficiency in cogeneration. These studies pay no regard, however, to issues of land use, monocultures of energy crops, and fertilisation (fossil based) thereof. Shifts from food crops to energy crops—and the effect of this on a national economy in terms of food supply—are hardly, if ever, addressed. Consequently, side factors such as energy input for crop cultivation bear substantial potential for optimisation [40, 41].

A special case of methane (SNG) production is the lignite gasification plant in North Dakota (USA) feeding up to 150,000 Nm^3 SNG/d to the pipeline system (See Sect. 4.4.6). Approximately 6,000 t/d of CO_2 separated from a Rectisol syngas cleaning are compressed to approximately 100 bar and transported via

pipeline approximately 300 km to the north where CO_2 is used in the local oilfields for enhanced oil recovery. Approximately 18 $/t are reimbursed for the CO_2 delivered. In comparing the repowering of H_2 against methane, Schüth came to the conclusion that on a basis of 1 kg hydrogen, either 20 kWh can be produced without any CO_2 emission, whereas hydrogen conversion to methane and subsequent combustion would result in 12.5 kWh and 5.5 kg emitted CO_2.

Methane has the advantage of being easily storable and existing infrastructures being available. Yet, the aforementioned 25 % energy loss for the methanation reaction constitutes a major drawback in all attempts to produce CH_4 from CO_2/H_2—that is, from renewable resources. Fossil fuel combustion (coal, oil, and natural gas) in power plants is expensive and results in high CO_2 emissions. In addition, plans to use fossil-fuelled power plants for covering peak loads only results in short run times, rendering this kind of power production uneconomic. As a consequence, subsidies are discussed. An alternative scenario will be discussed later on in this chapter. The high costs for hydrogen generation from renewables might be compensated to a large extent if the electrolysers were erected in central hydrogen generation plants very next to the caverns.

A different method is methane from biogas. The efficiency is quite the same as via gasification, but the plants can be much smaller and net CO_2 emissions are mostly avoided. However, translated to the scale of energy generation, biogas contribution can merely be an add-on; it would not be substantial. Table 8.3 compares the suitability of methane and hydrogen for long-time energy storage (several months) and names advantages and disadvantages of both approaches.

8.2.3 Renewable Methanol Production

Methanol is a liquid under ambient conditions, which can easily be stored, transported, and dispensed, similar to gasoline and diesel fuel. It can also be converted into fuel substitutes such as dimethyl ether (DME), a diesel substitute with a cetane number of 55. Alternatively, methanol can be converted into gasoline via the methanol-to-gasoline process or into diesel via the methanol-to-gasoline-and-diesel process, for instance. For these reasons, the term "methanol economy" was suggested, with the aim of characterising a future economy in which methanol replaces fossil fuels as a means of energy storage, ground transportation fuel, and chemical base material. In 1986, Friedrich Asinger proposed methanol as the energy and chemistry raw material of the future. In the 1990s, Nobel Prize winner George A. Olah started to promote the term "methanol economy" in order to make clear to everyone that there is a superior alternative to the hydrogen or ethanol economies so far proposed [43].

Like methane, the present production of methanol from H_2 and CO_2 is irrelevant on an industrial scale because of the price of hydrogen and the power for its production from water through electrolysis, respectively. Despite that, a few pilot plants were built in Japan (see Sect. 4.5). In Iceland, where cheap geothermal

Table 8.3 Comparison of methane and hydrogen for long-time storage of energy. (Adapted from [42])

	H_2	CH_4
Efficiency of	70–80 %	$H_2 \cdot 0.85 \sim 60 - 70\,\%$
– Production	Equal	Equal
– Power generation		
Infrastructure	(Additional gas)	(Replacement gas)
– Electricity	– Noncompatible	– Compatible
– Heat	– Noncompatible	– Compatible
– Traffic	– Noncompatible	– Compatible
Energy density (i.e., space requirement for storage)	10 MJ/Nm^3	33 MJ/Nm^3
CO_2 neutrality	Given	Given, where CO_2 stems from biomass, atmosphere, and nonenergetic CO_2 production
Safety	Not proven on the TWh scale	Proven on the TWh scale
Transformation costs	– Conversion of power → H_2 – Storage – Withdrawal of H_2 – Transport/pipelines	Injection only

power is available, the first commercial plant was built in 2011 with a production rate of 4,000 t of methanol per year [44, 45]. A second plant with a production rate of 100,000 t/a is in the process of planning [46]. The setup for the methanol synthesis is similar to the methanation process. Differences mainly arise from reaction design, reaction heat, and yield per pass, as compiled in Table 8.4.

The overall efficiency for power to methane has been determined as 62.0 % (based on 5 kWh/Nm^3 H_2 power consumption by the electrolyser) and 65.8 % for power to methanol [49]. Because power generation cannot be switched from fossil to regenerative energy from on one day to another, Cernol has proposed a combination of both types, in which different kinds of energy can contribute to varying degrees (Fig. 8.13) [50]. The combination of renewable power and fossil power seems to be, at least for a transition period, the best compromise between highly fluctuating (and therefore unreliable) renewable power and secured fossil power. As can be seen from Fig. 8.13, chemical storage is the core of this concept.

Canadian Blue Fuel Energy [51] plans to produce "renewable" methanol via green electricity from water power and CO_2 separated from NG. The resulting carbon footprint is substantially lower than that of ethanol from corn. Methanol has proven its suitability as fuel and fuel additive (see Sects. 6.3.1 and 6.3.2 in Chap. 6) and can be added to gasoline at almost any fraction.

Table 8.4 Comparison of methane versus methanol production processes

	Methane [47]	Methane (solar fuel) [34]	Methanol [48]
H_2:CO_2 ratio	4:1	79.5 %:20.5 %	3:1
$\Delta_R H^0$ (kJ/mol)	−131	−131	−50
η_{max} (%)	78	61.6[a]	85
Reactor design	Three phase	Packed bed	Packed bed
P (bar)	20	6	80
T (°C)	250	250	250
Catalyst	Ni	Ni	$Cu/ZnO_2/Al_2O_3$ (Süd-Chemie)
Yield per pass	40 %	NA	25 %
GHSV (h^{-1})[b]	2,000–3,000	4,000	10,500

[a] Overall efficiency with electrolysis to produce SNG with 90 vol% methane (according to Ref. [48])
GHSV Gas hourly space velocity; *NA* Not available

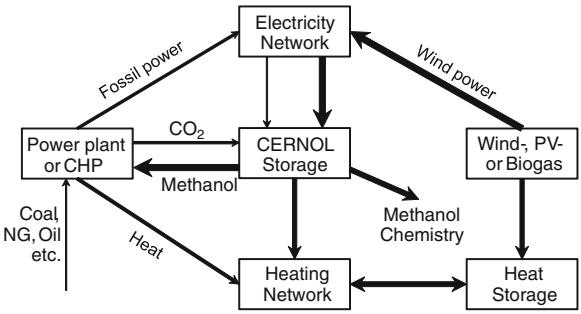

Fig. 8.13 Combination of conventional (fossil) and regenerative energy according to Cernol (adapted from Ref. [50]). *CHP* Combined heat and power; *NG* Natural gas, *PV* Photovoltaics

According to a GHGenius analysis of the product flow sheet, wind-power-based methanol provides an 84 % reduction in carbon intensity (14 g CO_2/MJ) versus a fossil-based gasoline (91 g CO_2/MJ) and a 77 % reduction versus U.S. corn ethanol (45–60 g CO_2/MJ), based on energy supply via NG. For water-power-based methanol, the carbon intensity would drop to 31 g CO_2/MJ. Methanol produced using average power from the grid in British Columbia, Canada provides a 65 % reduction in carbon intensity versus fossil-based gasoline and a 49 % reduction versus natural-gas-based U.S. corn ethanol [9].

To make use of the economy of scale, Bluefuel plans to develop a combination of a MegaMethanol plant and a Bluefuel plant (Fig. 8.14). Two streams of methanol are planned to be produced: (1) A very-low-carbon methanol stream with a carbon intensity of 14–32 g/MJ and (2) a MegaMethanol stream with a carbon intensity of 76 g/MJ. The product streams can be distributed either independently as gasoline blendstock or converted to gasoline via a methanol-to-gasoline process, for instance (see Sect. 6.4.1 in Chap. 6). The electrolysers (per Fig. 8.15) have a capacity of 650 MW_{el} for a yield of 1,485 tpd of methanol. Electricity is envisaged

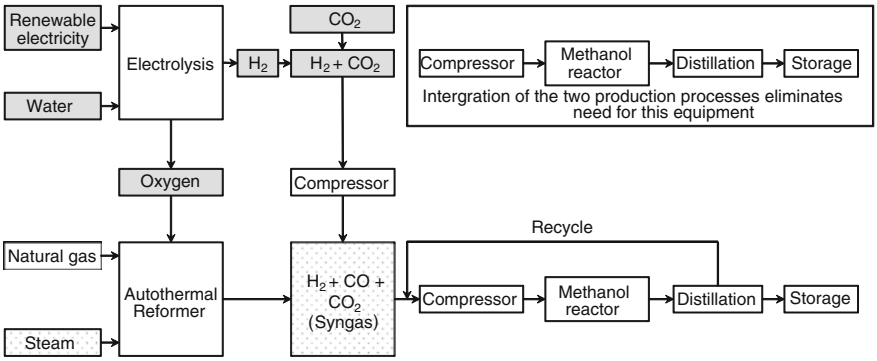

Fig. 8.14 Bluefuel scheme for a combined MegaMethanol plant and a Bluefuel renewable hydrogen/oxygen plant. (Adapted from Ref. [51])

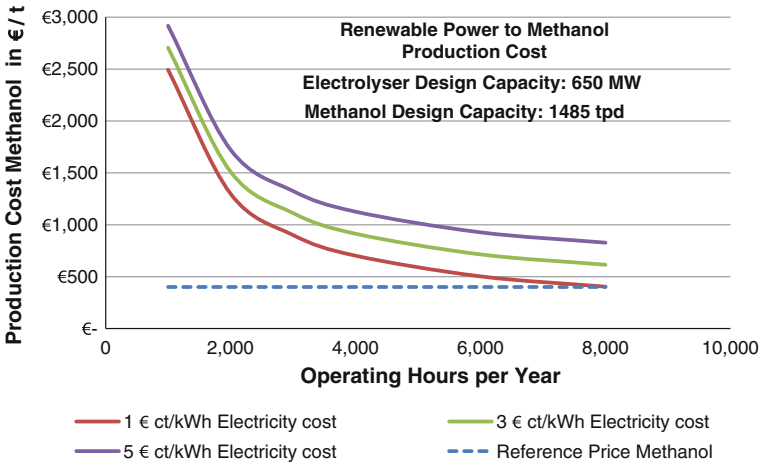

Fig. 8.15 Production costs of 'green' methanol as a function of operating time and water-power costs. A methanol market price level of $450/t is indicated (*dashed blue line*). (Courtesy of Air Liquide Global E&C Solutions)

to be provided by the British Columbia hydropower grid plus additional wind power.

The economic feasibility of this combination plant shows a methanol price below $900/t for operating times of more than 4,000 h/year and power cost between $0.03 and 0.05/kWh (see Fig. 8.15). A methanol market price level of $450/t (see Chap. 7) is indicated. At the current price levels of oil- and corn-based ethanol, methanol produced this way is cheaper on an equal energy basis, even if production costs sum up to $900/t, because HHV and carbon intensity have to be taken into account (see Fig. 7.1 in Chap. 7). The overall carbon footprint is lower, too.

Table 8.5 Physical state and volumetric energy of different energy carriers [21]

Energy carrier		Physical state	HHV (MJ/L)	LHV (MJ/L)
Methane		g, 1 bar	0.04	0.03
		g, 200 bar	11.1	8.9
		g, 350 bar	12.6	11.3
Methanol		l	17.9	15.8
Hydrogen	CHG	g, 1 bar	0.01	0.01
		g, 350 bar	3.3	2.8
Diesel		l	37.7	35.3
Gasoline		l	35.4	33.2
Gasoline (E10)		l	32.0	30.1
DME		l, 5 bar	23.4	21.3

HHV Higher heating value; *LHV* Lower heating value; *CHG* Compressed hydrogen gas; *E*10 Gasoline with 10 vol% ethanol and ROZ 95; *DME* Dimethyl ether

Figure 8.15 illustrates how power costs and operating hours have an effect on "green" methanol production costs. The average methanol price in 2012 was also used in Chap. 7 (350 €/t, approximately equivalent to $450/t).

8.3 Storage and Transport of Energy Molecules

The ability to store and transport the energy carriers methane and methanol, respectively, is the core topic in the overall process. The differences in physical state and volumetric energy density necessitate different requirements (Table 8.5).

For the distribution of methane and methanol, a well-developed NG and gasoline infrastructure is at hand. The first one consists mainly of pipelines distributing gas to the consumer. Methanol is mostly transported via trucks and tank wagons.

8.3.1 Methane Storage and Transport

Methane cannot be stored as a fluid under atmospheric pressure at room temperature. Instead, it is stored under a pressure of 100–200 bar in salt caverns, for instance. However, once injected, only 50–75 % of the gas can be withdrawn again. Hence, not more than this 50–75 % of gas is recoverable. In addition, one has to invest power for gas compression, which consumes approximately 4 % of the HHV of methane. Furthermore, energy has to be invested for cooling, while in the course of methane withdrawal the gas requires heating. In sum, these latter two processes consume another 15 % of the HHV, thus resulting in an overall efficiency of $\eta = 77$ % for storage, withdrawal, and transport over a distance of 500 km [49].

If gas is transported via pipelines, there is a pressure loss of approximately 1 % per 100 km, for which reason pipeline companies install compressor stations (the drive powers of which range between 1 and 30 MW). Typically, compressor stations are installed every 100–250 km. Gas compressions, as well as cooling and waste heat recovery, are major energy consumers. In sum, the energy uptake of one compressor station corresponds to approximately 0.2 % of the quantity of the transported gas (data from compressor station in Mallnow, Germany) [52].

8.3.2 Methanol Storage and Transport

Methanol storage is simple, like with other fuels. Because of the higher volumetric energy density compared to methane, less volume has to be stored and transported for the same amount of energy. Transportation via trucks and tank wagons requires 0.2–0.4 % per 100 km of the stored energy content (calculation with truck: 20 m^3 MeOH, 35 L diesel/100 km; with tank wagon: railcar [84 t] + ≤ 50 tank wagons [24 t wagon weight + 75 t MeOH] and 0.38 MJ · t^{-1} · km^{-1}, one-way). It has to be noted in this context that methanol, like methane, can easily be transported via pipeline grids, thus rendering it a useful medium to store and transport energy over long distances. Consequently, methanol is likewise suited for energy transportation via pipeline as an alternative to the electric power grid, as is in discussion for methane [53].

8.4 Energy Efficiency According to Application

Both methane and methanol are valuable compounds in the energy sector and base materials for the chemical industry. The main application in the energy sector is their use as fuel and as energy carrier for RE storage.

8.4.1 Fuel

Because a high volumetric energy density of the fuel is vital for use in vehicles, methanol as liquid has better properties than gaseous compressed methane, but both can be used as propellant:

1. Methanol in gasoline engines (directly and/or as methyl tert-butyl ether).
2. Methanol converted into DME in diesel engines.
3. Methane in NG vehicles.
4. Methanol in direct methanol fuel cells (DMFC) with an electric motor (see Sect. 6.5.2).
5. Methanol as hydrogen carrier in reformed methanol fuel cells with an electric motor.

The first three options do not require expensive adaptation of current vehicle technology, whereas fuel cell vehicles are not yet fully developed (Table 8.6). Figure 8.16 shows the relative theoretical ranges of each fuel calculated on the basis of 1 L diesel. Methane and hydrogen are compressed to 350 bar and DME is a fluid under a pressure of 5 bar. It should be noted that electric motors have better partial load properties than combustion engines.

Methanol has been used as fuel for decades, so its technical, operational, environmental, and safety characteristics in combustion engines are well explored. In 2011, approximately 17 million t of methanol (i.e., ~30 % of the global market) have been used in fuel and energy applications:

- Methyl tert-butyl ether
- Tert-amyl methyl ether
- Low direct blends (<3 %)
- High direct blends (M15, M60, M85)
- Biodiesel
- DME
- Fuel cells

Table 8.6 Conversion efficiency of different engines

Engine	η_{max} (LHV) (%)	Fuel
Gasoline engine	37	Gasoline, methanol
Diesel engine	45	Diesel, DME
Natural gas vehicle	42 [54]	Methane
RMFC + EM[a]	33 [55]	60 % methanol, 40 % water
DMFC + EM[a]	33 [56]	Methanol
Alkaline fuel cell + EM	71 [57]	Hydrogen

[a] Test phase

DME Dimethyl ether; *DMFC* Direct methanol fuel cells; *EM* Electric motor; *LHV* Lower heating value; *RMFC* Reformed methanol fuel cell

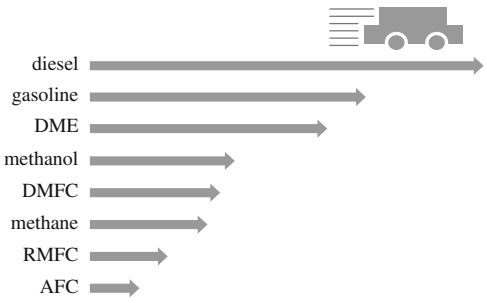

Fig. 8.16 Theoretical range of 1 L of a specific fuel in relation to 1 L of diesel. *DME* Dimethyl ether; *DMFC* Direct methanol fuel cell; *RMFC* Reformed methanol fuel cell; *AFC* Alkaline fuel cell

Table 8.7 Performance of General Electric gas turbine 109 FA in combined cycle mode with various fuels, 400 MW power

Gas turbine performance*	LNG	Distillate	Methanol
CC net output [MW]	385	394	394
CC net heat rate			
LHV [BTU/kWh]	6,083	6,743	6,079
HHV [BTU/kWh]	6,749	7,268	6,938
Gas turbine gross output [MW]	253	267	284
NO_x emissions at 15 % O_2 [ppm vol]	25	42	25
Water/steam injection [kg/h]	0	181	162

Heat rates as given in Ref. [60]

* 50 Hz Combined cycle, GE F-109A, 15 °C/59 °F

CC Combined cycle; *HHV* Higher heating value; *LHV* Lower heating value; *LNG* Liquefied natural gas

The main increase in worldwide methanol consumption from approximately 60 million t/a in 2012 to 95 million t/a in 2016 is considered due to methanol use as a fuel (increase from 20 million t/a in 2012 to 38 million t/a in 2016) [58].

8.4.2 Power Generation

Both methane and methanol can be used for power generation in combined cycle gas turbine plants, with conversion efficiencies of up to 68 % (60 % LHV). By using the heat loss in combined heat and power plants to generate power and heat, conversion efficiency can reach even 91 % (80 % LHV) [59]. Methane combustion does not need any adaptation of the gas turbines. The revamp costs for a large gas turbine to methanol as fuel instead of crude oil are in the order of magnitude of U.S. $3 million [49]. Leading gas turbine manufacturers are willing to execute and to guaranty the modifications and the performance of the gas turbines. Test work with gas turbines (Table 8.7) has demonstrated an efficiency increase of approximately 9 % compared to NG combustion, whereas NO_x emissions remain unaltered at the same (low) level of 25 ppm NO_x at 15 % O_2 [60].

8.4.3 Chemical Industry

Methanol is a base chemical with the most versatile applications (see Sect. 6.2). Methane as NG is a resource for synthesis gas, but its application as base chemical is restricted to form hydrogen cyanide (1997: 1.4 million t), which is barely traded worldwide [61]. In fact, methane has to be converted to methanol before it becomes useful in industrial chemistry.

8.5 Balancing of the Process Chain

Figure 8.17 shows the process chain of the power storage systems methane and methanol in terms of power-methane-power and power-methanol-power [24, 36, 59]. If methanol is used as fuel in a power plant and no transportation and transformation is necessary, the overall efficiency can be raised up to 38 % [62]. The comparison in shows that the overall efficiency of the power-to-power processes is evidently higher for methanol than for methane (Table 8.8).

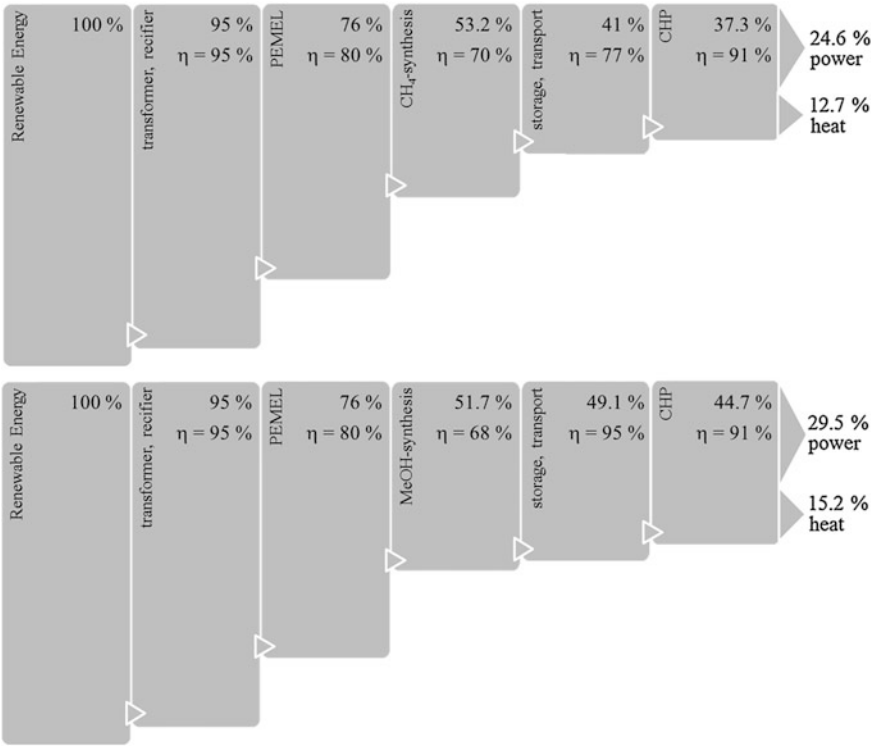

Fig. 8.17 Process chain for the power storage systems methane and methanol. Transport calculated for a distance of 500 km each. *PEMEL* Polymer membrane electrolysis; *CHP* Combined heat and power

Table 8.8 Comparison of process chain efficiencies of power-to-power processes

Storage material	Storage and transport efficiency (%)	CHP efficiency (%)	Power efficiency (%)	Heat efficiency (%)
Methane (SNG)	41	37.3	24.6	12.7
Methanol	49.1	44.7	29.5	15.2

CHP Combined heat and power; *SNG* Synthetic natural gas

8.6 Comparison of Storage of Surplus Power via Methane and Methanol

Storage characteristics of methane and methanol are compared here, based on the same basic data and for the same storage capacity; both measures of energy content are in TWh_{el}. A key question is the selection of the storage capacity. However, substantial differences were found in literature reports (Table 8.9).

Table 8.9 Literature survey on storage capacities for methane and methanol

Author	Ref.	Statements
Stolten	[4]	5.4 million tpa Hydrogen = 257 TWh_{el} = 46 million tpa methanol = 29 MegaMethanol plants
Stolten	[4]	90 TWh_{el} to provide storage capacity for 60 days as Reserve = 2,850,000 t methanol = 9.5 MegaMethanol plants
Stolten	[4]	15 TWh_{el} as a permanently filled reserve in the natural gas grid over a 1 year period (without caverns) = 1.6 MegaMethanol plants
DB Research	[9]	40 TWh_{el} after 2040, assuming 50 % of surplus power to be stored = 4.2 MegaMethanol plants
Beckmann et al.	[63, 64]	440 $TWh_{chem.}$ = 44 billion Nm^3 methane = 55 million tpa Methanol = 34 MegaMethanol plants
Sterner	[65]	20–40 TWh_{el} for > 50 % RE = 2.1–4.2 MegaMethanol plants

Table 8.10 Literature survey on surplus power generation

Author	Ref.	Statements
Sterner	[65]	170 TWh_{el} (scenario B: 100 % surplus energy, ideal grid extension)
UBA	[14]	90 TWh_{el} (scenario: 100 % surplus energy, ideal grid extension, ideal load management, ideal generation management)
		30 TWh_{el} (scenario: 85 % surplus energy)
Auer	[6]	40 TWh_{el} in 2040
Selected storage scenario (1)		• 100 TWh_{el} as surplus power in 2050 to be stored as methanol • 100 TWh_{el} = 11.5 million tpa methanol = 7 MegaMethanol plants (5,003 tpd methanol)
Selected storage scenario (2)		• 100 TWh_{el} as surplus power in 2050 to be stored as methane • 100 TWh_{el} = 6.05 billion Nm^3/a methane = 7 methane/SNG plants (109,500 Nm^3/h CH_4)

Table 8.11 Key parameters for production cost comparison of SNG against methanol

Variable	Unit	SNG	Methanol
TIC	Billion €	1.96	2.08
Cost of electrolysis	€/kWh	700	700
Electrolysis (% of TIC)	%	78	74
Power cost	€ct/kWh	1/3/5	1/3/5
Electrolysis performance	kWh/Nm^3 H_2	5	5
Electrolysis capacity	MW_{el}	2,190	2,190
Electrolysis efficiency	%	74.34	74.34
Product: SNG / Methanol	Nm^3/h / tpd	109,500	5,003
CO_2 purchase cost	€/t	40	40
O_2 sales	€/t	40	40
Depreciation/ROCE	Years/ %	15/10	15/10

ROCE Return on capital employed

A literature survey of surplus power generation showed large differences depending on the assumptions for the respective studies. By definition, surplus power cannot be fed into the national grid and must therefore either be stored (but the existing capacities are very limited) or exported, which is frequently done at negative prices to keep the power plants connected to the grid [66]. Germany exported 23 TWh_{el} in 2012, with a further increasing tendency [67]. In 2012, overall 150 GWh_{el} had to be disconnected from the grid because of oversupply. This is only a very small percentage against the total power production of approximately 741 TWh_{el}; however, in some local areas, up to 40 % of the regional power generation had to be disconnected—an amount that does not include offshore wind power production. It is expected that by 2030 in total 1,000 GWh_{el} have to be disconnected in order to not overload the grid [68]. Surplus power is in several studies calculated at marginal costs (between 1 and 5 €ct/kWh) [63, 64]. Based on the different figures for surplus power as summarised in Table 8.10, the size for the chemical storage was selected as 100 TWh_{el} for both cases:

Selected option for storage (1) Methanol surplus energy storage
Selected option for storage (2) Methane surplus energy storage

It is important to note that most of the storage capacities as listed in Table 8.9 are smaller in comparison to the surplus energy storage capacity of 100 TWh_{el}. This fact will play an important role in the comparison of the two alternatives.

8.6.1 Introductory Remarks for the Comparison

Despite power production that is fully based on RE (scenario B: 100 % surplus energy storage as H_2; i.e., based on the energy supply and demand situation in 2010, including the residual working lives of the nuclear plants; scenario B assumes a

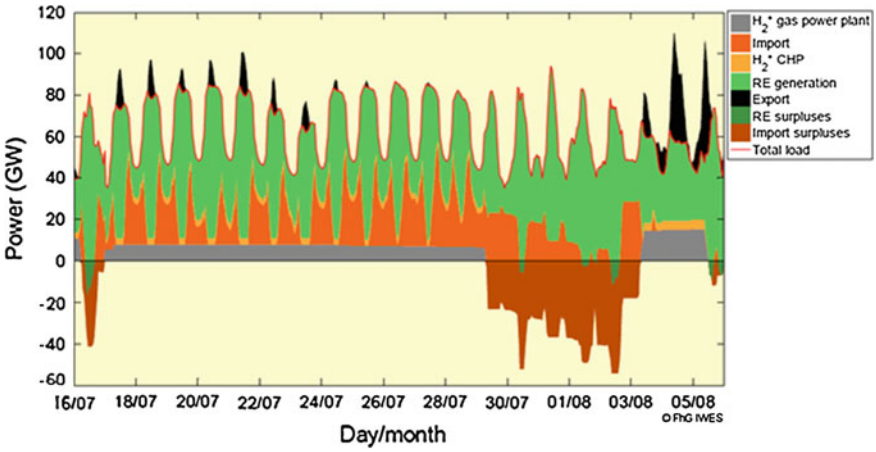

Fig. 8.18 Selected time series of the whole electricity system in Germany for the meteorological conditions in 2006. Calculated from chemical storage, estimated at a capacity in 2050 of 10 TWh_{el}, using scenario B in Ref. [65] (courtesy of the authors). See also Table 8.10

moderate cost increase versus scenario A, which works with a strong cost increase [65].), European grid integration, ideal network expansion, and load management, the need for a long-term energy storage remains necessary. Capacity and storage costs remain questions that are not yet answered, as can be derived from Tables 8.9 and 8.10. Figure 8.17 shows power production based on H_2 or CH_4.

Studies by the BMU Leadstudy 2010 showed that there are considerable differences in assumptions for the development of fuel prices until 2050 (Fig. 8.19) [69]. Comparing gross power consumption development until 2050 reveals substantial differences depending on the assumptions of the various studies, too (Fig. 8.20). The basic scenarios show a decline of gross power production of approximately 11 % from 2008 to 2030. In the period, after the power production remains roughly constant at a level of 535 TWh_{el}. Only the energy concept of 2010 (scenario II A) showed a further decline of power consumption due to efficiency increases. However, the new consumers, such as electric cars, heat pumps, and rail traffic, will (over)compensate for the efficiency increases. In addition, from 2030 on, water electrolysis for H_2/methane production will result in additional power consumption, resulting in an additional power demand of 100 TWh_{el} in 2050 (scenario: Baseline 2010 A with power production for H_2) [65].

The amount of chemical storage energy is highly dependent on the selected scenario, as can be seen from Table 8.9 and Fig. 8.18. The integration of the German grid into the European grid will reduce the necessary size, as well as the development/introduction of smart grid technologies [64]. However, the amount of surplus power will grow, depending on the further expansion of RE production in Europe. As a consequence, the difference between the surplus power produced and

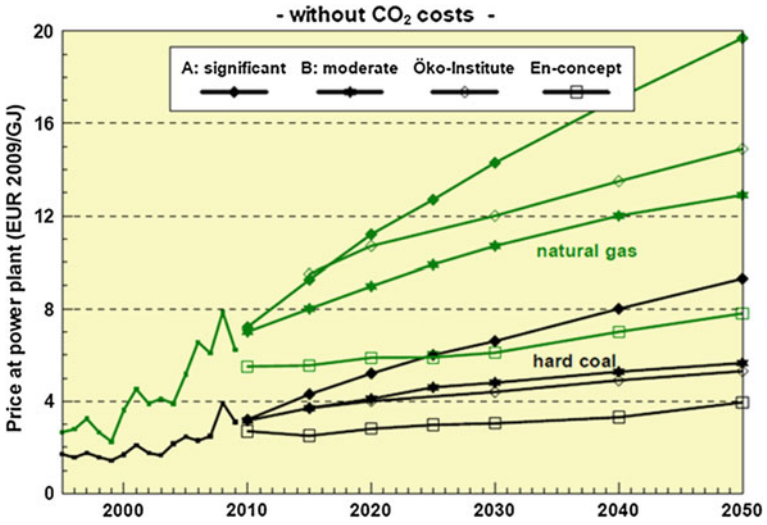

Fig. 8.19 Development of fuel prices at power plants according to different scenario options (A and B) and assumptions by other studies (Öko-Institut) and energy concepts of the German government in 2010 (En-concept) according to Ref. [69]. (Courtesy of the authors)

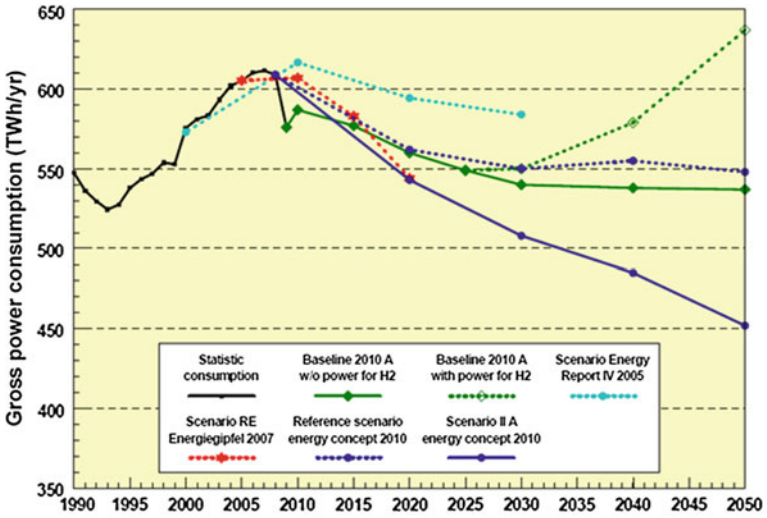

Fig. 8.20 Development of gross power consumption through 2050 according to different scenarios and assumptions (courtesy of the authors) [69]. *RE* Renewable energy. See text for scenario details

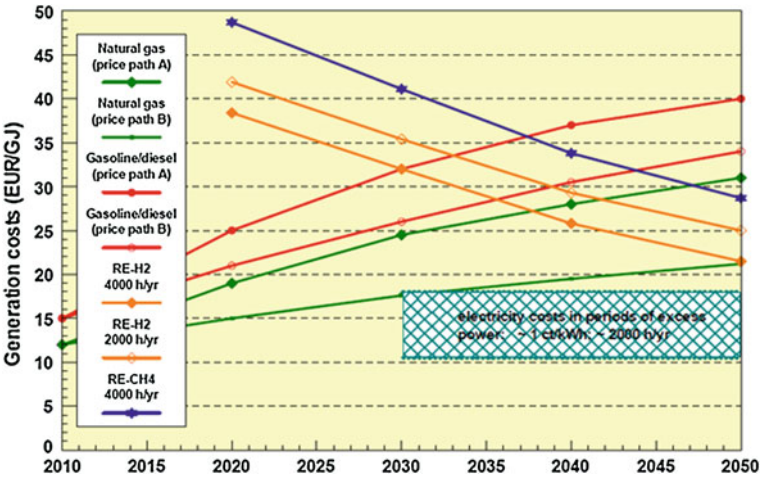

Fig. 8.21 Production cost for renewable hydrogen and methane (courtesy of the authors) [69]. *RE* Renewable energy. See text for scenario details

the storage power needed for the stabilisation of the international grid will be increased, demonstrating the need to make use of the surplus power for other chemical and energy use. The best option is to convert surplus power to methanol.

Figure 8.21 shows the expected fuel costs, ranging between 30–35 €/GJ on a full cost basis for the period between 2030 and 2040 [65]. Renewable hydrogen would become competitive against fossil fuels in about 2030 and against NG about 2040. For renewable methane, the break-even point would set in approximately 10 years later. The full costs for power generation in Fig. 8.20 were assumed to be from offshore wind plants: 7.9 ct/kWh in 2030, 6.2 ct/kWh in 2040, and 5.0 ct/kWh in 2050. The cost decrease is explained in terms of learning curves and economy of scale.

If surplus RE could be produced over a period of approximately 2,080 h per year at 1 ct/kWh, then (according to [65]) production costs between 10 and 18 €/GJ on a full-cost basis in the period after 2030 could be achieved (see Fig. 8.21). Thus, converting renewable electricity at 3–5 ct/kWh to methane and/or methanol would open the markets not only to economic repowering, but also to methanol as raw material for both fuels and chemicals, which is even more attractive.

There is also a positive effect of the turnaround in German energy policy, as can be seen from Fig. 8.22. In comparison to a fossil fuel scenario (business as usual), the differential cost for RE supply will substantially decrease compared to the expected rising costs of fossil fuels in the future.

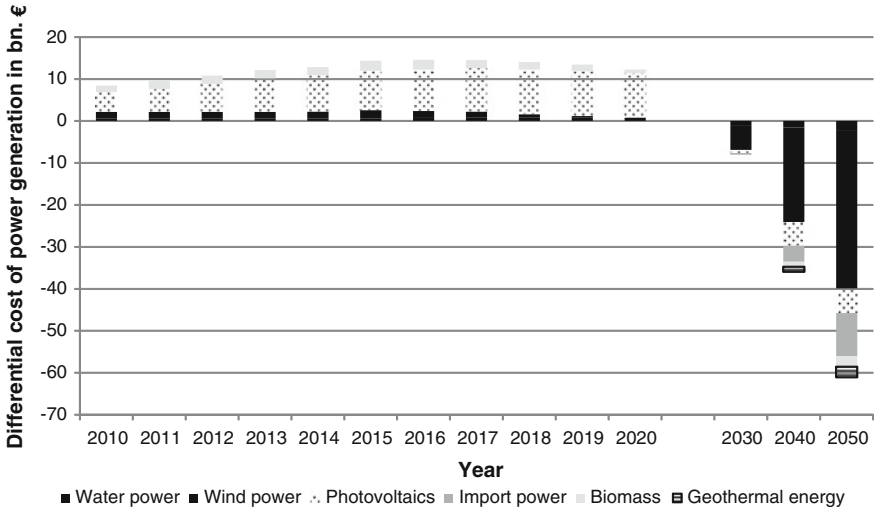

Fig. 8.22 Differential cost of power generation in billion €. (Adapted from [70])

8.6.2 Basic Assumptions for the Comparison of Methane Versus Methanol Storage

Taking 100 TWh_{el} surplus power as a basis (see Table 8.10), hydrogen production capacity can occur two different ways:

Storage scenario (1) 7 MegaMethanol plants each with 5,003 tpd methanol production

Storage scenario (2) 7 SNG plants each with 109,500 Nm^3 of SNG production

For purposes of clarity, an imaginable scenario (3) that combines methanol and methane production is not dealt within this treatise.

As will be outlined in more detail, plant capacities can deviate from the above selected sizes according to local optimisation, as economy of scale does not play an important role. Locations should be selected in different parts of Germany to optimise power supply, CO_2 supply, and product offtake as well as utilities and skilled manpower. Therefore, locations inside/directly linked to refineries/chemical complexes would be preferred. However, also smaller plants in areas with very limited power offtake capacity could be beneficial in order to avoid disconnections from the local grid as caused by fluctuating oversupply.

To compare the specific energy production costs (in €/GJ) of the two storage scenarios on a quantitative basis, one MegaMethanol plant (5,003 tpd) and one SNG plant (109,500 Nm^3/h) were selected (see Fig. 8.23 and Table 8.12). Both plants are based on the same power input of 2,190 MW_{el} per plant.

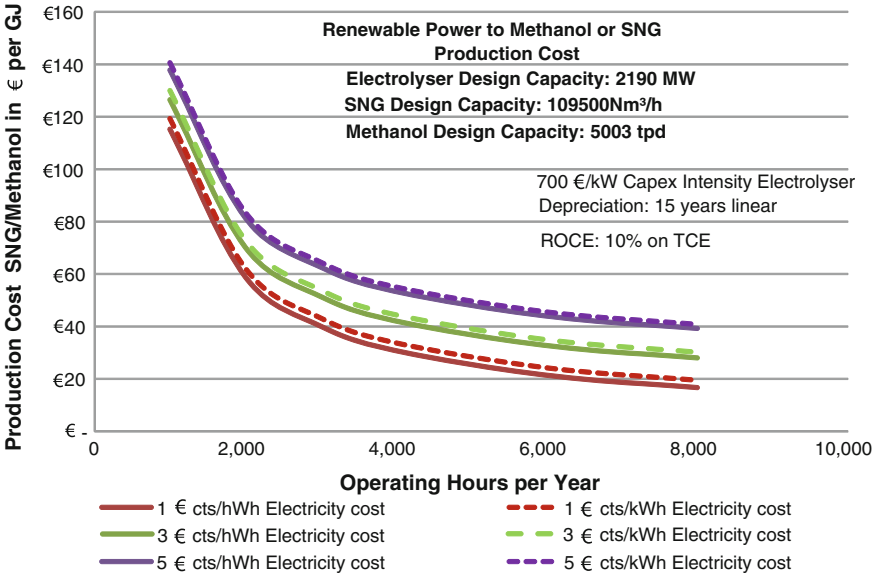

Fig. 8.23 Renewable power to methanol or SNG: Production costs for different power costs and working lives with assumed electrolyser costs of 700 €/kW in 2050 (adapted from [71]). *Capex* Capital expenditure; *ROCE* Return on capital employed; *TCE* total capital employed. Solid lines refer to SNG, dotted lines to Methanol

Table 8.12 Production costs in Euro-cents for SNG and methanol for different power costs and operating times

Operating time (h/a)	Process	Power cost 1 cent/kWh	Power cost 3 cents/kWh	Power cost 5 cents/kWh
4,000	SNG [€/GJ]	30.77	42.07	53.36
	Methanol [€/GJ]	33.77	44.43	55.09
6,000	SNG [€/GJ]	21.39	32.68	43.98
	Methanol [€/GJ]	24.26	34.93	45.59
8,000	SNG [€/GJ]	16.7	27.99	39.29
	Methanol [€/GJ]	19.51	30.18	40.84

8.6.3 Results of Comparison of a MegaMethanol Plant (5,000 tpd) with an SNG Plant for Methane Production (110,000 Nm^3/h)

Based on the same power input (2,190 MW_{el}), total installed cost (TIC) for both plant types, 15 years linear depreciation, and 10 % return on capital employed, the production costs for methanol and SNG in €/GJ are very similar, as can be seen from Fig. 8.23 and Table 8.12. The numbers in Table 8.12 refer to the values for

methanol/SNG costs in €/GJ at the different operating times and power costs as in Fig. 8.23, demonstrating how small the cost differences are. Other relevant figures/assumptions are assembled in Table 8.11. With a capacity of 2.1 MW per stack (type PEM, 30 bar pressure), about 1,000 stacks are needed to install the capacity of 2,190 MW_{el}. The cost of the electrolysers in total sum up to approximately 75 % of the TIC. There is nearly no economy of scale due to the numbering up of the individual stacks. The remaining TIC for the SNG/methanol synthesis is small (approximately 25 %), so the economy of scale will in most cases be of minor influence for the plant size compared to other parameters, such as power supply lines, offtake of products, and utilities.

8.7 Conclusion

There is no real difference between the overall efficiencies for the power storage systems based on methane or methanol (see Fig. 8.17). Both technologies are at a comparable level of development. The key technology to reduce the production cost of green methane and methanol in the future is the development of the electrolysis technology, especially the PEM technology, to higher efficiency, larger unit capacity, and (most importantly) significantly reduced cost. Large-scale chemical storage is required, according to various studies, when the renewable portion of power production increases beyond 50 % [14]. This development is expected to occur approximately from the year 2030 on. Thus, there is sufficient time to develop the necessary technologies, and studies demonstrate the high potential behind this development [71].

The consequences of reduced electrolyser costs may be illustrated with the following example. Under the condition that methanol is produced over 4,000 h per year at 1 €ct/kWh and that the electrolyser generates costs of 700 €/kW (which is approximately the average of both technologies, per Table 8.2), then the resulting methanol production cost is approximately 600 €/t. Reducing the electrolyser cost to 500 and 300 €/kW, respectively (thus in anticipation of technology improvements) decreases methanol production costs to 500 and 400 €/t, respectively. Increasing the efficiency of the electrolysis from 5 to 4 kWh/Nm^3 would result in a decrease of the specific generation cost (in €/GJ) of approximately 20 % [72]. One may believe that such cost reductions are overly optimistic. However, there is another important advantage of the PEM technology, which is its operability of up to 300 % of the nominal load for a limited time. At present, this is in the order of 1 h, but there is also a considerable potential for further developments. Consequently, under the fluctuating operating conditions with renewable energies, one could think of installing a reduced nominal capacity (i.e., reduced capital expenditure). For example, operating PEM electrolysis under fluctuating conditions up to 200 % of its nominal load, providing a hydrogen storage of suitable size (approximately 2 weeks), would allow for operating the downstream synthesis plant up to 8,000 h/year [72]. An increased

operating time from 4,000 to 8,000 h/year would reduce the specific energy production cost for methanol by 42 % (from 33.77 to 19.51 €/GJ).

There is a commercial 4,000 t/a methanol facility in Iceland and a 2,000 t/a pilot plant for methane production in Germany. In both facilities, experience is gathered under strongly fluctuating operating conditions. The major differences between methane and methanol lie in their different applications and as well as in the overall efficiency of energy storage in the individual chemical entities. In the energy sector, methanol has better properties for fuel utilisation compared to methane. However, the latter profits from the well-developed NG infrastructure. As an organic base chemical, however, methanol is unrivalled and its use in a wide range of applications is unparalleled. Regarding the core question—whether SNG or methanol (or both?) should be selected as storage molecules for the future chemical storage scenario—there are the following decisive facts:

1. There is no significant difference in the production cost for methane and methanol (Fig. 8.23).
2. Economy of scale is not a deciding factor for the technology choice.
3. Both methane and methanol can be produced on a large scale.
4. The amount of surplus power is significantly larger in comparison to the required storage volume beyond the year 2040 in Germany.
5. Surplus power is not charged from the EEG. On the contrary, it is sold at marginal cost (1–5 ct/kWh). The process window with generation costs between 10 and 18 €/GJ beyond 2040 (see Fig. 8.21) seems realisable.
6. Losses due to transport and compression/decompression of methane are considerably larger in comparison to methanol.
7. The costs to adapt a large gas turbine to methanol combustion are moderate: approximately $3 million has to be invested for a large-scale gas turbine.
8. The efficiency of a gas turbine is 9 % higher for methanol than for methane (see Table 8.10).
9. Methanol can be added to gasoline at 3 %. Gasoline consumption in the EU is 120 million t/a, allowing for 3.6 million t/a of methanol to be added and, in the case of "green methanol", having 5.4 million t/a of CO_2 (temporarily) being stored. Modern gasoline engines can accept up to 20 % methanol without engine changes.
10. Methanol has only half the specific energy content compared to gasoline. However, this disadvantage is largely compensated by significantly higher compression, resulting in a much higher specific power of an engine.
11. Green methanol can significantly contribute to achieve the EU goal of 20 % RE by 2020.
12. Green methanol can technically replace ethanol in gasoline engines. It is cost competitive against European ethanol on a €/GJ basis up to 800 €/t (see Fig. 7.1 in Chap. 7). The advantage would even be higher under present North American market conditions.
13. Green methanol from surplus power adds to supply security and price stability.

14. Methanol can easily be transported by road, railway, and pipelines, thus allowing for an easy and cost effective long-distance transport of renewable energies.
15. Methanol can be used as both energy and chemistry feedstock. Storage of energy in methanol produced from CO_2 efficiently closes the carbon loop by using regenerative energies. In this way, there is not only less dependence on crude oil, but also biomass can be produced for nutrition rather than transportation purposes, and public mobility on the basis of CO_{2+} sunlight comes into range.

Therefore, through the higher overall efficiency of methanol production compared to methane synthesis and in view of almost identical production costs of both entities, more energy per price unit is obtained from methanol than from methane (see Figs. 8.17 and 8.23).

References

1. M. Bertau, F.X. Effenberger, W. Keim, G. Menges, H. Offermanns, Chem. Ing. Tech. **82**, 2055–2058 (2010)
2. C. Pieper, H. Rubel, Electricity storage, making large-scale adoption of wind and solar energies a reality. Boston Consulting Group Report, 2010
3. J. Nitsch, B. Wenzel, Langfristscenarien und Strategien für den Ausbau erneuerbarer Energien in Deutschland—Leitscenarien. German Federal Ministry for the Environment, Nature Conservation and Nuclear Safety, Berlin, 2009
4. D. Stolten, T. Grube, M. Weber, Windstrom und Wasserstoff—Eine Alternative, 77. Meeting of the German Physical Society, Working Group Energy, 27.03.2012, Berlin, Germany, 2012
5. F. Behrendt, Chem. Ing. Tech. **83**, 1755 (2011)
6. J. Auer, Moderne Stromspeicher, Unverzichtbare Bausteine der Energiewende, DB Research, 03 Jan 2012
7. H. Splietthoff, A. Wauschkuhn, C. Schuhbauer, Chem. Ing. Tech. **83**(11), 1792–1804 (2011)
8. S. Bajohr, M. Götz, F. Graf, F. Ortfoll, Speicherung von regenerativ erzeugter elektrischer Energie in der Erdgasinfrastruktur, Fachberichte Rohrnetz, gwf-Gas/Erdgas, April 2011, pp. 200–210
9. S. Kohler, Siemens Publication Pictures of the Future, 2012, pp. 48–49
10. J. Nitsch, T. Pregger, T. Naegler, N. Gerhardt, B. Wenzel, Langfristszenarien und Strategien für den Ausbau der erneuerbaren Energien in Deutschland, DLR Stuttgart, Fraunhofer-IWES, kassel,IfnE Teltow; Studie im Auftrag des BMU, März 2012
11. Frankfurter Allgemeine Zeitung, Das Deutsche Stromnetz läuft über. 11 Jan 2013
12. M. Sterner, N. Gerhardt, Y.M. Saint-Drenan, M. Specht, B. Stürmer, U. Zuberbühler *Erneuerbares Methan—Eine Lösung zur Integration und Speicherung Erneuerbarer Energien und ein Weg zur regenerativen Vollversorgung*. Solarzeitalter 01/2010. (Eurosolar, Berlin 2010)
13. F. Schüth, Chem. Ing. Tech. **83**, 1984–1993 (2011)
14. T. Klaus, C. Vollmer, K. Werner, H. Lehmann, K. Müschen, *Energieziel 2050: 100% Strom aus erneuerbaren Quellen* (Federal Environment Agency, Dessau, Germany, 2010)
15. Waidhas, M, Dynamic electrolysis for grid surplus and frequency control. Presentation at the Dechema Kolloqium "Wind to Gas" Frankurt, 7 March 2013
16. http://www.iea.org/stats

17. F. Dormen, C. Pauly, G. Traufetter, Der Spiegel 22/2013, p. 74
18. German Renewably Energy Agency, Berlin, 2012
19. B. Lomborg, Der Spiegel 12/2013, pp. 122, 123
20. M. Specht, M. Sterner, F. Baumgart, B. Feigl, V. Frick, B. Stürmer, U. Zuberbühler, G. Waldstein, New routes for the Produktion of substitute natural gas (SNG) from renewable energy. FVEE Annual Meeting, Berlin, Germany, 2010
21. http://en.wikipedia.org/wiki/Heat_of_combustion and references cited there
22. H. Eilers, M. Iglesias Conzalez, G. Schaub, in *Chemical Storage of Electricity in hydrocarbon Fuels*. Reducing the Carbon footprint of fuels and petrochemicals, DGMK Conference, Berlin, 8–10 October 2012
23. M. Waidhas, Dynamic Electrolysis for Grid Surplus and Frequency Control, DECHEMA Kolloquium Wind-to-Gas, Frankfurt, 7.3.2013, 2013
24. T. Smolinka, M. Günther, J. Garche, Stand und Entwicklungspotenzial der Wasserelektrolyse zur Herstellung von Wasserstoff aus regenerativen Energien, Fraunhofer ISE/FCBAT (2011) (http://www.now-gmbh.de/fileadmin/user_upload/RE-Mediathek/RE_Publikationen_NOW/NOW-Studie-Wasserelektrolyse-2011.pdf), Berlin, 2010
25. DVGW-Arbeitsblatt G 262; Nutzung von Gasen aus regenerativen Quellen in der öffentlichen Gasversorgung. ISSN 0176-3490,2004
26. T. Kolb, Power-to-Gas (PtG), ein Baustein des künftigen Energiesystems. DECHEMA Kolloquium Wind-to-Gas, Frankfurt, 07 March 2013
27. B. Müller, K. Müller, D. Techmann, W. Arlt, Chem. Ing. Tech. **83**, 2002–2013 (2011)
28. BDEW, Energiemarkt Deutschland—Zahlen und Fakten zur Gas-,Strom- und Fernwärmeversorgung, 2010
29. Crotingo et al., 18 World Hydrogen Energy Conference, Essen, Germany, 2010
30. http://www.enertag.com/projektentwicklung/hybridkraftwerk.htm
31. Saur et al., Wind-Hydrogen Project: Electrolyser Capital—Cost Study. Technical Report, National Renewable Energy laboratory, Golden, CO, 2008
32. W.C. Chueh, C. Falter, M. Abbott, D. Scipio, P. Furler, S.M. Haile, A. Steinfeld, Science **330**, 1797–1801 (2010)
33. P. Sabatier, J. Senderens, Acad. Sci. **134**, 514–516 (1902)
34. S. Rieke, Energ. Wasser Prax. **9**, 66–72 (2010)
35. R. Grünwald, M. Ragwitz, F. Sensfuß, J. Winkler, Regenerative Energieträger zur Sicherung der Grundlast in der Stromversorgung. Office of Technology Assessment (TAB) at the German Parliament, Berlin, 2012
36. H. Krause, G. Müller-Syring, Integration von Wasserstoff in das Erdgasnetz. Power-to-gas—die Energiespeicherung der Zukunft. 4. Sächsischer Brennstoffzellentag, Leipzig, 2011
37. G. Müller-Syring, M. Henel, Power-to-gas, Ein Beitrag zur Energiewende. Technik-Dialog der Bundesnetzagentur, Schwerpunkt Speichertechnologien, Bonn, 16.März 2012
38. M. Sterner, Ph.D. thesis, Universität Kassel, 2009
39. T. Amon, B. Amon, V. Kryvoruchko, A. Machmüller, K. Hopfner-Sixt, V. Bodiroza, R. Hrbek, J. Friedel, E. Pötsch, H. Wagentristl, M. Schreiner, W. Zollitsch, Biores. Technol. **98**, 3204–3212 (2007)
40. J. Hill, Agron. Sustain. Dev. **27**, 1–12 (2007)
41. R. Rathmann, A. Szklo, R. Schaeffer, Renew. Energy **35**, 14–22 (2010)
42. B. Wenzel, J. Nitsch, Langfristscenarien und Strategien für den Ausbau erneuerbarer Energien in Deutschland. Entwicklung der EEG-Vergütung, EEG- Differenzkosten und EEG-Umlage bis 2030. On behalf of the German Federal Ministry for the Environment, Nature Conservation and Nuclear Safety, Teltow, Stuttgart, 2010
43. G.A. Olah, A. Goeppert, G.K. Surya Prakash, *Beyond Oil and Gas: The Methanol Economy* (Wiley-VCH, Weinheim, 2006)
44. C.N.K. Kumar, K. Tran, O.F. Sigurbjornsson, J. Whitlow, K. Alexander, WO2011061764, 2011
45. K. Tran, P. Wuebben, Vision of Renewable Methanol in the EU: Milestones and Timeline. Methanol Forum 2012, 29.09.2012, Houston, Texas, 2012

46. Landsvirikjun Corp., Press release, 23 Dec 2010
47. S. Bajohr, M. Götz, F. Graf, T. Kolb, Gas/Erdgas **153**, 328–335 (2012)
48. F. Pontzen, W. Liebner, V. Gronemann, M. Rothaemel, B. Ahlers, Catal. Today **171**, 242–250 (2011)
49. Data from Lurgi AG, personal communication, 2013
50. W. Seuser, G. Harzfeld, G. Balzer, E. Harzfeld, in *Fachhochschule Stralsund*. Windpower to Cernol- a hydrogen storage technology, Presentation at the Conference: Understanding Reality-Facing Challenges-Creating Future, Brussels, 24.November 2011
51. http://bluefuelenergy.com/ghgenius/ghgenius.html
52. Data from Erdgasverdichterstation Mallnow, Oberhausen, MAN Turbo AG, personal communication, 2009
53. VDB Verband der Bahnindustrie, Zahlen und Fakten: Bahnindustrie, 2010
54. G.E. Herdin, *Increasing Gas Engine Effiency* (World Energy Engineering Congress, Atlanta, 2000)
55. B.J. Bowers, J.L. Zhao, M. Ruffo, R. Khan, D. Dattatraya, N. Dushman, J. Beziat, F. Boudjemaa, Int. J. Hydr. Energy **32**, 1437–1442 (2007)
56. M. Müller, Regenerative Fuel Cells, in *Fuel Cell Science and Engineering*, vol. 2, ed. by D. Stolten, B. Emonts (Wiley-VCH, Weinheim, 2012), pp. 219–245
57. N. Hotz, M. Lee, C.P. Grigoropoulos, S.M. Senn, D. Poulikakos, Int. J. Heat Mass Transfer **49**, 2397–2411 (2006)
58. D. Johnson, IHS Global methanol market review, June 2012. Download from: http://www.ptq.pemex.com/productosyservicios/eventosdescargas/Documents/Foro%20PEMEX%20Petroqu%C3%ADmica/2012/PEMEX_DJohnson.pdf
59. H. Ghanbari, M. Helle, H. Saxén, Chem. Eng. Process. Process Intens. **61**, 58–68 (2012)
60. G.H. Shiomoto, D.E. Shore, Methanol Clean Coal Stationary Engine Demonstration Project. Executive Summary. California Energy Commision Report P500-86-004, 1986
61. G. Hagan, S. Cochrane, *HCN Market Research Report* (TLA Process Technologies, Miami, 1998)
62. Carbon-Clean Technologies AG, DE202010012734, 2012
63. M. Beckmann, C. Pieper, R. Scholz, M. Muster, Wasser und Abfall **14**(7–8), 47–55 (2012)
64. M. Beckmann, C. Pieper, R. Scholz, M. Muster, Wasser und Abfall **14**(9), 20–27 (2012)
65. M. Sterner, M. Jentsch, Energiewirtschaftliche und ökologische Bewertung eines Windgasangebots, Fraunhofer Institut für Windenergie und Energiesystemtechnik (IWES), Kassel, 2011
66. Frankfurter Allgemeine Zeitung, Der unheimliche Erfolg der Energiewende. 21 Feb 2013
67. Frankfurter Allgemeine Zeitung, Stromexporteur Deutschland vervierfacht Überschuss. 03 Apr 2013
68. Frankfurter Allgemeine Zeitung, Erdgassubstitut aus dem Bioreaktor, 04 Dec 2012
69. J. Nitsch, T. Pregger, Y. Scholz, T. Naegler, M. Sterner, N. Gerhardt, A. von Oehsen, C. Pape, Y.-M. Saint-Drenan, B. Wenzel, Langzeitszenarien und Strategien für den Ausbau der erneuerbaren Energien, in Deutschland bei Berücksichtigung der Entwicklung in Europa und global. “Leitstudie 2010”, German Federal Ministry for the Environment, Nature Conservation and Nuclear Safety, Berlin, 2010
70. M. Sterner, N. Gerhardt, M. Jentsch, M. Specht, B. Stürmer, U. Zuberbühler, Perspektiven des Energieträgers Methan. Methan aus Solar-und Windenergie, Solarzeitalter, 01/2010, Eurosolar, Berlin
71. T. Molinka, M. Günther, J. Garche, Stand und Entwicklungspotential der Wasserelektrolyse zur Herstellung von Wasserstoff aus regenerativen Energien. Kurzfassung des Abschlussberichts. NOW–Studie Fraunhofer ISE, 5 July 2011
72. A. Tremel, M. Walz, M. Baldauf, in *Use Case Analysis for CO_2-based Renewable Fuels*. 3rd International Conference on Energy Process Engineering, Frankfurt, Germany, 4-6 June 2013

Company Index

M. Bertau et al. (eds.), *Methanol: The Basic Chemical and Energy Feedstock of the Future*,
DOI: 10.1007/978-3-642-39709-7, © Springer-Verlag Berlin Heidelberg 2014

Subject Index

M. Bertau et al. (eds.), *Methanol: The Basic Chemical and Energy Feedstock of the Future*, DOI: 10.1007/978-3-642-39709-7,